

Государственное образовательное учреждение
высшего профессионального образования
**«Томский государственный университет
систем управления и радиоэлектроники»**

ТЕМАТИЧЕСКИЙ РЕФЕРАТИВНЫЙ СБОРНИК № 20-2/4

**“Radar Signal Processing”
(«Обработка РЛ сигналов»)**

Публикации в трудах конференций

Источник: *Digital Library IEEEExplore*

Язык: *английский*

Глубина поиска: *2007 гг.*

Дата формирования: *март 2011 г.*

Составитель: *В.И. Карнышев*

Томск – 2011

ТЕМАТИЧЕСКИЙ РЕФЕРАТИВНЫЙ СБОРНИК № 20-2/4

"Radar Signal Processing" («Обработка РЛ сигналов»)

Публикации в трудах конференций

"An End-to-End Wireless QoS Architecture Evaluation"

This work presents and evaluates an end-to-end wireless network QoS architecture, named DiffMobil. DiffMobil is composed by DiffServ over the IP core network and by the following modules over the circuit switched network: QoS negotiation, congestion control (composed by diagnosis and admission control) and flow control. DiffMobil [9, 11] can be implemented over any kind of wireless network: GPRS, UMTS, IMS/NGN. The concepts proposed by each module, do not depend on the network technology. As ns-2 (Network Simulator) [14] was used, experiments to evaluate the DiffMobil guarantees were conducted with simulations of service requirements by GPRS users. GPRS was the technology chosen because we have implemented a complete GPRS network over ns-2. Performance metrics of a GPRS environment simulated through ns-2 show that DiffMobil offers end-to-end QoS. [C8268]

"Node Compromise Modeling and its Applications in Sensor Networks"

Node compromise is the major and unique security issues in sensor networks. There are many security approaches that can be used to defend against node compromises, yet few researches were focused on their distribution models and defending against them. Knowing the distribution models of node compromise can help us defend against them efficiently and effectively. In this paper, we use probability theory to develop basic uniform model, basic gradient model, intelligent uniform model and intelligent gradient model of node compromise distribution based on the observations of different application environments. These models allow system to estimate the probability of node compromise. To explain how important of these models and how to apply them in security design, we introduced some applications that can be improved using our models such as detecting node compromise, key management and secure routing. [C8269]

"Implementation of advanced radar processes on TMS320C5x processors"

With respect to the advent of radar systems technology, necessity of using advanced and complex processing in the receivers, transfer of high volume of data and need of real time processing in relation to radar signals, appropriate processor must provide the required processing speed. This performance usually is provided with programmable digital signal processors. In this paper, first, processes such as pulse compression with phase coding method, clutter canceling with delay line canceller and Doppler filter bank methods are introduced, then several procedures of parametric and clutter map constant false alarm ratio along with combination of these two methods are described and finally possibility of implementation of these processes on a Texas Instrument DSP are investigated. [C8270]

"The Development of Embedded ECG Recorder Based on ARM9"

An embedded ECG recorder based on ARM9 and Linux RTOS is introduced in this paper. It is based on S3C2410X which is a 32-bit low power micro-controller manufactured by Samsung Company. We transplant Linux RTOS into S3C2410X and develop the application based on Linux. MiniGUI is adopted to design the user interface. This system could acquire ECG signals, display and analyze ECG and send alarm via GPRS when ECG signal is abnormal. [C8271]

"Sub-band interferometry on polarimetric SAR dataset"

Complex SAR image spectral analysis has been shown to provide interesting information about the scattering media, highlighting differences in behavior between homogeneous areas with a fully-developed speckle and point scatterers potentially presenting a more coherent radar spectral response. In the line of previously published works by other groups dealing with coherent scatterers, we have studied the statistics of their occurrence as a function of several parameters like frequency, resolution or polarization. The first step of our procedure consists in selecting two or more sub-bands in the Doppler spectrum (in the azimuth direction) or in the distance direction. The sub-bands are subsequently frequency-shifted in order to provide a nonzero

correlation. The resulting inter sub-band interferograms are explored to identify the points presenting a significant coherence and the relevance of the associated phase is investigated. The number of detected coherent scatterers, and the associated complex correlation coefficient is analyzed, with respect to the different polarizations, the width of the sub-bands and the distance between the sub-bands. Different polarimetric high resolution SAR datasets acquired with the ONERA airborne system RAMSES have been used. The large panel of RAMSES acquired datasets allows the exploration of the influence of frequency (P, L and X bands) and landscape. The theoretical approach will be detailed, and experimental results will be discussed. [C8272]

"Polarimetric temporal information for urban deformation map retrieval"

In this work, a preliminary study on the use of polarimetric persistent scatterers for differential interferometric applications within an urban environment is presented. The PolSAR measurements campaign that the RSLab of UPC is carrying on in the village of Salient using an X-Band ground-based SAR sensor is first described. The work is then focused on the additional information the knowledge of full scattering matrix [S] may provide with respect to the single polarization approach. The problem of instability of the polarimetric signature of urban targets is also analyzed. Finally, a solution based on the search of repeated patterns in the long-temporal profile of pixels' polarimetric signature is briefly introduced. [C8273]

"Search for Survivors Buried in Rubble by Rescue Radar with Array Antennas-Extraction of Respiratory Fluctuation -"

The authors have developed a Doppler-type ground penetrating radar (GPR) unit to find survivors buried in houses that have collapsed in an earthquake or other disaster. The purpose of this study is to improve the dynamic range of radar consisting of an array antenna so that it can quickly identify far-off survivors under rubble. The authors focused on time-variable elements from the respiration of a survivor awaiting rescue in order to remove clutter components, such as the rubble. A healthy individual's respiratory frequency varies from 0.2 Hz to 0.5 Hz, so the authors propose a signal processing method to extract these frequency elements in an effective manner. The authors also examine the effectiveness of this method experimentally. [C8274]

"An Experimental Study for a High-resolution 3-D Imaging Algorithm with Linear Array for UWB Radars"

Pulse radars with UWB signals are promising as a high-resolution imaging technique that can be used for a non-destructive measurement of surface details on reflector antennas and airplane signal. We previously proposed a fast 3-D imaging algorithm, SEABED, that utilizes a reversible transform between the time delay and the target boundary. However, data acquisition is time-consuming when obtaining a high-resolution image because it assumes a mono-static radar with 2-D scanning of an antenna. In this paper, we utilize linear array antennas and propose a fast and high-resolution imaging algorithm. We extend the reversible transform for mono-static radars to apply to bi-static radars to reduce the data acquisition time. The effectiveness of the proposed method is verified with numerical simulations and experiments. [C8275]

"A Wave Front Extraction Algorithm for High-Resolution Pulse Based Radar Systems"

The resolution of a pulse based radar system is restricted by the pulse width. Overlapping echoes in time domain of adjacent objects make a wave front evaluation of B-scans difficult. In this paper, a new algorithm for the wave front detection is proposed. Based on a reference impulse response of a large metal plate, the algorithm is able to determine the number of targets. Furthermore, two narrow adjacent spheres were detected as two different objects although the pulses of the two targets were overlapping. In the resulting radar image their shapes could be reconstructed. [C8276]

"Angle Accuracy of Antenna Noise Corrupted Ultra-Wideband Monopulse Receiver"

In the ultra-wideband monopulse receiver, the incident signal is received with two receiving antennas in sum and difference mode. The received signals' phase and energy are then compared to find the incident signal. The received signals, however, are susceptible to antenna noise. In this paper, we establish the relationship between the angle accuracy of the proposed receiver and the signal-to-noise ratio. The receiver modeled in this paper consists of two co-located ridged-horns, with their sum/difference signals received by cross-correlation receivers and processed by an ideal amplitude-comparison monopulse processor. The derived angle accuracy is compared with monopulse measurements at angles -5deg to +5deg at 1deg intervals. Measurements verify the derivations, showing a root-mean-square error of 0.43deg (measured) vs. 0.46deg (theoretical) at boresight; 0.13deg (measured) vs. 0.09deg (theoretical) at -5deg; and 0.17deg (measured) vs. 0.09deg (theoretical) at +5deg. [C8277]

"Pol-dinSAR: polarimetric SAR differential interferometry using coherent scatterers"

We investigate the impact of polarimetry and polarimetric effects on the Differential Interferometry (DinSAR) technique for the coherent backscattering reciprocal case, with the aim to obtain better accuracy and to extract additional information about the scatterer. Emphasis is given to the effects of Faraday and scatterer line-of-sight (LOS) rotations, and to the determination of the intrinsic scatterer scattering mechanism. [C8278]

"Footprint Adjustment On SFCW-GPR With Modified Dipole Array"

Antennas footprint is an important parameter for good detection result in ground penetrating radar (GPR) survey. The various condition of soil under which a target is buried may change the footprint of an antenna. An antenna with a capacity to adapt with different soil condition is therefore needed. This type of antenna is capable of keeping the footprint constant in different soil condition. The footprint of an antenna is related to the antennas dimension. In this paper, modified dipole array is proposed as an adaptive antenna for GPR. With RF switch circuit, we choose the element on the antenna that will be fed considering to footprint that will be produced. Resistive loading is used to reduce coupling level between elements in the array. The simulation results show that different active element produce different near field area. The size of near field area is proportional to the dimension of the element. [C8279]

"Comparison of the diffraction stack and time-reversal imaging algorithms applied to short-range UWB scattering data"

Comparison of different techniques for short-range UWB radar imaging has been performed based on experimental data. To acquire experimental data, a video-impulse radar with a specially developed antenna system with a single transmitter antenna and an array of receiver antennas has been used. Topology of the receiver array was made in such a way that the footprint of the receiver array does not have any sidelobes. [C8280]

"Evaluation and bias removal of multi-look effect on entropy/alpha/anisotropy"

Entropy, alpha and anisotropy ($H/\alpha/A$) of the polarimetric target decomposition has been an effective and popular tool for polarimetric SAR image analysis and geophysical parameter estimation. However, multi-look processing can severely affects the values of these parameters. In this paper, we evaluate the bias problem in $H/\alpha/A$ due to insufficient averaging. We found that the estimated bias is radar frequency dependent. A procedure for bias compensation is proposed. Data from L-band DLR/E-SAR and L-band JPL/AIRSAR, and X-band PI-SAR data are used for demonstration in this study. [C8281]

"Multidimensional speckle noise reduction in synthetic aperture radar images"

A new approach to filter speckle noise in multidimensional SAR data, based on the multiplicative-additive speckle noise model, is presented. This approach is based on processing the elements of the sample covariance matrix differently, according to the complex correlation coefficient. As it is demonstrated with experimental PolSAR data, the filter does not produce a loss of information, but an improvement of the capabilities to filter speckle noise. [C8282]

"Review of existing monographs and books on radar polarimetry and polariemtric SAR with the aim of justifying the need of updates"

Radar Polarimetry, Radar Interferometry and Polarimetric SAR Interferometry represent the current culmination in active 'Microwave Remote Sensing' technology, but we still need to progress considerably more in order to reach the limits of physical realizability. Whereas with radar polarimetry the textural fine-structure, target orientation, symmetries and material constituents can be recovered with considerable improvement above that of standard 'amplitude-only radar', by implementing 'radar interferometry' the spatial (in depth) structure can be explored. With Polarimetric Interferometric Synthetic Aperture Radar (POL-IN-SAR) imaging, it is possible to recover such co-registered textural and spatial information from POL-IN-SAR digital image data sets simultaneously, including the extraction of Digital Elevation Maps (DEM) from either Polarimetric (scattering matrix) or Interferometric (dual antenna) SAR systems. However, in order to further advance this promising technology, we require pertinent basic educational and advanced research texts plus application oriented books for the practicing engineering scientists and users. Hitherto there are not available satisfactory updated sets of basic books or application oriented handbooks. Therefore, in this paper a succinct review of the existing pertinent monographs, books and guides will be presented with the aim of identifying particular topics that still need to be covered. We do now require these urgently associated sets of revised and updated multi-lingual (English, Japanese, Korean, Chinese)

books. [C8283]

"Analysis of non-Gaussian POLSAR data"

In this paper we present a generalised Wishart classifier derived from a non-Gaussian model for polarimetric synthetic aperture radar (POLSAR) data. Our starting point is to demonstrate that the scale mixture of Gaussian (SMoG) distribution model is suitable for modelling POLSAR data. We show that the distribution of the sample covariance matrix for the SMoG model is given as a generalisation of the Wishart distribution, and present this expression in integral form. We then derive the closed form solution for one particular SMoG distribution, known as the multivariate K-distribution. Based on this new distribution, termed the K-Wishart distribution, we propose a Bayesian classification scheme, which can be used in both supervised and unsupervised mode. Modelling and classification is tested on airborne EMISAR data. [C8284]

"Classification comparisons between dual-pol and quad-pol SAR imagery"

We present a study of the polarimetric information content of dual-pol imaging modes, e.g. (HH, HV) and (VV, VH), and compare these against full quad-pol datasets. We discuss classification accuracies for various dual-pol datasets over several terrain/vegetation types with respect to the full quad-pol classification. The linear polarization modes implemented on space borne SAR systems are of primary importance. However, we also consider novel dual-pol modes, e.g. transmitting a circular polarization and receiving both H and V polarizations, and the so-call compact polarimetry models based on dual-pol data. Our primary emphasis is the inter-comparisons amongst the various dual-pol and compact polarimetric modes. [C8285]

"Analysis of fully polarimetric SAR data based on the Cloude-Pottier decomposition and the complex Wishart classifier"

An estimation of the number of clusters is proposed for fully polarimetric SAR data analysis, and a corresponding unsupervised segmentation algorithm is also given based on the Cloude-Pottier decomposition and the complex Wishart clustering. The Monte-Carlo Cross-Validation (MCCV) is used to estimate the optimal number of clusters to reveal the inner structure of the data. Since it is a quantitative estimation of the classification performance, the MCCV algorithm also has the potential capability to perform the unsupervised segmentation validation. The effectiveness of the MCCV estimation and the segmentation algorithm is demonstrated using ESAR data acquired. [C8286]

"Monitoring temperate glaciers by high resolution Pol-InSAR data: First analysis of Argentine E-SAR acquisitions and in-situ measurements"

This paper highlights the potential to measure temperate glacier velocities and surface characteristics by airborne interferometric and polarimetric SAR remote sensing. Indeed, a novel SAR airborne campaign took place in October 2006 over two Alpine glaciers. Simultaneously to the acquisition of repeat pass interferometric, polarimetric and multi-band data, in-situ measurements were carried out to provide useful information for the SAR synthesis, for backscattering analysis and for performance assessment. Analysis of the experimental data as well as early PolInSAR processing results regarding information extraction are presented. [C8287]

"Telemedicine Center"

This paper describes a stationary unit at the Telemedicine Center (TMC) which is one part of the advanced care and alert portable telemedical monitor. The TMC is software based on a JAVA server platform running on a Windows PC with a GPRS data link and installed in hospitals. It facilitates, tracks, monitors, and reports the patient condition anytime anywhere. It can run on the platform continuously and constantly and can be used to trigger emergency health alerts immediately when abnormalities are detected. Additionally, we help a physician identify useful information from a huge amount of sensor data collected by the body sensor network on a patient and hence to reduce communication costs. Another important is the sensor data can be auto-backuped in case of accidental broken . [C8288]

"The Hardware Design of Three-channel EIG Monitoring System Based on S3C2410X and GPRS"

A kind of ECG monitoring system, which can monitor ECG all the time and can give an alarm when the abnormal ECG signals are found, is described in this paper. The system is designed using S3C2410X and GPRS, and its software is designed based on Linux. The system can monitor the patient's ECG all the time. When the abnormal ECG signals are found, the system will send the short message automatically through GPRS. [C8289]

"An EGG wireless Monitoring Instrument Based on GPRS"

An ECG wireless monitoring system was introduced in this paper. The core unit of instrument is MSP430 micro-controller. The function of instrument includes ECG sampling, analysis and alarm. When the system detects the abnormal ECG from a patient, it will send an alarm message via GPRS wireless module. It is very important for the patient to be salvaged promptly. [C8290]

"Limits on the Resolution of Closely Spaced Multipath Signals"

Fundamental resolution limits of multipath replicas are presented. The results are not based on any specific resolution technique and therefore hold for any method. The resolution limit is a function of signal to noise ratio, signal waveform and the resolution success rate. As a specific example we consider the resolution of a radar chirp signal. We compare the limit with empirical results obtained by employing the Akaike Information Criterion and the Minimum Description Length criterion for model order selection. [C8291]

"Tracking a High Maneuver Target Based on Intelligent Matrix Covariance Resetting"

A high accurate tracking technique with the use of intelligent approach on matrix covariance resetting is proposed in this paper. In practice, the conventional Kalman filters have a fast convergence rate at the beginning. However, after some iteration the Kalman filter steps become very small. To overcome this defect and to make use of Kalman filter abilities, the matrix covariance resetting idea is used. The matrix covariance presetting usually is used to improve the tracking algorithm result especially for high maneuvering targets. To determine the optimal value of the unknown resetting parameter in each step, the intelligent fuzzy block is used. In this paper, an innovative technique is presented, which resets covariance matrix by using fuzzy logic. It is demonstrated by means of numerical acceleration examples that the tracking capability of the proposed method is essentially as good as that of the traditional methods, especially for high maneuver targets. [C8292]

"An Overview of Ultra-Wideband Technique Application for Medical Engineering"

As a novel technique, the UWB has many applications worth to researching on. This paper mainly describes current research on UWB equipments for medical applications. The unique features of UWB technique make UWB adapt to medical field. Based on introducing the key features of UWB technique, two existing main biomedical applications are presented. Then the safety of UWB medical equipments is discussed, which is fundamental of the biomedical applications. Finally a brief assessment of future trends for the UWB technique with a focus on biomedical applying engineer is provided, which is that the UWB technique has a wide application expectation for medical engineering. [C8293]

"The Analysis And Simulation Research of Distance Resolution and Ambiguity Property of LFM Signal"

The linear frequency modulation signal with bigger time-bandwidth product which is widely used in the pulse compression system radar. This paper is according to characteristic of the linear frequency modulation signal, and use the ambiguity function theory to analyse the characteristic. Gave out the course and result of the linear frequency modulation signal through matched filter. Hamming weighting the matched filter output response and simulation the output signal through weighting, and analyses the influence of window function to the matched filter output response and the distance resolution. [C8294]

"Target Detection Method of the LFM Radar Signal with Multiple Polarization Agility"

This paper discusses a linear frequency modulation (LFM) radar signal with multiple polarization agility for the full polarization radar system. The LFM signal is adopted inside each transmitted pulse and the range resolution can be improved through pulse compression technique. The polarization state of the transmitted signal can be changed among several polarization states, and the target can be discriminated from the interference signal through polarization estimation and detection. The signal processing method is introduced. The research results reveal that the target can be effectively detected based on their difference in polarization domain after the target and interference are separated in the range. [C8295]

"The Pattern Recognition of Radar Signal by Self-Adapted Wavelet"

Radar signal is unbalanced and usually mixed by noises. Wavelet transform is a power tool for analyzing unbalanced signal and multiresolution is the normal way. Also the choice of the wavelet bases is important. A new method for band limited wavelet construction is developed in the radar signal processing, which automatically locks on the frequency band that energy is concentrated. By the algorithm, an optimal scale

function is calculated according to the power spectrum of the learning radar signal, the corresponding wavelet can be calculated by two scale relation. With the scale and wavelet filter, the processing result will be the recognized pattern which is similar with the learning radar signal. The experimental results demonstrate the method is effective. Radar signal can be processed in real time. [C8296]

"Direct Decomposing Modulation Phase in GSM Passive Radar"

Direct decomposing modulation phase (DDMP) is presented for generating the quadrature GMSK (Gaussian filtered minimum shift keying) signals in GSM passive radar. We decomposed Integrated phases of the Gaussian filtered pulse response directly into two parts: the transient part and the stable part, analyzed the structures of this two parts in detail, and designed a simple realization scheme. Simulation results validate DDMP method. [C8297]

"A 0.35- μ m BiCMOS Automatic Gain Control IF Amplifier for Radar Receivers"

A monolithic automatic gain control (AGC) IF amplifier for radar receivers is designed in AMS 0.35- μ m SiGe BiCMOS process. The core circuit of this design is an AGC loop. According to the simulation results, this amplifier is able to process an input IF signal with a dynamic range of 40 dB and its output amplitude keeps a fixed value of 1.5 V. It provides a voltage gain up to 60 dB. This AGC amplifier works well over a frequency range from 175 MHz to 275 MHz with a passband ripple of less than 0.5 dB. This circuit consumes less than 100 mW at .a single 5-V supply and the layout takes 0. 8 mm². [C8298]

"Performance analysis of FIR digital filter design: RNS versus traditional"

This paper presents performance analysis of Residue Number System (RNS) based Finite Impulse Response (FIR) digital filters and traditional FIR filters. This research is motivated by the importance of an efficient filter implementation for digital signal processing. The comparison is done in terms of speed and area requirement for various filter specifications. RNS based FIR filters operate more than three times faster and consumes only about 60% of the area than traditional filter when number of filter taps is more than 32. The area for RNS filter is increasing at a lesser rate than that for traditional resulting in low-power consumption. RNS is a non-weighted number system without carry propagation between different residue digits. This enables simultaneous parallel processing on all the digits resulting in high speed addition and multiplication in RNS domain. Such compact and high speed real-time digital filters find applications in radar, communications and image processing systems. [C8299]

"Improving cooperation between Air Traffic Controllers: a design issue"

Reaching a high level of mutual awareness and comprehension in ATC electronic environments is usually considered as a challenge. The fact that the cognitive processes involved in the building of shared representations are by essence complex and hidden constitutes one of the trickiest reason of this difficulty among all the others. Thus, not only is the analysis of the current processes involved difficult in a "paper" environment (i.e. with paper strips and radar image) but when it comes to the design of an electronic stripping environment, basing the design on the adaptation of those processes may be difficult if not counterproductive. Actually, as any evolution of the environment modifies the activity in a non-deterministic way, it is quite difficult to anticipate to what extent those processes would remain adequate in an electronic environment. Instead of that option, applying an adapted design methodology may be a way to handle this issue. The purpose of this paper is to take a current instance of the ASTER project (assistant for terminal sectors) initially dedicated to the executive controller, aiming at providing assistance for the terminal sectors, i.e. sectors dealing with traffic inbound or outbound from one or several major airports, and outline the design process. In the first part of the paper, we will briefly introduce the ASTER concept and the VertiDigi HMI product. In a second step, we will focus on the cooperation issue and describe the way the design process was build in order to tackle this issue. [C8300]

"Airspace design process for dynamic sectorisation"

Air traffic control in core Europe reaches the limits of available airspace capacities. Therefore new roles are introduced to shift workload away from the executive (radar) controller, who operates at the limit and is the capacity bottleneck, towards a more planning oriented but yet adaptive control function, the multi sector planner. This multi sector planner will be responsible for the expeditious flow through several sectors. The new role will execute a set of actions on both, airspace and traffic flows to reduce workload for the sector team or balance workload between sectors, so that overall centre capacity is increased. One of the central support tools is fine-grained, tactical, dynamic airspace management in conjunction with tactical flow measures. The study presents the airspace design process and tools that have been applied for the development of the future airspace of the

Maastricht Upper Area Control Centre, based on the principles of dynamic airspace management. [C8301]

"Assessment of navigation errors on airborne state-based conflict resolution"

This paper focuses on the influence of navigation errors on state-based conflict resolution. Two well-established resolution manoeuvre classes have been investigated: the first one involves a turning point manoeuvre and has been selected as far as it minimizes the number of resolution manoeuvre stages and may be achieved through the autopilot lateral mode; the second one involves an offset manoeuvre and has been retained as far as it may be compatible with flight management system (FMS) functionality. The main throughput of the paper is the analysis of the sensitivity of the two resolution manoeuvre classes to navigation errors. The assessment is conducted through a set of radar encounters which have been modified and simulated by means of a point mass based aircraft dynamic model incorporating autopilot and navigation functionalities. This paper is an output of the AS STAR (advanced safe separation technologies and algorithms) project, sponsored by the European Commission within the 6th Framework Programme. [C8302]

"Assessment of controller situation awareness in future terminal RNAV operations"

The MITRE Corporation's Center for Advanced Aviation Systems Development (CAASD) was tasked by the Federal Aviation Administration (FAA) with defining and validating the performance-based air traffic management (ATM) concept to address the increasing need for improved capacity, efficiency, and productivity in the National Airspace System (NAS). A key enabler of this concept is the continued implementation and greater utilization of performance-based navigation provided by area navigation (RNAV) and required navigation performance (RNP) today and through the future. Implementation of new procedures and features, such as vertical profiles, are expected to reduce the active controlling task that is fundamental to air traffic control (ATC) operations and instead, increase monitoring of operations. This change is intended to leverage flight deck automation and reduce pilot and controller workload; however, it is critical to fully understand the human factors implications of making this shift, especially as traffic operations continue to grow. A human-in-the-loop (HITL) simulation was performed to evaluate changes in situation awareness for the feeder arrival controller position in a terminal radar approach control (TRACON) environment with conventional arrival operations and with future RNAV arrival operations when moderate and high levels of traffic were managed. An assessment of controller situation awareness was made based upon results from the situation awareness global assessment technique (SAGAT) and measurement of controller detection of pre-planned aircraft deviations from their assigned clearance. Workload was also measured using the NASA-task load index (TLX). Findings suggest that a change of controller situation awareness does occur as a result of the increased traffic levels managed. Assessing and mitigating this issue is under study by MITRE/CAASD, in particular through display and alerting automation for radar controllers. [C8303]

"Augmented reality for tower: using scenarios for describing tower activities"

The project 'augmented reality tools for tower' aims at studying the potential applicability of augmented reality (AR) in aerodrome operations. A careful understanding of tower activities is necessary in order to gain insights on the way controllers use the 'view out-of-the-window'. The present paper describes the work steps taken to deepen knowledge on tower activities and highlights the use of scenarios as useful means for describing contextual aspects of tower activities and for stimulating reflections on the design of AR displays. [C8304]

"Development of Underwater Security Sonar System"

A significant research project for developing an underwater security sonar system has been initiated in Japan to guard oil plants, harbors, airports, power plants, and LNG/Oil tankers against underwater terror attacks. In addition, it is planned to quickly establish means of scientifically searching for underwater smuggling of weapons and narcotics, poaching divers, illegal disposals and dead bodies, under the cloak of murky water. A model system was developed to provide empirical data and a means for evaluating detection and fusion algorithms. Major sensors of a littoral surveillance system properly include radar, optical cameras, infrared cameras, and an underwater acoustic surveillance system. We have systemized a wharf security system composed of two acoustic video cameras, a sector scanning sonar and supporting software in the first year of this 3 year program. [C8305]

"Optimal Acoustic Search Path Planning Based on Genetic Algorithm in Continuous Path System"

The design of efficient search path to maximize the Cumulative Detection Probability(CDP) is mainly dependent on experience and intuition when the searcher detect the target using SONAR in the ocean. Recently with the advance of modeling and simulation methods, it has been possible to access the optimization problem more systematically. In this paper, a method for the optimal search path calculation is developed based on the

combination of the genetic algorithm with detection algorithm. We consider the continuous system for search path, space, and time, and use the movement direction of the SONAR as a gene of the genetic algorithm. The developed algorithm, OASPP(Optimal Acoustic Search Path Planning), is shown to be effective, via a simulation, in finding the optimal search path for the case where the intuitive solution exists. [C8306]

"Buoy and Radar Observation Network around Taiwan"

The coastal ocean monitoring center (COMC) was assigned by the government offices to establish an coastal ocean monitoring network around Taiwan. It is composed by data buoys, radars, tide stations and coastal weather stations. All field stations are operational and have real time data transmission function. The purpose of this paper is to present the frame of this observation network and show observation results especially during past typhoons. This paper focuses on the introduction of data buoy and radar systems. The hardware and analysis method of data buoy and radar system are presented in this study. [C8307]

"Monitoring Coastal Processes and Ocean Wave Directional Spectra Using a Marine Radar"

We discuss the application of microwave radars to remote sensing of ocean waves and currents in the coastal zone. A new X-band marine radar family (coherent and noncoherent) operating at 10-m scales can map nearshore bathymetry, and measure ocean currents and wave spectra at distances out to a few kilometers. We present some examples of bathymetry experiments and recent empirical results in establishing the modulation transfer function that relates radar image spectra to ocean wave directional spectra, and allows such wave spectrum measurements. We discuss the plan for a real time operational system based on this technology. [C8308]

"Tsunami Detection using Multi-frequency Beam-Forming HF Radar"

We discuss a new multi-frequency beam-forming HF radar design for robust detection and tracking of tsunami waves from 200 km distances, providing continuous coverage of the tsunami approach to shore. The method works by mapping ocean currents at long range using traditional HF radar method of radial Bragg line Doppler shift measurement, then continuously looking for anomalous Doppler shift patterns and extremely high values due to the large orbital wave of the tsunami wave crest sequence. We discuss issues determining coverage quality improvement achievable using a multi frequency radar (MFR) in order to assure robust long range coverage. These issues include diurnal and seasonal changes in noise character due to ionospheric conditions, and the effect of local wind speed and sea state providing a sufficiently good sea echo signal at long range. Multiple frequency utilization assures this higher quality at no design cost compared to existing single frequency HF radars, using the ISR digital radar design. [C8309]

"Wideband Sonar Waveform Design using Linear FM Signals and Hermite-Rodriguez Functions"

A new approach for the design of wideband sonar waveforms using linear FM signals and Hermite-Rodriguez functions is proposed. The use of Hermite-Rodriguez functions make it possible to formulate the waveform design problem as an optimal parameter selection problem with a positive definite objective function and linear and bilinear constraints. Such a formulation is quite flexible and can accommodate both frequency and time domain design specifications and constraints. The approach used to solve the optimization problem is to convert the nonlinear and nonconvex complex-domain constraints to simple linear and bilinear real-domain constraints by introducing extra optimization variables. Some preliminary numerical results are presented to illustrate the effectiveness of the proposed method. [C8310]

"A Novel Method for Extraction of Micro-Doppler Signal"

The micro-Doppler effect may be generated by additional frequency modulations on the returned radar signal if the target contains rotating structures. The body image will be contaminated due to the existence of the micro-Doppler. In the paper, a simple method based on integral of dwell-time is introduced, which can be utilized to separate the signal of the rotating parts from that of the target body successfully. It makes the ISAR image clearer and also provides some information of the rotating parts, such as the radii and the rotation frequencies. Computer simulations are given to prove the effectiveness of the proposed method. [C8311]

"Optimal Polarization for SINR equation in partially polarized case"

For the SINR (signal-to-interference- and-noise-ratio) equation based on the polarization ellipse parameters in partially polarized case, an optimal polarization method called iterative optimal polarization (IOP) is presented. The iterative processes of IOP are described and shown. Simulation results show that the IOP is an effective method for searching the optimal polarization. After several iterations (4-6 steps), the final optimal value and

optimal point of the SINR equation can be obtained. The average relative errors between the optimum obtained with IOP and the actual optimum are very small. [C8312]

"Super-Resolution of Polarimetric SAR Images for Ship Detection"

Polarimetric SAR images are used for aerial and space imagery applications, such as target detection, tracking, and resource exploration. However, spatial resolution is limited due to the signal bandwidth and the antenna dimension. Super-resolution reconstruction is the process to reconstruct a high-resolution image from multiple low-resolution images. Polarimetric SAR provides multiple images of the same scene at the different channels (HH, VV, HV and VH). In this paper, the POCS method is applied to extract the information from LR images in different channels to generate the HR image. The multiplicative characteristics of noises in SAR images are utilized to construct the convex sets in POCS method. Ship targets are selected as detection object for super-resolution. Results from simulated and real data have validated the effectiveness of proposed method. [C8313]

"Realization of the Algorithms of a Multi-static TWSR"

The normal through-the-wall surveillance radar (TWSR) usually has one transmitting antenna (TA and one receiving antenna (RA), which is called monostatic TWSR. In this paper, a multi-static TWSR with one RA and many TAs is presented and this kind of TWSR works more efficiently than the normal one. FDTD method is used to numerically simulate the TWSR system and relative experiments have done. Besides, imaging process is carried out successfully on data of numerical simulation and imitating experiments of the multi-static TWSR by way of diffraction summation algorithm and frequency-wave number (f-k) algorithm. [C8314]

"Research on Subarray Partitioning of Planar Phased Array with Adaptive Digital Beamforming"

An approach of subarray partitioning for planar phase array radars with ADBF is presented. The architecture of subarray is optimized using genetic algorithm. With the optimized structure of the array, the sidelobe level of adaptive pattern has been well improved; meanwhile, the jammer was suppressed obviously in the direction of the jammer arrival for ADBF at the subarray level. That was demonstrated on 30x32 elements planar array. [C8315]

"Slowlight in semi-conductor amplifier Application to programmable time delays for the control of microwave signals"

Optoelectronics links in future radar systems require the generation and control of time delays for large frequency bandwidth (typically 20 GHz) microwave signals to be transmitted or/and processed. Compact structures wherein slow waves propagate have a role to play in a such context applying the so group delay generated onto the microwave signals. We present an original architecture to slow down the light in semi-conductor amplifier (SOA), based on a dual frequency optical beam interfering inside the gain medium of the SOA as wave mixing due to population oscillation. [C8316]

"An Efficient Method to Determine the Diagonal Loading Factor for PAM Communication System"

Minimum variance distortionless response (MVDR) beamformer are known to degrade due to the effects of imprecise knowledge about the steering vector and finite sample size. The diagonal loading method is a simple and efficient method that improves the robustness of beamformers. However, determining an ideal diagonal loading factor (DLF) is not a trivial problem, one that still has not been adequately addressed. Although beamformers are widely used in radar, sonar, and many other applications, in this paper, we consider only the pulse-amplitude modulation (PAM) digital communication applications. In this paper we take advantage of the binary feature in PAM digital communication system and present an effective method to determine the DLF. Since the binary feature is used, the new method does not require extra assumptions as in other methods. Numerical experiments show that the method improves the robustness of beamformers against mismatch caused by effects related to imprecise knowledge of the steering vector and finite sample size. [C8317]

"The Theory and Design of Provably Optimal Bandwidth Radar Absorbent Materials (RAM) using Dispersive Structures and/or Frequency Selective Surfaces (FSS)"

Performance coefficients, design tools and analysis is provided for the synthesis of optimal radar absorbent materials (RAM). The importance of equivalent circuits is emphasised. The basic theory is quite general and valid for metamaterial and frequency selective surfaces (FSS) composites containing piece-wise isotropic layered materials. [C8318]

"Adaptive Waveform Radar Enabled by S2-material Based Photonic Signal Processing Hardware"

An S2-material based photonic signal processor can perform wideband pulse compression over tens of GHz of instantaneous bandwidth in real-time. We utilize these capabilities to demonstrate wideband mismatched filtering showing 14 dB improvement in the peak-to-sidelobe-ratio when compared to the matched filter case. We proposed the utilization of this technology for adaptive waveform radar signal processing. [C8319]

"Unification of Descriptive Experiment Design and Worst-Case Performance Optimization-Adapted Regularization Paradigms for High-Resolution Reconstruction of Radar Imagery"

We address a new approach to solving radar imaging problems stated and treated as uncertain ill-conditioned inverse problems of nonparametric spatial power spectrum estimation via processing the finite number of independent observations of the degraded array data signals (one realization of the trajectory signal in the case of SAR). The idea is to adapt a statistically optimal minimum risk nonparametric power spectrum estimation approach to the radar imaging scenarios with model-level and system-level uncertainties. The proposed incorporation of the worst-case performance optimization-adapted robust regularization aggregated with the descriptive experiment design paradigm into the minimum risk nonparametric estimation strategy leads to a new unified doubly regularized minimum risk approach for robust adaptive high-resolution reconstructive imaging in the uncertain remote sensing scenarios. [C8320]

"Object Velocity Estimation Based on Asynchronous Data from a Dual-Line Sensor System"

This paper presents a 2 times 256 dual-line vision system for object velocity estimation based on the asynchronous output data. For real-time velocity estimation, a processing method has been developed and implemented on the digital signal processor. It exploits the sparse asynchronous data representation from the dual-line sensor with high temporal resolution (better than 100 mus) and low latency. The processing concept includes the object contours extraction, velocity estimation and scaling. Three approaches are used and evaluated for the velocity estimation. The first and second approaches use the mean and median object detection time, respectively for the object velocity calculation. In the third approach, the statistical linear fit RANSAC is used to extract the object time. This processing concept has been evaluated on object velocities that range from 1 to 22 m/s, for the three velocity estimation approaches and a comparative study has been provided. The experimental results included show a velocity estimation error < 1% using RANSAC. [C8321]

"The Evaluation of Performances of Automatic Method for the Object Detection in GPR Images"

The problem of automatic interpretation of GPR images containing several local objects has been considered. The method based on the Hough transform is used for object detection. The estimation of accuracy of the objects' coordinates determination and the evaluation of detection probability have been performed for the case of automatic interpretation of videopulse subsurface sounding results. The possibility of zero error for coordinate determination has been shown. The relations between object detection probability and false alarm probability are presented using the ROC curves. [C8322]

"Image Processing in Polarimetric SAR Images Using a Hybrid Entropy Decomposition and Maximum Likelihood (EDML)"

This paper presents a hybrid entropy decomposition and maximum likelihood (EDML) for synthetic aperture radar (SAR) image analysis and classification with the application of land use management. Entropy decomposition is an effective technique to obtain valuable decomposed parameters for image interpretation with analysis of the underlying scattering mechanisms. However, the main disadvantage of entropy decomposition is that the decision boundaries of the analysis plane are arbitrary. To overcome this problem, maximum likelihood technique is taken into consideration to help to determine the decision boundaries based upon Gaussian probability model. Hence, the hybrid EDML is developed to provide alternative way to improve the classification accuracy. The objective of this paper is to assess the use of polarimetric data for the image analysis and classification of land use management. It is illustrated using a well-known polarimetric AIRSAR data of San Francisco. In this paper, EDML technique is shown to have a superior result compared to other techniques. [C8323]

"A 210 GHz, Subharmonically-Pumped Active FET Mixer MMIC for Radar Imaging Applications"

A conversion loss of 8.5 dB is achieved for down-conversion of a 210 GHz RF signal in a sub-harmonically pumped mixer MMIC. The active FET mixer, realized in a 100 nm gate length metamorphic HEMT process, employs a dual-gate topology. The mixer achieves a 3-dB RF bandwidth from 188 to more than 210 GHz and is driven by a 10 dBm subharmonic LO signal. The combination with an integrated source follower stage results in a 2 GHz IF bandwidth. The mixer is dedicated to active imaging systems for concealed weapon detection

operating in the atmospheric window around 220 GHz. [C8324]

"A 77-79-GHz Doppler Radar Transceiver in Silicon"

This paper presents the first 77 GHz single-chip direct-conversion transceiver in silicon. The transceiver, fabricated in a 0.13 μm SiGe BiCMOS technology with f_T/f_{MAX} of 170/200 GHz, consumes 740 mW, and occupies 1.3 mm x 0.9 mm. The receiver achieves 25.6 dB conversion gain, 9 dB noise figure, 90 dB dynamic range, and an IP1dB of -24 dBm. The transmitter provides +5.8 dBm of saturated output power at 77 GHz, and a divide14, static frequency divider is included on-die. A tuned, 77 GHz clock distribution network is used to distribute the VCO signal to the divider, power amplifier, and down-conversion mixer. Successful detection of a Doppler shift of 55 Hz at a range of 4 m is shown. The phase noise at IF is shown to be superior to the VCO, suggesting noise correlation between the transmitter and receiver. [C8325]

"Metamorphic HEMT Amplifier Circuits for Use in a High Resolution 210 GHz Radar"

In this paper, we present the development of a W-band power amplifier (PA) circuit and a G-band low-noise amplifier (LNA) MMIC for use in a high-resolution radar system operating at 210 GHz. The power amplifier circuit has been realized using a 0.1 μm InAlAs/InGaAs based depletion-type metamorphic high electron mobility transistor (MHEMT) technology in combination with grounded coplanar circuit topology and cascode transistors, thus leading to a small-signal gain of 12 dB and a saturated output power of 20.5 dBm at 105 GHz. The low-noise amplifier MMIC was fabricated using an advanced 0.05 μm MHEMT technology and achieved a small-signal gain of more than 16 dB over the frequency band from 180 to 220 GHz together with a state-of-the-art room temperature noise figure of only 4.8 dB. Both amplifier circuits were successfully packaged into millimeter-wave waveguide modules and used to realize a 210 GHz radar, which delivers an instantaneous bandwidth of 8 GHz and an outstanding spatial resolution of 1.8 cm. [C8326]

"Ground and flight deck alternatives for terminal merging, sequencing, and spacing for arrivals"

Aircraft approach the terminal area on different arrival paths, merge and ultimately arrive at capacity-constrained runways on the ground. Upon entering the terminal area, air traffic control manually controls the aircraft in order to merge and sequence arrivals on different paths, and establish longitudinal spacing between aircraft. These operations are termed merging, sequencing, and spacing operations. New technologies available in air traffic control facilities and in the flight deck create the possibility of improving on the manual operations used today. Several alternatives are currently in operational trials. Unclear is what alternative will prove to be most desirable for implementation. This paper seeks to enumerate some alternatives, and their characteristics, and establishes a framework for assessment. [C8327]

"Using 4DT FMS data for green approach, A-CDA, at Stockholm Arlanda airport"

How is it possible to perform a Green approach to a large airport like Stockholm Arlanda? The answer is simple in theory but complicated in live trials. By letting the aircraft flight management system (FMS) communicate with the ground the air traffic controller could receive information about what the aircraft intends to do, i.e. what flight path it will take including the time at the different positions. By providing exact 4 dimensional data to the ground, the pilot and the air traffic controller have the same accurate information about the aircraft flight path. It is therefore realistic to think that Green approach concept "on time-first serve" could be applied. It should be stated already now that the during the trials performed, the FMS 4DT has only been collected for technical analysis and not for air traffic control purposes. To provide information about the future position of the aircraft to the air traffic controller is not a new idea. Traditionally, we have been using radar plots to calculate the aircraft position and predict its future flight path (also using fixed data from flight plans.) In these trial/simulations, the flight management system (FMS) data bus in the aircraft was connected to the VHF radio making the FMS information available to the ground as well. This paper discusses how a Green approach is performed during live trials with the special tools developed for this purpose, and the benefits achieved. The paper also provides a brief summary from the simulation that took place in Malmo, Sweden. This simulation addressed the Green approach concept in a much higher traffic density then could be achieved during live trials at Stockholm Arlanda. The work presented here is part of an ongoing European Commission funded North European ADS-B Network (NEAN) Update Program 2+ (NUP2+), with one main objective being to study the use of down-linked trajectory information. The technical aspect by using an aircraft derived trajectory was studied in NUP2+, which is due to finish in 2007. What can be performed to improve the use of 4 dimensional trajectory (4DT)? [C8328]

"General aviation Light Transport Aircraft avionics: Integration and system tests"

Avionics of current day aircrafts is termed as modular integrated full glass cockpit. Unlike lot of dials and gauges, the pilot will interact with multi function displays (MFD). This means that the systems are coupled with

multifunction displays, communication and navigation radios with control units, multi-mode interactive instruments for control and navigation, recording and fault management systems, airframe and health monitoring diagnostic capability. Pilot vehicle interface (PVI) is important measure of good avionics and cockpit layout, which implies the optimization of man machine interface, enhancement of economy and safety of flight operations. The paper presents the avionics architecture of a 14 seated light transport aircraft (LTA) for general aviation, which has the multi role commuter capabilities. LTA is a twin turbo-prop, multi role aircraft, with air taxi and commuter services as its primary roles. The avionics is built on the digital communication mode for both command and control with current requirements of TCAS, digital autopilot and AMLCD multipurpose glass displays. The LTA Avionics suite is grouped into six major groups based on the functionality: display system, communication system, navigation system, recording system, radar system and engine instruments and other cockpit displays. The paper also covers a details about the extensive tests carried out to prove the avionics design in terms of functionality, interoperability, interference and compatibility. Various practical integration and flight-test issues, methodology and details of the scenarios is presented in the paper. [C8329]

"Self-separation corridors"

This paper describes a concept called self-separation corridors (SSCs). This is an automatic dependent surveillance-broadcast (ADS-B) application that establishes self-separation corridors in high-altitude en route airspace. This concept enables traffic managers to create high-density corridors along specific airspace segments for suitably equipped aircraft for use during heavy sector congestion or limited access due to severe weather. An SSC is defined as a set of parallel routes in close proximity to one another, in which crewmembers accept responsibility for separation from other aircraft in the corridor. While in an SSC, pilots use on-board instrumentation to ensure proper spacing behind the lead aircraft. The on-board instrumentation also provides protection from deviations or blunders by aircraft on the parallel routes. This paper describes the primary SSC concept, proposed solutions, and suggested areas of research. [C8330]

"Analysis of RNAV arrival operations with descend via clearances at phoenix airport"

On 10 October 2006, two new area navigation (RNAV) arrival procedures for Phoenix Sky Harbor International Airport (PHX) were published which provide vertical guidance in the terminal area. The procedures largely overlay corresponding conventional procedures and established navigation patterns used by air traffic control (ATC). However, the inclusion of vertical guidance and routine ATC issuance of descend via clearances to leverage this guidance was expected to result in more continuous aircraft arrival descents inside the terminal area. More continuous descents enable prolonged flight under reduced engine thrust and associated fuel burn and environmental benefits. The MITRE Corporation's Center for Advanced Aviation System Development (CAASD) was tasked by the Federal Aviation Administration (FAA) to assess operational changes associated with the implementation of the new RNAV arrival procedures at PHX and estimate the resulting user benefits. Based on analysis of radar data recorded during eleven days of pre-and post-implementation operations, significant improvements in descent continuities were observed for aircraft descending via the new procedures. The improvements resulted in a 38-percent reduction in the time aircraft remained in level flight at key step-down altitudes in terminal airspace. Fuel burn benefits to users were estimated at \$0.5 million annually, and resulting reductions in CO₂ emissions were estimated at approximately 2500 metric tons annually. In addition to these currently realized benefits, improved participation coupled with procedure optimization efforts promise increased future user benefits. [C8331]

"Bearing Finding and Array Error Correction in Noncooperative Passive Detection"

Direction finding by MUSIC algorithm in noncooperative passive detection system is proposed. Basing on the method the array error is corrected by instrumental sensor method (ISM). In the method, firstly, the correlation signals of array received signals and the frequency-shift signals of direct signal are obtained; secondly, the signals near to estimation delay of correlation signals are selected as new received signals of the array; finally, MUSIC algorithm is used to find object's direction. It is proved that when the new received signals' length is 1, the method has highest estimation precision. Simulation result shows that theoretical derivation is correct and the method is effective. [C8332]

"A Framework for the Analysis of Multistatic Radar Systems with Multiple Transmitters"

The multistatic ambiguity function can be used as a tool for analyzing multistatic radar systems. It has been demonstrated that the multistatic ambiguity function can serve as a guideline for developing multistatic radar signal processing rules and waveform selection strategies in system configurations with a single transmitter and multiple receivers. In this work we extend the development of multistatic ambiguity function to radar systems with multiple transmitters and multiple receivers. [C8333]

"Diversity Aspects of Radar-Embedded Communications"

This paper discusses aspects of intra-pulse radar-embedded communications whereby a tag/transponder illuminated by a radar converts the illumination waveform into one of a set of K communication waveforms with which to convey information to a spatially separated receiver. Initial work based upon an expansion of the radar spectrum has demonstrated the potential for significant data-rate improvement relative to previous inter-pulse approaches while still maintaining a low probability of intercept. In this work, a general mathematical formulation for intra-pulse radar-embedded communications is presented. This formulation provides insight into options for even higher data-rates by utilizing additional degrees-of-freedom. [C8334]

"Application of Frequency Diverse Arrays to Synthetic Aperture Radar Imaging"

Cross-range resolution in spotlight synthetic aperture radar (SAR) is primarily a function of the angular extent ($\Delta\phi$) over which data is collected. One proposed means for improving cross-range resolution for a given $\Delta\phi$ is the use of frequency diverse array (FDA) techniques. The goal is to exploit an apparent increase in $\Delta\phi$ to improve cross-range resolution while retaining benefits of shorter synthetic apertures and integration times. [C8335]

"A waveguide/free-space measurement setup for panels and joints of large dielectric radomes"

The problem of characterizing panels and joints of large dielectric radomes is attacked in two ways. Small panel samples are placed in a waveguide setup, in order to measure the complex permittivity of its dielectric layers in their actual configuration. A proper free-space setup is instead used to directly characterize the transmission and scattering properties of the structures. Thanks to the use of TRL calibration and further signal processing, the developed system removes the effect of panel and joint edges as well as the scattering from the supporting structures without the necessity of an anechoic chamber. Experimental data are provided for a C-band panel, an uncompensated joint and the compensated one developed at the IEIT-CNR. [C8336]

"Closed-Loop Radar with Adaptively Matched Waveforms"

Adaptive and knowledge-based radar focus on improving the performance of the radar receiver through signal processing. However, rather than develop transmission waveforms and signal-processing techniques independently, it is useful to consider a closed-loop system complete with an adaptive radar transmitter. In this paper, we summarize and demonstrate a framework being developed at the University of Arizona for implementation of closed-loop radar with adaptive waveforms. This framework integrates a Bayesian channel representation, matched illumination techniques, and sequential hypothesis testing. The result is a closed-loop system that modifies its understanding of the channel based on measured data, customizes waveforms to hasten understanding of the channel, and draws conclusions (such as target classification) when sufficient understanding of the propagation channel is achieved. [C8337]

"A New Method for Estimating the Bandwidth using Two-Channel Narrowband Signals with Strong Interference"

Bandwidth is an important parameter in signal processing. A novel method for estimating the bandwidth using the linear phase relationship between two-channel narrowband signals is proposed. The two-channel model is based on the time-difference of arrival (TDOA) estimator. The second channel signal is a time delay copy of the first channel. The comparison between the proposed method and the general ones is presented. It is shown that the method is effective for signals corrupted by strong interference even at low SNR. [C8338]

"Cluster Sorting of Radar Signals Using Intra-pulse Feature"

Common parameters for signal description can hardly meet practical requirement of radar signal sorting and recognition. Aiming at the problem of signal sorting system, DCT (discrete cosine transform) features and BT (product of bandwidth and time width) feature are introduced to form a new description vector. DCT features not only can reflect modulation mode but also are not sensitive to noise. BT feature can reflect some parameters of modulation. Both of DCT features and BT feature are easy to get. At last, results of weighted dynamic cluster show that DCT features and BT feature are effective for sorting. [C8339]

"A Robust Method for Censoring the Interference-targets"

To avoid target signal cancellation, which decreases the output signal-to-interference-plus-noise ratio (SINR) of space-time adaptive processing (STAP) significantly, it is necessary to eliminate the data vectors contaminated by interference-targets from the training data vectors set. There often exist errors between the actual steering

vector and the assumed desired one for interference-targets (outliers) signals in nonhomogeneous clutter environments. The errors can cause distortion of main beam pattern, which leads the conventional reiterative censoring adaptive power residue (RAPR) method to degrade significantly in performance or even completely fail. An enhanced robust effective methodology is presented here, which first suppresses the mainlobe distortion to censor the strong interference-targets by diagonal loading the covariance matrix of training data vectors with a large value; and then eliminates the weak interference-targets coaligned with the desired signal vector. In addition, the new method achieves low computational complexity due to the recursive updating for inverse of covariance matrix. The computer simulation results show that the enhanced method is superior to the conventional RAPR method. [C8340]

"Noise-Linear Frequency Modulation Shared Waveform for Integrated Radar and Jammer System"

This paper presents an integration of radar and Electronic Warfare (EW) utilizing Noise-Linear Frequency Modulation (NLFM) waveform, which is capable of simultaneous operation of radar and EW function for target detection and jamming against the Linear Frequency Modulation (LFM) Pulse Compression (PC) radar. The basic properties, detection and jamming capability of the NLFM waveform are investigated. Analysis indicates that the NLFM waveform has better range resolution and sidelobe suppression than LFM PC and random signal waveform, and that it has higher jamming efficiency against LFM PC radar than normal noise jamming waveform. [C8341]

"Diagonal Loading Techniques to Relax Sample Support Requirement in Airborne Bistatic STAP"

In this paper, we concentrate on the employment of diagonal loading to relax sample size requirement of airborne bistatic STAP. Due to the independent motion effects of the receiver and transmitter, bistatic clutter generally appears more severely nonstationary in the range dimension than the counterpart of monostatic system. This leads to the shortage of IID training data samples and inadequate estimation of the clutter-plus-noise covariance matrix for bistatic STAP, which greatly degrades the performance of bistatic STAP. In this work, we first make a comparison of sample support in different bistatic scenarios and then propose to further abate the required sample support by combining the diagonal loading techniques with the reduced-dimension STAP algorithm. Simulation results manifest that the satisfying performance of bistatic STAP can be obtained by using the proposed method in the bistatic geometries where the training data is extremely insufficient. [C8342]

"Design of the High-powered Clutter Suppression System Based on ADSP-TS203"

The paper studies the design to implement moving target indication (MTI) and moving target detection (MTD) based on a piece of ADSP-TS203. Digital signal processor (DSP) provides great flexibility for the design of the software. After pulse compression, the radar echoes including clutter, noise and targets are transmitted to DSP for MTI and MTD. The system mainly adopts the arithmetic of three-pulse elimination to realize MTI. MTD can be completed by using a narrow-band-Doppler-filter group in frequency domain. At last, it's verified that this system can restrain clutter and distinguish the targets effectively, which has been tested on the hardware. Meanwhile, the improvement factor is also improved. The system can be widely used in radar signal processing. [C8343]

"Optimization of Orthogonal Discrete Frequency-Coding Waveform Based on Modified Genetic Algorithm for MIMO Radar"

A modified genetic algorithm (GA) is proposed to numerically design orthogonal discrete frequency-coding waveforms (DFCWs) which have good aperiodic autocorrelation and cross-correlation properties for orthogonal multiple input multiple output (MIMO) radar. Some of the designed results are presented, and their correlation properties are better than other known in the literature. The effect of Doppler frequency shift on the performance of these signals and ambiguity function are investigated. The simulation results and comparisons show that the proposed algorithm is more effective for the design of DFCWs with superior aperiodic correlation. [C8344]

"Signal-Clutter-Noise Power Ratio of Airborne Wideband Radar"

Received power of signal and clutter for airborne wideband radar is developed. Signal-clutter power ratio (SCR), signal-noise power ratio (SNR), clutter-noise power ratio (CNR), signal-clutter plus noise power ratio (SCNR) respectively for narrowband radar and wideband radar are given. Computer simulation shows, under the same conditions, wideband radar can provide better SNR, SCR and SCNR performance in one range resolution cell than narrowband radar, so wideband signal will be of more benefit to a target detector. [C8345]

"Geometry and System Aspects of Spaceborne/Airborne Hybrid Bistatic SAR"

Spaceborne/airborne hybrid bi-static SAR is a new kind of remote sensor raised in recent years, whose development is still at an early stage for its great difficulty. Due to the high differences between satellites' and aircrafts' velocities and altitudes, there are remarkable differences between the hybrid system and systems which have the symmetrical structure, such as spaceborne bi-static SAR and airborne bi-static SAR. Three basic and critical issues in the hybrid system are discussed, including geometry, Doppler properties and signal model. On the basis of the research work done in this paper, imaging algorithm of the hybrid system can be further designed in the next step. [C8346]

"LCMV Beamforming Algorithm Based on the Fractional Fourier Transform"

We propose a new method of LCMV beamforming based on the fractional Fourier transform (FrFT). This method encompasses the conventional linearly constrained minimum variance (LCMV) beamforming in the frequency domain or spatial domain as special cases. It is especially useful for applications involving chirp signals such as signal enhancement problems with accelerating sinusoidal sources where the Doppler effect generates chirp signals and a frequency shift and active radar problems where chirp signals are transmitted. Numerical examples demonstrate the potential advantage of the proposed method over the ordinary frequency or spatial domain beamforming for a moving target. [C8347]

"The Influence of Random motion Errors on Bistatic SAR Resolution"

In order to assess the quality of the system, this paper analyzes the effects of phase errors due to random motion on the resolution of airborne bistatic SAR. For zero mean random motion errors, an analytical result of RMS (root mean square) resolution is derived. Based on the derived model, Gaussian function is found to be the optimum weighting function on azimuth processing and the best achievable RMS resolution is obtained in closed form. [C8348]

"Adaptive Space-time-waveform Processing for MIMO Radar"

This paper presents a preliminary investigation into space-time-waveform adaptive for multiple input multiple output (MIMO) radar. Existing space-time adaptive processing (STAP) algorithms are extended to the waveform-time-space adaptive processing (WTSAP) case. We develop the signal model required to generate simulated data. Simulation results show a significant improvement in processor performance as compared to conventional phased array radar. [C8349]

"Heart Rate Analysis and Telemedicine: New concepts & Maths"

Our paper deals with some new aspects of ambulatory (Holter) ECG monitoring extending its indications and using for risk management purpose. Remote sensing consists of the transmittal of patient information, such as ECG, X-rays, or patient records, from a remote site to a collaborator in a distant site. Our earlier developed internet based ECG system was unique for on/off-line analysis of long-term ECG registrations. After the 5-year experience in a smaller region of Budapest, Hungary involving a municipal hospital and the surrounding outpatient cardiology departments and general practitioners, we decided to integrate into our new ECG equipment, the CardioClient the results. In the first clinical study of the four was a wavelet, non-linear heart rate analysis in sudden cardiac death patients using the Internet and the GPRS mobile communication. After the wavelet transformation by the Haar wavelet and the Daubechies 10-tap wavelet, the phase-space of the wavelet-coefficient standard deviation and the scale parameters showed an excellent separation in the scale-range of 3-6 between the two groups: in that region, the average scaling exponents was 0.14 ± 0.04 for Group-A, and 1.22 ± 0.27 for Group-B ($p < 0.001$). In the next study, we used the Internet database of long-term ambulatory, mobile, GPRS electrocardiograms for the for risk stratification of patients through the cardiovascular continuum. From our ambulatory mobile GPRS ECG database the following a priori groups were defined after a 24 months follow-up: G1: N=227 patients (without manifest cardiovascular disease, clusterized "boxes" based on the age, sex, cholesterol level, diabetes, hypertension); G2: N=89 patients (postinfarction group); G3: N=66 (patients with chronic heart failure) with (+) or without (-): all-cause death (acD), myocardial infarction (MI), malignant ventricular arrhythmia (MVA), sudden cardiac death (SCD). The actual vs. predicted values were analyzed with chi-square test. The best- significance levels ($p < 0.001$) were found with method in G1/MI+, G2/SCD+, G3/acD+, G3/SCD+ groups. In the third study a wavelet analysis of late potentials based on long-term, high-resolution, mobile, GPRS ECG data was performed. These pathological changes were also detected by the Haar and Daubechies_4 wavelets, but in a narrower space (110-128 ms and 180-240) and with lesser significance ($p < 0.01$). Late potentials were found in Group-A (N=21) in 18 cases with Morlet, 16 with Haar, 19 with Daub-4 analysis, and in 15 cases using all the 3 waves; for Group-B the data were 5, 9, 8, 5, respectively. In the fourth clinical study the prognostic value of the nonlinear dynamicity measurement of atrial fibrillation waves detected by GPRS Internet long-term ECG monitoring were analyzed. The multivariate

discriminant model selects the best parameters stepwise, the entry or removal based on the minimalization of the Wilks' lambda. Three variables remained finally: x_1 = CI mean-value at $\log r = -1.0$ (m9-14), x_2 = CI mean-value at $\log r = -0.5$ (m12-17), and x_3 = CD_cg. The Wilks' lambda was 0.011, chi-square 299.68, significancy: $p < 0.001$. [C8350]

"Architectural Challenges in Memory-Intensive, Real-Time Image Forming"

The real-time image forming in future, high-end synthetic aperture radar systems is an example of an application that puts new demands on computer architectures. The initial question is whether it is at all possible to meet the demands with state-of-the-art technology or foreseeable new technology. It is therefore crucial to understand the computational flow, with its associated memory, bandwidth and processing demands. In this paper we analyse the application in order to, primarily, understand the algorithms and identify the challenges they present on a basic architectural level. The processing in the radar system is characterized by working on huge data sets, having complex memory access patterns, and doing real-time compensations for flight path errors. We propose algorithm solutions and execution schemes in interplay with a two-level (coarse-grain/fine-grain) system parallelization approach, and we provide approximate models on which the demands are quantified. In particular, we consider the choice of method for the performance- intensive data interpolations. This choice presents a trade-off problem between computational performance and size of working memory. The results of this "upstream" study will serve as a basis for further, more detailed architecture studies. [C8351]

"A General Telematics Framework for Autonomous Service Robots"

Many environment and task specific methods and systems for building Service Robots exist. However vast strides in the evolution of smart device technologies and telematics create the need for a Telematic Framework that is generic, scalable, modular and dynamic. This Framework though generic in nature can be applied quite successfully to specific problems like robot navigation and sensor fusion as discussed here. The fundamental design aspects and implementation issues encountered during the development are discussed. Experiments were conducted and the results of the deployment of three major peripheral modules of the telematics framework namely the GSM/GPRS based communication module, GIS based decision support module and smart client integration modules (for GPS sensor) are reported in this paper. [C8352]

"A Combinatorial Procurement Auction for QoS-Aware Web Services Composition"

Business processes and application functionality are becoming available as internal web services inside enterprise boundaries as well as becoming available as commercial web services from enterprise solution vendors and web services marketplaces. Typically there are multiple web service providers offering services capable of fulfilling a particular functionality, although with different Quality of Service (QoS). Dynamic creation of business processes requires composing an appropriate set of web services that best suit the current need. This paper presents a novel combinatorial auction approach to QoS aware dynamic web services composition. Such an approach would enable not only stand-alone web services but also composite web services to be a part of a business process. The combinatorial auction leads to an integer programming formulation for the web services composition problem. An important feature of the model is the incorporation of service level agreements. We describe a software tool QWESC for QoS-aware web services composition based on the proposed approach. [C8353]

"A Fast RANSAC-Based Registration Algorithm for Accurate Localization in Unknown Environments using LIDAR Measurements"

The problem of accurate localization using only measurements from a LIDAR sensor is analyzed in this paper. The sensor is rigidly fixed on a generic moving platform, which moves on a plane. Practical on-line applications of localization algorithms impose constraints on the execution time, problem that is addressed in this paper and compared with other existing solutions. Due to the nature of the sensor adopted, the localization algorithm is based on a fast and accurate registration algorithm, which is able to deal with noisy measurements, outliers and dynamic environments. The proposed solution relies on the RANSAC algorithm in combination with a Huber kernel in order to cope with typical nuisances in LIDAR measurements. The robust registration is successively used in combination with an extended Kalman filter to track the trajectory of the LIDAR over time, hence to solve the localization problem. Simulations and experimental results are reported to show the feasibility of the proposed approach. [C8354]

"Study of Detection Technique Simulation of High Resolution Radar Based on BP Neural Network"

Technology applying neural network to detection of high resolution radar is advised. Firstly, it analyses the principle of detection technique of high resolution radar and the conception of "distance corridor". Secondly, it

introduces the basal principle of BP algorithm. The principle and structure of three layers BP neural network is analysed. Thirdly, the detection technology and algorithm of high resolution radar based on BP neural network is researched. The result of research of target detection technology based on BP neural network possesses superperformance, which is in view of four distance corridor and ten distance corridor, which are the neural network that possesses four input neurons and ten input neurons. At last, the research is carried out by Matlab, the result are visible and understandable. [C8355]

"Design of Perfect Reconstruction Cosine Modulated Filter Banks with Linear Phase"

This paper proposes an efficient iterative linearization method for designing a class of cosine modulated filter banks (CMFBs) with linear phase (LP) property satisfying perfect reconstruction (PR). In this paper, the design of the prototype filter is formulated as a quadratic-constrained optimization function of the prototype filter coefficients whose minimum point can be obtained using the Lagrange multiplier approach at each step. The main advantages of this method are simple design procedure and high computational efficiency. A design example is presented to demonstrate the effectiveness of this new method. [C8356]

"A Generalized Sidelobe Canceller Architecture for Reduced-rank Beam-space Post-Doppler STAP"

Based on the generalized sidelobe canceller (GSC), we propose a novel reduced-rank beam-space post-Doppler adaptive beamformer, where the blocking matrix are replaced by an architecture that consists of the novel combination of space-time channels. The number of space-time channels required by the new method is very small. Simulation results in ideal situations and with limited sample are presented. The approach can cancel clutter while maintain low sidelobe more efficiently. It has low sample support requirement, strong robust and convenient implementation. Performance analysis is carried out using simulated data. The results prove the effectiveness of the proposed approach. [C8357]

"CARE: Rocket Experiments for Investigation of the Radar Scatter Properties of a Dusty Plasma"

Summary form only given. The Charged Aerosol Release Experiment (CARE) will use a rocket payload injection of particulates in the lower ionosphere to determine the mechanisms for enhanced radar scatter from the electrons imbedded in an artificial dusty plasma in space. Natural dusty plasmas in the mesosphere near 85 km altitude have been shown to enhance radar scatter at VHF frequencies by 40 dB or more. The CARE program is designed to study the scatter processes near 200 km altitude in the ionosphere where densities are up to 1000 times larger. Numerical simulations of particulate transport in the upper atmosphere with charging by electron pickup or photodetachment have been used to predict the dusty plasma densities. These charged particle distributions provide initial conditions for particle simulations of plasma turbulence driven by the free-energy of the high-speed charged particle motion. Finally, radar signals scattered from the plasma irregularities are estimated using electromagnetic wave theory. The physical properties of the dusty plasma as will be determined using the radar echoes as well as in situ probes on the rocket payload and on secondary payloads launched after the dust has settled into the lower atmosphere. In addition, the NASA AIM satellite will measure the dust layer by-scattered sunlight and absorption. [C8358]

"A Novel Statistical Recognition Method Based on Hypersphere Model for Radar HRRP ATR"

Different from general Gaussian-distributed data, L2-normalized samples are applied to HRRP-based recognition to deal with the amplitude-scale sensitivity problem, therefore, geometrically speaking, power transformed HRRP samples spread on a unit hypersphere. This paper proposes a novel statistical recognition method for power transformed HRRP samples under the jointly multivariate Gaussian distribution hypothesis, in which the hyperspherical spread of HRRP samples and the effectively discriminating information contained in the noise subspace can be fully utilized without increasing computation complexity. The experimental results based on measured data show that our proposed method can greatly improve the recognition performance. [C8359]

"Implementation and Design of Auto Ranging System with Risk Estimation for Vehicles"

Based on the theory of optical-mechanical-electrical automatic ranging system of vehicles, paper has a discussion and research of the implementation and design of auto ranging system with risk estimation and decision. The hardware is based on MPC5200. And paper includes the design of hardware architecture, software architecture and key techniques, of hardware development, etc. The system adopts the laser-lidar ranging method to get a high precision. Paper focused on the signal processing of laser-lidar and waveforms selection of the detection system. [C8360]

"Synthetic Aperture PAU: a new instrument to test potential improvements for future SMOSops"

This paper describes some potential improvements that could be eventually implemented for future MIRAS (Microwave Imaging Radiometer by Aperture Synthesis) payloads of the follow-on missions of the ESA's SMOS (Soil Moisture and Ocean Salinity) mission. A ground-based instrument concept demonstrator has been designed and it is being implemented to validate these improvements. Both MIRAS and the (Synthetic Aperture Passive Advanced Unit, SA-PAU) are Y shaped arrays, but the receiver topology and the processing unit are significantly different. This paper identifies the elements in the MIRAS's design that could be improved and presents a new instrument (Synthetic Aperture PAU) that could be used to test some potential improvements for future SMOSops (SMOS operational system). [C8361]

"GAS: the Geostationary Atmospheric Sounder"

This paper presents the concept and initial breadboarding results of geostationary atmospheric sounder (GAS), which is being developed by Saab Space AB and Omnisys AB, Sweden, and funded by European Space Agency (ESA). GAS utilizes interferometric synthetic aperture radiometry to obtain desired spatial (30 km) and temporal (nowcasting) resolution for measurement of atmospheric temperature and humidity profiles under all weather conditions. These parameters are decisively important to meteorological and climate models at all time scales. [C8362]

"Estimation of 3-D Water vapor distribution using a network of compact microwave radiometers"

Quantitative precipitation forecasting is limited by the paucity of observations of water vapor in the troposphere. In particular, severe storms have been observed to develop in regions of strong and rapidly evolving moisture gradients. Conventional measurements of water vapor density profiles are obtained using in-situ probes on-board weather balloons, including radiosondes. These in-situ profile measurements have high vertical resolution, but have severe limitations in both temporal and spatial sampling. Lidars use differential absorption techniques to estimate water vapor with comparable resolution to that of radiosonde observations. However, lidars are expensive, and their operation is limited to clear-sky conditions due to the high opacity of clouds at optical wavelengths. Inversion of brightness temperatures measured by upward- looking, ground-based microwave radiometers allows the estimation of vertical profiles with high temporal resolution in both clear and cloudy conditions. However, assimilation of retrieved water vapor fields with improved spatial coverage has the potential for more substantial impacts on numerical weather prediction of convective storm initiation. Measurements using a network of multi-frequency microwave radiometers can provide information to retrieve the 3-D distribution of water vapor in the troposphere. [C8363]

"A Multi-parameter Synthetic Signal Sorting Algorithm Based on Clustering"

Radar signal sorting is one of important techniques in electron reconnaissance signal processing and generally uses PRI, RF, DOA, PW, PA and pulse-inner characteristics and so on parameters. Traditional signal sorting is a serial regulation detection system and has some limitation. Especially for a great lot of complicated data, it will be useless. Clustering is an important technique of data mining. It can divide data objects into several classes or clusters based on the comparability of data objects. So a multi-parameter synthetic signal sorting algorithm based on clustering is proposed in order to overcome the limitation of traditional radar signal sorting algorithm. This algorithm makes use of the clustering technique of data mining and combines with DOA diluting algorithm and PRI sorting algorithm, so it can be applied to signal sorting of general radar and special radar. In the end of paper, the simulated experiments show that the synthetic algorithm is effective. [C8364]

"Feature extraction of gable-roofed buildings from multi-aspect high-resolution InSAR data"

The achievable spatial resolution of state-of-the-art synthetic aperture radar (SAR) sensors enables the analysis of urban areas. The appearance of buildings in magnitude images is governed by effects of the inherent oblique scene illumination, such as layover, radar shadow and salient lines of bright scattering caused by direct reflection or multipath signal propagation. For example, in urban residential districts often salient pairs of parallel lines of bright magnitude are observed at locations of gable-roofed buildings. The first line (closer to sensor) is due to direct reflection of planar roof parts orientated toward the sensor. The second line can be related to signal caused by a dihedral corner reflector between ground and building wall. In this paper an approach is presented aiming at reconstruction of gable-roofed buildings by knowledge based analysis considering the mentioned SAR-specific effects. First, line and edge primitives are segmented and grouped to parallel line pair objects. Then for each of these objects geometrical and radiometrical features are extracted in the InSAR images. Based on the interferometric elevation data in the adjacent area of the primitives the projection from slant range into ground range geometry is done. After geocoding, building hypotheses are built from the fused set of extracted primitives from both aspect directions. The estimation of the building height is carried out by two complementing methods:

One is based on the extracted geometric parameters and the other on interferometric height data. The reconstruction results are quantitatively assessed by using a high resolution LIDAR surface model as ground truth data. [C8365]

"SRAL SAR radar altimeter for sentinel-3 mission"

The SRAL SAR radar altimeter is the core instrument of the topography mission carried on board the Sentinel-3 satellite which is planned to be launched in 2012. A detailed overview of this instrument is given in this paper in terms of architecture, functions, modes and performances. [C8366]

"Classification of stricken residential houses by the mid niigata prefecture earthquake based on POLSAR image analysis"

This report attempts to apply a hybrid classification technique based on POLSAR image analysis to detect the man-made residential houses in a local mountainous area stricken by the Mid Niigata Prefecture Earthquake. The present hybrid scheme includes the scattered power decomposition method based on physical scattering nature and the scattering feature extraction method using polarimetric correlation coefficient. From the results of the image analysis for actual POLSAR data, it is verified that the present hybrid scheme provides us accurate classification of the man-made targets even in the severe mountainous [C8367]

"An AMUSE-based Approach for Detection and Blind Separation of Multi-component Radar Signals"

The separation of multi-component radar signals is the key problem in the field of radar countermeasure etc. In the real time-vary signal scenario with short data acquired, an AMUSE-based second order statistics approach for effective separation of multi-component radar signals is presented using an effective blind signal processing model built for the intercepted radar signals. The efficacy of this approach is verified by simulation results. [C8368]

"The contribution of the european space agency to the ALOS PRISM / commissioning phase"

The Advanced Land Observing Satellite (ALOS) was launched on Jan 24th, 2006 by a Japan Aerospace Exploration Agency (JAXA) H-IIA launcher. It carries three remote sensing instruments: Advanced Visible and Near Infrared Radiometer type-2 (AVNIR-2), Panchromatic Remote-sensing Instrument for Stereo Mapping (PRISM) and Phased Array Type L-band Synthetic Aperture Radar (PALSAR). Within the framework of European ALOS Data European Node (ADEN), European Space Research INstitute (ESRIN) as part of European Space Agency (ESA), teamed up with JAXA for contributing to ALOS commissioning phase plan. This paper summarizes the strategy that ESA adopted to define and implement a data verification plan for mission operated by foreign nation, classified as so called ESA Third Party Missions (TPM). The verification of ALOS optical data from PRISM / AVNIR-2 instruments activities had begun four months after satellite launch on March 2007. GAEL Consultant (French company) has supported ESA / ESRIN for designing and executing the plan. A team of principal investigator's has been put together to provide technical expertise. This paper includes a description of the verification plan and summarizes the methodologies that were used for radiometric, geometric and image quality assessment. Preliminary results indicate that the radiometric calibration of the AVNIR-2 sensor agrees with Landsat 5 (L5) Thematic Mapper and the MEdium Resolution Imaging Spectrometer (MERIS) calibration to within 10%. The geometry accuracy of PRISM and AVNIR-2 product remains within specifications but some recommendations are provided to improve the quality of product. The preliminary results from the PRISM image quality assessment through computation of PRISM Modulation Transfer Function (MTF) raised few questions toward jpeg compression that degrades image. [C8369]

"Design of Automobile Collision Avoidance Warning System Based on LabVIEW"

This paper presents a warning system for automobile collision avoidance based on LabVIEW. The procedure is designed by LabVIEW7.0. The system adopts FMCW radar sensor and high-quality data acquisition card. This system can monitor the distance and velocity forward vehicle. According to the run law of vehicle, a simple formula for safety distance is set up. It can give the alarm when the collide danger is predicted, and it can assist the driver to brake control, thus some collision accidents will be avoided. It is flexible to design the programme, the different signal processing algorithm can be inputted and the better programme can be selected. The paper given the design method and main test data. [C8370]

"The C-SAR instrument for the GMES sentinel-1 mission"

The paper describes the C-SAR instrument for the GMES Sentinel-1 mission. After a brief introduction of the

Sentinel-1 instrument requirements a design description of the overall C-SAR instrument as well as of its major subsystems (i.e. the SAR Antenna Subsystem (SAS) and the SES Electronic Subsystem (SES)), is given. The paper concludes with an overview on the predicted instrument performance. [C8371]

"Simulation of Radar A/R Scope Based on Linux System"

Radar failure training simulator can provide a new training method for radar equipment repairing, and the simulation of radar A/R scope is an important part in developing radar failure training simulator. This paper uses Linux system, which has open source code, high stability, and good robustness, to develop the simulation part of radar A/R scope. On the basis of analyzing the display character of A/R scope, this paper introduces the object-oriented application program interface GTK+ and plotting tool Glade in Linux operating system, and also gives the simulating method, steps and result based on this system. [C8372]

"ICT Anti Collision Radar for Road Traffic"

The ICT radar is an information-communication technology system for early warning and collision avoidance on roads and motorways. This radar uses special sensor network, which-spanned over the moving vehicles and road obstacles-transmits automatically warning signals to the back of column and enables distant drivers to stop in time or to do such operations automatically. Large-scale simulations have been carried out, which show that in typical scenario the number of collisions decreases from some great number to zero as the radar usage increases from 0% to 100%. Even at 50% of random radar usage almost all huge collisions are excluded. Typical data of simulations are as follows: one lane road; 50 vehicles randomly spaced, distances drawn from normal distribution, next smoothed; average speed 90 km/h; reaction time of a driver-drawn from random distribution (mean 1 s); first vehicle in column suddenly stopped; model of collisions-domino-alike; protocol of radio communication-modified ALOHA; size of alert packet-100 bytes containing data: speed, acceleration, coordinates (GPS); kind of alerts: sharp brake, airbag explosion standing vehicle; transmission speed 8 Mb/s; average rate-1 packet/ms/node; time for reliable warning 0.1 s; range of warning 800 m; coverage area-triangular, backwards oriented; total number of scenarios-5.000. [C8373]

"Analysis of Radar Emitter Signal Feature Based on Multifractal Theory"

Fractal theory has applied to radar signal analysis, in which fractal dimensions such as Hausdorff dimension, box dimension, information dimension, similarity dimension, correlation dimension and so on always are used to depict the complexity of radar emitter signal. But single fractal dimension is not enough to describe a complicated fractal object, so multifractal is introduced to analyze radar emitter signal. Multifractal is the expansion of fractal dimension, which uses multifractal dimensions to describe growth features of fractal object in different levels and compensate the lack of single fractal dimension. Because radar emitter signal is a time series, the method to study time series multifractal can be adopted and the multifractal feature can be regarded as the basis of radar signal classification and recognition. Through simulating several typical radar signals and computing their multifractal dimensions, the simulation results validate that analysis of radar emitter signal multifractal feature has certain instructional meaning. [C8374]

"Technology Readiness Characteristics of 3G Subscribers in Indonesia: A Preliminary Study"

The technology of 3G (Third Generation) mobile communication was launched in Indonesian market in September 2006. Studies have been conducted to discover contents frequently accessed by subscribers and their satisfaction level to operators' services. However, little is known about the subscribers' technology readiness characteristic. Knowing this characteristic is important since it will help 3G operators designing a proper marketing program in widening the customer base. A preliminary survey was conducted to obtain this information and it was discovered that a significant number of users possessed technology readiness characteristics different than those originally presented in literature. [C8375]

"RADAR: Risk-and-Delay Aware Routing Algorithm in a Hybrid Wireless-Optical Broadband Access Network (WOBAN)"

We propose "risk-and-delay aware routing algorithm" (RADAR) for WOBAN. RADAR minimizes packet delay in the wireless front end of WOBAN and reduces packet loss for multiple failure scenarios: gateway failure, ONU failure, and OLT failure. [C8376]

"High-power stable single-frequency waveguide laser"

We demonstrate a waveguide laser providing over 20 mW in robust single-frequency operation using a 9-mm-long active waveguide. Overall cavity length is <60 mm including butt-coupled fiber-Bragg-grating mirrors. Power

scaling to 100 mW is discussed. [C8377]

"Study about Test Ammunition Terminal Effectiveness with the Velocity Radar"

The paper analyzes the fragment movement rule when the ammunition exploded. The mathematics model of the fragment radar echo signal is established on the basis of the principle of the movement targets modulating Doppler signal. The simulation data processing was achieved in using FFT method for the fragment echo signal. Quantitative analysis was realized about the influence for the signal processing precision by the fragment amount, the velocity difference value between the fragments and SNR. [C8378]

"Using Polynomial Phase Signal Modeling against Range False Targets"

A novel approach of extracting a true target component from radar superposing echoes on the premise of that a repeater jammer is detected, when radar is suffered from range false targets jamming, is presented based on multicomponent polynomial phase signals (mc-PPS's) modeling. For linear frequency modulation (LFM) waveform, the differences of the echoes' polynomial phase coefficients between a true target and a false target are analyzed first. Parameter estimation of the true target by using product high-order ambiguity function (PHAF) is described. After the desired parameters be estimated, the true target signal can be reconstructed. Validity of the method is verified by simulation results. [C8379]

"Design of LXIbus Interface Circuit for HF Ground Wave Radar"

According to the requirements of modularization and standardization, this paper presents the design principle of general purpose LXI bus interface for high frequency ground wave radar (HF GWR) based on LXI bus using DSP ADSP-21062, Ethernet controller DM9000A and dual-ported RAM (DPRAM). It describes the hardware design and data transmission mode in detail. With the advantages of high flexibility, integrity and speed, this interface circuit has been verified in practice. [C8380]

"TDC Based Radar Signal Reconstruction from Periodic Nonuniform Samples"

For the universal radar signal acquisition system design, to solve the problem of nonuniform sampling resulted from the fact that sample clock can't be divided exactly by radar pulse repetition frequency (PRF), a TDC (time-to-digital converter) based radar signal reconstruction method was presented. First, this paper proves that the nonuniform sampling can be modeled as periodic nonuniform sampling (PNS) process. Then assuming the time offsets are known, a new PNS reconstruction algorithm is derived. The new algorithm has the advantage that it can be used to perfectly reconstruct both even and odd order PNS signal. Besides, the algorithm can be calculated faster because it has a Hermitian Toeplitz matrix A . By integrating the TDC circuit in universal radar signal acquisition system, the sampling time offsets can be recorded, thus the real radar signal can be perfectly reconstructed from original non-uniform samples. Finally, the method is validated by computer simulation. [C8381]

"Wide-Band High Resolution Homing Sonar Echo Detect Based On Spread Spectrum Technology"

This paper propose and analyze high resolution auto-navigation sonar system based on DS/SS technology. Compare to traditional auto-navigation sonar system, the system have big time and frequency range, can provide high distance and speed resolution and good anti-interference capability. Paper discuss the principle of waveform design and enduce ambiguity function of DS/SS modulation signals. In the case of high-speed target, paper provided and proved a algorithm using CZT which can estimate Doppler frequency offset and target speed in very low SNR condition. [C8382]

"A Design of the Test According to Amplitude-frequency Characteristic in the Radar Antenna Control System"

In this paper, a design of the test according to amplitude-frequency characteristics and the advantages of the test system are introduced. It took the advantage of the control of single chip, improving its accuracy and sensitivity. [C8383]

"Experimental HF radar trial of real-time STAP"

An alternative multi-static HF radar architecture, known as the Forward-Based Receiver Augmentation (FBRA) system, has been developed and tested by the Defence Science and Technology Organization [1]. The experimental system has performed beyond expectations in a number of trials involving targets of interest. This is not only due to the impressive hardware capabilities, but also the advanced signal processing for clutter and

interference mitigation, particularly STAP which was shown to be indispensable for the successful operation of the system. This paper describes the real-time STAP algorithm in the FBRA system, and demonstrates its experimental detection performance on a cooperative aircraft target with flight path "ground truth" data available from on-board GPS logging equipment. [C8384]

"Use of frequency-randomized SAR waveforms for the detection and mitigation of small-motion effects in precision RCS measurement"

The use of SAR and ISAR imaging is an important tool in the laboratory RCS characterization of scattering patterns across signature critical platforms. Despite measures to the contrary, air turbulence and mechanical vibration can produce unwanted complex perturbations of the target during the imaging process. The slow sweep time of many laboratory stepped-frequency CW radars means that a target can undergo significant motion even during a sweep, leading to substantial and time-varying defocusing of range profiles, unsuited to conventional motion-correction schemes. Model code was written to provide simulations of representative complex motions for a string-suspended target. Comparison of images produced using monotonic and randomized waveforms could detail the presence and pattern of very small motion-related changes in RCS. The ability to do this was found to have a complex dependence on the relative lengths of the radar sweep time and the characteristic oscillation period of the motion. When the sweep time and oscillation period are comparable, it may be possible to accurately retrieve the target's entire motion history, from the phase perturbation recoverable from the difference of the monotonic and randomized waveforms in the raw frequency domain. This can then be applied back to the data as a motion correction. [C8385]

"Signal processing and waveform selection strategies in multistatic radar systems"

The multistatic ambiguity function has recently been used as a tool for analyzing multistatic radar systems. It was demonstrated that the multistatic ambiguity function with proper analytical foundation and corresponding graphic representation can serve as a guideline for developing multistatic radar signal processing rules. In this work we use this newly developed approach to combine optimal selection of weights for fusing signals from multiple receivers with waveform selection strategies in order to meet desired performance goals. We consider configurations with multiple receivers and one transmitter and demonstrate through examples that multistatic system performances can be significantly improved when selection of system parameters is based on shaping of the multistatic ambiguity function. This approach promises to be beneficial especially in scenarios with rapidly changing geometries, such as when the transmitter and/or receivers are moving, and when waveform diversity is applied, since the classical detection theory does not take into account the system geometry and waveform shape. [C8386]

"Sector interpolation for 3D SAR imaging with baseline diversity data"

SAR tomography is an emerging technique which can be used to derive full 3D SAR images of the observed areas. It is based on the Fourier elevation focusing of the signal acquired by means of baseline diversity. Unfortunately, the spatial baseline distribution is typically non-uniform, resulting in an unsatisfactory image quality. In this work, we improve the basic elevation focusing technique by reconstructing a set of uniform baselines data exploiting a light a priori information, i.e. the height sector which contains the scatterers. The validity of the method has been evaluated by carrying out simulated analyses for different scenarios. [C8387]

"Evaluation of a fully self-consistent methodology to correct attenuation and differential attenuation at C-band"

A methodology to correct reflectivity factor and differential reflectivity at C-band for rain attenuation is presented and evaluated. The methodology is based on a full self-consistency condition describing the interrelation between polarimetric measurements and attenuation or differential attenuation along the rain medium. Evaluation is performed both using C-band profiles generated from S-band radar measurements collected by the NCAR S-Pol radar as well as data collected at C-band by the Polar 55 C radar in Italy. Evaluation shows improvement in performance with respect to the available techniques. In particular, it shows the capability to remove any systematic bias that could arise from drop size distribution variability from attenuation and differential attenuation estimates. [C8388]

"Time-reversal waveform preconditioning for clutter rejection"

A time-reversal implementation of a transmit waveform preconditioning scheme for optimal clutter rejection in radar imaging is presented. Waveform preconditioning involves determining a map on the space of transmit waveforms, and then applying this map to the waveforms before transmission. Our work applies to antenna

arrays with an arbitrary number of transmit-and receive elements, and makes no assumptions about the elements being co-located. Waveform preconditioning for clutter rejection achieves efficient use of power and computational resources by distributing power properly over a frequency band and by eliminating clutter filtering in receive processing. By our time-reversal implementation we avoid the need to obtain an explicit model for the environment in order to compute the preconditioning operator. [C8389]

"Radar signal design using chaotic signals"

The use of chaotic signals in radar imaging applications present particular advantages as they behave like pseudo noise, have a wide band, and are easy to generate. A chaotic frequency modulated (FM) sine wave is an example of a chaotic signal that can yield higher transmitted mean power when peak-power limited transmitters are used. Unlike the random FM signal, the behavior of chaotic FM signals is not fully understood. In this paper, two approaches for analyzing the spectrum of chaotic FM signals are discussed. The first approach approximates the chaotic signal with noise and the second one, deals with the condition for the chaotic signal to remain chaotic after frequency modulation and consequently have a wide band spectrum. [C8390]

"Design and realization of a distributed vector sensor for polarization diversity applications"

Polarization is one type of waveform diversity that may be exploited to improve both radar and communication systems performance. Analytical results show that in order to obtain the best performance improvements, based upon the use of polarization diversity, knowledge of the full electric and magnetic field components is required. Vector sensor antennas are able to measure these components and thus they enable the exploitation of polarization diversity. This article describes a distributed approach to design a 6D vector antenna in a distributed fashion using both electric dipole and magnetic loops as constitutive elements. [C8391]

"Target classification by echo locating animals"

In this paper, the principal mechanisms by which bats are assumed to classify targets are reviewed. Particular attention is paid to the ways in which bats might extract information from echoes. Classification mechanisms differ fundamentally according to signal design. It is shown how bats design their emitted waveforms according to whether they need to classify on the basis of micro-Doppler or range profile information. Throughout, analogies are made with radar (and sonar) systems, drawing attention to some ways in which engineers might learn from the classification mechanisms proposed for echo locating animals. [C8392]

"Model order estimation for adaptive radar clutter cancellation"

Adaptive waveform design for radar clutter cancellation requires knowledge of the rank of the clutter subspace. In this paper, we compare the computed clutter subspace rank, r , using three methods: (i) the exponentially embedded family (EEF) estimator, (ii) Rissanen's minimum description length (MDL) estimator, and (iii) the statistical ranking and selection method (CWA). [C8393]

"MIMO noise radar-element and beam space comparisons"

The noise radar concept is extended to an array of K transmit antenna and M receive antenna. When independent noise sources are transmitted from each antenna the approach may be viewed as a special case of MIMO radar. Two transmission approaches, termed element space (ES) and beam space (BS), are considered together with both conventional and MVDR beamforming on receive. [C8394]

"Laboratory experiments for the evaluation of Digital Beamforming SAR features"

Digital beamforming (DBF) technique is a promising technique for future Synthetic Aperture Radar (SAR). In this paper, we present the preliminary experiments and investigate the crucial parameters for the optimization of the DBF SAR. The measurements were accomplished by a ground-based DBF SAR system for a single target. The demonstrator provides the raw data including the system response. SAR images were reconstructed with numerous spatial sampling distances, not only by DBF SAR processing, but also conventional mono-static SAR processing. The reconstructed images show that the minimum variation of the phase between the receive channel is crucial to obtain the theoretical improvement factor and achieve the wide area observation with fine resolution. [C8395]

"Distributed and Layered Sensing"

One can easily envision future military operations and emerging civilian requirements (e.g. intelligent unmanned vehicles for urban warfare, intelligent manufacturing plants) that will be both complex and stressing and will

demand innovative sensors and sensor configurations. The goal of our research into distributed and layered sensing is to develop a cost effective and extendable approach for providing surveillance for a variety of applications in dynamically changing military and civilian environments. Within distributed and layered sensing, we foresee a new sensor archetype. In this paradigm, sensors and algorithms will be autonomously altered depending on the environment. Radars will use the same returns to perform detection and discrimination, to adjust the platform flight path and change mission priorities. The sensors will dynamically and automatically change waveform parameters to accomplish these goals. Disparate sensors will communicate and share data and instructions in real-time. Intelligent sensor systems will operate within and between sensor platforms such that the integration of multiple sensor data provides information needed to achieve dynamic goals and avoid electromagnetic fratricide. Intelligent sensor platforms working in partnership will increase information flow, minimize ambiguities, and dynamically change multiple sensors' operations based upon a changing environment. Concomitant with the current emphasis on more flexible defense structures, distributed and layered sensing will allow the appropriate incremental application of remote sensing assets by matching resources to the situation at hand. In this paper, we discuss the electromagnetic compatibility (EMC) issues that must be addressed and understood as part of the development of a futuristic intelligence, surveillance and reconnaissance concept utilizing distributed and layered sensing waveform diverse systems. These systems involve the innovative integration of cutting edge technologies such as: knowledge-based signal processing, robotics, wireless networking waveform diversity, the semantic web, advanced computer architectures and supporting software languages. This concept is projected as an autonomous constellation of air, space, and ground vehicles that would offer a robust paradigm to build toward future deployments. The goal is to develop waveform-time-space adaptive processing for distributed apertures that could reduce EMC issues. [C8396]

"Image contrast and entropy based autofocusing for polarimetric ISAR"

In recent studies the possibility of extending autofocusing techniques to fully polarimetric ISAR systems has been proposed. The image contrast and entropy based autofocusing techniques have been proposed in the last decade as some of the most common techniques for obtaining well focused single polarisation ISAR images. In this paper, the two techniques are extended and applied to fully polarimetric ISAR data. A performance analysis is then provided and compared to single polarisation ISAR using real data. [C8397]

"A frequency diverse Doppler radar for range-to-motion estimation in urban sensing applications"

In this paper, statistical bounds on carrier diverse range estimation are provided. Single frequency (Doppler) radars cannot be used in range estimation due to their range ambiguities. An additional frequency can be used to increase the maximum unambiguous range to accepted values for indoor range estimation of moving targets. The target is assumed to have a linear translation motion profile. The dual frequency radar can also be used to estimate the actual target velocity, by conducting two different Doppler data measurements, separated by a time period, over which the target continues to exhibit the identical linear translation motion. The parametric model is developed, and the identifiability of the parameters is validated by the non-singularity of the Fisher information matrix. We provide Cramer-Rao bounds for the parameters and show their dependency on the observation period assuming partial knowledge of motion and noise parameters. [C8398]

"Code selection for radar performance optimization"

In this paper we consider the synthesis of radar waveforms in the presence of colored disturbance. We focus on the class of coded pulse trains and determine the best radar codes according to some established optimality criteria. We propose three coding methods. Two of them are based on the maximization of the detection performance under a control on the estimation accuracy of the target Doppler frequency. The third relies on the maximization of the detection performance under a binary constraint on the code alphabet. Two proposed techniques require the solution of non-convex optimization problems which are solved resorting to the theory of relaxation and semidefinite programming. At the analysis stage the performances of the new coding strategies are assessed also in comparison with a standard radar code both in terms of detection probability and target Doppler estimation accuracy. The results show that the proposed techniques may lead to codes whose performances are close to the benchmark curves. [C8399]

"One-step optimal measurement selection for linear gaussian estimation problems"

This paper considers the problem of choosing the optimal linear measurement for the estimation of a state vector X in a Bayesian context where the prior distribution for X is multivariate Gaussian. The motivation for this comes from waveform-agile active sensing systems that have the capability of choosing transmit or illumination waveforms in real time. The measurement is characterized by a measurement matrix B with an energy constraint along each row. Qualitatively, the optimal solution applies the available transmit energy to each of the

eigenmodes of the prior covariance of X , such that more energy is applied to modes with higher prior variance, in an attempt to bring the posterior variances down to a small common value. The allocation of the energy along the various eigenmodes requires the solution of a straightforward waterfilling problem. [C8400]

"Polarimetric ISAR autofocussing techniques: Comparison of results"

This paper briefly describes a number of scalar, partially polarimetric, and fully polarimetric ISAR image autofocusing approaches that are based upon the PPP and ICBA autofocusing techniques. All approaches are then compared and contrasted using real world data provided by the Defence Science and Technology Organisation of Australia. From this analysis the ICBA approach results in an improved image focus as defined by the image contrast, image entropy and image peak measures, whereas the performance of the PPP based approaches are mixed at best. [C8401]

"Multidimensional waveform encoding for spaceborne synthetic aperture radar systems"

This paper introduces the innovative concept of multidimensional waveform encoding for spaceborne synthetic aperture radar (SAR). The combination of this technique with digital beamforming on receive enables a new generation of SAR systems with improved performance and flexible imaging capabilities. Examples are high-resolution wide-swath radar imaging with compact antennas, enhanced sensitivity for applications like along-track interferometry and moving object indication, or the implementation of hybrid SAR imaging modes which are well suited to satisfy hitherto incompatible user requirements. Implementation specific issues will be discussed and performance examples demonstrate the potential of the new technique for different remote sensing applications. [C8402]

"Interferometric radar waveform design and the effective interferometric wavelength"

Interferometric radar systems are used by the research, commercial and military communities for applications ranging from topographic mapping to measuring subtle deformations of the Earth's surface for geophysical processes such as earthquakes, volcanoes and ice motion. These systems operate at a variety of wavelengths from 1 cm to 1 m depending on the application. As the number of users of the spectrum increases it is becoming increasingly necessary for these systems to alter their waveforms to have the necessary interoperable compatibility. In particular, notching of certain spectral bands within the radar transmit band may be required to avoid interference with critical users operating in the same band. For high accuracy applications it is necessary to account for how these waveform differences affect the interferometric phase and correlation. We have developed a formula for the effective interferometric wavelength that accounts for the effect of the transmitted waveform on the effective interferometric wavelength and the way the data is processed. [C8403]

"Waveform communalities between digital beamforming radar and MIMO"

In this paper an approach to the joint realization of digital beamforming radar and MIMO communications is presented. From a hardware point of view, both radar sensing and digital communications systems are based on similar radio frequency components. It will be shown that through a suitable signal design both applications can be simultaneously realized on one multiple antenna hardware platform. [C8404]

"Motion compensation for a frequency stepped radar"

A few hundred MHz synthetic bandwidth requires the transmission of many (~100) frequency stepped pulses when a small instantaneous bandwidth (<10 MHz) is available. The actual trend in radar imaging is towards wide instantaneous bandwidth (>50 MHz) thanks to improved technology. However the need of retrofit of narrow instantaneous bandwidth to HRR (high range resolution) seems to be still cost effective in the industrial context. In this case the processing time, combined with a large synthetic bandwidth, requires a proper motion compensation of radial target velocity and acceleration. Target kinematics parameters are estimated by minimization of a like-autocorrelation cost function; this technique is capable of detecting minima of aliasing created by uncompensated motion condition. Accuracies are estimated by Monte Carlo simulation and compared to those achievable by entropy and contrast based techniques. [C8405]

"Waveform design and modulation schemes for impulse communications and radar"

Ultrawideband impulse radio communication is based on the classical principles of pulse time modulation conveniently used for baseband transmission. In this paper, we present the principles of impulse waveform design, impulse time modulation for information transmission process, period-staggering modulation scheme for multiple access applications, and M-ary impulse modulation. Periodic and orthogonal non-sinusoidal impulse waveforms are generated in terms of the periodic and orthogonal sinusoidal waveforms. The conventional analog

and digital modulation schemes that are based on the use of sinusoidal carrier waveforms are applied to nonsinusoidal impulse waveforms. As illustrative examples, M-ary impulse modulation schemes are described, i.e., M-ary phase shift keying (M-PSK) and M-ary frequency shift keying (M-FSK). The design of a linear FM "chirp" impulse waveform for radar applications is presented too. [C8406]

"Canonical Framework for ATI and DPCA"

The topic of moving-target detection in clutter has been extensively studied, there are many methods, such as along-track interferometric (ATI) phase, displaced phase center antenna (DPCA) method, space-time adaptive processing (STAP), or some other metrics. A canonical framework is proposed that encompasses ATI and DPCA. The statistical test metric for ATI and DPCA is established in a simple form, via the definition of the complex central Wishart distribution, deduces the statistics of the test metric, the probability distribution of the test metric for ATI and DPCA have the complex central Wishart distribution of 1times1 case, namely the chi2-distribution. The theory foundation offers the possibility to construct the united multi-channel SAR GMTI detector, and derive the constant false-alarm rate (CFAR) detector tests for separating moving targets from clutter. [C8407]

"Precise Measurement of RCF in Colored Gaussian Noise"

A novel algorithm for precise measurement of RCF (radar carrier frequency) in colored Gaussian noise is proposed. The algorithm involves FFT, non-linear filtering, digital heterodyning, and decimation, phase-based frequency estimation. The algorithm has a reduced threshold relative to the existing methods and performance close to that of maximum likelihood estimation. In addition, the mean-squared error performance is within 0.3 dB of the Cramer-Rao bound (CRB) at signal-to-noise ratios (SNRs) above threshold. [C8408]

"Detection of Moving Target in FM Broadcast-Based Passive Radar"

Passive radar utilizes transmissions of opportunity to detect targets and estimate targets parameters. This paper systematically presents key techniques that concern the detection of moving targets in FM broadcast-based passive radar via ambiguity function. It addresses the common problems that exist in passive coherent radar, such as system design, interference cancellation and signal processing. Among which, the idea of automatic hardware cancellation is original. The efficacy of the proposed solution is demonstrated by offline processing real collected data sets. [C8409]

"Continuous coded waveforms for noise radar"

This paper describes a new class of continuous waveforms for noise radar that can be processed using earlier developed methods for reducing pulse compression sidelobes and equalizing compressed pulses before Doppler filtering. The proposed waveforms are based on codes that modulate sub-pulses which define the bandwidth of the waveform. For constant amplitude waveforms the codes are phase codes and the sub-pulses can consist of rectangular pulses with constant phase or linear phase. The proposed waveforms use many short codes to produce a code with a length that is the product of the shorter code lengths. The resulting long code can be arbitrarily long by introducing new shorter codes iteratively. The codes can be random or deterministic with low mismatch losses in the processing at the expense of a quasi-periodic but unpredictable waveform. [C8410]

"Shared-spectrum multistatic radar: Preliminary experimental results"

In this paper we present preliminary experimental results demonstrating the ability of the multistatic adaptive pulse compression (MAPC) algorithm to suppress the mutual-interference generated by shared-spectrum radar signals, thus enabling shared-spectrum radar. The MAPC algorithm, a waveform diversity technique wherein multiple known transmitted waveforms are adaptively pulse compressed using reiterative minimum mean-square error (RMMSE) estimation, has been shown to successfully suppress both range sidelobes and interference from multiple radars operating in the same spectrum. In this paper, we present initial experimental results from the adaptive pulse compression (APC) test bed that demonstrate the ability of MAPC to mitigate both the mutual interference from multiple radars and pulse compression range sidelobes when applied to measured data. [C8411]

"An Algorithm for 4-D Parameters Jointly Estimating of Near-Field Sources"

Source localization is an important problem in array signal processing and it is used to estimate the direction of arrival (DOA) of multiple sources. In this paper, we present a four-order cumulant based ESPRIT like method for passive localization of near-field narrowband non-Gaussian sources using a centrosymmetric cross array. The proposed method uses the multiple-rotational invariance among certain cumulant-domain signal subspaces for

4D parameter (carrier frequency, elevation, bearing and range) estimation of multiple sources. The method does not require any spectral peak search, only needs 1D parameter pairing, and can be applied to additive Gaussian noise environment. The performance of the proposed method is verified by computer simulations. [C8412]

"Speckle Reduction for Remote Sensing Images Based on Nonsubsampled Contourlet"

Existing speckle reduction methods for remote sensing images such as SAR cannot capture image edge detail information and reduce noise effectively at the same time. The nonsubsampled contourlet (NSCT) is built upon nonsubsampled pyramids and nonsubsampled directional filter banks and provides a shift-invariant directional multiresolution image representation. Therefore, a speckle reduction model based on NSCT is presented. Firstly original image with speckle noise was transformed into with additive noise by means of homomorphism transform, and then the NSCT was implemented, finally threshold denoising method was adopted to separate the noise and signal. A comparison between the above NSCT denoising method and conventional methods was carried out on remote sensing images contaminated by multiplicative noise and SAR original image. The experimental results show that the performance of the NSCT is superior not only in speckle reduction but also in edge preservation. [C8413]

"The Research of Network Planning Risk Element Transmission Theory Model Based on Neural Network"

In order to solve the network planning problem considering risk elements efficaciously, we redefine the network planning in this paper and transform the classical network chart to the new network chart based on combining neural network theory. On this basis, a risk classification is listed for the construction project, and we give the evaluation activity indexes using the expert assessment. Then, a risk classification is listed for the construction project. In order to get the total risk degree of all the network routes, after setting a certain weight and threshold value, we regard the indexes as the neural network input vector and calculate the risk degree of various activities. Thus, the total risk degree of all the network routes can be got. Finally, the model algorithm is illustrated with a case study. [C8414]

"Collaborative Detection Probability of Mobile Target for Coverage in Large-Scale WSN"

How to estimate the collaborative detection probability (CDP) for given certain number of sensors, characteristics of sensor and target is an important problem for coverage in large-scale WSN. A triangular analytical model (TAM) is developed to analyze CDP for a randomly deployment sensors in a 2-dimensional region. Making use of binomially stochastic distribution and normalization analysis methods, we theoretically characterize the relationship between the CDP for 3 collaborative sensors with the factors of sensor normalization node density (NND) and normalization specified path length (NSPL) on an assumption of target moving direction in parallel to X-axis, and work out a lower bounds on the CDP for 3 collaborative sensors at worst case on condition of NSPL no more than 1. The simulations of random deployment of sensors and target randomly moving direction show that the mobile target moving direction assumed in theoretical analysis has little influence on the detection performance analysis, and that the CDP for 3 collaborative sensors can be evaluated by the NND and the NSPL. [C8415]

"Research of Radar Signal Processor Based on the Software Defined Radio"

The paper addressed how to design the software radar signal processor based on the software defined radio structure, and discussed the reasons for using the DSP+FPGA and offered an insight into fix on the important parameters of software radio. Attention is concentrated on the construction of algorithm model, simulation the algorithm by Simulink, and some methods for algorithm and architecture mapping were discussed. The computer simulation of hardware model is provided; it changes the structure of hardware, and realizes the new function through the promotion or update of software. So the design and implementation of a velocity & distance-measuring radar signal processor based on the SR structure were studied. Evidences have shown that it especially suits the design of radar because of the similar structure and SR. [C8416]

"Binary Sequence Pairs With Two-level Autocorrelation Functions"

The uniqueness of the binary sequence pair with two-level autocorrelation functions (BSPT) is put forward in the paper and proved by using mathematic tools, which is of great importance in guaranteeing receiving uniquely when applying BSPTs. Some construction methods of BSPT are given. The infinite families of BSPTs are presented by applying construction methods given in this paper. [C8417]

"A new method to create a virtual third antenna from a two-channel SAR-GMTI system"

Two-channel SAR-GMTI systems are suboptimal for moving target motion parameter estimation. Indeed, the ATI phase estimate of the across-track velocity component for a moving target is biased to lower values depending on the target signal to clutter ratio and the target across-track velocity. Additional antenna diversity can introduce additional degrees of freedom that can eliminate the bias problem. Aperture switching is an accepted method to virtually increase the number of channels without adding new hardware. One such mode is the RADARSAT-2 toggle mode (S. Chiu and C. Gierull, 2006). This paper proposes a new processing method to create a similar effective phase center configuration as the RADARSAT-2 Toggle mode from already recorded two-channel SAR data. This is achieved by delaying and combining the recorded two-channel measurements. The combination operation manifests not only a third phase center halfway between the phase centers of the two-channel system, but also a different antenna length of the virtual third antenna which requires a modification of the DPCA-ATI processing algorithm. The DPCA-ATI performance of the new mode is assessed and compared to ATI from the original two-channel mode. [C8418]

"Polarization diversity for detecting targets in inhomogeneous clutter"

Polarization diversity has proved to be a useful tool for radar detection, especially when discrimination by Doppler effect is not possible. In this paper, we address the problem of improving the performance of polarimetric detectors for targets in heavy inhomogeneous clutter. First, we develop a polarimetric detection test that is robust to inhomogeneous clutter. We run this polarimetric test against synthetic and real data to assess its performance in comparison with existing polarimetric detectors. Then, we propose a polarimetric waveform-design algorithm to further improve the target-detection performance. A numerical analysis is presented to demonstrate the potential performance improvement that can be achieved with this algorithm. [C8419]

"Conditional and constrained joint optimization of RADAR waveforms"

In this paper we describe a methodology of jointly designing waveforms for a semi-cooperative, distributed radar system. Some radars have waveforms which are fixed and cannot adapt. The remainder of the group must optimize their emanations conditioned on the existence of the non-cooperative radars. We term this 'conditional joint optimization.' A special case is termed constrained joint optimization examines the problem when the RADAR configuration is completely cooperative. Only classic constraints such as phase-only, finite energy, etc. are considered. The overall metric that is used in the optimization is signal to interference plus noise ratio (SINR). We will show the results of a number of empirical experiments based on canonical spectra and knowledge aided sensor signal processing for expert reasoning (KASSPER) simulated data that show that a joint conditional design will outperform a non-cooperative, individually optimized RADAR network. [C8420]

"A novel polyphase code for sidelobe suppression"

A binary code sequence attained by modification of a Golay code is proposed. This code has sidelobes which are out of phase with the main lobe, a property which facilitates their removal. Unknown delay-dependent phase terms preclude the multiplexing of a Golay pair in frequency. However the modified Golay code is found to have an autocorrelation whose square is complementary with that of the code's original Golay partner. This enables complementary behavior to be achieved when the modified code is multiplexed at equal offsets both above and below the partner. Applications include sidelobe removal in radar returns. [C8421]

"Information theoretic radar waveform design for multiple targets"

In this paper we describe the optimization of an information theoretic criterion for radar waveform design. The method is used to design radar waveforms suitable for simultaneously estimating and tracking parameters of multiple targets. Our approach generalizes the information theoretic water-filling approach of Bell. The paper has two main contributions. First, a new information theoretic design criterion for designing multiple waveforms under a joint power constraint when beamforming is used both at transmitter and receiver. Then we provide a highly efficient algorithm for optimizing the transmitted waveforms, by approximating the information theoretic cost function. We show that using Lagrange relaxation the optimization problem can be decoupled into a parallel set of low-dimensional search problems at each frequency, with dimension defined by the number of targets instead of the number of frequency bands used. [C8422]

"Target tracking using particle filtering and CAZAC sequences"

When tracking targets in radar, the selection of the transmitted waveform and the method of processing the return signal are two of the design aspects that affect measurement accuracy. Increased measurement accuracy results in enhanced tracking performance. In this paper, we apply sequential Monte Carlo methods to propose matched filtering operations in the delay-Doppler space where a target is expected to exist. Moreover, in the case of thresholding the measurements, these methods are used to form resolution cells that have the shape of

the probability of detection contour. These methods offer an advantage over traditional radar tracking methods that form tessellating resolution cells to approximate the probability of detection contours, and exhaustively perform matched filtering operations over the entire delay-Doppler space. With the use of a Bjorck constant amplitude zero-autocorrelation (CAZAC) sequence, a high resolution measurement is attained and the use of thresholding is avoided. This is an advantage over commonly used waveforms such as linear frequency modulated chirps (LFMs). We examine the properties of Bjorck CAZACs and demonstrate improved tracking performance over LFMs in a single target tracking scenario. [C8423]

"Adaptive waveforms for target class discrimination"

This paper compares the performance of two matched-illumination waveform design techniques for distinguishing between M target hypotheses. The waveforms are implemented within a closed-loop, sequential-testing framework. In contrast to our earlier work, in this paper the target hypotheses are statistically characterized by power spectral densities. Thus, the waveforms are matched to the target class rather than to individual target realizations. As the class probabilities change in response to received data, the waveforms are adapted, which leads to faster decisions. [C8424]

"Orthogonal waveform support in MIMO HF OTH radars"

HF skywave radar performance and flexibility can benefit from transmission of multiple orthogonal waveforms in a multiple-input, multiple-output (MIMO) radar architecture. Several practical limitations need to be considered in such a design. One issue is that many HF radar transmit arrays are over-sampled spatially to allow for operation over a significant portion of the HF band. Transmission of orthogonal waveforms in this case can result in large reactive power and consequent equipment damage. Another issue is the ability to generate orthogonal waveform sets with sufficient cardinality at the low time-bandwidth products typical of aircraft surveillance operation. There are likely to be fewer waveforms than transmit elements and so some form of spatial rank expansion, from waveform to radiated signal, is required. Both of these issues are examined using Maric-Titlebaum frequency-hop codes as one example of an orthogonal waveform set. [C8425]

"Concurrent operation and cross-radar interference cancellation of two over-the-horizon radars"

It is known that improved target characterizations can be achieved by concurrently using multiple over-the-horizon radars (OTHRs) as compared to a single OTHR operating alone. However, a key limitation with OTHR radar is the selection of an appropriate operating frequency, given the rising demand on radar waveform bandwidth commensurate with the range resolution requirements. The authors have considered concurrent operations of two OTHR systems that use the same frequency band with different chirp waveforms, and a cross-radar interference cancellation technique has been developed. The purpose of this paper is to examine the performance of cross-radar interference cancellation in the presence of multiple target returns from both auto- and cross-radar reception modes. It is shown that, the interference between target returns corresponding to the same radar is negligible, whereas the residual error of cross-radar interference cancellation in the presence of signal returns corresponding to different radars takes a low value in a typical application scenario. [C8426]

"Characterization of diversity approaches for LFM stretch-processed waveforms"

Frequency diversity in linear frequency modulated (LFM) waveforms can introduce unintended range shifts among receive radars in a distributed environment. This can make it difficult to predict where interference will occur in those receive radars, particularly when multipath is considered. This paper introduces the concept of interference region in range-frequency space to characterize the interference levels at a receive radar caused by waveforms transmitted from different radars in a distributed architecture. Linear frequency modulated (LFM) stretch-processed waveforms provide wide bandwidth and high range resolution while imposing only modest demands on the digital processing capabilities of a radar system. For this reason they are the waveform family of choice for many current wideband radar systems, including synthetic aperture radar (SAR) systems. However, LFM waveforms do not easily lend themselves to applications that require orthogonality, such as distributed radar architectures. The widespread use of these waveforms and the processing advantages they provide make it worthwhile to examine schemes for their use in a distributed environment. The paper uses interference region analysis to assess the effectiveness of frequency diversity, upchirp-downchirp diversity and chirp slope mismatch using LFM stretch-processed waveforms in a distributed environment. [C8427]

"Computationally efficient waveform diversity"

In this paper, a new signal processing approach referred to as simultaneous range-Doppler (SRDreg) is presented. It applies fractional Fourier transforms in a manner that yields projections and slices of the cross-ambiguity function (CAF). Waveform diversity (WD) techniques often require extensive processing resources,

thus precluding WD from smaller, more mobile systems, or applications with limited resources. By employing SRDreg, the feasibility of WD in these applications is greatly increased. The projection and slice processing is used to detect targets and estimate their unambiguous range and Doppler in the CAF range-Doppler space. SRDreg detects peaks of the CAF in a processor-efficient manner, thereby reducing the computational load associated with traditional approaches since computing the entire CAF is avoided. The number of required operations is reduced to $O(N \log_2(N))$ as opposed to $O(N^2 \log_2(N))$. Since SRD* processing load is insensitive to waveform modulation and coding, orthogonal waveforms can be exploited to confer temporal, spatial, and spectral diversity to a sensor system, without incurring any processing penalty. Fundamentally, SRDreg offers waveform flexibility and increased processing efficiency, which can be applied to broaden the scope of applicability of WD to sensor systems. [C8428]

"The Strength Pareto Evolutionary Algorithm 2 (SPEA2) applied to simultaneous multi-mission waveform design"

This paper furthers the development of the application of evolutionary computation, specifically genetic algorithms (GAs) to the design of simultaneously transmitted orthogonal waveforms. The goal of the application is to determine a suite of "optimal" waveforms (in the Pareto sense) for a single platform radar system performing multiple radar missions simultaneously. The waveform suite is determined by applying the strength Pareto evolutionary algorithm 2 (SPEA2) developed by Zitzler, Laumanns & Theile (2002) to find waveform parameters that successfully realize a set of objectives particular to a variety of radar missions. The objectives to optimize are dictated by the particular missions of interest. The mapping of these objective functions to actual radar performance parameters is used in the SPEA2 algorithm to determine how best to simultaneously perform multiple radar missions such as GMTI, AMTI, SAR etc. using a single radar system in a Pareto optimal sense. Preliminary results are presented for a scaled down multi-mission multi-objective function scenario. [C8429]

"Energy-efficient Routing for Signal Detection under the Neyman-Pearson Criterion in Wireless Sensor Networks"

Energy-efficient routing for wireless sensor networks (WSNs) has been a topic of great interest for the last few years, but thus far routing for signal detection in WSNs has not attracted much attention. In particular, little research has focused on the Neyman-Pearson criterion which is the most well accepted metric for radar, sonar and related signal detection problems. In this paper, we formulate the problem of energy-efficient routing for signal detection under the Neyman-Pearson criterion, apparently for the first time. We hereby propose two different routing metrics that aim at a tradeoff between the detection performance and the energy consumption. In particular, the first one leads to a combinatorial problem of identifying a path which achieves the largest possible mean detection-probability-to-energy ratio, while the second one reduces to finding a route which minimizes the consumed energy while maintaining a predetermined detection probability. We further provide efficient algorithms for solving these problems based on state-of-the-art research from operations research. We also present simulation results which indicate the distinctive energy-performance balance achieved by each proposed routing metric. [C8430]

"Tracking Multiple Targets Using Binary Proximity Sensors"

Recent work has shown that, despite the minimal information provided by a binary proximity sensor, a network of such sensors can provide remarkably good target tracking performance. In this paper, we examine the performance of such a sensor network for tracking multiple targets. We begin with geometric arguments that address the problem of counting the number of distinct targets, given a snapshot of the sensor readings. We provide necessary and sufficient criteria for an accurate target count in a one-dimensional setting, and provide a greedy algorithm that determines the minimum number of targets that is consistent with the sensor readings. While these combinatorial arguments bring out the difficulty of target counting based on sensor readings at a given time, they leave open the possibility of accurate counting and tracking by exploiting the evolution of the sensor readings across time. To this end, we develop a particle filtering algorithm based on a cost function that penalizes changes in velocity. An extensive set of simulations, as well as experiments with passive infrared sensors, are reported. We conclude that, despite the combinatorial complexity of target counting, probabilistic approaches based on fairly generic models for the trajectories yield respectable tracking performance. [C8431]

"Skeleton-Based Tornado Hook Echo Detection"

We propose and evaluate a method to identify tornadoes automatically in Doppler radar imagery by detecting hook echoes, which are important signatures of tornadoes, in Doppler radar precipitation density data. Our method uses a skeleton to represent 2D storm shapes. To characterize hook echoes, we propose four shape features of skeletons: curvature, curve orientation, thickness variation, boundary proximity, and two shape

properties of tornadoes: southwest localization and the ratio of storm size to model hook echo size. To evaluate the hook echo detection algorithm, the hook echoes detected in several radar datasets by the algorithm are compared to those proposed by an expert. The effectiveness of the algorithm is quantified using a critical success index (CSI) analysis. [C8432]

"Collusion Attack-Resilient Hierarchical Encryption of JPEG 2000 Codestreams with Scalable Access Control"

This paper proposes a collusion attack-resilient method of encryption for access control of JPEG 2000 codestreams with hierarchical scalabilities. The proposed method generates one encryption key from one single key by multi-dimensional scanning to serve encryption keeping the scalability of codestreams. To avoid collusion attacks in which multiple users generate an illegal key from their own keys to overcome the access control, sufficient conditions are considered in this method. Moreover, a skip encryption is introduced to decrease the computational complexity and key management-and-de-livery cost of encryption. Simulation results show the effectiveness of the proposed method. [C8433]

"Morphological Processing of Severely Occluded Digital Elevation Images to Extract and Connect Stream Channels"

Recent advances in technology have enabled the acquisition of high-resolution topographic data by means of airborne laser swath mapping (ALSM), which can yield digital elevation models (DEMs) with horizontal resolutions of 1m. A DEM is a grayscale image wherein pixel value corresponds to elevation. Using ALSM imaging systems over forested terrain, we filter out the laser returns from the occluding foliage and estimate bare-surface DEMs. Extracting stream networks from DEMs is important for modeling many hydrological processes. We apply a sequence of morphological operations to an ALSM DEM to detect stream channels in forested terrain. We verify the accuracy of the results using a set of error measures over simulated terrain and also using GPS ground truth over real terrain. For linking disconnected stream segments, a measure of pixel connectivity is used. [C8434]

"SAR and SPOT Image Registration Based on Mutual Information with Contrast Measure"

In this study, we propose a novel robust mutual information (MI) based method to register SAR and SPOT images. Traditional MI based method can register SAR and SPOT images well. However, its robustness is not satisfying for local spatial information is absent. In our approach, first, local contrast of 5*5 windows centered at each point in both images is calculated, then the contrast value is assigned to each pixel and two contrast images are obtained. Finally, the SAR and SPOT images are registered by maximizing the MI between their contrast images. Experimental results show that compared with traditional MI, our approach is much more robust and acquires comparable or even higher accuracy. Meanwhile, compared with the MI with orientation information based registration (MIOI), another robust MI based method, our algorithm works much faster and more accurately. [C8435]

"Processing Fine Digital Terrain Models by Markovian Regularization from 3D Airborne Lidar Data"

Airborne laser scanner systems are based on the emitting/receiving cycle of a laser beam mounted on the nadir of an airplane. They provide 3D point clouds of the topography within an altimetric accuracy of generally less than 10 cm. The divergence of the emitted laser beam allows the recording of at least two distance measurements for each transmitted pulse. It is particularly interesting when surveying forest areas whereon both the top canopy and the ground are recorded at once. The aim of the paper is to describe a methodology for modelling the terrain from sparse laser ground points with a dense altimetric surface, without using classical interpolation algorithms. Our approach is based on the definition of an energy function that manages the evolution of a terrain surface in a Bayesian framework. The energy is designed as a compromise between a data attraction term and a regularization term. The minimum of this energy corresponds to the final terrain surface. We show some conclusive results of the retrieving of a realistic terrain. [C8436]

"Interferometric Synthetic Aperture Microscopy: Physics-Based Image Reconstruction from Optical Coherence Tomography Data"

Optical coherence tomography (OCT) is an optical ranging technique analogous to radar-detection of back-scattered light produces a signal that is temporally localized at times-of-flight corresponding to the location of scatterers in the object. However the interferometric collection technique used in OCT allows, in principle, the coherent collection of data, i.e. amplitude and phase information can be extracted. Interferometric synthetic aperture microscopy (ISAM) adds phase-stable data collection to OCT instrumentation and employs physics-

based processing analogous to that used in synthetic aperture radar (SAR). That is, the complex nature of the coherent data is exploited to give gains in image quality. Specifically, diffraction-limited resolution is achieved throughout the sample, not just within focal volume of the illuminating field. Simulated and experimental verifications of this effect are presented. ISAM's computational focusing obviates the trade-off between lateral resolution and depth-of-focus seen in traditional OCT. [C8437]

"Polarimetric Azimuthal Spectral Histogram Exposes Types of Mixed Scatterers and the Cause for Unexpected Polarimetric Averages"

Echoes detected by polarimetric weather radar in clear air contain signals from air and biological scatterers. Discriminating the various scatterer types from a composite echo is challenging due to variability in scatterers' quantity, azimuthal dependences of their polarimetric properties, and uneven mixing in resolution volumes. We use polarimetric spectral densities to estimate the volume content by constructing two dimensional (2D) histograms. The dimensions used to form image are Doppler velocity and polarimetric variable. The assimilation of these histograms in azimuth results in a 3D-azimuthal-spectral-histogram (3DASH). This representation allows us to use transparency for small occurrences to visualize the 3D-signatures of dominant content. The scatterer types have distinguishable signatures in 3DASH due to their diverse physical shapes, scattering properties, different headings, and speeds. 3DASH can help to understand what constitutes the polarimetric averages of the resolution volume. 3DASH can help provide resources for establishing intrinsic polarimetric values/functions for different types of biological scatterers, which are necessary for scatterer classification algorithms. [C8438]

"Robust Road Extraction for High Resolution Satellite Images"

Automatic road extraction is a critical feature for an efficient use of remote sensing imagery in most contexts. This paper proposes a robust geometric method to provide a first step extraction level. These results can be used as an initialization for other algorithms or as a starting point for manual road extraction. Results of the extraction are vectorized for GIS integration and for a better interaction with human experts that can refine the results. The algorithm is fast, has very few parameters and is only slightly affected by the image properties (resolution, noise). The algorithm is available in the open-source Orfeo toolbox. [C8439]

"Digital Implementation of Pulse Compression Technique for X-band Radar"

The performance of conventional pulsed radars is limited by its "time-bandwidth" product. In order to get high range resolution, a narrow pulse is required to be transmitted. However, this reduces the average transmit power resulting into shorter detection range. To mitigate this limitation of "time-bandwidth" problem, pulse compression technique is used. Pulse compression technique can be broadly classified as, FM chirp and phase coded. In FM chirp method, a longer duration frequency modulated pulse is transmitted, and on the receiver side matched filter is used to compress the echo signal. This also resolves the targets which may have overlapping returns. Earlier implementation of pulse compression was done using analog circuitry, which has its own limitations. With the availability of high speed digital equipment, it is now possible to implement it in digital domain. This paper presents a digital implementation of LFM pulse compression technique in X-band. Here, we used an arbitrary waveform generator to generate LFM pulse (chirp) at lower frequency band, which is up-converted to X-band by mixing with a carrier of 9.375 GHz for transmission. On receiver side, after translation to lower frequency band, data is acquired by analog to digital converter card and pulse compression algorithm was implemented in computer using MATLAB tool. Various tests were performed to verify pulse compression technique. [C8440]

"A coherent fiber-optic link with optical-domain down-conversion and digital demodulation"

Frequency down-conversion is an essential element of radar signal processing. Classical electronic down-conversion using heterodyne mixing, however, introduces unavoidable non-linearities resulting in inter-modulation distortion and conversion loss. In this paper we describe a hybrid optical/digital downconversion technique that is free of distortion and conversion loss. Experimental results are presented showing proof-of-concept operation limited to the dynamic range of the A/Ds that were available for the experiment. The ultimate goal is to attain an SFDR of 150 dB-Hz^{2/3} or higher across an instantaneous bandwidth of 1 GHz for a microwave carrier up to 100 GHz. [C8441]

"A Fuzzy Adaptive Fusion Algorithm for Radar/Infrared Based on Wavelet Analysis"

In order to improve tracking ability, a fuzzy adaptive fusion algorithm based on wavelet analysis for radar/infrared is proposed, which combines the merits of fuzzy logic and wavelet analysis. Fuzzy adaptive fusion algorithm is a powerful tool to make the actual value of the covariance of the residual consistent with its theoretical value. To overcome the defect of the dependence on the knowledge of the process and measurement noise statistics of Kalman filter, wavelet analysis is introduced, which needs no prior knowledge of the process and measurement

noise. And fuzzy inference system is applied for its simplicity of the approach and its capability of processing imprecise information. The simulation experiments on the novel adaptive fusion algorithm have been performed. The computational results show that the proposed algorithm can effectively strengthen the system robustness and improve the tracking precision. It is obvious that the algorithm has significant advantages over the traditional Kalman filter algorithms in tracking application. [C8442]

"Application of neural network in Infrared-Radar Dual-mode Guidance System"

In this paper a novel target tracking information differentiating system with the capability of real time tracking and accurately identifying is developed in infrared-radar dual-mode guidance system. We take advantage of neural network's well known capability of learning to perform the required classification without the assumption of probabilistic models for the input models to substitute the fuzzy rules in the information differentiating system. Since the neural network training based on expert knowledge database is conducted off-line, significant benefits of developing real time tracking capabilities are possible. Her supervising trained neural network is applied in the dual-mode guidance system, which outputs the confidence degree denoted as the weight value of target information in data fusion center according to the two input variables of measure noise and tracking error. The validity of this method is proved by simulation. [C8443]

"Application and Simulation of Kalman Filtering with Anti-Jamming"

Classifying the jamming of guidance system and inducing its characteristics; and the importance of jamming and anti-jamming in the missile guidance are analyzed. In order to make the missile dive target with higher speed and attack it in the limited time, designing Kalman filter based on missile and target relative movement modeling; researching the anti-jamming abilities and techniques. The result of simulation shows that it can obtain the anticipative effect under the certain of parameter selection and adjustment and this method has good value of theory and application. [C8444]

"Improved Multilayer Perceptron Design by Weighted Learning"

This paper presents new relevant results on the application of the optimization of backpropagation algorithm by a weighting operation on an artificial neural network weights actualization during the learning phase. This modified backpropagation technique has been recently proposed by the author, and it is applied to a multilayer perceptron artificial neural network training in order to drastically improve the efficiency of the given training patterns. The purpose is to modify the mean square error (MSE) objective function in order to improve the training efficiency. We show how the application of the weighting function drastically accelerates training convergence whereas it maintains neural network's (NN) performance. [C8445]

"Optimization of Fighter Aircraft Evasive Trajectories for Radar Threats Avoidance"

The problem of optimal evasive trajectories of fighter aircraft for radar threats avoidance is studied. At the core of the function is the tactical level trajectory planner that is highly integrated with the mission level planning system. The trajectory planner is described that can find an optimal or sub-optimal trajectory to penetrate through hostile enemy radar threats with a high survivable probability. Calculus of variations is introduced to deal with the flight constraints and an analytic solution for monostatic radar avoidance has been obtained. Based on the analytic solution, the concept of solution space has been proposed to generate evasive policy sets to cover the characteristic constraints. In the solution space, the Bayesian decision theory combined dynamic programming algorithm is adopted to get the global optimal solution to problem of multiple radars avoidance. The results are compared to other path planning methods, especially the methods of Voronoi diagrams and A*. [C8446]

"Ship Route Designing for Collision Avoidance Based on Bayesian Genetic Algorithm"

Maritime accidents frequently occurred because of human errors. It is important to generate safe route automatically in collision situations. Genetic algorithm is a new method for this purpose. However, the International Regulations for Preventing Collision at Sea have not been taken into account in previous researches. In this paper, Bayesian model is employed to calculate the post probability of each trajectory according to the rules and general practice of seaman. The fitness function is formed with path cost and information content. Experiments illustrate that evasion routes generated by Bayesian genetic algorithm are more rational than that of pure GA, considering the rules for preventing collision and general practice of seaman. [C8447]

"Information Fusion System with GPRS module for Monitoring the Status of Driver"

This paper presents the advanced system with GPRS module and information fusion approach for real-time

detecting the status of driver. It uses infrared cameras to simultaneously monitor the fatigue symptoms of driver for determining the fatigue status. The vision information consists of the trend of pupil change, the times of blinks, the times of yawns, and the angle between the head and the plumb line. The veracity of the system will be strengthened to determine the status of fatigue driving through information fusion technology. In addition, the system is capable of automatically drawing the conclusion that the driver is falling asleep and issuing different warning signals depending on the level of the fatigue status. The system will transmit the conclusion automatically to the traffic control department with GPRS module. [C8448]

"Research on Data Association in Three Passive Sensors Network"

In this paper, it is concerned with the static data association problem in the three distributed passive sensors network, in which each sensor can observe 2-dimensional angles (azimuth and elevation) of each target. A new fast data association approach is proposed in a multiple target dense environment with noise, missed detections, false alarm, and unknown number of the targets. Firstly, the data association of three sensors is transformed into the data association of two sensors about three groups, and the possible correct pairs of association are achieved by the statistic test. Secondly, the pairs of association which are detected by three sensors are got by the analysis method proposed in this paper, which is instead of m-D assignment. Lastly, the pairs of association which are detected by two sensors are got. The simulation results show that the proposed approach has higher association accuracy than the other conventional approaches. [C8449]

"Digital Signal Processing for A Level Measurement System Based on FMCW Radar"

A level measurement system based on FMCW radar is developed. The structure of the measurement system is introduced. The methods of digital signal processing for the system are investigated. FFT algorithm is employed to process frequency difference in low-accuracy situation. When the signal-to-noise ratio is high, the high accuracy measurement is obtained by the AR spectral estimation. An autocorrelation filter is applied to the measurement system to reduce the disturbances. The resolution of the system which employs the methods of signal processing reaches 1 mm. [C8450]

"ART and Fuzzy K-means Clustering Based Algorithm for Packet Classification"

Existing algorithms for packet classification always deal with a ready rule set. However, now a day, large classifiers' rule sets are huger and huger (say, 100 000 rules). Generated these rules by hand is so hard, and causes lots of redundant rules. In this paper, we present a two stage cluster based algorithm for packet classification, which aims to generate filter rules automatically for permitted packets. Based on the scheme, a three-field packet classification for permitted packets (sev-address, sev-port and protocol) is proposed. Experimental results show that the scheme can significantly reduce needed filter rules for permitted packets and the range of IP address lookup. [C8451]

"A Study of Information Fusion for UAV Based on RBF Neural Network"

We all know that it is very difficult to create accurate model for UAV navigation system because that this system is nonlinear system, at the same time, the environment information provided by information sources of multi-sensor in UAV is uncertain. Correspondingly, neural network can provide precise navigation information for UAV by fusing multi-source information that is uncertain, incomplete and mutually exclusive, accordingly to ensure navigation precise. This paper put forwards an information fusion method for UAV integrated navigation system based on RBF neural network. The simulation results show that this method can provide satisfactory navigation information. [C8452]

"Measurements of UWB Antennas Backscattering Characteristics for RFID Systems"

A measurement technique, which is carried out in indoor non-anechoic-chamber environment and can be employed to extract the backscattering characteristics of ultra-wideband (UWB) antennas for radio frequency identification (RFID) systems, is developed and presented in this paper. To validate the measurement technique, a type of UWB antenna, i.e., printed circular-disc monopole antenna (PCDMA), is simulated, fabricated, and measured. Backscattering characteristics of the PCDMA with three different kinds of terminations (i.e., open-circuit, short-circuit, and matched-load), including radar cross section (RCS) and UWB impulse response, are then extracted by the measurement technique. The measured results are theoretically verified by using the finite-difference time-domain (FDTD) method with Berenger's perfectly matched layer absorbing boundary condition (PML-ABC). [C8453]

"Theoretical and Experimental Analysis of a Rolled-Dipole Antenna for Low-Resolution GPR"

In this paper a rolled dipole antenna for low-resolution impulse ground penetrating radar (GPR) is theoretically and experimentally investigated. The antenna has been designed for transmission of monocycle pulses with duration of 5 ns (200 MHz central frequency) suitable for low-resolution GPR applications. The dipole is rolled to considerably reduce its length and resistive loading with the Wu-King profile is applied for suppression of late-time ringing, important for GPR. It is shown theoretically that the antenna radiates the pulse with no late-time ringing. Furthermore, by rolling the wires the antenna length is reduced by a factor of 4 with no evident negative impact on the antenna's characteristics. A shield for the antenna has been designed, constructed and integrated with the antenna. Furthermore, it has been found that a tapered bow tie can be combined with the antenna in such a way that a significant increase in the antenna efficiency is obtained, resulting in a unique hybrid of a dipole and a bow-tie antenna. [C8454]

"UWB Reference-Free Self-Positioning with Electrical Scanning Directional Antenna"

An Ultra-Wideband (UWB) self-positioning system and its architecture are presented. It consists of a pulse-based transceiver for ranging from the surrounding objects, an electrical scanning antenna for direction detection, and baseband positioning algorithms. Self-positioning can be performed by using the ranging and direction information based on reflected signals in a room environment. It can also determine its own position in the presence of some blocking objects by employing the so-called multi-layer reflection algorithm. This reference-free self-positioning system operated in an office meeting room is shown to be capable of achieving 30 cm positioning accuracy with the 70% bound. [C8455]

"Bistatic UWB Radar System"

A new GPR system using an optical electric field sensor was proposed. The system has a bistatic radar configuration, which is consisted from a TEM horn antenna as a transmitter and an optical electric field sensor as a receiver. The new system employs a time-domain data acquisition, and it made the data acquisition very fast. Laboratory measurements showed that a metallic sphere can be detected by the new system. Applications of this system will include landmine detection and through wall imaging. [C8456]

"Subsurface Imaging with UWB Linear Array: Evaluation of Antenna Step and Array Aperture"

This paper presents the investigation of antenna step and aperture size for an ultra-wideband (UWB) ground penetrating radar (GPR) with a linear array. The procedure includes the optimization of receiving array, verification of optimization results by EM simulation and experimental measurement for both surface and subsurface imaging. The imaging algorithm used for the evaluation combines the focusing of the array and the synthetic aperture radar technique in the mechanical scan direction. [C8457]

"Development of Antennas for Subsurface Radars within ACE"

The paper gives an overview of the joint activities of the ACE-2 partners in the area of antennas for surface penetrating radar. Main areas of joint research and development are discussed and main results of joint activities are presented. Special attention is given to experimental verification of proposed antenna designs. [C8458]

"Long Range and Ultra-Wideband Short Range Automotive Radar"

While radar based comfort systems like autonomous cruise control (ACC) and collision warning are available in many high and mid class models since several years, safety systems like pre-crash sensing, collision mitigation, or collision avoidance are just entering the market. For safety functions short range ultra-wideband radar sensors are used in addition to forward looking long-range radar to extend ACC to stop-and-go operation and to enable further features like pre-crash warning, parking aid, back-up warning, lane change aid, or emergency braking. The contribution give an overview on automotive radar sensors and applications for novel comfort and safety systems with special emphasis on ultra-wideband short range radar, addressing specifications, design, packaging, and the worldwide frequency regulation situation. [C8459]

"SiGe Circuits for Spread Spectrum Automotive Radar"

This paper presents circuits in SiGe bipolar technology for spread spectrum automotive radar applications in the band from 77 to 81 GHz. They cover the transmit and receive paths. The transmitter integrates a voltage controlled oscillator, a prescaler by 64, a 10 bit linear feedback shift register (LFSR), and a biphase modulator. The system has been optimized in order to achieve a range resolution less than 12 cm and an unambiguous range of 124 m. The quadrature receiver frontend consists of a single-ended low-noise amplifier (LNA), balanced-to-unbalanced converters, two fully differential direct-conversion mixers, LO buffer amplifiers, and a branchline coupler for I/Q generation. The presented systems show that millimeter-wave circuits in SiGe

technology can achieve high integration levels along with high performance. They are well suited for application in spread spectrum automotive radar systems. [C8460]

"A Double Stage IPCP Detector for UWB Radars"

Among ultra wide band (UWB) detectors have been introduced yet, single pulse detectors don't have good performance as two or multiple pulses detectors. Multiple pulses and multi-channel detectors increase calculation load and need faster processors than single or double-pulse detectors. Since they don't have equal detection performance for different number of target bright points, they are used in multi-channel architecture. In this paper, a double stage detector consisted of an Inter-Period Correlation Processing (IPCP) as first stage followed by another stage to detect targets missed in the first stage is proposed. The proposed detector improves IPCP detection performance without having multi-channel computational load. [C8461]

"Experimental Verification of Human Being Detection Dependency on Operational UWB Frequency Band"

The study investigates the effect of bandwidth and centre frequency of UWB radars on detection and resolvability of trapped victims. The study is limited to two person-under-test (PUTs) and does not set forth to perform statistical evaluation, but instead provides rough figures on appropriate frequency band to be used for human being detection purposes. It has been shown that for all considered cases, SNR increases with operational bandwidth and centre frequency and reaches its optimal values between 2-2.9 GHz and 4.5-6 GHz, respectively. HH antenna co-polarization is the preferred one, since it generally produces equal or higher SNR values than VV antenna co-polarization. The results show that it is easier to detect a standing victim; however such scenarios are not very likely occur in real-life conditions. It has been found that if a breathing human is blocking the propagation path of the human target response of another breathing human, the human target response of the latter is heavily attenuated (around 17 dB) and thus only the closer breathing human is detected. This study could, thus, not perform the down-range resolution assessment, as intended. Nevertheless, it demonstrated clearly that there is a need for multi-static radar configuration for increased probability of detection of trapped victims. [C8462]

"Using UWB Radios as Sensors for Disaster Recovery"

This paper considers the sub-problem of estimating the interior structure of a collapsed building by using embedded UWB radios as sensors. We created an extensive database of UWB propagation data through various building materials. Then, using this data and a novel algorithm, we demonstrate that we can indeed determine material type, thickness and cavity dimensions using UWB radios. This paper presents the algorithm and the evaluation results. As we show, for most common building materials such as concrete and reinforced concrete, the presented algorithm has a very small estimation error. [C8463]

"Narrowband Interference Suppression in UWB Impulse Radar for Human Being Detection"

Narrowband interference (NBI) is a major source of performance degradation in human being detection applications using impulse radar and stroboscopic samplers. Implementation of notch filters results in undesired ringing of the target response. Four methods are developed and their performance analysed: two variations of the approach that extracts the NBI and subtracts its contribution and two variations of the approach that filters the NBI out and restores the missing spectrum. NBI is modelled as modified GSM signal. It is shown that latter methods perform better both in terms of NBI suppression, but also in terms of signal waveform and energy preservation. [C8464]

"Improving the Speed of a Class of Single Frequency Estimation Algorithms"

Recently, a class of recursive algorithms for single frequency estimation has been developed based on the rotate-add-decimate (RAD) method. The computational bottleneck of the RAD approach is the calculation of the arctangent function required to create a frequency estimate at the end of each recursion. This work demonstrates speed gains are possible with minimal loss in mean squared-error (MSE) performance by deferring accuracy in the calculation of the arctangent function until the final recursion. [C8465]

"Recent Advances in Ultra Wideband Radar and Ranging Systems"

This invited paper describes advances in short pulse electromagnetics as applied to ultra wideband (UWB) radar and precision ranging. UWB sensors designed for perimeter intrusion detection, obstacle and collision avoidance and industrial safety applications was described. The design of a part 15 compliant, UWB radar development kit is also discussed. [C8466]

"Design Considerations For An Atmospheric Imaging Radar"

This paper describes the design requirements, tradeoffs and simulations involved with the design specifications of an Atmospheric Imaging Radar (AIR). Design constraints are discussed including size and portability. Radar details include the range of meteorological targets detectable, maximum range, and other criteria needed for the weather radar equation. A dual pulse repetition time waveform is used to improve the maximum unambiguous velocity and range. The trade-offs in volume, sensitivity and pulse integration are described in the radar design. Calculations are made and initial plots showing at least 15 dBZ sensitivity at 10 km are shown for a radar that will image a cone 16.5deg wide and 40 km long. [C8467]

"Shoreline Based Feature Extraction and Optimal Feature Selection for Segmenting Airborne LiDAR Intensity Images"

Modern airborne laser swath mapping (ALSM) systems measure both elevation and reflection intensity of the terrain. However, this intensity has been under utilized as a feature for image classification because it does not represent true terrain radiance. In areas with minimal topographic relief, such as beaches, we show that segmenting intensity images rather than elevation images has great potential for scene analysis. Several intensity-based features are extracted from ALSM data collected along a beach and partitioned into three classes to detect the water line. Class-conditional probability density functions are estimated for each feature to assess which are most informative. Results indicate significant class separation using centroidal features. Their classification performance is evaluated using a naive Bayes classifier and the area under receiver operating characteristic curves. The method presented provides a novel feature extraction and a systematic feature selection procedure for high-resolution ALSM intensity data. [C8468]

"Ground Penetration Radar Using Golay Sequences"

In most of the existing ground penetration radar (GPR) systems, the major problem is low signal-to-noise ratio (SNR) and the masking of the weaker returns by the strong side-lobes. These twin problems can be minimized to a large extent with the help of Golay sequences. Golay sequences are complementary sequences; the sum of these yield twice the value of the autocorrelation at zero lag and zero elsewhere. In terms of improved SNR and reduced sidelobe levels, the performance of these sequences is considered to be better than that of pseudorandom binary sequences (PRBS), Barker or other maximal length sequences. Some of the results from a bench-top Golay based GPR system using PRBS and Golay codes are presented. [C8469]

"Real-time Imaging of Human Bodies with UWB Radars using Walking Motion"

UWB (ultra wide-band) pulse radar is a promising candidate for surveillance systems used to prevent crimes and terror. The high-speed "SEABED" (shape estimation algorithm based on bst and extraction of directly scattered waves) imaging algorithm is deployed to apply UWB pulse radar in fields that require realtime operations. The SEABED algorithm is based on a reversible BST (boundary scattering transform) between the target shape and the received data. This transform does not require the iterative calculations needed by other algorithms such as the synthetic aperture method or the domain integral equation method. The SEABED algorithm assumes that omni-directional antennas are scanned to observe the scattered electric field in each location. However, in the field of surveillance systems, scanning antennas are impractical. In this paper, walking motion is used to replace scanning antennas. We propose a new algorithm to estimate the shape of a human body using the data provided by a human body passing stationary antennas. [C8470]

"UWB measurement, complex-amplitude texture, and Walled-LTSA array in plastic landmine visualization"

We describe the importance of ultra wideband (UWB) reflection measurement in the adaptive target visualization. We use a complex-valued self-organizing map (CSOM) to deal with complex-amplitude texture obtained by stepped-frequency UWB reflection measurement. We distinguish targets from clutter by paying attention to the difference in texture in space and frequency domains. In the technique, a wideband measurement is desirable to obtain precise texture. We employ a newly developed antenna, walled LTSA, with which we can construct a wideband, dense array for high-resolution imaging. [C8471]

"Recent Advances and Applications of M-Sequence based Ultra-Wideband Sensors"

Ultra-wideband (UWB) sensing is an upcoming technique to gather data from complex scenarios such as nature, industrial facilities, public or private environments, for medical applications, non-destructive testing and many more. Currently it is hard to estimate the full spread of future applications. The measurement approach

traditionally used is based on stimulation of the test objects by either short sub-nanosecond impulses or sine waves which are stepped/swept over a wide spectral band. This paper deals with an alternative approach, which uses very wideband pseudo-noise binary signals such as M-sequences for example. Such devices have a very high time stability, enable high measurement speed and do not burden the test objects with high voltage peaks. Furthermore, the device concept promotes monolithic circuit integration in a low cost semi-conductor technology. In what follows, the basic device concept and some extensions will be considered as well as some selected applications will be discussed. [C8472]

"The Research Activities of Ultrawide-band (UWB) Radar in China"

The UWB signals for radar applications can be generated from time domain or frequency domain. Because of the limited energy, the time domain UWB signal or impulse signal is usually applied for short range radar, such as ground penetrating radar(GPR) and through-wall-imaging radar(TWIR). In opposition to it, the frequency domain UWB signals can be applied both for short-and far-range imaging radar, such as GPR, TWIR or airborne UWB synthetic aperture radar(SAR). The UWB radar research has been carried out from 1980s in China. But its really flourishing and mature era was from the middle of 1990s. This paper reviews the Chinese archives and the most recent results in UWB radar both for time domain and frequency domain. [C8473]

"Detection and recognition of radar objects at sounding by high-power ultrawideband pulses"

By present, ultrawideband (UWB) radiation sources with megavolt efficient potential have been created. This is technical basis for development of UWB radars for remote object sounding. The paper gives special attention to analysis of investigation results of methods for detection and recognition of remote radar objects at sounding by high-power UWB pulses. To detect UWB signals at the noise and interference background, an approach based on the joint use of matched filtering and inter-period correlation processing is suggested. A genetic function method and parametric methods were developed for object recognition. Compression of the data bank is of importance in the latter methods. [C8474]

"UWB-GPR Data Processing for Identification of Anti-personnel Landmines under Rough Ground Surface"

A process for finding buried landmines by using GPRs is divided into two stages, detection and identification. In the detection stage, all buried objects including the desired landmines together with other clutter objects are detected. In the identification stage, the detected objects are classified and the landmines are differentiated from the other objects. In this research, we focus on the identification stage and propose a GPR data processing for identification of shallow(!) buried antipersonnel landmines. After suppressing the ground surface reflection, we extract features related to waveform correlation from the GPR data. As an identification algorithm, an approach based on a matched filter is employed. In order to check the identification performance, Monte Carlo simulations are carried out using dataset generated by a 2D-FDTD method. Results are shown in the form of ROC curves and AUC values, and effects of soil condition (i.e. ground surface roughness, inhomogeneity, and moisture in soil) on identification performance are assessed. [C8475]

"Vehicle Frontal Collision Warning System based on Improved Target Tracking and Threat Assessment"

A vehicle frontal collision warning system (FCWS) based on improved target tracking and threat assessment for collision avoidance is described in this paper. The system acquires longitudinal and lateral position of objects from radar and Lidar. Together with host's speed and angular velocity, the system tracks all the targets in front. The threat assessment, based on the knowledge of current state, provides a warning signal to the driver when a potential collision is detected. Extensive field tests show that, with the stable and accurate tracks, the warning system not only provides high accuracy in detecting potential collisions but also responds exactly in time to assist the driver. [C8476]

"Sensor Calibration Using the Neural Extended Kalman Filter in a Control Loop"

Sensor errors can adversely affect the behavior of a control system. When multiple sensors are used, a broken sensor can have its effects minimized by artificially inflating its error covariance. In this paper, a different approach to compensating for sensor errors in a multiple-sensor control system is introduced. The technique, referred to as a neural extended Kalman filter (NEKF), is developed for closed-loop control systems. The NEKF learns on-line from the same residual information used in the state estimator. The improvement in the sensor report is made by the neural network being added to the measurement model. In this work, the NEKF is applied to vehicle trajectory control problem with a position sensor and a velocity sensor. [C8477]

"A Low-cost Vehicle Detection and Classification System based on Unmodulated Continuous-wave Radar"

Vehicle detection and classification system is an important part of the intelligent transportation systems (ITS). Its function is to measure traffic parameters such as flow-rate, speed, and vehicle types, which are valuable information for applications of road surveillance, traffic signal control, road planning, and so on. This paper presents a novel low-cost vehicle detection and classification system which is based on a K-band unmodulated CW radar. This system utilizes time-frequency analysis, multi-threshold detection, and Hough transform as the major signal processing methods to extract speed and shape information of vehicles from Doppler signature they generate. It can perform vehicle detection, speed measurement, and vehicle classification simultaneously. Experimental results show that the proposed system and algorithms can provide promising performance and accuracy. [C8478]

"Feature Fusion for Robust Object Tracking Using Fragmented Particles"

Tracking people or objects across multiple cameras and maintaining a track within a camera is a challenging task in applications such as video surveillance. Some of the major challenges while tracking a target are illumination/scale changes and partial occlusion. In this paper, we propose a novel tracking framework using particle filter to efficiently track an object within a camera and a blob-based target association scheme for tracking across cameras. The proposed particle filter tracking algorithm uses a fragment-based approach to model the target and track it by fusing color and gradient features. Also, the proposed solution incorporates coarser level spatial information by fragmenting each particle and is shown to be beneficial for tracking under partial occlusion. A fast yet robust model update is employed to overcome illumination changes. Experimental results show (i) the robustness of the fragment-based tracking approach with respect to illumination/scale change and partial occlusion and (ii) tracking persons across two cameras. [C8479]

"Improving Arterial Performance Measurement Using Traffic Signal System Data"

The characterization of the performance of freeways in real time and on a historical basis has been successfully achieved for many years. The ability to characterize arterial performance has been more elusive. Currently numerous applications of traffic management and traveler information systems include freeways but lack the ability to extend their operation to major arterials. This paper describes methods for quantifying arterial performance using data from signal system loop detectors. Included in the array of metrics are traffic density, total delay, predicted travel time, and signal coordination effectiveness. Methods for determining performance in these areas are adapted for use in quantitatively evaluating arterials in real time. To assess them, methods are employed to analyze archived data for a segment of Barbur Blvd. in Portland, Oregon. Suggestions for future research are also included. [C8480]

"Localization of ahead vehicles with on-board stereo cameras"

This paper introduces a vision based algorithm that detects and localizes ahead vehicles elaborating images taken by a stereo camera installed on an intelligent vehicle. The algorithm is based on the analysis of stereo images, estimating the ground plane by least square fitting of disparity data, and segmenting the obstacles by a rule based split/merge strategy. Quantitative experiments on complex real world sequences validate the approach. The method is demonstrated to operate in real-time. [C8481]

"Improvement in SAR Image Classification using Adaptive Stack Filters"

Stack filters are a special case of non-linear filters. They have a good performance for filtering images with different types of noise while preserving edges and details. A stack filter decomposes an input image into several binary images according to a set of thresholds. Each binary image is filtered by a Boolean function. The Boolean function that characterizes an adaptive stack filter is optimal and is computed from a pair of images consisting of an ideal noiseless image and its noisy version. In this work the behavior of adaptive stack filters is evaluated for the classification of synthetic aperture radar (SAR) images, which are affected by speckle noise. With this aim it was carried out experiment in which simulated and real images are generated and then filtered with a stack filter trained with one of them. The results of their maximum likelihood classification are evaluated and then are compared with the results of classifying the images without previous filtering. [C8482]

"Radiomodule of VHF Reception Path"

Proposed in this paper is high-linear technological VHF radio module with controlled overload level and frequency protection. The original adaptation circuit of the path allows providing dynamic range expansion without cascades noise accumulation with reduced transfer. [C8483]

"Test bed for Remote Environmental Monitoring in Northwestern China"

In this paper we design the heterogeneous network instead of homogeneous one to reduce the load of single node and as a result it could eliminate probability of wireless sensor network (WSN) overload. For wide feasibility in China northwestern area we choose the Global System for Mobile Communications (GSM) to transmit monitoring data to server and implement a protocol stack like TCP to get a reliable short message service(SMS) from local telecom provider. Finally we show some test result of this test bed and discuss about the next step.

[C8484]

"Automatic extraction of LIDAR data classification rules"

LIDAR (Light Detection And Ranging) data are a primary data source for digital terrain model (DTM) generation and 3D city models. This paper presents an AdaBoost algorithm for the identification of rules for the classification of raw LIDAR data mainly as buildings, ground and vegetation. First raw data are filtered, interpolated over a grid and segmented. Then geometric and topological relationships among regions resulting from segmentation constitute the input to the tree-structured classification algorithm. Results obtained on data sets gathered over the town of Pavia (Italy) are compared with those obtained by a rule-based approach previously presented by the authors for the classification of the regions. [C8485]

"Robust Indoor Positioning Based on Received Signal Strength"

A positioning algorithm based on the relative order of the received signal strengths is discussed. This algorithm in conjunction with the ray-tracing propagation model can have promising performance for indoor environments without any needs for extensive set of a priori training. Enhancements to the positioning algorithm will be proposed and investigated. Two sets of experimental results with 802.11-based infrastructure and MICA2 motes are presented to demonstrate the system capability and performance in practice. [C8486]

"FIR-filter based equalization of ultra wideband mutual coupling on linear antenna arrays"

This paper describes a compensation method of ultra wideband mutual coupling using finite impulse response (FIR)-filters to equalize the frequency characteristic of antenna interactions. The result is a compensated far-field impulse response, which yields an radiated electric field similar to one caused by an ideal uncoupled antenna array. On the basis of an antenna array impulse response, which includes antenna interaction, a mathematical framework is derived to configure the FIR-filters. Finally, simulations are presented, where the preprocessed radiated electric field of an antenna array coincides with the electric field caused by a single isolated antenna without any coupling effects. [C8487]

"Multicarrier Coherent Pulse Shaping for Radar and Corresponding Signal Processing"

A new pulse shaping approach based on coherent superposition of multiple carriers in radar is introduced, by which a shorter efficient pulse width waveform can be formed. At the receiver end, breaking the echo into multiple corresponding frequency components, multiple series can be taken from those individual components, then recombining these components to achieve the signal processing gain. Three processing approaches are proposed for multicarrier Doppler processing, which will provide better Doppler estimate performances than that of conventional pulse Doppler radar. [C8488]

"Radar Reflected Signal Process of High Spinning Rate Projectiles"

By slotting at the bottom of the projectiles, the target characteristics such as the spinning rate and the attitude can be obtained by Doppler radar. The reflection of spin projectile is a nonstationary AM-FM signal. The index of AM represents the attitude of the projectile. And the modulation frequency shows the spinning rate. The model of the reflected waveform is given. Chirp-Z transform (CZT) is adopted to improve the measurement precision. The process approach and the complexity of CZT are present. Its time cost is in the same grade to FFT. Simulation results and perspective are also given. [C8489]

"Research on Rough Set-Neural Network and Its Application in Radar Signal Recognition"

The purpose of reconnaissance system's information processing is signal recognition, which is also a key step in the whole process of radar reconnaissance information processing. In order to solve the problem of radar signal recognition, a new type of recognition model is established which combines rough set and neural network closely in this paper. The model can be divided into these steps such as recognition information's pretreatment, sample data's reduction by rough set, neural network's learning and training and network's recognition to information

which is not identified. The model mixes rough set's strong rule extraction ability and the excellent classification ability of neural network through preprocessing initial information and reducing data and training network etc. The experimental results illustrate the model reduces subject factors in signal recognition, improves network's structure. Compared with traditional signal recognition methods, this model can manage to identify radar signal objectively and effectively without any transcendental information. [C8490]

"Research of High Precision Frequency Measure Algorithm Based on LabVIEW"

In order to get the frequency (f) of an intermediate frequency (IF) signal, during the measure of frequency modulated continuous wave (FMCW) radar, we often use the fast Fourier transform (FFT) for transforming time signal to discrete frequency signal, then we can get the frequency by the position of the frequency spectrum's peak. While the data was collecting, the collecting circuit does always not synchronize with the signal, what we collect is the truncated discrete signal, When we apply the discrete Fourier transform on this kind of signal, we can only get some discrete value of the continuous spectrum, the peak of the spectrum always has a departure with the envelope of the spectrum by using the not integral period sampling, and this causes the leak error. For improving the precision of the frequency measure, this paper presents a frequency measure algorithm by integrating automatic adjusting the sampling parameter and spectrum correction. By using this algorithm, we first adjust the sampling number based on current frequency for meeting the request of the integral period sampling, afterwards, the spectrum is further corrected by using the balancing of the energy rules, so we can get a more precise measure. [C8491]

"Application of Radial Basis Function Neural Networks in Complicated Radar Signal Measurement and Sorting"

An intelligent radar signal sorting system with a robust radial basis function (RBF) is presented in this paper. This system can automatically sort the random overlapped radar signal stream and separate the input pulse stream to individual radar pulse sequence. Because tradition Gaussian neural network uses Gauss function as its basis function and adopt gradient descending method to adjust parameters. So the tradition method is likely to produce some non-expectation in learning process. In order to solve the problem, the proposed RBF uses Log-Sigmoid function as its basis function, so it eliminates any risk of instabilities, and it has better learning properties and function approximation capabilities. This algorithm ameliorates the traditional algorithm and enhances the robust properties of learning process. For one thing, the method can adapt to the complicated electromagnetic environment demand due to its self-adapting capability. For another, it can overcome the difficulty that the data have too much noise due to the detection system faultiness. Simulation results demonstrate the obvious superiority of this algorithm. [C8492]

"Password-based Dynamic Group Key Agreement"

A password-based dynamic group key agreement protocol from tripartite Diffie-Hellman using pairing on elliptic curve is presented in this paper. In this scheme, due to all users share a common pre-distributed password, the setup of the key agreement is simplified and the performance is improved. In addition, each user establishes a relation between his left and right neighbors respectively in order to implement the fast joining and leaving operations. Under the DDH assumption, proofs are given to show that the proposed key agreement protocol is secure against passive attack. [C8493]

"Non-Contact Cardiopulmonary Sensing with a Baby Monitor"

Cardiopulmonary signals can be detected at a distance using simple Doppler radars operating in CW mode. Tests with and without audio modulation show the feasibility of measurements with this hardware, providing a maximum measured difference to the reference of just 1.6 bpm for heart rate. Tests show good correspondence of heart/respiration rate with the reference data. [C8494]

"Inter and Intra-Hemispheric EEG Coherence Responses to Visual Stimulations"

This study investigated whether the visual stimulation at extremely low frequency (ELF) could possibly induce changes in the electroencephalographic (EEG) responses. The functional connectedness was examined between the brain regions when the minimum variance distortion-less response (MVDR) coherence algorithm together with Wilcoxon signed-ranks test statistical method was applied. The results showed that functional significance of EEG alpha rhythms at parietal, and occipital cortex, respond to oscillatory 13 Hz and 16.66 Hz light stimulation, respectively. [C8495]

"Study of the Ballistocardiogram signal in life detection system based on radar"

In this article, our study of non-contact method via radar for monitoring the heart and respiratory rates of human subject is reported. The system is constructed which synchronously detects the electrocardiogram signals by the electrocardiograph and the ballistocardiogram signals by the non-contact life parameter detecting technology. Also, the detected signals are analyzed respectively in the time and frequency domain. The results show that the cycle of the ballistocardiogram is obvious in time domain and that the rhythm of the two kinds of signals keeps consistent. And their characteristic points in frequency domain are also the same. The clinical medicine usefulness of ballistocardiogram detected by the non-contact technology is approved and the credible evidence for the succeeding signal analysis and the clinical application is provided. Furthermore, the characters of the heartbeat signal detected by our system and the reasons for that are also discussed in detail in our paper.

[C8496]

"Lost Sample Recovering of ECG Signals in e-Health Applications"

This paper shows the interest of an interpolation method based on parametric modeling to retrieve missing samples in ECG signals. This problem occurs more and more with the emergence of telemedicine applications. The different links (fixed access network (PSTN), mobile access network (GSM/GPRS and future UMTS) or satellite interfacing (DVB-RCS technology)) involved in e-health applications are liable to induce errors on the transmitted data. These errors/losses can occur anytime and anywhere (according to the channel availability, memory overflows, protocols, etc) during a transmission process. Therefore the recovering of missing samples for biomedical signals is of great interest. The method used in this paper is based on a left-sided and right-sided autoregressive model, i.e., the interpolation algorithm uses the samples before and after the sequence of missing samples. An objective measure is used to assess the method performance. Results show that this interpolation method represents a really suitable technique to ECG signal reconstruction in a possible corrupted transmission. [C8497]

"Noise Considerations for Remote Detection of Life Signs with Microwave Doppler Radar"

This paper describes and quantifies three main sources of baseband noise affecting physiological signals in a direct conversion microwave Doppler radar for life signs detection. They are thermal noise, residual phase noise, and Flicker noise. In order to increase the SNR of physiological signals at baseband, the noise floor, in which the Flicker noise is the most dominant factor, needs to be minimized. This paper shows that with the consideration of the noise factor in our Doppler radar, Flicker noise canceling techniques may drastically reduce the power requirement for heart rate signal detection by as much as a factor of 100. [C8498]

"Recent Developments in Ground Based Millimeter Wave Radars"

This paper is a continuation to the paper entitled "Developments in Millimeter Wave Packaging brings down the Cost of Ground Based Perimeter Surveillance Radars" presented at Carnahan 2006, Kentucky, USA [1]. In this paper it presents the continuation in manufacturing techniques with focus on the antenna, followed by the development of a well known military techniques called "track-while-scan". This technique allows to track multiples intruders to extract the Doppler signature, while maintaining full capability in scanning the detection area to detect any new intruders. [C8499]

"Experience with Ranging Buried Cable Sensing"

The next generation of Guided Radar (GUIDAR) is based on Ultra Wide Band (UWB) radar signal processing. Just as spread spectrum technology has revolutionized the communications industry, UWB is dramatically changing radar signal processing. These advanced signal-processing techniques are adapted to leaky coaxial cable technology in the next generation GUIDAR to provide new features and enhanced performance. At the core of the new technology is an ultra high-speed digital correlator implemented in a Field Programmable Gate Array (FPGA). Complementary orthogonal codes based on Golay codes are used to produce thumbtack correlation functions simultaneously in multiple range bins. The net result is "near continuous wave (CW)" performance in forty to eighty 11.6-meter long-range bins with targets located within one meter along the length of cable. This is a dramatic improvement over the 3% duty cycle of the original GUIDAR and the typical 100 to 200 meter-long zones of current CW leaky cable sensors. Uncorrelated complementary codes are transmitted on each of two leaky coaxial cables. The responses from two parallel receive cables are digitized directly and down converted to baseband using quarter rate translation. The uncorrelated nature of the code allows the A and B sides of the processor to operate without interfering with each other. Synchronous sampling at twice the chip rate ensures that each target is observed in three adjacent sample bins. The phase and amplitude response in the three adjacent samples are combined to precisely pinpoint (within 1 meter) the locations of targets along the length of each of the two cables. The ability to precisely locate and track multiple simultaneous targets on each of two cables leads to numerous new features and performance benefits relative to existing leaky cable sensors.

With a separate calibrated threshold for every meter of cable, the sensor sensitivity is much more uniform and installation restrictions on burial depth, cable spacing and medium homogeneity can be relaxed. Potential sources of nuisance alarms can easily be located and overcome. The pinpoint location can be used to provide better CCTV assessment, target capture for video motion sensors and more effective response to intrusions. Through the use of parallel cables the sensor can be used to detect the direction of crossing and to classify targets such as small animals, people and vehicles. This patented next generation of GUIDAR technology represents a dramatic step forward from that which was introduced at the 1976 Carnahan Conference in Lexington Kentucky and the numerous CW leaky coaxial cable sensors that evolved from that work. This technology effectively addresses residential, commercial, industrial and governmental requirements, including those relating to Homeland Security, military operations and prisons. [C8500]

"Benefits of Wide Area Intrusion Detection Systems using FMCW Radar"

The history of perimeter protection is based on building fences. That basic concept evolved into detecting activity along the fences using a variety of sensors. Today a wide variety of fiber and wire-based sensors are available to mount on a fence, as well as many different types of IR, radar, optical, seismic and acoustic sensors to place along the fence line. Generally some camera support is provided, with the cameras programmed to point to pre-set locations along the fence. A more robust perimeter protection would consist of wide area sensors with the capability to look out beyond the fence to detect potential intrusion and track intruders to determine their intention. In looking beyond the perimeter, wide area sensors can provide precious time to plan and initiate the appropriate response. In addition, because they sweep a 360-degree circle, the sensors can provide continued tracking of the intrusion even after penetration of the perimeter, greatly enhancing the effectiveness and safety of the response team. The new wide-area concept consists of using modern radar technology for wide area detection of objects which are moving, and then using the precise location information from the radar to point a camera for assessment. Without having to continually stare at a bank of video monitors, the operator is presented with the location, direction of travel and identification and number of potential intruders, all in a matter of seconds. This paper first presents the features of this new wide area system, followed by an overview of radar technology and closes with a discussion on the benefits of the FMCW topology over pulse Doppler in security and surveillance applications. [C8501]

"Learning Imbalanced Data Sets with a Min-Max Modular Support Vector Machine"

To overcome the class imbalance problem in statistical machine learning research area, re-balancing the learning task is one of the most classical and intuitive approach. Besides re-sampling, many researchers consider task decomposition as an alternative method for re-balance. Min-max modular support vector machine combines both intelligent task decomposition methods and the min-max modular network model as classifier ensemble. It overcomes several shortcomings of re-sampling, and could also achieve fast learning and parallel learning. We compare its classification performance with resampling and cost sensitive learning on several imbalanced data sets from different application areas. The experimental results indicate that our method can handle class imbalance problem efficiently. [C8502]

"Resolving Wall Ambiguities Using Angular Diverse Synthetic Arrays"

Model-based algorithms that attempt to localize targets and estimate the structure within a building using data from external sensors have received much attention in recent years. The potential benefits to homeland security and urban warfare are exceedingly apparent. Accurately estimating the thickness and dielectric constant of the exterior wall could prove to be a critical first step in determining the layout within, i.e., the location of interior walls, doorways, stairwells, etc. However, data collection using a linear sensor arrangement yields an ambiguous two dimensional objective function for the wall parameters, rendering maximum likelihood methods ineffective. We show that a spatially diverse aperture obviates the wall parameter ambiguity and allows accurate estimation of thickness and permittivity using dynamic logic, an iterative model-based approach to maximum likelihood. [C8503]

"Effect of 8.43 Hz Frequency Magnetic Field on the Single Neuron"

Electromagnetic field (EMF) of the GSM cellular telephones affect on the living tissues thermally. In this communication system radiofrequency EMF is modulated by extremely low frequencies (ELF) -8,43 and 217 HZ. On the other hand bulk of investigations proves existence of non thermal effects of the ELF EMF on the biological systems. The current controversy lies on the possibility that the ELF-EMF could produce biological non-thermal effects. We present in vitro experimental data which show that neurons from the brain ganglia of the mollusk *HelixPomatia* are sensitive to ELF magnetic field of 8.34 Hz in the ranges of 0.2-10 mT. [C8504]

"IEEE 1641 signal modelling as a learning aid"

A requirement arose to specify test facilities for a complex radar system. For the digital and low frequency analogue parts of the system, there was no problem. However, the radar knowledge possessed by the engineer undertaking the assessment, one of the authors of this paper, was some 20 years out of date and gained when he was a maintainer rather than an engineer. What was needed was a better understanding of the nature and characteristics of a radar signal. This paper shows how a modeling tool for IEEE Std. 1641 (Signal & Test Definition) m was able to assist the engineer to gain the necessary knowledge to make a valid assessment.

[C8505]

"Radar Detection Through Wavelet Transform"

In this paper we intend to unite the wavelet theory with radar detection. To join both theories, we will use the connection between the wideband signal model and the wavelet transform. Once the wavelet transform is applied the echo signal received, we compare the wavelet coefficients of a scale j with a fixed threshold for a defined false alarm probability in that scale. From that comparison, the existence of target will be decided.

[C8506]

"L-VCONF: A Location-Aware Infrastructure for Battlefield Videoconferences"

Audio and videoconference technologies make complex coordination processes easier, especially when mobile participants need to synchronize their action in critical environments. The need for an infrastructure providing such a functionality may arise in complex scenarios where an IP network is not available, as for instance in battlefield or other critical environments. This paper describes L-VCONF, an architecture for geo-located conferencing based on a mobile/cellular network (i.e. GPRS, UMTS, WiMax technologies), quick-and-dirty mobile/cellular geolocation, SIP protocol and presence server. Our architecture supports IP audio/videoconferences enriched with geo-located coordination functionalities in complex environments. The approach described in the paper is robust w.r.t. uncertainty while handling location update notification for SIP presence server. [C8507]

"The Influence of Permittivity of the Crack-Type Defects to the Scattered Far Field (TM-Case)"

The influence of material's permittivity of two thin cylindrical inclusions illuminated by a plain TM-polarized electromagnetic wave and some geometric parameters of appropriate diffraction problem on the far radiation field have been investigated in the paper. [C8508]

"Building Learning Communities in Blended Classrooms Through an Innovative mLearning System"

Chinese classrooms have long suffered from a lack of interactivity. Many online classes simply provide recorded instructor lectures for students to listen to. This format only reinforces the negative effects of passive non-participatory learning. At a major university in Shanghai, researchers and developers actively seek technologic interventions that can greatly increase interactivity in online classes. They developed a cutting-edge mobile learning system that can deliver live broadcast of real-time classroom teaching to online students with mobile devices. This system allows students to customize means of content-reception.. The system also supports short text-messaging and instant polls. Through these venues, students can ask questions and make suggestions in real time, and the instructor can address them immediately. This paper describes this system in detail, and also reports results from a test implementation of the system with a blended classroom of 1000 students (250 campus and 750 online). [C8509]

"An Iterative Learning Algorithm for Multi-Channel Coherence Analysis"

An iterative learning algorithm for multi-channel coherence analysis (MCA) is developed in this paper. MCA is an extension of the well known canonical correlation analysis (CCA) that allows for more than two data channels to be analyzed. The many applications of CCA have motivated this extension to exploit the linear relationship between many data channels. This paper discusses fundamental differences between the two analysis techniques while reviewing the standard method for performing MCA. Discussion on why MCA correlations are not deemed "canonical" as they are in the two-channel case of CCA is also provided. The developed iterative learning for MCA is then demonstrated and its performance evaluated on a synthesized data set. [C8510]

"Angular Resolution Increasing in Processing of Radionavigation Signals"

Presented in this paper are the methods for radar objects imagery with increased angular resolution, as well as algorithms, which are necessary for information reprocessing. Results of numerical experiments using mathematical models are offered. Limits for increasing of angular resolution efficiency are determined depending

on signal/noise ratio. [C8511]

"Addition and Multiplication Statistics for Orthogonal Signal Processing in Multiple Antennas System"

Multiple configuration antennas system using ultra wideband orthogonal noise waveforms is considered for testation radar applications. System Signal Function of MIMO radar is determined using the time domain back-projection algorithm with addition and multiplication statistics. [C8512]

"Autodyne Signal at Reflection Factor Value Modulation"

Considered in this paper is the problem of signal generation on the amplitude variation taking into account frequency variations in autodyne oscillator under the influence of electromagnetic wave reflected from the object under control with reflection factor modulation. It is shown that autodyne response waveform may essentially differ for the modulation function law. The results of the theoretical analysis are confirmed by experimental investigation of the oscillators designed on the basis of hybrid integrated modules "Tigel-08" and "Tigel-08M" in millimeter waveband. Theoretical analysis carried out and experimental investigations results show that autodyne signal waveform with amplitude modulation of the electromagnetic wave reflected from the stationary object may essentially differ from the modulation function law. This feature should be taken into account at radio physical investigations of various substance features, in radio spectroscopy, as well as in short-range radar. [C8513]

"Elements of Fractal Radiosystems"

This paper proposes the design of wideband elements of fractal radio systems. [C8514]

"Analysis Features of Fast-Acting Radio Electronic Systems with Combined FM-AM Modulation"

Analysis features of combined FM-AM modulated signals in fast-acting radio electronic systems including radio frequency identification systems (RFID) and short range radar systems (SRRS) are shown in this paper. [C8515]

"Information Compression and Speckle Reduction for Multifrequency Polarimetric SAR Imagery using KPCA"

Multifrequency polarimetric SAR imagery provides a very convenient approach for signal processing and acquisition of radar image. However, the amount of information is scattered in many images, and redundancies exist between different bands and polarizations. Similar to signal-polarimetric SAR image, multifrequency polarimetric SAR image is corrupted with speckle noise at the same time. This paper presents a method of information compression and speckle reduction for multifrequency polarimetric SAR imagery based on kernel principal component analysis (KPCA). KPCA is a nonlinear generalization of linear principal component analysis using kernel trick. The NASA/JPL polarimetric SAR imagery of P, L, and C bands quadpolarizations is used for illustration. Experimental results show that KPCA has better capability in information compression and speckle reduction compared with linear PCA. [C8516]

"Neural Modeling Fields for Multitarget/Multisensor Tracking"

We describe a new approach for combining range and Doppler data from multiple radar platforms to perform multi-target detection and tracking. In particular, we assume azimuthal measurements are either coarse or unavailable, so that multiple sensors are required to triangulate target tracks using range and Doppler measurements only. The algorithm framework is based upon neural modeling fields, a biologically-inspired neural architecture, which yields advantages over conventional multi-target tracking algorithms by reducing the computational complexity during data association by several orders of magnitude. The algorithm is tested on synthetic multi-sensor data, and the results demonstrate that accurate tracks can be estimated by exploiting spatial diversity in the sensor locations. These results are promising, and demonstrate a surprising degree of robustness in the presence of nonhomogeneous clutter and uncertainty in the number of targets. [C8517]

"Performance Comparison of SOM Based Hybrid Hardware Classifiers"

This paper compares two hardware classifiers in various aspects. Both systems are hybrid network with SOM or Scalar SOM (SSOM) combined with Hebbian network. The SSOM is a simplified version of the SOM, which handles a single variable instead of vectors. The additional programmable network with the Hebbian learning capability, performs the category acquisition and naming. Two systems are described by VHDL and their classification performance as well as the circuit size and operating speed are compared. The results show that the SSOM based classifier exceeds the SOM based classifier in the circuit size and speed, while from the

classification point of view, the performance of the SOM based classifier is better. [C8518]

"Discretization of Continuous Interval-Valued Attributes in Rough Set Theory and its Application"

Rough set theory is a relatively new soft computing tool to deal with vagueness and uncertainty, and is regarded as a field of leading edge. But it cannot deal with continuous attributes, thus discretization is a problem which we cannot neglect. Discretization based on rough set has some particular characteristics, and consistency must be satisfied for discretization of decision systems. Existing discretization methods cannot well process continuous interval-valued attributes in rough set theory. A new approach is proposed to discretize continuous interval-valued attributes in this paper, which enhances the precision of classification and accurate recognition rate in pattern recognition. In the simulation experiment, the decision table was composed of 3 features and 17 radar emitter signals, and the recognition results obtained from this discretization algorithm show that the proposed approach is valid and feasible. The approach expands the application scope of rough set theory. [C8519]

"A Two-Stage Hybrid Space-Time Adaptive Processing Approach"

This paper presents a new two stage hybrid space-time adaptive processing (STAP) algorithm, which combine space-time multiple-beam (STMB) architecture and direct data domain (DDD) approach. The proposed two stage hybrid algorithm use the direct data domain approach as the first stage to suppress discrete interference in the range cell under test and use STMB method as the second stage to suppress the residue correlated interference. Therefore this approach takes advantage of the DDD and STMB method and alleviates their drawback, so it can suppress discrete interference and correlated interference simultaneously. [C8520]

"The Affection of MAC Protocols to Energy Consumption in the UWB-Ad hoc System"

Energy is the vital source for the UWB-Ad hoc system. For the characteristics of UWB-Ad hoc system, it has some particular requests to the MAC layer. Accordingly, it is necessary to find out the affection of MAC protocols to the performance of UWB-Ad hoc system. In this paper, kinds of MAC protocols that are all rate-controlled were studied. And performance curves were gotten. Also, a general model of the energy consumption was set up, which was the foremost contribution of this paper. The conception of average signal-to-interference-and-noise-ratio and two variables of energy consumption degree and capability were brought forward to give the measurement of QoS guarantee. Mass simulations proved the model and QoS guarantee sufficiently. [C8521]

"A new encoding transponders for SAR calibration"

A transponder can encode the signal transmitted by synthetic aperture radar (SAR). The reflected signal from the encoding transponder to SAR can be imaged with the background signals suppressed. One type of encoding transponder is to make the linear frequency modulation (LFM) signal transmitted by SAR inverted. To realize this aim, there are the analog mixing method and the digital undersampling method, which is put forward in this paper. The error models of these two methods are studied. Simulation experiments about an input LFM signal are carried out. The results prove that the precision of the digital undersampling method is better than that of the analog mixing method. [C8522]

"Adaptive S-method based ISAR imaging of maneuvering targets"

The range-Doppler imaging algorithm is a basic method for ISAR imaging, which is based on the uniform rotation of a target in a fixed plane. For maneuvering target, however, its rotational velocity and the axle often vary with time, so the second-order phase terms are induced to target echoes. Aimed at this situation, an adaptive S-method based imaging algorithm is proposed in this paper. First, translational motion compensation is implemented to the raw data. Then, this algorithm is applied to the echo of each range cell, to eliminate second-order phase terms and obtain ISAR imaging in the range frequency-Doppler domain. Since it only requires complex multiplications and adding, this algorithm has low computational complexity in practical use. In addition, due to the adaptiveness, it can adjust itself according to the returned signals, and reduce the influence of cross-terms for each range cell at the same time. The measured data has proved the validity of this algorithm. [C8523]

"ESPRIT super-resolution imaging algorithm based on external illuminators"

Passive radar imaging algorithm based on external illuminator requires large accumulated rotating angle of target. But in an actual circumstance, large rotating angle demands long time, which is hard to satisfy the request of real time, on the other hand, target reflectivity function differs at various aspect angles, moreover, when rotating angle increases, target reflectivity function differs seriously. In this paper, an ESPRIT based high resolution passive radar imaging algorithm is proposed to solve the problem which is that how to form a good

image at the instant of small rotating angle. In the method self-correlation matrix of the returned echoes is estimated firstly, then corresponding sine wave frequencies of the scattering-centers with the object is determined through eigenvalue decomposition, target location is deduced by the sine wave frequency, hence the reflectivity of the scattering-centers are computed. Computer simulation confirms the feasibility of the algorithm.

[C8524]

"HIPERMA: A high performance and reconfigurable processor for SAR applications"

In this paper, a high performance and reconfigurable MAC Array (HIPERMA) processor is designed for Synthetic Aperture Radar (SAR) systems. HIPERMA is composed of many coarse-grained reconfigurable units and can be configured to finish the algorithms based on matrix multiplication level. The processor maintains the performance of ASIC devices and flexibility of DSP, and also has inherent advantages over FPGA in terms of delay, area and configuration time. The measurement result shows it has a peak performance up to 20,000 MMACS based on SMIC 0.18 μ m six-metal CMOS process. [C8525]

"A new channel equalization method for airborne multi-channel SAR-GMTI system"

This paper investigates the channel equalization problem of airborne multi-channel SAR-GMTI system. A key problem for ground moving target indication is clutter suppression, which is sensitive to the correlation of channels. For the multi-channel system, there are differences among the characteristic of two channels and also the antenna amplitude patterns (phase as well as gain), which worsen the correlation of channels. This paper proposes a channel equalization method to improve the clutter suppression ratio. Theoretical analysis is illustrated with experimental airborne SAR data. [C8526]

"A novel approach to three-channel SAR-GMTI channel equalization and moving target detection and location based on real data"

Aiming at airborne three-channel SAR-GMTI system and its real data, a novel channel equalization method is presented, furthermore, in virtue of the method's good performance on compensating the clutter differences between different channels, a technique for moving target detection (MTD) and location is further proposed. This method first realizes signal equalization between inner channels utilizing the leaking signals, then implements range and azimuth time calibration and compensates the channel differences via iteration after range compression, after that, it realizes MTD by clutter cancellation and imaging, finally obtains target parameters by estimating moving target doppler shift. The technique proved its good performance in real data processing with the advantages of high channel equalization precision, little computations, good clutter cancellation and MTD performances and easiness to implement. [C8527]

"Non-statistical transformed data domain stap algorithm for non-homogeneous environment"

This paper introduces a new non-statistical STAP algorithm which is efficient and powerful in non-homogeneous environment. The traditional statistical algorithms using the estimated interference covariance are not optimal in heterogeneous clutter. The non-statistical approach which uses primary data only and is appropriate to extremely heterogeneous case is presented. The transformed data domain (TDD) algorithm which is more simple and efficient compared to the original direct data domain (D3) algorithm is proposed. The received space-time signal is transformed to beam-doppler domain and weight to minimize interferences is obtained in this space. The performance of the proposed non-statistical STAP is tested in SIRV clutter model environment and compared to that of the approach which employs traditional statistical algorithm. [C8528]

"A Real-time signal processing method for air-born three-channels GMTI"

In this paper, we briefly introduced the performance of several GMTI systems at first. After that, we prompted a method based on CSI algorithm for air-born three-channels GMTI signal processing, gave out the processing diagram of this method, analyzed the principle of cluster suppress, present an adaptive phase compensation method for each channel based on the minimum power criterion and analyzed the locating and velocity-estimation problem of moving targets. The presented method, which has been applied in actual furnishment, turned out to be efficient. [C8529]

"Algorithm for the latitude and longitude of an arbitrary pixel in air-borne strip mode SAR image"

As there are lots of advantages, synthetic aperture imagery is widely applied. Effective utilization of synthetic aperture imagery often requires precise latitude and longitude of each image pixel. In the case that the side-glance angle of beam is zero or small, a new algorithm has been developed to determine the latitude and longitude of an arbitrary pixel in an airborne strip mode SAR image without consideration of the hypsography.

The algorithm is precise and applicable. Error analysis of the algorithm is also made based on the parameters of a practical radar in the paper. [C8530]

"Research on jamming effect evaluation method of ISAR"

The inverse synthetic aperture radar (ISAR) is a high resolution imaging radar. Some methods used to evaluate the jamming effect of general radar are unsuitable to ISAR. Considering the principle of radar jamming and the theory of image disposal, the paper gives new evaluation methods of barrage jamming effect on ISAR. These methods can reflect clearly distortion degree of the jammed target during the whole jamming process. The results of simulation prove the methods are correct and effective. [C8531]

"Analysis of deception jamming to ISAR imaging system"

This paper presents a method of deception jamming to ISAR imaging system (Chen and Andrews, 1980). By series of simulations we will prove that when real target and fake target are moving in different trace the jamming is available and practical. [C8532]

"Parameter assessment for SAR image quality evaluation system"

Synthetic Aperture Radar (SAR) image due to its special imaging method has many different characters from optical image. In this paper, a objective image quality evaluation system is proposed with a set of parameters and relevant measurements that mainly based on SAR image itself. And this evaluation system is supposed to be used by both satellite-borne and airborne SAR system. [C8533]

"SAR deceptive jamming signal simulation"

Based on SAR jamming geometry model and radar waveform, the signal model on SAR deceptive jamming is presented, and the simulation method which is feasible in project is verified. The jamming signal is produced to protect single point or multi-points target, and is validated by SAR imaging algorithm. The method that is discussed in the paper isn't a limit to the occasion which the jamming station and the protective zone are situated in the main lobe, and it has practicality. [C8534]

"Separable space-time pattern synthesis for SBR sparse aperture array GMTI"

In this paper, a novel GMTI method is proposed for spaceborne sparse aperture radar using separable space-time processing. The extremely long baseline of a sparse aperture array can provide a narrow main beam at the cost of large number of grating lobes. To suppress ground clutter caused by grating lobes, a Doppler filter is applied at the output of the sparse array. An efficient, yet robust projection method is used to solve the Doppler filter coefficients, which is an ill-posed problem. More than -30 dB substantial gains can be achieved after sparse array beamforming and Doppler filtering. [C8535]

"On the influence of frequency-domain broadband beamformer on ISAR imaging"

Working on imaging mode, broadband phased array radar applies broadband signal. In order for spatial interference rejection, the radar should do broadband beamforming before imaging. However, the broadband beamformers may influence the performance of imaging. This paper first introduces the typical frequency-domain broadband beamformers, and then discusses the influence on pulse compression and ISAR imaging. Experiment results show that the impact of the frequency-domain broadband beamformers on ISAR imaging can be seemed as windowing the data in range and don't affect the performance severely. These beamformers are suit to practical broadband phased array ISAR imaging systems. [C8536]

"1-D high resolution range profiling technique for wideband solid state active phased array radar under active jamming situations"

High resolution one dimensional (1-D) range profile for wideband phased array radar is of great significance for ballistic missile recognition. It is always a matter of great interest for radar engineers to make an imaging radar function well in modern electronic warfare. Based on the stretch processing of LFM signal, the paper proposes a method named fully adaptive space-temporal ADBF at subarray level to achieve target imaging in active jamming situations. Computer simulation demonstrates the effectiveness of the current method. [C8537]

"Non-linear chirp scaling algorithm for one-stationary bistatic SAR"

This paper points out the non-linear property of the differential RCM along range direction in one-stationary

bistatic SAR, and compares it with the monostatic case. Then it deduces out a non-linear chirp scaling factor to identify the RCM of all targets in the swath. The complementary processes of a non-linear chirp scaling algorithm for one-stationary bistatic SAR are then described detailedly. Finally, the simulating results present here validate the correctness of the algorithm. [C8538]

"Moving target detection in airborne SAR by a combined wigner-STFT transform"

The detection and the motion parameters estimation of the moving targets is a key problem in imaging the moving target for Synthetic aperture radar (SAR). In this paper, a new method based on the combination of the Wigner-Ville distribution (WVD) and the short-time Fourier transform (STFT) has been proposed and applied to moving target detection for airborne SAR. It is demonstrated that the proposed method can eliminate the cross-terms of the WVD and improve the time-frequency resolution of the STFT simultaneously. Its performance is demonstrated by both simulation and experimental examples. Our results suggest that the proposed method provides a efficient technique in detecting the moving target for airborne SAR. [C8539]

"SAR ATR based on multi-subspaces of independent component analysis"

In this paper, a SAR (synthetic aperture radar) ATR algorithm based on multi-subspaces of Independent Component Analysis (ICA) is proposed. Features of each target SAR images are extracted by using ICA firstly, and then the Feature images of the target compose a subspace. All targets can compose multi-subspaces. Finally, we combine all the subspaces to a big new subspace by using PCA. We test our method on MASTAR database. The experiment result shows that the performance of this method is superior to other methods. [C8540]

"Radar automatic target recognition based on InISAR images"

A novel interferometric inverse synthetic aperture radar (InISAR) imaging method, include an efficient phase unwrapping approach, is proposed, which can work very well under very low signal noise ratio condition. Based on which, an InISAR image based target recognition method are proposed. The rotation and scale invariant features are extracted from the transformed InISAR images, namely, the polar images. The simulation results are provided to show the efficiency of the proposed methods. In addition, some system parameters, such as baseline length, target aspect, target speed, etc, are analyzed from the viewpoint of recognition performance. [C8541]

"Spatial decorrelation evaluation for interferometric SAR"

SAR interferometry based on image pairs acquired by different antennas enables the topographic mapping and ground moving target indication. Both the generated DEM accuracy and the clutter suppression performance are determined by the coherence of SAR image pairs. The baseline perpendicular to the SAR trajectory is one of the most important factors that affect the coherence, which varies with the property of the terrain. In this paper, the geometry between the perpendicular baseline and the terrain is researched, and the effect of terrain on coherence is presented. Then a more accurate formula for calculating the correlation coefficient is deduced in combination with the frequency characteristic of radar signals. The calculation results conform to the simulation results. [C8542]

"An improved road extraction method based on MRFs in rural areas for SAR images"

In the proposed general processing framework for road network extraction in synthetic aperture radar (SAR) images, this paper deals with automatic extraction of the road network. The general framework is based on road candidate detection, followed by optimization using a Markov random field description of road networks. The first part introduces the segment extraction technique in the road detection step. After introducing segment junction rules in the latter step, the major modification is the clique potentials of Markov random field that extracts the intersections of road networks, especially for T shape junctions. Advantage over previous extraction is proved by comparison of the experimental results. [C8543]

"Multi-scale feature analysis method for bridge recognition in SAR images"

Target recognition is an important field in remote sensing image processing. This paper handles with the problem of bridge recognition in Synthetic Aperture Radar (SAR) images. Based on features of bridges, rivers and land in different spatial resolution SAR images, a method of multi-scale analysis is proposed. The original data is split into low and middle resolution level. The bridge candidates are located in low level by automatically detecting river. And regions of interesting (ROI) are obtained in middle one. So, bridges are recognized by analyzing those regions. The example results indicate that the processing speed can be greatly improved and

the precision of recognition can also be ensured. [C8544]

"Research on jamming synthetic aperture radar technologies"

In this paper, fundamental theory of SAR imaging is introduced. Jamming SAR technology is analyzed and summarized. It contains mainly active jamming and passive jamming. Active jamming contains noise jamming and deception jamming. Passive jamming contains foil strip screen, microwave absorption material and camouflage reticulation. Jamming SAR theory is researched in detail. It based on SAR itself flaw. Emphasis puts on noise jamming, shift-frequency jamming and deception jamming. The result is these jamming methods very useful in practice. At last, author forecasts jamming SAR technology development in the future. [C8545]

"A fast segmentation scheme based on level set for SAR images"

In this paper, we propose a modified segmentation algorithm based on level set for synthetic aperture radar (SAR) images. The segmentation of SAR images is a difficult problem due to the presence of speckle which can be modeled as strong, multiplicative noise. One main drawback of previous the SAR image segmentation algorithm based on active contour model and level set is the computational expense inherent to solving the proposed nonlinear parabolic partial differential equation. The proposed algorithm is faster than the previous SAR image segmentation via standard curve evolution model. Experimental results are shown on both synthetic and real SAR images. [C8546]

"Two-dimensional PCA for SAR automatic target recognition"

In this paper, a new technique for synthetic aperture radar (SAR) automatic target recognition (ATR) is developed, which is builded upon two-dimensional principle component analysis (2DPCA). First, 2DPCA is applied to extract features in frequency domain, which is based on image matrix directly. Then support vector machine (SVM) is used for classification. Experimental results on MSTAR dataset show that the 2DPCA method both gives higher recognition rate, and are computationally more efficient than PCA. [C8547]

"Motion compensation technique for high resolution spotlight SAR"

Spotlight SAR is an efficiency way to obtain high resolution radar imagery. The non-stability of the aircraft motion during the long synthetic aperture time can make the imagery suffer the sever defocus, and there is phase error in the range direction in the high resolution SAR system. This paper presents a novel signal processing method to get high definition resolution spotlight SAR imagery, which can make an effective estimation on the aircraft position error, the phase error in range direction and the residual envelop error. The experiment results show that the proposed approach can get the high quality SAR image from raw data. [C8548]

"MTI processing based on dual frequencies-dual apertures spaceborne SAR"

Based on dual frequencies-dual apertures spaceborne SAR (synthetic aperture radar), a new SAR operation mode with four receiving channels is presented in this paper. High resolution imaging and moving target indication (MTI) are studied with this new mode. The coherent accumulation (CA) method, which combines dual channels data, is used to enhance the range resolution. With the data from all channels, the two aperture interferometric processing is executed to implement clutter cancellation. A pair of the clutter suppressed data are employed to implement double carrier frequency conjugated processing (DCFCP), then MTI processing is completed, followed by moving target imaging. The simulation results show the validity of the signal processing method and the feasibility of this new SAR mode. [C8549]

"A novel adaptive filtering algorithm for SAR speckle reduction"

The novel adaptive filtering algorithm based on the analysis of the detail images obtained from the wavelet decomposition of the original noisy image is proposed in the paper. The base idea is to compute the wavelet decomposition of the noisy image to reduce the amplitude of insignificant detail coefficients in the wavelet subspaces by selecting an adaptive filter window of size, the adaptive windowing algorithm was introduced where the window size is automatically adjusted depending on the samples statistics in the boundary of this window such as mean macrZ and standard deviation sigmaz, and then utilizing modified 2ndorder Lee filtering. One of the advantages of this approach over the traditional speckle filtering method is the fact that textures are preserved while speckle is reduced. Experimental simulations by real SAR images show it are effective. [C8550]

"An effective SAR-GMTI technique based on eigen-decomposition of the covariance matrix"

An effective multi-channel SAR-GMTI technique based on eigen-decomposition of the covariance matrix is

proposed. The variation of the sum of small eigenvalues of the covariance matrix is used to detect moving targets which can avoid clutter suppression. The radial velocity of the moving target is estimated by two steps. Firstly, using the interferometric phase of two SAR images to get the coarse radial velocity estimation, then the more precise radial velocity is obtained by searching the space-domain steering vector of the moving target. It overcomes the sensitivity of the interferometric phase to clutter and noise. The performance of the approach is analyzed in detail. The merit of the presented technique is demonstrated by simulated and measured SAR data. [C8551]

"Ground slow-moving target adaptive processing for Airborne Radar"

Airborne fire-control radar is mainly equipped with forward looking antenna, which is characterized by high flight velocity, short wavelength and low PRF. Consequently, on one hand, ground clutter of airborne fire-control radar is non-homogeneous in range and multi-ambiguous in Doppler frequency; on the other hand, Doppler frequency spectrum of the clutter varies quickly with the cone angle and the bandwidth of the mainlobe is much spread. We focus on the features of the clutter and the ground slow-moving target for airborne fire-control radar at first. Then it is pointed out that the mainlobe clutter is the most important factor which influences the detection performance. Finally, an adaptive processing algorithm, which is named FS-AMTI, is presented based on the frequency shift of the center of mainlobe clutter by adopting segmentation strategy. Experimental results with real data illustrate the good detection performance for slow-moving target of the proposed algorithm. [C8552]

"Study on imaging algorithm for missile-borne side-looking SAR"

A SAR image problem for missile-borne based on the platform anomaly movement is discussed in this paper. In this paper, a approximate illumination geometry has been defined and a new image model is presented. Image formation from missile-borne synthetic aperture radar (SAR) is limited by image degradations caused by missile's non-level straight line movement. In this paper we assume that the missile is uniformity and beeline motion in a synthetic aperture time due to the missile's high speed. A different reference range is adopted to cope with the range-dependent secondary range compression (SRC) to different synthetic aperture. By this approach, the SRC error can be reduced effectively. Finally, simulation results verify the correctness and validity of the proposed methods. [C8553]

"A novel imaging approach for multi-baseline SAR tomography"

MB-TomoSAR (multi-baseline SAR tomography) is the most promising technique to realize the real 3-D (three-dimensional) resolution of the observed target zones in future. In this paper, the state art of MB-TomoSAR is briefly reviewed firstly. Secondly, a more general MB-TomoSAR model is described, and a novel imaging approach of processing MB-TomoSAR data is proposed base on this general model. Thirdly, the emphasis is placed onto the simulation of MB-TomoSAR, and the method has been proved able to process the MB-TomoSAR data. Finally, a conclusion is given, and the new challenges on MB-TomoSAR in application are discussed. [C8554]

"Extension of range migration algorithm for airborne spotlight SAR with velocity variation"

To obtain the SAR images with high quality and the fast processing time in the airborne spotlight SAR with velocity variation, we propose a modified range migration algorithm (RAM) with resampling based on the extended Taylor approximation and the fast interpolation process. First, at the mixing stage of the reference signal and the raw data, we resample the azimuth position. Then, at the Stolt interpolation stage, we modify the original interpolation method. Finally, we test the effectiveness of the proposed method using a pulsed spotlight SAR simulator. [C8555]

"Improved RDM for SAR autofocus processing"

Reflectivity displacement method (RDM) is a classical algorithm of synthetic aperture radar (SAR) autofocus processing, whose performance degenerates with low contrast of the scene. This paper proposes an improved RDM for SAR auto focusing. Based on the relationship between the Doppler rate and the range, the proposed method can adoptively overcome the effect of the low contrast on the Doppler rate estimation and obtain fine autofocusing results. The experiments with real SAR data are used to show the effectivity of the proposed method. [C8556]

"New Binary ZCZ Sequence Sets with Mismatched Filtering"

New binary sequence sets with zero correlation zone (ZCZ) have been constructed on the basis of almost-perfect binary and almost-perfect ternary sequences and mismatched filtering. The obtained sequences have

energy efficiency close to 1 when length becomes large and in most of cases length of their ZCZ exceeds the upper bound of binary ZCZ sequences. These sequences can be used in quasi-synchronous code division multiple access (QS-CDMA) and radar systems to reduce multi-channel and multi-path interference. [C8557]

"High Performance Waveform Generator Design for Full-Coherent Millimeter-Wave Radar"

Millimeter-wave radar has attracted much attention as a replacement of some infrared or laser systems currently in use. In this paper, an approach of developing high performance waveform for full-coherent millimeter-wave radar is proposed. With good frequency configuration and optimal utilization of DDS (direct digital synthesizer), PLL (phase locked loop) and FPGA (field programming gate array), the developed radar waveform generator implemented with low complexity has the good performance of both spectrum purity (phase noise and spur level) and switching speed. The measurement results show that, in S/C band, the local oscillator's bandwidth is 480MHz and the minimum frequency step is 15MHz, the spur level is better than -65dBc, the phase noise level is better than -94dBc/Hz@1kHz, the maximum frequency switching time is less than 15μs. [C8558]

"A Practical Approach to Exploiting Coarse-Grained Pipeline Parallelism in C Programs"

The emergence of multicore processors has heightened the need for effective parallel programming practices. In addition to writing new parallel programs, the next generation of programmers will be faced with the overwhelming task of migrating decades' worth of legacy C code into a parallel representation. Addressing this problem requires a toolset of parallel programming primitives that can broadly apply to both new and existing programs. While tools such as threads and OpenMP allow programmers to express task and data parallelism, support for pipeline parallelism is distinctly lacking. In this paper, we offer a new and pragmatic approach to leveraging coarse-grained pipeline parallelism in C programs. We target the domain of streaming applications, such as audio, video, and digital signal processing, which exhibit regular flows of data. To exploit pipeline parallelism, we equip the programmer with a simple set of annotations (indicating pipeline boundaries) and a dynamic analysis that tracks all communication across those boundaries. Our analysis outputs a stream graph of the application as well as a set of macros for parallelizing the program and communicating the data needed. We apply our methodology to six case studies, including MPEG-2 decoding, MP3 decoding, GMTI radar processing, and three SPEC benchmarks. Our analysis extracts a useful block diagram for each application, and the parallelized versions offer a 2.78x mean speedup on a 4-core machine. [C8559]

"Double Periodic Arrays with Good Correlation for Applications in Watermarking"

Digital watermarking applications require constructions of double-periodic matrices with good correlations. More specifically we need as many matrix sequences as possible with both good auto and cross-correlation. Furthermore it is necessary to have double-periodic sequences with as many dots as possible. In this paper we present a method that increases the number of sequences, and another that increases the number of ones keeping the correlation good and double-periodic. Finally we combine both methods producing families of double-periodic arrays with good correlation and many dots. The method of increasing the number of sequences is due to Moreno, Omrari and Marie. The method to increase the number of dots was started by Nguyen, Lazlo and Massey, developed by Moreno, Zhang, Kumar and Zinoviev, and further developed by Tirkel and Hall. The very nice application to digital watermarking is due to Tirkel and Hall. Finally we obtain two new constructions of optical orthogonal codes and two new constructions of matrices: Construction A which produces codes with parameters $(n, \omega, \lambda) = (p(p-1), p-1/2, [p(p+1)])$, Construction B which produces families of code with parameters $(n, \omega, \lambda) = \{p^2(p-1), p(p+1)/2, [p(p+1)/4]\}$, max cross-correlation p , and family size $p+1$. Construction A' which produces matrices with parameters $(n, \omega, \lambda) = (p^2(p-1), p(p-1), \lambda(p)+3)$ Construction B' which produces matrices with parameters $(n, \omega, \lambda) = (p^2(p-1), p(p-1), \lambda(p)+3)$, max cross-correlation p , and family size $p+1$. [C8560]

"Variable Dimensional Local Shape Descriptors for Object Recognition in Range Data"

We propose a new set of highly descriptive local shape descriptors (LSDs) for model-based object recognition and pose determination in input range data. Object recognition is performed in three phases: point matching, where point correspondences are established between range data and the complete model using local shape descriptors; pose recovery, where a computationally robust algorithm generates a rough alignment between the model and its instance in the scene, if such an instance is present; and pose refinement. While previously developed LSDs take a minimalist approach, in that they try to construct low dimensional and compact descriptors, we use high (up to 9) dimensional descriptors as the key to more accurate and robust point correspondence. Our strategy significantly simplifies the computational burden of the pose recovery phase by investing more time in the point matching phase. Experiments with Lidar and dense stereo range data illustrate the effectiveness of the approach by providing a higher percentage of correct matches in the candidate point

matches list than a leading minimalist technique. Consequently, the number of RANSAC iterations required for recognition and pose determination is drastically smaller in our approach. [C8561]

"Semiautomatic registration between ground-level panoramas and an orthorectified aerial image for building modeling"

Aerial imagery and ground-level imagery are two complementary data sources for architectural modeling. How to integrate them is a critical issue in creating complete, photo-realistic and large-scale urban models. We describe a semiautomatic approach of detecting feature correspondences between ground-level images and the building footprint in an orthorectified aerial image. The ground-level images are stitched into panoramas in order to obtain a wide camera field of view. Line segments are extracted from ground-level images. Their corresponding segments on the building footprints are automatically detected through a voting process. Meanwhile the camera pose of the ground-level images is also obtained. Wrong correspondences are corrected through user interaction. Later, the height values of the building roof corners are computed and a piece-wise planar 3D model with photo-realistic facade and roof texture is then created. [C8562]

"Sequence Sets with Zero Correlation Zones using Mismatched Filtering"

In mobile communications, navigation and radar applications, good periodic sequences are normally used with matched-filter technique. However, from viewpoint of signal processing, there is no need to consider the filter coefficients as binary only. This paper proposes a method for constructing sets of sequences with zero correlation zone (ZCZ) for application in mismatched filtering. [C8563]

"Synthesis Results of the Periodic Discretely Coded Sequences with the Parameters Constraints Defined on the Basis of Cyclotomic Classes"

The results of the binary and ternary sequences synthesis by new methodology using a generalized coding rule over cyclotomic classes are presented. The effectiveness of the proposed methodology is shown by numerous examples. Synthesized new regular coding rules for characteristic and binary discretely coded sequences with the given constraints, imposed on the levels of the sidelobes of the correlation functions, on the peak factor, and on the characteristic sequences ensembles of a defined volume, have been synthesized. [C8564]

"Track association and fusion with heterogeneous local trackers"

Summary form only given. The problem of track-to-track association and track fusion has been considered in the literature where the local trackers assume the same target motion model and send their local state estimates to the fusion center on demand. Many issues arise when local trackers use different target motion models or even operate on different target state spaces. In this case, selecting an appropriate track association method at the fusion center is essential to the performance of the overall tracking system. In this paper, we examine several track association methods with different assumptions on the target distribution in a surveillance region. We found that the track association performance can be very different among these methods even when they have the same desired significance level of the correct association probability. We recommend to use the track association method that best approximates the likelihood ratio test with complete knowledge of the target distribution. In addition, existing track fusion techniques have to be modified to account for the model mismatch among some of the local trackers. The track association and fusion problem is illustrated by a two dimensional tracking example with both radar tracks and electronic support measures (ESM) tracks. [C8565]

"Track management and PMHT"

PMHT algorithm, as proposed, promises high performance multi target tracking in clutter with (relatively) modest computational resources. However, when applied to practical target tracking situations, a number of problems need to be overcome. PMHT assumes fixed number of tracks, and furthermore it assumes that all tracks are true tracks. No track quality measure is provided within PMHT to enable false track discrimination. In this paper we add the probability of target existence to PMHT processing, and accommodate a variable number of tracks. [C8566]

"Exploitation of multi-temporal SAR and EO satellite imagery for geospatial intelligence"

The simultaneous exploitation of multi- sensor imagery for geospatial intelligence applications is a challenging problem, and Image Analysts would benefit from tools that introduce automation and fusion into the exploitation process in a suitable manner. These tools should take advantage of the human cognitive ability to fuse and assimilate multiple sources and types of information; image fusion tools should be judged successful if they trigger new insight for the Image Analyst. This paper describes some relatively- simple methods for the

exploitation of synthetic aperture radar (SAR) and electro-optical (EO) commercial satellite imagery, with a focus on their integration into the geospatial intelligence workflow. Two examples of multi-temporal satellite imagery products produced by a DRDC Ottawa test-bed system, Image Analyst Pro, are presented. It is demonstrated that a high-resolution panchromatic EO image colourized by a SAR-derived degree of change is an effective intelligence product [C8567]

"Fire control-based adaptation in data fusion applications"

In military command & control applications, the information quality requirements are very context-dependent and seldom predefined. This leaves much room for adaptation. In this paper, the duration of the search & lock-on operations of the fire control radar is estimated and used as an adaptation trigger. The proposed estimation process aims at establishing a quantitative relationship between the quality of the tactical picture and the reaction time available for decision-making. Based on the target's time of flight, the defensive weapon properties, and the desired range of interception, admissible operational conditions and constraints for the fire control radar are derived to allow the weapon system to achieve its planned interception. These conditions and constraints are re-expressed in terms of tracking quality requirements. Then, adaptation mechanisms are used to select and tune the tracking algorithms and/or manage sensors in order to meet those requirements. [C8568]

"Gaussian mixture probability hypothesis density for visual people tracking"

This paper presents our work which involves the application of a recursive Bayesian filter, the Gaussian mixture probability hypothesis density (GMPHD) filter, to a visual tracking problem. Foreground objects are detected using statistical background modeling to obtain measurements which are input into the filter. The GMPHD filter explicitly models the birth, survival and death of objects by managing the number of Gaussian components and jointly estimates the time-varying number of objects and their states. A scene-driven method is proposed to initialize the GMPHD filter and model the birth of new objects. The results shows when a person or a group appeared, merged, split, and disappeared in the field of view, the GMPHD filter can track the number and positions at the most time. The scene-driven GMPHD filter can track the birth of new objects faster than the particle PHD filter. [C8569]

"Situation refinement for vehicle maneuver identification and driver's intention prediction"

In safety automotive applications the system must be capable of early recognizing the maneuvers performed by the driver and the intention associated with them in order to take preventive measures or trigger warning alarms. This is done by the situation refinement level in the fusion system that processes the data provided by the on-board sensors. By recognizing relationships between entities of the road environment the system can react with more efficiency to the current situation. For example the intention of a lane change, the detection of an overtaking maneuver, the estimation of the lane in which the detected vehicle is located, help the system to decide which action must be taken in order to prevent an unwanted situation. This paper focuses on the investigation of methods regarding the identification of the maneuvering type and the intention associated. [C8570]

"Quickest detection of statistical changes with application to tracking"

As part of the track-management process it is necessary to know when new tracks start and when old ones die. Thus some knowledge of the theory of detection of statistical changes is important, and the purpose of this talk is to give the audience some overview of what is available. Specifically, we shall discuss sequential testing, this information necessary as a precursor to an understanding of the procedure and performance of the Page "quickest" detection of statistical changes. We shall also discuss the Shiryaev test, which represents a more Bayesian point of view. We shall present applications to detection of target spawn based on monopulse radar data, and also to the track management of sonar targets whose aspect-dependent SNR is modeled as hidden Markov-the suboptimality of Page procedures for detection of a changes between HMMs is rather surprising. [C8571]

"Radar resources optimization by adaptive search domains priority assignment based on most threatening trajectories computation"

The main challenge of future phased array multifunction radar will be to optimise the radar time budget to avoid deleterious overload effects. For this purpose, we propose a new technique for priority assignment of Search Domains. Then, we have developed new algorithms for most threatening trajectories computation based on Calculus of Variations approach developed for "shortest path computation" in image processing. [C8572]

"Performance of the shifted Rayleigh filter in single-sensor bearings-only tracking"

The problem of single-sensor bearings-only tracking continues to present challenges to tracking algorithms, particularly in certain difficult scenarios such as ones with high bearing rates. In such scenarios, the performance of the recently introduced shifted Rayleigh filter (SRF) is compared with that of other techniques such as extended Kalman filter (EKF), unscented Kalman filter (UKF) and particle filter (PF). The results are also compared with the theoretical Cramer-Rao Lower Bound (CRLB). The SRF is a moment matching algorithm, and its key feature is that it generates the exact conditional distribution of target motion, given normal approximation to the prior. Simulations show that the SRF is superior to other moment matching algorithms such as EKF and UKF and is able to achieve comparable performance to PF while being orders of magnitude faster. [C8573]

"Service-Oriented E-Learning System"

Instead of building an e-Learning system from scratch, it can be assembled by choosing the required functionalities from a set of web services related to e-Learning. Web services eliminate many interoperability issues between components written and running on different hardware and software platforms. This study aims to construct a set of e-Learning web services. With these web services, new e-Learning system(s) can be constructed by choosing the services which are required. The developed web services include assessment, course management, grading, marking, metadata, registration and reporting web services. These web services are highly in demand as the functionalities for each of the web services are very useful and important in e-Learning systems. In Marking web service, rubrics can be defined to assist in assessment evaluation. In Metadata web service, learning object metadata (LOM) is applied to capture the description of the learning objects. [C8574]

"Multiscale Variational Threshold SAR Image Denoising Based on Quad-tree Complex Wavelet Packets Transform"

A new image transform, namely, the quad-tree complex wavelet packets transform (QCWPT) is introduced, which both has shift invariance and good direction analysis ability and other merits of the dual-tree complex wavelet transform (DCWT), and has the ability of analyzing the high frequency detail signal carefully like the wavelet packet transform (WPT). Furthermore, a novel image denoising scheme based on QCWPT was presented via setting multiscale variational thresholding method, which accords with the characteristic that the high frequency coefficient modules and the variance of the noise attenuate rapidly along with the decomposition scale increasing, the best complex wavelet packets basis was determined and processed at the largest scale. In numerical comparison with various methods, the presented scheme outperforms the traditional Wiener filtering, DCWT and QCWPT in terms of the equivalent number of looks (ENL), the figure of merit (FOM) and visual effects. Experiments also show that the presented scheme could not only remove the noises effectively, but also reserve the SAR image texture and edge details better. [C8575]

"Estimate and Track the PN Sequence of Weak DS-SS Signals"

This paper proposes a modified Sanger's generalized Hebbian neural network method to estimate and track the pseudo noise sequence of weak direct sequence spread spectrum signals. The proposed method is based on eigen-analysis of received signals. The received signal is firstly sampled and divided into non-overlapping signal vectors according to a temporal window, which duration is a periods of PN sequence. Then an autocorrelation matrix is computed and accumulated by these signal vectors one by one. The pseudo noise sequence can be estimated and tracked by the principal eigenvector of the matrix in the end. Because the eigen-analysis method becomes inefficiency when the estimated pseudo noise sequence becomes longer or the estimated pseudo noise sequence becomes time varying, we use a modified Sanger's generalized Hebbian neural network to realize the pseudo noise sequence estimation and tracking from weak input signals adaptively and effectively. [C8576]

"Why a Complex Valued Solution for a Real Domain Problem"

An insight into the potential benefits of using complex valued models for real valued data is provided. The problem itself is not new; it is however timely and important to revisit this issue, due to a plethora of modern applications based on multidimensional and multichannel measurements which can be cast into an equivalent problem in the field of complex numbers \mathbb{C} . The analysis and simulations highlight the duality between several classes of real domain problems and their complex valued representations. This is supported by case studies on image processing, modelling of point processes for brain prosthetics, and forecasting of vector fields. [C8577]

"Robust Adaptive Minimum Entropy Beamformer in Impulsive Noise"

This paper considers the problem of adaptive beamforming in alpha-stable (non-Gaussian) noise using the constrained minimum output entropy (MOE) based algorithm. Following the same rational that lead to the least mean p-norm (LMP), the weight update adjustment for minimum output entropy is constrained by statistics higher than second order. Also, the MOE algorithm is very robust to impulsive noise due to its M-estimator property derived from the fact that MOE constrains the output entropy. We explain these results analytically, and through simulations. [C8578]

"Stepped frequency chirp signal SAR imaging"

To achieve high range resolution using the stepped frequency chirp signal, two or more chirp waveforms are sequentially transmitted and received at stepped carrier frequencies in the whole bandwidth. An advantage of the approach has no increase in instantaneous bandwidth of the radar system. In this paper phase incoherent factor among sub-pulses trains produced by down frequency conversion mixer is put forward and analyzed. Which must be took into account when range bandwidth synthesis is processed. Frequency domain bandwidth synthesis is applied to SAR imaging combining with the phase incoherent factor estimate and compensation based on contract optimization autofocusing. Simulation results show the validity of the method. [C8579]

"Airborne ISAR imaging of ship side view"

In airborne ISAR imaging of ship targets, the complexity of the ship's rotation relative to the radar line of sight (RLOS) increases the difficulty in achieving high quality ship images. When imaging from long distance, the rotation induced by the tangential motion between the radar and the ship can always be neglected. The images obtained by exploiting the ship's own sway are generally the ship side view. However, when the rotation induced by the relative tangential motion cannot be neglected, the obtained images are the mixture of the ship top view and side view, which are not suitable for the ship recognition. In this paper, a method of obtaining the ship side view images under this circumstance is presented. Its main idea is to estimate the Doppler frequency derivative, which can be approximated by the chirp rate in a short imaging interval. A concentration measure is introduced to increase the estimation precision of the chirp rate in the dechirp process. The effectiveness of the proposed method is verified by the experiments on the simulation data. [C8580]

"The scheme and key components design of W-band coherent doppler velocity radar front-end"

This paper presents a scheme of W-band coherent Doppler velocity radar front-end, which can be used to measure the velocity of target ranging from 10 m/s to 2000 m/s. After the comparison of the advantage and disadvantage of several schemes, the scheme using the phase-locked dielectric resonator oscillator (PLDRO) and direct digital synthesis (DDS) is chosen. The two coherent X-band signals are produced by mixer and power-divider mechanism of the PLDRO and DDS. Then, transmitting signal and receiver LO is obtained by the 8th-order multiplier from the two X-band signals. The superheterodyne receiver is adopted to increase the system signal-to-noise ratio (SNR). The finished key components have good performance, indicating that the scheme increases the sensitivity and the resolution of the radar. [C8581]

"Operation mode for topside ionospheric sounding based on space-borne high frequency synthetic aperture radar"

Topside ionospheric sounding is significant for scientific research, especially on forecasting of some astronomical disasters. Current ionospheric topside sounding radars have low range resolution of tens of kilometers, but nearly have no azimuth resolution. The concept of synthetic aperture radar (SAR) is introduced to topside ionospheric sounding for improving the azimuth resolution. The operation mode based on space-borne high frequency SAR (HF-SAR) is presented in this paper. Theoretical analysis indicates that the azimuth resolution can be improved to tens of meters. The satellite orbit parameters are selected, and the main parameters of the radar system are preliminarily designed. The technique of Displaced Phase Centers Antenna (DPCA) is utilized to solve the confliction between the radar detection range and the pulse repetition frequency. [C8582]

"Vibrometry classification of moving vehicles using throttle signature analysis"

Any operating vehicle will emanate a degree of vibration due to the running engine and other machinery. These vibrations differ based on engine type, throttle-level, and vehicle structure and as such they constitute a unique signature for a given vehicle. The availability of remote vibrometry sensors, such as pulse laser radar, makes it possible to utilize this signature for remote automatic target identification. We propose a novel classification technique that is specifically tuned to identify vehicles whose engines have a variable amount of applied throttle based on a limited training set with known idle and full throttle values. The presented algorithm is real-time and operates reliably with short time duration samples of input data. Other benefits include a small training set and simple implementation based on linear algebraic techniques. It is also possible to adjust the technique to indicate

the degree of confidence in the result. We have achieved classification accuracy for a two class problem of 90% to 98%. [C8583]

"Advanced Multicast and Broadcast Content Distribution in Mobile Cellular Networks"

Recently 3GPP (Third Generation Partnership Project) has standardised MBMS (Multimedia Broadcast Multicast Services) enabling broadcast and multicast transmissions over GPRS (General Packet Radio Service) and UMTS (Universal Mobile Telecommunications System). Hence it makes an efficient usage of radio resources possible. 3GPP and 3GPP2 introduced the specification of IMS (IP Multimedia Subsystem) and MMD (Multimedia Domain), receptively, which both are responsible for resource, admission and charging control. It allows for cost efficient and flexible provision of enriched multimedia services over IP networks. Up to now the controlling IMS and MBMS are separated subsystems sharing no common interfaces. This paper introduces both systems and depicts ongoing standardisation activities regarding their interworking. Finally, it proposes a service provision architecture and describes required signalling flows which enable the provision of multicast streaming using the MBMS specifications not only as access bearer technology. Thus, we present a step towards the evolution of IMS enabling it with multicast and broadcast capabilities. [C8584]

"Follow-up control system of ultrasonic motor based on DSP"

According to advantages of ultrasonic motor (USM), a follow-up control system based on DSP-TMS320F2810 is presented in this paper. By analyzing output characteristic of USM, velocity of USM is mainly affected by frequency. So frequency is adopted as control variable in PID arithmetic. Time-varying input signal is followed by speed closed loop control, which forms inside loop. And the position of the motor is checked in time which makes outside loop. By experiments it is proved that the follow-up system has quicker speed tracking and exacter orientation compared to traditional analog follow-up system. [C8585]

"Automobile Advance Alarm System Based on Monocular Vision Processing"

While the interests in intelligent vehicle increase, many people are having concerns about systems that offer the information of distance and relative speed between two cars. This paper presents an algorithm to obtain efficiently the distance between two cars. [C8586]

"Heuristic Road Extraction"

The LiDAR system is used to gather 3D terrain information accurately and effectively. However, it is complicated to process the LiDAR data due to its irregularity and large number of collected data points. This paper proposes a novel method to extract urban road networks from 3D LiDAR data automatically. This method uses height and reflectance of LiDAR data, and clustered road point information. Geometric information of general roads is also applied to extract road points group correctly. The proposed method has been tested on urban areas which contain complicated road networks. The results demonstrate that the integration of height, reflectance and geometric information of roads is a crucial factor that distinguishes the proposed method in its ability to classify road points reliably and correctly. [C8587]

"A high linearity mixed signal down converter IC for C-band radar receivers"

A mixed signal receiver IC for C-band radars is presented. The design work has been focused on spectral purity and miniaturization. Miniaturization is achieved by minimizing peripheral components and control signals using internal calibration data and temperature compensation tables stored in RAM on-chip. This allows for the packaged chip to be used with a minimum of. The chip is manufactured by Austria Microsystems in their 0.35 um SiGe-BiCMOS process and utilizes digital IP-block included in the design kit. [C8588]

"Recognition Method of Radar Signal Based on Rough Set and Support Vector Machine"

A hybrid algorithm based on attributes reduction of rough set and classification principles of support vector machine (SVM) is presented in this paper. Firstly, the attributes reduction of rough set has been applied as preprocessor so that we can delete the redundant attributes and conflicting objects from decision making table but remain efficient information lossless. Then, the classification modeling and forecasting test based on SVM are realized. By this method, the dimension of data is reduced greatly, the complexity in the process of SVM classification is decreased highly, the occupied memory is cut down and the over-fit of training model is prevented at some extent, also the good classification performance is obtained. Finally, the simulation experiment of radar signal recognition and its results show this hybrid method is effective. [C8589]

"Novel robotic spacecraft simulator with mini-control moment gyroscopes and rotating thrusters"

A novel hardware-in-the-loop spacecraft simulator is introduced for the laboratory validation of guidance, navigation and control algorithms. This three-degrees-of-freedom robotic vehicle uses the principle of air-floating along a flat floor in order to reproduce in two dimensions the frictionless and weightlessness conditions of the orbital flight. For the first time in its class, to the authors' knowledge, the new spacecraft simulator uses miniature control moment gyroscopes for the attitude control and rotating thrusters for both attitude and translational control. A pseudo-GPS, a LIDAR and a fiber optic gyroscope are used as navigation sensors. The paper presents in details the design of the robotic vehicle and the results of preliminary experiments. [C8590]

"Navigation paradigm of a prehensive robotics assistance"

This article deals with a target tracking application for the disabled. The objective of this work is to track a wheelchair with a mobile platform and an embedded grasping arm (MANUS). We propose an approach based on an association of two Kalman filtering levels. The first level permits an estimation of the wheelchair configuration. The second is used to compute the mobile platform configuration in connection with its environment. The association of the two filtering process allows a robust tracking between two objects in movement. [C8591]

"Possibilistic multi-sensor fusion for humanitarian demining"

We propose a method for combining humanitarian mine detection sensors based on possibility theory. Firstly, different features are extracted from the sensor data. Possibility distributions are then derived from the features based on prior information. After that, the combination of possibility degrees is performed in two steps, on separate sensor level and between the sensors. Combination operators are chosen to account for the different characteristics of the sensors. The final decision is obtained by thresholding the fusion result. Promising results have been obtained on a set of real mines and non-dangerous objects. In particular a 100% mine recognition rate was achieved, with a limited number of false alarms. [C8592]

"Hand held dual sensor ALIS and its evaluation test in Cambodia"

Since 2002, we have developed a new hand-held land mine detection dual-sensor ALIS. ALIS is equipped with a metal detector and a GPR, and it has a sensor tracking system, which can record the GPR and Metal detector signal with its location. It makes possible to process the data afterwards, including migration. The migration processing drastically increases the quality of the image of the buried objects. ALIS uses two different GPR systems, namely VNA (Vector Network Analyzer) based GPR and an Impulse GPR VNA based GPR can provide better quality GPR images, although the impulse GPR is faster and light weight. ALIS evaluation tests were held in mine affected countries including Afghanistan, Croatia, Egypt and Cambodia. In the two-month evaluation test in Cambodia, ALIS worked without any problem. After some demonstrations and evaluation, we got many useful suggestions. Using these advises, we have modified the ALIS and it is now more easy to use. ALIS will be commercialized in 2007. [C8593]

"High resolution COSMO/SkyMed SAR data analysis for civil protection from flooding events"

The paper focuses on the multiple roles and advantages of the use of remotely sensed, especially COSMO/SkyMed, imagery in the context of flooding-event prevention and management, describing a support system for civil protection from floods and some of the image processing and analysis techniques involved in. [C8594]

"The SBAS-DInSAR technique as a tool for the observation of active volcanic areas: Results and future perspectives"

In this work we describe the application of the basic small BAseline subset (SBAS) technique, which exploits multilook interferograms, to a number of active volcanic areas. The use of such a technique reduces the amount of data to be processed and simplifies the analysis of geophysical phenomena occurring in extended areas (up to 100 km by 100 km). Moreover, it can be trivially extended in order to combine data acquired by different sensors with similar geometrical and electromagnetic characteristics, i.e., ERS and ENVISAT IS-2 mode, thus allowing an easy extension of the temporal observation window. The selected test sites for this study are Long Valley caldera, Mt. Etna and the Neapolitan Volcanic district (Mt. Vesuvio and Campi Flegrei caldera). Finally, we shortly analyze the implications of the use of forthcoming SAR sensors that operates in L- and X-bands. [C8595]

"Concept design of a near-space radar for tsunami detection"

Off-shore detection of tsunami waves is a critical component of an effective tsunami warning system (TWS). Even more critical is the off-shore detection of local tsunamis, namely tsunamis that strike coastal areas within minutes from the triggering quake. In this paper we propose a new concept for tsunami detection. NESTRAD (Near-Space Tsunami Radar) consists of a real aperture radar accommodated inside a stationary stratospheric airship providing continuous monitoring of tsunamigenic oceanic trenches. [C8596]

"Measurements of the effect of rain-induced sea surface roughness on the satellite scatterometer radar cross section"

Radar measurements of the sea surface, with satellite scatterometers that operate at Ku-band, will be affected by the presence of rain through modification of the sea surface roughness by rain impacts. This is in addition to wind driven roughness, atmospheric reflectivity and attenuation that affect the measured normalized radar cross section (NRCS). Numerous surface-based studies, using ocean platforms and wind-wave tanks, have shown the increase in the total NRCS can be significant and strongly dependent on radar frequency, incidence angle, polarization and wind speed [1],[2],[3]. Herein is the first study combining satellite based Ku-band data with high-resolution 3-D volumetric rain measurements, from simultaneous collocated NEXRAD data. The results to be presented were acquired during a significant rain event in the Gulf of Mexico just south of Houston, TX in May 2005. They are directly applicable to questions that are important to the interpretation of satellite derived wind vector estimates in the presence of rain of varying intensity and spatial distribution. This project is developing techniques to correct scatterometer derived wind- vector estimates. The acquisition of new knowledge on rain-splash effects is a necessary part of this effort. [C8597]

"Use of an application-specific dictionary for matching pursuits discrimination of landmines and clutter"

The HSTAMIDS handheld landmine detection system has been used in a number of humanitarian demining activities. Existing algorithms used with this system to assist human in discrimination process do a better job than the operator alone. However, they are unable to model mine and clutter signatures completely, leading to inaccurate mine confidence assignment. This paper presents a matching pursuits (MP) based landmine detection system using an application-specific dictionary. Prototypes for mine and clutter classes are built using MP decomposition of class members. A fuzzy K-nearest neighbor rule is used to assign confidence values for mine and clutter discrimination. The proposed algorithm is demonstrated on data acquired from three different landmines test sites. [C8598]

"Polarimetric feature fusion in GPR for landmine detection"

A polarimetric multi-feature framework for the detection of antipersonnel landmines with ground penetrating radar (GPR) is suggested. The features result from independently acquired and processed GPR measurements in co- and cross-polar configurations. The initial detection in the confidence maps is made independently after which the coordinates of the detected targets are co-located. The marginal feature distributions are normalized via Johnson's transform prior to the fusion process and a Maximum Likelihood based linear-quadratic classifier is used as a fusion rule. The framework makes use of secondary data acquired from an open test site to train the classifier. The framework performance is illustrated on the data acquired over a specifically designed test- site. [C8599]

"High resolution COSMO-SkyMed SAR images for oil spills automatic detection"

In recent decades SAR images have extensively been used for the observation and the characterization of the sea surface. A number of experiments have been carried out with airborne and spaceborne sensors. These show SAR's ability of detecting oil slicks and distinguishing them from similar oceanic features. A great amount of archived data is available in many spectral bands. In spite of this, nowadays C-band is the most widely used for the observation of the sea from a satellite. For this reason, in the last year we have developed OSAD (Oil Spill Automatic Detector), a system focusing on C-band. The availability of high resolution X-band images (supplied by COSMO-SkyMed satellites and managed by the Italian Space Agency) has encouraged further investigation aimed at extending the scope of this methodology to X band images with the final goal of employing it for detecting oil spills. X-SAR data (obtained from airplane multi-band experiments and from SIR-C X-SAR mission carried out by NASA's space shuttle in 1994) are analyzed in order to compare SAR images in different bands and spot locations contaminated by an oil slick. The COSMO- SkyMed constellation (supplying high spatial and temporal coverage of the Mediterranean basin) makes it possible to develop an operational oil spill survey system, particularly in protected areas and areas close to the coast. [C8600]

"Ridgelet transform with application in ground penetrating radar processing"

Ridgelet is the new development of wavelet dealing with line singularities in signals. In groundpenetrating radar (GPR) signal, the direct wave is a strong noise which has line singularity. In time-space domain, the useful information in GPR signal is badly polluted by strong direct wave so that the underground targets can not be recognized correctly. Ridgelet overcomes the disadvantages of wavelets in dealing with high dimensions that it can effectively represent singularities along lines or hyperplanes. Concerning the characteristics of GPR signals, the ridgelet transform is employed to remove the background noise and separate the direct wave. The simulation results for real GPR signals demonstrate its effectiveness. [C8601]

"Classification of radar emitter signals based on the feature of time-frequency atoms"

An effective approach based on the feature of time-frequency atoms for classification of the radar emitter signals is presented. Firstly, we introduce a fast matching pursuit (MP) algorithm, which using improved quantum genetic algorithm (IQGA) to reduce the time-complexity at each step of standard MP, to decompose the signal into a linear expansion of Gaussian chirplet time-frequency atoms. Then, the atoms characteristics are re-extracted to constitute the strong- discrimination atoms feature vector. Experimental results of atoms feature extraction of 5 typical radar emitter signals shows that the atom features have good performances of clustering the same radar signals and separating the different radar signals, which confirms the validity and feasibility of the proposed scheme of signals classification. [C8602]

"An electromagnetic coupling device for high speed running radar for non-destructive inspection"

The paper proposes an electromagnetic coupling device which improves the incidence efficiency of electromagnetic wave into the inspected objects when an electromagnetic wave (radar) is used for non-destructive inspection. The device enables a fast non-destructive inspection by a radar which is attached to the bottom of an inspection vehicle. That is, it enables the radar to run fast with a lift off the inspected objects. Here, as the inspected objects, we have railways and roads in mind and consider the detection of cavities under ground. [C8603]

"A kind of trading off algorithm of object classification based on intelligent data fusion"

A kind of trading off algorithm of target classification combined with double mode intelligent fusion is presented, Applying neuron-fuzzy technique to the synthesis of the complementary information between radar and infrared, through combining neuron-fuzzy technique with D-S evidence fusion theory, the ability of target classification could be improved. At the same time, according to the effective detection range of sensors, reasonably select the target features that can ensure the accurate target classification so that the computation load of the algorithm can be largely decreased compared to the infrared single model fusion. Simulation results illustrate that the trading off algorithm is effective. [C8604]

"Radar emitter signals classification using kernel principle component analysis and fuzzy support vector machines"

Field=03 In this paper, a novel approach based on QTFDs and kernel principle component analysis (KPCA) is proposed to extract features of radar emitter signals. Then, these discriminative and low dimensional features achieved were fed to a Support Vector Machines (SVMs) based on FCM (fuzzy c-means) clustering for multi-class pattern recognition. Experimental results show that the proposed methodology was efficient for the different complex radar emitter signals detection and classification. [C8605]

"A new method for recognising radar radiating-source"

A new method for recognising radar radiating-source is proposed in this paper. The sixth dimension of wavelet packet transform (Wpt6), the seventh dimension of wavelet packet transform (Wpt7), pulse repetition interval means (mPRI), and pulse repetition interval variance (sigma2PRI) are used as the gist for recognising radar radiating-source that is based on the characteristics of these parameters, and the RBPNN recognition is designed. By simulation, it shows that this new method can improve the recognition rate while it can improve the recognition velocity. [C8606]

"Feature extraction of radar emitter signals based on symbolic time series analysis"

An useful approach is proposed for intra-pulse feature extraction of radar emitter signals based on symbolic time series analysis (STSA). Embedding time-delay and modified Shannon entropy are used as two-dimensional feature vector to sort the interleaving radar signals. The time-delay feature can determine the length of symbol series. The entropy feature can quantitatively reveal deterministic information and complexity of radar intra-pulse modulation signals. In order to show the effectiveness and feasibility of the introduced approach, the

experimental results indicate that the features of seven typical radar emitter signals extracted by STSA have good characteristics of clustering and strong stability when SNR varies from 0 dB to 30 dB and the method of STSA for finding and quantifying information is computationally efficient, robust to noise and easy to use in engineering implementation and application. [C8607]

"Small-shaped space target recognition based on wavelet decomposition and support vector machine"

A kind of method for small-shaped space target recognition was proposed in this paper based on feature extraction with wavelet decomposition and formative support vector machine (FSVM) with sequential minimal optimization (SMO) algorithm. Firstly, the significance and characteristics of space target recognition were discussed and a two-stage recognition strategy was designed. And then aiming at the characteristics of small-shaped space target recognition, a new method was implemented based on feature extraction with wavelet decomposition and FSVM with SMO algorithm. Simulation results show the good performance of the algorithm proposed in this paper: the correct rate is more than 97% within 1360 simulation samples of ten classes of small shaped space targets; meanwhile the algorithm is characterized with high speed of near real time in both implementation of training and testing. [C8608]

"Bistatic scattering from bare soils: Sensitivity to soil moisture and surface roughness"

The sensitivity of bistatic scattering coefficient σ_{deg} to soil moisture (smc) is investigated on the whole upper half space by means of model simulations of the incoherent scattered fields. The achieved results, represented as maps of σ_{deg} as a function of azimuth and zenith angles, are evaluated by means of a quality index which takes into consideration the effect of roughness on smc measurement. [C8609]

"Delay/Doppler altimeter data processing"

The ESA Cryosat-2 mission will mount a de- lay/Doppler radar altimeter (DDA), named SIRAL, for the study of the trends in Earth's continental and marine ice fields. A DDA has many advantages over a conventional altimeter, retrieving a better resolution in the along track direction as a result of coherent processing of the backscattering energy. This permits the extension of applications to ice sheet monitoring as well as coastal studies, maintaining necessary precision for the open ocean. Operational SIRAL data processing for the Cryosat-2 mission is based on the precise wavenumber domain approach, following the strategy developed and verified for the Cryosat-1 mission [1]. A novel way of processing, supported by the chirp zeta transform (CZT) is here presented. Basically the CZT allows the Doppler beam formation to be directed toward the output surface samples in a single stage, increasing the computational efficiency of the processing at the expense of a slightly lower accuracy. The more precise wavenumber domain approach can be used to validate the method. The SIRAL sensor parameters and simulated scenarios will be taken as models to derive experimental results. [C8610]

"Merging of the stereogrammetry and interferometry techniques as relative bandwidth grows. Illustration with VHF Carabas SAR images"

SAR interferometry, requires the sensor separation to be below a critical baseline above which the coherency is lost as the ground projected frequency ranges do not overlap (frequency band shifting of one sensor -the delta-k system- is not addressed here). Indeed, as critical baseline increases with both wavelength and bandwidth, low frequency and/or wide band SAR systems have less stringent constraint for interferometric coherence, which is especially worthy for airborne acquisitions. However, as mentioned in earlier publications, the number of fringes apparent on an interferogram is (roughly) limited to twice the inverse of the relative bandwidth. Hence, wide band interferometry requires range migration evaluating for maintaining coherence, this range migration evaluation is similar to a stereogrammetric measure. As relative bandwidth grows, the two techniques merge, which can be illustrated from FOI Carabas VHF SAR data (of which the relative bandwidth is 111%). [C8611]

"Improvement of interferometric SAR coherence estimates by slope-adaptive range common-band filtering"

The accuracy of SAR interferometric coherence estimates depends on the precision of several processing steps. In particular decorrelation can occur if range common-band filtering does not perform optimally. Typically a planar surface is adopted which introduces additional decorrelation in case of sloped terrain. To take into account topographic variations a slope-adaptive range common-band filtering method has been developed. A DEM is used to simulate an unwrapped interferogram and the fringe rate is used as driver for the filter size in the range common-band filtering step. Tests with several spaceborne interferometric SAR datasets confirmed the

robustness of the method. The improvement of the coherence increased for increasing perpendicular baseline. As a consequence, the fringe visibility also greatly improved. To quantify the improvement of the coherence estimates with the slope-adaptive range common-band filtering, we considered the variation of classification in forest mapping, i.e. an application in which accurate coherence estimates are needed. With improved coherence the classified forest stem volume agreed better with forest maps derived from other remote sensing datasets.

[C8612]

"Polarimetric phase gradient autofocus"

In the past decade the use of fully polarimetric SAR (polSAR) systems has increased significantly due to their effectiveness in target classification and detection applications. While polSAR imagery has been extensively used to distinguish between different scattering mechanisms in a scene, there has been a lack of research in the exploitation of polarimetry to assist in image formation and in particular autofocus for fine resolution SAR. In this paper an extension of the phase gradient algorithm (PGA) for polSAR imaging is proposed and its effectiveness is tested on simulated and real data. [C8613]

"Tomographic processing of multi-baseline P-band SAR data for imaging of a forested area"

Recently, various attempts have been undertaken to obtain information about the structure of forested areas from multi-baseline synthetic aperture radar data. Tomographic processing of such data has been demonstrated but the quality of the focused tomographic image is limited by several factors. In particular Fourier-based focusing methods are susceptible to irregular and sparse sampling, two problems, that are unavoidable in case of multi-pass, multi-baseline SAR data acquired by an airborne system. We propose a tomographic focusing method based on the time-domain back-projection algorithm, which maintains the geometric relationship between the original sensor positions and the imaged target and is therefore able to cope with irregular sampling without introducing any approximations with respect to the geometry. We assess the tomographic focusing quality with the help of the impulse response of simulated point targets and an in-scene corner reflector. And, in particular, preliminary results obtained with the newly acquired P-band tomographic data set consisting of eleven flight tracks are presented. [C8614]

"Investigations on the TOPSAR acquisition mode with TerraSAR-X"

The paper reports about investigations on the implementation of the recently proposed TOPSAR acquisition mode with TerraSAR-X. Differently from ScanSAR, TOPSAR mode allows a wide swath coverage with nearly uniform signal to noise ratio (SNR), therefore avoiding scalloping and azimuth dependent SNR. To achieve this goal the antenna beam is steered within the different swaths in the along-track direction. TerraSAR-X can electronically steer the azimuth beam; however, angle quantization is introduced because of the limited number of available azimuth beams per data take. The effects of the TerraSAR-X angle quantization of the antenna steering are analyzed resulting in a negligible distortion. The maximum azimuth steering angle of TerraSAR-X allows the implementation of TOPSAR with the same coverage and resolution as the nominal TerraSAR-X ScanSAR mode, four range subswaths with 16 m azimuth resolution and a total swath of 100 km. Finally, TerraSAR-X TOPSAR interferometry capability and the possibility of using an inverse TOPSAR configuration are discussed. [C8615]

"Evaluation of the Bistatic Range migration processor"

The bistatic image formation process is more complex than the monostatic one, because the bistatic range equation consists of the sum of two hyperbolas. Several bistatic SAR processors have been presented in the last years. One of them is the bistatic range migration processor, which will be evaluated in this paper not only with regard to translational invariant configurations but also in view of variations from a model assumption. The bistatic range migration processor will be compared with a bistatic generic time domain SAR processor. The processing quality will mainly be evaluated by measuring the resolution and PSLR of point target responses.

[C8616]

"A SAR processing algorithm for TOPS imaging mode based on extended chirp scaling"

This paper presents an efficient phase preserving processor for TOPS (Terrain Observation by Progressive Scans) imaging mode. TOPS has been proposed as a new wide swath imaging mode, which solves the problems of scalloping and azimuth-varying ambiguities introduced by the conventional ScanSAR mode by means of steering the antenna along the azimuth direction. An algorithm based on ECS (Extended Chirp Scaling) is proposed, which uses sub-apertures and a new azimuth scaling step. The proposed solution is also efficient in the sense that it allows selecting the final azimuth image spacing by means of azimuth scaling, hence easing the forthcoming mosaicking of the different sub swaths. Simulations with point targets are used to validate

the processor. [C8617]

"Bistatic SAR imaging: A novel approach using a stationary receiver"

This paper introduces a novel approach to bistatic radar imaging. The proposed technique utilizes a synthetic transmit aperture and a stationary receiver to create a high resolution, 2-D bistatic SAR image of a given target scene. The technique can also be used to generate 3-D SAR images simply by utilizing a second, coherent receiver; hence operating in an interferometric bistatic SAR mode. The new technique is validated through both indoor and outdoor experiments. [C8618]

"Phase and temporal synchronization in bistatic SAR systems using sources of opportunity"

This paper discusses temporal and phase synchronization in SABRINA, a bistatic system that uses ENVISAT and ERS-2 as transmitters of opportunity. Phase synchronization and pulse alignment is achieved using a dedicated channel that receives a clean signal directly from the satellite. It is studied how to temporally align the acquired data with the satellite orbit using the apparent range migration history. [C8619]

"Space-based moving target positioning using radar with a switched aperture antenna"

Ground moving target indication (GMTI) by space based radar can effectively only be performed with a multi-aperture / multi-channel system or a satellite cluster [1]. To keep weight, power consumption, data rate and costs low, the technique of switching subapertures from pulse to pulse has been proposed. While the detection performance using STAP (space-time adaptive processing) has been analysed in several publications, the estimation performance and the mechanisms leading to good or bad aperture switching strategies, have not yet been treated sufficiently. In fact, aperture partitions well suited for detection must not necessarily be good for estimation. This paper is thought as a contribution to fill the knowledge gaps concerning repositioning algorithms and performance analysis. [C8620]

"Improvement of 3D radar backscatter model by matrix-doubling methods"

Radiative transfer models have been widely used to simulate the radar backscatter from forested areas. Most of these models are two dimensional. In order to take full account of spatial position of trees in a forest stand, a three-dimensional radar backscatter model of forest canopy was constructed by Guoqing Sun and Ranson in 1995[1]. The model takes into account only first-order scattering within tree crown and the double scattering between tree trunk (crown) and ground surface. The model predictions agree well with copolarized backscatter measurements, while it tends to underestimates the backscattering coefficients for cross-polarization, when there is strong volume scattering. In order to produce good estimations for cross-polarized component, the matrix-doubling method is employed in this paper to compute multiple-scattering within the crown. The comparison between the results of original model and that of modified model shows that the method is effective. The cross-polarization can be improved in different degrees according to the size and density of scatters within crown cell. [C8621]

"Feasibility of spaceborne bistatic radar missions for land applications"

This paper deals with a feasibility analysis of spaceborne bistatic missions for Earth Observation, with signals at microwave bands. The analysis, performed in the frame of a wider study financed by ESA, considers as input bistatic configurations, investigated in another paper, suitable for typical land applications i.e. soil moisture and vegetation biomass retrieval. Signal sources are GPS constellation and spaceborne SAR's. This analysis mainly encompasses the design of possible orbits implementing the desired bistatic configurations, and the characterization of the system performances. The latter are evaluated through several different parameters, grouped in two classes: target observation parameters, strictly related to the illuminator-target-receiver geometry at given epoch (e.g. signal to noise ratio, spatial resolution, observation angles) and system parameters such as: spatial coverage (measuring whether or not a point is accessible by the satellites in bistatic configuration), number of bistatic accesses to the target area, revisit time (indicating the delay between two successive bistatic acquisitions of the same area). [C8622]

"Position and orientation estimation of two airborne platforms towards each other"

The interest in bi- and multistatic radar has been growing over the last years as they offer various advantages. For instance the transmitter and receiver can easily be separated and therefore the survivability can be enhanced by deploying the transmitter further away from the scene. Bistatic radar can provide a cost effective solution as the transmitter and receiver can be built without the cost driving transmit/receive-modules. Beyond this, with large baselines it is likely to increase the signature from stealthy objects. Another interesting aspect of

bistatic imaging radar is the reduced dynamic range of difficult imaging environments such as urban ones. However, besides the benefits of bi- and multistatic radar one has to solve several technical problems [1]-such as the synchronisation and determining the relative position and orientation of both platforms towards each other. This paper discusses a method which allows determining these two fundamental parameters of an airborne bistatic SAR system and presents first simulations result, which confirms the method. [C8623]

"Performance results of the SHARAD instrument"

SHARAD (SHallow RADar) is a subsurface sounding radar provided by ASI as a Facility Instrument to NASA's 2005 Mars Reconnaissance Orbiter for the characterization of the upper part of the Martian crust. The design of the instrument reflects a balance of scientific requirements versus SHARAD mission and Hardware constraints. One of the most difficult point in SHARAD design was the choice of the radar wavelength, since longer wavelengths have the potential for deeper subsurface penetration at the expense of depth resolution. Shorter wavelengths enhance the ability to generate surface images and accurate profile. A radar sounder needs a system requirements for large dynamic range and precise sidelobe control. Very low range side-lobes are mandatory to allow detection of weak sub-surface echoes in presence of the strong surface return. The approach of limiting to the minimum the amount of processing performed on-board was selected in order to allow the pulse compression process (critical from the point of view of range side-lobes) to be performed on ground, using the computed instrument Point-Target-Response (PTR) as correlation reference waveform. One of the main goal of this paper is to describe the design of the experiment design of SHARAD and the selection of the instrument parameters. An assessment of radar performance has been obtained by using both on-ground and on- flight measurements. Some preliminary results from the mars mission have been reported. [C8624]

"Bistatic SAR interferometry using ENVISAT and a ground based receiver: Experimental results"

The Universitat Politècnica de Catalunya is developing a ground based bistatic system using ESA's ENVISAT and ERS-2 as transmitters. The spatial resolution of this configuration is similar to that of their monostatic counterpart, although foreshortening effects have a lesser impact. First single-pass interferometric images corresponding to a local test-site are presented and compared to a synthetic interferogram. [C8625]

"Experimental investigation of Digital Beamforming SAR Performance using a ground-based demonstrator"

Digital beamforming (DBF) technique is a promising technique for future synthetic aperture radar (SAR). In this paper, we present the preliminary experiment and results. The measurements were accomplished by a ground-based DBF SAR system for a single target. The system is evaluated by mono-static SAR operation first. Comparing between DBF SAR and mono-static SAR images the channel imbalance effect is investigated. Since the experiment provides the SAR raw data containing the system response, from this raw data we estimate the linear phase error due to the channel imbalance and compensate it. The reconstructed DBF SAR images show that the minimum variation of the phase between the receive channel is crucial to obtain the theoretical improvement factor. [C8626]

"The detection of multi moving targets for the airborne SAR"

In the airborne SAR system, the echo signal is modulated by the moving target's velocity and acceleration. A method based on the fractional Fourier transform and "clean " technique to detect multi moving targets is presented, and a fast auto-search algorithm is proposed. The results of simulation proved the multi targets resolution of this method. It can eliminate the influence of cross terms in time-frequency domain and identify the multi targets correctly as the detection SNR below -8 dB. [C8627]

"Adaptive CFAR detection of range-spread targets based on SAR raw data"

Conventionally, SAR automatic target detection (ATD) are often performed in SAR image domain. A novel scheme of SAR target detection in the state of non-imaging is presented. More precisely, this paper addresses adaptive detection of SAR possibly extended targets when implemented on range-compressed but azimuth-uncompressed SAR raw data, rather than the processed SAR image. The SAR target detection is established in the context of space-time adaptive processing (STAR) and the spatial-temporal steering vector of an airborne stripmap SAR is first derived by exploiting signature diversity, namely of the fact that SAR can change the transmitted signal as the azimuth varies. The generalized adaptive subspace detector (GASD) is employed to detect range-spread target from SAR raw data. Performance analysis of the proposed scheme is carried out via Monte Carlo simulation which shows the validity of the new scheme in possible realistic scenarios. [C8628]

"Research on real time range profile of marine targets and its characteristics"

Against dechirping pulse signals, this paper proposes a real-time range profile algorithm suitable for marine targets, and analyses the characteristics of range profile of marine targets with real raw data, the common ways to deal with the characteristics are given as well. Finally envelope alignment and exponential transformation used in radar recognition preprocessing are analyzed. [C8629]

"ISAR imaging with stepped-frequency chirp signal by de-chirping processing"

Inverse synthetic aperture radar (ISAR) imaging with stepped-frequency chirp signal (SFCS) is simulated by de-chirping processing. Time-frequency analysis and image processing techniques are applied together for motion compensation. Detailed algorithm steps and imaging simulation for high-speed moving target with an acceleration as large as 30m/s^2 are presented. Results indicate that SFCS signal has an much better performance than stepped-frequency continuous wave signal for imaging of target with ultra-high speed. [C8630]

"Improvements of ROPE in ISAR Motion compensation"

Motion compensation in inverse synthetic aperture radar (ISAR) usually consists of two parts: range alignment and phase compensation. In this paper, the rank one phase estimation (ROPE) algorithm is applied to the ISAR phase compensation. Its blind setting of zero Doppler frequency at the start is avoided greatly by circular shifting the poorly focused strongest scatterer in each range bin to the zero Doppler frequency. Moreover, the iteration is introduced to further increase the phase estimation precision of ROPE. Compared with PGA, a good phase compensation algorithm, the improved ROPE doesn't require a relatively focused image at the beginning, and can remove the high frequency phase errors and random phase errors effectively. The processing of ISAR real data verifies the good performance of the improved ROPE. [C8631]

"Two dimension chirp-Z transform for polar format imaging algorithm"

Spotlight SAR is an efficiency way to obtain high resolution radar imagery. The classic polar format algorithm (PFA) is the widely used method for spotlight SAR imagery reconstruction, but PFA need two dimension interpolation operation in SAR imaging, which has influence on the imaging precision and computation efficiency. This paper presents a novel polar format Algorithm based on two dimension CZT transform, which may avoid the interpolation operation to improve on imaging precision and computation efficiency. [C8632]

"Research on the technology of monopulse SAR ground moving target indication"

Synthetic aperture radar (SAR) is a sort of high resolution imaging radar but the image of moving objects are often smeared and displaced in azimuth. In this paper, ground moving target indication (GMTI) with a monopulse SAR is introduced. The present method makes it possible to indicate the moving target in imaging scene and correct the azimuth displacement with the focused data from the sum and difference monopulse channels. [C8633]

"ISAR Imaging with LFM waveforms"

This thesis demonstrates a technique involving Linear Frequency Modulation (LFM) waveform and Inverse Synthetic Aperture Radar (ISAR) processing to develop two-dimensional radar images of a missile target. The processing is combination of two high-resolution processes: development of a high-range resolution (HRR) profile in down range using LFM waveform, and the development of high-resolution profile in cross-range using the ISAR technique. With these two techniques complementing each other, images of targets' dominant scatterers can be extracted, processed and displayed. This method is a practical method to process LFM radar data, in order to imaging the target. And it is useful in checking various interference methods to ISAR imaging. [C8634]

"Design and realization of intermediate down-sampling for SAR based on FPGA"

Under the condition of meeting resolution, the SAR real-time image can satisfy the demands of the processing band by pre-filter and down-sample. Due to being in a special position in the signal processor, the ranger pre-filter needs very high operating speed and quick frequency response. The pre-filter principles and the methods are analyzed in this paper and the study is focused on the realization of range down-sampling using FPGA. This paper pay more attention to the range down-sampling which following the digital orthogonal mixing. After analyzing the polyphase arithmetic, a new method of down-sampling which is implemented in FPGA is put forward in this paper. Validated by simulation, circuit operates reliability and fulfils design demand. [C8635]

"An experimental independent bistatic radar system for wideband application"

The aim of this research is to develop techniques for bistatic ISAR as applied to target imaging. A scheme of an independent bistatic receiving system without dedicated data links was carried out under the support of national science foundation. The research defined a system configuration and assesses its potential performance via modeling. It was developed to support pulse compression of wideband waveforms for applications. The associated implementation issues introduced by electro-optical component characteristics were discussed. Coherent detection was used to implement difference mixing for subsequent digital processing. This system is independent since it requires no timing control signals for synchronization provided by illuminators, but the necessary reference signal is intercepted from the radar's sidelobe emissions. [C8636]

"Airborne SAR passive radar imaging algorithm based on external illuminator"

In this paper, we propose an airborne SAR passive radar imaging algorithm which makes use of the regular circular motion by an airplane to form a synthetic aperture in the case of only one external illuminator available. Due to collected data is non-uniform and sparse in the Fourier space, the target scattering function can be reconstructed from the echo data through coordinate conversion, interpolation and two-dimensional Fourier transform. Theory analysis and computer simulation confirm the effectiveness of the algorithm. [C8637]

"Two methods for enhancing the coherence in PolInSAR data processing"

Two methods for enhancing the coherence are reviewed in this paper. The first one is based on similarity parameter and the second one on a mathematical optimization model. Both methods can be used to fuse the polarimetric information and enhance the coherence effectively. This is helpful for the processing of interferometric data. The equivalence of these two methods is proved. A physical analysis is given to explain this equivalence. The experiment is used to verify the performance of both methods. [C8638]

"The design of waveform-generation applied to wide-band high resolution imaging radar"

Linear frequency modulated (LFM) signal is widely used in radar due to its good characteristic. Aimed at transmitted waveform design of SAR system, a scheme of the wide-band LFM signal based on DDS technique is presented in this paper. Some factors affecting its compressed performance are also discussed. Finally, experiments results show that the proposed scheme is available. [C8639]

"Design and implementation of SAR raw data BAQ based on FPGA"

SAR raw data rate is one of most important limiting factor of spaceborne SAR system, in this paper, a design method of SAR raw data real-time compression system based on FPGA is discussed in detail, which adopts Block Adaptive Quantization (BAQ) algorithm. By using less hardware logic resource, SAR raw data rate is reduced, and performance of this real-time compression system is enhanced greatly. In BAQ module, four-channel parallel processing logic architecture is designed to circulate the statistic of data block; the logic architecture of multipliers and comparers is optimized, and when time-division multiple BAQ modules mode is applied in both I and Q channels in multi-FPGA, the real time processing ability is enhanced geminately. Experiment indicates the highest clock is 149MHz, data throughput of single module is great than 1Gbps, and when compression ratio is 8/3, the signal distortion noise ratio (SDNR) is great than 14dB. [C8640]

"Airborne C-SAR (Synthetic Aperture Radar) real-time imaging system"

This paper presents the design of one real-time imaging system in airborne C-band Synthetic Aperture Radar. The real-time imaging algorithm based on subaperture-division is described in detail. In order to meet real-time signal processing the signal processing board with 8 ADSP-TS201S digital signal processors and 2GB SDRAM is designed. This system has excellent real-time processing ability and tremendous data throughput and high expansibility. Finally the raw data of other airborne SAR is used in our real-time imaging system. The image is shown and the processing time is estimated. The results validate the feasibility of our system. [C8641]

"Design of real-time processor for groundbased ISAR imaging"

ISAR real-time imaging algorithm, the hardware platform and the system structure of the processor are introduced. The high resolution ISAR images are given after imaging for the measured data from ground-based radar. The imaging results demonstrate the effectiveness of the proposed system. [C8642]

"Multi-DSPs SAR real-time signal processing system based on cPCI bus"

SAR real-time signal processing plays a significant role in SAR system, and has been taken as an important

means to obtain real-time and effective information in military application. This paper analyzes the basic system requirements in view of the SAR signal processing feature, and a universal design method of system architecture and software realization are presented. Finally, the actual result obtained from a Ku-band radar system is presented to prove that the system design method is feasible. [C8643]

"A simple implementation of multi-baseline INSAR"

Multi-baseline INSAR is a kind of technology that obtains terrain height information using multiple SAR images, therefore, it has a better performance than single-baseline INSAR. There are primarily two methods to increase the accuracy of terrain height estimation. One increases the quality of the interferometric absolute phase image by utilizing several single-look complex images. The other decreases the errors of the terrain height estimation through iterative ways. Integrating the former method and noise-immune phase unwrapping method, this paper presents a realistic method to implement multi-baseline INSAR. This method mainly includes two steps; the first one is about how to obtain multi-baseline interferometric absolute phase image whereas the second one is the unwrapping mechanism. Then, through simulation, the achieved results not only demonstrate the validity and practicability of the method, but also prove that the performance of the multi-baseline INSAR is much better than single-baseline INSAR. [C8644]

"Velocity determination of single sound source based on Doppler effect"

An algorithm is proposed for determination velocity of single moving sound source with uniform velocity and frequency. A synthesized sound signal is formed to simulating the moving sound source recorded by a fixed recorder, on which Hilbert transform is applied to obtain the instantaneous frequency of the sound signal. Utilize the Doppler effect as a model, which describes the relationship between the velocity and instantaneous frequency, to fit sampled instantaneous frequency by nonlinear least square, the velocity of a mobile can be obtained. Experimental results show that the accuracy of the obtained mobile's velocity is affected greatly by the background noise. Wavelet and EMD are used to reduce the noise in the noisy sound signal and instantaneous frequency, respectively. [C8645]

"On distance measurement using band-limited noise"

In many engineering fields, distance to target is fundamental and very important information, and often estimated or measured by using sound. To measure the distance to the target, time delay between reflected wave from transmitted wave is often used. However, it is difficult to measure short distance. Actually, ultrasonic range finders and ultrasonic level meters have minimum detectable range. Meanwhile, in the research field of microwave radar, a range finding method using standing wave is known for measuring short distances. It seems effective to use the standing wave of sound wave for measuring short distances. Moreover, in an actual situation of acoustic measurement, a random noise is very often utilized as well as a pure tone. Therefore, we focus our attention on audible sound and examine the distance estimation method using standing wave in audible sound. Specifically, we perform a computer simulation when audible sound, e.g., white noise, is used as a transmitted wave. [C8646]

"An improved fog-degraded image enhancement algorithm"

In fog weather, Images captured by outdoor surveillance system degrade significantly and suffer from poor contrast. This paper presents an improved algorithm for enhancing fog-degraded image contrast in which a moving mask is used. By assuming the pixels in a mask having same scene depth, the algorithm applies the modified partially overlapped sub-block histogram equalization to implement contrast enhancement in every mask. It involves two steps: first, sky region is segmented in order to restrain over-enhancement in the flat region and reduce noise; then, remove the sky pixels in masks and modify the histogram information in mask, thus the modified partially overlapped histogram equalization transformation function for enhancement can be gotten. This paper also proposes a novel fuzzy edge detection algorithm to evaluate above contrast enhancement effect. Experiments on many fog-degraded images demonstrate that the proposed improved algorithm is simple and effective in contrast enhancement of fog-degraded images. [C8647]

"Maneuvering target tracking using the optimal stochastic jump filtering algorithm"

The problem of maneuvering target tracking is addressed in this paper. Based on the 'current' statistical model, two-structured stochastic jump system is constructed in which the acceleration covariance switching to each other. The parameters are estimated with optimal stochastic jump filtering algorithm, and the tracking ability is improved much more after using the covariance non-linear adjustment. Finally, numerical simulation is performed and the simulation result demonstrates that this tracking algorithm outperforms original adaptive algorithm and improves the precision and tracking ability at the same time. [C8648]

"3D template based automatic landmine detection from GPR data"

In this paper, we present a 3D template based landmine automatic detection from GPR data. A 3D template is chosen and a 3D fuzzy template is designed. The choice of the 3D template is decided based on smooth changing position of the maximum amplitude at every C-scan as well as the threshold of its background average intensity. The 3D fuzzy template is extracted from 3D template crisp data. GPR similarity for both the 3D template as well as its fuzzy template is examined by crisp similarity measure and fuzzy similarity measure respectively. The cross correlation is applied as a similarity measure in crisp case while a fuzzy similarity measure, based on similarity of a measured data to a fuzzy rule, is applied in the fuzzy template case. Results of similarity applying both methods for automatic landmine detection are presented. The results show the promise of 3D fuzzy template and the fuzzy similarity measure in differentiating a landmine from other objects.

[C8649]

"Modeling of local search for track updates in phased array radar tracking"

A distinctive aspect of a phased array radar is that its beam can be positioned repeatedly, if necessary, in an allocation for a track update. When the first beam of the allocation fails to detect a return, a local search process is enforced by successively positioning the beam toward the predicted target position and its neighborhood until a successful track update is made. The local search can be characterized in terms of the events that can occur in the process and the probabilities of those events. In predicting the event probabilities, it is required to evaluate the expectation of a product of target detection probabilities of successive illuminations. In this paper, approximate but analytic and efficient expressions are presented for the expectation of a product of detection probabilities and angular measurement accuracy of detection for repeated beam-positioning.

[C8650]

"Development of the detection and reporting device for patients' getting out of bed using ultrasonic radar and power line communication"

We propose the detection and reporting device for confirming the safety of the patients at small nursing facilities or ordinary houses. The device combines the ultrasonic sensor which detects patients' getting out of bed with power line communication (PLC) as a reporting system. The ultrasonic sensor in this device detects elderly person's getting out of bed and lying down to bed. The effectiveness of the proposed device has been confirmed by the field experiments in welfare facilities for elderly people.

[C8651]

"Estimation of the 3D structure of road scenes from monocular images and range data"

This paper proposes a method for estimating the 3D structures of road scenes using a monocular camera and a laser scanner. In order to develop advanced driver assistance systems, it is necessary to obtain 3D information concerning obstacles in the road. However, it is generally difficult to obtain accurate 3D structures of road scenes over a wide field of view. Our proposed method estimates 3D structures both from a sequence of images taken by a monocular camera and from range data obtained by a laser scanner. It accurately estimates the camera motion by using both the images and the range data. Moreover, a particle filter is applied to achieve robustness in various scenes. By estimating the camera motion accurately, the 3D positions of feature points that are extracted in the image can be calculated accurately. In our experiments, it has been shown that the proposed method is capable of estimating camera motion in a real road scene and it is able to obtain 3D structure of a road scene accurately over a wide field of view.

[C8652]

"Using FRFT to estimate target radial acceleration"

Radial acceleration of radar target is characteristic of relative motion between radar and target, and is significant for maneuvering target recognition and tracking. To estimate radial acceleration from radar echo, fractional Fourier transformation (FRFT) was used in this paper. The acceleration estimation formula was deduced firstly, and then its estimation flow was given out. Differences in antinoise interference capability between FRFT, WVD-HT (Wigner-Ville distribution and Hough transformation) and WVD (Wigner-Ville distribution) in estimating chirp signal parameters were analyzed. Then the relation between acceleration measurement accuracy and angle search step was deduced, and lastly simulations were made, proving that the method can improve operational speed, control operational precision and be also of better antinoise interference capability than other methods.

[C8653]

"Experimental reaserch of unsupervised Cameron/ML Classification method for fully polarimetric SAR Data"

Fully PolSAR data provided by the NASA/JPL laboratory are widely used to classify PolSAR image. In this

paper, an unsupervised Cameron/ML approach is proposed to classify airborne fully polarimetric data collected by a research institute in China. Cameron's method is used to initially classify the PolSAR image firstly. Secondly the initial classification map defines training sets for the maximum likelihood (ML) classifier. The classified results are then used to define training sets for the next iteration. The advantages of this method are the automated classification, and the interpretation of each class based on scattering mechanism. Formula of Cameron classification for the very measured data is also obtained here. The experiment demonstrates the proposed approach dramatically improves the classification result compared with the Cameron method. [C8654]

"Measurements of length and velocity of vehicles with a low cost sensor radar Doppler operating at 24GHz"

This paper deals with both the implementation and the real-life characterization of a low-cost 24 GHz Doppler radar sensor, purposely designed for the traffic monitoring. To reduce industrial costs as much as possible a discrete-components technology has been adopted for the microwave front-end. Plastic packaged devices and fiberglass reinforced substrate are used in such a way as to fit with standard PCB manufacturing processes and automated assembly procedures. The signal manipulation is based on a state-machine algorithm and has been implemented in a 8051 family microcontroller unit. The realized sensor has a typical output power of 6 dBm and mounts a planar antenna with a 3 dB beam-width of plusmn4.5 degrees. The real-life measured performances shows a detection range in excess of 300 meters. [C8655]

"Automatic extraction of power transmission tower series from PolSAR imagery based on MRF model"

This paper describes a three-step algorithm for automatic extraction of power transmission tower series in full polarimetric SAR imagery. Firstly, the method uses a polarimetric whitening filter to combine the information in different polarimetric channels and reduces the speckle. Then the point-like targets are detected by an adaptive region classification CFAR detection approach, among which only a few are the potential power transmission towers. Finally, a graph linked the potential point targets is constructed and a Markov random field is defined on the constructed graph, the extraction result is obtained through an energy minimization process. The experimental result verifies the effectiveness of this algorithm. [C8656]

"Pixel-level image fusion based on multi-to-multi turbo iterative"

A pixel-level image fusion method based on multi-to-multi turbo iterative is proposed. An innovative multi-to-multi image fusion idea is introduced in this paper. Undoubtedly, it's impossible to cover all the information contained in several images by one image. So multi-to-multi image fusion system is much more reasonable than multi-to-one image fusion system. Based on this idea, getting several orthogonal images can provide a promising application in future. The local linear generative model method is expanded to get orthogonal images from the source images in this paper. In addition, turbo iterative essence is also adopted; two orthogonal fusion algorithms are used iteratively. The information from two algorithms is exchanged during the iterative process. This paper uses the wavelet based method and the expanded model based method which is mentioned above iteratively. Although the wavelet based fusion method can retain much detailed information, it is sensitive to noise. In contrast, the model based fusion method can control the noise well. With the multi-to-multi idea and turbo iterative being both adopted, the proposed image fusion method can get a better fusion result with more details and less noise. The experiments show a satisfying result. [C8657]

"An ant colony optimization approach for SAR image segmentation"

A novel SAR image segmentation algorithm, based on the Ant Colony Optimization (ACO) method is proposed in this paper. The method extended the ant colony algorithm to threshold optimization, two-dimension fuzzy entropy is used as objective function, and ant move direction is determined by the trail pheromone. Each ant in the colony will generate a path based on the relative positions of the nodes and feedback information about the best paths generated by previous colonies. The solution of each ant is improved by using a global optimization procedure. The proposed approach has been tested on different SAR images. Tests results show that, due to its ability of both finding good search paths and escaping from local minima, the proposed method could achieve a near-optimal solution to the SAR image segmentation problem. [C8658]

"Contour extraction based on improved GVF snake model in ASAR images"

This paper proposes an improved GVF Snake-based method which is applied to Envisat ASAR images to determine the interested object's boundaries. ASAR images have a lot of noise and speckle. But different from other low SNR images, they are also full of texture. While using GVF snake model, the result of the gradient

vector field in ASAR images becomes even worse. How to reduce the influence of the unimportant texture and the noise level while to preserve the image features is the key problem. To solve this, log Gabor wavelets that have the ability to preserve the phase data is introduced into the new scheme to correct the gradient vector flow. Results show that the new method can detect the contour of the interested object more accurately and false edges are removed. [C8659]

"Inferring radar mode changes from elementary pulse features using fuzzy ARTMAP classification"

A method for radar mode inference using fuzzy ARTMAP classification is presented. In this method elementary radar parameters, pulse width (PW) and pulse repetition interval (PRI) originating from a radar operating in a certain mode is input to a fuzzy ARTMAP classifier. Radar parameters were simulated at different signal-to-noise ratios (SNRs) to train and evaluate the fuzzy ARTMAP classifier without prior knowledge of radar operating modes. Thus fuzzy ARTMAP classification is used in the analysis of radar mode behavior. Training resulted in map field weights with high code compression and broad generalization of the input space. The choice of ARTa categories accurately correlated with the current radar mode input data presented to the classifier. It resulted in a 1.8% error in category choice (radar mode) at worst. Classifier training may be done on data with low SNR as the broad generalization during training will accommodate high SNR data without compromising accuracy during evaluation. Knowledge about the amount of radar modes and mode transition can also be gained by an initial training and evaluation (analysis) process to assign pseudo modes to a particular radar. The resultant modes can then be included into a fuzzy ARTMAP classifier by increasing the dimension of the predicted output, B to classify both radar class and operating mode. [C8660]

"Edge-enhanced speckle suppression using curvelet transform with an optimal soft thresholding"

Aiming at the problem that common curvelet may bring fuzzy edge when denoising, this paper proposes a novel edge-enhanced speckle suppression method using curvelet transform with an optimal soft thresholding. The method combines the original images' edge detection with the filtered image of each subband. In the edge area, first the edge information from the remnant image is extracted, and then the edge information is added to the filtered image. In the non-edge area, to increase the contrast with the edge and have a clean background, a mean filter is used to smooth the area. As a result, the edge enhanced image is gained. In order to reduce the affection of disadvantages from both hard thresholding and soft thresholding filtering to the curvelet coefficients, the method also adopts an optimal soft shresholding for filtering. The simulation results show that the de-noising method can significantly reduce the speckles while enhancing the edge and the structure of the original SAR images with more smoothness in background areas. [C8661]

"An Experimental and Theoretical Investigation into Capabilities of a UWB Microwave Imaging Radar System to Detect Breast Cancer"

An experimental and theoretical study concerning capabilities of an ultra wideband (UWB) microwave radar to detect breast cancer is presented. A simple phantom, consisting of a cylindrical plastic container with a low dielectric constant material imitating fatty tissues and a high dielectric constant object emulating tumour, is scanned over a circular cylindrical surface with an UWB probe antenna. Following the collection of an experimental data, spatial images of the breast phantom are formed using two different approaches. One neglects and the other one compensates for the signal drop with distance. The approach compensating for the received signal drop enables a successful detection of tumour targets with a diameter as small as 5 mm just by visual inspection of the produced image. In the theoretical investigations, a finite difference time domain (FDTD) method is applied to obtain a further insight into the experimental results. [C8662]

"Experimental Test Cases for Wireless Positioning Systems"

Ubiquitous mobile computing is a new and very interesting research topic with wide applicability in context-aware solutions and position-dependent provided services. One of the most significant elements of context-awareness in ubiquitous environments is mobile device localization. There have been a number of attempts to design systems for indoor localization using different wireless sensing techniques, although currently there is no conclusive method for this purpose. There is also a list of issues that prevent from obtaining a good positioning accuracy which are not often addressed by other articles. Therefore, we want to propose a set of test cases for wireless local positioning systems (WPS) based on radio signal strength we call positioning test cases. These tests could be used to compare different WPS implementations or to deploy a certain WPS implementation. [C8663]

"Multi-objective optimization for peer-to-peer multipoint video conferencing using layered video"

We present a multi-objective approach and corresponding formulations for the optimal operation of a peer-to-

peer multipoint video conferencing system. The system aims end-points with low bandwidth connections (i.e., single full-quality video in and out) and makes use of layered video to achieve that each participant can view any other participant's video at anytime. This may cause some of the peers receive lower quality video. Moreover, since the peers may have to forward the video they receive, this may cause larger delays for the peers that receive the video after it is forwarded by several peers. Objective formulations to determine the number of lower quality video receiving peers and the delay experienced by the peers are derived. A multi-objective optimization approach for minimizing both simultaneously is described. An extension that allows multiple video requests from the participants with sufficient bandwidth is proposed. Formulations to minimize the number of lower quality video receivers while maximizing the number of additional video requests are presented. A multi-objective optimization technique assigning importance weights to each of these objectives and its sensitivity to changes in the weights are shown. The use of multi-objective optimization techniques within a system is demonstrated through example scenarios. The effects of our optimization approach on the percentage of base quality receiving peers are examined through simulations. [C8664]

"Increasing data-bandwidth to instruction-set extensions through register clustering"

The conflicting requirements of performance and flexibility in today's embedded system market are forcing system designers to use more and more of the so called configurable or customizable processor cores. Such processors tend to meet the demanding performance constraints by accommodating application specific instruction set extensions (ISEs) which have, naturally, become a vital component of current processor customization flows. One major bottleneck in maximizing ISE performance is the limitation on the data-bandwidth between the general purpose register (GPR) file and the ISEs. For improved performance, it is desirable to have a large data-bandwidth from the GPRs to ISEs. However, the tight area constraints of modern embedded processors often restrict the GPR I/O of ISEs to save port area of the register files. This paper presents a novel approach to increase the GPR I/O of ISEs without significantly increasing the size of the GPR files. This is achieved by applying the concept of register clustering, common in many VLIW architectures, to single-issue processors with high performance ISEs. Such clustering often causes extra register moves in compiled code. This work also presents an algorithm to minimize such register moves. The benchmark results presented in this paper show that our solution can significantly reduce the area overhead of many-port GPR files without sacrificing the performance improvements through ISEs. [C8665]

"Accurate posterior probability estimates for channel equalization using gaussian processes for classification"

In this paper we propose to use Gaussian processes for classification (GPC) for solving the channel equalization problem. GPC provides not only accurate decisions as other nonlinear machine learning tools do, i.e. support vector machines or neural networks, but it also assigns posterior probabilities to each one of its output. This is a significant advantage of GPC with respect to other machine learning tools for channel equalization, because the channel decoder benefits from its soft outputs to provide significantly better error correcting capabilities for the entire communication system. As, for previous schemes, the channel decoder had to rely on the hard decisions given by the equalizer, because the output of these methods cannot be transformed into posterior probabilities. We show that the GPC equalizer is able to estimate posterior probabilities accurately in a variety of real digital communications channel. [C8666]

"A new bearings-only tracking algorithm for ground moving targets constrained to roads"

We propose a new recursive algorithm for tracking ground moving targets from multiple bearings-only measurements in clutter, collected by a ground moving observer. The scenario represents a target moving along a realistic road network with junctions, roads branching or crossing, where the probability of having measured the line-of-sight bearing, among the multiple observed ones, is less than the unity. This constrained motion estimation is performed using particle filters. Realistic simulations are presented to support our findings. [C8667]

"Amplitude Weighting of Linear Frequency Modulated Chirp Signals"

Linear frequency modulated chirp signals are used in radar system. The signals may be easily compressed to increase range of the radar. To obtain compressed signal with small sidelobes, weighting function must be implemented. The paper describes some methods of chirp signals weighting that may be useful especially for signals with low compression ratio. [C8668]

"Estimation of 2D-DOAs and angular spreads for coherently distributed sources using cumulants"

In this paper, a new 2D-DOAs and angular spreads estimation algorithm is proposed for coherently distributed

(CD) sources. Based on the newly designed array geometry, multiple CD sources model is developed. The respectively azimuth DOAs, elevation DOAs and their angular spreads of CD sources can be estimated by the proposed LS-VESPA-based algorithm, which first compute the cumulants using the specially designed guiding sensors, then estimate the invariance structured matrix by LS-VESPA algorithm, and finally obtain the parameters from the phase information and the module information of the approximation closed form of the steering vectors. The efficiency of the algorithm is validated by computer simulations. [C8669]

"Performance analysis of direct data domain approach and Esprit method for DOA Estimation"

In this study, we compared the performance of matrix pencil (MP) method and ESPRIT (estimation of signal parameters using rotational in-variance technique) method under varying number of snapshots taken. Matrix Pencil method applies the technique directly to the data to estimate the poles, and works well under the correlated signal case, as opposed to ESPRIT, a statistical subspace based estimation technique, will work after applying some additional spatial smoothing techniques to tackle the ill condition problem of covariance matrix. Simulation results are provided to show the performance of these two methods. [C8670]

"A space-frequency anti-jamming algorithm for GPS"

In this paper, we proposed a space-frequency GPS anti-jamming technique with constant beamwidth. The proposed method sets up a new data model by Fourier transformation. On the basis of the new model, the optimal output SINR can be obtained by using Capon beamforming similar to the only spatial domain. Also, in order to obtain the distortless GPS signal, the beampattern with constant beamwidth is generated by focusing transformation technique. [C8671]

"RCS and radar propagation near offshore wind farms"

The wind farm impact on marine radars has not been widely reported. Some past publications have touched on the subject but there has been no accurate model in place to readily examine the effects of different farm geometries, tower shapes and turbine sizes. This paper discusses the radar propagation modeling near offshore wind farms including the methods used to model individual turbine mono and bi-static RCS, and the multiple reflections of radar signals within the wind farm. An initial qualitative comparison between the results of the model and measured data is provided. [C8672]

"FDTD modeling of scattering from distant buried objects"

The purpose of this work is to study the propagation of the lateral wave over long distances in the earth and see what the scattering signal is at the radar system. This study is done through simulations with the finite difference time domain (FDTD) method [K.S. Yee, 1966; A. Taflov, 1995]. [C8673]

"Separation of multiple secondary surveillance radar sources in a real environment for the near-far case"

Multilateration systems based on secondary surveillance radar (SSR) systems and omnidirectional antennae are operational today (Bezousek, 1998 and Galat, 2004). Assuming the replacement of the single-element antenna by an array, we proposed new algorithms to discriminate overlapped signals in previous works (Petrochilos et al., 2002, 2004 and 2007); other solutions were also proposed in the literature (Roy and Kailath, 1989; Chaumette et al., 1993; and van der Veen and Tol, 1997). Unfortunately, all have either some shortcomings, or an expensive computational cost, or no simple practical implementation. Therefore, we proposed in the work of Petrochilos et al. (2005) a reliable, simple, and effective projection algorithm. Nevertheless, some issues were overlooked: in particular the relative power ratio between the signals to be separated may be important, which we study in this paper with real-life signals. [C8674]

"GPU based FDTD solver with CPML boundaries"

The use of graphical processing units has been recently documented for the implementation of the FDTD technique; however, little has been reported about the necessary additions to three dimensional GPU based FDTD codes to make the technique more useful for EM analysis and antenna design. This paper will detail the practical addition of a convolutional perfectly matched layer absorbing boundary to a three dimensional GPU accelerated FDTD code and present results of simulations with dielectric and conducting objects in the computational domain. [C8675]

"Application of particle swarm optimization (PSO) to single-snapshot direction of arrival (DOA)"

estimation"

This paper attempts to examine the feasibility of using an heuristic bio-inspired algorithm in DOA estimation. Specifically, particle swarm optimization (PSO) (Kennedy, et. al., 1995) [C8676]

"Tolerance manufacturing effects in crossfeed monopulse radars in presence of rough sea scattering"

In this paper the performances of a crossfeed system was analyzed in presence of stochastic rough sea scattering, whereas in other literature the crossfeeds monopulse have been analyzed only under the hypothesis of flat earth and perfectly smooth sea (Schenkel, 1987). Furthermore the effect of manufacturing tolerances in the passive network backing the antenna was considered. These errors can lead to small phase bias in the different monopulse channels, leading to inaccurate tracking. The different effects of these phase errors on standard and crossfeed monopulse radars were discussed. [C8677]

"Multipath return for radar targets over a rough surface"

A scattering formulation is described here which can be used to understand and predict the electromagnetic scattering from a target positioned over a (potentially) rough interface. It has application to the evaluation of radar performance in the presence of multipath [C8678]

"Nonlinear Target Identification and Tracking Using UKF"

In this paper, we implemented target identification algorithm using Dempster Shafer theory (DST) and tracking algorithm using extended Kalman filter (EKF) and unscented Kalman filter (UKF). A tracking filter is developed and simulated based on UKF to track nonlinear, ballistic and reentry targets. Comparison of EKF and UKF for nonlinear targets tracking are presented based on the simulation results. Simulated results gives more supporting points to use UKF for nonlinear target tracking rather using EKF. [C8679]

"Concept for measuring and compensating array deformation"

Phased array antennas are increasingly used in modern radar systems. Such systems are very liable to distortion of the relative phases between the radiating elements. For airborne, spaceborne, and naval phased array systems, vibrations of the array structure are an important source of phase distortions. In this paper, a system concept will be presented to measure array deformation and provide phase compensation information with which the received data can be corrected. Such realtime measurement and compensation of array vibrations may considerably improve the performance of operational systems. Therefore, a study was started to investigate the feasibility of this concept. Shaker experiments proved that the required measurement accuracy is within reach using off-the-shelf sensors and suitable signal processing. [C8680]

"Application of STAP technique to FMCW systems"

The fundamental assumption that is made while space-time adaptive processing (STAP) technique is considered is that the signal to be processed takes on the form of a sequence of coherent pulses. Frequency modulated continuous wave (FMCW) systems are in widespread use because of their numerous advantages due among others to its non pulse character. It seems extremely important to look for a possibility of using STAP procedures in FMCW systems to make them even more attractive. The paper presents a simple analysis of a proposed approach to achieve this goal. A structure of the signal processor is presented and assumptions necessary to be fulfilled are defined. Effects of the proposed approach implementation in HF, I, and X bands are evaluated on the basis of selected parameters of the appropriate FMCW-STAP systems. [C8681]

"Digital beamforming and multidimensional waveform encoding for spaceborne radar remote sensing"

This paper describes an active electronically scanned array (AESA) FMCW radar with eight transceivers. Each transceiver has its own direct digital synthesizer (DDS) for signal generation which enables digital beamforming on transmit as well as on receive. The coherent operation of the eight transceivers and the capability to perform digital beam forming on transmit and receive is demonstrated. [C8682]

"Investigation of MIMO SAR for interferometry"

In conventional interferometric synthetic aperture radar (SAR), the coherent combination of two SAR images reconstructed from two separated receive antennas is used for digital elevation model (DEM) or moving target indication (MTI), depending on the antenna constellations. In this paper we propose the novel system concept for

interferometric SAR (InSAR) based on Multiple-Input Multiple-Output (MIMO) configuration. A digital beam forming (DBF) SAR system based on multiple receive antennas is extended to MIMO SAR concepts. We investigate its performance and processing features, particularly, associated with the received signal quality and the transmitter diversity. Using orthogonal linear frequency modulated (LFM) signal, it is shown that space-time coding scheme can be applied to SAR system in multiple-input single-output (MISO) configuration. A simple Alamouti scheme enhances the signal-to-noise ratio (SNR) and extracts a spatial diversity. Combining this transmitter spatial diversity and digital beam forming on receive, we introduce the potential of high resolution wide swath (HRWS) observation for Interferometry. [C8683]

"Single-antenna projection algorithm to discriminate super-imposed Secondary Surveillance Radar Mode S signals"

This paper presents a novel, effective algorithm to discriminate and separate super-imposed SSR (Secondary Surveillance Radar) Mode S signals. Our goal is a blind separation of multiple SSR sources using a single channel receiver. Other algorithms perform sources separation exploiting space diversity or statistical properties, but with the practical inconvenience of the need for a multi-channel receiver. As today SSR stations are equipped with single-channel receivers (for Multilateration and Wide Area Multilateration applications, M-LAT, WAM) the proposed algorithm is aimed to be operationally useful. [C8684]

"Adaptive antenna configuration for unambiguous signal reconstruction in dual-channel SAR systems"

In a dual-channel SAR (synthetic aperture radar) system, two different approaches have been proposed in order to obtain at the same time wide range swath and high spatial azimuth resolution. The first one, based on the classical DPC (displaced phase centers) technique (Currie and Brown, 1992), requires a rigid selection of the PRF (pulse repetition frequency) value in order to guarantee uniform sampling of the SAR signal from the two receiving channels. The second approach, proposed in the work of Krieger et al. (2004) and Gebert et al. (2005) permits to correctly reconstruct the SAR signal even for nonuniform sampling. However the two approaches are able to completely suppress the signal of an ambiguous target having a Doppler centroid equal to PRF only if working with "uniform" PRF. This results in a degradation of the focused image quality that gets higher as the PRF moves away from its uniform value. This paper, starting from the approach proposed in the work of Krieger et al. (2004), describes how, in addition to a correct signal reconstruction, it is possible to make available different uniform PRFs for a complete suppression of the azimuth ambiguity. Through an adaptive selection of the dual-receive antenna configuration, it is possible to vary the phase centers displacement and, consequently, to vary the correspondent uniform PRF value. Using a phased array, the adaptive selection of the antenna configuration of either receiving channels, obtainable through a proper amplitude tapering, directly determines the level of accuracy achievable in the choice of the PRF. Such an antenna configuration adaptivity can be simply realized on board, hence permitting to real time reconfigure the system. This is particularly suitable in those SAR which need to operate with different PRF values. In this paper, for a given physical antenna, the performances of several tapering configurations are evaluated in terms of achievable uniform PRF and azimuth ambiguity level. [C8685]

"Knowledge-aided array calibration for registration-based range-dependence compensation in airborne STAP radar with Conformal Antenna Arrays"

We consider space-time adaptive processing (STAP) when the radar returns are recorded by a conformal antenna array (CAA). The statistics of the secondary data snapshots used to estimate the optimum weight vector are not identically distributed with respect to range, thus preventing the customary STAP processor from achieving its optimum performance. The compensation of the range-dependence of the secondary data requires the precise knowledge of the space-time steering vector. We propose a new knowledge-aided method based on the eigenstructure of the space-time covariance matrix for calibrating the gain and phase of each sensor in the CAA. Based on the calibrated space-time steering vectors, we can perform an accurate range-dependence compensation to obtain a valid estimate of the covariance matrix. End-to-end performance analysis in terms of signal to inference-plus-noise ratio loss shows that the method yields promising performance. [C8686]

"Real-Time Space-Time Adaptive Processing on the STI CELL Multiprocessor"

Space-time adaptive processing (STAP) has been widely used in modern radar systems such as ground moving target indication (GMTI) systems in order to suppress jamming and interference. However, its baseband signal processing part usually requires huge amount of computing power. This paper presents the real-time implementation of an STAP baseband signal processing flow on the state-of-the-art STI CELL multiprocessor which enables the concept of software-defined radar (SDR). SIMD vectorization is applied to speed-up the

kernel subroutines of STAP such as the QR decomposition, forward/backward substitution and fast Fourier transform (FFT). Benchmarking results of both the kernel subroutines and the overall flow are presented. Furthermore, based on the result of earlier benchmarking, optimized task partitioning and scheduling methods are proposed by us to improve the overall performance so that the overhead is reduced to the minimum. [C8687]

"Set of X-band distributed absorptive limiter GaAs MMICs"

A set of X-band absorptive limiter GaAs MMICs has been designed and realised using both the PPH25x foundry process from UMS and the PP50-10 process from WIN semiconductors. The innovative limiter concepts have been extensively characterised by both pulsed and CW measurements. Both passive and active topologies have been implemented. The passive limiter design has a typical small-signal insertion loss of 1.5 dB at 10 GHz, and it can withstand (absorb) up to 4 Watts (36 dBm) of CW power without degradation or damage, while keeping the output power level below 100 mW (20 dBm). The active limiter handles up to 10 Watts of CW input power, at the cost of higher small-signal insertion loss. For all designs the input reflection remains low for any input power level. The used GaAs surface ranges from 2 to 3 mm². [C8688]

"24GHz Software-Defined Radar System for Automotive Applications"

A software-defined measurement system is proposed and described in this work. The system makes use of a hybrid radar scheme of frequency modulation continuous wave (FMCW) and pseudorandom (PN) code pulse techniques. In this system, the FMCW measurement technique is deployed in obtaining the range value of a target while the PN code pulse radar technique is used to determine the inter-vehicle radar information for communication purpose. Different waveforms are generated in direct digital synthesizers (DDSs) and processed by different algorithms in a single digital signal processor (DSP). The switching between the PN code pulse and FMCW functions is controlled by software to improve the parametric resolution and ensure the communication function. Measurement results of our designed and fabricated K-band (24 GHz) prototype radar validate the proposed software defined radar system. The results of the radar compared with those of a reference laser meter suggest an accuracy of range value around 15 centimeters. The PN code information reflected from target is well collected and recovered. The work has demonstrated unique and reliable combined functions of the FMCW and PN code pulse platforms for automotive applications. [C8689]

"Signal Detection Algorithms Based on Non-Parametric Estimates of Density Function"

This paper presents a novel approach to design radar signal detection algorithms that are applicable when a priori information is limited. The problem is formulated as testing hypothesis on the kind of density function. A novel method that allows to adopt permutation test in a practical algorithm is suggested and researched. The developed new adaptive algorithm is based on non-parametric kernel estimates of the density function. The results are useful for applications of signal detection in surveillance and remote sensing radar systems. [C8690]

"Complex-Weighted OFDM Transmission with Low PAPR"

In this paper the novel method of complex weighting for peak-to-average power (PAPR) reduction of OFDM signal is addressed. Combination of different amplitude weighting factors (including rectangular, Bartlett, Gaussian, raised cosine, half-sin, Shannon, and subcarrier masking) with phasing of each OFDM subcarrier using random phase updating algorithm is studied. The impact of complex weighting of OFDM signal on the PAPR reduction is investigated by means of simulation and is compared for the above mentioned weighting factors. Results show that by either amplitude weighting or random phase updating the PAPR can be reduced. Applying both techniques together will further reduce the PAPR. For an OFDM system with 32 subcarriers and by Gaussian weighting combined with random phase updating, a PAPR reduction gain of 3.2 dB can be achieved. In order to reduce the complexity, grouping of amplitude weighting and/or phasing is applied. Results show that grouping of amplitudes weighting and phases reduces the hardware complexity while not much impacting the PAPR reduction gain of the method. For even further reduction of the PAPR, complex weighting method with dynamic threshold is investigated. Results show that the PAPR can be further reduced by factor of 4.8 dB. [C8691]

"Performance Analysis of FMCW Synchronization Techniques for Indoor Radiolocation"

A high precision localization system (HPLS) operating in the 5.8 GHz ISM band is presented. The system principle is based on the sequential exchange of frequency modulated continuous wave (FMCW) signals between identical radar stations. The round-trip time-of-flight (RTof) localization method requires exact synchronization of all involved stations. Consequently, accurate compensation of clock frequency drift is indispensable. We analyze the impact of clock deviation on synchronization accuracy and present a precise compensation method. The synchronization technique has been tested on a prototype system. Measurements

showed a 3D-position accuracy of 2.8 cm under laboratory conditions. [C8692]

"A study on RCS of missile models using the method of moments"

Simulation of electromagnetic signals scattered by objects is a complex issue, although its fundamentals have long been known. In the design of modern military aircrafts and vessels in general, advantages can be taken from their physical properties for reducing the intensity of radar signals, which are scattered back to the enemies. This leads to the definition of stealth plane or ship. A couple of design guidelines should be followed in order to achieve this goal. One of them is the geometric optimization of the vehicle shape. Much of the literature on this subject is classified; moreover, the computing burden to tackle such a design is quite demanding. In this work, a conventional PC running a commercial electromagnetic code based on a modified Method of Moments is used to analyze four different simplified missile models. Design rules are established in view of reducing the monostatic radar cross section (RCS) scattered signal. [C8693]

"Modeling of nonidealities in receiver front-end for a simulation of multistatic SAR system"

Novel concepts for synthetic radar (SAR) systems are designed to use the potential of multiple transmit or/and receive front-ends. The DBF SAR, HRWS SAR or MIMO SAR improve the quality of the radar image using multiple receiver signals and adequate signal processing algorithms. The processing algorithms are developed with assumption of an ideal transmit and receive system. The effects that could occur in the transmitter or receiver front-end disturb the received signal and resulting Radar image. This paper is a contribution to the investigation of the influence of nonidealities of the SAR receiver. Presented are VKA-representation models of HRWS SAR receiver developed simulation considers also effects resulting from quantization and digital beamforming processing (DBF). The VKA-representation enables description of the receiver in a compact and simple way. [C8694]

"A High Linearity Mixed Signal Down Converter IC for C-band Radar Receivers"

A mixed signal receiver IC for C-band radars is presented. The design work has been focused on spectral purity and miniaturization. Miniaturization is achieved by minimizing peripheral components and control signals using internal calibration data and temperature compensation tables stored in RAM on-chip. This allows for the packaged chip to be used with a minimum of. The chip is manufactured by Austria Microsystems in their 0.35 μm SiGe-BiCMOS process and utilizes digital IP-block included in the design kit. [C8695]

"Design of a [CDC-20 GHz] Buffered Track and Hold Circuit in InP DHBT Technology"

This paper describes the design and realization of a buffered track and hold (BTH) circuit fabricated in InP-InGaAs-InP double heterojunction bipolar transistor (DHBT) technology ($f_T = 180$ GHz). This BTH is intended for a single shot, 20 GHz bandwidth and 40 GS/s sampling frequency digitizer based on the non simultaneous spatial sampling principle. Based on a high speed switched emitter follower (SEF), the BTH can ensure 20 GHz bandwidth signal compatible with the targeted objectives. First experimental results in the frequency domain and a novel optimized architecture leading to a combination between the SEF and the Cherry Hooper design based buffer are also presented. [C8696]

"Modeling E-Mail Traffic for 3G Mobile Networks"

Traffic models are to provision the increasing load of packet switched traffic in mobile 3G networks. However, most traffic models were designed to fit the need of low delay wired connections. In this paper we propose a new traffic model for POP3 e-mail traffic generation in 3G mobile networks scenarios. The model is based on traces which were extracted in a live 3G network of a mobile operator. The main improvement of the model is the explicit modeling of the login process that takes place between the client and the server. We implemented the model in the network simulation tool ns-2 and based on this we simulated various scenarios to visualize the impact of a leading initialisation phase in high RTT environments. The results proof that the extension can reproduce the effect from the login in a more precise way. Finally a comparison between the measured and the simulated service footprints were compared. The new model performs better than common models in this scenario. [C8697]

"Tools and Practices for Measurement-based Network Performance Evaluation"

As networks and applications running on them become more complex, there is a need for an efficient framework supporting experimental performance evaluation based on real measurements. Towards this end, this paper presents: a) an advanced architecture for a traffic generation tool capable of producing complex traffic profiles, b) the architecture of a traffic analysis tool, and c) methods that allow for efficient monitoring and measurements of

delay and loss-oriented metrics in packet networks. The effectiveness of these tools and the applicability of the measurement methodology are illustrated through experiments that evaluate the performance of vertical handovers between GPRS and WLAN networks. [C8698]

"Enabling IMS with Multicast and Broadcast Capabilities"

The evolution of third generation cellular network focuses on the provision of enriched multimedia services and the support of QoS (quality of service) guarantees. The IMS (IP multimedia subsystem) is specified as subsystem providing resource, admission and charging control. Enabling GPRS (general packet radio service) and UMTS (universal mobile telecommunications system) to support multicast and broadcast transmissions, 3GPP (third generation partnership project) has recently standardised the MBMS (multimedia broadcast multicast services) framework. Up to now, IMS and MBMS are separated subsystems sharing no common interfaces in order to utilise each other. However, 3GPP is working currently on release 7 to integrate IMS and MBMS. In this paper we present an efficient integration of IMS and MBMS which supports several phases of unicast, multicast and broadcast transmissions. Furthermore, an integrated solution framework is introduced. Several end-to-end signalling procedures are finally discussed. [C8699]

"Teletraffic Analysis for the Performance Evaluation of De-Allocation/Re-Allocation Strategies in GSM/GPRS Cellular Networks"

A teletraffic analysis for the performance evaluation of the joint use of dynamic resource allocation (DRA), channel de-allocation (DAS), and channel re-allocation (RAS) strategies in GSM/GPRS networks is developed. In addition, an efficient DRA strategy with a link quality awareness policy, channel de-allocation and re-allocation policies as well as user prioritization (called DRA LA DAS RAS) is proposed. To the authors' knowledge, most related works have either studied link adaptation (LA) or dynamic resource allocation (DRA) strategies as independent topics but have failed to address their combined effect on GSM/GPRS systems. DRA LA DAS RAS uses both call degradation and call compensation techniques. Calls with the largest number of channels allocated and the worst link quality are degraded first. Conversely, calls with the lowest number of channels allocated and the best link quality are upgraded first. This allows upgraded calls to release resources more rapidly, making them readily available for new calls. Numerical results show that the proposed DRA LA DAS RAS strategy significantly improves system performance, i.e. up to 82% (74%) {58%} [37%] <27%> less blocking probability relative to the DRA (DRA LA with $p=0.75$) {DRA DAS} [DRA LA DAS with $p=0.75$] <DRA DAS RAS> strategy. [C8700]

"Enhancing Quality of Experience in Next Generation Networks Through Network Selection Mechanisms"

The evolution of telecommunications during the last decades has been enormous and as a result, nowadays, people find themselves before the challenge of 4G networks. Consequently, network selection techniques play a vital role in ensuring quality of experience (QoE) in heterogeneous networks. The main scope of this paper is the development of a process in order to compare packet-switched networks in terms of QoE offered and finally select the network that offers the highest standard of QoE. For this reason, main QoS parameters are identified and a scheme is proposed to identify each parameter's importance based on network performance. The proposed methodology combines the analytical hierarchy process (AHP) to decide the relative weights of evaluative criteria set according to the network's performance, as well as the grey relational analysis (GRA) to rank the network alternatives. The proposed methodology is then applied for GPRS and WLAN. [C8701]

"Enhanced Local Positioning Radar with Predictive Filters"

This paper presents two adaptive recursive tracking techniques for precisely localizing a mobile vehicle in an indoor industrial environment. An Extended Kalman Filter (EKF) and Unscented Kalman Filter (UKF), the corresponding algorithms and mathematical models are presented and analysed. Experimental range measurements generated from local positioning radar system are used to test the performance of these algorithms with respect to position and velocity root mean square errors. True and estimated trajectories of the mobile vehicle with associated means and error covariances are illustrated with the number of samples required in each case. Results obtained show that UKF outperforms EKF with respect to positioning accuracy and root mean square error. Both filters show comparable computational complexity with more robustness obtained by applying UKF for non linear estimation since there are no linearization errors as in the case of EKF. [C8702]

"Secure Interworking in Multi-Operator, Multi-Technology Wireless Communication Environment: Issues & Challenges"

Taking into account the recent advances in wireless communications with the deployment of various technologies that cover the same areas, secure interworking in multi-operator, multi-technology wireless communication environments is a critical issue that should be considered by all operators. This is primarily linked with risk analysis and it is the process that each operator should go through to determine the risk exposure. It indicates mainly the possibility of a damage that could happen either by intruders or by misuse of the resources. The goal of risk analysis is to determine the probability of potential risks and estimate the overall damage at an annual basis in order to define new policies and measures. This is the main contribution of this work. [C8703]

"Pilot Remote Experiment in the ERRL: Measurement of Scattering Parameters"

A remote laboratory platform enables the learners to access physical instruments at distant location and to perform experiments remotely via the Internet. This paper focuses on a pilot remote laboratory experiment on measurement of scattering parameters (s parameters) by using vector network analyzer (VNA) in the ERRL (European Remote Radio Laboratory) platform. The results of the pilot experiment are presented, and discussed shortly. [C8704]

"GPRS based Real-Time Reporting and Internet Accessible Sea Level Gauge for Monitoring Storm Surge and Tsunami"

Development and implementation of a real-time reporting and Internet-accessible sea level gauge is described. The paper addresses the application of mobile communication technology and particularly the use of General Packet Radio Service (GPRS) for accessing data from remote sea level gauge. By using a microcontroller and existing mobile phone network with a GPRS support, a continuous connection to the Internet is implemented for real time update of sea level data on a web server. The system provides a graphical illustration of the predicted fair-weather sea level, the current sea level, and the residual sea level (i.e., measured minus predicted fair-weather sea level). Thus, a cost-effective and easily maintainable platform is realized for real-time reporting of sea level and providing the requisite input for efficient implementation of any alert and warning mechanism in the event of oceanogenic natural disasters, particularly storm surges and tsunamis. The system described herein is operational in Goa, India since 24th September 2005. [C8705]

"Fast Fourier-domain modelling for a SAS simulator with application to time-variant targets, aspect-dependent occlusions, and Doppler effects"

This paper presents a new technique for the rapid computation of the far-field beampattern for the field scattered from a facet. We show how an affine transform and application of the warping property of the Fourier transform can be used to calculate the beampattern of an arbitrary triangular facet from the beampattern of a unit right-angle triangular facet. Thus, only a single beampattern needs to be calculated and stored; this is then interpolated as required. We describe how this technique can be applied to efficiently model time-variant facets, for example, the facets of a moving sea surface, or the visible region of a partially occluded facet. We also describe the incorporation of temporal Doppler effects. The fast Fourier-domain technique described in this paper has significantly improved the computational performance and memory footprint of our synthetic aperture sonar simulator. [C8706]

"Ambiguity Function and Cramer-Rao Lower Bounds for Passive Synthetic Aperture Sonar (SAS)"

The resolving power of passive SAS is addressed by computing and plotting its ambiguity function in the frequency/bearing plane. It is proven that, even in ideal conditions, the apparently better spatial resolution of passive SAS is due only to the better frequency resolution which results from the longer processing time. In other respects the computation of Cramer-Rao Lower Bounds (CRLB) for joint source bearing and frequency estimation is detailed. It is shown that, in realistic situations, i.e. when the source frequency is not known, the bearing accuracy (standard deviation) does not depend upon the own speed (and hence on the length of the synthetic aperture). In fact the true, and maybe the sole, practical interest of the many proposed passive SAS algorithms [2, 4] is that they may appear as manners to perform a coherent very long time integration, thus possibly allowing detection of weak coherent narrow band sources. [C8707]

"VHF PortMap Sea Surface Radar Observations in a Shipping Channel"

A new sea surface radar system is described, which gives a spatial resolution of 100 m and operating ranges to up to 3 km. The deployment of the dual-radar system at the Lido Entrance to the Venice Lagoon gave current flow data in the channel and provided detail of a complex counter-flow at the end of the channel where it debouches into the Adriatic Sea. This circulating flow near the end of the channel is similar to that observed in wide-mouthed natural channels and is bringing turbid water into the channel. The presence of the circulation at

the end of the channel has some consequences for sediment dynamics at the site. This deployment demonstrates the functionality of the PortMap radar in a busy shipping channel. [C8708]

"Bathymetric results from a multi-frequency InSAS sea-trial"

In this paper we present results from a multi-frequency interferometric synthetic aperture sonar (InSAS) sea-trial. The height estimate is generated using a maximum likelihood (ML) estimate combining the data from the hydrophones. To decrease the effect of the large variance of the phase difference estimates the broadband signal is divided into smaller subbands and combined to give a height estimate with much improved accuracy, albeit at a reduced resolution due to the reduction in system bandwidth. Results are shown for a three vertical element sonar, and the improvement obtained using multiple frequency bands sub-banded to give a lower variance in the height estimate. Multiple pings are also combined as multiple looks, further reducing the height variance. [C8709]

"Extended Towed Array Measurement: Beam-domain phase estimation and coherent summation"

Passive Synthetic Aperture (PASA) is a technique of increasing the length of a small array artificially through array towing motion and signal processing. This allows the user to obtain the advantage of a long array while maintaining the maneuverability of a short array. In recent years, there have been keen interests in improving the ETAM technique to overcome its disadvantage. In this paper, the Extended Towed Array Measurement (ETAM) technique [1] for passive synthetic aperture processing is investigated. It is shown that the overlap-correlator of ETAM is not effective in the presence of more than one source. A new approach of the overlap-correlator is proposed. This approach performs the phase correction factor estimation in the beam domain by correlating the beamformed output of the overlapped sections of the array. Using this approach, the technique is applied to simulated data and is shown to successfully detect two sources using only a single frequency band of processing. In addition, the new technique performs coherent summation of the synthetic aperture in the beam domain in a sub-aperture sense, instead of beamforming only after the array has been phase compensated and fully extended. The former approach ensures reduced sidelobes due to the effect of windowing at each sub-aperture beamforming step. This study has resulted in a beam domain PASA technique that overcomes original ETAM's problem of incorrect phase compensation in the presence of multiple sources. [C8710]

"A SONAR Simulation used to Develop an Obstacle Avoidance System"

Response time to a threat or incident for coastline security is an area needing improvement. Currently, the U.S. Coast Guard is tasked with monitoring the coastal areas using boats or planes, and SCUBA divers are deployed to inspect any potential underwater threats on the coastline or in a port. This can significantly hinder the response time to an incident. A solution to this problem is to use autonomous underwater vehicles (AUVs) to continuously monitor a port. The AUV must be able to navigate the environment without colliding into objects for it to operate effectively. Therefore, an obstacle avoidance system is essential to the activity of the AUV. Conventional underwater vehicles often use imaging or scanning SONARs for obstacle avoidance. The space and power available on a vehicle must be large enough to support these systems. Smaller underwater vehicles may not be able to accommodate a scanning SONAR system for use in obstacle avoidance. Thus, it is of great interest and need to determine the proper configuration of the SONAR system and its corresponding signal processing methods for the coastline security problem. This paper proposes a systematic approach to characterize the OAS performance in terms of environments, obstacles, SONAR configuration and signal processing methods via modeling and simulation. The SONAR simulator is based on modeling a set of circular piston transducers, and the echoes are created based on specular reflections. The ray-tracing algorithm used in the simulation considers reflections from planar, spherical, and cylindrical objects. The main contribution of the presented work is three folded: (1) help us understand better how the return signals are related to the obstacles and environment, (2) help us optimize the complexity of the transducers for coastline obstacle avoidance, and (3) help us better design the avoidance strategy needed for a specific scenario. [C8711]

"Dive into Myojin-sho Underwater Caldera"

In August 2005, we succeeded in operating AUV "r2D4", which was constructed in July 2003 as one of fruits of R-Two project, into Myojin-sho underwater Caldera in full autonomous mode. The caldera is located about 800 km in the south of Tokyo, and 8 km in diameter. There is an active underwater volcano Myojin-sho at the Northeastern part of outer rim of caldera, which erupted repeatedly in 1952. The Kuroshio current is usually running over the Caldera, so that current speed around it is sometimes more than 3 knots. It can be said that the diving of human occupied vehicle and remotely operated vehicle into Myojin-sho Caldera is very dangerous due to such hostile environment. The interferometry SONAR captured a clear image of the central cone in the middle of crater, and the in-situ chemical analyzer "GAMOS" detected high concentration of manganese ion

which indicates hydro-thermal activity in the crater. [C8712]

"Efficient Active Sonar Parameter Estimation Using Linear FM Signals via Hermite Decompositions"

Signals with finite time support are frequently encountered in sonar and radar processing. It is usually necessary to have a compact description of these signals' shape and time evolution. For this purpose, the Hermite series expansion is used in this paper to approximate an arbitrary enveloped linear frequency modulated (LFM) signal. The Hermite basis functions are based on the product of Hermite polynomials and a Gaussian function. The analytical expressions for the Fourier transform of LFM Hermite functions have been developed in this paper. It is proposed to use the Fourier transform of LFM Hermite functions for efficient computation of the wideband cross-ambiguity function (WCAF) for target parameter estimation in active sonar processing. Efficient two-dimensional (2-D) search methods are also proposed in this paper to obtain parameters from the WCAF. [C8713]

"Comparison of Ray Tracing Simulations and Millimeter Wave Channel Sounding Measurements"

Temporal-Angular channel sounding measurements of an indoor millimeter wave channel (60 GHz) is analyzed to determine the location of two dimensional clusters of arrivals at the receiver. The measurement scenarios are also emulated by a ray tracing tool. The results are similarly analyzed to verify possible agreements and determine the effectiveness of such tools in predicting cluster locations as well as ray arrival statistics within clusters in millimeter wave indoor channel. [C8714]

"Code-division multiple transmission for high-speed UWB radar imaging with array antennas"

In this paper, we introduced PN signals with Gold codes instead of the conventional short pulse for the UWB radar imaging, which enabled us to simultaneously transmit signals with multiple antennas. This radar system can obtain the observation data within a short time, which does not spoil the advantage of the high-speed imaging by the SEABED algorithm. We have derived the revised SEABED algorithm in order to deal with the antenna arrangement with a fixed receive antenna and multiple arrayed transmit antennas. This proposed radar system is suffered from the range sidelobes due to the auto-correlations and cross-correlations between PN codes. We found a sub-optimum set of sequences to suppress the range sidelobes. The quality of the estimated target image with the proposed sequences is high enough for most of applications. [C8715]

"Design and implementation of a golay-based GPR system for improved subsurface imaging"

A bench-top prototype GPR using Golay codes has been designed and implemented. The preliminary experimental results show a reasonable good improvement in terms of SNR. This work is still in progress. Improvements related to some of the other components and subsystems are underway. In particular, we are experimenting with innovative antenna designs having minimum influence on the transmitted waveform, and improved image processing algorithms. [C8716]

"A versatile through-the-wall doppler radar using BSS algorithms"

Doppler heart sensing radar has been developed for various healthcare and personnel detection applications. For through-the-wall sensing of personnel, the radar operator's cardiopulmonary activity may be detected due to reflection of the radar signal at the wall. This heart-motion signal may be considerably stronger than that from the subject of interest behind the wall. This paper presents a calculation of signal power expectations for detecting heart motion of both the radar operator and a subject behind a wall, and shows preliminary simulations using a blind source separation (BSS) algorithm to confirm the possibility of distinguishing these two heart-motion signals of widely different strength. [C8717]

"A power-efficient CMOS UWB signal-generation module"

This paper presents a new carrier-based ultra-wideband (UWB) transmitter architecture and its CMOS implementation. The new transmitter topology adopts a double-stage switching to enhance RF-power efficiency, reduce dc-power consumption and circuit complexity. Fabricated using a 0.18- μm CMOS process, the UWB signal generation module includes an UWB sub-nanosecond-switching single-pole single-throw (SPST) switch and a tunable impulse generator. Measurement results show that the generated UWB signal has variable 10-dB signal bandwidths from 0.5 to 4 GHz and tunable central frequency covering the entire UWB frequency range of 3.1 to 10.6 GHz. The CMOS module consumes less than 2 mW DC power. The proposed carrier-based UWB transmitter and the demonstrated module provide an attractive means for UWB signal generation for both UWB communications and radar applications. [C8718]

"Detection of buried metal structures using ground penetration radar techniques: A numerical study"

This paper investigates the resonance characteristics of metal structures based on numerical analyses. The complex natural resonances (CNR) are calculated using the FDTD method. Although CNRs are intrinsic to a metal structure, it is found that many factors affect their extraction from the scattered signals. We investigate some of these factors and point out useful guidelines that may be employed in the characterization of buried metal. [C8719]

"Multipath height finding in the presence of interference"

A new method is proposed for multipath target height finding with a non-coherent, narrowband radar in the presence of interference. The technique is based on an ultra-wideband fusion technique for sparse-band frequency processing originally developed for wideband imaging. It is illustrated with data collected during the mountaintop program. [C8720]

"Frequency domain feature extraction from synthetic aperture radar data"

Most feature recognition and classification algorithms for synthetic aperture radar (SAR) are done in the image domain, and thus do not explicitly exploit the scattering physics underlying the data. Feature extraction in the phase domain is based on electromagnetic scattering models which describe the sensor response to scene features. This idea of processing the SAR data using a filter matched to the phase history signature of a feature was introduced by Franceschetti (1997). Here, we extend the original concept for processing the raw signal to processing the spotlight mode SAR signal. We use a sensor model based on an experimental airborne SAR developed by MIT Lincoln Laboratory, the Lincoln Multimission ISR Testbed (LiMIT). To demonstrate the concept, line feature filters are applied to a simulation of a building from the LiMIT dataset. [C8721]

"Performance analysis on subsurface target depth detection using the E-Pulse Technique"

Numerical models of a hip prosthesis model sited within two different realistic human tissue models have demonstrated that the E-Pulse technique is capable of detecting target depth changes inside a frequency dependent lossy halfspace. The performance is highly related to the dielectric properties of the half space and the excitation frequency. The dispersive attenuation factor of the halfspace and the frequency response of the same target below two different halfspaces were also studied and it is concluded that the attenuation factor, the resonance frequency of the target and the Q factor of the resonant peaks are all closely related and directly affect the E-Pulse detection performance. [C8722]

"Human respiration rate estimation using body-worn ultra-wideband radar"

This paper demonstrates the use of UWB radar in non-contact monitoring of respiration rates. Based on the proposed propagation model, it was shown that the delay information of the first echo conveys useful information on the breathing signal. Critical system design parameters have been identified through a sinusoidal approximation of the antenna heights. With a simple signal processing algorithm, it was verified via simulation that the respiration rate could be accurately measured for very low SNR values. Specifically, the influence of human body/cloth movements on the estimation accuracy is investigated. In future, we will be looking into the potential of employing such a system for heart beat detection. [C8723]

"Evaluation of the Multicast Mode of MBMS"

Multicasting is an efficient way for delivering rich multimedia applications to large user groups as it allows the transmission of packets to multiple destinations using fewer network resources. Content and service providers are increasingly interested in supporting multicast communications over wireless networks and in particular over universal mobile telecommunications system (UMTS). To this direction, the third Generation Partnership Project (3 GPP) is currently standardizing the multimedia broadcast/multicast service (MBMS) framework of UMTS. In this paper, we present an overview of the MBMS multicast mode of UMTS. We analytically present the multicast mode of the MBMS and analyze its performance in terms of packet delivery cost under various network topologies, cell environments and multicast users' distributions. Furthermore, for the evaluation of the scheme, we consider different transport channels for the transmission of the data over the UTRAN interfaces and propose a cost based scheme for the efficient radio bearer selection that minimizes the packet delivery cost. [C8724]

"Towards Seamless Mobility Support with Cross-Layer Triggering"

This paper presents mechanisms for collecting and processing cross-layer information from mobile devices and networks. That information is further used to feed the handover decisions as a part of the seamless mobility support. This paper presents a mechanism called Trigger Management, developed within the EU's Ambient Network project, for collecting and processing cross-layer trigger information. The trigger management system is bound to the VERHO vertical handover controller system, enabling the handover decisions based on several input parameters. [C8725]

"Discovering Feasible Protocol Stack Combinations in Beyond 3G Systems: Information Model, Search Algorithms and Performance"

Beyond 3G wireless systems will be vested with dynamic reconfiguration capabilities capable of adapting their protocol stacks during runtime to optimize spectrum utilization and, thus, better meet the ever-changing service demands. For protocol stack reconfiguration to become a practical capability, a language for modeling, expressing and circulating data essential to reconfigurable protocol stacks is necessary. We present a generic object-oriented information model for describing the feasible combinations of protocol layers into protocol stacks. The model supports the derivation of an associated ontology specified in standard W3C semantic languages (OWL). We introduce a novel algorithm for discovering all the feasible protocol layer combinations that render valid protocol stacks, thus facilitating the selection of suitable ones. We assess the performance of a prototypical implementation of our algorithm used to discover feasible protocol stack combinations for the GPRS, UMTS and IMS access standards. Finally, we present our conclusions and provide directions for future work. [C8726]

"Tracking Multiple Dynamic Targets with Multidimensional Scaling"

We consider the problem of tracking multiple targets in the presence of imperfect and incomplete ranging information, focusing on the impact of target dynamics. The targets are assumed to describe independent, continuous and differentiable trajectories with non-stationary (dynamic) statistics, i.e., with variable velocities and accelerations. The impact of such dynamics onto the performance, computational complexity and memory requirements of two tracking techniques, namely, the Kalman filter (KF) and multidimensional scaling (MDS), is investigated. The main feature of the MDS-based tracking algorithm, which we proposed in an earlier work, is that tracking is performed over the eigenspace of a Nystrom-Gram kernel matrix constructed with no a-priori knowledge of the statistics of target trajectories. Consequently, tracking becomes a problem of updating the eigenspace given new input data, which is achieved with an iterative Jacobian eigen-decomposition technique. An advantage of this technique over the KF is that tracking accuracy is independent on target dynamics. Furthermore, the number of iterations required to update the eigenspace, is shown to grow only logarithmically with the target dynamics and with the number of simultaneously tracked targets. As a result, the MDS-based tracking algorithm with Jacobian eigenspace updating becomes more efficient than the KF as soon as a relatively small number of targets are simultaneously tracked, and/or target dynamics exceeds a certain threshold. [C8727]

"Utilizing the energy of each of the extracted poles to identify the dominant complex natural resonances of the radar target"

A novel technique, based on utilising the energies of the CNRs, has been introduced in this paper to identify the dominant poles, from a pool of extracted CNRs, of a simple PEC target in free space with different Signal-to-Noise ratios. The proposed dominant poles identification scheme does not require any knowledge of the modal order of the system. Applying this new technique to low Quality-Factor (Q-Factor) target and dielectric target will be the subject of further investigations. [C8728]

"Design of more affordable and reliable electronically-steered phased arrays"

Recent fundamental results (Speciale, 1996) in the theory of linear, multi-port networks enable cost-effective, higher-reliability designs for electronically-steered phased arrays. The referenced paper documents and proves that, by including a properly designed beam-forming network, it becomes possible to feed an array and steer its beam, using a much reduced number of expensive and critical phase- and amplitude-controlled sources, while at the same time completely eliminating the adverse effects of element coupling. Those new results are based on a generalization of the classical concepts of scalar image impedance, and of scalar image-transfer function for two-port networks, to the new concepts of multidimensional image-impedance matrix, and of multidimensional image-transfer function matrix for linear multi-port networks. [C8729]

"Portable High Resolution LFM-CW Radar Sensor in Millimeter-Wave Band"

This paper presents a portable radar sensor developed in the Universidad Politecnica de Madrid. The system

transmits a Linear Frequency Modulated Continuous Wave (LFM-CW) with two-antenna configuration for transmission and reception. The radar transmits at millimeter-wave band with a maximum bandwidth of 2 GHz and a transmitted power of 1 W. The system is modular, compact and lightweight. The sensor allows range intervals tuning and sampling the received signals with a constant rate. By this, it is particularly attractive for portable applications. Finally, the system performance has been tested in a traffic surveillance experiment. [C8730]

"Optimal Passive Source Localization"

In order to optimize the estimation of an object's position, this paper proposes a procedure for placing acoustical sensors in 3D space, using passive source localization. A standard performance measure in estimation theory is the Cramer-Rao Lower Bound (CRLB), which describes the lower bound of the variance of unbiased estimators. In the case of passive source localization, this bound depends on the sensor and source positions, as well as on the propagation speed and the assumptions made about the disturbance noise. A procedure for an optimal sensor placement, using this CRLB as the objective function, is described. In order to assure optimal coverage of a surveillance area, the average CRLB of multiple source positions (in this area) is minimized. [C8731]

"Target existence based resource allocation"

Assume an ESA (electronically steered antenna) radar. In between the surveillance mode operations (where the radar completes one scan of the surveillance area), this radar has spare time for (at least one) additional mode which could be optimized for various special requirements. The optimization is often translated to the choice of the next track to update. In this paper we propose a resource allocation scheme designed to minimize the time to confirmation of tracks following new targets, as well as to minimize the time to terminate tracks whose targets are lost or have disappeared from the view. The resource allocation cost is a function of the probability of target existence of individual tracks. Simulation results show that resource allocation based on this cost significantly increases the number of targets that can be reliably tracked in the sense of them being quickly followed by confirmed tracks upon arrival, and of their tracks being quickly terminated when the targets themselves disappear. The penalty of this approach is an increase in the root mean square target trajectory estimation errors of confirmed true tracks, as they are not updated as often. [C8732]

"Time allocation of a set of radars in a multitarget environment"

The question tackled here is the time allocation of radars in a multitarget environment. At a given time radars can only observe a limited part of the space; it is therefore necessary to move their axis with respect to time, in order to be able to explore the overall space facing them. Such sensors are used to detect, to locate and to identify targets which are in their surrounding aerial space. In this paper we focus on the detection schema when several targets need to be detected by a set of delocalized radars. This work is based on the modelling of the radar detection performances in terms of probability of detection and on the optimization of a criterion based on detection probabilities. This optimization leads to the derivation of allocation strategies and is made for several contexts and several hypotheses about the targets locations. [C8733]

"A fusion study of the FAVS sensors suite"

This paper presents a fusion process developed for the future armoured vehicle system (FAVS) technical demonstration (TD) project. One of the project objectives was to develop, optimize and demonstrate a multi-sensor suite mounted on an army vehicle to detect and identify targets while the platform was moving. The sensors consisted of a cooled infrared camera, millimetre-wave radar and a defensive aide suite. For the purpose of this paper, only the first two sensors were considered in the fusion study. This paper presents the sensor suite, the fusion process, a description of a field trial used to gather target detection data, and the results and analysis of the fusion process. [C8734]

"A novel framework for the network-wide distributed detection problem"

This paper presents a new framework for distributed target detection in wireless sensor networks (WSNs). In our previous work, for multiple networked sensors collaboratively detecting the presence or absence of a target in the sensor field, every sensor uses an identical threshold for local decision-making. In this paper, we propose a framework where the sensors in the network collaboratively decide and select non-identical thresholds to improve network-wide detection performance in a dynamic manner. This threshold selection scheme is based on a new statistical metric called false discovery rate (FDR). Assuming a signal attenuation model, where the received signal power decays as the distance from the target increases, various performance indices like system level probability of detection and probability of false alarm are studied. Analytical and simulation results are provided for system level probability of false alarm and probability of detection. Performance comparison

between the proposed approach and the classical identical local sensor threshold approach is provided to demonstrate the effectiveness of this scheme. [C8735]

"Multiple target tracking with asynchronous bearings-only-measurements"

An algorithm for detection and tracking of multiple targets using bearings measurements from several sensors is developed. The algorithm is an implementation of a multiple hypothesis tracker with pruning of unlikely hypotheses. Tracking conditional on each hypothesis can be performed using any suitable filtering approximation. In this paper a range- parameterized unscented Kalman filter is used. Each hypothesis describes a track collection with varying number of targets. Final track estimates are obtained by weighted clustering according to hypothesis probabilities and clustered track states. Simulation experiments include arbitrary setup of multiple targets and multiple moving receiver platforms (sensors). The main results are the asynchronous modeling of measurements arrivals which allows an effective and efficient processing in a Bayesian MHT framework. [C8736]

"Continuous-discrete filtering for dim manoeuvring maritime targets"

Real radar data containing a small manoeuvring boat in sea clutter is processed using a grid based finite difference implementation of continuous-discrete filtering. Both two dimensional diffusion and four dimensional constant velocity models are implemented using Gaussian and Rayleigh sea clutter models. Superior performance is observed for the constant velocity model and significant sensitivity is noted due to mismatches between actual clutter characteristics and Gaussian and Rayleigh models. A simple likelihood ratio thresholding technique is shown to provide a significant performance improvement. [C8737]

"A sequential ESM track association algorithm based on the use of information theoretic criteria"

In this paper, a sequential track association algorithm for multiple electronic support measures (ESM) sensors is proposed based on the application of clustering techniques. Association metrics are developed based on the use of the information theoretic criteria, in particular, the Akaike Information Criterion (AIC). The proposed association algorithm is able to handle track components of differing numbers of subcomponents including incomplete and erroneous ones. It has the advantage of not requiring any subjective threshold setting in deciding a non-association. Computer simulation and actual ESM processors are used to demonstrate the effectiveness and performance of the proposed association approach. [C8738]

"Ground target modelling, tracking and prediction with road networks"

A model for vehicle motion on a road network is developed using an enumeration of feasible routes. Combined with a generic stochastic model of distance travelled, a predicted pdf of vehicle position is derived as a mixture. This approach allows prior information on vehicle intent and behaviour to be included via the mixture weights. Illustrative examples are given using a second-order linear-Gaussian model for vehicle road speed. The value of road map data is shown via a tracking example with poor quality measurements and a substantial period prior to sensor activation. The tracking algorithm is implemented using a standard particle filter. In particular, the scheme has potential for revealing the likely paths taken by the vehicle. [C8739]

"Multisensor tracking and fusion for maritime surveillance"

Over the past several years, the NATO Undersea Research Centre has conducted extensive research in multisensor networks for undersea surveillance, culminating in the development of the DMHT tracker. In this paper, we discuss upgrades to this technology and its application to maritime surveillance. [C8740]

"Adaptive censored cell-averaging CFAR detection in distributed sensor networks"

This paper presents a new distributed CFAR (constant false alarm rate) detector based on the adaptive censored cell-averaging CFAR technique. In the scheme, every local decision of individual detector, resulting from the comparison between its sample in test cell and the estimate of clutter power level of its reference samples, takes the value zero or one. In local processor, the CCA-CFAR (censored cell-averaging) technique is utilized to get the local decision. Then, the fusion center makes the global decision based on the total local decisions, which are transmitted from each local sensor. The overall decision, which is zero or one, is obtained at the data fusion center grounded on "k/N" fusion rule. The results show that for the nonhomogeneous background caused by multiple interfering targets, this approach is more reality. Particularly in multiple target situations, it exhibits robustness than MOS (maximum order statistic), mOS (minimum order statistic), and OSOR (ordered statistics), ORAND in distributed sensor networks. Under Swerling 2 assumption, the analytic expression of false alarm and detection probability are derived. [C8741]

"Distributed data fusion algorithms for tracking a maneuvering target"

The focus of this paper is on examining the accuracy of two existing state vector fusion methods, weighted covariance fusion (WCF) and information matrix fusion (IMF), in a multi-sensor environment for computing the fused estimates from distributed Kalman filters tracking a single maneuvering target. Each sensor tracker utilized in the Reference Cartesian Coordinate System (RCCS) is described for target tracking when the radar measures range, bearing and elevation angle in the Spherical Coordinate System (SCS). Simulation results show that the IMF method has more efficient and robust capabilities of improving tracking accuracy than the WCF method.

[C8742]

"A distributed stand-in EW hunter-killer system"

DSTO Australia concluded a two year research program in March 2006 that demonstrated distributed, autonomous, self-organising stand-in sensor and effector systems. This paper describes research activities from this program including the development of miniaturised sensor and effector payloads, the development of novel algorithms for the fusion of data from distributed sensor payloads and the development of novel aircraft control algorithms to enable near optimal geo-location of pop-up emitters. The paper also describes field trials in which information products from these systems were injected into command support systems for integration and visualisation with other data to support situational awareness. A follow-on program has been approved and is also overviewed in this paper. [C8743]

"Distributed adaptive CCAWCA CFAR detector"

In the sense of likelihood ratio test (LRT), a new type of distributed constant false alarm rate (CFAR) scheme-CCA WCA(censored cell-averaging -R-weighted cell averaging) CFAR detector is presented. Its characteristic is that censored cell-averaging (CCA) CFAR algorithms are used in local processors to form the estimation of SNR of local observations, and then the estimation transmitted to the data fusion center (DFC). Finally, the fusion center makes the final decision based on the weighted cell averaging (WCA). Since the weights are adjusted according to different SNR adaptively, the proposed detector can be available in the case that the target echo and noise/clutter have different level for every sensor. In addition, it does not need a priori knowledge about the interference in order to perform well. Furthermore, unlike the OS-CFAF the tolerance of interfering targets is restricted in appointed k value's. Under Swerling 2 assumption, the analytic expression of detection probability and false alarm probability are derived. [C8744]

"Change detection methodology based on region classification fusion"

In this paper, several classification methods are presented and a fusion structure is included to improve the final classification performance. The definition of "layer" and the method to create it are then introduced. Based on "layer", a multiple level change detection algorithm is proposed, which gives the details of the changes in each region and is demonstrated to be an easy, effective and reliable method. Experimental results are provided using RADARSAT images, which have been registered with the automated registration algorithm of A.U.G. Signals that is currently available under the distributed processing system www.signalfusion.com. [C8745]

"Exploitation of bistatic doppler measurements in multistatic tracking"

The exploitation of bistatic Doppler measurements for multistatic tracking is considered. It is found through simulation, that, while the velocity estimation of the standard extended Kalman filter is improved in monostatic situations and multistatic situations where measurement errors are small, a degradation in performance is observed in multistatic situations where the measurement errors are realistically large. A bistatic modification to the alternate EKF of Bizup and Brown (2003) is proposed as a means of exploiting bistatic Doppler measurements in realistic multistatic situations. Simulation results confirm that the proposed filter outperforms the standard EKF and can produce significantly improved target velocity estimates when Doppler measurements are exploited in multistatic applications. [C8746]

"Sensor selection: the modified riccati equation approach compared with other selection schemes"

In this paper a comparison is made between a sensor selection algorithm (SSA) based on the modified Riccati equation (MRE) on the one hand, and a random sensor selection (RSS) or a fixed sensor selection (FSS) scheme on the other hand. The goal is to investigate the benefits the MRE SSA yields compared to the other selection schemes. The MRE SSA is capable of handling sensors with probability of detection $p_d < 1$ and performs sensor selection based on various expected performance criteria in a target tracking scenario. For all three selection schemes the particle filtering technique has been used for target tracking with an adaption for

missed detections in the case of $p_d < 1$. Results are compared using multiple runs with simulated data for a single, moving target and two stationary radars. One sensor yields range, Doppler and bearing information, the other range and bearing information. The analysis includes the quality of the state estimate and the sensor selection strategy. [C8747]

"Track to track fusion using out-of-sequence track information"

Fusing out-of-sequence information is a very important problem for multi-sensor target tracking systems. The challenge is in dealing with measurements that arrive from the various sensors at a central processor out-of-sequence; that is, signals arriving with a measurement relating to a time previous to the time of the current state. The problem of how to deal with these updates has received much attention in recent years and has been solved optimally and sub-optimally by various authors. Most of the solutions, however, treated only the problem of updating a track by out-of-sequence measurements (OOSM), but did not deal with the updating of a central track by local tracks. In this paper we adopt three solutions proposed by Bar-Shalom, for the OOSM problem, and adapt them to solving the out-of-sequence track (OOST) problem. We then demonstrate their application to the case of track-to-track fusion. [C8748]

"Ground target tracking using terrain information"

In this paper a hybrid Kalman filter is derived for the tracking of ground based targets. The propagation is performed using unscented Kalman filter equations, while the updates are performed using extended Kalman filter equations. The novel feature of this hybrid filter is that terrain information has been incorporated to improve the accuracy of state estimates. This information, termed trafficability, incorporates local terrain slope, ground vegetation and other factors to put constraints on the vehicles maximum speed. The estimated velocity vector is deflected based on the trafficability values of nearby locations. Simulations show that the use of trafficability can improve estimated accuracy in locations where the vehicle path is influenced by terrain features. [C8749]

"Multi level fusion with confidence measures for automotive safety applications"

The fusion of data from different sensorial sources is today the most promising method to increase robustness and reliability of environmental perception. The paper presents an approach for using fuzzy operators for the hierarchical fusion of processing results in a multi sensor data processing system for the detection of vehicles in road environments. Tracking and fusion of intermediate results is performed in several levels of processing (signal level, several feature levels, object level). To produce higher level hypotheses on the basis of lower level components, grouping rules using certain assignment decisions are used. In this paper this is seen as a classification procedure that is testing and assigning components step by step to a higher level feature or object. For these classifications a suitable combination of a fuzzy operator for fusion and membership functions for classification is proposed to meet the requirements of the hierarchical classification and the necessity to include confidence values for that. An example is given for the fusion of image and radar data in a vehicle detection algorithm. [C8750]

"Fusion of over-the-horizon radar and automatic identification systems for overall maritime picture"

Over-the-horizon (OTH) radar and automatic identification system (AIS) are commonly used in the surveillance of maritime areas. This paper presents a method, which includes tracking and association algorithms, for fusing the information from these two types of systems into an overall maritime picture. Data to be fused consists of asynchronous track estimates from the OTH system and measurements obtained from AIS. The data available at the fusion center, as output of real world systems, contained incomplete information, compared to theoretical tracking and fusion algorithms. A method to estimate the missing information in the input data is described. Results obtained using real data as well as simulated data are presented. This type of fusion provides overall pictures of maritime areas, with benefits for surveillance against military threats, as well as threats to exclusive economic zones. [C8751]

"Automatic ship positioning and radar biases correction using the hausdorff distance"

This paper describes a novel technique to obtain radar biases estimates that can effectively reduce mismatches in track association algorithms. This is accomplished by matching ship-borne radar images to geo-referenced satellite images. The matching is performed through the minimization of the averaged partial Hausdorff distance between data points in each image. The minimization rapidly yields robust latitude and longitude position estimates, as well as ship heading and radar biases. The accuracy of the measurements is improved by feeding them into a Kalman filter, which also yields estimates for the ship's velocity. The method can be employed for automatic radar calibration of bearing and range biases, while it also serves as an alternative effective position sensor for GPS-denied environments. [C8752]

"Multi-source semantic integration-revisiting the theory of signs and ontology alignment principles"

Current conceptual models for information fusion, including the JDL model do not consider the fact that their information sources are often based on different ontological bases. We therefore suggest that the Alignment functional process of the JDL model, which caters for space and time common referencing, be augmented with the notional aspect of common ontological alignment. We illustrate this with the semiotic triangle and show how symbols relate to conceptualizations which in turn refer to objects of interest within domains of discourse. We then discuss on the notion of ontology alignment and how it is substantiated in a perspective of communication between a source (an addresser) and a fusion node (an addressee). Finally, we discuss on the semantic distance as a result of aligning similar (but not congruent) concepts. [C8753]

"Tracking and fusion of surveillance radar images of extended targets"

Range and angle measurement errors may be correlated when centroid image processing is applied on radar images of extended targets. This paper describes how a model of the correlation between target heading and measurement error can be used to improve the accuracy of tracking filters. The performance of the presented tracking algorithms is tested using a trajectory generator based on jump Markov nonlinear systems. [C8754]

"An operator perspective on net-centric underwater warfare"

In March 2007, the Networked Underwater Warfare Technology Demonstration Project at Defence R&D Canada-Atlantic conducted an at-sea antisubmarine trial utilizing Net-centric warfare (NCW) constructs to demonstrate improved technologies for underwater warfare. User feedback was solicited during and after the trial for the purpose of documenting the manner in which the systems were used during the trial and gaining insight into their potential future usage in NCW activities. This paper describes some of the key issues raised and how they might be addressed in the future. Although some of the issues raised can be addressed through adjustments in the communications strategy, the way ahead for NCW will require a redefinition of the concept of operations for each platform and for the team in order to balance the advantages of the team and platform-centric approaches. [C8755]

"A Boolean Algebra of receiver operating characteristic curves"

A reasonable starting place for developing decision fusion rules of families of classification systems is using the logical AND and OR rules. These two rules, along with the unary rule NOT, can lead to a Boolean algebra when a number of properties are shown to exist. This paper examines how these rules for classification system families comprise a Boolean algebra of systems. This Boolean algebra of families is then shown under assumptions of independence to be isomorphic to a Boolean algebra of receiver operating characteristic (ROC) curves. These decision fusion rules produce ROC curves which become the bounds by which to test non-Boolean, possibly non-decision fusion rules for performance increases. We give an example to demonstrate the usefulness of this Boolean algebra of ROC curves. [C8756]

"Geolocation using video sensor measurements"

Ground target tracking using electro-optical and infrared video sensors onboard unmanned aerial vehicles has drawn a great deal of interest in recent years due to the evolution of inexpensive video sensors and platforms. We present algorithms for geolocation using pixel location measurements which are based on the perspective transformation and includes radial and tangential lens distortions. The covariance of geolocation error takes into account the errors in pixel location, intrinsic and extrinsic camera parameters, and terrain height. Pixel coordinates of the optical center, focal distances along the X and Y axes, lens distortion parameters, and the skew parameter constitute the intrinsic camera parameters. The extrinsic camera parameters include the sensor position and sensor attitude relative a local east-north-up coordinate frame. Numerical results are presented using simulated data. Our results show that the errors in the Euler angles used to represent the sensor attitude is the dominant source of geolocation error. [C8757]

"A case for service-oriented architecture in support of arctic C4ISR"

In this paper, we present the challenges that will be faced in maintaining Arctic domain awareness and the Arctic C4ISR issues that will result from these challenges. We have discussed the characteristics of the legacy client-server system and how it limits the exploitation of all available data. The characteristics of a Service-oriented Architecture that could address some of these issues are presented. Based upon our Service-oriented Architecture research and our experience in developing a test-bed to support sensor integration we have proposed an architecture that can contribute to addressing these Arctic C4ISR issues. Our experience and

results to date strongly suggest that the benefits derived by adapting a Service-oriented Architecture warrant the effort needed to fully develop this capability. [C8758]

"Drift aware wireless sensor networks"

The focus of wireless sensor networks is to develop low cost sensors with sufficient computing and communication capabilities to support networked sensing applications. The emphasis on lower cost led to sensors that are less accurate and less reliable than their wired sensor counterparts. Sensors usually suffer from both random and systematic (bias) problems. Even when the sensors are properly calibrated at the time of their deployment, they develop drift in their readings leading to biased sensor measurements. The drift in this context is defined as a unidirectional long-term change in the sensor measurement. Assuming that neighboring sensors have correlated measurements and noting that the instantiation of drift in a sensor is uncorrelated with other sensors and inspired by the resemblance of registration problem in radar target tracking with the bias error problem in sensor networks we devise a novel algorithm for detecting and correcting sensors drifts and show how it improves the reliability and the effective life of the network. [C8759]

"Radar target tracking using an IMM-EV estimators-based switching scheme"

In this paper, we propose a method of combining some interacting multiple model-extended Viterbi (IMM-EV) algorithms for target tracking. The objective of the proposed scheme is to take the maximum advantage of the combined strengths of some IMM-EV algorithms so as to achieve better performance and/or computational efficiency than the IMM and some tracking algorithms. Simulation results demonstrate the aforementioned goal can be achieved. [C8760]

"Optimal bayes joint decision and estimation"

Many problems involve joint decision and estimation, where qualities of decision and estimation affect each other. This paper proposes an integrated approach based on a new Bayes risk, which is a generalization of those for decision and estimation separately. Theoretical results of the optimal joint decision and estimation that minimizes the new Bayes risk are presented. The power of the new approach is illustrated by applications in target tracking and classification. [C8761]

"A distributed information fusion testbed for coastal surveillance"

MacDonald Dettwiler is leading a PRECARN partnership project to develop an advanced simulation testbed for the evaluation of the effectiveness of Network Enabled Operations in a coastal large volume surveillance situation. The main focus of this testbed is to study concepts like distributed information fusion, dynamic resources and networks configuration management, and self synchronising units and agents. This article presents the system architecture with an emphasis on our approach for distributed information fusion. [C8762]

"High Level data fusion system for CanCoastWatch"

In this paper, a goal-driven net-enabled distributed data fusion system is described for CanCoastWatch (CCW) project. Multiple sensors are deployed and managed to achieve the goals of situation assessment using a net-enabled architecture. The local tracks reported by multiple sensors are first integrated into global tracks. Decision making is then performed on basic sub-goals that can be directly derived from the fused global tracks. Finally, a goal-driven rule-based expert system uses the basic sub-goal decisions for goal reasoning. [C8763]

"Track-to-track fusion by a human operator for maritime domain awareness"

This work presents the results of a research activity to establish a framework in which a human operator can perform track-to-track fusion to produce a recognized maritime picture in support of maritime domain awareness. The work consists of three elements: 1) establishing the environment in which the operator will conduct the track-to-track fusion, 2) establish metrics that can be used to evaluate the effectiveness of the process used by the operator, and 3) conduct a trial to determine how the operator conducts fusion. The paper provided an overview of the context in which operators conduct track-to-track fusion. A survey of potential metrics was conducted and the ones that could be supported by the data captured during the trial were selected. The main findings of the trial are presented along with recommendation for future trials. [C8764]

"Gaussian mixture cardinalized PHD filter for ground moving target tracking"

The cardinalized probability hypothesis density (CPHD) filter is a recursive Bayesian algorithm for estimating multiple target states with varying target number in clutter. In particular, the Gaussian mixture variant (GMCPHD)

for linear, Gaussian systems is a candidate for real time multi target tracking. The present work addresses the following three issues: (i) we show the equivalence between the GMCPHD filter and the standard Multi Hypothesis Tracker (MHT) in the case of single targets; (ii) using a Gaussian sum approach, we extend the GMCPHD filter by employing digital road maps for road constraint targets. The utilization of such external information leads to more precise tracks and faster and more reliable target number estimates; (iii) we model the effect of Doppler blindness by a target state dependent detection probability, leading to more stable target number estimation in the case of low Doppler targets. [C8765]

"Trajectory clustering for coastal surveillance"

Achieving superior situation awareness is a key task for military, as well as civilian, decision makers. Today, automatic systems provide us with an excellent opportunity for assisting the human decision maker in achieving this awareness. Due to the potential of information overload one important aspect is to understand where to focus attention. Anomaly detection is concerned with finding deviations from normalcy and it is an increasingly important topic when providing decision support, since it can give hints towards where more analysis is needed. In this paper we explore trajectory clustering as a means for representing normal behavior in a coastal surveillance scenario. Trajectory clustering however suffers from some drawbacks in this type of setting and we therefore propose a new approach, spline-based clustering, with a potential for solving the task of representing the normal course of events. [C8766]

"A simple robust detection of weak target in noise radars"

This paper presents a concept of the simple robustification of correlation detector in the noise radar. The simulation results show that it is possible to increase the radar sensitivity in the non-Gaussian (impulsive noise) environment by several dB using nonlinear signal processing. Suggested method introduces only moderate losses (0.5-1.5 dB) in the case where input noise is purely Gaussian. [C8767]

"A low-Noise front-end with beamsteering capability at 35 GHz"

This paper presents a novel implementation of a 35-GHz front-end for beamsteering applications. The achieved low noise figure of only 2.5 dB enables reception of very low-power signals. The 35-GHz input signal is downconverted to 5 GHz. A controllable phase shift is added by utilizing an injection locked voltage controlled oscillator (VCO) to drive the mixer. The phase noise of the local oscillator's signal is reduced by using a cavity reference oscillator with very low phase noise for locking the VCO. A highly compact prototype has been build on RT/Duroid epsiv_r = 10.2 substrate and serves as test case for a future LTCC implementation. [C8768]

"A Ka-band, Magnetron based, scanning radar for airborne applications"

The design and characteristics of a Ka-band, magnetron based radar are described. Novel solutions used for the development of an electrically scanning slotted waveguide antenna array, a low noise digital receiver with a coherent on receiver technique implemented, and an advanced data acquisition and signal processing system are described. Possible applications of the radar are related to enhancing helicopter safety including detection of power lines and other obstacles, monitoring meteorological conditions on the direction of flight, and providing secure landing. [C8769]

"Multi-range and multi-pulse radar detection in correlated non-Gaussian clutter"

This work presents a multi-range cell and multi-pulse approach to radar detection problem. The derived detector performs clutter estimation using the neighboring range cells, clutter cancellation, threshold setting simultaneously and it eliminates the need for a separate CFAR operation. The radar clutter is modeled as compound-Gaussian and assumed to have fully-correlated unknown texture among the range cells in the window of interest. The target signal is composed of an unknown complex return and known Doppler steering vector. Generalized likelihood ratio test (GLRT) is derived by means of estimating the clutter texture parameter and complex target return. Performance of the detector is investigated by means of numerical analysis and Monte-Carlo simulations. [C8770]

"Use of the ground penetrating radar methods for paleontology on example of the mammoth fauna investigation"

In the paper, methods of ground penetrating radar (GPR) are investigated with the purpose of wild animal remains detection, in particular, borders of the mammoth valley and character of the bone fragments. Object of researches are radar methods and GPR systems, a method of detection of the mammoths burial zones, algorithms of processing and representation of the paleontologic data. GPR researches in total amount of 12,000

meters of the GPR profiles are carried out by Radar R&D on terrain "Lugovskoe" (25 kms from Khanty-Mansiysk). As a result of investigations, the congestion zone of the bone remain of mammoths are found out. From the results of experimental researches, the GPR method is practically approved for monitoring of subsurface media with the purpose of revealing the zones interesting for paleontology. The technique of GPR researches is fulfilled and its efficiency is appreciated. [C8771]

"A low-cost 24GHz Doppler radar sensor for traffic monitoring implemented in standard discrete-component technology"

This paper deals with both the implementation and the real-life characterization of a low-cost 24 GHz Doppler radar sensor, purposely designed for the traffic monitoring. To reduce industrial costs as much as possible a discrete-components technology has been adopted for the microwave front-end Plastic packaged devices and fiberglass reinforced substrate are used in such a way as to fit with standard PCB manufacturing processes and automated assembly procedures. The signal manipulation is based on a state-machine algorithm and has been implemented in a 8051 family micro-controller unit. The realized sensor has a typical output power of 6 dBm and mounts a planar antenna with a 3 dB beam-width of plusmn4.5 degrees. The real-life measured performances shows a detection range in excess of 300 meters. [C8772]

"Dispersion analysis of a planar negative group velocity-transmission line"

The existence of a negative group velocity region in a stub-loaded transmission line is investigated, focusing on the reshaping experienced by amplitude modulated signals propagating in it. [C8773]

"Adaptive algorithm for moving target detection and velocity estimation"

This paper presents new radar algorithm for detecting moving targets and measuring target velocities. The algorithm is based on calculating spectrum estimates by using the signals reflected from the adjacent range bins. Statistical hypothesis checking is fulfilled on the difference between the adjacent spectra. The decision-making on distinction between different spectral components is used for estimating velocity of the target. Efficiency of the algorithm is investigated by using statistical modeling. The algorithm is checked by processing a real radar data containing a signal on the background of reflections from rain. [C8774]

"W-band substrate integrated waveguide radar sensor based on multi-port technology"

A 94 GHz collision avoidance radar sensor based on multi-port technology is proposed. This sensor makes use of substrate integrated waveguide (SIW) multi-port circuit fabricated on alumina substrate. The use of integrated waveguide allows for a full integration of the radar sensor front-ends. A specific base-band circuit generates in-phase and in-quadrature signals used to obtain the relative speed of target (including the moving direction) and the distance by elementary signal processing. Simulation and measurement results validate the operating principle of the proposed sensor and also indicate excellent results for relative velocity measurement together with good accuracy of distance measurement. [C8775]

"Automotive 24 GHz pulse radar extended by a DQPSK communication channel"

An increasing number of cars are equipped with radar sensors for different applications observing the car environment. In order to improve the reliability of a single sensor and to gain additional information e.g. by triangulation, data from different sensors can be combined. One step further is to exchange sensor data between neighbouring cars by a data link to continuously transmit vehicle safety relevant sensor information. For this purpose it is necessary to establish an intervehicle communication (IVC) link. This task can be realized by independent communications links. A different attractive approach would be to partially use the hardware and the frequency spectrum of the existing radar sensors. This was the impulse to extend a pulse radar at a center frequency of 24.125 GHz by a communication transceiver in the same frequency band. The communication band, which is small compared to the radar spectrum, is placed in a range with low radar power spectral density. The pulse radar principle was chosen, because it is most common and key components, respectively RF-Frontends, are already available. The principle also provides short measurement times and high dynamic range. In the following the basic concept of the built prototypes and the signal processing of the radar and transceiver on FPGAs are described. The suitability of the system concept is discussed based on measurements and simulations. [C8776]

"Wideband ambiguity function and optimized coded radar signals"

A system efficiently combining radar and communication requires signals with a large time-bandwidth product to achieve high resolution for radar and high data rate. The narrowband approximation of this wideband signal

leads to errors. The narrowband conditions in literature are a gross indication of when the narrowband treatment of a signal is invalid. In this paper a mathematical expression is derived quantifying the error committed when applying the narrowband approximation. This expression decomposes the difference between wideband and narrowband correlation in two components: one only depending on the physical problem parameters (α , τ) and the signal bandwidth, duration, and carrier frequency; the other depending only on the particular signal assumed. This paper proposes a method to evaluate quantitatively when the narrowband approximation is inadequate, and a minimization algorithm to select a signal coding that minimizes the error caused by treating a wideband signal correlation with the narrowband approximation. [C8777]

"Analysis of the signal model for forward scattering radar in case of a small target"

This paper presents the signal model for forward scattering radar (FSR) in the case of a small target and presents the analyses of this model. The equations and graphs for waveform, instantaneous frequency, energy, autocorrelation function and spectrum are given. The empirical modes and Hurst parameter were also calculated and plotted. [C8778]

"Two-dimensional radar imaging with scattered PSK-modulated communication signals"

This paper presents an investigation on the applicability of array signal processing techniques on PSK-modulated data signals. A system design approach is presented and investigated that allows for two-dimensional radar imaging with scattered communication signals. The proposed system concept has been implemented in a simulation model. The applicability of different array processing techniques and their performance regarding resolution and dynamic range has been investigated. [C8779]

"Range Doppler detection for automotive FMCW radars"

The FMCW-Radar-Principle is widely used for automotive radar systems. The basic idea for FMCW-Radars is to generate a linear frequency ramp as transmit signal. The difference frequency between the transmitted and received signal is determined after downconversion. In order to detect range and velocity together, the information, extracted from one frequency ramp, is not enough, because it is ambiguous. Several subsequent ramps have to be generated to remove the ambiguity between the frequency portion produced by range and the doppler frequency. In this paper two methods are presented to perform this basic signal processing step. The two methods have the Fast Fourier Transform as basic calculation step in common, but the number of FFTs and their length are different. The requirements on bandwidth for the IF-Hardware and A/D-Converters are also determined by the algorithm for Range-Doppler-Detection. The CFAR (Constant False Alarm Rate)-Algorithm for target detection must also be adapted to the chosen method. Both methods have been verified with a 24 GHz radar prototype. The Radar-Frontend has been built with a newly developed SiGe-Radar-Chipset on Infineon's B7HF200-Process with a transition frequency of 200 GHz. [C8780]

"Performance analysis of RADARSAT-2 multi-channel MODEX modes"

It has been recognized that a two-aperture approach to ground moving target indication is sub-optimum and that target parameter estimation is often compromised by clutter interference or poor signal-to-clutter ratios. This paper investigates the ground moving target indication (GMTI) performance of several virtual channel concepts proposed for the RADARSAT-2 moving object detection experiment (MODEX). These are capable of increasing the spatial diversity of RADARSAT-2 by exploiting its very flexible antenna programming capabilities and allowing the two-channel SAR system to operate like a three or four channel radar. A high fidelity space-based radar moving target indication simulator (SBRMTISIM) is used to generate virtual channel raw GMTI data for analysis. Moving targets are detected using a combination of the factored space-time adaptive processing (factored STAP) and the cell-averaging constant false alarm rate (CA-CFAR) detector. The detection performance of virtual multi-channel MODEX modes are analyzed and compared with those of the standard two-channel MODEX mode and a true three or four channel space-based radar system. [C8781]

"Technology for ultra broadband reconfigurable beamformer and front-end"

This paper gives an overview of research results from FOI on integrated beamforming components and front-end for ultra wideband phased array. The feasibility of a flexible, wideband antenna array with frequency independent features has been demonstrated. Two objectives are to enable adaptation of beamwidths to different requirements, and to enable a frequency independent beamwidth over a wide frequency range. MMIC true-time delays and reconfigurable active power distribution working in the 2-18 GHz range are also presented. [C8782]

"A low-cost 24GHz doppler radar sensor for traffic monitoring implemented in standard discrete-

component technology"

This paper deals with both the implementation and the real-life characterization of a low-cost 24GHz Doppler radar sensor, purposely designed for the traffic monitoring. To reduce industrial costs as much as possible a discrete-components technology has been adopted for the microwave front-end. Plastic packaged devices and fiberglass reinforced substrate are used in such a way as to fit with standard PCB manufacturing processes and automated assembly procedures. The signal manipulation is based on a state-machine algorithm and has been implemented in a 8051 family micro-controller unit. The realized sensor has a typical output power of 6dBm and mounts a planar antenna with a 3dB beam-width of plusmn4.5 degrees. The real-life measured performances shows a detection range in excess of 300 meters. [C8783]

"Range Doppler detection for automotive FMCW radars"

The FMCW-radar-principle is widely used for automotive radar systems. The basic idea for FMCW-radars is to generate a linear frequency ramp as transmit signal. The difference frequency between the transmitted and received signal is determined after downconversion. In order to detect range and velocity together, the information, extracted from one frequency ramp, is not enough, because it is ambiguous. Several subsequent ramps have to be generated to remove the ambiguity between the frequency portion produced by range and the Doppler frequency. In this paper two methods are presented to perform this basic signal processing step. The two methods have the Fast Fourier Transform as basic calculation step in common, but the number of FFTs and their length are different. The requirements on bandwidth for the IF-Hardware and A/D-Converters are also determined by the algorithm for Range-Doppler-Detection. The CFAR (constant false alarm rate)-algorithm for target detection must also be adapted to the chosen method. Both methods have been verified with a 24 GHz radar prototype. The radar-frontend has been built with a newly developed SiGe-radar-chipset on inflneon's B7HF200-process with a transition frequency of 200 GHz. [C8784]

"Range migration algorithm with resampling in airborne bistatic spotlight SAR systems"

To obtain the SAR images with high quality in the processing of the airborne bistatic spotlight SAR systems in the spatial variant case, we propose a modified range migration algorithm (RMA) with resampling based on the extended Taylor approximation (ETA). After we analyze the azimuth positions of the transmitter and the receiver in the spatial variant case, we compensate the difference of the transmitter velocity and the receiver velocity at the mixing stage of the raw data and the reference signal. Then, the validity of the proposed algorithm is tested with some numerical simulations via a pulsed spotlight SAR simulator. [C8785]

"Appriou bio"

First Page of the Article [C8786]

"A Detection Method of Radar Signal by Wavelet Transforms"

In this paper, an effective detection method of radar signal is presented based on the wavelet analysis. The purpose of this paper is to provide the review of the wavelet analysis research and to detect radar target from radar echo. The theory of wavelet analysis is presented including continuous and discrete wavelet transform. Then specific application, namely radar target detection is presented. In this paper, using wavelet transform to preprocess the radar echo, we are able to obtain multiple data series at different scales of the wavelet transform. These multiple data series can then be used as input to sensors of independent component analysis for detection of a single independent source. The proposed method is applied to radar target detection using a real signal series. It is demonstrated that the method in combination with wavelet transform is effective with feasible result. It has greater theoretical significance and actual applied value in regarded to radar signal processing and target identifying in our aerial defense weapon system. [C8787]

"SAR Image Segmentation Based on Mixture Context and Wavelet Hidden-Class-Label Markov Random Field"

Because of the property that synthetic aperture radar (SAR) image includes plenty of multiplicative speckle noise, a new segmentation algorithm is proposed based on the mixture context and the wavelet hidden-class-label Markov random field (MRF). In our paper, a wavelet mixture heavy-tailed model is constructed, then the hidden-class-label MRF is extended to the wavelet domain to suppress the effect of speckle noise. Since the multi-scale segmentation with overlapping window is presented here, this segmentation method is utilized at the finest scale of stationary wavelet transform (SWT) domain, and the classical segmentation method is also utilized at the coarse scales of discrete wavelet transform (DWT) domain. Finally, a mixture context model is proposed to estimate inter-scale parameters and the optimal segmentation result is derived from a new maximum a posteriori

(MAP) classification. The experimental results show that our method achieves accurate SAR image segmentation result and preserves detailed boundary effectively. [C8788]

"Using a data fusion-based activity recognition framework to determine Surveillance System Requirements"

A technique is proposed to extract system requirements for a maritime area surveillance system, based on an activity recognition framework originally intended for the characterisation, prediction and recognition of intentional actions for threat recognition. To illustrate its utility, a single use case is used in conjunction with the framework to solicit surveillance system requirements. [C8789]

"ML Estimation of true Height in 2-D Radar Network"

In this paper, a method based on maximum likelihood to estimate the target true height in 2-D radar network is presented, and it is mathematically proved that the estimator is unbiased. The Cramer-Rao low bound (CRLB) of estimation error is also derived. Some conclusions are drawn based on simulations. It's concluded that the bearing error only has a bounded influence on CRLB, however, the influence on CRLB exerted by ranging error is unbounded. It's also found that CRLB is superlinear function of target-radar distance, and CRLB affected by target altitude or baseline length acutely as target altitude or baseline length is small. [C8790]

"Track Fusion with Road Constraints"

This paper is concerned with tracking of ground targets on roads and investigates possible ways to improve target state estimation via fusing a target's track with information about a road along which the target is believed to be traveling. A target track is estimated by a surveillance radar whereas a digital map provides the road network of a region under surveillance. When the information about roads is as accurate as (or even better than) radar measurements, it is desired naturally to incorporate such information (fusion) into target state estimation. In this paper, roads are modeled with analytic functions and its fusion with a target track is cast as linear or nonlinear state constraints in an optimization procedure. The constrained optimization is then solved with the Lagrangian multiplier, leading to a closed-form solution for linear constraints and an iterative solution for nonlinear constraints. Geometric interpretations of the solutions are provided for simple cases. Computer simulation results are presented to illustrate the algorithms. [C8791]

"A simple maneuver indicator from target's range-doppler image"

Tracking maneuvering targets presents a great challenge to airborne surveillance radar signal processing and sensor systems management systems. Smears caused by an uncompensated maneuver (either translational or rotational) affect target identification (ID) with distorted target images. An unexpected maneuver introduces large position estimation errors to a tracker and in the worst case loss of track. On the other hand, a sensor manager relies upon an expected performance of a tracker to schedule its resources so as to maintain target ID/tracker performance. To aid a sensor management cost function, we present a simple target maneuver indicator (TMI) specifically for the operational condition of target maneuverability. It relates the slope of a target's range-Doppler image to the underlying turn rate, if the target undergoes a maneuver. As an intermediate product of the range profile formation process, this approach provides an easy and quick indication of target maneuverability and, under favorable conditions, an estimate of such a maneuver (e.g., the turn rate), which can be incorporated into the tracking algorithm of the tracker. [C8792]

"A CMOS 22-29GHz Receiver Front-End for UWB Automotive Pulse-Radars"

The design of a CMOS 22-29 GHz pulse-radar receiver (RX) front-end for ultra-wideband (UWB) automotive radar sensors is presented. Fabricated in a 0.18 μm CMOS process, the 3 mm² RX chip achieves a conversion gain of 35-38.1 dB, noise figure of 5.5-7.4 dB and input return loss less than -14.5 dB in the 22-29 GHz band. The phase noise of the constituent QVCO is -107 dBc/Hz at 1 MHz offset from a center frequency of 26.5 GHz. The total dc power dissipation of the RX including LO/output buffers is 131 mW. [C8793]

"A Ka-band, magnetron based, scanning radar for airborne applications"

The design and characteristics of a Ka-band, magnetron based radar are described. Novel solutions used for the development of an electrically scanning slotted waveguide antenna array, a low noise digital receiver with a coherent on receiver technique implemented, and an advanced data acquisition and signal processing system are described. Possible applications of the radar are related to enhancing helicopter safety including detection of power lines and other obstacles, monitoring meteorological conditions on the direction of flight, and providing secure landing. [C8794]

"A simple robust detection of weak target in noise radars"

This paper presents a concept of the simple robustification of correlation detector in the noise radar. The simulation results show that it is possible to increase the radar sensitivity in the non-Gaussian (impulsive noise) environment by several dB using nonlinear signal processing. Suggested method introduces only moderate losses (0.5-1.5 dB) in the case where input noise is purely Gaussian. [C8795]

"Performance analysis of RADARSAT-2 multi-channel MODEX modes"

It has been recognized that a two-aperture approach to ground moving target indication is sub-optimum and that target parameter estimation is often compromised by clutter interference or poor signal-to-clutter ratios. This paper investigates the Ground Moving Target Indication (GMTI) performance of several virtual channel concepts proposed for the RADARSAT-2 moving object detection experiment (MODEX). These are capable of increasing the spatial diversity of RADARSAT-2 by exploiting its very flexible antenna programming capabilities and allowing the two-channel SAR system to operate like a three or four channel radar. A high fidelity space-based radar moving target indication simulator (SBRMTISIM) is used to generate virtual channel raw GMTI data for analysis. Moving targets are detected using a combination of the Factored Space-Time Adaptive Processing (Factored STAP) and the cell-averaging constant false alarm rate (CA-CFAR) detector. The detection performance of virtual multi-channel MODEX modes are analyzed and compared with those of the standard two-channel MODEX mode and a true three or four channel space-based radar system. [C8796]

"W-band substrate integrated waveguide radar sensor based on multi-port technology"

A 94 GHz collision avoidance radar sensor based on multi-port technology is proposed. This sensor makes use of substrate integrated waveguide (SIW) multi-port circuit fabricated on alumina substrate. The use of integrated waveguide allows for a full integration of the radar sensor front-ends. A specific base-band circuit generates in-phase and in-quadrature signals used to obtain the relative speed of target (including the moving direction) and the distance by elementary signal processing. Simulation and measurement results validate the operating principle of the proposed sensor and also indicate excellent results for relative velocity measurement together with good accuracy of distance measurement. [C8797]

"Adaptive algorithm for moving target detection and velocity estimation"

This paper presents new radar algorithm for detecting moving targets and measuring target velocities. The algorithm is based on calculating spectrum estimates by using the signals reflected from the adjacent range bins. Statistical hypothesis checking is fulfilled on the difference between the adjacent spectra. The decision-making on distinction between different spectral components is used for estimating velocity of the target. Efficiency of the algorithm is investigated by using statistical modeling. The algorithm is checked by processing a real radar data containing a signal on the background of reflections from rain. [C8798]

"Use of the Ground Penetrating Radar Methods for paleontology on example of the mammoth fauna investigation"

In the paper, methods of ground penetrating radar (GPR) are investigated with the purpose of wild animal remains detection, in particular, borders of the mammoth valley and character of the bone fragments. Object of researches are radar methods and GPR systems, a method of detection of the mammoths burial zones, algorithms of processing and representation of the paleontologic data. GPR researches in total amount of 12,000 meters of the GPR profiles are carried out by Radar R&D on terrain "Lugovskoe" (25 kms from Khanty-Mansiysk). As a result of investigations, the congestion zone of the bone remain of mammoths are found out. From the results of experimental researches, the GPR method is practically approved for monitoring of subsurface media with the purpose of revealing the zones interesting for paleontology. The technique of GPR researches is fulfilled and its efficiency is appreciated. [C8799]

"Comparison of bistatic signatures of octahedral and icosahedral reflectors in high-frequency domain"

In this paper, the bistatic polarimetric signatures of perfectly conducting octahedral and icosahedral reflectors with high dimensions with respect to the wavelength, are considered. A closed form solution for their fast computation is developed and results are compared. These particular faceted polyhedra, both composed by several identical elementary reflectors, should exhibit a large bistatic and monostatic radar cross section (RCS) over a wide angular range. The proposed method is based on coherent summations of the asymptotic solution of the trihedral corner reflector (TCR): the elementary reflector, evaluated for any incidence and observation angles.

This can be done with the help of geometrical optics (GO) to take into account shadowing effects. Physical optics (PO) and GO are used to derive the contribution of the TCRs in single, double and triple reflections. First order diffractions are also included in the analysis with the help of method of equivalent currents / incremental length diffraction coefficients (MEC/ILDC). [C8800]

"Joint influence of rain rate and turbulence on radar signal spectrum width"

This paper presents the developed model description and the calculation results of the joint influence that both rain intensity and turbulence produce on the spectrum width of the reflected signal in microwave frequency band. The model provides the possibility to calculate backscattered signal parameters at wide variety of the initial data. [C8801]

"Waveform design for radar-embedded communications"

This paper considers the embedding of a covert communication signal amongst radar backscatter by means of a tag/transponder that lies within the illuminated area of the radar. Past approaches have operated on an inter-pulse basis whereby a communication symbol/identifier is relayed to an intended receiver by imparting a Doppler-like phase-shift to each of a successive series of incident radar pulses. In contrast, the approach proposed in this paper operates on an intra-pulse basis whereby the incident radar waveform at the tag/transponder is "re-modulated" into one of a set of different waveforms each representing a different communication symbol. The particular design issues for these re-modulated waveforms are discussed and three general design methods are proposed. The effectiveness of the different methods is assessed in terms of the probability of communication error as a function of the respective powers of the embedded communication signal, the masking radar backscatter, and noise. The relative "covertness" of the resulting waveforms is also discussed. [C8802]

"An UWB Wall Scanner Based on a Shape Estimating SAR Algorithm"

This paper describes a complete pulse based high-resolution radar system. This includes the transmitting and receiving unit as well as the signal processing of the down-sampled echoes. The main focus of the hardware design was on the usage of low-cost components. The signal evaluation is based on the shape reconstruction of simple targets in order to use the proposed radar system for wall scanning applications, e. g. the detection of water pipes. [C8803]

"A SiGe-BiCMOS UWB Receiver for 24 GHz Short-Range Automotive Radar Applications"

This paper presents a SiGe receiver IC for 24 GHz short-range automotive radar based on pseudo-noise code modulation. An on-chip 48 GHz LC-VCO plus frequency divider generate the 1/Q clock signals for zero-IF down-conversion. The 24 GHz output signal of the first frequency divider is available off-chip as carrier for the accompanying transmitter IC. The IC includes two LNAs with built-in single-ended to differential conversion. On-chip coplanar transmission lines on a ground shield are used extensively throughout the IC for distribution of RF and clock signals. The 1.5x1.7 mm² receiver IC is implemented in a SiGe:C BiCMOS process with $f_t/f_{max} = 130/140$ GHz. The IC achieves a measured DSB noise figure below 7 dB across a 2.5 GHz DSB IF bandwidth, with a conversion gain of 39 dB. [C8804]

"Sensor Nodes for Doppler Radar Measurements of Life Signs"

Human life signs can be detected at a distance using mono-static Doppler radars operating in the CW mode. Phase stability of the measurement system plays an important role in successful life signs detection. In this paper it will be shown that small unwanted mechanical motions of the transmit antenna, result in unrecoverable phase errors in the received signal. To overcome this issue, we propose to use a bi-static radar with a sensor node receiver placed in the vicinity of the human subject. Theoretical and experimental results confirm the benefits of using sensor nodes. [C8805]

"A 26GHz Short-Range UWB Vehicular-Radar Using 2.5Gcps Spread Spectrum Modulation"

A 26 GHz short-range radar (SRR) system has been developed based on a 2.5 Gcps direct sequence spread spectrum (DSSS) technique combined with simple homodyne detection. Separate frequency-triplers have been provided with transmitter (TX) and receiver (RX) chips to cut off the carrier-leakage path from local signal. By using this configuration, carrier-leakage in TX signal can be significantly suppressed falling into the satisfactory range of the UWB regulation. The present radar system achieved the maximum detection range of 14 m with the resolution of 6 cm. TX, RX, and PN generator chipset has been developed using InGaP/GaAs HBT process, where f_t/f_{max} of 65 GHz/ 83 GHz were attained. [C8806]

"Study of Key Techniques Applied in Radars of Locating Enemy Artilleres"

The method for identifying a projectile navigating model using a Kalman filter is proposed. The process of locating enemy artillery using numeric analysis is introduced. The method for estimating locating errors is proposed firstly. Finally, the results of computer stimulation are presented. [C8807]

"The Short-Time Multifractal Spectral Analysis Based on the Singularity Exponents"

In this paper, a short-time multifractals models has been proposed, which is an extension of multifractals models. In the section 2, the mind of short-time multifractal spectrum has been introduced. In section 3, the short time multifractal spectrum based on the singularity exponents have been proposed. In section 3 is the calculation method of short time multifractal spectrum, and we analyzed the short-time multifractals characteristics of sea clutter, the simulation shows that the multifractal spectrum is time-varying, and the short-time multifractal spectrum is a new tools on complex fractal signal. [C8808]

"Adaptive Nulling Methods with Multiple Constraints for Transmitting DBF"

Adaptive nulling methods with multiple constraints for transmitting Digital Beamforming (DBF) of Uniform Linear Arrays (ULA) are proposed in the following three circs, with main lobe constraint only, with main and side lobes constraints, with main and side lobes constraints and given nulls constraint. And the optimum weight vector of transmitting DBF is derived by Lagrange multiplier approach and calculated with sample matrix inversion algorithm. The computer simulations show that the proposed methods are practicable and effective. [C8809]

"A Blanket Deception Jamming Rejection Approach Based on Jamming Sample Recognition"

Blanket deception jamming is characteristic of both noise jamming and deception jamming, which cause some traditional anti-jamming measures invalid such as sidelobe canceling and sidelobe blanking and so on. In this work, an approach of time-space cascade adaptive sidelobe canceling based on jamming sample recognition is presented. Even when the number of jamming is more than that of auxiliary channels, the suppression results is still very good. The computer simulations demonstrate the validity. [C8810]

"A Fully-Automated Measurement System for 77-GHz Mixers"

A fully-automated measurement system for 77-GHz mixers is presented. Power and frequency of LO signal plus up to three RF signals can accurately be configured. The RF signals are combined before being applied to the device under test (DUT) making single and dual tone measurements possible combined with the emulation of a blocking signal as important for transceiver applications. Thus, for the first time to the author's knowledge, it is possible to gain detailed insight into the large-signal behaviour of 77-GHz mixer circuits using an integrated low-cost solution. [C8811]

"A Wireless Location System for Sensing the Relative Position between Mining Vehicles"

In this paper a novel system and concept for sensing the relative position between mining vehicles is introduced. The localization is based on secondary radar like distance measurements between radar basestations on the excavator and transponders on the truck. Based on a novel geometry-matching algorithm it is possible to determine the relative position between truck and excavator precisely even in complex measurement and environmental conditions. The geometry-matching algorithm overcomes problems of usual triangulation based approaches because it efficiently reduces the risk to get an underdetermined set of geometric equations in conditions where measuring paths are shadowed or disturbed. The proposed concept allows for a steady and flexible control of all movements of the truck relative to an excavator and thus can contribute effectively to increase automation and productivity in future mining systems. The results of first full-scale experiments show the consistency and good performance of the proposed approach. [C8812]

"Measurement Augmentation to Compensate for Sensor Registration Using a Neural Kalman Filter"

Sensor measurement systems rely upon knowledge of the functional dynamics between system states and the measured outputs. Errors in sensor measurements come from a variety of sources, but standard systems can easily compensate for only some types of errors. There are well known techniques to compensate for errors that result from such issues as noise and sensor accuracy limitations, but other types of errors are not easily compensated for in standard systems. In target tracking, sensor registration, the result of sensor location and orientation self-reference errors, is a type of error that is not easily compensated for because it causes a deterministic bias or parameter drift, rather than random noise error. Previously, a modification of an adaptive

tracking technique based upon the neural extended Kalman filter was proposed as a technique to provide for on-line calibration for the sensor models. In this work, that technique has been improved by modifying the input vector of the neural network to make use of a combination of the target and ownship state variables. The result is an ability to correct for errors such as sensors registration using less computational complexity in the neural network than previously required. [C8813]

"A Framework for Low Data Rate, Highly Distributed Measurement Systems"

Specific types of distributed measurement and virtual instrumentation systems periodically acquire data from a large number of geographically distributed field terminal devices. Such systems are used in environmental monitoring or in monitoring of various commonalities such as electrical power distribution, gas or water networks. In this article we present a framework for low data rate, highly distributed measurement systems based on the publicly available GSM and GPRS services. By using the framework, it is possible to build a system which is capable to perform local measurements on a large number of geographically distributed measurement points, to collect measured data by using the mobile network, to store them on the server computer and to publish gathered data by providing XML web services interface. The framework is robust, scalable and suited for long-term autonomous operation. The tests showed that the framework is stable and operates properly. [C8814]

"Analytical Solution to Inverse Electromagnetic Scattering: Shape and Position Reconstruction of Dielectric Objects"

An analytical approach to inverse electromagnetic scattering is proposed. Inverse electromagnetic scattering problems deal with the reconstruction of the actual position, the shape, the dimensions and dielectric properties of a dielectric object inside a bounded space region. The technique is based on the use of a known incident field illuminating the space region containing the object. By using a set of measurements of the electrical field scattered by the object under test, an analytical solution can be derived. The solution method makes use of an equivalent source as scattered field's support. Such a source is considered a combination of non-radiating and radiating currents. Analytical results can be achieved by means of the singular system of the scattering operator in a very short computation time. [C8815]

"Through-the-Wall Radar Life Detection and Monitoring"

Technology that can be used to unobtrusively detect and monitor the presence of human subjects from a distance and through barriers can be a powerful tool for law enforcement, military, and health monitoring applications. To this end, ultra-wide band radar has shown promise for real-time subject imaging, and compact Doppler radar solutions have demonstrated potential for providing non-invasive detection and monitoring of cardiopulmonary activity for multiple subjects. These technologies work through walls and other obstructions, and can even leverage the presence of ambient radio signals to provide a covert means to detect, isolate, and physiologically monitor multiple human subjects from a remote position. Practical applications ranging from counter-terrorism to health monitoring require systems that are accurate, affordable, and easy to use. Current research efforts addressing these challenges through radio, signal processing, and sensor networking will be presented. [C8816]

"Some aspects of design and measurements results prediction for a Mobile Observation Point for a hydrocarbon pollution monitoring system"

The idea of mobile observation point (MOP) dedicated for a hydrocarbon monitoring system is presented. The main technical problems related to the monitoring system and MOP are described. Special attention was paid for a results of measurements prediction procedures. The main advantages and disadvantages of proposed solution are discussed. [C8817]

"A numerical evaluation of an optimal setup for a microwave axial tomograph aimed at the inspection of wood"

This paper presents the results of model based numerical simulations (Ansoft HFSScopy) used to analyze the scattering of the electromagnetic field on sample objects, in order to determine an optimal setup for a new microwave tomograph aimed at the inspection of wood trunks. Such a tomograph is targeted to obtain images of the cross section of dielectric cylinders. In particular, it was used to inspect wood slabs and trunks in order to search for defects and voids. For best results of the inversion (tomographic image reconstruction) algorithms, it is important that the measured data (samples of the scattered electric field) are collected under an optimal setup configuration of the sample, the illuminating and the pick-up antennas. [C8818]

"High Order Nystrom-PO Hybrid Method for 3D EM Scattering of Arbitrary Shape"

A novel hybrid method that combines high order Nystrom method and PO method is developed in this paper. It is shown that this method is capable of calculating the scattering properties of 3D conductor targets of arbitrary shape and can achieve desired accuracy. This method employs the simplicity and concision of the Nystrom method and PO method and it is suitable for computing the scattering properties of electrically large problems with fine scattering features. Various examples show the applicability of this method. [C8819]

"Bayesian Estimation of Covariance Matrices in Non-Homogeneous Environments"

In many applications, it is required to detect, from a primary vector, the presence of a signal of interest embedded in noise with unknown statistics. We consider a situation where the training samples used to infer the noise statistics do not share the same covariance matrix as the vector under test. A Bayesian model is proposed where the covariance matrices of the primary and the secondary data are assumed to be random, with some appropriate joint distribution. The prior distributions of these matrices reflect a rough knowledge about the environment. Within this framework, the minimum mean-square error (MMSE) estimator and the maximum a posteriori (MAP) estimator of the primary data covariance matrix are derived. A Gibbs sampling strategy is presented for the implementation of the MMSE estimator. Numerical simulations illustrate the performances of these estimators and compare them with those of the sample covariance matrix estimator [C8820]

"Influence of Random Carrier Phase on True Cramer-Rao Lower Bound for Time Delay Estimation"

The true Cramer-Rao lower bound (CRB) for the time delay estimation has been obtained for narrowband signals with the carrier phase as a deterministic parameter already. However, the carrier phase is usually a random parameter in noncoherent receiver in the applications such as radar, sonar and communication systems. And accuracy of the time delay estimation is affected by this nuisance carrier phase. In this paper, the true Cramer-Rao lower bound for the time delay estimation is derived and analyzed in the presence of a random carrier phase. The new bound is tighter than the one obtained under the condition that the carrier phase is not random. We show that this relation indicates the influence of the random carrier phase on the true CRB, and the penalty resulting from this random carrier phase increases severely with decreasing signal-to-noise ratio. The explanation about this influence is also given from the point of information theory. Simulations are provided to support the theoretical results [C8821]

"Sparse Manifold Learning with Applications to SAR Image Classification"

Nonlinear data-driven dimensionality reduction techniques have recently gained popularity due to the emergence of high dimensional data sets. The algorithmic complexity and storage requirements of these techniques, however, can make them prohibitive in resource-limited applications. It is therefore beneficial to reduce the number of exemplar samples required for performing an out-of-sample extension to a test point. In this paper, we propose a novel method for selecting a minimal set of exemplars and performing the out-of-sample extension. In the case of two-class target recognition with synthetic aperture radar (SAR) data, we compare the efficacy of the proposed approach with other approaches for selecting a subset of the available training samples. We show that the proposed algorithm outperforms the existing methods by providing low-dimensional embeddings that maintain interclass separability using fewer retained exemplars [C8822]

"Asymptotic Cramer-Rao Bound for Multi-Dimensional Harmonic Models"

The multi-dimensional harmonic model has attracted considerable attention for a variety of applications in signal processing. Stoica and Nehorai have derived the asymptotic (ie., for large analysis duration) Cramer-Rao lower bound (ACRB) which represents the minimal theoretical variance in the estimation of the model parameters for a one-dimensional harmonic model of order M. In this work, we generalize and analyze the ACRB associated to a M-order harmonic model of dimension P with $P > 1$ [C8823]

"Cramer-Rao Bounds for Range and Motion Parameter Estimations using Dual Frequency Radars"

In this paper, statistical bounds on dual-frequency range estimations are provided. Single frequency (Doppler) radars cannot be used in range estimation due to their range ambiguities. An additional frequency can be used to increase the maximum unambiguous range to accepted values for indoor range estimation of moving targets. The dual-frequency approach offers the benefit of reduced complexity, fast computation time, and real time target tracking. Indoor inanimate objects such as fans, vibrating machineries, and clock pendulums exhibit simple harmonic motions, whereas animate translation movements are typically linear. We provide Cramer-Rao bounds for the parameters defining both types of motions and show their dependency on the observation period and partial knowledge of motion and noise parameters [C8824]

"Threat Estimation of Multifunction Radars: Modeling and Statistical Signal Processing of Stochastic Context Free Grammars"

Multifunction radars (MFRs) are sophisticated sensors with complex dynamical modes that are widely used in surveillance and tracking systems. It is shown in this paper that the stochastic context free grammar (SCFG) is an adequate model for capturing the essential features of the MFR dynamics. We model MFRs as systems that "speak" according to a SCFG, and the grammar is modulated by a Markov chain representing MFRs' policies of operation. We then deal with the statistical signal processing problems of the MFR signal, especially the problem of threat evaluation (electronic support). Maximum likelihood estimator is derived to estimate the threat of the MFR and Bayesian estimator to infer the system parameter values. [C8825]

"An EM-Algorithm for Band-Toeplitz Covariance Matrix Estimation"

Toeplitz covariance matrix estimation has many uses in statistical signal processing due to the stationarity assumption of many signals. For some applications, further constraints may exist on the maximum lag at which the correlation function is non-zero and thereby giving rise to a band-Toeplitz covariance matrix. In this paper, an existing EM-algorithm for Toeplitz estimation is generalized to the case of band-Toeplitz estimation. In addition, the Cramer-Rao lower-bound for unbiased band-Toeplitz covariance matrix estimation is derived and through simulations it is shown that the proposed estimator achieves the bound for medium and large sample-sizes [C8826]

"Generating Binary Processes with all-Pole Spectra"

This paper presents an algorithm to generate autoregressive random binary processes with predefined mean and predefined all-pole power spectrum, subject to specific constraints on the parameters of the all-pole spectrum. The process is generated recursively using a linear combination of the previously generated values to bias the generation of the next value. It is shown that an all-zero filter whitens the process, and, therefore, the process has an all-pole spectrum. The process is also described using an ergodic Markov chain, which is used to determine the appropriate initialization and to prove convergence if the algorithm is not initialized properly. The all-pole parameter range for which the algorithm is guaranteed to work is also derived. It is shown to be a linear constraint on the all-pole parameters and their magnitude, subject to the desired mean for the process. The example and simulations presented elucidate and confirm the theoretic developments [C8827]

"Study on a Nonlinear Frequency Modulation Signal with Polarization-Coded Modulation"

This paper proposes a kind of complex radar signal with polarization agility based on nonlinear frequency modulation (NLFM) signals. This signal has the characteristics of NLFM signals and the anti-jamming ability and performance of low probability of intercept (LPI) can be improved by using the polarization-coded modulation technique. The mathematical expression of the signal is given and the methods of signal processing and target detection are discussed. The performance of the signal is analyzed and simulated when the target signal and the interference are in the different range cells, the results indicate that the target can be detected and the interference can be suppressed by two dimension signal processing when the target can be distinguished from the interference in polarization domain. [C8828]

"LFM extended target echoes detecting using Radon-Wigner Method"

LFM radar signal with sufficient bandwidth will lead to the high range resolution. When range resolution bin is smaller than the target to be detected, radar echoes will occupy multiple range bins. Dechirping and matched filtering are two pulse compression methods for wideband LFM echoes. This paper put forwards Radon-Wigner transform to detect multi- scatter target echoes. Analysis and computer simulation shows Wigner-Ville transformation of multi-scatter LFM signal will not produce the unwanted cross components, and each component in time-frequency spectrum plot are parallel. Radon-Wigner transform can converge the signal energy together to be detected, so it is a effective processing method. [C8829]

"Imaging of space objects using space-borne millimeter wave ISAR"

Imaging of space objects in orbit using space-borne millimeter wave Inverse synthetic aperture radar (ISAR) is investigated. The geometrical and kinetic relationship between the space-borne radar and the object is analyzed. Range walk and range dispersion have occurred during the pulse duration, caused by the high-velocity radial motion. A novel method for radial velocity compensation based on radon-ambiguity transform (RAT) is proposed. Computer simulation illustrates the feasibility of imaging space objects using space-borne radar. [C8830]

"Millimeter Wave Polarimetric Monopulse Radar Debugging System"

For testing millimeter wave polarimetric monopulse radar and testing algorithms for polarimetric radar, millimeter wave polarimetric monopulse radar debugging system is proposed in this paper. Polarimetric radar, as a kind of radar with strong counter-countermeasure capability, is more and more popular used nowadays. The cost of polarimetric radar is more expensive than traditional single-polarimetric radar. Millimeter wave polarimetric monopulse radar debugging system is a kind of assistant instrument. With it, the research cost and period both can be reduced. In the paper, the millimeter wave polarimetric monopulse radar debugging system is introduced in detail. Firstly, the conception of millimeter wave polarimetric monopulse radar debugging system is given; secondly, according to different functions, the debugging system is divided into three modules to be introduced; thirdly, the system key techniques and the performance are given. [C8831]

"Low Noise Low Cost Rx Solutions for Pulsed 24GHz Automotive Radar Sensors"

This work presents the performance of an integrated low noise amplifier (LNA) and Gilbert cell mixer integration and also a voltage controlled oscillator (VCO) performance. Differential topology was used to achieve the down converter. LNA measurements report 22.5 dB gain and about 3.2 dB noise figure at 24 GHz. Large signal results give IP1dBoF -15 dBm. The mixer measurements show very interesting results of 15 dB conversion gain and 5 dBDSB noise figure. This allows a down converter of 31.8 dB gain and 3.5 dBDSB noise figure which provides a dynamic range of 37 dB. The design of these circuits was performed considering temperature and process variations. Nevertheless, results obtained at 24 GHz have never been published using a standard 0.17 μm BiCMOS SiGe 170 GHz featuring 1.7 V B_{vceo} . [C8832]

"Diagonally Loaded Normalised Sample Matrix Inversion (LNSMI) for Outlier-Resistant Adaptive Filtering"

Instead of a "hard" decision on ignoring "outlier" training samples in constructing the covariance matrix estimate, we propose a "softer" method that reduces the impact of such abnormal data samples on adaptive filter performance. Specifically, we introduce a diagonally loaded covariance matrix estimate that is normalised by a generalised inner product (GIP), which is more robust against outliers. We demonstrate the efficiency of this technique on high-frequency (HF) over-the-horizon radar (OTHR) data [C8833]

"Simulation of ISAR Imaging for a Missile"

In this paper, physical optical (PO) method is introduced and applied to calculate the echo data from a missile illuminated by plane waves with arbitrary aspects and different frequencies for inverse synthetic aperture radar (ISAR) imaging. The missile is approximated by component disassembly method (CMD) and concept of scattering matrix is introduced in order to simplify complexity of the numerical calculation. Generated images of several incidence angles are analyzed by signal processing theory and can precisely represent the mirror scattering region and the rotation of the target. The results of the simulation indicate that PO method is simple and effective to calculate the radar echo of a missile for ISAR imaging. [C8834]

"Anti-Millimeter Wave Polarization Agile Active Jamming"

For anti-millimeter wave polarization agile active jamming, interpulse polarization coding technique, as a new polarization signal processing method, is proposed in this paper. The active jamming, as an effective technique to interfere traditional radar, is popular used nowadays. It often works with a single polarization antenna, so it can be identified by polarimetric radar. But a millimeter wave polarization agile active jamming is effective to deceit millimeter wave polarimetric radar. Therefore, a new recognition technique is necessary to be researched for anti-millimeter wave polarization agile active jamming. The purpose of the paper is to present an effective method for countermeasure to millimeter wave polarization agile active jamming. The interpulse polarization coding technology, as a new method using in millimeter wave polarimetric radar, is proposed and a new polarization demodulation method is given in the paper. The results of simulation prove the new method is effective to suppress millimeter wave polarization agile active jamming. [C8835]

"A Spatial Classification Model for Multicriteria Analysis"

This paper stresses that standard multicriteria aggregation procedures either do not assume any structure in data or this structure is in fact assumed linear. Nevertheless, many decision making problems are based upon a family of data with a well denned spatial structure, which is simply not taken into account. Hence, such aggregation procedures may be misleading. Therefore, we propose an alternative model where the aggregation of criteria assumes a certain structure, according to remote sensing data [C8836]

"The Potential Value of Decentralized Trunking as Regulatory Precedent for the Introduction of Dynamic Spectrum Access Technology"

One important way of obtaining the necessary regulatory permissions for dynamic spectrum access ("DSA") technologies from domestic government agencies and the International Spectrum Management Community is to demonstrate that there are policy and legal precedents for their introduction. A recent precedent centers on efforts in the U.S. to allow Unlicensed National Information Infrastructure devices to operate in the 5.25- 5.35 GHz and 5.47-5.725 GHz bands without causing interference to existing radio frequency operations (government radars) through the use of dynamic frequency selection ("DFS") and Transmit Power Control ("TPC"). Another, slightly older precedent is the U.S. Federal Communications Commission's policies and rules that permit the utilization of "decentralized trunking" in the VHF and UHF private land mobile radio ("PLMR") service bands. Under these rules, adequate "monitoring" (a.k.a., "listen-before-talk" or "LBT") is required in order to share spectrum under a decentralized trunking approach. This paper analyzes the potential value of this older precedent in advocating for broader regulatory acquiescence and near-term deployment of DSA technology. Arguably, in the U.S., a DSA radio system using technology to achieve decentralized trunking capabilities could be introduced onto shared channels in the PLMR bands without any major changes in the Commission's existing rules or policies. Using LBT functionality with advanced sensing algorithms, together with DFS and TPC capabilities, could promote shared access via decentralized trunking in the VHF PLMR band, where licensees often employ non-standard channel pairs or un-paired (simplex) channels, and the UHF PLMR band, which is often characterized as overcrowded but underutilized. However, some economic and regulatory barriers to the development of robust secondary market access to these spectrum bands may hinder the full potential of DSA technologies in these bands. [C8837]

"SIP-Based Handoff in 4G Mobile Networks"

It is commonly held that 4G mobile systems were founded on the Internet joined with diverse access technologies. Future network architecture is regarded as various overlapping wireless access segments. To efficiently support seamless mobility is the most critical challenge to integrate various wireless networks in future heterogeneous networking environment. The characteristics of the lower layer protocols are understandably invisible to SIP which provides mobility in the application layer. Hence, SIP is a promising nominee for managing mobility in heterogeneous networks. However, the performance of SIP-based mobility management is downgraded resulting from adopting TCP/UDP for signaling. In this paper, a soft handoff method, namely Bi-CoA, is proposed to shorten the service interruption time when the mobile node frequently handovers between WLAN and UMTS. The simulation results show that the solution proposed in this paper can efficiently support vertical handoff in future heterogeneous wireless networks. [C8838]

"Wearable System-on-a-Chip Pulse Radar Sensors for the Health Care: System Overview"

A new system-on-a-chip radar sensor for next generation wearable wireless interface applied to the human health-care and safeguard is presented. The system overview is provided and a summary of the feasibility study of the radar sensor is presented. In detail, the overall system consists of a radar sensor for detecting the heart and breath rates and a low-power IEEE 802.15.4 ZigBee radio interface, which provides a wireless data link with remote data acquisition and control units. Particularly, the pulse radar exploits 3.1-10.6 GHz ultra wide band signals, which allow a significant reduction of the transceiver complexity and, then, of its power consumption. The operating principle is highlighted and the results of the system analysis are summarized. Such a novel system-on-a-chip wireless wearable interface enables low-cost silicon technologies for contactless measuring of the primary vital signs and extends the capability in terms of applications for the emerging wireless body area networks. [C8839]

"Through-the-Wall Imaging and Sensing: An Electromagnetic Perspective"

In this paper we first briefly outline important areas of research in design of through-the-wall imaging and sensing systems from an electromagnetic perspective. Then we review some of our work in the applications of various polarization contrast techniques for detection of changes due to an object motion and/or orientation behind the wall. Finally, we discuss development of a low-profile wideband antenna array for a portable radar system that can be used in conjunction with polarization contrast algorithms. [C8840]

"Spectral Signature Classification Using A Support Vector Classifier For Real-Time Instrumentation"

The research WSR-88D (weather surveillance radar) locally operated by the National Severe Storm Laboratory (NSSL) in Norman has the unique capability of collecting massive volumes of Level I time series data over many

hours which provides a rich environment for evaluating our new post-processing algorithms. In this work, a Support Vector Machine (SVM) classifier is employed to identify tornado vortices based on their characteristic Doppler spectra and eigen analysis technique. A SVM-based classifier evades the pitfalls of the traditional statistical learning algorithms, such as neural networks, by setting up a convex optimization problem with a single global minimum. In addition, through the use of kernels and nonlinear mapping to higher dimensional spaces, the SVM classifier is able to effectively handle nonlinear classification problems. Finally, the SVM classifier has the added advantage of reducing overfitting by constructing a maximum margin separating hyperplane in a higher dimensional feature space which ensures a small generalization error bound . [C8841]

"Fourier Approach to Moving Target Indication and Detection in Multichannel SAR Data"

This paper outlines a solution to the multi-channel synthetic aperture radar (SAR) moving target indication and detection (MTI/MTD) by means of inverse systems approach. A novel model of the problem is presented and an approximate analytic solution to it will be given. It will be demonstrated how a moving target indicator can benefit from a multichannel SAR system as opposed to a traditional approach that separates MTI and SAR systems. It will be shown that the problem of separation of moving targets from stationary ones can be solved completely by using multi-channel approach and in such a way that a spatial distribution of the stationary targets does not play a role [C8842]

"Information Theoretic Measures for Change Detection in Urban Sensing Applications"

In through-the-wall radar imaging and surveillance applications, it is important for the imaging system to be able to automatically quantify and detect the changes in the imaged scene without the need for operator interpretation. In previous work [1], we considered two information theoretic measures, entropy and divergence, for this purpose. Preliminary analysis of these measures revealed that they can provide reliable notifications of changes in the scene. In this paper, we expand on this work by introducing two different classes of measures, namely, complexity and difference measures. Complexity measures, which includes entropy, quantify the amount of activity in the given scene. Difference measures, on the other hand, are effective at detecting the changes in the imaged scene. Our results, based on experimental data, show that the ratio of the norms is the most sensitive complexity measure and is useful for discriminating between populated and unpopulated scenes, whereas the Jensen-Renyi divergence measure is the most sensitive difference measure and can be applied for change detection in the scene. [C8843]

"Compensation behaviors in echolocating bats measured by a telemetry microphone during flight"

Some echolocating bat species are well known to compensate for the Doppler shifts in the echoes by changing their pulse frequencies so that the echo frequencies remain constant at which the bats can hear best. This behavior is termed "Doppler-shift compensation" and is an important behavioral adaptation for echolocating bats. In this study, we present the evidence for another compensation mechanism of echolocating bats, in which pulse intensity is adjusted in relation to the distance to a target resulting in maintenance of a constant intensity of the echo. Our custom-made telemetry microphone (Telemike) mounted on the back of the bat allowed us to observe not only the emitted pulses, but also the returning echoes which the flying bat actually listened to. The signal characteristics of pulse-echo pairs were analyzed combining with a high-speed video camera system as a bat flying toward the wall on which a landing mesh was attached in the flight chamber. We found that pulse intensity in bats intending to land exhibited a marked decrease by approximately 30 dB within 2 m of distance from the target wall, and the mean reduction rate was 6.5 dB per halving of distance. In contrast, the intensity of echoes returning from the target wall at the head of the flying bat halving of a nearly constant intensity while approaching the target wall. These findings provide direct evidence that bats are supposed to adjust pulse intensity to compensate for changes in echo intensity to maintain a constant intensity within the range necessary for optimal signal processing (echo-intensity compensation). [C8844]

"Remote Monitoring of Vehicle Diagnostics and Location Using a Smart Box with Global Positioning System and General Packet Radio Service"

This paper presents a distributed system for remote monitoring of vehicle diagnostics and geographical position. This is achieved by using on-board microcomputer system, called on-board smart box (OBSB), general packet radio service (GPRS) and a remote server. The OBSB which is equipped with an integrated global positioning system (GPS) receiver is empowered by a software application that manages the processes of local data acquisition and transmission of the acquired data to the remote server via GPRS. When programmed with speed limits in a certain geographical region, the OBSB allows the traffic control authority to supervise violations of speed limits from inside vehicles rather than outside supervision via certain check points. Appropriate vocal and text warning messages are issued when a vehicle exceeds the permitted speed limit at a certain location. A

prototype system is designed and implemented with a small number of sensors. On-road experiments have demonstrated the robustness, efficiency and applicability of the proposed system. [C8845]

"Distributed Collaborative Adaptive Sensing: A Unifying Theme for a Junior Level Embedded Systems Course."

A new junior level embedded systems course uses the notion of Distributed Collaborative Adaptive Sensing as a unifying theme. The content of the course is inspired by research in weather radar networks but is mapped to an imaging system for a more manageable and tangible application. "Big-picture" lectures present concepts and applications in modern embedded systems. The labs involve problem solving in sensor data acquisition, signal processing and networked computing. The Altera DE2 board with System on Programmable Chip (SOPC) development platform, the NIOS softcore [1] and other peripherals is used along with a digital camera [7]. Assessment of the outcomes and impressions of the course indicates a significant improvement over a more traditional embedded systems course. The course materials are available online [2]. [C8846]

"Development of diver detection and sensor integration for wharf surveillance software"

The underwater security sonar system is the port surveillance system which surveys over harbors and ships in order to protect harbor facilities such as wharfs, oil refineries, airports and vehicles, from the terrorism attack under or on the sea. For our surveillance system, it is required to develop the software which can perform "automatic detection of doubtful target" by processing the signal of sonars, and which can provide the high surveillance performance and usability by integrating the information of the sensors. For this purpose, we developed the algorithm for auto-detection and tracking of doubtful target. Also, we developed the algorithm for data acquisition and image processing specialized for the infrared camera for this system. [C8847]

"Vehicle Tracking and Distance Estimation Based on Multiple Image Features"

In this paper, we introduce a vehicle tracking algorithm based on multiple image features to detect and track the front car in a collision avoidance system (CAS) application. The algorithm uses multiple image features, such as corner, edge, gradient, vehicle symmetry property, and image matching technique to robustly detect the vehicle bottom corners and edges, and estimate the vehicle width. Based on the estimated vehicle width, a few pre-selected edge templates are used to match the image edges that allow us to estimate the vehicle height, and also the distance between the front vehicle and the host vehicle. Some experimental results based on real world video images are presented. These seem to indicate that the algorithm is capable of identifying a front vehicle, tracking it, and estimating its distance from the host vehicle. [C8848]

"Development of an Experimental Prototype Multi-Modal Netted Sensor Fence for Homeland Defense and Border Integrity"

Potential terrorists/adversaries can exploit a wide range of airborne threats against civilian and military targets. There is no effective, low-cost solution to robustly and reliably detect and identify small, low-flying airborne vehicles such as fixed-wing aircraft or unmanned aerial vehicles (UAVs) that might be carrying out chemical, biological or nuclear attacks, or smuggling drugs or illegal immigrants across the border. This paper presents a low-cost and low-power methodology for performing key 24/7 sentry functions that can be used for the protection and the surveillance of critical infrastructure from airborne threats. The methodology is based on joint multi-sensor fusion technology. It consists of a forward-based fence comprised of a mixture of selected low cost, low power, netted sensors including a simple radar, acoustic microphone array and optical (infrared and visible) cameras to detect, track and discriminate potential airborne targets. An experimental prototype end-to-end proof of concept system with deployable software, hardware and connectivity is built using COTS component. Multi-modal sensor fusion algorithms employing Kalman filter for target tracking and acoustic and image recognition algorithm for target classification are implemented. Results from field tests reveal reasonable detection and discrimination among candidate aircraft. [C8849]

"Doppler Effect on Location-Based Tracking in Mobile Sensor Networks"

Mobile sensor networks (MSNs) consist of large number of small and computationally impoverished devices deployed over an area to track mobile objects. Mobility is becoming an important feature of MSNs. Recently, sensors have begun to be deployed on mobile platforms such as robots. In this paper, we propose an evaluation of the mobility impact on MSN tracking efficiency. More precisely, we consider the Doppler effect on the results of several target location approaches. Two radar-based angle estimation techniques have been considered: Frequency-Modulated Continuous Wave (FMCW) Radar, and monopulse angle estimation. We also analyze the control of the uncertainty due to Doppler shift through a manipulation of the area coverage (i.e., number of

sensors per area coverage). [C8850]

"SAR Sea Ice Image Segmentation Based on Edge-preserving Watersheds"

This paper presents a hybrid method for the segmentation of SAR sea ice images, which consists of an initial watershed segmentation followed by a region merging. Iterative bilateral filtering is used to reduce speckle noise and suppress irrelevant image details, which can significantly alleviate oversegmentation of watersheds. Since edges are well preserved by bilateral filtering, the watershed algorithm is capable of precisely locating object boundaries. Final segmentation is accomplished by applying an iterative region merging on the watershed regions by taking into account local boundary strengths and regional statistics. The efficiency of the proposed method has been demonstrated on the segmentation of SAR sea ice images. In comparison with traditional watershed algorithm, our method achieves better performance in identifying filament structures such as leads. [C8851]

"Through-the-Wall Radar Imaging Experiments"

In this paper, we present full-polarization imaging results for different settings of calibrated reflectors and the contents of a typical office behind a typical exterior grade wall. An empty scene measurement was also performed to support coherent subtraction with the other scenes for clutter reduction. The images were generated using wideband synthetic aperture beamforming. The results are in agreement with the ground truth. [C8852]

"Multiple Signal Detection and Measurement Using a Configurable Wideband Digital Receiver"

A configurable wideband digital receiver with multiple signal detection capability is presented. The implementation of multiple signal detection scheme is often a challenge due to the timing and hardware constraints. The efficient multiple detection scheme presented in this paper employs hardware reuse by effective configuration and detects multiple signals before the next set of buffered data arrives for processing. Performance evaluation of the configurable receiver to detect up to five signals, their maximum attainable instantaneous dynamic range (IDR) and frequency detection error analysis are presented. [C8853]

"A Low-Cost Ultra-Wideband Indoor Ranging Technique"

This paper presents the development of a low-cost indoor ranging technique based on time-of-arrival (TOA) estimation, using short-pulse ultra-wideband (UWB) signals. The realized system includes two identical UWB transceiver devices, in which the receiver section is based on a tunnel diode detector and the pulse generation is performed by a common bipolar transistor driven in avalanche mode. An indirect measurement of the distance between the devices is obtained by measuring the frequency of the generated pulse train. A theoretical model of the system is described and a statistical analysis is presented, including the evaluation of the Cramer-Rao lower bound (CRLB) on the distance estimation. Furthermore the principle of operation of the realized system prototypes is described, along with some implementation issues. Finally experimental results are shown and discussed. [C8854]

"Estimation of Near-Field Parameters using Spatial Time-Frequency Distributions"

This work deals with the estimation of near-field parameters using passive sensor arrays. A transformation of the array data is proposed which allows the extraction of near-field time-frequency signatures from data containing a mixture of far- and near-field sources. Spatial time-frequency distribution matrices are then used as a means for solving the near-field parameter estimation problem. The estimation accuracy of the proposed approach is compared to existing methods via simulation analysis. An experimental validation of theoretical ideas is also presented. [C8855]

"Algorithm Extension of Cubic Phase Function for Estimating Quadratic FM Signal"

In this paper, an extended algorithm for parameter estimation of quadratic FM signal is derived by exploring the time diversity in the cubic phase (CP) function. The performance of the proposed algorithm is analyzed in terms of estimate bias and variance, and compared with other methods. Although the proposed algorithm employs a fourth-order nonlinearity which results in higher threshold SNR, it provides a number of advantages, such as low mean-square error (MSE) for the estimates at high SNR and simple extension for multicomponent signals. Extension to cubic FM signals is also discussed. The theoretical analysis is verified by the simulation results. [C8856]

"Configurable and Expandable FFT Processor for Wideband Communication"

A practical fast Fourier transform (FFT) processor can contain several millions of gates, so effective design techniques usually are required in order to guarantee high-speed products. A look-up table (LUT) methodology is developed and demonstrated on variable length (128-1024 point), variable bit-precision (6-12 b) FFT with uniform bit truncation and optimum bit truncation for wideband digital receiver in radar applications. The FFT processors are designed using a standard 130 nanometer CMOS process and operates down to 120 mV. The required processing time for the non-configurable 12-b 1024-point LUT FFT is 15.78 ns at a clock frequency of 470 MHz. The required time for configurable LUT 12-b 1024-point FFT processing is 61 ns. The configurable LUT FFT processor with short transform lengths can be expandable so that they can be used easily to form new FFT processors with longer transform lengths. The performance comparison of conventional FFT, LUT FFT, and configurable LUT FFT for digital wideband receiver application is discussed. [C8857]

"Local Information from Range-Speed Radar Sequences"

Radar observes targets, but they remain difficult to interpret due to the difficulty in analysing the radar range-speed sequences. The need for accurate analyses tools increases in case of extended target behaviour or multiple channel radars which give additional observation angles. Extended targets are targets with multiple scatterer responses which disturb each other and give a blurred target response. We investigate here the approach of deconvoluting the range-speed response with a point spread function and interpolate the range-speed positions to get the inner structure of the extended target. The deconvolution gives the individual elements of the extended target. The range-speed interpolation gives accurate position information. The positions and additional observation angle information are tracked with a filter. We demonstrate the approach with real radar measurements. [C8858]

"Profile Likelihood Estimator for Passive Scan-Based Emitter Localization"

This paper is concerned with the geolocation of a scanning emitter from time of intercept measurements of the rotating emitter beam. The problem of estimating the emitter location is cast into a profile likelihood estimation framework by treating the unknown scan rate of the emitter as a nuisance parameter. A grid search technique is developed for initializing iterative profile likelihood estimation algorithms. The grid spacing is determined from an estimate of the Lipschitz constant of the profile likelihood cost function. Maxima of directional derivatives of the cost function are fitted to a Weibull distribution to estimate the Lipschitz constant. The performance of the profile likelihood estimator is illustrated with simulation examples [C8859]

"A Generic ASIC Architecture for Real Time Time-Frequency Analysis of Non-stationary Large Bandwidth Signals"

Wide-band time varying digital signals are extensively used by GSM, TV relays or radars. Analyzing those signals requires building a time frequency representation (TFR) in real-time. Most of TFRs are derived from the Wigner-Ville TFR; unfortunately they are computationally too intensive for real time processing. In this paper we propose an alternative approach to design an ASIC which computes a particular TFR of an input signal in real-time that we named F-TFR. Our approach is based on gradual signal channelizing using modulation, FIR filtering and time-interleaving of the channelized signals. After a brief introduction, we describe in detail the F-TFR algorithm. Then, we study the corresponding hardware architecture introducing signal interleaving and equations adaptations which are necessary for hardware implementation. Finally, we present some typical signals analysis by F-TFR along with an hardware prototype. [C8860]

"Cognitive Dynamic Systems"

The first half of the paper addresses the rationale for why we need to study cognitive dynamic systems, with particular reference to two wireless applications: cognitive radio for communication, and cognitive radar for remote sensing. The second half of the paper discusses the issues involved in dynamic spectrum management and transmit-power control, which are of particular importance to cognitive radio. The iterative water-filling algorithm, in a noncooperative radio environment is discussed, and its virtues and limitations are highlighted. [C8861]

"Multisensor Dynamic Waveform Fusion"

Speech communication is significantly more difficult in severe acoustic background noise environments, especially when low-rate speech coders are used. Non-acoustic sensors, such as radar sensors, vibrometers, and bone-conduction microphones, offer significant potential in these situations. We extend previous work on fixed waveform fusion from multiple sensors to an optimal dynamic waveform fusion algorithm that minimizes

both additive noise and signal distortion in the estimated speech signal. We show that a minimum mean squared error (MMSE) waveform matching criterion results in a generalized multichannel Wiener filter, and that this filter will simultaneously perform waveform fusion, noise suppression, and crosschannel noise cancellation. Formal intelligibility and quality testing demonstrate significant improvement from this approach [C8862]

"Near-Real-Time Data Acquisition and Beamforming for UWB See-Through-Wall System"

An ultra-wideband See-Through-Wall (STW) imaging radar system has been developed that could allow the acquisition and processing of the collected radar data in real-time or near-real-time environment. In this paper, we have compared the performance of various Synthetic Aperture Radar image formation methods, and we will demonstrate the wall-correction preliminary results. Additionally, the design of a near-real-time FPGA-based beamforming processor will be presented and samples of our theoretical and experimental collected data. [C8863]

"Hilbert-Huang Transform (HHT) Processing of Through-Wall Noise Radar Data for Human Activity Characterization"

Different parts of the human body have different movements when a person is performing different physical activities. Also, there is great interest to remotely detect human heartbeat and breathing for applications involving anti-terrorism and search-and-rescue. Ultrawideband noise radar systems are attractive because they are covert and immune from interference. The conventional time-frequency analyses of human activity (usually including the short time Fourier transform (STFT), Wigner-Ville distribution (WVD), and wavelet analysis) are not generally adaptive to nonlinear and nonstationary signals. If one can decompose the noisy baseband signal containing human Doppler information and extract only the human-induced Doppler from it, the identification of various human activities becomes easier. We therefore propose to use a recently developed method, the Hilbert-Huang transform (HHT), since it is adaptive to nonlinear and nonstationary signals. When used with noise-like radar data, it is useful for covert detection of human movement. The HHT based signal processing can effectively improve pattern recognition and reject unwanted uncorrelated noise. [C8864]

"Improving Detection in Sea Clutter using Waveform Scheduling"

In this paper, we propose a method to exploit waveform agility in modern radars to improve performance in the challenging task of detecting small targets on the ocean surface in heavy clutter. The approach exploits the compound-Gaussian model for sea clutter returns to achieve clutter suppression by forming an orthogonal projection of the received signal into the clutter subspace. Waveform scheduling is then performed by incorporating the information about the clutter into the design of the next transmitted waveform. A simulation study demonstrates the effectiveness of our approach [C8865]

"Bivariate Gamma Distributions for Multisensor Sar Images"

This paper addresses the problem of estimating the parameters of a family of bivariate gamma distributions whose margins have different shape parameters. These distributions are interesting to detect changes in two synthetic radar aperture (SAR) images acquired by different sensors and having different numbers of looks. The estimators based on the maximum likelihood method and the method of moments are studied for these distributions. An application to change detection is finally discussed [C8866]

"Some properties of IIR power-symmetric filters"

Power-symmetric IIR filters have in the past been used in two-channel filter banks. If appropriately designed, such filters have allpass polyphase components, and this induces useful properties in the filter bank. For example, IIR orthonormal filter banks have in the past been designed in this way, and generate orthonormal basis functions. In this paper we study some theoretical properties of IIR power symmetric filters in a more general perspective. This includes the derivation of a general analytical form, and a study of pole locations [C8867]

"Through the Wall Imaging using Chaotic Modulated Ultra Wideband Synthetic Aperture Radar"

A novel chaotic modulated ultra wideband (UWB) synthetic aperture radar (SAR) imaging scheme and its post data processing technique are presented for through the wall surveillance applications. It is illustrated that the proposed radar has an excellent resolution performance due to the autocorrelation properties of chaotic signals. Through modeling room reverberation and target reflection, and deriving energy distribution at the receiver, detection performance is carried out to show the advantages of proposed radar. Electromagnetic (EM) simulations are performed in a through the wall scenario. Compared with the conventional UWB radar, the result

verifies the effectiveness and superiority of the proposed technique [C8868]

"Joint Model Selection and Parameter Estimation of GTD Model using RJ-MCMC Algorithm"

The Bayes principle is applied to the joint model selection and parameter estimation of GTD model to explore the prior information. An algorithm using RJ-MCMC is designed. It not only has better model selection and parameter estimation performance than the non-Bayes algorithms, but also solves the mixed parameter estimation problem in GTD model effectively. The advantage of this algorithm is especially evident at low SNR, for short data and with closely-spaced components. Simulations verify the effectiveness of this algorithm. [C8869]

"A Graph Reduction Method for 2D Snake Problems"

Energy-minimizing active contour models (snakes) have been proposed for solving many computer vision problems such as object segmentation, surface reconstruction, and object tracking. Dynamic programming which allows natural enforcement of constraints is an effective method for computing the global minima of energy functions. However, this method is only limited to snake problems with one dimensional (1D) topology (i.e., a contour) and cannot handle problems with two-dimensional (2D) topology. In this paper, we have extended the dynamic programming method to address the snake problems with 2D topology using a novel graph reduction algorithm. Given a 2D snake with first order energy terms, a set of reduction operations are defined and used to simplify the graph of the 2D snake into one single vertex while retaining the minimal energy of the snake. The proposed algorithm has a polynomial-time complexity bound and the optimality of the solution for a reducible 2D snake is guaranteed. However, not all types of 2D snakes can be reduced into one single vertex using the proposed algorithm. The reduction of general planar snakes is an NP-complete problem. The proposed method has been applied to optimize 2D building topology extracted from airborne LIDAR data to examine the effectiveness of the algorithm. The results demonstrate that the proposed approach successfully found the global optima for over 98% of building topology in a polynomial time. [C8870]

"Precise Registration of 3D Models To Images by Swarming Particles"

The precise alignment of a 3D model to 2D sensor images to recover the pose of an object in a scene is an important topic in computer vision. In this work, we outline a registration scheme to align arbitrary standard 3D models to optical and synthetic aperture radar (SAR) images in order to recover the full 6 degrees of freedom of the object. We propose a novel similarity measure which combines perspective contour matching and an appearance-based Mutual information (MI) measure. Unlike previous work, the resulting similarity measure is optimized using an evolutionary particle swarming strategy, parallelized to exploit the hardware acceleration potential of current generation graphics processors (GPUs). The performance of our registration scheme is systematically evaluated on an object tracking task using synthetic as well as real input images. We show that our approach leads to precise registration results, even for significant image noise, small object dimensions and partial occlusion where other methods would fail. [C8871]

"Symmetry-Aided Particle Filter for Vehicle Tracking"

Symmetry is an important characteristic of vehicle and has been used for detection tasks by many researchers. However, existing results of vehicle tracking seldom used this feature. In this paper, we combine the color histogram and the symmetry measurements to design a hierarchical-like particle filter for vehicle tracking. Experimental results show that the use of symmetry information will obtain better tracking performance than the conventional color histogram-based particle filters and effectively avoid some "hijack" problems. [C8872]

"Training and optimization of operating parameters for flash LADAR cameras"

Flash LADAR cameras based on continuous-wave, time-of-flight range measurement deliver fast 3D imaging for robot applications including mapping, localization, obstacle detection and object recognition. The accuracy of the range values produced depends on characteristics of the scene as well as dynamically adjustable operating parameters of the cameras. In order to optimally set these parameters during camera operation we have devised and implemented an optimization algorithm in a modular, extensible architecture for real-time applications including robot control. The approach uses two components: offline nonlinear optimization to minimize the range error for a training set of simple scenes followed by an online, real-time algorithm to reference the training data and set camera parameters. We quantify the effectiveness of our approach and highlight topics of interest for future research. [C8873]

"Methods for Seamless Vertical Handoff between UMTS and WLAN"

3G cellular networks and 802.11 wireless LANs have complementary advantages to each communication systems. Interworking between UMTS and WLAN can be used to pursue two advantages of both high speed access network and a broad cell coverage. How to reduce handoff latency between UMTS and WLAN is a so important issue, so in this paper we investigate the handoff latency and separate handoff delay into several parts in both upward handoff (from WLAN to UMTS) and downward handoff (from UMTS to WLAN). In order to reduce the handoff delay, we use cross-layer information between layer 2 and layer 3. [C8874]

"Verifying Behavior of L4 Microkernel based Mobile Phone"

The embedded mobile phone based on L4 microkernel are known to be difficult to predict their behavioral correctness since L4 microkernel communicates with various components for their execution. That means its correctness is not easy to guarantee by using traditional design and testing methods. In this paper, we propose a formal approach to prove the correctness of L4 based mobile platforms. [C8875]

"Investigation of the Effect of Fading Correlation on Performance of MIMO Systems Using an RCS Channel Model"

In this paper, the effect of receive and transmit antenna correlation on the performance (BER vs. SNR) of MIMO (multiple input multiple output) systems is determined by using an RCS (radar cross section) channel model. In this physical model, the scatterers existing in the propagation environment are modeled by their RCS so that the correlation of the receive signal complex amplitudes, i.e., both magnitude and phase, can be estimated. The proposed RCS channel model is then compared with classical models. [C8876]

"A Linear Programming Approach for Multiple Object Tracking"

We propose a linear programming relaxation scheme for the class of multiple object tracking problems where the inter-object interaction metric is convex and the intra-object term quantifying object state continuity may use any metric. The proposed scheme models object tracking as a multi-path searching problem. It explicitly models track interaction, such as object spatial layout consistency or mutual occlusion, and optimizes multiple object tracks simultaneously. The proposed scheme does not rely on track initialization and complex heuristics. It has much less average complexity than previous efficient exhaustive search methods such as extended dynamic programming and is found to be able to find the global optimum with high probability. We have successfully applied the proposed method to multiple object tracking in video streams. [C8877]

"Particle Filtering Algorithms for Tracking Multiple Sound Sources using Microphone Arrays"

A particle filtering algorithm using the parameters in the EM (expectation-maximization) algorithm is proposed for tracking multiple sound sources. Differently from the conventional EM based algorithms, the proposed algorithm can track multiple sound sources without knowing their starting points. Moreover, an idea of the group tracking is applied to the particle filtering algorithm so that better tracking performances can be obtained. Experimental results show the validity of the proposed algorithm. [C8878]

"Laplace Entropy and its Application to Time Delay Estimation for Speech Signals"

Time delay estimation (TDE) is a basic technique for numerous applications where there is a need to localize and track a radiating source. It is particularly challenging in the presence of noise and reverberation, and when the source signal is speech which is inherently nonstationary and random. The most important TDE algorithms for two sensors are based on the generalized cross-correlation (GCC) method. These algorithms perform reasonably well when reverberation or noise is not too high. In an earlier study of the authors, a more sophisticated approach was proposed. It employs more sensors and takes advantage of their delay redundancy to improve the precision of the TDOA (time difference of arrival) estimate between the first two sensors. The approach is based on the multichannel cross-correlation coefficient (MCCC) and was found more robust to noise and reverberation. In this paper, we show that this approach can also be developed on a basis of joint entropy. For Gaussian signals, we show that, in the search of the TDOA estimate, maximizing MCCC is equivalent to minimizing joint entropy. But with the generalization of the idea to non-Gaussian speech signals, the joint entropy based new multichannel TDE algorithm manifests a potential to outperform the MCCC-based method. Since there is no rigorous mathematical formula for speech entropy, we use the assumption that speech can be plausibly modeled by a Laplace distribution and develop a practical approximation of Laplace entropy for TDE of speech signals. The performance of the proposed new algorithm is investigated via simulations. [C8879]

"Bistatic Synthetic Aperture Hitchhiker Imaging"

We introduce a new bistatic synthetic-aperture imaging method for a radar system consisting of two receivers,

which will be referred to as hitchhikers, and a source of opportunity. We assume the receivers fly along arbitrary, but known, flight trajectories. We develop a correlation-based filtered-backprojection reconstruction method that preserves the visible edges of the target scene in the reconstructed image. We present an analysis of the computational complexity of the introduced method and demonstrate its applicability in numerical simulations. Potential applications of the proposed method include image formation using low earth orbiting and space-borne satellites as sources of opportunity. [C8880]

"Blind Separation of Human Heartbeats and Breathing by the use of a Doppler Radar Remote Sensing"

The combined use of a Doppler radar with digital signal processing technique gives an effective non-invasive remote sensing of heart beat signals. Initial results have showed that the proposed technique is very promising in successfully isolating desired heart beat signals from other mobile objects and other distortion effects characterizing the wireless channel. We concentrate in this paper on the harder problem of separating at low SNR the signals from two subjects in the same room. We show that preliminary results obtained by the real analytical constant modulus algorithm (RACMA) and the independent component analysis (ICA) on experimental data are very promising into this goal. [C8881]

"Event Driven Data Processing Architecture"

This paper describes a data processing architecture where events and time are in focus. This differs from traditional von Neumann and data flow architectures. New instruction codes are defined and special circuitry is introduced to express and execute event and time operations. This results in reconfigurable software controlled functionality together with real-time performance comparable to dedicated VLSI solutions. The architecture is demonstrated in a real-time radar jammer application. The architecture is promising also for applications as routers and network processors. A prototype system on silicon (SoC), complete with signal memory, instruction memory, four processing units in parallel and interfaces for digitized signals and host computer, is fabricated in 0.35 μm standard CMOS. Time events of signal data on two simultaneous 8-bit links can be programmed with a time resolution of one clock period. Measurements verified correct function and performance above 400 MHz clock frequency at 3.3 Volt supply. Power consumption is 3.6-Watt @320 MHz [C8882]

"New safety critical radio altimeter for Airbus and related design flow"

The latest generation of the ERT560 digital radioaltimeter (DRA) developed for the Airbus A380 is the result of Thales' 40 years experience. Over 40,000 radioaltimeters have been produced over that period based on dual technology, meeting the stringent requirements of the civil aircraft. This new version takes advantages of the FPGA technology to implement the main treatment of the equipment. The present article introduces the main capabilities of the ERT560 product and focus on the FPGA which is the key element of the safety critical analysis of the radioaltimeter. Then the paper presents the application of the new "design assurance guidance for Airborne Electronic Hardware (DO254) which has been raised in 2000 (this guide is the equivalent for the HW of the DO 178B for the SW). DO254 related activities are mainly developed such as a dedicated workflow, validation (give evidence of the completeness and correctness of all design life cycle outputs) and verification (evaluation of an implementation of requirements to determine that they have been met) and also verification tool qualification [C8883]

"2007 IEEE International Conference on Acoustics, Speech, and Signal Processing"

The following topics were dealt with: audio; electroacoustics; biomedical imaging; biomedical signal processing; multidimensional signal processing; information forensics; security; radar signal processing; machine learning for signal processing; multimedia signal processing; sensor array; multichannel signal processing; signal processing for communication; signal processing education; speech processing; and spoken language processing. [C8884]

"UWB Linear Quadratic Frequency Domain Frequency Invariant Beamforming and Angle of Arrival Estimation"

In this paper, we present Ultra Wide Band (UWB) frequency invariant beamforming and angle of arrival (AoA) estimation techniques. We propose a new linear quadratic (LQ) frequency domain frequency invariant beamforming strategy. Based on the proposed beamforming strategy, we give a Kalman filter based AoA estimation technique. Simulation results illustrate the performance of the proposed beamforming and AoA estimation strategies. [C8885]

"Estimation of 2-D Direction of Arrival with an Extended Correlation Matrix"

This paper presents a new subspace-based 2D direction of arrival (DOA) estimation algorithm for narrowband sources with high-resolution localization capabilities. DOA estimation is achieved by using the noise-subspace eigenvectors of a new extended correlation matrix (ECM). A 2-L shape antenna array is proposed. Unlike common planar and circular arrays, the novel antenna array with this special geometry requires no pair matching between the azimuth and elevation angle estimation also this key can remove the drawbacks of estimation-failure problems. The performance of the proposed approach is examined by a simulation study. The simulation results show a good estimate performance. [C8886]

"Advanced Methods of Multivariate Anomaly Detection"

The generic problem in anomaly detection is identifying unusual samples present in a large population. Each member of the population is described by a list of characteristics that define a feature vector. One statistical method that accounts for mutual correlations among the components has defined the standard for anomaly detection in communication, radar, and hyperspectral signal processing for several decades. This paper describes an advanced methodology that constructs nonlinear transformations to account for observed data distributions not amenable to a statistical description. The construction relies on a combination of stochastic methods and phenomenological constraints. Examples are taken from hyperspectral target detection. [C8887]

"Multiple Target Tracking Using Maximum Likelihood Probabilistic Data Association"

The maximum likelihood-probabilistic data association (MLPDA) target tracking algorithm is effective in tracking very low observable targets. A key limitation of MLPDA is that it is restricted to tracking a single target. We derive and implement a multiple target version of MLPDA called Joint MLPDA (JMLPDA). While the JMLPDA implementation presented in this paper is focused on a two-target case, this algorithm is extensible to any number of targets. The MLPDA and JMLPDA algorithms are combined to form a multi-target MLPDA tracking algorithm. Performance of the JMLPDA and the multi-target MLPDA algorithms are compared to a probabilistic multi-hypothesis tracker (PMHT) for two crossing targets, focusing on track management/update. Simulation results show that under conditions of heavy clutter, the multi-target MLPDA outperforms PMHT in terms of reduced track errors and longer track life. [C8888]

"Evaluation of Knowledge-Aided STAP Using Experimental Data"

Recent advances in knowledge-aided space-time adaptive processing (KA-STAP) have resulted in significant performance improvements for ground moving target indication (GMTI) radar systems. In particular, the use of prior knowledge including terrain, clutter discretized, and previously detected targets has been shown to be effective for mitigating the poor performance often encountered when operating in heterogeneous clutter environments. This paper provides an evaluation of KA-STAP techniques based on extensive processing of experimental data. Two major performance issues are addressed: high false alarm rates due to under-nulled clutter discretized and target cancellation due to corruption of the STAP training data by other targets in the scene. Each of these problems is demonstrated using experimental multi-channel X-band radar data. Methods for using prior knowledge to improve performance are presented and processing results using the experimental data are provided that show how KA-STAP can lead to significantly improved detection performance relative to conventional STAP processing. [C8889]

"Space-Time Adaptive Processing for Non-Sidelooking Airborne Radar with HPRF"

The primary differences in airborne radar clutter spectrum between non-sidelooking and sidelooking arrays are that its Doppler frequency of the clutter spectrum varies with the range and its clutter degrees of freedom (DOFs) are increased. In this paper, firstly a new clutter suppression approach for non-sidelooking airborne radar based on covariance matrix taper (CMT) is proposed at low pulse repetition frequency (LPRF) mode. Secondly a range ambiguous clutter suppression preprocessing method based on orthogonal projection technique is presented for non-sidelooking airborne radar with high pulse repetition frequency (HPRF). Finally the experimental simulation results indicate their correctness. [C8890]

"RFInD: An RFID-Based System to Manage Virtual Spaces"

We present RFInD, a cost-effective utilitarian system for locating objects using RFID technology. RFInD separates the notion of location from that of physical co-ordinates by using the abstraction of a virtual space. A virtual space is created by using RFID tags to label entities and locations in the physical space as references. RFInD manages the virtual space by using the references to create a spatial map, over which objects can be tracked and located. The target objects are labeled and embedded in a virtual space by associating them with proximate reference tags. RFInD creates the technology to automatically and efficiently manage these associations. In this work, we first characterize the capabilities of a commercially available RFID reader. We

show how to use these capabilities for two tasks, namely proximity detection and tag association. RFInD uses these capabilities as primitives to create virtual spaces, embed objects in the virtual space, and navigate the space to track the embedded objects. Further, our experiments establish the effectiveness of our approach in managing virtual spaces [C8891]

"Tork: A Variable-Hop Overlay for Heterogeneous Networks"

We present a new variable-hop peer-to-peer overlay that combines active stabilization and opportunistic maintenance to provide overlay nodes with a large range of hop-count versus peer bandwidth capabilities. Because of the variable-hop design, Tork is suitable for use in large-scale heterogeneous peer-to-peer networks where peers have a range of bandwidth capacities. For high-bandwidth peers Tork has O(1)-hop performance, and for low-bandwidth, most likely mobile peers, Tork has multi-hop performance. We further show that mapping overlay messaging to multi-destination routing in the underlay reduces Tork message overhead by up to 35% [C8892]

"Design of SPDT Switch, 6 Bit Digital Attenuator, 6 Bit Digital Phase Shifter for L-Band T/R Module using 0.7 μ M GaAs MMIC Technology"

The performance of modern radar systems with active phased array antennas is mainly driven by the performance of the microwave T/R modules. To reduce the size, weight, cost and power consumption, as well as to achieve better phase and amplitude accuracies for realizing low sidelobe levels with an accurate beam steering, T/R modules, now-a-days, employ MMICs (monolithic microwave integrated circuits) for implementing transmit/receive chain. The L-band SPDT switch, 6-bit digital attenuator, 6-bit digital phase shifter have been designed using GAETEC Hyderabad 0.7 μ m GaAs MESFET switch model to handle 30 dBm peak power. All the above components have been designed and simulated using Agilent ADS CAD tool interfaced with Academy Layout. The SPDT switch with insertion loss less than -1 dB, isolation greater than 60 dB and return loss better than 20 dB has been realized on a single 3.0 mm \times 2.35 mm GaAs chip. A 6-bit digital attenuator has a 31.5 dB attenuation range in 0.5 dB increments; 2.5° phase error and return loss better than 15 dB. The 6 bits are cascaded to form a complete attenuator on a double 3.5 mm \times 2.35 mm GaAs chip with 3 attenuator bits in each for a better yield. A 6-bit digital phase shifter with 9 dB insertion loss, return loss better than 15 dB has been realized on a two GaAs chips with size 4.0 mm \times 2.35 mm and 3.0 mm \times 2.35 mm and 3 phase bits in each chip for the better yield [C8893]

"Ontology-Based Pervasive Spatial Knowledge for Car Driver Assistance"

Deducing spatial knowledge for car driver assistance is of special importance for upcoming advanced driver assistance systems. Such systems can not only rely on car mounted sensors, but also require environmental tracking. We illustrate our approach of a distributed ad-hoc infrastructure that collects and disseminates tracking data of environmental objects and thus allows for vehicle- and ontology-based reasoning. We discuss, where such a system can facilitate in driver assistance systems, that require spatial knowledge [C8894]

"Multiresolution Subspace Beam Formation Using a Partially Coherent Model"

Traditional beam formation and waveform techniques rely on fixed apertures with single frequency assumptions that restrict the geometry of the aperture. This approach results constraints on the functionality of radar systems such as having simultaneous imaging and tracking ability, eliminating complex interference, and working with platforms that have limited bandwidth and processing resources. We propose an adaptive multiresolution orthogonalized sub-space beam formation method (AMOS) that allows optimization of apertures that may have non-uniform spacing with limited bandwidth. We combine this model with a partially coherent electromagnetic wavefront propagation model. We will show how this method compares to similar methods from a theoretical lower bound standpoint. [C8895]

"High Performance Space Computing"

This paper describes a fully programmable 6 processor die that was implemented in IBM's 130 nanometer 8SF process. It is capable of operating as two triple voted processors each with 6 Mbytes of Embedded Dynamic Random Access Memory (EDRAM) or 6 independent processors each with 2 Mbytes of EDRAM. In triple vote mode the processor counts and recovers from single event upsets. It supports external Double Data Rate (DDR) Synchronous Dynamic Random Access Memory (SDRAM), and has two Spacewire ports, a 4 Gbit input port, and a 4 Gbit output port. The processor core with memory performs approximately 2.5 Giga Floating Point Operations Per Second (GFLOPS) per Watt, with worst case input/output power its performance is approximately 1 GFLOPS per Watt. The processor's efficient messaging allows hundreds of processors to be applied to applications such as radar. [C8896]

"Unscented and Extended Kalman Estimators for non Linear Indoor Tracking Using Distance Measurements"

Industrial and logistic indoor tracking with accuracy in centimetre range is still a challenging issue. Many applications in mining, logistic, and navigation depend mainly on a precise determination of a mobile terminal. This work presents an indoor positioning approach using two recursive tracking algorithms for precisely localizing a mobile vehicle in a noisy environment. An extended Kalman filter (EKF) and unscented Kalman filter (UKF), the corresponding algorithms and mathematical models are presented and analysed. Experimental range measurements obtained from local positioning radar system are used to feed the filters. True and estimated trajectories of the mobile vehicle with associated means and error covariances are presented in more details. Results obtained shows that UKF is slightly more accurate and reliable. Whereas, EKF is easier to implement, converges faster when fed with a good initial estimate and more optimized for semi-linear tracking models.

[C8897]

"Indoor Navigation Based on Doppler Measurements"

Nowadays a lot of different services are brought to the user using wireless infrastructure. To enhance these services an information about the users actual position is often desirable. To obtain this information additional sensors have to be installed. As Doppler processing can easily be integrated in already existing indoor infrastructure, position finding systems based on Doppler measurements would be preferable. This paper presents a position finding system that relies on the simultaneous Doppler measurement of an object by four sensors at different positions. The four Doppler signals are evaluated to obtain position and velocity of a single moving target by iteratively solving a nonlinear system of equations. Methods to assess the obtainable accuracy as well as first simulation results will be discussed. A 4-channel CW-radar as a demonstration system is presented. [C8898]

"Analysis and Emulation of FM Radio Signals for Passive Radar"

Due to its high power levels provided, and its wide coverage, FM radio could be a good opportunity transmitter for passive coherent location (PCL) radar systems. In this paper we study the effectiveness of FM signals as radar waveforms by means of simulated and real data analysis. To this purpose, an emulation of FM radio transmitter is presented, whose outputs are compared with real FM data collected by an experimental digital receiver. In this way, we also achieve a reliable instrument to optimize target detection performance by a successive adaptive signal processing. To complete the analysis of opportunity waveforms, the signals' self-ambiguity functions and spectra are evaluated, so it is possible to improve the knowledge of how to select the most appropriate FM channel. Since emulated data differ from real data in means of the transmission channel, a statistical analysis of the real channel is presented. [C8899]

"Information Theory Based Radar Signature Analysis"

The ability to make radar signature databases portable for use within similar sensor systems is critical to the affordability of airborne signature exploitation systems. The capability to hybridize measured and synthetic signature database components will maximize the investment required to build complex radar signature databases. Radar target scattering response signatures and sensor related effects can be modeled and analyzed as a random process to enable sensor optimization. Information theory based methods are proposed as a means to identify those components within the signal subspace that are highly linked to target separability. Mutual information is developed as a measure of similarity to compare measured field data to modeled synthetic data. The approach is demonstrated using synthetic signature sets comprised of both "similar targets" and "dissimilar targets". [C8900]

"Technology Demonstration of Ka-band Digitally-Beam formed Radar for Ice Topography Mapping"

GLISTIN (Glacier and Land Ice Surface Topography Interferometer) is a spaceborne interferometric synthetic aperture radar for topographic mapping of ice sheets and glaciers. GLISTIN will collect ice topography measurements over a wide swath with sub-seasonal repeat intervals using a Ka-Band digitally-beamformed antenna. This paper will give an overview of the system design and key technology demonstrations including a 1m x 1m digitally-beamformed Ka-band waveguide slot antenna with integrated digital receivers. We will also detail the experimental scenario that we will use to demonstrate both the beamforming and interferometric performance of this system. [C8901]

"A Modulus Compensation Algorithm for Shape Self-Calibration of Paired Sensors Based

Antennas"

This paper is concerned with the array shape self-calibration problem when the array gain pattern of each sensor is spatially dependent and unknown. We adapt a constant modulus approach (CMA) to improve the precision in the sensor localization. We will see how this original method conducts to build particular antenna configurations appropriate for self-calibration. The performance improvement lies in a strong bias reduction.

[C8902]

"Three-Dimensional Ultrasound Imaging in Air using a 2D Array on a Fixed Platform"

Acoustic imaging has been used in a variety of applications, but its use in air has been limited due to the slow propagation of sound and high attenuation. We address the problem of ultrasound imaging of a scene in air with a 2D array under the constraint of a fixed platform. The presented system uses a single transmit pulse combined with a Capon beamformer at the receiving array under a near-field model to obtain three-dimensional images of a scene. Results from experiments conducted in a laboratory demonstrate that it is possible to detect position and edge information from which an object can be reconstructed. [C8903]

"TR-SAR: Time Reversal Target Focusing in Spotlight SAR"

We develop time reversal spotlight synthetic aperture radar (TR-SAR) for target focusing and ghost images removal in SAR. Conventional SAR is not designed for imaging targets in a rich scattering environment. In this case, ghost images due to secondary reflections appear in the SAR images. We show in this paper, how, from a rough estimate of the target location obtained from a conventional SAR image and using time reversal, TR-SAR focuses on the target with improved resolution, and reduces or removes ghost images. Verification with experimentally measured electromagnetic data demonstrates the success of TR-SAR. [C8904]

"Blind Adaptive Algorithm for M-Ary Distributed Detection"

In a parallel distributed detection system each local detector makes a decision based on its own observation, then transmits its local decision to a fusion center. Given fixed local decision rules, in order to design the optimal fusion rule for the M hypotheses, the fusion center needs to have perfect knowledge of the performance of the local detectors as well as the prior probability of the hypotheses. Such knowledge may not be available in practice. In this paper, we propose a suboptimal algorithm for M-ary decision fusion based on binary groupings of multiple hypotheses. Simulation results show that this method is effective in practice [C8905]

"High-Resolution Imaging using Capon Beamformers for Urban Sensing Applications"

A wideband synthetic aperture radar system based on beamspace Capon beamforming is presented for urban sensing applications. Various effects of signal propagation through building materials are incorporated into the beamformer design. Proof of concept is provided using real data collected in a laboratory environment. Comparison between data-independent and scene-dependent beamformers is provided. The results show that the beamspace Capon beamformer outperforms the nonadaptive delay-and-sum beamformer [C8906]

"A Subspace Method for MIMO Radar Space-Time Adaptive Processing"

In the traditional transmitting beamforming radar system, the transmitting antennas send coherent waveforms which form a highly focused beam. In the MIMO radar system, the transmitter sends noncoherent (possibly orthogonal) broad (possibly omnidirectional) waveforms. These waveforms can be extracted by a matched interbank. The extracted signals can be used to obtain more diversity or improve the clutter resolution. In this paper, we focus on space-time adaptive processing (STAP) for MIMO radar systems which improves the clutter resolution. With a slight modification, STAP methods for the SIMO radar case can also be used in MIMO radar. However, in the MIMO radar, the rank of the jammer-and-clutter subspace becomes very large, especially the jammer subspace. It affects both the complexity and the convergence of the STAP. In this paper, a new subspace method is proposed. It computes the clutter subspace using the geometry of the problem rather than data and utilizes the block diagonal property of the jammer covariance matrix. Because of fully utilizing the geometry and the structure of the covariance matrix, the method is very effective for STAP in MIMO radar.

[C8907]

"Non-Linear Prediction of Inverse Covariance Matrix for Stap"

For bistatic ground moving target indication radar, the clutter Doppler frequency depends on range for all array geometries. This range dependency leads to problems in clutter suppression through STAP techniques. In this paper, we propose a new approach of applying non-linear prediction theory to address the range dependency problem in bistatic airborne radar systems. This technique uses a non-linear function to obtain an estimate of the

range-dependent inverse covariance matrix. Simulation results suggest a non-linear fit for the model (nonlinear relationship between the inverse covariance matrices) and show an improvement in processor performance as compared to conventional STAP methods. [C8908]

"GLRT-Based Adaptive Doppler Processing for HF Radar Systems"

High frequency skywave and surface-wave over-the-horizon (OTH) radars are required to detect targets in the presence of powerful clutter and interference from man-made and natural sources. However, the received disturbances may be highly structured in the time domain (i.e. pulse-to-pulse) within the coherent processing interval (CPI). This provides scope for adaptive Doppler processing to enhance detection performance with respect to conventional FFT-based methods. This paper proposes a generalized likelihood ratio test (GLRT) based detector that not only possesses the valuable constant false alarm rate (CFAR) property invariant to disturbance scale-change, but also exhibits distinct advantages over the adaptive coherence estimator (ACE) and adaptive subspace detector (ASD) when unwanted signals are present. Here, we present the first experimental results for this detector in a HF surface wave radar Doppler processing application. [C8909]

"Characteristic Phase E-Sequences in Efficient Pulse-Compression Methods using Discrete Wavelet Decomposition"

We derive a family of sequences which obey a characteristic-phase constraint as it applies to finite sequences. We show these sequences are special cases of the well-known Welti sequences. We construct a transmit waveform which allows extremely efficient decomposition, whose outputs are simultaneously interpretable as adjacent correlation-filter outputs, and as lossless input signal representations. We discuss implementation of receive and transmit functions. [C8910]

"Multi-Channel Parametric Estimator Fast Block Matrix Inverses"

The optimal (adaptive) linear combiner (beamformer) weights for a sensor array are expressed in terms of the inverse of the multi-channel (MC) covariance matrix. Rather than form an estimate of the covariance matrix directly from the available data and inverting it, an alternative direct estimate of the inverse may be obtained by forming parametric MC linear prediction estimates and then expressing the inverse in terms of these parametric MC estimates. The resulting parametric estimate of the inverse is typically more accurate than inverting the estimate of the covariance matrix. This paper reveals, for the first time, the structure of the the inverse of the covariance matrix for the MC version of the covariance least squares linear prediction algorithm. The inverse structure involves products of triangular block MC Toeplitz matrices, which leads to fast computational solutions for the optimal weights. [C8911]

"Near-Field Source Localization via Symmetric Subarrays"

We propose a near-field source localization algorithm with one-dimensional (1-D) search via symmetric subarrays. By dividing the uniform linear array (ULA) into two symmetric subarrays, the steering vectors of the subarrays yield the 1-D (only bearing-related) property of rotational invariance in signal subspace, which allows for the bearing estimation using the generalized far-field ESPRIT. With the estimated bearing, the range estimation of each source is consequently obtained by defining 1-D MUSIC spectrum. This algorithm transforms two-dimensional (2-D) search involved in the parameter estimation to 1-D search, and it does not require high-order statistics computation in contrast with the traditional near-field high-order ESPRIT algorithm [C8912]

"Synthetic Aperture Radar Demonstration Kit for Signal Processing Education"

A synthetic aperture radar scale model has been developed to improve signal processing teaching. Based on low frequency ultrasound transmission, it is a low cost demonstration kit. The overall software is directly running on Matlabreg and allows easy and realtime modifications. This educational tool can be used to test different waveforms and show the effects of a real scene on the final image. It can also be used in a more advanced way to test different signal processing in order to improve image focusing or to reduce computation burden [C8913]

"Spreading Sequence-Based Non-coherent Sensor Fusion and its Resulting Large Deviation Exponents"

To address the coordination issue of sensors communicating with a fusion center, we propose a spreading sequence based non-coherent detection scheme for sensor networks to reduce the coordination between sensors to the largest extent. In this scheme, sensors employ independent spreading sequences to transmit their measurements. Non-coherent detection is conducted at the fusion center where only statistics regarding channel gains and sensor measurement uncertainties are needed. To evaluate the detector's performance, we first derive

the large deviation exponents of detection error probabilities and then compare them with the approaches assuming orthogonal channel allocation (e.g. TDMA/FDMA). Numerical and simulation results demonstrate the dependence of large deviation exponent on the asymptotic number of sensors per chip (defined as c), as well as the better performance of our proposed scheme than the one using non-coherent detection with orthogonal link, for some c [C8914]

"Different Sensor Placement Strategies for TDOA Based Localization"

This paper studies different optimization strategies for the sensor placement in source localization by using time differences of arrival. It continues the works in (B. Yang et al., 2005, 2006) and gives answers to some open questions there. In particular, we discuss the relationship between maximum Fisher information matrix, minimum Cramer-Rao bound, spherical codes, uniform angular arrays, and Platonic solids as well as their roles in optimizing the sensor placement. Various new optimum sensor array geometries are given [C8915]

"Blind Identification and Linear Quadratic Frequency Invariant Beamforming Based Angle of Arrival Estimation"

In this paper, we present wide band frequency invariant beamforming and angle of arrival (AoA) estimation techniques. We propose a new linear quadratic (LQ) frequency domain frequency invariant beamforming strategy. Based on the proposed beamforming strategy, we give a new AoA estimation technique using blind identification. Simulation results illustrate the performance of the proposed beamforming and AoA estimation strategies [C8916]

"Adaptive Polarized Waveform Design for Target Tracking using Electromagnetic Vector Sensors"

We develop an adaptive waveform design method for target tracking. In our method, at each time step, we optimally select the parameters, including the polarization of the transmitted signal waveform to improve the tracking accuracy. An array of electromagnetic vector sensors is employed to fully recover the polarimetric information from the reflected signals. We derive our approach under a framework of sequential Bayesian filtering. We apply a sequential Monte Carlo method to manipulate the nonlinear and non-Gaussian state and measurement models. We design a criterion for the waveform optimization based on a posterior Cramer-Rao bound [C8917]

"Performance Bounds and Algorithms for Tracking with a Radar Array"

Target tracking using a radar array system is considered. A signal model which includes the effects of path loss, signal delay, Doppler shift and angle-of-arrival is adopted. The conventional approach to radar tracking assumes that the raw measurements are processed to produce a collection of candidate target detections. We propose a new approach in which the raw received measurements are used for tracking. Performance bounds and a simulation analysis of filters developed for each model demonstrate the performance gains which can be achieved by tracking with raw sensor measurements [C8918]

"Waveform Optimization for MIMO Radar: A Cramer-Rao Bound Based Study"

A MIMO (multi-input multi-output) radar system, unlike standard phased-array radar, can transmit via its antennas multiple probing signals. This waveform diversity offered by MIMO radar enables superior capabilities compared with a standard phased-array radar. We consider MIMO radar waveform optimization for parameter estimation for the general case of multiple targets in the presence of spatially colored interference and noise. Numerical examples are provided to demonstrate the effectiveness of the approaches we consider herein. [C8919]

"SAR Processor based on a CFAR Signal or Interference Subspace Detector Matched to Man Made Target Detection in a Forest"

This paper deals with two new SAR processors based on CFAR subspaces detector. These two algorithms aim at improving man made target detection performances in a forest clutter by using electromagnetic scattering models. The implementation of the two detectors is described. An application on simulated data shows the interest of the two methods [C8920]

"Detecting and Tracking Moving Objects in Sequences of Color Images"

A statistical change detector, implemented as a zero-latency finite-memory filter, is used to identify anomalies in temporal pixel statistics. An F-distributed test statistic is computed for each pixel and used in a hypothesis test.

The tracker, with automatic track initiation and termination, uses a low-complexity pairwise joint probabilistic data association (JPDA) algorithm, which has been restricted to consider clusters (sub-problems) containing no more than two tracks. The track state and clutter model are augmented to include color. The detector and tracker are used to process sample video data [C8921]

"Incremental Learning of Stochastic Grammars with Graphical EM in Radar Electronic Support"

Although stochastic context-free grammars (SCFGs) appear promising for recognition of radar emitters, and for estimation of their level of threat in radar electronic support (ES) systems, well-known techniques for learning their production rule probabilities are computationally demanding, and cannot efficiently reflect changes in operational environments. Some techniques have been proposed for fast learning of SCFGs probabilities, yet, of those, only the HOLA technique can perform learning incrementally. In this paper, two incremental versions of the graphical EM (gEM) technique are proposed. The incremental gEM (igEM) and on-line incremental gEM (oigEM) allow for adapting production rule probabilities from new data, without having to retrain from the start on all accumulated training data. These new techniques are compared to HOLA using radar signal data. An experimental protocol has been defined such that the impact on performance of factors like the size of new data blocks for incremental learning, and the level of ambiguity of MFR grammars, may be observed. Results indicate that, contrary to HOLA, incremental learning of training data blocks with igEM and oigEM provides the same level of accuracy as learning from all cumulative data from scratch, even for small data blocks. As expected, incremental learning significantly reduces the overall time and memory complexities. Finally, it appears that while the computational complexity and memory requirements of igEM and oigEM may be greater than that of HOLA, they both provide a higher level of accuracy [C8922]

"Scaled Conjugate Gradient Method for Radar Pulse Modulation Estimation"

This paper addresses the problem of estimating a common modulation from a group of intercepted radar pulses. Estimated modulation profile operates as the basis for specific emitter identification (SEI). A robust M-estimation technique using scaled conjugate gradient algorithm for improving the frequency alignment of the pulses is proposed. In addition, postprocessing of the estimated modulation profiles for identification is considered. Simulation experiments are conducted in order to compare the performance with previously proposed methods. Results show that the proposed robust M-estimation technique provides improved performance at low signal-to-noise ratio regime due to better frequency alignment of the intercepted pulses [C8923]

"Detecting Curved Underground Tunnels using Partial Radon Transforms"

The Radon transform (RT) is known to be effective in detecting lines in noisy images, but it is not capable of detecting curves unless the curve parametrization is given. In this paper, partial Radon transforms (PRT) are investigated as a tool to detect curved features such as underground tunnels in ground penetrating radar (GPR) images. The algorithm applies the Radon transform to small batches of the total image and updates the tunnel position parameters as new batches are used. Missing data, as well as finding the ends of tunnels can be handled with the proposed algorithm. Performance analysis is given for various signal-to-noise ratios (SNR) and batch sizes. The effect of the curvature level on the performance is also analyzed. [C8924]

"Inversion of Circular Averages using the Funk Transform"

In radar, when the wavelength of the transmitted electromagnetic wave is considerably larger than the dimension of the antenna, the received signal is modeled as the integral of the mean reflectivity function of the illuminated scene over the intersection of spheres centered at the transmitter location and the surface topography. When the surface topography is flat the received signal becomes integral of the mean reflectivity function over circles which is also referred to as circular averages of the mean reflectivity function. Thus, reconstruction of the ground reflectivity from synthetic aperture radar data requires inversion of the circular averages. Apart from radar, circular averages inversion also arises in thermo-acoustic tomography and sonar. In this paper, we present a new inversion method for the circular averages that uses the relationship between the circular averages, hyperbolic X-ray and the Funk transforms. The method is exact and numerically efficient as compared to standard filtered backprojection algorithms. Numerical simulations demonstrate that the approach is practical. [C8925]

"Signal Properties of Squint Mode Bistatic SAR"

In this paper, the signal properties for the translational invariant case of bistatic synthetic aperture radar (SAR) based on the squint mode are deduced. Bistatic range history, point target response in time and frequency domains, Doppler properties and resolutions are presented in terms of the platform coordinates and the squint angles. The results are valid for large aperture and large squint angles. The accuracy of quadratic approximation

in bistatic SAR is also discussed. [C8926]

"Clustering Polarimetric SAR Image Under Deorientation Theory"

In natural complex terrain surfaces, scattering targets with random orientations produce random fluctuating echoes which lead to confused classifications by directly using target decomposition on polarimetric SAR (PolSAR) image. In order to reduce the influence, the target vector is transformed into the state with minimization of cross-polarization. Then a set of new parameters $u/v/w$ are used to characterize scattering mechanisms under the deorientation theory, and the fuzzy membership is adopted instead of "hard" division of parameter plan. Characterizing the sample coherency matrices as complex Wishart distribution, the PolSAR image is clustered based on Bayes maximum likelihood (ML) criteria. Experiment is carried out on an L-band NASA/JPL SIR-C PolSAR image over Danshui town, Guangdong, China. Comparison results with the popular used methods show that the proposed method provides a significant improvement in classification and the associated scattering mechanism of class is more accurate and beneficial for automatic terrain recognition. [C8927]

"Optimal Array Pattern Synthesis via Matrix Weighting"

We present new array beam pattern synthesis approaches via semidefinite relaxation (SDR) for arbitrary array. Compared to the conventional approaches of using weight vectors at the array output for array pattern synthesis, which we refer to as the vector weighting approaches (VWA), weight matrices are used at the array output by MWA for much improved flexibility for optimal array pattern synthesis, and globally optimal solutions can be determined efficiently due to convex optimization formulations. Numerical examples are presented to show the excellent performance of MWA. [C8928]

"Blind Extraction of Noisy Events using Nonlinear Predictor"

Existing blind source extraction (BSE) methods are limited to noise-free mixtures, which is not realistic. We therefore address this issue and propose an algorithm based on the normalised kurtosis and a nonlinear predictor within the BSE structure, which makes this class of algorithms suitable for noisy environments, a typical situation in practice. Based on a rigorous analysis of the existing BSE methods we also propose a new optimisation paradigm which aims at minimising the normalised mean square prediction error (MSPE). This makes redundant the need for preprocessing or orthogonality transform. Simulation results are provided which confirm the validity of the theoretical results and demonstrate the performance of the derived algorithms in noisy mixing environments [C8929]

"Maximum Likelihood Range Dependence Compensation for STAP"

We present a new method to estimate the clutter-plus-noise covariance matrix used to compute an adaptive filter in space-time adaptive processing (STAP). The method computes a ML estimate of the clutter scattering coefficients using a Bayesian framework and knowledge on the structure of the covariance matrix. A priori information on the clutter statistics is used to regularize the estimation method. Other estimation methods based on the computation of the power spectrum using for instance the periodogram are compared to our method. The result in terms of SINR loss shows that the proposed method outperforms the other ones. [C8930]

"Adaptive Radar Waveform Design for Multiple Targets: Computational Aspects"

In this paper we describe the optimization of an information theoretic criterion for radar waveform design. The method is used to design radar waveforms suitable for simultaneously estimating and tracking parameters of multiple targets. Our approach generalizes the information theoretic water-filling approach of Bell. The paper has two main contributions. First, a new information theoretic design criterion for designing multiple waveforms under a joint power constraint when beamforming is used both at transmitter and receiver. Then we provide a highly efficient algorithm for optimizing the transmitted waveforms, by approximating the information theoretic cost function. We show that using Lagrange relaxation the optimization problem can be decoupled into a parallel set of low-dimensional search problems at each frequency, with dimension defined by the number of targets instead of the number of frequency bands used. [C8931]

"Spectral Analysis of Polarimetric Weather Radar Data with Multiple Processes in a Resolution Volume"

A new approach for the clear air velocity estimation in weather radar is presented. A combination of nonparametric with parametric spectral analysis allows us to identify and extract multiple processes caused by different scatterer types within a single radar resolution volume. An example of clear air observed using an S-

band dual polarization radar is presented. Heretofore, migrating birds and wind-blown insects that are mixed within each resolution volume caused such data to be unusable for meteorological interpretation. In this paper, we construct power spectral densities of polarimetric variables. We use the polarimetric spectral densities to differentiate the scatterer types within the observed radar resolution volume. We demonstrate how our combination of non-parametric and parametric spectral analysis can be used to retrieve the true wind velocity in situations with severe contamination by biological scatterers [C8932]

"Low-Complexity Method for Transmit Beamforming in MIMO Radars"

MIMO radar is a new concept in which radar employs multiple waveforms to improve its performance. Previously, a transmit beamforming method was proposed for MIMO radars. This method allows optimization of the beampattern by altering the cross-correlation matrix of the transmitted waveforms. The optimization is based on minimization of a cost function, but the use of numerical methods in the algorithm leads to high computational complexity. Here we propose a new cost function for the beampattern optimization. For linear arrays and typical beampatterns, this cost function can be evaluated in closed form, thus reducing the computational complexity considerably. Simulation examples demonstrate that the proposed cost function also leads to faster convergence and lower approximation error [C8933]

"The Fast Correntropy Mace Filter"

In this paper, we implement the newly introduced correntropy MACE filter using the fast Gauss transform (FGT). The correntropy MACE filter is a nonlinear extension to the MACE filter using the correntropy function in a feature space nonlinearly related to the input. The correntropy MACE outperforms the traditional linear MACE in both generalization and rejection abilities. However, in practice, the drawback of the correntropy MACE filter is its computation complexity. This paper present a fast version of the correntropy MACE by using the FGT idea and validates the approximation with results in synthetic aperture radar (SAR) image recognition [C8934]

"A Global Motion Model for Target Tracking in Automotive Applications"

In common automotive radar tracking systems, simple linear models are used to track targets separately in longitudinal and angular direction relative to the own vehicle (or sensor) position. Under the special condition that the observed targets are straight ahead and moving nearly in the same direction as the observing vehicle, like in adaptive cruise control (ACC) systems, those models work well. In more general scenarios, where movements of other vehicles have to be tracked in all possible directions and all around the vehicle (e.g. in inner-city or intersection situations), the modeling is insufficient. In this paper we review the drawbacks of the commonly used models and present a more general motion model for automotive tracking systems. All necessary expressions for an implementation using an extended or unscented Kalman filter are given. Even if designed for radar systems, the state model is not limited to a special type of sensor. It can be used for ultrasonic or laser scanner systems as well as for vision-based systems with a different measurement model [C8935]

"A Low-Power CMOS Modulator for Ultra-Wideband Transmitters"

A low-power CMOS modulator for carrier-based ultra-wideband (UWB) transmitters is presented. The core of the circuit consists of an oscillator and two control switches. The oscillator sets the center frequency of the UWB signal. The spectrum of the baseband data pulse is frequency translated to the desired band without using an explicit mixer. Since in many pulse-based UWB systems, in particular those used in radar and low-data-rate communication applications, a short duration pulse with a low pulse repetition frequency (PRF) is used, the power consumption of the modulator can be reduced significantly by turning off the oscillator between the pulses. This is accomplished using a combination of two MOS switches. By manipulating the pulse width and phase delay of the pulse signals applied to these switches, the time and frequency domain specifications of the transmitted UWB signal are adjusted. A prototype UWB modulator is designed and simulated in a 0.18μm CMOS technology. Simulation results for operation in the UWB low band, i.e., 3.1 to 5 GHz are presented. [C8936]

"Detection with Adaptive Arrays with Irregular Digital Subarrays"

In this paper we combine advanced ABF algorithms like LSMI, LMI, CAPS, and concepts for adaptive guard channels with subarrayed planar arrays together with the theoretical results available in the field of adaptive detection (GLRT, ACE, AMF tests). The aim is to define a robust adaptive sidelobe blanking (ASB) detector against combined impulse and CW interference. For the selection of the thresholds we define the detection margin as a direction dependent tool instead of the commonly used main and guard channel antenna patterns. This criterion gives insight into the critical scenarios for detection. One result we obtain is that an ASB based on the GLRT together with a low sidelobe preserving ABF algorithm like CAPS has superior performance. [C8937]

"An Adaptive Beamforming Technique for Countering Synthetic Aperture Radar (SAR) Jamming Threats"

In a hostile environment synthetic aperture radar (SAR) is likely to be subjected to electronic countermeasures (ECM) to prevent target detection and classification. In practice, noise jamming may not always provide an effective ECM against the SAR because of the large power output required to obscure the SAR image. A potentially more potent threat is presented by deception or repeater jamming, which can exploit the SAR processing gain and prevent target identification and classification using relatively low power output. Such jammers are likely to be light, inexpensive and readily deployable. This paper presents an adaptive beamforming (ABF) for SAR technique which can provide robust and efficient suppression of both noise and deception jamming. The paper also includes results from experiments with SAR trials data containing jamming which demonstrate the effectiveness of the technique in a system offering using two spatial channels. [C8938]

"Time-varying autoregressive adaptive filtering for airborne radar applications"

Multivariate time-varying autoregressive models of order m (TVAR(m)) are introduced based on the Dym-Gohberg band extension technique for finite operator-valued matrices. For particular side-looking airborne radar scenarios (based on the KASSPER-II data set) and novel optimal time-varying transmit antenna pattern control, we demonstrate that model mismatch losses associated with relatively small TVAR order m ($m \sim 4$ to 8), are quite low (1.5 to 3 dB) inside the azimuth-Doppler range of interest, and allow for significant reduction in training sample support. [C8939]

"Direction of Arrival and Angular Velocities (DOAV) Estimation using Minimum Variance Beamforming"

The minimum variance distortionless beamforming (MVDR) is an excellent beamformer for estimating the location of a source when the background noise is Gaussian. This beamformer, also known as the Capon approach, is widely studied and used. In this paper, we investigate the use of the MVDR to estimate the angle of arrival and angular velocities by modeling the movement of the source emitting signal. As a result a four dimensional MVDR is proposed, to estimate the direction of arrival and angular velocities (DOAV) of moving sources, using a rectangular array of antennas. In order to estimate the emitting source parameters, a four dimensional search is required. In practice, this approach is costly and may not be suitable in realtime applications. To reduce the computational complexity of the approach, we exploit the geometry of the array, together with a parameter dimensionality decoupling technique to perform an initialization based on a subspace decomposition approach. This initialization results in two two-dimensional searches in parallel instead of the standard four-dimensional search. We further show that the initialization procedure fits well with the conventional MVDR concept. The performance of the subspace decomposition approach is demonstrated via simulations. We also investigate the effects of diagonal loading on a small sample size and how it can be used together with the MVDR initialization technique to enhance the performance of the overall MDVR approach. [C8940]

"Spotlight SAR Raw Data Simulation Using Frequency Scaling Algorithm"

SAR (synthetic aperture radar) raw signal simulation is an important tool for study and testing of different SAR processing algorithms and new SAR systems. In this paper, the system transfer function of spotlight-mode SAR is evaluated and its accuracy is described. And, frequency scaling algorithm (FSA) is employed to actualize the coupling relation between the range and azimuth in the 2-dimension frequency. An advantage of the frequency scaling algorithm is that it requires only FFT (fast Fourier transform) and complexity multiplication and avoids interpolation. [C8941]

"Self-Organizing Adaptive Radar Space-Time Adaptive Processing"

Self-Organizing Adaptive Radar Space-Time Adaptive Processing (SOAR-STAP) is discussed here. Some investigations have been done on applying SOAR concept to Sigma Delta -STA and D3LS-STAP. The advantages include computation load, sample support, converge rate, etc. SOAR-STAP converges faster than traditional STAP. For same computation time, the response pattern of SOAR-STAP is better than that of traditional STAP. In future, SOAR-STAP can be applied to conformal arrays, sensor robots, etc. The sensors of arrays may be developed independently and deployed incrementally, and then self-organize to form a large array with ability to self-calibrate and correct errors. [C8942]

"Adaptive Radar Detection: A Bayesian Approach"

In this paper we consider the problem of adaptive radar detection in Gaussian disturbance with unknown

spectral properties. To this end we resort to a Bayesian approach based on a suitable model for the probability density function of the unknown disturbance covariance matrix. We devise two detectors based on the GLRT criterion both one-step and two-step. The suggested decision rules ensure the same performance of the non Bayesian GLRT detectors when the size of the training set is sufficiently large. However they significantly outperform the counterparts in the presence of heterogeneous scenarios, where a small number of homogeneous training data is available. The analysis is also supported by results on high fidelity radar data from the KASSPER program. [C8943]

"Super-Resolution Direction-of-Arrival Estimation via Blind Signal Separation Methods"

In this paper, we present a novel high-resolution DOA estimation method based on second-order blind signal separation (BSS) techniques. In this approach, unlike other high-resolution methods such as MUSIC, finding DOA's doesn't involve searching for peak values in the estimated spectrum. Furthermore, in this algorithm, considering a uniform linear array (ULA), the angular distance between two sources is multiplied by $L-1$: L is the number of antenna elements in the array. Therefore, the proposed algorithm exhibits excellent resolution property compared to other techniques. Moreover, BSS techniques enable this approach to carry out source association along with DOA estimation. Here, we introduce the proposed algorithm and define the corresponding probability of resolution (PR). Simulation results demonstrate the superiority of the presented approach in comparison with the existing methods such as MUSIC. [C8944]

"Fast-Converging Adaptive Cascaded Cancellers Using A Novel Soft-Weighting and Reiteration(SWR) Technique"

We introduce a methodology that creates a new class of reduced-rank adaptive cascaded canceller algorithms. Two example algorithms illustrate the benefits of the proposed technique. It consists of combining a novel soft-weighting technique with an existing reiteration technique. Denoted as soft-weighting and reiteration (SWR), its use significantly improves the convergence performance of cascaded cancellers while preserving other desired algorithm characteristics, such as robustness. Example results are shown for the benchmark Gram Schmidt cascaded canceller and for the robust reiterative median cascaded canceller, but the technique is applicable to generic forms of cascaded canceller algorithms. Moreover, the resulting algorithms exhibit near-optimal sidelobe levels in their adaptive beam patterns, which can significantly reduces false alarms. We illustrate the improvements using simulated data and measured data from the MCARM space-time adaptive processing (STAP) airborne radar database. [C8945]

"Angle-Tracking Adaptive Array -- Adaptive-Adaptive Array Processing"

The optimal array, which maximizes the signal to interference plus noise ratio (SINR), is beam-formed by the following weigh vector: $W = c[R^{-1}s(\Phi)]^*$ where R is the covariance matrix of interference and receiver noise, and where $s(\Phi)$ is the steering vector from a desired direction Φ . The optimal array is well known and fundamental in the literature of adaptive array and signal processing but has not been actually applied to real radar because of huge computation burden for inverting R , which is on the order of $N^3/\Delta\tau$. Here N is the number of sensors in an array and $\Delta\tau$ is the update interval. Typically, $N = 1,000$ in a planar array and $\Delta\tau = 1$ mus. In order to reduce the computational burden, Brookner and Howells proposed the technique of adaptive-adaptive array, which transforms the large array of N sensors to a small array of $M+1$ beams of pointing to M interference sources and the desired direction Φ . The optimal array based on $M+1$ beams requires a computation burden only on the order of $M^3/\Delta\tau$. The adaptive-adaptive array in Brookner and Howells (1986) is an ingenious conjecture rather than a solid technique, because no solid method for tracking the directions of M interference sources is given. In this paper, the angle-tracking adaptive array (ATAA) in (Gu, 2006) is introduced to implement the adaptive-adaptive array processing. The ATAA offers an even higher SINR than the well-known optimal array at a computational burden only on the order of $N\ln M^2/\Delta\tau$. The ATAA is providing a solid basis for the adaptive-adaptive array and is superior over the well known optimal array in both SINR and computation burden, suggesting a remarkable new direction to the adaptive array processing in the eve of digital beam-forming era. [C8946]

"An Efficient Identification Algorithm for FIR Filtering with Noisy Data"

This paper is concerned with FIR filtering with noise-corrupted input-output measurements. With an analysis of the algebraic structure of the correlation matrix, it is shown that an unbiased estimate of FIR parameters can be obtained by solving a special bilinear equation. Then a bilinear equation method (BEM) is developed for solving the bilinear equation associated with the unbiased solution of the FIR filtering under the unknown ratio of the input noise variance to the output noise variance (NNR). Being different from the existing unbiased estimators, the main advantage is that the proposed method exploits much sufficiently the special structure of the correlation

matrix and obtains much accurate estimation for FIR filtering in the presence of input and output noises. Simulation results are presented to validate the good performance of the proposed method. [C8947]

"Thresholded samplers for UWB impulse radar"

This paper presents two novel methods for sampling the backscatter in an impulse radar system. The authors have called the two related methods for swept threshold and stochastic resonance sampling. The samplers are simple, mostly digital circuits which are not clocked, but instead utilize continuous-time signal processing. Since fine-pitch CMOS is not very good for analog processing, but instead has very fast digital logic, the samplers are well suited for this technology. An implementation in 90 nm CMOS is described and measurements which confirm a working 23 GHz sampler are shown [C8948]

"Adaptive WEighting of Signals via One Matrix Entity (AWESOME)"

We present the Adaptive WEighting of Signals via One Matrix Entity (AWESOME) algorithm for adaptive array beam pattern synthesis. The array geometry can be arbitrary. Compared to the conventional approaches of using data-adaptive weight vectors at the array output for beam pattern synthesis, which we refer to as the Vector Weighting Approaches (VWA), weight matrices are used at the array output by AWESOME for much improved flexibility for adaptive array beam pattern synthesis. Globally optimal solutions can be determined efficiently for AWESOME due to the convex optimization formulations. AWESOME can be considered as the Semidefinite Relaxation (SDR) of the VWA counterpart. Numerical examples are presented to show that AWESOME allows for strict controls of main-beam shape and peak sidelobe level while retaining the capability of adaptive nulling of strong interferences and jammers. [C8949]

"High Resolution Frequency MIMO Radar"

The frequency MIMO radar synthesizes a wideband waveform by transmitting and receiving multiple frequency signals simultaneously. This paper provides the efficient transmitter array configurations and signal processing methods to improve the cross range resolution and range resolution of the frequency MIMO radar after receiving beamforming. The key is to properly apply the weightings to the multiple subband returns to compensate the delay differences and phase shifts between them. To eliminate the ambiguous images, the nonuniform array and the auxiliary array layout are employed, and the round robin transmission scheme is utilized on the basis of the configuration of the main array plus the auxiliary array. Among them the "round robin" transmission scheme can obtain the best cross resolution at cost of decreasing the pulse repeat frequency. In the "round robin" transmission scheme, spatial diversity technique can be used to combat the target RCS scintillation. [C8950]

"A Two Stage GPS Anti-jamming processor for Interference Suppression and Multipath mitigation"

Global Positioning System (GPS) has found wide application in many areas. However, due to the low power of the received signal, GPS is susceptible to a variety of interferences and multipath. In this paper, a two stage GPS anti-jamming processor based on adaptive arrays is proposed. Firstly, the array received signals are projected onto the orthogonal subspace corresponding to interference to suppress interferences. Then the interference free signals are further processed by a conventional data-independent beamforming to enhance the GPS direct-path signal and mitigate GPS multipath signals. Simulation results are provided to demonstrate the performance of the proposed algorithm. [C8951]

"InSAR Remote Sensing Over Decorrelating Terrains: Persistent Scattering Methods"

Interferometric synthetic aperture radar, or InSAR, is a visual geodetic technique permitting detailed mapping of motion over wide areas. InSAR has been limited to regions without much vegetation, which shields the ground from the radar signals and contributes random motions to the observed deformation. The resulting "decorrelation" of the echoes precludes accurate displacement measurements in these areas. Decorrelation also occurs in interferograms with acquisitions separated too far in the sky. Yet certain points, denoted persistent scatterers, in a radar image are stable, do not decorrelate, and form a network of fiducial points that allow measurements in otherwise poor-quality interferograms. We have generalized an algorithm to find networks of stable points in natural terrain, rather than in urban areas, and applied the method to spaceborne satellite data. Using modern information theory to optimize persistent scatterer detection, we can now find many, many more such points than previously possible. We have applied this improved algorithm to the San Francisco Bay segments of the San Andreas and Hayward faults, and in both cases find that a large number of stable points are seen in the vegetated areas that have to date resisted InSAR analysis. Our method of integrating information theoretic estimation and detection theory to all parts of the method, improves the identification, filtering, and phase unwrapping of the observations. Identification of stable true-ground scattering points permits mapping of subtle surface motions and deformations and also of "bare-Earth" topography. [C8952]

"Range Migration Algorithm in Bistatic SAR Based on Squint Mode"

In this paper, the imaging model for the translational invariant case of bistatic synthetic aperture radar (SAR) is deduced, based on the monostatic squint mode. A derivation of the point target responses both in two-dimensional (2D) frequency and time domains is presented. Using these results, the range migration algorithm (RMA), which could solve the large squint angle in monostatic SAR, is transplanted to the bistatic case. Especially, the key operation of Stolt mapping is interpreted. The simulation results show that, the RMA in bistatic SAR could focus the bistatic large squint very well. [C8953]

"Affordable Naval Surveillance Radar Concept"

Current planned large surveillance radars for shipboard applications employing active aperture technologies are projected to be very expensive. The current planned radars for smaller ships, although less expensive, are limited in performance. This paper provides a new innovative naval surveillance radar architecture that promises to provide naval surveillance radars with high performance at lower cost. The radar uses a fairly inexpensive line array antenna for transmitting a broad beam and fairly inexpensive planar phased array antenna having digital beamforming in one dimension to form many narrow receive beams. The innovation is to rotate the antennas about 45 degrees on the ship relative to the local horizon so that the multipath and antenna sidelobes for most clutter and targets are minimized. For a mechanically rotating array, a transmitter can be located below deck and the transmission signal can be transferred through a passive rotary joint and passive line array antenna thus providing a simple low cost transmission system. On receive, the receive only phased array antenna can be fairly low cost and digital beamforming of multiple beams along the fan transmit beam can easily be accomplished. For non rotating radars, high power phase shifters would need to be employed in the transmit line array antenna to scan the beam. [C8954]

"A spectral slope-based approach for mitigating bistatic STAP clutter dispersion"

In this paper we consider the effects of bistatic clutter spectral dispersion on STAP techniques. A new spectral slope-based approach is presented for mitigating the bistatic geometry-induced performance loss by pre-processing the secondary data used for covariance estimation. Due to its capability to compensate both the clutter spectral centers misalignment and the trace slope variability over range, this approach is shown to yield further dispersion reduction with respect to previously proposed strategies thus improving the performance of STAP. [C8955]

"Clutter Rank of Multi-dimensional Sparse Array Radar"

The framework of estimating the clutter rank of multi-dimensional sparse array radar is presented in this paper. The whole array is first divided into several sub-arrays according to the Nyquist interval, and then the number of degree of freedom (NDOF) estimate theory is employed to estimate the clutter rank in each sub-array. Finally, the clutter rank of the overall system is obtained by adding them together. In 2D/3D arrays, the clutter correlation becomes 2D/3D band-limited process. The NDOF theory is thus extended to 2D/3D cases. The Nyquist interval in 2D/3D arrays with or without range ambiguity is also discussed. When no range ambiguity exists, the actual Nyquist interval is larger than the nominal one. And under some circumstances, the clutter ranks of the 2D and 3D array are approximately identical. [C8956]

"MESAR, Sampson & Radar Technology for BMD"

Over more than 20 years BAE Systems Integrated System Technologies Ltd. (Insyte) in the UK have been participating in the innovative Multi-function Electronically Scanned Adaptive Radar (MESAR) Programme. This has led to the Engineering Development and first of class production contract for the Sampson radar which is to be fitted for the UK T45 Destroyer as part of the PAAMS weapon system. The MESAR programme, which was jointly funded by UK MoD and Insyte, began in 1982 and has resulted in two radar equipments. MESAR1 was an S-band prototype active array multifunction radar which took part in three trials programmes in the period 1989-1995. The MESAR1 programme pioneered the development of Tx/Rx modules, digital adaptive beamforming and real time radar, radar control all of which were successfully demonstrated in trials. MESAR2 is an S-band pre-production active array multifunction radar which began development in 1995 and subsequently undertook a 2 year trials programme at a UK MoD trials range at Benbecula in the Outer Hebrides, Scotland. The objective of MESAR2 was to demonstrate the application of MESAR technology to Ballistic Missile Defence. The programme extended and evolved the technology developed in ME SARI and conclusively proved [C8957]

"Spatially Waveform Diverse Radar: Perspectives for High Frequency OTHR"

The application of multi-input multi-output (MIMO) radar concepts to HF over-the-horizon radar is considered to improve radar timeline management flexibility and to permit adaptivity on transmit. MIMO radar concepts in the literature are inconsistent and in this paper the taxonomy of MIMO radar is clarified and distinctions between different MIMO radar types drawn. The term "spatially waveform diverse radar" is introduced, and performance equivalences between element-space and beamspace orthogonality discussed. Finally, we outline significant constraints on the design of waveform sets for the case of transmit arrays where (at least for some part of the operational regime) the array inter-element spacing is less than one half wavelength. [C8958]

"Music-Enhanced CFAR for High Frequency Over-the-Horizon Radar"

To increase the number of location options for an HF surface-wave radar (HFSWR) there is significant interest in reducing the physical size of the receive array. Reducing the aperture results in a degradation of both sensitivity and azimuth information. Azimuth accuracy may be retained by the use of high-resolution methods (such as MUSIC) that have a significantly smaller beamwidth than standard beamforming. It is expected that the application of these high-resolution methods will help retain azimuth information with reduced aperture size. This paper evaluates the effects of reducing the physical aperture of the linear receive array used in HFSWR and using post-detection azimuth re-estimation by high-resolution methods to maintain azimuth resolution, accuracy, and hence tracking performance. This paper is limited to evaluating the effect of increased azimuth beamwidth and does not address the issue of reduced radar sensitivity. Data for the evaluation was obtained from an HFSWR system located at Cape Race, Newfoundland, Canada. The accuracy of the detection centroid for a full 16-element array is compared to the accuracy for a half-aperture 8-element array. It is shown that similar accuracy can be achieved from the shortened array employing the MUSIC-Enhanced CFAR compared to the full size array using the conventional CFAR processing. [C8959]

"Ultra-Wide Band Near-Field Imaging System"

An experimental ultra-wideband radar system prototype is presented for imaging objects located in the near field of the radar antennas. The system is primarily intended for through-matter, e.g. through-wall, target detection and imaging. The radar hardware is based on several novel technical solutions in the design of its electromagnetic (EM) and circuit components including a new antenna element with wide impedance and gain bandwidth. The same elements are employed for the transmit channel and the two-element receive array. The signal processing and target imaging algorithms are presented. Some results of indoor tests to image in 2-D the spatial position of a cylindrical object are reported. In particular, a brightest-spot recognition technique is demonstrated that uses a number of special radar calibration routines to set properly the time/range scale required for precise target localization and imaging while avoiding appearance of false target responses. [C8960]

"Modelling of Adaptive Multifunction Radars for Trials Planning and Acceptance"

Adaptive, electronically scanned, radars operating in a closed loop pose a particularly challenging problem for radar modelling as traditional probabilistic modelling cannot capture the emergent, highly non-linear behaviour of this class of radar. This paper describes a new suite of models originally designed to support the development of adaptive signal processing and radar control techniques in future multifunction radars. The ability of these models to predict the performance of the radar for site specific conditions is now being exploited to design trials for the ARTIST programme and shows considerable potential to support future radar procurements. [C8961]

"Time-Domain Planar Near-Field Measurement Simulation for Wideband RCS and Antenna"

This paper describes an UWB RCS/antenna planar near field (PNF) measurement system under construction to get the wideband RCS or the impulse response and transient characteristic of UWB antenna. A metal plate's bistatic RCS measurement under TD-PNF was simulated and also was compared with the FD-PNF measurement result. The results show good agreement. Unlike the conventional antenna or RCS time domain test system, the UWB radar signal instead of the no-carrier short time pulse was used to excite the antenna that can avoid the decrease of the dynamic range. FDTD is used to calculate the transient E-field of MtimesN points in a fictitious plane just like the actual PNF sampling signals in the time domain (TD). The calculated results can be considered the actual oscilloscope's sampling output signals. Through time domain near to far field transform, we get the almost same radiation pattern comparing to the FD measurement and the software simulation results. [C8962]

"Hitchhiking bistatic radar: principles, processing and experimental findings"

An experimental low cost bistatic hitchhiking radar has been developed at FFI utilizing the transmission of a civilian ATC radar. It uses off-the-shelf components in the receiver to produce close to real time traces of targets of opportunity. The processing enables positioning in 2D with good suppression of nearby clutter by continuously

monitoring the clutter variation. [C8963]

"Obtaining a 35x Speedup in 2D Phase Unwrapping Using Commodity Graphics Processors"

Graphics processing units (GPUs) are a powerful tool for numerical computation. The GPU architecture and computational model are uniquely designed for high-resolution high-speed grid-based calculations. This capability can be utilized to accelerate certain classes of compute-intensive radar signal processing algorithms. Characteristics of a problem well-suited for computation on a GPU include high levels of data parallelism, low control logic, uniform boundary conditions, and well-defined input and output. We describe the implementation of two-dimensional multigrid least-squares weighted phase unwrapping on a GPU and demonstrate a large speedup over C and MATLAB implementations. Details of the GPU computation are provided. Background information on the GPU architecture and its applicability to general-purpose computation is discussed. [C8964]

"Human Tracking Using Doppler Processing and Spatial Beamforming"

We present a continuous-wave Doppler radar with a multi-element receiver array for tracking humans. Joint Doppler processing and spatial beamforming are used to resolve multiple movers in the Doppler and direction of arrival (DOA) space. The improvement in the performance of the multi-element array compared to a previously developed two-element system is evaluated through Monte Carlo simulation. In an array of limited size, the sidelobes of the strong targets prevent the detection of weaker targets. To overcome this limitation, the monopulse, CLEAN and RELAX algorithms are investigated in conjunction with software beamforming. The improvement in the performance of the radar towards the detection of multiple targets is evaluated by simulation. Measurements are conducted using a 4-element receiver for different targets in line-of-sight and through-wall scenarios. [C8965]

"Signal Detection using the Correlation Coefficient in Fractal Geometry"

Using the Fractal Geometry in Signal processing has been extended nowadays. They have found several applications in signal detection and recognitions. They use the chaotic feature of the noise and clutter and try to distinguish between the noise, clutter and the desired target. Recent works show that lots of clutters like sea and ground clutters have fractal behavior so this kind of approach to the signal detection has been extended these days. In this paper we have used the Box-Counts of a signal rather than the Fractal dimension of a signal as will be defined later in the text. By applying the new defined concept we have developed different methods of signal detection. We use the correlation coefficient of the Box-Count and the time domain range for different ranges. By using the difference in the behavior of these coefficients when we have or don't have a target, we can set statistics from these variables and set up some detectors to determine whether the received signal contains a target or not just by comparing the statistics with some thresholds. One of the applications of the method is in high resolution radars. The received signal contains the Range Profile of the target which is unknown in our point of view. So using matched filters cannot be such helpful. In this paper the proposed detectors can act much better the common detectors of these signals. We have shown the advantage of the new methods. They bring us about 3 db increases in SNR. [C8966]

"DSP Based Implementation of Direction of Arrival for Wideband Sources"

There is a need for the computation of direction of arrival (DOA) for wideband sources for number of applications. There are number of algorithms available in the literature for wideband case however we focus on Coherent Signal Subspace method proposed by Wang and Kaveh. Most algorithms available in the literature follow some variation of CSS algorithm thereby increasing computational complexity in an effort to get more accurate, statistically stable and unbiased DOA. We are interested in computing DOA for wideband sources in real time. We chose CSS algorithm and investigated possibility of implementing it using commercially available digital signal processor (DSP) in an effort to achieve real time capability. DSPs offer flexibility, ease of development of embedded system, reduces design cost and offers use of high-level programming language such as C. In this work, we propose a DSP based architecture for detecting and estimating the DOA of wideband sources. It is known that DOA algorithms require computation of eigenvalues and eigenvectors. It would be best to find computational friendly algorithm for the computation of eigenvalues and eigenvectors. In this work eigenvalues and eigenvectors are computed using well known Householder and QR algorithms. CSS algorithm is then implemented in C and executed on DIOPSIstrade 740 by Atmel. DIOPSIstrade 740 (D740) is a high performance dual-core processing platform for real time applications. The CSS algorithm was then parallelized and a parallel architecture was then developed. This paper presents parallel architecture using DIOPSIstrade 740 (D740) and computes performance parameters. [C8967]

"An Experimental Study on Using Electronically Scanning Microwave Radar Systems on Surface

"Mining Machines"

Using a series-model of an automotive short range radar sensor (SRR) and a recently completed experimental radar system, field tests have been performed in a surface mine. It was examined, to what extent low-cost electronically scanning radar sensors can provide useful data for assistance systems in large scale mining machines. The series SRR sensor using mono-pulse principles for cross range measurement, proved to be useful to supervise the safety zone of a bucket wheel excavator. The more complex and sophisticated experimental radar system using digital beam-forming for cross range processing, can clearly detect and map the contours of trenches and escarpments. The overall promising results refer to many more potential applications for electronically scanning radar in surface mining and motivate to adapt the experimental sensor for such applications. [C8968]

"Wavelets: a Versatile Tool for the High Frequency Surface Wave Radar"

Widely used in image processing, wavelets seem to be a promising versatile tool for the high frequency surface wave radar (HFSWR). HFSWR is based on the ability of HF waves (3 MHz to 30 MHz) to propagate along the earth curvature. HFSWR can detect targets up to few hundred kilometers beyond the horizon. The two main applications of the HFSWR are the maritime surveillance of the exclusive economic zone (EEZ) and the remote sensing of the sea. Beside the classical noise which affects all radar signals, the detection capabilities of HFSWR suffer from two limitations: the sea clutter and the ionospheric clutter which are target masks. However sea clutter can be used to perform remote sensing of the sea. In this paper we are studying how wavelets may contribute to the improvement of radar signal processing. We consider general de-noising feature for radar signals, we carry out a wavelet-based improvement of remote sensing of oceanographic parameters and we show the first results of a wavelet-based processing for ionospheric clutter mitigation. [C8969]

"Adaptive estimation of unknown phase offset between sub-arrays in distributed aperture systems"

It has been recently shown that angle-dependent complex phase and gain offsets between separately calibrated distributed subarrays can be compensated for during beamforming via a modification of a subspace detection approach. In addition to normal estimation and detection losses associated with such an adaptive filter, an additional loss is incurred using this approach. This loss is derived analytically and compared with previously simulated losses. [C8970]

"Optimising bistatic HF radar configurations for target and environmental signature discrimination"

HF radars are large and expensive systems whose performance is strongly dependent on the scattering geometry. There have been several cases where such radars have been poorly deployed, with consequent failure to achieve the surveillance objectives. This paper formulates the problem of radar site configuration in terms of objective mission-related metrics and outlines the optimisation procedure. [C8971]

"Tracking Possibly Unresolved Targets with PMHT"

In tracking scenarios with high target density, it is possible that two (or more) targets may be close enough to be unresolved by the sensor. In this case, the unresolved targets produce only a single measurement, and this may cause the tracking algorithm to incorrectly terminate track on one of the targets. This paper presents an extension of the probabilistic multi-hypothesis tracker (PMHT) to allow for the possibility of unresolved targets. The extended algorithm is compared with the standard PMHT, and with the joint probabilistic data association algorithm for unresolved measurements. [C8972]

"Angle-Only Tracking of Manoeuvring Targets using Double Sets of Multiple Range Models and Probability Mass Diffusion"

This paper presents a solution to the problem of tracking of manoeuvring targets by angle-only measurements from a single, manoeuvrable platform. The solution combines the properties of accurate range estimates of non-manoevring targets with the ability to track manoeuvring targets in an all recursive setting. While previous methods use combinations of recursive and batch processing and/or threshold type manoeuvre detection, the proposed solution has these properties inherently, with a "soft" manoeuvre detection mechanism. The solution, in this paper, is based on a combination of two previously presented ideas, the Multiple Range Models and the recently presented Probability Mass Diffusion filter. In the paper the general problem of angle-only tracking is discussed and the basics of the proposed solution are given. Performance is shown by Monte Carlo simulations of a wide range of target scenarios. [C8973]

"A Kirchhoff Integral Approach to Radar Propagation Modelling and its Application to the Estimation"

of Clutter"

Anomalous propagation, such as that experienced in evaporative ducts, can have a marked effect upon microwave radar clutter. Not only is the clutter strength affected by a change in propagation losses, but the backscatter coefficient is affected through the dependence of grazing angle upon propagation conditions. It is shown that a Kirchhoff integral approach to anomalous propagation can provide an effect means of calculating both propagation loss and grazing angle, hence providing a useful tool for clutter calculations. [C8974]

"RF Photonics for Radar Front-Ends"

Recent developments in RF photonic component technologies can have a significant impact on future radar system architectures. In this paper, current performance of low noise figure and high dynamic range RF distribution links and delay lines, low phase noise RF oscillators, and fast tunable RF filters developed using photonic technologies are highlighted. Performance comparisons with electronic RF front-end technologies are provided including size, weight and power considerations. Finally, other RF photonic technologies applicable to radar systems and further photonic device improvements required for more pervasive radar system use are discussed. [C8975]

"Netted Radar Theory and Experiments"

In this paper, the performance netted radar is evaluated in terms of the ambiguity function. A three dimensional netted radar ambiguity model has been formulated. A software tool has been developed to assess the netted radar ambiguity and resolution properties. Simulation results show that the degradation of range and Doppler resolution are strongly dependent on system and target geometry. We then introduce the design and realization of an experimental netted radar being developed to explore practical performance. This paper describes the system development, testing and calibration and results of initial field testing. [C8976]

"The Signal and Interference Environment in Passive Bistatic Radar"

We present a review of the properties of some signals that may be used as illuminators of opportunity in passive bistatic radar systems. It is shown that such signals are not ideal for radar purposes, though modern digital modulation formats are to be preferred, since their ambiguity performance is better and in general does not vary with time. However, with any type of signal the ambiguity performance is also a strong function of bistatic geometry. We also consider the direct signal, multipath and interference environment, and show both by analysis and experiment that this will in general be severe, requiring of order 80 dB or more of suppression to achieve acceptable target detection results, and even then an effective receiver noise figure of order 20 -30 dB should be used in performance calculations. [C8977]

"Optimal Receiver Trajectories for Scan-Based Radar Localization"

Scan-based radar localization is a passive emitter localization technique for stationary pulsed radars with rotating antenna. In scan-based localization knowledge of the radar sweep rate is used to determine the subtended angle of the radar location from a pair of receivers. A collection of subtended angles is utilized to estimate the radar location. The paper first presents a maximum likelihood estimator for scan-based localization and an iterative Gauss-Newton implementation for it. The Cramer-Rao lower bound (CRLB) for the radar location estimate is derived. Based on the optimization of the CRLB, a practical technique for determining optimal receiver trajectories is developed. The effectiveness of the developed technique is illustrated with several simulation examples. [C8978]

"Error Exponents for Neyman-Pearson Detection of Markov Chains in Noise"

A numerical method for computing the error exponent for Neyman-Pearson detection of two-state Markov chains in noise is presented, for both time-invariant and fading channels. We give numerical studies showing the behaviour of the error exponent as the transition parameters of the Markov chain and the signal-to-noise ratio are varied. Comparisons between the high SNR asymptotics for the time-invariant and fading situations will also be made. [C8979]

"Enhanced Multi-Target Tracking with Doppler Measurements"

In many radar or sonar tracking systems, where the state of interest typically includes target position and velocity components, target Doppler measurements may be available in addition to the target position measurements. Using measurements of Doppler information directly in target trajectory estimation leads to a nonlinear filter implementation. In this paper we investigate the methods of using Doppler measurements to improve tracking performance while maintaining the tracker implementation in the linear domain. Two new methods, namely, the

one point track initialisation and the Doppler data association are proposed. By applying these two methods on the linear multi-target integrated probabilistic data association algorithm (LMIPDA), we improve tracking performance in terms of reduced number of false tracks and computational load. The merits of the proposed approaches are demonstrated via an active sonar underwater multi-target tracking scenario. [C8980]

"High Maneuver Target Tracking Based on Combined Kalman Filter and Fuzzy Logic"

In this paper, a new combined scheme is presented to overcome some drawbacks of the high maneuvering target tracking problems by using the mixed fuzzy logic and the standard Kalman filter. This scheme is consist of two important aspects; at first absolute value of difference between last target course and the present observation target course and the second aspect is the absolute value of measurement residual. The results compared with the augmented method and another combined fuzzy logic method which have been reported respectively. Simulation results show a high performance of the proposed innovation method and effectiveness of this scheme in high maneuvering targets tracking problems. [C8981]

"Design Challenges for an Autonomous Cooperative of UAVs"

The Defence Science & Technology Organisation (DSTO), which is part of the Australian Department of Defence, is developing a research capability that uses small, inexpensive, autonomous uninhabited air vehicles (UAVs) to detect, identify, target, track, and electronically engage ground-based targets such as radars. The UAVs, which act autonomously and cooperatively, use a geographically distributed and heterogenous mix of relatively unsophisticated electronic warfare (EW) sensors and other miniaturised payloads networked together to deliver a distributed situational awareness picture that can be shared across the command echelons. If the many design challenges are overcome, the cooperation and networking of these platforms and payloads could provide results superior to those of the significantly more expensive, platform-centric systems, but with the added advantage of robustness. This paper outlines the challenges relating to autonomy, supervision, and control that the developers face and reports on the development of DSTO's multi-UAV cooperative to date. [C8982]

"UAV Team Formation for Emitter Geolocation"

In this paper we study a scenario in which uninhabited aerial vehicles (UAVs) are tasked with locating a group of active emitters. The time difference of arrival (TDOA) technique is used by the UAVs to geolocate the active emitters. As TDOA requires at least three UAVs to perform geolocation, an algorithm to team three or more UAVs and task this team to geolocate an emitter is required. We discuss two approaches for teaming the UAVs, which we have developed and tested via simulation. The first approach is a simple heuristic that assigns the closest three UAVs to the highest priority emitter. This approach was simple and efficient to run, but improvements in performance could be made. Because TDOA works best when the UAVs are angularly separated evenly around the emitter, the next teaming algorithm developed takes into account the geometry between all UAVs and emitters. It assigns a cost for each UAV team and emitter combination based on the current angular separation of the UAVs around an emitter, and by how much each UAV team can perfect its geometry in a given time period. Two search techniques are explored, which search the solution space for efficient solutions. Results from simulation tests of the two approaches indicate that the second algorithm on average geolocates the emitters in the simulation faster than the heuristic approach, and provides an efficient solution to this UAV teaming and allocation problem. [C8983]

"Track Registration for Multistatic Radars with Multipath"

Bistatic radars deployed in built-up areas, suffer from the effects of multipath due to the presence of reflecting walls. When the geometry of the reflecting surfaces are accurately known, it is possible to identify and utilize radar measurements from the various multipath signals but only if the radar receivers are well registered. Given a 2-D scenario with a single moving target, a smooth reflecting wall, a radar transmitter and two noncollocated radar receivers, we investigate the observability of target state and sensor biases for the following multipaths: (i) direct path: transmitter-target-receiver, (ii) transmitter-wall-target-receiver, (Hi) transmitter-target-wall-receiver, (iv) transmitter-wall-target-wall-receiver. Each radar receiver has a known location and measures range (propagation path length), azimuth, and doppler but has unknown range and azimuth biases in its measurements. Results show that measurements from different multipath signals can be identified. Furthermore, a selection of these measurements can be combined to carry out track registration. [C8984]

"Data fusion without data fusion: localization and tracking without sharing sensitive information"

It is now well known that data-fusion can improve detection and localisation of targets. However, traditional data fusion requires the sharing of detailed data from multiple sources. In some cases, the various sources may not be willing to share such detailed information. For instance, current allies may be willing to share some level of

information, but only if they can do so without revealing their secrets. We show here that, at least for localisation and tracking of targets, data-fusion can be performed without the need to actually combine the data in question, so that no party learns the information of another. Such an approach would allow co-operation between parties that share mutual interests, and yet do not completely trust each other. The particular application on which we concentrate is localisation and tracking of a target using multiple sensors (radars or sonars, or other devices). We show that multiple sensors can be used to refine a target's position estimate, or even obtain a position estimate where no single sensor has enough information to do so (e.g., each has only range information), without sharing the details of the sensor, such as its position, or accuracy of its estimates. [C8985]

"Ionospheric Propagation Effects on Ground and Space Based Radars"

This paper discusses the application of EM propagation theory to account for observations of scintillation from equatorial satellite beacon and radar measurements of transionospheric propagation. Satellite beacon measurements from the wideband satellite experiment are used to calculate the degradation caused by scintillation in the radar coherent integration process. Coherent integration will be required in any space based radar to achieve separation in Doppler of moving targets from the large return of the earth. Measurements of ionospheric scintillation in the equatorial region taken with the VHF/UHF ALTAIR radar in the Marshall Islands are described. These measurements support the use of the strong scatter limit of the parabolic wave equation that accounts for certain features of the observations. A technique is illustrated to calculate realizations or sample functions of wide bandwidth radar signals that have passed through the ionosphere. This technique gives realizations that are consistent with the ALTAIR observations. Results are given for radar performance of target detection for several different radar signal combining techniques. [C8986]

"Characterization of Zero-Doppler Clutter Removal Techniques for ISAR Applications"

Inverse Synthetic Aperture Radar (ISAR) processing is used to generate high-resolution images. This work considers an outdoor test range whereby the ISAR processing induces zero-Hz Doppler clutter (ZDC) effects which adversely impact image quality by either (1) masking actual target responses, or (2) inducing responses not directly attributable to target features. Techniques for removing adverse ZDC effects have been developed and are generally user dependant and/or target specific. This work aims to identify key ZDC reduction mechanisms and characterization metrics to be exploited for more generic applications. Two characterization techniques are considered: pixel-average percentage difference and image cross-correlation of pre-ZDC and post-ZDC processed data. The impact of data windowing is also investigated using various window widths and types. [C8987]

"A New Method for Compensation of SAR Range Cell Migration Based on the Pulse Z-Transform"

A new phase preserving SAR processor that solves the range dependent range cell migration problem is presented and verified theoretically in this paper. The operations involved are only Fourier transforms and multiplications. No interpolation is used, and the processor achieves $O(M \cdot \log_2(M) \cdot N \cdot \log_2(N))$ floating point operations where M and N are arbitrary numbers of data samples in azimuth and range. The SAR processor works for squint mode as well as broadside SAR operation. [C8988]

"A New Approach to Achieving High-Performance Power Amplifier Linearization"

Digital baseband predistortion (DBP) is not particularly well suited to linearizing wideband power amplifiers (PAs); this is due to the exorbitant price paid in computational complexity. One of the underlying reasons for the computational complexity of DBP is the inherent inefficiency of using a sufficiently deep memory and a high enough polynomial order to span the multidimensional signal space needed to mitigate PA-induced nonlinear distortion. Therefore we have developed a new mathematical method to efficiently search for and localize those regions in the multidimensional signal space that enable us to invert PA nonlinearities with a significant reduction in computational complexity. Using a wideband code division multiple access (CDMA) signal we demonstrate and compare the PA linearization performance and computational complexity of our algorithm to that of conventional DBP techniques using measured results. [C8989]

"Polarization Diversity Using Mutual Information"

An information-theoretic criterion is introduced for waveform polarization type selection in a synthetic aperture radar (SAR) configuration. The criterion is based on the concept of mutual information (MI). Specifically, the MI criterion (MIC) minimizes the MI between the radar return signal at two distinct instants of time: one is the just-received return due to the last-transmitted pulse with known polarization type, and the other is the to-be-received return due to the pulse to be transmitted next with to-be-determined polarization type. In that manner, the polarization type selected for the pulse transmitted next will result in the collection of the largest amount of

new information, as measured by a formal criterion. The MIC involves the radar system model and the probabilistic definition of the clutter, interference, and noise processes. In particular, when all these processes are proper Gaussian processes, the MIC attains a simple analytic form. The formulation and simulation-based results are presented in the context of a first-order radar system model, for simplicity, but the MIC can be extended to cover more complex models in a straightforward manner. In addition, the MIC is applicable to other radar modes and sensor types. The results presented show that the MIC is an effective method for polarization type selection in a SAR. [C8990]

"Map-Aided Secondary Data Selection"

Here, we present the results of an investigation on a secondary data screening approach that uses the National Land Cover Dataset along with the Digital Elevation Model to compute a feature vector for each secondary data range. By combining both knowledge sources, we created a feature vector for each range which is essentially a map of the terrain radar cross section as function of azimuth angle. We present the loss in signal-to-interference plus noise ratio, due to the use of an estimated covariance matrix versus a known covariance matrix, for two scenarios: Los Angeles and KASSPER '02. On one hand, our results reveal that map-aided training does not offer a consistent improvement in performance over selecting secondary vectors based on range from the cell-under-test (CUT). On the other hand, the results also reveal that the use of map-aided training does not degrade performance. Thus, one can use map-aided training without the fear of degrading performance while maintaining the potential of improved capability in scenarios where similarity scoring reveals differences between the feature vectors of the CUT and the secondary data ranges. [C8991]

"Adaptive IIR Filtering via a Recursive Total Instrumental Variable Algorithm"

Adaptive IIR filtering in the case where noise exists in both the input and output of the system amounts to solving over-determined normal equations. In this paper a recursive total instrumental-variable (RTIV) algorithm is proposed for tracking the total least-squares (TLS) solution of the normal equations in the over-determined instrumental-variable methods. It is shown that the weight vector in the RTIV algorithm converges to the direction parallel to the singular vector associated with the smallest singular value of the augmented cross-correlation matrix. Moreover, the estimated parameters of the adaptive IIR filter are optimal in the TLS sense and its noise rejection capability is superior to that of the least-squares based algorithms. The appealing behavior of the RTIV algorithm for noisy adaptive IIR filtering is substantiated by simulation results. [C8992]

"Maximum-likelihood based range-dependence compensation for coherent multistatic STAP radar"

We study the performance of space-time adaptive processing (STAP) applied to coherent multistatic radar. The radars we consider are passive (receive only) but are synchronized in order to allow coherent processing of the data among the different radars. One of the major benefit of multistatism is that the full velocity vectors of the targets can be measured. Furthermore, we study the feasibility of estimating the clutter covariance matrix, required to compute the STAP filter. We show that range-dependence effects cause the usual sample matrix inversion (SMI) scheme to fail and we propose a method able to cope with arbitrary multistatic geometries. [C8993]

"Multiple Constraint Space-Time Adaptive Processing Using Direct Data Domain Least Squares (D3LS) Approach"

In this paper, a new direct data domain least squares (D3LS) approach is developed for multiple target detection in space-time adaptive processing (STAP). The advantage of the D3LS technique is that it does not rely on any statistical information of the interference as opposed to conventional STAP algorithms. The modified version of D3LS when more than one target is in a radar scenario will be discussed. This is equivalent to forming multiple beams simultaneously while suppressing all other interference at the radar receiver. Numerical simulations show that multiple beams are directed towards target directions correctly and maintain their gain constraints along those directions such that the target signal intensities or complex amplitudes can be estimated. [C8994]

"Accurate Target Geolocation using Cooperative Observers"

We consider the problem of geolocating a target using relatively simple ground-based sensors with a high degree of accuracy. We show that by using cooperative receivers, it is possible to achieve the desired level of accuracy for a stationary target by utilizing time difference of arrival measurements. We then extend this approach to provide a recursive solution for tracking moving targets using the unscented Kalman filter. Simulation results indicate improved performance over traditional geolocation results with a single receiver. [C8995]

"Parameter Optimization for Load-Optimal Agile Beam Radar Tracking"

Parameter optimization for agile beam radar tracking is considered to minimize radar resources that are required to maintain a target under track. The parameters to be optimized include the track-revisit interval as well as the sequence of pairs of target signal strengths and detection thresholds associated with successive illumination attempts in each track-revisit. The cost to be minimized is the radar energy resources required per unit time over a given number of track-revisits. This formulation is compared to the optimization problem where the cost is the total radar resources required over a specified tracking period. [C8996]

"Training Method for Ground Bounce Removal with Ground Penetrating Radar"

Downward looking ground penetrating radar (GPR) has been considered a viable technology for landmine detection. For such a GPR with the antennas positioned very close to the ground surface, the reflections from the ground surface, i.e., the ground bounce, are very strong and can completely dominate the weak returns from shallowly buried non-metallic mines. Hence, one of the key challenges of using GPRs for landmine detection is to remove the ground bounce as completely as possible without altering the landmine return. The ground bounce varies with surface roughness and soil conditions and leads to performance degradation for many ground bounce removal algorithms without reference data selection. In this paper we introduce NHD-based reference data selection methods for ground bounce removal. Experimental results are provided to illustrate the performance of the proposed method. [C8997]

"Mobile Platform Self-Localization"

This paper proposes a detailed bearing-only algorithm for mobile platform self-localization with respect to three beacons or landmarks whose positions are known. The derivation process of the mobile platform position is split into two stages, where the first stage determines the location region of the platform whereas the second stage fine-tunes this coarse location into one point within this region and calculates the platform heading. Previous approaches to self-localization either have applicability limitations or do not propose a formulation that provides a clear insight into the behaviour of the platform position solution in terms of platform/beacon geometry. [C8998]

"Challenging Issues in Multichannel Radar Array Processing"

This paper is focused on multichannel radar array processing and addresses some challenging issues concerning: the adaptation in nonstationary and nonhomogeneous environments, the value of Space-Time Adaptive Processing (STAP) in an operational High Frequency (HF) radar system, the benefits resulting from the joint use of multiple (not colocated) transmitters and receivers, and the parallel implementation of the multichannel processor. The work follows on where the importance of a multichannel processing is demonstrated with reference to airborne, ground-based, and Over The Horizon (OTH) radar systems. [C8999]

"An ECCM Scheme for Orthogonal Independent Range-Focusing of Real and False Targets"

This article develops a radar signaling scheme providing full immunity against a repeat jammer. Resistance against the jammer is achieved by employing the concept of pulse diversity where the radar continuously emits either modified version of previous waveforms or new pulses following a specific orthogonal structure. This structure enables the radar to successfully separate the signals being reflected off the real targets and the false reflectors being emulated by the jammer, resulting in full independent range-focusing. The method permits combination of various types of pulses and also offers waveform diversity. [C9000]

"Cramér-Rao Bound for Multiple Target Tracking Using Intensity Measurements"

The paper investigates the recently proposed ultimate Cramer-Rao lower bound (CRLB) for tracking multiple targets (Ristic et al., 2004). There are three main contributions: (1) The effect of interaction between targets is analysed; (2) The multi-target CRLB is verified via Monte Carlo simulations; (3) The broader implication of the CRLB is illustrated in the context of a wireless sensor network. [C9001]

"Coherent Integration With Range Migration Using Keystone Formatting"

We have developed and demonstrated the Keystone format to simultaneously remove linear range migration for all targets regardless of their velocities. Higher order motion and under sampling foldover can be removed by hypotheses. The authors present an approach to radar matched filtering which can produce simultaneous high range and high Doppler resolution matched filter outputs. The new matched filter coherently integrates the radar data even though the target scatterers move through many range resolution cells during the coherent integration time. [C9002]

"Forward-based Receiver Augmentation for OTHR"

An experimental multi-static HF radar is described that augments conventional over-the-horizon radar (OTHR) by placing multiple forward-based receiver systems within line-of-sight of targets of interest. With sufficient and appropriately located forward-based receiver sites the radar can generate target tracks that are independent of the uncertain ionospheric state and the system has low incremental cost compared with a complete OTHR. Each site in the multi-static system consists of a ten element linear array with a direct digital HF receiver per element architecture and the receiving components have sufficient dynamic range and spectral purity to operate in the footprint of the direct OTHR transmitter signal. The system uses custom receivers that integrate the frequency management function with the radar receiver function. Signal processing algorithms include real-time STAP and adaptive CFAR. Inter-site communications is achieved using a low-cost 802.11 b wireless communications network where the longest path in this network is 37 km. The system has performed beyond expectation for the desired target class. [C9003]

"Application of the Coherent Pixels Technique (CPT) to urban monitoring"

During the past years, Remote Sensing has become a powerful tool for earth observation. In particular, SAR differential interferometry (DInSAR) has shown to be a very reliable technique for deformation phenomena monitoring, being able to achieve millimetric accuracies. It is the aim of this paper to present and show the potentials of the UPC's advanced DInSAR algorithm, the coherent pixels technique (CPT). Deformation results of different studied areas will be presented, revealing the performances of DInSAR for risk management as well as for the understanding of much geological processes. [C9004]

"Multipass SAR Processing for Urbanized Areas Imaging and Deformation Monitoring at Small and Large Scales"

A new processing chain that allows monitoring ground deformations, both at small scales and large scales, is discussed. Core of the chain is the spatial differencing (SD) algorithm that allows very quick estimation of the small scale (low resolution) mean deformations velocity and residual topography by means of the use of spatial differences between adjacent and non-adjacent pixels. Small scale deformation time series is then generated by using the Enhanced spatial differences (ESD) that permits separating atmospheric phase contribution, linear and non-linear deformation velocity and residual topography. Deformations and target localization at large scales (full resolution) is provided by the application of a multi-dimensional (4D) imaging (differential-tomography) that exploits the complex nature of the received signal to focus the data in the space-time domain. [C9005]

"UWB and mm-Wave Communications Systems"

First Page of the Article [C9006]

"Extraction of Bridge Features from high-resolution InSAR Data and optical Images"

Modern airborne SAR sensor systems provide geometric resolution in the order well below half a meter. By SAR interferometry from pairs of such images DEM of the same grid size can be obtained. In data of this kind many features of urban objects become visible, which were beyond the scope of radar remote sensing only a few years ago. However, because of the side-looking SAR sensor principle, layover and occlusion issues inevitably arise in undulated terrain or urban areas. Therefore, SAR data are difficult to interpret even for senior human interpreters. Furthermore, the quality of the InSAR DEM may vary significantly depending on the local topography. In order to support interpretation SAR data are often analyzed using additional complementary information provided by maps or other remote sensing imagery. In this paper a fusion of high-resolution InSAR data and one aerial image is discussed for the example of a scene containing bridges that are core elements of infrastructure. The aims are improvement of the 3D visualization of the scene and the extraction of the main parameters of the bridges' geometry. [C9007]

"Statistical Polygonal Snakes for 3D building reconstruction using High Resolution SAR data"

In this paper, the polygonal active contour method is adapted to the case of synthetic aperture radar (SAR) images of urban areas. The statistical criterion is modified to be able to deal with multiple images in order to improve the segmentation of buildings. A criterion is proposed and is then implemented and tested over real high resolution SAR images containing urban areas. A discussion about the benefits of this approach is done and further work about 3D statistical active contour is introduced. [C9008]

"Damage mapping for the 2004 Niigata-ken Chuetsu earthquake using Radarsat images"

The building damage detection technique which we have developed has been successfully applied to past events such as the earthquakes in Kobe in 1995, India in 2001, and Bam in 2003 by using the compound index, z -value, a value derived from the correlation and difference in intensities between pre-and post-event SAR images. This technique was applied to the Japan earthquake areas affected in the Niigata-ken Chuetsu, Japan earthquake of October 23, 2004 by using one pair of radarsat images taken before and after the earthquake. However, it was not possible to identify any significant distribution of damaged buildings. In this study, we examined the reasons for that and proposed a new technique that uses two pairs (pre-seismic and co-seismic) of SAR images to identify smaller building damage ratios in less densely built-up areas as compared to previous techniques. The main idea is to minimize the effects of signal noise and temporal changes of the earth's surface on building damage estimation by calculating the difference values of the two pre-event images and one post-event image. From a macroscopic point of view, the distributions of both difference values of the z -values and the correlation coefficients in built-up areas were in good agreement with damage reported in survey reports. In Yamakoshi village, located in the highlands, we could also identify large-scale landslides with accuracy as good as that of interpretation from aerial photos. [C9009]

"Target recognition by means of spaceborne C-band SAR data"

The relative low resolution (~ 25 m times 5 m on the ground) of spaceborne C-band SAR data as acquired e.g. by ESA sensors ERS and Envisat can be significantly increased (up to sub-meter precisions (Perissin and Rocca, 2005)) by processing coherently long series of images. Moreover, by analyzing the amplitude of the radar signal, the main radar characteristics of urban targets can be estimated and a system for automatic recognition of a set of scattering structures can be developed. In this work, we present the methodology and the results obtained on the test-sites of Milan and Shanghai by combining data acquired from ascending and descending passes and from parallel satellite tracks. [C9010]

"Towards a Complete Processing Chain of Multibaseline Airborne InSAR Data for Layover Scatterers Separation"

Interest is continuing to grow in exploiting the advanced multibaseline operation of synthetic aperture radar interferometry (InSAR) to solve layover effects, that can degrade conventional InSAR topographic mapping. In this work we report about experiments of the functionality of "layover-free" or "higher-order" interferometry with the dual-baseline single-pass SAR interferometer AER-II. Estimation of the number of multiple layover scatterers, i.e. of the interferometric order, and model-based spatial spectral estimation are integrated to process the three-antenna non uniform array data. Results are discussed for a bridge over the valley test site. [C9011]

"A 79GHz SiGe-Bipolar Spread-Spectrum TX for Automotive Radar"

A 79GHz spread-spectrum TX, implemented in a SiGe bipolar process, consists of a VCO, a prescaler, a PRBS generator, and a biphasic modulator. The sequence length of the PRBS is 1023 bits at a bit rate of 1.235Gb/s. The chip provides an output power of -1dBm and draws 750mA from a 5.5V supply [C9012]

"Broadband RF and Radar"

First Page of the Article [C9013]

"A Novel Positioning Algorithm in Wireless Sensor Networks Based on Indoor Connective Information"

Localization information of individual nodes is crucial for many advanced functions including routing, querying in wireless sensor networks. Most of the existing localization algorithms in wireless sensor networks are designed for outdoor environment and few of them can get a reasonable localization precision in indoor environment. This paper presents a novel indoor localization scheme which uses the spatial connective information to filter distorted messages, so as to improve the positioning precision. We establish an indoor positioning dome system, make performance comparison with other schemes and fully prove the advantages of our proposed indoor scheme. [C9014]

"Intelligent Radar Management Techniques in High Frequency Surface Wave Radar"

This paper has highlighted and provided some background as to why HFSWR has been a leader in intelligent radar techniques as without them the robust radar performance cannot be achieved. The use of basic Intelligent Radar Techniques has provided the ability for the radar to operate in a complex environment effectively and robustly. However the high level of complexity combined with the experience also leads to a general conclusion

that real time evaluation and modelling of radar performance against the chosen goals could enhance the efficacy of the radar, but to achieve this goal an extra layer of analysis and control software is required to exploit the ground work laid by the current and very effective system. [C9015]

"mm-Wave Tranceivers and Building Blocks"

First Page of the Article [C9016]

"A Bandpass $\Delta\Sigma$ DDFS-Driven 19GHz Frequency Synthesizer for FMCW Automotive Radar"

A 19GHz frequency-modulated continuous-wave TX based on a bandpass $\Delta\Sigma$ DDFS-driven RF frequency synthesizer is presented. Implemented in a 0.25 μ m SiGe process, the synthesizer draws 63mA from a 2.5V supply while achieving a 512MHz FM deviation with a 200Hz FM rate at a center frequency of 19GHz. The measured phase noise of the frequency synthesizer is -113.68dBc/Hz at 1MHz offset frequency from a 19GHz carrier [C9017]

"A 90GHz 65nm CMOS Injection-Locked Frequency Divider"

Two injection-locked 2:1 frequency dividers for automotive radar applications achieve locking ranges from 82 to 94.1 GHz and from 34.3 to 42.1 GHz and consume 4mW and 8.4mW, respectively. The cascade of the two dividers can be locked from 79.7 to 81.6GHz. The 1mm²chip is implemented in a 65nm CMOS process. [C9018]

"A 23-to-29GHz Differentially Tuned Varactorless VCO in 0.13 μ m CMOS"

A differentially tuned varactorless VCO is implemented in a 0.13 μ m CMOS process. The frequency is continuously tunable from 23.2 to 29.4GHz (23.6% range differential and 3.3% range for common-mode tuning) using a single-ended (1.5V max) tuning voltage. Measured phase noise at 26.6GHz is -96.2dBc/Hz (3MHz offset) and the open-drain output buffer delivers -11dBm (single-ended) to a 50 Ω load. The 0.3 \times 0.4mm²core consumes 43mW (6.5mW in the output buffer) from a 1.2V supply. [C9019]

"Cell Decomposition for Building Model Generation at Different Scales"

Usually, 3D building reconstruction is realized by systems, which either apply constructive solid geometry (CSG) or boundary representation (B-Rep) to model the respective buildings. We present an alternative approach based on cell decomposition, which can be used efficiently for building reconstruction at different scales. Firstly, building polyhedrons are constructed from airborne LIDAR data and given outlines of the respective buildings. In this context, cell decomposition is used to guarantee topological correct representations and the simple implementation of constraints between different building parts like co-planarity or right angles. As it will be demonstrated in the second part of the paper, cell decomposition is also advantageous if large scale building models have to be generated for example based on the analysis of terrestrial LIDAR data. [C9020]

"Moving Target UWB Radar Demonstration using Real-Time Sampling"

Moving target bistatic 2D UWB radar trial with two receiving antennas using modification of time-domain back-projection technique with use of 50 GHz equivalent sampling oscilloscope in comparison of two channel 1 GHz real time sampler is presented. Sub nanosecond first derivate Gaussian pulse with peak-peak amplitude 1.2 V was used. As a target a metal barrel was chosen and his movement by shifting with 5 cm step simulated. Using real-time sampler was the goal. Acquired data were processed and the radar images shown. [C9021]

"Doppler Radar System for Small Objects Localization"

This paper addresses design of a localization system using Doppler radar. First the hardware requirements are discussed. A lot of attention is paid to logarithmic amplifier issues as it plays a key role in the final design. Then the time-frequency analysis is presented as an option for signal processing. [C9022]

"Comparison of Pulse and Continuous Wave Propagation Through the Wall"

Knowledge of UWB pulse propagation in and through walls is needed for precise structure analysis and radar sensing. In this paper some experimental results (insertion loss, delay) of pulse propagation through the wall are shown. The methodology of time domain measurement is presented as well. Attenuation of the same wall was measured also in frequency domain. Comparison of spectral components wall attenuation measured using time domain techniques and continuous wave measurements is also done. Dependency of signal delay and attenuation on wall-antennas distance is investigated. [C9023]

"Simulated Transient Radiation Characteristics of Optimized Ultra Wideband Printed Dipole Antennas"

In case of particular ultra wideband applications (i.e. radar, positioning, etc.), it is crucial to know the transient responses of antennas. This paper picks up the threads of the previous work, where the optimization process searches for the dipole shape, which accomplishes two required parameters-good matching and minimal distortion. The particle swarm optimization method was used in the process of dipole shape optimization. As a result, the optimized ultra wideband dipole is perfectly matched and minimally distorts the applied signal. The main part of the paper presents the transient radiation characteristics of optimized dipoles with common dipole element shape, such as the ideal dipole, dipole with balun transformer and monopole with planar ground plane. [C9024]

"Tumor Estimation In Tissue Sensing Adaptive Radar (TSAR) Signals"

Tissue sensing adaptive radar (TSAR) is a microwave imaging technique that has been proposed as a modality for early stage breast cancer detection. A considerable challenge for the successful implementation of this technique is the reduction of clutter that is present in the scattered fields. In this paper, a method to estimate the tumor response contained in the late time scattered fields is presented. The method uses a parametric function to model the tumor response. A maximum-a-posteriori (MAP) estimation approach is used to evaluate the optimal values for the estimates of the parameters. Accurate identification of the tumor response permits the segregation of the clutter from the late time response. The ability of the algorithm to estimate a tumor response using simulated TSAR data is demonstrated. [C9025]

"Vehicle Positioning in Underground Mines"

This paper describes the problem of locating a vehicle relative to a digital map of an underground mine. The mines of interest produce potash, and they are at a depth of approximately 1000 meters, being relatively large, covering an area greater than 10 kilometers by 10 kilometers. A major application of vehicle positioning is in tracking ground penetrating radar. Ground penetrating radar is used to ascertain the current condition of the mine ceiling and evaluate its risk of delamination (i.e. collapse). A ground penetrating radar system is driven along a tunnel and measurements are logged. It is necessary to record position information along with the radar signal, and this can be an expensive task without a positioning system, since there are many kilometers of mine tunnels. Two possible problem solutions are proposed each using different absolute measurements. For the first case the distance to the mine walls is used. In the second case an existing wireless ethernet network furnishes the positioning system with distances from local access points. The system model is the same for both formulations and uses a state space representation. Both formulations also make use of inertial measurements such as acceleration. A particle filter, which is a recursive Bayesian technique using sequential Monte Carlo sampling, is used to estimate the state and, therefore, the position of the vehicle. [C9026]

"A New Differential Clutter Map Processing in Modern Surveillance Radars"

In this paper we propose a new differential clutter map processing to reduce the false alarms from stationary ground clutter, sea clutter and improve the detection probability of the slow moving target with low Doppler frequency shift. The proposed clutter map is a scan to scan processing which receives the echo signal from Doppler filter bank tuned at lowest Doppler frequency, processes it and delivers the processed signal to the CFAR processing. The simulation results show that the false alarm rate is reduced by more than -30 db. The Clutter map also increased the probability of detection of low speed target, slower than 100 Km/hr. [C9027]

"IEEE 802.11 WLAN Based Real-Time Location Tracking in Indoor and Outdoor Environments"

In this paper we propose an IEEE 802.11 wireless LAN (WLAN) based location tracking system for indoor and outdoor environments. The system is implemented using the received signal strength indication (RSSI) measurements and training-data based estimation techniques. Methods for acquiring, filtering and interpreting wireless data are discussed with emphasis on how they will be applied to wireless tracking. Training-data based estimation is performed by taking a series of RSSI measurements at known training points and then approximating the current location using the nearest neighbor algorithm. Propagation-based distance estimation is based on the Log-distance path loss model. Experiments are conducted for both training and propagation models to estimate the distance of the user from a known access point in indoor and outdoor locations. The experimental results that show the indoor and outdoor location estimation using the propagation model and training data are presented. [C9028]

"Simulation Tools for Interpretation of High Resolution SAR Images of Urban Areas"

New powerful spaceborne sensors for monitoring urban areas have been designed and are ready for launch. More detailed SAR images will be soon available and, consequently, new tools for their interpretation are needed, above all when urban scenes are illuminated. In this paper, the authors propose some tools for the study and the analysis of high resolution SAR images based on a SAR raw signal simulator for urban areas. Comparing simulated SAR images with the real one, interpretation of SAR data is improved and fundamental support of the employed tools is further assessed. [C9029]

"Raster to Vector in 2D Urban Data"

The aim of this work is to propose a refined approach to urban object recognition and extraction exploiting a priori information about geometrical features of the urban objects. In particular, the proposed procedure shows that it is possible to improve the characterization of elements of the urban scene by assuming that they fit to some geometrical models. Advantages includes the possibility to manage urban object as vector files, to compare object presence and shapes in multi- temporal remotely sensed data sets, and finally to compare and fuse remotely sensed data with Geographic Information vector layers. [C9030]

"Object-Oriented Classification of LIDAR-Fused Hyperspectral Imagery for Tree Species Identification in an Urban Environment"

The objective of the current study was to develop a methodology for the identification of tree species in an urban environment by using Quickbird multispectral data, AISA hyperspectral data, AISA Eagle hyperspectral data and Leica ALS50 LiDAR data. For this research, object-oriented classification was performed using eCognition Professional. The classifications were performed on each of the images available with and without the aid of LiDAR. Elevation and intensity data was used to create images segments as well as user-defined class rules. Classes included honey locust, white pine, crab apple, sugar maple, white spruce, American basswood, pin oak and ash. Initial results indicate fusing LiDAR data with these imageries showed an increase in overall classification accuracy for all datasets. Increases in overall accuracy ranged from 12 to 24 percent over classifications based on spectral imagery alone. There were some more substantial increases in some individual species accuracies, particularly classes that consisted of smaller objects such as saplings or shrubbery. [C9031]

"Joint combination of point cloud and DSM for 3D building reconstruction using airborne laser scanner data"

More and more cities are looking for service providers able to deliver 3D city models in a short time. Airborne laser scanning techniques make it possible to acquire a three-dimensional point cloud leading almost instantaneously to digital surface models (DSM), but these models are far from a topological 3D model needed by geographers or land surveyors. The aim of this paper is to present the pertinence and advantages of combining simultaneously the point cloud and the normalized DSM (nDSM) in the main steps of a building reconstruction approach. This approach has been implemented in order to exempt any additional data and to automate the process. The proposed workflow firstly extracts the off-terrain mask based on DSM. Then, it combines the point cloud and the DSM for extracting a building mask from the off-terrain. At last, based on the previously extracted building mask, the reconstruction of 3D flat roof models is carried out and analyzed. [C9032]

"Reconstruction of the 3D Stereo Buildings from Polarimetric SAR Images in Two Converse Flights"

The height and location of the three dimensional (3D) objects can be retrieved from polarimetric SAR images in multidirectional flights, and the 3D stereo objects can then be reconstructed. Polarimetric SAR image describes the objects via polarization synthesis, and presents much richer information than mono-polarized SAR image. Furthermore, multi-aspect flights of polarimetric SAR can see the 3D stereo objects in different angles and become feasible to invert the height and location of the objects. This paper presents an attractable approach for reconstruction of the 3D stereo buildings from two converse flights of airborne PI-SAR images (at X band with spatial resolution 1.5 m). [C9033]

"3D Visualisation and Physical Feature Extraction of Urban Areas using Multibaseline POL-InSAR Data at L-Band"

This paper extends two single polarization multi-baseline interferometric SAR spectral analysis techniques to the fully polarimetric configuration. These new algorithms enhance the height estimation of scatterers by calculating optimal polarization combinations and allow to determine their physical characteristics. First experimental results show the retrieval of building height and their polarimetric properties by means of single-baseline polarimetric

datasets. Dual-baseline observations permit the solution of the layover problem by separating two contributions within one resolution cell. The algorithms are tested using multibaseline Pol-InSAR data acquired by DLR's E-SAR system. [C9034]

"An Integral Detection Scheme for Moving Object Indication in Dual-Channel High Resolution Spaceborne SAR Data"

Upcoming SAR satellite missions like TerraSAR-X or RADARSAT-2 will deliver high resolution dual channel SAR data with large coverage. These new missions-together with rising interest in area-wide traffic monitoring-motivate spaceborne GMTI as an attractive alternative to conventional traffic data acquisition. However, a moving object appears distorted in the SAR image since the well-known stationary world assumption in the SAR focusing process is violated. In this paper, a detection approach is presented, which considers simultaneously the effects of azimuthal and radial motion of an object. The mathematical framework of this detector combines information of the measured signal, the expected signal, and their variances. Furthermore, the performance of the proposed algorithm is analysed using experimental airborne SAR data. [C9035]

"Urban Land Cover in Rome, Italy, monitored by single-parameter multi-temporal SAR images"

This paper reports on monitoring land cover in the urban and sub-urban area of Rome, Italy, by multi-temporal ERS 1-2 SLC SAR images. The identification of the SAR image parameters, including backscattering, degree of interferometric coherence and textural pixel-based features to be exploited in classification, is discussed. The information extracted from the SAR images is fused and processed by a Multi-Layer Perceptron (MLP) neural network (NN) to produce land cover maps. The network topology has been carefully designed, paying special attention to the number of hidden units. Once trained, the net's performance has been validated over a statistically significant ensemble of patterns independent of the learning set. The net has been used for the automatic classification of a large area in two different years, 1994 and 1999, thus obtaining a map of hot spots corresponding to areas where changes had occurred. [C9036]

"Estimating instantaneous false alarm rate in a CFAR system by Bayesian and empirical Bayesian methods"

In this paper it is shown that the instantaneous false alarm rate in a constant false alarm Rate (CFAR) system fluctuates from scan to scan and that Bayesian and Empirical Bayesian estimators can be applied to decrease the error between the actual and the assumed false alarm rate. The instantaneous false alarm rate is a random variable and its probability density function is derived for different system configurations. Bayesian estimators are applied in cases where analytical expressions of the mean and variance of the instantaneous false alarm rate can be derived. The mean square error in the estimated false alarm rate is shown to be less than the mean square variations of the instantaneous false alarm rate. Empirical Bayesian estimators are introduced and applied to cases where statistical properties of the false alarm rate are unknown. Empirical Bayesian estimators rely on past data to estimate the current false alarm rate and it is shown that they will converge asymptotically to the equivalent Bayesian estimators as the amount of past data gets large. [C9037]

"Cancellation of Doppler Distortion in Pulse Compression for Targets Moving in an Arbitrary Direction"

It can be shown that the hyperbolic frequency modulated waveform is Doppler-invariant only when the Doppler factor is a constant number, i.e., the target has a constant velocity and along the direction from the radar to the target. If the target moves in an arbitrary direction, the degradation of the pulse compression caused by the mismatch between the reflected signal and the matched filter may still exist. In this paper we demonstrate that the Doppler effect caused by the moving target in an arbitrary direction can be approximated by a target with an initial velocity and a constant acceleration along the direction from the radar to the target, which results in a frequency shift in the reflected waveform. Therefore a bank of matched filters with pre-selected values of frequency shifts can be utilized to compensate for the Doppler effect. Numerical examples with target moving in an arbitrary direction are presented to illustrate this effect, which have been successfully compensated by shifting the frequency response of the matched filter. [C9038]

"Computationally Efficient Angle Estimation Using Maximum Likelihood In A Digital Beam-Forming Radar"

We present a new signal processing method that uses maximum likelihood estimation (MLE) to estimate target angle-of-arrival (AOA) for a digital beam-forming phased array radar. We describe the motivations for abandoning conventional monopulse estimation, and contrast our proposed method to other recently proposed

MLE approaches. In particular, we describe a method which eases the computational burden associated with maximum likelihood AOA estimation, making it feasible for use in real-time signal processors for phased array radar systems. We discuss improvements in beam-shape loss and AOA estimate accuracy for search radar applications. [C9039]

"A Novel High Resolution ICA-Based TOA Estimation Technique"

In this paper, a novel high resolution time of arrival (TOA) technique is proposed for multipath wireless environments. The technique is based on frequency domain independent component analysis (ICA). The proposed technique has applications in radar, sonar, wireless local positioning system, and, mobile adhoc networks (MANETS). The proposed algorithm is compared to the traditional techniques such as delay lock loop (DLL) and super-resolution multiple signal classification (MUSIC). Simulations are conducted to compare performance measures that include: (1) sensitivity to bandwidth, (2) resolution: Capability of resolving closely spaced reflections in a multi-path environment, (3) sensitivity to number-of-observations, and (4) sensitivity to signal-to-noise ratio (SNR). Simulation results confirm that the proposed algorithm leads to lower sensitivity to SNR, number-of-observations, and, bandwidth. In addition, the technique possesses a high resolution and can be simply implemented via FPGA (field programmable gate array) and DSP (digital signal processor). [C9040]

"A New Doppler-Tolerant Polyphase Pulse Compression Codes Based on Hyperbolic Frequency Modulation"

The conventional polyphase pulse compression codes including Frank code, P1, P2, P3 and P4 code suffer severe signal loss in performance under Doppler environment. This paper proposed a new polyphase pulse compression codes which are conceptually derived from the step approximation of the phase curve of the hyperbolic frequency modulated chirp signal. Comparing with the above conventional codes and the sidelobe-optimized polyphase $P(n,k)$ code, the peak value of this new polyphase codes degrades much slower and the range resolution as well as maximum sidelobe level are almost constant when Doppler frequency increases. The main disadvantage of this polyphase code is the relatively high sidelobe level without Doppler effect, which can be addressed by applying the proper window function. The desired Doppler-tolerant property of this new polyphase codes is very attractive for radars employing digital signal processing. [C9041]

"A Co-Channel Signal Detector Based on Phase Tracking for Pulse Doppler Radar"

Doppler processing is routinely applied to isolate targets from noise, clutter and interference in conventional pulse-Doppler radar. If a target is co-located in range and azimuth and has a similar radial velocity (co-channel) as another target (or interference), that target may not be detected. This is because only amplitude or power information is used in the detection stage, which does not provide sufficient information to discriminate co-channel signals from each other. In this paper we propose a detector which can resolve co-located targets (or target with interference) with similar Doppler frequencies. Instead of only using phase information for the coherent integration, our proposed detector tracks the phase modulation differences of the co-located, co-channel, targets. The amplitude information of the targets can also be estimated and forwarded to the tracker. One application of this method is HF radar where a target may have a Doppler frequency similar to a Bragg line-first order sea clutter. The Bragg lines are generally dominant at all ranges and exist in all directions. Conventional processing fails to discriminate when targets radar features are similar to the Bragg lines. Simulations of the proposed method show promising results that targets with Doppler frequencies near Bragg lines can be detected. [C9042]

"Adaptive Regularized FOCUSS Algorithm"

The sparse solutions obtained via the regularized version of FOCUSS (focal underdetermined system solver) are governed by the choice of a proper regularization parameter. Based on the principle of adaptive regularization algorithm (ARA) and regularized FOCUSS (R-FOCUSS) algorithm, this paper proposes an adaptive regularized FOCUSS (AR-FOCUSS) algorithm for solving an underdetermined linear system. Simulation results show that AR-FOCUSS is less sensitive to the choice of regularization parameter than R-FOCUSS, and the former outperforms the latter under the same conditions. [C9043]

"Adaptive MIMO radar system in clutter"

In this paper we describe an adaptive CFAR algorithm for detection in a MIMO radar system operating in K-distributed clutter. We provide a statistical description of the signal processing and therefore we report the results in false alarm rate and detection. Moreover the incoherent algorithm taken into account is compared with a coherent way of processing the same data in order to provide a deeper understanding. [C9044]

"CMOS Transceivers at 60 GHz and Beyond¹"

The integration of millimeter-wave transceivers in CMOS technology can benefit from sophisticated signal processing and calibration techniques already in use at lower frequencies. This paper describes a CMOS heterodyne receiver with on-chip LO and frequency divider that achieves a noise figure of 6.9-8.3 dB while consuming 80 mW. A frequency divider is also presented that operates from 64 to 70 GHz in 0.13- μ m CMOS technology with a power dissipation of 6 mW. [C9045]

"Noisy Component Extraction (NoiCE)"

Existing blind source extraction (BSE) methods are limited to noise-free mixtures, which is not realistic. Based on a rigorous analysis of the existing BSE methods, we address the problem of noisy component extraction (NoiCE) which provides BSE in the presence of noise. As a byproduct in BSE after deflation, we may also obtain the asymptotic identification of the a priori unknown observation noise disturbance. By yielding an asymptotically efficient filter in the presence of an unknown observation noise, our approach may also be viewed as a robust approach to noisy component extraction. Simulation results are provided which confirm the validity of the theoretical results and demonstrate the performance of the derived algorithms in noisy mixing environments. [C9046]

"Elevation Filtering in Wide-Aperture HF Skywave Radar"

Use of 2D arrays in HF skywave radar to provide elevation angle of arrival information has the potential to improve coordinate registration and provide for elevation filtering. This latter capability can be used to filter out propagation occurring off disturbed ionospheric layers which can introduce Doppler spreading in backscattered ground return, obscuring low radial speed targets. Filtering capability via a 2D wide-aperture HF receive antenna is demonstrated using real-world data with multiple ionospheric propagation paths. [C9047]

"Short-data-record Adaptive Detection"

The classical problem of detecting a complex signal of unknown amplitude in colored Gaussian noise is revisited in the context of adaptive detection with limited training data via the auxiliary-vector (AV) filter estimation algorithm. Based on statistical conditional optimization criteria, the iterative AV algorithm starts from the target vector and adding non-orthogonal auxiliary vector components generates an infinite sequence of tests that converges to the ideal matched filter (MF) processor for any positive definite input autocorrelation matrix. Computationally, the algorithm is a simple recursive procedure that avoids explicit matrix inversion, decomposition, or diagonalization operations. When the input autocorrelation matrix is replaced by a conventional sample-average estimate, the algorithm effectively generates a sequence of MF estimators; their bias converges rapidly to zero and the covariance trace rises slowly and asymptotically to the covariance trace of the familiar adaptive matched filter (AMF). For finite data records, the generated sequence of estimators offers favorable bias/covariance balance and members of the sequence are seen to outperform in probability of detection (for any given false alarm rate) all known and tested adaptive detectors (for example AMF and the multistage Wiener After algorithm). While the issues treated refer to general adaptive detection procedures, the presentation herein is given in the context of joint space-time adaptive processing for array radar. [C9048]

"Knowledge Aided Detection and Tracking"

Proper use of knowledge of the environment can assist in the detection and tracking of targets within a radar system. Referenced research shows that knowledge-aided (KA) algorithms using terrain data enhances radar performance in the filtering, detection and tracking stages of processing. This paper addresses the development and experimental demonstration of a new post detection filtering algorithm that uses digital terrain elevation data to identify shadowed regions where ground targets are not observable. This knowledge is used to eliminate false alarms from within these regions prior to track processing. A demonstration experiment is described and improvements on the order of 9.4 dB are reported. [C9049]

"Inverse Precision Velocity Update for Monopulse Calibration"

A critical function of a radar system is to precisely locate moving targets for identification and targeting. The moving target location is determined with respect to the actual boresight of the radar antenna performing the angle measurements. The accuracy of these angle measurements is often limited by bias errors (e.g., radome errors, sum and difference channel isolation and imbalances, and harmonization errors) which are not related to the signal-to-noise ratio of the received radar return. In effect, the bias errors preclude accurate monopulse angle measurement to a target, even if the target is clearly visible by the radar. A new technique is proposed which avoids these limitations, deriving a correction for the electrical boresight of a monopulse antenna mounted

on a moving platform. It exploits highly accurate velocity measurements from currently available low-cost INS/GPS systems with carrier phase measurements. The measured velocity coupled with advanced multichannel processing of a monopulse SAR mode provide independent pointing error estimates from many pixels. This patented technique has been named Inverse Precision Velocity Update (or Inverse PVTJ) for monopulse calibration. The angle estimates from a selected set of pixels are weighted and averaged to obtain a precise estimate of the monopulse beam pointing for accurate moving target geolocation. [C9050]

"Detection of defects in wood slabs by using a microwave imaging technique"

In this paper, an experimental set up based on interrogating microwaves is used to obtain images of the cross section of dielectric cylinders. In particular, a microwave tomographic configuration is used to inspect wood slabs in order to search for defects and voids. The measured data (samples of the scattered electric field) are inverted by using an efficient reconstruction technique, which is able to handle the ill-posedness of the inverse scattering problem. The developed experimental apparatus is validated in this paper by means of several numerical simulations. Preliminary experimental results are also reported. [C9051]

"An Overlapped Scan Method for Enhanced 3D Radome Characterization"

An aircraft's nose cone is a protective cover for the aircraft that not only provides aerodynamic stability, but also typically serves as an electromagnetically transparent shield for a radar that is located behind it. Formally known as a radome, these thin, multilayer fiberglass covers have desired electrical performance parameters to ensure proper radar signal transmission and reception. Of particular importance are the transmission efficiency and horizontal beam deflection as seen throughout the radome. Over time, radomes deteriorate in response to moisture, bird strikes, lightning strikes, aging, delaminations, and the like. There is to date, however, very little literature on visualizing, localizing, and characterizing transmission efficiency errors of radomes in a 3D rendering based on measured data. This paper introduces a new method for accomplishing this by introducing a new mathematical technique for processing received signals of adjacent scans. [C9052]

"Ground Penetrating Radar: A Smart Sensor for the Evaluation of the Railway Trackbed"

Ground Penetrating Radar (GPR) has become an increasingly attractive method for the engineering community, in particular for shallow high-resolution applications such as railway trackbed evaluation. It is a non-destructive smart sensing technique, which can be applied dynamically to achieve a continuous profile of the trackbed structure. Due to recent hardware and software improvements, real time cursory analysis can be performed in the field. Based on collected field data, the present paper investigates the applicability of the GPR smart sensor system in terms of the railways trackbed assessment and concludes on the capability of the GPR sensing technique to assess adequately the ballast quality and the trackbed formation. [C9053]

"Compression Waveforms for Non-Coherent Radar"

Non-coherent pulse compression (NCPC) was suggested recently. It was described using on-off keying (OOK) signals based on Manchester-coded binary pulse compression sequences (e.g., Barker, Ipatov). The present paper expands the discussion on waveform choice for both periodic and a-periodic cases, and on detection performances of this method. OOK transmitter and a receiver based on envelope-detection, suggested for the NCPC system, are simpler to implement than a binary phase-coded transmitter and a coherent receiver with I&Q synchronous detector, required for coherent pulse compression. NCPC can be used in simple radar systems where Doppler information is not required, in direct-detection laser radar systems and in ultra wide band (UWB) radar. Non-coherent processing has drawbacks in cases of reflections from multi-scatterer targets. The drawbacks and means of mitigating them are considered in section II. [C9054]

"Ambiguity and sidelobe behavior of CAZAC coded waveforms"

CAZAC (Constant Amplitude Zero Autocorrelation) sequences are important in waveform design because of their optimal transmission efficiency and tight time localization properties. Certain classes of CAZAC sequences have been used in Radar processing for many years while recently discovered sequences invite further study. This paper compares several classes of CAZAC sequences with respect to both the periodic and aperiodic ambiguity function. Some computational results for different CAZAC classes are presented. In particular, we note the fact that so-called Bjorck CAZACs have sidelobes at different locations when different shifts are considered. We take advantage of this fact by using an averaging technique to lower sidelobe levels. [C9055]

"Achieving Real-Time Efficiency for Adaptive Radar Pulse Compression"

The adaptive pulse compression (APC) algorithm has been shown to effectively suppress the range sidelobes

resulting from large scatterers to the level of the noise thereby unmasking nearby small scatterers and yielding substantial sensitivity improvement over deterministic filtering techniques. However, implementation in a real-time system is limited by the relatively high computational complexity of the algorithm. As such, this paper considers dimensionality reduction techniques as a means to reduce this computational cost in order to enable real-time operation. In general, numerous different methods exist to decompose the minimum mean-square error (MMSE) framework upon which the APC algorithm is based. In this paper dimensionality reduction is achieved either by segregating contiguous blocks of the received signal samples or by decimating the received signal. Each of the two approaches then facilitate the approximation of the original MMSE cost function of APC by the sum of lower dimension MMSE cost functions thus yielding filters that require a lower computational cost to implement. The reduced dimension algorithms, collectively denoted as the fast adaptive pulse compression (FAPC) algorithm, substantially reduce the computational cost of APC while still maintaining much of its performance benefit.

[C9056]

"Performance of Pulse Compression Code and Filter Pairs Optimized For Loss and Integrated Sidelobe Level"

This paper describes a method for finding code/filter pairs with very low mismatch filter losses. These losses remain nearly constant with changing filter length. In addition it has been found that substantial improvements in sidelobe levels are obtained. The filter performance of these codes is compared to the filter performance of known codes. [C9057]

"Phased-Array and Radar Breakthroughs"

Many think that radar is a mature field, nothing new to happen, it having been around a long time. Nothing can be further from the truth. When I entered the field in the '50s I thought the same thing. The MIT Radiation Lab. Series 28 book volume set summarizing the highly classified World War II work on radar was just published and provided the definitive coverage and there was to be nothing more to learn. How wrong I was. Since then many amazing new developments have taken place. Things are moving even faster now. We live in exciting times. Phased array radars and radars have seen in recent years breakthroughs that lead to capabilities not possible only a few years ago. This is exemplified by the development of GaAs integrated microwave circuits called monolithic microwave integrated circuits (MMIC) which makes it possible to build active electronically scanned arrays (AESAs) having lighter weight, smaller volume, higher reliability and lower cost. MMIC allows the construction of AESAs for applications not feasible before. This integration has reached the point where it is possible to now build a low cost 35 GHz phased array for a missile seeker costing \$40/element (total cost of array including all electronics divided by number of elements). The advances provided by Moore's Law has now made it is feasible to do digital beam forming with all its numerous advantages. One advantage of digital beamforming is the ability to lower the search power and occupancy by up to a factor of two. Another advantage is that it makes it possible to achieve the performance of a fully adaptive array without having to do a large matrix inversion, i.e., it makes adaptive-adaptive array processing or equivalently principal decomposition feasible. Also covered will be: the potential for GaN and SiC chips which have the capability of a factor of ten higher peak power than GaAs chips; arrays with instantaneous bandwidths of up to 33:1; SiGe low cost T/R modules; low cost MEMS arrays; meta- materials which provide negative refractivity possibly allowing focusing beyond the diffraction limit; a real radar application for Multiple-Input Multiple-Output (MIMO) as opposed to fantasy has been demonstrated by Lincoln Laboratory MIT which allows the coherent combining of two radars to achieve a 9 dB increase in sensitivity; the ability to build microwave tubes that are smaller, more power efficient, lighter, require lower voltages and have lower cost. [C9058]

"Army Radar Requirements for the 21st Century"

The paper presents a subjective view of what the Army surface based radar user will be asking of radars in the future. In addition to the primary advantages offered by radars, such as "all-weather capability, wide area coverage, and three-dimensional accurate position information, the user wants more. These desires include passivity or at least a low radio frequency signature and more information regarding object identification. In addition, they want the radar to perform multiple functions and missions, seamlessly participate in network operations, and at the same time be very reliable, low maintenance and not cost very much. The paper discusses the rationale behind the requirements and provides some insight into ways to achieve the objectives.

[C9059]

"Statistics of Clutter Residue in MTI Radars with IF Limiting"

In an MTI (moving target indicator) radar, when the received signal from clutter exceeds the IF (intermediate frequency) dynamic range, i.e., limits in the IF bandpass limiter, the radar literature states that good MTI

performance cannot be achieved. Close examination of clutter sequences shows that when the dynamic range of the radar is exceeded, occasional large spikes of clutter residue do occur but good clutter rejection is obtained in most of the clutter cells. This paper provides insight into the cause of the spikes of clutter residue and presents the statistics of the residue for two-pulse, three-pulse, and four-pulse MTI filters. The percentage of clutter-limited cells with good MTI performance supports the conclusion that most of the clutter-limited cells do exhibit good MTI performance. The infrequent residue spikes have a distinct pattern at the output of the clutter filter that is markedly different from targets. With the insight of the time domain view, this paper suggests that false alarms can be avoided with the use of a binary detection scheme and that by using an m-out-of-n detection criteria, clutter rejection performance can be as good as that for linearly processed signals. [C9060]

"Future Surface Radar technology: From Air Defence to Air and Missile Defence"

This paper describes how Air Defence radars are evolving from general Air Defence missions (single-mission radar) to Air and Missile Defence missions (multi-mission radar) in order to cope with new threats for Homeland Defence and External Theatre Defence. After a description of the radar requirements for general Air Defence and Missile Defence, Missile Defence impacts on radar sensors are explained. It is shown that conventional Air Defence radar cannot completely meet at the same time both Air Defence and Missile Defence requirements. The present multi-mission, multifunction MASTER A developed by Thales is described. The final parts explain the Thales portfolio evolution from MASTER A to M3R and the related S Band product policy. [C9061]

"2-D Angle of Arrival Estimation with Two Parallel Uniform Linear Arrays for Coherent Signals"

In this paper, a previously proposed estimator is extended to estimate two dimensional (2-D) angles of arrival of multiple highly correlated and coherent signals by using forward /backward spatial smoothing techniques. The special structure of the two parallel uniform linear arrays (ULAs) is exploited to estimate 2-D angles of arrival as polynomial roots. The computation complexity of the proposed method is discussed. Simulation results show that the proposed method can achieve higher resolutions and lower root mean square errors compared with DOA matrix method. [C9062]

"Adaptive Pulse Compression: Preliminary Experimental Measurements"

Preliminary experimental results from the adaptive pulse compression (APC) test bed are presented. A recently proposed adaptive processing technique has been shown via simulation to improve upon current pulse compression techniques through a process known as reiterative minimum mean-square error estimation (RMMSE). The RMMSE technique forms the basis of the APC and the Multistatic APC (MAPC) algorithms. In this paper, we present experimental results demonstrating the feasibility of these approaches. Several polyphase waveforms have been implemented in an experimental test bed. Initial results show that small non-linearities in the waveform generation process have only a marginal impact on the estimation performance of the algorithms. A discussion of the APC test bed followed by experimental results demonstrating the performances of the APC and MAPC algorithms are presented. These initial experimental results indicate that the APC approach is able to successfully mitigate pulse-compression sidelobes on measured data, and that the MAPC algorithm can successfully mitigate both the mutual-interference from shared-spectrum radar signals and pulse compression sidelobes on measured data. [C9063]

"Sequential Monte-Carlo techniques and vision-based methods for road signs detection"

This paper presents a model-based method for road signs detection and tracking. The object is described by a CAD model and tracked through the sequence. The detection and tracking problem is modeled using the estimation theory of hybrid processes, in which each sign of the database is described as a distinct mode. The proposed state-space modeling is here strongly nonlinear. Hence, one develops a Multiple Hypothesis Particle Filter solution that is based on the theory of the Sequential Monte-Carlo Methods. This solution is then applied in real time to real road image sequences. [C9064]

"Development problems of large area, web accessible, environmental pollution monitoring system"

The main purpose of the paper is to present the www hydrocarbon pollution monitoring system which is under development at the Warsaw University of Technology (WUT). The dedicated system server collects data from mobile GSM/GPRS accessed observation points, and delivers information on potential pollution to the authorized www clients. The emergency alarm information is planned to be send directly to palmtop/mobile phone equipped emergency teams to assure short response time to environment contamination. The moving observation points property and country wide GSM operator coverage makes the system flexible and universal. The principles of system realization are presented. The structure of the system and some problems concerning its development are discussed. Two realizations of system software are presented and compared: one with the use of Microsoft

.NET IDE, and the other with LAMP/WAMP approach. [C9065]

"MonoPulse Angle Measurement For An Airborne Side-Looking Phased Array PD Radar"

For airborne phased-array radar, target angle measurement generally utilizes monopulse method in sum (Sigma) and difference (Delta) beams. This paper discusses a monopulse angle measurement method in Doppler-domain, which compares the Doppler filter output amplitude of Sigma channel with that of Delta channel, and gets the angle bias by finding the angle bias-table of Sigma channel and Delta channel. And then get the positive or negative of the bias by comparing the phase between Sigma channel and Delta channel. Practical results show the effectiveness of this method. [C9066]

"A Comprehensive Review of Quasi-Orthogonal Waveforms"

Quasi-orthogonal waveforms which exhibit low cross-correlation responses have the potential to enhance radar performance. Intra-pulse, phase coded or frequency modulated waveforms, sharing the same frequency band, are of greatest interest. A review of quasi-orthogonal waveform design and performance is presented including bounds on auto and cross-correlation performance. [C9067]

"Tracking High-Speed Targets Using a Pulse Doppler Stepped-Frequency Waveform"

This paper develops a computationally efficient processing technique using fast Fourier transforms (FFT), averaging, and weighted least squares fits to track high-speed targets with a pulse Doppler waveform that is stepped in frequency. The measurements will be unambiguous in Doppler for high-speed targets of interest, but highly ambiguous in range before tracking. First, a range-Doppler matrix is formed using motion compensated data. Then, the effect of the range, radial velocity, and radial acceleration of the target on the processed data is approximated by a polynomial series, and the parameters are estimated using a weighted least squares fit. Monte Carlo simulations of the algorithm when four or more cpis of data are processed are in reasonable agreement with the theoretical predictions. [C9068]

"The Frequency Selection Consideration for the Low Orbit Space Based Radar"

Space based radar (SBR) has been researched intensely for many years, because it can provide global surveillance without time and space limit. But the enormous expenses delay its realization. In order to decrease its cost and improve its performance, a lot of works have been done, such as the radar system design, the signal processing method research and the constellation design for the world-wide coverage, etc. But few works have been done about the detailed consideration of the frequency selection of SBR. In fact, the frequency selection is closely related to the SBR's functions, performance and cost. Here, the system characteristics are analyzed for the monostatic SBR in low earth orbit with different frequencies, including L, S, C and X bands. The size and weight of the antenna and the power consumption of the system are considered. The SBR has some different modes of operation according to the different missions, including SAR mode, searching mode and tracking mode. And the wide area searching mode makes demand of the largest power aperture product (PAP). To realize the certain area coverage rate which is according to a certain angle coverage rate (ACR) in space, the SBR needs the corresponding PAP. The weight and primary power of the SBR can be estimated based on the needed PAP. [C9069]

"Spectrogram-Based Methods for Human Identification in Single-Channel SAR Data"

Radar offers unique advantages over other sensors, such as visual or seismic sensors, for human target detection and identification. Radar can operate far away from potential targets, and functions during the daytime as well as nighttime in virtually all weather conditions. In this paper, we examine the problem of human target detection and identification using single-channel synthetic aperture radar (SAR) data. A 12-point human model, together with kinematic equations of motion for each body part, is used to calculate the expected target return and spectrogram. The unique characteristics of the human spectrogram are analysed and used to design a prototype for an automated gender discrimination scheme. Simulation results show a 83.97% detection rate for males and 91.11% detection rate for females. Inherent deficiencies of spectrogram-based methods are discussed. Future work will focus on the development of an alternative solution for overcoming these deficiencies. [C9070]

"Amplitude Weighting of Linear Frequency Modulated Chirp Signals"

Linear frequency modulated chirp signals are used in radar system. The signals may be easily compressed to increase range of the radar. To obtain compressed signal with small sidelobes, weighting function must be implemented. The paper describes some methods of chirp signals weighting that may be useful especially for

signals with low compression ratio. [C9071]

"CZT-Based High Performance Frequency Estimation"

Accurate and high-performance frequency estimation of a noisy sampled sinusoid sequence with short time length and adjacent overlapping has been attracting top focus in the field of signal processing. Based on the CZT of a single-tone sequence, this paper presents a novel improved Rife CZT-interpolated frequency estimator, which develops an improved Rife algorithm on the symmetry of CZT Linear Spectrum Model by the magnitude relationship between peak and its adjacent CZT coefficients. Computer Monte -Carlo simulations show that the algorithm is effective and the proposed estimator outperforms the traditional Rife-Jane's estimator in accuracy, the CRLB-approximation RMSE of estimation and discriminating capability for adjacent overlapping. It is also shown that the CZT-based estimator has as lower SNR threshold as to about -12 dB and good estimation performance even in the case of very short samples, which is quite suitable for applications of strict stationary requirement. [C9072]

"Detecting Features using Random Sample Theory"

This paper aims to detect features in 2-D and 3-D highly noisy images using random sample theory fast and with high detection performance. The proposed method yields faster results than standard feature detection algorithms, such as the Hough transform (HT) or its variants, while keeping the the performance level of HT. Proposed method first finds possible feature areas by creating random hypothesis and testing them. Features are re-estimated by only searching these possible areas which reduces the total search space. The proposed algorithm is tested on both simulated and experimental subsurface Seismic and GPR images for searching linear features like pipes or tunnels. Results show that the proposed algorithm can detect features accurately and much faster than conventional methods. [C9073]

"Reducing the Transmission Power Requirements of the Multimedia Broadcast/Multicast Service"

The multimedia broadcast/multicast service (MBMS) was designed to support the economical distribution of multimedia content to large numbers of receivers in 3rd generation cellular networks. In this paper we present and evaluate an MBMS extension that reduces the transmission power requirements while increasing the number of potential users of such services, by supporting the distribution of multiple variants of the same content to heterogeneous receivers. We first describe the standard MBMS model, along with its state management and signaling procedures, as well as our extended MBMS model, in terms of the modifications that it imposes on the standard. We then present an analytical and simulation evaluation of the transmission power requirements of our approach against alternatives based on standard MBMS, showing that our approach maximizes the number of potential users, without excessive transmission power requirements. [C9074]

"Prototype of a Reconfigurable 94GHz Smart Radar Sensor"

With the introduction of millimetre wave radar systems in various commercial applications, including collision avoidance, cruise control, autonomous navigation and imaging, it is now clear that a "one size fits all" approach to radar system development is not effective. This paper describes the implementation of a reconfigurable millimetre wave system comprising a coherent 94 GHz front end, a fast arbitrary waveform generator based modulator and a fast digitiser which, with their associated software, will allow for the development and evaluation of modulation and signal processing techniques which can be adapted to various radar based tracking and imaging requirements. [C9075]

"A Holographic Approach to Image Processing"

In this document, a distributed image processing based on the mathematics of holographic storage is presented. This work was inspired by the distributed principles between wave propagation and subsequent interference patterns seen in holograms. We then analyzed the mathematics to produce a general mathematical description of the holographic process. From a generalized case of this analysis we are able to propose this way for works in some engineering fields such as radar, control and neural networks. [C9076]

"Electromagnetic Target Recognition with the Fused MUSIC Spectrum Matrix Method: Applications and Performance Analysis for Incomplete Frequency Data"

The aim of this paper is to apply an electromagnetic target recognition method, which is based on the use of fused MUSIC spectrum matrices, to the case of incomplete frequency domain data. The aforementioned method was suggested recently and successfully applied to both canonical and complicated targets in the presence of complete frequency domain data [1]. However, most of the real world applications involve the use of severely

incomplete frequency data, especially missing low frequency information. In this paper, the performance of mentioned target recognition method is investigated for various incomplete frequency bands and for a group of five small-scale aircraft targets. As a result, the mentioned target recognition method is demonstrated to give still high correct decision rates even when the frequency band is reduced by 300 MHz at low frequency end and at the signal-to-noise ratio is decreased down to -5 dB level. [C9077]

"Development of a Software Testbed for Integrated Navigation Systems"

In today's navigation systems different types of sensors are integrated. This integration may include inertial sensors, global navigation satellite systems, radar altimeter, barometric altimeter, digital terrain maps and etc. Mostly a Kalman filter is designed to fuse the sensor data and to calculate the navigation data. In order to validate and test the integration algorithm, a comprehensive software testbed has to be developed. In this paper, we develop such a testbed for integrated navigation systems where the sensor data is modeled with real time errors. Using this testbed it is possible to try different scenarios in the software environment for any navigation system whereas to test such scenarios with the hardware systems is too costly and even may be impossible. This testbed is also suitable for performing Monte-Carlo simulations and covariance analysis. A well-known terrain referenced navigation algorithm, TERCOM, is tested with this software testbed. [C9078]

"A Sparse Signal Representation-based Approach to Image Formation and Anisotropy Determination in Wide-Angle Radar"

We consider the problem of jointly forming images and determining anisotropy from wide-angle synthetic aperture radar (SAR) measurements. Conventional SAR image formation techniques assume isotropic scattering, which is not valid with wide-angle apertures. We present a method based on a sparse representation of aspect-dependent scattering with an overcomplete dictionary composed of elements with varying levels of angular persistence. Solved as an inverse problem, the result is a complex-valued, aspect-dependent response for each spatial location in a scene. Our formulation leads to an optimization problem for which we develop a tractable, graph-structured approximate algorithm. We present experimental results on realistic electromagnetic simulations demonstrating the effectiveness of the proposed approach. [C9079]

"Adaptive Censored CFAR Performance in Nonhomogeneous Correlated Clutter"

In this work, performance analysis of CFAR radar processors in nonhomogeneous partially correlated Gaussian background is studied using binary integration detectors. In nonhomogeneous background, a new algorithm is proposed to find the homogeneous region that the test cell is located. CFAR analysis is performed in this region and the probability of false alarm results are compared with the design value. [C9080]

"LPI Radar Sinyallerinin Ozimge Yaklasimi ile Siniflandirilmasi Classification of LPI Radar Signals via Eigenimage Approach"

Low Probability of Intercept (LPI) Radar signals have the property of wide bandwidth, low peak power to make them difficult to be detected by Electronic Support Measures (ESM) receivers. In this study, the detection performances of LPI Radar signals with Wigner-Ville Distributions are examined by treating each distribution as an image. The classification can be performed with an image processing algorithm, eigenimage approach over Wigner-Ville Distributions. [C9081]

"On Performance of S-band FMCW Radar For Atmospheric Observation"

First Page of the Article [C9082]

"Classification of Cylindrical Targets above Perfectly Conducting Flat Surfaces by Statistical Neural Networks"

This paper evaluates the radar target classification performance of neural networks. A set of features are derived from scattered fields calculated by using the image technique formulation and Moment Method (MoM). Statistical neural networks that utilize the feature set are proposed for target classification. The database contains a finite number of samples of three cylindrical targets at certain angles. A portion of the database is used to train the network and the rest is used to test the performance of the neural network for target classification. This work aims to find the right target above a perfectly conducting (PEC) flat surface from the scattered field values. [C9083]

"Non-Parametric Radar Detection In Homogeneous And Non-Homogeneous Environments"

In this study, non-parametric constant false alarm rate (CFAR) radar processors are investigated. Performance analysis of the system, which uses generalized sign test in its detector, is done in homogeneous and non-homogeneous environments. Also the performance of the system is compared with the performance of the cell averaging constant false alarm rate (CA-CFAR) detector in the homogeneous and non-homogeneous environments. [C9084]

"Design of V-shaped Array Geometry"

In this study, a new design method is proposed for V-shaped planar array geometry for two-dimensional azimuth and elevation angle estimation. The proposed method is similar to filter design in signal processing. This method determines the V-shaped array geometry which gives the best 2-D angle estimation performances for the specified design parameters. The best geometry is determined by using Cramer-Rao Bound (CRB) and performance comparison is done with other planar array geometries. [C9085]

"Experimental Comparison of Two Automotive Radars for use on an Autonomous Vehicle"

Many of the requirements for autonomous sensing of moving vehicles are the same as those for automatic cruise control radars, whose development is now sufficiently mature to be on offer to the consumer car market. This paper investigates the suitability of these radars for use on an autonomous vehicle, and describes a capability assessment of two specific radars for such a task. [C9086]

"Optimal Beampattern Synthesis of a Polarized Array"

Utilizing the polarization information in waveforms about targets enables improving the performance of radar systems. We consider the optimal synthesis of the polarized beampattern of an array of antennas, each having two orthogonal electric dipole elements. We control the amplitudes and phases of the electric fields emitted from these dipole antennas to synthesize the electromagnetic beam with desired power and polarization patterns. The problem is formulated in a convex form which is thus efficiently solvable. We compare the performance of two synthesizing methods: (i) separate design of the two co-aligned dipole antenna sub-arrays; and (ii) joint design of the cross-dipole antenna array. Our results indicate that these two separate designs have the equivalent capability of suppressing the sidelobe power density, whereas the joint design has the additional advantage of controlling the beam polarizations. The results are also demonstrated by numerical examples. [C9087]

"MIMO Radar waveform Design"

Recently the radar community has been discussing "multiple-input multiple-output (MIMO) radar" that utilizes multiple transmitters to transmit independent waveforms. MIMO radar offers the potential for significant gains, e.g., diversity gain and spatial resolution gain. Since the employed radar waveform plays a key role in determining the accuracy, resolution, and ambiguity in performing tasks such as determining the target range, velocity, shape and so on, it is meaningful to investigate waveform design specially for this newly proposed MIMO radar. This paper summarizes some of our recent results on MIMO radar waveform design, mainly for identification and classification of extended radar targets. Our waveform design considers optimizing two criteria: maximization of the mutual information (MI) and minimization of the minimum mean-square error (MMSE). In this process, we are also interested in identifying the relationship between the waveforms obtained under the two criteria, given different a priori knowledge of the target's second-order statistics. [C9088]

"Detection of Small Aircraft with Doppler Weather Radar"

We present a method that can be performed in parallel to reflectivity estimation in weather radar and that allows one to detect small aircraft. Though small aircraft and large birds might produce comparable reflectivity signals their spectral signatures are considerably different. A small aircraft with propellers can be recognized from its spectrum via modulations produced by Doppler shifts from rotating parts. Generally such a spectrum has an elevated spectral floor compared to the spectrum of a resolution volume without an airplane. The spectral floor level is used for detection. The method is demonstrated on a clear air case observed with Doppler weather radar on March 6, 2007 at elevation 0.5° . [C9089]

"Fast Encoding of Synthetic Aperture Radar Raw Data using Compressed Sensing"

Synthetic Aperture Radar (SAR) is active and coherent microwave high resolution imaging system, which has the capability to image in all weather and day-night conditions. SAR transmits chirp signals and the received echoes are sampled into In-phase (I) and Quadrature (Q) components, generally referred to as raw SAR data. The various modes of SAR coupled with the high resolution and wide swath requirements result in a huge amount of data, which will easily exceed the on-board storage and downlink bandwidth of a satellite. This paper addresses

the compression of the raw SAR data by sampling the signal below Nyquist rate using ideas from Compressed Sensing (CS). Due to the low computational resources available onboard satellite, the idea is to use a simple encoder, with a 2D FFT and a random sampler. Decoding is then based on convex optimization or uses greedy algorithms such as Orthogonal Matching Pursuit (OMP). [C9090]

"Feature Detection in Images by Adaptive Random Sampling"

Random sample theory is an effective tool for detecting features in images. This paper presents an adaptive random sampling scheme that clusters random samples into candidate features. The required trial number is reduced by adaptive sampling, thereby reducing the run time of the algorithm. The proposed method quickly finds rough regions in the image that may include features using adaptive random sampling and re-estimates the features using the Hough Transform (HT) within the smaller regions. The proposed algorithm is tested on both simulated and experimental subsurface seismic and GPR images to search for linear features like pipes or tunnels. Faster results are obtained as compared to standard feature detection algorithms, such as the HT or its variants, while maintaining the similar performance level as the HT. [C9091]

"Mapping Ocean Currents With IKONOS"

The velocity of sea surface gravity waves depends on the wave wavenumber, k , and the surface current, U . The surface current can thus be inferred from the displacement of waves in a sequence of ocean surface images. This has been demonstrated using both marine radars and aerial video to image the ocean waves. In this paper we describe the implementation with IKONOS satellite images. We discuss special considerations for obtaining and processing satellite images: the need for precise co-registration of the images; the optimum sun angle for imaging ocean waves; the optimum oceanographic conditions; and the use of multi-spectral bands to edit non wave surface features (e.g., whitecaps). In the test case a current velocity map was produced at 200 m grid spacing. The rms error in the velocity estimates is 10 cm/s. [C9092]

"Doppler Resilient Golay Complementary Pairs for Radar"

We present a systematic way of constructing a Doppler resilient sequence of Golay complementary waveforms for radar, for which the composite ambiguity function maintains ideal shape at small Doppler shifts. The idea is to determine a sequence of Golay pairs that annihilates the low-order terms of the Taylor expansion of the composite ambiguity function. The Prouhet-Thue-Morse sequence plays a key role in the construction of Doppler resilient sequences of Golay pairs. We extend this construction to multiple dimensions. In particular, we consider radar polarimetry, where the dimensions are realized by two orthogonal polarizations. We determine a sequence of two-by-two Alamouti matrices, where the entries involve Golay pairs and for which the matrix-valued composite ambiguity function vanishes at small Doppler shifts. [C9093]

"Statistical Characteristics of Harris Corner Detector"

In this study, a method is proposed to calculate the bias and mean square error matrix of Harris detector calculated corners. The main result is presented in a theorem and the performance of the algorithm is shown on an example. [C9094]

"Bayesian Covariance Matrix Estimation with Non-Homogeneous Snapshots"

We address the problem of estimating the covariance matrix M_p of an observation vector, using K groups of training samples $\{Z_k\}_{k=1}^K$, of respective size L_k , whose covariance matrices M_k may differ from M_p . A Bayesian model is formulated where we assume that M_p and the matrices M_k are random, with some prior distribution. Within this framework, we derive the minimum mean-square error (MMSE) estimator of M_p which is implemented using a Gibbs-sampling strategy. Moreover, we consider simpler estimators based on a weighted sum of the sample covariance matrices of Z_k . We derive an expression for the weights that result in minimum mean square error (MSE), within this class of estimators. Numerical simulations are presented to illustrate the performances of the different estimation schemes. [C9095]

"Limitations of Spectral Correlation Based Detectors"

This work explores the capabilities of spectral correlation based detectors for partially or completely unknown signals corrupted by Gaussian noise. The main contribution is twofold: Firstly, the cyclostationary model is shown to be less suitable for detection purposes than the stationary model. Secondly, analytic approximations are derived for the detection and false alarm probabilities, under the assumption of long observation time. [C9096]

"Estimation of the Hit Probability and its Effect on the Performance of Frequency Hopping Radar System"

It was found that, the frequency hopping, FH, technique minimizes sensitivity of radar system to jamming and interference and may solve some of the ambiguity and resolution problems. In the present work, at first, a theoretical introductory to summarize the subject of FH technique, slow frequency hopping (SFH) as well as fast frequency hopping (FFH) is given. Fast frequency hopping will be considered rather than SFH because its performance is significantly better. The frequency hopping procedure will be carried out pseudo randomly according to the Gamma random distribution which is proved here to have better correlation properties. Expectation of the hit probability of the used FH sequences of the radar signal, as well as the range ambiguity function, will be calculated and evaluated as a measure of the system performance. The simulation output has proved that the FFH radar system can achieve a nearby ideal performance. [C9097]

"A Plastic W-Band MEMS Phase Shifter"

A plastic, W-band MEMS phase shifter realized in a WR-10 waveguide architecture with built-in deformable diaphragms has been successfully demonstrated. A prototype device has been fabricated based on a two-cavity Iris filter design with two 1.6 mm in diameter deformable membranes on one side. Experimental results show that a total phase shift of 110deg at 95 GHz has been achieved under membrane deformation from -50 μm to +150 μm with corresponding insertion loss of 2.9 dB and 3.48 dB, respectively. This concept and approach could potentially open up a new class of opportunities in low-cost plastic components for millimeter-wave systems, including electronically scanned radar. [C9098]

"Time Reversal Target Classification from Scattered Radiation"

This paper proposed the M-ary hypothesis testing algorithm for classifying radar backscatter signals from hidden targets in a rich scattering environment using time reversal. The target recognition algorithm is to be designed to distinguish measurements of the radar backscatter from an unknown object as belonging to one of a set of M classes. The proposed time reversal target classifier is, in essence, a correlator that calculates the cross-correlation of the normalized target signature waveforms with a data dependent quantity obtained from measurements. The algorithm requires a priori empirical statistical knowledge of the scattering channel, which is dependent of configurations of the scatterers in the environment. By incorporating time reversal, the proposed algorithm provides a significant performance improvement compared with the conventional method. Proof of concept is provided using electromagnetic data collected in a laboratory environment. [C9099]

"Adaptive Technique for Clutter and Noise Suppression in Weather Radar Exposes Weak Echoes Over an Urban Area"

We present an adaptive spectral technique for ground clutter and noise suppression in weather radar echoes. This technique is especially good for detecting weak echoes that are either submerged in noise or masked by the residuals from ground clutter if standard techniques for clutter suppression are used. Our technique is demonstrated on two clear air cases observed with Doppler weather radar on February 22, 2007 and March 6, 2007. Adaptively suppressed ground clutter and noise allow exposure of a feature over an urban area, which we interpret as a "bird highway" between two lakes and along the river. [C9100]

"Maximizing Detection Performance with waveform Design for Sensing in Heavy Sea Clutter"

In this paper, we consider a radar system capable of adaptively adjusting its transmitted waveform to mitigate the effect of the environment and improve detection performance. We thus bring the potential of waveform agility to bear on the challenging problem of target detection in heavy sea clutter. Using a two-stage procedure, we first estimate the statistics of the sea clutter in the vicinity of a predicted target. A phase-modulated waveform is then designed and transmitted so as to maximize the generalized likelihood ratio at the predicted target location, thus improving the signal-to-clutter ratio (SCR). Employing the compound-Gaussian (CG) model, we exploit a subspace-based approach to further mitigate sea clutter and deliver improved detection performance. Simulations illustrate the effectiveness of our method. [C9101]

"Improved Tracking of Airborne Targets Hidden in the Blind Doppler using Particle Filter"

In airborne tracking, the blind Doppler makes the target undetectable, resulting in great tracking difficulties. In this paper, we sum up two types of the blind Doppler cases under constant velocity constraint: targets' intentional tangential flying to radar and unintentional flying also leading to the blind Doppler. We propose an improved particle filter by introducing two different levels of noise to the movement model and one of them is a random acceleration noise. This acceleration selection added to the sampling step makes the constant velocity

model efficient in dealing with maneuvering motions (i.e. escape turns). We compare the proposed particle filter with the extended Kalman filter and previous particle filter solution. Simulation results show that the proposed method outperforms previous ones in tracking accuracy and continuity. [C9102]

"Aerial Lidar Data Classification using AdaBoost"

We use the AdaBoost algorithm to classify 3D aerial lidar scattered height data into four categories: road, grass, buildings, and trees. To do so we use five features: height, height variation, normal variation, lidar return intensity, and image intensity. We also use only lidar-derived features to organize the data into three classes (the road and grass classes are merged). We apply and test our results using ten regions taken from lidar data collected over an area of approximately eight square miles, obtaining higher than 92% accuracy. We also apply our classifier to our entire dataset, and present visual classification results both with and without uncertainty. We implement and experiment with several variations within the AdaBoost family of algorithms. We observe that our results are robust and stable over all the various tests and algorithmic variations. We also investigate features and values that are most critical in distinguishing between the classes. This insight is important in extending the results from one geographic region to another. [C9103]

"Wireless LAN Positioning based on Received Signal Strength from Mobile device and Access Points"

Most of the WLAN positioning systems use Received Signal Strength (RSS) as an important information to estimate the location of a mobile station. In fact, RSS can be obtained at the access points or at the mobile device, and most of the previous works use either way to collect this information. In this paper, we propose a new WLAN positioning approach by making use of the RSS collected at both the access points and mobile device. Besides, our new approach is positioning algorithm independent, which means the user can apply any location estimation algorithm with our new data acquisition approach. With our new data acquisition approach, our experiments had shown that the accuracy of location estimation can be improved by 12.84% to 38.23% on the average, as compare to the previous work which only uses the RSS information from either access points or the mobile device. [C9104]

"Extension of Automotive Radar Target List Simulation to consider further Physical Aspects"

In this paper, we present extensions to the existing model which consider the effects of multipath propagation and multiple reflections in order to bring the simulated target lists a step closer to reality. [C9105]

"Automatic Registration for Model Building using Variable Dimensional Local Shape Descriptors"

A new set of variable dimensional local shape descriptors for 3D registration is proposed and applied to 3D model building from range images. The descriptors are based on a large set of properties represented as high dimensional histograms. The novelty of the method is two fold: first, it offers a generalized platform for a large class of local shape descriptors; second, unlike previously devised descriptors that are of low dimensionality and compact size, these descriptors are high dimensional and highly discriminating. The new approach suggests investing more into descriptor generation and comparison and in return gaining a higher percentage of inliers in the set of hypothesized point matches across the images being registered. This in turn drastically reduces the required number of RANSAC iterations for finding the alignment between two images, as is confirmed by experimentation in a 3D model building application. It is also shown that the correct choice of properties can increase the effectiveness of feature correspondences, thereby increasing the possible acquisition angle between overlapping images. [C9106]

"A Fast SAR Target Recognition Approach Using PCA Features"

The real-time ability and recognition rate are two primary goals for evaluating the performance of an SAR image target recognition system. This paper concentrates on the analysis of key factors which influence these two goals. According to the analysis, a fast SAR target recognition approach is proposed, which utilizes a self-organizing neural network trained with the Hebbian rule to extract the principal component features and a multi-layer neural perceptron network as the classifier. The experimental results show that it consumes little memory and runs very fast with a considerable recognition rate, thus can be used in a real-time application. [C9107]

"Modeling Attack Distribution in Sensor Networks"

Attack is the major and unique security issues in sensor networks. There are many security approaches that can be used to detect attacks, yet few researches were focused on modeling these attacks' distribution. Knowing the distribution models of attacks can help us detect and defend against them efficiently and effectively. In this paper,

we use probability theory to develop basic uniform model, basic gradient model of attack distribution based on the observations of different application environments. These models allow system to estimate the probability of a node to be attacked. To explain how important of these models and how to apply them in security design, we introduced some applications that can be improved using our models such as detecting attacks and secure routing. [C9108]

"The Application of KL Transform to Remove Direct Wave in Ground Penetrating Radar Records"

In ground penetrating radar (GPR) records, because of different kinds of noises, especially direct wave of ground surface, the real target is not seen clearly in the radar echo section, which makes the detection of real targets difficult. Considering that the direct waves among traces are not change greatly and have strong correlation, so it can be restrained by certain methods. KL transform often be used to pick up coherent noises and random noises in multi channel seismic records[U 4]. In this paper, KL transform is used to GPR data processing, which fully uses the different second-order statistic characteristics of their correlations on the direct wave, target signals in multi channel GPR data. The target signals are successfully separated form noises according to the corresponding relation of the eigenvalue's magnitude of the correlation matrix and correlation strength of each component in the multi channel GPR data. [C9109]

"Weighted Support Vector Machine Segmentation of SAR Images Based on MARMA model"

Synthetic aperture radar (SAR) is a coherent sensing device. Existing algorithms for processing optical images are not suitable for SAR images because of speckles noise in SAR images. This paper introduces the support vector machine (SVM) segmentation of SAR images based on multiscale autoregressive moving average (MARMA) model, which can capture the statistical scale-dependency of SAR images. Firstly, the multiscale sequences of SAR image are constructed. Secondly, the paper investigates how to establish MARMA model and how to extract the multiscale stochastic characteristics of the different SAR texture images. Finally, the paper classifies the characteristics vector using generalized weighted SIM. Experiments show that the proposed algorithm is efficient. [C9110]

"Spectrum Analysis of Radar Signals with Usage of Kravchenko Windows"

The purpose of the report is to obtain new Kravchenko windows on the basis of a direct product in a time-domain of a window of the Hamming, Gauss, Chebyshev, Blackmann-Harris and atomic functions sets $f_{upN}(n)$ in l/m of a degree, to define their parameters and to execute comparison with the present classical and constructed windows. To justify expediency of application of the obtained windows in a spectrum analysis of multifrequency radar signals with a large volume range of amplitudes on the basis of comparison of parameters and parameters, and as visual comparison of outcomes of computer simulation. [C9111]

"Conception of Scaling, Fractional Dimension and Deterministic Chaos in Radio Physics and Radio Electronics"

It has been briefly reported how the new synergetic approach on the basis of fractional measuring, fractal dimension, scaling, fractals and deterministic chaos has been developing in IRE RAS as applied to problems of modern non-linear radio physics and radio engineering. New challenging information technologies development and introduction on the basis of fractal radio physics and fractal radio electronics principles relates with training of specialists for these scientific fields. [C9112]

"The Signal Digital Processing in the Millimeter Band FMCW Radar"

The frequency-modulated continuous wave-radars-(FMCW-radars) are widely applied in the car road safety systems, the aircraft altimeters, the fusion plasma microwave diagnostics and in other ranging systems of different usage. The most optimal choice in terms of the "cost-quality" criterion for the radars that function at tens of meters distances is a transceiving set homodyne circuitry preference. The Gunn oscillators and Schottky diode barrier mixers usage in such radar sets let one create solid-state midget microwave detectors of different purposes. However, designing the transceiving set-based measuring system, one is confronted with a number of difficulties, depended on the high requirements over the transmitted waveshape and the generator and reception path gain frequency responses linearity. [C9113]

"Construction of 2D Filters for Digital Signal and Image Processing on Basis of the Kravchenko Weight Functions and R-Operations in Millimeter Range"

Various two-dimensional weight functions (windows) are applied to processing and the analysis of radar images in millimeter range. For construction of two-dimensional filters it is necessary to synthesize them on some basic

areas which geometry has essential value. It influences physical characteristics of filters, and also results of processing of multivariate signals. We shall notice, that classical methods allow to synthesize 2D filters only on the elementary basic areas. On the basis of the theory of R-functions it is possible to describe the equation of basic area of the reference areas of the any shape at an analytical level. Such approach allows to build two-dimensional weight functions (windows) on reference areas of non-standard geometry. [C9114]

"Mobile Robot's Map Reconstruction Based on DSMT and Fast-Hough Self-Localization"

This paper presents a new tool based on DSMT (Dezert-Smarandache Theory) and fast-Hough self-localization which is applied to autonomous mobile robot's map reconstruction. Uncertainty from sonar information is fused and managed in rebuilding grid map effectively with DSMT, since fast-Hough self-localization from laser information overcomes some shortcomings of classical Hough transformation including high amount of computation and low precision of localization. When a virtual mobile robot evolves in the virtual environment with different outline features, the result can adequately testify that the new tool owns better performance to rebuild map. In general, this research provides an approach for studying autonomous navigation of mobile robot or unmanned land vehicle (ULV) in unknown environment, also provides a human- computer interactive interface to manage and manipulate the robot remotely. [C9115]

"Initialization Procedure for Radar Target Tracking without Object Movement Constraints"

The tracking of radar targets in automotive applications often relies on certain constraints to the movement of objects. For example, the objects of interest in an ACC system (adaptive cruise control) are other vehicles that are positioned straight ahead and moving in approximately the same direction as the observer. In this case, a single radar measurement (distance to target, bearing angle and Doppler velocity) contains -neglecting measurement noise -full information about the position (by distance and angle) and the movement state. Thus, the initialization of tracks can be done based on a single measurement. Without the mentioned assumption, no information about the movement direction of the object is contained in a single measurement. Theoretically, at least two measurements are necessary to extract information about the object movement direction. But due to severe measurement noise and quantization, even three or more measurements may contain misleading information about the movement state. In this paper we present an initialization procedure for radar target tracking without any constraints to object movement. In the first cycles of a new track, the state estimation is computed by a linear regression method. After that, the track state is handed over to a Kalman filter which does the tracking for the rest of the track's lifetime. [C9116]

"The Contour Analysis of Low-Sized Complex-Shaped Objects Based on R-Functions, Atomic Functions and Wavelets"

The parameter processing of radar signals plays a great part in various fields of physics and engineering. The contemporary level of the development of the radar systems gives the opportunity to obtain rather complete information about an examining object. The great part in this process plays the processing of gained radar images, as they represent the main information, concerning the shape and the parameters of an object. Therefore, the main problems are the following: the rise of resolvability, the improvement of the quality of gained images as well as the creation of new fast-acting algorithms of radar information processing. [C9117]

"CFAR Matched Detector of Signals in Autoregressive Noise"

The generalized likelihood ratio test (GLRT) for detecting a target signal in autoregressive (AR) noise whose covariance matrix is unknown is presented. We proposed a new constant false alarm rate (CFAR) matched detector whose structure does not depend on noise covariance matrix and level and its performance penalty is small. The evaluation of its performance shows that the loss measured with respect to the corresponding optimum structure with known noise covariance matrix is kept within a few dBs. [C9118]

"Brownie: Searching Concealed Real World Artifacts"

This paper presents Brownie that searches the location of a sensor attached artifact and returns the location with a location expression. Contain expression between artifacts are intuitive location expression to indicate. If you search your book, a contain expression (e.g., the cabinet contains your book.) is more intuitive than other location expression (e.g., the distance from your book to the cabinet is within 2 meters.). There are two requirements to create contain expressions. The first requirement is detection of contain expressions. In every day life, there are sensor attached artifacts and normal artifacts that are not attached sensors. It is difficult to detect normal artifacts which contain sensor attached artifacts. The second requirement is tracking of contain expressions. It is difficult to track normal artifacts that contain sensor attached artifacts. To satisfy the two requirements, we introduce a camera for environment, and ultrasonic and acceleration sensors for an artifacts.

To satisfy detection of contain expressions, the combination algorithm of the camera and ultrasonic sensors is introduced. To satisfy tracking of contain expressions, the combination algorithm of the camera and acceleration sensors is introduced. We conducted experiments to confirm that Brownie satisfies two requirements. [C9119]

"Acoustic Micro-Doppler Gait Signatures of Humans and Animals"

A micro-Doppler active acoustic sensing system is described. We report its use in acquiring gait signatures of humans and four-legged animals in indoor and outdoor environments. Signals from an accelerometer attached to the leg support the interpretation of the components in the measured micro-Doppler signature. The acoustic micro-Doppler system described in this paper is simpler and offers advantages over the widely used electromagnetic wave micro-Doppler radars. It can be implemented in custom integrated circuits and embedded in a multi-modal wireless sensor network for autonomous detection and classification. [C9120]

"Peer-to-peer Multipoint Conferencing using Layered Video: Multi-objective Optimization for Extra Requests"

A multi-objective optimization formulation for considering multiple view requests in a peer-to-peer multipoint video conferencing system is described. The system aims end-points with varying bandwidth connections to the Internet and makes use of layered video to assure that each participant can view any other participant's video at anytime. However, this may cause some of the peers to receive lower quality video. We allow multiple video requests from the participants with sufficient bandwidth. Formulations to minimize the number of lower quality video receivers while maximizing the number of additional requests are presented. A multi-objective optimization assigning importance weights to each of these objectives is described and explained with a practical scenario. Sensitivity analysis of the optimization approach, to changes in the weights is made. [C9121]

"Constant Envelope Orthogonal Frequency-Division Multiplexing Phase Modulation for Radar Pulse Compression"

Constant envelope orthogonal frequency-division multiplexing (CE-OFDM) is evaluated as a potential wideband radar pulse compression modulation using ambiguity function analysis. [C9122]

"Collector Receiver Design for Data Collection and Localization in Sensor-driven Networks"

We consider a sensor network in which the sensors communicate at will when they have something to report, without prior coordination with other sensors or with data collection nodes. The burden of demodulating the sensor data, and localizing the sensor which is communicating, falls on a network of collector nodes which are perpetually monitoring transmissions from the sensor network. This model allows the random deployment of very large numbers of sensor nodes with minimal capabilities, while shifting the complexity to a network of collector nodes. While the philosophy is similar to prior work on "imaging" sensor nets, the key difference is that the communication model is now sensor-driven, rather than collector-driven. The two major technical challenges addressed in this paper are as follows: (a) Are there simple physical layer implementations of the collector receiver for jointly solving the tasks of detection of a sensor transmission, estimation of the direction from which it comes, and demodulating the data? (b) Given that the collectors are not time synchronized well enough to permit the use of time-difference-of-arrival techniques for sensor localization, how well can the sensors be localized with spatial information alone, assuming that each collector node has a relatively small number of antennas? The results reported in this paper indicate that the preceding issues can be addressed satisfactorily with appropriate design of the collector physical layer, together with Bayesian combining of the spatial information extracted by each collector. [C9123]

"Constant False Alarm Rate (CFAR) Detection in Weibull Environment"

In this work, the performance of N pulse radar receivers which use Post Integration (PI) and Binary Integration (BI) algorithms is analysed in homogeneous Weibull environment. It is assumed that the shape parameter of the Weibull distribution is known a priori. If the scale parameter is known a priori, PI and BI receivers, otherwise the same receivers integrated with CFAR processor which estimates the scale parameter are considered. The performance of the considered models are analyzed and compared with different shape parameters. For PI-CFAR model, the sensitivity of the model is analyzed for the case when the shape parameter value of the real data is different from the design value. [C9124]

"Application of Topographic State Constraints in Ground Target Tracking"

In this work, tracking performance affects of the application of topographic state constraint information was investigated in a ground target tracking scenario utilizing a GMTI radar by using unscented Kalman filter based

VS-IMM algorithm as well as VS-SIR particle filter and the tracking results of the aforementioned filters were compared to the results achieved by an unconstrained IMM filter. It was observed that application of topographic state constraints helped the performance of tracking algorithms for tracking onroad targets. However, it was also seen that constrained trackers showed error spikes greater than those of the unconstrained filter when either targets left roads or approached junctions. [C9125]

"Detection in Heterogeneous Radar Clutter"

Classical algorithms that were derived with Rayleigh clutter assumption yield increased false alarm rate under Weibull clutter. In this study, a method for radar thresholding in range-heterogeneous Weibull radar clutter is proposed. The method employs expectation-maximization (EM) algorithm in estimation of the parameters and sets the threshold according to these estimates to yield the desired false alarm rate. Due to the mathematical complexity of the shape parameter estimation, an algorithm that uses a predefined shape parameter set is proposed. Performance of the algorithm is analyzed and it is shown to perform successfully even under spiky clutter conditions. [C9126]

"Texture Classification by Using Wavelet Domain Association Rules"

Texture is an important characteristic for analysis of many types of images that including natural scenes, remotely sensed data and biomedical modalities. Texture classification aims to assign texture labels to unknown textures, according to training samples and classification rules. In this study, multi resolution approaches such as wavelet transform and association rules are hybridized for efficient texture classification. The wavelet domain and the intensity domain (gray scale) association rules were generated for performance comparison purposes. The performed experimental studies show the efficiency of the proposed system. [C9127]

"Method of Compound Object Identification in Microwave Band by Scattered Field Interference Pattern"

There is proposed and investigated the method of compound object identification by scattered field amplitude and phase parameters in the made of coherent-pulse probing signal spectral scanning. [C9128]

"Proportionate-Type Steepest Descent and NLMS Algorithms"

In this paper, a unified framework for representing proportionate type algorithms is presented. This novel representation enables a systematic approach to the problem of design and analysis of proportionate type algorithms. Within this unified framework, the feasibility of predicting the performance of a stochastic proportionate algorithm by analyzing the performance of its associated deterministic steepest descent algorithm is investigated, and found to have merit. Using this insight, various steepest descent algorithms are studied and used to predict and explain the behavior of their counterpart stochastic algorithms. In particular, it is shown that the μ -PNLMS algorithm possesses robust behavior. In addition to this, the ϵ -PNLMS algorithm is proposed and its performance is evaluated. [C9129]

"Analysis of scattered by rain precipitation radar signals in MMW-band"

In the paper direct radar signals and by rain medium scattered radar signals are considered. An algorithm for such analysis, use rain normalized volumetric scattering cross section area and attenuation coefficient, is proposed. Summarized scattered by rain medium radar signal can reach a half of direct radar signal, calculated use attenuation coefficient only. [C9130]

"Echo Signal Frequency Averaging as Method of Forming the Stable Criteria of Compound Object Identification in Microwave Band"

There is proposed the method of forming the stable criteria of radar compound object identification in the microwave band. This method is based on distraction of interference interaction of local reflection areas of the object shaping surface. [C9131]

"Approach to Optimum Performance in Random Spreading CDMA by Linear-Complex LAS Detectors"

In this paper, we first present a BER upper bound for the family of LAS detectors. Then the upper bound is applied to analyze the performance of local maximum likelihood (LML) detectors in large random spreading CDMA (LRS-CDMA) channels where user number A' and spreading gain N tend to infinity and K/N keeps a constant. The LRS-CDMA channels are shown to possess the LML characteristic. In the regime of $K/N < 1/2$ -

$1/(4\ln 2)$ and $N\sigma^2$ equal to a constant where σ^2 is the noise power, an LML point is almost surely a global maximum likelihood (GML) point and the asymptotic multiuser efficiency of all the LML detectors converges almost surely to one. Given a practical CDMA system with fixed finite K and N , we then propose to construct a quasi-LRS-CDMA channel where bits are extended by a factor of B and spread by unit-length BN -chip sequences and each user transmits B extended bits. Simulation results show that in the regime of $BK > 1000$, $K/N < 1.0$ and SNR ges 4 dB, while their average per-bit complexity is less than $0.79BK$, the LAS detectors can achieve the BER indistinguishable from the large-system limit BER of the GML detector. [C9132]

"The Estimation and Removal of Unknown Background Signatures in Raman-Shift Spectra via SWTPE"

We present a technique, called the sliding-window technique for pedestal estimation (SWTPE), for estimation and removal of unknown arbitrarily-varying noisy background (pedestal) from Raman-shift spectra that may contain Raman-signatures of chemical agents. ROC plots depicting P_{dles} 0.8 vs. P_{fages} 0.1 are presented for two example backgrounds to demonstrate the performance of the algorithm. [C9133]

"Joint Detection and Identification of an Unobservable Change in the Distribution of a Random Sequence"

This paper examines the joint problem of detection and identification of a sudden and unobservable change in the probability distribution function (pdf) of a sequence of independent and identically distributed (i.i.d.) random variables to one of finitely many alternative pdf's. The objective is quick detection of the change and accurate inference of the ensuing pdf. Following a Bayesian approach, a new sequential decision strategy for this problem is revealed and is proven optimal. Geometrical properties of this strategy are demonstrated via numerical examples. [C9134]

"Minimax Robust Waveform Design for MIMO Radar in the Presence of PSD Uncertainties"

In this paper, we consider the problem of mini-max robust waveform design for multiple-input multiple-output (MIMO) radar based on mutual information (MI) and minimum mean square error (MMSE) estimation for target identification and classification. Recognizing that a single, precise characterization of target power spectral density (PSD) is rare in practice, we assume the PSD lies in an uncertainty class of spectra bounded by known upper and lower bounds, which markedly relaxes the required target a priori knowledge. Based on this band model, we develop minimax robust waveforms for MIMO radar under both MMSE and MI criteria. These robust waveforms bound the worst-case performance at an acceptable limit, and also could insure performance will be sufficiently good for any PSD in the uncertainty class. Our findings also indicate that the MI and MMSE criteria lead to a different minimax robust waveform solutions, which is in contrast to the case of the perfectly known target PSD. [C9135]

"Comparison between DPCA Algorithm and Inertial Navigation on the Ixsea Shadows SAS"

In this paper, we present some results obtained with the Shadows system, the new synthetic aperture sonar, by IXSEA. First sections are a slight presentation where we expose the performances and specifications of Shadows. We present the results obtained on the lateral sonar by using first the algorithm of DPCA, second the simulation of DPCA parameters by using the navigation data. Hence we present some results obtained by comparing the two methods. The data were recorded by the Shadows system in La Ciotat Bay during summer 2006. [C9136]

"Design of a Communication Service System for Vehicle Monitoring"

To develop a general and high compatibility communication service system is the key to build vehicle monitoring centre successfully. In this paper, a design method of the general communication service platform based on GIS/GPS/GPRS for vehicle monitoring system is proposed, which uses non-blocking I/O technology, J2EE design mode and open source technology. The application in practice indicates the high efficiency, stability, reliability, and expansibility of this communication platform. [C9137]

"The Design of Vehicle Emergent Calling System Based on GPRS"

Combining with the working principle of Intelligent Transport System, and with the purpose of enhancing the security of modern traffic, this paper brings forward a project of building a kind of automobile emergent calling system which starts-up with the starting of airbag, the wireless data transport modem, which is droved by serial interface, transmitted the acquired data to the remote monitoring center. The design of the hardware circuit implement, the design of software and the design of building monitor and control center are demonstrated. And

finally, the key technique of the system is also discussed. [C9138]

"Past, Present and Future of RFID"

RFID has a history which began with radar in the 1920s and 1930s. Later, transistors made it possible to include lots of chips on a single circuit leading to the tags in use today. The components and functionality of RFID, both active and passive systems, will be explained. The current push for RFID was instituted by Wal-Mart. But, everything has not proceeded according to plan. Presently, there are many instances where the return-on-investment for using RFID is just not there. The presenter will discuss a number of conditions that must exist for RFID to have a healthy future. [C9139]

"A New Guidance Law Based on Information Fusion and Optimal Control of Structure Stochastic Jump System"

Based on multisensor information fusion theory and optimal control theory of structure stochastic jump system, a new guidance law is proposed for air-to-air missiles based on information fusion of active radar and infrared sensor, and its validity is testified by analysis on simulation by building digital model of missiles. Compared with proportion navigation law and extended proportion navigation law based on radar or infrared through many Monte Carlo simulations, the results show that the new guidance law reduces errors of tracking target and has smooth trajectory and small over-load, and it is important to theory and engineering application. [C9140]

"Agenda-at-a-glance"

{no data available} [C9141]

"Time-orthogonal-waveform-space-time adaptive processing for distributed aperture radars"

Distributed aperture radars represent an interesting solution for target detection in environments affected by ground clutter. Due to the large distances between array elements, both target and interfering sources are in the near field of the antenna array. As a consequence the characterization of both the target and the clutter is complicated, combining bistatic and monostatic configurations. Using orthogonal signaling the receivers can treat the incoming signals independently solving separately bistatic problems instead of the initial multistatic problem. Recent works have demonstrated the benefits of the use of frequency diversity space time adaptive processing for distributed aperture radars. This paper modifies the waveform diversity signal model, resorting to a time orthogonal signaling scheme, which does not present the coherence loss exhibited by frequency diversity. [C9142]

"Research on Cooperative Control Method of Saturation Attack"

Saturation attack can effectively improve operational effectiveness of anti-ship missile, and it can help to increase penetration probability and destroy targets as possible as it can. Cooperative control of saturation attack has many advantages and it is necessary to study the problem. Accordingly, the paper expatiates on developments of guidance law to control impact time/impact angle and cooperative route planning. Further more, the paper fully discusses the key problems, such as guidance law on impact time/impact angle, time-to-go estimation methods, cooperative route planning control methods and the internal relations between the numbers of launching missiles and hitting probability. In a word, the research of time cooperative control methods of saturation attack is both extensive application backgrounds and a series of challenges. But there are many problems to be solved. [C9143]

"Real-Time Robot Joint Variable Extraction from a Laser Scanner"

This paper describes a customized iterative closest point (ICP) algorithm for robot excavator bucket pose estimation and joint angle evaluation using a laser scanner. The proposed ICP variant handles noise, occlusion and partial- overlapping. The method has been tested on a Takeuchi mini-excavator and proved to be reliable with minimal workspace error. The angle estimations were found to be accurate. A comparison has been provided between the angle estimation results and the measurements from joint angle sensors. [C9144]

"Satellite Recognition Base on Wavelet Denoising in HRRP Feature Extraction"

Wavelet denoising is proposed to be used in radar high resolution range profile (HRRP) feature extraction because the HRRP is sensitive to the target pose. It is proposed that wavelet denoising is used to process the HRRP before extracting features, and noise threshold is used as the detecting threshold of strong scattering centers. Denoised HRRP shows that the wavelet threshold denoising can eliminate the influence of the spurious

scattering centers outside of target region and reserve the original HRRP characteristics of target region well. Experimental results show that wavelet denoising enhances the HRRP features stability and recognition rate greatly. [C9145]

"Polarimetric Monopulse Radar Intelligent Emulator"

For debugging polarimetric monopulse radar and testing polarization algorithms, a new polarimetric monopulse radar intelligent emulator is proposed and designed in this paper. The polarization information, as a basic character of the target echo, plays an important role in modern radar detection nowadays. The polarization algorithms are developed with rapid speed. It is not realistic to test all algorithms on real radar in research stage. Therefore, the polarimetric radar emulator is required. The functions of radar emulator are as follows: recording the valuable experiment data for researching, playing the experiment data as a radar receiver for radar signal processor debugging, running some polarization programs with real experiment data to test the programs. In the paper, the polarimetric monopulse radar intelligent emulator is introduced in detail. Firstly, the index of emulator is given; secondly, the emulator is divided into 3 modules to be introduced; thirdly, the system architecture and key techniques are analyzed; finally, the performance of emulator is given. [C9146]

"A Novel Feature Extraction Approach for Radar Emitter Signals"

Feature extraction is the crucial technology to deinterleave and recognize the new system radar emitter signals. In this paper, a novel time-frequency atom feature extraction approach is presented. Based on the over-complete multiscale dictionary of Gaussian Chirplet atoms, adopting match pursuit (MP) to decompose signals and the improved quantum genetic algorithm (IQGA) to reduce the search time for MP, the optimal Chirplet atoms to represent the feature information of the radar emitter signals can be obtained. The validity and feasibility of the approach was proved by using fewer Chirplet atoms to acquire more accurate feature information compared with Gabor atoms approach. [C9147]

"A SAR Imaging Algorithm with Stronger Anti-jamming Capability"

This paper analyzed the imaging processing gains of the CS imaging algorithm (CS) and the RD imaging algorithm (RD) on both the signal and the oppressive jamming. According to above analysis, the conclusion is drawn that the anti-jamming capability of RD is better than that of CS. However, CS fits the spaceborne SAR imaging with large range cell migration well. The echo data are processed through the pre-filter to improve the anti-jamming capability of CS. The anti-jamming capability of RD is identical with that of the pre-filter processing CS algorithm (pre-filter processing CS). Finally, the simulated data and the real data are processed respectively. The simulation result verified the validity of the analysis. [C9148]

"Research on LEO Satellites Time Synchronization with GPS Receivers Onboard"

Precise relative navigation of spacecraft is required for its critical movement, such as rendezvous and formation flying-key aspects of many current and future space missions. Potential applications of interest include the capabilities to detect and track slowly moving ground vehicles (ground moving target indication (GMTI)) and perform synthetic aperture radar (SAR) imaging, with the requirement to provide GMTI and SAR data to users in a timely manner. Extensive research has been carried out on terrestrial applications of global positioning system (GPS) time transfer. For low earth orbit (LEO) satellites, such missions can use the GPS signals for relative positioning and data time tagging. This paper focuses on linking these two key applications-the use of GPS in LEO for relative navigation and precise formation flying, and time and frequency transfer between LEO satellites. As an example, the research investigates co-orbiting satellites A and B of gravity recovery and climate experiment (GRACE) at a separation of about 200 km. The observations of GPS receivers onboard both GRACE A and B satellites are transferred into receiver independent exchange format (RINEX) format (1 Sept. 2003). The orbit of both satellites is then computed using the zero-difference precise point positioning technique. The RMS orbital difference between the results obtained and the precise orbits from GFZ is below 0.07 m. Two methods are proposed to compute the time difference between GPS receiver onboard satellites A and B respectively. One uses onboard GPS RINEX observations and the GRACE orbit from GeoForschungsZentrum Potsdam (GFZ) which has a large relative latency, the times between A and B in multi-channel common-view mode are compared. Another method computes the clocks of A and B by use of GPS observation onboard and the computed orbit. The times between A and B are then compared. Results indicate that a RMS accuracy of 2-3 nanoseconds (ns) can be achieved. This suggests that GPS-has the capabilities of high-precision time transfer between LEO satellites. [C9149]

"Improved Methods for Frequency Measurement of Short Radar Pulses"

A method for measuring the frequency of short radar pulses is presented. In our experiment, two frequency

synthesizers were used as a signal source, a double balanced mixer as a phase detector and a fast sampling oscilloscope (1 Gs/s) was used for data acquisition/display. Therefore our method is relative in nature. Since this method is based on waveform measurements, also even shorter pulses and their frequency deviations can be measured or at least detected and evaluated. In our test setup, 18 ns pulses can be produced. A waveform of such short pulses cannot be measured using a conventional oscilloscope, but a dedicated high-speed sampling device. [C9150]

"Anti-Full Polarization Active Jamming"

For anti-full polarization active jamming, a new polarization signal processing technology is proposed in this paper. The single polarization active jamming can be identified by polarimetric radar, but the full polarization active jamming is effective to deceive polarimetric radar. Therefore, the new detection technology is necessary to be adopted against full polarization active jamming. The purpose of the paper is to present a new method for anti-full polarization active jamming. The polarization coding technology, as a new method used in polarimetric radar, is proposed and a new polarization demodulation method by included angle of polarization state between transmitter signal and echo signal on the Poincare polarization sphere is given in the paper. [C9151]

"Ultra Low Phase Noise 1 GHz OCXO"

Modern radar equipment, commercial and defense communication systems, point-to-point and point-to-multipoint microwave digital radios, microwave sources require excellent stability, extremely low phase noise frequency sources in UHF band. Existing HF OCXO at 100 MHz can achieve -90 dBc/Hz phase noise at 10 Hz offset from the carrier and -125 dBc/Hz at 100 Hz offset. The goal of this work was to create a 1 GHz OCXO with temperature stability performance of SC-cut (1E-8 or better), with the similar to 100 MHz phase noise close to the carrier, and noise floor reaching -150 dBc/Hz, while providing +7 dBm of output power. The goal was accomplished by integrating in a small SMD package (20 x 25 mm), or Europack (36 x 25 mm) high performance, low frequency, SC-cut reference OCXO, low noise off-the-shelf Phase Lock Loop (PLL) IC, and ultra low noise 1 GHz VCXO. Reference OCXO implemented in DIP 14 compatible format was described in previous papers. The key solutions for this development were optimization of the phase noise performance both close to the carrier frequency and on the noise floor, and design of a VCXO. The VCXO is based on a 3rd overtone 200 MHz AT-cut crystal resonator with relatively high Q, passive band-pass filter, tuned on the fifth harmonic of the 200 MHz VCXO, and a free-running L-C oscillator, which is injection locked to the above mentioned fifth harmonic of the VCXO. Dual stage multiplication of the lower frequency VCXO (100.00 MHz, and 111.111 MHz), and additional measures of phase noise reduction far away from the carrier were also investigated. [C9152]

"The benefits of matched illumination for radar detection of ground based targets"

This paper compares the radar detection performance of a narrow band rectangular pulse, linear chirp and nonlinear stepped frequency waveform approximating to a matched target illumination against two target types (a farm tractor and a main battle tank) in the presence of clutter (soil/sand, rocks and woodland). [C9153]

"An approach for interference detection and rejection from other sensors by using Hough Transform and image processing"

This paper presents some results of studies on radar interference rejection using a Hough-Transform-based technique and image processing. If target detection is done by comparing the magnitude of each bin with a threshold produced by a CFAR algorithm, a number of radar systems operating at the same frequency band can cause reciprocal interference, thereby affecting detection and increasing false alarm probability. In this work we will refer to this interference as to "other sensor interference" (OSI). The goal of this work is the definition of methods to detect and remove the interference patterns from radar raw video images. We show that the substitution of interferences with samples estimated from cells (cross range samples) in close proximity of the OSI-affected samples allows CFAR algorithms performance to be improved. [C9154]

"The peak sidelobe distribution for binary codes"

Low aperiodic-autocorrelation peak sidelobe levels (PSLs) relate to enhanced range resolution for binary-phase-coded radar and communication waveforms. Typical methods to identify the minimum-attainable PSL for a given code length N require exhaustive calculations whose computational burden grows exponentially with N . In this project, exact PSL histograms were determined for computationally practical lengths. These histograms may lead to ways to estimate PSL distributions for computationally impractical lengths. Plots of the lower four moments for N between 1 and 45 showed that the moments can be approximated closely by aN^k . Histograms for $N = 45$ were compared to a binomially-distributed PSL PDF model based on statistically independent sidelobes. The

independent-sidelobe model agreed closely with truth for middle-to high-PSL values, and only varied significantly from truth for PSLs one or two units away from the lowest achievable PSL. Future work will examine ways to develop the PDF from the moments accurately enough to estimate minimum PSL for a given N, and ways to account for sidelobe dependence in the probabilistic model. [C9155]

"Air target detection and tracking using a multi-channel GSM based passive radar"

This paper presents a summary of the hardware system design and associated signal processing schemes of a multi-channel GSM based passive radar and most importantly presents new experimental results to demonstrate the multichannel GSM based passive radar ability to detect and track the Doppler frequency of aircraft target as well as measure the aircraft target bearing. [C9156]

"Optimal sparse waveform design for HFSWR system"

High frequency surface wave radar (HFSWR) systems operate in heavily congested high frequency (HF) band. It is very difficult to find continuous clear channels for the wide-band HFSWR systems. Both the conventional frequency modulated continuous wave (FMCW) and the frequency modulated interrupted continuous wave (FMICW) are not able to solve the problem. The sparse waveform design can mitigate the interferences influence by discontinuous spectra waveforms; however, it gives rise to high range side lobes, which can't be suppressed by traditional spectral weighting. In this paper, we investigate a genetic algorithms (GAs) based sparse waveform optimization approach for HFSWR systems. Simulation results show an optimal transmitting sparse waveform solution. [C9157]

"Multistatic SAR image reconstruction based on an elliptical-geometry radon transform"

We propose a geometry and inversion methods for a multistatic, downlooking SAR mode using simple antennas. The resulting generalized Radon transform takes line integrals over ellipses of changing aspect ratio. We apply the method of approximate inverse to the inversion of this transform and show the results of the numerical inversion. [C9158]

"Cross-eye jamming of monopulse radar"

Radar seeking missiles present a serious threat towards ships and aircraft. In cross-eye jamming a missile seeker is deflected by signals from two onboard antennas transmitting out of phase with signals of nearly equal strength. The limits on cross-eye performance imposed by scattering have been studied when scattering takes place far from the propagation path. It will be shown that a digital cross-eye system with several antenna units can be seriously affected by scattering from sea waves and terrain. [C9159]

"Novel pulse-sequences design enables multi-user collision-avoidance vehicular radar"

A new, so-called chaotic pulse-sequence radar (CPSR) has been developed and implemented for short-range vehicular radar, designed to warn the driver of close-by overtaking vehicles (so-called 'blind-spot' warning). It employs a novel design of randomized signal generation and processing which overcomes problems of long-range returns from large reflecting structures and high-levels of interference from both similar and dissimilar radars in the same frequency channel/band. The new technique involves generation of long, non-deterministic pulse trains, composed of a large number of successive, relatively-short pulse-sequences having specially designed correlation properties, separated by random gaps. The statistically-defined unpredictability of such composite pulse trains required in a multi-user scenario is derived from a very large number of pulse-sequences processed in the radar receiver to obtain near-vehicle range estimates. Field tests of a prototype radar confirm good and reliable performance of the technique, including its interference rejection capabilities. [C9160]

"Multichannel parametric detectors for airborne radar applications"

We consider the problem of detecting a multichannel signal in the presence of spatially and temporally colored disturbances. The parametric Rao and GLRT detectors, recently developed by exploiting a multichannel autoregressive (AR) model for the disturbance, have been shown to perform well with limited or even no range training data. The performance of the parametric detectors, however, has been evaluated through the limited computer simulations. The disturbances were generated to follow the exact multichannel AR processes and independently from each other with the same distribution whereas the disturbances in an airborne radar environment do not follow the exact multichannel AR model. In this paper, we evaluate the detection performance of the parametric Rao and GLRT detectors using airborne data obtained from the multi-channel airborne radar measurement (MCARM) database. This data contain typical clutter found in airborne radar systems, and cover a variety of scenarios including dense-target or heterogeneous environment. Numerical

results show that the parametric Rao and GLRT detectors work well with limited or even no range training data in an airborne radar environment. [C9161]

"Waveforms in virtual tomographic arrays"

Distributed sensing systems incorporating RF tomography allow a trade-off between spatial and spectral diversity, however a large number of widely spaced sensors is conventionally thought to be required. A practical method of reducing the number of sensor nodes is introduced via the concept of the virtual tomographic array. Furthermore, the geometry of this virtual array is electronically reconfigurable. Optimal resource allocation is accomplished instantaneously, with dynamic control based upon matching sensing modalities to site specific target and clutter observables. [C9162]

"Knowledge base technologies for waveform diversity and electromagnetic compatibility"

Waveform diversity in multistatic radar systems can enhance distributed radar system performance. Dynamically changing the electromagnetic emanations of radar and communications systems however poses an electromagnetic compatibility (EMC) challenge. Data are provided illustrating how waveform diversity improves multistatic radar system performance. An approach for maintaining EMC in a dynamically changing environment is provided along with an example knowledge base (KB) solution. [C9163]

"Feasibility study of a low-cost system-on-a-chip UWB pulse radar on silicon for the heart monitoring"

In February 2002 the FCC authorized the marketing of a new class of radiofrequency devices: the ultra-wide-band (UWB) systems. One of the most interesting applications for which the UWB systems are addressed is related to the medical imaging. This paper addresses the feasibility study of a novel fully integrated 3.1-10.6 GHz UWB radar on a standard silicon technology for the heart wall monitoring. A theoretical frequency-dependent model of the losses of the electromagnetic radiation in the channel (the human chest) in which the radar operates has been derived. The preliminary specifications of each building blocks have been derived by basic theory in the conditions of the addressed scenario. System simulations have been carried out by means of the Ptolemy simulator within Agilent ADS2005ATMin order to claim the preliminary theoretical study. The CAD analyses have shown that the correlator-based radar topology allows us to approach the realization of such a system-on-a-chip pulse radar in a modern silicon technology (as such as the standard CMOS 90 nm). [C9164]

"Varying FM rates in adaptive processing for distributed radar apertures"

Previous work in waveform diversity for distributed apertures for target detection has focused largely on orthogonal transmissions. This paper investigates an alternative approach; implementing waveform diversity based on differing slopes of the linear FM pulse to the application of target detection for a distributed radar aperture system in the presence of noise and clutter. This paper add develop the required signal model corresponding to the proposed system, accounting for the cross-coupling between the linearly FM pulses. This paper determines whether applying this type of waveform diversity will result in improved performance in the discrimination of the target from noise and interfering sources and compare the performance whether this method is a feasible solution. A crucial step is the optimization of the FM rates using sequential quadratic programming. [C9165]

"Waveform design for distributed aperture using Gram-Schmidt orthogonalization"

In this work, we consider a distributed aperture radar system and present a method for clutter rejecting waveforms and reflectivity function reconstruction. This work generalizes the monostatic radar waveform design method for range-doppler imaging, developed in [1], [2] to distributed aperture radar systems. The designed waveforms also lead to a filtered backprojection type reconstruction of the reflectivity function which can be efficiently implemented in a parallel fashion. [C9166]

"Real-time PRF selection for medium PRF airborne pulsed-doppler radars in tracking phase"

This paper proposes a new method to select optimal pulse repetition frequency (PRF) sets for use in tracking mode of medium PRF airborne pulsed-Doppler radar. Neural networks algorithm is used to map from engagement variables to the optimal PRF set. On-line computation during flight can be made real-time after off-line training of the neural network. The training sets for the neural network need to be generated by selecting optimal PRF set for the possible engagement scenarios from which range-Doppler clutter map is calculated to check the decodability and detectability for all PRF candidates. The PRF sets generated by the method must guarantee the maximum detectability inside the target tracking window as well as maintaining good decodability.

Simulation result shows that the proposed method has much better range-Doppler detection performance compared to the previous algorithms by applying different optimal PRF set to different engagement scenarios and target positions. [C9167]

"How will waveform diversity affect electromagnetic compatibility?"

This paper will provide a general overview of the new research area called waveform diversity (WD), and its potential impact to the EMC community. The scope of research that is considered WD is broad in both technical content and application. The two main application areas are radar and communications across the RF spectrum. WD is beginning to transition from theory to operational systems, and the effect on RF design and EMC analysis may be significant. This paper will describe WD, what has motivated people to research it, and potential effects to the EMC community. [C9168]

"Discrete Suppression with $\Sigma\Delta$ -STAP"

This paper presents the hybrid algorithm of SigmaDelta-STAP and direct data domain(D3) which is robust to the discrete interferer. SigmaDelta-STAP provides high performance result with the relatively low complexity of calculation. It also requires small number of training sample to estimate covariance matrix. However this algorithm is vulnerable to the discrete interferer which is target-like interferer with high SNR. This paper shows that SigmaDelta-STAP can suppress discrete interferer signal in conjunction with direct data domain (D3) method which is an effective method to eliminate non-correlated interference such as discrete interferer in the non-homogeneous environment. [C9169]

"A Nested Multi-static HF Radar Testbed for the New York Bight and Beyond"

Surface currents are envisioned to be an integral component of the Integrated Ocean Observing System (IOOS) and High Frequency (HF) radar technologies provide the means to measure these data across multiple scales. The Rutgers University Coastal Ocean Observation Lab (COOL) has continuously operated a nested network of HF radars since 1998 as part of a sustained coastal observatory centered on the New York Bight. Components of this network include 25 MHz, 13MHz, and 5 MHz Tx /Rx shore stations and offshore buoy mounted Tx stations. These components are linked through GPS synchronization technology to provide fully nested multi-static surface current coverage. Data from these systems are supporting a growing number testbed activities and large science campaigns. Testbed activities focus on extending the present surface current mapping coverage closer to the beach with the development of new nearshore wave and current applications. Additional software and hardware modifications are beginning to extend the environmental monitoring to full maritime domain awareness by transitioning the sites to a dual-use mode that include hard target detection and tracking. The HF radar data has most recently supports two science campaigns, the Shallow Water 2006 (SW06) Joint Experiment supported by the Office of Naval Research and the Mid-shelf Front Experiment supported by the National Science Foundation (NSF). Both campaigns have used the HF radar as a resource for adaptive sampling. During the SW06 experiment, HF radar data was incorporated into daily reports along with other observation and forecast data to support the science fleet offshore. In addition to the adaptive sampling application, the mid-shelf front experiment takes advantage of the 5.5 year dataset within the study site. Long term means show a significant cross-shelf transport pathway south of the Hudson Shelf Valley that could possibly feed the mid-shelf front. These Rutgers systems fit into a larger effort across the entire Mid-Atlantic Bight (MAB) region from Cape Hatteras, NC to Cape Cod, MA. HF radar groups across this region have now formed a consortium for the operation and maintenance of the entire network, including system hardware, data management, and product delivery. Through this consortium the existing pockets of systems, of which Rutgers is one, can be operated as one regional system that spans over 1000 km of coastline. This network consists of 11 long-range sites providing total vector coverage across a large portion of the region from Cape Hatteras NC to the apex of the New York Bight. Additional funded sites for Moriches, NY and Block Island, RI, will extend the coverage north to Cape Cod, MA and Nantucket MA. In addition there are four higher resolution sub-systems made up of 15 sites in operation in the Chesapeake Bay, New York Harbor, the Long Island Sound and the Delaware Bay estuaries. In addition to scientific research and education applications, the United States Coast Guard Research and Development Center has identified the Mid-Atlantic Bight as a testbed for the new search and rescue planning tool, SAROPS. [C9170]

"A Structured Approach to Passive Sonar Track Association"

The presence of multiple, apparently independent track segments originating from the same target complicates the track-level passive sonar picture. If some of these segments can be shown to have common origin, they can be associated into a single composite track, simplifying that picture. The process could also provide additional information about the target, such as range or classification. Track association is typically a manual process,

relying on the expertise of a human sonar operator. If a method could be found to reliably apply numerical scores to the degree of apparent relationship between pairs of tracks, those scores could be used to assist an operator in the track association process or as inputs to a fully automated track association process. This paper outlines the construction of a test based on the sample correlation coefficient and describes the result of its application to tracks produced by a probabilistic data association filter (PDAF) from a set of towed array sensor data. [C9171]

"Comparative Theoretical Performance of Maneuverable Unmanned Vehicles versus Conventional Towed-Arrays for Passive Sonar"

This paper considers the potential for passive acoustic target detection using a maneuverable unmanned underwater vehicle (UUV) equipped with towed line array. The objective is to assess target detection performance as a function of vehicle maneuverability, environmental variability, and array length. Detection performance is evaluated by mapping the search region onto a graph wherein vehicles are constrained in their trajectories as function of their maximum turning angle. Detection range, as a function of location on the graph, is encoded on the edge weights between nodes. With this framework, the UUV trajectory which maximizes the probability of at least one target detection along a transit through the region can be determined using the computationally efficient Dijkstra algorithm. Increasing UUV maneuverability is shown to significantly improve detection performance given known environmental variability since the optimal trajectory is able to visit more favorable locations, or "hot spots" with respect to environmental conditions. Moreover, it is shown that in sufficiently variable, but known, environmental conditions, a maneuverable UUV with short array is competitive to a much longer non-maneuverable array. [C9172]

"Target Detection Using HF Radar Data"

High frequency (HF) radar systems have a potential to detect targets which are located beyond the optical horizon on the sea surface. Unfortunately sea clutter may be strong enough to prevent such detection. In this work we present results of applying space-time adaptive processing (STAP) to this problem. Real, registered signals were used for numerical experiments. [C9173]

"Measurements of the Effect of Rain-induced Sea Surface Roughness on the Satellite Scatterometer Radar Cross Section"

Radar measurements of the sea surface, with satellite scatterometers that operate at Ku-band, will be affected by the presence of rain through modification of the sea surface roughness by rain impacts. This is in addition to wind driven roughness, atmospheric reflectivity and attenuation that affect the measured normalized radar cross section (NRCS). Numerous surface-based studies, using ocean platforms and wind-wave tanks, have shown the increase in the total NRCS can be significant and strongly dependent on radar frequency, incidence angle, polarization and wind speed [1], [2], [3]. Herein is the first study combining satellite based Ku-band data with high-resolution 3-D volumetric rain measurements, from simultaneous collocated NEXRAD data. The results to be presented were acquired during a significant rain event in the Gulf of Mexico just south of Houston, TX in May 2005. They are directly applicable to questions that are important to the interpretation of satellite derived wind vector estimates in the presence of rain of varying intensity and spatial distribution. This project is developing techniques to correct scatterometer derived wind-vector estimates. The acquisition of new knowledge on rain-splash effects is a necessary part of this effort. [C9174]

"Advances in Lidar Transmitter Sources for Ocean-Atmosphere Remote Sensing"

Pulsed, tunable alexandrite lasers in combination with harmonic generators and Raman wavelength shifter form a powerful and versatile tool for lidar (light detection and ranging) remote sensing. Such an integrated laser system can generate any wavelength from ultraviolet to infrared with the necessary beam qualities required for lidar measurement. This paper presents the development of injection seeded alexandrite ring lasers and linear cavity alexandrite lasers that can be deployed in ocean-atmosphere lidar remote sensing. [C9175]

"New Application of Wavelet Transform for Internal Wave Detection SAR and Optical Image: A Case Study in Japan Waters"

We observed the internal wave features in ERS1/2 SAR and ASTER images data over Japan waters, during 1993-2004 period. The internal wave features were shown in the Tsushima Strait, coast of Izu Peninsula, coast of Ibaraki in east of Honshu, coast of Sado Island in west of Honshu, and southwest and south of Hokkaido. The internal wave feature characteristics in image suggest tidal generation source. At these places, packets of non-linear internal waves were formed over shelf break areas such as ridge and sill. Various wavelet transform, e.g.

Haar, Daubechies, Symlet, Coif, Biorthogonal, and Meyer wavelet, are tested comparably to study the internal wave detection in image using multi resolution analysis. Though all of wavelet families can be used for internal wave packet detection, the decomposed feature tends to follow the wavelet function, which compress the first wave crest. To solve this problem, we propose new wavelet function constructed from Damped Oscillation Function. So far this method show good result. Finally, we show the application of KdV model to calculate the nonlinear speed of the internal wave, which can be use to predict the generation of strong current when internal waves occur. [C9176]

"Satellite Data Visualization on the Ocean Motion Website"

The NASA-sponsored OceanMotion Web site (<http://www.oceanmotion.org>) documents humankind's experiences, observations and investigations of ocean surface currents. In addition to the information resources posted on the website, there are also investigations that lead students to explore patterns and relationships through data products (color-coded images, time series graphs and data tables). These investigations are done through an interactive browser interface that provides access to a wealth of data. This paper focuses on use of surface current data and models in student investigations to illustrate application of basic science principles. Skills developed using data to discover patterns and relationships will serve students in other courses as well as empower them to become stewards of the Earths environment. [C9177]

"MARCOAST-Operational Marine Oil Spill and Water Quality Monitoring Services"

The MARCOAST partnership, supported by the european space agency (ESA) under the global monitoring for environment and security (GMES) service element programme is providing operational oil spill and water quality monitoring services, using products derived from satellite remote sensing data combined with models and in-situ measurements. This paper provides a brief overview of the ESA GMES service element programme, describes the services being offered by the MARCOAST partnership, and discusses how the MARCOAST project is meeting the key challenge of making the transition from research to operational application of satellite remote sensing data. The aim of this paper is twofold: To raise awareness of the purpose, aims and future plans of the ESA/EC GMES programme, in terms of the development and provision of marine services, and to provide a technical overview of the operational services offered by MARCOAST, so that Oceans '07 participants can take a view on their potential utility with regard to their own operational needs. [C9178]

"Resolving Coastal Ocean Eddy Activity in Surface Velocity Signatures from Wellen Radars and an Acoustic Doppler Current Profiler"

A dual-station high frequency Wellen Radar (WERA), transmitting at 16.045 MHz, was deployed along the east Florida Shelf and is currently operated and maintained by the University of Miami's Rosenstiel School for Marine and Atmospheric Science. From September 2004 to June 2005, a bottom-mounted acoustic Doppler current profiler (ADCP) obtained subsurface current measurements within the radar footprint along the shelf break at 86-m depth. The RMS differences ranged from 0.1 to 0.25 ms⁻¹ between the surface and 14 m depth indicating good data. Monthly time series analyses indicated numerous current reversals during the 9-month deployment. When utilized in conjunction with the ADCP subsurface measurements, WERA enables 3-dimensional snapshots of coastal oceanographic features. Given the high temporal and spatial resolution of the WERA system, an increased understanding can be gained in the coastal ocean regime aiding the ability of ocean models at predicting complicated features in the domain. [C9179]

"Multistatic Target Tracking for Non-Cooperative Illuminating by DAB/DVB-T"

Digital Audio/Video Broadcasting (DAB/DVB-T) [1] is already available in a large area. The advantage of using these signals for passive air surveillance is the disposability of a large range of illuminators sending an easily decodeable digital broadcast signal. In the considered multi-static scenario, one observer provides bistatic Time Difference of Arrival (TDoA) and Doppler measurements. To build a 3D multi-target tracker, information of different illuminators has to be fused. The main task is to handle ghosts, which arise due to the association problems between illuminators, targets and measurements. For real-time applications the runtime of the algorithm is another important issue. As a solution, we present a Multi Hypothesis Tracking (MHT) filter working on different stages. The first stage includes a primary tracking directly on the measurements; the second stage works on 2D-estimates and addresses the association problem; the final stage yields 3D information. Numerical results will include performance analysis via Monte-Carlo simulations and comparison to the trace of the covariance matrix. Estimation errors in the x/y-plane and height will be considered separately. [C9180]

"Wave and Tidal Power measurement using HF radar"

HF radar systems have been used extensively worldwide to provide surface current measurements for scientific,

vessel traffic management, environmental, offshore engineering, search and rescue and other applications. Wave measurement with such systems is beginning to be used in operational systems. Many validations have been carried out demonstrating the accuracy of the parameters measured. This paper addresses the potential application of these systems within the marine renewables industry. Wave and tidal power measurements are presented. [C9181]

"HF Radar Observation of Wave Directional Spectra in a Strong Current Regime"

Dual Wellen HF Radar (WERA) systems have been observing near-surface currents and wave parameters over the Southeast Florida shelf since June 2004 as a part of the Southeast Atlantic Coastal Ocean Observing System (SEACOOS). The region of coverage includes the Florida Straits and the Florida Current (FC) which typically has maximum surface velocities approaching 2 ms^{-1} . The echo-Doppler spectra are also routinely recorded and archived at both stations which allows post-processing to extract surface wave directional spectra using an iterative approach as implemented in Seaview Sensing reg software. Both WERA sites operated continuously during the passage of Hurricane Jeanne over the Florida Straits on 25 Sept 2004. Although it passed $\sim 200 \text{ km}$ to the north of the measurement domain, the local mean winds exceeded 20 ms^{-1} and rotated over 270° . The near-surface currents during the passage of Hurricane Jeanne reflected the influence of the wind as well as the Florida Current. The effect of the wind on the near surface flow was seen in easterly and southerly flow over the shallow shelves near Florida and the Bahamas respectively as well as relatively slow flow in the center of the Florida current. Maximum current velocities were only 130 cms - 150 - 60 cms^{-1} less than typical values. The interaction of these wave fields from differing directions with the high lateral shear of the western edge of the Florida Current was observed every 10 minutes.. The wind-wave component of the spectrum was observed to respond rapidly to the rotating wind-field, but effects of the horizontal shear were observed in the off-wind angle of the wind-wave peak. Tower frequencies were often observed at large angles to the local wind. [C9182]

"Radio Frequency Interference Suppression Techniques in FMCW Modulated HF Radars"

High-frequency (HF) radars are operated in the 3-30 MHz frequency range and need to share the frequency bands with other radio services. Due to their over-the-horizon (OTH) capabilities, HF radars play an important role in remote sensing and surveillance. The propagation conditions of the electromagnetic wave depend on the earth's ionosphere and mainly follow a daily cycle. Communication paths between the HF radar and other radio services, some thousands of kilometres off, open and close with a high variability. Special care must be taken to dynamically adapt the HF radar's characteristics to the varying electromagnetic environment. The impact of a frequency modulated continuous wave (FMCW) HF radar on other radio services is not very strong, because of its low transmit power and utilisation of the radio spectrum. However, strong signals from other radio services can significantly reduce the performance of the oceanographic measurements. Several radar control and signal processing steps are discussed in this paper. All together form an effective procedure to reduce the impact of Radio Frequency Interference (RFI) on the oceanographic measurements. [C9183]

"Coastal applications of X-band radar to achieve spatial and temporal surface wave monitoring"

In this paper wave data from two different coastal stations will be discussed with respect to spatial inhomogeneities in the wave field. Effects of the changes in the local topography and strong tidal currents are reproduced in the radar data. The discussion will focus on the potentials of these data to monitor spatial and temporal variabilities of the sea state in coastal approaches. As an example, dissipation, refraction, and reflection of waves will be analysed. [C9184]

"Tsunami Monitoring by HF Ocean Radar: Time and Space Scales"

HF coastal ocean radars are ideal instruments for detection of surface currents in coastal waters and have had wide application for monitoring tidal and wind driven surface currents. This paper addresses the questions of spatial and temporal scales for optimal detection of tsunami properties by HF radar at the shelf break and on the continental shelf itself. Two approaches are used in this evaluation. One is a stylized tsunami wave approaching a shelf which has parallel bathymetry contours and a shelf with uniform depth. In this case the non-linear effects at the edge of the shelf are the same at all points along the shelf edge, and the subsequent wave train emerging onto the shelf has parallel wave fronts. The second approach is a case study of a real section of shelf-edge and shelf bathymetry. In this case numerical modelling indicates that there is a complex pattern of surface currents at the shelf break which varies in space and time. The subsequent wave train has a complex wave front which can be considered to be generated from point sources along the shelf edge. These wave fronts are shaped by local shelf bathymetry as well as interference of waves from the originating source points at the shelf edge. In the case of real bathymetry there are complexities in the surface current field which will produce different outcomes

for direction-finding and phased array types of HF radar facilities. Because of its ability to resolve spatially complex current patterns, the phased array system is preferred for tsunami observation networks. [C9185]

"Coastal Eddies in the Ocean Wind Field as Observed by Single and Multifrequency HF Radars on Monterey Bay, California"

Coastal wind eddies at the 10-40 km scale have been studied over Monterey Bay, California by Archer, Ludwig et al. using shore and buoy anemometers and satellite images. Most frequent in the evening and early morning hours, these, typically cyclonic, eddies are often responsible for fog in the Santa Cruz area. We have previously demonstrated the ability of multifrequency HF radar (4.8 to 21.8 MHz) to map the ocean wind field. Observations over a year time span indicate standard errors of prediction of 1.7 m/s for wind speed and 25deg for direction with biases of 0.1 m/s and 0.3deg respectively. By combining HF radar wind vector estimates with shore based anemometer data in the WOCSS surface wind field model we are able to form detailed (3 to 5 km resolution) images of eddies over Monterey Bay and to follow their development and decay. We discuss the requirements for making wind field maps with HF radars and demonstrate how the changing array of multiple radar sites can be used to produce HF radar wind field maps. We report observations of 10-20 km cyclonic eddies in the northern and eastern parts of Monterey Bay. [C9186]

"Node-Replacement Policies to Maintain Threshold-Coverage in Wireless Sensor Networks"

With the rapid deployment of wireless sensor networks, there are several new sensing applications with specific requirements. Specifically, target tracking applications are fundamentally concerned with the area of coverage across a sensing site in order to accurately track the target. We consider the problem of maintaining a minimum threshold-coverage in a wireless sensor network, while maximizing network lifetime and minimizing additional resources. We assume that the network has failed when the sensing coverage falls below the minimum threshold-coverage. We develop three node-replacement policies to maintain threshold-coverage in wireless sensor networks. These policies assess the candidature of each failed sensor node for replacement. Based on different performance criteria, every time a sensor node fails in the network, our replacement policies either replace with a new sensor or ignore the failure event. The node-replacement policies replace a failed node according to a node weight. The node weight is assigned based on one of the following parameters: cumulative reduction of sensing coverage, amount of energy increase per node, and local reduction of sensing coverage. We also implement a first-fail-first-replace policy and a no-replacement policy to compare the performance results. We evaluate the different node-replacement policies through extensive simulations. Our results show that given a fixed number of replacement sensor nodes, the node-replacement policies significantly increase the network lifetime and the quality of coverage, while keeping the sensing-coverage about a pre-set threshold. [C9187]

"On Sequences with Good Correlation Properties: A New Perspective"

The so-called merit factor approach (MFA) to radar binary sequence design has led to several theoretical contributions in fairly diverse research areas including information theory, computer science, combinatorial optimization, and analytical number theory. However, the pragmatic motivation of this approach is shown here to be questionable. Specifically, the MFA -which basically aims at minimizing the clutter effect on radar performance -implicitly assumes the use of a least-squares (LS) receiver that is optimal only when there is no clutter. This apparent inconsistency in the problem formulation can be eliminated by using a more general optimal instrumental-variables (IV) receiver in lieu of the LS receiver. The IV receiver proposed here is shown to reject clutter much more efficiently than the LS receiver. Additionally, the binary sequence design problem associated with the IV receiver is shown to have an interesting form that is likely to attract the attention of the readers previously interested in the MFA. [C9188]

"Evolution of GSM into the Next Generation Wireless World"

GSM is the most widely deployed 2nd generation digital cellular standard, with over 2 billion subscribers in some 213 countries and adding about 1000 new users per minute! Originally developed in the 1980s, and first deployed in 1991, GSM is a TDMA+FDMA system, providing wide area voice communications using 200 KHz carriers. Subsequently, GSM evolved into a 2.5G standard with the introduction of packet data transmission technology (GPRS) and higher data rates via higher order modulation schemes (EDGE). More recently, GERAN standards organization has been evolving further to coexist with and provide comparable services to 3G technologies. In this paper, we first provide an overview of the traditional 2G and 2.5G GSM, and then discuss the so-called "GERAN Evolution" into the 3G world. We conclude by detailing a few selected aspects of the GERAN Evolution. Overall, we aspire to demonstrate that GERAN is a vibrant, living and growing technology that exploits the latest advances in communications and signal processing. [C9189]

"Optimal Sniffers Deployment On Wireless Indoor Localization"

Location determination of indoor mobile users is challenging due the complex and volatile indoor radio propagation signals. A radio-frequency (RF) based indoor localization system, like RADAR or ARIADNE, typically operates by first constructing a lookup table mapping the radio signal strength at different known locations in the building, and then a mobile user's location at an arbitrary point in the building is determined by measuring the signal strength at the location in question and searching the corresponding location from the above lookup table. Usually, the mobile's signal strength is measured by three or more sniffers deployed inside the building. Obviously, the number of sniffers and their positions greatly affect the localization performance. This paper presents a detailed analysis and experimental results that explore the impact of the sniffers deployment on the performance of the indoor localization. The results demonstrate that the best localization performance is obtained when the center of gravity of the equilateral triangular (formed by three sniffers) coincides with that of the floor plan; and in order to provide optimal localization for all positions of a large floor, it is necessary to deploy more than three sniffers in a semi-mesh style such that any position in the building is always covered by three nearby sniffers. [C9190]

"Satellite Target Recognition Algorithm Based on BP Neural Networks"

For high resolution range profile (HRRP) is sensitive to pose and translation, back-propagation (BP) algorithm is proposed to be used to process even rank central moments of HRRP in target recognition. Wavelet denoising is used to enhance the signal noise rate (SNR) of HRRP. Then central moments are extracted from the denoised HRRP. Even rank central moments can be used as features for target recognition because they are more stable and the dimension is reduced. BP algorithm is used to process the central moments feature vector. The experimental results based on real satellites data show that the proposed method achieves good recognition performance based on its low storage and computational complexity. [C9191]

"Parameter Estimations of SAR Moving Target Based on DPCA-FrFT Algorithm"

The DPCA-FrFT algorithm is used in this paper to realize the localization and velocity estimations in both ground range direction and azimuth direction when it comes to a two-aperture radar system. The moving point target's echo model of two-aperture SAR system is established. Then, the linear frequency-modulated characteristics of moving target's DPCA signal is elaborated. According to this characteristics, fractional Fourier transform is adopted to detect the moving target and estimate parameters. Because of the good capability of DPCA technique for clutter cancellation and the nice effect of FrFT for chirp signal detection, the DPCA-FrFT algorithm can suppress the clutter and realize the localization and velocity estimations well in different signal-to-noise ratio conditions. The simulation results validate the effectiveness of this algorithm. [C9192]

"Challenges for Autonomous Mobile Robots"

Summary form only given. This talk will have two parts. In part one, we will review recent progress in mobile robotics, focusing on the problems of simultaneous mapping and localization (SLAM) and cooperative navigation of mobile sensor networks. The problem of SLAM is stated as follows: starting from an initial position, a mobile robot travels through a sequence of positions and obtains a set of sensor measurements at each position. The goal is for the mobile robot to process the sensor data to compute an estimate of its position while concurrently building a map of the environment. We will present SLAM results for several scenarios including land robot mapping of large-scale environments and undersea mapping using optical imaging sensors. We will also describe work on cooperative navigation for networks of autonomous underwater vehicles (AUVs) and autonomous sea-surface vehicles (ASVs). In the second part of the talk, we will provide an overview of MIT's entry in the 2007 DARPA Urban Challenge. The goal of this effort is to produce a car that can drive autonomously in traffic. Our team has developed a novel strategy for using a large number of inexpensive sensors mounted on the vehicle periphery. Lidar, camera, and radar data streams are processed using an innovative, locally smooth state representation that provides robust perception for real-time autonomous control. A resilient planning and control architecture has been developed for driving in traffic, comprised of an innovative combination of well-proven algorithms for mission planning, situational planning, situational interpretation, and trajectory control. These innovations are being incorporated in two new robotic vehicles equipped for autonomous driving in urban environments, with extensive testing on a DARPA site visit course. [C9193]

"A New Approach to Geometrical Feature Assessment for ICP-Based Pose Measurement: Continuum Shape Constraint Analysis"

This paper presents a generalization of closest- point constraint analysis called continuum shape constraint analysis (CSCA) that can be used to assess the suitability of whole objects or object features for range data

scanning and subsequent pose estimation. "Directional CSCA" (D-CSCA) is proposed to specifically address pose estimation accuracy via the ICP (iterated closest-point) family of algorithms. Constraint analysis based on noise amplification index (NAI) is used. In the D-CSCA formulation, the continuum nature of the underlying shape registration renders the resulting gradient matrix and NAI thereof as pure properties of the feature, dependent on viewpoint but independent of the viewing instrument. [C9194]

"Comparisons between HF radar and SAR current measurements in the Iroise Sea"

In coastal oceanography, currents are difficult to measure with a good temporal and spatial resolution. Nevertheless, precise knowledge of these currents is crucial for certain applications such as pollution monitoring. Up until now, very few instruments have been able to provide current measurements. Although techniques based on HF radar and satellite-based Synthetic Aperture Radar(SAR) are promising, comparisons between these two approaches must be carefully formulated since the approaches differ in terms of scattering geometry, radiation frequency, and antenna footprint. In this document, we present a brief review of these two approaches as well as a comparison between them using data acquired over the Iroise Sea in France. Since the dominant source of currents in this area is tidal in nature, we also compare the results to the currents predicted by the tidal model MARS2D. The results are encouraging: the SAR-derived currents (specifically, the component of the current in the radial direction along the SAR beam) are qualitatively similar to the equivalent projected radial components deduced from HF measurements and MARS2D output. It must be noted, however, that the HF radar results may be compromised by the presence of island, and the SAR results may be compromised owing to the sensitivity to wind waves. [C9195]

"Offshore wind mapping using synthetic aperture radar and meteorological model data"

We introduce an iterative maximum a posteriori probability (MAP) method for combining meteorological model output with synthetic aperture radar for offshore wind field estimation. The MAP approach is demonstrated for 40 ENVISAT ASAR scenes collected for 2004-2006 over the UK Irish Sea. The CMOD4 and CMOD5 geophysical model functions are compared and retrievals using MAP and a simpler directon based windspeed algorithm are validated against in situ mast observations. In particular the CMOD5 MAP algorithm shows promising results showing a RMSE of 2.09 ms-1. [C9196]

"Remote Sensing of the Sea and Target Detection Improvement Using a Wavelet-based Extraction of Sea Echoes from High Frequency Radars"

High frequency radars (HFR) use HF waves (3 MHz to 30 MHz). They interact with the sea surface and are well-suited radars to perform remote sensing of the sea. Moreover, HFR coverage range is not limited by the radio horizon: it is possible to keep watch over the sea up to few hundred kilometers from the coast line (surface wave mode) or up to few thousands kilometers (space wave mode). Oceanographic parameters (i.e. wave height, surface current velocity, wind direction and wind velocity) are derived from the so-called sea spectrum. Moreover, HFR can be used for maritime surveillance of the Exclusive Economic Zone (EEZ). In that case, the sea spectrum is an unwanted signal because it can mask targets. So, sea spectrum extraction is an important topic of HFR signal processing since it is a key point for remote sensing accuracy and target detection features. Wavelet-based processing allows an efficient extraction. [C9197]

"Features and Limitations of the Modular Oceanography Radar System WERA"

The WERA system (wave radar) is a shore based remote sensing system to monitor ocean surface currents, waves and wind direction. This long range, high resolution monitoring system based on short radio wave radar technology. The vertical polarised electromagnetic wave is coupled to the conductive ocean surface and follows the curvature of the earth. This over the horizon oceanography radar can pick up back-scattered signals from the rough ocean surface (Bragg effect) from ranges of up to 200 km. The physical background, technical concept and environmental boundary conditions are explained. Results for various installations from all over the world demonstrates the features and flexibility of the system: high resolution monitoring (range cell size of 300 m) over a range of 60 km or long range applications with 3 km range cell size, all generated with the typical high temporal resolution of 10 minutes. The technical performance depends on the site geometry, system configuration and the environmental conditions. These aspects will be discussed to enable interested users to estimate the potential of this technology for their specific application. [C9198]

"Detection/Imaging of Buried Objects: Using Spatial/Angular Diversity with Distributed/Embedded Sub-Surface Sensors for Reduced Mutual Coupling and Suppressed EM Emissions"

The proliferation of strategic subsurface sanctuaries has increased the need for enhanced remote sensing

techniques providing for the accurate detection and identification of deeply buried objects. A new RF Tomographic Technique is proposed in this concept paper for developing RF CAT Scans of buried objects using spectral, spatial/angular, and polarization diversity. This imaging technique uses an embedded ring of subsurface radiators, delivered by earth-penetrating, non-explosive, electronic "e-bombs", as the source of strong underground radiated transmissions and uses distributed surface-contact sensors to collect the tomographic data for relay to a circling UAV and transmission to a remote control site (using layered sensing). Three-dimensional imaging algorithms are being developed to detect, image, and characterize deeply buried targets. Distributed transmitters and receivers significantly increase unwanted mutual coupling and EM emissions that interfere with signal reception. However, by embedding the transmitters underground, reduced mutual coupling and EM emissions (and improved signal-to-noise ratios) can be achieved. Simple surface SAR experiments over deep mine shafts have been performed to validate the 3D processing algorithms using 2D surface SAR sensor data. WIPL-D models have also been used to simulate the embedded and distributed sensors and to verify the significant enhancement in the received signal-to-noise ratio obtained by burying the radiating ring under the surface sensors. [C9199]

"RF Electromagnetic Penetration of the Nasa Space Shuttle Endeavour Performed with an Ultra-Wideband System"

This paper summarizes a joint NIST-NASA measurement effort to thoroughly evaluate the electromagnetic penetration of the shuttle Endeavour. NASA is concerned about the effects that microwave imaging radar systems might have on critical avionics systems on its fleet of space shuttles. As part of a multifaceted effort, a portable, NIST-developed ultra-wideband measurement system was deployed at the Kennedy Space Center to evaluate electromagnetic penetration over the frequency range of 30 MHz-6 GHz at selected locations inside Endeavour. The measurements were performed inside a large metal hangar, which exhibited robust reverberant behavior. A combination of reverberant chamber techniques and time/frequency signal processing permitted the evaluation of electromagnetic penetration at six different locations inside the orbiter. [C9200]

"HF radar measurements in Liverpool Bay, Irish Sea"

A phased array HF radar systems transmitting at 13 MHz with sites at Form by Point, north of the Mersey outflow, and on the North Wales coast near Abergele has been operational since August 2005. Data on a 4 km grid are recorded every 20 minutes, with hourly data telemetered to the Proudman Oceanographic Laboratory by telephone land line. The data are compared with two in situ acoustic Doppler current profilers (ADCPs, measuring both currents and waves) at sites A and B and an in situ wave buoy at site A. A thirty turbine wind farm is in the radar field of view. The semi-diurnal tides are the dominant physical process in Liverpool Bay. There also appears to be a persistent circulation, relating to the density field, with day to day wind driven (surge) currents not as important as in some shelf sea regions. The tidal currents have been compared with results from a 1.8 km grid 3D numerical model. The agreement is good over most of the spatial coverage but in the north-west corner the radar currents, although exhibiting a very well defined tidal signal, are considerably larger than the model currents. Also of note there is significant energy at tidal frequencies (presumably non coherent) in the tidal residual currents, which is also seen in the ADCP records. Tests on the data quality and further comparisons of the HF radar currents and waves with observations and numerical model estimates (including the wind-driven component) were presented. One eventual aim is to test the feasibility of assimilating the current information into the models. [C9201]

"Waveform Diversity and Electromagnetic Compatibility"

Waveform diversity in multistatic radar systems can enhance distributed radar system performance. Dynamically changing the electromagnetic emanations of radar and communications systems however poses an electromagnetic compatibility (EMC) challenge. Data are provided illustrating how waveform diversity improves multistatic radar system performance. An approach for maintaining EMC in a dynamically changing environment is also provided. [C9202]

"High Order Spectral Estimation Methods in Ground Penetrating Radar Applications"

In ground penetrating radars (GPR) using stepped frequency continuous wave (SFCW), for an estimation of objects depth the inverse discrete Fourier-transformation (IDFT) of signals (image and real parts) on an output of the receiver is applied. As a result frequencies of spectral components corresponds to time delays (or to depths) of signals reflected from buried objects. In applications, in particular, in engineering geology surveys at the decision of problems with use of SFCW GPR, the spectrum width of a probing signal is choosing so that dispersive properties of medium not strongly deformed signals. [C9203]

"Frequency-Dependent Attenuation and Velocity Characteristics of Magnetically Lossy Materials"

In many situations, the magnetic properties of sub-surface materials are often considered unimportant when compared to their 'dielectric' characteristics (i.e., permittivity and conductivity). However, if significant amounts of magnetic minerals exist, such as magnetite, hematite, maghemite and/or iron in its free state, then the relaxation phenomena of these magnetically lossy particles can have an overriding effect on the complex effective permittivity spectrum of the material. In this paper, the effective permittivity, attenuation and propagation characteristics of a range of nano-to-micro scale quartz/magnetite mixtures are investigated with the aim of determining how lossy magnetic minerals affect the macroscopic properties of the material as a whole. In addition, the measured results are compared to popular 'dielectric-based' mixing models (such as the Complex Refractive Index Model CRIM) and the nature of the magnetic relaxation mechanisms is discussed from the aspect of composite mediums. Results indicate that even relatively small amounts of magnetite can have a considerable effect on both signal attenuation and wave propagation velocity and that the current range of mixing models are inadequate for the description of magnetically lossy mixtures. [C9204]

"Solving the full nonlinear inverse problem for GPR using a three step method"

In order to extract accurate quantitative information out of Ground Penetrating Radar (GPR) measurement data, one needs to solve a nonlinear inverse problem. In this paper we formulate such problem as a nonlinear least squares problem which is non convex. Solving a non-convex optimization problem requires a good initial estimation of the optimal solution. Therefore we use a three step method to solve the above non-convex problem. In a first step the qualitative solution of the linearized problem is estimated to obtain the detection and support of the subsurface scatterers. For this first step Synthetic Aperture Radar (SAR) is proposed. The second step consists out of a qualitative solution of the linearized problem to obtain a first guess for the material parameter values of the detected objects. The method proposed for this is Algebraic Reconstruction Technique (ART), which is an iterative method, starting from the initial value, given by the first step, and improving on this until an optimum is achieved. The final step then consists out of the solution of the nonlinear inverse problem using a variational method. [C9205]

"FirstArrival Traveltimes Inversion Based on Minimal Number of Parameters in shallow crosswell GPR Tomography"

Ground-penetrating radar is often used for the characterization of subsurface properties. In this paper, we present a cross-well tomographic inversion algorithm of first-arrival traveltimes which uses only a limited number of parameters. This methodology has been developed for media with significant contrast of electrical permittivity, for example for near-surface sedimentary media. The aim is to determine the distribution of the electromagnetic wave velocity between two wells. We consider that the media can be decomposed into several homogeneous layers, with horizontal or gently dipping interfaces. It is described by a vector of parameters which includes one velocity and one or two thicknesses per layer. This methodology allows to obtain a 1D velocity profile of the medium between the two wells. This inversion scheme was tested on synthetic data. The head waves which appear due to the velocity contrasts are taken account in the inversion. Our inversion methodology was also tested on real data and the obtained velocity models were compared to those obtained using surface acquisition data only. Our results show that the velocity profiles issued from cross-well and surface acquisition appear to be very similar. [C9206]

"Characterization of inhomogeneous cylinders from transient data"

In this paper we propose a non linear inversion approach, which is able to characterize a scattering system from the knowledge of the transient scattered field measured when only one electromagnetic source is used to illuminate the objects. Such a source radiates a double-frequency Gaussian incident pulse, that is a pulse shape whose spectrum assumes its maximum value around two different frequencies. The inversion problem is formulated in the frequency domain rather than directly in the time domain and an iterative method is exploited to retrieve the unknown permittivity and conductivity profiles. The proposed strategy works in the canonical two-dimensional scalar case and its reconstruction capabilities are tested against experimental data concerning inhomogeneous targets. [C9207]

"Subsurface localization of interfaces"

The localization of a slab embedded within a homogeneous half-space is dealt with. A multi-frequency plane wave incidence is assumed and the locations of the slab interfaces are represented as the support of "distributions". A linear model of the electromagnetic scattering is adopted and the inversion is regularized by means of the Singular Value Decomposition (SVD) tool. Numerical tests performed via SVD allow to analyze the

reconstruction capabilities of the reconstruction algorithm, i.e. the maximum depth of investigation and the resolution limits, which depend on the properties of the investigated medium and on the exploited work frequency band. Experimental results are shown. [C9208]

"A Full Waveform inversion Algorithm for Interpreting Crosshole Radar Data"

Ground-penetrating radar (GPR) is a useful tool for civil and environmental engineering fields because of its high resolving power and non-destructive measurements. This paper presents a method of full-waveform inversion of borehole GPR data for imaging permittivity structures. The inversion algorithm is based on a conjugate gradient search for the minimum of an error functional relating to the difference between measured and predicted data. A small model perturbation in the functional can be efficiently calculated by propagating the data error back into the model in reverse time and correlating the field generated by the back-propagation with the corresponding incident field at each point. A finite difference time domain (FDTD) method is used for solving Maxwell's equations to obtain incident electromagnetic wavefields. Back-propagated wavefields satisfy adjoint Maxwell's equations, which are stable in reverse time and can be solved by the same FDTD scheme. The imaging scheme is applied to crosshole radar configuration, thereby demonstrating its capability to reconstruct permittivity structures. Tests on a two-dimensional synthetic model produce good images of target scatterers and show stable convergence. [C9209]

"Electromagnetic scattering by buried cylinders"

A spectral-domain method, for the solution of the two-dimensional electromagnetic plane-wave scattering by a finite set of perfectly conducting or dielectric cylinders buried in a dielectric half-space, has been developed. The scattered field is represented in terms of a superposition of cylindrical waves, and use is made of the plane-wave spectrum to take into account the reflection and transmission of such waves by the interface. The problem is solved for both the near- and the far-field regions, for TM and TE polarizations. The validity of the approach is confirmed by comparisons with results available in the literature. The technique is applied to scatterers of arbitrary cross-section simulated by a suitable configuration of circular cylinders. Our method is employed to study the scattering from buried objects of a pulsed plane wave, that may have a rather general shape in the time domain, by performing a sampling of the incident-field spectrum, and solving the problem in the frequency domain. [C9210]

"Time-frequency domain signature analysis of GPR data for landmine identification"

In this paper, the problem of detecting buried antipersonnel (AP) landmines is tackled in the broader context of target identification: determining relevant features, extracted from impulse ground-penetrating radar (GPR) signals, which can be used to classify landmines. These features are extracted in the time-frequency domain using the Wigner-Ville distribution (WVD) and the wavelet transform (WT). Radar data are collected using the MINEHOUNDTM hand-held dual-sensor system over two types of soil and for different landmines and objects. The Wilk's lambda value is used as a criterion for optimal discrimination. Results show that time-frequency signatures from WVD contain more valuable information than the features extracted using WT. Therefore, they could improve landmine and false alarm classification and help to differentiate between two different landmines. [C9211]

"Constraining GPR data inversion using hydrodynamic laws for noninvasive soil hydraulic and electric property determination"

We constrain full-wave inversion of time-lapse radar data using hydrodynamic modeling to simultaneously identify the shallow subsurface hydraulic properties and continuous vertical electric profiles. Radar data are acquired in the frequency domain using a vector network analyzer combined with an off-ground monostatic antenna. This permits to accurately filter antenna effects and to derive Green functions from which the inversion is initiated. In order to demonstrate that enough information is contained in the radar data so as to ensure unique estimates, hydrodynamic events were simulated for three different textured soils, namely, coarse, medium, and fine. The corresponding time-lapse radar data were subsequently computed and inverted to find back key soil hydraulic parameters, i.e., Γ , B_i , n , and K_s in Mualem-van Genuchten's model. For the three scenarios considered, the three hydraulic parameters were exactly retrieved, and hence, the corresponding time-dependent electric profiles as well. Provided that the soil-specific relations between the soil water content and its electric properties and the hydrodynamic initial and boundary conditions are known, the proposed method appears to be promising for proximal mapping of the shallow subsurface hydraulic properties and monitoring of the water dynamics at the field scale. [C9212]

"Design and construction of a large test site to characterize the GPR response in the vadose zone"

In this work Ground Penetrating Radar (GPR) and Time Domain Reflectometry (TDR) measurements are carried out on a test-site. The test site consists of a pit filled with gravel and sand in which a pipe system for water inflow is buried. The data are collected under different water charge conditions and the water level is monitored by piezometers. TDR measurements are performed at various depths using a multilevel probe system. GPR measurements are performed by using the single-offset reflection method with a system equipped with 250 MHz and 500 MHz antennas. The results pertaining to the water table depth estimations, obtained by calibrating time GPR section with TDR velocity data, have shown a good agreement with the piezometric responses. [C9213]

"Evaluating GroundPenetrating Radar use for water infiltration monitoring"

Ground-Penetrating Radar (GPR) was used to monitor water infiltration in sand. Water was injected down an 81 cm long tubed hole with a piezometer recording the depth of water and a tap valve used to adjust it to 15 cm $\Gamma_B \pm 2$ cm above the bottom of the tube. During the 20 minutes of infiltration two GPR antennas (transmitter and receiver) were recording a trace every second from an offset position on the surface. The signal, enhanced by differential correction allows to trace the evolution of top and bottom limits of the water bulb in space and time. Comparison with hydrodynamic model of the infiltration process proves that the GPR reflections trace the wetting front and not the saturation bulb. An exact, quantified estimation of the evolution of the top border of the wetting zone is provided. For the bottom border, further work on the estimation of the velocity of radar wave in the infiltration bulb will be needed. [C9214]

"Determination of soil permittivity from GPR data and a microwave tomography approach: a preliminary study"

In this paper we present a new strategy to retrieve the dielectric permittivity of the soil starting from B-Scan GPR data, gathered on a pipe buried on purpose and processed by means of a microwave tomography algorithm. The validation will be performed by making use of synthetic data, obtained from an FDTD code. The results of the proposed approach shall be compared with those achieved from the hyperbolas of the radar traces and from the Hough Transform based approach. [C9215]

"An Investigation into the Implementation of ADI-FDTD Subgrids in FDTD GPR Modeling"

The implementation of subgrids in the traditional finite-difference time-domain (FDTD) method is often required, especially when structures of fine geometry need to be modeled. Since the FDTD method is conditionally stable, different time-steps should be employed in the main grid and in the subgrid. To overcome the requirement for time interpolation at the boundary between the two grids, an unconditionally stable method, the alternating-direction-implicit (ADI-FDTD) method, has been used in the subgrid. As a result both the main FDTD grid and the subgrid use the same time-step. This paper presents an investigation into the performance of an ADI-FDTD subgrid when it is implemented into the conventional FDTD method. [C9216]

"Advanced forward modeling and tomographic inversion for leaking water pipes monitoring"

The timely detection of damage and leakage from pipelines is of extreme importance both environmentally and from a economic perspective. Accordingly, we address the problem of imaging leaking pipes by exploiting single-fold, multi-receiver GPR data. In particular, we devise a tomographic imaging method which, taking advantage of the available knowledge on the investigated 'scenario' (pipe position and size), allows us to detect the presence of a leakage already in its first stages of development. In order to properly design the features of the imaging approach, and test its capabilities in controlled conditions, we make use of synthetic data generated with an advanced full-wave 2.5D Finite-Difference Time-Domain forward modeling solver capable of accurately simulating real world GPR scenarios. Numerical examples obtained in this way show the effectiveness of the developed imaging method. [C9217]

"Estimation of Electromagnetic of Libyan soil Properties by Stepped Frequency Radar"

A vector network analyzer was used to measure the electromagnetic properties of two types of Libyan soil. The vector network analyzer was used to act as a stepped frequency ground probing radar. The frequency that was covered is from 1 to 3 GHz. A TEM horn antenna was used for transmission and reception. From the experiments the attenuation and time delay was measured. Then conductivity, permittivity and moisture content were estimated from the measurements. The samples were taken before and after it rained by a week following a long dry season. The experiments gave a reasonable estimation of the parameters and showed that clay retained its moisture for a longer period that sandy soil. [C9218]

"Localization of thin metallic scatterers by experimental data"

The problem of detecting and localizing "small" scatterers by the knowledge of the field scattered under a known illumination is dealt with. According to the distributional model shown in Ref. [2], the problem is cast as the inversion of a linear integral operator acting on 6-distributions whose supports are representative of the scatterers' locations. In this paper, we present some experimental results of such an approach. To this end, we perform the reconstructions by exploiting experimental scattered field data collected in controlled conditions at the Electromagnetic Diagnostic Laboratory of the Second University of Naples. The multi-static/single-view/multi-frequency and the multi-static/multi-view/multi-frequency configurations are both considered. [C9219]

"Localization of small PEG spheres by multiview/single-frequency data: numerical results"

In this paper the problem of determining the number and the locations of "small" PEC spheres from the knowledge of the scattered far-field is addressed. A multi-view/single-frequency configuration is considered. The multiple scattering between the spheres is neglected and their locations are represented as the supports of Γ, \tilde{B} -functions. This allows to cast the problem as the inversion of a linear integral operator with the Γ, \tilde{B} -functions being the unknowns of the problem. The inversion of the linear integral operator is achieved by means of the Truncated-Singular Value Decomposition (TSVD). The performances of the linear inversion algorithm against the model errors (i.e. for situations where the multiple scattering is not negligible) and the presence of an Additive White Gaussian Noise (AWGN) are investigated by numerical simulations. [C9220]

"Experimental Verification of LOZA-V GPR Penetration Depth and Signal Quality"

Experimental GPR survey data obtained in Yingshan and Tianmo parks (Beijing) are presented. The purpose was to estimate actual penetration depth and signal quality of LOZA-V GPR in generic Chinese soil conditions. This subsurface monopulse radar, using spark discharge transmitter and resistively loaded dipole antennas, reliably detects underground objects at 14-20 m depths without sophisticated signal processing. [C9221]

"Metal-sheet test to estimate shape and frequency content of the radar pulse"

Appropriate GPR data processing and inversion require a reliable estimation of the radar pulse. In particular the knowledge of the shape and frequency content of the wavelet sent into the ground is an important issue not only for processing an interpreting reflection profiles, but also for GPR tomography, especially for amplitude tomography. Common practice considers the nominal antenna frequency as a measure of the bandwidth of the radar wavelet in the air, which in turn is assumed to be equal to the peak (dominant) frequency. Raising the antenna above a totally-reflecting metallic slab is the simplest way to gain information on the shape of the radar pulse in the air. This is the experimental calibration method generally used for correcting zero-time drift and to obtain a reference signal for amplitude analysis. This method was applied in this study to extract information on the frequency content of the emitted radar wave. Experimental errors related to ambient noise and positioning inaccuracies impose great care for a correct extraction of the needed attributes. The same test was also useful to gain insights into the influence of the filters applied in the acquisition stage. [C9222]

"Design of a GPR for deep investigations"

This paper describes the design steps in producing a GPR for deep, mainly geological and environmental investigations. A phase coded spread spectrum pulse is used with high power transmitters to an antenna array. The receiver has a real time data converter with a correlator giving 125dB dynamic range. Initial results are shown. [C9223]

"GPR Antenna Test Facility at IRCTR-IB"

This paper describes the GPR antenna test facility developed at the research branch of IRCTR at ITB Indonesia called IRCTR Indonesian Branch (IRCTR-IB). The facility consists of a GPR test range, a PC-controlled scanner, a UWB sensor, and measuring equipment. The test range was constructed as a wooden sandbox of 3 m Γ B—3 m Γ B—1.6 m and filled with dry sand with relative permittivity of 5.1. The scanner is used for accurate antenna positioning above the sand and fully controlled from a PC. A control software has been developed to allow automatic data acquisition and antenna positioning, important for measurements of antenna footprints. The measuring equipment consists of a vector network analyzer, a sampling converter and pulse generators to allow accurate measurements in frequency as well as time domain. [C9224]

"A prototype for the WISDOM GPR on the ExoMars mission"

This paper will describe a GPR prototype for the WISDOM-(Water Ice and Subsurface Deposit Observations on Mars) experiment on the ExoMars mission. The operation principle as well as the instrument design is explained. Simulations of the radar response to realistic geologic models of the Martian sub-surface are presented.

Measurements with a commercial GPR system in Mars analog geology on earth are shown. [C9225]

"MARSIS Data Inversion Approach"

In this paper we describe an inversion approach in order to analyze data from the MARSIS (Mars Advanced Radar for Subsurface and Ionosphere Sounding) instrument on Mars Express. The inversion process allows the dielectric constant of the subsurface material to be estimated provided the dielectric constant of the surface is known. In addition, if impurity are present, it is possible to estimate the dielectric constant of any inclusions as well as the percentage amount of material in the inclusions relative to the host material provided knowledge of the host material up to the depth where the interface has been detected is available. The data inversion method is based on the analysis of the surface to subsurface power ratio and the relative time delay as measured by MARSIS. The data inversion has been performed at several frequencies in order to estimate the frequency dependent parameters affecting the behavior of the radar echoes. It is necessary that the surface and subsurface interfaces have the same roughness in order to estimate the Subsurface Fresnel reflectivity. As a preliminary approach, only flat surface have been selected. MOLA (Mars Orbiter Laser Altimeter) has already provided detailed data on the visible Martian surface and a simulator, with a facet model, has been utilized to use MOLA data in order to verify the correct selection of the frames that will be used for the data inversion (absence of clutter echoes). [C9226]

"Calibration report of the SHARAD instrument"

The Mars Shallow Radar Sounder (SHARAD) is an HF (20 MHz) Sounding Radar embarked onboard the Mars Reconnaissance Orbiter (MRO) spacecraft. SHARAD on-ground calibration activities have been limited to the characterization of the SEB (SHARAD Electronic Box), not having been possible to perform extensive characterization of the flight antenna nor end-to-end calibrations on ground. Scope of the present document is to define the activities to be carried out in-flight in order to ensure SHARAD products calibration. The calibration needs are assessed and an overall calibration strategy is then defined, leading to the identification of the data sets to be collected and relevant processing to be applied. The document also address how to exploit the available calibration data (from both on-ground and in-flight calibration) to correct SHARAD products, and the organization of the calibration database. [C9227]

"Sounding Mars with SHARAD & MARSIS"

MARSIS (Mars Advanced Radar for Subsurface and Ionosphere Sounding) is a low frequency nadir looking sounding radar selected by ESA as a payload of the Mars Express mission, whose primary Scientific Objective is to map the distribution of water both solid and liquid, at global scale on the Martian crust. MARSIS is the first instrument to be able to detect what lies beneath the surface of Mars (up to about 5Km). The Mars Shallow Radar Sounder (SHARAD), a facility instrument provided by the Italian Space Agency (ASI), is embarked on board the NASA Mars Reconnaissance Orbiter spacecraft. SHARAD began science operations on October 3rd 2006: it has been collected data from surface and subsurface. This instrument penetrates to roughly half a kilometre below Mars' to search for information about underground layers of ice, rock and, perhaps, melted water. In this paper, some interesting comparisons between these sounders are proposed. Data confirm that MARSIS and SHARAD are complementary instruments. [C9228]

"Investigation of Convenient Antenna Designs for Ultra-Wide Band GPR Systems"

This paper proposes the planar and 3-dimensional ultra-wide band (UWB) antenna types suitable for hand-held and vehicle mounted impulse GPR systems. On this scope, bow-tie, spiral, TEM horn, dielectric-loaded Vivaldi, multi-sensor adaptive and array model antenna configurations are designed, simulated and measured. The numerical and experimental results are presented with performance comparisons. [C9229]

"Improved Bow-Tie Antenna for Pulse Radiation and Its Implementation in a GPR Survey"

In our previous works we developed an improved UWB bow-tie antenna for high-resolution GPR applications. The antenna has been designed to detect small shallow-buried objects for which it should be able to transmit short pulses with very small late-time ringing. It has been shown theoretically that in comparison with conventional bow-tie or dipole antennas, this antenna radiates significantly stronger pulses in its broadside direction with very small late-time ringing. In this paper, experimentally we compare the antenna with a resistively-loaded planar dipole which is commonly used for GPR. It has been found that the antenna exhibits superior characteristics in terms of significantly larger amplitude of the transmitted pulses and much smaller late-time ringing. Furthermore, the antenna has been implemented in a commercial GPR system and tested in real GPR surveys. In this paper we demonstrate that the implementation of this antenna results in clear B-scan images which allow one to easily observe the detail of the shallow subsurface. [C9230]

"Shape reconstruction of three dimensional buried objects from stepped frequency data"

In this communication the problem of reconstructing the shape of 3D buried targets from stepped frequency GPR data is addressed by exploiting an improved formulation of the Sampling Methods (SM). These latter are simply and efficient methods which may retrieve the geometrical features of dielectric or metallic targets from multiview, multistatic data measured at a fixed frequency. However, while accurate results may be achieved when full-aperture data are available, their effectiveness is quite unsatisfactory in case of aspect-limited data and lossy media, which is the usual case in GPR applications. In order to overcome this drawback, we propose a new formulation, which is able to improve the reconstruction of the deeper part of the investigated region and it is an original extension of the SM to the case of multi-frequency data. [C9231]

"Vertical and Horizontal Resolution of GPR bow-tie antennas"

Since the characteristics of the detected reflections depend on the issued signal properties, a key factor for carrying out a successful GPR survey is to know as much as possible about the transmission features of the antennas. This information is essential when deciding the antenna and which is the most appropriate parameter configuration setting for a specific study. These characteristics vary for the different available GPR equipments. Numerous experimental tests have been developed in this way. In this paper we present the first results of set of experiments about the resolution capabilities of two commercially bow-tie antennas (1GHz and 800 MHz). The propagation media was air in this first study and the experimental results are compared with the theoretical estimations. The obtained conclusions are the first step in order to establish the real bounds for the detection capability of these antennas. [C9232]

"A Clutter Canceller for Continuous Wave GPR"

In this work an innovative clutter canceller for Continuous Wave GPR (Ground Penetrating Radar) has been designed and implemented. An IQ modulator has been used to build up the central part of the device. The IQ modulator replaces more expensive components like digital controlled phase shifters and attenuators. This device also have wider dynamics with respect to linear vectorial modulator. To prove the feasibility of the system, the effect of signal feedthrough for IQ modulators is studied. Tests and measurements of the complete device are exposed. [C9233]

"The broadband device for nondestructive measurements of dielectric permeability of lossy media"

The opportunity of creation of the device and a corresponding method for measurement of complex dielectric permeability of solid, liquid, loose environments in ultra short wave and in microwave ranges without breaking of their structure is investigated. The given problem is actual in many areas, including geophysics, radio physics, underground radio sounding and the like. For nondestructive materials testing it is necessary to use only flat constructions of the measuring cell, for example, as unbalanced strip line (SL), slot line or coplanar waveguide. Use of shielded coplanar waveguide (SCPW) as a measuring cell of the complex dielectric permeability tester is base. Results of development of a broadband Instrument on basis SCPW for measuring an electrical parameters of lossy materials, methods of its calibration and testing are presented. [C9234]

"Analysis of a non Electrical Resistive GPR Antenna"

In order to avoid oscillations in a GPR antenna, logarithmic resistive patterns throughout the arms of the dipoles are used. This consumes the energy generated by the transmitter, but significantly reduces the efficiency of the antenna and of the radar. This work analyses the possible effects of eliminating resistors by simulating the delayed potentials from the electromagnetic equations. The antenna is modelled as a modified transmission line with open end. A new transmitter is required to avoid the generation of new pulse reflections from the antenna arms. With that, the efficiency of the radar would increase and the broadcast electromagnetic pulse would be more symmetrical. [C9235]

"Look-Ahead Radar and Horizon Sensing for Coal Cutting Drums"

Safe and efficient coal extraction requires advanced radar subsystems that can be mounted on cutting drums of coal mining machines. A look-ahead radar (LAR) must solve the radio geophysics problem of transmitting an electromagnetic (EM) wave through at least 6.1 m (20 ft) of coal to detect an air- or water-filled void. An up- or down-looking radar must determine the distance to the coal bed sedimentary rock boundary. The reflected EM wave from the void or boundary rock must be processed in real time in the radar electronics to determine the physical distance to the void or coal bed boundary. The distance determination requires the in situ measurement of the coal electrical conductivity or relative dielectric constant. Up or down (horizon) sensing enables selective

cutting near the undulating sedimentary rock boundaries of the coal bed to address coal quality and ground control issues. Both sensors require subsystems for dynamic electric power generation, real-time measurement of antenna rotation angle, detection of weak coal-boundary reflected EM waves concurrently with the suppression of the significant larger first air-coal reflected wave, processing to determine distance through coal, and RF modem transmission of measured data from the cutting drum to the body of the mining machine and along the segmented or coiled-tubing drill pipe. This paper describes the development of the GPR subsystems and field test results. [C9236]

"Hardware implementation of an SAD based stereo vision algorithm"

This paper presents the hardware implementation of a stereo vision core algorithm, that runs in real-time and is targeted at automotive applications. The algorithm is based on the sum of absolute differences (SAD) and computes the disparity map using 320 times 240 input images with a maximum disparity of 100 pixels. The hardware operates at a frequency of 65 MHz and achieves a frame rate of 425 fps by calculating the data highly parallel and pipelined. Thus an implemented and basically optimized software solution, running on an Intel Pentium 4 with 3 GHz clock frequency is 166 times outperformed. [C9237]

"Displaying LiDAR Data for Interactive Web-Based Modelling of the Environment"

The increasing commercial availability of highly accurate LiDAR scanning offers remote sensed data accurate enough for generalized and distant views of the environment. From this data, bare earth digital terrain models (DTMs) can be processed semi-automatically, then draped with aerial imagery. The paper describes an approach developed in the VEPs project that switches on the LiDAR data for trees and buildings removed from the DTM in the 3D Scene. This data can then be used to visually judge the appropriate height and form of buildings and trees. A set of web-based interactive tools have been developed to enable users to freely adjust the scale and mass of structures and vegetation to match the selected point cloud area, substantially improving the quality of presence and accuracy of the resulting model. Issues are raised in obtaining equally accurate data of what is proposed from Planners and Developers. [C9238]

"Towards Fog-Free In-Vehicle Vision Systems through Contrast Restoration"

In foggy weather, the contrast of images grabbed by in-vehicle cameras in the visible light range is drastically degraded, which makes the current applications very sensitive to weather conditions. An onboard vision system should take fog effects into account. The effects of fog varies across the scene and are exponential with respect to the depth of scene points. Because it is not possible in this context to compute the road scene structure beforehand contrary to fixed camera surveillance, a new scheme is proposed. Weather conditions are first estimated and then used to restore the contrast according to a scene structure which is inferred a priori and refined during the restoration process. Based on the aimed application, different algorithms with increasing complexities are proposed. Results are presented using sample road scenes under foggy weather and assessed by computing the contrast before and after restoration. [C9239]

"Real-time Planar Surface Segmentation in Disparity Space"

An iterative Segmentation-Estimation framework for segmentation of planar surfaces in the disparity space is implemented on a Digital Signal Processor (DSP). Disparity of a scene is modeled by approximating various surfaces in the scene to be planar. The surface labels are estimated during the segmentation phase of the framework with help of the underlying plane parameters. After segmentation, planar surfaces are separated into spatially continuous regions. The largest of these regions is used to compute the estimates for the plane parameters. The iterative process is continued till convergence. The algorithm was optimized and implemented on TMS320DM642 based embedded system that operates at 3 to 5 frames per second on images of size 320 x 240. [C9240]

"Voice over Internet Protocol on Mobile Devices"

Voice over internet protocol (VoIP) is a way to carry out a telephone conversation over a data network. VoIP products promise converged telecommunications and data services that are cheaper, more versatile and provide good voice quality as compared to traditional offerings. Although VoIP is widely used, VoIP on mobile devices is still in its infancy. Currently, there are a number of VoIP solutions for mobile phones. However, VoIP solutions developed using Java 2 platform micro edition(J2ME) are not available. Java based solutions are widely compatible with many devices. In this paper, strong focus has been granted to cross-device compatibility through the use of the widely supported J2ME framework. The implementation details of VoIP client using J2ME are illustrated. [C9241]

"Opinion"

{no data available} [C9242]

"A Fast Flow Control and Approach Queuing Monitor using FDP in Excel Environment"

Flow control monitor is relating to huge amount of flight data processor (FDP) and radar data processor (RDP) message to any en-route center. Under current high flow density situations, most major airports have encountered flow control problem. Approach queuing based on the estimated time of arrival (ETA) from FDP and revised by RDP on the metering fixes in the terminal control area (TCA) of a major airport may be constructed. This paper presents a simple method to reconstruct FDP message onto excel program to queue the approach flight to the destination airport. The queuing process reads all daily scheduled flights from flight plans at a major airport, and settles an initial queuing chart. The flow control software will check the necessary separation and constraints to allocate arrivals and departures in a maximum accepting rate. Once flow congestion in certain time slot may occur, the queuing monitor will send alert signals to the air traffic control (ATC) to determine appropriate separation solutions. To demonstrate the proposed method, Taiwan domestic flow control monitor on Taipei Sung Shan Airport (TSA) is tested using historical data for simulation. In Taiwan, typical short flights are operated that FDP data may be adopted for flight observation. This paper proposes a simple sequencing and rescheduling method to extend the flow control surveillance range as long as 60 minutes. Standard ATC separation rules and queuing rules are applied. The excel software can refresh any FDP change with 2 seconds. The simulation results appear feasible for flow control and observation for approach flights. In the future, the ADS-B data can be used to update the approach flight data for better performance. [C9243]

"Wireless Telemedicine Physiological Monitoring Center Based on Virtual Instruments"

This paper presents a new model of wireless telemedicine physiological monitoring center, which is developed by the Laboratory Virtual Instrument Engineering Workbench (LabVIEW) and integrates current general packet radio service (GPRS) technology and signal processing with DSP processor. At the patient's location, a wireless PDA-based monitor is used to continuously acquire the patient's vital signs, including heart rate, ECG, SpO₂ and so on. Through the internet, the patient's physiological signals can be transmitted in real-time to a telemedicine monitoring central management unit, and the unit can access the data and the case history of the patient, either by the central management unit or the wireless devices. This paper presents our prototype implementation of signal processing based on a high-performance DSP-based personal server. The results also show that the wireless telemedicine physiological monitoring center model is superior to the currently used monitors both in mobility and in usability, and, therefore, is better suited to patient transport. [C9244]

"A Novel Algorithm for Estimating Vehicle Speed from Two Consecutive Images"

In this paper, we present a new algorithm for estimating individual vehicle speed based on two consecutive images captured from a traffic safety camera system. Its principles are first, both images are transformed from the image plane to the 3D world coordinates based on the calibrated camera parameters. Second, the difference of the two transformed images is calculated, resulting in the background being eliminated and vehicles in the two images are mapped onto one image. Finally, a block feature of the vehicle closest to the ground is matched to estimate vehicle travel distance and speed. Experimental results show that the proposed method exhibits good and consistent performance. When compared with speed measurements obtained from speed radar, averaged estimation errors are 3.27% and 8.51% for day-time and night-time test examples respectively, which are better than other previously published results. The proposed algorithm can be easily extended to work on image sequences [C9245]

"Comparison of Shunt and Series/Shunt nMOS Single-Pole Double-Throw Switches for X-Band Phased Array T/R Modules"

This paper compares the performance of shunt and series/shunt single-pole double-throw nMOS switches designed in a 0.13 μm SiGe BiCMOS process for X-band phased array transmit/receive modules. From 8.5 to 10.5 GHz, the worst case return loss, insertion loss, and isolation are 14.5, 1.89, and 20.5 dB, respectively, for the reflective shunt switch, and 22.2, 2.33, and 22.5 dB, respectively, for the absorptive series/shunt switch. Both switches exhibit an IIP₃ of about 28 dBm and dissipate no dc power. The performance of these switches are comparable to other CMOS switches found in triple well technologies, on non-standard substrates, using special device structures, or using extra dc biases [C9246]

"4G Self-Configurable System Based on Neural Networks"

This work present the study on two types of neuronal networks for a fourth generation (4G) self-configurable

wireless communications system. Simulations were made in MATLAB to study the behavior of two types of neuronal networks, back propagation network (BPN) and radial basis function (RBF) trained to discriminate signals taken from three systems of wireless communication of second (2G) and third generation (3G). When the results are observed it seems that designed network BPN, generates a smaller error of recognition in addition of which it contains a smaller number of neurons than network RBF, this reduces the system time response in addition of which it allows a saving in the memory use [C9247]

"Vector field characterization in ERS-1 imagery of sea ice"

The nonrigid motion of sea ice is an essential component when describing global climatology models. With the availability of sequential ERS-1 satellite imagery, we estimate high resolution motion and describe the differential characteristics of motion. This characterization is subsequently used to locate critical points, also known as coherent structures, in the flow, thereby reducing the large vector field into a collection of important feature points which essentially describe the flow pattern. In this paper, we build on previous work in an attempt to enhance the characterization of the flow field via visualization and quantification of these coherent structures. We show that the statistical quantification of these structures can provide a greater clarity in our understanding of the physical dynamics taking place within the sea ice [C9248]

"SiGe Circuits for Automotive Radar"

This paper presents circuits in SiGe bipolar technology for automotive radar applications at 77 GHz. They cover the transmit and receive path of typical radar sensors and include a voltage-controlled oscillator with integrated power amplifier and frequency divider, an active mixer and a low-noise amplifier [C9249]

"An X-band Transmission Line Based CMOS VCO with FM Modulation"

An X-band voltage-controlled oscillator (VCO with frequency modulation (FM) capability is realized in a 0.18μm 1P6M CMOS technology. The characteristics of the VCO modulated by a 100KHz triangular waveform are presented and investigated. The passive components of the VCO are implemented by two-dimensional (2-D) complementary-conducting strip transmission lines (CCS TLs), varactors and metal-oxide-metal (MOM) capacitors for substrate coupling consideration. The measured VCO with free running phase noise of -83.2 dBc/Hz at 100KHz offset from the carrier. The compact VCO chip size is 330 times 450μm² excluding pads. Furthermore, the modulation bandwidth is up to 400MHz of the proposed VCO with direct FM modulation which could improve range resolution in a radar system [C9250]

"16-26GHz Low Noise Amplifier for short-range automotive radar in a production SiGe:C technology"

Short-range radar is a technology that potentially can help to enhance road safety. Recently, in the USA as well as in Europe, frequency bands around 24GHz have been opened up for automotive radar applications. This paper describes a low noise amplifier (LNA) in a production 0.25μm SiGe:C BiCMOS IC technology. The input and output impedances are matched to 50Ω (single-ended). The LNA has 11dB gain and 4.2dB noise figure at 24GHz and has excellent performance for frequencies between 16-26GHz. The 0.45times0.55mm² IC dissipates 20mW from a 3.3V supply [C9251]

"A Low-Power Micromixer with High Linearity for Automotive Radar at 77 GHz in Silicon-Germanium Bipolar Technology"

A direct-conversion micromixer realized in a modern SiGe:C bipolar technology for application in automotive radar systems at 77 GHz is presented. The mixer exhibits a minimum conversion gain of 15 dB and a maximum noise figure of 16.5 dB over a frequency range from 75 GHz to 85 GHz. The 1dB input related compression point is at -3dBm and the RF and LO matching is better than -20 dB and -10 dB, respectively. The total DC current consumption is 34 mA at 5.5 V [C9252]

"Development of the Hand held dual sensor ALIS and its evaluation"

GPR has been thought a useful sensor for detection of buried land mines, but no GPR has been practically deployed in humanitarian demining. Since 2002, we have developed a new hand-held land mine detection dual-sensor ALIS. ALIS is equipped with a metal detector and a GPR, and it has a sensor tracking system, which can record the GPR and Metal detector signal with its location. It makes possible to process the data afterwards, including migration. The migration processing drastically increases the quality of the image of the buried objects. ALIS uses two different GPR systems, namely VNA (Vector Network Analyzer) based GPR and an Impulse GPR. VNA based GPR can provide better quality GPR images, although the impulse GPR is faster and light weight.

ALIS evaluation tests have been held in mine affected countries including Afghanistan, Croatia, Egypt and Cambodia. In the two-month evaluation test in Cambodia, ALIS worked without any problem. After some demonstrations and evaluation, we got many useful suggestions. Using these advises, we have modified the ALIS and it is now more easy to use. ALIS will be commercialized in 2007. [C9253]

"Multi-frequency ground-penetrating radar method for revealing complex sedimentary facies"

We attempted to resolve deltaic facies in Taylor Valley, Antarctica by using pulses centered near 120, 300 and 880 MHz, the latter of which has not yet been tried in this setting. The 120 MHz profiles clearly defined gross material changes, while the 300 MHz profiles added significant resolution to the topset, foreset and bottomset beds. The additional, higher frequency provided only about 2.5 m penetration however, the 10-15 cm pulse length revealed and defined multiple, fine-scale features that were not observed with the lower frequencies. The dip of these features is, in some instances, opposite to that of larger features profiled with the lower frequencies. Profiling with 880 MHz not only confirmed the greater complexity of the sedimentary architecture, but also allowed more robust interpretation of depositional processes. Generally, we recommend pulses centered near 300-400 MHz for detailed sedimentary profiling to about 6m depth. [C9254]

"Applications of GPR to archaeology and geology: the example of the regio III in Pompeii (Naples, Italy)"

GPR investigations has been collected in Pompeii, in an area of the regio III not yet fully excavated. In this area, as in many other parts of this roman city, large portions of archaeological features are still buried under thick volcanic deposits. The radar survey has been conducted on the top of a long scarp parallel to Nola Street. This site was chosen because some remains are well visible on the front of the scarp, so they can be use to calibrate the radar sections. The results allowed us to reconstruct the subsurface structure of the area, and to locate the main roman ruins buried in the volcanic deposits. Moreover, the analyses of the radar sections highlighted the geometry of the volcanic deposits overlain the roman ruins, and made possible the correlation between the shallow geological stratigraphy and the reflectors sequence shown in the radargrams. [C9255]

"Inversion of dispersive APVO GPR curves: a thin-layer approach for fracture characterization on a vertical cliff"

Reliability of stability assessment of prone to fall rock masses suffers from the lack of information about the geometry and the properties of the fracture networks. GPR profiles associated to Common Mid-Point (CMP) data, all recorded on the cliff wall, recently proved their efficiency to image correctly the extension of fractures with a satisfying resolution. However, besides velocity, CMP data also contain information generally not used, i.e. Amplitude and Phase variations of the reflectivity for a given reflector as function of Offset (APVO) and frequency. In this study, we analyzed the potential of these curves in the context of thin layers, where multiple reflections generate interferences and complex patterns. We notably present an inversion of real APVO curves derived from a CMP profile acquired directly on a limestone cliff wall. The reflected wave was primary deconvoluted in order to correct wave propagation effects and to evaluate radiation patterns. In a second step, APVO curves were inverted considering a neighborhood algorithm. This procedure permitted to obtain the Jonscher parameters describing the complex permittivity of the thin-layer and of the limestone formation, as well as the aperture and depth of the studied fracture. [C9256]

"Ground penetrating radar imaging of a 4th Century Roman Fort, Humayma, Jordan"

A suite of geophysical surveys were conducted on and around the site of a 4th Century Roman fort in Southern Jordan from 2002-2005 as part of the Humayma Excavation Project. Presented here are the results of the ground penetrating radar (GPR) data. Data were collected in a series of 1-m-spaced profiles within the 150m by 200m Fort and collated to generate 3D volumes. These GPR data volumes are sliced horizontally at optimized depths to yield map-view images of buried structures that have been and will be used to guide future excavation and develop usage plans. Data yielded good detail of interior structures (walls and potential tiled floors) and exterior features (defensive ditches, claviculae, the Via Nova). Ongoing excavations will provide additional information as to the specific nature of the observed features. [C9257]

"Geophysical investigations in the Castle of Crotona (Calabria Region, Italy)"

This work is about geophysical investigations carried out in the Carlo V king's castle, in Crotona village (Calabria Region, Italy). A magnetic method (M), ground penetrating radar (GPR) and electrical resistivity tomography (ERT) surveys have been used to locate buried remains and old walkway. Each interesting area was investigated with a map survey, which is obtained acquired along several parallel profiles. Therefore, a 2D

magnetic maps and a 3D GPR and resistivity data have been obtained. Finally, the ERT and GPR results showed some features associated to buried military walkway. [C9258]

"Incorporating near-surface layering in GPR data inversion for improved surface water content estimates"

We analyze the retrieval of soil surface dielectric permittivity in presence of shallow dielectric contrasts using full-wave inversion of off-ground monostatic ground-penetrating radar (GPR) data. Shallow soil layers affect the surface reflection and lead to constructive or destructive interferences which result, respectively, in overestimated and underestimated surface dielectric permittivity values. Synthetic GPR Green's functions were generated for a series of model configurations with different contrasts and different layer thicknesses. Green's function inversions were then performed to retrieve the initial parameters and analyze the sensitivity of the different parameters in the inverse problem. Two global optimization algorithms were used and compared, namely, a genetic algorithm and the multilevel coordinate search. The results showed that, depending on the contrast and layer thickness, it is not always possible to identify the original soil model. This depends in particular on the width of the frequency range. Both algorithms led to comparable results and did not converge properly in all cases, given their standard parameterization. Yet, the proposed method appears to be promising to improve real-time mapping of surface water content using off-ground GPR and full-wave inversion. [C9259]

"Low Frequency GPR in Difficult Terrain"

Many subsurface investigations are requested in areas unsuitable for most geophysical methods. In some instances, difficult terrain prevents surface coupling with transmitters, receivers, or other instrumental components. In other instances, such as in urban areas, spatial restrictions prohibit the use of seismic methods. Ground penetrating radar (GPR) is one method that can be used to attempt data collection in these difficult areas. In this paper, we will demonstrate the application of low frequency GPR to map a sloping bedrock surface configuration in an urban setting with the aforementioned site limitations. The sloping bedrock surface with a relief of approximately 21.5 meters underlies a stabilized slide area resulting from a failed retaining wall. 40-MHz and 100-MHz antenna systems were employed on boulder rip-rap (used to stabilize the slide area) and within an apartment house complex. Seismic refraction and surface wave investigations were performed to help constrain the GPR data interpretation and to provide bedrock integrity information. [C9260]

"Masonry investigation through Very Large Bandwidth CW-SF radar"

In this paper, a number of experimental tests aimed to evaluate the potential of Very Large Bandwidth Continuous Wave Step Frequency (CW-SF) radar for investigating masonry structures, are reported. Furthermore, an innovative polarimetric technique able to detect the double-bounce signal due to corner inside a masonry is proposed and tested. [C9261]

"Directional Borehole Radar Calibration"

We are developing an innovative low noise borehole radar system that is designed for a single borehole providing 3D imaging capabilities. Harsh and changing operating environments are challenges to the electronic design. Low noise systems are particularly sensitive to operating conditions. After a brief introduction, testing and calibration methods are introduced. Included are new measurement results and figures depicting the practical results achieved so far. [C9262]

"Analysis of Dipole Antenna Eccentered in a Borehole for Borehole Radar"

In this paper, we analyze response of borehole radar that use an electrically small dipole antenna in an eccentric borehole. Our approach is an extended version of the pseudoanalytic formulation, which was previously applied for analysis of an induction logging tool. In order to verify the calculation method, we did two experiments. The first one is measurement of monopole antenna response inside an eccentric air cylindrical layer in another water cylindrical layer on a ground plane, when a wave is incident on the antenna. The second experiment is crosshole measurement in a field test site. We controlled position of a dipole antenna in a borehole, and made it eccentered in a water-filled borehole. In both experiments, we compared the calculated data and the experimental one, and we will show the validity of the developed pseudoanalytic formulation. [C9263]

"General representations of electromagnetic interferometry"

The theoretical and experimental developments in interferometry have advanced spectacularly over the last five years and are still expanding at a rapid pace. With interferometry we mean the retrieval of the Green's function by cross-correlating or cross-convolving two (wave) field recordings. Over the last year several contributions

have included interferometric representations for media with losses, in absence of wave phenomena, like in thermal and electromagnetic diffusion or viscous flow, and for moving media. In this paper we use the reciprocity theorems of the time-correlation and time-convolution types to formulate general representations for electromagnetic fields and waves, and give explicit expressions for different possible GPR applications involving controlled or uncontrolled sources, which can be transient or noise sources. [C9264]

"Array-Based GPR for Shallow Subsurface Imaging"

Recently we have reported development of an UWB array-based time-domain Ground Penetrating Radar for landmine detection. The radar is designed to be used within a vehicle-mounted multi-sensor system for humanitarian demining and produces 3D images of subsurface by ID mechanical scanning. In this paper, we demonstrate imaging capabilities of the developed system. The imaging capability of the radar is realized via electronic steering of the receive antenna footprint in cross-scan direction and synthetic aperture processing in along-scan direction. Imaging via footprint steering allows for drastic increase of the scanning speed. [C9265]

"Influence of Mode Conversion at Borehole on Direction Finding with Dipole Array Antenna"

We investigate influence on DOA estimation with the circular dipole array antenna in a borehole (CAB), when the TE plane wave incident on the CAB. According to calculation of electromagnetic fields of the TE plane wave, vertical component of the electric field is excited by the cylindrical layers around the antenna, and these phenomena are called mode conversion in this paper. This increases error of DOA estimation, if we assume that the TM wave is incident on the CAB like in [4] during the array signal processing. We introduce the index $\Gamma_{Bi}(t)$ in order to represent quantity of component excited by the mode conversion. According to the experiment in air and field experiments, we confirmed that the mode conversion occurs, and this would influence DOA estimation with the CAB. [C9266]

"Using GPR to Monitor Cracks in a Historical Building"

The paper treats the application of GPR to detect and monitor cracks induced on a historical building by a landslide. The data were acquired on a floor inside the building with profiles 10 cm apart recorded at three different times. A 2GHz bipolar antenna was used, which allows the acquisition of multi-component data. The data were processed to produce vertical profiles and a 3D cube for each component and survey. The interpretation of the profiles is in good correlation with the structure of the floor. The profiles and time slices have detected two different kinds of anomalies, only a few of which can be due to utilities and the metallic mesh. The others were associated with cracks induced by the landslide. The time slice obtained from the last survey shows anomalies not detected before. [C9267]

"Principle of a direction sensitive borehole antenna with advanced technology and data examples"

Underground, in mines it is important to get spatial information about the geology on limited profiles. In low conductive material, like salt, ground penetrating radar (GPR) is a valuable method to find structures in the environment. For radar measurements in boreholes a direction sensitive antenna can solve the problem of getting spatial information. A new development of a direction sensitive antenna with an advanced technology to calculate the direction increases the resolution of this method. The idea of this technique will be illustrated and examples of measurements are shown. [C9268]

"Analysis of Directional Borehole Radar Measurement Data"

We developed a new directional borehole radar system with an array of optical electric field sensors as receivers. The system was tested in a field test site in order to assert its ability to detect three dimensional (3D) location of a subsurface tunnel. In this paper, the result is shown with a comparison to a result obtained by RAMAC directional borehole radar system. It is found that the optical electric field sensors are able to obtain highly coherent signals, that is necessary for the accurate estimation of a target azimuth direction, over the RAMAC system. The mutual coupling effect that deteriorates the coherence is also discussed. The azimuth estimation of the subsurface tunnel, which is located 5.5m apart from the tunnel, showed good agreement with the actual direction to an error of within 10 degree. [C9269]

"SHARAD radar signal processing technique"

SHARAD (SHallow RADar) is the sub-surface sounding radar provided by the Italian Space Agency (ASI) as a facility instrument to NASA's 2005 Mars Reconnaissance Orbiter (MRO). SHARAD has been launched on August '05 and has started its nominal observation phase since November '06. Primary objective of its investigation is to map, in selected regions, dielectric interfaces to depths of up to one kilometer in the Martian subsurface and to

interpret these interfaces in terms of the occurrence and distribution of expected materials, including rock, regolith, water, and ice. SHARAD which is a wideband low-frequency nadir-looking pulse limited radar sounder is expected to map Mars surface with a theoretical range resolution of 15 m in free space propagation, an along-track horizontal resolution of 300-1000 m and an across-track horizontal resolution of 1500-8000 m, depending on spacecraft altitude and terrain roughness. These performances can be reached by means of a focused synthetic aperture processing. The processing chain has been specifically designed and developed by CORISTA within SHARAD Ground Data System development activities with the aim of generating Level 1B products. This paper will be focused on of Level 1B SHARAD data processing description. Some results will be presented using SHARAD first data. [C9270]

"Complex Wishart Distribution Based Analysis of Polarimetric Synthetic Aperture Radar Data"

Multi-look, polarimetric synthetic aperture radar (SAR) data are often worked with in the so-called covariance matrix representation. For each pixel this representation gives a 3 times 3 Hermitian, positive definite matrix which follows a complex Wishart distribution. Based on this distribution a test statistic for equality of two such matrices and an associated asymptotic probability for obtaining a smaller value of the test statistic are given and applied to change detection, edge detection and segmentation in polarimetric SAR data. In a case study EMISAR L-band data from 17 April 1998 and 20 May 1998 covering agricultural fields near Foulum, Denmark, are used. Soon the Japanese ALOS, the German TerraSAR-X and the Canadian RADARSAT-2 will acquire space-borne, polarimetric data making analysis based on these methods important. [C9271]

"Derivation of Soil Surface Roughness Dynamics from Multi-temporal and Multi-parametric Air-borne PolSAR-data"

The dynamics of soil surface roughness is important to a number of land surface processes. The potential of multi-temporal and multi-parametric PolSAR-data for soil surface roughness estimation is investigated to determine its temporal development. The study is based on weekly quadpol L-Band E-SAR backscatter data, which was collected over the agri-phenological cycle in the course of the AgriSAR 2006 campaign. For ground truthing, the soil surface roughness was measured using photogrammetric imaging techniques. Two ground truth roughness indices (rms-height s , tortuosity index TB) and three polarimetric roughness estimators (anisotropy A , circular polarization coherence γ_{RRLL} and the real part of the circular polarization coherence $Re[R_{RLL}]$) were compared. While most of the comparison outlined weak correlations, best and sufficient results were obtained between s and $Re[R_{RLL}]$. Multi-temporal roughness maps were derived from this relationship, which are further affected by the presence and development of particular plants. [C9272]

"Performance Estimation of Similarity Measures of Multi-Sensor Images for Change Detection Applications"

Change detection of remotely sensed images is a particularly challenging task when the available data come from different sensors. Indeed, many change indicators are based on radiometry measures, operating on them differences or ratios, that are no longer reliable when the data have been acquired by different instruments. For this reason, it is interesting to study the performance of those indicators that do not rely completely on radiometric values. A series of similarity measures for automatic change detection was investigated and their performance compared using optical and SAR images covering a period of several years. We could observe that the considered change detection algorithms perform differently but that none of them permits an "absolute" measure of the changes independent of the sensor. [C9273]

"Dynamical Analysis of Hydrological Indexes Extracted from Remote Sensing Imagery: An Introductory Study"

A new intelligent computational paradigm based on filtering techniques modified to enhance the quality of reconstruction of the physical characteristics of environmental electronic maps extracted from the large scale remote sensing imagery is proposed. First, the problem-oriented modification of the previously proposed fused Bayesian-regularization enhanced radar imaging method is performed to enable it to reconstruct remote sensing signatures of interest. Second, the extraction of the so-called hydrological electronic maps and the analysis of its dynamics are proposed. Finally, simulation results of hydrological remote sensing signatures reconstruction from enhanced real-world environmental images are reported to verify the efficiency of the proposed approach. [C9274]

"Cross-band Inverse Synthetic Aperture Radar (ISAR) Image Fusion"

Research on image fusion is making rapid progress recently, because multiple looks of the same target from

different aspects will increase the available knowledge and allow more useful target information to be extracted. Studying on the physical principle of constructing radar images, especially inverse synthetic aperture radar (ISAR) images, make the fusion from multiple individual images generated by radars at multiple locations becomes possible. However, it is a challenge for image fusion if the source images are of different geometric resolutions, which are determined by radar system parameters, for example, the bandwidth of transmitted signals. This paper analyzes the influences caused by the different image resolutions, modifies the data fusion method proposed by previous research, and applies the modified method to an actually measured database. The performance of the modified image fusion algorithm is evaluated by the image attribute rating (iar) curves. The results show that the data collected by radars working at X-band and Ka-band can be fused successfully, and the information contained in the signals at these two frequency bands are complementary to each other. Therefore, the fusion improves target feature detection and thereby enhances target recognition. [C9275]

"Hilbert-Huang Transform (HHT) Analysis of Human Activities Using Through-Wall Noise Radar"

Various parts of the human body have different movements when a person is performing different physical activities. There is a need to remotely detect human heartbeat and breathing for applications involving anti-terrorism and search-and-rescue. Ultrawideband noise radar systems are attractive because they are covert and immune from interference. The conventional time-frequency analyses of human activity are not generally applicable to nonlinear and nonstationary signals. If one can decompose the noisy baseband reflected signal and extract only the human-induced Doppler from it, the identification of various human activities becomes easier. We propose a nonstationary model to describe human motion and apply the Hilbert-Huang transform (HHT), which is adaptive to nonlinear and nonstationary signals, in order to analyze frequency characteristics of the baseband signal. When used with noise-like radar data, it is useful covertly identify specific human movement. [C9276]

"Super-resolution Processing of SAR Images by Match Pursuit Method Based on Fourier Dictionary"

In this paper, we extend the application of the March Pursuit method to SAR super-resolution processing. Firstly, based on the SAR attributed scattering model, a Fourier dictionary with fast implicit algorithm is constructed in phase history domain. Secondly, with given dictionary the representation coefficient is got by Orthogonal March Pursuit algorithm. Thirdly, in light of the fast implicit algorithm of Fourier dictionary, By IFFT to the coefficient, larger scale phase history data is built. Finally, By IFFT to the larger scale phase history data, higher resolution image is obtained. Simulation experiments and computational results of measured MSTAR data demonstrate that March Pursuit based on Fourier dictionary can be implemented speedy and stably, it can provide super-resolution at the same time. [C9277]

"Sub-wavelength Microwave Radar Imaging for Detection of Breast Cancer Tumors"

This paper presents a novel approach to the detection of tumors of size well below a centimeter using a sub-wavelength ultrawide band (UWB) microwave radar imaging technique. Our approach exploits the principle of phase-shifting mask (PSM) and is implemented using a time-reversal (TR) algorithm based on the transmission-line matrix (TLM) method. A 0.5-mm diameter tumor was detected and located using a 200-ps UWB pulse in a realistic inhomogeneous two dimensional breast model. The breast model was derived from magnetic resonance imaging data and simulated using the TLM method. [C9278]

"Cross-Polarization Radar Integrated Debugging Platform"

For debugging cross-polarization radar and testing polarization algorithms, new cross-polarization radar integrated debugging platform is proposed in this paper. The polarimetric signal processing are developed with rapid speed nowadays, but cost of polarimetric radar is so expensive that most programs and algorithms can't be tested by real radar usually. Last but not least, most radar experiments are one-off, but these are not enough for research. For resolve these problems, a kind of multifunctional integrated device is required. In the paper, the cross-polarization radar integrated debugging platform is designed in detail. Firstly, the index of integrated debugging platform is given; secondly, the debugging platform is divided into 3 modules to be analyzed; thirdly, the key techniques are analyzed; finally, the performance of platform is tested. [C9279]

"Multi-Frequency Antenna design for Space-based Reconfigurable Satellite Sensor Node"

The paper investigates the antenna design to be applied in the ESPACENET sensor node. The project involves a network of autonomous pico satellites working at a large number of communication standards and as passive radar sensors for earth observation. They would form the next generation of "eyes in the skies "; looking out for natural disasters, helping in the survey and effective utilization of natural resources and also form a seamless

network of global communication which will have the potential to evolve itself with the growing demands of tomorrow's world. We discuss the need for a multiple frequency broadband antenna which would help cover a larger range of microwave frequencies enabling the antenna to work as both a communications antenna and a sensor device. [C9280]

"Road Border Recognition Using FIR Images and LIDAR Signal Processing"

This paper addresses the detection and tracking of road borders in non cooperative environments. A 2-dimensional scanning LIDAR is used to improve the reliability of the FIR camera based road border recognition. In order to detect the road borders we apply a Kalman-filter based model fitting strategy. Extracted measurements of the FIR images are transformed into the vehicle coordinate system in order to provide a precise description of the road course ahead. The model description in a common coordinate system -the vehicle coordinate system -allows an easy compensation of the ego-motion and a direct and straight forward fusion of the different sensor data. Both the detection and the estimation were developed and enhanced for the intended sensor configuration. The corresponding mathematical derivations are presented in this paper. Using the range values, delivered by the LIDAR, a more stable estimation of the pitch angle can be achieved. The realization of that is shown in detail. This is used to define the ROI in which the image processing is carried out. [C9281]

"Integration of Arm-equipped Mobile Robot GRYPHON for Humanitarian Demining Operation"

Our project to develop arm-equipped mobile robot GRYPHON for humanitarian demining operation will be introduced. The mobile base of the GRYPHON is the off-the-self buggy vehicle and it is modified to be tele-operated by wireless control system. The GRYPHON is mounted specially designed robot arm of about 4m long with counterweight at the rear side of the arm. The arm is equipped with 2 dof wrist mechanism and mine detector including metal, GPR (Ground Penetrating Radar), and NQR (Nuclear Quadropole Resonance) sensors. The GRYPHON can be manually driven from the base camp to the mine field and it is changed to the tele-operated mode at the site. It is then accessed to the border of the mine field and measures the surface of the ground by stereo-vision to generate the scanning trajectory for the arm. Execution of the scanning is then done to generate signal map of the terrain. The deminer judge the generated signal map and marks some of the suspicious points on the CRT screen of the control box located far away from the GRYPHON. The GRYPHON then automatically marks the locations of the ground by paint or paddles to show the places for the final prodding operation. The dynamo of the buggy vehicle is designed to provide all the electric power required for this operation in full day. [C9282]

"Robust Satellite Techniques (RST) for Oil Spill Detection and Monitoring"

Satellite remote sensing is an useful tool supporting the management of marine technological hazards, especially for what concern oil discharge. Nowadays, the most reliable satellite techniques are based on SAR (Synthetic Aperture Radar) active sensors operating in the microwave region of the electromagnetic (EM) spectrum. Such methods (even if not in whatever wind condition), assure good sensitivity for oil spill detection and high spatial resolution for a detailed description of the polluted area. Unfortunately, they cannot be used for real-time monitoring at all latitudes because of a revisiting cycles which ranges from few days up to 5 weeks moving from polar to equatorial zones respectively. Passive optical sensors on board meteorological satellites could be, in principle, also used for oil spill monitoring provided that suitable data analysis techniques (still lacking) are developed. In fact, thanks to a time resolution which is better than of few hours (up to few minutes) and despite their lower spatial resolution (not better than 250 m in the visible spectral range) they could represent the unique possibility when a timely detection is crucial in order to mitigate the damages. In this paper a new satellite technique for oil spill detection and monitoring is discussed. It is based on the general RST (Robust Satellite Techniques) approach applied to AVHRR1 observations in the Thermal Infrared (TIR) region of the EM spectrum. The proposed approach, which exploits the analysis of multi-temporal satellite records, seems able to detect the anomalous signals on the sea due to the oil polluted areas with excellent reliability (0% of false alarms) and good sensitivity in different observational conditions. It is applied in this paper to the "San George" Argentina -Uruguay oil spill event occurred in February 1997. Preliminary results so far achieved confirm the reliability of the proposed approach which promises to offer new (economically sustainable too) opportunities for building a real-time monitoring system for oil spill at the global scale. [C9283]

"A Novel Methodology for Parameter Retrieval from Multi-temporal Data Demonstrated for Forest Biomass Retrieval from C-band SAR Backscatter"

A methodology for parameter retrieval from multi-temporal Earth observation data is proposed and applied to forest biomass retrieval from C-band SAR backscatter. The potential of single observation C-band SAR data to

map forest biomass is limited mainly due to a low sensitivity and the dependence of C-band scattering on many other parameters. In this contribution a methodology to retrieve forest biomass from multi-temporal C-band SAR observations is presented. The method was applied to map forest biomass over a large area in Central Siberia using significant stacks of ENVISAT ASAR Wide-Swath data. The resulting forest biomass map is assessed by comparison with available inventory data. The quality achieved appears very promising. [C9284]

"A Duopoly Pricing Game for Wireless IP Services"

This paper addresses the behavior of the selfish service providers in the form of IP sinks providing high-speed IP access. Service providers compete for mobile users by adjusting the price they charge for their services. Their aim is to maximize the total collected profit. Mobile users are also selfish choosing the service provider offering the best quality of service and price combination. As the service providers come closer to each other, we show the existence of three critical phase transitions in their behavior. Depending on the separation between them, there may exist a unique Nash equilibrium, or a continuum of Nash equilibria, or no Nash equilibrium. We completely characterize the pricing strategies of service providers at Nash equilibria. We also prove that the total social welfare in the presence of selfish providers is close to the maximum social welfare that can be reached through non-selfish optimization. [C9285]

"Characterization of the Temporal and Spatial Variability of Soil Moisture through Multi-Temporal Analysis of ASAR Observations"

In this paper, synthetic aperture radar (SAR) based soil moisture retrieval results are presented using observations acquired over the Tibetan Plateau. Two different time series based methods are used for the retrieval of soil moisture. With method I, soil moisture is retrieved through scaling of the backscatter (σ_{ao}) observations between the maximum and minimum observed σ_{ao} at a specific location. For method II, soil moisture is retrieved using the integral equation method (IEM, Fung et al. 1992), for which a site-specific effective surface roughness parameterization is obtained through model inversion using minimum observed σ_{ao} . The retrievals are validated against ground measurements and showed that using method I and method II soil moisture can be estimated with accuracies up to 0.056 and 0.035 cm³cm⁻³, respectively. [C9286]

"Investigation on Genetic Algorithm for Countermeasure Technique Generator"

Development of successful electronic countermeasure (ECM) techniques against target track radars is a time-consuming and expensive process. Recently, Nunez et al. reported a genetic algorithm (GA) optimization method for ECM techniques generation; this paper outlines the current effort to implement the approach with an operational radar system and to establish a methodology for arbitrary ECM signal generation in a closed-loop system. While this effort employs GA, the method applies equally to other optimization techniques. After defining the GA fitness function for a generic range gate pull off (RGPO) technique, the ECM signal is implemented with a very fast digital arbitrary waveform generator. The RGPO signal is injected into the radar environment, and the tracking radar response is measured and scored for optimization. The method is suitable for more sophisticated ECM signals and will be studied in future work. [C9287]

"Statistical Model of the Signal Scattered from Sea Surface at the Grazing Feed Angles"

Experimentally obtained dependences of the lifetimes of the spikes and silent intervals in the signal scattered from the sea their spectrums and final probabilities of the existence including and simultaneous operation using several frequencies and polarizations allow using the proposed statistical model to fulfill the imitation of the noise conditions for the multifrequency and multipolarization radars. The proposed approach could be useful both for the theoretical analysis of the operating characteristics of the systems for the detection of the objects against a sea background and for the working-off the perspective algorithms of the radar information. [C9288]

"Comparison of 3-D and 2-D DCT Based Filtering of Multichannel Images"

A common feature of multichannel images of different origin and spectral bands is that they exhibit a high degree of mutual correlation of their components. At the same time, information content and noise properties in component images are more or less different. For the noise removal from such images, two general approaches are possible. The first one assumes component-wise (2-D) filtering; the second approach presumes vector (3-D) processing. Component wise filtering is, in general, simpler whilst 3-D processing that is able to take into account the inter-channel (inter-band) correlation of data is potentially more efficient. [C9289]

"Interpretation of an Influence of the Transmitter and Receiver Bistatic SAR Tracks to Resolution"

Remote sensing of a surface by the bistatic model allows obtaining more information about surface conditions.

Practically all remote sensing problems are solved on basis of ambiguity function analysis of a system. Here a qualitative variables of such system is determined by a resolution or by an ambiguity function width on the fixed level. The resolution of the bistatic SAR as the monostatic has an objects space discrimination in all directions even if is used unmodulated sounding signal and a selection degree mainly depends on a phase function variation rapidity where return signal is processed. [C9290]

"Polarization-Spectral Indication of the Objects"

The experimental study of the features of the polarization-spectral structure of the signals scattered from the sea surface, hydrometeors, lots covered of flora and above-sea objects allowed to ascertain that for the acquiring signals of the object the appreciably high level of the correlation at orthogonal polarizations than for the noise is typical. This condition could be used for the indication of the low-speed objects against a background of lots covered of flora. Since the signal scattered from the object at the polarization orthogonal to the transmitted partially coherent to the signal at the matched polarization, the latter could be used as reference for the realization narrow-band tracking of the orthogonally polarized signal component. [C9291]

"Results of Computer Imitation Modeling of Immunity of Correlator Affected by Active Continuous Interferences at the Processing of Wideband Noise or LFM Sequences of Pulses"

Recently the more complex conditions of radar exploitation are connected with saturation of some areas with many radio engineering systems creating complex interference situation. The purpose of this work is: an analysis and estimation of immunity of the multi-channel correlator under matched processing of sequences wideband noise pulses (NP) in condition of the influence of the active continuous interferences (CI) of different types and parameters using criterion of immunity on signal level; a selection of dangerous types of such CI and revision of the conditions of their setting up; a revealing the peculiarities and advantage of the using the noise signal of the given structure with a large time-bandwidth product and small power spectrum density for ensuring of immunity of its correlating processing in condition of the active continuous interferences. [C9292]

"SaS Process Location Parameter Adaptive Estimator Based on Data Censoring"

The task of location parameter estimation by means of adaptive censored procedure in SaS noise environment is considered. Based on the carried out research it is proposed to use the percentile coefficient of kurtosis and median absolute deviation as parameters able to describe processes with SaS pdf in case of absence of a priori knowledge about its statistical characteristics. The new formula is presented to evaluate the censoring parameter of the investigated estimator. Based on comparative analysis it is shown that the proposed adaptive procedure allows one to obtain the smallest variance among the considered robust and adaptive estimators for $\alpha = 0.9$. The proposed adaptive estimate can be put into basis of noise suppressing filter to be applied in image homogeneous regions in case of mixed noise. [C9293]

"DCT Local Adaptive Filtering of Images Corrupted by Fluctuative Noise with a Priori Unknown Statistical Properties"

A DCT based locally adaptive filter has been proposed and applied for processing of real and imaginary components of bispectrum for solving a problem of unknown signal shape (waveform) reconstruction. The bispectrum is a 2-D complex function and in its real and imaginary components a strongly non-stationary noise is present. Thus, the filter designed can be also effectively applied to processing different kind of images for which non-stationary noise with a priori unknown local statistical properties is present. The modifications of DCT based filters have been successfully used for removal of pure multiplicative, speckle and film-grain noise. [C9294]

"Results of Laboratory Test of Immunity of Correlator Affected by Active Continuous Interferences at the Processing of Wideband Noise Pulses Sequences"

Works concern to computer modeling of immunity of noise and LFM radars affected by single-frequency interference that is its influence on a form of output correlation effect depending on time of accumulation. The different influence of single-frequency interference is examined for both noise and LFM-signals as well as SAR-image. Advantage of application of matched correlating processing of a noise signal is quality shown for neutralization of influence of single-frequency interferences by means of increase of accumulation time. The presented experimental investigation of immunity of noise radar affected by wideband or/and single-frequency interference. The aim of the presented work is: estimation of immunity of correlator matched with a noise pulse under influence of active (mutual and intentional) continuous interferences with application of local criterion of immunity at signal level; detection of the decorrelating factors bringing with a real correlator. [C9295]

"All-Optical High-Frequency Electrical Chirped Pulse Generation using a Nonlinearly Chirped Fiber Bragg Grating"

In this paper, two novel approaches to optically generating high-frequency chirped electrical pulses with tunable chirp rate using a tunable nonlinearly chirped fiber Bragg grating (NL-CFBG) are proposed. In the first approach, a high-frequency electrical chirped pulse is generated based on optical spectral shaping and nonlinear wavelength-to-time conversion using a tunable NL-CFBG. In the second approach, two ultrashort pulses at different wavelengths are dispersed at an NL-CFBG. The beating of the two differently dispersed pulses at a high-speed photodetector generates a chirped electrical pulse with tunable chirp rate. The NL-CFBG used in the proposed systems is produced using a simple technique based on strain-gradient beam tuning. Mathematical models to describe the chirped electrical pulse generation are developed, which are verified by numerical simulations. The first approach is also verified by a proof-of-concept experiment. [C9296]

"High-Accuracy Doppler Signal Processing: Techniques and Applications"

In this paper, Doppler signal processing having a large potential for further developing and gaining new applications have been demonstrated. This has been illustrated by several examples related with the estimation of the SAR platform orientation angles from the radar returns, improving quality of SAR images based on a high-accuracy estimation of the Doppler rate, and retrieving 3D topography of Earth surfaces by using conventional squint-mode SAR systems, where sub-Hertz accuracy of the Doppler centroid measurements is realized. Among other promising applications of high-accuracy Doppler measurements, InSAR systems can be mentioned, including those intended for high-resolution imaging the Moon and other space objects with Earth-and space based radars. [C9297]

"A Low-Cost Millimeter-Wave Six-Port Double-Balanced Mixer"

A low cost millimeter-wave narrowband six-port double-balanced mixer circuit is proposed. Due to the symmetry and specific properties of the six-port, the mixer exhibits very good suppression of harmonic and spurious products. The mid operating frequency is selected to be 77 GHz, which is dedicated to collision avoidance radar for automobile applications. The simulation results show a conversion loss less than 4 dB and a very good linearity over a wide input power range. The 1 dB compression point and the third-order input intercept point are respectively 7.25 and 17 dBm. [C9298]

"System Design of a 77 GHz Automotive Radar Sensor with Superresolution DOA Estimation"

This paper introduces a novel 77 GHz FMCW automotive long range radar (LRR) system concept. High resolution direction of arrival (DOA) estimation is an important requirement for the application in automotive safety systems. The challenges in system design regarding low cost and superresolution signal processing are discussed. Dominant interferences to the MUSIC DOA estimator are amplitude and phase mismatches due to inhomogeneous antenna patterns. System simulation results deliver design guidelines for the required signal-to-noise ratio (SNR) and the antenna design. Road traffic measurements with a demonstrator system show superior DOA resolution and demonstrate the feasibility of the design goals. [C9299]

"Improved Noise Parametr Estimation and Filtering of MM-Band SLAR Images"

Blind (automatic) techniques for determination of noise characteristics of Ka- and X-band SLAR images obtained from the Institute of Radiophysics and Electronics of UNAS and A.I. Kalmukov Center of Earth Radiophysical Sensing. New modification on a filter based on a discrete cosine transform applied in sliding blocks is described. Filter efficiency is considerably improved by taking into account noise type and statistical characteristics. [C9300]

"To the Question About Estimation of Residual Fluctuation of Signal on Output of Correlation Receiver of Noise Radar"

It is shown in paper, that by virtue of random nature of signal being used in noise radars, a response on the output of correlator has an additional noise constituent unconnected with thermal noise of receiver. The value of this additional fluctuation is inversely proportional to the base of noise signal that it is necessary to take into account at development of noise radars. The value estimation of additional noise constituent in the present paper is done for stationary ergodic Gaussian noise signals with uniform and Gaussian spectrum. [C9301]

"Ka-Band Ground-Based Noise Waveform SAR"

We present main results of design and investigations of Ka-band ground based interferometric SAR which uses continuous noise waveform as a probe signal and may operate in both monostatic and bistatic regimes.

Synthetic aperture antennas enable to design a portable, light weight, easy to mount device with high speed of operation suitable for SAR imaging in quasi-real time while Ka-band noise waveform signals provide all-weather high resolution, high electromagnetic compatibility and interference immunity. Experiments have shown a rather high stability and repeatability of the measurements due to both the high quality of the equipment and advanced signal processing methods. The SAR system designed is an innovative instrument for solving new tasks of precise remote monitoring of various large objects, such as sealing of big halls, dams, bridges, TV towers, hangars, etc. [C9302]

"Performance of Falcon-I: Developed Low-Power and High-Sensitivity Cloud Profiling FM-CW Radar at 95GHz"

We have developed a low-power and high-sensitivity cloud profiling radar, named FALCON-I, transmitting frequency modulated continuous wave (FM-CW) at 95 GHz for ground-based observations. Millimeter wave at 95 GHz is used to realize much higher sensitivity than lower frequencies to small cloud particles. An FM-CW type radar realizes similar sensitivity with much smaller output power to a pulse type radar. Two 1m- diameter parabolic antennas separated by 1.4 m each other are used for transmitting and receiving the wave. The direction of the antennas is fixed at the zenith at this moment. The radar can observe clouds up to 20 km in height with the range resolution of 15 m and the angular resolution of 0.2 degree. Simultaneous observations of FALCON-I and a pulse type radar, SPIDER, show good performance of FALCON-I. Sensitivity of FALCON-I is -32 dBZ in radar reflectivity factor at 5 km, which is only 3 dB worse than that of SPIDER although its output power is 1/3000 to SPIDER. Ranging resolution of 15 m is realized for FALCON-I, which is 1/10 of that of SPIDER. Using developed FALCON-I, we observed clouds in various regions and oceans in the last three years. [C9303]

"Direction of Arrival Estimation using Advanced Signal Processing"

Accurate estimation of signal direction of arrival (DOA) has many applications in communication and radar systems. For example, in defense application, it is important to identify the direction of possible threat. One example of commercial application is to identify the direction of emergency cell phone call such that the rescue team can be dispatched to the proper location. DOA estimation using a fixed antenna has many limitations. Its resolution is limited by the mainlobe beamwidth of the antenna. Antenna mainlobe beamwidth is inversely proportional to its physical size. Improving the accuracy of angle measurement by increasing the physical aperture of the receiving antenna is not always a good option. Certain systems such as a missile seeker or aircraft antenna have physical size limitations; therefore, they have relatively wide mainlobe beamwidth. Consequently, the resolution is quite poor. Also, if there are multiple signals falling in the antenna mainlobe, it will be difficult to distinguish them. Instead of using a fixed antenna, an array antenna system with innovative signal processing would enhance the resolution of signal DOA. It also has the ability to identify multiple targets. Two types of signal processing methods, model based and eigen-analysis estimation techniques, are presented in this paper. The model based approach models the observed data as the output of a linear shift invariant system driven by zero mean white noise. The signal's DOA can be estimated by evaluating the model parameters. This approach has properties similar to the maximum entropy spectrum estimation. Some of the problems in the maximum entropy method, such as the line splitting effect, are also observed in this method. Two different processing algorithms are used to obtain the model parameters, and they are: 1. least mean square (LMS) and 2. sample matrix inversion (SMI). The eigen-analysis method based on temporal averaging has been investigated by many authors in the past (Schmidt, 1986). However, temporal averaging requires average over multiple time samples to estimate the covariance matrix. Sometimes, the radar system prefers to have an estimated covariance in a single snapshot. We propose eigen-analysis based on spatial smoothing so that we can have estimated covariance in a single snapshot. Performances based on several different spatial averages are discussed in this paper. Extensive computer simulations are used to verify the processing algorithms. For narrowband signals, both processing algorithms provide enhanced resolution and have ability to resolve multiple targets as long as the number of targets is less than the system's degree of freedom. SMI provides better performance than the LMS method due to the fact that this method is relatively immune to excessive mean square error. However, for multiple wideband waveforms, sometimes the array antenna has difficulty to resolve them, especially if signals are impinging the antenna with narrow spatial separation. This problem can be solved by extending the array antenna to a space time adaptive processor (STAP) (Guerri, 2003). STAP is basically replacing the single weight at the output of each array element by an adaptive filter. Statistical analysis of the performance of the processing algorithms and processing resource requirements are discussed in this paper. [C9304]

"Solving Multi-path Time Delay Estimation Problem in the Presence of Additive White Gaussian Noise Using a Genetic-Algorithm"

In practical world, there always exist problems of multi-path time delay estimation (MTDE) and it is an important problem in the fields of sonar, radar, digital communication and geophysics. We consider the problem of estimating the arrival times of overlapping ocean-acoustic signals from a noisy received waveform that consists of attenuated and delayed replicas of a known transient signal. We assume that the transmitted signal and the number of paths in the multipath environment are known. Many existing time-delay estimation algorithms perform poorly due to converging to local optimum points. In this paper, an efficient genetic-algorithm (GA) is applied to deal with the above problem. To the best of our knowledge this study is the first attempt to solve time delay estimation (TDE) using an evolutionary technique, genetic-algorithms. The performance of generic-algorithm is examined for different signal-noise scenarios. Our simulation results show that the time delays are estimated well based on the genetic-algorithm. [C9305]

"Non-bayesian fault detection/isolation with nuisance parameters and constraints"

The problem of statistical non-bayesian fault diagnosis (detection and isolation) is addressed in the paper. The goal is to discuss how to deal with nuisance parameters and how to integrate the constraints in the statistical decision-making process. To illustrate the theoretical results, the problem of navigation system integrity monitoring is considered. [C9306]

"ROC Analysis with Matlab"

The contribution is focused on essentials of ROC and Cost analysis and their support by Matlab software. In the contribution there are mentioned basic facts on ROC and COST curves theory and shown results of Matlab-based solution, mainly samples of graphical outputs, simplified and schematised due to size of images in the paper. More detailed solution of selected practical problems will be demonstrated during presentation. Source files can be obtained from the author. [C9307]

"A Mixed Fast Particle Filter"

Particle filtering algorithm has been widely used in solving nonlinear/non-Gaussian filtering problems. In this paper, a new particle filter is proposed, which is based on the unscented Kalman filter (UKF) and the extended Kalman filter (EKF), and takes a divide-and-conquer sampling strategy. It first uses a mixed Kalman filter, which combines UKF and EKF, as proposal distribution to generate part of the particles, and then uses the transition prior for another part. The experiment results show that this new particle filter can reduce time cost in addition to giving higher accuracy compared to other particle filters. [C9308]

"Experiment of Phase Unwrapping Algorithm in Interferometric Synthetic Aperture Sonar"

Two-dimensional (2-D) phase unwrapping, which defined as the estimation of unambiguous phase data from a 2-D array known only modulo 2π radian, is a key technique in the interferometric synthetic aperture sonar (InSAS). Unfortunately there are no a set of approaches of final word on phase unwrapping especially in the real dates. Recently, an InSAS prototype is developed and the lake trials were fulfilled. The phase unwrapping algorithms in the InSAS system were analyzed and their advantages and limitation were also studied with the results of data of Lake Trail. The results we derived from the lake trail will make foundation for further research. [C9309]

"Application and Analysis of Time Domain Cross Correlation for Traffic Flow Speed Measurement"

Radars are common means to measure vehicle speed. They are fast and accurate, however measure only instantaneous velocity not speed of the traffic flow. Therefore they are not suitable to help determine the busy degree of traffic. A novel method of traffic flow speed measurement using video based on time domain cross correlation is introduced. It provides 'flow speed', a much better parameter determining whether there is a traffic jam or how fast one can cover that road under the observed situation. With regard to the 'False-Peak' problem, effect of the sequence length on correlation result is presented, together with formulas used to calculate proper sequence length both accurately and approximately. Test results demonstrate the signification of sequence length on improving cross correlation result and good accuracy suitable for estimation of road busy degree. [C9310]

"Analysis of Sidelobe Elevation for Polyphase Complementary Codes through the Non-ideal System"

Complementary phase-coded signals have found widespread use in radar systems utilizing pulse compression technique due to their unique autocorrelation properties. However, nonzero sidelobe values appear when the complementary signals pass through the system with limited bandwidth. This paper gives a detailed discussion

on the impact of passband cutoff frequency, passband ripple, transition bandwidth, and minimum stopband attenuation of FIR digital filter on sidelobe elevation. At last this paper gets some useful conclusions which are conducive to system design optimization and sidelobe suppression research. [C9311]

"EM characterization of bituminous concretes using a quadratic experimental design"

This paper describes the characterization of bitumen concretes by measurement cells, within the ground-penetrating radar frequency band, on mixtures defined by a specific experimental design. This one is from a fractional Γ ,BS plan (41. 24) which limits the design to 32 mixtures. The parameters, classically used and chosen by road specialists for this specific study, are the nature of the aggregates, the binder richness modulus, the compaction, the maximum size of the aggregates and the continuity of the granulometry. The model, associated with the experimental design, tends to fit a multiple linear regression describing the relationship between measures and the chosen parameters. Two successive levels of calculation have been realized, independently for either the real part and the imaginary part of the relative permittivity. Globally, The first calculation, taking into account all the parameters and their interactions, shows, in the frequency band [100-1300 MHz], that the model explains about 84 % of the measured permittivity. When limiting to a reduced design, keeping only the significant parameters and interactions, results tend to about 85%. [C9312]

"An innovative on-board processor for the real-time GPR monitoring of railway substructure conditions"

The SAFE-RAIL system and the relevant processing unit are hereafter described as a success case for the solution of an electromagnetic inverse problem in real-time applications. The SAFE-RAIL system on-board processing unit is conceived for providing functionalities for real-time exploitation of raw data deriving from microwave sensing action through innovative GPR equipment. In particular, the main objective, as per European STREP project SAFE-RAIL statements, is focused on automatic interpretation of microwave sensed data relevant to rail-track subsurface, aiming at characterizing the ballast and sub-ballast layer properties with consequent extraction in real-time of geophysical parameters. A neural network based approach has been exploited as an efficient way for solving the inverse problem through a "learning-by-examples" approach. The capability of the SAFE-RAIL system in matching real-time performance requirements has been investigated. System operability and cost-effective implementation issues have also been deeply addressed. [C9313]

"The inspection of large retaining walls using GPR"

In hilly regions, retaining walls along roads and motorways are numerous. In some cases the knowledge of the details of the construction is limited. If rehabilitation work becomes necessary, a detailed knowledge of all details of the construction is desirable for an improved planning. In a pilot study a GPR inspection of retaining walls was carried out. This included the development of an apparatus for the controlled positioning of the radar antennas on the faces of the walls as well as an evaluation of different antennas and acquisition parameters for this application. This paper describes the approach for data acquisition, acquisition and processing parameters and the results obtained on a retaining wall situated at a Swiss motorway. [C9314]

"A Stakeholder Led Accuracy Assessment System for Utility Location"

In the UK alone there are many millions of miles of underground utilities and records concerning their location are often inaccurate, incomplete, or non-existent. As well as posing significant health and safety problems to construction personnel, this problem brings with it large social and financial costs. This has led to increasing use of Ground Penetrating RADAR (GPR) for utility location, but without detailed consideration of its efficacy in terms of location accuracy. Therefore, Mapping the Underworld (MTU), a multi-university research project aimed at ensuring improved accuracy in utility location, has been actively engaged in stakeholder consultation. As well as providing much useful data on stakeholder needs, this is also providing a methodology for the assessment of GPR utility location in terms of the factor of most importance to them-the degree to which the equipment provides location within their own accuracy requirements. Also, in order to provide consistency in the assessment methodology, MTU intends to construct a state-of-the-art test facility for assessing location equipment accuracy within tight tolerances. This will yield a combined methodology for reliable testing of location equipment, coupled to an accuracy assessment system weighted in a manner acceptable to stakeholders. [C9315]

"GPR signal attenuation vs. depth on damaged flexible road pavements"

The findings of a GPR survey carried out on damaged flexible road pavements built on embankments and in cutting sections were reported. The survey was carried out to recognize correlations between: (i) types of damage, (ii) height of embankments or depth of cutting sections, (iii) traffic load and (iv) GPR scan results. Two

types of damages, inducing loss of load bearing capacity, were investigated: transversal cracks and ramified cracks. Sixteen sites were chosen, describing the different combinations of the variables to be analyzed. The sites were selected among secondary non-urban roads in the area of L'Aquila (central Italy). Road integrity was evaluated by a GPR quantitative analysis (GPR signal attenuation vs. depth), using an antenna array with a nominal frequency of 1600 MHz. It investigates media till a depth of 1.5 m which is also the maximum depth of influence of the induced traffic stress. The results carried out from two sets of scans (affected and unaffected parts) were compared in order to identify GPR signal changes. These changes made it possible to trace the causes of the damage to the road pavement vs. embankment height, cutting depth and traffic load. [C9316]

"Author Index"

{no data available} [C9317]

"Prediction of structural damages of road pavement using GPR"

A new methodology has been proposed to extract the hydraulic permittivity fields in sub-asphalt structural layers and soils from the moisture maps observed with GPR. It is effective at diagnosing the presence of clay or cohesive soil that compromises the bearing capacity of sub-base and induces damage on the road. The numerical algorithm has been yet discussed in the 11th International Conference on Ground Penetrating Radar [5]. Here some experimental confirms have been presented. [C9318]

"Characterizing Railroad Ballast Using GPR: Recent Experiences in the United States"

Recent work has been conducted in the United States with 2 GHz horn antennas to characterize railroad ballast. There were a number observations made during the course of the project that derive from gaining a more thorough understanding of ballast and the interaction of GPR with the ballast matrix. The major observations from over 238 km of track data at four different geographical locations include: (1) it cannot be assumed that there will be a reflection from the bottom of clean ballast or that there will be a reflection from the ballast-subballast interface; (2) the presence of a strong reflection in the data generally, but not always, infers moderately-fouled to clean ballast above the reflecting boundary; and (3) no observable ballast-subballast interface reflections are generally, but not always, associated with gradational fouling or a fully-fouled ballast section. [C9319]

"2007 15th International Conference on Digital Signal Processing"

The following topics were dealt with: biomedical signal and image processing; design and implementation; adaptive filtering; detection and estimation theory and applications; machine learning; bioinformatics and genomic signal processing; array processing, radar and sonar; image and multidimensional signal processing; information forensics, security and data fusion; multimedia signal processing and joint source-channel coding; nonlinear signal processing; time-frequency and time-scale signal processing; sensor array and multichannel systems; speech and language processing; blind equalization and source separation; computer vision and pattern recognition; musical signal processing. [C9320]

"Conference Information"

{no data available} [C9321]

"Road-Shape Recognition Using On-Vehicle Millimeter-wave Radar"

In this paper, we present a method for estimating road shape using on-vehicle millimeter-wave radar. The radar detects not only the backscatter from vehicles but also from stationary objects such as crash barriers and sound barrier walls that are generally installed along roads. This indicates that we can estimate road shape by collecting information on the distribution of these objects. We adopt the multiple signal classification (MUSIC) algorithm for increasing the azimuth resolution. Moreover, to apply the MUSIC algorithm into real-time radar systems, the computational cost is reduced by introducing the technique of bi-iteration singular value decomposition (Bi-SVD). The estimated road shapes exhibit good agreement with the actual shapes. Therefore, this technique is expected to improve the reliability of driving support systems. [C9322]

"Two-Dimensional Generalized Partial Response Equalizer for Bit-Patterned Media"

The use of bit-patterned media is one of the approaches being investigated to extend magnetic recording densities to 1 Tbit/in² and beyond. In patterned media, track pitch may be small causing adjacent tracks to have significant interference on the replay waveform from the main data track. To mitigate the effect of such inter-

track interference (ITI), we propose the use of a two-dimensional (2D) generalized partial response (GPR) equalizer. We select both the equalizer and the partial response target using the minimum mean squared error (MMSE) criterion. However, we avoid the need for a 2D Viterbi algorithm by imposing a constraint on the 2D target that forces the adjacent track contributions (in the ideal case) to zero. Simulation results show that this 2D equalizer significantly improves the bit error rate (BER). In this work, the effect of a 2D GPR equalizer on the performance of a patterned media system in the presence of track misregistration (TMR) is also investigated. Based on the simulation results, the 2D equalization method appears to be more tolerant to TMR than the conventional GPR. The main drawback of the proposed method is the need for simultaneously acquiring the signals from three adjacent tracks. [C9323]

"2007 IEEE Intelligent Vehicles Symposium"

The following topics are dealt with: vehicle environment perception; cooperative cognitive automobiles; collision avoidance; automated vehicles; communications and networks; sensors; vehicle control; driver assistance systems; decision and expert systems; information fusion; integrated safety systems; image processing; radar signal processing; lidar signal processing. [C9324]

"Vehicle Identification Using Near Infrared Vision and Applications to Cooperative Perception"

Vehicles will be in the next future equipped with V2V telecommunication means to exchange data, such as the presence of an obstacle on the road, or an emergency braking notification. Vehicles are also more and more equipped with perception systems (cameras, laser scanners, radars) that enable them to explore the immediate environment, including other vehicles. We propose in this paper an on-board optical vehicle identification system to enable telecom and perception systems to cooperate. The optical identification identifies which vehicle, in the scene captured by the perception system, is sending information via telecom. [C9325]

"A Multilevel Traffic Incidents Detection Approach: Identifying Traffic Patterns and Vehicle Behaviours using real-time GPS data"

This paper presents a multilevel approach for detecting traffic incidents causing congestion on major roads. It incorporates algorithms to detect unusual traffic patterns and vehicle behaviours on different road segments by utilising the real-time GPS data obtained from vehicles. The incident detection process involves two phases: (1) Identifies of road segments where abnormal traffic pattern is observed and further divides the 'abnormal segments' into smaller segments in order to isolate the potential incident area; (2) Performs a hierarchical analysis of the vehicles' GPS data, using predefined rules to detect any occurrence of abnormal behaviour within the 'abnormal' road section identified in phase 1. The strength of such approach lays in isolating road segments sequentially and then analysing vehicle data specific to the identified road segment. In this way, the processing of vast data is avoided which is an essential requirement for the better performance of such complex systems. The approach is demonstrated using a simulation of motorway segments near Coventry, UK. [C9326]

"Monocular Video serves RADAR-based Emergency Braking"

Much work was carried out recently for emergency braking based on radar signals. The key step for emergency braking is the reliable detection of obstacles. Moving objects are verified as such by tracking the radar signal. However, discarding so-called phantom objects remains a challenge for stationary objects. This leads to the question of sensor fusion for more reliable verification of obstacles. In this paper we propose a novel method using a monocular camera, such as the night view camera in the Mercedes S class. Our two goals in this paper are the verification of obstacles and the detection of obstacle boundaries. This allows analysis of the situation for carrying out emergency braking. The verification of obstacles is done by analyzing the scaling of obstacles as they get closer to the camera. The perspective image motion of the ground plane serves as a counter hypothesis to detect phantom objects. Obstacle boundaries are found by graph cut segmentation on these two motion fields. [C9327]

"Short Range Radar Signal Processing for Lateral Collision Warning in Road Traffic Scenarios"

This paper introduces signal processing algorithms of single-sensor-multi-target-tracking, sensor data fusion, and multi-sensor-multi-target-tracking developed for designing a novel lateral collision warning function. In order to improve the perception of road vehicles, an experimental vehicle has been equipped with arrays of three short range radar sensors on both sides. With the aid of such sensor arrangements, lateral objects (e.g. cars, trucks, bicycles, guard rails) can be detected and tracked. Thus, imminent collisions in the lateral area may be prevented by warning the driver when the ego-vehicle inadvertently drifts towards another vehicle on the adjacent lane or towards the road boundary, or when another vehicle approaches the ego-vehicle in a dangerous manner. [C9328]

"Finite Array Observations-Adapted Regularization Unified with Descriptive Experiment Design Approach for High-Resolution Spatial Power Spectrum Estimation with Application to Radar/SAR Imaging"

We address a new approach to solving array radar/SAR imaging problems stated and treated as uncertain ill-posed inverse problems of nonparametric estimation of the power spatial spectrum pattern (SSP) of the wavefield scattered from an extended remotely sensed scene via processing the discrete measurements of a finite number of independent observations of the degraded data signals (one realization of the trajectory signal in the case of SAR). The problem is treated in the framework of the worst-case statistical performance optimization-adapted regularization (WOR) method aggregated with descriptive experiment design (DED) paradigm. Our approach is based on the optimization of worst-case statistical performance of the resulting finite-dimensional fused WORDED estimator of the SSP. The DED-formalized projection schemes as well as the weighting "degrees of freedom" of the WOR strategy are incorporated into the optimization procedure subject to the statistical operational worst-case performance constraints imposed on the desired solution operator. [C9329]

"The Use of Non-Uniform Sample Phases for Array Synthesis"

The non-uniformly sampling procedure and the Fourier transform properties permit to control the shape of an antenna array pattern. The problem found in this analysis is usually the appropriate use of the array factor phase for further control of the pattern. In this work, a new technique will be presented that provides the control of shaped beam patterns using also the phase of the non- equidistant samples of the array factor. Considering the phase, the ripple structure of an array pattern has more oscillations, which yields a function with a smaller transition region between the beam zone and the sidelobe zone. Another advantage of the phase usage is to obtain different array excitations that produce the same pattern amplitude. [C9330]

"Robust Adaptive Beamforming: When the Worst Case is the Best We Can Do"

First Page of the Article [C9331]

"Adaptive Interference Suppression for Civil Aviation VHF Air-to-Ground Communication Based on Constant Modulus Array"

VHF air-to-ground communication is very important for the communications between air traffic controllers and pilots in civil aviation. However, due to various kinds of reasons, radio interference exists in the VHF communication link and has posed a great threat to the civil aviation safety. In this paper, we first establish a practical data model for the problem of interest, then a blind signal extraction (BSE) method based on constant modulus array is proposed to suppress the interference. Simulation results are provided to demonstrate the performance of the proposed method. [C9332]

"Synchronization Signal Design for OFDM Based On Time-Frequency Hopping Patterns"

In an OFDM system, channel estimation can be considered as sampling the time-frequency response of the channel through a number of known pilot symbols placed across the time-frequency plane. Sampling theory dictates that the pilot insertion frequency must be above the Nyquist rates in both time and frequency to avoid aliasing of the delay-Doppler response. Based on the regularly spaced pilot pattern, we can derive alternative patterns that preserve the non-aliasing property by hopping the scan lines in either time domain or frequency domain, but not both. From this extended set of patterns, we find ones with properties that, in addition to channel estimation, can achieve responsively other synchronization tasks such as initial time-frequency offset estimation and device identification. The ambiguity function analysis frequently used in radar signal design leads to a periodic time-hopping pattern based on the costas array that has minimal coincidences with its circular time-frequency shifts, which can be used for the identification of multiple devices. The hopping in time also greatly increases the pilot's time support, thus enabling the quick initial acquisition of timing and frequency offset with very short observation. [C9333]

"Routing for Emitter/Reflector Signal Detection in Wireless Sensor Network Systems"

In this paper, we consider energy-efficient routing for detection in wireless sensor networks (WSNs). Energy-efficient routing for WSNs has been intensely studied recently, but routing for signal detection in WSNs has not attracted much attention. Moreover, we are not aware of any previous work on routing for detection in WSNs that specifically considers the Neyman-Pearson criterion which is the most accepted metric for radar, sonar and related signal detection problems. By deploying a simple but illustrative model for target detection in WSNs, we

formulate a problem of energy-efficient routing for signal detection under the Neyman-Pearson criterion. We propose a routing metric which aims for a route with the maximum mean detection-probability-to-energy ratio, and describe methods for solving the resulting optimization problem. This proposed metric, striving for a balance between the consumed energy and detection performance, is effective for finding the optimal routing that values such an energy-detection tradeoff. [C9334]

"Feature Detection in Highly Noisy Images using Random Sample Theory"

A novel feature detection algorithm utilizing random sample theory is proposed for 2D and 3D images. The proposed method works on both binary and gray-scale images and yields faster results than standard feature detection algorithms, such as the Hough Transform (HT), while keeping the performance level of HT. The proposed method creates random hypothesis features and tests them to select candidate features in the image. The selected candidate features are then re-estimated within a smaller search space around the candidate feature. The proposed algorithm has been tested on both simulated and experimental subsurface seismic and GPR images to locate linear features like pipes or tunnels. Results show that the proposed algorithm can detect features accurately and much faster than conventional methods. [C9335]

"VoIP Performance in SIP-Based Vertical Handovers Between WLAN and GPRS/UMTS Networks"

This paper experimentally analyzes the handover performance of VoIP sessions in a wireless overlay of 802.11 WLANs and GPRS/UMTS networks when mobility is handled at the application layer by SIP. It also assesses the impact of handovers on the VoIP call quality perceived by the user by means of the extended E-model. The study reveals that good performance values are achieved when handing over from GPRS/UMTS to WLAN. Additionally, acceptable quality is obtained for handovers from WLAN towards UMTS. On the other hand, unacceptable values are achieved when moving towards GPRS. The main reason is the delay experienced by SIP messages when traversing the cellular network. [C9336]

"Quantitative analysis of texture parameter estimation in SAR images"

This paper deals with the validation of a previously developed texture model for SAR data as well as its associated parameter estimation algorithm. The mentioned model is named the Anisotropic Gaussian Kernel (AGK) model and allows the description of the possibly nonstationary and anisotropic behaviour of texture on heterogeneous areas of SAR images. The parameter estimation performance is evaluated over simulated data. We also investigate about the validity of our model over experimental data, by means of dissimilarity measures. [C9337]

"Poster Session 6d: Antennas 1"

First Page of the Article [C9338]

"Oral Session 7a: Multistatic Radar 2"

First Page of the Article [C9339]

"Oral Session 6b: SAR/ISAR 3"

First Page of the Article [C9340]

"Poster Session 6c: Environment 2"

First Page of the Article [C9341]

"Poster Session 7d: Antennas 2"

First Page of the Article [C9342]

"Oral Session 8a: Radar Systems 3"

First Page of the Article [C9343]

"Oral Session 7b: Environment 1"

First Page of the Article [C9344]

"Poster Session 7c: Target Recognition"

First Page of the Article [\[C9345\]](#)

"Oral Session 6a: Radar Systems 2"

First Page of the Article [\[C9346\]](#)

"Poster Session 4c: Radar Systems 2"

First Page of the Article [\[C9347\]](#)

"Poster Session 4d: SAR/ISAR 2"

First Page of the Article [\[C9348\]](#)

"Oral Session 4a: ECCM"

First Page of the Article [\[C9349\]](#)

"Oral Session 4b: Detection and Tracking 2"

First Page of the Article [\[C9350\]](#)

"Poster Session 5c: Radar Systems 3"

First Page of the Article [\[C9351\]](#)

"Poster Session 5d: Detection and Tracking 3"

First Page of the Article [\[C9352\]](#)

"Oral Session 5a: Antennas"

First Page of the Article [\[C9353\]](#)

"Oral Session 5b: SAR/ISAR 2"

First Page of the Article [\[C9354\]](#)

"A normalized Fractionally lower-order moment algorithm for Space-Time Adaptive Processing"

A new space-time adaptive processing algorithm is proposed for clutter suppression in phased array radar systems. In contrast to the commonly used normalized least mean square (NLMS) algorithm which uses the second order moments of the data for adaptation, the proposed method uses the lower order moments of the data to adapt the weight coefficients. The normalization is also performed based on the data sample dispersion rather than the variance. Processing results using simulated and measured data show that the proposed algorithm converges faster than the NLMS algorithms in Gaussian and non-Gaussian clutter environments. It also provides better clutter suppression than the NLMS algorithm under heavy-tailed, impulsive, non-Gaussian environments. It in turn improves the target detection performance. [\[C9355\]](#)

"Detection Probability of WCDMA Based Cellular Radar System"

Cellular radar is basically a kind of passive radar system. It uses the signal of a base station in a wireless communication system as an 'opportunity of illumination' to detect a target. The meaning of detection in cellular radar is slightly different from other conventional radar systems. It means, we must consider not only the detection criterion of radar system but also that of wireless system to constitute the concept of detection for cellular radar. A radar system regards that the signal is detected if the received signal voltage exceeds the threshold, while in WCDMA system the received signal is said to be detected when PN acquisition succeeds. It is obvious that the cellular radar system fails to obtain sufficient information of targets without guarantee of those two detection criterions. Therefore, we widely need to combine them and consider simultaneously. It is also important to measure how well a system can detect a target, so we define the detection probability. In this paper, we analyze necessity of two detection criterions and provide a novel definition of detection for the cellular radar. Computation of the detection probability in a certain radar environment is also involved. [\[C9356\]](#)

"Blank Page"

First Page of the Article [C9357]

"Back Cover Page"

First Page of the Article [C9358]

"Fusing ladar and color image for detection grass off-road scenario"

It is necessary to extend the intelligent vehicle to navigate from structured environment to rough terrain, which is a great challenge for environment modeling. Ladar and camera are the most widely used sensors, but each of them has shortcoming. In this paper, SVM method is used to fuse the information from ladar and color camera. After registration, ladar point is represented by its position and neighbored pixels in the image. The height of the object as well as the H and S components of the color of the pixels are selected to represent the terrain. Grass and non-grass terrain are recognized based on the features. Experiment shows this method is simple and efficiency. [C9359]

"Vehicle centroid estimation based on radar multiple detections"

Automotive radar application is a focus in active traffic safety research activities. And an accurate lateral position estimation from the leading target vehicle through radar is of great interest. This paper presents a method based on the regression tree, which estimates the rear centroid of leading target vehicle with a long range FLR (Forward Looking Radar) of limited resolution with multiple radar detections distributed on the target vehicle. Hours of radar log data together with reference value of leading vehicle's lateral offset are utilized both as training data and test data as well. A ten-fold cross validation is applied to evaluate the performance of the generated regression trees together with fused decision forest for each percentage of the training data. As a result, compared with the current approach which calculates the mean of lateral offset, the regression tree and decision forest approach yield more accurate position estimation of the lateral offset from a single leading target vehicle with radar multiple detections. [C9360]

"Data fusion performance evaluation for range measurements combined with cartesian ones for road obstacle tracking"

This paper deals with the assessment of centralized fusion for two dissimilar sensors for the purpose of tracking road obstacles. The aim of sensor fusion is to produce an improved estimated state of a system from a set of independent data sources. Indeed, for a robust perception of the environment, seen here as obstacles, several sensors should be installed in the equipped vehicle: camera, lidar, radar, etc. In our case, the motivation for this work comes from the need to track road targets with lidar measurements combined with radar ones. Thus, the aim is to combine effectively radar range measurements (i.e. range and range rate) with lidar Cartesian measurements for a "turn" scenario. Centralized fusion, i.e. measurement fusion, for two dissimilar sensors is considered here for assessment which is based on Cramer- Rao Lower Bound (CRLB), the basic tool for investigating estimation performance as it represents a limit of cognizability of the state. In the target tracking area, a recursive formulation of the Posterior Cramer-Rao Lower Bound (PCRLB) is used to analyze performance. Many bound comparisons are made according to the scenarios used and various sensor configurations. Moreover, two algorithms for target motion analysis are developed and compared to the theoretical bounds of performance: the extended Kalman filter and the particle filter. [C9361]

"A robust method to determine relevant target vehicle using vehicular radar"

In order to solve the problem of the instability in the selection of relevant target, caused by the complexity of the measurement environment of vehicular radar, a robust method to determine the relevant target using vehicular radar is proposed. Based on analyzing the measurement environment, the method uses the principle of the nearest object in the same lane for target pre-selection. The Kalman filter is applied to predict the target information and the relevance verification of the pre-selected target is done by the consistence checking. The target decisions are made through a "relevant target life cycle" method. The verification tests show that by efficiently eliminating the effects of ghost objects, other disturbances and the bumping and swinging of vehicle, the proposed method can accomplish the determination of relevant target under different conditions. [C9362]

"RADAR 2008-First call for papers"

First Page of the Article [C9363]

"Poster Session 8d: STAP and ECCM"

First Page of the Article [\[C9364\]](#)

"Oral Session 9a: Target Recognition 2"

First Page of the Article [\[C9365\]](#)

"Oral Session 8b: Environment 2"

First Page of the Article [\[C9366\]](#)

"Poster Session 8c: Passive Radar"

First Page of the Article [\[C9367\]](#)

"Oral Session 10b: STAP"

First Page of the Article [\[C9368\]](#)

"Blank Page"

First Page of the Article [\[C9369\]](#)

"Oral Session 9b: SAR/ISAR 4"

First Page of the Article [\[C9370\]](#)

"Oral Session 10a: Passive Radar"

First Page of the Article [\[C9371\]](#)

"Hardware efficient frequency estimation and tracking using signal autocorrelations"

This paper proposes an algorithm for efficient frequency estimation and tracking. The proposed algorithm can be implemented with a small number of multiplications. This is important because in most hardware implementations (e.g. in FPGA) the number of multiplications is the most expensive for silicon area optimization. A correlation based pulse-pair (PP) method, which is an efficient technique for frequency estimation, is used for the initial frequency estimation. It is known that the PP method has a very low number of multiplications, and is ideally suitable for FPGA type hardware implementations, especially at high frequencies. The disadvantage of using the PP method is that the method requires inverse tan operation in the implementation that makes the technique computationally unattractive. In this paper, a new efficient recursive technique for implementing inverse tan operation is proposed. Method for proper frequency estimation and tracking of signals with time varying instantaneous frequencies is also discussed in the paper. [\[C9372\]](#)

"UWB antennas: Design and application"

Since FCC released the extremely wide spectrum with emission masks for commercial ultra-wideband (UWB) applications in 2002, much effort of research and development has been paid for the design of UWB antennas for a variety of applications from wireless or wired communications to non-communications such as imaging, location, and radar systems. Many UWB antennas have been developed to cover the ultra- wide operating bandwidth of the UWB systems with acceptable performance. Currently, the prospective applications of UWB technology are becoming clearer and clearer. The majority of UWB R&D activities have been focused on how to meet the specific requirements of forthcoming UWB systems. This paper will review the R&D of UWB antennas since 2002. The important milestones of the UWB antenna designs will be introduced. The issues how to apply UWB antennas in the promising UWB systems will be highlighted. Many state-of-the-art designs will be updated. [\[C9373\]](#)

"Tunnel-accessed NATs for always-best-connected and application mobility"

We describe the design, implementation and performance of a Remote NAT that can be used to provide an 'always-best-connected' service. In this service a mobile host will connect through the best possible network. Switching between the networks (even with IP address changes) will be transparent to the application. The solution that we propose is different from traditional mobility solutions like MSOCKS and Mobile IP and requires

no support from the networks to which the mobile host connects. The solution involves an 'ABC daemon' on the mobile host and a 'remote NAT' that is used to provide a consistent interface to the remote host during a connection oriented application. We also describe the prototype implementation and preliminary experimental results. [C9374]

"3D map generation for biometric applications using a network of multi-static radar sensors"

In this paper, we describe a novel algorithm based on diffraction tomography for 3D map generation using the received backscattered radar electro-magnetic (EM) field from different spatially distributed multi-static radar sensors. Each sensor at a given time will transmit a radar waveform and the other sensors including the one transmitted will receive the waveform that is backscattered from the objects. A data cube of received data will be created at each sensor by changing the location of sensors. This data cube is used in generating the 3D object profiles at each sensor and then the fused 3D map will be outputted which will contain the fused 3D object profiles or structure obtained from each sensor. If there are more than one object in the field of interest there would be inter object backscattering. This would result in receiving mixed signals. This mixed signal might cause problems in the generation of the 3D map/structure. So to reduce the effect of inter object backscattering we use the probabilistic based blind source separation (BSS) technique for convolutive mixture separation. Before applying the mixture separation technique, we estimate the number of sources. For this we have developed a technique. In this paper, all these techniques are described and also results using real radar backscattered data are provided. A description of how this 3D maps can be used for biometrics is also provided. [C9375]

"Radar 2007 The Institution of Engineering and Technology International Conference on Radar Systems"

First Page of the Article [C9376]

"Copyright"

The following topics are dealt with: radar systems; multistatic radar; detection and tracking; synthetic aperture radar; target recognition; waveform design; ECCM; antennas; passive radar; and space-time adaptive processing. [C9377]

"The IET Radar 2007 International Conference on Radar Systems [CBook of Abstracts]"

First Page of the Article [C9378]

"Blank Page"

First Page of the Article [C9379]

"Target tracking and interception in wireless sensor networks with compensation of communication delay"

A predictive guidance algorithm that adapts to the network-induced communication delay in Wireless Sensor Network Guided Guidance Systems (WSNCGSSs) is proposed. In this algorithm Multi-Step Predictor (MSP) is used before the conventional Pure Proportional Navigation (PPN) is applied in the guidance loop. The predictor compensates for communication delay and provides PPN with more accurate target estimates. Simulations show that delay compensation can improve the target interception performance significantly. [C9380]

"T6-High Frequency Over-the-Horizon Radar Applications I Oceanography"

{no data available} [C9381]

"A OFDM module for a MB-OFDM receiver"

The rules defined by FCC, for marketing and operation of UWB products, permitted the use of orthogonal frequency division multiplexing (OFDM) to implement UWB communications. MB-OFDM is taking place as good approach to UWB, for instance for wireless USB. The latest generations of FPGAs, including DSP capabilities, embedded processors and special features for I/O streaming, are being efficiently used in wireless high-data rate applications. Therefore, FPGAs can be used for UWB technology implementation. This paper discusses the implementation of a specially tailored FFT to demodulate OFDM in a UWB receiver. Special emphasis is put on the design to fulfill the critical time requirements. [C9382]

"Improvements in Data Management Practices within West Florida Shelf Coastal Ocean Monitoring and Prediction System"

In this paper, we describe the improvements that are being carried out in data management practices within West Florida Shelf Coastal Ocean Monitoring and Prediction System (COMPS). COMPS, has been in operation since 1997 providing near real-time weather and numerical ocean circulation models data needed for public, federal, state and local emergency management officials and researchers via Internet (<http://comps.marine.usf.edu>). COMPS program has grown since 1997, and presently we maintain twelve coastal and eight offshore buoy weather monitoring stations located along the coast and offshore of the West Florida Shelf. In addition to in-situ weather monitoring platforms, we also maintain a Hi-Frequency radar network that provides surface currents up to 200 km from the shore. With the growth in the COMPS program, and its participation in various Regional and National Ocean observing system data management related activities and projects, we took a project to make improvements in data management practices and COMPS web site. Preliminary results are presented here. [C9383]

"A Simulation of the Synthetic Aperture Radar Observation of a Manufactured Object in Sea Clutter using Finite Differences"

A simulation of the synthetic aperture radar (SAR) observation of a complex sea scene is proposed. The observed sea patch consists of sea clutter and a metallic, steady object. The simulation process is based on a local, discrete calculation using the finite difference method in the time domain. This approach turns out to be relevant when considering precise, complex scenes such as depicted in the study, despite a few drawbacks that are enlightened in the article. Antenna synthesis is performed upon a series of simulations using finite differences, and leads to the formation of a SAR image of the studied scene. [C9384]

"Maintaining track continuity in GMPHD filter"

The data association between objects and measurements is a challenging task in multiple-object tracking because of computationally expensive. This challenge can be overcome by the probability hypothesis density (PHD) filter. Recently, the Gaussian mixture probability hypothesis density (GMPHD) filter has been proposed as a closed-form of the PHD filter. However, the GMPHD filter does not include track continuity during the period of tracking. In this paper, we present a method for maintaining the continuity of state estimates of objects in the GMPHD filter. The set of labels from Gaussian components is used to create hypotheses for label association process and the Hungarian algorithm is applied to search for the best hypothesis association. The results show that the method is robust and efficient. [C9385]

"Architecture optimization of a finite impulse response filter using toggle-based power estimation"

In this paper one way of reducing the power consumption and the area of a finite impulse response (FIR) filter is presented. Using a standard toggle-based power estimation method combined with gate-level simulations and circuit synthesis we showed that we can achieve a significant area and power reduction from the beginning by carefully selecting the right architecture and optimizing the VHDL code description of the module. The analysis was made based on the unity delay model and not on the physical extracted layout for an actual submicron technology (130 nm) but this method can be utilized successfully for other technologies. [C9386]

"Improved ISAR imaging based on local polynomial fourier transform"

In this paper the local polynomial Fourier transform is introduced. Theoretical analysis and comparisons on the SNR ratio achieved by using the local polynomial Fourier transform, the short time Fourier transform, and the Fourier transform are presented to illustrate the merit of the local polynomial Fourier transform. Improved performance for radar imaging using the local polynomial Fourier transform is demonstrated, compared with that using the short time Fourier transform and Fourier transform. [C9387]

"Robust supergain array in noise fields"

The supergain array is known to be highly sensitive to slight errors in its array parameters. A method which offers robustness against array perturbation errors is presented. The beamformer weights which optimizes the array gain can be obtained by incorporating the perturbation error statistics in the covariance matrix of the noise field. In addition, the proposed method is equivalent diagonal loading if the perturbation errors are isotropic and uncorrelated. [C9388]

"Poster Session 2c: Radar Systems 1"

First Page of the Article [C9389]

"Poster Session 2d: SAR/ISAR 1"

First Page of the Article [C9390]

"Oral Session 2a: Multistatic Radar 1"

First Page of the Article [C9391]

"Oral Session 2b: Detection and Tracking 1"

First Page of the Article [C9392]

"Poster Session 3c: Environment 1"

First Page of the Article [C9393]

"Poster Session 3d: Detection and Tracking 2"

First Page of the Article [C9394]

"Oral Session 3a: Target Recognition 1"

First Page of the Article [C9395]

"Oral Session 3b: Waveform Design"

First Page of the Article [C9396]

"Poster Session 1d: Detection and Tracking 1"

First Page of the Article [C9397]

"Programme"

First Page of the Article [C9398]

"Blank Page"

First Page of the Article [C9399]

"Radar 2007 The Institution of Engineering and Technology International Conference on Radar Systems-Committee/Members"

First Page of the Article [C9400]

"Table of Contents"

First Page of the Article [C9401]

"Oral Session 1b: SAR/ISAR 1"

First Page of the Article [C9402]

"Poster Session 1c: Multistatic Radar"

First Page of the Article [C9403]

"Keynote Address"

First Page of the Article [C9404]

"Oral Session 1a: Radar Systems 1"

First Page of the Article [C9405]

"Building Corner Feature Extraction Based on Fusion Technique with Airborne LiDAR Data and Aerial Imagery"

Generally, automatic building corner or linear feature extraction from urban area aerial imagery is based on traditional computer vision corner or edge detection techniques. However, challenges and difficulties remained due to the complex characteristic of objects in urban images. Visually, the linear features in airborne LiDAR are much more distinct than those in aerial imagery, however, common criticisms arising from the low horizontal accuracy of LiDAR data. To overcome these difficulties, this study proposes a building corner extraction algorithm based on information fusion technology by integrating aerial imagery and airborne LiDAR data. According to experiment results, the proposed method can obtain the distinct building corners not only with the characteristics of uniform spatial distributed pattern based on Voronoi graph theory, but also with the shape, length, and height constrained conditions derived from LiDAR linear features. The proposed algorithm resolves the heterogeneous remote sensing data registration difficulties between LiDAR data and raw aerial imagery. [C9406]

"A Notion of Diversity Order in Distributed Radar Networks"

We introduce the notion of diversity order in distributed radar networks. Our long-term goal is to analyze the trade-off between distributed detection and centralized detection using co-located antennas. In contrast with the asymptotically high Signal-to-Noise Ratio (SNR) definition in wireless communications, we define the diversity order of a distributed radar network as the slope of the probability of detection (PD) versus SNR curve at PD=0.5. In this paper we restrict our analysis to noise-limited systems. We evaluate the diversity order of fully distributed systems, and prove that for the OR rule, the gain in diversity is only logarithmic in the number of distributed sensors, denoted K. The AND rule does not lead to any gain in diversity order. We finally present some recent results, and provide preliminary analysis regarding the characterization of a Diversity-Multiplexing tradeoff in distributed radar detection. [C9407]

"RF Tomography with Application to Ground Penetrating Radar"

RF tomography and ground penetrating radar are combined to detect and identify hidden targets, such as underground facilities and hard and deeply buried targets. Past experience in below-ground imaging is described, current measurement results are presented, and future plans are discussed. [C9408]

"Multi-Channel Fast Parametric Algorithms and Performance for Adaptive Radar"

Airborne radar systems employing radar sensor arrays utilize multi-channel (MC) signal processing techniques for optimal detection and localization of targets. The detection and localization statistics have mathematical structures that typically require the inverse of an estimated covariance matrix in order to be evaluated. Due to the size of sensor arrays and the number of pulses in a coherent processing interval (CPI), the dimension of the covariance arrays is very large (1000s) and the computational burden of estimating and inverting such large arrays has led to the development of parametric methodologies that significantly reduce both the computational requirements and the amount of measured data to create the inverse co-variance matrix estimate. Recent developments have indicated non-stationary covariance estimates may provide enhanced detection performance over stationary covariance estimates. This paper outlines the fast computational structure possibilities of both stationary and non-stationary covariance inverse structures in one-dimensional and multi-channel cases. [C9409]

"Doppler Resilience, Reed-Muller Codes and Complementary waveforms"

While the use of complementary waveforms has been considered as a technique for providing essentially perfect range sidelobe performance in radar systems, its lack of resilience to Doppler is often cited as a reason not to deploy it. This work describes and examines techniques both for providing Doppler resilience as well as tailoring Doppler performance to specific aims. The Doppler performance can be varied by suitably changing the order of transmission of multiple sets of complementary waveforms. We propose a method which improves Doppler performance significantly in specific Doppler ranges by arranging the transmission of multiple copies of complementary waveforms according to a suitable choice from the first order Reed-Muller codes. We provide both a theoretical analysis and computer simulations of the Doppler response of waveform sequences constructed in this way. [C9410]

"A Net Track Solution to Pose-Angular Tracking of Maneuvering Targets in Clutter with HRR Radar"

Maintaining track continuity is a challenging task for large area persistent surveillance with high target density, rapid target maneuvering, and low target-to-clutter ratio. When the sensor revisit interval is long, measurement-to-track association becomes rather difficult. Although maneuvering targets can be discriminated via Doppler processing, clutter still masks moving targets at certain aspect angles. This creates a blind zone for GMTI (ground moving target indicator) radar, which may extend as large as 25% of the azimuth angles. For high-value targets that may undergo evasive maneuvers, a net track solution coordinating multiple looks from a netted set of sensors is set forth in this paper to ensure continuous monitoring. Target visibility therefore needs to be factored into netted radar platform coordination and sensor systems management. For ground targets, their heading is mostly aligned with the longitudinal axis. The target pose thus carries kinematic information about the direction of velocity vector that can be used to assist tracking of maneuvering targets. In this paper, the range profiles of high range resolution (HRR) radar are used for pose angular estimation of maneuvering targets in clutter. A pose-sensitive classifier provides matching scores that are converted into likelihoods and updated over time in a probabilistic manner. Pose angular tracking from individual sensors in the network is fused to cover the blind zone encountered by individual sensors. A software simulation environment that produces range profiles based on the RF signatures of moving targets is used in the study. Simulation results for pose angular tracking in clutter are presented to illustrate the net track solution concept and its performance. [C9411]

"Waveform Diversity for Different Multistatic Radar Configurations"

The multistatic ambiguity function has recently been proposed as a tool for analyzing and designing multistatic radar systems. It was demonstrated through examples that multistatic radar system performances can be improved by shaping the multistatic ambiguity function through waveform selection and adequate weighting of different receivers during pre-detection fusion. In this work we study sensor repositioning as a third way of shaping the multistatic ambiguity function. We provide some preliminary simulation results that illustrate how significant improvements in radar system performances can be achieved by combining waveform selection, receiver weighting and sensor placement strategies. These results can serve as a guideline for future multistatic fusion rule development. [C9412]

"Knowledge-Aided, Physics-Based Signal Processing For Next-Generation Radar"

In this paper we describe knowledge-aided signal processing to improve the performance of radar systems operating in complex clutter environments. The paper describes two paradigms based on either direct or indirect application of prior knowledge. A physics-based, knowledge-aided, parametric approach to clutter estimation is discussed. We provide numerical analysis demonstrating the performance enhancements offered by the proposed methods relative to baseline techniques when operating in the presence of heterogeneous clutter. [C9413]

"Auxiliary-Vector RADAR on MCARM Data"

Derived from statistical conditional optimization criteria, the auxiliary-vector (AV) detection algorithm starts from the target vector and adding non-orthogonal auxiliary vector components generates an infinite sequence of tests that converges to the ideal matched filter (MF) processor for any positive definite input autocorrelation matrix. When the input autocorrelation matrix is replaced by a conventional sample-average estimate, the algorithm effectively generates a sequence of estimators of the ideal matched filter that offer exceptional bias/covariance balance for any given finite-size observation data record. In this work, the AV algorithm is evaluated on collected airborne phased-array radar data from the MCARM program and is seen to outperform in probability of detection (for any given false alarm rate) all known and tested adaptive detectors (for example AMF, generalized likelihood ratio test, the multistage Wiener filter algorithm, etc.). [C9414]

"Knowledge-Aided Space-Time Adaptive Processing"

A fundamental issue in knowledge-aided space-time adaptive processing (KA-STAP) is to determine the degree of accuracy of the aprioriknowledge and the optimal emphasis that should be placed on it. In KA-STAP, the a priori knowledge consists usually of an initial guess of the clutter covariance matrix. This can be obtained either by previous radar probings or by a map-based study. In this paper, we consider a linear combination of the aprioriclutter covariance matrix with the sample covariance matrix obtained from secondary data, and derive an optimal weighting factor on the aprioriknowledge by a two-step maximum likelihood (ML) approach. The performance of the two-step ML approach is compared with that of the convex combination (CC) approach and is evaluated using the KASSPER data. [C9415]

"Two-Dimensional Mixed Autoregressive Models for Space-Time Adaptive Processing"

We introduce a new class of parametric models for two-dimensional (space-time) adaptive processing for (slow-

time) stationary multivariate interference (clutter). This class is based on maximum-entropy (ME) extensions (completions) of partially specified block-Toeplitz covariance matrices. We derive exact solutions for the ME extensions and also provide computationally advantageous suboptimal solutions for efficient STAP filter design. The efficiency of the proposed parametric models is illustrated by an airborne radar scenario provided by the DARPA KASSPER dataset. [C9416]

"A Comparison of MIMO and Phased Array Radar with the Application of Music"

The utilization of diversity in radar systems has shown improvements over conventional phased array radars in many aspects of the system performance including target detection probability, number of targets, and beam-pattern. We present here the application of the MUSIC algorithm to MIMO radar and the associated benefits of increasing the diversity to its performance for a single target and two closely spaced targets, but also show that a system with diversity can perform worse than that of a phased array system due to the directional transmit beamforming gain available to the phased array. [C9417]

"Multitaper Array Processing"

Thomson's multitaper approach generates estimates of the power spectrum by averaging individual "eigenspectra" obtained using a set of orthogonal window functions. The multitaper method is designed to work with very low sample support, typically a single snapshot of data, making it very attractive for the analysis of nonstationary or transient signals. This paper explores the use of the multitaper approach for spatial spectrum estimation in passive sonar. Several examples are given, and the problem of processing non-planewave signals is briefly discussed using an example motivated by a deep water propagation experiment. [C9418]

"Improved consistent estimation on Krylov subspaces"

An improved construction of the optimum minimum variance unbiased estimator on a reduced-dimensional subspace is proposed that uniquely relies on the sample estimate of the observation covariance matrix. Unlike traditional subspace realizations based on directly replacing the true covariance matrix with the sample covariance matrix, the proposed implementation is based on an estimation of the Krylov subspace that is consistent under a limited number of samples per observation dimension. By allowing for arbitrarily large-dimensional samples, our approach not only generalizes the conventional subspace estimator but also models appropriately finite sample-size situations, in which it is shown to present a significantly superior performance. [C9419]

"A Novel Approach for Multiple Moving Target Localization Using Dual-Frequency Radars and Time-Frequency Distributions"

Accurate range estimation and tracking of moving targets is an important task in urban sensing applications. A dual-frequency radar, which estimates the range of a target based on the phase difference between two closely spaced frequencies, has been shown to be a cost-effective approach to accomplish both range-to-motion estimation and tracking. This approach, however, suffers from two drawbacks: it cannot deal with multiple moving targets, and has poor performance in noisy environments. To overcome these drawbacks, we propose, in this paper, the use of time-frequency signal representations. High signal-to-noise ratio (SNR) is obtained by focusing on the moving target instantaneous Doppler frequency law provided by the power localization properties of time-frequency distributions. The case of multiple moving targets is handled by separating the different Doppler signatures prior to phase estimation. [C9420]

"A Modulation Based Approach to Wideband-STAP"

In this paper, a new method for processing wideband radar data is presented. To perform the full degree of freedom wideband processing, 3-D space-time adaptive processing (STAP) needs to be implemented, which involves intense computational burden. One approach in this case is to do subband STAP processing and combine these outputs. In this paper, instead of traditional subband processing, incoming wideband data signal is modulated by multiple carriers, combined, and filtered prior to processing using narrowband STAP. This method offers a significant decrease in computation burden compared to the subband method. [C9421]

"Optimal Beamforming with Mobile Robots"

Detection using distributed networks have received significant attention in the space-time adaptive processing literature. The paper examines the use of a new dimension-the mobility of robots to improve the output signal-to-interference-plus-noise-ratio (SINR) of an array of antennas. It is proposed that by optimizing over the positions of the antennas in the plane, the SINR can be significantly improved, extending the well-known

method of beamforming using optimal complex weights. Initial simulations using a simplistic system scenario show that large gains in SINR are indeed possible when combining the optimal weights and local optimal positions of the receiving antennas. [C9422]

"Time Reversal Synthetic Aperture Radar Imaging In Multipath"

Conventional spotlight synthetic aperture radar (SAR) assumes a single reflection of transmitted waveforms from targets [1]. Multiple reflections of targets due to surrounding scatterers appear as ghosting artifacts in conventional SAR images, which obscures true target image and leads to poor resolution. In this paper, we develop image formation techniques using time reversal, time reversal SAR (TR-SAR), to remove ghosting artifacts and achieve high resolution. The TR-SAR algorithm is tested using phase history data collected by a rail-mounted SAR sensor operated by Raytheon. [C9423]

"A Graph-Theoretic Approach for Constraining Floor Plan Estimation from Radar Measurements"

This paper addresses the problem of floor-plan estimation using a limited number of stand-off radar aspect angles, time-delay measurements and wall-penetrations. While most floor-plan estimation work has focused on local methods for reconstructing wall positions within a building, i.e. imaging methods, this paper approaches the problem by incorporating global constraints into the solution. This is done by associating each room in the building with a node on a directed graph that encodes its adjacency to the other rooms. Floor plan reconstruction methods are presented for both cases where the topology of the building is known or unknown. [C9424]

"Application of GPRS Techniques for Wide-Area Power Quality Monitoring"

This paper tries to use USB and personal digital assistant to develop a novel power quality (PQ) monitoring platform and then integrates GPRS technique into the proposed PQ platform to realize wide-area PQ monitoring. The works of this paper can be divided into three parts. First, a small-scale PQ monitoring platform with appropriately designed I/O interfaces and peripherals is designed and implemented. Next, a GPRS module which can be integrated into the designed PQ monitoring platform is developed. Finally, a web server with well-designed database used to record abnormal PQ data is designed. The proposed GPRS based wide-area PQ monitoring system can be used for PQ monitoring with minimum cost and maximum efficiency. All the functions implemented in this paper can realize the novel, real-time and wide-area PQ monitoring. Experimental results demonstrate the validity of the proposed system. [C9425]

"A Closed Form Expression for the Number of Costas Arrays of Arbitrary Order"

We give a closed form expression for the number of Costas arrays of arbitrary order by counting them as lattice points in the chambers of a related hyperplane arrangement and suggest how recent algorithmic breakthroughs might be used to find them. [C9426]

"Compressive Sensing for GPR Imaging"

The theory of compressive sensing (CS) enables the reconstruction of sparse signals from a small set of non-adaptive linear measurements by solving a convex ℓ_1 minimization problem. This paper presents a novel data acquisition and imaging algorithm for ground penetrating radars (GPR) based on CS by exploiting sparseness in the target space, i.e., a small number of point-like targets. Instead of measuring conventional radar returns and sampling at the Nyquist rate, linear projections of the returned signal with random vectors are taken as measurements. Using simulated and experimental GPR data, it is shown that sparser and sharper target space images can be obtained compared to standard backprojection methods using only a small number of CS measurements. Furthermore, the target region can even be sampled at random aperture points. [C9427]

"Stereo-Vision-Based Moving Object Tracking via Robust Linear Filtering"

Vision-based tracking sensors typically provide nonlinear measurements of the targets Cartesian position and velocity state components. In this paper we derive linear measurements using an analytical measurement conversion technique which can be used with two (or more) vision sensors. We derive linear measurements in the target's Cartesian position and velocity components and we derive a robust version of a linear Kalman filter. We show that our linear robust filter significantly outperforms the extended Kalman Filter. Moreover, we prove that the state estimation error is bounded. [C9428]

"Distributive Target Tracking in Wireless Sensor Networks under Measurement Origin Uncertainty"

This paper addresses the problem of tracking a single target under measurement uncertainty due to clutters and

missed detections in wireless sensor networks. By adopting the particles' representation of the probability density function of target state, this paper develops a particle filter (PF) and probabilistic data association filter (PDAF) hybrid tracking algorithm, name as PF-PDAF. PF-PDAF extends the well-known PDAF to the general nonlinear system. Based on the hierarchical sensor network architecture, the distributive PF- PDAF is also implemented. Moreover, the posterior Cramer-Rao lower bound (PCRLB) is computed to provide a theoretical bound on the tracking performance of the developed algorithms. Simulation results are provided. [C9429]

"Communication and Localization for a Cooperative eSafety-System"

The core concept of the project, presented in this paper, is to enable the future availability of a modular cooperative system that will bring together sensor and communication technologies permitting to all road users (vehicles, motorcycles, bicycles, pedestrians) to take an active part in the reduction of the number of accidents that involve vulnerable road users. For this, legacy detection technologies, such as infrared or radar are enhanced by a RF-based communication. [C9430]

"Target Tracking with Range and Bearing Measurements via Robust Linear Filtering"

In this paper we provide a robust version of a linear Kalman filter for target tracking with nonlinear range and bearing measurements. Moreover, we prove that the state estimation error is bounded in a probabilistic sense. We compare our approach with the current state of the art in converted radar measurement based linear filtering. [C9431]

"Cramer-Rao Bound and Maximum Likelihood Estimation of Covariance Matrices With Non-Homogeneous Snapshots"

We consider the problem of estimating the covariance matrix R of an observation vector, using K groups of snapshots $Z_k = [z_{k,1} \dots z_{k,L_k}]$, of respective size L_k , whose covariance matrices R_k are randomly distributed around R , and hence are different from R . The Cramer-Rao bound (CRB) for estimation of R is derived as well as its maximum likelihood estimator (MLE). We illustrate the behavior of the CRB in the two opposite cases, namely $K = 1$ where all snapshots share a common covariance matrix, and $L_k = 1$ where each snapshot has a different covariance matrix. We also discuss the influence of the degree of heterogeneity on the estimation performance. [C9432]

"Derivation and Analysis of an Adaptive Detector With Enhanced Mismatched Signals Rejection Capabilities"

We consider the problem of adaptive radar detection with a view to provide a detector with high sidelobe signals rejection capabilities. Towards this end, we consider a modification of the adaptive beamformer orthogonal rejection test by enforcing the presence of a fictitious signal under the null hypothesis, orthogonal to the presumed target signature in the whitened space. We derive the generalized likelihood ratio test for this problem and provide analytical expressions for its probability of false alarm and probability of detection, for both matched and mismatched signals. The new detector is shown to offer very good performance in terms of mismatched signals rejection. [C9433]

"Morphological Component Analysis and STAP Filters"

STAP is an adaptive filtering algorithm that works on space-time radar data to suppress the effects of clutter and jamming and achieve both target identification and parameter estimation in airborne and space based radar [1][2]. The signals to which STAP processes are applied consist of three basic parts, target, clutter and jamming. In morphological component analysis (MCA) [3] the component signals are separated by assuming that each signal component can be sparsely represented in some suitable dictionary. It is assumed that expansions of a given signal component in the dictionaries of the other signal components are non-sparse. The MCA algorithm seeks a solution through an optimization method that implements this sparse-representation idea. This approach was applied to the analysis of ISAR images in [4]. In this paper we consider the basic STAP equations as a problem in multi-channel morphological component analysis (MMCA) [5] [6] [7]. The method is illustrated by application to the KASSPERI datacube. [C9434]

"Multibeam Amplitude Comparison Problems for MIMO Radar's Angle Measurement"

Amplitude comparison angle measurement is a practical technology for its simple structure and low complexity. MIMO radar can view a broad angular sector and form multiple simultaneous joint-beams. It is very suitable to implement multi-beam amplitude comparison angle measurement in MIMO radar. As the accuracy of angle measurement depends directly on the half-power beamwidth of the antenna pattern, we make detailed analysis

on the joint-beam properties for MIMO radar, and derive the mathematical expressions of the half-power beamwidth and peak sidelobe level. We also provide an effective method for allocating the multibeam directions in this paper. [C9435]

"Waveform Design for MIMO Radar with Space-Time Constraints"

We consider the problem of designing waveforms for MIMO-radar, where both the temporal and spatial characteristics of the waveform need to be determined. In other words, we design a set of different waveforms transmitted by different antennas. In previous works design procedures were presented where the resulting waveforms were constrained only by transmit power. Here we extend this work to include arbitrary linear constraints in the form of a space-time basis for the waveforms. We demonstrate that properly selecting and applying these constraints leads to waveforms with better temporal and spatial response (e.g., range response and beam pattern) than using previously proposed design procedures. [C9436]

"Time Reversal Transmission in MIMO Radar"

Time reversal explores the rich scattering in a multipath environment to achieve high target detectability. MIMO radar is an emerging active sensing technology that uses diverse waveforms transmitted from widely spaced antennas to achieve increased target sensitivity when compared to standard phased arrays. In this paper, we combine MIMO radar with time reversal to further improve the performance of radar detection. We establish a radar target model in multipath rich environments and develop likelihood ratio tests for the proposed time-reversal MIMO radar (TR-MIMO). Numerical simulations demonstrate improved target detectability compared with the commonly used statistical MIMO strategy. [C9437]

"Coherent Change Detection Statistics for Multiple Polarization SAR Images"

Given a pair of multiple polarization synthetic aperture radar (SAR) images collected at different times, the basic change detection problem is to determine pixels in the image that have changed during the time between images. A change detection statistic is computed for each pixel in the image to indicate whether a change has occurred. In this paper, we present a generalization of the coherent change detection (CD) statistic used for scalar valued SAR data to multiple polarization SAR data. Our generalized CD statistic is based on a test for statistical independence. We do not make any restrictive assumption regarding the underlying SAR data. A theoretical analysis of change detection performance is presented and comparisons are made with previous work. [C9438]

"Wavefront Adaptive Raymode Processing for Over-the-Horizon HF Radar Clutter Mitigation"

Detection of surface targets using over-the-horizon radar (OTHR) is extremely challenging due to ionospherically-induced Doppler spread clutter. In particular, low Doppler targets are often masked by ground clutter arriving via multipath propagation at different elevation angles, each with a different ionospheric Doppler shift. The wavefront adaptive raymode processing (WARP) approach presented here exploits the azimuthally distributed nature of the clutter return and adaptively estimates the "crinkly" spatial wavefront arriving on each raymode by using its distinct Doppler spectral characteristics. Rather than the plane-wave beamwidth of the array aperture, the raymode resolution of WARP is limited by the wavenumber-extent-spatial-aperture (WESA) product of the clutter return. Thus it is possible to spatially separate clutter raymodes using limited array apertures. Using simulated radar data, WARP is shown to provide a signal-to-clutter-plus-noise ratio (SCNR) improvement of as much as 30 dB over conventional processing for targets buried in Doppler spread clutter. [C9439]

"Comparison of Radar-Based Human Detection Techniques"

Radar offers unique advantages over other sensors in the human detection problem, such as remote operation during virtually all weather and lighting conditions. Many radar-based human detection systems today employ Fourier analysis, such as spectrograms. However, spectrograms perform poorly in high clutter environments. Also, an inherent SNR loss is caused by the implicit assumption of linear target phase. In this paper, human modeling is used to derive a more accurate non-linear approximation to the true non-linear target phase and the likelihood ratio is optimized over unknown parameters to enhance detection performance. Performance is compared both analytically and through MATLAB simulations. [C9440]

"Target of Imaging Observation Based on The Wavelet Transform and GPR"

A data analysis methods for frequency modulation continuous-wave ground penetrating radar targets near-fields images using wavelet transform are proposed. And discussing the instant characteristic of zero intermediate

frequency detected from frequency modulation continuous-wave ground penetrating radar echo signals using wavelet transform. Based on the wavelet transform algorithm features: constant Q, fit algorithm and fit mother wavelet improved the accuracy of echo signals' time- difference detecting and the image bound of target. And obtained the better results from the computing simulation. [C9441]

"On the Swept-threshold Sampling in UWB Medical Radar"

The non-invasive techniques to measure vital signs have received much attention lately. They exhibit several advantages compared to the traditional invasive techniques. One such technique can be based on radar principles. In this paper we scrutinize the statistical properties of a medical radar developed on a single CMOS chip, which operates in the ultra wideband from 3.1 GHz to 10.6 GHz. A key part of the chip is based on a new technique for sampling at very high frequencies called swept- threshold sampling. This is based on multiple pulse emissions, accumulation and range-gating. We derive expressions for the bias and variance of swept-threshold sampling and show that the bias is a strong function of noise power and input value, but independent of the swept-threshold parameters for a fixed input range. The variance is shown to be proportional to the quantization step size and standard deviation of the noise process. Finally, simulation results are provided as proof of concept, and they show that the derived theoretical equations for bias and mean square error are valid. [C9442]

"A Clutter Reduction Technique for Microwave Reconstruction of Shallow Underground Targets"

This paper presents a signal pre-processing technique for the stepped-frequency ground penetrating radar that is aimed at suppressing clutter related to antenna effects and variation of the ground surface response. Both the ground bounce and the clutter can obscure shallow underground objects such as landmines making difficult their detection. At the preprocessing stage, the measurement system has been calibrated using a free space and metal sheet as standards. Both the modulus and the phase of the signal obtained for metal sheet have been approximated by polynomials, and this synthetic signal is used to derive approximate transfer functions of the antenna. This technique utilizes calibration measurement for only one position of the metal sheet and yet reduces clutter related to the antenna effects. Besides, the calibration simplifies further subtraction of the ground surface response. The 2-D image of the subsurface is built then using B-scan data from which the ground bounce is eliminated. The performance of the method is demonstrated in several examples employing the frequency-domain data collected by a transmitting-receiving antenna pair. [C9443]

"Application of S-method to Multi-component Emitter Signals"

S-method (SM) is an effective time-frequency distribution for multi-component analysis. It keeps high time-frequency resolution and removes cross-term among components. So, this paper applies SM to process multi-component emitter signals. First, the factors that affect the performance of SM are discussed. Then, an on-line multi-component emitter signal analysis method is given to process the intercepted emitter signal continuously. At last, SM is used to analyze a manmade multi- component emitter signal. The cross-term reduction performance and noise suppression ability of SM is considered in the experiment. Experimental results show that SM is an effective multi-component emitter signal analysis method with good performances of owning high time-frequency resolution, avoiding cross-term among components and keeping good analysis ability at low signal to noise ratio. [C9444]

"Development of a high resolution UWB Sensor for Estimation of Transfer Function of Vocal Tract Filter"

UWB sensor has been considered as a good candidate for non-invasive medical imaging of human body. In this paper an FCC compliant UWB pulsed radar sensor is proposed. The transmitter transmits a pulse using a broadband monopole antenna. The pulse shape is similar to fifth derivative of Gaussian bell shape. The homodyne receiver is designed such that it correlates the received signal with a known template signal. The radar is capable of measuring millimeters of target motion. This radar is used for measurement of windpipe wall and glottal structure motions. Also corresponding acoustic signals can be measured using a simple microphone. These data are used in estimation of transfer function of the vocal tract filter (VTF). The transfer functions obtained for an individually pronounced sound element can be further used in applications like speech regeneration, voice recognition and background noise filtering. [C9445]

"3D Organization of 2D Urban Imagery"

Working with New York data as a representative and instructive example, we fuse aerial ladar imagery with satellite pictures and Geographic Information System (GIS) layers to form a comprehensive 3D urban map. Digital photographs are then mathematically inserted into this detailed world space. Reconstruction of the photos'

view frusta yields their cameras' locations and pointing directions which may have been a priori unknown. It also enables knowledge to be projected from the urban map onto georegistered image planes. For instance, absolute geolocations can be assigned to individual pixels, and GIS annotations can be transferred from 3D to 2D. Moreover, such information propagates among all images whose view frusta intercept the same urban map location. We demonstrate how many data mining and visualization challenges (e.g. identify all photos containing some stationary ground target, observe some structure from multiple perspectives, quantify match between two pictures, etc) become mathematically tractable once a 3D framework for analyzing 2D images is adopted. Finally, we close by briefly discussing future applications of this work to photo-based querying of urban knowledge databases. [C9446]

"Extracting information from shadows in SAR imagery"

The presence of speckle noise presents considerable challenges in interpreting SAR imagery. Despite the very high resolution that is on offer with modern SAR systems, the extraction of reliable intelligence from SAR imagery in an automated and robust manner has faced considerable difficulties. Shadow regions in SAR imagery are unique in terms of absence of speckle and any distortion from imaging artefacts. This paper presents a series of work that has aimed at exploiting the information in SAR shadows. Earlier work looked at combining shadow features with target features obtained with single look imagery. This provided for better target classification and led to a technique for estimating heights for urban structures. However, it is with multiple perspective imagery that SAR shadows have proved really effective. Using shadow delineation alone, information from different look angles over a sequence of SAR images is combined together to provide very reliable and unambiguous estimates of building dimensions. Another remarkable success has been the detection of moving targets from their shadows over a sequence of SAR images. The images of moving targets are blurred and distorted making it difficult, if not impossible, to detect the moving targets in SAR imagery. However, the target shadows are undistorted. Initial results with short-range data have been successfully replicated with detecting moving targets at much longer ranges. In all of these cases performance will be affected where clutter background is weak, dynamic range is poor or shadows from different objects overlap. Nevertheless, this paper has highlighted a range of applications from target detection and location to urban scene analysis where SAR shadows have been shown to provide a highly effective way of extracting information from the imagery. [C9447]

"Survivability Index for GSM Network"

The cellular mobile technology has been emerged astonishingly over the last decade. Global system for mobile (GSM) is most dominant among various cellular standard. It was developed in Europe and deployed in many parts of world. Now a day it carries critical business and social information of many subscribers thus proper quantification of quality of service must be done. In this work, survivability index (SI) has been proposed for above purpose. Survivability is one of many words which were coined as a measure of degree to which a system is able to provide critical services. Traditionally, survivability of cellular systems is measured in terms of one of following parameters: the number of functioning units, the maximum traffic capacity, blocking probability and the service restoration time, etc [1][2]. The available measures of survivability do not cover many inherent features simultaneously. This work is a step towards development of a compact and effective measure of cellular network survivability. SI has a weighted sum form which takes into account following features of a cellular network (i) blocking probability, (ii) dropping probability, (iii) voice quality, in terms of carrier to cochannel interference ratio (C/P) and (iv) availability. Its analysis has also been done for GSM network by considering two different failure scenarios. The evaluation of a GSM network has also been for different failure scenarios. [C9448]

"Digital Beamforming Antenna for Synthetic Aperture Radar"

Future SAR instruments such as the high resolution wide swath (HRWS) SAR incorporate digital beamforming techniques to overcome fundamental limitations of conventional SAR and to offer advanced modes defined by software. The European and German Space Agencies ESA and DLR are currently conducting interlinked studies of critical Digital Beamforming SAR antenna items, including several breadboarding activities. An overview of the developments and results is presented. [C9449]

"An Architecture for the Interoperability of Multimedia Messaging Services between GPRS and PHS Cellular Networks"

This paper proposes an architecture integrated with P-mail Deluxe Protocol (PDX) and Multimedia Message Service (MMS) to provide the Interoperability of the multimedia messaging between Personal Handy System and General Packer Radio Service (GPRS) networks. The proposed architecture includes an MMS-P-mail Gateway (MPG), within three messaging services units, i.e., multimedia messaging relay, adaptation and configuration unit. Through the MPG gateway provides bi-directionally seamless routing, protocol conversion, reformatting, and

transmission of the multimedia message. The proposed architecture leverage on the integration with PHS and GPRS networks to expand the MMS usage volume. An implementation of the MPG is described in this paper as an illustration of the feasibility of the proposed architecture. [C9450]

"A New Class of Interlaced Complementary Codes Based on Components with Unity Peak Sidelobes"

A new class of biphase complementary code sets is proposed. Individual codes in each set have maximum sidelobes of unity magnitude. The individual codes could have gaps of zeros but they are interlaced together without gaps in the final scheme. A number of such codes, as presented in this paper, use Barker codes as building blocks with additional elements from $\{+1, -1, 0\}$. An extension to polyphase interlaced complementary codes with unity peak sidelobes components is also discussed. The main drawback of regular complementary codes longer than 4 is that they have peak sidelobe magnitude greater than unity. In the presence of frequency selective fading or other factors, inexact sidelobe cancellation results in non-zero sidelobes at the output. This is minimized in the proposed schemes by using codes that have peak sidelobes of unity magnitude as the individual codes in the sets. A figure of merit is proposed to measure the frequency use efficiency of the proposed codes as well as other multi-frequency codes. [C9451]

"Keystroke Patterns Classification Using the ARTMAP-FD Neural Network"

This paper presents the development of a keystroke dynamics-based user authentication system using the ARTMAP-FD neural network. The effectiveness of ARTMAP-FD in classifying keystroke patterns is analyzed and compared against a number of widely used machine learning systems. The results show that ARTMAP-FD performs well against many of its counterparts in keystroke patterns classification. Apart from that, instead of using the conventional typing timing characteristics, the applicability of typing pressure to ascertaining user's identity is investigated. The experimental results show that combining both latency and pressure patterns can improve the equal error rate (ERR) of the system. [C9452]

"Study on the Division Tactics of Top Swimming Athletes Home and Abroad in the 400m Freestyle Swimming Race"

In swimming competition, a rational disposition of physical strength is seen as a major factor in deciding the final outcome. Among various items in swimming competition, the issue of physical distribution over the 400 m race has aroused the most extensive controversy. In this paper, concerning the achievements of elite athletes home and abroad in 400 m freestyle swimming race, the principle of variation coefficient in statistics has been adopted and calculation is conducted in regard to the newly-defined speed coefficient. The features and disciplines in the tactics application of those top athletes are analyzed from a new angle about the adoption of phase speed pattern. It is hopeful that this paper could provide some valuable suggestions about the puzzle of physical distribution over the swimming competitions for swimming coaches in the process of their instruction. [C9453]

"Subspace-Based Method for Multiple-Target Localization Using MIMO Radars"

The concept of multiple-input-multiple-output (MIMO) radar is recently proposed inspired by recent advances in MIMO communications. The subspace-based method for multiple-target localization is proposed in this paper. It is shown that the "effective source" covariance matrix is almost always nonsingular under mild conditions in the MIMO radar configuration. The performance of the proposed method is validated by numerical simulations. [C9454]

"Application of Doppler Spectrum for Retrieval of Statistical Parameters of Sea Waves"

The experiment for studying of microwave backscatter by the rough water surface during the flight above the Gorky water storage basin was performed. A Doppler radar (10GHz) with a knife-like beam (1deg-16deg) was installed at a helicopter and was oriented vertically downward. The analysis of the experimental data has confirmed that the width of the Doppler spectrum depends on the direction of wave propagation. The new algorithm for determination the correlation coefficient between the vertical component of the orbital velocity and water surface slopes, as well as the variance of orbital velocity was developed using the width of the Doppler spectrum of the reflected radar signal for the case of moving radar. The experimental data processing has confirmed the effectiveness of retrieval algorithm and demonstrated the possibility to determine the average phase velocity of sea waves, the average wavelength, and the significant wave height. [C9455]

"Super-imposed Mode S signals: Single-antenna Projection Algorithm and processing architecture"

This paper presents an effective algorithm to discriminate and separate superimposed SSR (secondary

surveillance radar) mode S signals. The algorithm is an adaptation of the PA (projection algorithm) [1,3,4] that perform a blind separation of the multiple SSR sources using a single channel receiver. As present-days SSR stations only have a single-channel receiver, the proposed algorithm is operatively useful, specially for multilateration and wide area multilateration applications, (M-LAT, WAM). The algorithm is evaluated with real recorded data and also simulated signals generated by a complete simulation of a typical MLAT Rx station, from the RF to the digital section. We discuss as well the estimation of the time of arrival for each overlapped signal, that is necessary for the timing. Finally we propose a possible architecture for the signals separation block of the digital processor of the receiving station. [C9456]

"Improvements of radar clutter classification in air traffic control environment"

The use of adaptive technologies may prove useful in the processing of radar signals. The proposed radar clutter classifier is aimed to improve the detection of snow clutter presence in data acquired by a ground radar system in an air traffic control environment. Each plot detected in the radar image is processed in order to extract a series of features which are then used to discriminate between targets or snow clutter. The data set used in simulations has been extracted from a measurement campaign carried out in presence of snow in Italian airports, with the help on an expert operator who manually classified a set of plots as target, or clutter. Two sets of features have been tested, one of which is derived from moments of inertia, and the second one is a specifically designed feature vector, which has been selected as to follow the reasoning scheme of a trained human observer. Three different classifiers have been tested and compared in the final stage: a Bayes classifier, a multilayer perceptron and a radial basis function network. Results indicate the best configuration exhibits a correct classification rate of about 95%. [C9457]

"Enhanced Model Order Estimation using Higher-Order Arrays"

Frequently, R-dimensional subspace-based methods are used to estimate the parameters in multi-dimensional harmonic retrieval problems in a variety of signal processing applications. Since the measured data is multi-dimensional, traditional approaches require stacking the dimensions into one highly structured matrix. Recently, we have shown how an HOSVD based low-rank approximation of the measurement tensor leads to an improved signal subspace estimate, which can be exploited in any multi-dimensional subspace-based parameter estimation scheme. To achieve this goal, it is required to estimate the model order of the multi-dimensional data. In this paper, we show how the HOSVD of the measurement tensor also enables us to improve the model order estimation step. This is due to the fact that only one set of eigenvalues is available in the matrix case. Applying the HOSVD, we obtain $R+1$ sets of n-mode singular values of the measurement tensor that are used jointly to improve the accuracy of the model order selection significantly. [C9458]

"Statistical Modeling and ML Parameter Estimation of Complex SAR Imagery"

Accurate statistical models for the complex pixels forming fine-resolution synthetic aperture radar (SAR) images are needed for several engineering applications, including coherent signal detection in SAR clutter, automatic target recognition, and automatic SAR RCS calibration without calibration targets. We derive the maximum likelihood estimator for the parameters of a complex generalized Gaussian distribution and show that it can be efficiently computed. Applying this to fine-resolution SAR images representing a wide variety of scene contents, we show that this model very accurately captures both the central regions and tails of the data distribution. [C9459]

"Slow-Time MIMO STAP with Improved Power Efficiency"

This paper concerns a multiple-input multiple-output (MIMO) generalization of space-time adaptive processing (STAP) to mitigate radar clutter subject to multipath propagation between transmit and receive arrays. Slow-time MIMO transmit channels are phase-coded to be orthogonal post-Doppler processing at the receiver ("slow-time"); and are easily implemented without receiver modification before range pulse-compression. Slow-time MIMO STAP methods coherently combine orthogonal received waveforms, steering virtual transmit nulls in cone angles responsible for multipath clutter [1]. A potential problem with MIMO STAP is the occurrence VSWR peaks over the course of a dwell. Herein, we consider sub-array designs that improve power efficiency by reducing VSWR. [C9460]

"MIMO Radar: Joint Array And Waveform Optimization"

In this paper, techniques for the optimization of multiple-input multiple-output (MIMO) radar waveform correlations and array geometries are investigated. The primary focus of this study is improved angle-estimation performance. This performance can be characterized by the Cramer-Rao angle-estimation bound and by the threshold point. The threshold point indicates the signal-to-noise ratio (SNR) at which the angle-estimation

performance of an estimation statistic deviates from the Cramer-Rao bound performance. Approximation techniques for estimating the threshold are introduced. Examples of joint waveform and array geometry optimization are presented. [C9461]

"A Handheld Texel Camera for Acquiring Near-Instantaneous 3D Images"

A Texel camera is a device which synchronously captures depth information via a ladar and digital imagery of the same scene. The ladar and digital camera are co-boresighted to eliminate parallax. This configuration fuses the ladar data to the digital image at the pixel level, eliminating complex post-processing to register the datasets. This paper describes a handheld version of a Texel Camera which can be used to create near-instantaneous 3D imagery. The hardware configuration of the Texel Camera, issues and method associated with ladar/camera calibration, and representative imagery are presented. [C9462]

"Design of FIR LS Hilbert Transformers Through Fullband Differentiators"

This paper presents some new explicit expressions for the impulse responses of the case 3, case 4, and differentiating Hilbert transformers. The proposed closed-form design is based on the fullband least-squares differentiator and relations between differentiator and Hilbert transformer. The obtained simple formulas give an efficient way to determine tap-coefficients of designed Hilbert transformers even with a hand calculator. Several numerical examples and comparison with McClellan-Parks algorithm prove the efficiency of this approach. [C9463]

"Performance Analysis of the NAMF Test in Heterogeneous Non-Gaussian Radar Clutter Scenarios"

An important issue in radar space-time adaptive processing (STAP) is the selection of training data for estimation of the unknown disturbance covariance matrix. In this paper, we address the training data selection issue and analyze the performance of normalized adaptive matched filter (NAMF) in heterogeneous non-Gaussian radar clutter scenarios. Simulations of the probability of detection (PD) versus signal-to-interference-plus-noise ratio (SINR) for the NAMF are conducted using Mountain Top data, which exhibit non-Gaussian statistics. To select the training data representative of the interference, we apply adaptive beamforming and show that PD versus SINR for NAMF is robust with respect to a wide range of variation in the beamformer output. To mitigate heterogeneous clutter, the self-censoring reiterative fast maximum likelihood (SCRFML) algorithm is employed to regularize the eigen spectrum underlying the unknown disturbance covariance matrix. We demonstrate that the NAMF detection performance can be significantly improved with the application of SCRFML. [C9464]

"A robust detector for impulsive noise environment"

This paper proposes a robust detector for detection of known signals in impulsive noise environment. The impulsive noise is assumed to be present in addition to the usual additive white Gaussian noise and is modeled as a uniformly distributed random variable that appears with a certain probability. In the paper the detector for the aforementioned noise model is derived and its performance is investigated. It is shown that the detector outperforms the usual matched filter detector in case the impulsive noise is present while the performance is similar to that of matched filter in absence of the impulsive noise. [C9465]

"Coverage in radar networks"

In this paper the coverage performance of a radar network is examined in which four different forms of processing concept are applied to the same data collected. It is found that the coverage performance can be strongly dependent on the form of the processing concept used and on the number of the nodes (for a given false alarm rate). [C9466]

"Regional Variance Dependant Sub-frame Reduction for Face Detection in High Definition Video Frames"

Statistical learning based face detection systems search multiple scale sub-frames of an image or frame of a video stream with a trained classifier to detect face objects. If the frame is large there will be a large number of these sub-frames. Sections of the frame with a regional variance below a predefined threshold do not need to be searched as it is not possible for a face to exist in these spaces. A preprocessing system to eliminate these low variance regions of a frame is presented in this paper. A top down quad-tree deconstruction of the frame is used to accomplish this task. Regional variance is computed and tested to determine if a given quadrant should be further broken down. If below a predefined threshold that region will be eliminated in a mask image. This

procedure is continued until all sections are eliminated or a defined tree depth is reached. The resulting mask image is then smoothed and subjected to thresholding, merging the remaining valid search areas. The resulting filled mask is then used to determine whether a given sub-frame should be sent to a Viola-Jones face detection cascade. Preliminary results show promise in reducing the number of sub-frames that must be considered for detection, increasing the speed of the detection system. [C9467]

"3D Scene Reconstruction through a Fusion of Passive Video and Lidar Imagery"

Geometric structure of a scene can be reconstructed using many methods. In recent years, two prominent approaches have been digital photogrammetric analysis using passive stereo imagery and feature extraction from lidar point clouds. In the first method, the traditional technique relies on finding common points in two or more 2D images that were acquired from different view perspectives. More recently, similar approaches have been proposed where stereo mosaics are built from aerial video using parallel ray interpolation, and surfaces are subsequently extracted from these mosaics using stereo geometry. Although the lidar data inherently contain 2.5 or 3 dimensional information, they also require processing to extract surfaces. In general, structure from stereo approaches work well when the scene surfaces are flat and have strong edges in the video frames. Lidar processing works well when the data is densely sampled. In this paper, we analyze and discuss the pros and cons of the two approaches. We also present three challenging situations that illustrate the benefits that could be derived from this data fusion: when one or more edges are not clearly visible in the video frames, when the lidar data sampling density is low, and when the object surface is not planar. Examples are provided from the processing of real airborne data gathered using a combination of lidar and passive imagery taken from separate aircraft platforms at different times. [C9468]

"Adapting to Change: The CFAR Problem in Advanced Hyperspectral Detection"

Newer, realistic models of targets and backgrounds used in hyperspectral detection do not always lend themselves to a CFAR (constant false alarm rate) formulation. Several advanced techniques are considered here. It is found that incorporating a particular empirically validated method of target evolution permits an exact CFAR version of a large class of advanced detectors based on elliptically contoured distributions. Other validated detectors are considered, for which no closed form normalization exists to convert them to CFAR form. For these a geometrical approach to achieving approximate CFAR performance is described and analyzed. [C9469]

"In Situ Adaptive Feature Extraction for Underwater Target Classification"

This research compares the performance improvements of image-based sonar target classification algorithms when they are adapted to changing clutter environments. The distribution of seabed pixels in the sonar imagery is modeled as a correlated, K-distributed random variable allowing for a quantitative representation of seabed environments in the various testing scenarios. Parameterized environments comprising various target-like seabed textures are generated synthetically and used to examine adaptive classification performance. Results demonstrate that optimizing classifier parameters respective to specific environments improves overall classification performance compared to optimizing classifier parameters against a pooled dataset that includes all possible environments. [C9470]

"On Data-Adaptive Waveform Design for MIMO Radar"

We consider the problem of signal design for MIMO radars, where the transmit waveforms are adjusted based on the characteristics of the radar scene. A model for the radar returns which explicitly incorporates the transmit waveforms is presented. The waveforms are designed to optimize the estimation of the radar scene. An adaptive design can provide improved estimation performance compared to fixed designs such as the one employing a set of orthogonal waveforms. [C9471]

"MIMO Radar Ambiguity Optimization Using Frequency-Hopping Waveforms"

Recently, the concept of MIMO (multiple-input- multiple-output) radars has drawn considerable attention. In traditional SIMO (single-input-multiple-output) radar, the transmitters emit coherent waveforms to form a focused beam. In MIMO radar, the transmitters emit orthogonal (or incoherent) waveforms to increase the spatial resolution. These waveforms also affect the range and Doppler resolution which can be characterized by the ambiguity function. In traditional (SIMO) radars, the ambiguity function of the transmitted pulse characterizes the compromise between range and Doppler resolutions. In the MIMO radar, since many transmitting waveforms are involved, their cross-ambiguity functions enter into the signal design problem. In this paper, frequency hopping codes are used to generate these orthogonal MIMO radar waveforms. A new algorithm for designing the frequency hopping codes is proposed. This algorithm makes the energy in the corresponding ambiguity functions evenly spread in the range and angular dimensions. [C9472]

"Parameter Estimation and Number Detection of MIMO Radar Targets"

This paper considers the problem of target parameter estimation and number detection of multi-input multi-output (MIMO) radar targets. Cyclic optimization algorithms are presented to obtain the maximum likelihood (ML) estimates of the target parameters and a Bayesian information criterion (BIC) is used for target number detection. Specifically, an approximate cyclic optimization (ACO) approach is first presented, which maximizes the likelihood function approximately. Then an exact cyclic optimization (ECO) approach that maximizes the exact likelihood function is introduced for target parameter estimation. The ACO and ECO target parameter estimates are used with the BIC for target number determination. Numerical examples are presented to demonstrate the effectiveness of the proposed approaches for target parameter estimation and target number detection. [C9473]

"Signal Covariance Matrix Optimization for Transmit Beamforming in MIMO Radars"

MIMO radars use multiple waveforms simultaneously to improve performance. A beamforming method that exploits this waveform diversity has been proposed previously. This method works by optimizing the covariance matrix of the waveforms to obtain an approximation of a desired beampattern. The previous method uses gradient descent to optimize the beampattern with the constraint on the power of each antenna element. We show how this method can be extended to obtain rank-deficient covariance matrices and also to handle the total power constraint. The conjugate gradient method is used in addition to the gradient descent. In this paper, we also propose converting the constrained beampattern optimization problem into an unconstrained one. This can be done by using the method of Lagrange multipliers, but also removing all constraints and then scaling the result so that the total power constraint is satisfied. Using this approach, the beampattern optimization can be written as a least squares problem. [C9474]

"Performance Prediction and Verification for the Synchronization Link of TanDEM-X"

The paper describes the synchronization link of the two satellites of the TanDEM-X mission. The synchronization link is established to track the oscillator phase noise difference which- after appropriate processing-can be used to compensate the effect of oscillator phase noise. A signal model based on the synchronization link hardware is presented which is then used to derive an analytical expression for the compensation phase including effects such as instrument drift, Doppler, antennas, and receiver noise. Specifically the influence of the synchronization link RF hardware on the quality of the derived compensation signal is crucial for the performance. Therefore the synchronization link RF hardware of the TerraSAR-X satellite is characterized to obtain realistic data. These measurements will be used for the calibration of the synchronization link, i.e. to remove systematic errors due to temperature drifts of the instrument. [C9475]

"Prediction and detection of Faraday rotation in ALOS PALSAR data"

Faraday rotation can degrade the quality of low- frequency spaceborne SAR data, making an estimation and correction of these effects a prerequisite for data quality continuity. In this paper, methods for predicting and estimating Faraday rotation are presented and tested on ALOS/PALSAR data. A first example for unambiguous detection of Faraday rotation in SAR is shown. In addition, the improvement after correcting for FR is proven using a real data example. [C9476]

"Full motion compensation for LFM-CW synthetic aperture radar"

Small, low-cost, high-resolution SAR systems, such as the Brigham Young University (BYU) muSAR, are made possible by using a linear frequency modulated continuous wave (LFM-CW) signal. SAR processing assumes that the sensor is moving in a straight line at a constant speed, but in actuality a UAV or airplane will deviate, often significantly, from this ideal. This non-ideal motion can seriously degrade the SAR image quality. In a continuous wave system this motion happens during the radar pulse which means that existing motion compensation techniques, which approximate the position as constant over a pulse, are limited for an LFM-CW SAR. In this paper, the LFM-CW SAR signal model is presented and processing algorithms are discussed. The effects of non-ideal motion during the SAR signal are derived and new methods for motion correction are developed which correct for motion during the pulse. These new motion correction algorithms are verified with simulated data and with actual data collected using the BYU muSAR system. [C9477]

"Individual T/R module characterisation of the TerraSAR-X active phased array antenna by calibration pulse sequences with orthogonal codes"

TerraSAR-X is a high resolution synthetic aperture radar (SAR) satellite due for launch in 2007. Its active

phased array X-Band antenna hosts 384 transmit/receive modules controlling the beam steering in azimuth and elevation direction. Precise modelling of the antenna is only possible if the actual characteristics of each individual transmit/receive module are known. TerraSAR-X has been equipped with an innovative characterisation mode based on the so-called PN Gating method. Individual and simultaneous characterisation of all transmit/receive modules is realised under most realistic conditions with the same power loads like in the nominal mode. This paper shows the results of PN Gating measurements on a satellite SAR system. [C9478]

"Analysis and improvement of polarimetric calibration techniques"

This work presents an analytical study of the Quegan's PolSAR data calibration algorithm. As it shall be demonstrated, the solution proposed by Quegan based on certain approximations, gives in certain situations, biased crosstalk ratios u , v , w and z . An improved Quegan's calibration algorithm is proposed and tested. [C9479]

"Characterization of local regularity in SAR Imagery by means of multiscale techniques: application to oil spill detection"

Thanks to their capability to cover large areas, in all weather conditions, during the day as well as during the night, spaceborne Synthetic Aperture Radar (SAR) techniques constitute an extremely promising alternative to traditional surveillance methods. Nevertheless, in order to assure further usability of SAR images, specific data mining tools are still to be developed to provide an efficient automatic interpretation of SAR data. The aim of this paper is to introduce texture analysis performed in the framework of time-frequency theory, as a means to detect oil spills in the sea surface. In particular, an algorithm permitting a precise quantitative characterization of the border between the oil spill candidate and the sea, will allow a novel classification of oil spills and look-alikes. [C9480]

"ALOS PALSAR products verification"

ALOS, an enhanced successor of the Japanese Earth Resources Satellite 1 (JERS-1), was launched from JAXA's Tanegashima Space Center in January 2006. An important contribution to the ALOS mission is the verification of PALSAR products to be distributed by the European ADEN node using the PALSAR processor developed by JAXA. A total of 28 ALOS PALSAR products have been analysed with respect to radiometric, geometric and polarimetric quality (including effects of Faraday rotation caused by the ionosphere) and a summary of the results is shown in this paper. [C9481]

"Calibration of the SHARAD Instrument"

The Mars Shallow Radar Sounder (SHARAD) is an HF (20 MHz) Sounding Radar embarked onboard the Mars Reconnaissance Orbiter (MRO) spacecraft. SHARAD on-ground calibration activities have been limited to the characterization of the SEB (SHARAD Electronic Box), not having been possible to perform extensive characterization of the flight antenna nor end- to-end calibrations on ground. Scope of the present document is to define the activities to be carried out in-flight in order to ensure SHARAD products calibration. The calibration needs are assessed and an overall calibration strategy is then defined, leading to the identification of the data sets to be collected and relevant processing to be applied. The document also address how to exploit the available calibration data (from both on- ground and in-flight calibration) to correct SHARAD products, and the organization of the calibration database. [C9482]

"Inversion of soil moisture content from L- and P-band AIRSAR polarimetric SAR data"

Improvements of polarimetric inversion algorithms is presented in this paper. The confounding influence of roughness and vegetation cover on the estimation of the soil moisture contents is considered in the inversion algorithm that estimates volumetric moisture contents and roughness parameters simultaneously from the pertinent combination of polarization measurements. The estimation of the soil moisture contents from polarimetric SAR data is investigated using L- and P-band AIRSAR polarimetric SAR data collected over the Jeju Island, Korea. Results indicate that the estimation of the soil moisture contents can be expanded to a wider range of terrain types by using both L- and P-band polarimetric SAR data. [C9483]

"An improved time-frequency phase adjustment technique for ISAR"

The time-frequency method is a promising phase adjustment technique for inverse synthetic aperture radar (ISAR). Usually, the time-frequency method estimates the translational Doppler frequency and thus the translational Doppler phase by detecting the peaks of the time-frequency representation at different times. Unfortunately, it has some defects, such as the sensitivity to noise and target scintillation, and the aliasing of the

time-frequency representation due to undersampling. In order to remove these limitations, we develop an improved time-frequency method. It estimates the translational Doppler frequency from the envelope correlation of the instantaneous slices of the time-frequency representation. Compared with the traditional time-frequency method, this technique can estimate the translational Doppler frequency more accurately. Moreover, we develop a preprocessing method to avoid the aliasing of the time-frequency representation due to undersampling.

[C9484]

"The fractional Fourier transform and its application to high resolution SAR imaging"

The fractional Fourier transform (FrFT), which is a generalized form of the well-known Fourier transform, has opened up the possibility of a new range of potentially promising and useful applications including radar involving the use and detection of chirp signals, pattern recognition and Synthetic Aperture Radar (SAR) image processing. The Chirp Scaling Algorithm (CSA) is one of the most important and well-known radar imaging algorithms. It is attractive because of its excellent focusing ability and implementation simplicity. Benefiting from the inherent structure of the FrFT for non-stationary digital signal processing and analysis, especially for chirped-type signals, a new version of the CSA based on the Fractional Fourier Transform (FrFT) is developed. The introduced Fractional Chirp Scaling Algorithm (FrCSA) applied the Fast Fourier Transform (FFT) instead of the fractional Fourier transform (FrFT) in the azimuth direction for the analytical development tractability purposes only as it is numerically tractable in both dimensions. To demonstrate the resolution and focusing enhancement in the azimuth dimension using the FrCSA and also to be able to perform azimuth fractional filtering, noise removal and flight path nonlinearity compensation, a closed form expression for the azimuth fractional transformation is required. In this talk we present the mathematical derivation for a closed-form expression of the azimuth-fractional Fourier transform of the new FrCSA with application to high resolution imaging. Results to real SAR data images will show significantly enhanced features using the FrFT-based azimuth expression instead of the classical FFT-based one within the fractional chirp scaling algorithm or any other chirped-type SAR imaging algorithm. [C9485]

"Evaluation of the altimetric information from RADARSAT-1, ASTER and SRTM data for topographic mapping in the Amazon Region"

Brazilian Amazon is a vast territory rich in natural renewable and non-renewable resources. Due to the adverse environmental condition (rain, cloud, dense vegetation, poor access), topographic information is still poor, and when available needs to be up-dated or re-mapped. In this paper, the feasibility of using altimetric information for topographic mapping through orbital stereoscopic (ASTER, RADARSAT-1) and interferometric (SRTM-3) DEMs (digital elevation models) was investigated for two regions in the Brazilian Amazon: Tapajos National Forest (flat terrain) and Serra dos Carajas (mountainous relief). The quality of information produced from these data was evaluated regarding field altimetric measurements. Precise topographic field information acquired from differential global positioning system (DGPS) was used as Ground Control Points (GCPs) for the modeling of the stereoscopic DEMs and as independent check points (ICPs) for the calculation of altimetric accuracies of the products. The investigation has shown that the accuracy of the altimetric information derived from Fine RADARSAT-1, ASTER and SRTM-3 DEMs met the requirements for a semi-detailed (1:100,000-map) scale as requested by the Brazilian standard for cartographic accuracy. Furthermore, SRTM-3 DEM was more accurate than stereoscopic DEMs. The additional great advantage of using SRTM-3 is the free access data. However, updated planimetric information is also necessary for cartographic production. Thus it is suggested a combination of altimetry derived for SRTM-3 and planimetry from high-resolution SAR (Fine RADARSAT-1, PALSAR) or if possible optical data (ASTER, SPOT) for topographic mapping at semi-detailed scale in similar environments of the Brazilian Amazon, where terrain information is seldom available or presents low quality. [C9486]

"Joint time-frequency analysis for radar signal and imaging"

The Fourier transform has been widely used in SAR signal and image processing. In most cases, SAR signals exhibit time-varying behavior in the Doppler spectrum. Thus, a joint time-frequency analysis (JTFA) for SAR signals is more useful. In this paper, we introduce three important issues with JTFA for radar signal and imaging: (1) time-frequency based image formation; (2) time-frequency analysis of ground moving targets; and (3) time-frequency analysis of micro-Doppler signatures. [C9487]

"Characterization of scatterers by their anisotropic and dispersive behavior"

Synthetic Aperture Radar (SAR) images built from received signals are high-resolution maps of the spatial distribution of the reflectivity function of targets. Conventional radar imaging assumes that all the scatterers are considered as bright points (isotropic for all observation angles and white in the frequency band) [1]. Recent studies based on multidimensional Time-Frequency Analysis describe the angular and frequency behavior of

scatterers and show that they are anisotropic and dispersive [2]. Another useful information source in radar imaging is the polarimetry. Studies based on multidimensional wavelet and coherent decompositions allow to represent the angular and frequency polarimetric behavior and show the non-stationarity of this behavior. The aim is to characterize scatterers by time-frequency analysis and polarimetry. [C9488]

"Subaperture analysis of polarimetric SAR imagery"

In this paper we investigate the nonstationary behavior of individual polarimetric parameters, e.g. entropy, anisotropy, alpha angle, orientation angle, helicity, etc. We distinguish between parameters that depend solely on the eigenvalues of the standard Cloude-Pottier polarimetric decomposition (span, entropy and anisotropy) and the others that depend on the scattering mechanisms, i.e. the Cloude-Pottier eigenvectors. After producing a series of azimuth subaperture polarimetric images, we apply the polarimetric decomposition to each subaperture frame and identify subaperture frames that show nonstationary scattering. Comparison of several specific targets, both discrete and distributed, will highlight aspects of polarimetric variability with respect to the SAR view angle. We illustrate our results using EMISAR L-band polarimetric SAR data. [C9489]

"The cross Time-Frequency Distribution Series for Synthetic Aperture Radar (SAR) applications"

Joint Time Frequency Analysis (JTFA) is a powerful analysis tool in SAR image processing. At the heart of this process are the Time-Frequency Representations (TFR's) such as the Wigner-Ville distribution (WVD), which is difficult to use because of its large cross-product terms. The pseudo-WV TFR reduces the cross terms by smoothing the integration defining the WV transform. The Time-Frequency Distribution Series (TFDS) mitigates the unwanted cross product terms by averaging only those expansion terms close to the signal. The cross-Wigner-Ville Distribution (CWVD) is a generalization of the cross correlation function to the time-frequency (TF) plane. Likewise, the cross- pseudo-WV and the cross-TFDS can be defined and applied to pairs of signals. The cross-TFDS is shown to reduce the cross terms seen in the cross-WV distribution. Two examples are shown using SAR data. [C9490]

"Complex scene analysis from Time-Frequency statistics of POLSAR data"

This article presents a statistical approach for the study of PolSAR images using Time-Frequency (TF) correlation properties. PolSAR information is analyzed using a linear time- frequency (TF) decomposition which permits to describe a scene polarimetric behavior for different azimuth angles of observation and frequencies of illumination. A TF signal model is proposed and studied using two statistical descriptors related to the signal stationary aspect and coherence in the time-frequency domain. These indicators are shown to provide complementary information for an enhanced description of the scene. [C9491]

"A low-cost imaging radar: DRIVE on board ONERA motorglider"

UAVs from different countries and with different payloads have proven their capabilities within military applications. Future UAV employment in the civilian areas of surveillance (pollution, natural risks prevention, fire prevention), monitoring (traffic control, environmental monitoring, earth observation) and communication relays becomes unavoidable. Many payload configurations may be used in UAV operations, but compared to systems working in other spectral regions (such as optical or infrared sensors), radar has the main advantage to be able to operate in all-weather condition. A concept of low-cost imaging Ka-Band radar is presented in this paper. This radar is integrated into under-wings pods that are fixed on a STEMME S10VT motorglider. This radar concept combines real aperture in the cross-track direction, by the antennas geometrical aperture, and synthetic aperture in the along-track direction, realized with the aircraft motion. Radar front-end uses FMCW technique which allows to reduce the power emission to a few Watts. In addition, the use of the millimeter band induces antennas size reduction, and makes possible the radar integration into pods. Thus, radar particularities are a low-size, a low-weight and a low-cost basis, making this radar suitable for future integration on board small vehicles, such as UAV. The radar definition and specifications will be detailed, together with the first results obtained on Fall 2006. Two ways of operating the radar will be presented: An application as vertical sounder, using horn antennas, and an application as SAR radar, using rectangular antennas. The two cases will be illustrated by samples of acquisitions results. The DRIVE radar has been developed and built to fly on board an UAV vehicle. Indeed, this radar is designed and will be used by ONERA as a UAV radar test bench. Current airplane used for testing applications is a STEMME S10-VT motorglider as the geometry of this airplane may be representative of a MALE UAV-: wingspan is 23 m large and weigh is about 900 kilograms. DRIVE Project started at ONERA on January 2005, and first flights happened in the beginning of 2006. DRIVE radar uses FMCW techniques and operates in Ka Frequency Band: Central frequency is 35 GHz and bandwidth is about 800 MHz width. [C9492]

"Image quality analysis of the vibrating sparse MIMO antenna array of the airborne 3D imaging"

radar ARTINO"

ARTINO is a new radar system, integrated in a small mobile and dismountable experimental UAV. The side-looking geometry of usual SAR systems produces shading effects of the scene to be imaged. ARTINO overcomes this restriction with the ability to image the direct overflowed area (Nadir looking) in three dimensions. The effects caused by vibrations of the used sparse MIMO antenna array- which is embedded in the wings of the airplane- are discussed with respect to the 3D imaging quality. A correction approach within the image formation process is presented, too. [C9493]

"A space-time minimum cost flow phase unwrapping algorithm for the generation of persistent scatterers deformation time-series"

We have investigated the phase retrieval capability of the Extended Minimum Cost Flow (EMCF) phase unwrapping (PhU) approach in the framework of the Persistent Scatterers Interferometry (PSI) algorithms for the generation of deformation time-series. The presented technique exploits an appropriate selection of full resolution interferograms obtained via a triangulation step carried out in the Temporal/Perpendicular baseline plane, where the available SAR image sequence is represented. Moreover, the phase unwrapping procedure is implemented via the cascade of two steps, based on the conventional Minimum Cost Flow (MCF) algorithm, that allows us to exploit both the spatial characteristics and the temporal relationships among the produced interferograms. The presented experiments, carried out by analyzing a set of 43 ERS SAR images relevant to an area of the city of Rome (Italy), confirm the effectiveness of the exploited PhU approach. [C9494]

"A new framework for multi-pass SAR interferometry with distributed targets"

This paper focuses on multi-pass spaceborne synthetic aperture radar interferometry (InSAR) in presence of distributed scattering, paying particular attention to the role of target decorrelation in the estimation process. This phenomenon is accounted for by splitting the analysis into two steps. In the first step we estimate the interferometric phases from the data, while in the second step we use these phases to retrieve the physical parameters of interest, such as LOS displacement and residual topography. This approach is suited both to derive the performances of InSAR with different decorrelation models and for providing an actual estimate of LOS motion and DEM. Results achieved from Monte-Carlo simulations and a set of repeated pass ENVISAT images are shown. [C9495]

"The family of atomic functions and digital signal processing in synthetic aperture radar"

The report consists of two parts. In the first part, the sampling analysis of weight windows is conducted on the basis of atomic functions (AF) and their application in problems of the classical method of synthetic aperture radar (SAR) is considered. The second part contains fundamentals of a modified method of synthesizing the aperture. The modified ambiguity function for different signals is probed. The lacks of the Ambiguity function are detected at a modified method. The paths of elimination of the indicated lacks are offered by introduction of weight processing in a technique of the modified method. The expediency of application of weight windows based on AF in reduced problems is empirically justified. [C9496]

"Intellectual multisurvey processing of radar information"

Intellectual system algorithms of low-sized air objects detection against radar clutters are offered. These algorithms, based on predicate algebra techniques, provide automation of multisurvey information processing and increase detection efficiency due to accumulation of signal (power) and logic information in analyzed resolution cell and its neighborhood. Thus processing speed (data-rate) is increased and online data processing. [C9497]

"A three dimensional SAR system on an UAV"

Applications of small unmanned aerial vehicles (UAVs) have increased steadily over the past years. Applications are found in Earth observation, reconnaissance, monitoring, and surveillance missions using imaging systems. The big advantage of radar sensors is their all-weather capability. Especially imaging radars possess several benefits over optical systems, as they are not affected by rain, snow, fog, or the time of day. The advantages using small unmanned platforms come at the cost of having to deal with restrictions on weight and volume. Hence, these parameters are the predominant design drivers for UAV sensor developments. This paper presents the concept, the technical realization and the status of a 3D imaging radar system suitable for small UAVs. ARTINO (Airborne Radar for Three dimensional Imaging and Nadir Observation) combines a real aperture, realized by a linear array of nadir pointing antennas, and a synthetic aperture, which is spanned by the moving airplane. [C9498]

"Annealed Differential Evolution"

Differential evolution (DE) has recently emerged as a leading methodology for global search and optimization over continuous, high-dimensional spaces. It has been successfully applied to a wide variety of nearly intractable engineering problems. However, the DE and its variants usually employ a deterministic selection mechanism that always allows the better solution to survive to the next generation. This often prevents DE from escaping local optima at the early stages of search over a multi-modal fitness landscape and leads to a premature convergence. The present work proposes to improve the accuracy and convergence speed of DE by introducing a stochastic selection mechanism. The idea of a conditional acceptance function (that allows accepting inferior solutions with a gradually decaying probability) is borrowed from the realm of the simulated annealing (SA). In addition, the work proposes a center of mass based mutation operator and a decreasing crossover rate in DE. Performance of the resulting hybrid algorithm has been compared with three state-of-the-art adaptive DE schemes. The method is shown to be statistically significantly better on a six-function test-bed and one difficult engineering optimization problem with respect to the following performance measures: solution quality, time to find the solution, frequency of finding the solution, and scalability. [C9499]

"New potentials of differential SAR tomography: Volumetric differential interferometry and robust DEM generation"

A new interferometric SAR mode has been recently introduced termed differential interferometry (Diff-Tomo). In this paper, two new potentials coming from the joint elevation-velocity resolution capability of Diff-Tomo are introduced. The first concerns differential measurements and elevation profiling of volumetric scatterers with non-rigid motion and possible temporal decorrelation. The second concerns estimation of terrain elevations which is robust to some temporal decorrelation effects. Simulated results are reported as a first preliminary probing of performance and limits of these methods. [C9500]

"Advances in real time lidar spectroscopy"

We summarize the resolution limits and potential sensitivity of existing Hoar-spectrometer systems. The spectral resolution of these systems is limited primarily by the phase space area (etendue), which depends on the width and convergence angle of the laser beam's image on the spectrometer input slit. Decreasing the beam's image width can be achieved with conventional optics at the expense of an increase in convergence angle, which often results in a loss in coupling efficiency due to mismatching with the spectrometer's phase space area. We describe how this limitation has been overcome using suitably designed optical fiber bundles. We also discuss both theoretical and computer modeling predictions of the variation in telescope-to-spectrometer coupling efficiency with range for lidar spectrometers. Finally we compare the performance of photon counters and intensified CCD arrays and discuss methods of range-gating their outputs. [C9501]

"Lidar method for determination of quartz concentration in the tropospheric mineral aerosols"

We present a lidar method that enables the determination of quartz concentration in mineral aerosols. The method combines the Raman scattering lidar using a 466 cm⁻¹ quartz line with a high-spectral resolution lidar (HSRL). The methodology and experimental results are described. [C9502]

"Developing a GeoSTAR science mission"

The geostationary synthetic thinned aperture radiometer (GeoSTAR) is a new instrument design that has been under development at the Jet Propulsion Laboratory in the form of a proof-of-concept prototype. It is intended to fill a serious gap in our Earth remote sensing capabilities—namely the lack of a microwave atmospheric sounder in geostationary orbit. Such sensors have long been part of low-earth-orbiting (LEO) operational weather satellites and research satellites and have had a major impact ranging from numerical weather prediction to climate research. A similar capability in GEO is highly desired because of the advantageous observing point GEO offers, with continuous views of the entire visible Earth disc—crucial for the observation of hurricanes and other rapidly evolving atmospheric phenomena. GEO also enables full resolution of the diurnal cycle, which is particularly important in the study of atmospheric processes and climate variability where clouds and convection play a role, since those phenomena are known to have strong diurnal variability and are difficult to sample properly with sun synchronous LEO satellites. The GeoSTAR prototype produced the first interferometric radiometric images obtained at sounding frequencies in early 2005, and subsequent tests have demonstrated that the system exhibits excellent stability, accuracy and sensitivity and performs even better than predicted. This can be characterized as a breakthrough development. The technology required to implement GeoSTAR is at a level of maturity that a space mission can be contemplated. Such a mission is recommended by the U.S. National Research Council in its recent Decadal Survey of Earth missions and is being considered by both NASA

and NOAA for the coming decade. Recent studies indicate that it is indeed feasible to implement a GeoSTAR mission in the 2014-16 time frame. We discuss possible mission scenarios as well as the science benefits that would ensue. The benefits are particularly significant in the area of tropical cyclones and severe storms, where there currently is a dearth of observations. With a geostationary microwave sounder it is possible to obtain the 3-dimensional distribution of temperature, water vapor and liquid water continuously and regardless of cloud cover, and atmospheric stability indices such as lifted index (LI) and convective available potential energy (CAPE) can be derived nearly everywhere. That will make it possible, for example, to detect severe-storm precursor conditions even if the area is under cloud cover. Recent progress in radiative transfer models now also makes it possible to obtain those parameters in the presence of moderate precipitation, and rain rates and snow rates can be derived as well. Aircraft based field campaign observations have also shown that a microwave sounder can be used to derive measures of convective intensity and precipitation in deep-convective systems from scattering due to ice particles formed by such systems. This can be used to estimate the intensity of tropical cyclones and can be used to detect sudden intensification and weakening in near-real time. [C9503]

"Improved receiver architecture for future L-band radiometer missions"

Microwave radiometer measurements are a viable technique for measurement of soil moisture and ocean salinity. Therefore, there is a strong interest in new L-band remote sensing radiometers. For example, European Space Agency's SMOS (soil moisture and ocean salinity) satellite is currently under development. SMOS applies Noise Injection Radiometer subsystem for the measurement of the average brightness temperature of the scene. This paper proposes the use of reference channel control method for the future L-band radiometer missions, e.g., for potential SMOS follow-on mission. According to analysis, significant improvement in radiometric resolution (up to 40%) would be achieved compared to traditional antenna channel noise injection architecture. The proposed system is based on the use of an active cold load (ACL) as cold reference. [C9504]

"Multi baseline SAR acquisition concepts and phase unwrapping algorithms for the TanDEM-X mission"

The TanDEM-X (TerraSAR-X add-on for Digital Elevation Measurement) mission will start in 2009 with the aim of generating a global Digital Elevation Model with high accuracy corresponding to HRTI-3 specifications (12 m posting, 2 m relative point-to-point height accuracy for flat terrain). To achieve this goal, a second satellite similar to TerraSAR-X will fly close to TerraSAR-X in a controlled Helix configuration for 3 years to jointly acquire interferometric SAR data in bistatic mode. According to the current mission concept, there will be at least two complete coverages of the global land surface, each one running one year. The different coverages will have different heights of ambiguity to allow multi-baseline phase unwrapping. For the sake of a homogenous data quality the second acquisition will be shifted by half the swath width with respect to the first coverage. Finally difficult terrain will be covered two more times with different acquisition geometries (i.e. different look direction and/or incidence angles). This paper presents first study results of phase unwrapping algorithms foreseen to process SAR data from the bistatic TanDEM-X configuration. [C9505]

"Spaceborne multi-dimensional SAR imaging: Current status and perspectives"

Multi-Dimensional (MultiD) SAR imaging is a modern technique, based on coherent SAR data combination, aimed to space (full-3D) and space deformation-velocity (4D) analysis. It extends the concept of SAR interferometry and differential interferometry and offers new options for the analysis and monitoring of ground scenes. With this regard, we discuss the current status and the results obtained by processing ERS real data, we investigate perspectives related to the next generation multi-static satellite formations, and we show some sample results regarding 3D and 4D theoretical performance bounds. [C9506]

"Lidar, sun photometer and polar nephelometer measurements: Remote sensing of aerosol size distribution properties"

We are developing new sensors to measure aerosols using lidar, automated Sun photometers, and in situ polar nephelometers. The lidar measurements are based on a ground system using a 532 nm laser. The sun photometer are based on a custom Sun tracking design. The aerosol phase function measurements are based on a custom polar nephelometer system developed at the University of Hawaii. Results from our first joint field experiment using these new systems will be discussed. [C9507]

"A new type of lidar for atmospheric optical turbulence"

We are developing a new type of lidar for measuring range profiles of atmospheric optical turbulence. The lidar is based on a measurement concept that is immune to artifacts caused by effects such as vibration and defocus.

Four different types of analysis and experiment have all shown that a turbulence lidar built from commercially-available components will attain a demanding set of performance goals. The lidar is currently being built for testing scheduled in 2007. [C9508]

"Disaster monitoring by extracting geophysical parameters from SAR data"

The fractal geometry proved to be the most appropriate mathematical instrument in describing natural scenes, by means of few effective and reliable geophysical parameters. In this paper we use fractal concepts to model and to identify geometrical changes occurred in areas hit by disasters. We present an overall framework employing fractal based models, algorithms and tools to support identification of natural area changes due to natural or man-made disasters. The proposed framework includes a SAR raw signal simulator, which is of key importance to improve the comprehension of the mechanisms underlying SAR image formation. In addition, we consider, as a case study, the simulation and detection of lava flows in a volcanic scenario. The potentialities of our technique for the discrimination between different types of lava are presented and discussed. [C9509]

"ICC's project for DInSAR terrain subsidence monitoring of the catalonian territory"

The Institut Cartografic de Catalunya (ICC) has initiated a project for continuous subsidence monitoring of the Catalan territory using an automatic advanced DInSAR processor (DISICC). Data used in this project are acquired by ERS-1/2, ENVISAT, and the future ALOS, TerraSAR-X and Radarsat 2 satellites. The processor performs the co-registration, interferogram generation, filtering, topographic cancellation, linear deformation model adjustment and non-linear displacement estimation, allowing the generation of classical and advanced DInSAR results combining information from different orbits and satellites. The project consists of the usage of 10 different ERS/ENVISAT frames, 5 descending and 5 ascending, completely covering the desired area, which is about 31.930 Km². The data temporal frame comprises images acquired from 1992 to 2006. [C9510]

"Multidimensional radar waveforms a new paradigm for the design and operation of highly performant spaceborne synthetic aperture radar systems"

This paper introduces and analyses the innovative paradigm of multidimensional waveform encoding for spaceborne synthetic aperture radar (SAR). The combination of this technique with digital beamforming on receive enables a new class of highly performant SAR systems employing novel and highly flexible radar imaging modes. Examples are adaptive high-resolution wide-swath SAR imaging with compact antennas, enhanced parameter estimation sensitivity for applications like along-track interferometry and moving object indication, and the implementation of hybrid SAR imaging modes that are well suited to satisfy the hitherto incompatible user requirements for frequent monitoring and detailed mapping. Implementation specific issues will be discussed and examples demonstrate the potential of the new technique for different remote sensing applications. [C9511]

"SBRAS-an advanced simulator of spaceborne radar"

An application-oriented spaceborne radar advanced simulator (SBRAS) is presented in this paper. SBRAS is initiated by the technical and economical requirements to verify formation-flying distributed satellites synthetic aperture radar (SAR) scheme and simplify the instrument hardware design. The simulator develops a full flow of signal processing including formation design, SAR raw data simulation of nature scene, imaging, InSAR processing, digital elevation model (DEM) generation and performance analysis. A user-friendly GUI is provided. [C9512]

"Extinction-to-backscatter ratios of lofted aerosol layers observed during the first three months of CALIPSO measurements"

Case studies from the first three months of the Cloud and Aerosol Lidar and Infrared Pathfinder Spaceborne Observations (CALIPSO) measurements of lofted aerosol layers are analyzed using transmittance [Young, 1995] and two-wavelength algorithms [Vaughan et al, 2004] to determine the aerosol extinction-to-backscatter ratios at 532 and 1064 nm. The transmittance method requires clear air below the layer so that the transmittance through the layer can be determined. Suitable scenes are selected from the browse images and clear air below features is identified by low 532 nm backscatter signal and confirmed by low depolarization and color ratios. The transmittance and two-wavelength techniques are applied to a number of lofted layers and the extinction-to-backscatter ratios are compared with values obtained from the CALIPSO aerosol models [Omar et al, 2004]. The results obtained from these studies are used to adjust the aerosol models and develop observations based extinction-to-backscatter ratio look-up tables and phase functions. Values obtained by these techniques are compared to Sadeterminations using other independent methods with a goal of developing probability distribution functions of aerosol type-specific extinction to backscatter ratios. [C9513]

"ADM-Aeolus: The first space-based high spectral resolution Doppler Wind Lidar"

The 'Living Planet Programme' of the European Space Agency (ESA) is gaining momentum. Six Earth Explorer missions are currently being implemented including ADM- Aeolus, ESA's Doppler Wind Lidar (DWL) mission. The Aeolus mission will demonstrate the capability of a space- borne high spectral resolution DWL to accurately measure wind profiles in the troposphere and the lower stratosphere (0- 30 km). The Mission thus addresses one of the main identified deficiencies of the current Global Observing System (GOS). From the backscattered frequency-shifted laser light it will be possible to obtain about 3,000 globally distributed horizontal line-of-sight (HLOS) wind profiles daily. The accuracy of the Aeolus winds, in cloud-free regions and above thick clouds, is expected to be comparable to that of radiosonde wind measurements. Additional geophysical products that will be retrieved from the Aeolus measurements are cloud and aerosol optical properties. Aeolus HLOS wind profiles will find wide application in Numerical Weather Prediction (NWP) and climate studies, improving the accuracy of numerical weather forecasting, advancing our understanding of tropical dynamics and processes relevant to climate variability and climate modelling. Impact experiments, assimilating synthetic Aeolus wind data into operational NWP models, have already been performed. One focus has been the forecast performance in regions known to be particularly sensitive to the accuracy of the initial conditions. The tentative results show that the largest benefits from Aeolus HLOS winds can be expected over the oceans and in the Tropics. In view of other lidar missions in space, the potential of a long-term database of cloud and aerosol optical properties is being studied. An additional topic is the potential benefit of wind profile observations in the lower stratosphere. Ground-based and airborne campaigns are being prepared for the validation of the Aeolus Airborne Demonstrator (A2D)-a high spectral- resolution DWL instrument with technology very similar to Aeolus. This paper provides an overview of the Aeolus mission, the science and application activities being performed in support of the mission and the potential benefit of such observations in a wider context. [C9514]

"Numerical simulation of electromagnetic-wave propagation for land mine detection using GPR"

The ground penetrating radar (GPR) has demonstrated good potential for the remote imaging of surface-laid or shallow-buried landmine-like objects (typically ~ 5-30 cm) and its use is currently receiving much attention. It has turned out to be a promising alternative technology for low dielectric contrast objects, a difficult detection situation that is often encountered in practise (e.g. detection of plastic mines in dry or sandy soils environment). This paper examines numerically the imaging of buried objects using ultrawide-band (UWB) time domain radar. We develop a simplified model to characterize the system, air-ground-buried targets-antennas and simulate the electromagnetic wave propagation and scattering at a bandwidth of 0.5-2.5 GHz. All the elements need to be modelled simultaneously in order to obtain an accurate estimation of our radar performance and surface response to the incoming radar pulses. The final goal is to improve the detection rate of plastic antipersonnel mines, reducing the false alarm level. We show some simulated results in 2D and 3D assuming plane waves and afterwards we introduce a model for our GPR antennas to characterize the real source. [C9515]

"An efficient electromagnetic approach to train the SVM for depth estimation of shallow buried objects with microwave remote sensing data"

Present paper deals the fusion of image analysis with electromagnetic and support vector machine (SVM) optimization approach to estimate the depth of shallow buried metallic and dummy mine (i.e., without explosive) objects with microwave remote sensing data at X-band (i.e., 10 GHz). The objects were buried under dry and smooth sand. For this purpose, a monostatic scatterometer at X-band has been indigenously developed, which consists a transmitter and receiver mounted on the stand of the sand pit and when operated it moves over it in X- and Y- axis. An algorithm has been proposed for identification of suspected region first i.e., region of interest (ROI) that contains buried objects in the image by proposing a quantity "detection figure" (D), which further proceed for depth estimation of buried objects. Algorithm includes image processing, electromagnetic multi layer interaction and SVM approach. The convolution-using image processing techniques has been applied to avoid the overlapping of the return signal. The support vector machine (SVM) approach has been analyzed for estimation of depth and an efficient method based on electromagnetic multiplayer interaction concept has been proposed to train the SVM. The depth estimated for Al sheet gives better result than dummy landmine, but the estimated depths results for both objects are in good agreement with actual depths. The present approach may be quite helpful to develop an automatic satellite data based information systems to estimate the depth of various shallow buried objects with satellite or air-borne radar data. [C9516]

"First steps towards multimodal georeferencing of 3D VHR optical and X-band SAR imagery"

With the advent of new, more widely available very high resolution (VHR) SAR and optical sensor satellite constellations, the issue of jointly exploiting the corresponding imaging data in the best possible way naturally arises. Our ultimate goal is the pixel-level fusion of these modalities and their visualization in a 3D context, i.e.

draped over terrain data, itself obtained from interferometric SAR processing. In this paper, we investigate the issues associated with adapting tools originally developed for low-resolution C-band SAR imagery to high-resolution X-band SAR imagery (both spaceborne). Specifically, we consider the issues associated with SAR interferometry (InSAR) and more particularly those associated with complex interpolation and phase unwrapping. We found that the existing chirp-Z transform complex interpolator previously used at low resolution is perfectly suitable for handling VHR SAR data. We also found that, while the selected phase unwrapping procedure works well when the resolution is reduced by averaging, it is deficient at full resolution, in part due micro-reliefs and specific phase responses. [C9517]

"Enhancement of radar based DEMs using 3D techniques"

Digital elevation models may contain several errors, what causes uncertainty about the reliability of the data. Reliable use of elevation data requires that uncertainty associated with the data be accounted for and that the errors responsible for this uncertainty are identified, quantified and removed. Several studies have proposed assorted methods to detect and quantify, and also to remove different kinds of errors. However, these automatic procedures apply algorithms that are specialized in detecting errors with particular characteristics, producing good results only when the model contains predominantly these specific types of errors. In this context, this paper presents a methodology and a tool for enhancing digital elevation models, named DEMEditor. Visual interpretation plays an important role in this work, which exploits user's knowledge about the data in the decision-making process about areas to be enhanced in the digital elevation model. The background of the user allows the identification of any type of error, relieving the need for automatic detection algorithms that specialize in detecting errors with particular characteristics. [C9518]

"Genesis of a new NASA InSAR mission concept, and natural hazards applications"

The National Research Council's Decadal Survey for Earth Science identified InSAR (Interferometric Synthetic Aperture Radar) observations among the highest priorities for new NASA Earth missions. A system making observations required by the solid Earth, vegetation, and ice/climate science communities is recommended. In response, analyses are underway to evaluate efficient combinations of science objectives and mission/instrument scenarios. The InSAR component can be satisfied by a new radar instrument concept capitalizing on existing technology and hardware, including a large commercial mesh reflector antenna and transmit/receive modules developed for the UAVSAR airborne radar. This InSAR system satisfies key science objectives and addresses several shortcomings of existing InSAR capable satellites. To reduce temporal decorrelation, L-Band (23 cm) wavelength is used. A 300 km wide-swath scanSAR mode with 8 day repeat enhances study of ice dynamics, pre/post earthquake deformation, volcano monitoring, and other dynamic phenomena. With a minor orbit change, global biomass surveys are possible using multipolarization. Key challenges are involve scheduling to optimize conflicting observational requirements of various science communities served. [C9519]

"Dynamic persistent scatterers interferometry"

This paper presents the concept of Dynamic Persistent Scatterers Interferometry (PSI) processing, which enables the sequential estimation of parameters. The method is based on the Integer Least Squares (ILSQ) PSI concept and makes use of the estimation vector and corresponding variance-covariance matrix of the initial estimation epoch. In addition, the concept of multi-modal adaptive estimation and testing is applied. The algorithm systematically adds a new acquisition or set of acquisitions to an existing stack, updates the solution of the previous run, and analyzes whether the behavior of the (pre-) selected points fits the expected one. [C9520]

"Ground deformation retrieval of urban and suburb areas based on multi-baseline DInSAR algorithm: A case study in Cangzhou City (China)"

This paper aims at ground surface deformation retrieval in wide areas including urban and suburb areas based on multi-baseline DInSAR algorithm proposed by Mora. Several progresses are made in order to extract good results. Firstly, a new complex network is presented to restrain noise influence on delaunay triangular network. Secondly, Based on a model coherence function, linear deformation velocity increments and height error increments between neighboring high coherent points (HCPs) are resolved. In order to integrate increments in network, least squares adjustment method and error controlling method are used to obtain stable parameters estimation. At last, by Combining complex and delaunay networks, wide areas deformation is investigated, from center urban areas to suburb areas. The algorithm is performed to investigate the subsidence of CangZhou City, Hebei province (China) during the time of 1993-1997 by using 9 scenes of ERS SAR data. The experiment results show serious subsidence in the region and are validated by leveling data and groundwater wells data. [C9521]

"TerraSAR-X and TanDEM-X: Revolution in spaceborne radar"

Commercially available imagery is and will remain indispensable to civilian and military organizations gathering various types of geo-spatial information. Whether fulfilling international agreements, providing military contingents in international peacekeeping or humanitarian missions, or conducting joint technical exercises with other countries-a reliable access to timely, high resolution remote sensing data is an essential basis for well-informed decision making, particularly in time-critical situations. Today, organizations with those needs customarily resort to high resolution data acquired by optical sensors-often a lengthy operation. The radar satellite TerraSAR-X, and at a later stage together with TanDEM-X with its complementary near-real time data acquisition capabilities, offer a whole new approach to the use of space-borne datasets for mapping purposes in time-critical situations. [C9522]

"Verification of the TerraSAR-X system"

The paper discusses the areas covered by the TerraSAR-X Calibration/Verification-Plan. By means of a commissioning phase planning tool the data take requests required for characterization, calibration and verification are sequentially arranged. The status of the individual data takes is tracked from request planning to the final image analysis. All data take requests and results are supervised and summarized in a so-called verification matrix. In the end the paper gives an overview about the commissioning phase schedule and the repeat cycle based planning. [C9523]

"RadSTAR L-band imaging scatterometer- performance assessment"

L-band Imaging Scatterometer (LIS), developed at NASA/Goddard Space Flight Center as part of the RadSTAR initiative, is an airborne imaging radar that combines phased array technology and digital beam forming techniques for the measurement of important scientific parameters. The instrument operates at 1.26 GHz, horizontal polarization, and employs a real-time processor capable of synthesizing multiple beams over a scan range of +/-50 degrees. LIS was flight tested in May 2006 and in January 2007 on board of the NASA P3 aircraft over the Delmarva Peninsula, VA. In this paper we describe the RadSTAR system and present some preliminary analysis of the radar data collected during the test flights. [C9524]

"Advanced control and processing capabilities in the aquarius scatterometer flight electronics"

The Aquarius mission requirement for 0.1 dB scatterometer measurement stability has driven the radar's control and processing hardware design. Two new aspects of the flight electronics that contribute toward the overall stability will be discussed in this paper: 1) a high-rate radar timing mode for verifying performance on the ground, and 2) an onboard processor for flagging echoes corrupted by radio-frequency interference (RFI). [C9525]

"Status and perspectives of GNSS-R at ESA"

This paper presents an overview of the activities currently being undertaken by the European Space Agency in the field of GNSS reflectometry. Furthermore, the salient features of Europe's Galileo project with respect to the applicability of the signals for the purpose of GNSS-R are given. Furthermore, the prospects for the near future in terms of experiments and applications are given and finally there is a review of the potential for GNSS-R space missions. [C9526]

"Oceanpal®: Monitoring sea state with a GNSS-R coastal instrument"

Oceanpalreg is a coastal instrument developed at Starlab for operational remote sensing of the ocean surface, with potential direct applications to snow/ice mapping and soil moisture monitoring. The instrument is based on the exploitation of global navigation satellite systems (GNSS) and their augmentation systems (WAAS, EGNOS). The emitted signals provide an exceptional source of opportunity for passive remote sensing of the Earth. The use of GNSS reflections (GNSS-R) for sea-surface monitoring is a bistatic radar technique only requiring a receiving system. The concept has already been implemented for coastal platforms (few meters above the water), aircraft (1km to 10 km) and is being studied for space platforms (LEO, orbiting at 500-1000 km). The potential applications include sea-state, sea-surface altimetry and surface roughness, both for scientific and operational oceanography. We report on a recent long-term experimental and demonstration campaign, carried out at the Oceanpalreg Coeli station in the Barcelona Port during the period 2004-2007, with a real time web-based service. This campaign has been made possible through collaboration with the Barcelona Port Authority Environmental Monitoring Department (APB). The instrument was installed on a breakwater near the main entrance of the port, at 23 m over the sea-surface. We describe in this paper the successful long-term comparison between the data obtained by Oceanpal instrument and the observables recorded by two nearby

buoys. Data used for this analysis cover a period of over one year, allowing a definitive evaluation of the performances of this GNSS-R based coastal instrument for SWH retrieval. We also review results from a weeklong phase altimetry campaign at the port of Vilagarcia. [C9527]

"The repeat-pass interferometric SAR by Pi-SAR(L)"

This paper describes the system and experiment of Pi- SAR(L) repeat pass interferometric SAR. To obtain a high- quality interferometric image, it is necessary to make two flights on the same pass and observe in the same direction. We built a flight control system utilizing the preinstalled autopilot. This system measures position and altitude precisely with using a differential GPS, and controls the flight pass to be within virtual tube of 10 m diameter. The antenna rotation mechanism was also installed to control the observation direction. The repeat-pass flight has been conducted many times. The flights were stable and the deviation was within a few meters for both horizontal and vertical even in the gusty condition. The SAR data were processed in time domain based on range Doppler algorithm to make the complete motion compensation. The interferometric image processed after precise phase compensation is shown. [C9528]

"High resolution millimeter wave SAR interferometry"

High resolution millimeter wave synthetic aperture radar (SAR) interferometry is presented using the MEMPHIS multi-baseline InSAR system. A complete processing chain is used to generate digital elevation models starting from the radar raw data. A deeper focus is laid on the phase unwrapping step, which is achieved using the multi-baseline properties of the system. In November 2006, an experiment was realized including two test sites in Switzerland; the actual results are presented and discussed. [C9529]

"Altimetric calibration experiences in the Western Mediterranean"

Since many years, space borne radar altimeters have brought a powerful contribution in monitoring the dynamic sea surface topography, and in understanding better the ocean circulation and its impact on the earth system. Today, altimetric satellites are observing the whole oceans, measuring the sea surface height with a rms precision of 3-4 cm at 1 Hz sampling, as demonstrated by TOPEX/POSEIDON, launched in 1992, by Jason-1, launched in 2001 and by ENVISAT, launched in 2002. Such a high level error budget was achieved thanks to the tremendous improvements which have been obtained in radar performances as well as in precise orbit determination. Indeed, applications of altimetry in oceanography and geodesy requires very precise measurements of the satellite-sea level range, along with appropriate environmental corrections, but also an accurate knowledge of the satellite position with respect to the Earth reference. One campaign has also been made in June 2003 at the Ibiza island area (Martinez-Benjamin et al., 2003). The marine geoid has been used to relate the coastal tide gauge data from Ibiza and San Antonio harbours to off-shore altimetric data. A technical Spanish contribution to the calibration experience has been the design of GPS buoys and GPS catamaran taking in account the University of Colorado at Boulder and Senetosa/Capraia designs. We present a synthesis of the sea level results results obtained from the altimeter calibration campaign at Ibiza island on June 2003 using the direct measurements from GPS buoys and the derived marine geoid. The main objective of the marine campaign was to check the value of Ibiza Island as a permanent calibration site in the western Mediterranean Sea, to complement the Corsica site in the network of altimeter calibration sites. [C9530]

"ALTICORE-A consortium serving european seas with coastal altimetry"

In this paper, we describe the ALTICORE (value added satellite ALTImetry in COastal REGions) initiative, a consortium aiming at providing high quality coastal altimetry over some European seas. Taking the Ligurian Sea in the NW Mediterranean as an example, which acts as a test zone for this work, we show the improvement in availability and quality of ENVISAT data, through our processing, when compared with the official altimetric products delivered by AVISO. We also introduce the building concepts of solutions for data search, extraction, update and delivery based on web-services. This grid-type infrastructure is being designed within ALTICORE. [C9531]

"Status of GNSS reflectometry related receiver developments and feasibility studies within the German Indonesian Tsunami Early Warning System"

In the frame of the German Indonesian Tsunami Early Warning System (GITEWS) project a multi-frequency Global Navigation Satellite System (GNSS) Occultation & Reflectometry & Scatterometry (GORS) space receiver is developed. It is based on commercial off-the-shelf (COTS) GNSS receiver technology, as the core instrument for a future tsunami detection constellation of small low Earth orbit (LEO) satellites. For use in reflectometry, scatterometry and radio-occultation measurements as well as high-precision navigation applications, specific adaptations of the GNSS receiver firmware are desirable, which require a close interaction between scientists

and the receiver manufacturer. Within the GITEWS project GFZ has set up a team consisting of GFZ, DLR and JAVAD GNSS (JAVAD) to adapt and extend their new generation GNSS receivers for advanced scientific space applications. Specific adaptations address the improvement of the cold start time-to-first-fix, the selection of optimal tracking loop parameters and channel slaving for monitoring of reflected signals. Besides pseudorange, phase and signal-to-noise measurements, the modified receiver allows output of in-phase (I) and quadrature-phase (Q) accumulations at 5 msec intervals (200 Hz). As a major step forward compared to current space receivers, the new receiver supports tracking of the civil L2C signal of the GPS constellation. An overview of the current status is given and first results are discussed. Within GITEWS the feasibility of a tsunami detection mission is studied, including the constellation mission design, the options for operating the system and the ways to develop an end-to-end system for the quick response to tsunami events. In parallel simulation studies of the GNSS signals reflected to a LEO satellite are carried out. This will be realised by a Zavorotny and Voronovich scattering model with a two-scale model approach using an Elfouhaily sea wave spectrum. An overview of the current activities is given and first results are discussed. [C9532]

"TOGA, a prototype for an optimal orbiting GNSS-R instrument"

Remotely sensing the Earth's surface using GNSS (Global Navigation Satellite System) signals as bi-static radar sources is one of the most challenging applications for radiometric instrument design. As part of NASA's Instrument Incubator Program, our group at JPL is building a prototype instrument, TOGA (Time-shifted, Orthometric, GNSS Array), to address a variety of GNSS science needs. Observing GNSS reflections is major focus of the design/development effort. The TOGA design features an electronically steered antenna (ESA) array which forms simultaneous high-gain beams in multiple directions. Multiple FPGAs provide flexible digital signal processing logic to process both GPS and Galileo reflections. A Linux operating system based science processor serves as experiment scheduler and data post-processor. This paper outlines the TOGA design approach as it applies specifically to observing science quality GNSS-R signals from low Earth orbit. [C9533]

"Modeling and analyzing InSAR phase profiles at building locations"

The improved ground resolution of state-of-the-art synthetic aperture radar (SAR) sensors suggests utilizing SAR data for the analysis of urban areas. Even in the case of InSAR, for building recognition usually the analysis is triggered mainly from features detected in the magnitude images. However, considering InSAR data significant phase profiles in range direction at building locations are observable. In this paper a simple model for these characteristic profiles in layover areas is proposed. The model takes into account that in layover areas a mixture of several signal sources contribute to the interferometric phase of a range cell. At building locations a combination of contributions from ground, wall, and roof is observed. The resulting phase profiles are characterized by sensor and illumination parameters as well as object parameters. In the first part of this paper, simulated phase images at building locations based on a given surface profile in range direction are presented. In the second part, real InSAR data sets of the airborne sensors AeS-1 (Intermap) and AER-II (FGAN-FHR) with a slant range resolution of 38 cm respectively 94 cm are used to calculate interferometric phase truth data which are then compared with the simulation results. [C9534]

"Using airborne laser altimetry to improve river flood extents delineated from SAR data"

Flood extent maps derived from SAR images are a useful source of data for validating hydraulic models of river flood flow. The accuracy of such maps is reduced by a number of factors, including changes in returns from the water surface caused by different meteorological conditions and the presence of emergent vegetation. The paper describes how improved accuracy can be achieved by modifying an existing flood extent delineation algorithm to use airborne laser altimetry (LiDAR) as well as SAR data. The LiDAR data provide an additional constraint that waterline (land-water boundary) heights should vary smoothly along the flooded reach. The method was tested on a SAR image of a flood for which contemporaneous aerial photography existed, together with LiDAR data of the un-flooded reach. Waterline heights of the SAR flood extent conditioned on both SAR and LiDAR data matched the corresponding heights from the aerial photo waterline significantly more closely than those from the SAR flood extent conditioned only on SAR data. [C9535]

"Some polarimetric aspects of processing sea surface M-ATI SAR data"

A brief review is presented of published work on detection and imaging techniques based on matrix group theory for the scalar non-polarimetric two channel along track interferometer and the vector polarimetric two channel across track interferometer. The relevance to ATI of the vector theory for the across track interferometer is discussed as is the problem of extending the theory to the case of the ATI with N beams. Difficulties in developing detection and imaging methods for the general case of N beams have lead to attempts to develop an alternative approach based on linear filtering. It is assumed that image modulations are a result of local

fluctuations in mean intensity which can be described by a spherically invariant statistical process with a compound distribution. The unmodulated background consists of Gaussian scatterers. These scatterers and the modulated ones have different Doppler spectra and maximising the normalised standard deviation of the filtered image maximises the visibility of the image modulations. Polarimetric aspects of this approach are discussed and experimental results obtained with an airborne four beam M-ATI are presented illustrating aspects of the discussion. [C9536]

"The EarthCARE mission: Mission concept and lidar instrument pre-development"

The earth clouds, aerosols, and radiation explorer mission has been selected as the 6th earth explorer mission of ESA's living planet programme [1]. A suite of four instruments, active and passive, will be embarked on the same satellite to measure cloud and aerosol properties simultaneously with TOA radiances in order to derive TOA fluxes in relation to clouds and aerosols. [C9537]

"Initial CRAM aerosol retrievals from CALIPSO and supporting airborne HSRL measurements"

The successful launch of the Cloud-Aerosol Lidar and Infrared Pathfinder Satellite Observation (CALIPSO) and Cloud-Satellite (CloudSAT) satellites on April 28, 2006, placing two new active remote sensing systems (lidar and radar) in space, heralded a new era in spaceborne earth observations. Not only will they provide new information unique to active sensing satellites, but by positioning them in orbit with the A-Train constellation of satellites, joining the passive sensing satellites AURA, PARASOL and AQUA, this will enable myriad synergistic active-passive sensing opportunities. CALIPSO and CloudSAT have both successfully completed their payload checkouts and initial validations; some six months of data have already been collected and data are now beginning to be distributed to the scientific community (e.g., CALIPSO Level 1 and 2a data released on Dec. 8, 2006). Thus there are sufficient data, with more arriving daily, to fuel years of scientific studies addressing questions critical to more fully understanding the earth-atmosphere system and assessing weather-climate change issues. The Constrained Ratio Aerosol Model-fit (CRAM) technique for aerosol retrieval is examined in the context of CALIPSO data, and temporally/spatially coincident High Spectral Resolution Lidar (HSRL) data is studied with respect to its potential to provide external context to the retrievals and to verify aerosol models upon which the CRAM technique relies. [C9538]

"Physical parameter extraction over urban areas using L-band POLSAR data and interferometric baseline diversity"

Estimating the number of backscattering sources is an important issue in analyzing multibaseline interferometric SAR data. This paper extends model order selection algorithms to process polarimetric multibaseline InSAR observations. These methods are applied to urban environments using fully polarimetric dual-baseline InSAR data of Dresden city acquired by DLR's E-SAR system. Experimental results for single polarization and polarimetric set-ups are presented and discussed. [C9539]

"Highly accurate DSM reconstruction using Ku-band airborne InSAR"

We present a newly developed airborne InSAR system incorporating a novel phase unwrapping algorithm, capable of retrieving a highly accurate Digital Surface Model (DSM). The SAR sensor system, with a spatial resolution of 30 cm, is carried on an airborne platform which has 2 antennas placed in a baseline length of 1 m. We have established a DSM reconstruction processing technique, which includes the new "Iterated Conditional Modes-Minimum Cost Flow" (ICM-MCF) phase-unwrapping algorithm. The ICM-MCF algorithm finds a locally optimal configuration of unwrapped phases under a well-characterized statistical model of the terrain and noise. An experimental field observation was carried out in Tsukuba, Japan. The DSM was generated, and the height accuracy of the SAR-DSM was evaluated by comparing with laser profiler data. For 50 cm x 50 cm mesh, an accuracy of better than 50 cm in height was confirmed. [C9540]

"A novel optimization approach to forest height reconstruction from multi-baseline data"

The paper deals with the problem of reconstructing the height of forests from polarimetric/multi-baseline SAR data. The approach consists of optimizing an objective functional defined as the distance between the measured data and the data predicted by the model at the actual estimate of the unknowns. We indicate the role of global optimization on the performance of the forest height reconstruction algorithm. As global optimizer, a multilevel single-linkage method, which incorporates a local optimization into the global search, is exploited, thus offering computational efficiency and reliability. The performance of the method are illustrated against numerically simulated data. [C9541]

"Height dependent motion compensation and coregistration for airborne SAR tomography"

SAR tomography (SARTom) is an imaging technique that allows multiple phase centers separation in the vertical (height) direction. It is performed after standard 2D SAR repeat-pass processing and operates on a stack of coregistered SAR images. Theoretically, the coregistration between two images is height dependent and the use of a reference height (or a DEM) is needed, although not ideal in the case of volumetric target (multiple phase centers in one resolution cell). In this paper, the drawbacks related to the choice of this reference in a tomographic context are analysed and a height dependent coregistration approach is proposed. In order to do this, it is also necessary to remove processing corrections related to the reference height, such as motion compensation, and make them height dependent. The inclusion of the height dependency during the tomographic SAR processing results in a better quality of the final tomograms in terms of pseudo-power and phase centers separation. The results of the proposed approach are validated on real data acquired by the E-SAR system of the German Aerospace Centre-DLR. [C9542]

"SAR imaging based upon nonswitchable antenna array and noise signals"

The work is devoted to elaborating a new method for SAR image generating using noise/random signals and nonmoving & non-switching antenna array suggested in Lukin (2006). The main idea of that antenna array consists in the extraction from the total signal of one channel receiver the signals received by a single element of the array. This signals separation is based upon decorrelation properties of noise/random signals. Attractive advantages of the suggested antenna array and the method for SAR imaging consist in no need in either mechanical motion or electronic switching of the antenna array elements, which simplify its design and lower the cost. Analytical evaluations for main performance of such antenna array are given for its various implementations. The related SAR imaging algorithm is described in detail. Some results of computer modeling of SAR imaging using this antenna array are presented. Advantages and constraints of the method and array suggested are discussed. [C9543]

"Image fusion using a NSDFB-based contourlet packet"

In this paper, a new contourlet packet (CP) is constructed based on a complete wavelet quadtree followed by a nonsubsampling directional filter bank (NSDFB). By combining the finer approximation characteristic of wavelet packet with the invertible characteristic of NSDFB, the proposed CP can give more accurate reconstruction of images than WP. After the proposed CP transform on the fusing images, the low-frequency subbands are compared to preserve the coefficients whose module are minimum, local inner-product rule is performed on the high-frequency subbands of the images. Then the fusion image can be obtained by taking an inverse CP transform. The experiment results show the superiority of the method to Contourlet, Wavelet packet, NSCT, stationary Wavelet, complex wavelet and WBCP based fusion methods, both in image clarity and standard deviation, information entropy, average gradient, average cross [C9544]

"The arm detection based on Rao test method"

Firstly, aim at the different radar echo characteristic of anti-radar missile (ARM) and its aircraft, a correlative canceller is proposed to restrain the aircraft signal through estimating its Doppler frequency. Then based on the assumption of autoregressive (AR) process noise, a detection algorithm is derived to implement the ARM target detection through Rao test. Simulation experiments show that the correlative canceller can restrain aircraft signal and the ARM signal is lossless; the Rao test method is simple and realizable, however, it almost has the same performance as that of generalized likelihood ratio test (GLRT). Lastly, the boundary of error rate for choosing reference signal is obtained through simulation. [C9545]

"An efficient weighted L_p algorithm for the design of non-uniform filter banks"

In this paper, we propose a simple weighted L_p algorithm for the design of non-uniform integer decimated filter banks. By choosing proper L_p criteria at pass-band and stop-band of the prototype filter and minimizing the p power of error function with an iterative method, ripples characteristic of the prototype filter can be efficiently controlled and non-uniform filter banks with high stop-band attenuation can be designed. An example is given to demonstrate the effectiveness of the proposed method. [C9546]

"Image fusion using a contourlet HMT model"

In this paper hidden Markov tree (HMT) based image fusion methods are investigated. Considering the failure of wavelet in representing the geometry of image edges in dimension 2, here a new contourlet HMT model for image fusion is proposed. Because the CHMT model efficiently captures all dependencies across scales, space and directions through a tree structured dependence network, it can give more accurate description of images.

Moreover, the CHMT has a simple tree structure with fewer parameters than wavelet HMT (WHMT), which enables efficient training using the expectation maximization (EM) algorithm. Inputting the contourlet coefficients of source images to train the CHMT model, we can get the edge probability density functions. Local inner-product fusion rule is performed on the high-frequency directional sub-bands, which is acquired by the product of the high-frequency directional coefficients by the edge probability density function of CHMT. The low-frequency sub-bands are compared to preserve the coefficients whose module are minimum. The experiment results show the superiority of the proposed image fusion method to WHMT and contourlets, both in image clarity, implementation speed, standard deviation, average gradient and average cross entropy. [C9547]

"Simulation of pulse compression performance under influence of background noise in modern surveillance radar"

In this paper, simulation of pulse compression performance in radar systems under influence of Gaussian noise and low angle Weibull land clutter have been presented. Peak side lobes (PSL) of optimized biphasic pulse compression codes (OBPCC) of lengths ranging between 5-30 have been discussed. Optimization of peak side lobes is processed using Genetic algorithm optimization tool. Simulation of pulse compression performance at signal to noise ratio (S/N) varying between 5 to 30 dB is introduced. Comparative study shows that for low values of S/N, the peak side lobe level for OBPCC under influence of background noise is equal to its correspondence of ideal biphasic codes used in pulse compression radar, leading to enhancement of detection capability, range resolution and compression ratio of modern surveillance radar systems. [C9548]

"Evolutionary Filter for Mobile Robot Global Localization"

Mobile robot global localization aims to determine the robot's pose in a known environment in absence of initial robot's pose information. This article presents an evolutive localization algorithm known as Evolutive Localization filter (ELF). Based on evolutionary computation concepts, the proposed algorithm search stochastically along the state space the best robot's pose estimate. The set of pose solutions (the population) represents the most likely areas according the perception and motion information received. The population evolves by using the observation and motion errors derived from the comparison between observed and predicted data obtained from the probabilistic perception and motion model. The resulting global localization module has been tested in a mobile robot equipped with a laser range finder. Experiments demonstrate the effectiveness, robustness and computational efficiency of the proposed approach. [C9549]

"Dwell scheduling of multifunction phased array radars based on genetic algorithm"

A dwell scheduling model which takes the time and energy constraints into account is founded from the viewpoint of scheduling gain. Dwell scheduling strategy design is turned into a nonlinear programming procedure. A dwell scheduling algorithm is then given based on the genetic algorithm. Simulation results demonstrate that compared with the conventional adaptive scheduling method, the proposed algorithm not only increases the scheduling gain and the time utility of the system but also decreases the task drop rate. [C9550]

"An IMM-based adaptive-update-rate target tracking algorithm for phased-array radar"

This paper addresses the problem of adaptive-update-rate target tracking in the phased-array radar. A novel IMM-based adaptive-update-rate method is proposed. The update interval is proportional to the inverse square root of the position residual. A controllable parameter is introduced in the formulation of calculating the update interval which can be used to balance the tracking precision and the system load. Simulation results demonstrate the effectiveness of the proposed algorithm. [C9551]

"Multiscale bandelet image compression"

The estimation of basis shapes, the partition of image and the optimization of geometric flows are three key issues in the implementation of the second Bandelets proposed by peyer. Compared with other polynomial geometric flows, linear geometric flows are commonly used because of its simplest structure and least parameters to store. However, the actual structure of edges and contours can only be considered as lines in a local region. So the size of partition blocks should be small so as to the geometric regularities in each block can be approximated as linear. The geometric regularities mainly appear in the high frequency subbands of images, so in this paper we proposed a multi-scale Bandelet transform based on complete wavelet packet decomposition. And a fixed size of image partition is employed in each high frequency subbands. In relative to the second generation Bandelet, it has quick implementation and comparable performance. [C9552]

"SAR image denoising based on wedgelet and dual-tree complex wavelet transform"

Image denoising based on wedgelet transform and dual-tree complex wavelet transform (WDT-CWT) is proposed in this paper. Wedgelet transform is a new method that has a good performance in approximating edges. The limitation of wedgelet transform is that it smoothes the flat region excessively, leading to the loss of some texture features. To reduce this limitation, we employed dual-tree complex wavelet transform (DT-CWT) to improve the detection of texture information. Through a combination of the wedgelet transform and DT-CWT, we develop a detector of texture, edge and direction information. The experimental results show that WDT-CWT outperforms many traditional approaches both visualization and in terms of evaluation values. [C9553]

"Deriving filter parameters using dual-images for image de-noising"

This paper presents a novel technique to derive the filter parameters for removing signal dependent noise (SDN) in the image. In order to remove SDN, many de-noising algorithms rely on a prior knowledge of noise parameters, especially the variance σ_{man}^2 , and the gamma value γ of the specific imaging technique. This paper proposes a technique to automatically derive the signal variance σ_{mf}^2 and use this parameter to construct the Local Linear Minimum Mean Square Error (LLMMSE) filter without the need to know the values of σ_{man}^2 and γ . Two image instances of the same noisy scene are used to calculate the signal variance which is then used to construct the LLMMSE filter. Experiments with both the "Lena" image and real-life far-infrared (FIR) vein pattern images showed that the proposed technique can predict the signal variance consistently, and the constructed LLMMSE filter performs well in removing the signal dependent noise. [C9554]

"Wrapper approach for feature subset selection using GA"

In this paper, wrapper based approach is presented to feature subset selection of ground penetrating radar (GPR) echo signal using genetic algorithm in conjunction with constructive learning algorithm. GPR echo signal inherently has the non-stationary characteristic and the target echo signal is deteriorated by the clutter. Firstly, WP-based preprocessing algorithm is used to clutter reduction and feature extraction. Then wrapper based approach is adopted to find optimal feature subset, and at meanwhile obtain the result of classification. Experiment result based on GPR landmine data shows the feasibility and advantage of the presented algorithm. [C9555]

"Modeling of varying geometrical scenarios of bistatic radar"

In this paper, a bistatic clutter geometrical model is proposed. The model can accurately describe the geometrical relationship between the bistatic radars and the clutter scatterers, and it can be applied in any bistatic geometrical scenarios. On the basis of analyzing the geometrical relationship between the bistatic radars and the clutter scatterers in varying geometrical scenarios, the paper formulates mathematical expressions to describe the geometrical relationship. The method for deducing the expressions is introduced in detail. Finally, the Doppler-azimuth trajectories are provided with to examine the model via four bistatic geometrical scenarios and compared with that of multichannel airborne radar measurements (MCARM). The results prove that the model is accurate. [C9556]

"Implementation of STAP system for dual-channel airborne radar"

Real time processing is a technical challenge for high precision implementation of space time adaptive processing (STAP) system with tremendous dataflow. Considering the requirements, the design objective is to decrease latency and to increase throughput of system. The compact parallel implementation of STAP system for dual-channel airborne radar is studied in this paper. Different scheduling methods are tested in two designed architectures based on the selected platform called as RLPGS structure and RLSPG structure. The real system demonstrates well on a single processing board, the performance meets the system requirement. [C9557]

"A cyclostationarity based iterative algorithm for multi-component chirp signal parameter estimation"

This paper is concerned with the problem of estimating the phase parameters of multi-component chirp signals embedded in additive noise. An iterative algorithm based on cyclostationarity is proposed. The main characteristics of the proposed algorithm include reduction in error propagation effect, increase in estimation accuracy and operation over a wider range of phase parameter values. Simulation results demonstrate that the new iterative algorithm has better performance as compared with the conventional cyclostationary estimation method. [C9558]

"Best least squares solution for Prony model"

In this paper the nonlinear least-squares estimation (NLSE) of the parameters of Prony model, with condition

meeting in the optimization is both necessary and sufficient, is presented. The necessary condition for stationary of the summed squared error is expressed generally with an auxiliary parameter vector then defined uniquely by some way, such that the solution is sole and globally optimal. An equivalent condition involving only the exponents, with the coefficients suppressed, is developed. This condition is interpreted in the geometric language of abstract vector spaces, thus recognition for geometric structure that the best solution would meet is acquired. The condition still in effect requires solution of nonlinear algebraic equations, and a fully effective linear iterative method is proposed for this purpose. Finally, the procedure is illustrated with a simple example, and the result compared with one's of Pro-ESPRIT method. [C9559]

"SAR image segmentation based on spatially adaptive weighted possibilistic c-means clustering"

Due to the influence of speckle in synthetic aperture radar (SAR) image, statistical dependencies among neighboring pixels should be considered in SAR image segmentation. The spatially adaptive weighted possibilistic c-means (SAW-PCM) clustering algorithm is proposed in which spatial information is introduced into PCM approach to directly adjust the membership. The relationship between the neighboring pixels is described through Markov random fields (MRF). To preserve detail information in SAR images, the directional neighborhood system set is established. The selection of neighborhood systems is based on similarity measurement (SM) between wavelet energies of comprehensive result of steerable wavelet transform. Among the different neighborhood alternatives, the one with the highest SM value is chosen to compute the weight value. The experimental results on real SAR images demonstrate the merit of the proposed method, especially in the preservation of details within a SAR image. [C9560]

"Properties of HF RADAR Compact Antenna Arrays and Their Effect on the MUSIC Algorithm"

Detailed analysis of the compact antenna array patterns and the internal signal processing within the MUSIC algorithm leads to a goodness-of-fit quality metric for the output radial current velocities and bearings produced by the HF RADAR system. To achieve this, some theory behind the MUSIC direction finding algorithm, describing its Direction of Arrival (DOA) metric, is first presented. MATLAB simulations are conducted and statistics are collected on the DOA metrics. The magnitudes of these metrics are directly related to the quality of the bearings produced by the MUSIC algorithm. Quality of measured antenna patterns is paramount to the accuracy of the MUSIC algorithm bearing output. Ambiguities, as well as other aspects of the measured antenna patterns that are detrimental to quality, are discussed. This research provides HF RADAR users with a practical quality metric for the radial current velocities and their associated bearings produced by the HF RADAR system. [C9561]

"Surface Current Mapping in the Lower Chesapeake"

Two CODAR 25 MHz radars with co-located transmit/receive antennas have been installed in the lower Chesapeake Bay. Antenna patterns have been measured at both sites and initial quality control tests have included comparisons of measured and ideal baseline data. [C9562]

"An Efficient Algorithm for the Radar Recognition of Ships on the Sea Surface"

In this paper, an efficient algorithm is proposed to the angular-diversity radar recognition of ships with noise effects taken into consideration. The goal is to identify the similarity between the unknown target ship and known ships. The content of this paper is divided into two parts. In the first part, the angular-diversity radar recognition of ships is given by transformation based approaches, i.e., the principal components analysis (PCA), with noise effects taken into consideration. The goal is to identify the similarity between the unknown target ship and known ships. In the second part, the linear discriminant algorithm (LDA) is utilized to increase the recognition rate. Initially, the angular-diversity radar cross sections (RCS) from a ship are collected to constitute RCS vectors (usually large-dimensional). By changing the elevation angle or the ship type, different RCS vectors are obtained to produce a high-rank covariance matrix. By choosing some of the largest eigenvalues and their corresponding eigenvectors, all the RCS vectors are projected onto the eigenspace (usually small-dimensional). Similarity between the unknown target ship and known ships can be identified in the eigenspace with high recognition rate. This will reduce the complexity for radar recognition of RCS characteristics from ships. However, the separating ability for such an elementary recognition is usually poor. This poor separation of radar target recognition will make the prediction results unreliable. The PCA gives the major features for the projected data of the two classes. While the LDA gives the best separation for the projected data of the two classes. To enhance the separating ability of radar target recognition, the projection features on the PCA space are further projected onto the LDA space and the recognition is performed on the LDA space. Our simulation shows that the separating ability for RCS based recognition of targets is greatly increased by using the LDA in the radar recognition process. In addition, the use of LDA in the recognition process increases the ability to tolerate noise

effects. This study will be helpful in many applications of radar target recognition. [C9563]

"Data Exploration for Multidisciplinary Research"

The metadata oriented query assistant (MOQuA) is a web application for exploring complex collections of data via a highly interactive and intuitive interface. MOQuA development has been motivated by the evolution of climate and ecosystem studies towards highly interdisciplinary research programs that depend on data drawn from a variety of sources. Present generations of earth science data systems are not structured to support exploration through a data space that is simultaneously rich in measured parameters, yet sparse in geographic and temporal coverage. We have implemented MOQuA for the Autonomous Ocean Sampling Network 2003 field program data set, which includes observations from a diverse collection of platforms such as drifters, autonomous underwater vehicles and ships, fixed measurement assets (such as moorings and radar), and remote measurements from satellites and aircraft. It also includes output from three oceanographic models. Measured and derived data are stored in several formats, residing within numerous data management systems. [C9564]

"Bathymetric Capabilities of the HISAS Interferometric Synthetic Aperture Sonar"

Multibeam echo-sounders have until now been the leading technology in seabed mapping, but typically have resolutions of around half a metre. Recently, synthetic aperture sonar (SAS) technology has matured to a commercial level, delivering sidelooking imagery with a resolution of a few centimetres to a range of several hundred metres. High resolution sidelooking imagery makes interferometry an extremely interesting technique for bathymetric processing. In this paper we discuss the theoretical accuracy in relative height mapping of the new HISAS interferometric SAS and compare the results with processing of simulated data. We also demonstrate SAS interferometry on real data collected with a prototype SAS mounted on a HUGIN AUV. Different filtering techniques are applied to the data, illustrating the trade-off between resolution, robustness and smoothness. [C9565]

"Sea clutter measurement with airborne synthetic aperture radar"

In this paper, we consider the surface motion as an important factor governing behaviours of the sea clutter observed in SAR images. Therefore, we propose a model for SAR-acquisition of time varying scenes. Then we derive from this model the 2nd order statistical properties of an acquired scene in terms of a time-dependant reflectivity q . We also introduce the sea surface elevation and we complete the reflectivity description by applying small slope approximation (SSA) of the wave scattering from rough surface. [C9566]

"Surface Current Measurements During Safe Seas 2006: Comparison and Validation of Measurements from High-Frequency Radar and the Quick Release Estuarine Buoy"

The National Oceanographic and Atmospheric Association's (NOAA) 2006 Safe Seas Oil Spill Drill, conducted just outside the Golden Gate, was a prime opportunity to test the value and effectiveness of three recently deployed 13 MHz coastal radars that are part of the Central and Northern California Ocean Observing System. These Coastal Ocean Dynamic Application Radar (CODAR) systems were deployed by the Coastal Ocean Currents Monitoring Program (COCMP) to measure surface currents up to 85 km offshore from Point Reyes to just north of Half Moon Bay. CODAR systems measure surface currents by transmitting radio waves over the ocean and use the Doppler-shifted return sea echo to extract surface current velocities. Safe Seas 2006 was the first demonstrated use of High-Frequency Radar (HFR) to assist in oil-spill response in real time. Surface current maps were posted to the web hourly during the simulated oil spill to monitor surface current structure during the 48-hour exercise. NOAA's Quick Release Estuarine Buoy (QREB) was also deployed at the location of the simulated oil spill to obtain oceanographic environmental data in real time. The QREB is equipped with an Acoustic Doppler Current Profiler (ADCP), which provided a vertical profile of currents near the location of the simulated spill. In an effort to determine the reliability of the data produced from both measurement devices during the exercise, HFR total vector data from the three coastal systems were compared to the data acquired by the QREB surface bin located at approximately 3 m depth. Also, to verify individual HFR site performance, radial data from each site were compared with their respective radial components from the QREB data. Total-vector comparison results reveal strong correlation in both the cross-shore ($R^2 = 0.69$) and along-shore ($R^2 = 0.90$) components with RMS differences of less than 0.09 m/s. Both instruments also observed the same dramatic shift in along-shore current-direction during the two-day exercise. Radial comparisons revealed strong correlation as well for the two HFR systems that acquired data at the QREB location. Endpoints of recovered drift cards released during the exercise also qualitatively correlate with trajectories produced from the HFR current maps. Further, tidal analyses were performed on the QREB and HFR data, utilizing Pawlowicz's widely accepted T-Tide algorithm, to further validate measurements made by these instruments. Despite the short data set, these

analyses showed pronounced signals of K1 and M2 constituents in good agreement between the QREB and HFR instruments. The consistent comparison results described in this paper show that HFR can add significantly to the effectiveness of surface current mapping over a large area during oil spills and can complement the QREB measurements to enhance oil-spill response. [C9567]

"VDatum and Strategies for National Coverage"

VDatum is a software tool being developed by the National Ocean Service that allows users to vertically transform geospatial data among a variety of ellipsoidal, orthometric and tidal datums. This is important to coastal applications that rely on vertical accuracy in bathymetric, topographic, and coastline data sets. The VDatum software can be applied to a single point location or to a batch data file. Applying VDatum to an entire data set can be particularly useful when merging multiple data sources together, where they must first all be referenced to a common vertical datum. Contemporary technologies, such as lidar and kinematic GPS data collection, can also benefit from VDatum in providing new approaches for efficiently processing shoreline and bathymetric data with accurate vertical referencing. VDatum is currently available for Tampa Bay, New York Bight, Delaware Bay, Louisiana's Calcasieu River and Lake Charles, central California, Puget Sound, Strait of Juan de Fuca, and north/central North Carolina. In addition, VDatum development is near completion for Chesapeake Bay, Mobile Bay to Cape San Bias, Southern California, Long Island Sound and New York Harbor, and projects are also commencing for an area from New Orleans to Mobile Bay, the Gulf of Maine and the Pacific Northwest. Given the numerous applications that can benefit from having a vertical datum transformation tool, the goal is to develop a seamless nationwide VDatum utility that would facilitate more effective sharing of vertical data and also complement a vision of linking such data through national elevation and shoreline databases. [C9568]

"Estimates of Radial Current Error from High Frequency Radar using MUSIC for Bearing Determination"

Quality control of surface current measurements from high frequency (HF) radar requires understanding of individual error sources and their contribution to the total error. Radial velocity error due to uncertainty of the bearing determination technique employed by HF radar is observed with both direction finding and phased array techniques. Surface current estimates utilizing Multiple Signal Classification (MUSIC) direction finding algorithm with a compact antenna design are particularly sensitive to the radiation pattern of the receive and transmit antennas. Measuring the antenna pattern is a common and straightforward task that is essential for accurate surface current measurements. Radial current error due to a distorted antenna pattern is investigated by applying MUSIC to simulated HF radar backscatter for an idealized ocean surface current. A Monte Carlo type treatment of distorted antenna patterns is used to provide statistics of the differences between simulated and estimated surface current. RMS differences between the simulated currents and currents estimated using distorted antenna patterns are 3-12 cm/s greater than those using perfect antenna patterns given a simulated uniform current of 50 cm/s. This type of analysis can be used in conjunction with antenna modeling software to evaluate possible error due to the antenna patterns before installing a HF radar site. [C9569]

"Neural Network Based Approaches for Detecting Signals With Unknown Parameters"

The detection of gaussian signals with unknown correlation coefficient, ρ_{hos} , is considered. A strategy for designing mixture of experts in composite hypothesis test is proposed. It is based on designing a single multi-layer perceptron (MLP) trained with ρ_{hos} varying uniformly in $[0,1]$ to approximate the average likelihood ratio (ALR), and evaluate it for fixed values of ρ_{hos} , so as to identify different variation subintervals of ρ_{hos} , attending to the single MLP performance. Taking into consideration the relation that exists between MLP structure and the boundaries it is capable to build, we propose to train different MLPs with different sizes for each subinterval (MLP1 and MLP2, for the lower and higher half, respectively) for improving detection capabilities controlling computational cost. To improve the approximation implemented by MLP1, a radial basis function neural network (RBFNN) trained for the lower subinterval of ρ_{hos} has been combined with MLP2. As the functions approximated by the RBFNN and the MLP are equivalent but different, a combination strategy has been proposed based on thresholding the networks outputs and applying them to an OR logic function. Although this scheme does not outperform the 2MLPs, the reduction in computation cost is very important. [C9570]

"Considerations in Marine Sand Mining and Beach Nourishment"

Beach nourishment restores beaches and enhances both their recreational value and their utility in shore protection. Increasing population in coastal areas and competition for land use has reduced the availability of terrestrial borrow pits while older sand pits have been exhausted. This situation has driven the search for borrow or mining sites offshore. Presently, almost all the marine sand mining along the Atlantic and Gulf coasts of the

U.S. is to obtain material for publicly funded, beach nourishment. Much of this activity is in waters subject to federal jurisdiction. The demand for construction aggregate in metropolitan and developing coastal areas suggests that there might be an additional demand on offshore sand resources. Marine sand mining, as any type of dredging, disrupts habitat and can disturb transitory fishes and marine mammals. By altering the configuration of the sea floor, sand mining modifies wave transformation and, possibly, nearshore currents. Removing a large quantity of offshore sand and placing it in the nearshore zone alters habitat and sediment-transport processes. For over a decade, there has been a series of studies concerned with the potential environmental consequences of offshore sand mining and subsequent beach nourishment. A more recent set of projects developed and tested a suite of protocols for monitoring dredged and nourished areas. The field study testing the draft monitoring protocol was conducted in the active, sand-mining region of Sandbridge Shoal, offshore of Virginia Beach, Virginia. Results indicate that repopulation of dredged areas is enhanced by leaving patches of undisturbed bottom within the dredged region. No negative impacts on macrobenthos or demersal fishes were noted. Changes in wave transformation resulting from modifying the bottom topography are relatively small and, as the sand-mining sites tend to be in waters greater than 10 m deep, usually only occur during storms. In some instances, dredging shoals may decrease inshore wave height by diminishing the concentration of wave rays caused by refraction on the shoal. Shore-based radar may offer advantages for monitoring waves in the near shore. Agencies involved with individual sand-mining programs should consider participating in consortia managing local, coastal observing systems. Location and elevation/depth (x,y,z) data with sufficient metadata is the basic dataset necessary for determining and monitoring changes in the shore and seafloor surface. The data can be acquired as profiles or, especially in nearshore regions, swath-bathymetry surfaces. Profiles should be spaced to capture changes in topography. On-shore and off-shore measurements should be synoptic or nearly so. Although there are valid and strong scientific and management reasons for implementing a standardized, minimum monitoring protocol for marine sand mining, there appears to be little will for such a program. The obvious problem is cost coupled with the question "who pays?" Costs continue beyond the actual monitoring project. If data are in an electronic format, someone must maintain the computer system and the web site. In the case of beach nourishment projects, although the locality or agency sponsoring the project would carry the immediate expenses, eventually the cost would work down to the tax payer. For commercial mining of construction aggregate, the cost would wind up with the "end user." There are additional problems. The question "why monitor?" must be answered. If the data are collected solely to satisfy a monitoring requirement and are stored, unused the exercise cannot be justified. Widely and easily accessible monitoring data would help determine common factors contributing to the performance of sand mining and beach nourishment projects and would be beneficial in improving the predictive models. [C9571]

"E-SLAM solution to the grid-based Localization and Mapping problem"

A new solution to the simultaneous localization and modelling problem is presented. It is based on the stochastic search of solutions in the state space to the global localization problem by means of a differential evolution algorithm. A non linear evolutive filter, called evolutive localization filter (ELF), searches stochastically along the state space for the best robot pose estimate. The proposed SLAM algorithm operates in two steps: in the first step the ELF filter is used at a local level to re-localize the robot based on the robot odometry, the laser scan at a given position and a local map where only a low number of the last scans have been integrated. In a second step the aligned laser measures together with the corrected robot poses are used to detect when the robot is revisiting a previously crossed area. Once a cycle is detected, the Evolutive Localization Filter is used again to re-estimate the robot poses in order to integrate the sensor measures in the global map of the environment. The algorithm has been tested in different environments to demonstrate the effectiveness, robustness and computational efficiency of the proposed approach. [C9572]

"Combined use of complementary pairs of sequences with orthogonal sequences of different length"

Complementary pairs of sequences (Golay sequences) are currently being applied to multiple fields of engineering. This paper describes the way in which to combine these sequences with other sequences of different length in the same physical transmission channel by generating pairs of sequences which are not Golay but are orthogonal to them. This new set of sequence pairs can be efficiently generated, thereby rendering their implementation suitable for logic devices. The possibility of attaining a combined use of sequences of different lengths, with no interference between them, in the same application will be demonstrated, so allowing the use of each sequence for different purposes. This technique offers a wide range of uses, especially among them, in communications, transmission channel identification and multisensor arrays. [C9573]

"Utilization of LIDAR and NOAA's Vertical Datum Transformation Tool (VDatum) for Shoreline Delineation"

The National Oceanic and Atmospheric Administration (NOAA), an organization of the U.S. Department of Commerce, is mandated to map the United States' coastal boundary, defining the nation's legal shoreline. This paper presents a new methodology for extraction of shorelines from lidar data. The methodology incorporates NOAA's vertical datum transformation tool (VDatum) for transforming lidar data to a specified tidally-based datum for shoreline extraction. The VDatum utility comprises geoid models, fields representing departures of an orthometric datum from local mean sea level, and hydrodynamic models portraying tidal regimes for accurate demarcation of coastal lines. The procedure presented here minimizes the variability and subjectivity that have plagued more traditional shoreline delineation techniques. The semi-automated routine allows for consistent, non-interpreted shorelines to be derived, providing significant advantages over proxies such as the high water line, beach scarps, and dune lines. This technique is invariant to coastline type, and has provided good results for a range of margins, such as a sandy or rocky. Additional advantages include the ability to derive multiple tidally-based shorelines from a single dataset and greater flexibility in data acquisition. Perhaps most importantly, the lidar data can be collected in a manner to support a variety of Integrated Ocean and Coastal Mapping (10CM) applications, including nautical charting, storm surge/tsunami modeling, coral reef mapping, ecosystem monitoring, and coastal mapping. [C9574]

"Demonstration of a Novel Man-Portable Magnetic STAR Technology for Real Time Localization of Unexploded Ordnance"

We report results of field tests of the first prototype of a novel man-portable Magnetic Scalar Triangulation and Ranging (STAR) technology. The new magnetic sensor system technology is being developed with support from the Strategic Environmental Research and Development Program (SERDP) to provide an easily deployable magnetic sensor system for real-time, point-by-point Detection, Localization and Classification (DLC) of magnetic targets such as Unexploded Ordnance (UXO) and buried mines. The STAR technology is based on a multi tensor gradiometer approach that uses magnetic gradient tensor magnitudes, i.e., "gradient-contraction-type" parameters to perform DLC of magnetic targets. The magnetic STAR sensor uses the scalar functions to triangulate a magnetic UXO-type target's position vector and to calculate the target's magnetic signature vector. The vector components of an object's magnetic signature provide a basis for real time classification of its type, i.e. UXO-like or not. In order to provide proof of principle of the STAR concept and demonstrate its advantages for high mobility magnetic sensing applications, we designed, constructed and field-tested a prototype man-portable STAR Gradiometer. The portable gradiometer's hardware and software are completely self-contained and provide a practical and user friendly capability for real time DLC of magnetic targets. Target DLC parameters: e.g., range, bearing, elevation and magnetic signature are correlated with Global Positioning System time and position data and displayed in near real time (total delay < 3 seconds) on a heads-up display that clips onto the operator's safety glasses. Interactive software controls data acquisition, performs signal processing to remove residual motion noise effects and runs the STAR Algorithm to generate and display the target's DLC parameters. Field tests have demonstrated proof-of-principle of the STAR concept and conclusively demonstrated that the technology has unique advantages for DLC by highly mobile sensing platforms. While being carried and operated by a single individual, the portable sensor has demonstrated very robust, motion noise resistant performance even while undergoing rotational motion of more than 40 degrees per second. The field test results very strongly indicate that the man-portable STAR technology can provide a wide variety of highly maneuverable sensing platforms (including Autonomous Underwater Vehicles) with uniquely effective, motion-noise-resistant magnetic sensing modalities for DLC of magnetic targets such as UXO and underwater mines. [C9575]

"Reliable Seabed Characterization for MCM Operations"

Seabed type has a major influence on mine countermeasures (MCM) operations. In this paper an accurate and efficient seabed characterization method is presented. The basic classification is performed by wavelet-based decision trees, while a data fusion algorithm based on Dempster-Shafer Theory of Evidence is used to combine the information provided by multiple observations from the same or different sensor platforms. Markov Random Field filtering of the resulting belief maps is finally used to provide cleanly delimited seabed segmentations. The technique is demonstrated using data obtained by NURC during recent sea experiments with NATO partner nations. [C9576]

"Data quality and sampling requirements for reliable wave measurement with HF radar"

HF radar systems located on the coast can provide measurements of surface currents and waves. The maximum range of these measurements depends on the signal to noise in the radar backscatter spectrum. Previous work, comparing radar with buoy wave measurements, has shown that a second order peak signal to noise of 15dB can provide reliable measurements of the directional wave spectrum. However recent evidence suggests that this is not sufficient and some ideas for a more robust measure are discussed. For radar and buoy

measurements averaging is required in order to reduce the variance in wave parameter estimates. The work of Sova (1995) on the impact of temporal sampling variability in radar Doppler spectrum estimation on wave measurement is reviewed. The implications of this for various sampling strategies that have been used for radar wave measurements is discussed and compared with the corresponding sampling variability of wave buoy measurements. The impact of increased averaging will be demonstrated using WERA data from the Eurorose Fedje experiment. [C9577]

"Generalization of Trapezoidal Vague Set and Its Use for Analyzing the Fuzzy System Reliability"

In this paper, definition of trapezoidal vague set (A. Kumar et al.) is generalized and by considering several cases it is shown that definitions of triangular vague set (S.M. Chen, 1997), trapezoidal vague set (A. Kumar et al.), triangular fuzzy number (G.J. Klir and B. Yuan, 1995), (H-J. Zimmermann, 1996) and trapezoidal fuzzy number (G.J. Klir and B. Yuan, 1995), (H-J. Zimmermann, 1996) are the particular cases of the definition of trapezoidal vague set introduced in this paper. Also arithmetic operations between two trapezoidal vague sets are introduced. Further new methods are developed for analyzing the fuzzy reliability of series and parallel systems. The developed methods are applied to analyze the fuzzy reliability of a radar warning receiver. [C9578]

"Evaluation of Edge Detection Techniques towards Implementation of Automatic Target Recognition"

The vision of Automatic Target Recognition (ATR) is through an integrated command identification architecture that combines non-cooperative and cooperative identification sensors and systems. The ATR implemented shall support development of situational awareness i.e., overall, general knowledge of the tactical battlefield environment, including the location of friendly, neutral, and enemy forces and plan of action for battle. The required operational capability will then be achieved by combining onboard data from multiple sensors and systems with indirectly supplied off board information. Edge Detection is one of the major image-processing requirements for achieving efficient and accurate target recognition in difficult domains. The on-board sensors used on combat aircraft are Electro-optic Targeting Sensors (EOTS), Infra-red (IR) sensors, Radar, Synthetic Aperture Radar (SAR) and Inverse SAR (ISAR) providing vast amount of images with different characteristics helpful for detecting targets. This paper concentrates on the assessment of advanced edge detection techniques on all types of sensor input images obtained for the implementation of automatic target recognition for air-to-air, air-to-sea and air-to-ground applications. This paper also describes the approach towards implementation of automatic target recognition for the entire range of sensor inputs. The proposed algorithm for automatic target recognition is for implementation on airborne systems with potential use on ground stations. [C9579]

"Wireless Content Management (WiCoM) for Mobile Device"

A Content Management System (CMS) is a software system used for the management of computer files, image media, audio files, electronic documents and Web contents. A Wireless CMS in contrast is administered through a mobile device wirelessly. This paper details the development of a wireless content management system (WiCoM) which works in real time, using wireless programming and J2ME development platform. The focus of our work is to enable secure cyber content administration using smart mobile device. The novelty of the WiCoM system is-it provides cost-effective implementation of real-time news reporting system and e-commerce sites. [C9580]

"Polyphase Sequences Design-Using MSAA"

Sequences having the minimum peak aperiodic autocorrelation sidelobe level one (1) are called Barker Sequences. Such sequences have been used in numerous real-world applications such as channel estimation, radar and spread spectrum communication etc. Unfortunately, the longest known biphasic and quadriphasic Barker sequences are of lengths 13 and 15 respectively. In this paper Modified Simulated Annealing Algorithm (MSAA) is used to design thirty-two phase sequences, which have good autocorrelation properties. Some of the synthesized results are presented here. The properties of the sequences up to length 24 have Barker properties which were not reported in literature earlier. The sequences of lengths from 4 to 289 have autocorrelation properties better than Frank codes. The synthesized 32-phase sequence sets are promising for practical application to radar and spread spectrum communication systems. [C9581]

"Quantitative Evaluation of Location Systems Techniques for Short-Range RF-Based Sensor Networks"

The use of wireless sensor networks has been proposed for a large spectrum of location-dependent applications. Because of the current restrictions on processing power, power supplies and sensor hardware, most of the

current systems struggle between accuracy and complexity. Seeking to provide the current location of nodes with a minimum additional cost to each sensor nodes, several location tracking systems have proposed different techniques based on received radio signal strength. In this paper we present a quantitative evaluation of several location tracking systems techniques based on radio signal strength indication through trace-driven simulations. Our work shows that previous assumptions on the limitations of these techniques do not consider the transmission of messages with several signal strengths which improves considerably the accuracy of these systems. [C9582]

"Capacitive coupling return loss of a new pre-ionized monopole plasma antenna"

Plasma antenna has unique properties like low RCS and variable impedance; however, previous plasma antenna uses 500 MHz RF power to generate a plasma column, which is limited in energy efficiency and bandwidth. Here we introduce a new type of plasma antenna that generates plasma column with pre-ionization from a DC high voltage, and signal is coupled to the plasma antenna via capacitive coupling. This device greatly increases the overall energy efficiency and bandwidth of the plasma antenna. The electron density of the plasma is nearly constant in entire length, and is tunable in some degree by the DC current. Two plasma antenna of 1 m and 60 cm have been built and tested against same length metal antenna, the results are similar. Positive gain can be achieved at X-band. This device also shows a few obvious resonance lines where signal are absorbed strongly by the plasma. Return loss and radiation pattern of such antenna is reported. [C9583]

"Consideration of Crustal Deformation in the Adjacent Area of Plate Boundary"

Southwestern Ryukyu Arc and Eastern Taiwan region are characterized by subduction and collision of the Philippine Sea Plate and Eurasian Plate, Huatung Longitudinal Valley is a huge valley running between the cities of Hualian and Tainan in Eastern Taiwan with approximate length of 130 km. This valley is also located in between central mountain range and coastal mountain range. Since 1998, Tokai University has started to measure seismological activities with Dahan Institute of technology (DIT), a Taiwan Technology University, also measuring GPS and electronic distance meter (EDM) data to monitor the crustal movement in the northern part of test area. We have performed a repeat-pass differential interferometric analysis using the ENVISAT/ASAR data. In addition, we propose a crustal movement extraction approach useful when insufficiency of the successful SAR image pairs. [C9584]

"Reconstruction of Super-resolution Spectra for the Beamformed Data in HF Skywave Radar"

For economy, the digital beamforming (DBF) is used to transform a huge array outputs into the bearing ones at several expectable directions in HF skywave radar. However, as the target signal phases on the different array elements are mixed in the beamformed data, the resolvable super-resolution spatial spectra of the coherent targets within a beamwidth can not be directly constructed by the existing algorithms any more. Therefore, in this paper, an improved method for the reconstruction of these spatial spectra is investigated to solve the underlying problem. A so-called pseudo-inverse processing is used to transform the beamformed data to the equivalent array data on the peak of the detected target range-velocity spectra. Then, combined with the Toeplitz construction and the multiple signal classification (MUSIC) algorithm, the coherent targets are resolved and the azimuth estimates are improved. Since the window weighting is usually used in the beamforming, the different weighting effect on the pseudo-inverse processing is also discussed. [C9585]

"Wavelet-Based ECG and PCG Signals Compression Technique for Mobile Telemedicine"

One of the emerging issues in telehealth care system is how effectively the limited and well established mobile technologies that are now almost globally usable are exploited. The main challenge is to develop a mobile telemedicine system to transmit biosignals directly to a specialist in an emergency medical care unit for monitoring/diagnosis using an unmodified mobile telephone which provides the patient's information on the spot without unnecessary delays in seeking care, access to health facility and provision of adequate care at the facility. To provide a practical mobile telemedicine in GSM/GPRS/EDGE/UMTS limited capacity for transmitting the cardiac data for the diagnosis of cardiovascular diseases (CVD) which are widespread health problems with unpredictable and life-threatening consequences in most regions throughout the world, the implementation of biosignals compression technique is focused in this paper. Therefore, a new and simple target data rate (TDR) driven Wavelet-threshold based cardiac signals compression algorithm is presented for mobile telemedicine applications. The performance of the compression system is assessed in terms of compression efficiency, reconstructed signal quality and coding delay. This algorithm is tested using MIT-BIH ECG databases and qdheart PCG database records and the experimental results are compared with other Wavelet based ECG coders. The presented algorithm is less complex because it does not require QRS detection, amplitude and period normalization and period sorting. [C9586]

"Acoustic Doppler sonar for gait recognition"

A person's gait is a characteristic that might be employed to identify him/her automatically. Conventionally, automatic for gait-based identification of subjects employ video and image processing to characterize gait. In this paper we present an Acoustic Doppler Sensor(ADS) based technique for the characterization of gait. The ADS is very inexpensive sensor that can be built using off-the-shelf components, for under \$20 USD at today's prices. We show that remarkably good gait recognition is possible with the ADS sensor. [C9587]

"Resolution limits of closely spaced random signals given the desired success rate"

Fundamental limitations on estimation accuracy are well known and include a variety of lower bounds including the celebrated Cramer Rao Lower Bound. However, similar theoretical limitations on resolution have not yet been presented. We exploit results from detection theory for deriving fundamental limitations on resolution. In this paper we discuss the resolution of two zero mean complex random Gaussian signals with a general and predefined covariance matrix observed with additive white Gaussian noise. The results are not based on any specific resolution technique and thus hold for any method and any resolution success rate. The theoretical limit is a simple expression of the observation interval, the user's pre-specified resolution success rate and the second derivative of the covariance matrix. We apply the results to the bearing resolution of two emitters with closely spaced direction of arrival impinging on an array of sensors. The derived limits are verified experimentally by model order selection methods such as the Akaike Information Criterion and the Minimum Description Length. [C9588]

"Radiation, scattering and receiving of pulse signals for subsurface object identification"

In many papers there are approaches for solving subsurface sensing and identification of subsurface objects based on FDTD methods with original method of identification (Pockok et al., 1998, Rao et al., 2002). There are not efficient for complex objects and lengthy object (its geometrical size is larger than pulse longitude). In this paper a numerical model for calculating far field scattered by complex objects is described. An evaluation is based on analytical evaluations. The results for some testing objects are represented. [C9589]

"Localization of the reflecting centers using multifrequency and multiposition antenna scanning"

The problem of processing for multifrequency and multiposition cross-section scanning data has been considered. The method of quasisolution searching with compromise model of interaction of the reflecting centers and antenna has been used. The accuracy properties of the method have been analyzed. [C9590]

"Research on Multi-mode Fusion Tracking of OTHR Based on Auction Algorithm"

In OTHR's tracking system, we will estimate the state of a discrete-time, linear stochastic system whose observation process consists of a finite set of known, non-linear measurement models. MPDA is capable of exploiting multipath target signatures arising from discrete propagation modes that are resolvable by the radar, but it is very time-consuming and will bring multipath tracks. In this paper, a multi-mode fusion tracking of OTHR based on auction algorithm (A-MFT) is proposed, which effectively solve the problem of multi-mode measurements. When tracking a single and non-maneuvering target with four possible measurements, simulations in clutter environment show that the computing speed of the algorithm proposed in this paper is greatly higher than that of MPDA, and the tracking precision just a little lower than that of MPDA, further more, A-MFT will not bring multipath tracks and do not need consequent track association. [C9591]

"A Method of Radar Signal Separation"

Radar signal separation is an important link in the chain of information processing for air-defense, which is the process of extracting unknown independent radar signals from unknown sensor measurements. Sometimes, the source signals and the method of combination are unknown, and hence the problem is related to the problems of blind deconvolution and blind equalization. Blind signal separation is sometimes referred to as independent component analysis, as it generalizes principal component analysis to produce independent signals rather than simply uncorrelated signals. Based on the frequency localization of Morlet wavelet and genetic algorithm, this paper presents a method of radar signal separation. Some examples are given. The results of separation demonstrated this method is effective and low sensitivity to noise. [C9592]

"Multitarget association and tracking in 3-D space based on particle filter with joint multitarget probability density"

This paper addresses the problem of 3-dimensional (3D) multitarget tracking using particle filter with the joint

multitarget probability density (JMPD) technique. The estimation allows the nonlinear target motion with unlabeled measurement association as well as non-Gaussian target state densities. In addition, we decompose the 3D formulation into multiple 2D particle filters that operate on the 2D planes. Both selection and combining of the 2D particle filters for 3D tracking are presented and discussed. Finally, we analyze the tracking and association performance of the proposed approach especially in the cases of multitarget crossing and overlapping. [C9593]

"A New Multi-objective Fully-Informed Particle Swarm Algorithm for Flexible Job-Shop Scheduling Problems"

A novel Pareto-based multi-objective fully-informed particle swarm algorithm (FIPS) is proposed to solve flexible job-shop problems in this paper. Firstly, the population is ranked based on Pareto optimal concept. And the neighborhood topology used in FIPS is based on the Pareto rank. Secondly, the crowding distance of individuals is computed in the same Pareto level for the secondary rank. Thirdly, addressing the problem of trapping into the local optimal, the mutation operators based on the coding mechanism are introduced into our algorithm. Finally, the performance of the proposed algorithm is demonstrated by applying it to several benchmark instances and comparing the experimental results. [C9594]

"SAR Image despeckling using grey system theory"

Speckle noise appears in synthetic aperture radar (SAR) images owing to the SAR imaging mechanism. This paper investigates and proposes a novel method on SAR images despeckling via grey system theory. In the method, we dynamically select one referential sequence to stand for inner region pixels, and a group of comparative sequences to represent the pixels to be enhanced. Then, edge pixels are distinguished from non-edge pixels via the grey relational degrees between the two kinds of sequences, and kept unchanged; while the noise and inner region pixels, taken as non-edge pixels, are adjusted to some new values. Experimental results show that the method, when being applied to both simulated and real SAR images, has a good performance in peak signal-to-noise ratio (PSNR) improvement, and outperforms most of the conventional filters: mean filter, median filter, Lee filter, Kuan filter and Frost filter. [C9595]

"SPHERE-A Simulation Platform for Heterogeneous Wireless Systems"

This paper presents SPHERE, a Simulation Platform for Heterogeneous wiREless systems, and describes its motivation, methodology and implementation approach. This advanced system level simulation platform emulates simultaneously the transmission of GPRS, EDGE Multi-slot, HSDPA and WLAN at the packet level, which allows conducting novel investigations on common radio resource management for beyond 3G systems or on the optimization of radio resource management techniques. This paper presents the simulation platform, validates it and introduces its research potential. [C9596]

"Web Interface for Querying/Searching RDF Database"

The resource description framework (RDF) is a language for representing information about resources on the web. However, RDF can also be used to describe other data and relationships between objects in the data. Many applications in the signal/image processing (SIP) community (such as radar imaging, electromagnetics, etc.) generate large amounts of data. Researchers would like to have online access to this data as well as the ability to easily explore and mine the data. Our application's RDF metadata representation is similar to that of a conventional database, and users can use forms to search the database, or use the standard RDF query language SPARQL, to create queries. In most cases, all the data as well as the RDF description of the data resides on secure Department of Defense (DoD) major shared resource center (MSRC) resources. In order to provide a web interface for exploring this data, we need a secure way to access the user data. Towards this goal, we use the user interface toolkit (UIT) to provide a web application that allows users to browse and search the RDF metadata of large SIP databases securely and conveniently on their desktop. The UIT uses the same Kerberos technology and Secure ID cards that are used to access all MSRC machines and provides an application programming interface (API) for building clients to access computing resources in the DoD high performance computing and modernization program (HPCMP). [C9597]

"Technical Challenges of Supporting Interactive HPC"

Users' demand for interactive, on-demand access to a large pool of high performance computing (HPC) resources is increasing. The majority of users at Massachusetts Institute of Technology Lincoln laboratory (MIT LL) are involved in the interactive development of sensor processing algorithms. This development often requires a large amount of computation due to the complexity of the algorithms being explored and/or the size of the data set being analyzed. These researchers also require rapid turnaround of their jobs because each iteration directly

influences code changes made for the following iteration. Historically, batch queue systems have not been a good match for this kind of user. The Lincoln Laboratory Grid (LLGrid) system at MIT-LL is the largest dedicated interactive, on-demand HPC system in the world. While the system also accommodates some batch queue jobs, the vast majority of jobs submitted are interactive, on-demand jobs. Choosing between running a system with a batch queue or in an interactive, on-demand manner involves tradeoffs. This paper discusses the tradeoffs between operating a cluster as a batch system, an interactive, on-demand system, or a hybrid system. The LLGrid system has been operational for over three years, and now serves over 200 users from across Lincoln. The system has run over 100,000 interactive jobs. It has become an integral part of many researchers' algorithm development workflows. For instance, in batch queue systems, an individual user commonly can gain access to 25% of the processors in the system after the job has waited in the queue; in our experience with on-demand, interactive operation, individual users often can also gain access to 20-25% of the cluster processors. This paper will share a variety of the new data on our experiences with running an interactive, on-demand system that also provides some batch queue access. [C9598]

"A new method for joint estimation of three-dimensional parameters of coherent signals"

A new method is proposed to estimate the frequency and 2-D arrival angles of coherent signals over a wide frequency band, which is called time-space smoothing DOA algorithm (TSS-DOA). Firstly the time-space smoothing matrix is constructed by temporal data and spatial data of two uniform parallel linear arrays and smoothing technique, and then 3-D parameters of coherent signals can be obtained from its eigenvalues and the corresponding eigenvectors. The algorithm can precisely estimate 3-D parameters of coherent signals, and doesn't need the multidimensional spectrum peak search with smaller computational load and parameters paired automatically. In addition, it can still estimate correctly 3-D parameters of signals when signals have the same one or two dimensional parameters. Simulation results show that the proposed algorithm is effective. [C9599]

"To improve the GMAP for speckle filtering by consideration of the correlation of SAR images"

Synthetic aperture radar (SAR) images are corrupted by speckle noise, which degrades the quality and interpretation. One of the most traditional speckle filters, the Gamma maximum-a-posteriori (GMAP) speckle filter, is based on the first order texture models in SAR images, i.e. the local mean and local variance, without the consideration of the correlation present in the SAR images. To enhance the speckle filtering effects, this work presents an improved GMAP filter based on a new model which is able to take the correlation present in images into account. The final experimental results show that our proposed algorithm can get better performance in terms of the speckle suppression and the fine details preservation. [C9600]

"2007 International Symposium on Intelligent Signal Processing and Communications Systems Proceedings"

The following topics are dealt with: coding theory; speech and audio signal processing; wireless personal communication; system on chip; SoC; direct of arrival estimation; image enhancement and filtering; CDMA; TDMA; OFDM; radar tracking; radar detection; image denoising; feature extraction and detection; information theory; spectral estimation; image segmentation; wireless ad hoc and sensor network; FPGA; embedded system; parameter estimation; channel estimation; image coding; analog circuits; digital filters; filter bank; video coding and transmission; MIMO communication; motion estimation; multimedia management; computational intelligence; image fusion; communication protocols; face detection; PCA; ICA; SVD; optical-signal processing; radar signal processing. [C9601]

"GPS smart jammer suppressin algorithm based on spatial APES"

Smart jammer is one of the most threat interferences for the GPS receiver, so a smart jammer suppression algorithm is proposed in this paper, which combines spatial amplitude and phase estimation(APES) method and high resolution coherent subspace estimation method. The new method can resolve the problem that spatial APES is unable to cancel multiple coherent interferences, and also provide the accurate GPS signal estimate. Simulation results show that the feasible of the proposed method. [C9602]

"The SIP High Productivity Toolset for Parameter Sweeps and Monte Carlo Runs"

Many high performance computing tasks take the form of parameter sweeps. The same task is run many times with different sets of input parameters. For example, a researcher may run thousands of radar signature jobs over various azimuth and elevation angles. Keeping track of the status of the overall situation can be daunting and tedious, leading the user to manually track the state of all the jobs. Time that could otherwise be spent on analysis is spent managing the parameter sweep itself. The signal and image processing high productivity toolset

(SIPHPT) automates much of the parameter sweep management activity. With the user supplying a single configuration (setup) file, the SIPHPT provides utilities to submit jobs, verify proper job setup, and monitor overall status. The SIPHPT creates underlying master scripts to manage the jobs. In the event jobs do not complete successfully, the exact same commands (and setup file) can be used to submit and monitor the jobs again. The master script will only run jobs that have not yet been successful. The SIPHPT thus provides utilities to reduce manual job management activity associated with large parameter sweep jobs, availing users more time to concentrate on analysis. We describe the SIPHPT and provide information on where to find it on Department of Defense (DoD) high performance computing (HPC) Aeronautical Systems Center (ASC) and Army Research Laboratory (ARL) Major Shred Resource Center (MSRC) systems. [C9603]

"Unbiased plain gradient algorithm for adaptive 11R notch filter with constrained poles and zeros"

An unbiased plain gradient (UPG) algorithm for a constrained adaptive IIR notch filter (ANF) is presented in this paper. The proposed algorithm employs the bias removal technique to remove the bias existing in the estimate of the filter parameter, resulting in good estimation. The computer simulation results have shown that the proposed technique is unbiased. [C9604]

"FPGA SAR Processor with Window Memory Accesses"

In the paper, we present a design of FPGA SAR processor with four 1D FFT processing elements, double internal RAM buffers and double external SDRAM modules. Without traditional corner turn phase, we propose a data layout scheme mapping one row of logical matrix into a rectangular window in physical banks of SDRAM in order to increase the practical I/O throughput between SDRAM modules and SAR processing elements. In addition, we theoretically analyses the optimal window size to minimize the total number of opening/closing pages when performing 2D FFT by balancing the number of handling physical pages between row accesses and column accesses. The experimental results show our window layout approach achieves 650 MB/s of effective bandwidth, reaching nearly 82% of peak bandwidth, with 58.1% increases compared to traditional Corner Turn approaches. The proposed SAR processor has been implemented in an FPGA test-bed, outperforming related works in both of computing speed and image scale. [C9605]

"A time-domain beamformer for UWB through-wall imaging"

A time-domain beamformer using ultra-wideband short-pulse (UWB SP) signal for through-wall imaging (TWI) applications is proposed in this paper. The impact of the wall on the performance of through-wall radar imaging, such as wave refraction and velocity change, is considered in the design of the beamformer. Proof verifying the proposed beamformer is provided using the finite-difference time-domain (FDTD)-simulated high fidelity through-wall radar data. Simulation results demonstrate that hidden targets behind the wall can be located accurately in both range and angle by using the presented time-domain beamformer. [C9606]

"Experimental consideration on the synthetic range-profile processing by stepped-frequency radar"

In radar system, separation of the target from the background clutters requires high range and cross-range resolution. To improve the range resolution, shorter pulses and wideband-FM pulses are utilized. However, they tend to complicate system architecture and to increase implementation cost due to the necessity of a wideband receiver. The synthetic range-profile (SRP) processing has been proposed to realize high range resolution without using the wideband receiver. The principle of the processing is that the echoes of stepped-frequency pulses are synthesized by IDFT in the frequency domain. This enables us to obtain short pulses in the time domain. This paper proposes the SRP radar composed of high-speed wideband exciter, which generates the stepped-frequency pulses. Through experiments, effectiveness of the proposed system is verified. [C9607]

"Tropospheric signal delay estimation in repeat-pass SAR Interferometry with QR-factorization"

In this paper we analyze the reason why the QR-factorization is a very useful method for estimate the atmospheric delay in the unwrapped step of the SAR interferometric processing. We compute the solution of phase delay parameter model and confront the result with the GPS data metrics and the result from the Saastamoinen model. It is important to develop the new method for estimate the atmospheric phase delay and errors unwrapping procedure without the GPS or metrological data. [C9608]

"On the concatenation of LDPC and RS codes in magnetic recording systems"

In this paper, we investigate the sector failure rate (SFR) and the burst-error correction capability of two coding solutions in magnetic storage systems. The two-level solution involves concatenating an outer RS code with an inner LDPC code whereas the one-level solution is an RS-only or an LDPC-only system. Although the outer RS

code incurs an additional rate loss, it is expected to gain in the presence of burst errors. The rate of the LDPC code and the i -level of the RS code can be chosen optimally to suit the operating condition of the channel. These solutions have also been studied in various technical papers in literature. Previously mentioned performance measures are used to evaluate strengths and weaknesses of these two solutions. [C9609]

"A new variable step-size equivariant adaptive source separation algorithm"

In this paper, variable step-size blind source separation (BSS) algorithms are investigated. Since it is hard to achieve both fast convergence and stable tracking performance for a given step-size, step-size is crucial for the equivariant adaptive source separation (EASI) algorithms. Firstly, the measurement of the independence for the output signals is analyzed, then, a new EASI algorithm whose step-size is changed adaptively by mutual information is proposed. Computer simulation results show that the new algorithm has satisfactory convergence and stable tracking performance. [C9610]

"A novel method of interference suppression for civil aviation air-ground communication based on blind signal extraction"

An algorithm of interference suppression for the Very High Frequency (VHF) air-ground communication in civil aviation is presented in this paper. Based on the analysis of the civil aviation VHF air-ground communication characteristics, the blind signal extraction (BSE) model for the civil aviation VHF air-ground communication is established, and the interference suppression scheme is proposed. The blind signal extraction is introduced, then an extraction method based on the kurtosis and the adaptive deflation is adopted to realize the suppression of the interference. Simulation results are also presented to show the validity of the proposed method. [C9611]

"Localization with orientation using RSSI measurements: RF map based approach"

Localization of RFIDs in the indoor environment will entail determining both the position and the orientation of the user. This paper develops estimator using RSSI measurements to predict the position and orientation of a transmitter in an indoor environment. The best estimator tried was an K-nearest neighbours model that gave an accuracy of approximately 83% for position prediction and 93% for orientation prediction. It was also found that the RSSI values change throughout the day, meaning that an adaptive estimator is necessary for localization. [C9612]

"Characterisation of an L-band digital noise radar"

This paper experimentally evaluates the dynamic range of a digital radar at L-band employing both direct digital synthesis and direct RF sampling, thus minimizing analogue components. Noise-like radar waveforms and pulse to pulse waveform agility are utilized to improve the signal to noise ratio and reduce the sidelobe levels to improve the dynamic range of the radar system. [C9613]

"Ultra wideband forward scattering radar: Concept and prospective"

Initial stages of progress in the research on Ultra-Wideband Forward Scattering Radar are presented in this paper. The system's concept and high potential for several practical applications are investigated. kwjUltra-Wideband radar forward scattering radar [C9614]

"Low noise wideband optical mixing and optical up-conversion architecture"

Radar requirements differ from commercial Radio-Over-Fibre (ROF) systems. High signal to noise ratio (SNR) and spurious free dynamic range (SFDR) in a photonic beam forming architecture are paramount. The architecture described in this paper uses phase modulation to overcome previous limitations. It provides high SNR, low-distortion mixing, enabling optical systems to be used in radar, beamforming and similar applications. [C9615]

"Results from TerraSAR-X geometric and radiometric calibration"

As TerraSAR-X, due for launch in June 2007, will be an operational scientific mission with commercial potential, product quality is of crucial importance. The success or failure of the mission essentially depends on the calibration of the TerraSAR-X system ensuring the product quality and the correct in-orbit operation of the entire SAR system. This paper describes the calibration procedures for TerraSAR-X and the dedicated activities to be performed during the five months commissioning phase. Results from on-ground tests are discussed with respect to geometric and radiometric calibration of the TerraSAR-X system. [C9616]

"A novel nonlinear technique for sidelobe suppression in radar"

Sidelobes can be completely removed if the returns from two pulses based on Golay complementary sequences are combined after pulse compression. However these pulses cannot be sent simultaneously via frequency separation because of a phase term which is dependent on the unknown range. We propose to transmit one of the sequences at two offsets, above and below the carrier frequency. This facilitates recovery of the square of the autocorrelation function independently of signal phase. A modification to the Golay pair results in sequences having complementary squares of autocorrelation sequences. This enables complementary behaviour with frequency offset pulse pairs. The nonlinear squaring operation introduces small manageable cross-terms in place of sidelobes. [C9617]

"Review of the state of the art of UK AESA technology and the future challenges faced"

The UK Ministry of Defence is starting to introduce in to service the next generation of radar technology. This technology brings with it the potential for significant improvements in performance for airborne, ground based and naval applications as well as benefits for through life capability maintenance. However there are a number of challenges facing the implementation of advanced radar technology that can make these benefits difficult to realise. To address these challenges, the UK MoD is currently undertaking a number of advanced research and technology demonstration programmes aimed at in-service equipment and future upgrade programmes. This paper summarises the current state of UK MoD funded next generation radar programmes and highlights the key challenges faced. These challenges represent opportunities which the wider community can address. [C9618]

"Spatial variant apodization on subsurface imagery acquired along circular trajectories"

Stepped Frequency Continuous Wave Radar (SFCW) systems have become during the last decade a popular design architecture for Subsurface Radar (SR) applications. Due to its data acquisition methodology, the collected reflections must be imaged using Fourier techniques. This process can produce the presence of sidelobes, reducing the Signal to Noise Ratio (SNR) of the displayed data. This paper proposes the use of Spatially Variant Apodization (SVA) techniques for sidelobe elimination on SR data acquired along circular trajectories. The SVA approach was tested on real data yielding promising results. [C9619]

"T/R module design and production processes for airborne radar systems"

E-scan radar for airborne applications has now reached a stage of maturity in several European companies and has demonstrated significant performance improvements with high reliability and affordable costs. T/R modules are a key component of E-scan radars and have transferred out of the development laboratory and through the initial production stage into radar production. Adequate technical performance for T/R modules is now taken for granted, so the focus is now upon achieving lower production cost and mass, together with repeatability of performance and reliability in volume manufacture. This paper discusses the key drivers that enable successful transfer into large scale production of T/R modules. [C9620]

"Impact modelling of wind farms on marine navigational radar"

The impact of wind turbines on radar systems is of increasing concern. This paper addresses the problem of the offshore wind farm and presents a methodology used to model the interference of wind turbines with pulsed marine navigational radar. It will show the ability to model some of the main issues such as; target spreading, sidelobe detection and the appearance of ghost targets. A comparison between the results from the model and measured data taken near the North Hoyle wind farm in North Wales, UK is provided. [C9621]

"Passive radar detection using wireless networks"

We report the first results of simulation and experiments on the utilisation of 802.11 wireless network transmissions in a passive radar system. Target detection of a range of objects has been simulated and then experimentally demonstrated. Waveform analysis shows that some of the modulations used within the transmission sequence have suitable properties for target localisation. These initial results suggest this technique has a high potential for the basis of a widely available low cost passive surveillance system. [C9622]

"DRM signals for HF passive bistatic radar"

The concept of using digital HF signals in a passive radar configuration is discussed. Ambiguity functions of these signals are presented and a comparison of the waveform's properties is made with other signals of interest in passive radar in terms of their radar parameters. The ambiguity functions show no ambiguities, approach the ideal thumbtack shape and are thus potentially very useful for passive radar applications. For 5 s integration

times the signals have a processing gain in excess of 40 dB. Expected coverage is examined in terms of the signal to interference ratios expected for an array of receivers and compared to the coverage obtained using a single surveillance channel. It is concluded that to support the detection ranges of which HF is capable, a phased array surveillance receiver is required to reduce the effects of interference from the transmitter. [C9623]

"Lossy compression of voltage level samples before detection in distributed passive bistatic radar systems"

Distributed passive radars confront the high dynamic range challenge by splitting the receiver physically to provide high SNR samples of the transmitter as well as reduced cochannel interference. The receivers are mutually coherent and must therefore exchange voltage level data for computation of the cross-ambiguity function. The data bandwidth required for fullprecision (16 bit) data is about 2 Mbps to support for a single channel. This data bandwidth demand can stress the cost and latency of distributed passive radars. Therefore we investigate the effect the sensitivity of a passive radar system using several methods to compress the voltage level samples prior. [C9624]

"A geometrically based multipath channel model for passive radar"

The presence of multipath on the signals of opportunity used by passive radar can have a significant impact on their performance. Therefore, the availability of meaningful and representative models for the multipath environment experienced by a passive radar is an important element for both the development of appropriate signal processing techniques and for a reliable performance assessment. A geometrically based multipath channel model for passive radar is derived in this paper, that is able to account for different scenarios in terms of both transmitter and receiver antenna location. The derived model is used as the basis for a channel simulator, that is described in this paper, that allows to evaluate the realistic performance of passive radar systems. [C9625]

"Options for mitigation of the effects of windfarms on radar systems"

This paper follows on from a previous paper 'Windfarm characteristics and their effect on radar systems' [1] and considers various options for the mitigation of these previously described windfarm effects. Options include terrain screening, modifications/upgrades to existing radar, new radar designs, data fusion schemes utilising data from multiple sensors, stealthy wind turbines and windfarm layout. [C9626]

"Windfarm characteristics and their effect on radar systems"

Generating electricity from renewable energy sources is a major part of the UK Government's strategy to tackle climate change and to develop business opportunities. It has set ambitious targets of generating 10% of all UK's energy from renewable sources by 2010 with an aspiration to double this by 2020 [1]. Wind energy is expected to be a key contributor to these targets. There are concerns, however, that the construction of windfarms will have a negative effect on both Air Traffic Control (ATC) and Air Defence (AD) radars and many windfarm developments fail due to objections from radar stakeholders. This paper explores the effects, on radar system components, of the echo signals received as a result of radar illumination of a windfarm and their impact on the overall performance of a radar system. [C9627]

"Reducing clutter in airborne radars equipped with electronically scanned array antennas"

An airborne radar's antenna beam pattern interacts with the terrain beneath the platform to create unwanted clutter returns. A novel display format for depicting this interaction was used to identify fundamental differences between traditional, mechanically scanned antennas and contemporary active electronically scanned array (AESA) antennas. It was observed that the elevation sidelobes of an AESA are deflected away from the vertical when the antenna's mainbeam is steered electronically in azimuth; this can reduce the clutter caused by the altitude line. A technique is then proposed for reducing the clutter within the system by exploiting this phenomenon of deflected elevation sidelobes and the theory is supported with results from flight trials. [C9628]

"Measurement of the wind vector over sea by an airborne radar altimeter, which has an antenna with the modified beam shape"

In this paper, a possibility of recovering the wind vector over sea using an airborne radar altimeter in a short-pulse scatterometer mode, which has a nadir-looking wide-beam antenna with the modified beam shape forming an egg-shaped footprint, and in conjunction with simultaneous range Doppler discrimination techniques, is discussed, and a measuring algorithm of the sea surface wind speed and direction is proposed. [C9629]

"Polarisation filtering for small target discrimination in ground clutter"

The Electronic Warfare and Radar Division (EWRD) of the Defence Science and Technology Organisation (DSTO) has initiated a number of studies investigating the exploitation of polarimetric analysis for the detection of small targets in strong ground clutter. This paper presents the results of experimental trials and associated signal processing research where an understanding of the scattering mechanisms present is used to design discrimination filters in the polarisation domain. It is shown that these physics-based filters provide highly efficient detection and identification of a variety of manmade targets immersed in strong clutter environments.

[C9630]

"Analysis of calibrated sea clutter and boat reflectivity data at C- and X-band in South African coastal waters"

The temporal characteristics of low grazing angle sea clutter and boat reflectivity are considered for both fixed and stepped frequency waveforms under a range of environmental conditions and geometrical configurations. Detectability of boats using an asymptotically optimal detector is evaluated empirically, as well as the influence of the local sea on boat reflectivity. Measurements were conducted with a calibrated, coherent, staring, pulsed radar system at C- and X-band frequencies ranging from 6.9 GHz to 10.3 GHz. [C9631]

"CFAR loss and gain in K-distributed sea-clutter and thermal noise"

Setting the detection threshold in a radar operating in a maritime environment is critically dependent upon the characteristics of the sea clutter. Analysis is presented in this paper of the performance of the cell-averaging CFAR in K-distributed sea clutter. It is demonstrated that in spatially uncorrelated, spiky clutter the CFAR loss is very high, but may be reduced in some circumstances by increasing the radar system noise level. It has previously been reported [5] that in spatially correlated clutter the CFAR loss may be reduced by optimising the cell averager length, which in some cases leads to a 'CFAR gain' rather than a loss. Here, it is shown how added thermal noise affects this performance. [C9632]

"High grazing angle X-band sea clutter distributions"

This paper investigates the statistical properties of sea clutter at grazing angles higher than traditionally used for airborne maritime radar surveillance, i.e. 10° - 45° . Specifically, we study the spatial distribution of X-band, high resolution and high grazing angle polarimetric sea clutter data. We found that among the VV, HV, and HH polarisations, the VV data is least spiky and the K distribution usually provides a good fit. The HH data is spikiest and its distribution exhibits a sudden departure from the K distribution in the upper tail region, which usually requires the KA or similar distributions to achieve a better fit. Due to drawbacks of the KA distribution, this paper proposes a combination of two K distributions to fit the distribution of sea clutter with spikes. Referred to as the KK distribution model, it is found to provide the best overall fit. [C9633]

"Load balancing for typical radar systems with overlapping surveillance space"

Dwell scheduling has been an important issue for radar systems. This research explores the on-line dwell scheduling issue over multiple transmitters/receivers in radar systems. We investigate the minimization of the maximum load in the system to balance workloads over multiple transmitters/receivers. Two on-line algorithms are proposed and analyzed against adversaries. Algorithm GREEDY, which assigns an incoming dwell task to the available transmitters/receivers, is shown to be a 3-competitive algorithm against the adversary. The online algorithm, denoted by Algorithm FIXED, by assigning the arriving dwell task to a pre-defined transmitters/receivers is proved to be a 2-competitive algorithm. The capability of the proposed algorithms is evaluated by a series of experiments. Although Algorithm FIXED outperforms Algorithm GREEDY against adversaries in the worst cases, Algorithm GREEDY outperforms Algorithm FIXED if the dwell tasks are uniformly distributed in the behavior in experiments. [C9634]

"Investigating possible bistatic configurations for ship wake imaging through simulation"

We consider the context of marine surveillance and ocean imaging with bistatic radar. Since these systems are not yet mainstream and somewhat costly, not much experience has been accumulated yet in the literature and their usefulness is still under debate. We propose an approach to find potentially interesting bistatic configurations that could be used in the future to monitor the ocean, and especially ship wakes. First, we review the important acquisition parameters and how their choice might influence the final image. These considerations are then validated through simulation for frequencies above 1 GHz. [C9635]

"Modelling sea clutter temporal correlation in detection calculations"

The calculation of target detection performance in a combination of K-distributed sea clutter and radar system noise has, to date, been limited to the case where the clutter speckle component is independent from pulse to pulse (as sometimes occurs with frequency agility). Recent advances in computational techniques reported here allow the speckle and noise to have different correlation times, thereby allowing fixed frequency and limited frequency agility radars to be modelled at all ranges and at all clutter to noise ratios. [C9636]

"Optimisation of bistatic HF surface wave radar configurations"

HF surface wave radars are increasingly being deployed in bistatic configurations, usually via the mechanism of overlapping the coverage of two monostatic radars and sharing signals, but sometimes as intrinsically bistatic radar designs. In either case, the advantages which may attach to bistatic scattering geometries may easily be compromised by suboptimum positioning of the transmitting and receiving systems. Here we address the problem of finding the optimum spatial configuration for a given palette of radar missions, taking account of target signatures, clutter, noise, propagation and geographical constraints on the siting of the radar facilities. [C9637]

"Application of HRRP even rank central moments features in satellite target recognition"

Because high resolution range profile (HRRP) is sensitive to pose and translation, HRRP even rank central moments are proposed to be used as a kind of stable target feature in satellite target recognition. HRRP SNR is enhanced by wavelet denoising, then translation-invariant central moments are extracted. In order to reduce the feature vector dimension, even rank central moments are proposed to be used alone. Nearest neighbor fuzzy classifier (NNFC) that is very fit for combined features is introduced to process the central moments features vector. Experimental results with real satellite data show that good recognition performance is obtained. [C9638]

"Radar interoperability with modern multi-function radars-a case study"

This paper addresses the interoperability of modern multi-function radars operating in close proximity to 'conventional' radar systems. The paper introduces the 'measures of performance degradation' used in the Sula System approach, discusses the timescales relevant to the interoperability study, provides typical case study visualisations for the fictitious scenario and introduces some potential mitigation techniques to improve interoperability. [C9639]

"Beam pattern synthesis for spaceborne sparse aperture radar"

An effective aperture based approach is proposed for the beam pattern synthesis of a sparse aperture array by frequency diversity and post-data processing. The beam pattern by synthesizing signals received by sparse apertures is aliased with many grating lobes caused by undersampling in the effective aperture. To mitigate grating lobes, extra sampling points should add in the effective aperture to improve the sampling period. Two strategies are considered in this paper: first, by frequency diversity on M subapertures, the sampling points can be improved by a factor of M ; second, by synthesizing K pulses on the entire coherent processing integral (CPI) data cube, a synthesized array can be achieved and the sampling points can be improved by K times. With the total MK sampling points improved, the peak sidelobe level (PSL) can be reduced to -25dB with the given parameters. However, the performance is, to some extent, sensitive to position errors. Experimental simulations show the optimized effect. [C9640]

"Precise full wave analysis of the slot coupled circular microstrip patch antennas"

An aperture coupled circular microstrip patch antenna is analyzed. A full wave spectral domain method of moment along with a reciprocity analysis of a single aperture coupled microstrip element is applied. Both the electric surface current on the circular patch and the equivalent magnetic current on the aperture are considered. Results on effects of different feed line stub length, aperture length, different feed substrate permittivity and thickness on input impedance and resonant frequency of the antenna are provided. [C9641]

"Performance analysis of sidelobe blanking system in presence of mutual coupling"

Sidelobe blanking (SLB) devices are used in connection with the radar system to reduce the number of false alarms due to impulsive interference. This paper studies the impact of the mutual coupling between the primary and the secondary antenna on the probability of blanking a sidelobe jammer interference via an SLB device. Performance curves are presented and the role of the different jammer and mutual coupling parameters thoroughly investigated. [C9642]

"Fractal feature based radar signal classification"

Automatic target recognition (ATR) using radar, is a much researched area with a demand for better and more accurate classification algorithms. In the present work, the local fractal dimensions of a synthetic aperture radar image have been used as features to classify ground targets. The performance of the fractal feature based ATR algorithm was compared with that of three other established ATR algorithms, viz. the simple yet powerful template matching ATR algorithm, the Gaussian model based Bayesian classifier, and the recently proposed principal component analysis based nearest neighbour algorithm. The fractal feature based classifier was shown to outperform all the other algorithms. [C9643]

"Features influence on targets classification performance using the high range resolution profiles (HRR profiles)"

In this paper, we propose the aircrafts supervised classification using the high range resolution profiles (HRR Profiles), extracted from ISAR images. [C9644]

"Time-frequency analysis of late time electromagnetic transients from radar targets"

Radar target recognition based on late time target resonance detection has been widely reported in the literature. Determination of the commencement of the late time period is crucial when extracting such resonance information because including the early time components significantly degrades the accuracy of the extraction due to the time-varying behaviour in this portion of the signature. In this paper an investigation of the late time commencement point is carried out in the Time-Frequency domain using the example of a wire scatterer. [C9645]

"Hidden Markov Models in radar target classification"

A classification technology is presented that uses Hidden Markov Models (HMMs) to classify simulated and real radar signals from five classes of targets: personnel, tracked vehicles, wheeled vehicles, helicopters and propeller aircrafts. Similar to techniques that have been well proven in speech recognition, the time-varying nature of radar Doppler data is exploited. The method classifies the different targets by their different Doppler characteristics. The purpose of this paper is to make a comparison between three kinds of HMM Methods: 1. HMM with continuous outputs (CHMM) 2. HMM with discrete outputs (DHMM) 3. Semi-continuous Hidden Markov Models (SCHMM) [C9646]

"Performance results for a knowledge-aided clutter mitigation architecture"

This paper describes performance results for a knowledge-aided (KA) space-time adaptive processing (STAP) architecture. The knowledge-aided parametric covariance estimation (KAPE) method forms the basis of the architecture. We employ high-fidelity simulated data from the DARPA KASSPER program in the analysis. For the scenarios considered, the KA-STAP architecture provides substantial performance improvement over traditional, post-Doppler STAP. [C9647]

"Bistatic JDL-STAP for ground moving target detection"

Optimum STAP requires knowledge of the true interference covariance matrix. In practice, this matrix is not known and is estimated from training data that must be target-free and statistically homogeneous with respect to the test data. These conditions are often not satisfied, which degrades the detection performance. Single-data-set algorithms have been proposed to circumvent this problem, which works solely on the test data. In this paper, we study the issues associated with applying reduced-dimension techniques to these algorithms in a bistatic radar system. Simulation results show an improved detection performance against conventional STAP algorithms in heterogeneous environments. [C9648]

"Bistatic STAP using DVB-T illuminators of opportunity"

In this paper, we examine the feasibility of applying Space-Time Adaptive Processing (STAP) to bistatic passive radars using noise-like signals in general and Digital Video Broadcasting-Terrestrial (DVB-T) illuminators of opportunity in particular. We show that by working on the appropriate mixing product, we make the application of classical STAP methods and nonhomogeneity detection possible. We finally confirm these theoretical results by simulations created from real measurements. [C9649]

"A rare event approach to the detection of target-like signals in CFAR training data"

A new method based on the existence of rare events (RE) is proposed to detect the presence of nonhomogeneous samples in a set of Constant False Alarm Rate (CFAR) training data. Two RE schemes designated as the mean-to-mean ratio (MMR) and the variance-to-variance ratio (VVR) tests are proposed. No a priori knowledge of the nonhomogeneity topology is assumed. Analysis using Monte-Carlo method based on Rayleigh clutter and Swerling I target models is presented. Target-like interferences which seriously degrade the detection performance of the cell-averaging CFAR detector can be detected with a higher probability by RE detectors. [C9650]

"Developments to a multiband passive radar demonstrator system"

The system and design issues of a multiband passive radar demonstrator developed by BAE Systems Advanced Technology Centre have been reported [1], together with some initial results from measurement trials. Further enhancements have been implemented at system, hardware and software levels to improve the overall performance of the demonstrator, through the introduction of analogue cancellation circuitry, computer control of RF band selection and switching, and faster run time signal and data processing. This paper briefly summarises the original multiband passive radar demonstrator, then outlines the rationale for the various enhancements, their practical implementation, and the supporting analysis, simulation and modelling. Results from recent trials of the enhanced demonstrator with civil aircraft 'targets of opportunity', that confirm the improved detection performance and multiband operation, are presented and discussed. [C9651]

"Passive Bistatic Radar (PBR) demonstrator"

We present a system characterisation of a Passive Bistatic Radar (PBR). The system under investigation exploits 'illuminators of opportunity', which in this case are commercial, non-cooperative, VHF FM broadcast transmissions. The paper demonstrates the detection of large passenger-jet aircraft over central London. The merits of FM broadcast transmissions are also analysed in a radar context. Furthermore, a system characterisation with performance predictions is presented. [C9652]

"Robust radar detection of moving ground targets with STAP"

Airborne radar sensors are able to detect small and slow moving ground targets using short dwell times by distinguishing the weak target signature from the dominant ground clutter signal. The capability of a Ground Moving Target Indication (GMTI) sensor is principally governed by the Probability of Detection (PD). Other capabilities such as geolocation, tracking and recognition are derived from these detection data. One method used to enhance the PD for platforms with multiple phase centres is Space Time Adaptive Processing (STAP). In this paper we report an experimental assessment of a robust STAP algorithm [1, 5, 6] using the QinetiQ Enhanced Surveillance Radar (ESR) data. From our results it is apparent that robustness may be introduced if a selective training methodology is employed to estimate the data covariance. Results are given for both Pre- and Post-Doppler STAP [C9653]

"Suppressing radio frequency interferences with adaptive beamformer based on weight iterative algorithm"

By comparing the disadvantages and advantages of conventional algorithms of adaptive beamformer, we put forward an adaptive beamformer based on weight iterative algorithm for suppressing RFI according to the distributing properties of radio frequency interference (RFI) in different range cell. We get the initial weight vector of the adaptive beamformer by using the algorithm of minimum variance distortionless response (MVDR). The other weight vectors are computed by the algorithm of linearly constrained minimum variance (LCMV) based on the last time weight vector. The covariance matrix of the two algorithms, i.e. MVDV and LCMV, are constructed with the array snapshots in the far range cells which have not useful radar echo. Thus the free degree of antenna array is increased. The feasibility of the adaptive beamformer is proved by using it to process the actual radar data. [C9654]

"Space-Time Adaptive Processing in the presence of non-Gaussian sea clutter"

Space-Time Adaptive Processing (STAP) is an optimum technique for target detection in the presence of Gaussian clutter [1,2]. However, for high resolution sea surveillance radar, clutter statistical properties are different [5]. Therefore classical STAP must be redefined. It can be done in the framework of the theory of Spherically Invariant Random Process (SIRP). In this paper a simple method of improving STAP performance in the presence of non-Gaussian clutter is proposed. Results are validated using simulated data. [C9655]

"Modulus spatially variant apodization algorithm for radar images"

In this paper, a non-linear adaptive sidelobe control algorithm is discussed and a modulus spatial variant apodization (MSVA) algorithm is proposed. This algorithm could provide a method different from spatial variant apodization (SVA) mainlobe differentiation, which uses modulus to differentiate mainlobe. Good result is obtained. Experimental study is conducted to this algorithm by simulations and actual radar image. The result validates effectiveness of this algorithm. [C9656]

"A robust CFAR algorithm in non-homogenous environments"

A new constant false alarm rate (CFAR) detection processor is presented that exhibits a robust CFAR performance in the condition of non-homogenous environment. Its performance would be independent of background noise power. Since the processor can track noise power variation and adopt itself to the new background conditions. The new CFAR algorithm, called as Adaptive Switching CFAR (AS-CFAR) is analysed and simulated CFAR to demonstrate its improved robustness in non-homogenous environments. [C9657]

"The error statistics of surveillance radar position measurements"

This paper examines the error statistics of 2D radar position measurements when targets are extended relative to the resolution of the system. Monte Carlo simulations are used to show how the common assumption that range and angular errors are uncorrelated fail in some cases. It fails in surveillance systems that apply centroid image processing on extended targets. It is shown that there may be correlation which depends on the aspect angle of the target. Two new models that include this correlation are proposed. The proposed models can be used to improve the performance of target tracking and data fusion algorithms. [C9658]

"Naval environment propagation characteristics and clutter suppression in a multi sensor tracker"

This paper outlines the diverse approach taken to design sensors and a system which performs in Naval propagation and clutter conditions, for the Seawolf Mid Life Update Multi Sensor tracker. It describes the design solution for an I band monopulse radar, a Ka band monopulse radar and a Long Wave Infra Red (LWIR) Electro Optical sensor. It then describes how the three sensor are fused to provide a system with world wide naval environment capability. [C9659]

"Permutation test algorithms for nonparametric radar detection"

In this paper, we present two new permutation test algorithms for applications to radar detection. The first algorithm is a direct realization of the permutation test definition with very high computational complexity in the most cases, the second algorithm is based on histogram computations and, consequently, computationally very efficient. As is well known, detectors based on permutation tests have constant false alarm rate (CFAR) characteristic under clutter with the exchangeability property. The exchangeability property means that the multidimensional distribution of a block of clutter (noise) samples is invariant under permutations of its arguments. [C9660]

"Multipath cancellation on reference antenna for passive radar which exploits fm transmission"

In this paper we address the problem of multipath cancellation in the reference signal used in passive radar, which exploits FM transmitter as source of opportunity. The presence of multipath echoes in the reference signal is demonstrated to strongly affect the detection performance of passive radar. Based on the well-known CMA approach, new multi-dimensional techniques are derived for the adaptive equalization of the reference signal. The effectiveness of the proposed techniques is demonstrated with reference to typical simulated scenarios. The proposed strategies are shown to be very appealing solutions for multipath cancellation in the reference signal for passive radar. [C9661]

"Order statistic and Maximum Likelihood distributed CFAR detectors in Weibull background"

we consider a fuzzy distributed system in which the local detectors do not produce a binary decision but a value (between 0 and 1) of the membership functions. In this case, we consider the problem of the distributed Maximum Likelihood (ML) and Order Statistic (OS) constant false alarm rate (CFAR) detections using various fuzzy fusion rules in Weibull clutter. Computer simulation is used for performance evaluation of these distributed detectors using fuzzy fusion rules such as "Algebraic Product", "Algebraic Sum", "Union" and "Intersection". The results indicated robust and superior performance of algebraic product in the homogenous and non-homogenous situations. [C9662]

"A novel approach to range profile estimation of a moving vehicle by road monitoring radar"

A wideband signal is generated from a sum of narrowband signals. As a result, the Doppler shifted signal received from a vehicle can be compensated for using specially designed auxiliary signals. This enables vehicle range profile estimation and classification. [C9663]

"Antijamming method based on orthogonal codes jittered and random initial phase for SAR"

Corresponding to the disability of Synthetic Aperture Radar (SAR) to suppress Terrain Scattered Jamming, this paper proposes an anti-jamming method based on jittering orthogonal codes and random initial phase. Orthogonality between neighbor slow moments' pulse codes leads to disability of jamming to get coherent match filtering gain of range direction, at the same time, random initial phase at each slow-moment leads to disability of jamming to finish azimuth match filtering. Experiment testifies the ability of this method to suppress jamming from the directions of range and azimuth. [C9664]

"Real Time STAP for UESA Radar"

We present results on the implementation of Circular Array Space Time Adaptive Processing (C-STAP) algorithms in Lockheed Martin Orincon Defense's Real-Time Interactive Programming and Processing Environment (RIPPEN). Full and reduced rank Linearly Constrained Minimum Variance Multiple Quadratic Pattern Constraint (LCMV-MQPC) algorithms are implemented in RIPPEN to support portability, rapid hardware implementation, analysis, and optimization on PC and Mercury Systems. Measures for required algorithm overhead are developed and evaluated. The complexity of STAP algorithms requires metrics drawn from full implementation and experimentation. In particular, the interplay between covariance matrix size, rank reduction techniques, available DSP chip cache memory, and matrix inverse and multiplication operations are considered. [C9665]

"Impact of measurement-to-track data association errors on RCS-based target classification"

This paper develops a method for quantifying the impact of measurement-to-track data association errors on the performance of RCS-based classification schemes. First, it develops a means for assessing the impact of misassociations on the estimated mean and variance of the track SNR. This is done for both single-target and multiple-target tracking scenarios. Then, it develops an approach for quantifying the impact of errors in the estimated mean and variance on classification performance. As such, the user can easily relate the number of misassociations to the probability of error in the classification scheme, given specific target information and a particular decision region. Furthermore, this approach could prove useful to those designing RCS-based classification schemes. For example, the decision region could be intelligently modified to reduce the overall probability of error if certain types of misassociations are anticipated. Future work will explore revisions necessary to accommodate multi-modal SNR distributions and more sophisticated SNR estimators. [C9666]

"Study on sar jamming measures"

The objective of this paper is to build some typical jamming models, to evaluate the performance of different jamming modes, and finally to develop a simulation system of SAR countermeasures. For this purpose, the mathematic models of various SAR jamming modes are analyzed firstly; secondly the whole image processing from raw data simulation to jamming mode choosing are carried out, where the optimal jamming measure can be chosen out according to the three evaluation indexes discussed in this article. The simulation experiments demonstrate that the simulation system is accurate and useful to increase the survival probabilities of ground targets. [C9667]

"An efficient reduced-rank STAP based on PASTd algorithm"

In this paper, the projection approximation subspace tracking deflation (PASTd) algorithm is investigated in the context of the reduced-rank STAP (RR-STAP), where a recursive approach is employed to estimate the clutter subspace. Instead of a direct use of the classic PASTd algorithm in the RRSTAP, a modified PASTd adapted to the STAP is applied. With respect to the conventional eigenvalue decomposition (ED) approach, the presented algorithm is computationally more efficient and meanwhile able to achieve comparable convergence effectiveness. The presented methodology is validated by the Monte Carlo simulation. [C9668]

"Ionospheric clutter modelling for VHF passive radars operating at high latitudes"

Passive VHF and UHF radars which prosecute FM and television broadcasts above 50 MHz at latitudes greater than 40 degrees will occasionally be subject to large amounts clutter from the ionosphere. Conventional pulsed, active radars can mitigate against auroral clutter by appropriate gating of the transmitter waveforms and receiver samples. However, passive radars, as CW systems cannot. In this report we describe the basic features of meter

scale ionospheric clutter, describe how its magnitude can be estimated, and how its effects may be mitigated. [C9669]

"Regularisation methods for covariance matrix estimation in low sample support stap"

The interference covariance matrix in space time adaptive processing is usually estimated from training data that is drawn from adjacent range gates to the cell under test. The sample support required to achieve good detection performance may not be available in practice due to many factors such as system design or clutter heterogeneity. In this paper, we address this problem by proposing and evaluating a number of covariance matrix regularisation methods that attempt to reduce the bias of the eigenvalues of the estimated covariance matrix and hence improve the signal detection performance. [C9670]

"An ECCM signaling approach for deep fading of jamming reflectors"

This article develops a radar signaling scheme to combat a repeat jammer. The signaling design is based upon emission of radar pulses following a specific orthogonal structure, where both pulse diversity and coding techniques are combined. The construction, through simple one-step matched-filtering, ensures that signals emitted by a jammer are placed in a deep fade, allowing for easier identification of false reflectors. [C9671]

"Air Target Identification-concept to reality"

This paper summarises our journey with radar-based Non-Cooperative Air Target Identification (NCTI) from initial concepts through to practical implementation by military users. Thus we will discuss the underpinning ideas and particularly the difficulties associated with making the techniques work in practice and the solutions we have found. We will discuss the three main approaches: Jet Engine Modulation (JEM), High Range Resolution Profiling (HRRP) and Range-Doppler Imagery (RDI). These are described well in [2]. Difficult issues such as robust database generation and confidence measures-at the heart of current research-will be considered also. [C9672]

"A novel approach to residual video phase removal in spotlight SAR image formation"

An ad hoc residual video phase (RVP) removal algorithm is developed for a spotlight SAR system employing dechirp-on-receive, and working with the polar format algorithm (PFA). In comparison with the existing RVP compensation approach, just two additional complex multipliers are required in the new algorithm to accomplish the range resampling of the polar formatting, in the meantime of RVP removal. [C9673]

"Moving target detection for synthetic aperture radar via shadow detection"

In this paper a novel technique is presented for detecting moving targets in SAR imagery by tracking the shadow of the target over multiple looks instead of using the target direct energy return. Unlike the SAR image of a moving target that is blurred and displaced, the shadow of the target is displayed at the true target location. The detection performance using shadow is primarily independent of the target radar crosssection and depends upon the clutter to noise signal level. A change detection method is developed that provides detection via identification of the target shadow as an outlier from a background distribution. The background is inferred from a sequence of SAR images. It is shown that simple temporal averaging by alignment of the image for estimating the background works reasonably well with SAR images offering good shadow contrast. The technique was successfully demonstrated initially using real radar data from a short range spotlight SAR system. Results against weaker shadow signals at longer stand-off range have also proved very encouraging showing a moving target being detected at 10 km standoff range. [C9674]

"Constrained adaptive beamforming for electromagnetic interference cancellation for a synthetic aperture radar"

Imaging capability of a Synthetic Aperture Radar (SAR) could be seriously limited or denied by an electromagnetic interference signal impinging on the antenna array during imaging. The use of antenna nulling techniques shall cancel the effects of interferences over the collected SAR data. Despite the greater Signal to Interference plus Noise Ratio (SINR) obtainable using an antenna nulling interference cancellation technique, nulling the antenna pattern in the direction of arrival of the disturbance could modify the antenna main lobe gain during the synthetic aperture, resulting in a distorted focused image even after interference cancellation. Thus, forming a SAR image while suppressing an interference can potentially destroy large regions of the image. In this paper we analyse several constrained spatial techniques aiming to reduce the interference level without significantly affecting the image quality. [C9675]

"Airborne Multi-frequency-Band SAR system and its information processing"

This paper describes the design of a Multi-frequency Band (MFB) SAR system and the flight tests, and discusses the methods of image formation, registration and fusion. Some experiment results are also presented. The MFB SAR system works in time-division mode so as to improve the compatibility of subsystems and to decrease the volume and the weight of the system. The MFB SAR images of the same scene are presented and some conclusion is made from the flight tests. Nonlinear Chirp Scaling algorithm is used to form the MFB SAR images. The problems of motion compensation for P-band SAR are analyzed. A new registration method is introduced based on subsection phase correlation, which can rectified the coordinates of the MFB SAR images with registration error less than 1 pixel. Finally, the MFB SAR images are fused based on the GHM multi-wavelet transform. [C9676]

"Pedestrian detection based on automotive radar"

Automotive radar sensors are able to measure the target range, azimuth angle and radial velocity simultaneously with high accuracy and update rate even in multiple target situations. Target recognition of radar objects is still a technical challenge and one of the most important topics to support future advanced driver assistance systems (ADAS). There is especially a large interest to distinguish between radar echo signals from human beings and from other objects in the target recognition scheme. Therefore, this paper elucidates the motion sequence of a walking pedestrian and describes this complicated process in a suitable technical model with different reflection points and related Doppler frequencies. Based on some measurements with a 24 GHz radar sensor several signal features are generated, which are used for the target recognition procedure. [C9677]

"On the application of pattern recognition to identification of simple targets based on resonance and polarization diversity"

In this paper, target radar features based on extracting the polarization matrix of each of the radar target's complex natural resonances (CNRs) in the time domain is investigated. These resonance frequencies and their complex residues (amplitudes) in a co- and cross-polar configuration form a polarization matrix decomposition of the target in late time and are also related to the principal dimensions of the target and their relative physical orientation. We have developed and investigated new radar target features, whereby, for incident circular polarization we generate horizontal and vertical complex residue patterns for each known target at the first few dominant resonance frequencies over a number of aspect angles. [C9678]

"Interrupted SAR waveforms for high interrupt ratios"

SAR operations typically require long flight lengths to provide the coherent sequences needed for cross-range imaging. For multi-function radars with SAR modes it is usually necessary to interrupt the SAR data collection sequences to support other essential radar modes. These data interruptions can require interruptions totalling up to 50% of the radar timeline. This paper analyses the simulation of antenna patterns at rates of data interruption, typically with 50% data loss. This paper compares the effects of high data interruption on SAR antenna patterns for both periodic and randomly spaced data interruptions. For spotlight mode SAR, the use of pattern averaging can be used to reduce the pattern sidelobes for the cases of randomly spaced data interruptions. [C9679]

"Lateral velocity estimation for automotive radar applications"

Automotive radar sensors are applied to measure the target range, azimuth angle and radial velocity simultaneously even in multiple target situations. But it is also possible to calculate the lateral velocity by a single radar measurement. Based on some analytical and experimental results it is shown in this paper that the lateral velocity of a radar target can also be measured precisely even in a single observation situation. This additional information of lateral speed is of much interest in all target tracking procedures, especially for typical city traffic situations and for advanced driver assistance systems (ADAS). [C9680]

"Bistatic radar using a spaceborne illuminator"

A bistatic radar has a physically separated transmitter and receiver. This paper investigates a bistatic radar system which uses a spaceborne Synthetic Aperture Radar (SAR) transmitter on board the European Space Agency's Envisat satellite and a stationary, ground based receiver. The advantages of this variant of the bistatic configuration includes the passive and therefore covert nature of the receiver, its relatively low cost, in addition to the possibility of using a non-cooperative transmitter. [C9681]

"Four-order bi-static imaging algorithm and auto-combination technique in constellation SAR"

system"

A bi-static SAR imaging algorithm based on four-order expansion and an auto-combination technique to improve both azimuth and slant range resolution in constellation SAR system have been described in this paper. The whole processing can be simply divided into two steps: bi-static SAR imaging and sub-image combination. Quantitative analysis and simulations are provided as well. [C9682]

"High resolution ISAR images of non-cooperative targets with a new spatially variant apodization method"

An Inverse Synthetic Aperture Radar (ISAR) obtains images of radar targets by means of an advanced signal processing. The image quality is usually measured by two parameters: resolution and sidelobe level. Sidelobe level is commonly reduced by lineal apodization (or windowing), this signal processing technique is simple but its mayor drawback is resolution loss. [C9683]

"Metamaterials-from magnetism to invisibility"

Metamaterials are artificial electromagnetic materials, that can be designed to have properties that are difficult or impossible to achieve with conventional, naturally occurring materials. Built from microstructure that is small compared to the wavelength of operation, metamaterials can be designed with effective permittivity and permeability values that can be large or small or even negative at any selected frequency. The engineered response of these artificially constructed metamaterials has had a dramatic impact on the physics, optics, and engineering communities, as we can now make practical materials exhibiting physical phenomena such as a negative refractive index, that were previously only theoretical exercises. In this paper, I will review the development of metamaterials, and discuss their use to control electromagnetic fields and hence to make lenses with sub-wavelength resolution and a cloak of invisibility. [C9684]

"Modified frost speckle filter based on anisotropic diffusion"

The demand for speckle reduction of synthetic aperture radar (SAR) images is to smooth the speckle noise while preserving the structure information of the original images. This paper provides a new method derived from Frost filter kernel for SAR images speckle reduction based on anisotropic diffusion. The anisotropic diffusion is the edge-sensitive diffusion, so it is introduced into the conventional Frost filter to get the better edge preservation for the speckled images. The final experimental results for both the synthetic speckled images and the real SAR images show that the proposed algorithm can get better performance in terms of the extent of the speckle suppression and the fine details preservation. [C9685]

"Digital radar"

A radar architecture is described in which radio frequency (RF) pulse waveforms are generated digitally in the transmitter and target returns are digitised without analogue down-conversion in the receiver, thereby eliminating most of the analogue components found in typical radar systems. This architecture, which has a number of important advantages over conventional radar systems, can be implemented using broadband digitisation technologies developed recently for the communications industry. [C9686]

"Exhaustive search for long low autocorrelation binary codes using length-increment algorithm"

important in many applications and their construction is a hard computational problem. Here a new exhaustive search algorithm is developed to find all optimal aperiodic binary sequences which are faster than simple one and it achieves its efficiency through a combination of the following four devices: (1) A branch-and-bound search strategy; (2) Search logic that avoids codes redundant relative to two PSL-preserving operations; (3) A fast recursive method for computing autocorrelation functions of binary sequences; (4) A simple scheme for partitioning and parallelizing, made possible by the fixed upper bound on psl. kw]Exhaustive search, Low autocorrelation binary sequence, Pulse compression. [C9687]

"SAR image enhancement by dominant scatterer removal"

In the paper the effective method of SAR image enhancement is presented. A strong scatterer produces sidelobes in range and cross-range dimension forming characteristic cross-shaped pattern centred on dominant scatterer. The presence of these sidelobes decreases the overall image quality and can mask weak scatterers close to the strong one. The proposed method is based on adaptive removal of modelled strong scatterer echoes from raw radar data. After removal the raw radar signal is reprocessed, and strong scatterers are then added to the final image. The method has been tested both using simulated and recorded data, showing its great

potential. [C9688]

"Sensors as intelligent robots"

The desire to anticipate, find, fix, track, target, engage, and assess, anything, anytime, anywhere (A2F2TE4A) by the US Air Force will require changes to how we modify, build, and deploy radar systems. The radar systems of the future must be intelligent and integrated within sophisticated systems of heterogeneous sensors that operate on many hypotheses at the same time. Within this paper we make a case that an intelligent system of sensors is obtainable in the near future and provide a futuristic scenario illustrating how some current technologies will play a role in obtaining this capability. [C9689]

"Caesar: Demonstrating AESA capability option for eurofighter captor radar"

The Euroradar consortium has developed a new antenna and associated hardware/software modifications which enable E-scan capability to be exploited by the existing Captor radar, while retaining all features and capabilities of the original system. The Captor Active Electronically Scanned Array Radar (CAESAR) upgrade package is accommodated within the Eurofighter Typhoon front fuselage and retains existing aircraft interfaces. The benefits of agile beam operation have been successfully demonstrated in two phases of flight trials, most recently on a Eurofighter Typhoon in early 2007. Most crucially, future advances in radar system supportability will benefit directly from experience on the CAESAR programme. [C9690]

"Shadow enhancement in SAR imagery"

Shadow cast by features on ground can be an important aid in object classification in synthetic aperture radar (SAR) images. Synthetic aperture imaging causes a fundamental limitation to shadow clarity due to the fact that the illuminator is moved during the data collection. This leads to a blend of echo and shadow, or geometrical fill-in in the shadow region. The fill-in is most dominant for wide beam synthetic aperture imaging systems. By treating the shadow as a moving target and compensating for the motion during the synthetic aperture imagery, we avoid the geometrical shadow fill-in. This new technique, referred to as the fixed focus shadow enhancement (FFSE) can be used directly as an imaging method on raw SAR data or as a post processing technique on the complex SAR image. In this paper, we demonstrate the FFSE technique on publicly available SAR data. [C9691]

"Despeckling SAR images in the undecimated wavelet domain based on scale correlation and GMRF model"

A new adaptive filtering algorithm in the undecimated wavelet domain based on several adjacent scales correlation is proposed in this paper. Moreover, the Gaussian Markov random field (GMRF) model is used to characterize the inner-scale contextual dependence of wavelet coefficients. In the end, both the simulated speckle images and the real SAR images are used to validate the performance of our new algorithm. [C9692]

"Polarimetric hot spot processing for ISAR image autofocusing"

In recent studies the possibility of extending autofocusing techniques to fully polarimetric ISAR systems has been proposed. One of the first techniques for ISAR image autofocusing still in use is the Hot Spot processing. In this paper, the Hot Spot technique is extended and applied to fully polarimetric ISAR data. A performance analysis is then provided and compared to single polarisation Hot Spot by using real data. [C9693]

"Investigating the effect of a target's time-varying Doppler generating axis of rotation on ISAR image distortion"

ISAR imaging has potential in assisting with the classification of non-cooperative targets. Blurred ISAR imagery may however lead to misleading classification results. Much research has been done to understand some of the causes of distortion in ISAR imaging mostly under the limited assumption that a target's axis of rotation is constant over the CPI. This paper investigates how the target's time-varying Doppler generating axis of rotation, caused by the complex 3D motion of a target at sea, contributes to ISAR image blurring. Quaternion algebra is used to aid the characterisation of a time-varying Doppler generating axis of rotation on the migration through cross-range cells. Real motion data of a sailing yacht is used to examine the effects of 3D rotational motion on ISAR imagery of point scatterer like simulated targets and the associated blurring. Simulation results show that small yaw rate perturbation during side-view ISAR imaging intervals gives rise to significant changes in the direction of the Doppler generating axis which results in scatters migration through cross-range cells. [C9694]

"Dual polarization wide-band interleaved spiral antenna array"

A new way to design dual polarization wideband spiral antenna array is presented. The proposed technique consists of two interleaved arrays, one for each polarization. The position of every spiral antenna is optimized through a genetic algorithm so that each array is nearly the size of the platform while having low sidelobes. Both resulting arrays have the same properties and are steerable. This method also helps to increase the bandwidth. A 200-elements spiral array (spiral of width 0.25m) with dual polarization is shown, its beam can be steered $\pm 30^\circ$, over more than two octaves (2.36:1). The physical rejection of the sidelobes (i.e. without weighting) is about -10 dB. The planar extension is also introduced. [C9695]

"Optimal fast-time beamforming with linearly-independent waveforms"

Optimal radar transmitter and receiver architectures are proposed for increasing the degrees of freedom for beamforming optimisation by transmitting linearly independent waveforms from each element of a phased array radar. This effectively encodes clutter returns with a spatial signature which enhances clutter-rejection performance in the spatial processing. The theory which enables the exploitation of these additional degrees of freedom is developed for a general set of linearly independent waveforms and considered in the context of both conventional beamforming applications as well as novel applications. [C9696]

"ISAR motion compensation using entropy metrics"

Radar imaging using an ISAR system requires the estimation of the targets kinematic parameters in order to be used for motion compensation. A focused and legible image requires this step. Some of the popular methods that perform this compensation are based on an entropy metric. This metric is relatively simple to use but requires a lot of computations (i.e. it can be quite slow) and it can also yield a false estimation due to local minima. In this work the authors introduced the use of a conditional entropy metric that helps with the problem of local minima and also propose the use of working with low resolution images to increase the speed of the estimation. Results are shown using real data. [C9697]

"SPIKE a Physical Optics based code for the analysis of antenna radome interactions"

This paper presents a new physical optics based radome code SPIKE which has been used by SELEX S&AS to assess the impact of radomes on antenna performance. After a brief summary of the mathematical basis of the code some advantages of Physical Optics such as the ability to predict 2nd flashlobes and calculate the near fields in the vicinity of the antenna are demonstrated. Finally a comparison of flight trials data with results obtained from SPIKE in conjunction with a radar detection model GARD is made. [C9698]

"An efficient set of features for pulse repetition interval modulation recognition"

Pulse repetition interval (PRI) modulation recognition is one of the essential processes in Electronic Support (ES) receivers. The recognized PRI modulation type and other measured pulse train parameters usually reveal the functional purpose of the radar and are of good use in emitter identification. In this paper, a novel feature set for PRI modulation recognition is proposed. The selected features exploit both the statistical and the sequential information of pulse intervals to describe specific modulation types. After feature extraction, a relatively simple multi-layer neural network is employed for classifying different PRI modulation types. With simulations, the feature set is shown to be capable of identifying all well-known PRI types. [C9699]

"Maximising the benefits of sophisticated electronic countermeasures systems"

As electronic countermeasure systems become more complex, the time taken between the equipment being specified, designed, developed and eventually fielded has lengthened significantly. During this development, advances in radar processing are likely to change the requirements for countermeasure waveforms, and the original specification from which the system was designed may no longer be appropriate. The hardware within modern countermeasure systems is designed in a flexible manner that will support the generation of waveforms not explicitly defined during the specification process. However, the functionality of this hardware is constrained by the inflexible nature of the support tools that prevent novel waveforms from being defined within the system. This paper provides background to the evolution of countermeasure systems and their support tools, and continues to discuss more flexible approaches to the definition of countermeasure waveforms such that maximum benefit can be gained from modern technology in an ever-changing environment. [C9700]

"Diffusive CFAR & its extension for Doppler and Polarimetric data"

A new CFAR is introduced based on non-linear PDE (Partial Differential Equation) operators & geometric flows (Laplace-Beltrami & Mean Curvature Flows). This "Diffusive CFAR" smoothes Radar noisy data but preserves discontinuities. This kind of CFAR is well adapted for Radar detection in Littoral Area, where probability of

detection in sea/ground clutter transitions and crest line (most threatening areas) could be non optimal by use of classical CFAR. We introduced these new CFAR in the framework of Information Geometry by taking into account radar signal statistics. We propose diffusive CFAR extension for Doppler & Polarimetric data. Finally, real time implementation is described based on "short-kernel" methods. [C9701]

"Impact of amplitude and phase mismatch in main beam jamming cancellation for active antenna with sub-array structure"

The paper describes the effect of amplitude and phase mismatch in main beam jamming cancellation performance achievable with radar system equipped with an active antenna having a sub-array structure. [C9702]

"GLRT based adaptive detection for MIMO radars"

In this paper, the problem of adaptive target detection using temporal coherent pulse train in presence of clutter is considered for MIMO radars. We have formulated this problem as a hypothesis test. For clutter with unknown statistics two adaptive decision rules have been developed using two-steps generalized likelihood ratio test (GLRT). The performances of the proposed detectors have been evaluated using Monte-Carlo simulations. The results show the superiority of the MIMO radars with temporal coherent processing over the conventional phased arrays due to both angular spread and a newly presented phenomenon which is called Doppler spread in this paper. [C9703]

"Cooperation between tracking and radar resource management"

This paper will discuss closely integrating the Tracker and Radar Resource Management processes within phased array radar. Several techniques are discussed and, where possible, basic analyses and figures of merit are given. In particular an analysis of time-agile track initiation in land clutter suggests significant benefits for slow moving targets. [C9704]

"Beamforming in terrain scattered jamming"

Terrain scattered jamming is a recent problem for mainly airborne radars with low sidelobe array antennas. Modern jammers with array antennas can analyse the terrain scattering scenario and adapt the jamming signals and beam patterns to enhance the jammer effectiveness. Reciprocity between the radar antenna and the jammer antenna via terrain scattering can be used to control both radar and jammer functions and to optimise performance. The effectiveness of both functions is analysed by simulations. [C9705]

"Radar detection and classification of jamming signals based on cone classes"

This paper deals with the problem of detecting and classifying a radar signal (target signal or jamming) in the presence of Gaussian disturbance. The jamming signal is modelled as belonging to a cone whose centre vector is the true target steering vector. Two different detection/classification approaches are analysed (the well-known ACE and GLRT approaches), yielding both to a two block device. The performance of the two decision algorithms are evaluated analytically, where possible, and by Monte Carlo simulation, otherwise. Some numerical results are reported along with some concluding remarks. [C9706]

"Performance of multichannel parametric detectors with MCARM data"

We consider the problem of detecting a multichannel signal in the presence of spatially and temporally colored disturbances. The parametric Rao and GLRT detectors, recently developed by exploiting a multichannel autoregressive (AR) model for the disturbance, have been shown to perform well with limited or even no range training data. In this paper, we evaluate the detection performance of the parametric Rao and GLRT detectors using airborne radar data obtained from the Multi-Channel Airborne Radar Measurement (MCARM) database. The data contain typical clutter found in airborne radar systems, and cover a variety of scenarios including dense-target or heterogeneous environment. Experimental results with the MCARM data show that the parametric Rao and GLRT detectors can provide good detection performance with limited or even no range training data in real radar environments. As such, these detectors offer useful solutions to detection problems in dense-target or heterogeneous environments. [C9707]

"Performance bounds for tracking algorithms based on a time-varying third-order nonlinear model"

The problem of deriving accurate algorithms for tracking of maneuvering targets is central in many applications, such as radar and sonar. Assuming that a certain model is indeed capable of describing the unknown system, it

is still important to have a measure of the achievable accuracy. Clearly, the Cramer-Rao inequality has been applied to a large number of different parameterized models to obtain a lower bound of the variance of any unbiased estimate of the true system parameters. Also, in a tracking scenario it is of great interest to be able to quantify the best possible performance that can be achieved. For this purpose certain time-varying Cramer-Rao lower bounds, CRB's are derived in the following. These bounds are based on the assumption of a third-order model which incorporates both time-varying and time-invariant parameters. In addition, possible measurement nonlinearities are taken into account. The so obtained CRB's depend on not only the unknown filter parameters but also certain second-order statistics, namely the variance of the (presumably random) target acceleration and the measurement noise. In general, it is of great importance to be able to quantify the impact of different values of these quantities, which typically are unknown in practice. The tracking behavior of the computationally efficient Recursive Prediction Error Method, RPEM based on the considered nonlinear three-state filter model, is exemplified and compared to the CRB's that have been derived here. [C9708]

"Performing inversion of HF radar backscatter ionograms"

The knowledge of the ionosphere's real state is very important for the over-the-horizon (OTH) radars. Those radars use the ionosphere as propagation channel, so we need to know its behaviour. A new inversion method to get the electronic density profile of the ionosphere from backscatter ionograms is presented. This method uses the elevation angle information to stabilize the inversion. [C9709]

"Wake vortex detection & monitoring by X-band Doppler radar: Paris Orly radar campaign results"

In order to improve the capacity of airports to handle the expected increasing amount of traffic, the knowledge about the safety issues for wake vortexes mitigation has to be improved. Currently, safety distances are very conservative and depend only on category size of aircrafts, without taking into account local wind nowcasting. The final goal is to develop a Wake Vortex Alert System for controllers to ensure operationally in all weather conditions adaptive appropriate not oversized separation rules. In a first step, it is necessary to perform long time data collections of wake vortex sensor signature on large European airports. [C9710]

"Sensor data association test methodology for the seawolf midlife update programme"

The SeaWolf Mid-Life Update (SWMLU) programme is a major upgrade to the UK Royal Navy's principal point defence weapon system. The upgrade includes the addition of an Electro-Optic (EO) sensor to upgraded radars. The processing of sensor data into a coherent fused picture is a key element of the overall system design. [C9711]

"Constrained adaptive detection of range spread targets"

In this paper we consider the problem of detecting range spread targets in the presence of steering vector mismatches and Gaussian disturbance with unknown covariance matrix. To this end we resort to the Generalized Likelihood Ratio (GLR) principle and devise several detectors accounting for possible mismatches between the actual and the nominal steering vector. At the analysis stage, we assess the performance of the new algorithms, both in the matched and mismatched signal cases, also in comparison with a previously proposed GLR Test (GLRT) designed assuming that the nominal and the actual steering vectors coincide. The results show that the new tests may achieve performance improvements over the previously proposed GLRT when the mismatch is present. Moreover they exhibit an acceptable performance loss in the matched signal case. [C9712]

"A hybrid D3 -Sigma Delta STAP algorithm in non-homogeneous clutter"

This paper presents a knowledge based hybrid algorithm using Sigma-Delta STAP which is practical and powerful in non-homogeneous environments. In the hybrid algorithm, statistical and non-statistical direct data domain (D3) algorithms are combined to obtain the advantages of both approaches. In this paper a new revised D3algorithm which uses a maximum SINR strategy is presented. The residual interference after the D3process is further suppressed by the efficient $\Sigma\Delta$ STAP algorithm. The performance of the hybrid algorithm using D3- $\Sigma\Delta$ STAP is tested in SIRV clutter environment and compared to that of the method which employs JDL as a statistical algorithm. [C9713]

"System simulation for a multi-function phased array radar"

This paper describes a system simulation which operates in non real-time to provide full closed-loop operation of the ground based multifunction phased array radar simulation system (MFRSS) in support of ballistic missile defence experiments against countermeasure. This system simulation provides capability to evaluate the system

performance of multifunction phased array radar, and key algorithms verification and validation such as target modelling, multi-target imaging, target recognition and resource scheduling. [C9714]

"Sharing false alarm rate information between disparate sensors"

This paper describes a method of improving the performance of networked sensors, such as radars or Electronic Support Measure (ESM) systems by allowing them to share local area false alarm data. This achieves more efficient operation than sharing tracks or plots, since lower-level information can be shared, but avoids the communications overheads of sharing data before plot extraction. [C9715]

"Multistatic and/or Quasi Monostatic Radar Measurements of propeller aircrafts"

Forsvarets forskningsinstitutt (FFI) has developed an experimental multistatic radar that has been participating in a NATO trial in Livorno fall 2005 under the NATO RTO SET078 TG46-Multiband radar for air defence. Results from the multistatic and/or monostatic radar measurements of the propeller aircrafts over sea and land are presented. [C9716]

"The effect of land clutter statistics on automatic gain control"

Modern radars are rarely able to sample the full dynamic range of observed land clutter. Therefore designers must employ gain control to make best use of the receiver hardware. This paper considers suitable land clutter models for use in the development of automatic gain control for high-resolution radar. The clutter statistics observed by the radar also have an impact on other areas including detection and target classification, but this paper concentrates on the problem of controlling the front-end gain of the radar receiver. [C9717]

"Radar target-ground interaction"

An investigation of the X-band (10GHz) Electro-Magnetic (EM) scattering of a complex vehicle in-situ is reported. The aim of this work is to characterise radar multi-path effects in Synthetic Aperture Radar (SAR) imagery, and further to demonstrate how an appropriate choice of polarimetric basis can allow its mitigation. Ground-target multi-path effects reduce the interpretability of imagery by adding artefacts. Additionally, multi-path impacts on Automatic Target Recognition (ATR), because for any given situation it will not be clear what kind of ground should be employed for the training database. [C9718]

"Accurate and efficient analysis of the EM environment due to naval radars"

The application of computational Electromagnetic (EM) tools to analyse the effects of radar systems on large, complex platforms are presented in this paper. In particular, significant cost and time savings are achieved early in the design process with the accurate modelling of applications such as RF hazards and the siting/installed performance of radars. The effectiveness of computational analysis is dependent upon on both the sophistication of the EM software and the quality of the CAD in containing perhaps physically small but electromagnetically significant detail. An example is given of the effect of a surveillance radar onboard the UK Aircraft Carrier (CVF). [C9719]

"Ground SAR system with tunable distance limits and low sampling rate"

This paper presents an experimental synthetic aperture radar (SAR) system which is under development in the Universidad Politecnica de Madrid. The proposed system uses a linear frequency modulated continuous wave (LFM-CW) radar with two antenna configuration for transmission and reception. The radar operates at millimetre-wave band with a maximum transmitted bandwidth of 2 GHz. The advantage is that the system allows to tune different interval ranges and sampling the received signals with a constant rate. The proposed system will use a car as mobile platform to obtain high resolution radar images of any ground area next to a straight road. [C9720]

"Detecting moving targets in multiple-channel SAR via double thresholding"

Well executed SAR images are picture-like and it is possible to identify various kinds of targets, e.g., trucks, ships, etc. However, from a single SAR image, it is not possible to determine which surface targets are moving. In many applications, it is imperative to detect objects that are moving and track them through stop-go-stop motion. We have developed a technique for detecting moving surface targets in a single frame of multi-channel SAR image using phase-interferometry. In this paper, we present results using airborne SAR data. [C9721]

"Prediction of low incidence angle propagation effects in ISAR images of sea targets"

In this paper we deal with the prediction of high-resolution radar cross section (ISAR images) in sea scenarios for low incidence angle conditions. In this contribution, we describe a computer program to predict high-resolution ISAR images including the effects caused by low incidence angle propagation (multipath, evaporation duct, atmospheric gases absorption...) and ship and sea surface dynamics. [C9722]

"Accurate moving target location in SAR imagery"

The Non-Linear Synthetic Aperture Radar (SAR) technique uses a combination of platform manoeuvre and novel processing to separate the effects of a target's radial velocity and cross-range displacement, giving accurate estimates of both. The technique provides high resolution (sub metre) images free from the distortion caused in conventional SAR imagery by moving targets, and allows the accurate location of both stationary and moving objects. [C9723]

"Retrieving evaporation duct heights from measured propagation factors"

The knowledge of refractivity is very important for coverage prediction. This problem is common above sea, where the particular atmospheric conditions lead to atmospheric ducts which strongly modify the range of the radar compared to the standard atmosphere coverage. The most common duct which is almost always present is the evaporation duct. The aim of this paper is to present two inversion methods to retrieve the evaporation duct height from the propagation factor measured along the propagation path during the Vampira campaign 2004. The two inversion methods considered are the simple quadratic regression and the least-squares support vector machine. [C9724]

"Sparse array systems for ultralight UAV radar"

Sparse array imaging systems (developed in ultra sound medical imaging) using a co array can be deployed on small UAVs to eliminate grating lobes on a wideband radar. This allows the use of thin film antennas under the aircraft wing using a split transmit and receive aperture. Simulations show side lobes equivalent to an array of 2 times the linear dimension. Apodization reduces sidelobes to -100dB, but a secondary lobe is apparent at $0.5-0.8\pi$. Z Transform apodization will reduce the secondary lobe. It can be eliminated entirely using sub kernel convolution with the Z transform. [C9725]

"Vivaldi Antennas: Wideband radar antennas simulation and reality"

Multiple applications sharing a single multiple-aperture array is a driver for research into wideband antenna design. Vivaldi antennas are inherently wideband and are known to have good RF characteristics, are inexpensive and easy to manufacture, and have a flat profile enabling construction of compact arrays. This paper investigates a wideband antipodal Vivaldi antenna over a 20:1 frequency range, with a focus on the key parameters needed to achieve ultra-wideband performance. We discuss tradeoffs and interdependencies of different parameters including the antenna shape, the dielectric material and the substrate thickness. We compare simulated results of Vivaldi antennas (using CST Microwave Studio) with measurements of prototypes. [C9726]

"Netted radar hough detector in randomly arriving impulse interference"

In this paper, two Hough Detectors, decentralized and centralized, with the polar Hough transform (PHT) that operate in the presence of randomly arriving impulse interference (RAII) are proposed and studied. The usage of the Hough transform (HT) in systems for air traffic control enables to detect more effectively the target trajectory in the presence of RAI. The study of the signal processing employed in detectors is carried out using Monte-Carlo simulations in MATLAB computing environment. The results obtained show that the detection probability of the multi-sensor centralized Hough detector is higher than that of the decentralized detector. [C9727]

"Quantifying the benefits of complex radar resource management techniques for airborne electronically scanned radars"

This paper describes a study aimed at quantifying the performance improvement achievable through use of complex radar resource management schemes, instead of basic schedulers, for an electronically scanned airborne surveillance radar system. Through computer simulation of representative scenarios, it is demonstrated that a highly adaptive approach, based upon an entropy metric, enables a radar to establish tracks at significantly longer ranges whilst maintaining overall surveillance performance. [C9728]

"AMSAR active phased array antenna"

The European AMSAR programme (Airborne Multi-role Solid-state Active Array Radar) undertaken by GTDAR, a company owned by Thales (France), SELEX SAS (UK) and EADS (Germany) under contract to the French Authorities acting on behalf of the French, German and United Kingdom Ministries of Defence, aims to demonstrate the capabilities of AESA (Active Electronically Scanned Array) based airborne radar systems. The programme started in 1993 bilateral with France and UK whereas Germany joined 1995 during Phase 1. Phase 2 started in 1999 and is divided into three Sub-phases 2A, 2B and 2C with a duration planned to at least 2010. The main objectives are the demonstration of airborne AESA technology in flight, including real time AESA Software and Adaptive Beam-Forming (ABF) techniques. The programme content as well as current achievements are described in this paper. [C9729]

"Dynamic simulation of a new deployable antenna structure for space application"

Dynamic simulations are very important for the design of new deployable structures for space applications. We present here a new kind of deployable structure, which can be used as a backbone for a large deployable paraboloidal reflector antenna. Through a simplified rigid multi-body model with certain constraints, dynamic simulations of the deploying processes are carried out. The structure can be deployed successfully. The calculation model of the structure is with a packaging ratio to be 0.038, with a density to be 0.156Kg/m². It reveals that such a structure has a great potential to be used in a large deployable mesh antenna or other deployable structures for space applications. [C9730]

"Design of a low cost microstrip patch antenna for GPS applications"

A compact MSA for GPS application at 1575 MHz, having 8 slits is presented. The said MSA is designed and simulated in IE3D and measurements are made using Agilent Vector Network Analyser E5062A. [C9731]

"Scanner 4000/4100: Synthesis, design and manufacture of an artificial lens for an air surveillance antenna"

The synthesis and design of a metallic lens in the aperture of a large flared horn antenna is reported. The lens provides sufficient correction of the quadratic phase error in the aperture of the horn to obtain ample antenna gain, while it simultaneously shapes the phase in the aperture such that a modified cosecant squared far-field pattern is obtained in the cross-sectional plane of the flared horn. The reflection from the lens due to the incident cylindrical wave (propagating between the flares of the horn) shall be weaker than -25dB to maintain a stable antenna pattern within the desired bandwidth. Otherwise, the amplitude and of phase distribution in the aperture of the horn will be perturbed by the reflected field (returning subsequent to reflections from the inner surfaces of the horn). The aperture distribution would then be strongly dependent upon the exact location of the lens (located in the vicinity of the aperture). As the depth of the horn is 44 wavelengths, the perturbations due to the reflected field from the metallic lens would also become highly frequency dependent. A low reflection off the lens thus relaxes the mechanical requirements of its exact location, and is as such a prerequisite for a successful electrical design and for the series production of the antenna. [C9732]

"Through-the-wall radar using multiple UWB antennas"

In this paper, we present a study of short range radar for through-the-wall detection and tracking of human beings. New concepts envisaged here are based on an Ultra Wide Band (UWB) waveform and on the use of numerous separated antennas. A full wave 2D simulator using the FDTD method has been performed in order to deliver synthetic data for studying signal processing algorithms. These algorithms, although well known in some other contexts, are here applied to UWB TTW imaging and detection and some quasi real time formulations are proposed. Results are presented on a test configuration computed by the simulator. [C9733]

"A 77-GHz MMIC power amplifier driver for automotive radar"

A SiGe 77 GHz power amplifier driver combining two three-stage amplifier MMIC is reported. The measured small signal gain of the chip varies from 16 to 18 dB from 75 GHz to 80 GHz with 3.37 dBm saturated output power at 77 GHz. The 3 dB bandwidth is between 70 and 82 GHz. The maximum small signal gain is around 17.9 dB at 79 GHz. This chip is fabricated using 0.25 μ m SiGe BiCMOS process. The power divider and combiner improve the linearity and relax the output power requirement of the amplifier unit and therefore this circuit is suitable to be used as a driver in the 77/79 GHz automotive radar transmitter. [C9734]

"An estimation of radar cross sections of small vessels at HF"

In this paper, we estimate the radar cross sections (RCS) of ships with Gross Registered Tonnage (GRT) of about 1000 tons ("small vessels") for HF radar operating between 3 and 5 MHz. The estimation is focused on

the RCS of ships at aspects close to the end-on (rear- or bow-on) directions. The conclusion of the estimation is that the RCS of the small vessels at aspect angles of up to 250 from the end-on directions are about 25-30 dBm². [C9735]

"Speed estimation experiments for ground moving targets in UWB SAR"

This paper presents an iterative method to estimate the Normalised Relative Speed (NRS) of ground moving targets in Ultra Wideband (UWB) wide beam Synthetic Aperture Radar (SAR) using one antenna. The number of iterations depends on the separation between processed NRS and true target NRS. The NRS estimate is based on a chirp rate estimator in azimuth direction of the SAR image. The paper derives an analytical expression of the azimuth phase information based on the moving target NRS and the NRS used in the image formation. The method has been tested on real data from the CARABAS-II SAR system showing good results. [C9736]

"Resource allocation modelling using methods of feasible directions in phased array radar systems"

In this paper, we report on recent progress results on optimal real-time resource allocation in phased array radar systems. A recently proposed resource allocation approach, Q-RAM, is considered and is observed to generate non-optimal results. We identify the shortcomings of this method and firstly extend it using Karesh-Kuhn-Tucker (KKT) optimality conditions for the single-resource-type case to obtain a globally optimal algorithm. We later generalize this further for the multiple-resource-type case. However, this particular approach has its origins in quality-of-service domain and is fundamentally limited to sampled cost functions. The availability of empirically obtained sampled convex tracking performance curves for phased array radar, and the feasibility of continuous approximations to these curves lead our study to the consideration of well formulated alternative methods from optimization literature belonging to the Methods of Feasible Directions. We apply in particular the Gradient-Projection Algorithm for the more general multiple resource type case. Our experimental studies using simulated radar performance curves show that superior performance can be obtained in closeness to optimal and execution speed. Closeness to optimality improvement becomes significant in particular for dense target scenarios with large number of targets. [C9737]

"On the effects of quantization on mismatched pulse compression filters designed using L-p norm minimization techniques"

In [1] the authors introduced a technique for generating mismatched pulse compression filters for linear frequency chirp signals. The technique minimizes the sum of the pulse compression sidelobes in an L_p-norm sense. It was shown that extremely constant sidelobe levels (better than 60 dB) can be achieved for minimal mismatch loss and broadening of the compression peak. This paper reports on an investigation into the effect of quantization on pulse compression filters designed using the abovementioned technique. Simulation results for 8-bit and 16-bit implementations of a pulse compressor system are presented. [C9738]

"Polarimetric frequency agile FMCW RCS measurement radar"

Assessment of the frequencies and polarizations behaviour of the Radar Cross Section (RCS) of moveable targets with an unpredictable trajectory and/or targets with unrepeatable behaviour is difficult using single frequency/polarisation measurements. The variations of the RCS require a large number of measurements in order to acquire a representative RCS of the target over the spectrum of frequencies and different polarisations. The paper presents a RCS measurement radar system developed to measure RCS at different frequencies and polarizations, the relevant meteorological and oceanographic data and target movement simultaneously thus making it easy to assess RCS results and measurement quality. The system was developed for the Royal Norwegian Navy. [C9739]

"SCANTER 4000/4100: A multi purpose surveillance radar"

This paper presents the background for and the main features of the multi purpose SCANTER 4000 and SCANTER 4100 surveillance radar systems, recently being developed at Terma A/S for air and sea surveillance. The SCANTER 4000 system is for stationary applications, while the SCANTER 4100 radar system is intended for use on a moving platform, e.g. a vessel. The paper describes the highlights in terms of the measured performance obtained and gives an overview of the radar system. [C9740]

"An unsupervised multi-feature framework for landmine detection"

A multi-feature framework for the detection of antipersonnel landmines with Ground Penetrating Radar (GPR) is suggested. The features result from independently acquired and processed GPR measurements. The initial

detection in the confidence maps is made independently after which these detection coordinates are co-located. The marginal feature distributions are normalized via Johnson's transform prior to the process of their fusion. A Maximum Likelihood based classifier is used as a fusion operator. The operator takes a quadratic form due to the enforced normality of the feature distributions. The framework trains the classifier using secondary data acquired at an open site. The framework's performance is illustrated using the data acquired over a specifically designed test-site. [C9741]

"Array signal processing using digital subarrays"

Subarrays constitute a step in the direction towards full digitisation of array antennas. An overview of the problems of digital processing with subarray outputs and a description of several mitigation techniques is given. We present rules for designing subarrays, for forming sum and difference beams, clusters of scanned beams at subarray level, and for forming a guard channel. The grating effects of subarrays on adaptive beamforming and STAP are described and demonstrated by examples. Finally we describe the problems of applying superresolution methods with subarrays. [C9742]

"UHF radar system tested on the Bridge of Yangtze River"

This paper presents a field test of UHF radar system on the Bridge of Yangtze River in China. Recently a set of UHF radar system has been developed for vessel surveillance and estimation of surface velocity profile across the river. The radar operates at 300MHz to match the dimension of water wavelengths. Another aim of ship surveillance is to protect the pier against ship collision. The transmit power of the radar is under 5W and the maximum range is 2km. This paper gives the design methods and waveform parameters of the system, some results of field test are also presented. [C9743]

"Optimal search and optimal detection"

The application of optimal search and optimal detection to radar is summarized. Optimal search and optimal detection distribute limited search effort (energy and time) in the optimal manner in both space and time to maximize target detection performance and to minimize target search energy and time. A savings of several dB of power-aperture or search time is obtained for most radars. [C9744]

"Experimental results on moving target detection by focusing in UWB low frequency SAR"

The main objective of this paper is to present and evaluate a method to detect moving targets in Ultra Wideband (UWB) low frequency Synthetic Aperture Radar (SAR). Moving target detection at low radar frequencies is associated with long integration time and has to handle azimuth focusing for reliable detection. The examined method tests different hypotheses on relative speeds in the area of interest. The optimum step size between the hypotheses is found from a point target approximation. Experimental results show that the ability to detect moving targets increases significantly. In this study, the improvement of the Signal-to-Clutter Noise Ratio (SCNR) is up to approximately 20dB using a single antenna. The focusing method allows initial estimates in speed of moving targets. The SAR data, which is used in our experiments, was collected by the airborne UWB low frequency CARABAS-II system. [C9745]

"SharpEye A 'New Technology' marine radar"

For over sixty years radar has been used as a tool to aid the safe navigation of ships at sea. Despite numerous improvements which have helped to produce a clearer radar picture and the addition of valuable tools to help the navigator, the radar sensor has remained essentially unchanged for the whole of this period. Recent changes introduced by the International Maritime Organisation (IMO) to the regulations covering the carriage of S-Band radar by commercial shipping are deliberately designed to encourage the introduction of 'New Technology' radar sensors. This paper describes one implementation of a 'New Technology' radar and discusses the challenges that face the radar designer in the price conscious marine radar market. [C9746]

"Maximum likelihood CFAR for lognormal clutter with censored samples"

In this paper the structure of Maximum Likelihood (ML) CFAR for lognormal clutter is derived assuming that some reference samples are censored to avoid destructive effect of interfering targets. It is shown that under some acceptable approximations we will achieve in a simple structure for this detector which is suitable for real time processing. The proposed detector is compared with non censored ML CFAR (i.e. logt CFAR) via simulation. It is shown that while the proposed detector is a little weaker than logt CFAR in homogeneous clutter, in non homogeneous clutter it outperforms the logt CFAR. [C9747]

"Power line RCS measurement at 94 GHZ"

A 94GHz FMCW radar has been developed for an obstacle detection and warning system for civil helicopters. Validity of the radar is demonstrated by flight experiments. Power line RCS is measured at the distance farther than 500m to determine specifications for a practical radar. Measured results have shown that the RCS becomes more than 15dB larger than that for short range observation. It has also been shown that the RCS variation with incident angle by Bragg scattering still remains even for long distance observation. [C9748]

"Cross modulation cancellation for airborne phased array radar"

The control of spurious signals, caused by cross modulation of two or more strong signals, is a demanding driver on the linearity of transmit/receive modules and subarray channel receivers in active electronically scanned array (AESA) antennas used with airborne radars. This paper proposes a method for the suppression of the spurious signals caused by cross modulation and presents simulation results to quantify its performance. The effects of potential errors on the suppression achieved are considered and a method is proposed for reducing these effects. With adaptive equalisation filtering, suppression of up to 30 dB can be achieved in the presence of realistic errors. [C9749]

"Urban target classifications using time-frequency micro-Doppler signatures"

Moving target indicators (MTI) find important applications in urban sensing. While motion detection can be achieved using simple CW radars, characterization of moving targets can be provided by estimating the key parameters of the target micro-Doppler signature. For indoor sensing, this signature has underlying instantaneous frequency features, which may depend on the radar viewing angle. This paper considers typical animate and inanimate moving objects and presents time-frequency motion classifiers using quadratic time-frequency distributions. The distinctions between the different target micro-Doppler parameter values and bounds are delineated. [C9750]

"Weight and layout optimized arrays using least angle regression"

We utilize a variable selection method called least angle regression for finding weight and layout optimized sparse wideband arrays. As opposed to previously reported methods for finding sparse arrays, the proposed method is attractive in that it optimizes both weights and layout simultaneously, and finds a solution in bounded time proportional to the number of elements and excitation samples of the array. In the case of no sparsing the method yields weights whose beampattern is equal to the least squares solution. For a 64-element linear array, with parameters based on a realistic medical ultrasound imaging system, a 6 dB improvement in the peak sidelobe level was observed for an array sparsed to 48 elements compared to the fully sampled unity-weighted array. [C9751]

"Global mapping of height of bright band"

Radar observations of the melting layer of precipitation have been made since the dawn of radar meteorology. It has been known since then that the melting of precipitation is often associated with an enhancement of the reflectivity of weather targets. The primary cause of the enhancement is a rapid increase in the dielectric constant of hydrometeors at the top of the melting layer followed by an increase of the velocities of melting snowflakes toward the end of the melting process [3]. The radar bright band results mostly from melting of snowflakes as they fall through the 0 degC isotherm. As the ice is gradually transformed to liquid, the refractive index and, hence, the back-scattering cross section increase, and the radar echo intensity increases to a maximum at ap 200 m below the 0degC isotherm. The decrease of echo intensity below the bright band level is mostly the result of decreases of particle concentration caused by increases of terminal velocity as the particles melt. 2A23 TRMM data provides information about the height of bright band (HBB) as well as the height of freezing. HBB is generally close to the height of freezing (usually within plusmn 2 km). In this paper, data from the TRMM PR are used to generate monthly maps of the height of bright band (HBB over the globe for the year 2000, 3 dB thickness of BB is developed, HBB over ocean and land and during some events such as hurricane are examined. [C9752]

"Performance analysis of maximum likelihood CFAR detection for Gaussian mixture type clutter"

In a previous work, we have proposed to use a generalized Gaussian Mixture (GM) distribution for modelling the sea clutter. In this work, we analyze the performance of the proposed method for the CFAR and non-CFAR cases. In order to evaluate the performance of the proposed method, we derive the probability of false alarm Pfa. The Cramer Rao Bound (CRB), which is used to predict the performance of a given system is also given. [C9753]

"Estimation of the Frequency of Sinusoidal Signals in Laplace Noise"

Accurate estimation of the frequency of sinusoidal signals from noisy observations is an important problem in signal processing applications such as radar, sonar, and telecommunications. In this paper, we study the problem under the assumption of non-Gaussian noise in general and Laplace noise in particular. We prove that the Laplace maximum likelihood estimator is able to attain the asymptotic Cramér-Rao lower bound under the Laplace assumption which is one half of the Cramér-Rao lower bound in the Gaussian case. This provides the possibility of improving the currently most efficient methods such as nonlinear least-squares and periodogram maximization in non-Gaussian cases. We propose a computational procedure that overcomes the difficulty of local extrema in the likelihood function when computing the maximum likelihood estimator. We also provide some simulation results to validate the proposed approach. [C9754]

"Resolution of Closely Spaced Deterministic Signals with Given Success Rate"

Fundamental limitations on estimation accuracy are well known and include a variety of lower bounds including the celebrated Cramer Rao Lower Bound. However, similar theoretical limitations on resolution have not yet been presented. We exploit results from detection theory for deriving fundamental limitations on resolution. The results are general and are not based on any specific resolution technique and therefore hold for any method and for any resolution success rate. We show that for signals with additive white Gaussian noise the resolution is given by a simple expression related to signal to noise ratio, the signals waveforms and the resolution success rate. As an example, we discuss the resolution of two sinusoids with closely spaced frequencies. The result is compared with the empirical performance of the Akaike information criterion, and the Minimum Description Length criterion for model order selection. [C9755]

"Source localization in view of urban sensing applications"

An analysis of the effect of sensor positions and the number of sensors on source location estimates in urban environments is performed. The sensors are uniformly distributed on a circle around a building in which the source is to be localized. Location estimates are obtained via trilateration and multilateration. Source location errors, as a function of the number and positions of sensors, are derived under equal range errors assumption, and the asymptotic behavior of location errors is observed. [C9756]

"Generalized almost-cyclostationary processes and spectrally correlated processes: Two extensions of the class of the almost-cyclostationary processes"

In this paper, two recently introduced classes of nonstationary processes are reviewed: The class of the generalized almost-cyclostationary (GACS) processes and the class of the spectrally correlated (SC) processes. GACS processes exhibit multivariate statistical functions that are almost-periodic functions of time whose Fourier series expansions have coefficients and frequencies that can depend on the lag shifts of the processes. SC processes exhibit spectral components with different frequencies that are correlated. Both GACS and SC processes include as special case the almost-cyclostationary (ACS) processes. GACS and SC processes arise in communications and radar-sonar applications when ACS processes are transmitted and there exists relative motion between transmitter and receiver and/or surrounding scatterers. Problems arising in the statistical function estimation and in sampling continuous-time GACS and SC processes are addressed. [C9757]

"Single snapshot projection based method for azimuth/elevation directions of arrival estimation"

In this paper we address the problem azimuth/elevation directions of arrival estimation using a uniform rectangular array URA. A new low computational cost projection approach, based only on a single snapshot is proposed. It consists of two one dimensional (1-D) search Procedures using projection matrices constructed from the rows and the columns of the data matrix, such approach is followed by a pair matching method. Simulations results show that the new method is effective when the signal-to-noise ratio (SNR) is high. [C9758]

"Radar cross section of a semi-elliptic channel in a ground plane loaded by multi -dielectric layers"

An analytic solution to the problem of scattering of a plane electromagnetic wave by a lossy or lossless dielectric confocal elliptic shell loading a semi-elliptic channel is derived. The incident, scattered and transmitted fields in every region are expressed in terms of complex Mathieu functions. Applying the boundary conditions at various faces and interfaces along with the partial orthogonality properties of angular Mathieu functions, the unknown scattered and transmitted field coefficients are obtained and written in matrix form. The presented numerical results show a good agreement with the published data especially for the case of a lossless dielectric shell

loading a semi-circular channel. [C9759]

"Underdetermined audio source separation using fast parametric decomposition"

In this paper, we consider the problem of underdetermined blind source separation using modal decomposition. Indeed, audio signals and, in particular, musical signals can be well approximated by a sum of damped sinusoidal (modal) components. Based on this representation, we propose a two steps approach consisting of a signal analysis (extraction of the modal components) followed by a signal synthesis (pairing of the components belonging to the same source) using vector clustering. Our contributions in this paper are a new separation method with relaxed assumption and reduced computational cost compared to other existing algorithms. Simulation results are given to assess the performance of the proposed algorithm. [C9760]

"Enhancing UCA-ESPRIT for non-circular sources"

UCA-ESPRIT is a subspace-based algorithm that is applicable to uniform circular arrays (UCAs). It is a closed-form algorithm that provides automatically paired estimates of the azimuth and elevation angles of multiple farfield plane waves incident on the circular array. Work (M. Haardt and F. Romer, 2004) has shown how ESPRIT type algorithms can be enhanced when the signals incident on the array are non-circular signals such as BPSK or ASK. These enhancements were applicable only to arrays with centrosymmetric manifolds. This paper shows how UCAs can take advantage of the non-circular source enhancements (which include better estimator performance and the ability to resolve a higher number of sources) despite the fact that the UCA is not a centrosymmetric array. [C9761]

"Adaptive neuro-fuzzy inference system for speckle noise reduction in SAR images"

An adaptive neuro-fuzzy inference system (ANFIS) based method is proposed for speckle noise reduction in synthetic aperture radar (SAR) images. Before using active RADAR (radio detection and ranging) and SAR imageries, the very first step is to reduce the effect of speckle noise. Reduction of speckle noise is one of the most important processes to increase the quality of radar coherent images. Filtering is the common method which is used to reduce the speckle noise. For this purpose, two ANFISs are trained and outputs of these systems are converted to one output through a mean calculator in this work. Performance of the proposed method is compared with performances of state-of-the-art methods in the literature for speckle noise reduction. Results are presented by filtered images and a table. [C9762]

"A hybrid MOMFD-FDTD ground penetrating radar modeling technique to detect multiple buried objects"

A hybrid method is presented for modeling realistic ground penetrating radar systems to detect multiple underground conducting or dielectric targets. The model combines the method of moments solution of the frequency domain thin-wire electric field integral equation to treat the dipole antennas and the finite difference time domain technique to handle medium stratification and buried targets. The capabilities of the moment method solution of the thin-wire electric field integral equation and general finite difference time domain solution of Maxwell's equations regarding the scattering of arbitrary shape objects in multilayered media are combined to efficiently simulate the electromagnetic behavior of the system. Some problems of practical interest are simulated using the proposed method and the capabilities of this technique to detect multiple buried arbitrary shape targets are discussed. [C9763]

"Ladar scan preprocessing for robust motion estimation"

Two-dimensional laser radars (2D-ladars) are sensors extensively used in mobile robotics for map building, self-localization, and obstacle detection due to their accuracy and reliability. Due to their fast sampling of the environment they also perfectly suit incremental ego-motion estimation, that is, to find how the position of the vehicle changes in short periods of time only by comparing sensor readings. Some of the most accurate methods dealing with this problem rely on a consistent computation of derivatives of range scans provided by the ladar. In practice, edges in the environment and sensor noise lead to inconsistencies in this computation. In this work we introduce an approach in the frequency domain, which robustly detects the continuous contour patches in the scan and then filters out the noise in those sections. In contrast with other methods based on batches of filters and heuristic rules, our approach employs spectral information to automatically select the filter parameters. We validate our method with experimental results on real environments. [C9764]

"Adaptive ML-CFAR detection for correlated chi-square targets of all fluctuation models in correlated clutter and multiple target situations"

The problem of adaptive CFAR detection of a pulse-to-pulse partially correlated target with 2 K degrees of freedom in a pulse-to-pulse partially Rayleigh correlated clutter and multiple target situations is addressed. The target and the clutter covariance matrices are modeled as first-order Markov processes. The probability of detection for the mean level (ML) detector is shown to be sensitive to the degree of correlation of the target returns and the degree of correlation of the clutter returns as well. [C9765]

"An improved CFAR detector using wavelet shrinkage in multiple target environments"

In constant false alarm rate (CFAR) detection, the noise level in the cell under test (CUT) is estimated by combining the outputs of reference cells. In nonhomogeneous environments, estimator should be immune to the presence of nonhomogeneities among the reference cells. Here, we propose a wavelet CFAR detector that can automatically censors nonhomogeneities of reference cells. This detector is a combination of a pre-processor for denoising of input signal and a conventional CA-CFAR detector. The detection performance of WT-CA-CFAR processor is compared with the CA- and CML-CFAR detectors for homogeneous and multitarget situations. The results show that the WT-CA detector acts like the CA-CFAR in a homogeneous background and performs robustly in presence of interfering targets. [C9766]

"Rapid-fluctuating Radar Signal Detection with Unknown Arrival Time"

We study the rapid-fluctuating radar signal detection, where the arrival time of the received signal, i.e., the range cell index of the target, as well as the complex amplitude of the signal and the noise are unknown. We show that even in additive white gaussian noise (AWGN) environment, uniformly most powerful invariant (UMPI) test does not exist. Instead, the UMPI detector in known SNR is used as an upper performance bound for performance evaluation of any invariant detector performance. In addition, we derive generalized likelihood ratio (GLR) detectors for this signal in AWGN with unknown noise variance and also in clutter with unknown covariance matrix. The GLR test statistic for AWGN represents the ratio of the maximum power over all cells to the total power. The GLRT for a clutter environment is also a power ratio which is the maximum over all range cells of the Euclidean norms of the spatially whitened observed sequence. Simulation results demonstrate that the performance of the proposed GLR test in AWGN is very close to the upper bound performance, i.e., to the UMPI test in known SNR. [C9767]

"Serial Acquisition of DS-CDMA Signals using Smart Antennas and Adaptive Thresholding Constant False Alarm Rate Processing"

This paper proposes an adaptive pseudonoise (PN) code acquisition system that adopts smart antennas and a cell averaging constant false alarm rate (CA-CFAR) processor to achieve reliable PN code acquisition in the presence of fading and interference. Hence, the decision threshold is adjusted according to the varying environment in order to improve the detection performance. The performance of the proposed system has been assessed theoretically by deriving closed form expressions for the probability of detection and probability of false alarm. The mean acquisition time is also obtained, and simulation results have been presented to verify the derived theoretical analysis. [C9768]

"A Novel Threshold Optimization Technique for CFAR Detection in Weibull Clutter using Fuzzy-Neural Networks"

This work provides an effective approach based on adaptive neuro-fuzzy inference system to the solution of constant false alarm rate (CFAR) detection for Weibull clutter statistics. The optimal detection thresholds of the ML-CFAR (maximum-likelihood CFAR) detector in Weibull clutter with unknown shape parameter are obtained using fuzzy-neural networks (FNN) technique. The genetic learning algorithm (GA) is applied for the training of the FNN threshold estimator. The proposed FNN-ML-CFAR algorithm proved to be efficient particularly in the case of spiky clutter. Experimental results showed the effectiveness of an adaptive neurofuzzy threshold estimator under different system conditions and it is also shown that the FNN-ML-CFAR detector can achieve better performances than the conventional ML-CFAR algorithm. [C9769]

"Automatic Censoring Detection Using Binary Clutter-Map Estimation for NonGaussian Environments"

In this paper, we propose an automatic censoring detector using binary clutter map estimation, for multiple target situations and compound dominated-clutters. The proposed censoring procedure dynamically discards the unwanted samples by implementing an adaptive pre-thresholding, for the incoming clutter echoes. Thus, the obtained decisions are sent serially into a shift register to form the binary clutter map (BCM) estimation. Finally, the logical states of the clutter map register are used to yield the background level estimation. To show the

robustness of the clutter map-based detection scheme, the effects of speckle correlation and interfering targets on the censoring efficiency are analyzed. [C9770]

"Independent Component Analysis of POLSAR Images. Relative Newton-Based Approach"

We propose here a new method for POLSAR image analysis. The method is based on a new PCA-ICA model in which the relative Newton-based approach for performing ICA is developed. The basic idea of ICA with relative Newton method consists in approximating the negentropy by taking account of the orthogonality constraint of the extracted components. This concept is recognized for its robustness and gives consequently very good theoretical results. The approach is well justified from the mathematical point of view. However, its implementation requires being more flexible because of the number of the estimated parameters. The purpose of this paper is to try to open new issues, in future research, in the concern of working out a new method for SAR image analysis that accumulate the advantages of the proposed method while avoiding its disadvantages. [C9771]

"Estimation of Motion Parameters of Moving Target using Wigner Distribution"

The purpose of this paper is to estimate unknown motion parameters, acceleration and initial velocity, from the radar signal corrupted by random noise. The principal attack of the approach is to use the (pseudo)-Wigner distribution which is computed from the noisy observation data. Parameters are estimated by least-squares method for the noisy instantaneous frequency of returned signal. Numerical simulations are presented to verify the efficacy of the proposed method. [C9772]

"Determination of Earth Surface from TRMM Satellite Images"

The Precipitation Radar (PR), on board of the TRMM satellite, provides many information and measurements related to the weather above the Earth. Images are produced from reflectivity measurement of different particles and materials. Determination of Earth surface level is required when investigating detection methods using TRMM PR data, such as detection of oil and underground water below the Earth surface. In this paper, two techniques were proposed for detecting exact Earth location from TRMM satellite rays reflectivity. First technique is based on satellite reflectivity images and the second one is based on the reflectivity data itself. The former performed better than the latter in estimating the Earth surface level. This finding can facilitate oil and underground water detection. [C9773]

"Invariant Detection of a Constant Magnitude Signal with Unknown Parameters in White Gaussian Noise"

In this paper, we use invariant tests for the detection of a complex signal with unknown phase variation and unknown amplitude in additive white Gaussian noise (AWGN). We show that in this problem, the uniformly most powerful invariant (UMPI) detector exists only if the signal-to-noise-ratio (SNR) is known. We derive the UMPI detector in known SNR and use it as the upper performance bound for any invariant test. In addition, we derive the generalized likelihood ratio (GLR) detector and evaluate its performance against the UMPI performance bound. We show that the GLR detector asymptotically approaches the UMPI test in large SNRs. Simulation results illustrate the close performances of the two detectors even at low SNRs, while in contrast of the UMPI test the SNR is unknown in the proposed GLR test. In order to understand, why the knowledge of SNR is not so important in this detection problem, we also derive the GLR test for the case of known SNR. Interestingly, the resulting GLR detector (derived for the case of known SNR) turns out equivalent with the one derived for unknown SNR, i.e., the knowledge of the SNR is not used in any of GLR tests. This reveals why the knowledge of the SNR is not so useful in this detection problem. [C9774]

"Issues in the Design of Equiripple FIR Higher Order Digital Differentiators using Weighted Least Squares Technique"

Weighted least square method proposed by S. Sunder and V. Ramachandran for the design of a digital differentiator is studied and implemented for an odd length differentiator of single and higher order. The response of the differentiator, variation of mean square error, and normalized difference of envelop function are studied for different iterations. Issues related to convergence of the WLS method are discussed. It is observed that the number of samples used while implementing the WLS algorithm has a significant influence on the results. A low value of the number of samples increases the tendency of the algorithm to converge towards a solution. However, the estimate of the error in the solution is misleading as the actual error in such cases is more than the estimated value. [C9775]

"Gaussian vs differentiated gaussian as the input pulse for ground penetrating radar applications"

The input signal for ground penetrating radars (GPR) is as important as the radar hardware such as the antenna and the receiving unit. The pulse duration, peak value and pulse profile are the main time domain features of a pulse that have to be considered in GPR applications. The most popular pulse signal used in GPRs is the Gaussian pulse and in this paper its performance is compared with that of the differentiated Gaussian pulse. The clutter level and the scattered signal strength of the GPR response are assessed in the comparison. [C9776]

"Towards an enhanced driver situation awareness system"

This paper outlines our current research agenda to achieve enhanced driver situation awareness. A novel approach that incorporates information gathered from sensors mounted on the neighboring vehicles, in the road infrastructure as well as onboard sensory information is proposed. A solution to the fundamental issue of registering data into a common reference frame when the relative locations of the sensors themselves are changing is outlined. A description of the vehicle test bed, experimental results from information gathered from various onboard sensors, and preliminary results from the sensor registration algorithm are presented. [C9777]

"Building an IMS Client test bed with open source tools"

Requirements are growing faster than ever. Keeping a product in sync with ever growing requirements is a big challenge and IMS is a classic example for the above statement. 3GPP IMS standards are evolving and the client side requirements bulge every month. It is important to ensure an IMS client is tested during the time of development with a platform that simulates the IMS network. As it is an expensive proposition to rely on operator's live network for testing and a live network cannot simulate error conditions, an IMS client test bed becomes essential. This paper explains our experiences in using open source elements like OpenIMSCore, OpenIkeV2, Strongswan, Open Sigcomp and SIPp to build an IMS client test bed. This paper describes vividly, a test bed that can be used to test an IMS client across usecases that include simple 3GPP call flow, call flow with signaling compression, call flow over TLS, call flow with security and a call flow from a device behind NAT with STUN server. The test bed is built to accommodate IMS clients operating on varied access types like LAN, GPRS/EDGE/UMTS and Wi-Fi. [C9778]

"Radiating element characteristics effect on the scanning performance of phased array antenna for tracking purpose"

A comprehensive study of finite phased array of Patch antennas and Vivaldi antennas is presented for missile seeker radar, with emphasis on the active admittance and scanning performance. The search, detect and track a high velocity target at a long distance by missile seeker is becoming more and more difficult as the target RCS becoming smaller due to application of stealth technology. Active phased array as missile seeker due to its potential to offer high power is a possible solution. For smaller array configuration of both patch and vivaldi, VSWR vs. scan angles, Active Admittance vs. scan angles are calculated using MATLAB 6.5 showing small variation with scan angles from 0 to 45. Also the patch and vivaldi array designs have been simulated showing the radiation pattern of single antenna and planar four element array using CST Microwave Studio, Version 5 in KCSTC (Kalpana Chawla Space Technology Cell), IIT Kharagpur. [C9779]

"Target prediction in Forward Scattering Radar"

This paper describes aspects of ground target detection using a Forward Scattering Radar (FSR). The problem of extracting the Doppler signature in different interference environments is addressed. Hilbert Transform and Wavelet have been used to predict the existence of target. The paper begins with a brief description of the system, followed by a more detailed analytical study of predicting the presence of target in FSR. A practical experimentation has been realised to evaluate the proposed algorithm. [C9780]

"A new signal detection with unknown doppler in an unknown background using spectrogram"

The current methods of detecting targets operate based on interference, clutter, noise, parameters and/or on signal Doppler specifications. There is no optimum detector for a general environment in unknown Doppler shifts. In this paper based on the combination of tolerance interval technique and time-frequency signal analysis, a new method is presented to introduce a new detector. The method is non-parametric, signal is analyzed in time-frequency domain by its spectrogram and the time interval of signal presence is determined. Finally, the adaptive thresholding is utilized and signal detection is fulfilled. [C9781]

"Optimal radar bistatic angle by statistical analysis of scattering patterns"

In this work, we introduce the concept of optimal bistatic angle such that the scattered radar target signal has a robust strength level irrespective of the target aspect. The concept involves statistically analyzing the scattering patterns as a function of the target aspect to a fixed and known incident radar direction. Henceforth, statistical quantities like mean and standard deviation are used to obtain statistics patterns for radar scattering patterns of an ellipsoid, a cylinder, and a square shape targets. Since different targets are likely to have different optimal angles, we propose using the optimal angle concept to improve the signal-to-noise ratio of a target of interest. This benefit can be further exploited in a radar target classification process. [C9782]

"Polarization studies in the UWB radar target response using joint Time-Frequency analysis"

The polarization dependent nature of ultra wideband (UWB) scattering from a radar target is studied using time-frequency (TF) analysis. The UWB frequency responses of the target under linear and circular polarization incidence are studied. The results demonstrate that the Q-factor of the resonant peaks vary as the incident polarization changes, indicating that different layer SEM poles are extracted for different polarization incident states. [C9783]

"Remote Sensing Signature Fields Reconstruction Via Robust Regularization of Bayesian Minimum Risk Technique"

The robust numerical technique for high-resolution reconstructive imaging and scene analysis is developed as required for enhanced remote sensing with large scale sensor array radar/synthetic aperture radar. The problem-oriented modification of the previously proposed fused Bayesian-regularization (FBR) enhanced radar imaging method is performed to enable it to reconstruct remote sensing signatures (RSS) of interest alleviating problem ill-posedness due to system-level and model-level uncertainties. We report some simulation results of hydrological RSS reconstruction from enhanced real-world environmental images indicative of the efficiency of the developed method. [C9784]

"Implementation of Batch-Based Particle Filters for Multi-Sensor Tracking"

In this paper, we demonstrate fixed-point FPGA implementations of state space systems using Particle Filters, especially multi-target bearing and range tracking systems. These trackers operate either as independent organic trackers or as a joint tracker to estimate a moving target's state in the x-y plane. For the efficiency of the particle filter, we consider factorized posterior approximations based on the Laplacian approximation, which uses a Newton-Raphson search. We delineate the computation and memory resources needed for real-time performance of the range and bearing particle filter trackers. Our implementations are demonstrated using the Xilinx System Generator. As part of the FPGA implementation, a floating-point, soft- and hard-core implementation of the Newton search algorithm is also developed. [C9785]

"Waveform Preconditioning for Clutter Rejection in Multipath for Sparse Distributed Apertures"

The idea of preconditioning transmit waveforms for optimal clutter rejection in radar imaging is presented. Waveform preconditioning involves determining a map on the space of transmit waveforms, and then applying this map to the waveforms before transmission. The work applies to systems with an arbitrary number of transmit- and receive-antenna elements, and makes no assumptions about the elements being co-located. Waveform preconditioning for clutter rejection achieves efficient use of power and computational resources by distributing power over a frequency band in an effective way and by eliminating clutter filtering in receive processing. [C9786]

"Wavefront Adaptive Sensing for Radar Spread Clutter Mitigation"

In spatially inhomogeneous, Doppler-spread radar environments, adaptive processing is often precluded because neither the target wavefront is sufficiently known nor is signal-free training data available. This paper presents a new clutter mitigation method designed to overcome these challenges by combining minimum variance (MV) adaptive beamforming and blind source separation (BSS) for distributed sources. Wavefront adaptive sensing (WAS) is a hybrid adaptive beamforming approach which uniformly maximizes gain against clutter by avoiding MV signal cancellation due to mismatch at high SNR and poor BSS threshold performance at low SNR. Simulation results are presented for target detection in a multi-mode spread-Doppler over-the-horizon radar scenario. [C9787]

"Perfectly balanced binary sequences with optimal autocorrelation"

We have found in our recent work that the coding gain of a coded OFDM system can be maximized if the out-of-phase autocorrelation of the encoding sequence is zero for initial lags. The number of lags with zero

autocorrelation depends on the channel length. We are interested in unbiased sequences and consider perfectly balanced binary sequences (BBSs) only. Our main goal in this paper is to obtain BBSs with best possible autocorrelation. We also study the properties of difference sets associated with BBSs and prove the non-existence of BBSs under commonly used difference sets. [C9788]

"Mobile Chatting Server for GPRS networks"

This paper addresses the extension of single mobile-to-mobile to multiple client supporting server design capable of acting as a an hand held mobile server, routing the messages between clients, through general packet radio ser- vices(GPRS) networks without involving internet based servers. Extension is achieved by adding multi-threading architecture in the server. An SMS, containing the server's IP, is sent to the selected client by the server using Wireless Messaging API. Thinlet based user interface is used to develop the client and server applications. The paper describes an application example of Real-time chatting between two clients through our mobile chatting server. [C9789]

"A Lower Bound for Sequential Estimators"

A popular class of parameter estimation method is based on a sequential/iterative scheme. In this framework, each component is estimated one by one and at each iteration the underlying model is based on the estimation of a single component corrupted by a structured interference (the other components) and by an unstructured Gaussian noise. So, in the context of the bearing estimation problem, we derive the deterministic Cramer-Rao Bound, called Interfering CRB (I-CRB), associated with this model. In particular, we show that for low Interference to Noise Ratio (INR), the I-CRB reaches the CRB for a single component (without structured interference). Inversely, for high INR, the I-CRB is equal to the Prior-CRB where we assume the exact knowledge of the structured interference. In addition, we show that in the closely-spaced bearings, the I-CRB has two typical regimes depending of the INR. [C9790]

"Laser range finder based obstacle tracking by means of a two-dimensional Kalman filter"

This article presents a implementation of a two- dimensional tracking filter in an automotive application. A headway alert system is a considered application for this tracking system, whose key component is a Kalman filter estimating and filtering two-dimensional trajectories of vehicles and various other obstacles that may occur in a traffic scenario. A reliable tracking system is essential for developing a robust headway alert application to identify obstacles and to avoid false warnings. The data, on which the Kalman filter algorithm is based on, is provided by a prototype laser range finder mounted in front of the host car and delivering range and angular data from obstacles in front. These data are filtered and combined with ego-motion data from the host car to decide whether to warn the driver about a potential threat. [C9791]

"Radar Estimation of Building Layouts Using Jump-Diffusion"

Estimating buildings layouts using exterior radar measurements is a challenging task involving the electromagnetic modeling, many unknown parameters, and limited number of sensors. We propose using the jump-diffusion algorithm as a powerful stochastic tool that can be used to determine the number of walls, estimate their unknown positions and other parameters. We improve the convergence rate of the jump-diffusion algorithm by developing an iterative procedure that first finds low- resolution estimates, which are then used to initiate our more accurate estimation. Our efficient usage of the available frequency bandwidth, improves the computational speed that otherwise would be hampered by the forward electromagnetic modeling. [C9792]

"Hybrid Adaptive Receive Processing for Multistatic Radar"

For multiple radars operating within the same spectrum, the resulting mutual interference can severely degrade sensitivity. Recently, the multistatic adaptive pulse compression (MAPC) algorithm has demonstrated the ability to partially suppress multistatic interference to better estimate the illuminated range profiles. This estimation is accomplished by jointly determining, in an MMSE sense, the range cell complex amplitudes associated with each of the received radar waveforms. As the number of received radar signals increases, the residual error after the application of MAPC increases as well. However, instead of jointly estimating all the received signals, one may wish to selectively minimize the residual error for a particular received radar (e.g. the monostatic returns from the co-located transmitter). In this paper, selective error minimization is achieved by utilizing a MAPC-based variant of the CLEAN algorithm. The resulting hybrid CLEAN algorithm is shown to provide significant sensitivity improvement over MAPC alone. [C9793]

"Adaptive Sensing of Dynamic Target State in Heavy Sea Clutter"

We propose an adaptive estimation method for the spatio- temporal covariance matrix of sea clutter. The motivation is to enable adaptive detection approaches that rely on accurate estimation of this matrix. The method involves vectorization of the equations for the dynamical system model governing the temporal evolution of the clutter matrix followed by a multiple particle filtering approach to deal with the high dimensionality of the formulation. The estimated sea clutter covariance matrix is applied to the problem of detection of a small target in heavy clutter; effectiveness is demonstrated via simulations. [C9794]

"Variational Bayes Data Association Filter"

We propose a sequential variational Bayes method, which is a recursive formulation of variational Bayes method, extended for online learning. We derived a novel data association filtering method for multiple targets, named variational Bayes data association filter (VBDAF). To estimate multiple targets' states, data association is an important problem, when data don't have unique labels and we can only associate data and targets probabilistically. EM algorithms or variational Bayes methods have been used for estimation problems with missing values such as data labels, but they are batch formulations. JPDAF have been widely used for multiple targets tracking. It is an extended filtering method based on sequential Bayes methods such as Kalman Filter, and approximation in the sense of finite mixture distributions, where VBDAF is approximate in the sense of KL divergence. We demonstrate VBDAF, in application of online multiple target localization. [C9795]

"The Integrated Coral Observing Network: Sensor Solutions for Sensitive Sites"

The National Oceanic and Atmospheric Administration's (NOAA) Integrated Coral Observing Network (ICON), has been operational since 2000 and works closely with most US Government and many international environmental partners involved in coral reef research. The ICON program has pioneered the use of artificial intelligence techniques to assess near real-time data streams from environment sensor networks such as the SEAKEYS Network (Florida Keys), the Australia Institute of Marine Science Weather Network, NOAA's Coral Reef Ecosystem Division network in the Pacific, and its own Integrated Coral Observing Network (ICON) of stations in the Caribbean. Besides its innovative approach to coral monitoring station deployments, the ICON program recently pioneered techniques for the near real-time integration of satellite, insitu and radar data sources for purposes of ecological forecasting of such events as coral bleaching, coral spawning, upwelling and other marine behavioral or physical oceanographic events. The ICON program has also ushered in the use of pulse-amplitude- modulating fluorometry to measure near real-time physiological recording of response to environmental stress during coral bleaching, thus providing even better ecological forecasting capabilities through artificial intelligence and data integrative techniques. Herewith, we describe these techniques, along with a report on new coral calcification instrumentation augmenting the ICON sensor array. [C9796]

"Adaptive Transmit/Receive Schemes for Mimo Radar"

In this paper we consider the issue of adaptive transmission and detection for MIMO radars operating under clutter with unknown covariance. In particular, we show that the availability of a set of secondary data allows defining constant-false-alarm rate (CFAR) receivers starting upon a family of previously known non-adaptive structures. We also show that, if the clutter correlation remains constant in several scans, an adaptive waveform selection procedure can also be implemented. The results show that the adaptive transmit/receive structures perform satisfactorily in comparison to their non-adaptive counterparts, the loss being in the order of 2-3 dB's for customary values of the system parameters. [C9797]

"Mimo Radar, Theory and Experiments"

In this paper the data acquired with the UCL radar network are analyzed and the properties of the received multistatic signals are investigated. Under a specific design of the experiment geometry, the statistical properties of the received signals are also studied. [C9798]

"Mimo SAR Imaging: Signal Synthesis and Receiver Design"

A multi-input multi-output (MIMO) radar can be used to form a synthetic aperture for high resolution imaging. To successfully utilize the MIMO synthetic aperture radar (SAR) system for practical imaging applications, constant-modulus transmit signal synthesis and optimal receive filter design play critical roles. We present in this paper a computationally attractive cyclic optimization algorithm for the synthesis of constant-modulus transmit signals with good auto- and cross- correlation properties. Then we go on to discuss the use of an instrumental variables approach to design receive filters that can be used to minimize the impact of scatterers in nearby range bins on the received signals from the range bin of interest (the so-called range compression problem). Finally, we present a number of numerical examples to demonstrate the effectiveness of the proposed approaches. [C9799]

"Cross-Channel Interference in Surveillance Radar Networks"

In this paper we evaluate the impact of the presence of an interfering radar on the target direction of arrival (DOA) pseudo-monopulse and ML estimation performed by the reference radar. The importance of the use of codes in a radar network is highlighted in a simple scenario of two surveillance radars. [C9800]

"Application of a Surface Reconstruction Method for Material Penetrating UWB Radar"

Although there exist a lot of imaging methods which were especially developed or adapted for pulse based radar data, the obtained image is often not satisfying. This paper describes the implementation of a surface reconstruction algorithm for ultra-wideband (UWB) radar systems. It was applied to real radar data and it will be shown that even in the case of overlapping echoes of the object and the wall, the object can be clearly distinguished and identified. [C9801]

"Polarimetric Analysis of Radar Signature of a Manmade Structure"

Identification of manmade structures from radar images has always been a difficult task, especially for single-polarization radar. Fully polarimetric radar, however, can provide detailed information on scattering mechanisms that could enable the target or the structure to be identified. Complexity remains stemming from overlaps of single bounce scattering, double bounce scattering and triple and higher order bounce scattering from various components of manmade structure that makes physical interpretation a challenge. In this paper, we will present an interesting example using polarimetric SAR data of the Great Belt Bridge, Denmark, to illustrate the capability of polarimetric SAR in analyzing radar signatures. Polarimetric target decomposition is used to differentiate the multiple bounce scattering contributions contained in the polarimetric SAR images. Two C-band Danish EMI SAR data takes, the first obtained during the bridge's construction and the second after its completion, are used to extract the scattering characteristics of the bridge deck, bridge cables and supporting structures. [C9802]

"Multi-Band and Reconfigurable Front-Ends for Flexible and Multi-Functional RF Systems"

This report summarizes some of the recent results at FOI with respect to multi-band and reconfigurable front-ends for flexible and multi-functional RF systems. Firstly, we report on a frequency agile X-band smart skin digital beamforming antenna based on using an 8-10 GHz tunable active filter and an image rejection mixer in a receiver GaAs MMIC. Secondly, we have also investigated the possibility of using RF MEMS based reconfigurable matching networks for realizing tunable bandpass LNAs with even wider tuning ranges (e.g. 6-10 GHz could be possible according to our simulations). Finally, we study a system concept for a Ka-band multi-functional electronically steerable antenna (ESA) on a small UAV based on using sub-arrays with low-loss MEMS phase shifters. The results show that adequate RF performance (in terms of 2 dB of average losses at 35 GHz) can be possible to achieve with a Ka-band 4-bits MEMS phase shifter design made on quartz. [C9803]

"An Unsupervised Segmentation Using SPAN/H/γ/A initialization for Fully Polarimetric SAR Data Analysis"

In this paper, an unsupervised segmentation method is proposed for fully polarimetric SAR data. We use the parameter SPAN combined with the H/γ/A to perform the initialization, and the Wishart test statistic is used reduce the number of clusters. The output number of clusters is determined by the data log-likelihood algorithm. We try to keep the definition of SPAN as long as possible during the segmentation procedure. The experimental results show that the proposed segmentation algorithm is very fast, but the performance of the segmentation still need further investigation. [C9804]

"Threshold optimization for distributed CFAR detection in Weibull clutter using genetic algorithms"

The use of genetic algorithms (GAs) tool for the solution of constant false alarm rate (CFAR) detection for Weibull clutter statistics is considered. An approximate expression of the probability of detection (PD) of the ordered statistics (OS)-CFAR detector in Weibull clutter is derived. Optimal threshold values of distributed maximum likelihood (ML)-CFAR detector and distributed OS-CFAR detector with a known shape parameter of the background statistics are obtained using GAs. For the ML-CFAR distributed detection, we consider also the case when the shape parameter is unknown. A performance assessment is carried out, and results are given as a function of the shape parameter of the Weibull distribution and of the system parameters. [C9805]

"Influence of phase on Cramer-Rao lower bounds for joint time delay and Doppler stretch estimation"

The Cramer-Rao lower bounds for joint time delay and Doppler stretch estimation have been obtained for

wideband signals with known phase already. However, the carrier phase is usually unknown in non-coherent receivers in the applications such as radar and sonar. And accuracy of the joint estimation of time delay and Doppler stretch will be affected by this unknown phase. In this paper, starting with a general wideband signal model with unknown phase, the Cramer-Rao lower bounds for joint time delay and Doppler stretch estimation are derived by using Fisher information matrix. The bounds obtained under unknown and known phases are compared and the relations between them are offered. Further explanations about the relations are also given from the view of information theory. Simulations are provided to support the theoretical results. [C9806]

"High resolution SAR imaging with enhanced focusing capabilities using the fractional fourier transform"

The fractional Fourier transform (FrFT), which is a generalized form of the well-known Fourier transform, has only started to appear in the field of signal processing decade ago. This has opened up the possibility of a new range of potentially promising and useful applications. In this paper we apply the new FrFT-based Chirp Scaling Algorithm (CSA) to a high resolution small target imaging and compare its performance with the classical CSA based on the Fast Fourier Transform (FFT). Simulation results show that the FrFT-based CSA can offer significantly enhanced features compared to the classical FFT-based approach. [C9807]

"A Monte Carlo simulation for two novel automatic censoring techniques of radar interfering targets in log-normal clutter"

In this paper, we present two novel algorithms for automatic censoring of radar interfering targets in log-normal clutter. The proposed algorithms consist of two steps: removing the corrupted reference cells (censoring) and the actual detection. Both steps are performed dynamically by using a suitable set of ranked cells to estimate the unknown background level and set the adaptive thresholds accordingly. The proposed detectors do not require any prior information about the clutter parameters nor do they require the number of interfering targets. The effectiveness of the proposed algorithms is assessed by computing, using Monte Carlo simulations, the probability of censoring and the probability of detection in different background environments. [C9808]

"Target Signal Extraction by Adaptive Signal Decomposition Methods"

Adaptive signal decomposition method is recently used for the interference reduction and target extraction. Two useful method, the adaptive chirplet decomposition (ACD) and empirical mode decomposition (EMD), are proposed in this paper. Using both simulative and experimental signals, they are compared in terms of Physical meaning, adaptiveness, sensitivity to signal type, interpretation of method, complexity of algorithm and computing time. In most cases, EMD is a better choice. [C9809]

"A Novel Beam Deflection Method for Wide Angle Laser Scanning"

A novel optical structure consisting of two concentric dielectric interfaces for all-static projection of a laser spot array over a wide angle is demonstrated. Spot size growth within the waveguide is simulated, and verified experimentally. [C9810]

"Obstacle detection based on a four-layer laser radar"

In the case of indoor/urban navigation, obstacles are typically defined as surface points that are higher than the ground plane. However, this characterization cannot be used in cross-country and unstructured environments, where the notion of "ground plane" is often unmeaning. The paper proposes a new obstacle detection algorithm based on a four-layer laser radar (LD_ML) which is applied to an autonomous land vehicle (ALV) in rough terrain. An obstacle is defined by the cluster gradient and height of candidate obstacle points. The obstacle detection algorithm is proposed by analyzing obstacles characterization, which includes four steps: First, obtain the candidate obstacle points through gradient condition; second, collect candidate obstacle points according to the rule of the nearest distance; third, decide a cluster whether it is an obstacle or not according to the cluster height; finally, estimate and predict the position of obstacles. The experiment results testify the algorithm is reliable and stable. [C9811]

"Apodisation, denoising and system identification techniques for THz transients in the wavelet domain"

This work describes the use of a quadratic programming optimization procedure for designing asymmetric apodization windows to de-noise THz transient interferograms and compares these results to those obtained when wavelet signal processing algorithms are adopted. A systems identification technique in the wavelet domain is also proposed for the estimation of the complex insertion loss function. The proposed techniques can

enhance the frequency dependent dynamic range of an experiment and should be of particular interest to the THz imaging and tomography community. Future advances in THz sources and detectors are likely to increase the signal-to-noise ratio of the recorded THz transients and high quality apodization techniques will become more important, and may set the limit on the achievable accuracy of the deduced spectrum. [C9812]

"Target identification and signal processing of millimeter-wave"

In this process, the control of DSP is the most critical, which controls the dual-channel analog/digital converter to transform the signal of millimeter wave radar in the first half cycle of one clock, whereas the signal of millimeter wave radiometer in the last half cycle. When the signal processing and target identification is finished, the results are returned to the high-speed memory, or to the computer display through the general serial interface of DSP. Regarding to passive detection and identification, 12-bit high-speed A/D converter in TMS320LF2812, of which the highest sampling conversion time is 80 ns, is used to distance ranging, feature extraction and target identification of MMV targets. The outputs of MMW high-stability oscillator, which go by the modulator, pour into the millimeter wave power amplifier. In the receiver mixer, echo signal and high-stable original signal are mixed to produce the difference frequency signal. [C9813]

"Enhanced Resolution for Sparse Aperture Radar Imaging Using Super-SVA"

High resolution imaging formation is one of the most important tasks for synthetic aperture radar (SAR). In this paper, a novel technique is proposed to form resolution-enhanced image from sparse aperture data. By iterative spatially variant apodization (SVA) processing on each of the sparse spectrums, a full aperture spectrum can be achieved and a high resolution image is recovered. [C9814]

"Detection Probability of WCDMA Based Cellular Radar System"

Cellular radar is a kind of passive radar system. It uses the signal of a base station in a wireless communication system as an 'opportunity of illumination' to detect a target. We must consider not only the detection criterion of radar system but also that of wireless system to constitute the concept of detection for cellular radar. It is obvious that the cellular radar system fails to obtain sufficient information of targets without guarantee of those two detection criterions. Therefore, we widely need to combine them and consider simultaneously. It is also important to measure how well a system can detect a target, so we define the detection probability. In this paper, we analyze necessity of two detection criterions, provide a novel definition of detection for the cellular radar and compute the detection probability. [C9815]

"An Iterated Extend Kalman Particle Filter for Multi-sensor based on pseudo sequential fusion"

In order to overcome the flaw that it is hard to get the optimization importance density function in the particle filter. The IEKF and the sequential fusion were integrated with particle filter. Then, the particle filter was introduced to radar/infrared Multi-sensor target fusion tracking. The main idea is use the system state transition matrix and the error covariance matrix which are gained from the IEKF and the sequential fusion to construct the importance density function of the particle filter. So the importance density function can integrates the latest observation into system state transition density, and the proposal distribution can approximates the posterior distribution reasonably well. The simulation results show that the iterated extend Kalman particle filter based on sequential fusion can significantly improve the accuracy of state estimation. [C9816]

"Durian Maturity Identification using Radar Equation Based on Support Vector Classification"

This paper presents a method to identify the maturity of durian using radar equation. The measurement system consists of two identical square patch antennas acting as a transmitter and a receiver. The return loss of the transmitter and the transmission coefficient at the receiver are measured using network analyzer. These measured data are used to determine the ratio of the effective reflection coefficients for two different frequencies at the interface between air and durian. In this step, the radar equation is applied. In this experiment, ten mature and ten immature durians are chosen by an experienced farmer. The measured data of fourteen durians are used for training the system using the support vector classification. The measured data of another six durians are used for testing the system. The results show that the performance of the system is acceptable. [C9817]

"Producing Pulse Compression Codes with Proper Auto Correlation Function, Regarding Pulse Shape"

Using radar with short pulses has some advantages like increasing range resolution and Doppler tolerance. Reducing pulse width has some disadvantages in addition to benefits, like peak power problem in power amplifiers. Coding and pulse compression in radar signals have an advantage of short pulses and also solve

peak power problem. In this paper we will show that deleting some bits from pulse compression code like maximum length code, leading to code with proper merit factor. Designing codes is usually performed with assumption of rectangular pulse shape. Our target in this paper is producing good pulse compression codes in non-rectangular pulse. [C9818]

"DSAC report 'specification and measurement of radar performance'-have we fully exploited its findings?"

The report 'Specification and Measurement of Radar Performance' [1] was commissioned by the Defence Scientific Advisory Council (DSAC) and summarised in a presentation to Radar 2002 by Professor Simon Watts. There have been some significant developments in the way projects are specified and managed in the 5 years following the report. So what has changed and what can still be learnt? The paper presents some advances, particularly in the area of synthetic test environments as a tool in support of through-life capability management (TLCM) that allow real-world trials to be reduced and focussed on the really difficult-to-simulate issues. [C9819]

"The architecture and operating characteristics of a multi-frequency HF surface wave radar-part two"

The HFSWR described in part one of this paper [1] uses simultaneous multi-frequency operation to obtain robust performance during its normal operation. To examine the nature of the radar and its environment, the high quality multi-frequency data generated and then stored, is analysed in more detail, particularly to generate measured target HF RCS profiles which are presented in this paper. The results suggest there is an ability in part to distinguish different target categories. This, and the supporting evidence, is commented on. [C9820]

"Sidelobe suppression of LPI phase-coded radar signal"

Sidelobe suppression is one of the major subjects in LPI phase-coded signal processing. Low sidelobe level is essential for target detection. Traditional sidelobe reduction techniques are not effective for phase-coded signal unless large calculation is involved. What's more, traditional sidelobe suppression filters are generally not applicable when target is eclipsed. In this paper, a novel sidelobe reduction method based on code agility is proposed, which can apply to all kinds of phase-modulated sequences including seriously eclipsed radar echo without heavy computation. [C9821]

"Application of neural network to pulse compression"

To solve the existing dilemma between making good range resolution and maintaining the low average transmitted power, the pulse compression technique is used. It is necessary for the pulse compression processing to give low range sidelobes. The traditional pulse compression algorithms based on 13-element Barker code such as direct autocorrelation filter (ACF) has been developed, and the neural network (NN) algorithms were issued recently. However, the traditional algorithms cannot achieve the requirement of high signal-to-sidelobe ratio, and the normal NN such as backpropagation (BP) network usually produces the extra problems of slow speed and sensitive to the Doppler frequency shift. In this paper, a pulse compression technique based NN will be studied. In the following, this approach is applied to real data and practical problems will be considered. [C9822]

"Space debris radar imaging"

For space debris radar imaging with the dimension smaller than radar range resolution, only SRDI (Single Range Doppler Interferometry) was discussed before. A single range matching filtering approach for space debris radar imaging is proposed in this paper. The proposed approach is to obtain 2-D image of space debris by using a range cell to transversely echo data and matching filter the signals with different turning radius. Investigations and simulations show that: of the proposed approach, its computational burden is less than that of SRDI, and its imaging effect is better. [C9823]

"A new method of the high-resolution wide-swath SAR"

A new method of the high-resolution wide-swath SAR is advanced in this paper. It realizes high resolution and wide swath SAR imaging at the same time. It is based on waveform diversity SAR technique and improves the integrated range ambiguity ratio. It also eliminates the blind zones. Moreover the data rate isn't increased. [C9824]

"Extended envelope correlation for range bin alignment in ISAR"

Range bin alignment is the initial step for translational motion compensation in Inverse Synthetic Aperture Radar (ISAR) images. Envelope correlation with the use of reference profiles is widely known for this step. Here, an extension based on a sub-integer alignment is proposed. The Nelder-Mead algorithm is used for the optimisation step. The approach is compared with Global Range Alignment (GRA). Despite the performances of the two techniques are similar, the proposed algorithm is more robust in special cases. Live data from a high resolution Linear Frequency Modulated Continuous Wave (LFMCW) millimetre-wave radar are used to validate the technique and make the comparisons. [C9825]

"Improved synthetic aperture radar imaging for high resolution applications"

The fractional Fourier transform (FrFT), which is a generalized form of the well-known Fourier transform, has opened up the possibility of a new range of potentially promising and useful applications including radar involving the use and detection of chirp signals, pattern recognition and Synthetic Aperture Radar (SAR) image processing. [C9826]

"Digital pulse compressor design for ultra-low range sidelobes for use within the eclipsed region"

A novel pulse compression technique is described, which allows extremely low range sidelobes to be maintained within the eclipsed regions of a pulse Doppler radar. The technique allows more efficient use of the radar's time, by allowing data to be recovered from the eclipsed regions, reducing the need for multiple waveforms to provide complete surveillance coverage. Theoretical modelling results are presented. [C9827]

"Optimum steady-state filter for periodic nonuniform sampling system"

This paper presents an optimum steady-state filter as an explicit solution to the periodic nonuniform sampling (PNS) tracking system. Closed-form, generalized filter gains and relationships for PNS tracking are obtained through solving coupled Riccati equations. A time proportion parameter is introduced. Together with the Tracking Index, it plays a fundamental role in steady-state analysis of time-variant Kalman Filter. Analytic solution is obtained for the first-order model while numerical solution for the second-order case. Using steady-state PNS filter gains, a constant-gain filter (CGF) is constructed to avoid overburden of computation without much performance loss. [C9828]

"The Gauss-Newton algorithm applied to track-while-scan radar"

The Gauss-Newton (GN) algorithm is the minimum-variance non-recursive estimation procedure invented by Gauss in 1809 [3, 4, 7]. Mathematicians refer to it by that name; statisticians refer to it as nonlinear regression; astronomers call it differential correction. In 1959 Swerling reworked Gauss' non-recursive algorithm into a recursive format [9], giving rise to the Bayes-Swerling filter. In 1960/61, Kalman and Bucy published their algorithm [5, 6], which, in the absence of process noise, can be derived from Swerling's recursive format [7]. The huge advances in computing power and affordability of RAM since the early 60's have made it desirable that we re-examine Gauss' original algorithm which avoids the problems and/or limitations incurred by either the Swerling or the Kalman recursive formats, and at the same time opens up tremendous flexibility in terms of access to internal filter values. This paper examines the GN algorithm and how it has been applied to Track-While-Scan (TWS) radar. A companion paper in these proceedings discusses the application of GN to Passive Coherent Location (PCL) radar [8]. [C9829]

"System level modelling of space based MTI performance"

Moving target indication (MTI) has been performed from airborne platforms for many years over both the land and sea. Multi-phase centre space based radars offer the potential to perform the same functions from space. This paper describes, from first principles, a simple monostatic system level performance model of the area coverage rate that could be achieved by a space based radar. This is then used to identify the important system performance drivers for further work. [C9830]

"A robust adaptive detection scheme for radar Doppler processing"

Adaptive detection procedures offer significant advantages with respect to conventional (data-independent) processing, particularly in structured interference environments that are commonly encountered in practical radar applications. This paper illustrates the use of adaptive Doppler processing for main beam interference cancellation, where it is the temporal (pulse-to-pulse) structure rather than the spatial structure of the interference that is exploited to achieve performance gains relative to conventional Fast Fourier Transform (FFT) based approaches. The experimental performance of a generalized adaptive detector, that exhibits robustness against mismatched targets as well as unwanted signals in structured interference environments, is compared

against conventional FFT-based Doppler processing and modern adaptive detection schemes that have also been derived using the generalized likelihood ratio test (GLRT) methodology [1]. [C9831]

"Eliminating ghost images for stepped-frequency train of LFM pulses"

Range ambiguity due to inappropriate frequency step size between successive pulses and "ghost image" phenomenon due to pulse expansion in single pulses, are two drawbacks of stepped-frequency waveforms (SFWF) in obtaining synthetic high range resolution (HRR) profiles. A new Least Square (LS) synthetic range profiling algorithm is proposed in this paper. Compared with the traditional algorithms, it can reduce range ambiguity, restrain ghost images, and decrease the signal-to-noise ratio (SNR) loss as well. The field experimental profiling results are also presented. [C9832]

"Performance evaluation for imaging laser radars with focal plane array"

Recent advances in lasers and optical detectors have made feasible the development of laser radar systems capable of providing real time images, one need regarding the growing interest on automatic target recognition applications. These imaging applications require the use of a focal plane array rather than a scan mechanism. In this paper we describe, from a new quantum point of view, the different contributions of signal and noise involved in incoherent laser radars systems based on a focal plane array in reception. This model allows evaluating the performance of these systems. A comparison with a real incoherent radar is also given. [C9833]

"Decentralized processing in radar networks"

In this paper we apply a sub-optimum algorithm to a radar network with a double threshold for detection and we report the results for two types of decision rules. The algorithm presented nearly maintains detection performance in the presence of jamming and is achieved without any of the countermeasures more commonly adopted. Furthermore we show that the detection loss due to the sub-optimum algorithm is not large. This leads to a trade off between losses and increased tolerance to electronic countermeasures (ECM). [C9834]

"Optimized implementation of a parallel DSP architecture for real time stacked beam radar signal processing"

This paper presents a parallel processing architecture, based on four TMS320C44 VME-bus DSP boards, for real time implementation of six clutter map constant false alarm rate (CM-CFAR) detectors together with a height finding extractor. The latter is based on a centroidal interpolation of the angular location of the target. The optimal processing speed has been achieved by fully exploiting the capacity of the 'C44 processor. The implemented configuration is well adapted for two dimension stacked beam surveillance radar. The overall parallel processing scheme interconnections and the real time implementation results are presented and discussed. [C9835]

"Range Doppler correlation for time-orthogonal distributed aperture radars"

Distributed aperture radars represent an interesting solution for target detection in environments affected by clutter. Due to the large distances between array elements, both target and interfering sources are in the near field of the antenna array. Recent works have demonstrated the benefits of combining frequency diversity and space time adaptive processing for distributed aperture radars. Using orthogonal signaling the receivers can treat the incoming signals independently, solving several bistatic problems instead of the initial multistatic problem. However, a well known problem in bistatic radar is the dependency of the clutter Doppler center on range. We analyze the benefits of joint use of waveform diversity and adaptive techniques to counteract the non-stationarity of the clutter Doppler. [C9836]

"Clutter modeling and analysis for spaceborne bistatic radar"

This paper presents a new clutter model for bistatic spaceborne radar, which takes the influences on clutter and STAP performance into account of the elliptic orbits of the satellites, the curving surface of earth, the earth rotation, the range ambiguity and the geometry of bistatic/multistatic radar system. Based on the model proposed in this paper, an analysis of the characteristics of ground clutter is given. The simulation results show that the Space-Time distribution of clutter would vary with range and time, which along with range ambiguity would result in serious performance degradation in clutter cancellation. And the performance of GMTI is poor due to the serious Doppler frequency ambiguity and inadequate spatial resolution if the elements of the receiving array are all mounted on one satellite, which could be resolved with the elements of the receiving array mounted on many sparsely distributed small satellites along with the non-simultaneous space-time samples technique. [C9837]

"Radar and communication waveform: Wideband ambiguity function and narrowband approximation"

Aiming for a system combining radar and communications, along with high performance requirements, imposes a waveform characterized by a large time-bandwidth product. The assumption of a wideband signal model for the radar problem and wideband ambiguity function seem then a forced solution, but it is then relevant to identify the exact conditions and the sustainable degradation of performance that allow instead the use of the narrowband approximation. The need to use wideband representation depends on the waveform parameters bandwidth and duration. Certain types of future state-of-the art radar should take into account this representation. [C9838]

"Waveform diversity for distributed and layered sensing"

Waveform diversity in distributed radio frequency (RF) sensor systems offers the potential for breakthrough performance enhancements in the detection and identification of natural and manmade objects. This paper discusses advances in relevant technology and emerging applications to radar. [C9839]

"Helicopter-borne mtd radar development and flight test for moving clutter measurement"

Helicopter-borne multi-mode radar experimental model has been developed for air surveillance and navigation mission study. In this paper, the radar system is designed and implemented with the key system and subsystem specification, and the various field tests are conducted for performance evaluation. Key subsystems are the planar array antenna, coherent transceiver, and multi-DSP based radar signal processor for pulse compression, MTI and MTD, CFAR, and compensation processing of shifted clutter spectrum. Through the helicopter-borne radar flight test using real-time radar data acquisition system, the Doppler shift of clutter spectrum due to the platform motion is measured and analyzed in terms of the various operational parameters. [C9840]

"Predictive density of millimeter-wave backscattering based on Gamma mixture model"

In this paper, we investigate a predictive density distribution of millimeter-wave (MMW) backscattering from terrain for the purpose of the estimation of MMW clutter distribution. In order to derive the density, the product model represented by speckle and texture is applied, where the distributions of the speckle and texture are modelled as the Gaussian and the Gamma mixture models, respectively. For the estimation of the mixture parameters, the expectation-maximization technique is applied. The applicability of the predictive density is demonstrated with experiment data at 94GHz band. [C9841]

"Spectrally efficient radar systems in the L and S bands"

In the L and S bands radar is extensively used in the UK for aeronautical, maritime and weather surveillance on both fixed and mobile platforms. In recent times, however, there has been a desire within the communications industry to access parts of the radar L and S bands. This tendency will certainly continue in the future under pressure from the (civil) communication market. This paper outlines the research carried out and the conclusions of a study into spectrally efficient radar technology funded by the UK communications regulator Ofcom. [C9842]

"The spectrum of scattered radar signals from complex ground targets"

This paper records the spectrum of some types of radar pulses scattered by complex ground based targets. A frequency-domain full wave Electromagnetic (EM) model of targets reveals significant distortion of the spectrum of the scattered signal in relation to that of the incident signal in many cases. Scattering is examined in monostatic cases only. The results lead into a deeper understanding of the scattering mechanisms and the quantification of echoes of complex ground targets. This can lead one to categorise ground targets differently from other features such as surface clutter and target shadows. [C9843]

"Frequency coded waveforms from chaotic time series"

This paper discusses the construction of frequency coded radar waveforms formed by using a chaotic time series for the frequency coding. These codes provide wide bandwidth, and, hence, high range resolution, and also provide orthogonality. The paper uses simulation results to investigate the properties of these waveforms, including spectral properties, sidelobe levels, range resolution and orthogonality. This study was motivated by the need for a system of coded waveforms that provide both cross-correlation orthogonality and high range resolution. An advantage of these frequency coded waveforms over phase coded waveforms is that bandwidth (and hence range resolution) is independent of pulsewidth. [C9844]

"Recognition of convoys with airborne adaptive monopulse radar"

A technique for recognition of extended targets on the ground, in particular convoys, by air- or spacebased radar is presented. The technique is based on adaptive monopulse in conjunction with space-time adaptive processing for clutter and interference rejection. It is demonstrated that the standard deviation of the azimuth and radial target velocity estimates of the space-time adaptive monopulse can be exploited to recognise a potential spatial extension of a moving target. [C9845]

"Multiperspective micro-Doppler signature classification"

Multiperspective automatic target recognition is considered to assist underlying classifiers by providing more views of the target. For the first time data from netted radar has been analysed for micro-Doppler signature content and a multiperspective dynamic time warping classifier developed. Despite limitation in the multiperspective data, identification is achieved with a probability of correct classification of 0.99. The results are contrasted with a monoperspective approach. [C9846]

"SAR active-decoys jamming based on DRFM"

The problem of how to realize the SAR active-decoys jamming is studied. Principles of the SAR active-decoys jamming are presented through analyzing range deception and azimuth deception, respectively. Thereby, two novel realization schemes are proposed. They can both realize active-decoys jamming effectively and only need measuring the angle between the radar and the jammer. The two realization schemes can be realized conveniently based on DRFM but they content the different deceptive demands respectively. Generally, we recommend the second one because it generates more decoys and it's easier to realize. Their validities are proved by the simulated results. [C9847]

"Inversion of residual errors to improve insar data acquisition, processing and interpretation"

The quality of the InSAR products has improved remarkably during the past few years. However, in order to further enhance the accuracy of the InSAR products and obtain results close to the real parameters further tuning of the InSAR processing is needed. In this work efforts have been made to improve upon the interpretation and analysis of the repeat pass space borne InSAR system data by quantifying and inverting the error sources. In an innovative way, error evaluation at every important step in the InSAR signal processing has been carried out and small algorithms have been incorporated to inverse the errors, thus fine tuning the InSAR signal processing. [C9848]

"A ground vehicle classification approach using unmodulated continuous-wave radar"

Vehicle classification is of great importance to the development of Intelligent Transportation Systems. In this paper, a novel ground vehicle classification approach using unmodulated CW radar is proposed. The radar is set up to look forward down to the road; vehicles are modelled as body targets composed of multiple scattering centers. Analysis shows that the spatial distribution of scattering centers can be derived from the Doppler signature of radar echo. Hough Transform is performed to estimate the distribution which is then used for classification. In experiments, vehicles are classified into three types at an average accuracy of 94.8%. [C9849]

"Waveform diversity: Past, present, and future"

This paper reviews important aspects of waveform diversity development, and discusses how waveform diversity, distributed processing, spatial diversity, and knowledge-based processing can be integrated for optimum surveillance system performance. A next-generation surveillance concept is proposed, which is composed of a distributed constellation of autonomous sensors. [C9850]

"Fine micro-Doppler analysis in ISAR imaging"

In ISAR imaging, it's well known that rotating parts of a target such as wheels or rotors induce additional features in the Doppler frequency spectrum. These features are called micro-Doppler effect and appear as sidebands around the central Doppler frequency. They can provide valuable information about the structure and motion of the rotating parts and may be used for target identification. In this paper, we propose a fine analysis of the Doppler returned by reflectors of a rotating wheel. Thanks to the micro-doppler signature we are able to extract information on its geometrical features (position, orientation). The method has been performed on simulated and experimental data and provides satisfactory results. [C9851]

"Neural network based for automatic vehicle classification in forward scattering radar"

The paper is dedicated to the continuation and improvement of the vehicle classification method of SISAR micro-sensors for ground vehicles previously presented in RADAR2004 and RADAR2005 [1-2]. In spite of a number of theoretical research efforts in the application of SISAR for target classification [1-4], there are only few research concentrate on the classification processing to confirm the feasibility of SISAR's practicality. This paper begins with an overview and summary of the authors' previous research. Then a new research topic in the improvement of the classification performance for various scenarios using Neural Network is proposed. Finally experimental results, conclusions and recommendations are presented. [C9852]

"The architecture and operating characteristics of a multi-frequency hf surfacewave radar-part one"

To successfully operate a High Frequency Surface Wave Radar (HFSWR) the current understanding of the HF environment dictates a holistic approach to the problems encountered. The use of a Multiple-Input Multiple-Output (MIMO) architecture combined with strong frequency management techniques and multi-frequency operation can provide the quality of data required for robust tracking. The use of COTS technology, especially wideband HF digital receivers and digital waveform generators allows for the implementation of the required techniques in a practical system. Part one of this paper describes the basic MIMO system architecture, general operational characteristics and the tracking performance of an operational multi-frequency monostatic HF surfacewave radar. Part two of the paper exploits the quality of the tracking performance of the radar to extract target RCS characteristics. Other technical details of the multi-frequency operating characteristics are also presented. [C9853]

"Platform concept: A breakthrough in surface radar architecture"

This paper describes how a platform concept can optimise future surface-based radar developments. After an overview of the general trends and drivers in the surface radar market, the paper demonstrates that the only way to reduce development cost, manufacturing cost and time-to-market whilst offering new, intelligent and innovative radar solutions, is to implement a product platform strategy. The global, modular and open standard-based architecture of the SR3D platform developed by Thales is described. The benefits of such an approach are explained and the operational advantages for both the customers and the endusers are illustrated. [C9854]

"Demonstrating the concept of using synthetic environments in radar acceptance and procurement"

This paper describes an experiment into the use of a synthetic environment (SE) in a radar acceptance and procurement procedure. The concepts and benefits of using an SE are discussed and a suite of models which can produce realistic synthetic radar data is described. An account of baseband, in-phase and quadrature (IQ) data, generated by the QinetiQ radar model Generic Engagement Environment Simulation Suite (GEnESiS), being injected into a fully operational and integrated radar's receive chain, is given. The final track output of the radar is shown and the metrics that could be used to assess radar performance are discussed. [C9855]

"HF radar ship detection and tracking using WERA system"

High frequency (HF) radars are capable to detect and track targets at extremely long ranges. The signal environment that includes external noise, different kinds of clutter and interference will significantly limit the detection performance and system capability. This paper considers a new approach to solve the ship detection and tracking problem in a complex HF radar signal environment. It uses a conventional constant false-alarm-rate (CFAR) detection procedure but the thresh-olding scheme is based on regression analysis of power spectrum values along range and Doppler cells. The ship tracking scheme includes the model in polar coordinates that uses tracking state vector consisted of range, azimuth and velocities and fixed-coefficient filter parameters to get smoothed tracks. The proposed detection and tracking schemes have been tested using real HF radar data from WERA system. [C9856]

"RADARSAT calibration operations at the Canadian Space Agency: Maintaining RADARSAT-1 performance and preparations for RADARSAT-2"

This paper describes the image quality control activities performed at the Canadian Space Agency on RADARSAT-1, and presents the preparations for calibration support activities for RADARSAT-2. Radiometric calibration and image quality performance of the RADARSAT-1 SAR is monitored routinely since its commissioning in 1996, based on imagery of the Amazon and of Precision Transponders. Antenna elevation beam patterns and SAR impulse response are still maintained within initial design goals after more than 11 years. Efforts have now been undertaken for the provision of complementary validation data to support the RADARSAT-2 calibration, maintained by MacDonald Dettwiler and Associates Ltd (MDA). [C9857]

"TanDEM-X: A satellite formation for high-resolution SAR interferometry"

TanDEM-X (TerraSAR-X add-on for Digital Elevation Measurements) is an innovative spaceborne radar interferometer mission that was approved for full implementation by the German Space Agency in spring 2006. This paper gives an overview of the TanDEM-X mission concept, summarizes the basic products, illustrates the achievable performance, and provides some examples for new imaging modes and applications. [C9858]

"A combination of NLOS radar technology and LOS optical technology for Defence & Security"

This paper describes a new system specifically designed for Defence & Security applications combining Non-Line-Of-Sight radar technology and camera technology. After a description of the new challenges caused by limited regional conflicts and terrorism, an innovative ground-based solution built with an UHF radar, called Ground-Alerter-One, and an IR camera is presented. Details on the frequency band choice are given. The design principles are explained and some results of operational trials conducted during the last few months are presented. [C9859]

"Multidimensional waveform encoding for synthetic aperture radar remote sensing"

This paper introduces and analyses the innovative concept of multidimensional waveform encoding for spaceborne synthetic aperture radar (SAR). The combination of this technique with digital beamforming on receive enables a new class of highly performant SAR systems employing novel and highly flexible radar imaging modes. Examples are adaptive high-resolution wide-swath SAR imaging with compact antennas, enhanced parameter estimation sensitivity for applications like along-track interferometry and moving object indication, and the implementation of hybrid SAR imaging modes that are well suited to satisfy the hitherto incompatible user requirements for frequent monitoring and detailed mapping. Further advantages arise for fully polarimetric operation where it becomes possible to reduce the PRF by a factor of two. Implementation specific issues will be discussed and examples demonstrate the potential of the new technique for different remote sensing applications. [C9860]

"Is radar still the king?"

In origin known as RDF (Radio Direction Finder) the RADAR (the term was coined in 1941 as an acronym for Radio Detection and Ranging) even if it was at a very first stage of development, had an invaluable role in major battles all along the second World War. [C9861]

"A Hybrid Kalman/ γH^∞ Filter for Maneuvering Target Tracking"

In air surveillance systems, Kalman filter and its derives have been largely used for real-time multiple target tracking, where minimization of calculation burdens is greatly desired. While non-maneuvering targets can be accurately tracked by using a Kalman filter with a constant velocity model, a maneuvering target might be mis-tracked since prediction errors increase significantly. The H^∞ filter is the robust filter, which does change its characteristics depending on the parameter. In order to track accurately not only non-maneuvering but also highly maneuvering target, we propose, in this paper, a variable γH^∞ filter with an acceleration term when a maneuver is detected. [C9862]

"Brightness Temperature Maps Retrieval for the SMOS Space Mission: Regularized Inversion and Bias Reduction"

Synthetic aperture imaging radiometers (SAIR) are powerful sensors for high-resolution observations of the Earth at low microwaves frequencies. Within this context, the European Space Agency is currently developing the SMOS mission devoted to the monitoring of soil moisture and ocean salinity at global scale from L-band space borne radiometric observations obtained with a two-dimensional interferometer. This contribution is concerned with the reconstruction of radiometric brightness temperature maps from interferometric measurements provided by SMOS. [C9863]

"A Multi-Level Mobile Video Surveillance Notification System"

This paper describes a multi-level mobile video surveillance notification system that provides access to the monitoring system from anywhere there is a mobile handset with wireless connectivity. The system automatically identifies motion abnormalities within the monitored scene and starts recording any suspicious movement. The output is recorded in a lightweight animated GIF file. The system provides multiple levels of alerts (by Email, SMS or Phone Call) based on the amount of motion activity at the monitored scene. The output file can be sent to the user using MMS or stored on the server and accessed via a URL that is exchanged to the user via SMS.

The system is fully configurable from the user handset application, making it suitable for various surveillance environments. [C9864]

"A New Algorithm for FOA and 2-D AOA Estimation"

In this paper, a new algorithm for frequency of arrival (FOA) and two dimensional (2-D) angles of arrival (AOAs) signal parameters estimation is proposed, which is based on two parallel uniform linear arrays (ULAs). Three subarrays are constructed by taking the special structure of the array. The proposed method is simple and does not require initialization or pairing matching. The key component is that the three eigenvalue matrix pencils obtained share the same signal subspace. We obtain the correct $(f, \Gamma, B, \Gamma^* B^*, f)$ through a simple search procedure by exploiting the above property. Simulation results and comparisons with other existing algorithms are carried out to demonstrate the performance of the proposed method. [C9865]

"On Tracking Maneuvering Targets in 3-Dimensional Space with Online Observed Colored Glint Noise Parameter Estimation"

In this paper a comprehensive algorithm is presented to alleviate the undesired simultaneous effects of observed glint noise distribution, colored noise spectrum, unknown noise parameter, and nonlinearity of the system on tracking of the maneuvering targets in 3-dimensional space. Particle filter is used as a nonlinear state estimator to deal with the nonlinearities of the observation equations. To identify the dynamics of the maneuvering targets a new switching scheme is proposed to be substituted for the conventional interacting multiple model approach. The method is strictly causal and can be implemented for an online tracking system. The algorithm performance has been verified by illustrating some simulation results. [C9866]

"A Performance Comparison of Two Time Diversity Systems using TM-CFAR Detection for Partially Correlated Chi-Square Targets in Nonuniform Clutter and Multiple Target Situations"

In automatic detection, performance of time diversity systems is proved to be sensitive to how the multiple-pulse sample echoes, from commonly encountered nonhomogeneities, are accumulated within the same receiver. Based upon the "non conventional time diversity system" (NCTDS), we derive exact expressions for the probabilities of false alarm and detection of a pulse-to-pulse partially correlated chi-square target with $2K$ degrees of freedom for the trimmed mean constant false alarm rate (TM-CFAR) detector. Because of the complex mathematics induced by the "conventional time diversity system" (CTDS), detection performance of this system is carried out using Monte Carlo simulations. The obtained results show that, while the NCTDS achieves a better nonuniform clutter resilience than the CTDS, the latter outperforms the former in multiple target situations. Hence, when both nonhomogeneities are concomitantly present, the two systems performances become nearly similar. [C9867]

"Fuzzy Neural Network Approach for Estimating The K-distribution Parameters"

This paper provides a novel approach based on neuro-fuzzy inference system for the estimation problem of the K-distributed parameters. The proposed method is based on a network implementation with real weights and the genetic algorithm (GA) tool is applied for an off-line training of the fuzzy-neural network (FNN) shape parameter estimator. Moreover, the proposed estimator combines the Raghavan's and ML/MOM (maximum-likelihood and moments) methods and the experimental results are presented to demonstrate the validity of the approach. It is shown that such the FNN estimator is successful with a lower variance of parameter estimates when compared with existing Raghavan's and ML/MOM approaches. [C9868]

"Sonar Images from Well-Known Simulated Raw Data"

Sonar is a technique used to observe the underwater scene over large distances. Active sonar is mainly used for imaging or for bathymetry. With modern sonar both uses are now possible. To form a high resolution three-dimensional image, an active side-scan sonar is used. To develop algorithms in order to obtain an image, we need experimental data. One of the difficulties in the analysis of sonar data is the lack of seabed in order to repeat an experiment exactly in the same environment. To overcome these problems, a sonar signal simulator can be used. In this paper, we describe processing sequences including a sonar signal simulator, micro navigation and Synthetic Aperture Sonar (SAS) algorithms. Many simulators use a perfect platform motion. Here, the platform path can be modified. Nevertheless, it is possible to have the accurate position of the platform for each sample, which is not possible with experimental data. [C9869]

"Adaptive MRIMM algorithm for tracking manoeuvring target using a phased array radar"

In this paper, tracking a manoeuvring target with a phased array is considered. A new algorithm, called the Adaptive Multi Rate Interacting Multiple models (AMRIMM) algorithm is presented. The AMRIMM algorithm adds

to the MRIMM the ability to select the next update time adaptively, according to the motion of target. In this algorithm, the manoeuvring model operates at full rate, while the non manoeuvring model operates at half rate. A discrete wavelet transform is used to solve the problem raised by the difference in the update rate between the two models. The performances of the AMRIMM algorithm are compared to that of the MRIMM algorithm and the IMM algorithm that use a fixed update time, via Monte Carlo simulations. [C9870]

"A passive, multi-static radar system"

In this paper, a passive multi-static radar system that utilizes broadcast high definition television (HDTV) transmissions is described, and results collected from a deployment in Washington DC are presented. [C9871]

"The dependence of radar target detectability on array weighting function"

This paper assesses the dependence of target detectability in the presence of clutter on the transmitting and receiving antenna array weighting functions for airborne, medium pulse repetition frequency radar. Target detectability is best for functions which result in the lowest average sidelobe levels. [C9872]

"Detection of narrowband radar signals having a broadband digital receiver"

In this paper an adaptive prewhitening method is proposed to obtain an uniform transfer function of the used broadband receiver. Then we describe a new detection scheme which is based on extreme value statistics. The discussed methods are applied to real data measured by the PALES experimental system. [C9873]

"Target detection using orthogonal netted radar system (ONRS)"

An Orthogonal Netted Radar System (ONRS) is a networked system consisting of multiple radars, each of which uses an orthogonal set of coding waveforms, and operating at the same carrier frequency. ONRS can simultaneously operate in a monostatic and a multistatic mode, and thus possesses the advantages offered by both a monostatic and a multistatic radar system. The principles and structure of ONRS are described in this paper. The detection schemes using ONRS and an initial performance analysis is carried out. [C9874]

"Ground clutter cancellation in MIMO and multistatic noise radars"

In this paper, ground clutter cancellation in a multi-channel noise radar is presented. The radar system under consideration consists of K independent noise transmitters working in the same frequency band and L receivers. Independent cancellation of clutter echoes originating from successive transmitters is not fully effective therefore joint cancellation of all clutter echoes is proposed. [C9875]

"Improving resolution using multistatic radar"

Multistatic radar is an emerging concept which offers a variety of potential gains in target information. The availability of multiple down-range information from different target perspectives have significant potential for improved overall resolution when this data is fused, since monostatic radars typically have a significantly worse crossrange resolution in comparison to down-range resolution. In this paper the concept of monostatic and bistatic radar resolution is reviewed, before we examine how this concept changes when we consider the output of a multistatic radar system. We then investigate what methods might be used during fusion to provide improved resolution. We conclude by demonstrating these multistatic methods using a radar system designed and built at UCL. [C9876]

"A common view GPSDO to synchronize netted radar"

The paper describes the development of a time transfer standard for use with networked radar systems. The system is based on common view GPS satellites and utilizes low-cost commercially available equipment. Some practical design issues are discussed and plans for future research are outlined. [C9877]

"Efficiency of adaptive threshold detector of pulse-doppler radar"

Detection performance of airborne multi-channel radar that operates under clutter conditions is reviewed. The potential energy loss arising from determination of adaptive threshold calculated by mean magnitude of the signal envelope or median estimator is found. Minimum digit number providing acceptable digitization loss is estimated. [C9878]

"Low cost networked radar and sonar using open source hardware and software"

Experimental and educational applications of radar and sonar hardware would often be facilitated by access to a flexible, digital transceiver. This hardware should be easily reconfigured to implement different transmit waveforms, and sampling requirements. It would be possible to compromise very wide bandwidth in such an environment. This paper reports on the development of a digital transceiver based on Open Source hardware and software from the GnuRadio project. [C9879]

"Adaptive beamforming passive radar based on FM radio transmitter"

One of the major problems in continuous wave bistatic radar based on FM radio transmitter is direct path interference(DPI). This is the signal received directly from a transmitter by the receive channel antenna. The DPI and the reflected signal are coherent, have similar structure except for the mutual delay and Doppler frequency shift. To detect targets it is necessary to suppress or remove the DPI signal. First of all, the DPI signal based on FM radio transmitter is analyzed. Secondly, the approach based on adaptive nulling array processing is introduced in detail to solve this problem. Finally, associated signal processing schemes of the FM-radio-based passive radar is discussed. Simulation results by applying real collected data show the proposed method is effective. [C9880]

"Signal synchronisation in SS-BSAR based on GLONASS Satellite emission"

This paper presents the issue of synchronisation in Space-Surface Synthetic Aperture Radar (SS-BSAR). GLONASS Satellite System is considered as the transmitter of opportunity. Experimental testing of the synchronisation algorithm is also presented and verified. [C9881]

"A statistical method for processing SAR Multichannel ATI sea surface images"

A statistical analysis is presented of the process whereby weighted complex-valued Multichannel ATI (MATI) images of the sea surface are linearly combined so as to maximise or minimise the visibility of selected image features in the resulting filtered image. It is assumed that the modulated features are a result of local fluctuations in mean intensity which can be described statistically by a compound distribution. The background consists of unmodulated Gaussian scatterers. These scatterers and the modulated ones have different (and finite) Doppler spectra. It is shown that with these assumptions, maximising (or minimising) the normalised standard deviation of the filtered image maximises (or minimises) the visibility of the image modulations whatever the spectra may be or the compound distribution. This result means that it is not necessary to know the shape or pattern of the images modulations in order to enhance them. The analysis presented in this paper is aimed particularly at horizontally polarised images. A result is presented showing the effectiveness of the technique. [C9882]

"Diffraction techniques in rcs prediction of an aircraft model"

Aircraft or ship is of interest as a target in radar wavelength of X-band in the optical RCS regime. In this region, analytical approximate techniques are used for RCS modeling. Physical Optics (PO) is a popular method on which many efficient computer codes are based. Alternative ray based methods are Geometrical Theory of Diffraction (GTD) and its extension Equivalent Currents (EC) which take diffraction into account. In this paper, RCS estimation results of GTD/EC are compared to PO for some geometry. It is concluded that although PO codes are very efficient, they fail at describing diffraction. Finally the RCS of an aircraft model is estimated using hybrid GTD-EC method at X-band. It is deduced that the implemented method is suitable in case of echo area estimation of electrically large bodies having no fine features. [C9883]

"An improved scheme for the frequency domain $\Sigma\Delta$ -DPCA"

In this paper, the frequency domain $\Sigma\Delta$ -DPCA processing (F- $\Sigma\Delta$ -DPCA) is investigated in detail, and an improved scheme for the F- $\Sigma\Delta$ -DPCA is proposed, which can significantly reduce the computational burden. In practice, due to the sum and difference beam pattern designed independently and other system errors, the clutter suppression of the time domain $\Sigma\Delta$ -DPCA processing (T- $\Sigma\Delta$ -DPCA) is significantly degraded. However, the F- $\Sigma\Delta$ -DPCA adaptively calculates the optimum gain ratio for motion compensation within each Doppler cell, which is robust to system errors. Theoretical analysis and simulation results are presented to validate that, the F- $\Sigma\Delta$ -DPCA can achieve superior performance of clutter cancellation than the time domain processing, and the improve approach is feasible for real-time application. [C9884]

"Comparison of MIMO radar concepts: Detection performance"

In this paper, four different array radar concepts are compared: pencil beam, floodlight, monostatic MIMO, and multistatic MIMO. The array radar concepts show an increase in complexity accompanied by an increase in diversity. The comparison between the radar concepts is made by investigating the detection performance for a

surveillance task in various environments, including an urban environment. [C9885]

"Detecting personnel in wooded areas using MIMO radar"

This paper discusses the problem of detecting personnel in wooded areas using radar. Radio wave propagation at high frequencies suffers severe attenuation in forests which means low-frequency radar is required. However, stand-alone compact low-frequency radars have a poor angular resolution, which suggests use of a distributed radar system. A proposed solution to the problem is the use of multiple-input multiple-output (MIMO) radar. This approach exploits the angular diversity of widely spaced transmit and receive antennas to combat dynamic range and multipath problems associated with the complex scattering environment present in the forest. We assess the feasibility of the concept through simulation of radio propagation in a forest using a simple point scatterer model and a more detailed radio frequency scattering approximation using a CAD model of a forest. [C9886]

"DEM alignment and registration in interferometric SAR processing and evaluation"

Interferometric synthetic aperture radar (InSAR) processing, if lacking high quality ground control points (GCPs), may produce large errors in the final DEM. Some kind of alignment or registration can reduce these errors. This paper evaluates the accuracy of InSAR processed digital elevation models (DEM), against a high resolution DEM. InSAR DEMs were aligned and least-squares registered with USGS, 1/3 arc second NED. The accuracy evaluations after registration show InSAR DEMs alignment and registration can eliminate DEM errors caused by lack of accurate GCPs. In some cases, this process improves the accuracy of the InSAR DEM even more efficiently than including GCPs into InSAR processing. [C9887]

"ASCAT scatterometer ocean calibration"

The European Organisation for the Exploitation of Meteorological Satellites (EUMETSAT) is responsible for the absolute calibration of the new Advanced scatterometer (ASCAT), onboard MetOp-A, which mainly relies on the use of transponders. An alternative calibration method, which uses scatterometer measurements over the ocean, is presented here. The method is based on the knowledge of the backscatter signal modulation by the ocean surface, which is derived from previous C-band scatterometer missions, and on the use of numerical weather prediction wind output as calibration reference. The method proves to be very useful in providing guidance to EUMETSAT calibration efforts and provides continuity of the C- band scatterometers. Moreover, the ocean calibration results in very good quality winds. As such, within the framework of the EUMETSAT Ocean & Sea Ice Satellite Application Facility, the Royal Netherlands Meteorological Institute has released a demonstration ASCAT 25-km wind product, which is available at <http://www.knmi.nl/scatterometer> since 28 March 2007. [C9888]

"Scattering from sahelian grassland: a coherent modeling"

A coherent scattering formulation is developed for radar remote sensing of Sahelian grassland. This African vegetation is composed of shrubs and annual grass. The proposed model includes a vegetation generator tool in order to create vegetation structure with realistic architectures and botanical information. This is important in the development of the coherent scattering model, since the relative position of plant elements needs be preserved as accurately as possible. To correctly account for the coherent attenuation through the crown layer, the crown shape of shrubs must be considered. The crown shape is highly irregular, but for the most part can be encompassed in an ellipsoidal or cylindrical volume depending on the ground truth data. Thus, the extinction of the coherent wave is then calculated only when traveling within the crown volume. On the other hand, the grass generator models the grass as a set of cylindrical stalks and blade leaves arranged in a semi- deterministic fashion. Since grass blades are thin, multiple scattering among adjacent elements can be neglected at microwave frequencies. Backscatter statistics are acquired via a Monte Carlo simulation over a large number of realizations. Depending on the season, it is shown that contribution from soil and grass are the dominant components of the overall backscatter. [C9889]

"On SAR hurricane wind speed ambiguities"

Radar backscattered signals over the ocean are dampened in extremely high winds, which leads to a wind speed ambiguity problem during the process of wind retrieval from synthetic aperture radar (SAR). This problem was firstly studied by Shen et al. (2007), where we proposed a wind speed ambiguity removal scheme for the two wind speed solutions that may exist for any given normalized radar cross section (NRCS) and wind direction. This approach is based on the operational geophysical model function (GMF) CMOD5. Recently, new C-band GMFs for high wind have been developed, among which, a HH polarized GMF was established for the first time. In this study, the wind speed ambiguity problem will be studied within the context of the available high wind GMFs, which are, CMOD5, CMOD4HW, HWGMF_V and HWGMF_H. For the wind retrieval from HH polarized SAR

images, a hybrid empirical polarization ratio is generally adopted. To compare the different behavior of various GMF models, this polarization ratio is used to transform the HH polarized GMF into a W field. Although the wind speed ambiguity problem is found in most GMFs, the saturation wind speed where radar backscattered signals start to decrease is different for the various GMFs. We show that consideration of the wind speed ambiguity problem is important for high wind retrieval from SAR images, especially for category 5 hurricanes. [C9890]

"Dependency analysis of normalized radar cross section of ocean surface on ocean winds using an airborne dual-frequency polarimetric SAR"

The normalized radar cross section (NRCS) of ocean surface is measured from three directions of illumination by an airborne dual-frequency synthetic aperture radar (SAR) with L- and X-band, and the dependency of the NRCS and the polarimetric ratio on the relative wind direction is analyzed. In X-band, the NRCSs in parallel polarizations represent the dependency on the relative wind direction. The NRCS in HH polarization of X-band has difference between upwind and downwind condition, though that in VV polarization the NRCSs for upwind and downwind condition are almost same. The wind dependency of the NRCS in L-band is smaller than that of X-band. The polarimetric rate in X-band shows the wind dependency with small difference between upwind and downwind conditions, though that in L-band is not apparent. The results suggest the possibility of measurement of ocean winds only using the polarimetric SAR in X-band. Moreover, the small dependency of the NRCS in L-band suggests the possibility of the wind speed measurement over the ocean. [C9891]

"Determine the location of a thermal front in the Iroise Sea by using HF radar data and tide model results"

The Iroise Sea is a shallow sea, located on the North West European Shelf close to Western Brittany (France) and North of the Bay of Biscay. Due to strong gradients in the bathymetry close to the coast and strong local winds, tidal currents can reach up to 3.5 m/s during spring tide and induce a strong vertical mixing along the coast. During summer, solar radiation and thus warming of the sea surface, together with mixing along the coast, and thus colder temperatures in this area, leads to a formation of a thermal front, where the differences between the sea surface temperatures on both sides can reach up to 3degC. During the SURLITOP experiment, that took place from August to November 2005, two HF radar stations have been installed at the French coast. Both stations were working simultaneously at a working frequency of 12.4 MHz and a measurement cycle of 12 min. The surface current fields processed from the radar data have been interpolated to a regular 2times2 km grid. For the same period, tide model simulations (MARS 2D) have been processed with the same temporal and spatial resolutions. Because the model has been run under barotropic conditions, the location of the front, which is induced by density gradients, can not be reproduced. In contrast to the model, the radar measures the total circulation including the baroclinic signal, so that the difference between radar data and model results can be exploited to find the location of the thermal front. To validate this result, satellite remote sensed sea surface temperature data have been used. The result is very promising, as the region of highest differences between radar data and model results coincide with the location of the thermal front. The location of the front itself can be determined by the narrowness of the isotherms. Also the structures of the front isotherms and the strongest gradients of the currents are very similar. Thus it is possible, to determine the location and dynamics of a thermal front by using HF radar data in combination with model results, if the model is working under barotropic conditions. [C9892]

"Refocusing through single layer building wall using synthetic aperture radar"

Through-wall imaging using synthetic aperture array technique is studied by employing ultra-wideband antennas and for wide incidence angles. The effect of the building walls on the target image distortions is investigated by simulations and measurements. It is shown that using the idea of match filtering, the effect of the wall can be compensated for and point target response can be reconstructed. A controlled experiment within the laboratory environment is performed to verify the methods, presented. It is shown that for an ultra-wideband system operating over frequency band of 1-3 GHz highly distorted images of two point targets in close proximity of each other behind a wall can be resolved after refocusing. A dual-frequency synthetic method is also presented that can improve the cross-range resolution of the refocused image. [C9893]

"Half-space born approximation modeling and inversion for cross-well radar sensing of contaminants in soil"

Detection of dense non-aqueous phase liquids (DNAPLs) is a practical interesting problem in geophysics. This problem involves forward modeling, subsurface sensing and object reconstruction. An analytical forward model-HSBA-in the frequency domain containing dyadic Green's function solution to describe the cross-well radar sensing in infinite soil media is developed. First order Born approximation is employed to linearize this inverse

scattering problem. The forward model is validated by both frequency domain computational models and laboratory experiments that are collected using cross-well radar method that uses broadband antennas in subsurface to illuminate the inhomogeneous field and receive scattered electromagnetic (EM) waves. A shape-based inversion algorithm is proposed for contaminant pool localization and reconstruction, in which the shape of the object is assumed priori and represented by a low-order differentiable parametric function. The characteristics of the object-location, size and dielectric contrast to the background medium-are obtained by an iterative non-linear optimization. The inversion method using synthesized data by numerical experiments gives promising preliminary results. [C9894]

"Exact electromagnetic modeling of the scattering of realistic sea surfaces for HFSWR applications"

As a long term objective we would like to define the required conditions to detect oil spills, using high frequency surface wave radar (HFSWR). Assuming that the presence of oil spills on the sea surface modifies the surface tension which in turn affects the dynamics of the sea, we would like to determine the minimal surface tension which makes this phenomenon observable on a Doppler spectrum. For this purpose we have developed a simulator based on a realistic modeling of the sea and of its temporal variation as well as on an exact modeling of the interactions between the electromagnetic waves and the environment. We have chosen to implement a full wave model called ELSEM3D, developed by ONERA. This tool is based on the method of moments (MoM) which can be accelerated by the fast multipole method (FMM). The issues of such a modeling are numerous: computational time due to the number of temporal realizations required to generate a Doppler spectrum and the dimension of the scene. In this paper, we will discuss the issues raised by this study and outline how we can overcome them. We will also present some simulated Doppler spectra for different sea states and radar configurations. [C9895]

"Differential absorption microwave radar measurements for remote sensing of atmospheric pressure"

The accuracy of numerical weather model predictions of the intensity and track of tropical storms may be improved by large spatial coverage and frequent sampling of sea surface barometry. The feasibility of a microwave radar operating at moderate to strong O₂ absorption bands in the frequency range of 50~56 GHz to remotely measure surface barometric pressure may provide such capability. At these radar wavelengths, the reflection of radar echoes from water surfaces is strongly attenuated by atmospheric column O₂. Because of the uniform mixture of O₂ gases within the atmosphere, the total atmospheric column O₂ is proportional to atmospheric path lengths and the total atmospheric column air, and thus, to surface barometric pressures. Recent research has developed a technique based on the use of a dual-frequency, O₂-band radar to overcome many of the difficulties associated with techniques requiring larger frequency separation. The ratio of reflected radar signals at multiple wavelengths are used to minimize the effect of microwave absorption by liquid water, water vapor in the atmosphere and the influences of sea surface reflection over the frequency of operation. Langley Research Center (LaRC) has developed a radar based on this measurement technique to estimate barometric pressure. This paper will present an overview of the differential absorption measurement concept and will discuss a radar instrument to verify the differential O₂ absorption measurement approach. Results of instrument functional testing and initial measurements will be presented. [C9896]

"Sampling quantization analysis and results for FMCW SAR"

One of the advantages of Frequency Modulated Continuous Wave (FMCW) radars is the relative low required sampling frequency even when transmitting high bandwidths. This is a consequence of the inherent homodyne configuration of the radar front-end. A simple way to reduce further the data rate is to use few bits per sample. The paper analyzes the effects of low bit sampling in FMCW Synthetic Aperture Radar (SAR) data. A low number of bits used to sample the FMCW deramped signal could produce spurious peaks and intermodulation products of the sinusoidal signal. However, it is shown in the paper that, for typical value of signal to noise ratio in FMCW systems, white noise suppresses the spurious products. Simulation results and verifications on real data collected with the FMCW SAR system built at the Delft University of Technology are presented. [C9897]

"Exploiting full-waveform lidar data and multiresolution wavelet analysis for vertical object detection and recognition"

A current challenge in performing airport obstruction surveys using airborne lidar is lack of reliable, automated methods for extracting and attributing vertical objects from the lidar data. This paper presents a new approach to solving this problem, taking advantage of the additional data provided by full-waveform systems. The procedure entails first deconvolving and georeferencing the lidar waveform data to create dense, detailed point clouds in which the vertical structure of objects, such as trees, towers, and buildings, is well characterized. The point

clouds are then voxelized to produce high-resolution volumes of lidar intensity values, and a 3D wavelet decomposition is computed. Vertical object detection and recognition is performed in the wavelet domain using a multiresolution template matching approach. The method was tested using lidar waveform data and ground truth collected for project areas in Madison, Wisconsin. Preliminary results demonstrate the potential of the approach.

[C9898]

"Detection of foliage-obscured vehicle using a multiwavelength polarimetric lidar"

Foliage obscured man-made targets detection and identification is of great interest to many applications. In this paper, the backscattered laser signals from a multiwavelength polarimetric lidar were used to detect a vehicle hidden inside a vegetated area. The polarimetric reflectance data from the lidar at two separate laser wavelengths at 1064 nm and 532 nm revealed distinct target characteristics from both the vehicle and the vegetation. The results from this case study demonstrated the validity of the proposed lidar detection technique. Furthermore, the results could potentially lead to a lidar detection and identification technique for a wide variety of foliage-obscured man-made targets under various application scenarios. [C9899]

"A geophysical model function for windsat polarimetric radiometer wind retrievals using linear polarizations"

In this paper, we develop a novel geophysical model function (GMF) for the WindSat radiometer relating the vertically (V-pol) and horizontally (H-pol) polarized brightness temperature (TB) to the ocean surface wind field. The brightness temperature data from the 10, 18 and 37 GHz channels were used in this analysis. The brightness temperature combination of the form (AV-H) is found to be mostly independent of the atmospheric variations, where A is a constant number for each frequency. The GMF was developed empirically using the collocated wind vectors from the QuikSCAT scatterometer retrieval as truth and the WindSat's (AV-H) TB's. We examined the characteristic of the GMF and explored the opportunity to improve our current WindSat wind direction retrieval that utilizes only 3rd and 4th Stokes measurements, by integrating this GMF. The strength of the wind directional signals is encouraging for moderate wind speed at 8 m/s and higher. [C9900]

"A comparison of models for retrieving high wind speeds"

Based on polarization ratio from ENVISAT ASAR, we compared the wind vectors retrieved from CMOD5 with $\alpha = 0.6$, $\alpha = 0.5$, our polarization ratio, VV HWGMF with our polarization ratio and HH HWGMF with results from QuikSCAT and buoy, respectively. We found that CMOD5 with $\alpha = 0.5$ polarization ratio is best one for retrieving high wind speed from RADARSAT SAR; and error between QuikSCAT and HH HWGMF is the least. The polarization ratio and GMF for high wind need be improved. [C9901]

"Automatic extraction of salient geometric entities from LIDAR point clouds"

This paper introduces a modularized tool for the processing of LIDAR data based on the analysis of neighbor relationships between LIDAR points with the goal to extract planes, lines, and points in 3D. The tool's functionalities will be exemplified by the application of reconstructing building roofs. Detecting buildings within digital surface models is one further step to enhance the results of fully- and semi-automatic software tools which handle huge LIDAR point clouds. The functionalities comprise the sorting of point coordinates to improve efficiency, the retrieval of LIDAR point topology by triangulation of points, the extraction of 3D planes by "plane growing" and the determination of lines, points and roof outlines based on the 3D planes by statistical estimation and hypothesis testing of their parameters. [C9902]

"Automatic feature extraction from airborne lidar measurements to identify cross-shore morphologies indicative of beach erosion"

Airborne lidar data were acquired along St. Augustine Beach, Florida six times between August 2003 and June 2006. To identify sub-aerial morphologies indicative to beach erosion, the data sets were mined extensively by extracting several morphological features using cross-shore profile sampling. For each profile, the features were grouped into erosion or accretion classes and their class-conditional probability density functions (PDFs) estimated via Parzen windowing. PDF separability was ranked using symmetric and normalized measures of relative entropy (i.e. divergence). Results were compared to a simple median metric. The more interclass separation provided by a feature, the greater its potential as an indicator for erosion or accretion. Over short time periods (>1 month), beach slope and beach width ranked highest by providing the most separation and therefore high potential as indicators for erosion. Over longer time periods (>1 year), deviation-from-trend, which is the shoreline's deviation from the natural strike of the beach, ranked highest. This is significant in that the pier region's deviation from the natural trend is believed by coastal researchers to be a strong contributing factor to it

being an erosion "hot spot". The method we have developed provides a systematic framework to mine high-resolution airborne lidar data over beaches, detect erosion-prone areas, and numerically rank a feature's potential as an indicator for erosion. [C9903]

"Application of Polarimetric SAR images acquired in square-loop flights"

We acquired several data sets of polarimetric SAR data in Sendai, Japan by airborne Pi-SAR system for fundamental research of radar polarimetry and interferometry. Among these data acquisitions, two data sets were acquired in multiple flight paths in a short time period, and polarimetric SAR image acquired from different angles are available. We found very clear azimuth incident angle dependency of the polarimetric SAR images. In addition, a square-loop flight was carried out in the same location in January 2004. The incident angle dependency of the SAR image in polarimetry in X-band is very clear in these SAR images. We found that the phase difference in orthogonal circular polarization has significant dependency on the azimuth incident angle. The data sets also has a very good potential for SAR radargrammetry. We discussed the possibility of application of polarimetric SAR data acquired from multiple directions. [C9904]

"Coherence dependency of the PALSAR POLInSAR on forest in japan and amazon"

PALSAR PolInSAR capability was evaluated. One of the important capabilities that the PolInSAR offers is to estimate the forest height. For one-year and more months after the launch of the ALOS on Jan. 24 2006, PALSAR observed several test areas using the polarimetry modes repeatedly. We applied the PolInSAR method to retrieve the forest heights of the four test sites in Japan and Amazon. In this paper, we introduce an applied method and results. The results show that the forest tree height can be estimated with good accuracy. [C9905]

"Multibaseline POLInSAR coherence modelling and optimization"

This paper analyzes a POLInSAR coherence model with respect to polarization diversity. The coherence constituents are identified and examined. Extending POLInSAR to multiple baselines, two general multibaseline coherence optimization methods are introduced. The coherence model is utilized to discuss the advantages and applications of these newly developed multibaseline coherence optimization methods. [C9906]

"Disaster monitoring and environmental alert in taiwan by repeat-pass spaceborne SAR"

The prevailing complex geological and ecological conditions of Taiwan have drawn considerable attention from various geo-ecological communities because of their vulnerability to produce various natural hazards at different scales. Located in the tropical/subtropical zone of the Pacific Rim, its ecological and rugged mountainous properties are environmentally sensitive making monitoring and observations especially difficult because of the high population density. For example, in terms of natural hazard mitigation tectonically active regions are used for analyzing the cause of abundant risk events, such as earthquakes, landslides and land subsidence. In fact Taiwan is well suited as a test site for studying those geologically disastrous processes. Implementing novel techniques of space remote sensing has proved to be an effective means in recent years for greatly improving our understanding of these phenomena. In this paper we report on the monitoring of such events using multi-modal polarimetric and/or interferometric SAR images at C and L band from ERS, JERS-1, RADARSAT-1, ENVISAT, and from the recent ALOS satellite. For crustal and surface deformation, we used radar image pairs with long temporal baselines and large areas of coverage for investigating deformation over Western Taiwan. Pre-seismic and co-seismic deformation patterns are spatial-temporally analyzed. The other topic deals with the coastline changes observed from a sequence of ERS-1/2 SAR images within the years of 1996 to 2005. Waterlines were extracted using multi-scale procedures of edge detection and were corrected with tidal motion data. Substantial analyses were carried out in conjunction with ground surveys and lidar mapping. The topographic feature changes due to large scale landslides triggered by torrential rains were also monitored. In addition, the SAR interferograms were used to analyze the deposition changes along the riverbeds and riverbanks for short-intervals using optimal baselines. Summary and remarks on the implementation of such multi-modal polarimetric and/or interferometric SAR imagery for environmental monitoring are provided. [C9907]

"PolSAR image filtering based on feature detection using the wavelet transform"

This paper elucidates a new approach for speckle reduction in polarimetric synthetic aperture radar ("PolSAR") images based on the stationary wavelet transform. Noisy wavelet coefficients are thresholded using an entropic thresholding technique. Principal Component Analysis and Sum of Squared Coefficients methods are used to detect significant coefficients based on the entire polarimetric covariance matrix. [C9908]

"Building feature extraction via a deterministic approach: application to real high resolution SAR"

images"

Interpretation of high resolution SAR (synthetic aperture radar) images is still a hard task, especially when man-made objects crowd the scene under detection. This paper contributes to the analysis of this kind of data by adopting an approach, based on a scattering model, for the retrieval of buildings height from real SAR images and presenting first numerical results. [C9909]

"Estimation of physical properties of persistent scatterers using JERS-1 data"

The physical properties of persistence scatterers (PS) are estimated utilizing variety means. Two urban areas of Seoul and Busan in Korea are processed using L-band HH-polarization JERS-1 data. The linear and one-year periodic deformations are monitored. The size and brightness variation of PSs are also estimated. In addition, the concurrence of PSs and the point-like targets are examined and disagreement between the positions of both types of scatterers is identified. [C9910]

"Snow wetness monitoring using multi-temporal polarimetric ASAR data and multi-layer hybrid model"

This paper presents a method to characterize snow cover using multi-temporal dual polarization ASAR/ENVISAT data. At first, variations of electromagnetic backscattering of snowpack depending on melting are explained and validated by a multi-layer model. It is demonstrated that it is crucial to exactly model the distribution of Liquid Water Content inside snow pack in C-band. Consequently, a new mapping algorithm based on the French weather model CROCUS is proposed in order to estimate the spatial variability of layered snowpack profile. [C9911]

"Change detection and analysis with radarsat-1 SAR image"

In the present paper, according to data analysis, the problem of change detection has been addressed with unsupervised change detection with multi-temporal single-channel single-polarization RADARSAT-1 SAR images. Method proposed in this paper is based on four main steps: (1) Data preprocessing. SAR images are rectified and calibrated to Gauss-Kruger projection firstly. Moreover they are co-registered to ensure the condition of good accuracy of change detection. (2) Change detection. The window log-ratio approach is adopted to compare multi-temporal SAR data, because of the multiplicative speckle in the images. Then a proper window is selected to average pixels from the two SAR data in log-ratio process instead of pixel by pixel. (3) Selection of optimal threshold value. Minimum error threshold is applied to find the optimal threshold. (4) Change detection map can be obtained by segmentation of window log-ratio image. Experiments show the approach deal well with change detection in water area. [C9912]

"SAR-based estimation of the baltic sea ice motion"

The ice season in the northern part of the Baltic Sea varies from a few weeks up to 4-5 months depending on the location and the winter. As a long-term average the Baltic Sea is ice covered for about 45% of its surface area at the annual maximum. Due to the relatively narrow basins, the deformation rate remains rather high throughout the winter. The ice thickness measurements show that in the Bay of Bothnia over one third of the ice cover is thicker than 1 m in the later stages of the ice season during a typical winter. Modeling the state and development of the Baltic ice cover has been an active research area which have resulted in operative ice models. The current operative ice model run at the Finnish Ice Service (FIS) models the following parameters: ice motion and concentration, mean ice thickness, ridged ice thickness, ridged ice concentration, compressive region, and deformed ice fraction. Some case studies have been made to validate the results. However, a more systematic forecast evaluation is needed, the final goal being the data assimilation to integrate the EO data into the numerical ice model. In this paper we present an algorithm which estimates the ice motion field from two successive RADARSAT-1 SAR images. A large number of RADARSAT-1 ScanSAR Wide mode SAR images, usually over 100, is received at FIS every winter. The same sea areas are visible in the images with a time interval of 1-3 days. [C9913]

"Simulation studies of forest structure using 3D lidar and radar models"

The use of lidar and radar instruments to measure forest structure attributes such as height and biomass are being considered for future Earth Observation satellite missions. Large footprint lidar makes a direct measurement of the heights of scatterers in the illuminated footprint and can yield information about the vertical profile of the canopy. Synthetic Aperture Radar (SAR) is known to sense the canopy volume, especially at longer wavelengths and is useful for estimating biomass. Interferometric SAR (InSAR) has been shown to yield some forest canopy height information. There is much interest in exploiting these technologies separately and together

to get important information for carbon cycle and ecosystem science. More detailed information of the electromagnetic radiation interactions within forest canopies is needed and backscattering models can be of much utility here. A three-dimensional (3D) coherent radar backscattering model and a 3D lidar backscatter models were used to investigate the use of large footprint lidar, SAR and InSAR for characterizing realistic forest scenes. The tree height indices derived from lidar waveform and heights of InSAR phase centers were compared. Results will address the possible synergies between lidar and radar data in terms of forest structural information. [C9914]

"Inversion model validation of ground emissivity. Contribution to the development of SMOS algorithm"

SMOS (Soil Moisture and Ocean Salinity), is the second mission of "Earth Explorer" to be developed within the program "Living Planet" of the European Space Agency (ESA). This satellite, containing the very first 1.4 GHz interferometric radiometer 2D, will carry out the first cartography on a planetary scale of the moisture of the grounds and the salinity of the oceans. The forests are relatively opaque, and the knowledge of moisture remains problematic. The effect of the vegetation can be corrected thanks a simple radiative model. Nevertheless simulations show that the effect of the litter on the emissivity of a system litter + ground is not negligible. Our objective is to highlight the effects of this layer on the total multi layer system. This will make it possible to lead to a simple analytical formulation of a model of litter which can be integrated into the calculation algorithm of SMOS. Radiometer measurements, coupled to dielectric characterizations of samples in laboratory can enable us to characterize the geological structure. The goal of this article is to present the step which we chose to validate this analytical model. [C9915]

"Quad-polarimetry and interferometry from repeat-pass dual-polarimetric SAR imagery"

New space-borne polarimetric SAR systems employ, or will employ, dual-pol imaging modes as well as full quad-pol imaging, e.g. PALSAR, RADARSAT-2, TERRASAR-X. Therefore questions arise as to the capabilities (and limitations) of these various dual-pol SAR imaging modes. One novel offshoot of our work on dual-pol SAR image analysis and polarimetric decompositions of dual-pol data was the idea to collect two dual-pol images employing geometry appropriate for parallel repeat-pass interferometry. The polarizations of the dual-pol collections differ, e.g. one is (HH, HV) and the other (VV, VH). Using the example of transmitting either horizontal (H) or vertical (V) polarizations, one collects all four polarimetric channels, but only two per pass. Except for the interferometric repeat-pass nature of the SAR image collections the polarimetric information should be identical to standard quad-pol SAR imagery. The relevant open questions concern the interferometric baseline and temporal decorrelations between the repeat-pass dual-pol images. [C9916]

"Multi-baseline polarimetrically optimised phases and scattering mechanisms for InSAR applications"

An interesting, but rarely used technique in polarimetric SAR interferometry is the enhancement of interferometric coherence by projection into an optimal polarimetric state. In particular, newly developed methods for polarimetric optimisation of multi-baseline coherences provide the possibility of simultaneous constrained coherence optimisation for more than one baseline. This technique can significantly improve the usefulness of long-term interferometric pairs and time-series, and appears, therefore, of interest to various fields of application. The aim of this paper is to discuss the correct derivation of multi-baseline differential interferograms with polarimetrically optimised coherence and to outline several possible areas of application, particularly in the field of differential interferometry and permanent scatterers. [C9917]

"Technique of remote sensing image processing in active faults survey"

The paper employed image fusion technology for SAR image and ETM+ multi-spectrum image, combined enhancement technology of multi-spectrum texture characters and spectrum characters to process SAR image, ETM+ image, SPOT-5 image and high precision DEM data. Then, with the help of high resolution image and three-dimensional image of the fault, the paper analyzed the characters of the active fault's remote sensing image. [C9918]

"Need for developing repeat-pass differential POLSAR interferometry"

Radar Polarimetry, Radar Interferometry and Polarimetric SAR Interferometry represent the current culmination in active 'Microwave Remote Sensing' technology, but we still need to progress very considerably in order to reach the limits of physical realizability. Whereas with radar polarimetry the textural fine-structure, target orientation, symmetries and material constituents can be recovered with considerable improvement above that of standard

'amplitude-only' radar; by implementing 'radar interferometry' the spatial (in depth) structure can be explored. With Polarimetric Interferometric Synthetic Aperture Radar (POL-IN-SAR) imaging, it is possible to recover such co-registered textural and spatial information from POL-IN-SAR digital image data sets simultaneously, including the extraction of Digital Elevation Maps (DEM) from either Polarimetric (scattering matrix) or Interferometric (dual antenna) SAR systems. Simultaneous Polarimetric-plus- Interferometric SAR Imaging offers the additional benefit of obtaining co-registered textural-plus-spatial three-dimensional POL-IN-DEM information, which when applied to Repeat-Pass Image-Overlay Interferometry provides differential background validation and environmental stress-change information with highly improved accuracy. However, hitherto only single-polarization-channel repeat-pass IN-SAR was developed and considered; and therefore the aim of this paper is to scrutinize and determine why and for what specific problems fully polarimetric differential RP-POL-IN-SAR imaging is required. [C9919]

"Comparison of similarity measures of multi-sensor images for change detection applications"

Change detection of remotely sensed images is a particularly challenging task when the available data come from different sensors. Indeed, many change indicators are based on radiometry measures, operating on their differences or ratios, that are no longer reliable when the data have been acquired by different instruments. For this reason, it is interesting to study the performance of those indicators that do not rely completely on radiometric values. A series of similarity measures for automatic change detection has been investigated and their general performance compared using optical and SAR images covering a period of about six years. We could observe that the considered change detection algorithms perform differently but that none of them permits an "absolute" measure of the changes independent of the sensor. Also the dimensions of the windows, for the estimation of the pixel statistics and of the similarity measure, affect the final results. [C9920]

"Large scale change detection techniques dedicated to flood monitoring using ENVISAT wide swath mode data"

Semi-automatic flood extraction procedures based on change detection techniques appear particularly adapted to plain flood monitoring and mapping. The change detector was specifically elaborated to analyse ENVISAT ASAR wide swath mode data pairs, which appear very well adapted to flood monitoring over wide areas. The algorithm is based on two analysis levels: an enhanced ratio for strong changes over large homogeneous and flat areas combined with a ratio calculated from the two raw images which aims to keep the raw data's thematic precision. Slope and aspect effects are also eliminated by the use of a digital elevation model during the processing. This change detection analysis was performed on 35 data pairs acquired within the framework of the flood DRAGON project. The first set of results is very promising and robust using HH polarization. Change detection between data with W polarization or with different polarization (HH versus W) has to be fully validated but results are promising. [C9921]

"Mapping of wind-thrown forests using VHF/UHF SAR images"

SAR images from the Swedish airborne CARABAS-II and LORA systems have been visually analyzed over simulated wind-thrown forest at both single tree and stand level. In ideal conditions, the results show that LORA is more accurate than CARABAS-II at detecting wind-thrown trees, regardless of tree size and direction of the fallen trees relative to flight heading. Furthermore, the visible single trees in the LORA images appeared more distinct than in the CARABAS-II images, which could be explained by the high resolution in the LORA images. Based on visual interpretation, it is likely that the detection of wind-thrown forests could be improved using VHF/UHF SAR images acquired both prior to and after a storm event. [C9922]

"Bistatic border effects modelling in forest scattering"

Simulating forest scattering by electromagnetic waves has been proposed with both coherent and incoherent models. However, to our best knowledge, most models consider a description of the forest as infinite in the horizontal plane and layered vertically. Such description is relevant in most cases, but fail when border effects are present near the boundaries: the shadowing effects as well as the reinforcement ones, which are present in true SAR images, are absent in the synthetic images. The purpose of this study is to present a coherent scattering model taking into account forest regions of finite extent and benefit from its polarimetric, interferometric and bistatic capabilities to bring out interesting outlooks about border effect in the bistatic case. [C9923]

"Conditional copula for change detection on heterogeneous SAR data"

A new preprocessing technique is presented in this paper to perform automatic change detection in multitemporal multimodal remotely sensed images, mainly synthetic aperture radar (SAR) ones. This technique is dedicated to the case where the two acquisitions, before and after a major disaster, are different for some

reason (different sensor, modality of acquisition or climatic conditions). A measure, based on the local statistics of the images between the two dates, has proved to be a relevant change indicator. Nevertheless, the measure is valid when the two observations have been acquired with a similar point of view only. When the modalities of acquisition differ, local statistics tend to be too different, from one image to the other, to be relevant to the ground evolution without mixing to the normal changes. The technique, that overcomes this constraint, is based on the assumption that some dependence exists indeed between the two images. This dependence is modelled by the copula theory and used to perform an estimation of the local statistics that would have been observed if the modality of the first image had been similar to the other. It yields an estimation of local statistics of the first image, through the point of view of the latter. Then, usual comparison of those statistics may be applied to perform change detection. Some results are shown on a pair of ERS images and pairs of SPOT/ERS acquired before and after a flood. [C9924]

"Obtaining a ship's speed and direction from its Kelvin wake spectrum using stochastic matched filtering"

The Kelvin wake of a ship is directly linked to the ship's speed, heading and hull shape. This wake can be visible in high resolution synthetic aperture radar images or optical images. Whenever it is possible, analyzing it can provide elements to identify the ship and track its course. We propose a strategy based on the generalized Radon Transform and the Stochastic Matched Filtering where the locus of the wake signature in the 2D spectrum of the image is to be detected. [C9925]

"Comparison and evaluation of polarimetric change detection techniques in aerial SAR data"

This article aims at providing a comparison of polarimetric change detection indices from a practical point of view. Six polarimetric change detection indices were tested on L band EMISAR data over Norway. Tests included quantitative evaluation of change maps compared to a ground truth of changes, and qualitative evaluation by visual inspection. Contrast ratio and the Wishart test gave the best results among the tested indices. [C9926]

"Detecting changes in polarimetric SAR data with content-based image retrieval"

In this study, we extended the potential of a Content- Based Image Retrieval (CBIR) system based on Self-Organizing Maps (SOMs), for the analysis of remote sensing data. A database was artificially created by splitting each image to be analyzed into small images (or imagelets). Content-based image retrieval was applied to fully polarimetric airborne SAR data, using a selection of polarimetric features. After training the system on this imagelet database, automatic queries could detect changes. Results were encouraging on airborne SAR data and may be more useful for spaceborne polarimetric data. [C9927]

"Vegetation modelling for height inversion using InSAR/Pol-InSAR data."

The random volume over ground model has been extensively used for forest height inversion using Pol-InSAR data. Two different forest models are proposed to better represent the forest structure for height inversion using Pol-InSAR. The first one takes into account a vertically varying mean extinction coefficient and the second one considers contributions localized in a finite height interval. [C9928]

"Forest monitoring with JERS-1/SAR and ALOS/PALSAR"

JERS-1/SAR images taken in 1990's and ALOS/PALSAR images taken in 2000's are used and examined the deforestation status during ~14 years. Many trees had been fallen by a typhoon hit in 2004 in a test site, Tomakomai. There is also a plantation area and the site show active change during the term. The forest stands could be roughly classified for four types, forest stands, vacant, where almost all trees were carried out, and two types of transitional stands from a forest to a vacant. Many deforested areas are easily detected by using the difference of backscattering coefficients between two images, if fallen trees have been carried out from the stands. The change from the normal forest to the vacant stands causes 3.1dB decrease in the σ_{HH} . On the other hands, transitional stands show almost same backscattering as the normal forest stands, although. Three- component scattering model shows surface scattering component accounts for 50% over the vacant stands, while volume scattering component accounts for ~60% over the forest stands. But the model doesn't show the clear difference between transitional forest site and normal forest. The temporal changes of the forest during 14 years are also examined for the plantation area. One stand show gradual increase of σ_0 and the values seem to be saturated around 17.4 tons/ha (~5 m in average height). [C9929]

"Spatial patterns of the canopy stress during 2005 drought in Amazonia"

In the last decades, the detection of drought occurrences and assessment of its severity using satellite data are becoming popular in disaster, desertification, crop production, phenology, land cover change and climate change studies. To detect the drought effects on different vegetation types, many methodologies have been developed, mostly relying on the use of vegetation indices. This communication reports the first attempt to assess the capability of MODIS NDVI, Enhanced Vegetation Index (EVI) and Normalized Difference Water Index (NDWI) from 2000 to 2006 time-series to detect the 2005 drought in Amazonia. To reach this objective, monthly composites of the MOD13A2 product were generated from period. Then, monthly anomalies were calculated, considering anomalous values when lower than -1 standard deviation (sd) or higher than 1 sd. Rainfall data provided by the Tropical Rainfall Measuring Mission (TRMM) was also acquired for the same time-series with the objective of supporting the understanding of vegetation response with the precipitation. Water deficit data calculated based on the TRMM data were also used to guide the sampling scheme. A land cover map for South America updated with natural land cover changes detected by the Near Real Time Deforestation Detection Project (DETER) was used as a mask to avoid false anomalies in the Brazilian Amazon. In general, NDWI and EVI showed to be sensitive and consistent for the temporal series used. NDVI presented a high variability and though a difficult interpretation. Critical months in the NDWI and EVI series coincided with the months with higher water stress calculated based on the TRMM data. EVI also showed to detect changes in the canopy structure. These preliminary results suggest that this is a strong methodology to be used in the spatial analysis of the extent of the drought effects in the vegetation. Literature data will be incorporated in this research for validation purposes. [C9930]

"Using MODIS and GLAS data to develop timber volume estimates in central Siberia"

Mapping of boreal forest's type, structure parameters and biomass are critical for understanding the boreal forest's significance in the carbon cycle, its response to and impact on global climate change. The biggest deficiency of the existing ground based forest inventories is the uncertainty in the inventory data, particularly in remote areas of Siberia where sampling is sparse, lacking, and often decades old. Remote sensing methods can overcome these problems. In this study, we used the moderate resolution imaging spectroradiometer (MODIS) and unique waveform data of the geoscience laser altimeter system (GLAS) and produced a map of timber volume for a 10degx12deg area in Central Siberia. Using these methods, the mean timber volume for the forested area in the total study area was 203 m³/ha. The new remote sensing methods used in this study provide a truly independent estimate of forest structure, which is not dependent on traditional ground forest inventory methods. [C9931]

"Analysis of airborne SAR data (L-band) for discrimination land use/land cover types in the Brazilian Amazon region"

The objective of this paper is to show the potential of multi-polarized mosaic-images from a MAPSAR (L-band) simulation campaign performed in the Amazon region (test site Tapajos) in order to discriminate land use/land cover classes. An Enhanced-Frost filter was used and the thematic discrimination was done by an algorithm for attribute extraction based on Bhattacharya distance. A comparison was made among the radiometric aspects of the SAR mosaic for 10 thematic classes obtained, converting these B-distances to JM distance values. This allowed to define which individual or multiple polarizations are more appropriate for the identification of thematic classes. [C9932]

"backscatter and interferometry for estimating above- ground biomass in tropical savanna woodland"

Tropical savannas cover 15% of the Earth's land surface and are important ecosystems in the global Carbon cycle due to their high productivity. SAR interferometry and backscatter are investigated for estimating biomass in a tropical savanna in Belize, Central America. Single-pass InSAR data used are C-band (AIRSAR) and X-band (Intermap); SAR backscatter data used are fully polarimetric L and P band (AIRSAR). Results show that both C-band and X-band InSAR show a clear trend in vegetation patterns although both underestimate vegetation heights due to the heterogeneity of the vegetation cover. The scattering phase centre is lowered more for the X-band due to larger ground- level contribution. High P and L-band backscatter values are observed for areas containing high biomass vegetation, but also for leafy palmetto that have relatively low biomass. [C9933]

"Detection of forest changes using ALOS PALSAR satellite images"

A controlled experiment has been performed to quantify the ability to detect clear-cuts using ALOS PALSAR data. The experiment consisted of 8 old spruce dominated stands, each with a size of about 1.5 ha, located at a test site in southern Sweden. Four of the stands were clear-felled and the remaining stands were left untreated for reference. A time series of PALSAR images was acquired prior to, during, and after treatment, including 7

fine beam single polarization (FBS, look angle 34.3deg, HH-polarization) SAR images. The results clearly show that the clear-felled stands could be separated from the reference stands. The drop in backscattering coefficient between the reference and the clear-felled stands was on average 2.1 dB. This implies that ALOS PALSAR data potentially can be used for large-scale mapping of changes in forest cover. [C9934]

"Estimation of the bidirectional reflectance distribution function of subarctic boreal forest using C-band SAR"

Surface albedo is acknowledged as an important variable in climate research. Monitoring of Earth's surface albedo in a global scale is practical only with satellite observations. However, satellite-based albedo research in the boreal regions is hampered by continual cloud contamination in the optical wavelengths, as well as long periods of low sun elevation. As the surface albedo can be calculated from the Bidirectional Reflectance Distribution Function (BRDF) of an area, new methods to improve the accuracy of BRDF calculation and remove cloud contamination effects are needed to enhance the accuracy of future climate studies. This study explores the possibility of estimating the BRDF of boreal forest using C-band synthetic aperture radar (SAR) data. The principle of the estimation is based on the knowledge that the BRDF of boreal forests depends on structural parameters such as NDVI or LAI, and that similar structural information can be derived from SAR imagery. The results of the study show that the estimation of BRDF from C-band SAR is possible at least under certain conditions, the proposed estimation method yielded a coefficient of determination of 0.68 for the small-scale study area in Northern Finland. [C9935]

"Detection of May 2006 Saharan dust outbreak over Granada, Spain, by combination of active and passive remote sensing"

During May 2006 a severe Saharan dust outbreak affected the Iberian Peninsula. During this event that lasted almost a whole week a large amount of mineral particles were present in the atmospheric column. In this work we present some results on this particular event that has been monitored at Granada, Spain (37.16degN, 3.6degW and 680 m a.m.s.l.) using different types of instrumentation. To investigate the optical properties of atmospheric aerosols, we used a combination of passive and active remote sensing, including Lidar system and radiometers, together with in situ techniques to characterize the physical properties of the aerosol. Features of the mineral aerosol outbreak are discussed in combination with other external information sources like back trajectory analyses. Our analyses are based mainly on the information obtained on the columnar properties of the atmospheric aerosol, although considerations were done on the atmospheric aerosol characteristics at the surface boundary layer. [C9936]

"Inversion algorithms comparison using L-band simulated polarimetric interferometric data for forest parameters estimation"

Polarimetric SAR interferometric data can provide estimates of forest biomass density. There are different approaches to deal with the inversion problem, such as neural networks and the traditional optimal estimation approach. This paper presents a study to evaluate their performance by means of quantitative indexes addressing both the computation time and the retrieval accuracy. Better forest parameters estimates have been obtained when neural networks algorithms were used. [C9937]

"Examination of hygroscopic properties of aerosols using a combined multiwavelength elastic-Raman lidar"

Water vapor is an important greenhouse gas due to its high concentration in the atmosphere (parts per thousand) and its interaction with tropospheric aerosols particles. The upward convection of water vapor and aerosols due to intense heating of the ground leads to aggregation of water particles or ice on aerosols in the air forming different types of clouds at various altitudes. The condensation of water vapor on aerosols is affecting their size, shape, refractive index and chemical composition. The warming or cooling effect of the clouds hence formed are both possible depending on the cloud location, cover, composition and structure. The effect of these clouds on radiative global forcing and therefore on the short and long term global climate is of high interest in the scientific world. A major interest is manifested in obtaining accurate vertical water vapor profiles simultaneously with aerosol extinction and backscatter in the meteorological and remote sensing fields all around the globe in an effort to understand the hygroscopic properties of aerosols. In previous work, simultaneous measurements of RH with backscatter measurements from a surface nephelometer were used to probe the hygroscopic properties of aerosols. However, most of these measurements were not able to probe the high RH domain since such high RH is rare for surface altitudes. For this reason, experiments using a 355 nm raman water vapor and aerosol lidar at the ARM site were used. Capable of providing simultaneous backscatter and RH profiles, and performing the experiments under low altitude cloud decks insured stable well mixed layers as well

as probing RH profiles to above 95% which is required for the differentiation of different aerosol hygroscopic models. [C9938]

"The vertical distribution of Saharan dust over the western and central Mediterranean through dust modelling and lidar observations"

Aerosol extinction vertical profiles during Saharan dust events measured by two EARLINET lidar stations in the western and central Mediterranean during a two-year period (2001-2002) are compared to profiles forecasted by the dust regional atmospheric model (DREAM) that currently operates dust forecasts over the Mediterranean region. 35 Saharan dust cases were successfully captured in Barcelona (Spain) with a 1064 nm backscatter lidar and 45 Saharan dust cases in Naples (Italy) with a 351 nm Raman lidar. The objective of the present study is twofold: (1) to evaluate the skills of the model to forecast the dust vertical distribution in the Mediterranean basin and (2) to study the synoptic pattern dependence of the Saharan dust events over the western and central Mediterranean. The comparison between the modeled and the measured mean annual aerosol extinction vertical profiles shows a rather good agreement between model forecasts and lidar data. However, below 2000 m the extinction measured by the lidar systems is not captured by DREAM due to the significant influence of local anthropogenic aerosols in the boundary layer. The main synoptic patterns responsible for all the measured events of Saharan dust were identified and classified for both sites. It was found that the main synoptic situations in which the Saharan dust reaches the Mediterranean basin are anticyclonic systems located in North Africa (both for dust transport over the western and the central Mediterranean) and a low pressure system located in Portugal (for the western Mediterranean) and in central Europe (for the central Mediterranean). In the presence of low pressure, the altitude of the dust plume is higher in the western than in the central Mediterranean and this is probably related to geographical factors. [C9939]

"Wetlands map of Alaska using L-Band radar satellite imagery"

We have used two seasons of L-band SAR imagery to produce a thematic map of wetlands throughout Alaska. The classification was developed using the Random Forests statistical decision tree algorithm. Input data included mosaics of summer and winter JERS-1 SAR imagery with associated image collection dates, summer and winter SAR backscatter texture, elevation, slope, proximity to water, and geographic latitude. The accuracy of the resulting thematic map was quantified using extensive ground reference data. The overall aggregate accuracy calculated based on all classified pixels was 89.5%, with individual per-tile aggregate accuracies ranging from 80% to 97%. As the first high-resolution large-scale synoptic wetlands map of Alaska, this product provides the basis for improved characterization of land-atmosphere CH₄ and CO₂ fluxes and climate change impacts associated with thawing soils and changes in extent and drying of wetland ecosystems. [C9940]

"Two-dimensional surface river flow patterns measured with paired riversondes"

Two RiverSondes were operated simultaneously in close proximity in order to provide a two-dimensional map of river surface velocity. The initial test was carried out at Threemile Slough in central California. The two radars were installed about 135 m apart on the same bank of the channel. Each radar used a 3-yagi antenna array and determined signal directions using direction finding. The slough is approximately 200 m wide, and each radar processed data out to about 300 m, with a range resolution of 15 m and an angular resolution of 1 degree. Overlapping radial vector data from the two radars were combined to produce total current vectors at a grid spacing of 10 m, with updates every 5 minutes. The river flow in the region, which has a maximum velocity of about 0.8 m/s, is tidally driven with flow reversals every 6 hours, and complex flow patterns were seen during flow reversal. The system performed well with minimal mutual interference. The ability to provide continuous, non-contact two-dimensional river surface flow measurements will be useful in several unique settings, such as studies of flow at river junctions where impacts to juvenile fish migration are significant. Additional field experiments are planned this year on the Sacramento River. [C9941]

"Multi-track PS-InSAR datum connection"

InSAR data acquired from independent overlapping tracks can be exploited for a reliability assessment of the Persistent Scatterer InSAR (PS-InSAR) technique. This is obtained by means of the datum connection of multiple tracks, simultaneously evaluating the misclosures between multi-track PS-InSAR estimates. Due to a different viewing geometry, many of the detected PS will physically not be the same. However, their estimates may still refer to the same deformation signal. The existence of independent observations of the same deformation signal provides a powerful tool to increase the redundancy and evaluate the reliability. The datum connection can be subdivided in two steps. The first step consists of the conversion of PS locations to a common datum. Secondly, the PS-InSAR parameter estimates (velocities, displacements, heights) are connected. In stead of the conventional approach of separately geocoding each track, we propose the use of a common radar datum

defined by the acquisition geometry of the 'master track'. Multi-track datum connection has been applied in the Groningen region, the Netherlands, which is affected by subsidence due to gas extraction with displacement rates up to 7 mm/year. The main reservoir is (partly) visible in 6 independent overlapping ERS tracks from 1992 (ascending and descending). Datum connection resulted in a consistent set of PS-InSAR deformation estimates. Additionally, the deformation signal was decomposed in horizontal and vertical movements, utilizing the different viewing geometries of the tracks. [C9942]

"The Comparison of the V-Fold and the Monte-Carlo cross validation to estimate the number of clusters for the fully polarimetric sar data segmentation"

In this paper, the cross validation algorithm is used to estimate the number of clusters for the unsupervised classification of fully polarimetric SAR data. Three different cross validation algorithms are applied for comparison, which are the dispersion measure method, the V-fold cross validation (VFCV) and the Monte-Carlo cross validation (MCCV). Our current experiments show that the dispersion measure method appears generally unable to provide a reliable estimation. The VFCV and the MCCV algorithms seem to be more effective than the dispersion measure method. Moreover, the VFCV is much faster than the MCCV, but the MCCV may be able to provide better estimation than the VFCV. [C9943]

"InSAR monitoring of landslides on permafrost terrain in canada"

In this study we used differential InSAR techniques to monitor landslide slide and permafrost activity at a site along the Mackenzie Valley Pipeline Corridor. Our results that motion are about 3 times more on exposed burnt slopes than the adjacent areas. The maximum activity is in September, probability related to gradual accumulated increases in soil temperatures. [C9944]

"Analysis of the temporal behavior of coherent scatterers (CSs) in ALOS PaISAR data"

Coherent scatterers (CSs) are scatterers detected by using spectral correlation properties and characterized by a deterministic scattering behavior. In this paper we investigate, for the first time, the temporal behavior of CSs using quad-pol data acquired by ALOS/PaISAR. In this sense, we can evaluate the stability of the deterministic scattering nature of individual scatterers. [C9945]

"An investigation of PN sequences for multistatic SAR/InSAR applications"

This paper investigates the performance of pseudo-noise (PN) sequences as pulse compression waveforms in the radar imaging of distributed targets. Multiple transmitter schemes such as multi-static synthetic aperture radar (SAR) and multi-baseline interferometric SAR (InSAR) provide high resolution images for remote sensing applications at lower costs. PN sequences are a natural choice for such systems. The performance of different PN coding schemes such as the maximal length sequences (m-sequences), Gold sequences and shifted m-sequences are compared. [C9946]

"Calibration and performance analysis of the PAU- RAD instrument"

This paper presents the calibration of the PAU-RAD instrument: a novel pseudo-correlation radiometer with digital beamforming, it consist on a Wilkinson power splitter and two receiving chains whose outputs are cross-correlated. To types of calibration are required: an internal hardware, relative calibration to perform the phase and an amplitude correction, and internal radiometric calibration. The simplified and unified calibration procedure is presented using internal well-known temperatures. [C9947]

"Validation of a backscatter model of a river ice covers using Radarsat-1 images"

Simultaneous microwave radar data and measurements field at some study sites on river ice were collected over the Athabasca River during winter 2006. These data will be employed to validate an electromagnetic model developed to simulate the backscatter of river ice cover. This model is based on radiative transfer theory which is solved by doubling matrix methods". This numerical method accounts for scattering effects due to the volume, boundaries, boundary-volume interactions and coupling between layers. Three ice types were formed on this river (columnar ice, snow ice and frazil ice). The measurements collected from the extracted ice cores included the ice thickness, ice type, ice densities, and size and form of the scatters embedded in the ice cover. These measurements will be used as inputs data for the model developed to its validation with the Radarsat-1 images and to understand the interaction of radar signal with the different ice types formed on the river. [C9948]

"Hurricane wind field estimation from seawinds at ultra high resolution"

Although SeaWinds was not originally designed to observe tropical cyclones, new higher resolution products resolve much of the horizontal structure of these storms. However, these higher resolution products (reported at 2.5 km) are inherently noisier than the standard 25 km products and the high rain rates often associated with hurricanes corrupt the wind estimates. Fortunately, these storms have structure which can be exploited using a model. This paper develops a new procedure for hurricane wind field estimation from the SeaWinds instrument at ultra high resolution. We develop a simplified hurricane model to provide prior information to be used in maximum a posteriori probability (MAP) wind estimation. Using the hurricane model ameliorates the effects of rain and noise on the scatterometer measurements and directly provides useful hurricane parameters such as the eye center location and intensity. [C9949]

"Multibaseline POL-InSAR analysis of urban scenes for 3D modeling and physical feature retrieval at L-band"

This paper generalizes a multibaseline interferometric SAR signal model taking polarization diversity into account. Based on this formulation, two high-performance spectral analysis techniques are extended to the multibaseline POL-InSAR configuration. These new algorithms enhance the height estimation of scatterers by calculating optimal polarization combinations and allow to determine their physical characteristics. Applying the methods to urban scenes, experimental results show the retrieval of building height and polarimetric properties by means of single-baseline polarimetric datasets. Dual-baseline observations permit the solution of the layover problem by separating two contributions within one resolution cell. The algorithms are tested using multibaseline Pol-InSAR data acquired by DLR's E-SAR system over Dresden city. [C9950]

"Application of persistent scatterer InSAR and GIS for urban subsidence monitoring"

The purpose of this paper is to demonstrate the application of C-band ERS-1/2 and ENVISAT radar images to investigate the urban subsidence due to groundwater extraction. Cities in Australia without groundwater being over-extracted are compared to cities in Australia and China with groundwater being over-extracted. The persistent scatterer InSAR results are interpreted and compared to investigate the effect of groundwater extraction to urban subsidence. The GIS software is used to interpret the persistent scatterer InSAR results. The combined methods between persistent scatterer InSAR and GIS allow an integration of information from various sources and hence improve the efficiency for interpreting the data. A total of 15, 18 and 27 images of ERS-1/2 images acquired from August 1992-December 1996, April 1992-April 1997 and August 1992-July 2002 for Canberra, Sydney and Newcastle respectively are chosen to be investigated with persistent scatterer InSAR. Together with the above images, ten ERS-1/2 images from June 1992-December 1996 and nine ENVISAT images from December 2003-June 2006 acquired over Perth (Australia) and Northern China respectively are also chosen for similar investigation. The results show that the deformation rate from the cities with groundwater over-extracted, are significantly larger than the cities without groundwater over-extracted. The results have demonstrated the effect of groundwater extraction to urban subsidence. [C9951]

"Mapping subsurface geology in Arid Africa using L-band SAR"

Using L-band SAR data from JERS-1 and ALOS, we produce regional mosaics of Sahara in order to map subsurface geology. A first mosaic of eastern Sahara using more than 1600 JERS-1 scenes allowed the discovery of unknown paleo-rivers, faults, and impact craters. On-going work concerns a new L-band high-quality mosaic of the entire Sahara, based on ALOS/PALSAR data. [C9952]

"LIDAR detection of plankton in the ocean"

For a variety of oceanographic applications, airborne LIDAR is very attractive, because of its ability to cover large areas in a short amount of time and at low cost compared with traditional research vessel surveys. One application we have investigated is the detection of plankton in the ocean. We have found that zooplankton layers can be detected, structure within those layers can be tracked, and relative estimates of abundance can be made. This paper describes the NOAA LIDAR and some of the results related to detection of zooplankton in the upper ocean. [C9953]

"Wavelet polarimetric SAR signature analysis of sea oil spills and look-alike features"

Marine dark features in SAR imagery related to oil spills, biogenic look-alikes and low wind areas are analyzed by means of the wavelet polarimetric signature (WASP) tool. The WASP encapsulates in a graph the dependency of the wavelet variance on dyadic scale and polarization state. Experiments on SIR-C/X-SAR C-band data showed the effectiveness of this analysis in characterizing textural features of the areas of study. [C9954]

"CALIPSO-AERONET Combined Application for Weather and Climate Research"

In this paper, a new method is proposed, which combine CALIPSO lidar data with AERONET data to acquire the unstable aerosol information in Taiwan. First, introduce a CALIPSO retrieval arithmetic to obtain the aerosol optical depth, and then compare the differences between CALIPSO and AERONET. By combining these two techniques we could not only have the precise site data from AERONET, but also own the change information of aerosol in southeast China from CALIPSO. Different from AERONET, we can also display the spatial properties of aerosol from CALIPSO lidar backscatter data, such as, the strength of aerosol in each layer and their change with time in the aerosphere. [C9955]

"What optech's bathymetric LiDAR sees underwater"

This article presents early results of the FUDOTERAM project using bathymetric LiDAR data acquired with the SHOALS-3000, the latest bathymetric LiDAR system from Optech. The survey area is in the coastal zone along the northern shore of Chaleurs Bay, in the western Gulf of St. Lawrence, Canada. The project aimed to apply the SHOALS- 3000 to geological mapping, sedimentary process monitoring and marine habitat mapping. This paper focuses on the sedimentological part of the study and presents the early raw data obtained to produce a bottom type classification based on some simple parameters, roughness, slope angle and direction. Two methods are evaluated for analysis of the SHOALS-3000 waveforms, the Moment Method and the Gaussian Mixture Model, and the latter is used as an approach to model the bottom type signal. [C9956]

"Study on inversion models for the severity of winter wheat stripe rust using hyperspectral remote sensing"

For Large-scale farming of agricultural crops, it is needed to detect diseases of crops in early time. After that, measurements can be taken to prevent and cure the diseases. Hyperspectral remote sensing data, of which spectrum resolution is less than 10 nm, include a mass of diagnosing spectrum information, which can be used to non-destructively detect disease stresses in green vegetation. In 2002-2003 and 2004-2005, a series of field experiments were conducted to collect the canopy spectral reflectance of winter wheat in the selected field. Canopy reflectance spectra were acquired by ASD FieldSpec Pro TM spectrometer in different severity regions of diseased winter wheat interval 7~10 days, meantime, in the same regions, the disease index (DI) were gained by the field survey. The results showed that while DI increased, the spectral reflectance of the canopy gradually increased in the red valley region. The DI was highly correlative with the hyperspectral variables such as R672, vegetation indices $(R553-R672)/(R553+R672)$, $(R808-R672)/(R808+R672)$, $(R808-R976)/(R808+R976)$, slope of red edge $(D\lambda_{red})$, sum of 1st derivative value within red edge (SDr), the vegetation indices SDr/SDg , SDr/SDb , $(SDr-SDg)/(SDr+SDg)$, $(SDr-SDb)/(SDr+SDb)$. Here, R denotes reflectance. Number in subscript is wavelength (nm). SDb and SDg denote sum of 1st derivative value within blue edge and green edge respectively. The coefficient between vegetation index SDr/SDg and DI is the largest. Linear and non-linear regression methods were used to build the inversion models. Using 2002-2003 data to test all above models, the models consisted of the variable of SDr/SDg has the highest predicable precision. Therefore, the model is the best one for inversion about severity of winter wheat yellow rust by hyperspectra. The conclusion has important-mean to guide people to cure the disease of crops and increase yields of crops and ensure security of food supplies. [C9957]

"Cantarell natural seep modelling using SAR derived ocean surface wind and meteo-oceanographic buoy data."

The Cantarell Seep is the most significant natural seep discovered in the Southern Gulf of Mexico. The trajectory of the oil seep, driven by sea surface winds and ocean currents, can sometimes impinge on the environmentally sensitive Mexican coast. For this reason it is necessary for the implementation of slick impact models to determine and track oil slick behaviour on sea surface as an aid to contingency planning. The focus of this study was to improve the confidence of the Cantarell natural seep impact model by utilizing SAR derived ocean surface wind field data and in situ meteo-oceanographic buoy data. The advantage of the SAR wind is that the data provides high resolution, wide-area coverage, up to 500 km by 500 km in the case of RADARSAT-1. The accuracies are +/- 2 m/s for wind speed and +/- 25deg for wind direction. The buoy is stationary and only provides wind data for that location but the instruments are more sensitive and provide higher accuracies than the SAR. The buoy information is recorded in one-minute intervals, transmitted to shore by microwave communication and the accuracies are +/- 0.7 m/s for wind speed and +/- 3deg for wind direction. Our approach was to combine the two data sources to provide better coverage and accuracy for oil slick modeling. [C9958]

"Statistical classification methodology of SHOALS 3000 backscatter to mapping coastal benthic

habitats"

The scanning hydrographic operational airborne LiDAR survey (SHOALS) consists of a bathymetric LiDAR system which provides high precision measurements of water depth. Even though the acquisition is focused on depth accuracy, the return signal, i.e. waveform, contains other relevant information because of integration signatures from the water surface, the water column and the sea-bed. This paper highlights the benthic characterization in extracting statistical parameters derived from the bottom backscatter. In applying multivariate analysis (K-means), it is significantly proven that signals derived from habitat, described as statistically homogeneous throughout ground-truth analysis, are (1) similar within an intra-habitat view, while they are (2) different between themselves. [C9959]

"Morphological segmentation of Lidar Digital Elevation Models to extract stream channels in forested terrain"

Our paper proposes an approach for the extraction of stream channels from Airborne Laser Swath Mapping (ALSM) data. Recent advances in technology have led to high-resolution topographic data acquisition by means of airborne lidar (i.e. ALSM), which can yield Digital Elevation Model (DEM) datasets with horizontal resolutions of 1 m and vertical rms errors in the range of 10-15 cm. The extraction of a stream network from a DEM plays a fundamental role in modeling spatially distributed hydrological processes and flow routing. We apply morphological filtering to an ALSM DEM to detect and characterize stream channels in forested terrain. Since the size and shape of morphological Structuring Elements (SEs) is known to strongly affect filtered results, we test for accuracy by developing a set of error measures over simulated terrain. We subsequently apply the filter to actual ALSM data. For linking disconnected stream segments, a measure of pixel connectedness known as the Connectivity Number is used. The method presented is shown to enable systematic characterization and comparisons of streams, even in heavily forested terrain. [C9960]

"A study on optical and SAR data fusion for extracting flooded area"

This article proposes a method of fusing the optical data before the flood and SAR (synthetic aperture radar) data during the flood. The main goal of this study is to evaluate the capability of data fusion to combine the information from Landsat ETM image with Radarsat SAR image for water body and flooded area extraction. The Landsat ETM data will basically provide the information of landform and background information which includes the normal water extent. The Radarsat SAR data however was taken during flood will provide information mainly on water body extent and flooded area. In the result image, flooded area was significantly enhanced. We can distinguish the flooded area and normal water area easily. [C9961]

"Object-based classification of multi-sensor optical imagery to generate terrain surface roughness information for input to wind risk simulation"

Geoscience Australia is conducting a series of national risk assessments for a range of natural hazards such as severe winds. The impact of severe wind varies considerably between equivalent structures located at different sites due to local roughness of the upwind terrain, shielding provided by upwind structures and topographic factors. Terrain surface roughness information is a critical spatial input to generate wind multipliers. It is generally the first spatial field to be evaluated, as it is utilised in both the generation of the terrain and topographic wind multiplier. Landsat imagery was employed to generate a terrain surface roughness product for six major metropolitan areas across Australia. It was necessary to investigate the applicability of multi-sensor approaches to generate a regional/national terrain surface roughness map based on the Australian/New Zealand wind loading standard (AS/NZS 1170.2). This paper discusses the methodology that developed a procedure to derive terrain surface roughness from various multi-source satellite images. MODIS, Landsat, and IKONOS imagery were acquired (from 12 September-26 November 2002) covering a significant portion of the New South Wales, Australia. An object-based image segmentation and classification technique was tested for seven bands of MODIS, six bands of Landsat Thematic Mapper, and four bands of IKONOS. Eleven terrain categories were identified using this technique which achieved classification accuracies of 79% and 93% over metropolitan (Sydney) and rural/urban areas respectively. It was revealed that the object-based image classification enhances the quality of the terrain product compared to traditional spectral- based maximum likelihood classification methods. To further improve the derivation of terrain roughness classification results, an integrated textural-spectral analysis merged Synthetic Aperture Radar and optical datasets provided in a study by [1]. A comparison with results derived from textual-spectral classification showed considerable improvement over the results from earlier classification techniques. [C9962]

"An algorithm to improve the NEXRAD rain rate estimates"

A Doppler WSR-88D radar (NEXRAD) is currently operating in Cayey (East of PR, at 886 m). Reflectivity and

rain rate (Z-R) relationships were developed using a dense network of rain gauges to validate radar estimates. These equations intent to correct the radar estimates for seasonal effects. Equations were derived for wet and dry seasons over Puerto Rico. To minimize the errors due to beam block and clutter, equations were derived with 20 rain gauges located 15 km or less from the radar location. [C9963]

"Reflectivity retrieval in a networked radar environment: Demonstration from the CASA IP1 radar network"

A network-based reflectivity retrieval technique has been developed within the Center for Collaborative Adaptive Sensing of the Atmosphere (CASA). The concept of a networked- radar system is simultaneous observations of the same precipitation event by multiple radars operating at the attenuating frequency such as X-band and scanning in a low elevation plane. This paper presents the preliminary demonstration of the network-based retrieval using data from the first Integration Project (IP1) radar network in Oklahoma. Electromagnetic waves backscattered from a common volume in a networked radar system are attenuated differently along the different paths. The CASA networked-retrieval method is based on a set of governing integral equations describing the backscatter and propagation of common volume with constraints of total path attenuation. The method has been implemented in a multiprocessor environment, which operate simultaneously and collaboratively to meet the real time requirement of CASA. The performance of the implemented retrieval algorithm such as computation requirement will be presented. Comparison of the CASA networked retrieval is made against the conventional attenuation correction based on the principle of coupling the specific attenuation, differential propagation phase and reflectivity. The preliminary results show good agreement with conventional differential phase base attenuation correction. [C9964]

"Piece-wise variance method for signal-to-noise ratio estimation in elastic/Raman lidar signals"

A straightforward signal-to-noise ratio (SNR) estimator for elastic/Raman lidar channels and related noise-induced errorbars is presented. The estimator is based on piece-wise estimation of the mean signal power and noise variance component under analog detection. The piece-wise estimator results are compared with those obtained from a previously published SNR parametric estimator under high and low SNR scenarios. [C9965]

"Design methodology of a ceilometer lidar prototype"

This article presents step-by-step applied methodology to design a 905-nm 5-kHz rep. rate diode-laser biaxial lidar ceilometer prototype beginning from the definition of initial specs, and related trade-offs to the first measurement tests. It is shown how key variables such as the received and background power, the range-dependent signal-to-noise ratio (SNR), the integration time, and the overlap factor have been simulated and analysed by means of parameter tuning inside acceptable state-of-the-art goal intervals. Main emission and reception subsystems as well as some auxiliary mechanical subsystems (adjustment parts and protection/subjection) are discussed. Finally, preliminary test measurements on topographic targets and storm clouds carried out with the ceilometer prototype are presented. Future improvements and trade-offs are also discussed. [C9966]

"Lidar application in selection and design of power line route"

Light detection and ranging is a relatively new technology, developed to complement traditional remote sensing technology. Digital aerial image provides reflectance information for land cover while LIDAR data provide more accurate geometrical information. There is much potential for fusing these two sources to achieve increased accuracy and utility for feature detection and classification. In order to assist Guangxi Electric Power Design Institute to improve their efficiency in power transmission line selection and design, field survey work, and reduce the cost, we have recently carried out the first power line project by using LIDAR and high resolution digital camera in China. The use of coloring LIDAR points by RGB of digital images makes it possible for obtaining high quality of in-room surveying, feature detection and classification. In addition, high quality and high resolution of DEM, DSM, DOM and visualization provides our customer not only with better selection and design of power line route, and reduced survey work, but also significant savings by 10 percent reduction of power line construction. [C9967]

"Comparison of measured scattering coefficient of dry soil at X-band with the scattering coefficient estimated using the dielectric constant"

The soil is one of the natural earth material which is produced by withering of rocks. The soil is mix of sand, silt and clay with air pores. The compactness of soil depends upon the percentage of these constituents and the pore size. The dry soil has its dielectric constant which is independent of frequency and so the scattering

coefficient also will be independent of frequency for pure dry sand. But in nature it is not so, it always has some percentage of moisture in it. The moisture will be due to presence of water which will be a combination of bound water and free water. More the percentage of moisture more is the presence of free water. But for dry soil there is no water and for natural dry soil the free water is very small and mostly it is bound water. The scattering coefficient will be different although soil is close to dry and also will vary with frequency due to presence of small quantity of free water present. The scattering coefficient has been measured for HH, VV, HV, VH polarizations. Separately using the values of the soil constituents the dielectric constant is estimated for pure dry sand. Using this dielectric constant the scattering coefficient is estimated for different polarization. For estimation of scattering coefficient the small perturbation model is used which is applicable for slightly rough surface. The measured values of scattering coefficient is compared with estimated values of scattering and the error analysis is done. [C9968]

"A new high-altitude airborne millimeter-wave radar for atmospheric research"

A high-altitude airborne millimeter-wave radar for atmospheric research is being developed by the National Center for Atmospheric Research. The radar will be mounted on the High-Performance Instrumented Airborne Platform for Environmental Research (HIAPER). We present simulations of the minimum detectable signal, the reflectivity accuracy, the polarimetric purity, and the expected accuracy of cloud liquid water retrievals to describe the expected performance of the radar. We also describe the phased approach to implementing the system which starts with a W-band Doppler radar, and through phases, adds pulse compression, polarimetric capability, and a second wavelength (Ka-band) radar. [C9969]

"A time domain clutter filter for staggered PRT and dual- PRF measurements"

In this paper, a method for clutter filtering and the estimation of spectral moments from non-uniformly sampled Doppler weather radar signals is presented. The method uses a parametric model for the received signal. The spectral moments of both clutter and precipitation echoes are estimated using the maximum likelihood estimator. Unlike the current frequency domain techniques where non-uniformly sampled signals are zero-padded to be uniform sequences, the likelihood function used in this algorithm can be constructed directly from the non-uniformly sampled data. Therefore an accurate estimation of spectral moments even in case of clutter-to-signal ratio as high as 60 dB can be obtained. The proposed method is illustrated on simulated radar signal time series and measurements collected using the staggered pulse repetition time (PRT) and dual pulse repetition frequency (PRF) transmission schemes from the CSU- CHILL and collaborative adaptive sensing of atmosphere (CASA) IP1 radars. [C9970]

"Dual-polarization spectral decompositions: Application to radar parameter estimation and quality control"

Spectral decompositions of dual polarization observation allows for extending of analysis of polarimetric radar data to the new dimension, namely Doppler frequency domain. In this paper it is shown how this new paradigm can be used for improving quality of radar data. On an example of the CSU- CHILL observations it is demonstrated that this analysis can be used to design a spectral filter that allows for both ground clutter mitigation and radar sensitivity improvement. [C9971]

"Application of single drop scattering algorithms to rain related retrieval"

Since many years radars are known as valuable tools to retrieve rain. Applying well established relations for different types of radar allows accessing many rain parameters. For calculating the scattering function, the flattening of rain drops constitutes a non-negligible error source. In this contribution, different algorithms are applied to calculate the scattering function or the cross section of rain drops. Their results are compared to each other. A point matching algorithm serves as reference. To this reference, results from a Mie scattering algorithm, and-for backscatter-the Rayleigh approximation and an algorithm correcting the backscatter cross section according to the Rayleigh approximation for drop flattening are compared. The findings from this inter-comparison are presented for transmitting frequencies of 10 GHz, 24 GHz and 94 GHz. [C9972]

"Wave measurements under the typhoon by 9.25MHz ocean radar"

National Institute of Information and Communications Technology (NICT) is developing 9.25 MHz ocean radar for measuring the sea surface currents and ocean waves on the offshore. This study clarifies the validity and accuracy of observing ocean waves, when the typhoon passed through the observation area, with 9.25 MHz ocean radar. In addition, we compare inversion algorithms for 9.25 MHz ocean radar wave measurements. This study compares the performance of two inversion techniques due to Kojima and Hashimoto, and Howell and Walsh. [C9973]

"Adaptive bayesian algorithm for vegetated field parameters extraction by using multi-frequency and multi-polarimetric SAR images"

This paper proposes an alternative inversion algorithm for extracting soil and vegetation parameters from multi-frequency, multi-polarimetric SAR data. The alternative approaches aim at identifying a useful modelization of the soil and vegetation response to radar signal and then indicate a possible solution to the extraction of soil moisture and vegetation water content. The core of the algorithm is based on the determination of probability density functions (pdfs) through a Bayesian methodology and has been initially developed for bare soils and tested on numerous data sets. The purpose is to apply this inversion algorithm to fields that have different levels of vegetation cover and considering different theoretical and empirical approaches. In fact, as already stated, a single approach, theoretical or empirical model, cannot be often applied on a wide number of cases. This paper addresses a possible solution based on two alternative different modelizations. [C9974]

"Mapping and monitoring land cover in Corumbiara area, Brazilian Amazonia, using JERS-1 SAR multitemporal data"

This paper discusses the use of a JERS-1 synthetic aperture radar (SAR) time-series for mapping and monitoring land cover in a test site in the region of Corumbiara, Rondonia State, western Brazilian Amazonia. In order to support JERS-1 data analysis, land cover maps were obtained by digital classification of Landsat TM images acquired from 1993 to 1997 period, following a procedure based on image segmentation, unsupervised classification, and post-classification image edition. The comparison of these products with JERS-1 images shows that clean deforested areas are well identified presenting a low backscattering response as expected. However areas that have been cleared and even burned but with remaining forest material left on the ground present high backscattering response opposed to expected. Considering these observations and user interpretation expertise, JERS-1 SAR images can be used to map and monitor land cover changes in Amazonia. [C9975]

"Land cover analysis at a regional scale exploiting low and medium resolution ENVISAT ASAR Data: Application to Poyang Lake Area (Jianxi Province, P.R. China)"

Located in Jiangxi Province, Poyang Lake is the largest freshwater lake in China and constitutes a major hydrological subsystem of the middle Yangtze river (Changjiang) basin in central China. An impressive amount of low to medium resolution ENVISAT data covering the Poyang Lake's 2004 and 2005 hydrologic years were acquired and analysed within the framework of the flood DRAGON project. Land cover mapping was realized synergistically using: 1) a land cover map derived from a colour composition containing seasonal ENVISAT ASAR Global Monitoring Mode image sums, and; 2) a land cover map derived from a colour composition containing filtered, seasonal ENVISAT ASAR wide swath mode image sums. Confronted and validated with the hydrodynamic characterization derived from Landsat reference data, these preliminary classifications lead to a land cover map with 13 classes covering 20,000 km² (170 km from north to south and 120 km from East to West) and was realized at a 1/200 000 scale, but can be used from 1/150 000 to 1/500 000. The results highlight the great potential of ASAR medium and low resolution products for wide-area mapping. Worldwide, large archives of such data already exist which should enable access to the prerequisite amount of data required for such large-scale, land cover characterization. [C9976]

"A novel method for estimating offshore wind fields using synthetic aperture radar and meteorological model data"

Synthetic aperture radar (SAR) provides a promising method for offshore wind field estimation, particularly in the context of important for offshore wind farm development. This paper introduces an iterative maximum a posteriori probability (MAP) method for combining meteorological model output with synthetic aperture radar for offshore wind field estimation. The MAP approach is demonstrated for 40 ENVISAT ASAR scenes collected for 2004-2006 over the UK Irish Sea. Both the CMOD4 and CMOD5 geophysical model functions are implemented and retrievals using MAP and a simpler direction based windspeed algorithm are validated against insitu mast observations. The CMOD5 MAP algorithm in particular shows promising results with an estimates on average within 2 observations. [C9977]

"Computation of wind direction from SAR images without external a priori information"

We present here the follow-up of a previously published work [1], where we described a wavelet based method to characterize the sea surface backscatter structures present in the SAR images. The method relies on the ability of the two-dimensional continuous wavelet technique to detect the spatial structure of the marine

atmospheric boundary layer and to isolate wind-related cells and features. The analysis of the cells' geometry, moulded by the radiometric characteristics of the sea surface, permits the identification of the wind direction inside the cells and thus the computation of the wind speed through standard algorithms. About twenty SAR images (ERS-2 and ASAR Wide Swath) over the Mediterranean Sea have been analyzed, and the results compared with NSCAT and QuikSCAT satellites wind fields. These images cover a wide range of meteorological conditions, from low (2 m/s) to moderate winds (12 m/s), presenting many kinds of signature, i.e. wind cells, atmospheric gravity waves, convective structures and radiometric flatness. The main difference of this method, with respect to the majority of those already proposed, is that it does not require a-priori information about the wind direction as well as any periodicity of the backscatter structures. The aliased wind directions are estimated from the texture of the SAR reconstructed map, while the dealiasing is possible due to the asymmetries present in the detected backscatter structures. The resulting SAR derived wind fields have been compared with those provided by satellite scatterometers. Results indicate a good score in detecting the wind direction (ap 70%). The developed methodology, once tested over an adequate quantity of images to derive statistically reliable results, could be routinely used to enrich SAR images with the wind field, as well as to characterize other backscatter structures displayed by SAR not depending directly on the wind. [C9978]

"Use of tandem pairs of ERS-2 and ENVISAT SAR data for the analysis of oceanographic and atmospheric processes"

Currently the European satellites ERS-2 and ENVISAT are flying on the same orbit with a time separation of 30 minutes. In this presentation pairs of the respective synthetic aperture radar data are analyzed with respect to different atmospheric and oceanic processes. The presented results were obtained in the framework of the ESA AO project COTAR. The tandem configuration exists since the launch of ENVISAT in 2002. In the presentation an overview will be given of the available image pairs acquired over the ocean on a global scale. Combinations of ERS-2 SAR data with both image mode and wide swath mode scenes provided by the ENVISAT ASAR are considered. The two SAR images enable the analysis of the change of radar cross section within half an hour. This temporal separation is very interesting for oceanographic applications because there are many processes like atmospheric fronts, convective cells, ocean tides, etc., which are detectable on this time scale. In the presentation tandem pairs acquired over the research platform FINO west of the island Borkum in the North Sea will be presented. The area is of high practical interest because of the planned Offshore Windpark Borkum West. The platform provides wind measurements at different heights and additional oceanic information to support the planning activities for this windpark. The dynamics of atmospheric structures is analysed. It is well known that the near surface wind field is a dominating factor for the normalized radar cross section of the sea surface. For this reason SAR scenes are well suited to study atmospheric effects with high spatial resolution. It is shown that the use of tandem pairs enables the study of processes like the propagation of an atmospheric fronts or the evolution of convective cells. Both effects are illustrated with different examples using additional information from in situ measurements. Furthermore existing techniques for the estimation of the wind field in 10 m height from SAR data are applied to both images. The evolution of the spatial structure of both wind speed and wind direction is analysed. The observations are related to some theoretical issues like, e.g., the Taylor hypothesis. Particular emphasize is put on the connection between the spatial and the temporal structure of the wind field. This topic is of high practical relevance, e.g., in the context of offshore windenergy exploitation. Additional applications like ship tracking, oil spill detection and the study of ocean wave field dynamics are briefly discussed as well. [C9979]

"Measurements of eddies in the ocean surface wind field by a mix of single and multiple-frequency HF radars on monterey bay california"

To properly assess the impact of global climate change and plan for remediation, accurate regional climate models are necessary, functioning on 10 km size scales rather than the typical 100 km scales. Examples of 10 km size scale phenomena are coastal wind eddies at 10-40 km scales, studied over Monterey Bay, California by Archer, Ludwig et al. using shore and buoy anemometers and satellite images. Most frequent in the evening and early morning hours, these, typically cyclonic, eddies are often responsible for fog in the Santa Cruz California area. We have previously demonstrated the ability of multifrequency HF radar (4.8 to 21.8 MHz) to map the ocean wind field. Observations over a year time span indicate standard errors of prediction of 1.7 m/s for wind speed and 25deg for direction with biases of 0.1 m/s and 0.3deg respectively. Combining HF radar wind vector estimates with shore based anemometer data in the WOCSS surface wind field model allows formation of detailed (3 to 5 km resolution) images of wind eddies over Monterey Bay and observation of their creation and decay. We discuss requirements for wind field observations with HF radars and demonstrate how multiple radar sites can be used to produce HF radar wind field maps. We report observations of 10-20 km cyclonic eddies in the northern and eastern parts of Monterey Bay. [C9980]

"Validation of a new empirical SAR algorithm"

A new empirical algorithm-CWAVE [1] was developed at the German aerospace center (DLR). A global dataset of two years (September 1998 to December 2000) of ERS SAR data was reprocessed to more than one million SAR imageries. Met ocean parameters like significant ocean wave height (H_s), wind speed (U_{10}) and mean wave period (T_m-10) are derived from the SAR images using the CWAVE algorithm [1]. The results are compared to collocated ERS altimeter data and in situ measurements from NOAA buoys and observations taken onboard the vessel Polarstern. It is shown that the SAR derived H_s is comparable in quality to altimeter measurements and can thus be used for real time assimilation. [C9981]

"IDRA: A new instrument for drizzle monitoring"

IRCTR is currently developing a high resolution radar aimed at the observation of rainfall and drizzle parameters for use in hydrological studies and in studies of the effect of the increase in anthropogenic aerosols in the radiation budget. Much effort has been done at obtaining a high sensitivity to be able to detect low reflectivity phenomena like drizzle. The radar is placed in the Cabauw meteorological super-site, allowing synergy with other instruments to further improve its capabilities. [C9982]

"Global analysis of a 2 Year ERS-2 wavemode dataset over the oceans"

Starting in 1991, the ERS-1 and (later) ERS-2 satellites have collected wavemode data over the global oceans whenever no image mode data acquisition was requested. Wave- mode data are full resolution SAR data covering small areas of size 5 km times 10 km every 200 km along the orbits thus forming a dataset giving information from all global oceans daily. In the scope of the WAVEATLAS ESA AO Project, ESA provided two years (Sep. 1998-Nov. 2000) of raw ERS-2 wave mode data to DLR which were processed into more than one million single look complex images, so-called imageries, using DLR's BSAR processor. The algorithms CWAVE and LISE were applied to estimate wind and wave parameters such as significant wave height, wind speed and sea surface elevation fields together with several single wave parameters. The paper presents global statistics with emphasis on wave parameters, namely significant wave height, single wave crest height, and wave height. Areal and seasonal distribution of high sea states is discussed and the relevance of the analysis for extreme sea state mapping is pointed out. As far as possible, the results are related to existing theoretical knowledge and compared to observational data (Hogben atlas) as well as model results. The outcome of this processing will be compiled into a new unique atlas on global waves and extreme events. It is planned to extend the atlas back to 1991 when ERS-1 was launched and forward to present times thus covering a more than 15 years period.

[C9983]

"Validation of an X-Band SAR Wind Algorithm by SIR-C/X SAR Data"

Space borne radar systems are capable of providing wind field information over the ocean. Radar instruments are of high value for operational applications because of their all weather and daylight capabilities. Synthetic aperture radar (SAR) instruments as flown on the European satellites ERS-2, ENVISAT or the Canadian platform RADARSAT are of particular interest for applications where high resolution two- dimensional information on the near surface wind field is needed. All these operate in C-band. The respective wind field algorithm CMOD was tuned to this wavelength. New research focussed on high speed cases to be able to measure wind speeds above 20 m/sec and on the W to HH polarisation ratio. For future missions like TerraSAR-X, to be launched in May 2007 new wind field algorithms tuned to X-band are needed. The TerraSAR-X instrument has a spatial resolution of up to 1 m and additional features like multi polarisation which make it a very interesting tool for oceanographic applications. In this paper a new X band wind field algorithm, XMOD1.0 is introduced. The algorithm is based on the detection of wind streaks in the SAR images and scatterometer measurements of [1]. Data from the SRTM mission flown on the shuttle in February 2000 and SIR C/X SAR in 1994 are used to test the algorithm. Results are validated against in situ data and model data from ECMWF. The potential of SAR measurements to support the optimal siting, the design, as well as the operation of offshore wind parks is shown. Applications for offshore wind farming of the TerraSAR-X mission will be discussed. The platform FINO 1 was chosen as a primary test site to calibrate and validate wind fields for X band satellite images. For the development, optimisation and validation of the retrieval algorithms comparisons with in situ data, e.g., acquired at the FINO platform will be carried out. The respective calibration and validations strategies will be summarized.

[C9984]

"A grid based weather radar data retrieval and processing framework."

In this paper, we describe the implementation of a distributed data retrieval and processing strategy enabled by using grid computing technologies and applied to distributed collaborative adaptive sensing environments. Underlying the grid computing and storage infrastructure there is a data dispersion algorithm to guarantee

pervasive data management. Experimental results show that the proposed framework integrates successfully radar networks to grid infrastructures, while providing higher resources utilization than typical storage strategies. [C9985]

"Intercomparison of spanish advanced lidars in the framework of EARLINET"

To extend and reinforce the action of the EARLINET- ASOS project, a nucleus of Spanish advanced lidars was created. Four systems were intercompared satisfactorily in terms of backscatter coefficients at two elastic wavelengths. [C9986]

"Phase shifter system using vector modulation for xband phased array radar applications"

This paper presents the design and implementation of a complete phase shifter system using vector (polar) modulation, suitable for solid-state phased array radar applications, providing a cost effective solution which overcomes the main constraints involved with traditional systems. The performance characteristics for three intermediate frequencies were measured. In addition, measurements at X- band were performed using frequency up-converters. Finally a four channel prototype was built to evaluate the network connectivity of the phase shifter. [C9987]

"Real-time three-dimensional radar mosaic in CASA IP1 testbed"

This paper reports on a real-time three-dimensional radar mosaic technique for Collaborative and Adaptive Sensing of the Atmosphere (CASA) Integrated Project 1 (IP1) testbed. The technique exploits the dual-polarization capability of the IP1 radar network for the improvement of multi-radar composite fields. In particular, the copolar correlation and the attenuation derived from the differential propagation phase are injected to the interpolation process to derive a weighting scheme and a data quality index field for the composite fields. This technique is also served as a front-end that drives the composite reflectivity fields to the CSU DART now-casting algorithm. [C9988]

"Speed measurements with a continuous wave lidar prototype"

The UPC lidar group is developing a Doppler wind lidar based on the "edge-technique". Such systems use the slope of a high resolution optical filter as frequency discriminator. A laboratory prototype, able to measure the speed of solid targets emitting continuous wave radiation and using a Fabry-Perot interferometer as optical filter, has been built. A tuning control has been included to compensate drifts between the emitted frequency and the filter resonance frequencies in order to assure maximum sensitive measurements. The design of the system and different results concerning the performance of the tuning control system and speed measurements will be presented. [C9989]

"A wind speed and fluctuation simulator for characterizing the wind lidar correlation method"

Aerosol distribution in the atmosphere is used as a wind-tracer by lidars since it is drifted by the wind and respond to its changes. Two methods are used: the correlation and the Doppler method. This first one is easier and cheaper to implement than the latter. It makes it competitive for retrieving wind speed profiles or estimating wind turbulence. However, its accuracy decreases significantly as the distance from the optical radiation source increases, hence the need to characterize the method by means of wind field profile simulations and validate it by comparing the retrieval of real wind velocities with that of cooperative instruments such as radiosoundings. In this paper, the bases of a 2D lidar signal simulator are presented. The relationship between wind fields and the aerosol concentration dynamics, and the way they relate to lidar signal returns is explained. The first results of the application of the correlation method for the retrieval of wind velocities from real data at the UPC are presented and compared to radiosoundings measurements. [C9990]

"Lidar determination of the frequency of variations of the boundary-layer top"

The frequency of thermals up- and downdraft, during the day, and that of gravity waves, during night, are retrieved by applying a fast Fourier transform to the temporal evolution of the boundary-layer height as obtained by lidar measurements. The principal components of each obtained spectrum of frequency are related to the dominant processes occurring at the convective and nocturnal boundary-layer tops. The formation of lee-waves systems during special meteorological conditions determined the oscillation of the boundary-layer height. Fluctuations at the nocturnal boundary-layer height can occur even if the conditions through the layer depth are statically stable. These oscillations are principally due to wind shear and buoyancy (gravity) waves at the altitude of the nocturnal boundary-layer top. [C9991]

"Statistical considerations on the extinction error variance for the raman lidar inversion algorithm"

At the basis of the Raman lidar extinction inversion algorithm is the derivative of the logarithm of the ratio between the atmospheric nitrogen number density and the range-corrected Raman power return. While its computation is straightforward under ideal (noiseless) conditions, this is not the case under low signal-to-noise ratios, for which the observation noise may lead the logarithm to singular values. This work presents an analytical-statistical overview of the inversion problem and related error bars, tentative noise limiting criteria, and justifies the approximations at play to estimate the inversion error by means of error-propagation techniques for high signal- to-noise ratios. Simulation examples consider a 532/607-nm elastic-Raman system. [C9992]

"Rainfall estimation and rain gauge comparison for x-band polarimetric CASA radars"

The Center for Collaborative and Adaptive Sensing of the Atmosphere (CASA) developed and deployed four polarimetric and Doppler-capable distributed, collaborative and adaptive X-band radars in Oklahoma with the capability to detect and track tornadoes and storms in the lower troposphere with high spatial and temporal resolution. This paper presents an analysis of the performance of X-band rainfall estimation composite algorithms and the conventional reflectivity-rainfall relationship. The polarimetric estimators are developed by different combinations of radar products including horizontal equivalent reflectivity (Z_h), differential reflectivity (Z_{dr}) and specific differential phase (K_{dp}). The Micronet Little Washita rain gauge network is used for validating rainfall estimates of the KCYR CASA radar. In addition, NEXRAD WSR-88D KFDR radar data are analyzed and compared with the rain gauge network and the CASA radar estimates. Fourteen hours of data collected during August 2006 from three different storms are analyzed. Both convective and stratiform events are represented in the radar data analysis. An accuracy of point radar measurement is assessed for different rain intensities. Results demonstrate an improvement in hourly rainfall accumulation estimation for average rainfall intensities beyond 5 mm/hr with the use of polarimetric estimators. An increase in absolute difference standard error with distance by the use of absolute difference in radar and rain gauges estimates is also evaluated. [C9993]

"Radar network characterization"

The use of dense networks of small radars for weather sensing is being investigated by the Engineering Research Center for Collaborative Adaptive Sensing of the Atmosphere, with a first test-bed of this new paradigm well underway. The potential benefits of closely-deployed, overlapping, short-range weather radars are easy to see intuitively, and can be summarized as a greater ability to mitigate the effects of the Earth curvature and sense close the ground in all of the network domain, an increased spatial and temporal resolution, the capability of performing multiple-radar measurements, and the capability of adaptively tasking the individual radars according to the meteorological scene, while using less complex radar units. Virtually all of these potential benefits are governed by the trade-offs generated by the characteristics of the particular radar units employed and their spatial distribution, creating different data outcomes depending on the individual radar capabilities, the radar network layout, and the resulting number of radars with overlapping coverage. [C9994]

"Radar imaging of urban areas by means of very high resolution SAR and interferometric SAR"

In remote sensing applications the monitoring of urban areas by means of SAR sensors has been grown to a valuable and indispensable tool. Whereas SAR imaging with a spatial resolution down to one meter is widespread, a resolution down to 10 cm and below is offered only by a very few SAR sensors worldwide. In this contribution the potential of high resolution and very high resolution radar imaging of urban areas by means of SAR and interferometric imaging will be demonstrated and discussed. Limits of these techniques and open problems will be addressed as well. The corresponding data were acquired with PAMIR, the X-band SAR/GMTI demonstrator of FGAN-FHR. [C9995]

"Building characterisation in VHR SAR data acquired under controlled EMSL conditions"

The upcoming availability of new very high resolution SAR imagery from satellite sensors (e.g. Radarsat-2, TerraSAR-X, COSMOSkyMed) has renewed interest in extraction of scene parameters for the characterisation of urban areas. In order to properly face this problem, we have defined a structured and hierarchical research strategy that follows a systematic approach to 3-D building characterisation in VHR SAR data. This research strategy, starting from a theoretical analysis based on the literature, aims at a more depth understanding of the backscattering behaviour in VHR SAR urban images on the basis of empirical tests on different experimental setups. These setups include trials in the EMSL, with the outdoor Linear Synthetic Aperture radar (LISA) and a final validation and tuning of the results on VHR SAR from airborne and satellite platforms. This paper describes the proposed research framework in general, and presents the results obtained from the first set of EMSL experiments aimed at analysing the effect of the viewing and aspect angles, i.e. the orientation of the building

structure with respect to the SAR's azimuthal direction. [C9996]

"Evaluation of first generation CASA radar waveforms in the IP1 testbed"

The Center for Collaborative Adaptive Sensing of the Atmosphere (CASA), an engineering research center (ERC) established by the National Science Foundation (NSF) deployed its first generation network of four low-power, short-range, X-band, dual-polarized Doppler weather radars known as NE-TRAD. The short range CASA radars will have range overlay and velocity folding problems with conventional pulse-pair processing. The first testbed of X-band radar systems (developed within the ERC) in central Oklahoma called IP-1 (Integrated Project 1) have a low unambiguous velocity due to their short wavelength, and increasing the PRF will result in multiple trip overlays since storms can extend over a large distance. In addition the radar observations at short ranges are contaminated by ground clutter. This paper describes the waveforms for the individual radar nodes based on NETRAD operational requirements such as scan speeds, volume coverage pattern and system/hardware limitations to resolve range and velocity ambiguities. A dual PRF waveform has been suggested for operational use based on a simulation study. This paper presents an evaluation of the waveform from data collected by the first generation CASA radars. [C9997]

"Low cross-polarization antenna array for CASA's student test bed radar"

A series-fed aperture-coupled antenna array is designed using a substrate with a relative permittivity of 1.2 and a thickness of 1.75 mm for the patch antenna. A substrate with a relative permittivity of 6.15 and a thickness of 0.625 mm is used for the feed lines. The array was designed to achieve a sidelobe level lower than 20 dB and a cross-polarization lower than 30 dB. The array presented is a center-fed array composed of two sub-arrays of 6 elements. This configuration makes the array a 4-port array, having two ports for horizontal polarization (H and H₁₈₀), and two for the vertical polarization (V and V₁₈₀). The cross-polarization and sidelobe levels achieved are -39.11 dB, and 19.3 dB respectively. The half power beam width (HPBW) is around 9deg and the front-to-back ratio (FBR) is -15.84 dB. Isolations SHV and SHV₁₈₀ are -26.61 dB and -23.08 dB respectively. [C9998]

"Simulation of minimal infrastructure short-range radar networks"

Distributed networks of short-range radars offer the potential to observe winds and rainfall at high spatial resolution in volumes of the troposphere that are unobserved by today's long-range weather radars. One class of potential distributed radar network designs includes Off-the-Grid (OTG) weather radar networks. These are short-range radar nodes designed to be deployed as part of an ad-hoc network and to limit their reliance on existing infrastructure. Independence of the wired infrastructure (power or communications) would allow OTG networks to be deployed in specific regions where sensing needs are greatest, such as mountain valleys prone to flash-flooding, geographic regions where the infrastructure is susceptible to failure, and underdeveloped regions lacking urban infrastructure. This paper will present a system model and simulation framework for the design of OTG networks. The model estimates the energy requirements of the three major system functions, sensing, communicating and computing, as well as power generated from the solar panel. The simulation will be used to develop an energy cost function to be used in control decisions. [C9999]

"Implementation of a new refractivity estimation algorithm on a network of S-band radars"

The retrieval of the surface-layer moisture field can be obtained by estimating the refractive index of air, measured in parts per million and referred to as refractivity. A technique developed to estimate the refractivity using radar has been demonstrated with validated results from field experiments [1], [2]. This technique utilizes the measured change in phase from stationary ground targets, which will be primarily due to changes in refractivity at warmer temperatures given a stable radar frequency. While this technique has been successfully demonstrated on individual radars, there is no clearly defined method of combining multiple radar estimations beyond gridding and averaging. Recently, however, a new algorithm was proposed as an alternative approach, especially when dealing with multiple radars [3]. The new algorithm uses a minimum least squared error approach, with a smoothing constraint and a method to address phase wrapping. This paper will explore the implementation of this constrained least squares (CLS) approach with data collected during a refractivity field experiment during the summer of 2006 in Colorado. It will also explore the implications of running the CLS algorithm in real-time, and briefly discuss future directions. [C10000]

"Mapping subsidence in Tianjin area using ASAR images based on PS technique"

By identifying temporarily stable natural reflectors or persistent scatterers (PS), PSInSAR (Persistent Scatterers for SAR Interferometry) technique can analyze this subset of pixels in SAR images, even with long temporal and space baselines, to get high accuracy deformation measurements. We implement the PSInSAR process that is briefly summarized in this paper and apply this method in Tianjin area to detect the deformation phenomena

using ENVISAT ASAR images. Calibration of ASAR images helps us select more PSC and using calibrated backscattering coefficient threshold we can discard the pixels whose amplitude are relatively stable while whose backscattered signals are weak and incoherent. Results obtained by processing 14 images show the distribution and the relative deformation value of the displacement field. The estimated linear velocities of PS are not accurate enough because of the relatively small number of images. [C10001]

"Earthquake damage detection using remote sensing data"

In this study, we propose a new earthquake damage detection method based on a combination of the results estimated by using earthquake information (magnitude and location of source) and the change of the earth's surface observed by SAR. As a map produced by the detection method has less noise than a coherence ratio image, we found that the proposed method has better detection ability than that which only uses the change of coherence value. [C10002]

"ASAP, towards a PARIS instrument for space"

The technological aspects of the Altimetric and Scatterometric Applications of PARIS (ASAP) sensor are presented in this paper. This sensor is based on the PARIS concept, which makes use of GPS signals reflected on the ocean's surface in order to measure the surface's properties (altitude and roughness). The ASAP instrument is a hardware real-time PARIS receiver with the aim of being an intermediate step between the airborne GOLD-RTR receiver developed at our institute and a future spaceborne PARIS instrument. [C10003]

"Perspective of remote optical measurement techniques (ROMTs)"

This article presents an intercomparison between four different ROMTs: differential optical absorption spectroscopy (DOAS), differential absorption LIDAR (DIAL), Fourier transform infrared spectroscopy (FTIR), and tunable diode laser absorption spectroscopy (TDLAS). The main focus is on the TDLAS technique, where the main laser-diode typologies and modulation schemes, namely, wavelength modulation spectroscopy (WMS) and frequency modulation spectroscopy (FMS), are reviewed. At present, new promising modulation schemes with range resolution capability are being investigated. Among them, analog frequency modulation (FM) and digital pseudo-random schemes are discussed. [C10004]

"DInSAR monitoring of land subsidence in Orihuela City, Spain: Comparison with geotechnical data"

An advanced DInSAR technique called Coherent Pixels Technique (CPT) has been used to measure the subsidence existing in Orihuela city (Spain) during the period 1993-2001 due to ground water level fall. The estimated subsidence, with values lower than 7 cm, is highly influenced by soil geotechnical conditions like the deformable soil thickness. In addition, the wells location is an important subsidence factor because they are directly related to a decrease of the piezometric level. [C10005]

"Student developed meteorological radar network for the western part of Puerto Rico: First node"

This paper summarizes the work being done in developing a student designed radar network in western Puerto Rico. Modifications to a commercially available Raytheon MK2 marine radar are presented as well as the sensitivity expected. [C10006]

"Improvement and validation of MODIS performance in automated detection and extent estimate of wildfires"

Global MODIS Fire products (MOD14) are routinely generated by automated application of the Giglio algorithm (Giglio et al., 2003, Remote Sensing of Environment 87, 273-282) on daytime and night-time data collected up to four times a day. We present here the results and the validation of an Improved Giglio Algorithm for the Detection of Italian Fires (IGADIF). IGADIF presents substantial innovation in the computing of (two) physical parameter estimates at sub-pixel resolution: the top fractional temperature present in candidate Hot-Spot pixels, and the total area involved in the burnout. GIS validation of IGADIF and MOD-14 results are conducted considering two independent sets of ground truth data, the record of fire extinguishing operations carried out by the Italian National Firemen Corps (NFC), and the burn scars obtained from ASTER. [C10007]

"3-D tsunami coastal hazard mapping in Sri Lanka by very-high resolution, airborne and spaceborne remote-sensing"

Following an inter-Government agreement established between Italy and Sri Lanka in the aftermath of the great

2004 Indian Ocean tsunami, the operational project 'HyperDEM' was designed for mapping in 3-D the coastal areas of Sri Lanka, aimed to easing and speeding-up emergency mapping in tsunami- prone areas. The work, based on integration of airborne Lidar and spaceborne Radar campaigns, started in autumn 2005 and was accomplished in summer 2006 after acquisition of the outstanding data volume of ca. 2.7 TeraBytes. Some examples of results, and technical hints on methodological solutions adopted in solving operational problems are presented here. Upon completion of the work, the Government of Sri Lanka was provided with ca. 2'500 sq.km of Digital Elevation Models of the coastal areas, ca. 1'800 of which at the exceptional resolution of 1 metre and the elevation precision of 0.3 metres, and c.a. 700 at the resolution of 30 metres vs. an elevation precision of 2.6 metres. [C10008]

"Intercomparison of Calibration techniques for the 1064nm channel on a Nd:YAG elastic lidar"

The need for accurate calibration is apparent for accurate retrievals of backscatter at 1064 nm. Due to the low molecular scattering in comparison to the aerosol component, it is not possible to use a Rayleigh calibration procedure which is suitable for the 355 and 532 nm channels and an alternative approach is needed. In particular, a modified cirrus cloud calibration method is considered which uses the fact that the cirrus cloud scatter is spectrally independent together with an approach to properly estimate the backscatter at cloud base. We find that the calibration accuracy can be taken within 15% which is reasonable agreement with the uncertainty in the backscatter color ratio between 532 nm and 1064 nm. [C10009]

"Comparison of SRTM-NED data to LIDAR derived canopy metrics"

Forest canopy height derived from the SRTM-NED were compared to three LIDAR vegetation metrics for the Sierra Nevada forest. Generally the SRTM-NED was found to under estimate the vegetation canopy height. The SRTM SAR signal was found to penetrate, on average, into 44% of the canopies. The residual errors as a function of LVIS canopy height and cover were found to generally increase with height and cover. Likewise, the RMSE was found to initially increase with canopy height and cover but saturates at 50 m height and 60% cover. [C10010]

"Numerical simulation of a heterodyne Doppler LIDAR for wind measurement in a turbulent atmospheric boundary layer"

This study concerns the modeling and the design of a monostatic heterodyne pulsed LIDAR. The heart of the system is constituted of a 1.55 μm able to produce high pulse repetition frequency. The aim of this work is to assess its efficiency to perform accurate wind speed measurements in the low atmospheric boundary layer, from a 2-D scanning pattern, in the presence of refractive turbulence. A complete LIDAR numerical simulation technique has been developed. Its main originality is the integration of both optical and fluid dynamics numerical methods to take into account the signal coherence loss due to refractive turbulence and speckle effect as well as the fine structures of the wind field. The wind speed profiles along each line-of-sight are retrieved from the return signal using a low-order autoregressive model. An adequate averaging model is then used estimate horizontal components of the wind speed for altitudes up to 150 m. [C10011]

"Coherent lidar modulated with frequency stepped pulse trains for unambiguous high duty cycle range and velocity sensing in the atmosphere"

Range unambiguous high duty cycle coherent lidars can be constructed based on frequency stepped pulse train modulation, even continuously emitting systems could be envisioned. Such systems are suitable for velocity sensing of dispersed targets, like the atmosphere, at fast acquisition rates. The lightwave synthesized frequency sweeper is a suitable generator yielding fast pulse repetition rates and stable equidistant frequency steps. Theoretical range resolution profiles of modulated lidars are presented. [C10012]

"Semi-automatic true orthophoto production by using LIDAR data"

Light Detection and Ranging (LIDAR) has been used for years with a variety of applications, including the efficient creation of digital terrain models (DTMs) for large-scale, high- accuracy mapping. LIDAR technology offers fast, real-time collection of 3-D points so that allows the production of higher-accuracy orthophotos than traditional stereo-compilation methods. The technology is moving quickly toward offering more efficient collection techniques for applications such as city modelling and true orthophoto production. Traditional orthophoto production suffers from the fact that buildings (and any other objects above ground) are not correctly placed in the orthophoto. True orthophoto production overcomes these deficiencies by taking the digital surface model (DSM) into account. However, the resulting true orthophotos still suffer from occluded areas and unsharp edges of buildings and roads. The experimental investigations with different data sets show that it is essential to use

high quality DSMs to produce high quality true orthophotos. In this paper, aspects of the improvement of true orthophoto production will be discussed: (a) in the first approach which has been widely used in photogrammetry, the DSM is used for generating true orthophotos and (b) in comparison to the DSM based method, semi-automatically collected vector data of buildings are superimposed on DTM and are used as input data for generating true orthophotos in the second approach. The processes and problems of both true orthophoto production procedures will be investigated in detail and results include the comparison of true orthophoto productions based on DSM (from LIDAR data) and DTM plus vector data. For the experimental investigation, a LIDAR data set for downtown Stuttgart is used. [C10013]

"An airborne multi-angle power line inspection system"

This paper gives a brief description of an Airborne Multi-angle Power Line Inspection System (AMPLIS). AMPLIS is composed by 3 CCD cameras, a Position and Orientation System (POS), a stabilized platform, the data collection and control subsystem. It can be equipped on a helicopter and fly along the lines at a speed of about 100km/h at a relative height of 100 m over the power lines. AMPLIS is capable of detecting the distance between the power lines and the ground surface with an accuracy of less than 0.5 m. It can automatically find the dangerous objects beneath the lines which can greatly decrease the man power and cost in power line inspection. It has been successfully tested with good performance in Wuhan, China, 2005. [C10014]

"Extracting tree crown properties from ground-based scanning laser data"

The spatial organization of above-ground plant material plays an important role in controlling not only plant functional activities like photosynthesis and evapotranspiration, but also the photo-vegetation interactions. To improve our understanding of such interactions, the acquisition of highly detailed information about the 3D architecture of individual plants and communities of plants is required. Recently, Light detection and ranging (LiDAR) sensors, both at the ground and the airborne-level, have emerged as useful tools for mapping 3D plant structure. One such ground-based instrument is the Intelligent Laser Ranging and Imaging System (ILRIS 3D), which was developed at Optech Incorporated. This laser scanner, generates a 3D digital reconstruction of any scene, by actively emitting laser pulses and recording the time elapsed for the return of a pulse, thereby measuring the distance of any given object. It is the objective of this research to utilize the ILRIS 3D to measure structural, and biophysical information of individual trees for use as direct inputs into complex radiative transfer models. The key parameters under investigation are crown dimensions (i.e. shape, area, and volume), crown-level gap fraction (GF) and crown-level leaf area index (LAI). The ILRIS 3D was used to acquire 3D point clouds of an artificial 6' Ficus tree, in a controlled laboratory environment. Measured XYZ point cloud data was segmented to retrieve laser pulse return density profiles, which subsequently were used to estimate gap fraction and LAI. Gap fraction estimates were cross-validated with traditional methods of histogram thresholding of digital photographs ($r^2 = 0.96$). Crown LAI estimates were compared with the actual values ($r^2 = 0.95$, RMSE = 0.45). The next challenge was to implement the developed algorithms to real crowns, namely olive (*Olea europaea* L.) orchards in southern Spain. Individual tree-level ILRIS 3D data was collected from 24 structurally diverse crowns. Crown dimensional profiles were extracted for ILRIS data that was collected from a horizontal view (i.e ground-based) and a nadir view (i.e from platform 12 meters above ground). Preliminary retrievals from the olive orchards dataset is described here, while current ongoing field measurements are being conducted to validate the findings. Successful demonstration of extracting crown-level structural parameters like gap fraction and LAI from ground-based LiDAR will be important new information that can be used for detailed radiative transfer modeling in olive orchards and likely lead to more robust inversion algorithms. [C10015]

"Retrieving 3D canopy structure from synergistic analysis of multi-angle and lidar data"

Recent empirical studies have shown that multi-angle data can be useful for predicting canopy height, but the physical reason for this correlation was not understood. The research presented here puts forth a physical explanation for this phenomenon. We employ the use of Radiative Transfer, more specifically canopy spectral invariants, which can decouple spectral and structural parameters in a vegetation canopy. As a case study we compare canopy heights predicted from a multivariate analysis of 28 (7 cameras* 4 bands) and LVIS canopy heights and a multivariate analysis of 7 directional escape probabilities and LVIS canopy heights. We find that the 7 directional escape probabilities can provide approximately the same amount of information about canopy height as 28 spectral/angular reflectances from AirMISR. Finally we speculate that multi-angle data does not allow for extraction of canopy height but in fact requires synergy between Lidar sensors. [C10016]

"Modeling fractional shrub/tree cover and multi-temporal changes in mire ecosystems using high-resolution digital surface models and CIR aerial images"

The objective of this paper is to assess increase and decrease of forest area and estimate shrub encroachment

between 1997 and 2002 in open mire land using CIR aerial images, DSMs derived from it and LiDAR data. The present study was carried out in the framework of the Swiss Mire Protection Program, where changes of forested area are a key issue. The study area is located in the Pre-alpine zone of Central Switzerland. In a first step, high-quality DSMs were automatically generated from CIR aerial images of 1997 and 2002. This DSM generation is based on high accuracy, intelligent matching methods developed at ETHZ which are able to produce very dense and detailed DSMs that allow a good 3D modeling of both deciduous and coniferous trees and shrubs, and multi-temporal analysis of their growth pattern. In a second step, tree layers from both years were generated combining canopy height models derived from the DSMs and LiDAR DTM with a fuzzy classification of spectral information (NDVI) of CIR aerial images. In a third step, on the basis of these tree layers fractional tree/shrub covers were produced using explanatory variables derived from the DSMs in logistic regression models. Bias (due to different quality of input data) was estimated by analyzing the distribution of the fractional model differences. The corrected models reveal a general decrease of tree/shrub probability that indicates a decrease of forest and other wooded areas between 1997 and 2002. On the other side, the models also indicate real shrub encroachment and tree growth in open mire land. The study stresses the importance of high-resolution and high-quality DSMs and highlights the potential of fractional covers for ecological modeling.

[C10017]

"Integration of first and last return LiDAR with hyperspectral data to characterize forested environments."

The fusion of active LiDAR and passive optical hyperspectral data allows us to characterize the forest environments in ways that have not been possible previously with only one data source. This paper describes an airborne platform configured to collect data from multiple sensors simultaneously. Data from the platform have been applied to describe forest environments both in terms to species and structure. Integration of the data yields information and characterization of forest environments than has been possible in the past. [C10018]

"Bathymetric retrieval from manifold coordinate representations of hyperspectral imagery"

In this paper we examine the accuracy of manifold coordinate representations as a reduced representation of a hyperspectral look-up table for bathymetry retrieval. The approach is based on the extraction of a reduced dimensionality representation in manifold coordinates of a sufficiently large representative set of hyperspectral imagery [4]. The manifold coordinates are derived from a scalable version [4] of the isometric mapping (ISOMAP) algorithm [12] [11]. In the present work and in [5], these coordinates are used to establish an interpolating look-up table for bathymetric retrieval by associating the representative data with ground truth data, in this case from a LIDAR estimate in the representative area. The compression of look-up tables could also readily be applied to look-up tables generated by forward radiative transfer models [9]. In this paper, we analyze the approach using data acquired by the PHILLS [6] hyperspectral camera over the Indian River lagoon Florida in 2004. Within a few months of the PHILLS overflights, SHOALS LIDAR data was obtained for a portion of this lagoon, principally covering the beach zone and in some instances portions of contiguous river channels.

[C10019]

"The use of ASAR data for class cover identification from small swatches"

In this work we address the problem of land cover classification in advanced synthetic aperture radar (ASAR) images. The derivation and assessment of texture features for ASAR image segmentation is investigated using full multidimensional co-occurrence matrices as features. Expansion of local patches in terms of Walsh functions helps identify the optimal distance for the calculation of the co-occurrence matrices. The defined distance agrees with the one chosen by performing exhaustive tests where many distances were tried and the best was chosen from the training data. The well known chi-square test of statistical significance has been used for classification.

[C10020]

"Evaluation of ASAR and optical data synergy for high resolution land cover mapping in Portugal"

This paper aims at presenting the usefulness of combining satellite optical data from the visible and infrared wavelengths with longer wavelength radar data for land cover mapping in Portugal. This is a ground-breaking study in a geographical region that does not experience continuous intra-annual dreadful atmospheric contamination that commonly justifies radar usage. In this study we exploit the ability of ASAR images as an extra input feature for land cover classification together with the most used satellite optical data, i.e. Landsat. The goal of this paper is three-fold: 1) compare single date classification of ASAR data with Landsat data for land cover mapping; 2) evaluate the usefulness of multi-temporal ASAR measurements for land cover classification improvement; and 3) to compare a final map accuracy assessment with the classification scores attained with training and test sample sets. We conclude that ASAR imagery does not individually improve

overall classification accuracy, but their synergy with Landsat data or in a multi-temporal context show up specific advantages; statistically sound accuracy assessment of final map bends optimal classification accuracies attained with test sampling observations. [C10021]

"COSMO-SkyMed active calibrator: A sophisticated tool for SAR image calibration"

In the framework of the COSMO-SkyMed mission¹, Space Engineering has designed and manufactured four Active Calibrators (AC). An AC has a twofold function: 1) re-radiating the received radar signal with the required Radar Cross Section (RCS) and polarisation; 2) acquiring the received Synthetic Aperture Radar (SAR) pulses amplitude for successive elaboration. The AC will be used as a tool of the COSMO-SkyMed Calibration / Validation facility during the SAR commissioning phase to validate the on-board SAR and during the normal phase to maintain stable the image quality figures. The Active Calibrators will be operated together with a set of Passive Calibrators, characterised by a fixed RCS. The former ones have the great benefit of providing much higher RCS figures and recording capabilities than the latter ones. This paper describes the characteristics and performance of this Active Calibrator. [C10022]

"Overview of the active TerraSAR-X calibrators and first results"

This paper describes the development and system concept for an active and highly integrated, digitally controlled SAR system calibrator. For precise and high-quality SAR data, precise ground targets are necessary for external calibration of the SAR data. Compared to passive targets, active radar targets like transponders offer more features. The recording of the transmitted radar signals from the satellite becomes possible and allows additional data analysis and data correction. A total of 18 active transponder and receiver systems and 16 receiver only systems were fabricated for the TerraSAR-X calibration campaign in summer 2007 [1], [2], [3]. TerraSAR-X is the first German spaceborne X-band SAR satellite mission. [C10023]

"The role of performance modelling in active phased array SAR"

Phased array antennas play an important role in many radar applications and their use has increased during recent years in space-based remote sensing applications. Their success is mainly due to high agility in reconfiguring pattern, quick steering capability along both elevation and azimuth axis, easy packaging on spacecraft, low sensitivity to T/R module failures, high achievable directivities. In the frame of SAR systems implementation and calibration activities, a SAR simulator is required to support engineering activities devoted to scenario definition, performance assessment, estimation of error effects on signal Tx/Rx/Cal chain. Such a tool shall also implement an electromagnetic antenna model which is required to predict antenna performance, in terms of beam shape, directivity and sidelobe levels, with high accuracy and reliability, by keeping into account characterisation data provided at various levels (both pre-flight and in-flight), mutual coupling, VSWRs, insertion losses, amplitude and phase errors. This paper discusses preliminary results achieved by mean of a SAR simulator which implements a non-electromagnetic antenna model developed by Alcatel Alenia Space Italia for SAR instrument calibration and phased array antenna pattern prediction, which is based on array factor computation by mean of fast Fourier transform applied on the excitation matrix, where nominal excitation values are corrected on the base of near field pre-flight and in-flight measures. In particular, the predicted beam is achieved by matching together both information on antenna configuration (operative frequency, bandwidth, element spacing, number of T/R modules, TDLs, failures), data coming from near field measures (pre optimisation and post optimisation holograms) and in-flight telemetries. This paper presents the former results obtained by loading pre-flight measured data, and shows the high accuracy achieved in directivity computation, beam shape prediction and pointing angle-estimation, by comparing such results with those achieved by mean of an electromagnetic validated model. The tool, developed in Matlab, operates a correction of nominal antenna excitations by applying over them a pre-distortion array obtained by opportunely sampling the near field holograms acquired during pre-flight tests and correcting such information to compensate for probe to AUT distance. The effect of correction is evident both along azimuth and elevation cuts, even if the elevation pattern shows some discrepancies over far sidelobe regions. In any case, the general good matching toward validated analyses demonstrates the effectiveness of such approach which offers high accuracy even with low computational complexity. Furthermore, the model is designed to account for in-flight deviations from nominal behaviour, like those due to module failures or component degradation. The model loads calibration data and status telemetries and updates its database in order to predict the whole sets of beams in the most accurate way. As a project and analysis tool, the model also implements the possibility to cycle over independent variables to perform statistical analyses. In such way, the effects of frequency variations, graceful degradation, pointing deviations, amplitude/phase and random errors may be analysed and predicted in terms of expected values and variances. [C10024]

"A comparison of internal calibration schemes for spaceborne single-pass InSAR applications"

In this paper, first compared different receive channel schemes for InSAR application, then the main principal and technique of three practical internal calibration schemes are analyzed and compared, especially the famous SIR-C and X-SAR internal calibration system. Based on these different schemes, a new internal calibration scheme using microwave over fiber link is subscribed. [C10025]

"Emissivities of rough surface over layered media in microwave remote sensing of snow"

The rough surfaces in Greenland are exhibited as sastrugi. The roughness heights are less than 8 cm for much of the year except in late winter and spring, when they increase to 25 cm or less. Roughness profiles were also related to snow and firn ventilation. WindSat, launched in January 2003, was the first spaceborne polarimetric radiometer to measure all 4 elements of Stokes vector, viz., the vertical polarized brightness temperatures, the horizontal polarized brightness temperatures, and the real and imaginary part of the cross-correlations of the vertical and horizontal polarizations. It was shown by Tsang (1984, 1990) that azimuthal asymmetry will create nonzero third and fourth Stokes parameter in passive microwave remote sensing. Thus the third and fourth Stokes parameters contain information of the azimuthal structure. Usually the third and fourth Stokes parameters are quite small between 0.5 K to 1 K over land and less than plusmn2.5 K over ocean. However, measurements of third and Stokes parameters over Greenland show surprising values of 10 K for the third Stokes parameter and between -10 K and 20 K for the fourth Stokes parameter. In this paper, we use physically based electromagnetic model to study the passive polarimetric remote sensing of snow in Greenland by consider the scattering and emission from a random rough surface over multi-layered media. We consider the random rough surface varied in only one horizontal direction so that azimuthal asymmetry exists in the 3-D problem. Dyadic Green's functions of multilayered medium (Tsang et al., 2000) is used to formulate the surface integral equation so that the polarization dependence of emission and scattering is accounted for systematically. The surface integral equations are solved by using the method of moments in conjunction with fast numerical algorithms such as the multilevel UV method. Numerical results of brightness temperatures are illustrated for all four Stokes parameters to demonstrate the signatures of sastrugi in passive microwave remote sensing. To account for the large third and fourth Stokes parameters, we also consider the case of anisotropic scatterers in volume scattering. Full multiple volume scattering are studied with numerical solutions of the radiative transfer equations for non-spherical scatterers with preferred orientation. [C10026]

"Empirical SWE retrieval using airborne microwave and in situ snow measurements"

We examine the response of microwave brightness temperatures to snow water equivalent over a wide range of snowpack conditions observed during the Cold Land Processes Experiment (CLPX) in 2002 and 2003. Spatially intensive measurements of snow were collected over the CLPX study areas within the Colorado Rocky Mountains. The NOAA Earth System Research Laboratory's Polarimetric Scanning Radiometer (PSR) was operated to obtain coincident high-resolution (150-500 m) multiband microwave imagery of the snowpack. Together, a robust data set of over 2300 collocated in situ and remotely sensed observations were obtained for this analysis. For each point we modeled brightness temperatures using observed snow properties and the Helsinki University of Technology (HUT) snow emission model. Using observed and modeled data, we developed multiple regression algorithms to retrieve snow water equivalent (SWE). The algorithms use brightness temperature differences between 10.7, 18.7, and 21.5 GHz with 37 GHz and 89 GHz. Results show that the CLPX microwave data are consistent with a) historically established data and, b) after removal of cases with macro vegetation or possible wet snow, with theoretically derived curves for microwave dependence on SWE. [C10027]

"ComRAD active / passive microwave measurement of tree canopies"

The NASA/GSFC and George Washington University network analyzer-based multifrequency truck-mounted radar system has recently been upgraded with the addition of a dual-polarized 1.4 GHz total power radiometer. The system, now called ComRAD for Combined Radar/Radiometer, can function as a ground-based instrument simulator for L band space missions such as Hydros, Aquarius, and SMOS. In late summer 2006 ComRAD was deployed to the field to begin a series of coordinated active/passive L band measurements over small stands of deciduous and coniferous trees in order to improve our understanding of the microwave properties of trees and their effect on soil moisture retrieval algorithms. This paper describes the preliminary measurements obtained at the start of a three-year planned field measurement effort. [C10028]

"A statistical and theoretical study about radar sensitivity to crop growth from S to X band"

In this work, we show the correlation study carried out on the data collected on a maize field in the Swiss region named Central Plain, by the multifrequency RASAM scatterometer. This agricultural field was monitored over long periods, at a wide range of frequencies and observation angles, so that the correlation between

backscattering and crop height, biomass and soil moisture could have been studied under several plant and observation conditions. Moreover, we describe some recent refinements applied to the vegetation scattering model developed at Tor Vergata University, and we evaluate the accuracy of extended comparisons between model outputs and RASAM signatures. The Tor Vergata model is finally applied to give a theoretical basis to the experimental correlation findings. [C10029]

"Speckle noise reduction in SAR imaging using lattice filters based subband decomposition"

A new speckle reduction algorithm based on lattice filters for SAR imaging is presented. In the new method, the subband decomposition of the speckled image is performed using lattice filters. The noisy image is decomposed into subband images using high-pass and low-pass filters having lattice structure, then a threshold value is estimated according to noise variance in each subband and soft-thresholding is applied on the subband images. The despeckled image is obtained from the thresholded subband images using the inverse lattice filter. The proposed speckle reduction method is applied to RADARSAT/SAR images. The performance of the proposed method has also been compared with median filtering, and discrete and stationary wavelet transform based speckle reduction methods. Results show that the proposed method may be used efficiently for speckle noise reduction in SAR images. [C10030]

"Combination of one-class remote sensing image classifiers"

This paper presents simple but powerful combination methods of dedicated one-class classifiers (OCCs) for efficient remote sensing image classification. The mean and product combination rules are applied to the probabilistic outputs generated by OCCs, and the performance is illustrated in a urban monitoring application in which multi-sensor (optical and SAR) data and multi-source (spectral and contextual) features are available. Two OCCs are used as core parts: the classical mixture of Gaussians (MoG) and the support vector domain description (SVDD) classifier. The obtained results by combining SVDD classifier outputs show a clear improvement in the accuracy, and more robustness to high dimensional samples compared to both MoG and stacked approaches. [C10031]

"Ground-based microwave interferometric measurements over a snow covered slope:an experimental data collection in Tyrol (Austria)"

This paper reports on some results obtained during an experimental campaign carried out for monitoring a snow covered alpine mountainside and based on the use of a ground based interferometer working at C band. The effect of the interaction between radar signal and a dry snow cover on interferometric phase has been investigated on the bases of a simple model, representing the snow cover as a homogeneous lossless dielectric layer over the soil. Measured differential phases have been converted into snow depth estimations and compared to ground truth data. Coherence behaviour has been also investigated to evaluate the effectiveness of the proposed technique. As previously documented from other researchers, the potential of the technique has been demonstrated but limits to its applicability were found to be analysed thoroughly. [C10032]

"Deconvolution algorithms in image reconstruction for aperture synthesis radiometers"

In remote-sensing applications the inclusion of subgrid-scale variability in coarse resolution data still remains an elusive challenge. This paper is devoted to the development of an appropriate downscaling technique for future Aperture Synthesis Radiometer's images. A comparative study of different deconvolution algorithms has been performed and particular emphasis is made on the use of least-squares Lagrangian methods and Fourier Wiener filtering. Results show that with this technique it is feasible to improve the spatial resolution of brightness temperature images from the Spatial Sensor Microwave Imager (SSM/I) radiometer and from an upgraded version of the Soil Moisture and Ocean Salinity (SMOS) End-to-end Performance Simulator (SEPS). [C10033]

"Uplift rates from river profiles: methodology and case study, Oriente, Cuba"

The thrusting of the Cuban Oriente block onto the Bahamas platform and the transform movement between the Caribbean and North American plate cause oscillating uplift in the east of Cuba, manifesting itself in tilted blocks, coral reef terraces and rivers cutting deep into the bedrock. Objectives of this work are to identify active tectonic boundaries and derive relative uplift rates in Oriente using power-law scaling relation between channel slope and contributing drainage area to obtain a more detailed picture of the tectonic processes of the study area. Geomorphological interpretation and analysis of river profiles shows an inhomogeneous distribution of relative uplift rates within the Cuban Oriente block. This method allows for the estimation of deformation over large areas, the localization and the quantification of vertical displacements. [C10034]

"Structural lineaments in a volcanic island evaluated through remote sensing techniques The case of Santiago Island (Cape Verde)"

The remote sensing data (optical and radar) was used with the purpose of identify the structural lineaments that crosscut the geological formations that composed the bedrock of the south part of Santiago island (Cape Verde). Besides tectonics, this study also provided new insights to the understanding of the hydrogeological system of the volcanic island. [C10035]

"Study of ground surface displacement estimation using ALOS/PALSAR D-InSAR interferometry"

The area of Southwestern Ryukyu Arc and Eastern Taiwan are characterized by collision and subduction of the Philippine Sea Plate under the Eurasian Plate. Huatung Valley is a huge valley formed by plate motion and existing between the cities of Hualian and Taitung with approx. length of 130 km. Since 1998, Tokai University has started seismological activity measurements with Dahan institute of technology (DIT). DIT measuring GPS and electronic distance meter (EDM) data to monitor the crustal movement in the northern part of test area. We have performed a repeat-pass differential interferometric analysis using the ENVISAT/ASAR data in 2005 and 2006. In addition, we propose a crustal movement extraction using successful ALOS/PALSAR image pairs in 2007. [C10036]

"Ortho-rectification and terrain correction of polarimetric SAR data applied in the ALOS/Palsar context"

Methods for terrain correction of polarimetric SAR data were studied and developed. Ortho-rectification resampling and amplitude correction utilized Stokes matrix data. The Stokes matrix of thermal noise was subtracted before amplitude normalization. Application of an azimuth-slope correction algorithm resulted in slightly narrower distribution of orientation angles compared to input data. [C10037]

"Stratospheric ozone layer observations over tsukuba, Japan by NIES ozone DIAL."

The paper presents results from differential absorption lidar (DIAL) observations of the vertical profiles of ozone, aerosols, and temperature at the National Institute for Environmental Studies (NIES) in Tsukuba (36degN, 140degE), Japan. Currently, the lidar system uses 308/355 nm (DIAL) for lower stratospheric ozone measurements. The 355 nm is also used for aerosol measurements. The lidar system is a part of the International Network for the Detection of Atmospheric Composition Change (NDACC). The version 2 algorithm was used for accurate determination of ozone, aerosols, and temperature profiles. Methods for correcting systematic errors have been applied to the algorithm. Aerosol corrections have been applied to the temperature and ozone calculations. The mean vertical ozone profiles of the NIES ozone lidar were compared with those of SAGE II; they agreed well within a 5% relative difference in the 20- to 40-km altitude range and within 10% up to 45 km. The long-term variations of ozone obtained by the NIES ozone lidar also showed good agreement with those by the ozone sondes and SAGE II at 20 km, 25 km, 30 km, and 35 km. The temperatures retrieved from the NIES ozone lidar and those given by the National Center for Environmental Prediction (NCEP) agreed within 7 (K) in the 35- to 50-km range. [C10038]

"Return from insects in the clear-air convective boundary layer"

The Microwave Remote Sensing Laboratory (MIRSL) at the University of Massachusetts operated its S- band Frequency Modulated Continuous Wave (FMCW) radar during the International H2O Project (IHOP_2002) over the months of May and June 2002. The radar operates at very high spatial and temporal resolutions, 2.4 m and 5 s, respectively, which allows the segregation of scatter from different scattering mechanisms. Rayleigh scattering from particulate scatterers (i.e. dust and insects) dominated the return, however Bragg scattering from turbulence was also significant, especially at the top of the afternoon convective bounday layer (CBL). Scattering from insects was isolated using a 5x5 median high-pass filter. The majority of reflectivity measurements from particulate scatterers ranged from -30 dBZ to -10 dBZ, however intense point-scatterers (> 0 dBZ) skewed the distribution which resulted in mean values much greater than the median values. There is a strong diurnal signal in the backscatter: minima in the morning and at dusk and a maximum mid-afternoon and in the nocturnal boundary layer. The strong diurnal signal suggests that with targeted allocation of radar resources return from insects can be used to monitor the clear-air CBL of the central Great Plains of North America. [C10039]

"Classification of satellite images applied to geological mapping (Douro Region-Northeastern Portugal)"

Optical and microwave remote sensing data, from the northeastern of Portugal, was used to the discrimination of lithologies outcropping in that region. Classification techniques was applied and from the results it can be

concluded that the optical data performed a better discrimination than the radar data. In this last case, a texture analysis shows that the mean (with matrix of 5*5) gave the best results. [C10040]

"Recognizing salt-structures on the basis of geophysical and remote sensing data: the case of monte real salt-structure (onshore west-central portugal)"

Remote sensing data from Monte Real sub-basin (onshore West-Central Portugal), collected by the LANDSAT 7 ETM+, JERS-1 (SAR) and Envisat (ASAR) satellites, are used with the purpose to give new insights relatively to the Monte Real salt-structure. The recognized pattern of the diapir and of the structural lineaments is in agreement with the geophysical and geological data. [C10041]

"New polarimetric calibration proposal and its evaluation using ALOS PALSAR calibration campaign measurements"

We propose new polarimetric calibration algorithms using two reference targets: a polarization-preserving reflector and a polarization rotating one. In this method, iteration procedure is adopted for accuracy improvement in deriving transfer matrices of radar transmitting and receiving antennas, FR(Faraday rotation) matrix and actual scattering matrix of observed target. Availability of this method was evaluated by measured results obtained in calibration campaign of PALSAR(phased array type L-band synthetic aperture radar) boarded on ALOS(advanced land observing satellite). It is proved that the proposed method can derive each matrix component separately. [C10042]

"Polarimetric Calibration Experiment of ALOS PALSAR with Polarization-Selective Dihedrals"

Polarization-selective dihedrals are developed for polarimetric calibration of the PALSAR. The PALSAR is the first spaceborne polarimetric SAR boarded on the ALOS satellite launched in January 2006. This paper presents calibration experiments of PALSAR with the dihedrals in the ALOS initial calibration and validation phase. The reflectors are deployed in open fields of Tomakomai forest, to be imaged by not only the PALSAR but also the airborne polarimetric SAR, Pi-SAR. [C10043]

"Transpolarizing surfaces for polarimetric SAR systems calibration"

A novel transpolarizing or crosspolarizing surface has been proposed to be applied in polarimetric SAR calibrating systems, like trihedrals, since they can not provide initially a crosspolar response. So the trans-surface has been designed and measured in an anechoic chamber, providing good results for normal incidence. [C10044]

"ALOS PALSAR Calibration and Validation Results from Sweden"

In 2006 calibration activities for ALOS PALSAR were conducted in Sweden. Four five-metre trihedral corner reflectors and three smaller dihedral reflectors were deployed and operated during eight months. 23 PALSAR scenes were acquired over the calibration site allowing an evaluation of the quality and temporal stability of the data. Results show that the co-polarized data have been stable during the whole calibration period with variations in the trihedral responses lower than 0.7 dB. The measured resolution in azimuth was 4.4 m and in slant range 4.7 m for single polarization images and 9.5 m for polarimetric data. For the cross-polarized data large variations in the dihedral responses were found. It is assumed that this is caused by a larger sensitivity to pointing errors. For the polarimetric data, estimation of Faraday rotation gave values ranging from 0.1deg to 3deg. [C10045]

"Evaluation of the interaction between SAR L-band signal and structural parameters of forest cover"

The objective of this paper is to evaluate the interaction between backscatter (sigmadeg) from polarimetric L-band SAR data (collected by the airborne sensor R99-B/SIPAM) and biophysical parameters of the primary forest and secondary succession sites. The area under study is located in the region of Tapajos (Brazil), where SAR data were collected in May 2005. Another approach under investigation is the evaluation of the contribution from basic backscatter mechanisms, using the Freeman-Durden decomposition technique, applied to complex SAR images, where the physiognomic-structural characteristics of the forest stands give a significant contribution. In brief, it was possible to verify that the variable "tree height" has better relations with the backscatter values, when compared to other biophysical variables, especially when the model also includes variations of the incidence angle of the stripes imaged. The decomposition technique showed that the volumetric scattering component has the strongest influence on the SAR response at primary and secondary tropical forests. [C10046]

"SHARAD design and operation"

This paper describes the operating principles and the design of the Mars shallow radar sounder (SHARAD), an HF sounding radar devoted to the mapping of sub-surface features of Mars and currently operational on board the NASA/JPL's Mars reconnaissance orbiter spacecraft. Compared to its predecessor MARSIS, currently operating from ESA's Mars Express, SHARAD is characterised by an higher carrier frequency (20 MHz vs a max of 5 MHz for MARSIS) and a much wider signal bandwidth (10 MHz vs 1 MHz of MARSIS). This allows SHARAD to achieve a finer range resolution (15 metres unweighted in free space) at the expenses of ground penetration, which makes the instrument ideal to probe the shallow subsurface layers (to depths of hundreds of meters) which cannot be resolved from the surface by the much far- reaching MARSIS. SHARAD uses a 85 usec chirp signal with a PRF of 700 Hz and a peak power of 10 W, and radiates by means of a 10 meters fiber foldable tube (FFT) dipole antenna, with a wide-band matching network in charge of impedance matching with the transceiver. The most challenging requirement (especially considering the large fractional bandwidth of the system) is the level of the range sidelobes, which shall be below -55 dBc after the 6th lobe, to allow proper detection of the weak subsurface echoes in presence of strong surface returns. On this side, the design takes advantage from the wide download bandwidth made available by the MRO Spacecraft to keep the on-board processing to a minimum level (basically, only a programmable coherent presuming), and leave most of the processing (range compression and synthetic aperture) on ground. In this way it is easy to use Tx chirps and Rx transfer functions characterised on- ground as reference for range correlation, with the range sidelobes limited, basically, only by the stability of the RF hardware. The limited amount of on-board processing also helped in limiting the complexity of the instrument design and, therefore, its mass and power consumption. SHARAD uses a very simple architecture, with the transmit chirp generated directly on the RF frequency (using a digital chirp generator) before being amplified to the transmit level by a class C amplifier. The receiver is even more essential, providing direct amplification of the received signal (with programmable gain and band filtering) to an A-to-D converter operated in downsampling mode by digitising the signal at 26.6 MHz rate. In this way, the complete 10 MHz signal bandwidth can be represented unambiguously with only an acceptable amount of oversampling (30%) minimising the required hardware. Instrument control and processing tasks are performed by the same AD-21020 DSP (with the help of a couple of FPGAs). The presuming can be varied from 1 to 32 in powers of two steps, and the resolution of science data can be selected to be 4, 6 or 8 bits, to allow optimisation of the data rate vs the operating scenarios. The receive window position can either be controlled in open loop, using an a priori knowledge of S/C orbit and surface topography (which demonstrated to be a very robust approach) or in closed loop. [C10047]

"Parameter based SAR simulator for image quality evaluation"

A SAR simulator for image quality evaluation is presented. This simulator can be used for the estimation of SAR image quality performance from the simulated raw data and the verification of the SAR payload design parameter associated with the image quality parameters. Evaluation of SAR image quality is achieved by analyzing the error effect of system parameter using the developed simulator. [C10048]

"Robust forest height extraction using polarimetric SAR interferometry"

Recently, many researches have demonstrated that polarimetric SAR interferometry is the most promising technique for forest parameter extraction. In this paper, we present a robust forest height extraction technique based on reliable phase estimation. The more accurate interferometric phase estimation can be attained with the reliable ground phase and canopy phase using three-stage inversion process and ESPRIT technique, respectively. We show the validity of the method by applying it to L-band simulated polarimetric and interferometric SAR data. The experimental results are also provided to give the availability of this method. [C10049]

"Satellite eye for the galathea 3 ship expedition: global tour 2006-2007"

Satellite Eye for Galathea 3 (www.satelliteeye.dk) contains education at the internet for secondary and upper secondary schools and the public. The Galathea 3 ship expedition circumnavigated the globe starting from Denmark 11 August 2006, visiting Greenland, Azores, South Africa, Australia, Solomon Islands, New Zealand, Antarctica, Chile, Galapagos, the Caribbean, the Northeastern USA and finishing in Denmark 25 April 2007. During the entire expedition satellite images were ordered along the ship track, downloaded, processed, archived and used for education. The satellite images are displayed in Google Earth along with 10 minute observations of air and sea parameters observed at the ship (<http://galathea.oersted.dtu.dk>). This material forms basis for 9 running projects along the entire route and 24 site-specific cases. Observations from several science projects onboard will be used in the site-specific cases. One of the continuous study cases is chlorophyll observed from

Envisat MERIS. As an example: in the upwelling zone near Namibia a very high level of chlorophyll was observed from MERIS. The ship route consequently was changed slightly the day after in order to traverse the area with the highest amount of chlorophyll. Chlorophyll observed onboard (in-situ) two days later show high amounts. In addition, in the science project on the carbon cycle a significant emission of CO₂ was observed. The students can use the data online in the classroom. Students from several classes were onboard for part of the expedition and these classes in particular used the Satellite Eye teaching material. In Google Earth satellite images of many themes are shown. These include sea ice, sea surface temperature, ocean wind, wave height, sea surface level, ozone, clouds and radar images of ocean and land. Also high spatial resolution land cover mapping of the visited harbors and their surroundings are included. The case studies uses the image processing software LEO Works developed through the ESA project EDUSPACE, the European Earth Observation web site for Secondary Schools (<http://www.eduspace.esa.int>). For each theme a thorough educational material has been developed in Danish and English. ESA has granted a large amount of Envisat as well as PROBA images and third mission data from SPOT and Landsat. Also data from NOAA, NASA, JAXA and QUICKBIRD were used. [C10050]

"Combined use of InSAR and ICESat / GLAS data for high accuracy DEM generation on antarctica"

This study aims to use ICESat /GLAS data for correction of DEM made from Interferometric SAR data instead of traditional ground control points (GCPs) collected by ground survey. GLAS is a laser altimeter system and it can measure the earth surface topography with ultimate vertical accuracy (plusmn14 cm) and high spatial accuracy (plusmn15 m). Therefore, we can treat GLAS data for the reference of height and position on Antarctic ice sheet. We applied this method at south of Breivika. The elevation values derived by ERS-1/2 InSAR DEM have insufficient height accuracy compared to GLAS data due to insufficient baseline estimation, ice flow appeared in the fringe pattern, and difficulty of phase unwrapping, which is RMS plusmn284.0 m compared with GLAS data. After the correction of InSAR DEM using GLAS data, it improved to plusmn32.6 m. Next, we validated this result using the 28th JARE (Japanese Antarctic Research Expedition) GPS survey result. The RMS height difference between JARE GPS result and corrected InSAR DEM showed plusmn39.5 m. The result showed that our correction method works quite well and we can produce spatially dense and high accuracy DEM along with Antarctic coast line. The one remaining problem is how to reduce the effect of ice flow appeared in the fringe pattern. [C10051]

"Extraction of forest parameters in a mire biotope using high-resolution digital surface models and airborne imagery"

The objective of this paper is to spatially predict tree/shrub genera using generalized linear models (GLM), color-infrared (CIR) aerial images, ADS40 images, digital surface models (DSMs) and field samples. The present study was carried out in the framework of the Swiss Mire Protection Program, where extraction of forest parameters for description of present state of a mire ecosystem and as indicators for changes are of high importance. In a first step, high-quality DSMs were automatically generated from CIR aerial images for two test sites, both located in the Pre-alpine zone of Central Switzerland. In a second step, tree layers were then generated combining canopy height models derived from the DSMs and LiDAR DTM with a fuzzy classification of CIR aerial images. In a third step, on the basis of these tree layers, fractional tree/shrub covers were generated using explanatory variables derived from the DSMs and logistic regression models. Then tree genera were predicted for the pixel values (tree/shrub probability > 0.3) of the fractional covers using a multinomial regression model and additional spectral information as provided by Leica ADS40 data for one test site and CIR aerial images for the other test site. Overall, prediction of tree genera was less satisfactory when only using CIR aerial images. In contrary, up to six different tree genera were predicted with high accuracy using explanatory variables derived from ADS40 images. The study stresses the importance of high-resolution and high-quality DSMs and highlights the potential airborne remote sensing data for ecological modeling purposes. [C10052]

"Polarview@FIMR: WWW-based delivery of baltic sea ice products to end-users"

Sea ice information for navigational purposes is essential in the Baltic Sea. Winter navigation is made possible by the use of icebreakers, ice-strengthened vessels and by restricting navigation. Thus the icebreakers need detailed ice information for route planning. The smoothness of traffic has been possible due to better ice monitoring, where use of Earth observation data has become more and more important. For this purpose the FIMR PolarView web pages have been set up and they contain information to aid navigation in the area of the Baltic Sea. One such future SAR-based product could be the ice motion estimated from successive SAR images. For this purpose an algorithm for the ice motion detection has been developed at FIMR. Also the presentation of the existing products will be developed, for an example also the animations of the SAR-based ice thickness charts and ice predictions will probably be available in near- real-time next winter. [C10053]

"A physically consistent stochastic model to observe oil spills and strong scatterers on SLC SAR images"

A speckle model to characterize low backscatter areas and areas with strong scatterers in marine SLC SAR images is presented. The model allows using high resolution speckled SAR images instead of dealing with multi-look SAR images where, at the expense of a poorer spatial resolution, the speckle is mitigated. The new approach is based on the use of the three parameters of the generalized K probability density function. This speckle model embodies the Rayleigh, the Rice and the K-distribution scattering scenes, which are descriptors of scenes dominated by Bragg scattering, scenes in which a dominant scatter is present and scenes with a non-Gaussian signal statistic, respectively. A large data-set of ERS 1/2 SLC SAR images, provided by the ESA under the Project C1P-2769, is employed. Results show the effectiveness of the approach. [C10054]

"Identification of oil spills based on ratio of alternating polarization images from ENVISAT"

We propose here a method to identify surface film in SAR images using the Alternating Polarization ratio images from ENVISAT. This ratio is lower in polluted areas than in non-polluted areas due to the difference in relative contributions of the non-Bragg scattering to the total radar signal. [C10055]

"Use of quikscat ku-band scatterometer data for retrieval of seasonal snow characteristics in Finland"

The feasibility of using scatterometer data from the spaceborne QuikScat instrument for retrieval of snow characteristics in Finland has been studied. QuikScat data for the winters of 1999-2000 through 2005-2006 have been used along with in situ data for 21 test sites. [C10056]

"Microwave remote sensing of alpine snow"

In the alpine zone snow is a dominant factor for more than half of the year and has strong influence on the ecosystem and economy. The knowledge of snow coverage, structure, liquid water content etc. is important and useful for many applications ranging from flood management to avalanche warning. Remote sensing from space has good potential to address these needs. Within ASSIST, Alpine Safety, Security and Information services and Technologies, these topics are also of interest. Two snow related products were identified that can be produced on an operational base with the available satellite systems to be ingested into the ASSIST service. Avalanche maps, mapping the contours of avalanches, and snow cover maps, mapping the snow covered area. The produced products are in good agreement with validation data. Unfortunately the current available satellite systems (mainly c-band SAR that is applicable) are not very well suited for snow related applications due to the small influence of the dry snow on the microwave signal at C- band. To overcome this limitation the CoReH2O mission was designed. With its X- and Ku-band system and repeat rates of 3 and 15 days it has high potential for alpine snow applications. Additional microwave signature measurements at these frequencies with standardized and reproducible snow characterization information will be needed for model development and validation. Recent developments allow a more quantitative snow characterizations and will be considered in the SnowScat project in combination with traditional snow characterization methods. [C10057]

"Bora events over the adriatic sea and black sea studied by multi-sensor satellite imagery"

Bora events over the Adriatic Sea and Black Sea are investigated by using synthetic aperture radar (SAR) images acquired by the Advanced Synthetic Aperture Radar (ASAR) onboard the Envisat satellite, optical and infrared images acquired by the MODIS sensor onboard the Terra satellite, and sea surface wind data acquired by the scatterometer onboard the Quikscat satellite. Quantitative information on the sea surface wind field is extracted from the ASAR images by using the CMOD4 wind scatterometer model. It is shown that SAR images yield information of the spatial structure of bora events over coastal waters with high spatial resolution that cannot be obtained by other spaceborne instruments. Furthermore, by using ASAR data in combination with MODIS data we are able to detect cyclonic atmospheric eddies, which are often generated by lateral wind shear associated with bora events. [C10058]

"X-band backscatter from the ocean at low-grazing angles"

In 2005 and 2006, we mounted an X- band Doppler radar on ships that operated in the South China Sea and off the coast of New Jersey, respectively. The measurements were made only at W polarization in 2005 but at both HH and W polarization in 2006. On average, VV normalized radar cross sections, $\sigma_0(VV)$, behaved at grazing angles between 1 and 2 degrees in much the same manner that they do at higher grazing angles. In particular, they showed the second-harmonic dependence on the angle between the antenna-look direction and

the wind direction that is characteristic of scatterometry. $\sigma_0(HH)$, on the other hand, showed little evidence of the second harmonic component, maximizing with the antenna looking into the wind and minimizing in the opposite direction. For both polarizations, σ_0 was generally well above that expected from Bragg scattering and the polarization ratio $\sigma_0(VV) / \sigma_0(HH)$ was much smaller. Surface signatures of internal waves (IW) off the New Jersey coast were much weaker when the antennas looked in the direction of internal wave propagation than when they looked opposite this direction. Interestingly, for the nonlinear internal waves found in the South China Sea, the opposite phenomenon occurred: W signatures were stronger looking in the direction of IW propagation than opposite to it. [C10059]

"Oil spill segmentation of SAR images via graph cuts"

Segmentation of dark patches in SAR images is an important step in any oil spill detection system. Segmentation methods used so far include 'adaptive image thresholding', 'hysteresis thresholding', 'edge detection' (see [1] and references therein) and entropy methods like the 'maximum descriptive length' technique [2]. This paper extends and generalizes a previously proposed Bayesian semi-supervised segmentation algorithm [3] oriented to oil spill detection using SAR images. In the base algorithm on which we build on, the data term is modeled by a finite mixture of Gamma distributions, with a given predefined number of components, for modeling each one of two classes (oil and water). To estimate the parameters of the class conditional densities, an expectation maximization (EM) algorithm was developed. The prior is an M- level logistic (MLL) Markov Random Field enforcing local continuity in a statistical sense. The methodology proposed in [3] assumes two classes and known smoothness parameter. The present work removes these restrictions. The smoothness parameter controlling the degree of homogeneity imposed on the scene is automatically estimated and the number of used classes is optional. To extend the algorithm to an optional number of classes, the so-called alpha-expansion algorithm [4] has been implemented. This algorithm is a graph-cut based technique that finds efficiently (polynomial complexity) the local minimum of the energy, (i.e, a labeling) within a known factor of the global minimum. In order to estimate the smoothness parameter of the MLL prior, two different techniques have been tested, namely the least squares (LS) fit and the coding method (CD) [5]. Semi-automatic estimation of the class parameters is also implemented. This represents an improvement over the base algorithm [3], where parameter estimation is performed on a supervised way by requesting user defined regions of interest representing the water and the oil. The effectiveness of the proposed approach is illustrated with simulated SAR images and real ERS and ENVISAT images. [C10060]

"SAR simulation of ocean scenes covered by oil slicks with arbitrary shapes"

The identification of oil slicks on the ocean surface from SAR data requires quantitative sound models accounting for the most important characteristics (ocean spectrum, slick viscosity, slick shape, and so on). In this paper we present the implementation of an innovative SAR raw signal and image simulator, which is able to reproduce images relative to ocean surfaces covered by oil slicks with arbitrary shapes. The attention is mainly focused on slicks with fractal contours. The fractal Weierstrass-Mandelbrot function is used to generate slicks with fixed fractal dimension. A box counting technique is employed to evaluate the fractal dimensions of the generated slicks and the corresponding SAR images. Radiometric properties of the area covered by oil are also estimated in order to show how the simulated data provide a powerful set for processing algorithms. [C10061]

"Mapping and modelling the snowmelt and greening pattern in southern norway by combining microwave and optical remote sensing sensors"

Southern Norway has strong climatic gradients and is well suited for studying snow melt and greening patterns. In this study we combine snow cover maps with phenological maps for the early May period for the years 2004 and 2006. The snow cover area maps are based on both microwave (ASAR) and optical (MODIS) sensors. The phenological maps are based on NDVI thresholds from the MODIS sensor. The onset of growing season 2004 was among the earliest recorded over the last 30 years. On May 8, 2004 30% of the study area was covered by snow and 29% had unfolded leaves on trees. The onset of the growing season in 2006 was slightly later than average, and on May 4, 2006 64% of southern Norway was covered by snow and the phenophase of unfolded leaves had not started yet. [C10062]

"Retrieving land cover information from MERIS and MODIS Data: a comparative study for landscape characterization in Portugal"

This is a preliminary study in the framework of an ongoing research work that aims at comparing the aptitude of MERIS and MODIS images for land cover mapping at regional scale. Overall and per class accuracies achieved with a Maximum Likelihood classification of MODIS and MERIS images acquired during August 2005, are used as a measurement of their adequacy for land cover characterization in Portugal. Attained results show that

differences in spatial and spectral resolutions of used images do not produce overly disparities in land cover classes' discrimination. Still, the separation between such numerous land cover classes is hampered by landscape fragmentation of the territory at such spatial resolution. [C10063]

"The role of spatial interactions for prediction of the spectral structure of the atmospheric phase screen"

The atmospheric phase screen is one of the main error sources that affect the precise phase measurements in many fields of earth remote sensing. The atmospheric effects can be mitigated if a precise knowledge of the power spectral density of the process is available and if same sample observations can be retrieved on a sparse grid. At smaller scales, where interactions are no longer isotropic, the behaviour is not easily predicted by the ultimate dissipative behaviour of turbulence eddies. We start by assuming that the propagation of the electromagnetic wave in the lower atmosphere can be represented by a ray travelling in a layered medium where the refractive index is constant along each layer. In a turbulent atmosphere, the interaction among eddies induces a diffusion process that propagates with different rates in both vertical and horizontal direction with the final effect of ruling the number of effective layers in the atmosphere. In this way, the overall path travelled by the electromagnetic wave is governed by the accumulated number of such effective layers whose interactions play a primary role in our model. A good model for the interactions among different layers is the linear interaction model. The power spectrum of the process can be found by solving a differential equation with given initial conditions. It can be demonstrated that an asymptotic power law decay is found under binomial competitive interactions and that, at a smaller scale, the behaviour observed in the observed data is naturally induced by the interaction process itself. The model predictions have been tested using samples of the atmospheric phase screen extracted from Synthetic Aperture Radar interferograms. To this end, the model parameters have been estimated from the data set and the predicted spectrum has been compared with the measured one. [C10064]

"Qualitative approaches to rapidly identify completely submerged rice due to tropical cyclone using satellite data"

The objective of the present study is to identify completely submerged rice areas due to tropical cyclones using remotely sensed data. The Kendrapara district of Orissa state hit by a tropical cyclone on 30th October 1999 is considered as study area and for this area, pre event (October 11, 1999) visible- near IR image and pre (October 11, 1999) and post event (November 2, 1999 and November 4, 1999) Radarsat images were procured. The pre event IRS ID LISS III (resolution = 22 m) image of Kendrapara district was geometrically corrected and classified into several landuse and landcover classes. Supervised classification technique was used for landuse/landcover classification. This landuse/landcover map is assumed to be accurate and is used as a base map in the present study. Pre and post event Radarsat-SAR images were also geometrically corrected. Further preprocessing included speckle noise removal, data calibration and incidence angle adjustment. Based on literature, a threshold of -16.5 db (DN value =100) was chosen to classify each pixel in pre Radarsat-1 SAR image as water or non-water. The landuse/landcover map was used to identify the rice regions in the pre and post-event Radarsat images. Application of the threshold allows for the determination of the submerged rice areas. To determine the validity of a single threshold, water pixels in pre event Radarsat-1 SAR images were extracted corresponding to the base map. A histogram of these values suggests that a single value threshold approach may not be fully accurate. To overcome these limitations, two alternative approaches, namely image histogram and change in db were formulated. For both approaches, the rice pixels in pre and post event Radarsat- SAR images were extracted corresponding to base map rice pixels. In case of image approach, a histogram was plotted for the DN values of the pre and post Radarsat-1 SAR rice pixels. This allows the qualitative identification of the submerged rice areas. Using change i- n db approach, pixel-to-pixel change in db in pre and post event Radarsat-1 SAR images in rice pixels was calculated. Analysis of these values allows for the identification of different effects of submergence on the rice area. This type of analysis will help policy makers in determining the extent of submergence and could serve as a tool for rapid assessment of damage and help expedite release of relief funds and aid proper allocation of funds to the affected areas/people. [C10065]

"Uncertainty analysis in advanced differential interferometric SAR processing"

The DInSAR technique enables to determine with precision the surface displacements, using a combination of multiple interferograms. The DInSAR processing steps generate different kinds of errors, which propagate in the entire chain. This work is focused on a particular type of error generated during the DInSAR processing: the unwrapping related errors. The errors generated during the unwrapping process and the use of a procedure to automatically detect and correct them are presented in this work. By an iterative process and exploiting the SVD least squares method for outliers rejection, this procedure determines the phases values associated with each SAR image, starting from a stack of interferograms. It works on previously selected pixels and provides good results with high observation redundancy. The effectiveness of the procedure is illustrated by using ERS SAR

data acquired over Barcelona (Spain). [C10066]

"ASAR parallel-track PS analysis in urban sites"

In this work we present a methodology for developing a Permanent Scatterers (PS) analysis jointly exploiting data acquired from parallel orbits to estimate height and deformation trend of multi-angle urban targets. The methodology allows applying the PS technique also in areas where the number of ASAR acquisitions per single track would prevent to get reliable estimates. Preliminary experimental results achieved in the Shanghai test site confirm the promising potential of the proposed methodology. [C10067]

"CoRe-H2 O-A dual frequency SAR mission for hydrology and climate research"

Taking into account the needs for improved, spatially detailed observations of snow and ice in climate research, hydrology, and glaciology, the satellite mission COld REgions Hydrology High-resolution Observatory, CoRe-H2O, was proposed to ESA. As payload a co- and cross-polarized Ku-band (17.2 GHz) and X-band (9.6 GHz) SAR was selected, because of its sensitivity to dry snow, thin sea ice, and the metamorphic state of snow, firn and ice on glaciers and ice caps. A cost-effective ScanSAR scheme with parabolic reflectors (each with multiple beams) is proposed fulfilling the requirements for swath width, spatial resolution and radiometry. The mission has been selected by ESA for further scientific and technical studies in the frame of the Earth Explorer Satellite Programme. [C10068]

"Increased export of grounded ice after the collapse of northern Larsen ice shelf, Antarctic Peninsula, observed by Envisat ASAR"

Time series of satellite radar image data of Envisat ASAR were used to study the retreat of ice shelves and glaciers at northern Larsen Ice Shelf, Antarctic Peninsula, up to March 2007. After the disintegration event in March 2002, the small remaining ice shelf section of Larsen B decreased further in area. The retreat of grounded glacier ice continued also. The glacier velocities above previous Larsen B increased further since 2004, but the acceleration has been smaller than in the first two years after the collapse in 2002. Ice export increased rapidly after the glaciers started to calve directly into the ocean. The sea level contribution due to discharge of grounded ice above the disintegrated ice shelf sections amounts to about 6% of the present glacier and ice sheet contribution to sea level rise. [C10069]

"Generation of ENVISAT ASAR Mosaics accessible on-line"

This paper describes the routine generation of ASAR mosaics at ESRIN and their distribution via Web map servers. ASAR products are automatically collected from various processing sites to be geocoded and mosaicked on the GRID Processing on Demand system at ESRIN. New mosaics are automatically transferred to an OpenGIS Web map server where they can be directly visualized at full resolution by external users. The generation of mosaics involves several processing steps including antenna pattern correction and compensation of incidence angle depending on vegetation type. Several map projections are supported including polar stereographic projections (Arctic and Antarctic's) as well as Plate Carre acute projections (entire World). [C10070]

"Error analysis of Envisat ASAR level 2 algorithm based on simulation technique"

In ESA's Envisat ASAR level 2 algorithm, it is assumed that the synthetic aperture radar (SAR) image cross spectra of mixed ocean waves were the summation of SAR image cross spectra of wind waves and that of swells. But our previous studies show that in addition to this, the cross spectra of mixed waves consist of an extra term (see the companion paper submitted to this symposium). Just this term leads to an inherent error of this algorithm which has not been considered yet. This paper presents an error analysis of Envisat ASAR level 2 algorithm for ocean wave spectra retrieval in different significant wave height, wavelength, wave direction and wave component conditions based on simulation technique. It shows that the inherent errors (1) change with above parameters, and are always positive which mean the retrieved ocean wave height are overestimated; (2) increase for larger significant wave height; (3) increase for smaller wavelength; (4) increases for smaller propagation angle respect to azimuth direction. (5) increase for more wind wave component. Therefore, Envisat ASAR level 2 algorithm only works in small wave height, or large wavelength, or large propagation angle, or few wind wave component conditions. [C10071]

"The value of SAR Multi-polarization data in delivering annual crop inventories"

The outcome of a multi-year project carried out across sites within Canada has been the development of a method to deliver crop inventories using the integration of SAR and optical satellite data. Although multi-temporal

optical imagery can classify crops at the target accuracy, SAR data will be valuable in boosting accuracies and ensuring operational delivery of this annual inventory. [C10072]

"ASAR instrument performance and product quality evolution"

ENVISAT ASAR is successfully operating since March 2002 and resulting ASAR products are operationally distributed to the user community since December 2002. This paper provides an update of the ASAR performance, from the instrument status to the product quality assessment. [C10073]

"Comparison of geometric optics and diffraction effects in radar scattering from steep and breaking waves"

To address the issue of radar scattering from steep and breaking ocean waves, we developed an efficient and fast 2-D numerical full-wave approach to model both wave evolution and radar scattering from these waves. It enabled us to reproduce the main features of the temporal and polarization behavior of the radar signal such as sea spikes. In addition, to better understand the contribution of multiple scattering that might emerge from radar scattering on steep and breaking waves, we have modeled scattering using a ray-tracing approach that not only provides the ray picture but also supplies both the ray amplitude and the ray phase. This approach eliminates diffraction effects from consideration, leaving only geometric optics effects that include multiple reflections. As a result, angular dependencies of the scattering cross section based on the ray approach were calculated and compared with corresponding values from the full-wave approach. Generally, better agreement between these two approaches is obtained for forward scattering directions than for backscattering directions. Ray simulation for a backscattering direction does not reproduce the HH/W ratio with the spikes observed in the full-wave solution. This indicates that diffraction effects are critical for explaining important features of backscattering from breaking waves. The role of multiple reflections from the breaking wave profile in creating spikes with an anomalous HH/W ratio proved to be negligible. [C10074]

"The RADARSAT constellation payload design"

The Canadian Space Agency completed the definition phase of the RADARSAT Constellation, a constellation of three satellites that will ensure C-band data continuity with RADARSAT-2. The first satellite is scheduled to enter in operation toward the end of the RADARSAT-2 mission, for a full implementation of the constellation in 2014-15. The RADARSAT Constellation is designed to improve significantly the availability of SAR data for main Canadian Government departments, the main applications areas being maritime surveillance, ecosystem monitoring and disaster management. An important constraint on the mission was to reduce significantly the cost of SAR data, which forced the use of new approaches in the payload design. The paper presents the initial payload design process and three techniques investigated to improve its performance. [C10075]

"Retrieval of wind speed using an L-band synthetic aperture radar"

Retrieval of wind speed using L-band synthetic aperture radar (SAR) is both an old and new endeavor. Although the Seasat L-band SAR in 1978 was not well calibrated, early results indicated a strong relationship between observed SAR image intensity and wind speed. The JERS-1 L-band SAR had limited usefulness over the ocean. Most recent wind retrievals from spaceborne SARs have been at C-band for ERS-1/2, Radarsat, and Envisat. With the launch of the sophisticated multi-polarization Phased Array L-band Synthetic Aperture Radar (PALSAR) on the Advanced Land Observing Satellite (ALOS), we renew the investigation of wind retrieval from L-band. [C10076]

"Probability density function of ocean surface slopes from radar observations"

Airborne radar observations of the sea surface at C-Band and small incidence angles are used to investigate some properties of the surface slope probability density function (pdf). The method is based on the analysis of the variation of the radar cross-section with incidence angle, assuming that the backscatter can be described by the Geometrical Optics theory. First, we show that roughness properties with scales larger than 12 cm can be analyzed in our configuration (C-Band, incidence 7 to 16deg). The radar data are then analyzed in terms of filtered mean square slope under the assumption of a Gaussian slope pdf. Dependence with wind speed of the upwind and total mss are analyzed and compared to various published studies. Finally an analysis of the radar data under a non-Gaussian assumption for the slope pdf is proposed, by applying the compound model suggested by [1]. [C10077]

"Airborne Ku-band radar remote sensing of terrestrial snow cover"

Preliminary analyses of the POLSCAT data acquired from the CLPX-II in winter 2006-2007 are described in this

paper. The data showed the response of the Ku-band radar echoes to snowpack changes for various types of background vegetation. We observed about 0.4 dB increase in backscatter for every 1 cm SWE accumulation for sage brush and agricultural fields. The data also showed the impact of surface hoar growth and freeze/thaw cycles, which created large snow grain sizes and ice lenses, respectively, and consequently increased the radar signals by a few dBs. [C10078]

"The SARALPS-2007 measurement campaign on X and Ku-Band Backscatter of snow"

The retrieval of snow parameters, and snow water equivalent in particular, are key parameters in hydrology and climate research. Theory, ground-based signature research and analysis of spaceborne scatterometry suggests that the high-frequency combination of Ku- and X-band active microwave sensors is an excellent tool for the retrieval of snow physical properties. In order to validate this, a snow measurement campaign was carried out with the University of Cranfield's portable Ground-Based Synthetic Aperture Radar (GB-SAR) System during the winter of 2006/7 at two test-sites in the Austrian Alps close to Innsbruck. Fully polarimetric X- and Ku-band backscatter signatures were acquired over a range of incidence angles (~20deg-70deg), with the active sensor operating predominately in SAR mode, but occasionally also in InSAR mode. Microwave signatures and snow properties were measured on seven different dates. Detailed complementary meteorological and snow metamorphic conditions were also recorded. [C10079]

"Ship signatures in synthetic aperture radar imagery"

Ship signatures in synthetic aperture radar (SAR) imagery have been matched to Automatic Identification System (AIS) data to yield a large database of known ships for ship signature analysis. This paper focuses on ship radar cross section and ship length derived from the ship signature length. Cross-polarization is an attractive option for ship detection. [C10080]

"A multi-scattering and multi-layer snow model and its validation"

Microwave scattering from snow is difficult to model due to the complexity and heterogeneity of natural snow. In this paper, we developed a multi-layer, multi-scattering model based on recent theoretical advances in snow and surface modeling. In the proposed multi-layer model, Matrix Doubling method is used to account for scattering from each snow layer; and Advanced Integral Equation Model (AIEM) is incorporated into the model to describe surface scattering. Comparisons were made between the model predictions and field observations from truck-mounted L- and Ku-band scatterometers (frequencies are 1.25 GHz and 15.5 GHz) at Local-Scale Observation Site (LSOS) of NASA Cold-land Processes Field Experiment (CLPX) during Third Intensive Observation Period (IOP3). It was found that model predictions were in good agreement with field observations with proper particle size selected. Analysis on scatterer shape, multiple scattering and snow stratification effects were also made based on model simulations. [C10081]

"Atmospheric vertical profiles obtained by Lidar over Évora during CAPEX project"

CAPEX is a European project to investigate aerosol particles, radiation, cloud properties, precipitation and radioactivity over Portugal. During the campaign, carried out during the first fortnight June 2006 at Évora, Portugal (38deg34' N, 7deg54' W, 293 m a.s.l.), synoptic conditions favoured the arrival of air masses coming from Europe, Northern Africa and Mediterranean basin at several levels. In this study, two complex profiles, including layers coming from Europe and Sahara desert, are analyzed by a combination of Lidar and Cimel CE-318-4 data. Good agreements were found between them. [C10082]

"Development of web-based SAR processor for education"

Recently, synthetic aperture radar (SAR) processing algorithms have become more complicated due to the variety of observation modes of SAR sensors. Understanding the basics of the SAR processing technique is necessary to work out new approaches using the new sensing modes. A web-based SAR processor using Ajax technology is proposed for easy use in an educational computer system with various limitations. This paper presents the concept and the implementation method of this software and shows processing examples. [C10083]

"A low cost testbed for synthetic aperture techniques"

This paper describes a testbed for synthetic aperture techniques. The developed testbed uses only off-the-shelf components providing the students and the researchers with a low cost environment for development and testing of new algorithms. The applicability of the platform is demonstrated with acoustic images of point-like and extended targets. [C10084]

"Vehicleborne bistatic synthetic aperture radar imaging"

A complete vehicleborne Bistatic Synthetic Aperture Radar (SAR) imaging experiment is presented in this paper. Some new technologies were used to solve synchronization problems. An algorithm named the Glide Window Echo CFAR was used to realize time synchronization and collect the echo. High stable local oscillator was employed to achieve frequency and phase synchronization, and the PRF was adjusted adaptively in the Data Acquisition Device in the receive station. Finally, the Range-Doppler algorithm with range migration correction was using to image the certain scene successfully. [C10085]

"Lidar education at Georgia Tech"

The lidar research team at the Georgia Tech Research Institute (GTRI) is developing an educational program with many components including academic classes, short courses, classroom teaching materials, hands-on laboratory demonstrations, and web-based resources. We are currently developing a textbook for introductory instruction on the basic principles of lidar systems. [C10086]

"Remote sensing information visualization using volume based objects in world wind"

Visualization of remotely-sensed meteorological data has traditionally consisted of two dimensional maps. However, the technological advancements in recent years have allowed data to be collected in new and unique ways and with greatly increased range and density. In particular, data are now collected at discrete locations within a volume, as opposed to points on a surface. The data volume, as opposed to an image, necessitates a different form of visualization. Unlike common techniques that stick on two dimensional maps, the main focus for the new techniques is showing the precipitation and other meteorological data in a more intuitive manner. This paper will introduce one of several possible ways to visualize a volume dataset. In this particular case rain intensity values gathered by NASA's TRMM satellite deliver a stereotypic volume dataset. [C10087]

"Application of bootstrap techniques for the estimation of Target Decomposition parameters in RADAR polarimetry"

The precise estimation of the eigenvalues of PolSAR responses is essential in the derivation of Target Decomposition parameters such as the Cloude-Pottier parameters (Entropy, Anisotropy and average angle Alpha). However, sample eigenvalues are strongly biased for small sample sizes leading to underestimated Entropy and overestimated Anisotropy values. In this paper, we investigate the use of a particular bootstrap technique for the correction of the bias. Bootstrap techniques are attractive because they can deal with very small sample sizes under minimal assumptions on the signal distribution. Here, we are using the jackknife bias correction technique which has been successfully applied to various signal processing problems. Monte-Carlo simulations reveal that the jackknife bias correction directly applied on the Cloude-Pottier parameters lead to better bias reduction. [C10088]

"Multi-waveform radar for ice sheet measurements and classroom demonstration"

The Center for Remote Sensing of Ice Sheets (CReSIS), at the University of Kansas, is a Science and Technology Center established by the National Science Foundation (NSF) in 2005, with the mission of developing new technologies and computer models to measure and predict the response of sea level change to the mass balance of ice sheets in Greenland and Antarctica. As part of a senior undergraduate capstone design course we designed and simulated a wideband, push-broom, multi-waveform radar for fine-resolution airborne ice sheet surface elevation measurements. A prototype of this system was developed and its response was measured. The prototype will serve as a teaching tool and a design platform for the final instrumentation package to be used on an uncrewed aerial vehicle (UAV) being developed at the University of Kansas. In this paper we will present the objectives of the project, design details, simulation results, and testing results from experiments delay line and point targets. [C10089]

"MERIT Erasmus Mundus: an opportunity for international cooperation in Remote Sensing education in Europe"

MERIT is a research-oriented Joint European Master on Information and Communication Technologies funded by the Erasmus Mundus program of the European Community. Its well funded scholarship scheme offers an outstanding opportunity for students, professors and researchers from non-European countries to participate in education programs (e.g remote sensing) in Europe. [C10090]

"Vertical profile reconstruction with Pol-InSAR data of a subpolar glacier"

The last decade has seen an increasing demand for accurate mapping and wide-coverage monitoring of glaciers and ice sheets in order to measure and predict their response to global climate change and their contribution to sea level rise. This in turn requires a more complete understanding of their properties including topography, accumulation rates and vertical profiles. One promising new technique for vertical profile reconstruction using polarimetric interferometric SAR (Pol-InSAR) data is polarization coherence tomography (PCT) and for the first time, PCT is adapted here to a glacier scenario. The inversion algorithm to reconstruct vertical ice profiles is applied to both simulated data to assess its accuracy and sensitivity to input parameters, and to airborne Pol-InSAR data at L- and P-band and InSAR data at X-band collected using DLR's E-SAR system over the Austfonna ice cap in Svalbard, Norway. [C10091]

"Performance analysis of a hybrid bistatic SAR system operating in the double sliding spotlight mode"

A bistatic synthetic aperture radar uses a separated transmitter and receiver flying on different platforms to achieve benefits like exploitation of additional information contained in the bistatic reflectivity of targets, reduced vulnerability for military applications, forward looking SAR imaging or increased RCS. A particular constellation, where the transmitter is in space and the receiver near or on the earth surface (e.g. aircraft, tower) is called a hybrid bistatic SAR system. Besides technical challenges, like the synchronization of transmitter and receiver, the overlap of the two antenna footprints is of vital importance. Due to the extreme platform velocity differences, SAR modes with flexible steering of the antenna beams are necessary. The sliding spotlight mode offers such a beam steering, where the antenna footprint velocity can be chosen slower or faster than the platform velocity. If both transmitter and receiver use this mode it is called double sliding spotlight mode, which will be investigated in this paper using the example of the satellite TerraSAR-X and the airborne SAR system PAMIR. Several aspects like the ground resolution, Doppler frequency and Doppler-bandwidth will be analyzed. [C10092]

"Surface deformation analysis of the Campi Flegrei caldera, Italy, by exploiting the ENVISAT ASAR data with the SBAS-DInSAR technique"

We have investigated the deformation affecting the Campi Flegrei caldera (Italy), from 2002 to the end of 2006, by analyzing ENVISAT ASAR IS-2 data. This study has been performed by exploiting the SBAS-DInSAR algorithm that allows us to detect earth surface displacements and to investigate their temporal evolution via the generation of deformation time series. The presented analysis highlighted the renewed volcanic activity that started on mid-2005; moreover, we have combined the ascending and descending data in order to separate the vertical and east-west components of the detected displacements. The obtained results have been confirmed by the leveling data collected by the Osservatorio Vesuviano. [C10093]

"Ship detection with the fuzzy c-mean clustering algorithm using fully polarimetric SAR"

A fuzzy c-mean clustering algorithm to detect ships is proposed using fully polarimetric SAR data. The algorithm is unsupervised. It does not need the statistical decision and the performance is not data specific, as often arises with CFAR methods. A distance measure, based on a complex Wishart distribution, is applied using the fuzzy c-means clustering algorithm. The algorithm makes use the statistical properties of polarimetric data, and takes advantage of a clustering algorithm. It is thus expected that the algorithm could include fully polarimetric backscattering information for ship detection. Its effectiveness is demonstrated by applying it to detect the targets in a set of AIRS AR data. [C10094]

"Performance analysis of bistatic SAR configurations"

In this work we analyze the properties of integration time and azimuth coverage of bistatic SAR configurations. The kinematics of antennas is modelled as a motion at a constant velocity along a linear path. Orbits can be at different heights above the ground and have crossing projections on a horizontal plane. Footprints on the reference ground plane move at different velocities. Performances of bistatic SAR configurations are compared to those of monostatic ones. [C10095]

"Synchronization techniques for the bistatic spaceborne/airborne SAR experiment with TerraSAR-X and PAMIR"

The separation of transmitter and receiver makes bistatic SAR (synthetic aperture radar) systems preferable to conventional monostatic systems in several applications. However, this separation also leads to difficulties in image processing and in synchronization of the involved systems. For the upcoming hybrid bistatic SAR experiment with the TerraSAR-X satellite as transmitter and the airborne SAR/GMTI system PAMIR as receiver the synchronization issues are discussed in this paper and possible solutions are presented. [C10096]

"Elevation-dependent motion compensation for frequency-domain bistatic SAR image synthesis"

While numerically more efficient, frequency domain SAR image synthesis is less easily adaptable to the irregular real airborne trajectories than time-domain image synthesis. Trajectory nonlinearities have another consequence: The image focusing depends on the terrain elevation, hence motion compensation for irregular trajectories on mountainous areas must take into account terrain elevation data. Bistatic SAR processing is elevation-dependent even if the trajectory are perfectly linear (with the exception of the case where both aircrafts follow the same flight line). Terrain elevation can only be ignored at distance very large with respect to the elevation fluctuations, which is only the case in airborne bistatic SAR imaging when the area flown over is extremely flat. We describe here how the monostatic elevation-dependent motion compensation for omega-k algorithm is adapted to bistatic omega-k synthesis algorithm. [C10097]

"Influence of mechanical antenna distortions on the performance of the HRWS SAR system"

High-Resolution Wide-Swath (HRWS) Synthetic Aperture Radar (SAR) is a multi-static spaceborne Radar. The performance of the Radar system is improved by the mean of DBF on receive in azimuth and in elevation. This requires an relieve antenna array with large number of elements. In this paper the performance of large antenna array under the influence of plane distortions is analyzed. Presented is the influence on the array factor of symmetrical, unsymmetrical and random mechanical distortion. The paper considers also the influence on the performance of the antenna distortion on the High-Resolution Wide-Swath (HRWS) Synthetic Aperture Radar (SAR) in elevation. [C10098]

"Processing disdrometer raindrop spectra time series from various climatological regions using estimation and autoregressive methods"

A large data set of rain drop size distribution (RSD) measurements collected with Joss-Waldvogel (JWD) and 2D video disdrometers (2DVD) in UK, Athens, Japan and USA are analyzed. The objective of this work are manifold: i) show the differences of a wide climatological DSD-derived moments; ii) retrieve from this disdrometer data set the driving parameters of the normalized gamma RSD and perform a sensitivity analysis of these results by using different best-fitting techniques; iii) exploit the correlation structure of the estimated RSD parameters as input of a vector autoregressive stationary model in order to simulate time series (or horizontal profiles) of RSDs and, consequently, of either rain rate or path attenuation; iv) characterize the distribution of the inter-rain duration (or dry periods: DP) and rain duration (or wet periods: WP) to design a simple semi-Markov chain to represent the intermittency feature of rainfall process. The overall stochastic procedure to randomly synthesize (or generate) RSD time series is named Vector Autoregressive Raindrop Markov Synthesizer (VARMS) model. This stochastic RSD generation tool may find useful applications both in hydro-meteorology and radio-propagation. [C10099]

"Preliminary quantitative analysis of S-band FNCW radar data from atmospheric observation"

For more than three decades, S-band, frequency-modulated, continuous-wave (FMCW) radars have been used to study the structure and dynamics of the atmospheric boundary layer (ABL). With tremendous sensitivity and spatial resolution compared to their pulsed counterparts, these systems have been successfully applied to detection of clear-air turbulence in the lower atmosphere. In this study, data collected during field experiments by the University of Massachusetts' high-resolution S-band FMCW radar is used to illustrate and discuss system performance. S-band FMCW radar is sensitive to both Bragg scatterers (from spatial variations in radio refractive index of air) and Rayleigh scatterers (strong point-like echoes from nonatmospheric targets), and in the convective boundary layer Rayleigh echo appears to dominate the observed vertical profile of mean reflectivity. A postprocessing technique, which is based on single-lag covariance differences between the clear-air echo and Rayleigh echo, is applied to time-series of backscattered power to estimate clear-air component of the backscatter and remove the influence of Rayleigh scatter on the vertical profiles. The preliminary results of a quantitative analysis (mean and statistical distribution) of radar reflectivity are presented and compared with theoretical predictions about the convective ABL. [C10100]

"Compact PolInSAR for vegetation characterisation"

In this paper, we analyse the potential associated with a compact polarimetry (CP) P band spaceborne SAR system. Indeed, this architecture allows polarimetric acquisition without the usual reduction in swath. The CP data is shown to be almost equivalent to the full polarimetric data over extended targets, and the PolInSAR analysis can be performed without a significant loss of performance. [C10101]

"Cloud particle size measurements in Arctic clouds using lidar and radar data"

The ratio of the lidar and radar scattering cross section is sensitive to cloud particle size. High Spectral Resolution Lidar (HSRL) provides robustly calibrated scattering cross sections without the uncertainties introduced when conventional lidar data are corrected for attenuation. This paper explores the use of HSRL data and 35 GHz radar data for measuring particle size, particle phase, number density and the water content of Arctic clouds. [C10102]

"Characterizing the radiation fields in the atmosphere using a cloud-aerosol-radiation product from integrated CERES, MODIS, CALIPSO and CloudSat data"

CloudSat and CALIPSO cloud and aerosol information is convolved with CERES and MODIS cloud and radiation data to produce a merged 3-dimensional cloud and radiation dataset. [C10103]

"Cloud Profiling Radar Performance Eastwood Im"

The Cloud Profiling Radar (CPR), the primary science instrument of the CloudSat Mission, is a 94-GHz nadir-looking radar that measures the power backscattered by clouds as a function of distance from the radar. This instrument has been acquiring global time series of vertical cloud structure at 500-m vertical resolution and 1.4-km horizontal resolution since June 2, 2006. In this paper an overview of the radar performance during the first year in flight is provided. [C10104]

"Potential of forest height estimation using X band by means of two different inversion scenarios"

Polarimetric SAR interferometry (Pol-InSAR) is a powerful remote sensing method for forest height estimation by using the random volume over ground model (RVoG). At higher frequencies implementation of forest height estimation in X band is limited to less dense and low forest types where X band is able to penetrate through the volume to the ground. However, the penetration depth at X band is insufficient to cover all forest types. In the paper, forest height inversion at X band using two different approaches is demonstrated with focus on the impact of extinction on forest height estimation. [C10105]

"X-band extinction in boreal forest: Estimation by using E-SAR POLInSAR and HUTSCAT"

In this paper we study the extinction coefficient of boreal forest by utilizing airborne E-SAR X-band POLInSAR and HUTSCAT X-band profiling scatterometer measurements. By combining E-SAR VV-pol coherency with HUTSCAT tree height measurements we calculate forest extinction coefficients by RVoG model inversion and compare the results with extinction values obtained from HUTSCAT measurements. For retrieval of the extinction coefficient we propose robust RVoG model inversion procedure and discuss the model inversion conditions. Our results show, that extinction coefficient for boreal forest is quite low even for X-band, especially from nadir looking instruments. The extinction coefficient of forest canopy retrieved from HUTSCAT measurements is 0.15 dB/m and retrieved from E-SAR and HUTSCAT measurements is 0.9 dB/m. [C10106]

"The use of multidimensional copulas to describe amplitude distribution of polarimetric SAR data"

The paper focuses on a flexible model of multidimensional probability density function (pdf) dedicated to describe amplitude distribution of polarimetric SAR data. The model is based on the copula theory for characterizing the dependency between polarimetric channels (HH, VV, HV/VH or the target vector components). The benefit in using copula theory is to extend correlation concept to a wider dependence one, which may not be linear. From this point of view, the model is more flexible than the classical Wishart distribution. But it may include it. The other benefit in using the copula model is to separate the dependence concept from the shape of the marginal pdfs. Hence, this multidimensional characterization may be linked to classical 1D gamma pdf, or to a more flexible Pearson system of distributions. In the case of high resolution data, pdf shapes are becoming of heavy tailed and the Fisher system of distributions seems to be an interesting alternative for such a model. Any parametric 1D model may be used. The paper mainly focuses on the model itself and more precisely on the technique required to construct such multidimensional dependence function. The difficulties arise for copula on 3D in which the dependency is not homogeneous between the components (the link between HH and VV may not be of the same behavior as the one between HH and HV). Illustrations are given on classification and despeckling. Classification will be performed by a stochastic estimation maximisation (SEM). Despeckling will be achieved by a maximum A posteriori technique. [C10107]

"Segmentation of polarimetric SAR data using contour information via spectral graph partitioning"

A new method for segmenting polarimetric Synthetic Aperture Radar (POLSAR) data is proposed. Image segmentation is formulated as a graph partitioning problem. Spectral graph partitioning-known to provide perceptually plausible image segmentation results using one or more cues (e.g., similarity, proximity, contour

continuity)-is applied on POLSAR image data. The degree of similarities between pairs of pixels are calculated based on contour information. Graph partitioning is performed using the Multiclass Spectral Clustering method that minimizes the normalized cut cost function to ensure minimal similarity between partitions. The resulting segmentation is an approximation to the global optimal solution. C-band POLSAR data acquired by CV-580 are used for testing the performance. The results are found to closely agree with manual segmentations. [C10108]

"Comments on hybrid-polarity SAR architecture"

Recent work on compact polarimetry is reviewed in the context of the fifty-year history of polarimetric diversity. One promising form of this genre is hybrid-polarity (CL-pol), in which a synthetic aperture radar (SAR) transmits circular polarization and receives on two orthogonal mutually-coherent linear polarizations. The CL-pol technique is compared and contrasted to alternative compact polarimetric schemes. Useful characteristics that are unique to the hybrid-polarity architecture are described, especially rotational invariance and polarimetric calibration. [C10109]

"Unsupervised classification of polarimetric SAR data using graph cut optimization"

The paper presents a new framework for the classification of polarimetric SAR data. The underlying model introduces cyclic conditional dependencies among the class labels assigned to neighboring observations as a mechanism to regulate the spatial homogeneity of classification results. Classification is posed as an inference problem, and is solved by coherently integrating expectation maximization and graph cut optimization. Results based on real SAR data are presented. [C10110]

"Dual-polarization and dual-frequency radar scattering from ice crystals"

Dual-polarization and dual-frequency radar observables are simulated at 3, 35, and 94 GHz frequencies for remote sensing of clouds. Their use in ice crystal classification, ice water content and particle size estimation are evaluated. [C10111]

"POLINSAR for FOPEN using flashlight mode images along circular trajectories"

The airborne radar system RAMSES collected data over the Sweden forest to investigate the capabilities of detection at P-band and influences of different SAR parameters like resolution, central frequencies, and look angle. During this campaign, circular trajectories have been performed in order to analyze the presence of anisotropic scattering from the targets at P-band. We show the treatment of two circular trajectories using the Flashlight imaging mode and its ability to collect several SAR data with different look angles. The scope of this paper includes a general description of the operating mode of flashlight SAR images in the interferometric mode and the use of it for FOPEN purpose. The capabilities of detection of such polarimetric images have already been investigated, but without using the interferometric mode [1]. It had been shown that using circular trajectories at P-band was necessary to detect targets: first in our configuration detection was very difficult because the forest was very dense, secondly the targets were very sensitive to the orientation angle of the radar, which should not be the case at lower frequencies. Moreover, polarimetry and polarimetric interferometry are useful tools once the acquisition conditions ensure that detection is possible. Now, the full polarimetric and interferometric information are used in order to explore the potential of the POLINSAR circular mode to yield high detection rate. [C10112]

"Impact of surface heterogeneity on surface soil moisture retrievals from passive microwave data"

Water and energy fluxes at the interface between the land surface and atmosphere are strongly depending on the surface soil moisture content which is highly variable in space and time. The sensitivity of active and passive microwave remote sensing data to surface soil moisture content has been investigated in numerous studies. Recent satellite borne mission concepts, as e.g. the SMOS mission, are dedicated to provide global soil moisture information with a temporal frequency of 1-3 days to capture the high temporal dynamics of surface soil moisture. Passive satellite microwave sensors have spatial resolutions in the order of tens of kilometres. The paper investigates the impact of land surface heterogeneity on soil moisture retrievals from L-band passive microwave data at different spatial scales between 1 km and 40 km. The impact of sensor noise and quality of ancillary information is explicitly considered. A synthetic study is conducted where brightness temperature observations are generated using simulated land surface conditions. The soil moisture retrieval uncertainties resulting from the heterogeneity within the image pixels as well as the uncertainties in the a priori knowledge of surface temperature data and due to sensor noise, is investigated. [C10113]

"Volume and double-bounce decorrelation effects in the OVog model for Single-Tx PolInSAR"

The formulation of the complex interferometric coherence for the oriented volume over ground model (OVog) has been recently proposed for the case of dominant double-bounce mechanism from the ground when the interferometer is operated in single-transmit (bistatic) mode. This paper analyzes the two contributions to the total coherence function: the volume and the double-bounce terms. The study is performed by observing the model predictions of the coherence loci for several agricultural crop scenarios and with system parameters corresponding to the TanDEM-X mission. For low vegetation depths (up to 1 m) neither of the two contributions is negligible when the ground-to-volume ratio is low. However, when the backscattering returns from ground and vegetation are similar, i.e. ground-to-volume ratios around 0 dB, the volume decorrelation terms does not affect the coherence so much. As predicted by theory, higher vegetation layers yield an increase of the influence of the volume term and more differences between polarimetric channels. [C10114]

"Urban land cover classification: potential of high and very-high resolution SAR imagery"

A comparative study on the complexity of the urban environments in SAR imagery at different spatial resolutions is presented. Two datasets have been considered, including the city of Rome, Italy imaged in decametric resolution and the Frascati area (Rome, Italy) acquired in very high spatial resolution (~2 m) at L-band in a fully polarimetric mode. The different characteristics of the radar sensors require careful managing of the corresponding product capabilities to maximize the various pieces of information contained in the variety of scattering mechanisms. [C10115]

"Application of random set-based clustering to landmine detection with hyperspectral imagery"

We apply a population-based classifier to Long Wave HyperSpectral Imagery (LWHSI) for the purposes of landmine detection. In LWHSI, there are many environmental factors that are correlated with groups of samples (pixels in an image) in sample populations (individual images). These factors greatly affect samples' values making it difficult for standard classification models to perform well on a consistent basis. Population-based classifiers capture information correlated with sample populations. We perform classification experiments over a range of LWHSI imagery and compare results between the population-based classifier and standard kNN. After analysis, we show that the use of population-correlated information in LWHSI greatly improves classification results and consistency. [C10116]

"High resolution DSM generation from ALOS PRISM"

PRISM carried at ALOS satellite is expected to generate worldwide topographic data in respects of its high resolution and stereoscopic observation. The algorithms for generating digital surface model (DSM) and ortho-rectified image (ORI) have been developed for those objectives in Earth Observation Research Center / Japan Aerospace Exploration Agency (EORC / JAXA). During first one year following the successful ALOS launch, the capabilities of the algorithm have been widely tested. In this paper, the performance analysis intermediate results of DSM and corresponding ORI processing are described. First, the geometric model analysis of PRISM sensor is presented with the experimental results of the orientation processing. Then, the performance analysis of DSM and ORI generated with the PRISM geometric model is presented. The accuracy assessment results of generated DSM are presented from the comparison with high accuracy and high resolution reference DSM data sets of LiDAR DSM and Aerial Photo DSM. The accuracy assessment results of generated ORI are presented from the comparison with GCP. [C10117]

"The mega capture of the negro river, central amazonia, brazil: a novel feature revealed by SRTM data"

In Central Amazonia, Brazil, the Solimoes and Negro rivers converge to form the Amazonas, the largest river in the world. Interferometric-derived topographic data, generated during the Shuttle Radar Topography Mission (SRTM), indicate that the present-day lower course of the Negro River is the result of a mega fluvial capture governed by neotectonics. The data indicated that the ancient confluence of the Negro River with the Solimoes River was located where today is the mouth of Manacapuru River, 60 km west of the present location in the vicinity of the city of Manaus. [C10118]

"A wavelet based targets detection method for high resolution airborne SAR data"

A wavelet based automatic targets detection method for high resolution airborne SAR data is described in this article to receive faster and more accuracy detection. This method is based on the assumption that man-made objects are easily detectable at low resolution because their scattering is more persistent than that of natural objects. The algorithm involves an improved wavelet soft threshold filter (IWSTF) and a wavelet based RCCFAR detector. In order to retain the target feature, the wavelet soft threshold filter is improved by the strategy used in the enhanced Lee filter. Instead of using a global threshold, we adopted an adaptive threshold calculated

according to the detail coefficients in each scale. To accelerate the RCCFAR detector, two RCCFAR detectors are used. One is first applied to the approximate coefficients to make a coarse detection. The other one is applied to the filtered images in those regions which are regarded as candidate targets. Performance of the algorithm is assessed by some high resolution airborne SAR image and it shows that the algorithm can effectively reduce false alarms caused by speckles. [C10119]

"Urban subsidence observed by InSAR in Tianjin Region"

In this paper, we present the results of D-InSAR technique and conventional leveling at selected area in Tianjin city, using 8 ENVISAT SAR images between 17 October 2003 and 17 February 2005. The D-InSAR results show that the subsidence rate reached over 5 cm/year (7 cm within 16 months) in highly sinking area, and it is consistent with leveling results. D-InSAR is able to provide more details of urban subsidence, and it is supplement to leveling surveys in those areas with sparse leveling benchmarks. [C10120]

"SAR images classification using case-based reasoning method"

In this paper, we investigate a case-based reasoning (CBR) method for the classification of multi-temporal SAR images with the aid of ancillary information. Our scheme for the problem of multi-temporal SAR images classification comprises four main steps, including SAR image processing, construction of case library, case-based classification and post-classification processing. During the construction of case library, we employ a spatial-temporal analysis technique to remove fake cases, which can guarantee cases with high confidence. In the implementation of case-based classification, we propose a similarity assessment and use it for the case-based matching. After that, we investigate an object-oriented post-classification method which takes the shape of land use region into account, as a result, it leads to a more meaningful classification, and the regenerate land use image or map can be easier compared and combined with usual GIS data. Multi-temporal ENVISAT ASAR images from 2004 to 2005 are used in our experiments, where their resolution are 12.5 times 12.5 m. The study site is located in Beijing, China. During our experiments, we use the land use map of 2004 to assist the construction of the case library. The results of our experiments indicate that the CBR method is very promising for the classification of multi-temporal SAR images, where the overall classification accuracy can reach up to 80%. [C10121]

"Combining modern techniques for urban 3D modelling"

This paper will give an insight into modern ways of buildings modelling considering the case of TU Delft's campus with the use of classic photogrammetry tools and terrestrial laser scanning data. In addition we will use airborne LIDAR (Light- Imaging Detection and Ranging) for generating of extrusion models. The used methods aim to obtain models which can be used in Geographical Information Systems supporting different level of details. The detail factor may vary from pure city models, which are only blocks containing no facade information, to more complex 3D models with facade information as a texture and/or geometry. In our paper we will make some comparisons using a building model and discuss upon its information type and the achieved accuracy. Further more we will show an application example for the extrusion models. [C10122]

"Two-dimensional synthetic aperture radiometry over land surface during soil moisture experiment in 2003 (SMEX03)"

Microwave radiometry at low frequencies (L-band, ~ 1.4 GHz) has been known as an optimal solution for remote- sensing of soil moisture. However, the antenna size required to achieve an appropriate resolution from space has limited the development of spaceborne L-band radiometers. This problem can be addressed by interferometric technology called aperture synthesis. The Soil Moisture and Ocean Salinity (SMOS) mission will apply this technique to monitor global-scale surface parameters in the near future. The first airborne experiment using an aircraft prototype of this approach, the Two-Dimensional Synthetic Aperture Radiometer (2D-STAR), was performed in the Soil Moisture Experiment in 2003 (SMEX03). The L-band brightness temperature data acquired in Alabama by the ID- STAR was compared with ground-based measurements of soil moisture and with C-band data collected by the Polarimetric Scanning Radiometer (PSR). Our results demonstrate a good response of the 2D-STAR brightness temperature to changes in surface wetness, both in agricultural and forest lands. The behavior of the horizontally polarized brightness temperature data with increasing view-angle over the forest area was noticeably different than over bare soil. The results from the comparison of 2D-STAR and PSR indicate a better response of the 2D-STAR to the surface wetness under both wet and dry conditions. Our results have important implications for the performance of the future SMOS mission. [C10123]

"A method to retrieve soil moisture using ERS Scatterometer data"

Soil moisture is a key component in the hydrologic cycle and climate system. It is an important input parameter for many hydrologic and meteorological models. Taking the advantage of the multi-incident angles of the ERS Wind Scatterometer(WSC), a new soil moisture retrieving method, that significantly improves the surface backscattering presentation, is proposed in this study based on the Advanced Integral Equation Model (AIEM) and the Water-Cloud model. It utilizes the correlations in each backscattering components (bare soil and vegetation) for the simultaneous measurements of each incident angle pairs to reduce the effect of surface roughness and vegetation scattering on soil moisture estimation. The result is validated by using the ground measurements from the Intensive Observation Period (IOP'98) field campaign in 1998 of GAME/Tibet in the end of this paper, and the time series of the estimated soil moisture shows a consistent trend with those sampled on the ground. [C10124]

"Assessing pine barrens soil moisture regimes using Synthetic Aperture Radar (SAR) techniques"

The evaluation of soil moisture parameters within various soil regimes is somewhat difficult and challenging. Spatial and temporal invariability often complicates this process. The following study presents a format in which the spatial and temporal variations that govern upper surface (0-5 cm) soil moisture regimes within ecologically sensitive regions such as "Pine Barrens" can be studied. Based on in situ measurements, coupled with satellite derived analysis, radar backscatter, surface roughness, incidence angles, relative beam modes, and nominal area coverage, comparable soil moisture data between simulated and measured values within the upper surface (0-5 cm) soil moisture regime can be analyzed. [C10125]

"Ku-band, polarimetric, combined, short pulse scatterometer-radiometer system for stationary fixed platform, vessel and airborne applications"

In this paper a Ku-band (~15 GHz), dual polarization, combined scatterometer-radiometer system is described. The system allows carry out polarimetric (vv, vh, hh, hv), simultaneous and coincident microwave active-passive measurements of the observed surface (soil, vegetation, snow and water surface) parameters. The originality of the developed system is in the spatial-temporal combination of microwave active and passive channels of observation and its possible application for short distance sensing (the minimum operational range for the scatterometer is ~6 m) from low altitude platforms under far field conditions for both radar and radiometric observations. [C10126]

"Usage of multitemporal filtering of SAR images for change detection"

A methodology for change detection of artificial features using multitemporal series of SAR data is presented. The methodology uses time averaging of data from ERS-2 and Envisat yielding improved radiometric quality which highly improves the photointerpretability. The methodology is tested in several scenarios in the context of security applications when data needs to be gathered during cloudy season when optical satellites are unable operate. The results have been validated with very high resolution optical data from summer season. [C10127]

"Accuracy comparison of Differential Interferometric Synthetic Aperture Radar using LiDAR Digital Elevation Model"

This paper describes about accuracy of differential interferometric synthetic aperture radar (DInSAR) using different resolutions of external digital elevation models from ERS-1/2, STRM, LiDAR. For DInSAR technique, external DEMs have to have correct surface information. Typical DInSAR processes used the space-bone SAR data such as SRTM, ERS-1/2, JERS, and RADARSAT. However, they did not remove the vegetation and non-terrain feature. It is the cause of errors in final result using non-correct DEM. For improved accuracy of DInSAR results, in this paper, LiDAR DEM which has high spatial resolution with removed non-terrain data is used and compare with other DEMs. [C10128]

"Modeling of soil roughness using terrestrial laser scanner for soil moisture retrieval"

The present work reports the bases of an ongoing research whose main objective is the development of a methodology to characterize surface roughness models using terrestrial laser scanning devices. The classical measurements take the profile as the valuable information on roughness variations but a brand new paradigm is applied here where an original three-dimensional, multi-scale framework leads towards an accurate characterization of patterns and roughness for different surfaces. Terrestrial laser scanners are able to provide a complete picture of the roughness properties over the spatial scale of a Synthetic Aperture Radar satellite resolution cell. The paper describes the methodology for measuring the roughness of different surfaces and analyzes parameters what can be used as ancillary data in soil moisture retrieval from satellite datasets. [C10129]

"Change detections from sar images for damage estimation based on a spatial chaotic model"

Because of its all-weather and all-time characteristics, SAR images are particularly effective to monitor disaster events. When a disaster occurs, the image acquired from a SAR sensor changes dramatically. As a result, damage estimation for natural and human-made disasters from SAR images can be achieved by applying a change detection technique. Theoretically, SAR signals can be characterized as a chaotic phenomenon because that the scattering signals within a resolution cell are summed up coherently. Accordingly, SAR signal can be represented by a spatial chaotic model and characterized by its fractal dimension. In this paper, based on the spatial chaotic model, a simplified SAR image change detection procedure is proposed. The proposed method is then applied to estimate the flood-damage area caused by flooding events. Experimental results reveal that the proposed method is an effective and efficient tool for damage estimation from SAR images. [C10130]

"Monitoring of mining induced land subsidence using L- and C-band SAR interferometry"

In this study, we applied InSAR technique to Zonguldak Hardcoal Basin in Republic of Turkey using JERS-1/SAR, RADARSAT and PALSAR data in order to monitor mining induced surface displacement. [C10131]

"Second-order motion compensation in bistatic airborne SAR based on a geometrical approach"

Common efficient SAR processing algorithms are based on nominal operational conditions. Unfortunately, due to atmospheric turbulences and maneuvering errors, these conditions are often violated in real SAR systems. Hence, a crucial problem in most airborne SAR systems is the compensation of motion errors; if not corrected, the image quality will considerably degrade. A first-order motion compensation (MoCo) technique was developed at our institute, based on a precise knowledge of the position and the velocity of the transmitter and the receiver. The problem arose while proceeding with our processing algorithm, since the reconstructed image was better focused but not completely focused. Our paper proposes a second-order MoCo technique that will considerably improve the reconstruction of the SAR image. While the first-order MoCo considered the range and azimuth times, the second-order MoCo approximation will consider the frequencies. Experiments with different sets of bistatic airborne SAR data are performed based on this solution, and some promising results are given. [C10132]

"Deformation monitoring over a large area via the ESD technique with data takes on adjacent tracks"

Enhanced spatial differences (ESD) is a new processing chain for monitoring ground deformations at small scale over wide areas. Core of the processing is the spatial differencing (SD) step that performs a quick preliminary estimation of the mean deformation velocity and residual topography via spatial differences. We show the results achieved by applying the ESD algorithm to data collected over adjacent tracks for ERS and ENVISAT. [C10133]

"Research on differential interferometry for spaceborne bistatic SAR"

Differential interferometry (D-InSAR) for spaceborne bistatic SAR is studied. According to advantages of the system, particularities and superiorities of D-InSAR based on spaceborne bistatic SAR are discussed first. Then, solid baseline is decomposed and the model of "three-pass" D-InSAR is established. Afterwards, the theory of data fusion is introduced to D-InSAR and a new method is put forward to avoid the max detection error. A simulation experiment accompanied by very good result is shown in the end. [C10134]

"Translational variant bistatic SAR signal space-time feature and processing method"

In this paper, we discuss the translational-variant feature of translational-variant bistatic SAR configuration using the space Taylor's expansion in section II. In section III, a new translational-variant bistatic SAR imaging method is proposed, which uses scaled IFFT technique to eliminate the translational-variant feature of SAR space resolution. Finally, some numerical experiments are conducted to demonstrate the feasibility of this method and discuss the depth-of-focus of the scaled IFFT bistatic SAR imaging algorithms. [C10135]

"Optimizing interferogram generation, pixel selection and data processing for high non-linear deformation monitoring with Orbital DInSAR"

A necessary step for every DInSAR technique is to properly select the data from which deformation information will be calculated. Two main processes must be done in this sense, the interferogram set creation and the quality pixel selection. In this paper we will present advances concerning both issues: a new method for selecting a high quality and reduced interferogram set solving an equivalent minimum spanning tree system and a pixel selection criterion based in region growing type algorithms. Furthermore, in order to avoid errors when dealing with highly non-linear deformation patterns, a temporal block differential processing is proposed.

[C10136]

"A bistatic SAR interferometric simulator for fixed receiver configurations"

Bistatic SAR systems are an emerging research field. In which context, the Universitat Politècnica de Catalunya is developing a ground based bistatic system using ESAs ENVISAT and ERS-2 as transmitters. In this paper we characterize the bistatic interferometric phase and the different sources of decorrelation. We will also present a bistatic interferometric simulator which is able to generate realistic synthetic bistatic interferograms. The simulator is validated with real data obtained with our bistatic acquisition system, named SABRINA. [C10137]

"Comparison between MARSIS & SHARAD results"

MARSIS (Mars advanced Radar for subsurface and ionosphere sounding) is a low frequency nadir looking sounding radar selected by ESA as a payload of the Mars Express mission, whose primary Scientific Objective is to map the distribution of water both solid and liquid, at global scale on the Martian crust. MARSIS is the first instrument to be able to detect what lies beneath the surface of Mars (up to about 5 km). MARSIS operates with a very high fractional bandwidth: 1 MHz bandwidth allows a vertical resolution of 150 m in vacuum which corresponds to 50-100 m in the subsurface, depending on the electromagnetic wave propagation speed in the crust. The center frequency of the pulses transmitted by MARSIS can be set to 1.8 MHz, 3 MHz, 4 MHz and 5 MHz. On day side operations, it operates only in 4 MHz and 5 MHz due to the ionosphere plasma frequencies of Mars cutting off all frequencies lower than 3 MHz. All the four carrier frequencies are available for subsurface sounding on night side. The Mars Shallow Radar Sounder (SHARAD), a facility instrument provided by the Italian Space Agency (ASI), is embarked on board the NASA Mars Reconnaissance Orbiter spacecraft. SHARAD began science operations on October 3rd 2006: it has been collecting data from surface and subsurface. This instrument penetrates to roughly half a kilometer below Mars' surface to search for information about underground layers of ice, rock and, perhaps, melted water. SHARAD operates with a center frequency of 20 MHz and 10 MHz bandwidth. These parameters allow vertical resolution on the order of 10-20 m. The carrier frequency of 20 MHz guarantees the capability of SHARAD to operate in day side as well as in night side. Both MARSIS and SHARAD use the principle of a Synthetic Aperture Radar (SAR) to achieve a fine along-track resolution. In particular, MARSIS is an unfocused SAR with best along-track resolution of 2 km; data coming from SHARAD can be processed with focusing algorithm (Chirp Scaling Algorithm), resulting in a best horizontal resolution of 300 m. This paper provides a comparison between MARSIS and SHARAD images in different zones of the Mars' surface. From the preliminary analysis it has been evident that MARSIS detects signals from subsurface interfaces at 3 km of depth, while the signals received by SHARAD in the same zone and at the same depth are much weaker compared with the background noise. However, SHARAD radar-grams show subsurface interfaces at 100-200 m of depth: these interesting targets can not be discriminated by MARSIS because of its coarse vertical resolution. At the same time, SHARAD data add to MARSIS data scientific information about the upper portions of the crust of Mars. [C10138]

"Radar interferometry for 3-D mining deformation monitoring"

Geodetic information of terrain can be measured using remote sensing techniques such as photogrammetry, airborne laser scanner (ALS) and interferometric synthetic aperture radar (InSAR). They are considered to be relatively more cost-effective than and complementary to conventional ground-based surveying methods. Our previous studies demonstrated the capability of using differential InSAR for underground longwall mining subsidence monitoring in New South Wales, Australia. The mining subsidence (vertical surface deformation) was measured using DInSAR with the assumption of negligible horizontal deformation. However, the ground surveying data shows that the underground mining activity may induce horizontal surface deformation. Therefore, both ascending and descending orbits and different swath modes of ENVISAT/ASAR data are used in this paper to quantify the vertical and horizontal vectors of mining deformation. [C10139]

"Six years of land subsidence in Shanghai revealed by JERS-1 SAR data"

Differential interferometric synthetic aperture radar (SAR) (DInSAR) has proven to be very useful in mapping and monitoring land subsidence in many regions of the world. Shanghai, China's largest city, is one of such areas suffering from land subsidence as a result of severe withdrawal of groundwater for different usages. DInSAR application in Shanghai with the C-band European Remote Sensing 1 & 2 (ERS-1/2) SAR data has been difficult mainly due to the problem of decorrelation of InSAR pairs with temporal baselines larger than 10 months. To overcome the coherence loss of C-band InSAR data, we used eight L-band Japanese Earth Resource Satellite (JERS-1) SAR data acquired during 2 October 1992 to 15 July 1998 to study land subsidence phenomenon in Shanghai. Three of the images were used to produce two separate digital elevation models (DEMs) of the study area to remove topographic fringes from the interferograms used for subsidence mapping. Six interferograms

were used to generate 2 different time series of deformation maps over Shanghai. The cumulative subsidence map generated from each of the time series is in agreement with the land subsidence measurements of Shanghai city from 1990-1998, produced from other survey methods. [C10140]

"A stability analysis of the lambda estimator for solving the ambiguity problem in persistent scatterer interferometry"

Persistent Scatterer Interferometry is a well-known technique to obtain displacement rates in urban areas from a stack of SAR interferograms. Besides the original method introduced by A. Ferretti, C. Prati and F. Rocca in the late 1990's, which estimates the displacement rates and DEM corrections by an ensemble coherence maximization approach (periodogram) based on a common master image, several other algorithms have been introduced in the past few years. One of these approaches has been developed at DLR It incorporates the Least-squares AMBiguity Decorrelation Adjustment (LAMBDA) method that was originally developed for fast GPS double difference ambiguity estimation. In this paper different parameters are tested to investigate robustness and performance of this estimation method. At first the effects of a reduced number of observations and varying reference points on the estimation with LAMBDA are analyzed while in the second part a direct comparison between LAMBDA and ensemble coherence maximization (periodogram) is performed. [C10141]

"Correction of tropospheric water vapour effect on ASAR interferogram using synchronous MERIS data"

The water vapour in troposphere has been identified as one of the major errors in SAR interferograms, which can cause a spatial delay during two non-simultaneous acquisitions. The microwave-signal propagation path delay due to water vapour may reduce the reliability of deformation measurements. In this paper, it aims to assess the water vapour effect on interferograms, and apply synchronous MERIS data to reduce the effect on ASAR interferograms. Due to the co-existence of MERIS and ASAR on board of ENVISAT satellite, they can acquire data co-located in the same time and space. So it has a unique advantage to combine MERIS and ASAR data to reduce the tropospheric water vapour effect on ASAR interferograms. However, the method is not so well operational, and still existing some problems need to be further discussed, such as: how to deal with the cloud coverage over MERIS water vapour image; and how to register MERIS to ASAR from different reference systems, and so on. These will be discussed in this paper, and novel ideas are proposed to deal with them. The discussions are based on the application of the test site in the middle and lower reaches of Yangze River, southwest Hubei province, China. [C10142]

"Point target interferometry for natural and artificial scatterers"

The Coherent Targets Monitoring technique is providing superior ground deformation mapping compared with standard interferometry based on one pair of Master/Slave scenes. This is because using a larger data set it is possible to estimate and correct for additional phase error sources. Also the point targets detected as coherent targets are generally characterized by stronger signal that provides more accurate phase information than the clutter present in the rest of the scene. This paper reviews previous work in SAR noise estimation and shows the advantages of point targets versus distributed targets. Results from the Turtle Mountain/Frank Slide site show that the measured phase/deformation errors at the point target positions are within the estimated range. Corner reflectors with a high SNR are expected to improve the accuracy of the method. [C10143]

"Evaluation of accuracy in PS-based radar interferometry with simulated data"

This paper analyzes the relationship between the noise level in interferometric phases at permanent scatters (PS) and the accuracy in deformation measurements with the PS-based differential SAR interferometry (PS-DInSAR). The study is carried out based on interferograms that are simulated with parameters of 26 ERS-1/2 SAR scenes over Shanghai. The results show that in the cases of high phase signal to noise ratio (noise level lower than ± 0.5 rad), the accuracy of the deformation rates estimated with PS-DInSAR can be up to about ± 2 mm/a, and the accuracy of the estimated elevations is about ± 1 m. The accuracies decrease with the increase of the noise level of the phase data. When the noise level is ± 0.8 rad, the accuracy of deformation measurements decreases to ± 1 cm/a and that of elevation measurements decreases to ± 3 m. [C10144]

"Glacier displacement field estimation using airborne SAR interferometry"

This paper deals with the methodology in the processing of airborne SAR data to measure glacier displacement fields. The possibility to retrieve a 2D displacement map of the deformation in slant-range geometry with an airborne platform is discussed. A new extended multisquint approach is proposed to simultaneously estimate

residual motion errors and the along-track displacement of the glacier, while the across-track displacement is obtained by means of differential interferometry. Experimental results are shown with data acquired by the Experimental SAR (E-SAR) of the German Aerospace Center over the Aletsch glacier in the Swiss Alps.

[C10145]

"Persistent scatterer density improvement using adaptive deformation models"

Because the quality assessment of Persistent Scatterers (PS) is dependent on the deformation model chosen, PS may be falsely rejected due to model imperfections. To accept these PS, more advanced deformation models should be used. Two methods applying adaptive deformation models are proposed. The first is based on a sequential scheme of alternative hypothesis testing of extended deformation models within the integer least-squares framework. The second uses an iterative scheme of global deformation modeling based on previous PS results. Application of the techniques to a salt mining area in The Netherlands confirms the increase in the number of detected PS. [C10146]

"Application of a coherent modeling on Sahelian grassland"

The validity of a coherent Sahelian-grassland scattering model is determined by comparing the model predictions with satellite measurements of a representative site. This model considers the realistic botanical structure of grassland. The site Agoufou, located in the Northern Mali, was selected as the test target. This site is governed by a semi-arid tropical climate. Its vegetation is mainly composed of shrubs and annual grass. HH polarization backscattering data was collected over an entire growing season at different incidence angles by means of the ENVISAT ASAR. Simulations provided by the coherent model show a good agreement with measured data having a correlation coefficient equal to 0.92. Model predictions show that the HH polarization component is higher than the W polarization component during all growing season. Significant parameters are shown to be the grass density, the soil moisture content and the grass moisture content. The most sensitive parameter is the ground soil moisture content. Moreover, it is observed that the variation of the backscattering coefficient for all parameters can be represented by a linear regression function. [C10147]

"Study of millimeter-wave radar for helicopter assisted landing system"

This paper discusses the development of an algorithm used to simulate the effectiveness of millimeter-wave radar in imaging a rough terrain, for the purpose of helicopter assisted landing. Using an externally generated terrain and the physical optics approximation, the algorithm computes the backscatter response of the terrain when illuminated by a real aperture antenna. Results are presented from simulating terrains with different macroscopic features, such as a hump, ditch or a slope. It is shown that operating at millimeter-wave, more specifically at W-Band frequencies, is ideal for such an application where a compact sensor is required to achieve high resolution imaging. [C10148]

"A simulator for SAR sea surface waves imaging"

This paper describes a synthetic aperture radar (SAR) sea surface waves simulator. The simulator, based on the velocity bunching (VB) theory, has been developed and implemented modularly and its use can also assist microwave remote sensing courses. The present version of the software is run in classes at National Oceanographic Centre of Southampton (NOCS), UK and at the Università di Napoli Parthenope, Italy. [C10149]

"The effect of polarization ratio on RADARSAT wind vector retrievals"

In this presentation, the polarization ratios were calculated from AIRSAR polarimetric SAR data and ENVISAT ASAR dual-polarization data; and their empirical CC parameters which depend on incidence angle were obtained. Five C band HH polarization RADARSAT-1 SAR images are used to validate these polarization ratios and we found that the empirical parameter $\alpha = 0.5$ is superior to other possible parameter α values.

[C10150]

"Pulse electromagnetic sounding of the petroleum- containing layered medium"

In this research, propagation of super wide-band pulse in a frequency dispersive medium representing the oil-saturated collector. The capability of their use for geonavigation in techniques of lateral drilling is discussed on the basis of the results of simulation obtained. The complex dielectric constant of oil-saturated rock was calculated on the basis of refraction mixing dielectric model, the oil, sodium chloride solution, methane, quartz and bentonite being contained in each layer. The thin cylindrical vibrator of finite dimensions was used as antenna, being excited by voltage the like one period sinus pulse of nanosecond duration. The time-domain structure of pulse propagation in a plane-layered medium was calculated. Attenuation of power flow pulse

reflecting from oil-bearing bed was studied. The gain-frequency characteristic relating to each particular layer was analyzed proving the medium of petroleum collector to operate like a low-pass filter. [C10151]

"Validation of the soil dielectric spectroscopic models with input parameters based on soil composition"

In this paper, a comparative analysis of dielectric spectrum predictions for moist soils in the microwave band was carried out, regarding a well known and prevalent semiempirical dielectric model proposed in [1]-[3], on the one hand, and recently developed generalized refractive mixing dielectric model [5], on the other hand. The analysis is based on the measured dielectric data borrowed from [4], in which a set of soils measured includes all of grain-size distributions that are observed in nature, with measurements being performed over the range from 40 MHz to 17 GHz. In the case of the soil measured in [4] that has an intermediate position in terms of its texture parameters, input data for the semiempirical model were attained, using the texture and soil mineralogy data available in [4], and dielectric spectra predictions both for the dielectric constant and loss factor were calculated. Simultaneously, with the use of the dielectric data of [4], input parameters for the generalized refractive mixing dielectric model were derived, and dielectric predictions for the same moistures were calculated. Comparative analysis based on the measured data together with both predictions showed the semiempirical dielectric mixing model to generate dielectric constants and loss factors that have a noticeable bias relative to the measured ones, correlation coefficients being on the order of 0.93. At the same time, the GRMDM predictions appeared to correlate with the measured values with noticeably better accuracy both in the frequency and moisture domains. As a result, the ability to make accurate predictions for dielectric spectra with the use of the SDMM was shown to be doubted, regarding the moist soils, which falls out of the scope of soils measured and fitted to develop the SDMM in [1]-[3]. On the contrary, the GRMDM [5] has proved to be able to make predictions for the dielectric spectra of moist soils with the same error as that of initial dielectric measurements. [C10152]

"Semi-Analytic Mode Matching (SAMM) algorithm for efficient computation of nearfield scattering in lossy ground from borehole sources"

The 3D semi-analytic mode matching (SAMM) algorithm is used to determine nearfield scattering from underground targets in lossy soil, where the source is a dipole placed within a borehole in the ground. Scattering is described by moderately low-order superpositions of spherical modes placed at multiple user-specified coordinate scattering centers (CSCs); the mode coefficients are found numerically by least-squares fitting all boundary conditions at discrete points along the relevant interfaces while at the same time obeying radiation conditions. SAMM results are compared with a completely different method: the Half-Space Born Approximation (HSBA). Good agreement between methods serves as algorithm validation. [C10153]

"Polarimetric microwave emission from snow surfaces: 4th Stokes component analysis"

The effect of ice on polarimetric 4th Stokes component observations is investigated using WindSat data over Antarctica. The difference in the magnitude of the signal observed during (July 2003) and summer (February 2004) months are investigated using a second harmonic sine function of the azimuth look angle. The seasonal variations are further investigated by a time series of the 4th Stokes component for a location in Wilkes Land in east Antarctica and compared with a time series observed by the ERS scatterometer (ESCAT) from a previous work. The paper discusses the potential of a polarimetric radiometer in providing information about scattering and thermal properties of a snow ice pack. [C10154]

"Development of a baseband signal ATI-SAR simulator for ground moving target indication"

Along-track SAR interferometry has long been used to measure ocean surface currents with small velocities. There is a significant potential to employ this technique to detect slow ground moving targets with small radar cross-sections. In this paper, we present the development of a baseband signal simulator on ground moving target indication with along-track SAR interferometry. We summarize current state-of-the-art along-track SAR interferometry techniques and algorithm developments for ground moving target detection, and consider the case of an airborne SAR operated in the stripmap mode. And then we propose to investigate and develop advanced techniques for potential civilian and military applications in Australia. [C10155]

"Remote sensing of glacier by ground-based radar interferometry"

The Belvedere Glacier, east face of Monte Rosa, has been investigated for many decades because of a long history of outburst threatening the village of Macugnaga and, in the latest years, a surge-type evolution, responsible for the formation of a large depression at the foot of the east wall of Monte Rosa, which hosted a supraglacial lake named "Lago Effimero" in summer 2002. In this contribution, a Ground Based SAR (GB-SAR)

interferometer was employed for determining the ice-flow velocity of the illuminated part of the Belvedere Glacier in order to enhance the understanding of ice flow mechanics and hopefully reduce the glacier hazard. The deformation field and the velocities measured by the GB-SAR sensor have been validated with data by more conventional ground-based measurements. [C10156]

"Introduction of a grid-based filter approach for InSAR phase filtering and unwrapping"

This work presents a phase unwrapping (PU) algorithm for SAR interferometry based on an approximate grid-based filter (GbF). This PU algorithm, which makes use of state space techniques, performs simultaneously noise filtering and phase unwrapping. The formulation of this technique provides independence from noise statistics and is not constrained by the non-linearity of the problem. Results obtained with synthetic and real data show a significant improvement with respect to conventional PU algorithms in some situations. [C10157]

"Frequency domain imaging algorithm for spaceborne/airborne hybrid bistatic SAR"

A frequency domain imaging algorithm for the hybrid spaceborne/airborne BSAR is presented. The key point of deriving the algorithm is the analytical evaluation of the system point target response's 2-D spectrum. To overcome the difficulty of resolving analytical solution for the stationary phase point, the spectrum's phase is approximated by two-order Taylor expanding around the point, which is not only in the neighborhood of the system's corresponding stationary phase point but also can be obtained analytically. Thus the approximated analytical spectrum is pretty close to the actual one. In the imaging algorithm, both range-dependent range cell migration and azimuth-dependent range cell migration are compensated in two steps: Inverse Scaled Fourier Transform which can be realized through the chirp z-transform and phase multiplication. The validity of the algorithm is demonstrated by experiment with the simulated data. [C10158]

"Automobile-based Bistatic SAR processing and experimental results"

In recent years, the interest in bistatic synthetic aperture radar (SAR) has rapidly increased and many bistatic SAR models and processing methods are presented. But some technical problems of bistatic SAR, such as synchronization (in both time and frequency) and the imaging processing of bistatic raw data, have not been resolved sufficiently. To verify bistatic SAR system synchronization plan and imaging processing algorithm, the University of Electric Science and Technology of China (UESTC) developed an Automobile-Based Bistatic SAR system because of its convenience, and carried out a series of experiments. Comparing with airborne monostatic SAR imaging processing, some special problems should be considered. In this paper, we introduce the Automobile-based Bistatic SAR system and discuss the corresponding imaging processing method. [C10159]

"Shape from shading of SAR imagery in fourier space"

A new shape from shading technique is presented in this study. This technique is a further development of Pentland's linear shape from shading technique (1990). The equations and geometric modeling are extracted for SAR imagery. However, the modeling can be easily adapted for optical images as the geometric modeling is much simpler than SAR images due to the fact that the geometric transformation from 3D object space to 2D image space in optical imagery is modeled by a well-estimated orthogonal projection or perspective projection itself. This solution for shape from shading problem employs linear estimation of the reflectance model using Taylor expansion. As there are one known image intensity and two unknown surface gradients for every pixel, there is no direct solution. By using a global approach and solving all the image pixels at the same time, it is possible to estimate an answer and overcome the ambiguity problem in the incidence angle estimation. For this purpose, the Fourier transform of the expanded reflectance model will be taken and as the Fourier transform of the surface gradients is a linear function of the surface height, the number of equations and unknowns will be equal and the system is soluble. In the proposed algorithm, an iterative approach is used to improve the accuracy of the estimated surface height. Iteration starts with a low resolution digital terrain model (DTM) of the area for the initial guess of the surface gradients and based on the equation system in Fourier space, the iteration continues until a threshold is reached or the number of iterations exceeds a tolerance. The technique is tested on a Radarsat image from Death Valley area and the results are shown and validated with the available DTM of the area. Based on the results, it seems that the proposed method is sensitive to the noise. The noise problem should be carefully considered either during the reflectance modeling or during solving the problem in the Fourier space as a filtering problem. [C10160]

"ISAR imaging of helicopter"

Conventional envelope alignment method of ISAR imaging assumes that the target is a rigid body, and therefore, the correlation between one-dimensional range profiles at neighboring time slots gives a larger value compared to correlation between time separated range profiles. But this is not the case for targets such as helicopter which

have rotating body parts. In this paper, an envelope alignment algorithm for helicopter target ISAR imaging is proposed. For every range profile, correlation with other range profiles are done, and the range profiles with larger correlation value are used to provide an initial estimate of the target motion parameters by polynomial fitting. Then the estimated parameters are averaged to get a better estimation. The position of the rotor signals are obtained by taking the difference of the range profiles in the slow time domain. The rotor signals are then suppressed by zero-force windowing technique. Simulation results have shown the effectiveness of this algorithm. [C10161]

"Scattering from 2D-dielectric random surfaces effect of roughness and moisture of seedbed surfaces upon the bistatic scattering coefficient"

We propose a statistical model to describe the seedbed surfaces and we study the roughness and moisture influence upon the backscattering coefficient and the scattering patterns by means of Monte-Carlo predictions. For each realization, the scattering amplitudes are obtained by the C method. [C10162]

"Disaster monitoring and environmental alert in Taiwan by repeat-pass spaceborne SAR"

The prevailing complex geological and ecological conditions of Taiwan have drawn considerable attention from various geo-ecological communities because of their vulnerability to produce various natural hazards at different scales. Located in the tropical/subtropical zone of the Pacific Rim, its ecological and rugged mountainous properties are environmentally sensitive making monitoring and observations especially difficult because of the high population density. For example, in terms of natural hazard mitigation tectonically active regions are used for analyzing the cause of abundant risk events, such as earthquakes, landslides and land subsidence. In fact Taiwan is well suited as a test site for studying those geologically disastrous processes. Implementing novel techniques of space remote sensing has proved to be an effective means in recent years for greatly improving our understanding of these phenomena. In this paper we report on the monitoring of such events using multi-modal polarimetric and/or interferometric SAR images at C and L band from ERS, JERS-1, RADARSAT-1, ENVISAT, and from the recent ALOS satellite. For crustal and surface deformation, we used radar image pairs with long temporal baselines and large areas of coverage for investigating deformation over Western Taiwan. Pre-seismic and co-seismic deformation patterns are spatial-temporally analyzed. The other topic deals with the coastline changes observed from a sequence of ERS-1/2 SAR images within the years of 1996 to 2005. Waterlines were extracted using multi-scale procedures of edge detection and were corrected with tidal motion data. Substantial analyses were carried out in conjunction with ground surveys and lidar mapping. The topographic feature changes due to large scale landslides triggered by torrential rains were also monitored. In addition, the SAR interferograms were used to analyze the deposition changes along the riverbeds and riverbanks for short-intervals using optimal baselines. Summary and remarks on the implementation of such multi-modal polarimetric and/or interferometric SAR imagery for environmental monitoring are provided. [C10163]

"Investigation of H.264 intra coding for SAR image"

In this paper we investigate the performance of H.264 intra coding for synthetic aperture radar (SAR) image. The results show that H.264 intra coding is a high performance coder for the SAR image. However, when the SAR image is despeckled, H.264 Intra coding is not so efficient than the wavelet based image coder, such as JPEG2000 and SPIHT. Then more efficient representation is needed when H.264 Intra Coding is used to code the despeckled SAR image. [C10164]

"Optimum design of antenna pattern for spaceborne SAR performance using improved NSGA-II"

Optimization of antenna array using in SAR system is considered in this study. A robust evolutionary algorithm, non-dominated sorting genetic algorithms (improved NSGA-II), is applied on a spaceborne SAR antenna pattern design. The system consists of two objective functions with two constraints. Pareto front are generated as a result of multi-objective optimization. After being validated by a test problem ZDT4, the algorithms were used to synthesis antenna radiation pattern. The good results with low ASR and high directivity are obtained. [C10165]

"An advanced airborne multisensor imaging system for fast mapping and change detection applications"

The advanced airborne multisensor imaging system (AAMIS) has been developed for a light fixed wing aircraft. It integrates a suite of state-of-the-art electro-optical (EO), thermal, hyperspectral, and Lidar imaging instrument packages for simultaneous active ranging and passive imaging that covers the electromagnetic (EM) spectrum of the visible and near infrared range and the long-wave infrared range. AAMIS has been tested for today's fast mapping and change detection needs. It demonstrates leading performance in providing comprehensive

geometric and geophysical aerial image products with high spatial, spectral, radiometric, temporal and range resolutions. High resolution innovative data products collected by AAMIS sensors are presented. These include 3.5 cm resolution orthomosaics for a complete 15 km times 25 km large area coverage, 1 ft resolution hyperspectral images with contiguous 10 nm spectral resolution for the 410-820 nm range, 0.02 K resolution thermal images in a large 1 k by 1 k frame video format, and 20 cm range accuracy 3D Lidar mapping products. [C10166]

"Effects of attitude error on spaceborne ScanSAR mosaic"

Attitude stability is a very important parameter for the platform design of scanning synthetic aperture radar (ScanSAR) satellite. In this paper, the effect of satellite attitude error on the Doppler parameters is derived in detail. And the effects of Doppler centroid frequency error on spaceborne ScanSAR mosaic in azimuth are analyzed, to provide a theoretical guideline for the design of spaceborne ScanSAR system, as verified by simulations. [C10167]

"A combined sensor system of digital camera with LiDAR"

In order to utilize the advantages of the high height accuracy of laser ranging and the good planimetric accuracy of processed digital camera imagery, the feasibility of a combined sensor system of LiDAR with digital camera using area or line array CCDs is first analyzed in this paper. The hardware composition of the combination system is given and the algorithm of integrally processing LiDAR points cloud and digital camera image is illustrated. Software development and availability for the processing at all stages of the work flow, is the key to the full utilization of such an integrated system. [C10168]

"A high resolution SAR sensor for space and airborne applications"

This paper discusses the general layout to achieve a flexible SAR radar design with the potential for extremely high resolutions. [C10169]

"Cassini RADAR: investigation of titan's surface parameters by means of Bayesian inversion technique and gravity-capillary waves modelling of liquid hydrocarbons surfaces"

During the first two years of the Cassini mission, a great amount of data dealing with Titan's surface has been collected. In particular, the analysis derived from the SAR imagery reflects the complex Titan's surface morphology. In fact, in the different Cassini radar images a certain number of areas with peculiar features has been identified, such as: dark and bright areas (Ta, T3), periodic structure ("sand dunes") and, above all, hydrocarbon lakes [2],[11]. The proof for the presence of hydrocarbons lakes on Titan has been obtained during the T16, the radar pass performed on Titan by the Cassini spacecraft on 22 July 2006 [12]. In this paper, the investigation of Titan's surface parameters (physical and morphological) has been carried out by the means of Bayesian inversion technique, and simulations of the wave motion for the hypothesized hydrocarbons liquid surfaces has been performed. [C10170]

"Closed form expressions for scattering matrix of simple targets in multilayer structures"

Scattering matrix of a simple target embedded in multilayer planar structure is derived. The structure is excited by an elliptically polarized plane wave incident at an oblique angle. The calculation of the electromagnetic fields is performed in spectral domain. The scattering matrix of a planar electric dipole printed on upper interface and surrounding by free-space is evaluated. The obtained results agree with those existing on the literature for normal incidence case. [C10171]

"Dielectric spectroscopic model for tussock and shrub tundra soils"

In this paper, the measured microwave dielectric data are presented for some soils collected in the tussock and shrub tundra area located on the North Slope, Alaska, near Toolik Lake, at N 68deg 38', W 149deg 35' with an elevation of 730 m. The measured samples represented the organic rich soil picked up from the middle and base of tussock, organic poor soil from the depth of 20 cm in the valley between tussocks, and organic rich soil from the depth of 20 cm in the shrub tundra site. The measurements were carried out in the range of frequencies from 0.5 to 16.0 GHz and temperatures from -30degC to +25degC. On the basis of that data, the spectroscopic model of complex dielectric constant was developed for the moist soils measured, using the methodology of the generalized refractive mixing dielectric model [1]. This model takes into account contributions from the organic/mineral contents of soil, soil ice, free liquid soil water, and bound soil water arising due to interaction of soil water molecules with the surface of organic/mineral and ice particles. The complex dielectric constants for all the types of soil water observed were shown to follow the Debye formulas, with a single relaxation frequency for

every distinct type of soil water. The temperature dependences were obtained for the parameters of the generalized refractive mixing dielectric model, including the parameters of soil water Debye relaxation, that is, the low and high frequency limits of dielectric constant and relaxation time, as well as the ohmic conductivity relating to every component of the soil water. The previously unknown physical phenomenon of liquid soil water transformation into a transition type of bound water, instead of ice, was observed in the range of temperatures below -6degC, which appeared to arise in the organic rich soils studied. The results obtained can be considered as a substantial contribution to the soil dielectric database, to be employed in the physically based data processing algorithms for radar and radiometry remote sensing of the northern circumpolar region. [C10172]

"A UAV avionics system to facilitate VHF depth sounding and SAR"

An avionics system for an autonomous UAV platform supporting VHF depth sounding and SAR is under development. The system is divided into navigation, communication, and data processing or logging. This design provides accurate position, velocity, acceleration, and attitude data. It supports over-the-horizon communication via an Iridium satellite link. The data collected by this system will allow for motion effects of the UAV to be compensated for, to enable SAR image formation. [C10173]

"Surface clutter analysis and ranging sidelobe level requirements for spaceborne meteorological radars"

Pulse compression techniques are very attractive in the development of new-generation spaceborne meteorological radars, because it has the advantages to reduce the transmit power requirements and improve the measurement precision by increasing incoherent average samples. Compared with TRMM, which employed a pulsed-CW signal, it is very important to analyze the effect of surface clutter from ranging sidelobes of the returned signal after pulse compression. In this paper, the effect of surface clutter with different antenna sidelobe levels and different ranging sidelobe levels are analyzed in details. Based on the analysis of surface clutter, the requirements for antenna sidelobe level and pulse compression range sidelobe level are proposed. [C10174]

"Scientific use of TerraSAR-X"

TerraSAR-X is a new German radar satellite scheduled to be launched in May, 2007. Its lifetime will be five years. It carries a high frequency X-band SAR sensor that can be operated in three different modes and various polarizations. The Spotlight-, Stripmap- and ScanSAR-modes provide high resolution images for detailed analysis as well as wide swath data whenever a larger coverage is required. These high geometric and radiometric resolutions together with the single, dual and quad-polarization capability are innovative and unique features with respect to space borne systems. Additionally several incidence angle combinations will be possible and double side access can be realized by satellite roll maneuvers. The satellite will be positioned in an 11 days repeat orbit. The revisit time in the very high resolution Spotlight mode is 2.5 days for 95% Earth's surface visible to TerraSAR-X. [C10175]

"UAV based collision avoidance radar sensor"

In this paper, the critical requirement for obstacle awareness and avoidance is assessed with the compliance of the equivalent level of safety regulation, and then the collision avoidance radar sensor system is presented with the key design parameters for the requirement of the smart unmanned aerial vehicle in low-altitude flight. Based on the assessment of various sensors, small-sized radar sensor is selected for the suitable candidate due to the real-time range and range-rate acquisition capability of the stationary and moving aircraft even under all-weather environments. Through the performance analysis for the system requirement, the conceptual design result of radar sensor model is proposed with the range detection probability and collision avoidance mode is established based on the time-to-collision, which is analyzed by collision scenario. [C10176]

"Matching stereoscopic SAR images for radargrammetric applications"

The aim of this paper is to present our studies about extraction of 3D information from radar images. Several radargrammetric methods allow DEM (digital elevation model) generation from SAR images and we take a special interest to stereoscopic method. The main idea is to match image stereo pairs, to create a disparity map from one image to the other and to compute elevation thanks to the incidences angles. [C10177]

"A multi-sensor approach and ranking analysis procedure for oil seeps detection in marine environments"

Accidents involving oil spills from petroleum exploration, production, and transportation facilities have stained the history of major companies. The implementation of monitoring systems as an aid to contingency planning is

crucial to guarantee proper environmental performance in offshore activities. On the other hand, natural oil and gas seeps have historically provided invaluable information to oil explorers in frontier areas. The use of Synthetic Aperture Radar (SAR) orbital systems is commonly used for oil slicks detection in the marine environment. Such information can be applied to petroleum exploration (oil seeps detection) and environmental assessment (oil spills monitoring). In combination with SAR satellite images (RADARSAT-1 and ENVISAT ASAR), and essential meteorological and oceanographic data, the proposed technology enhances the detection of oil slicks in the ocean surface based on radar texture. [C10178]

"Bistatic SAR Raw Data Simulation for Ocean"

Bistatic SAR is a potential and effective tool for ocean remote sensing, and the simulation of bistatic SAR raw data from ocean surface plays a great role in the understanding of the mechanism of bistatic SAR ocean surface imaging. In this paper, a bistatic SAR raw data simulation model for ocean surface is presented, which includes bistatic scattering simulation and ocean echo data simulation. In our research, based on IEM scattering model, a stochastic multiscale scattering model is improved by applying the second order nonlinear modulation model, and the speckle noise and coherent time character of ocean surface are simulated in the SAR raw data simulation. [C10179]

"Morphological tools for range-interval segmentation of elastic lidar signals"

This article presents a preliminary semi-automated range-interval segmentation toolset for the identification of: 1) the apparent range of full overlap, 2) the clear-sky level (i.e., the molecular level), and cloud layers (cloud-base, cloud-peak, and cloud-top range), and 3) apparent homogeneous extinction intervals. [C10180]

"New inversion algorithm for raman lidar without derivative of the inelastic signal"

A new algorithm for extracting the backscattering coefficient profiles from elastic and inelastic lidar signals is presented. It re-formulate the Raman lidar equation, provided by the interaction of the laser light with the atmospheric nitrogen, in order to obtain the exponential of the integral of the extinction coefficient at the elastic wavelength instead of the extinction coefficient profile, as it is traditionally made, assuming the usual wavelength-dependent relationship between the Raman and Elastic extinction coefficients, and then substitutes that quantity into the elastic lidar equation to obtain the backscattering profile. That circumvents the calculation of the derivative of the noisy inelastic lidar signal with the main advantage of the extraction of backscattering coefficient profiles, one of the final products, without requiring any smoothing or filtering of the original signals. Several examples of the new method applied to profiles obtained with the CIEMAT lidar system, located in Madrid (SPAIN), are analyzed and the results are compared with other algorithm calculations. In conclusion, an improvement of the reliability and accuracy of the retrieved data was observed in the cases analyzed. [C10181]

"Kuroshio-induced cold eddy streets in the lee of isolated islands"

Cold eddy streets formed in the lee of isolated islands were investigated in relation to the Kuroshio current. Multi-temporal SAR images acquired over a one-month period revealed island wake patterns, such as meandering disturbances and eddy streets. These patterns corresponded to the Kuroshio path, indicating a Kuroshio-island interaction. We constructed high-spatial-resolution sea-surface temperature (SST) images for the time when the Kuroshio impinged on the islands by regressing the LANDSAT infrared images on the AVHRR-derived SST. The images revealed low-SST island wakes, some of which included cold eddy streets. A numerical simulation was performed to investigate their formation mechanism. The simulation qualitatively reproduced the cold eddy pattern, with eddy-driven mixing developing a mixed layer down to 100 m, causing the low-SST island wakes. The shedding frequency and distance of the model-produced eddies were close to those of the Karman vortex theory, suggesting that Karman-like cold eddy streets developed behind the islands when the Kuroshio passed. [C10182]

"Inversion of a layered rough surface model: maximizing the number of retrievable parameters for the design of future subsurface sensing radar systems"

We previously applied an optimization technique known as Simulated Annealing (SA) to the inverse problem associated with a 3D two-layer dielectric structure with slightly rough interfaces and showed that simulated annealing methods are capable of globally minimizing cost functions with many local minima [1]. Nonlinearity of the cost function is a major factor that decreases the performance of the inversion algorithm. With a fixed set of measurement and inversion parameters, as the number of unknown model parameters increases, the cost function nonlinearity becomes more severe, decreasing the efficiency of inversion and making the annealing process perform like an inefficient brute force search. The focus of this work is on strategies to choose the optimal set of measurement parameters for retrieval of the largest possible number of parameters of a layered

dielectric structure. [C10183]

"Forest inventory applications using optical and RADARSAT-2 images in Mexico"

There is a need in Mexico for accurate and up to date forest inventories due to concerns related with sustainable development programs. Forest inventories in the past have been incomplete and are not useful at regional levels. The national forest inventory is scheduled to be updated soon -optical remote sensing techniques and traditional field surveying are envisaged. There are no operational applications of radar remote sensing for forest management within government agencies or academic institutions in the country. Forest land cover is dynamical due to urban area growth, illegal logging and forest clearing for agricultural purposes in many regions. A previous land cover project combined Landsat-ETM and RADARSAT-1 imagery in Central Mexico, where forest areas are frequently foggy. A current project involves testing the potential benefits of combining polarimetric radar and optical data for forest applications. RADARSAT-2 imagery will be used as part of the Science and Operational Applications Research Program. The project aims to evaluate combined optical/radar approaches to improve forest inventory at regional scales. As a first step the total forested area is determined from optical SPOT 5 images. We show preliminary results from the optical data which are being validated on the field. As RADARSAT-2 imagery become available, polarization signatures for forest parameters will be obtained. Further work will evaluate the complementarities with optical signatures in determining forest species. [C10184]

"Estimation of forest stem volume using ALOS PALSAR satellite images"

A first evaluation of ALOS PALSAR data for forest stem volume estimation has been performed at a coniferous dominated test site in Sweden. In total, 7 Fine Beam Single polarization (FBS, look angle 34.3deg, HH-polarization) and 7 Polarimetric (PLR, look angle 21.5deg, HH-, HV-, VH-, and W- polarization) SAR images were used. In total, 56 forest stands with stem volume in the range of 45-650 m³ ha⁻¹ (average 325 m³ ha⁻¹) were analyzed by relating backscatter intensity to field data. The estimation accuracy of stem volume at stand level was calculated in terms of root mean square error (RMSE). For the best case investigated an RMSE of 30% was obtained using one of the FBS images acquired in the winter season. The corresponding RMSEs for the PLR images with HH-, HV-, VH-, and W-polarization were 65%, 65%, 62%, and 81%, respectively. The better results for FBS compared to PLR mode could be explained by particularly favorable weather conditions at image acquisition, or by the higher ground resolution in the FBS images, which makes small stands less sensitive to errors in geocoding. [C10185]

"The active-passive remote sensing for aerosol optical depth retrieval"

In this paper, a hybrid retrieval method of aerosol optical depth based on the combination of active and passive optical remote sensing is proposed. Two methods to retrieve the atmospheric optical depth are introduced: the so-called dark pixel method is used for retrieving the aerosol optical depth from MODIS; the other one is used by CALIPSO lidar data. After analyzing the two methods, the combined MODIS and CALIPSO method is applied for the aerosol optical depth, the primary experimental results show that these data are in agreement with each other in time-space evolution trend. [C10186]

"Automatic recognition of coastal and oceanic environmental events with orbital radars"

An automatic classification procedure was developed able to identify different oceanic events, detectable in orbital radar images. The procedure was customized to be used in the southeastern Brazilian coast, since the classification training and test used examples extracted from 402 RADARSAT-1 images acquired in this region. Different sets of spectral, geometric and contextual (meteo-oceanographic and location) features of selected low backscatter patches were evaluated. Machine learning procedures (neural networks, decision trees and support vector machines) were used to induce classifiers to differentiate between seven classes, belonging to two categories. The classification procedure involves two steps: first the features area classified in one of two categories-oil spill or meteo- oceanographic phenomena. In the second step, the identification of tree classes of oil spills and four classes of meteo- oceanographic phenomena is done. The oil spill related classes are associated to operational exploration and production spills, ship releases and others. The meteo-oceanographic phenomena include biogenic oils and/or upwellings, algae blooms, low wind areas and rain cells. The models induced by support vector machines and neural networks achieved good results, allowing the operational implementation of the proposed procedures. [C10187]

"Surface signature of ocean convection in the Greenland sea as detected by SAR and enhanced by statistical pattern analysis"

The aim of this work is to present a process to enhance the image feature of the surface signature produced by

the SAR sensor of the convective chimney discovered in March 2001 in the Greenland Sea. The procedure developed to extract the feature is described and some examples of the results of this study are presented and discussed. [C10188]

"Extreme wind conditions in tropical cyclones observed from synthetic aperture radar images"

Both atmospheric and oceanic processes play an important role in the dynamics of tropical cyclones. Due to the relatively small amount of in situ data available for extreme events like hurricanes or typhoons remote sensing techniques play an important role in the measurement of the relevant geophysical parameters. In this paper some recent results on SAR observation of extreme wind conditions are summarized. The study is based on the use of ENVISAT ASAR wide swath images. The objective of this study is to investigate the performance of SAR to improve the existing model for the retrieval of information on wind field under extreme wind and wave conditions using information from a parametric Holland type model. [C10189]

"Measurement of extreme wave height by ERS-2 SAR and numerical wave model (WAM)"

The Synthetic Aperture Radar (SAR) onboard the European Satellite ERS-2 is operated in wave mode over the global oceans whenever no image mode data acquisition is requested. In the present paper new SAR algorithms to derive sea state at German Aerospace Center (DLR) are shortly introduced and used to determine SAR derived ocean parameters from wave mode data. Global Significant wave height statistics on a 3deg by 3deg grid derived by an empirical method (CWAVE) is presented in this paper for sea state analysis. A severe North Pacific storm that produced significant wave height above 10 m along the northern great circle shipping route is presented in the paper. The sea state generated is analyzed in more detail using the empirical method to derive significant wave height and compared to the ocean wave model WAM. [C10190]

"Brightness temperature validation for SeaWinds radiometer using Advanced Microwave Scanning Radiometer on ADEOS-II"

After the launch of NASA's SeaWinds scatterometer in 1999, a radiometer function was implemented in the Science Ground Data Processing Systems to allow the measurement of the Earth's microwave brightness temperature. This paper presents the validation of the SeaWinds radiometer (SRad) ocean brightness temperatures using the Advanced Microwave Scanning Radiometer (AMSR) as a brightness temperature standard. Results are presented which compare collocated and simultaneously measured ocean brightness temperatures while operating on Japan's ADEOS-II satellite. [C10191]

"A quadtree algorithm for high squint SAR imaging"

In this paper, a quadtree algorithm is used for high squint SAR image reconstruction. It is very difficult for current SAR-imaging algorithms to be used directly in high-squint configurations. This is due to the large range-cell migration and the nonnegligible cubic-phase term in the signal. Every preceding problem is eliminated by using backprojection at the expense of substantially greater processing time. The quadtree image formation technique is a computationally efficient approximation to standard convolution backprojection algorithm. A quantitative analysis and simulations show that this algorithm can process the SAR data with a high squint angle. [C10192]

"Statistical description of tropospheric delay for InSAR: Overview and a new model"

This paper focuses on statistical modeling of water vapor fluctuations for InSAR. The structure function and power spectral density approaches are reviewed, summarizing their assumptions and results. The linking equations between these modeling techniques are reported. A structure function model of zenith tropospheric propagation delay is then derived from a two-regime power spectral density function presented in literature. The novelty lies in the fact that a closed form expression is derived and a free model parameter is allowed, which may be tuned to available measurements or, in the absence of these, to atmospheric statistics. The latter approach is used to compare the derived model with previously published results. [C10193]

"Mixture model for the segmentation of the InSAR coherence map"

In this work, we classify the interferometric SAR (InSAR) coherence map into three classes using the Bayes' theorem. The segmentation procedure is performed using a mixture modelling of the coherence map. The multimodal density of the mixture comprises three component functions characterizing different land surface categories (lake, bare soil, urban ...). This work is an ameliorated segmentation approach of that published by the authors in R. Abdelfattah, et. al., (2006). We test the performance of the proposed mixture model on a dataset about regions with different geophysical characteristics and different time interval between the acquisitions. The results of this study could be used as a supervised learning step for an automatic land cover

classification algorithm. This new method classifying the image considering the corresponding InSAR coherence map is particularly powerful for the detection of layover and shadow regions. [C10194]

"High resolution SAR imaging along circular trajectories"

After a first series of full circle SAR acquisitions in L and P-bands during a 2004 joint FOI-ONERA campaign in Sweden, ONERA experimented in 2006 high resolution (15 cm) polarimetric, full circle acquisitions in France and Germany using its X-band sensor. In order to cope with narrower antenna pattern and aircraft attitude fluctuations, a steerable antenna was used. Furthermore, an experimental setup for retrieving high accuracy trajectory was installed. This paper describes the processing of this signals. [C10195]

"Image coregistration in SAR interferometry only by means of arithmetic operations"

An alternative interpolation technique for SAR image coregistration in interferometric processing is formulated and described. The proposed algorithm is based on the 1-D Farrow interpolator and, when combined with an adequate implementation, it involves a smaller computational burden than the conventional method and yields high accuracy. Basically, this technique enables to carry out the coregistration without resorting to a set of functional weights, and it only requires arithmetic operations and 2-D FFTs. This paper includes several results and comparisons that confirm its validity: the proposed technique is combined with two different polynomial interpolation procedures (Taylor and Chebyshev); bounds on its interpolation error in the 1-D and 2-D cases are derived; and, additionally, it is tested numerically with a synthetic image. [C10196]

"Investigation of creation methods of digital elevation model"

The investigation of the existing techniques of phase unwrapping has been carried out. [C10197]

"DEM calibration concept for TanDEM-X"

The TanDEM-X mission [1] comprises two fully active synthetic aperture radar satellites operating in X-band. The primary goal of this mission is the derivation of a high-precision global Digital Elevation Model (DEM) according to HRTI level 3 quality [2]. This requires accurate calibration of the interferometric system parameters. Content of this paper is the development of a general concept for this calibration, which comprises the determination of instrument and baseline errors, an adjustment concept and the distribution of control points. This concept has a key incidence on mission aspects like the data acquisition plan and the data take adjustment procedure. [C10198]

"Frequency impact on the bistatic radar scattering from an ocean surface"

In this paper we study the frequency impact on the normalized bistatic cross section (NBCS) of the sea surface. Numerical simulations are presented and analyzed in the frequency range from 1 to 14 GHz (L- to Ku-band). We treat this problem with the unifying scattering model denoted small slope approximation (SSA). The computations were made assuming the surface-height spectrum of Elfouhaily et al. for fully developed seas. Numerical results are obtained and discussed in both forward and fully bistatic configurations for different sea states and polarizations. [C10199]

"Simultaneous wind and rain retrieval for ERS scatterometer measurements"

Using collocated ESCAT, TRMM PR, and ECMWF data, the effects of rain on the ESCAT wind-only retrieval has been evaluated. For high incidence angle measurements, the additional scattering of rain causes estimated wind speeds to appear higher than expected. It is also noted that the selected directions of the rain-corrupted wind vectors generally point along swath in heavy rain, regardless of the true wind. A simultaneous wind/rain retrieval method (SWRR) is developed using a simple wind/rain backscatter model. Validation shows that SWRR method significantly improves the wind vector estimates at high incidence angles in heavy rain cases. It also provides an estimate of the surface rain rate. [C10200]

"Calibration of SMOS geolocation biases"

The Soil Moisture and Ocean Salinity (SMOS) mission aims at observing two variables critical for a large scientific community, from biosphere dynamics to climate monitoring. The mission should also provide information on root zone soil moisture and vegetation and contribute to significant research in the field of the cryosphere. The original design, 2D interferometric radiometer at L-band, and principle of measurement makes SMOS a challenge at various technical levels. Moreover, stringent requirements on the estimated variables make the complete processing of SMOS data even more challenging. One of these requirements is concerned with the

ability to accurately localize all the footprints of the instrument on the surface of the earth. Based on simulation and sensitivity studies with respect to the final retrieval of soil moisture, this accuracy requirement has been established so that the localization error on each footprint presents a zero mean and a standard deviation of 400 m. This high accuracy is mainly due to the need for knowledge of open water within a footprint, not to bias soil moisture estimation. This accuracy is highly challenging and unprecedented for sensors of this class and resolution. The on board devices that will help characterize the geolocation of the SMOS products include stellar sensor and gyroscopes, which can achieve an accuracy consistent with the requirements in terms of standard deviation. But the overall localization budget is also contaminated by an important bias, due to the mechanical deployment of the instrument antenna arms after launch, and to the launch shift that impacts all the alignments on the satellite (mechanical shift of stellar sensor due to shocks and vibrations, moisture desorption in mechanical brackets...). The purpose of this study is to characterize these biases, obviously inaccessible to on ground measurement and expected not to evolve once in orbit, so that they can be accounted for in the ground processing prior to initiate the soil moisture retrieval. [C10201]

"The effect of rain on retrieval of C- and Ku-band scatterometer surface winds during Hurricanes Lili (2002) and Isabel (2003)"

The Imaging Wind and Rain Airborne Profiler (IWRAP) and Simultaneous Frequency Microwave Radiometer have been flown aboard the NOAA WP-3D "Hurricane Hunter" aircraft for the past five (2002-2006) hurricane seasons. IWRAP is a conically scanning, high resolution C- and Ku-band Doppler radar that profiles from the aircraft to ocean at four incidence angles. The microwave return from the ocean is used to infer ocean surface vector winds via scatterometry. The UMass Simultaneous Frequency Microwave Radiometer (USFMR) is a C-band radiometer that measures integrated rainfall rate and ocean surface wind speed. The combination of these two instruments allows for the determination of the effect of rain on scatterometer derived surface vector winds. Our focus is on scatterometer retrievals at an incidence angle of 50deg during Hurricanes Lili (2002) and Isabel (2003). The measurements were carried out under the Coupled Boundary Layers and Air-Sea Transfer (CBLAST) program and are the highest resolution radar measurements of the lower atmospheric boundary layer in powerful hurricanes. The retrievals at C-band use the CMOD5 geophysical model function (GMF) while those at Ku-band use one which is a synthesis of the QSCAT- 1 GMF and one developed using IWRAP data. As has been reported, the effect of rain at Ku-band is a dramatic decrease, even for wind speeds greater than 20 m s⁻¹. The atmospheric attenuation dominates these results. At C-band the primary effect is a decrease in azimuthal modulation which is especially important at high wind speeds where this modulation decreases in the absence of rain. [C10202]

"Impact of SAR impulse response function in interferometric measurement"

The stable point network (SPN) is a persistent scatterer interferometric technique developed by ALTAMIRA INFORMATION in 2001. The technique makes use of both ERS SAR and/or ASAR differential phase measurements to generate long term terrain movement and precise height maps with the same resolution as the original SAR images. The algorithm is capable to use all the available phase information even in conditions of large baselines or platform instabilities giving place to large Doppler centroid variations. Such behaviour is handled by precise location estimate of the scatterer within the pixel and accurate elevation extraction which permits the exact location of the radar measurement in ground geometry. However not all the SPN interferometric measurements within a pixel have a direct correspondence in the real scene. Some points presented as measurement points may not be related to existing structures on ground but directly generated by the processing itself. For instance, several artifacts can be created in the Synthetic Aperture Radar images due to the signal acquisition system. Azimuth ambiguities are one of them. They may appear as strong targets in low backscattering areas like forest or water. Secondary lobes of strong targets are also an issue. Since low level signals can be masked by the side lobes of higher level signals. They cannot be handled like standard scatterers and present completely different geometric behaviour not related to their position in the radar image. This paper discusses the way to identify those artifacts and analyses their impact on SPN measurements compared to their reference points (centre of the main lobe). [C10203]

"Polarimetric, combined, short pulse scatterometer-radiometer system at 5.6GHz"

In this paper a C-band (~5.6 GHz), dual polarization, combined scatterometer-radiometer system is described. The system allows carry out polarimetric (vv, vh, hh, hv), simultaneous and coincident microwave active-passive measurements of the observed surface (soil, vegetation, snow and water surface) parameters. The originality of the developed system is in the spatial-temporal combination of microwave active and passive channels of observation and its possible application for short distance sensing (the minimum operational range for the scatterometer is ~6 m) from low altitude platforms under far field conditions for both radar and radiometric observations. [C10204]

"Accuracy and resolution analysis of the pencil beam radar scatterometer onboard China's HY-2 satellite"

The Ku-band scatterometer onboard HY-2 (SCAT/HY-2) is a pencil-beam radar employing pulse compression techniques to ensure number of the independent measurement samples and the resulted precision of the backscattering coefficient for each resolution cell. In this paper, the system specifications of SCAT/HY-2 are introduced. The signal processing scheme, including pulse compression, resolution cell regroup and the area weighted incoherent average of the backscattered power, is presented and analyzed. Based on the analysis of the resolution cell after pulse compression processing, the radiometric accuracy and surface resolution of the SCAT/HY-2 for all the azimuth angles will be simulated. Simulation and analysis results shows that SCAT/HY-2 can satisfy the specification requirements of HY-2 satellite. [C10205]

"A distributed approach to efficient time-domain SAR processing"

This paper presents a distributed approach for time-domain focusing, which significantly enhances the overall efficiency by distributing the computational load across a (potentially large) number of networked computers. The system described includes the so-called master, responsible for pre-processing, the distribution of fragments of raw-data data and the collection of processed image fragments. Fragments of raw-data are passed to so-called slaves, any number of which can be connected to the master, which are responsible for the focusing itself. Master and slave actively communicate over the network to organise the entire process in a scalable manner. In this way, time-domain processing can be accelerated by a factor that is virtually linear in the number of participating slaves. This paper summarises the current status of software development, realised in a platform-independent way using the IDL and Java languages. Additionally, some preliminary evaluations of performance, scalability and the required network infrastructure are given. Some examples of SAR data, acquired by the airborne sensor E-SAR of DLR, and processed with the system described are shown. [C10206]

"Target separation in SAR image with the MUSIC algorithm"

The aim of this work is to exploit the MUSIC algorithm performance in order to enhance target separability in range and azimuth, i.e. achieve point targets separation inside a resolution cell. Simulations have been done in order to plan and check the feasibility of a super-resolution experiment that took place in September 2006 on the test site of Oberpfaffenhofen (Germany). The data set has been acquired with the E-SAR system of the DLR in X-band. The targets to be separated were seven small corner reflectors that have been placed in a way that their response falls in one or, at maximum, two resolution cells of the standard Fourier SAR image. A post-processing implementation of the MUSIC algorithm has been proposed allowing, in the already focused SAR image, to retrieve the targets geometry. Conditions and analysis of the results have been carried out. [C10207]

"Relationship between antenna pointing stability and spaceborne ScanSAR scalloping calibration"

Based on uniform weighting antenna model, the Doppler center frequency error from instability of antenna pointing is derived in detail for spaceborne scanning synthetic aperture radar (ScanSAR) system. And the effects of Doppler center frequency error on image radiometric correction are analyzed. The basic precision of the antenna pointing stability is present for the offsets of ScanSAR image radiometric correction, which is verified by simulations. [C10208]

"Design of GMTI combining networks"

Multichannel radar systems are of choice for ground moving target indication (GMTI) since they allow for a joint space-time processing of the received data that enables an efficient suppression of ground clutter returns. The design of the receiving sensor group is driven by the performance specifications of the intended GMTI modus, which usually requires the sensor array to consist of a few hundred up to a few thousand elements. Though desirable, a full digital processing of all receiving channels is practically not feasible due to both hardware constraints and computational load. The formation of sub-arrays using a proper combining network before A/D conversion reduces the number of processing channels while maintaining the advantages of the full array. In this paper the impact of the combining network design on the GMTI performance of a simulated airborne multichannel radar system is investigated. [C10209]

"Semi-automatic fast recognition of areas of interest for SAR image interpretation"

The framework of this study is focused on semiautomatic fast recognition of areas of interest for SAR images. The intended goal is to label regions in an image as fastly as possible, into classes significant for a given application. The proposed approach defines the information extraction as a two-level procedure. First, a

segmentation technique is applied to obtain an image partition in homogeneous regions, this property being of a crucial interest for the rest of the process. Then, several measures are computed over regions, considered at this level as "objects", in order to identify at which typical class of land-cover they can be attached. Among a large set of measures experimented, we will point out the most pertinent ones for the considered SAR images. In this paper, we focus more on "forest"/"field" areas extraction in SAR images, and show that the discrimination results obtained here are more precise than in a "classical" purely raster classification process. The proposed approach can be extended to discriminate other classes from high resolution SAR images. [C10210]

"Elimination of oil spill like structures from radar image using MODIS data"

Oil-spill detection from radar imagery is a complicated task in Estonian coastal sea where look-alikes caused by ice, upwelling events, cyanobacterial blooms may occur. We compared SAR image with the MODIS optical imagery and look-alikes caused by upwelling event and cyanobacterial bloom were detected from images of August 7, 2007. Analysis of MODIS imagery from years 2000-2006 showed that during the ice free period upwellings occur frequently in the Gulf of Finland and they are strongest during summertime stratification period. Cyanobacterial blooms occurred in July and August in Estonian coastal sea. Some ice cover is present in Estonian coastal sea every winter. [C10211]

"Application of 3D-SAR nearfield imaging algorithms to GPR data"

This contribution addresses the utilization of near field 3D-SAR imaging algorithms applied to radar data from an ultra wideband (UWB) ground penetrating radar (GPR) system. The measured data were collected at the test field of the multi sensor mine signature (MsMs) group at the European Joint Research Centre (JRC) in Ispra/IT. The layout of this test field was designed for the more difficult problem of detecting targets representing anti-personnel mines. The 3D-SAR imaging algorithms can be implemented in time-domain or frequency domain. This contribution focuses on the time-domain implementation. The influence of the quality of the 3D-SAR imaging algorithm on the performance of an automated detection process is evaluated. [C10212]

"Target recognition in SAR images with Support Vector Machines (SVM)"

This paper addresses object recognition problem in SAR images with SVM classifier; the work has been mainly focused on feature vector definition. Actually, each object is represented by a feature vector and SVM aims to estimate the best hyperplanes that separate classes in the feature space. Very robust definition of feature vector is proposed and tested on real data (MSTAR database). Confusion matrices prove that a very good recognition rate is reached, even for mixed incidence angles configuration. [C10213]

"The extraction of ocean wind, wave, and current parameters using SAR imagery"

Recently satellite SAR techniques have become essential observation tools for various ocean phenomena such as wind, wave and current. The CMOD4 and CMOD-IFR2 models are used to calculate the magnitude of wind at SAR resolution with no directional information. Combination of the wave-SAR spectrum analysis and the inter-look cross-spectra techniques provides amplitude and direction of the ocean wave over a square-km sized imagette. The Doppler shift measurement of SAR image yields surface speed of the ocean current along the radar looking direction at imagette resolution. In this paper we report the development of a SAR Ocean Processor (SOP) incorporating all of these techniques. We have applied the SOP to several RADARSAT-1 images along the coast of Korean peninsula and compared the results with oceanographic data, which showed reliability of space-borne SAR based oceanographic research. [C10214]

"Phase distortion modelling due to motion in wave scattering mechanism applied to SAR images analysis"

In SAR image processing, taking phase distortion in radar signals into account is equivalent to considering motion as information embedded in it. In the aim of doing this, a model based on Gaussian linear frequency modulation is introduced, adapted to quantification and estimation of phase distortion. This model is based on three parameters, the Doppler frequency modulation rate K , the analysis time T_a and the Doppler frequency f_d , and allows practically a local representation of any quasi-punctual target echo. [C10215]

"Spaceborne SAR raw signal simulation of ocean scene"

According to fractal ocean surface model, electromagnetic scattering model under Kirchhoff approximation and the raw signal simulation procedure of dynamic scene based on time domain, spaceborne synthetic aperture radar (SAR) raw signal of ocean scene is generated. The SAR images obtained from the echo of both simple cosine wave and complex fractal ocean surface are in accordance with the tilt modulation and the velocity

bunching theoretically, and also with the statistical properties of real ocean SAR images, which validate the simulation procedure. The raw signal could be the input data of studying along-track InSAR (ATI) for ocean current measurements. [C10216]

"Combined wavelet and curvelet denoising of SAR images using TV segmentation"

Synthetic aperture radar (SAR) images are corrupted by speckle noise due to random interference of electromagnetic waves. The speckle degrades the quality of the images and makes interpretations, analysis and classifications of SAR images harder. Therefore, some speckle reduction is necessary prior to the processing of SAR images. The speckle noise can be modeled as multiplicative i.i.d. Rayleigh noise. The discrete curvelet transform is a new image representation approach that codes image edges more efficiently than the wavelet transform. On the other hand, wavelet transform codes homogeneous areas better than curvelet transform. In this paper, two combinations of time invariant wavelet and curvelet transforms will be used for denoising of SAR images. Both of the methods use the wavelet transform to denoise homogeneous areas and the curvelet transform to denoise areas with edges. The segmentation between homogeneous areas and areas with edges is done by using total variation segmentation. Simulation results suggested that these denoised schemas can achieve good and clean images. [C10217]

"CAESAR-XInSAR: A new software for interferometric SAR processing"

In order to meet the need of the development in interferometric SAR, especially the development of Permanent Scatterers InSAR(PS-InSAR) in these years, we develop a new software called CAESAR-XInSAR at the Remote-Sensing Satellite Ground Station, CAS. Both conventional InSAR and PS-InSAR are considered in this system. It supports the interferometric processing from SAR SLC data to end products of DEM or surface deformation map. It is organized in different modules and developed in Visual C++ 6.0 environment on PC under windows operating system. It is currently at the stage of the development from scientific platform to operational system. In this paper, the organization and the modules of this system are described and the results from CAESAR-XInSAR are also processed in the end. [C10218]

"Evaluation of the single and two data set STAP detection algorithms using measured data"

Traditional space time adaptive processors for radar target detection require a training data set which is usually drawn from adjacent range gates. Clutter heterogeneity, however, can severely limit the available training sample support and consequently degrade the detection performance. The SDS algorithms, on the other hand, overcome this problem by operating solely on the test data without recourse to training data. In this paper we evaluate both of these approaches, in particular the AMF and MLED, using the MCARM data set. We illustrate the performance degradation of the AMF that results from the clutter heterogeneity and the corresponding advantage of the MLED. We also show that a calibration step of the spatial steering vectors results in significant performance improvement of all of the algorithms considered here. [C10219]

"ISAR imaging of targets with moving parts using micro-doppler detection on the range profile image"

In ISAR imaging, most works have assumed the target to be a rigid body, a body without any rotating, vibrating or moving parts. The rotation of structures in a target, such as the rotor of a helicopter or the turret of a tank target, may induce frequency modulation on the returned signals and generate sidebands about the center frequency of the target's body Doppler frequency, known as the micro-Doppler phenomenon. In this paper we present a new method based on range grouping of the target's range profile for the separation of the rotating or moving parts from the target's body. The method is carried out on the Range Profile Image, different from other methods that do the separation at the signal level. [C10220]

"Steerable filter based multiscale registration method for JERS-1 SAR and ASTER images"

It is a challenging problem to automatically register the SAR and optical satellite images in remote sensing applications. In this paper, a novel intensity based multiscale registration method using steerable Simoncelli filters is proposed to register JERS-1 SAR and ASTER images. The mutual information is used as the similarity measure, and a hybrid search technique is used to do the parameter optimization. The experimental results showed that the proposed registration scheme is competent for JERS-1 SAR and ASTER images, though the robustness of this scheme should be verified further more. [C10221]

"Coherent-stable scatterers detection in SAR multi-interferograms: Feature fuzzy fusion in Alpine glacier geophysical context"

SAR interferometry (InSAR) performs two acquisitions (spatially separated by the baseline) of the signal back-scattered by the resolution cell which contains height and/or displacement information. Repeat pass spaceborne interferometry provides multi-interferograms which can be used to extract such information either by combining the multi-temporal results of conventional interferometry or by a different approach based on specific targets: the coherent stable scatterers (CSS). In this paper a two-step approach is proposed to obtain specific features from multi-temporal InSAR data sets. The first step consists in extracting image attributes related to the useful information. The second step consists in merging the attributes using an interactive fuzzy fusion technique. The interactive fuzzy fusion is proposed to provide end-users with a simple and easily understandable tool for tuning the detection results. The method is applied on a data set of five co-registered ERS 1/2 tandems from the French Alps (the Mont-Blanc region), including two temperate glaciers: the Argentiere and the Mer-de-glace. The results illustrate how the end-user can combine the proposed attributes to detect the presence of CSS or distributed stable scatterers usefull for multi-temporal analysis. [C10222]

"Similarity measures between SAR and optic data"

With the development of remotely-sensed multisensor satellites like Pleiades Cosmo-Skymed that have the particularity of providing both SAR and optic data, new techniques in image processing are needed. These techniques must take into account the complementarities and differences in nature of these data. A preliminary operation for advanced techniques that use multisensor images such as fusion, classification, etc. is registration. In the case of SAR and optic data, we can do automatic registration if we exactly know the sensor parameters and have a digital terrain model (DTM) or a digital elevation model (DEM) at our disposal. If we do not have an exact knowledge of these parameters, the registration becomes difficult. Another approach to achieve the automatic registration which does not need sensor parameters will rely on comparison measures between both data. In this paper, we present a comparison of several similarity measures between multisensor SAR and optic images used in matching algorithms. An evaluation of these measures for synthetic data based on their distributions is given. Then results on real images are analyzed. [C10223]

"Unsupervised change detection by multichannel SAR data fusion"

In the contexts of environmental monitoring and disaster management, multichannel synthetic aperture radar (SAR) data present a good potential, thanks both to their insensitivity to atmospheric and Sun-illumination conditions, and to the improved discrimination capability they may provide as compared to single-channel SAR. In this paper an unsupervised contextual change-detection method is proposed for two-date multichannel SAR images, by adopting a data-fusion approach. Each SAR channel is modelled as a distinct information source and Markovian data fusion is used by introducing a suitable Markov random field model. The task of the estimation of the model parameters is addressed by combining the expectation- maximization algorithm with the recently proposed "method of log-cumulants." The proposed technique is experimentally validated on SIR-C/XSAR data. [C10224]

"Advanced D-InSAR techniques applied to a time series of airborne SAR data"

This paper presents airborne differential SAR results using a stack of 14 images, which were acquired by the experimental SAR (E-SAR) system of the German Aerospace Center during a time span of only two and a half hours. An advanced differential technique is used to retrieve the error in the digital elevation model and the temporal evolution of the deformation for every coherent pixel in the image. The two main limitations in airborne SAR processing are analyzed, namely the existence of residual motion errors (inaccuracies in the navigation system in the order of 1-5 cm), and the accommodation of the topography and the aperture during processing. The SAR focusing chain to process the data is also presented, together with the modifications in the differential processor to deal with the remaining baseline error. The detected deformation of a corner reflector and of several agricultural fields allows validating the proposed techniques. [C10225]

"An autofocus approach for residual motion errors with application to airborne repeat-pass SAR interferometry"

Airborne repeat-pass SAR data are very sensible to sub-wavelength deviations from the reference track. To enable repeat-pass interferometry a high-precision navigation system is needed. Due to the limit of accuracy of such systems, deviations in the order of centimeters remain between the nominal and the processed reference track causing mainly undesirable phase undulations and misregistration in the interferograms, referred as residual motion errors. Up to now only interferometric approaches, as multi-squint, are used to estimate those deviations to compensate for such residuals. In this paper we present for the first time the use of the Autofocus technique for residual motion errors. A very robust autofocus technique has to be used since the accuracy of the estimated motion has to be at millimeter scale. Because we deal with low-altitude-strip- map mode data we

propose a new robust autofocus technique based on the WLS (Weighted Least-Squares) phase estimation and Phase Curvature Autofocus (PCA) extended to the range- dependent case. We call this new technique WPCA (Weighted PCA). While the multi-squint approach is only able to estimate the baseline variation from coregistered images, the autofocus approach has the advantage of being able to estimate motion deviations independently for each image. Repeat-pass data of the E-SAR system of the German Aerospace Center (DLR) are used to demonstrate the performance of the proposed approach. [C10226]

"Research of influence of transients, non-equidistance of the taken readings, divergence of beams on characteristics of interferometric SAR"

There is under consideration a combined influence of the transients in the filters of the radar system selective circuits, non-equidistance of the taken readings and divergence of the beams at the distance up to the earth surface reflecting elements that is comparable with a synthetic antenna aperture value. There is taken into account influence of the above-mentioned factors on the resolution capability of the radar system for the earth remote sensing. The transients lead to swinging of the SAR antenna pattern; the other indicated factors result in widening of the synthetic antenna pattern. There are given the corresponding relationships and diagrams that make it possible to take into account the influence of the above-mentioned factors and determine the ways for reduction of the destructive factors influence on the synthetic antenna pattern. [C10227]

"X-band airborne differential interferometry over the Perugia area"

In this paper we show the results of an airborne differential SAR interferometry (DInSAR) experiment carried out over the Perugia area, center of Italy, by using the X-Band OrbiSAR system. Measurements on corner reflectors allowed us evaluating the system detection capability. [C10228]

"A new method for moving target indication and detection in multi-channel SAR data"

A new and fast algorithm for MTI/MTD processing is presented. This algorithm is based on a formation of SAR images from each channel and using these for separation between moving and stationary targets. First, the problem is described by means of a generalized model. Then, an inverse problem is formulated and some of its approximate solutions by means of the Fourier transform are given. The approximate solutions are used to show how one can resolve stationary targets and moving ones completely regardless their distribution in space or reflectivity. The only criterion used is the velocity of a target. Further, it is shown how moving targets and stationary targets can be separated from processed, that is focused, SAR images. [C10229]

"Localizing metallic small spheres by a linear distributional approach"

The problem of determining the number and the locations of "small" metallic spheres from scattered far-field measurements under plane waves incidence is considered. The problem is formulated by neglecting the mutual scattering between the spheres and by representing their locations as the support of delta-functions. This allows to cast the problem as the inversion of a linear integral operator we tackle by means of a Truncated Singular Value Decomposition. The performance of the inversion scheme are analyzed for both the cases of a multi-view/single-frequency and a single-view/multi-frequency configuration by exploiting synthetic exact data. [C10230]

"Measurement and analysis of depolarization generated by scattering over constructive obstacles at 5.8 GHz"

The interest on the scattering due to constructive obstacles appears in different knowledge areas, mainly radar theory and mobile communications. In radar terms, a target can be identified by means of its scattering pattern. Those patterns are also useful in radio communications, in order to obtain confident models for planning the deployment of networks. If co- polar scattering itself gives an important amount of knowledge, the definition of the obstacle is better done when cross-polar data is incorporated. In order to characterize the scattering patterns due to constructive walls, a measurement campaign has been developed, using an automated system, which integrates the mechanical movement to the vector network analyzer control. The aim of the campaign was to check the reflection behavior of different constructive materials. All the experimental work has been performed at the frequency band around 5.8 GHz. Materials considered are a metallic surface, used as a reference, a brick wall, and a chip wood panel. All sample sizes are large enough to ensure that the 3-dB illuminated area, an ellipse with a major axis of 80 cm, falls within the limits of the slabs, thus reducing any diffraction effects on the edges of the samples. As measurements were performed in co-polar and cross-polar polarizations, both co-polar scattering pattern analysis and depolarization index computations could be made. By means of cross-polar measurements, depolarization indexes can be extracted. This magnitude indicates the percentage of the incident

wave that is reflected in the orthogonal polarization. The values obtained for the chip wood panel are between 2 and 3%, and those corresponding to the brick wall are clearly polarization-dependent, being 8% for parallel incidence and 0.4% for perpendicular incidence. [C10231]

"Simulation of LIDAR-based aircraft wake vortex detection using a bi-gaussian spectral model"

A new spectral model of the return signal from a LIDAR Doppler wake vortex detector is proposed. It has been experimentally discovered during ground-based and flight test campaigns but suffered a lack of theoretical evidence. Using high resolution fluid simulations of wake vortices, we highlight the physical meaning of this model. Comparisons with the traditional single Gaussian model show the superiority of this new approach is consistent with previous experimental results. [C10232]

"Fusion of support vector machines for classifying SAR and multispectral imagery from agricultural areas"

A concept for classifying multisensor data sets, consisting of multispectral and SAR imagery is introduced. Each data source is separately classified by a support vector machine (SVM). In a decision fusion the outputs of the preliminary SVMs are used to determine the final class memberships. This fusion is performed by another SVM as well as two common voting schemes. The results are compared with well-known parametric and nonparametric classifier methods. The proposed SVM-based fusion approach outperforms all other concepts and significantly improves the results of a single SVM that is trained on the whole multisensor data set. [C10233]

"Multiband CFAR detection of thermal anomalies using principal component analysis"

This paper deals with the problem of CFAR detection of thermal anomalies in multispectral satellite data. The goal is to extend the algorithm proposed in [1], and successfully applied to MODIS data from band 21, to the case of multiband investigation. A multiple-channel model has been designed, where data from MODIS bands 21 and 31 are projected into a new coordinates system by adopting the principal component analysis (PCA). A preliminary statistical analysis has been performed on both the principal components of data to verify that the Weibull distribution can be adopted for background. Subsequently, a Kendall test has been used to check the level of dependency of the projected data and it has shown that channels independence can be assumed with high significance level. After PCA, a CFAR detection is applied to projected data and thanks to data independence the single detections are combined with an AND rule. The outcome of the AND operation gives the thermal anomalies detected in both channels with an assigned overall probability of false alarm (PFA). The Multiband CFAR algorithm has been applied to a 256 x 256 MODIS image from bands 21 and 31 and results have been compared with those from NASA-DAAC MOD14. [C10234]

"Detecting moving targets in dual-channel high resolution spaceborne SAR images with a compound detection scheme"

Traffic data acquisition from space has evolved to an important task over the last years. Future SAR satellite missions will provide high resolution dual-channel SAR data and therefore a possibility to collect traffic parameters of a large area from space. In this paper a detection approach for vehicles will be presented, which considers simultaneously the effects moving objects suffer from in the SAR image. The performance of the proposed detection scheme is analyzed using experimental airborne SAR data. [C10235]

"A new method for Doppler centroid estimation for spaceborne SAR based on chirp scaling algorithm"

We introduce a new method to estimate the Doppler centroid accurately based on chirp scaling algorithm after investigating the performances of curvature factor C_s and the effective FM rate K_s regarding to Doppler ambiguity number (DAN) and finding that C_s and K_s will lose their functions if a wrong DAN is used and the generated image definition will be degraded. So relations between definition evaluation functions (such as entropy and variance) and the DAN can be used to find the correct DAN which makes the entropy minimum or the variance maximum. Radarsat raw data is used to test the proposed method and find that the performance of using variance is better than that of using entropy. [C10236]

"Unsupervised land cover classification of SAR images by contour tracing"

The potentiality of synthetic aperture radar (SAR) images for land cover mapping is an important area of research. For single band, single polarized SAR images, information is available in the form of intensity and texture only. Land cover classification of SAR images requires exploitation of spatial relationship of pixels also, in addition to pixel level segmentation. SAR images can be segmented successfully if the regions with

homogeneous intensity and texture areas can be identified and grouped together. So far, contour tracing has been used only in demarcating sea and land. Identifying contours in a domesticated area with a mixture of water, urban and vegetation areas require complex analysis of the spatial distribution of pixels. In this paper, we have presented an unsupervised classification algorithm using maximum a posteriori (MAP) segmentation for SAR images in which SAR image is classified into monotone, texture and edge regions. Monotone and textured regions are labeled as land cover types like water, urban and vegetation areas using K-means classification. SAR image of the region with latitude varying from 77.86deg to 77.91deg and longitude varying between 29.89deg and 29.85deg of Haridwar region, India is considered for segmentation. We have compared the segmented image obtained by this methodology with the topographic map of the corresponding region. The water, urban and vegetation areas are clearly recognized with the proposed classification approach which represents a very good agreement with the original topographic sheet. [C10237]

"The equivalence of Cameron's unit disc and Poincaré's sphere for symmetric scattering characterisation and classification"

Cameron's coherent target decomposition and classification is able to represent a symmetric scatterer onto a unit disc in the complex plane, and assign it to one of the six symmetrical elemental scatterer classes. Recently, Touzi et al. proposed a variation of Cameron's method by introducing a coherent analysis. Moreover the Poincaré's sphere, was used instead of the unit disc for representing symmetric scattering because it was considered a more suitable domain. The aim of this work is to demonstrate the equivalence of using Poincaré's sphere domain and Cameron's unit disc, in term of characterisation and classification of symmetric scattering types. [C10238]

"The analysis and compensation for the unwrapped phase error raised by the dynamic baseline of DSS-INSAR"

The DSS-INSAR (distributed small satellite INSAR) applies the interferometry to the carrier platform which is made up of small satellites flying in a certain formation. It aims to retrieve DEM (digital elevation map) with quite high precision globally. In fact, every small satellite in the flying formation is dynamically circling around a reference central point along a certain track. Therefore, the baselines generated by the flying satellites are also unstable. However, the stability of these baselines is very crucial to get elevation measurement with high precision. Therefore, it is valuable to analyze the influences of the above-mentioned baselines on unwrapped phases. This article demonstrates the errors of unwrapped phases introduced by dynamical baselines of DSS-INSAR and provides effective solutions to compensate those errors in detail. In the first beginning, this article deduces the relationship between the across-track baseline, the along-track baseline and the orbit elements, respectively. Then, it analyzes the unwrapped phase error introduced by the dynamical baseline of DSS-INSAR. Finally, it provides a very effective model which can be used to compensate the error. [C10239]

"Offset Phase Estimation in Multi-Channel InSAR DEM Reconstruction"

Interferometric SAR (InSAR) systems are able to estimate height profiles of the Earth surface. For the involved estimation problem, Maximum A Posteriori (MAP) statistical technique and Markov Random Field image models have been used, showing to be effective in case of multiple interferograms, obtained via different baselines/frequencies. In this paper, we face the problem of unknown phase offsets presence affecting real interferograms, which makes impossible to retrieve correct height estimations. We present a procedure to estimate these offset values, based on statistical estimation and we test it both on simulated and real data, showing the effectiveness of the method. [C10240]

"A multi-baseline InSAR DEM reconstruction approach without ground control points"

Distributed spaceborne interferometric synthetic aperture radar (DS-InSAR) system includes more than one baseline, so it is also called multi-baseline InSAR system. It offers additional observation information for the derivation of position and height of object, compared to the single-baseline InSAR system. Based on the additional information it offers, a new DEM reconstruction approach of multi-baseline InSAR system is proposed. At first, theory of the approach is introduced and DEM reconstruction equations are derived. Then, error sensitivity analysis is made by first order approximation of Taylor expanding, which is validated by Monte-Carlo simulation. The results show that theoretical error analysis formula can give support for analysis and design of the system directly and the DEM accuracy is very sensitive to the interferometric phase difference error. [C10241]

"Parallel computation of synthetic SAR raw data"

For modern SAR data acquisition, bi- and multistatic SAR missions become increasingly important. Established methods for processing monostatic SAR signals need to be adapted to new algorithms for signal processing. In order to support the evolution and development of these new algorithms simulated SAR raw data of arbitrary bi- and multistatic SAR scenarios are essential. This paper refers to a modular SAR simulator, which is able to simulate complex bi- and multistatic SAR scenarios. It focuses on the geometrical simulation approach of the simulator and the computationally intensive synthesis of SAR raw data. The main part describes the parallel implementation of the radar lobe footprint scan and of the succeeding SAR raw data generation executed on a compute cluster. An example will be shown, which compares the simulation of the same SAR scenario on three different compute systems and their runtimes. [C10242]

"Region feature extraction based on improved regularization method in SAR image"

The noise existed in synthetic aperture radar (SAR) image weakens the detailed features of region of interest (ROI) such as target and shadow. It also leads to the serious performance reduction of subsequent target detection, classification and recognition. The conventional regularization method could enhance target features in SAR image; however, the high computation complexity limits the real-time application of it. An improved regularization method is introduced in this paper, which increases processing speed of region feature extraction for SAR image significantly. It is theoretically proved that, by optimizing SAR projection operator, computation complexity could be reduced from $O(M^3N^3)$ to $O(MN)$ without ability losing of the region-based feature enhancement. MSTAR SAR image data is employed for algorithm experiment. The result shows that our method can increase target-to-clutter ratio significantly while restraining the noise in ROI, and then extract target and shadow from background clutters in SAR image more accurately. [C10243]

"Fine micro-Doppler analysis in ISAR imaging"

In ISAR imaging, it's well known that rotating parts of a target such as wheels or rotors induce additional features in the Doppler frequency spectrum. These features are called micro-Doppler effect and appear as sidebands around the central Doppler frequency. They can provide valuable information about the structure and motion of the rotating parts and may be used for target identification. In this paper, we propose a fine analysis of the Doppler returned by reflectors of a rotating wheel. Thanks to the micro-Doppler signature we are able to extract information on its geometrical features (position, orientation). The method has been performed on simulated and experimental data and provides satisfactory results. [C10244]

"Dyadic resolution multilook image generation by wavelet packet transform correlation of complex SAR signals"

We present a signal processing approach for generation of multilook SAR intensity images at dyadic scales of resolution. Orthogonal subband decomposition inherent in discrete wavelet packet transform is utilized in shift-invariant manner to produce multiresolution complex SAR images. The symmetry of detailed subband spectra is utilized in separating the disjoint spectra to produce multilook image. Analytical results and sample imagery of diffused reflection are presented. [C10245]

"Spotlight-mode SAR data focusing using a modified wavenumber domain algorithm"

In this paper, a modified version of the wavenumber domain algorithm (MWDA) is analytically presented and formulated. It is capable of processing the spotlight-mode SAR data. MWDA combines the high accurate focusing of the wavenumber domain algorithm (which is also called range migration algorithm) and the interpolation-free requirement. To avoid costly interpolation manipulation, the inverse scaled Fourier transform (ISFT) is substituted for Stolt mapping. The subaperture processing is used to circumvent the limitation that the pulse repetition frequency (PRF) is not high enough to sample the signal in azimuth. [C10246]

"Reconstruction of the building objects from multi-aspect high-resolution SAR images"

In this paper, an approach to the automatic reconstruction of 3D simple building objects from multi-aspect metric-resolution SAR images is proposed. The edge detector of constant false alarm rate (CFAR) and a parallel Hough transform technique are first employed to extract the parallelogram-like image of the building walls in SAR image. A set of probability density functions is presented to describe the extracted random wall-images and their multi-aspect coherence. Then the maximum-likelihood estimation of object is derived from its multi-aspect object-images. A hybrid priority criterion is defined to evaluate the reliability of reconstruction result, based on which, an automatic reconstruction algorithm is further devised to match object-images of different aspects and finally reconstruct the building objects. Four-aspect Pi-SAR images over Sendai, Japan are adopted for reconstruction. The results show the fidelity of the whole process chain and the feasibility of 3D objects automatic reconstruction from multi-aspect SAR images. [C10247]

"Clutter analysis of high resolution millimeter-wave SAR-data in the spatial and wavelet domain"

This paper presents the analysis of high resolution millimeter SAR clutter data, measured in a joint Swiss-German flight campaign. The generalized Gaussian function and the Kolmogorov-Smirnov test are considered to test the hypothesis of Gaussian clutter process. 35 GHz and 94 GHz data are compared. The results are presented in the time and wavelet domain, as the wavelet domain is an import transform domain for the development of terrain classification, target recognition and data compression algorithms. [C10248]

"A velocity vector estimation algorithm tested on simulated SAR raw data"

This paper presents an improved method for estimating the velocity vector of a moving target from SAR raw data. The velocity estimate is carried out without a priori information by a recursive procedure coupling Along Track Interferometry (ATI) for the range component to the Impulse Reference Function (IRF) analysis for the azimuth component. To develop and test the estimation scheme, a dual channel SAR raw data simulator has been built and the retrieval algorithm has been implemented, taking into consideration the coupled effect of the two velocity components. Significant statistics have been generated by considering different targets and backgrounds, simulating scenes with constant backscatter, vehicles in a shrubs environment and ships at sea. [C10249]

"DEM estimation from multi-Baseline ENVISAT- ASAR interferometric data through maximum likelihood techniques"

In this paper, two techniques for estimating accurate height profiles of the ground, using multi-baselines interferometric synthetic aperture radar (In-SAR) data and an a-priori inaccurate digital elevation model (DEM) of the observed scene, are analyzed. The methods are both based on maximum likelihood (ML) estimation: the first estimates directly the quota of each pixel of the image, independently from the other pixels, while the latter estimates the parameters of the local planes which best approximate, in the ML sense, the height profile in a small neighborhood of each pixel. The inclusion of this contextual information allows improving the estimation accuracy. Results on simulated and real ENVISAT-ASAR data are presented. [C10250]

"Error analysis of ICESat waveform processing by investigating overlapping pairs over Europe"

Full waveform laser altimetry is a recently developed method to obtain a complete vertical profile of the height of objects in the footprint as illuminated by a laser pulse. The richness of the signal also complicates the processing. One way to improve the processing strategy is to analyze differences of waveforms that should be very similar because they were obtained at approximately the same time and location. Such waveform pairs are still difficult to find. Here it is shown how to use the archive of ICESat space-borne altimetry data over Europe to determine a set of tenths of thousands of at least partial overlapping waveform pairs. The differences in the values of the waveform parameters, median energy, waveform extent, relative returned energy and intensity distribution are determined and discussed. As a case study, three typical pairs of almost perfectly overlapping waveforms are shown, where considerable differences are still occurring. In all three cases an explanation for these differences is found and discussed. Further analysis of the waveform pairs in this database is expected to considerably improve automatic processing of full waveform data. [C10251]

"Semiautomatic reconstruction of building height and footprints from single satellite images"

Extraction of man-made structures from satellite images is one of the essential issues in remote sensing and many techniques were proposed for building extraction from high resolution satellite images. However, most of them rely stereo analysis or additional data sources such as LIDAR for retrieval of 3D building information. This paper proposes a semiautomatic approach that extracts 3D building information from single satellite images. In this approach, after measuring boundaries of a building roof we determine the building height by projecting building shadow onto the image space until the projected shadow matches the actual shadow. Then we extract building footprints by translating roof boundaries along the direction of vertical edges to the amount determined by the building height. To increase the level of automation, we devised a technique that adjusts the height so that the projected shadow matches the actual shadow and determine building height automatically. We also devised a technique to extract roof boundaries by clicking only two corner points. A panchromatic IKONOS image and Quickbird image over Deajeon area were used to test proposed algorithms and a IKONO stereo pair was used to get reference building heights. While building heights determined manually showed the accuracy of an RMS error of 1.66 m, the heights determined automatically showed an RMS error of 1.86 m. The results show that 3D building information can be extracted from single satellite images and that the automation approaches proposed in this paper worked. [C10252]

"Uncertainty analysis of flood disaster assessment using radar imagery"

Flood is a paroxysmal natural disaster, which results in vast damage to economy in China every year. Precise loss evaluation is an effective method to alleviate the loss. The inundated area, on which loss evaluation is based, is the most fundamental element to evaluate the loss caused by floods, and is a critical step to control the precision of the loss evaluation. Satellite SAR imagery is broadly used in monitoring and evaluating flood disaster. Spatial resolutions of radar images and ground scale are crucial to the extraction of inundated area in the process of disaster monitoring. In order to calculate the error of the statistic of submerged areas in the process of remote sensing disaster monitoring using Radarsat imagery, we take the Airborne SAR image as ground truth data and calculate the error brought by radarsat data, we get the explicit error finally. By performing the test and precision appraisal of the remote sensing monitoring process aiming at the same study area and the same disaster event, and promotes the precision and credibility of remote sensing monitoring. [C10253]

"Variational-based speckle noise removal of SAR imagery"

In this paper we present a variational method for synthetic aperture radar (SAR) speckle removal. Variational method is a newly developed technique for the removal of SAR's multiplicative noise. For an image, we could define an energy functional. The energy evolves as the original image changes, and the minimum energy corresponds to the speckle reduced result. Partial differential equation (PDE) technique is used to get the minimal solution. Our energy functional makes use of the statistical information of the multiplicative noise since it follows a Gamma law with mean $\mu = 1$ and variance $\sigma^2 = 1/M$ for M-look SAR. Our energy is a regularization term with two constraints. The regularization term is the integral for the norm of image gradient; two constraints are the mean of noise should be 1 and the variance of noise should be $1/M$. We use the method of Lagrange multipliers, Euler-Lagrange equation and heat flow method to obtain the minimizer of the energy. ERS Precision Image (PRI) data are to demonstrate our algorithm. Numerical result shows that the speckle reduced image preserves edges and point targets while smoothes homogenous regions in the original image. The algorithm is computationally efficient and easy to implement. [C10254]

"Geological lineament and shoreline detection in SAR images"

In this paper, an algorithm for unsupervised detection of linear structures, in particular, the geological lineament and shoreline, as seen in Synthetic Aperture Radar (SAR) satellite images is proposed. Methodologies to extract linear features consist of three stages. First, the refined local statistics filter is used to remove the speckle noise on the raw image. The likelihood ratio edge detector and local non-maximal suppression are performed on the result images for edge enhancements and detection. In the second stage, mathematical morphology techniques are used to reconnect the fragmented lines and remove the uninterested patterns in the binary image which is produced by thresholding the enhanced image after edge detection. Spatial statistics including spatial mean and spreading coefficient of each cluster (object) in the binary image are calculated in order to simply classify their shapes. The clusters with large spreading coefficient will be remained and others will be removed. Finally, in the third stage, the edge features detected will be described by chain code method and polygonal approximation. The last stage contains many substeps such as edge thinning and curve pruning. [C10255]

"A multiprocessing framework for SAR image processing"

This paper introduces a framework developed for image processing of synthetic aperture radar (SAR) images. It encapsulates features of modern hardware architectures, including symmetric and asymmetric multiprocessing, within an easy and intuitive to use application programming interface (API). The multiprocessing part is designed for unified usage of different architectures reaching from multicore processors to cluster of workstations to grids of clusters. So an application using the framework can be ported from one architecture to another without any changes in the source code. The framework builds the bottom layer of the processing system developed for the German Aerospace Center's (DLR) new airborne SAR sensor, the F-SAR [1]. [C10256]

"Three dimensional SAR image focusing from non-uniform samples"

Multiple SAR signals acquired along different orbits can be exploited for reconstructing a three dimensional (3-D) reflectivity profile of the scene along azimuth, range and elevation co-ordinates. For the 3-D image formation, the problem of the non-uniform spacing of the orbits has to be considered. In this paper we propose a technique based on two steps: 1) a preprocessing step, in which the samples of the multi-pass signal is computed on a grid which is uniform in the elevation direction, starting from its unevenly spaced samples; 2) a 3-D image focusing based on a simple 3-D convolution operator. The technique proposed has the main advantages of preserving numerical efficiency and allowing to easily include information on the signals bandwidth in the pre-processing step, in such a way to regularize the problem and obtain stable solutions. [C10257]

"Inland lake monitoring using low and medium resolution ENVISAT ASAR and optical data: Case study of Poyang Lake (Jiangxi, P.R. China)"

Poyang Lake, one of the most regularly flooded areas in China, can be considered as a key natural flood control and reduction element within the Changjiang middle basin. Within the Flood DRAGON Project, part of the MOST-ESA DRAGON Programme, Poyang Lake's water extent was monitored based on 64 ENVISAT low and medium resolution ASAR and MERIS Full Resolution data, over a two and half year period. It's the first time that such an amount of ENVISAT data was exploited in monitoring inland lake water extent variations. This original integration approach permitted: lake-surface variation analysis, yearly submersion-time estimation, and the recognition of three hydrological sub-systems. The results highlight the great potential of ENVISAT and more largely of Earth Observation Medium Resolution data in monitoring and managing large inland water bodies. This approach can be applied worldwide in a global climate change context. [C10258]

"Analysis of urban land use pattern based on high resolution radar imagery"

The actual process of rapid urbanization is associated with various ecological, social and economic changes in both the urban area and the adjacent natural environment. To keep up with the effects and impacts of this development, effective urban and regional planning requires accurate and up-to-date information on the urban dynamics. Recent studies have proven the applicability of high resolution optical satellite data for the acquisition of some of the requisite spatial and socio-economic information. Although radar data is more reliably available than optical imagery, high resolution radar imagery has barely been employed for urban applications so far. This fact is mainly due to a lack of civil space borne radar systems featuring a ground resolution which is suitable for the analysis of urban structures. Additionally significant difficulties concerning the interpretation of according data over highly structured urban areas occur. The german TerraSAR-X system will provide radar imagery with a spatial resolution comparable to actual high resolution optical platforms. This study investigates the potential use of high resolution radar data in the context of urban applications. Thereby a concept-that was developed on the basis of SAR data recorded by DLR's airborne E-SAR system-will be adapted to an analysis of TerraSAR-X imagery. It introduces a temporally and spatially robust approach towards an automated analysis of the urban structure. For that purpose data sets of single-polarised X-band imagery are analysed by means of an object-oriented classification. This study includes the development of an improved image segmentation procedure in order to create meaningful spatial entities. Moreover, it contains the definition and application of a rule base for the detection of built-up areas, the derivation of the urban land cover and the generation of additional value-added information related to the urban structure. [C10259]

"Improving interferometric radar measurement accuracy using local meteorological data"

Permanent monitoring of potential rock-slide area can be done using interferometric radar measurements where the accuracy is limited by the variation of the velocity of light, i.e. variation of the refractive index. Using differential interferometric measurements, the measurement accuracy can be very good if the distance between the reference and the potential rock-slide area is small. However, if the distance to the reference is large or if using a reference is not possible, the measured accuracy is dependent on the variation of the refractive index. Using meteorological data at the radar site, the refractive index can be estimated locally. The results show that the meteorological data can improve the interferometric radar measurement accuracy. [C10260]

"Identification of inland fresh water wetland using SAR and ETM+ data"

The main aim of this paper was to explore the potential of SAR data, in combination with optical remote sensing data, in identifying inland fresh water wetland from crop, especially rice paddy. The test area is a part of Hongze Lake, the fourth biggest fresh water lake in China. It is one of important wetlands for migratory birds in China. Due to unreasonable exploitation of wetland resources, the lake is facing a great loss of wetland. In Hongze lake watershed, Jiangsu Provincial Sihong Hongze Lake wetland ecological reserve was established for the preserve of wetland ecosystem and rare species in the watershed. In the processing of the dataset, clustering algorithm ISODATA was employed firstly to generate initial classification results for sample selection. Then, 1500 samples were taken in total by using stratified random sampling. These samples were superimposed on the screen on top of rectified aerial images. The land cover class at each point was determined based on field investigation and visual interpretation. 900 samples of them were for training and the other for the assessment of classification accuracy. Attributes of samples such as the digital number values of six bands of ETM+(TM1-5, 7), texture, DEM and 4 components of principal components analysis of six bands of ETM + data, were fed into the CART (Classification and Regression Tree) algorithm for the generation of knowledge rules. Because the training observations were evenly distributed among classes, the class assignment at each terminal node was determined by the majority of per-class observations at that node. Then, decision tree classifier was applied to the imagery of ETM+ for the classification of landuse/cover in the whole study area. RADARSAT SAR C-band

was classified into four classes: lowest backscatter, low backscatter, medium and high backscatter. The results from two data sources were combined by using rules. The results showed that the combination of the SAR data and the optical remotely sensed data have achieved the highest classification accuracy (92.3% of total classification accuracy). The results also confirmed the value of classification tree in the identification of fresh water wetland. It was illustrated that radar data was a good complementary data source for the identification of wetland. [C10261]

"Typhoon monitoring/operational forecasting and services 2005 in China"

Typhoons bring about serious damage to China. The forecasters of CMA predict typhoon track and rainfall intensity with numerical model, satellite images, radar data, automatic station data etc. There are 7 landfalling typhoons in China in 2005. Among these typhoons, Haitang has some characters of high intensity, strong wind, long maintenance over land etc. Its track and rainfall were predicted with numerical model successfully. Typhoon Matsa move towards northwest after landfall, overlapping with the astronomical tide forming strong storm surge. Warnings and disaster prevention and preparedness were in time but there was certain rainfall forecasting bias existed when Matsa move towards north and northeast. [C10262]

"SAR measurements of surface displacements at Augustine volcano, Alaska from 1992 to 2005"

Augustine volcano is an active stratovolcano located at the southwest of Anchorage, Alaska. Augustine volcano had experienced seven significantly explosive eruptions in 1812, 1883, 1908, 1935, 1963, 1976, and 1986, and a minor eruption in January 2006. We measured the surface displacements of the volcano by radar interferometry and GPS before and after the eruption in 2006. ERS-1/2, RADARSAT-1 and ENVISAT SAR data were used for the study. Multiple interferograms were stacked to reduce artifacts caused by different atmospheric conditions. Least square (LS) method was used to reduce atmospheric artifacts. Singular value decomposition (SVD) method was applied for retrieval of time sequential deformations. Satellite radar interferometry helps to understand the surface displacements system of Augustine volcano. [C10263]

"Small scale surface deformation detection of the Gulf of Corinth (Hellas) using Permanent Scatterers technique"

The Permanent Scatterers (PS) technique, invented by Politecnico di Milano research team, is an approach that minimises the undesirable noise components in the classic InSAR technique, such as spatial and temporal decorrelations, signal delay due to tropospheric and ionospheric disturbances, orbital errors as well as topographical errors. This approach is suitable for the measurement of near vertical displacements of the order of ~1 mm per year. It exploits almost all of the available SAR interferometric data over an area and requires availability of natural and/or artificial permanent scatterers. In this study we describe the implementation of the PS technique, called PerSePHONE (Permanent Scatterers Project Held by the Observatory, National, of Hellas). Its development has been based on a number of algorithmic adaptations, as well as new approaches in PS candidate selection. An example of this implementation is shown for the case of the Corinth Rift area (Hellas). [C10264]

"Effect of salinity on the dielectric properties of geological materials: implication for soil moisture detection by means of remote sensing"

This paper deals with the exploitation of dielectric properties of saline deposits for the detection and mapping of moisture in arid regions on both Earth and Mars. We then present a simulation and experimental study in order to assess the effect of salinity on the permittivity of geological materials and therefore on the radar backscattering coefficient in the [1-7 GHz] frequency range. Dielectric mixing models were first calibrated by means of experimental measurements before being used as input parameters of analytical scattering models (IEM, SPM). Simulation results will finally be compared to field measurements (Pyla dune, Death Valley, Mojave Desert) and will be used for the interpretation of SAR data (AIRSAR, PALSAR). [C10265]

"Evaluation of the influence of land cover on the noise level of ERS-scatterometer backscatter"

In this study we assess the impact of different land cover types on the azimuthal noise of backscatter signal using multi-year ERS-scatterometer data. Results indicate a strong response of the azimuthal noise level to the different land cover types like rainforests, lakes, rivers, floodplains, coastal areas, permanent snow or ice, urban areas, and deserts as well as topography. Complex topography with high standard deviation in heights, ridge-shaped features oblique to the satellite track on the surface, and water-contaminated areas are the main causes of the high azimuthal noise in scatterometer measurements. The azimuthal noise fluctuations generally show a minimum over rain forests and maximum over sand deserts. Changes in the level of azimuthal noise of

backscatter signal clearly reflect changes in land cover or surface roughness. [C10266]

"A semi-empirical backscattering model for estimation of leaf area index (LAI) of rice in southern China"

Most paddy rice in southern China grows in warm, humid and rainy areas where it is hard to acquire optical remote sensing data. In this study, a semi-empirical backscattering model was proposed to estimate leaf area index (LAI) of rice in the area using ENVISAT Advanced Synthetic Aperture Radar (ASAR) alternating polarization data. Ground measurements of LAI, water content and height of rice in the test site were collected and the model fitted at the same time as the acquisition of ASAR data. LAI estimated from the model was compared with ground measurements to evaluate the accuracy of the model. The results showed that the model provides a promising alternative to optical remote sensing data for predicting LAI of rice in southern China. [C10267]

"Potential of X-band spaceborne synthetic aperture radar for precipitation retrieval over land"

Numerous space-borne X-band Synthetic Aperture Radars (X-SAR) systems will be launched by European agencies in the coming decade commencing this year. Those X-SARs can measure precipitation over land, thereby significantly augmenting the sensors that comprise the Global Precipitation Mission (GPM). This will incur relatively little incremental cost because they have already been funded. X-SAR measurements are especially beneficial over land where rainfall is difficult to measure by means of microwave radiometers that depend on scattering by frozen hydrometeors associated with that rain. The improved horizontal resolution of the retrievals will match the higher spatial resolution of mesoscale and general circulation models that will become available in the coming decade. [C10268]

"Soil parameter estimation and analysis of bistatic scattering X-band controlled measurements"

In this paper, we will present well controlled experimental bistatic X-band measurements of rough surfaces, which have been recorded in the Bistatic Measurement Facility (BMF) at the DLR Oberpfaffenhofen, Microwaves and Radar Institute. The bistatic measurement sets are composed of soils with different statistical roughness and different moistures controlled by a TDR (Time Domain Reflectivity) system. The BMF has been calibrated using the Isolated Antenna Calibration Technique (IACT). The validation of the calibration was achieved by measuring the reflectivity of fresh water. In the second part, the first validation of the specular algorithm by estimating the soil moisture of two surfaces with different roughness scales will be reported. Additionally, a new technique using the coherent term of the Integral Equation Method (IEM) to estimate the soil roughness will be presented, as well as evaluation of the sensitivity of phase and reflectivity with regard to moisture variation in the specular direction. [C10269]

"Application of C and Ku-Band scatterometer data for catchment hydrology in northern latitudes"

Spatially continuous soil moisture information is on high demand globally. A database which is available from active microwave data (ERS scatterometer, C-band, 50 km) has been assessed over two large basins (Mackenzie and Lena) in northern latitudes. This information was combined with snowmelt patterns which can be derived based on diurnal thaw-refreeze of the snow cover from a further scatterometer (Quikscat, Ku-band, 25 km). Relative soil water information has been averaged over each basin and compared to discharge measurements for the summer periods 1996-2000. A correlation (logarithmic function) of 0.78 is observed for the Lena basin. The Mackenzie is much more complex and thus the relationship is less obvious. This is also reflected in the snowmelt data. Whereas 80% of basin area undergoes melting at the same time in the Lena basin in 2000, at maximum 40% can be observed for the Mackenzie during the same year. Maximum runoff in the Lena basin is observed when snowmelt ceases for the entire basin. This is delayed by three weeks for the Mackenzie although increased runoff can be observed already after 70% of the basin is snow-free. [C10270]

"Integration of L-band SAR data into land surface models"

Land surface process modelling might be limited due to lack of reliable model input data. Key surface variables as land cover information or soil moisture conditions have been proven to be observable by remote sensing systems. The integration of remote sensing data into land surface process models might therefore help to improve their simulations results. Longer wavelength SAR data has a higher sensitivity to soil moisture content than higher frequency systems. Recent (ALOS) and planned (e.g. TerraSAR-L) SAR systems are therefore expected to provide valuable information about soil moisture dynamics. The present study investigates the potential to retrieve land cover information and geophysical parameters from L-band SAR data. The retrieval results are assimilated into a state-of-the-art land surface model to evaluate the merit of L-band SAR data assimilation. [C10271]

"Polarimetric measurements of radar backscatters of a wet-land rice field throughout a growth period at L- and C-bands"

Backscattering coefficients and phase-difference statistics of a wet-land rice field in Suwon, Korea are measured using a ground-based polarimetric scatterometer at 1.9 and 5.3 GHz throughout a growth year from transplanting period to harvest period (May to October in 2006). The ground truth data including bio-mass, plant height, and leaf-area index (LAI) are also collected for each measurement. The measured backscattering coefficients and phase difference statistics are analyzed based on the growth age for each polarization, frequency, and incidence angle. It is found that the hh-polarized backscattering coefficients have wider sensitivity region than the w-polarized backscattering coefficients with respect to the rice growth age. [C10272]

"Ground calibration of SMOS: NIR and CAS"

Ground calibration of the calibration subsystems of MIRAS (Microwave Imaging Radiometer using Aperture Synthesis) has been performed. The MIRAS instrument is the payload of European Space Agency's (ESA) Soil Moisture and Ocean Salinity (SMOS) mission. The calibration subsystems are Calibration Subsystem (CAS), which is a noise distribution network, and Noise Injection Radiometer (NIR), which measures the noise levels of CAS and the average incident brightness temperature. This paper presents the used measurement approaches, related uncertainties, and the calibration results for the NIR and CAS. The results show that in spite of uncertainties, the characterization methods allow accurate ground calibration of the two subsystems. The performance of both subsystems meet the requirements. [C10273]

"The ALOS Kyoto & Carbon Initiative"

The ALOS Kyoto & Carbon Initiative is an international collaborative project led by the JAXA Earth Observation Research Center (EORC). It forms the continuation of JAXA's on-going JERS-1 SAR Global Rain Forest and Global Boreal Forest Mapping project (GRFM/GBFM) into the era of the Advanced Land Observing Satellite (ALOS). The ALOS K & C Initiative has been set up to support the data and information needs required by international environmental Conventions; Carbon Cycle scientists and Environmental Conservation programs (referred below to as the CCCs). Led and coordinated by EORC JAXA, the Initiative is being undertaken by an international Science Team and focuses primarily on defining and optimizing the provision of data products and validated thematic information derived from in-situ and satellite sensors focusing on data acquired from the Phased Array L-band Synthetic Aperture Radar (PALSAR) on-board the Advanced Land Observing Satellite (ALOS). The objective of the ALOS K & C Initiative is to define, develop and validate thematic products derived from ALOS PALSAR data that can be used to meet specific information requirements relating to the CCCs. A key component of this work has been the development of a systematic data acquisition strategy for ALOS which comprises fixed, systematic global observation plans for PALSAR. The strategy is implemented as a top-level foreground mission and with a priority level second only to that of emergency observations. With emphasis on acquiring repetitive and consistent data over continental scales, it ensures that adequate data will be collected to allow the required thematic output products to be developed on a timely basis. The K & C Initiative is based on the three coordinated themes relating to global biomes; Forests, Wetlands, Deserts and Semi-Arid Regions, and a fourth theme dealing with the generation of regional ALOS PALSAR Mosaics. A key word for the Initiative is regional- scale applications and- product development, with data requirements in the order of hundreds or thousands of PALSAR scenes for each prototype area. Each theme has identified key products that can be generated from the PALSAR data including land cover, forest change mapping and forest biomass and structure analysis; global wetland inventory compilation and landscape change determination; and freshwater resources and desertification. Each of the products developed will be generated using a combination of PALSAR imagery, in situ measurements and ancillary datasets. An international Scientific Advisory Panel has been established to maintain the scientific relevance of project design and to ensure alignment with other relevant international efforts (e.g. GOF/GOLD, IGOL, GTOS/TCO). The panel consists of scientists active in the fields of carbon modeling and biophysical parameter retrieval; SAR and image processing, as well as and representatives from GOF, TCO, FAO, space agencies, universities and public research institutions. [C10274]

"ALOS PALSAR for characterizing wooded savannas in Northern Australia"

With the successful launch of Japan's advanced land observing satellite (ALOS) phased array L-band SAR (PALSAR) and the recent provision of a Japanese earth resources satellite (JERS-1) synthetic aperture radar (SAR) mosaic for north Australia, significant opportunities for characterizing, mapping and monitoring the structural diversity and biomass of wooded savannas in Australia have been provided. This paper gives an overview of research undertaken and preparations being made to support such mapping in the state of Queensland. Preliminary observations on the integration of ALOS PALSAR and Landsat-derived foliage

projective cover (FPC) for mapping woody regrowth and dead standing trees are presented. [C10275]

"Some results of the MIRAS-SMOS demonstrator campaigns"

In this paper, some results of the MIRAS-SMOS demonstrator campaigns are presented. The follow two campaigns were held: an image validation campaign at IRTA side and a flight demonstrator campaign at Finland. The ultimate objective of the airborne demonstrator is to demonstrate its imaging capabilities by applying improved calibration and inversion algorithms to natural low-contrast targets. [C10276]

"Corn monitoring and crop yield using optical and RADARSAT-2 images"

In agriculture, soil and crop conditions change from day to day and throughout the growing season. Agricultural targets also vary spatially with differences observed from field to field, as well as within individual fields. The heterogeneity of corn-growing conditions in Mexico makes accurate data for crop type, crop condition and crop yield prediction difficult to obtain. Yield predictions are needed by the federal government to estimate, ahead of harvest time, the amount of corn required to be imported in order to meet the expected domestic shortfall. In this project a methodology for the estimation of corn yield ahead of harvest time is developed which uses radar and optical remote sensing and which specifically considers the corn-growing situation in Central Mexico. Radar based crop type classification requires data sets with multiple polarizations. Recent research to assess relative classification accuracies of multi-polarized combinations for target crops using airborne data has been reported. In addition to identifying crop type and variety, identifying crop growth stage is valuable. Crop condition, loosely defined as the vigor or health of a crop in a particular growth stage, is related to crop productivity and yield; however, the relationship is complex. Main crop condition indicators include biomass, height, leaf area and contents of plant water, chlorophyll and nitrogen. Crop-type and crop-condition mapping are among the applications that are expected to benefit the most from the technical enhancements embodied by RADARSAT-2. The potential of RADARSAT-1 data for these applications has been rated as "limited", whereas for RADARSAT-2 data this potential is anticipated to be "strong". The Science and Operational Applications Research for RADARSAT-2 Program (SOAR) is promoting the evaluation of Synthetic Aperture Radar (SAR) capabilities by providing images to selected research projects which include the present one. objectives of this project are: a) use RADA- RSAT-2 data and optical data to determine cultivated areas and monitor crop condition for obtaining better estimations of crop yield; b) obtain polarization signatures from RADARSAT-2 data for corn and relate these to Leaf Area Index and photosynthetic active radiation (PAR) crop parameters and vegetation indexes, to establish indicators of crop condition and produce estimates for crop yield; c) use field data collected for three key corn crop growth stages over 300 pilot plots during 2001-2006, and increase the number of plots to build a database to support accuracy studies using RADARSAT-2 data. The expected benefits of this project are: to obtain knowledge about crop type, crop condition and crop yield with better accuracy than with current methodologies; to support national corn farmers associations; to design agriculture related activities within State agriculture plans; to support the corn product industry and aid government decision making. Relevant results and economical impact will imply operational usage of RADARSAT- 2 data in the agricultural sector in Mexico. [C10277]

"Sensitivity of multi-temporal high resolution polarimetric C and L-band SAR to grapes in vineyards"

In the follow-up of the BACCHUS project, aimed at establishing a reference high quality geographic information system for vineyards, an airborne SAR survey has been carried out in fall 2005 in the Frascati area, near Rome (Italy) to investigate on the potential of radar remote sensing in vineyard monitoring. This contribution reports on the polarimetric very- high resolution C and L-band SAR data acquisition campaign supported by ESA and carried out by the DLR E-SAR on two dates in October 2005. The possible relation between the observed variations of backscattering at different polarizations and the harvest of the grapes is discussed. [C10278]

"Remote sensing data assimilation for regional crop growth modelling in the region of Bonn (Germany)"

The study investigates the possibilities to improve the performance of CERES-Wheat crop growth model by assimilating information derived by optical and SAR Earth observation data. Biophysical parameter retrieval was done with the water cloud model for SAR data and the CLAIR model was applied to multispectral imagery. The CERES -Wheat model was calibrated using ground truth information. The re-initialization method with an adjustable planting date was selected as assimilation strategy. Modelling results generally improved by using all different kind of remote sensing data. However, best results were achieved by using information of the optical sensors only and not by a synergetic time series of all available data. [C10279]

"Polarimetric analysis of maritime SAR data collected with the DSTO ingara X-Band radar"

Fine resolution spotlight synthetic aperture radar (SAR) imagery collected on a circular flight path is used to investigate the variation in ship detection performance with respect to three fundamental radar parameters: the transmit/receive polarisation combination, the incidence angle and the azimuth angle. The polarisation combinations examined are HH, HV, VV, RR and cross-slant 45deg. Three different incidence angles are considered-50deg, 60deg and 70deg-corresponding to collection geometries for high altitude maritime surveillance systems. Performance is assessed using a simple target-to-background contrast measure. Results are compared with preliminary results from a four component decomposition of the Mueller matrix. While the latter and cross-slant 45deg show promise, in general HH is shown to have the best performance. [C10280]

"Very high resolution interferogram acquisition campaign and processing"

The ONERA RAMSES system is a flexible SAR system in constant evolution, developed mainly as a test bench for new technologies and to provide specific data for TDRI (Target Detection, Recognition and Identification) algorithm evaluation. It is flown on a Transall C160 platform operated by the CEV (Centre d'Essais en Vol). This paper gives an overview of the latest upgrading to acquire large data set without on board deramp-on-receive mode and then present the acquisition campaign at X band for very high resolution single pass interferometric multi-baseline mode. The multi-baseline mode used is a ping-pong mode where four antennas are used. The goal of this campaign was to acquire interferometric data in very high resolution mode, better than 0.3 m along slant range axis with a large slant range swath of 2400 m. [C10281]

"Theoretic error analysis of split-gate tracker in satellite radar altimetry"

A theoretical analysis of the altimeter split-gate height tracker error is carried out in this paper. The principles of altimeter split-gate tracker are reviewed, and the discriminative curve of the tracker is derived. It is shown that the antenna parameters have little influence on the slope of discriminative curve. The height noise of the tracker is analyzed, assuming there is no other noise in the instrument. It shows that the AGC gate noise contributes much in the overall tracker noise in high sea state condition, so a long AGC gate is preferable. Finally, the 1s-averaged height noise level in a typical sea state (SWH=4 m) is calculated, and the error specification (<2 cm) is proved to be met. [C10282]

"Integrating point, curve and area descriptors into geospatial databases for metric resolution SAR image analysis"

Image understanding and retrieval for metric SAR data needs to be tackled by specific algorithms in order to exploit the specific metric scale scene characteristics and the typical sensor phenomenology. A composite approach is developed to this end. Extraction, characterization and simplification/grouping algorithms are employed together with super-resolution for isolated bright scatterers, scatterer alignments and uniform backscatter and texture areas to populate a geospatial database. The generated descriptors can be navigated via different data viewers for scene understanding and data retrieval applications. Examples on real metric SAR data are given. [C10283]

"A FEXP model Short Range Dependence analysis for improving oil slicks and low-wind areas discrimination in sea SAR imagery"

Starting from a consideration of the Long Range Dependence (LRD) behavior of sea SAR image spectra, an overview is given of the LRD approaches currently being used to achieve reliable sea surface anomalies discrimination from high resolution sea SAR images. In this paper, the problem of SAR image analysis to discriminate oil slicks from low wind areas on the sea surface is addressed by employing fractional exponential (FEXP) models and short range dependence (SRD) parameters. The presented method demonstrated reliable results when applied to European remote sensing 2 (ERS-2) SAR precision images (PRI) and ERS-2 SAR ellipsoid geocoded images (GEC) of the Atlantic and the Pacific Oceans. [C10284]

"Robust change analysis of SAR data through information-theoretic multitemporal features"

Multi-temporal analysis of Synthetic Aperture Radar (SAR) images has gained an ever increasing attention due to the availability of several satellite platforms with different revisit times and to the intrinsic capability of the SAR system of producing all-weather observations. As a drawback, automated analysis in general and change detection in particular are made difficult by the inherent noisiness of SAR imagery. Even if a pre-processing step aimed at speckle reduction is adopted, most of algorithms borrowed from computer vision cannot be profitably used. In this work, a novel pixel feature suitable for change analysis is derived from information-theoretic concepts. It does not require preliminary de-speckling and capable of providing accurate change maps from a couple of SAR images. The rationale is that the negative of logarithm of the probability of an amplitude level in

one image conditional to the level of the same pixel in the other image conveys an information on the amount of change occurred between the two passes. Experimental results carried out on two couples of multi-temporal SAR images demonstrate that the proposed IT feature outperform the Log-Ratio in terms of capability of discriminating changes. [C10285]

"Multiscale filtering of SAR images using scale and space consistency"

A new approach for speckle reduction in SAR images based on the stationary wavelet transform is proposed. Noisy wavelet coefficients are reduced via a shrinkage function that depends on a statistical modeling of the normalized wavelet coefficient probability density functions. Consistencies between coefficients across scales and space are also reinforced using consistency rules. The approach is particularly robust in cases of correlated speckle noise. [C10286]

"An innovative algorithm for radar altimeter acceleration bias compensation"

In this paper, the characteristics of the alpha-beta filter in altimeter height loop are analyzed. The "acceleration lag bias" is firstly described and the previous approaches are reviewed, and then, an innovative algorithm is designed to compensate the error. Finally, a numerical simulation is presented to test the effectiveness. It is shown that bias can be almost totally compensated by the algorithm. [C10287]

"Snow avalanche detection and classification algorithm for GB-SAR imagery"

This paper presents an algorithm for the automatic detection and classification of snow avalanches using GB-SAR imagery. The algorithm has been validated extensively in two different test sites in Sion (CH) and Alagna (I), respectively. Results show an important reduction on the images to manually supervise and minimal false negative rate. The real-time availability of the location and extent of the avalanche events provided by this system has demonstrated to be of high interest to ski resort administrators, allowing a more efficient management of the resources available to prepare the tracks. [C10288]

"Optimal configurations of bistatic radar for retrieving soil moisture and vegetation biomass"

The possible contribution of bistatic radar measurements to estimate bare soil moisture and vegetation biomass is investigated by a simulation study based on well established electromagnetic models (both coherent and incoherent components). The best system configuration, in terms of observation directions, polarisations and frequency has been singled out by predicting the retrieval accuracy. This has been evaluated using the Cramer-Rao lower bound to identify optimal configurations for single polarisation and multipolarisation receivers, as well as in case the bistatic measurements are complemented by monostatic ones. [C10289]

"ALOS PALSAR radar observation of tropical peat swamp forest as a monitoring tool for environmental protection and restoration"

Tropical peat swamp forests are threatened by large scale deforestation and canal drainage. Oxidation and forest fire cause enormous carbon emissions. Most remaining areas are located in Indonesia. Time series of historical JERS-1 SAR data reveal the extent and nature of recent disturbances, such as those caused by excess drainage and severe ENSO. Since the dynamics of flooding and drought events can be observed well by the recently launched ALOS PALSAR instrument, important information relevant for detection of ecosystem disturbance and evaluation of restoration efforts can be obtained. [C10290]

"Microwave radar remote sensing of Plinian volcanic ash clouds for aviation hazard and civil protection applications"

The potential of ground-based microwave weather radar systems for volcanic ash cloud detection and quantitative retrieval is evaluated. A prototype algorithm for volcanic ash radar retrieval (VARR) is discussed. Starting from measured single-polarization reflectivity, the statistical inversion technique to retrieve ash concentration and fall rate is based on two cascade steps: i) classification of eruption regime and volcanic ash category; ii) estimation of ash concentration and fall rate. An application of the VARR technique is finally shown taking into consideration the eruption of the Grimsvotn volcano in Iceland on Nov. 2004. Volume scan data from a Doppler C-band radar, located at 260 km from the volcano vent, are processed by means of the VARR algorithm. Examples of the achievable VARR products are presented and discussed. [C10291]

"A new tracker for ocean-land compatible radar altimeter"

Satellite radar altimeter is an active microwave remote sensor for obtaining ocean topography, as well as the

marine and land ice mass fluxes at a global scale. Because the echo properties of ocean, land and pole ice are very different, the on-board tracker of radar altimeter should have the ability to handle the distinct signals automatically. In this paper, a new tracker for ocean land compatible, the model compatible tracker (MCT), is proposed. In MCT, two track algorithms, MLE (Maximum likelihood Estimate) and OCOG (off center of gravity), cooperate in parallel. Therefore, not only the good accuracy but also the robustness can be realized in real time on board. So MCT is very suitable for the ocean-land compatible radar altimeter. The principle of MCT, the cooperation strategy for the two algorithms, the adaptive bandwidth technique, and the realization of MCT are discussed in this paper. [C10292]

"An interferometric imaging altimeter applied for both ocean and land observation"

This paper introduces an interferometric imaging altimeter system designed for both ocean and land observations. This sensor combines the functions of interferometric radar altimeter and SAR together and is aimed to provide centimeter- level accuracy of topography for ocean and meter-level accuracy of topography for land. With the interferometry technique, a wide swath of 80 km is achieved, and with the synthetic aperture technique, a resolution of 100 m for land observation is achieved. System design is outlined and some preliminary results are presented. [C10293]

"Lidar DEM for characterizing the volcanic landforms of tatun volcanoes in metropolitan taipei"

Tatun volcano group is a cluster of dormant volcanoes surrounding metropolitan Taipei. Rugged terrain, monotonic lithology and dense vegetation covers are adverse factors for mapping the geological structures. In this study, airborne lidar survey was conducted to obtain a bare ground DEM with 2 m grid and with an accuracy of decimeters. Shaded-relief images, pit-patterns and drainage networks are then derived from these DEMs for visual interpretation. 51 volcanoes are thus recognized. Two fissures running through the highest volcano in this area, namely Mount Seven-Stars, are extending 2000 m and 1000 m, respectively. The largest width and depth of the opening of the ruptures is located in the west flank of the volcanic cone. The slope angle of the east-wing of the volcanic cone is 36deg, whereas the angle of the west-wing is only 24.5deg. The opening of the west fissure is larger and its extension is longer than the east one. Thus, the west side can be subjected to an active extensional process of strain. The fissures could be resulted from the ongoing regional extension of the Tatun volcanic area due to the plate subduction and collision of the Eurasian plate and the Philippine sea plate. [C10294]

"Relationship between wind vectors and L-band radar cross sections examined using PALSAR"

The relationship between ocean wind vectors and L-band normalized radar cross sections (NRCS) is examined using the Phased-Array L-band Synthetic Aperture Radar (PALSAR). We used PALSAR ScanSAR images with a wide range of incidence angles from 17deg to 43deg. More than 6,000 match-ups, each consisting of the NRCS, incidence angles, wind speeds and wind directions, were collected. The NRCS exhibits a power-law relationship with respect to the wind speed. The coefficients of the power law can be derived as a function of the incidence angles. Based on this relation, the wind speeds are then inversely estimated from the NRCS and the incidence angles. A comparison with the truth winds reveals -0.23 m/s bias and 2.63 m/s rms error, demonstrating the feasibility of L-band scatterometry. Collecting more match-ups and further considering wind-direction dependence, which was not included in this study, would lead to the derivation of a robust L-band model function. [C10295]

"Land use changes driven by 2008 beijing olympic playground constructions and depicted by landsat temporal data"

Landsat TM/ETM+ data in May or June are used to depict the land use changes from 1988,1994, 2001, 2003, 2005, 2006 respectively inner Beijing six ring express road and specially to watch the land use changes from the beginning of Beijing Olympic playground area housebreaking in 2002. The great changes are identified in terms of land use change and usage replacements. [C10296]

"A comparison of the methods for the urban land cover change detection by high-resolution SAR data"

The land cover change detection method using the standard deviation of the backscattering coefficient was suggested. Comparing with the previous method using spatial information such as correlation coefficients, it reduced the commission errors in the agricultural areas. It was found that the detection accuracy increased when the target area was large, but each changed target was difficult to detect for crowded and complex urban areas, even though high-spatial resolution airborne SAR data was used. [C10297]

"Canadian Space Agency's Hurricane Watch Program: Archive contents, Data Access and improved planning strategies"

The Canadian Space Agency's Hurricane Watch program monitors tropical cyclones worldwide and acquires RADARSAT-1 Synthetic Aperture Radar imagery to provide experimental datasets to the scientific research community interested in surface wind field studies. The current HW archives spans from 1999 to 2006 and contain a variety of tropical cyclones from around the world. The images show various storm development stages, and morphological characteristics. To further promote the initiative, CSA is about to provide processed images to the scientific community through an Announcement of Opportunity. In this paper, we will demonstrate how simulations of extensive acquisition plans over the Atlantic basin can provide an improved planning strategy to increase the number of valuable images. [C10298]

"Implementation of 3D discrete wavelet scheme for space-borne imagery classification and its application"

A three dimensional discrete wavelet transform (3D DWT) expands planes of the 2D DWT into volume data. The 3D DWT scheme has advantages of analyzing spectral characteristics in the order of frequency and analyzing changes of spatial information and spectral information simultaneously. Nonetheless, few researchers have attempted to classify multi-spectral images using the 3D DWT. This study aims to apply the 3D DWT to the classification of multi-spectral images and synthetic aperture radar image. To classify these images, we employ two numerical values: The 3D wavelet coefficients and the energy of each band. And then we evaluate their results quantitatively with those of traditional classification techniques including the 2D wavelet scheme. Therefore, the results show that the classification technique of the 3D DWT is more effective than that of traditional techniques, especially in complicated imagery. The accuracy of the 3D energy in SAR imagery is higher. This study provides new numerical values to classify images effectively. Furthermore, these values can be extended to the image retrieval and pattern recognition in high-resolution imagery and this scheme can be employed in image dataset obtained at other times. [C10299]

"The Sentinel-3 mission and its topography element"

In the frame of GMES Program, ESA is currently starting the implementation phase of Sentinel-3 mission, which is intended to provide sustained Ocean and Land observation data over a period of 15 to 20 years. The Topography element of this mission will serve primarily the marine operational users but will also allow the monitoring of sea ice and land ice, as well as inland water surfaces, using novel observation techniques. The launch date for this mission is currently foreseen mid 2012. [C10300]

"An assessment of the Ka band interferometric radar altimeter for monitoring rivers and lakes with the WatER mission"

The Water Elevation Recovery (WatER) satellite mission was recently proposed and supported by a large international scientific community. It is dedicated to the determination of land surface water extent, elevation and slope, and also ocean mesoscale and submesoscale phenomena, using a Ka band Radar Interferometer (KaRIN) as its primary instrument. This instrument is able to provide the appropriate space-time sampling required to observe full signatures of the parameters characterizing these phenomena. However, determining these parameters to the accuracy desired for hydrologic applications is challenging. [C10301]

"Wind jet transition and its localized impact on wave height distribution along the Pacific Coast of Northern Japan"

We present a case study of low-level wind jets induced in sequence by orographic effects off the Pacific coast of northern Japan during 7-11 June 2003, and demonstrate that the transition of the wind jets causes areal differences of the wave height variations along the coast. First, we analyze SeaWinds scatterometer wind measurements. Under the easterly wind, a strong wind jet formed after passing by Cape Erimo. As the wind shifted to the southeast, the wind jet started to decay. In turn, the southerly wind along the coast led to another wind jet in the lee of the easternmost tip of the Sanriku coast. Then, we identify onsets and decays of the wind jets from time series of wind speed at meteorological stations. Finally, we demonstrate that the transition of the wind jets has local impacts on wave height variations. Significant wave heights measured by altimeters were correlated positively with local wind energy, i.e., squares of wind speeds. Accompanying the wind jet formation/decline, significant differences of wave height variations became marked among wave observation stations located along the coast at intervals of up to 50 km. [C10302]

"Simultaneous X-band radar and Ka -band radiometer observations of the ocean"

Simultaneous microwave radar and radiometer observations of the ocean were conducted from aircraft during the ShoWEx'99 experiment. Both radar and radiometer wind dependences show similar signal growth with wind speed increase (except for the radiometer at vertical polarization and a near-Brewster angle). Analysis of the low-wind data shows that wind speed is a poor characteristic of the sea surface state in calm conditions because the wind field itself is quite non-uniform in space and time. Under such conditions both radar and radiometer data show strong scatter versus mean wind speed, but they are still well correlated with each other. We conclude that both active and passive instruments respond to the local variations of the sea surface roughness, which are not related to the mean wind speed at low winds. Our comparison shows that the best correlation is between the radar looking at 40-60deg and the near-nadir looking radiometer, which agrees with the theory of scattering/emission from a rough surface. [C10303]

"Integrated satellite tracking of pollution: A new operational program"

The Canadian Ice Service (CIS) new operational program ISTOP (Integrated Satellite Tracking Of Pollution) is designed to effectively use SAR satellite imagery from Canada's Radarsat-1 as an aid in marine oil spill detection. [C10304]

"Statistical characterization of radar sea scatter for breaking wave detection"

Radar backscatter data are collected using a coherent, dual-polarized radar from a fixed tower in the ocean. Statistical analysis is performed to investigate the 1D and 2D probability density functions of backscatter intensity, Doppler frequency, coherence function and polarization ratio. The fraction of sea spike coverage generally increases with wind speed but the trend of increase is modified by the intensity of background swell condition. Parameterizations of sea spike coverage combining both wind and wave factors show some apparent advantage than parameterizations with wind or wave factors alone. [C10305]

"High resolution millimeterwave SAR for the remote sensing of wave patterns"

High resolution imaging of the ocean swell was performed using data collected with the polarimetric millimetre wave synthetic aperture radar MEMPHIS. The data, representative for a region off the south Spanish Atlantic coast in spring, have been evaluated using imaging and non-imaging statistical methods. The influence of high resolution processing on the clutter statistics for the Ka- and the W-band is discussed. [C10306]

"A case study on swell modulation caused by surface winds using spaceborne Synthetic Aperture Radar"

In an ERS-SAR image of the sea off Kii Peninsula on 30 March 1996, we found an atmospheric front formed by the sheltering effect of land topography and swell modulation in the sheltered/non-sheltered areas. From the SAR image, high- resolution wind speed and SAR-wave spectrum are retrieved. In the frequency range higher than the peak frequency, the SAR- spectra of the non-sheltered area have energy density higher than that of the sheltered area. The difference between the spectra of sheltered/non-sheltered areas is well explained by the simulated SAR spectra using the SAR-derived winds and a wind wave development formula suggest that the observed swell modulation is caused by the surface wind. This is a preliminary report and a full paper will appear elsewhere. [C10307]

"Oceanic Rainfall Retrievals using passive and active measurements from SeaWinds Remote Sensor"

The SeaWinds sensor was launched onboard two satellite missions. The first was the QuikSCAT mission launched in mid 1999 by NASA, and the second was the ADEOS II mission launched by JAXA in late 2002. SeaWinds operates at a ku-band frequency of 13.4 GHz, and was originally designed to measure the speed and direction of the ocean surface wind vector by relating the normalized radar backscatter measurements to the near surface wind vector through a geophysical model function. In addition to the backscatter measurement capability, SeaWinds simultaneously measures the polarized radiometric emission from the surface and atmosphere, utilizing a ground signal processing algorithm known as the QuikSCAT / SeaWinds Radiometer (QRad / SRad). This paper presents an oceanic rainfall retrieval algorithm that combines the simultaneous active radar backscatter and the passive microwave brightness temperatures observed by the SeaWinds sensor. The retrieval algorithm is statistically based, and has been developed using collocated measurements from SeaWinds, the Tropical Rainfall Measuring Mission (TRMM) Microwave Imager (TMI) rain rates, and the National Center for Environmental Prediction (NCEP) wind fields. The rain is retrieved on a wind vector cell (WVC) measurement grid that has a spatial resolution of 25 km. Examples of the rain estimates from SeaWinds are presented, and

comparisons are made with the standard TRMM 2A12 rain data product. Validation results demonstrate that SeaWinds rain measurements are in good agreement with the independent microwave rain observations obtained from TMI. Further, by applying a threshold on the retrieved rain rates, SeaWinds rain estimates can be utilized as a rain flag. In order to evaluate the performance of the SeaWinds flag, comparisons are made with the Impact based Multidimensional Histogram (IMUDH) rain flag developed by JPL. Results emphasize the powerful rain detection capabilities of the SeaWinds retrieval algorithm. Due to its broad swath coverage, SeaWinds affords additional independent sampling of the oceanic rainfall, which may contribute to the future NASA's Precipitation Measurement Mission (PMM) objectives of improving the global sampling of oceanic rain within 3 hour windows. Also, since SeaWinds is the only sensor onboard QuikSCAT, the SeaWinds rain estimates can be used to improve the flagging of rain-contaminated oceanic wind vector retrievals. The passive-only rainfall retrieval algorithm (QRad /SRad) has been implemented by JPL as part of the level 2B science data product, and can be obtained from the Physical Oceanography Distributed Data Archive (PO.DAAC). [C10308]

"QuikSCAT and SSM/I ocean surface winds for wind energy"

Ocean surface winds observed by satellite scatterometer (QuikSCAT) and passive microwave (SSM/I) provide valuable information for wind energy applications. In wind energy two long-term aspects on the offshore wind climate is of concern. One is the 20-year average necessary for the estimation of produced wind power during the life-time of a wind turbine (i.e. wind resource assessment); the other is the month-to-month variation in produced wind power (i.e. wind-indexing). In the present study, the offshore wind resource is estimated from QuikSCAT wind maps. The offshore wind climates at the North-European mid-latitudes and in the Atlantic trade belt zone are compared. Distinct differences are identified and these agree well with independent data from meteorological masts in the two regions. Seven years of twice daily observations from QuikSCAT are used for the offshore wind resource assessment. Wind-indexing is based on long-term trends observed in wind climate statistics. It is customary to observe winds and produced power in parallel in order to keep track of performance. Wind-indexing is based on long-term wind observations and the present study investigate variation in offshore and land-based variations during 18 years observed from SSM/I, other wind observations, model results and produced wind power. Very interestingly it is found that the offshore wind climate is different from wind climates over land in the North-European mid-latitudes. [C10309]

"Towards a high-resolution ASCAT scatterometer wind product"

In scatterometry, the wind vector retrieval problem is ambiguous, i.e., the inversion procedure does not result in a unique wind solution. To remove such ambiguity, a spatial filter is applied over the ambiguous wind field. Such filtering methods succeed in most of the cases. However, as the resolution increases both the noise and the direction ambiguity in retrieved winds increases, leading to arbitrary local minima wind solutions. Exploiting the full wind vector probability density function of the wind inversion, and adopting spatial meteorological balance constraints in a 2D-Var ambiguity removal (AR) alleviates the problem of arbitrary minima and noise, and provides a spatially consistent scatterometer wind field at high resolution. In other words, the method has the advanced filtering properties needed for maintaining small-scale meteorological information in scatterometers, while reducing noise. The method can be adopted in the context of 3D- or 4D-Var data assimilation systems. Moreover, these findings will be used to develop a high resolution (12.5-km sampled) coastal wind product from the new ASCAT scatterometer. [C10310]

"Evaluation of X-band polarimetric radar estimates of drop size distributions from coincident S-band polarimetric estimates and measured raindrop spectra"

Recent research has demonstrated the value of polarimetric measurements for the correction of rain-path attenuation at X-band radar frequency and the estimation of rain parameters including drop size distributions (DSD). The issue this study is concerned with is to what degree uncertainties in attenuation correction can affect the estimation of DSD. Since attenuation correction uncertainty enhances with rain path our hypothesis is that DSD retrieval uncertainty at X-band may deteriorate with range. In this study we evaluate the relative accuracy of X-band DSD retrieval against DSD estimates from S-band radar observations and in-situ disdrometer spectra. We present comparisons of various techniques for estimating DSD model parameters from attenuation-corrected X-band dual-polarization radar data. Coincident X-band (XPOL) and S-band (S-Pol) dual-polarized radar measurements from the International H2O experiment (IHOP) as well as coincident X-band polarimetric radar (MP-X) measurements over disdrometer during a Typhoon storm case in Japan are used to assess the accuracy of the different DSD retrieval algorithms applied to X-band radar. [C10311]

"Waveform coding for dual polarization weather radars"

Polarimetric variables are an essential part of algorithms for improved rainfall rate estimation, attenuation

correction and hydrometeor identification. In such systems the transmit polarization state changes according to some fixed pattern that is repeated. The simultaneous mode and alternating mode waveforms are commonly used in weather radars. In the simultaneous mode of operation the horizontal and vertical polarization states are transmitted simultaneously and samples of both horizontal and vertical co-polar return are obtained. A drawback of the current implementation of simultaneous mode is its inability to measure cross-polar parameters such as linear depolarization ratio. In this paper a technique to estimate cross-polar signals with a simultaneous mode waveform is presented. In this method, the horizontally and vertically polarized transmit waveforms are coded with orthogonal phase sequences. The performance of the phase coded waveform is determined by the properties of the phase codes. This paper presents the performance of the cross-polar and co-polar parameter estimation based on the simulation as well as data collected from CSU- CHILL radar. [C10312]

"Wide area traffic monitoring with the PAMIR system"

This paper presents some Scan-MTI results, which were obtained with the SAR-GMTI system PAMIR developed at FGAN-FHR. The Scan-MTI mode was designed to rapidly monitor wide areas for ground moving targets. The scan operation enables detection of targets from different aspect angles with a high revisit rate. This mode is particularly adapted to perform an efficient traffic monitoring, as well. [C10313]

"Survey of bathymetry and current fields by radar image series acquired by shore based x-band radar"

The error source in assessing the bathymetry by the Dispersive Surface Classifier method is discussed in this paper. The accuracy of the method is high in the deeper areas and is reduced behind the slopes. The identification of systematic correlation of the absolute value of the error with the slope was not possible. The spatial correlation of the error illustrates that the direction of the wave field influences the two neighboring cells in the same direction. [C10314]

"Pol-InSAR Results from ALOS-PaISAR"

The launch of JAXA's ALOS in January 2006 provides-for the first time since the SIR-C/X-SAR mission's in the 80's-the opportunity to acquire Pol-InSAR data from space. Indeed, PaISAR (i.e. the SAR instrument onboard of ALOS) is able to operate in a quad-pol mode-declared by JAXA as an "experimental mode"-that allows the acquisition of Pol-InSAR data in a repeat- pass mode. In this sense, ALOS-PaISAR allows the application, validation and development of Pol-InSAR inversion techniques on a much wider range of sites distributed world-wide and accessible to a much wider scientific user community than possible with airborne sensors. In this paper we present the analysis of fully- and/or dual-polarimetric and interferometric data sets acquired by ALOS/PaISAR during its CAL-VAL and operational data acquisition phase and discuss the potential and the limitations for different polarimetric interferometric applications. More developed applications as forest height estimation from single- and multi-baseline Pol-InSAR ALOS-PaISAR data inversion-addressed in the frame of JAXA's Karbon & Kyoto initiative-as well as novel applications regarding coherent scatterer's detection and interpretation in urban environments are discussed. The impact of critical mission and operation design parameters as spatial coverage, repeat-pass time, observation scenario, and orbit control are evaluated and discussed. [C10315]

"PALSAR CALVAL summary and update 2007"

This paper summarizes the geometric and radiometric calibration results of the PALSAR achieved during the ALOS initial calibration phase, which covers five months between May 16 2006 and October 23, 2006, and the half-year of the operational phase. All the PALSAR modes, FBS (fine beam single), FBD (Fine beam dual), SCANSAR, DSN (band limited SAR), and POL (Full polarimetry) were calibrated and validated using in-total 500 calibration points collected world widely and distributed target data from the Amazon. Through the characterization of the PALSAR, antenna pattern determination, and polarimetric calibration, we performed the adjustments of the PALSAR radiometric and geometric model installed on the SAR processor (SIGMA-SAR). Using the reference points, we finally confirmed that the geometric accuracy of the FBS, FBD, DSN, and POL modes is 9.3 m, that of SCANSAR is 70 m, and radiometric accuracy is 0.64 dB. Polarimetric calibration was successful that amplitude balance of VV/HH is 0.025 dB and the phase balance is 0.32 degrees. [C10316]

"Advanced land observing satellite (ALOS): On-orbit status and platform calibration"

The Advanced Land Observing Satellite (ALOS) was launched on January 24, 2006. Since then, it has been operated successfully on orbit, delivering a variety of high-resolution images in numerous quantities and contributing to disaster management support many times. This paper reviews the last 15 months' operations and on-orbit status of the ALOS spacecraft, with the flight data analysis of the bus subsystems and the mission subsystems. A particular emphasis is given to the assessment, calibration and validation of the mission-related

platform performances such as orbit determination and control accuracies, attitude determination and control accuracies, attitude stability, and pixel geolocation determination accuracy. Efforts to improve these performances are also reported. [C10317]

"Synthetic range profile focusing via contrast optimization"

In stepped frequency radar, target motions produce range profile distortion. Specifically, the target radial velocity causes range profile shift, point spread function symmetric spreading and peak reduction, whereas the target radial acceleration is responsible for both asymmetric and symmetric point spread function spreading. This paper proposes a contrast-based technique for estimating the target motion parameters and therefore for reducing range profile distortions. [C10318]

"The RA-2 individual echoes processing description and some scientific results"

The RA-2 in its nominal operation provides averaged waveforms at the rate of 18 Hz (one averaged waveform over 100 individual echoes, every 0.0557 seconds). It has also the capability to provide limited bursts of individual, unaveraged echo sample data in phase (I) and quadrature (Q), at the full PRF rate. In this concept the full-rate data are stored, for a short burst, into an internal buffer memory, in parallel to the normal averaging and other functions of the instrument. The buffered data are subsequently read out at a much lower rate and appended to the normal science data. These Individual Echoes (IE) are, therefore, not processed onboard in the same way that the nominal RA-2 waveforms are. Recent studies have demonstrated that through the full rate data it is possible to discover some behaviour than cannot be seen with the averaged data. Moreover, it is the first time in altimetry that we have echoes that contain the information of the phase. This is a great potential for new science studies. This paper describes the algorithm applied on-ground to the IE of the RA-2 Burst Waveforms to reproduce the same process done by the instrument on-board (except for the averaging). Once this algorithm is applied to the IE they will be in the same condition than the normal RA-2 telemetered average waveform, but at 100 times higher surface sampling and with the phase information. The final objective of this work is the use of the IE fully processed and instrument calibrated for calibration, validation and science exploitation purposes. We will present results of studies carried out using these IE. The blurring on the averaged waveforms depends on the total movement of the range window [1], which in turn depends on slope of the terrain, the orbit slope and ultimately, how well the on-board tracker tracks that particular waveform shape. In early studies using ERS data, the blurring on the averaged waveforms has been estimated by simulating the ERS range window movement during-tracking. Using individual echoes there is no longer the need to do so, we can directly use these echoes. The IE will be averaged in the correct way and compared to the averaged waveform provided in the nominal RA-2 product. Changes on the retracked epoch and slope of the leading edge can be assessed for different type of waveforms over different surfaces. In particular we will present results of the analysis of the behaviour of IE over the "Salar D'Uyuni" in Bolivia, to better understand biases in retracking of specular echoes. The results can be used to improve the current understanding of retracked elevations over sea ice and help to improve tuning of current sea ice retracking schemes for the EnviSat RA-2 instrument. ESA has run a study on this topic to seed the use of individual echoes by scientists. This study is completed and reconstructed echoes will be made available for the first time to the scientific community. Final results from the technical and scientific application of individual echoes and S band data are described in [3]. [C10319]

"An advanced concept of radar altimetry over oceans with improved performances and ocean sampling: AltiKa"

This paper describes the AltiKa project: the mission, the instrument design, the altimeter parameters, the anticipated performances, the key technologies involved, the whole payload design and budgets, and the microsat configuration. A status of AltiKa development is also given. [C10320]

"Re-tracking of SAR altimeter ocean power-waveforms and related accuracies of the retrieved sea surface height, significant wave height and wind speed"

This paper describes the simulation of the power-waveforms acquired in by a radar altimeter operating in SAR mode over ocean surfaces, including the effects of the radar transfer function and of the geophysical ocean parameters, namely the sea surface height (SSH), the sea surface wave height (SWH) and the surface wind speed (WS). The performances of the SAR mode with respect to the retrieval of the ocean geophysical variables (SSH, SWH, WS) are then computed using the Cramer-Rao estimation bounds. It is shown that the radar to ocean range estimation provided by the SAR mode is improved by more than a factor of two compared with conventional Ku band altimeters. Improvements on SWH and wind speed are also discussed. [C10321]

"Prototype of NASA's global precipitation measurement mission ground validation system"

NASA is developing a Ground Validation System (GVS) as one of its contributions to the Global Precipitation Mission (GPM). The GPM GVS provides an independent means for evaluation, diagnosis, and ultimately improvement of GPM spaceborne measurements and precipitation products. NASA's GPM GVS consists of three elements: field campaigns/physical validation, direct network validation, and modeling and simulation. The GVS prototype of direct network validation compares Tropical Rainfall Measuring Mission (TRMM) satellite-borne radar data to similar measurements from the U.S. national network of operational weather radars. A prototype field campaign has also been conducted; modeling and simulation prototypes are under consideration. [C10322]

"Surface clutter suppression for ice sounding radars by coherent combination of repeat-pass data"

This paper formulates a new approach for ambiguous surface clutter suppression for ice sounding radars. While surface clutter from the non-orthogonal direction is reduced by means of Doppler and/or SAR processing, the residual surface contributions from across-track may still mask the reflection of internal layers and the bedrock, both coming from the nadir direction. The suggested approach involves several repeated acquisitions separated by certain baselines. It uses a geometry model to derive a synthesized sparse array diagram with adaptive nulls in the direction of the ambiguities. Initial performance evaluations for a P-band space-borne mission indicates that clutter can be suppressed by 30-40 dB. The approach can potentially be demonstrated with airborne sounder data in case precise navigation and motion compensation is ensured. [C10323]

"Rain microphysics estimation using X-band dual polarization radar measurements"

Rain microphysics retrieval has been proposed and demonstrated mainly at S-band where attenuation effects are usually negligible. Recent advances in attenuation correction techniques enable rain microphysics retrieval also using attenuating frequencies, such as X- and C-band. Most up to date attenuation correction methodologies are based on the use of a constraint represented by the total amount of the attenuation encountered along the path, which is distributed over each range bin contained in the path. The inner self-consistency of radar measurements can be exploited to improve the attenuation estimate obtained using those techniques. In fact, based on the self-consistency principle, an optimization procedure can be devised to obtain the best estimate of specific and cumulative attenuation as well as of specific and cumulative differential attenuation. The main goal of the study is the examination of the drop size distribution retrieval from X-band radar measurements after attenuation correction. The study is based both on simulated and measured data. Simulations based on the use of profiles of gamma drop size distribution parameters obtained from S-band observations are used for quantitative analysis. Examples of the DSD parameter retrievals using radar measurements corrected for attenuation and differential attenuation are also shown. [C10324]

"Preliminary design of the spaceborne dual-frequency precipitation radar for the global precipitation measurement"

The dual-frequency precipitation radar (DPR) installed on the Global Precipitation Measurement (GPM) core satellite is being developed by JAXA and NICT. This paper describes the results of preliminary design of the DPR instrument. [C10325]

"Simulation of SAR image cross spectra from mixed ocean waves"

A 6-parameter frequency spectrum with two peaks and a cos-2s type spreading function is used to simulate the mixed waves. The spaceborne and airborne synthetic aperture radar (SAR) image cross spectra of mixed waves in different significant wave height, wave length, wave direction and wave component are then calculated by using Engen's nonlinear transformation formula. Analysis based on above simulation indicate that (1) the cross spectra of mixed waves dilate in range direction and shrink in azimuth direction (the so-called azimuth cutoff effect); (2) the cutoff effect increases for waves with larger wave height, or for waves with shorter wave length, or for waves propagating closer the azimuth direction, or for waves containing more wind wave component, or for spaceborne SAR; (3) the cross spectra split into two parts for waves propagating along range direction (the so-called double-peak phenomenon); (4) the direction ambiguity of ocean waves can be removed by using the imaginary part of cross spectra; (5) in addition to the contribution of wind wave part and swell part of the mixed waves, the cross spectra of mixed waves consist of an extra term which leads to an inherent error when using ESA's Envisat ASAR level 2 algorithm to retrieve ocean waves (see the companion paper submitted to this symposium). [C10326]

"Multi-look polar decomposition of polarimetric SAR images"

This paper focuses on the multi-look polar decomposition of SAR images. Standard polar decomposition is generally used in single look polarimetry to decompose a bi-static or mono-static polarimetric scattering matrix

into a product of an Hermitian matrix (boost) and a unitary matrix (rotation). An extension of this use in the framework of multi-looked polarimetry is proposed here. This new approach consists in decomposing the scattering matrix into boost and rotation components before vectorisation, then in averaging to generate boost and rotation coherency matrices separately, with new inferred parameters; the boost and rotation entropies, and concurrent dominant scattering mechanisms (alpha boost and alpha rotation). This multi-look extension of polar decomposition may allow for the definition of a new classification strategy for remote sensing data. [C10327]

"The dependence of polarimetric decomposition parameters on biophysical forest parameters, frequency and methodology"

The increasing availability of fully polarimetric SAR data provides a large potential for the assessment of biophysical forest parameters. Aiming at an inversion of polarimetric parameters into forest parameters, this study shows the sensitivity of polarimetric decomposition theorems (Pauli- and H-lambda decompositions) to biophysical forest parameters, especially forest density. Effects of non-biophysical parameters on the estimation of decomposition parameters are also shown. The investigations were carried out on fully polarimetric data at L-band (1.3 GHz) and P-band (350 MHz) acquired in 2003 in a preAlpine region in Switzerland with the German E-SAR (Experimental SAR) platform. [C10328]

"Experimental validation of a Kirchhoff based shape reconstruction algorithm in realistic conditions: a test case for buried pipes"

A two dimensional shape reconstruction algorithm is applied to experimental GPR in-situ measurement data. The reconstruction algorithm is based on the Kirchhoff approximation and is exploited to process data collected under a multimonostatic configuration by a pulsed GPR. Thus the need to pass from time domain measurements to frequency domain data suitable for the inversion algorithm is also addressed. [C10329]

"Bistatic foliage penetration modelling"

This paper aims at presenting a model able to study the impact of the target presence under vegetation and to assess the detection feasibility. In a first part the model is described. We will then get at the analysis of results for several set of radar configurations to illustrate the potentiality of detection by means of shadows. [C10330]

"Grecosar, a SAR simulator for complex targets: Application to urban environments."

This paper presents a preliminary study about the scattering properties of urban-like scatters based on simulated SAR images. A simple target performed by a box of gypsum located over a perfectly conducting flat plane is analyzed for different views in both ISAR and SAR fully-polarimetric modes. The results are analyzed with the Pauli decomposition theorem and they show that the scattering response of such a target is dominated by a strong scatter, which polarimetric behavior depends on the relative orientation of the target with respect to the radar. Tests with interferometry shows that the height of the box can be reasonably retrieved despite of model simplicity. [C10331]

"A neural approach to unsupervised classification of very-high resolution polarimetric SAR data"

Analysis of L-band polarimetric SAR data has not been extensively carried out for undulating, heterogeneous and fragmented landscapes, where classification can become quite challenging. This paper reports results of a study on the pixel-by-pixel unsupervised classification of very-high resolution polarimetric images by self-organizing neural networks. [C10332]

"Properties of polarimetric sea clutter at 35 GHz"

The FGAN operated MEMPHIS radar was used to measure the backscatter behaviour of sea clutter at 35 GHz. The resulting fully polarimetric, carefully calibrated reflectivity data were analysed with respect to their temporal and spatial characteristics. Temporal decorrelation is fast, accordingly the polarimetric persistence is very low. As to spatial statistics, several well-known probability density functions like redistribution or log-normal are compared to each other. It is found that none of them is ideal. There is always a number of outliers that statistically behave differently. By eliminating them the goodness of the fit can be improved. [C10333]

"Bayesian classification of hydrometeors from polarimetric radars at S- and X- bands: algorithm design and experimental comparisons"

Dual-polarized weather radars are capable to detect and identify different classes of hydrometeors, within stratiform and convective storms exploiting polarimetric diversity. A model-supervised Bayesian method for

hydrometeor classification (BRAHC), tuned for S- and X- band, is described in this study. The critical issue of X-band radar data processing is the path attenuation correction, usually negligible at S-band. During the IHOP experiment (Oklahoma, 2002) two dual-polarized radars, at S- and X- bands, were deployed and jointly operated with closely matched scanning strategies, giving the opportunity to perform experimental comparisons between coincident measurements at different frequencies. Results of hydrometeor classification and water content estimates at S- and X- bands are discussed and the impact of path attenuation correction is quantitatively analyzed. [C10334]

"Glacier volume changes using ASTER optical stereo. A test study in Eastern Svalbard"

Currently, one of the major methodological gaps in the observation of glaciers from space is the measurement of volume changes of mountain glaciers and small ice caps. Here, we present a case study of comparing a photogrammetric digital elevation model derived from ASTER satellite optical stereo to contour lines from a topographic map from the 1970s. For two small ice caps in Eastern Svalbard, Kvalpyntfonna and Digerfonna, we obtain an overall thickness change of about -0.5 m/yr between 1970 and 2002. From comparison of different methods and quality checks we estimate the error of this number to be in the order of 5-10%. [C10335]

"Retrieval of ice thickness distribution in the seasonal ice zone from L-band SAR"

Airborne polarimetric and interferometric synthetic aperture radar (Pi-SAR) observation, conducted in the southern Sea of Okhotsk in February 2005, provided the opportunity to validate the retrieval of ice thickness distribution. In conjunction with the airborne SAR observation, in-situ ice thickness and ice- surface roughness measurements were carried out in the same area with ship-borne electromagnetic (EM) inductive sounding and supersonic profiling, respectively. Based on the analyzed results of data acquired in this experiment, this paper examines the possibility of ice thickness retrieval from the L-band SAR backscattering data in the seasonal ice zone (SIZ). [C10336]

"Interpretation of C-band SAR backscattering coefficient time series for the Baltic Sea landfast sea ice using a 1-D thermodynamic snow/ice model"

We have compared time series of C-band HH-polarization backscattering coefficients (σ_{deg}) of the Baltic Sea land-fast level ice with results from a 1D high-resolution thermodynamic snow/ice model (HIGHTSI). The σ_{deg} time series were obtained from ENVISAT synthetic aperture radar (SAR) images acquired in February 3-April 7, 2004, and February 6-April 30, 2006. Typically the HIGHTSI results greatly helped to interpret the σ_{deg} behavior with changing weather conditions. There were some cases where detailed ground truth, combined with theoretical σ_{deg} modeling, would have been needed for interpretation of the σ_{deg} trends. From the point of view of operational Baltic Sea ice monitoring with SAR images, the most interesting observation was the large variation of level ice σ_{deg} with changing weather conditions. [C10337]

"A new algorithm to calculate sea ice concentration from the SSM/I 85GHz observations"

A new algorithm has been developed to calculate sea ice concentration from any set of passive microwave observations. It was applied to estimate total ice concentration and partial concentration of three ice types using SSM/I 85 GHz observations. The essence of the algorithm is a mathematical optimization technique to determine the best solution from multi-channel observations of a heterogeneous footprint that contains ice types of highly complex and overlapped brightness temperature. Results were validated against ice concentrations from Radarsat image analysis; an operational product from the Canadian Ice Service (CIS). They have proven the successful performance of the algorithm. [C10338]

"GPR missions on mars"

Recently in order to investigate the distribution of water, liquid and solid, in the upper portions of the crust of Mars planet two different instruments are active, the Mars Advanced Radar for Subsurface and Ionosphere Sounding (MARSIS) and SHAallow RADar (SHARAD). Both the instruments are a low frequency (1.8-5MHz for MARSIS and 20 MHz for SHARAD) Ground Penetrating Radar (GPR) in altimeter configuration which uses the synthetic aperture technique. The main differences between the two instruments are the spatial resolution (150 m vertical resolution, 5-10 Km along track resolution for MARSIS and 15 m vertical resolution, 300-500 m along track resolution for SHARAD) and the penetrating capability (about 5 Km for MARSIS and 1 Km for SHARAD). After the instrument data acquisition from the Martian surface an appropriate processing shall be performed in azimuth (unfocused for MARSIS and focused for SHARAD) and range dimension to produce the scientific final data. In this work will be presented an efficient procedure to detect the possible subsurface presence using the available surface topography data. After the performance evaluation of this technique an example of application will be presented on real SHARAD data [C10339]

"Focusing problems of subsurface imaging by a low-frequency SAR"

ONERA radar RAMSES was recently upgraded with low frequency band (P-band, 435 MHz). In P-band, frequencies penetrate through the ground and through forest canopy. Unfortunately, the formation of the subsurface radar images presents a number of new specific challenges that include algorithm validity, calibration methods, radio-frequency interference, and image focusing and analysis. This paper addresses the aspects of focusing images from an airborne low frequency SAR of buried targets in a lossy and dispersive soil. The hydrological model (Richards' equation) was used to model the multilayer case. [C10340]

"GPU-based framework for interactive visualization of SAR data"

Synthetic aperture radar data presents specific problems for interactive visualization. The high amount of multiplicative speckle noise has to be reduced. The high dynamic range of the amplitude data must be mapped to the lower dynamic range of display devices in a way that makes image features appropriately visible. In addition to interactive navigation in the data, it is desirable to allow interactive selection of despeckling and dynamic range reduction methods and adjustment of their parameters. Graphics processing units (GPUs) can be seen as ubiquitous parallel coprocessors with extreme computational power. In this paper, we propose a GPU-based framework for interactive visualization of SAR data. Data management techniques are used to make full use of the GPU. We reworked well-known despeckling and dynamic range reduction techniques for the GPU programming model and implemented them in our framework. Both navigation in large data sets and adjustment of processing parameters are fully interactive. [C10341]

"Active remote sensing applications to disaster management with implications to spectrum management"

Spaceborne active sensors have been used for years to study the Earth's surface and atmosphere. The intent of this paper is to present the unique types of active remote sensors and their characteristics that apply to disaster management; and to present a status of current frequency spectrum use and needs of spaceborne active sensors, along with any issues or concerns. [C10342]

"Retrieval of fully polarimetric mueller matrix under Faraday rotation effect at P band in space-borne polarimetric SAR observation"

Spaceborne microwave observation of subcanopy and subsurface requires the SAR (polarimetric synthetic aperture radar) technology at lower microwave frequencies, such as P band. However, SAR observation at P band is remarkably influenced by Faraday rotation (FR) effect through ionosphere. An example in this paper illustrates why the measured polarimetric data with FR at P band cannot be directly applied to terrain surface classification. We further present that the parameters u , v , H , a , A for terrain surface classification derived from the polarimetric data without FR, which are recovered from the data with FR, can be applied to the surface classification, even there is a plusmn $\pi/2$ ambiguity error unresolved. Based on gradual change of FR degree along geographical location, a method to eliminate the plusmn $\pi/2$ ambiguity error is designed. Thus, the polarimetric scattering vector and Mueller matrix without FR and plusmn $\pi/2$ ambiguity can be fully inverted from the measured polarimetric data with FR. [C10343]

"Ice flow estimation of Shirase Glacier by using JERS-1/SAR image correlation"

We applied an image correlation method to the Japanese Earth Resources Satellite-1 (JERS-1) synthetic aperture radar (SAR) data obtained from 1996 to 1998. The obtained ice flow velocity was systematically larger on the western streamline than on the eastern streamline from the grounding line towards the downstream region. The differences were 0.28 km/a in 1996 and 0.33 km/a in 1998, which were significantly larger than the error estimate of 0.04 km/a. The ice flow direction was about 312deg at the grounding line and changed to 327deg at 10 km, 346deg at 20 km and 2deg at 30 km downstream from the grounding line. The total deflection attained 38deg towards east. [C10344]

"An improved methodology to map Snow Cover by means of Landsat and MODIS imagery"

In this article we propose a methodology to determine snow cover by means of Landsat-7 ETM+ and Landsat-5 TM images, as well as an improvement in daily Snow Cover TERRA- MODIS product (MOD10A1), between 2002 and 2005. Both methodologies are based on a NDSI threshold > 0.4 . In the Landsat case, and although this threshold also selects water bodies, we have obtained optimal results using a mask of water bodies and generating a pre-boundary snow mask around the snow cover. Moreover, an important improvement in snow cover mapping in shadow cast areas by means of a hybrid classification has been obtained. Using these results

as ground truth we have verified MODIS Snow Cover product using coincident dates. In the MODIS product, we have noted important commission errors in water bodies, forest covers and orographic shades because of the NDVI-NDSI filter applied to this product. In order to improve MODIS snow cover determination using MODIS images, we propose a hybrid methodology based on experience with Landsat images, which provide greater spatial resolution. [C10345]

"Assimilating spaceborne radar and ground-based weather station data for operational snow-covered area estimation"

An enhanced method for snow-covered area (SCA) estimation for boreal forest zone is presented. The method combines TKK developed spaceborne radar-based SCA estimation with ground-based weather station observations. The purpose is to improve the reliability of SCA estimates near and after the end of snow-melt season. The SCA estimates acquired with the enhanced method are compared with optical satellite data-based (MODIS) SCA data. Investigations were carried out for snow-melt seasons of 2004-2006. The results show a significant increase in accuracy when the enhanced SCA method is applied. Correlation between the radar-based and optical reference data increases from 0.919 to 0.937 and RMS-error improves from 0.151 to 0.140 when the new method is employed. [C10346]

"Diurnal SAR variability due to ice and snow air interface wetness overnight changes."

For a water content over 8%, the transmitted component of a SAR beam becomes negligible. The electromagnetic wave interaction with the interface discontinuity is then determined by the scattering efficiency of surface roughness rms and correlation height. It is illustrated by the difference of contrast observed on images acquired from a same scene one late in the afternoon after a warm day and the development of a wet interface, and the other, early in the morning after a cool night and growth of frost flower in place of the wet interface. The increased the rms height of newly formed crystals reduce the angle dependence of the backscattered signal and therefore the contrast on the scene, however, the increased volume scattering in snow covered areas seems to be the main factor causing a resolution difference on the ridge network between images recorded on morning and at the end of the afternoon. A detailed survey of the air-snow or air-ice interface of the snow cover and ice blocks surfaces. Surface wetness, snow wetness content and surface roughness are documented. Radar data measured on a variety of snow and ice interfaces are presented and analyzed. We show that the presence of a wet film on snow and ice surfaces produces an increased forward scattering whereas interfaces covered with newly crystallized ice display an enhanced backscattering. [C10347]

"Robust measurement of glacier surface motion from multiscale speckle tracking using local constraints"

A grown importance in long-term operational glacier monitoring has emerged, mainly due to the connection of glacier recession to climate changes. Up to now, mainly two types of methods have been used for the estimation of glacier flow velocities: Image matching and differential interferometry (DInSAR). Although the principal potential of DInSAR for glacier velocity estimation has been shown in several case studies, its successful application is often limited by phase noise, described by the coherence. Additionally, the glacier velocity is often too large to be analysed by means of DInSAR since this method can be too sensitive to correctly track the large displacements occurring during a typical data acquisition interval of one month. SAR amplitude images are not limited by phase stability problems like in DInSAR and can reliably be acquired on a regular basis. In this work, a novel algorithm for computing the velocity field and motion parameters from a sequence of SAR amplitude images are presented. The algorithm is based on the vector relaxation combined with standardized cross-covariance matrix information and cross-correlation techniques. The cross-correlation is used to indicate the candidate motion vectors for each pixel. After this step, by a relaxation operation local smoothness constraints are introduced into the estimated flow pattern, leading to a more homogeneous velocity estimation. In order to handle fast motion and reduce the mismatches, the mentioned algorithms are applied in different scales and linked using anisotropic diffusion equation in case of multiscale cross-correlation. This significantly improves the reliability of the motion detection in the presence of noise, inherent in case of SAR data. [C10348]

"Passive microwave signatures of autumnal sea ice types from ship-based observation"

Surface-scale passive microwave signatures of newly formed sea ice were collected using ship-based radiometers in the Southern Beaufort Sea and Amundsen Gulf between mid October and mid November 2003. Sea ice in the region was highly spatially and temporally variable. Over a heterogeneous area of open water and thin ice, polarization ratios showed multimodal frequency distributions and the differences between surface and satellite radiometric data were large. However, differences were small over a homogeneous area of snow-covered first-year ice during late fall and the corresponding histograms showed unimodal distributions. Our

results suggest that sub-pixel heterogeneity is a critical factor in characterizing the mixture rules used in passive microwave sea ice algorithms. [C10349]

"P-sounder: an airborne P-band ice sounding radar"

This paper presents the top-level design of an airborne, P-band ice sounding radar under development at the Technical University of Denmark. The ice sounder is intended to provide more information on the electromagnetic properties of the Antarctic ice sheet at P-band. A secondary objective is to test new ice sounding techniques, e.g. polarimetry, synthetic aperture processing, and coherent clutter suppression. A system analysis involving ice scattering models confirms that it is feasible to detect the bedrock through 4 km of ice and to detect deep ice layers. The ice sounder design features a digital signal generator, a microstrip antenna array, a conventional RF-architecture with a central transmitter, four receivers, and internal calibration loops. In 2008 the first data acquisition campaign will take place in Greenland. [C10350]

"Potential of a C-band SAR mission with 12-day repeat cycle to derive ice surface velocity with interferometry and offset tracking"

The goal of this contribution is the assessment of the potential of a C-band SAR mission with repeat-pass interval of 12 days-as the intended European satellite system Sentinel-1-to derive ice surface velocity using SAR interferometry (InSAR) and offset-tracking. For this purpose we investigated ERS-1 SAR data acquired during the ice missions in 1992 and 1994 in 3-day repeat-orbits at Nordaustlandet in the northeast Svalbard archipelago. In 12-days winter InSAR pairs phase decorrelation is mainly observed in areas of high strain rates and, in certain cases, because of snow melting or redistribution through snowfall or wind. Velocity maps derived from these image pairs were found useful to enhance in regions of slow glacier flow the mapping of the surface ice-flow divides previously determined from optical imagery and topographic information. Range-azimuth offset-tracking investigations suggest that the expected error of this method is on the order of 50 m/year and that spatial coverage is generally satisfactory. Application of dual-azimuth offset-tracking, use of HH polarization and enhanced spatial resolution, feasible with Sentinel-1, could enhance the expected error. [C10351]

"The problem of parameter estimation for spatially correlated polarimetric ground clutter at millimeterwave frequencies"

Most mathematical methods commonly used to estimate the parameters of a probability density function are based on the assumption of independent identically distributed (iid) data. However, the analysis of the reflectivity values of polarimetric ground clutter has shown that there may be a considerable amount of correlation depending on the type of clutter. For this analysis the estimated autocorrelation function, the Bartels test, and the runs up and down test for randomness are used. [C10352]

"Design of FMCW millimeter-wave radar for helicopter assisted landing"

This paper discusses the design and construction of a compact, ultrafast, monostatic frequency modulated continuous wave (FMCW) millimeter-wave radar, operating at 94.75 GHz, intended to be used as a helicopter assisted landing sensor. A high speed direct digital synthesizer is used to generate the baseband FM signal. Custom transmitter/receiver baseband boards are designed to up/down-convert the frequency modulated (FM) signal to an appropriate IF before it can be connected to the W-band RF frontend. A high-gain lens horn antenna is used in the RF frontend, in conjunction with other waveguide-based W-band components. A Xilinx FPGA is used in the backend data processing, preferred over conventional DSPs because of its speed. The whole system is packaged in an aluminum casing, with dimensions of 9' x 11' x 11' and weighing under 20 lbs. [C10353]

"A ship detection method for dual polarization SAR data based on whitening filtering"

Recently, as the rapid growing use of dual polarization spaceborne SAR data for ship detection, it seems necessary in practice for us to find a favorable detection algorithm, however, which is still scarce in literatures. In this paper, based on the application of the whitening filter, we proposed to design a dual polarization CFAR (Constant False Alarms Rate) detection method for ship detection, with the verification of its CFAR property. Preliminary detection results of real Envisat/ASAR Alternating Polarization (AP) mode data were shown in the last section to validate the detection method. [C10354]

"Comparison of parameter estimation accuracy of distributed-target polarimetric calibration techniques"

The accuracy with which distributed-target polarimetric calibration algorithms estimate crosstalk and the ratio of

Tx-to-Rx channel imbalance is compared. The algorithms investigated are minor variants of previously-published algorithms but rederived for notational and definitional consistency. Numerical simulations were used to assess the algorithms' performance in the absence of noise. Results indicate that the imbalance parameter is generally accurately-estimated but that crosstalk estimation accuracy varies greatly. [C10355]

"Signatures of polarimetric parameters and their implications on land cover classification"

Knowledge-based or rule-based classification schemes provide robust classification of normally a few major classes. In order to determine optimum polarimetric parameters for such classification schemes, a study has been performed, where the separability between different sets of major classes using many different polarimetric parameters has been investigated using airborne, C- and L-band polarimetric SAR data. [C10356]

"An approach to classify polarimetric P-band SAR images for land use and land cover mapping in the"

In this paper the potentiality of polarimetric P-band SAR data for Amazon tropical forest land cover mapping is assessed. The classifying approach is based on the Iterative Conditional Mode (ICM) algorithm, taking into account several specific distributions to SAR data. Distinct land cover classes are modeled considering different distributions. The results show that the P-band data is not capable to discriminate the nine classes initially used. However this capability improves significantly when classes having similar vegetation structure are grouped. The HV image is effective in differentiating primary and very old regeneration forest areas from other land cover classes, while W image increases the classification of bare soil and crop/pasture areas. The results show the importance of polarimetric information for the classification of several land use classes. [C10357]

"Degree of polarization for weather radars"

Future operational weather radars are likely to implement hybrid polarization, an operating mode that involves transmitting 45deg slant polarization and receiving the horizontal and vertical components of the backscattered field. In this work, the degree of polarization at slant send is theoretically considered and experimentally evaluated from fully polarimetric signatures in order to assess its potential for use in next generation operational weather radars. [C10358]

"Polarimetric optical tools and decompositions applied to SAR images"

Radar polarimetry aims to determine the scattering properties of a target or scatterer. For this purpose, the scattering matrix can be analyzed and represented in several ways using various techniques to extract information about the scattering mechanisms. Polarimetry and ellipsometry are techniques which both study the properties of the polarization of the scattered waves but traditionally refer to different wavelengths: optical wavelengths for ellipsometry, and high-frequencies radio waves for radar polarimetry. This paper deals with natural targets in the general bistatic case, for which the 16 parameters of the Mueller matrix are independent. We try to answer the following questions: how to deduce the radar polarimetric parameters from the optical measurements of a Mueller ellipsometer? What are the polarimetric parameters traditionally devoted to optical images, and in which extent is it possible to apply and interpret them in the case of SAR images? [C10359]

"Design and development of a signal and data processor test bed for a passive radar in the FM band"

This paper describes the design and development of the signal and data processing chain required by a Passive Covert Radar (PCR) exploiting a single non co-operative frequency modulated (FM) commercial radio station as its transmitter of opportunity. The processing chain is proved to: 1) efficiently remove interference and clutter from the received signal, 2) detect targets and extract their bistatic range, bistatic Doppler and azimuth, 3) track targets in the Cartesian domain via the use of particle filtering. The whole processing sequence has been tested using emulated FM radio signals and scenarios as an input to receiving channels. Detection and tracking performance of the passive radar have been assessed comparing the performance of the signal and data processor test bed to the truth data feeding the test bed itself. [C10360]

"Simultaneous radar observations of tropical cyclones by space-based and ground-based radar"

Megha 2700, S-band ground-based Doppler weather radar (DWR) located on the east coast of India, is capable of providing long range detection and characterization precipitation and severe storm such as tropical cyclone over Bay of Bengal. The location of the radar is in coverage area of Tropical Rainfall Measurement Mission (TRMM) satellite. Precipitation radar (PR) operating at Ku-band (13.8 GHz) aboard the TRMM has capability of providing vertical structure of tropical cyclones. Although tropical cyclones can be frequently observed by PR,

and their vertical structure can be studied, it is not so frequent that they are observed by most existing Ground based weather Radars (GR). The authors take this opportunity for performing inter-comparison between the two radars and inter-compare vertical profile of reflectivity (VPR) of tropical cyclone which were simultaneously observed by the Megha 2700 DWR and PR. This work can be useful not only in cross-monitoring severe tropical cyclone activity in a long range over Bay of Bengal, but also as ground validation study of TRMM, and even to the future global space based precipitation mission such as Global Precipitation Measurement (GPM), which is planned to fly over the globe in the near future. [C10361]

"Comparison of NOWRAD, AMSU, AMSR-E, TMI, and SSM/I surface precipitation rate Retrievals over the united states great plains"

This paper compares surface precipitation rates retrieved for the United States Great Plains (USGP) during the summer of 2004 using the Advanced Microwave Sounding Unit (AMSU) aboard the United States NOAA-15 and -16 satellites with similar precipitation products produced by AMSR-E aboard the NASA Aqua satellite, SSM/I aboard the United States DMSP F-13, -14, and -15 satellites, TMI aboard the NASA TRMM satellite, and a doppler radar product (NOWRAD) of the Weather Services International Corporation (WSI). AMSU surface precipitation rates were retrieved using neural network algorithms trained with either a cloud-resolving MM5 physical model for 106 global storms (the AMSU/MM5 algorithm), or summer NEXRAD radar data for the USGP (the AMSU/NR algorithm). Observed correlation coefficients between $\log_{10}(X + 0.01)$ for NOWRAD surface precipitation rates X (mm/h) at 0.25-degree resolution and those for other sensors were, in declining order, 0.82, 0.79, 0.78, 0.71, and 0.68 for TMI, SSM/I, AMSU/NR, AMSR-E, and AMSU/MM5, respectively. Higher correlation coefficients were obtained when TMI was regarded as truth: 0.86, 0.83, 0.82, 0.80, and 0.78 for SSM/I, AMSU/NR, NOWRAD, AMSU/MM5, and AMSR-E, respectively. Other sensor comparisons include false alarm statistics for all pairs of sensors, rms and mean differences with respect to NOWRAD, precipitation-rate distribution functions, and observed correlations between NOWRAD and AMSU/MM5 precipitation and hydrometeor water path retrievals. [C10362]

"Distributed target detection in SAR images using improved chaos-based method"

Detection of distributed targets such as internal wave or ship wake on sea surface in Synthetic Aperture Radar (SAR) images is an important application of ocean microwave remote sensing. The chaotic characteristic of sea clutter gives some clues to targets detection on sea surface. Speckle, the inherent noise of SAR image, will affect the predictive accuracy of sea clutter adversely and reduce the detection performance of radar. In order to apply the chaotic characteristic of sea clutter to targets detection in SAR images more effectively, an improved chaos-based detection method is proposed in this paper. First, speckle noise is suppressed by undecimated wavelet transform (UWT), and then targets are detected on the basis of the chaotic characteristic of sea clutter from the denoised SAR images. Experimental results prove that the method proposed in this paper is effective for the distributed targets detection in SAR ocean images. [C10363]

"TerraSAR-X Mission Status"

TerraSAR-X is Germany's first national remote sensing satellite being implemented in a public-private partnership between the German Aerospace Centre (DLR) and EADS Astrium GmbH, with a significant financial contribution from the industrial partner. This radar satellite, which is to be launched in June 2007 will supply high-quality radar data for purposes of scientific observation of the Earth for a period of at least five years. At the same time it is designed to satisfy the steadily growing demand of the private sector for remote sensing data in the commercial market. This contribution will describe first the public-private partnership scheme, the roles and responsibilities of the partners as well as the overall project organization. The mission and system design will then be described, followed by a brief overview of the satellite, the related Ground Segment and the applied data policy. The contribution will then focus on the actual mission status. Finally a brief outlook will be given on the activities to come. [C10364]

"Observational data set in support of falling snow retrieval algorithm development"

The Canadian CloudSat/CALIPSO Validation Program (C3VP) was a field campaign held during the winter of 2006-2007. The C3VP provided an opportunity for the Global Precipitation Measurement (GPM) mission team to participate in cold-season northern latitude data collection activities in advance of GPM's launch. The GPM team collaborated by providing instrumentation and scientists in order to advance the development of falling snow detection and snow rate retrieval algorithms. This paper will describe the field campaign, present some observations, and provide early analysis from the resulting measurements. [C10365]

"The Gauss-Newton algorithm in passive aircraft tracking using doppler and bearings"

Passive Coherent Location (PCL) radar systems capitalise on illuminators of opportunity such as TV broadcast stations, in order to obtain RF backscatter from targets such as aircraft. In this paper it is envisaged that an array of receivers is available, each of which measures both the bearing to an airborne target as well as the Doppler shift of the signal induced by the target's motion. These bearing and Doppler values are then processed by the method invented by Gauss in 1809 called the Gauss-Newton (GN) algorithm [2, 3, 6], which is discussed in further detail in an accompanying paper in these proceedings [7]. Results are presented, based on an extensive simulation study for various target types and varying numbers of receivers. [C10366]

"Impact of air target altitude and co-channel interference to coverage area of GSM and DVB-T based passive radar"

In this paper, the coverage area of a passive bistatic radar system is considered in a case of air target with different altitudes. Illumination of the target is carried out either by GSM-900 base stations or by DVB-T broadcasting stations existing in Finland. Direct path and co-channel interference, propagation attenuation at different antenna heights and target altitudes as well as antenna radiation patterns are taken into account in the estimation of the coverage area. The estimated coverage area is expressed as a function of receiver location with different altitudes of target and with different attenuation values of interference cancellation. The results show that the coverage area depends on the target altitude only if the altitude is very low, and co-channel interference cancellation has a significant role especially in the case the illumination of the target is carried out by GSM-900 base stations. [C10367]

"Modification of the beam mismatch correction algorithm"

In August 2001, the orbit of the Tropical Rainfall Measuring Mission (TRMM) satellite has been boosted from the altitude of 350 km to 400 km to extend its life time. The time delay between transmission of pulses and reception from rain/surface echoes occurs by one inter pulse period (IPP) (Takahashi and Iguchi, 2004). Due to this time delay, one pulse transmitted at N-1th angle bin is received at the receiving time gate of the next angle bin N. So the mismatch occurs between the transmitting antenna beam direction and the receiving antenna beam direction. This causes antenna gain reduction by 6 dB and leakage of rain/surface echo from the N-1th angle bin to the Nth angle bin. In this paper, the modified beam mismatch correction algorithm is tested numerically, then it's applied to the standard algorithm of TRMM/precipitation radar to reduce the correction error of the current beam mismatch correction algorithm. [C10368]

"Adjustment of cross-track dependence of TRMM Precipitation Radar observation"

The Tropical Rainfall Measuring Mission (TRMM) is NASA's first mission dedicated to observing and understanding tropical rainfall and its effects on global climate. The Precipitation Radar in TRMM is the first spaceborne instrument designed to obtain three-dimensional maps of precipitation reflectivity. Such measurements yield information on the intensity and distribution of rain, rain type and storm depth. An advantage of space radar is that the scattering volume has similar size at any location. However, it has been a challenge to compare data to the one that is collected from the Tropical Rainfall Measuring Mission (TRMM) precipitation radar (PR) for varying scan angles. Intercomparisons between ground radar and spaceborne radar on a point-by-point basis can be a difficult task. Errors result from the mismatch between ground radar and spaceborne radar resolution volume, spatial alignment, and operating frequencies as well as the limited number of the data set collected instantaneously by both instruments. Differences in viewing aspects and resolution that result from the measurement of return signals from different volumes of the precipitation medium contribute to the intercomparison error. A study of the characteristics of the region of the bright band from TRMM-PR vertical profile measurements on a global scale indicates that while bright band height varies widely, the distribution of bright band structure does not vary around the globe. The results show that the average profile of the bright band vertical profile using bright band height as a reference point around the globe has unique profile and do not changes around the globe for large data set. This unique profile can be used to adjust the radar observation error due to different parameters. The TRMM-PR vertical resolution becomes poorer with increasing distance of the TRMM-PR samples from the nadir. Studying the model profile at the nadir profile and other profiles that are off-nadir ray can be used to build the statistical model that can be used to adjust the effect of the scanning cross-track at angle far from the nadir-ray, and the results are presented. [C10369]

"Analysis of densely observed TRMM/PR data during 180-degree yaw maneuver"

The Tropical Rainfall Measuring Mission (TRMM) satellite performs 180-degree yaw maneuver (yaw-around) when the solar beta angle which is the angle between the satellite orbit plane and the direction to the sun crosses the 0-degree. The yaw- maneuver is completed about 16 minutes (about 7000 km in flight length on the Earth) in the TRMM case. During the yaw-around, the precipitation radar (PR) onboard TRMM continues

nominal observation (but data processing is limited to level-1 algorithms). Therefore very dense observation is realized during the yaw-around. Since nearly fixed target (rain echo and surface echo) is observed by different incident angles in a short time, new information can be obtained that cannot be obtained nominal observation. On the incident angle dependency of the sea surface echo, we can avoid the uncertainties comes from the changes in the target. Range profiles of the sea surface echo of different incident angles are compared with the long-term global average data. The same approach can be used to quantitative estimation of bright band structure such as blurring effect of the off-nadir incident angles. A case study on 24 January, 2000, which is the stratiform rainfall case over Borneo Island and the range of the incident angle is about ± 6 degrees, shows that significant difference cannot be seen among data and that the echo strength of each height concentrate within 3-dB. However, the range profiles of the surface echo underneath the stratiform rainfall show quite different angle bin dependency from the reference echo profiles near the rain area. For convective echoes, the nonuniform beam filling (NUBF) effect can be estimated by the different incident angle data and the data which location is slightly offset from the center. More reliable path integrated attenuation (PIA) can be obtained from different incident angle data and the NUBF can be estimated both by the range profiles of surface echo of off-nadir angle bin data with an approach by Takahashi et al. (2006) and their change with the location within a footprint.

[C10370]

"The TanDEM-X mission: Overview and status"

TanDEM-X opens a new era in space borne radar remote sensing. The first bistatic SAR mission, is formed by adding a second, almost identical spacecraft, to TerraSAR-X and flying the two satellites in a closely controlled formation with typical distances between 250 and 500 m. Primary mission objective is the generation of a consistent global digital elevation model with an unprecedented accuracy according to the HRTI-3 specifications. Beyond that, TanDEM-X provides a highly reconfigurable platform for the demonstration of new SAR techniques and applications. This paper gives an overview of the TanDEM-X mission concept, summarizes the capabilities of the system, illustrates the achievable performance, and provides some examples for new imaging modes and applications. The mission has been approved for full implementation by the German Space Agency with a planned launch in spring 2009. [C10371]

"First results of ground moving target analysis in TerraSAR-X data"

Summary form only given. The advanced high-resolution German SAR satellite TerraSAR-X is scheduled to be launched at the end of May 2007. Due to its daylight and weather independent applicability in combination with a large spatial coverage and a short acquisition time, SAR has become a promising tool for traffic monitoring in recent years. Ground moving target indication (GMTI) techniques shall be applied to TerraSAR-X data in order to demonstrate the capability of a space borne SAR sensor to monitor traffic flows on highways. A series of GMTI experiments were to be carried out during the commissioning phase of the TerraSAR-X satellite. In first trials, cars, which are equipped with special radar reflectors and GPS receivers, were to be used as moving target references that are imaged in TerraSAR-X data takes. In a follow on experiment, arbitrary cars on motorways were to be imaged simultaneously by TerraSAR-X and by an airborne high-resolution camera. Car tracks extracted from the series of the optical images shall serve as a reference for the evaluation of the TerraSAR-X moving target data in this case. The paper presents first results of the data evaluation. An experimental GMTI processing system is used to detect and measure moving targets in both single-channel and dual-channel data. The dual-channel data, which enable the application of well established GMTI methods like the along-track interferometry (ATI) or displaced phase centre array (DPCA) techniques, are acquired either in the so-called "aperture switching" mode with virtual multiple receiving channels or in the dual-receive antenna (DRA) mode with physically separated receiving channels. The paper reports on the analysis of the first experimental GMTI data by using different detection and measurement strategies. This includes the adapted processing of the SAR raw data with respect to the moving target signals, the incorporation of GIS data in the detection and measurement process and the application of different detectors for across- and along-track velocity components of the moving cars. The quality of the data is thoroughly analyzed and conclusions are drawn for the development and the performance of a fully automatic GMTI processing system for TerraSAR-X. Furthermore, an outlook on the planned experiments is given. [C10372]

"Linear versus non-linear analysis of relevant scatterers in high resolution SAR images"

With the increase of synthetic aperture radar (SAR) sensor resolution, SAR images could include a large variety of interesting real man-made structures. Therefore, a more detailed analysis and a finer description of SAR images of urban areas are needed for a better understanding of the scene. Nevertheless, recognizing scenes using high resolution SAR images requires the capability to identify relevant signal signatures (called also descriptors), depending on variable image acquisition geometry, arbitrary objects poses and configurations. Among feature extraction methods, we propose to use principal components analysis (PCA) and/or independent

components analysis (ICA), in order to exploit deeper the nature of SAR signatures. In this paper, both a description of our work and a presentation of our preliminary classification performance results will be provided. [C10373]

"Stochastic models of SLC HR SAR images"

The paper presents two algorithms for texture primitive feature extraction on Single Look Complex (SLC) and Polarimetric Synthetic Aperture Radar (PolSAR) SLC data. We assume the data to be modeled by a Gauss-Markov Random Field (GMRF): a complex GMRF model for characterizing the spatial correlation in SLC data and an extension of the model for inter-band correlation characterization. The complex GMRF characterizes the spatial relationship of a two-dimensional complex signal, i.e. SLC SAR data. The extended model characterizes the spatial interaction and the inter-band pixels correlation between the polarimetric complex channels. The Bayesian approach permits to deal with model fitting and selection in a direct way. The results are presented on a polarimetric E-SAR L band scene of Mannheim, Germany. [C10374]

"Unsupervised segmentation of SAR images using Triplet Markov fields and fisher noise distributions"

This paper deals with SAR data segmentation in an unsupervised way. The model we propose is a combination of the nonstationary triplet Markov field recently introduced and the Fisher distributions. The first one allows modeling the different stationarities present in a given image. The second one has the advantage that is well adapted to this kind of data. We present an original technique based on Iterative Conditional Estimation method, to estimate the parameters of the model we propose. Application examples on simulated data and real SAR images are presented as well. [C10375]

"TerraSAR-X interferometry: report on a first assessment"

The German radar sensor TerraSAR-X will be launched by the middle of the year 2007 and will provide high-resolution data with also high radiometric and geometric accuracy. First interferometric results can be reported at the time of the conference. Various interferometric tests and a prediction on the performance of the monostatic interferometry will be described in the course of the presentation. Unfortunately, no data are available at the moment. [C10376]

"TerraSAR-X calibration-first results"

As TerraSAR-X, due for launch in 2007, will be an operational scientific mission with commercial potential, product quality is of crucial importance. The success or failure of the mission essentially depends on the calibration of the TerraSAR-X system ensuring the product quality and the correct in-orbit operation of the entire SAR system. The paper describes the in-orbit calibration procedure for TerraSAR-X and dedicated activities performed during the commissioning phase. First results could not be described because TerraSAR-X was not launched up to the time of uploading the full paper. [C10377]

"In-orbit SAR performance of TerraSAR-X"

TerraSAR-X is the first German Radar satellite for scientific and commercial applications. The project is a public-private partnership between DLR and EADS Astrium GmbH. TerraSAR-X consists of a high resolution Synthetic Aperture Radar at X-Band. The radar antenna is based on active phased array technology that allows the control of many different instrument parameters and operational modes (Stripmap, ScanSAR and Spotlight) with various polarizations. Following the TerraSAR-X launch, it is planned a six month Commissioning Phase covering the characterization and verification of the SAR mission. Within this phase, the Overall SAR System Performance takes care of the correct working and interaction of all SAR system elements essential for obtaining an optimum SAR Performance. [C10378]

"TerraSAR-X payload data processing-First Experiences"

In February 2007 the German TerraSAR-X satellite will be launched and the TerraSAR-X mission will enter its approximately 5 months commissioning phase. At that time, the challenging developments on both sides, the advanced high-resolution multi-mode SAR instrument on the one hand and the corresponding sophisticated TerraSAR-X ground segment on the other hand will prove correct interaction and functioning. Screening and processing of the SAR data is the task of the DLR developed TerraSAR Multi Mode SAR Processor TMSP. Preceded by data reception, transcription including decryption and followed by archiving, cataloguing and product delivery, processing of the data by the TMSP is the central part of the SAR data workflow implemented in the Payload Ground Segment PGS. Space and ground segment have been subject to intense complete system

testing on ground. Here, the compatibility of SAR instrument commanding, SAR instrument operations and subsequent SAR data processing has been successfully proven for the various acquisition modes of the sensor. Compliance of specified and measured product performance has been investigated as far as possible utilizing simulated point target SAR data. However, the real challenge will be the screening and SAR processing of TerraSAR-X data acquired in orbit and linked down to the receiving station. Therefore, the complete reception and processing chain will be properly tuned and adjusted to the properties of the received TerraSAR-X payload data. The TMSP algorithms have to be configured, e.g. thresholds for calibration pulse analysis, estimation window sizes for SAR data analysis, parameterization of estimation algorithms. Also the configuration of product variants with respect to resolution and radiometric quality will be checked and refined. This paper presents the very first experiences in reception, transcription, screening and processing of TerraSAR-X data with respect to performance, throughput and quality. During the TMSP checkout phase the compatibility of instrument commanding and SAR processing have to be verified and the accordance of SAR performance prediction and the obtained product performance and quality have to be investigated. First characteristics of the SAR data with respect to raw data statistics, calibration pulse analysis and Doppler centroid measurements will be shown. As far as available examples of SAR image products featuring the different image modes, Stripmap, ScanSAR and Spotlight at different incidence angles and polarizations will be displayed and a first estimate of product performance parameters will be given. [C10379]

"TerraSAR-X value added image products"

The space mission TerraSAR-X is the first German space project implemented under a Public Private Partnership (PPP). Cooperation partners are the German Aerospace Centre (DLR) and EADS Astrium GmbH. Within this construct, DLR will be responsible for the scientific use of the TerraSAR-X data, whereas commercial marketing will be undertaken exclusively by Infoterra GmbH, a wholly-owned EADS Astrium subsidiary. In a co-operation between Infoterra GmbH and Joanneum Research, Value Added products and processors have been developed for TerraSAR-X data. These products are mainly oriented at the area of interest or are mapping products which represent a higher level of image processing in terms of radiometric correction and orthorectification, mosaics, subsets and merges. In this paper, these products are described. Further, an insight into the automated and semi-automated production chain is provided. [C10380]

"Quality of orthorectified TerraSAR-X products"

Summary form only given. The German Aerospace Center (DLR) has developed the TerraSAR-X Ground Segment. One part is the geocoding system that provides orthorectification capability for multi-resolution, multi-polarisation and multi-frequency data. Besides an ellipsoid corrected product a new product called Enhanced Ellipsoid Corrected (EEC) will be offered that considers digital elevation models (DEM) of a moderately coarser resolution than the 1 up to 3 m resolution of the TerraSAR-X modes. SRTM/X-band DEMs with approximately 25 m spacing will be the backbone for this operational and fully automated service. As optional product an geocoded incidence angle mask (GIM) is available providing information about the incidence angle of the radar beam, as well as about layover and shadow areas. High precision terrain correction using high resolution DEMs, tie-pointing and image adjustment will be implemented in an experimental processor. This paper gives detailed information on the image quality, which is examined in detail based on the first available geocoded TerraSAR-X products. Therefore radiometric and geometric aspects will be investigated. It is to be shown that the orthorectification step does not tamper the original radiometric properties. The geometric accuracy of the orthorectification mainly depends on the quality of the used DEM. Besides the SRTM/X-band DEM additional elevation data like SRTM/C-band, ERS-derived and GLOBE data are used for EEC generation. The achieved pixel location accuracies will be presented. The quality characteristics of the Geocoded Incidence Angle Mask- depending also on the used DEM-are described. Moreover the high precision orthorectified image (called geocoded terrain corrected-GTC) will be examined with regard to pixel location accuracy. A high resolution laserscanning DEM, tie-points and image adjustment will be used for this analysis. Furthermore information regarding processing performance will be given. [C10381]

СПИСОК ЛИТЕРАТУРЫ

C8268. de L. P. Duarte-Figueiredo F. An End-to-End Wireless QoS Architecture Evaluation. / de L. P. Duarte-Figueiredo F., Loureiro A.A.F. // 2007. ISCC 2007. 12th IEEE Symposium on Computers and Communications. - Las Vegas, NV, 1-4 July 2007. - P. 715-720. ↑

- C8269.** Xiangqian Chen. Node Compromise Modeling and its Applications in Sensor Networks. / Xiangqian Chen, Makki K., Kang Yen, Pissinou N. // 2007. ISCC 2007. 12th IEEE Symposium on Computers and Communications. - Aveiro, 1-4 July 2007. - P. 575-582. ↑
- C8270.** Abdellahi F. Implementation of advanced radar processes on TMS320C5x processors. / Abdellahi F., Jazi M.D. // 2007. ICJET 2007. International Conference on Information and Emerging Technologies. - Karachi, 6-7 July 2007. - P. 1-5. ↑
- C8271.** Yanzheng Li. The Development of Embedded EGG Recorder Based on ARM9. / Yanzheng Li, Shuicai Wu, Jia Li, Yaiping Bai, Song Zhang. // 2007. CME 2007. IEEE/ICME International Conference on Complex Medical Engineering. - Beijing, 23-27 May 2007. - P. 230-233. ↑
- C8272.** Nouvel J.F. Sub-band interferometry on polarimetric SAR dataset. / Nouvel J.F., Dubois-Fernandez P., Angelliaume S., Mimoun D. // 2007. IGARSS 2007. IEEE International Geoscience and Remote Sensing Symposium. - Barcelona, 23-28 July 2007. - P. 188-191. ↑
- C8273.** Pipia L. Polarimetric temporal information for urban deformation map retrieval. / Pipia L., Fabregas X., Aguasca A., Lopez-Martinez C., Mallorqui J.J., Moraline O. // 2007. IGARSS 2007. IEEE International Geoscience and Remote Sensing Symposium. - Barcelona, 23-28 July 2007. - P. 192-195. ↑
- C8274.** Akiyama I. Search for Survivors Buried in Rubble by Rescue Radar with Array Antennas-Extraction of Respiratory Fluctuation -. / Akiyama I., Yoshizumi N., Ohya A., Aoki Y., Matsuno F. // 2007. SSRR 2007. IEEE International Workshop on Safety, Security and Rescue Robotics. - Rome, 27-29 Sept. 2007. - P. 1-6. ↑
- C8275.** Kidera S. An Experimental Study for a High-resolution 3-D Imaging Algorithm with Linear Array for UWB Radars. / Kidera S., Kani Y., Sakamoto T., Sato T. // 2007. ICUWB 2007. IEEE International Conference on Ultra-Wideband. - Singapore, 24-26 Sept. 2007. - P. 600-605. ↑
- C8276.** Hantscher S. A Wave Front Extraction Algorithm for High-Resolution Pulse Based Radar Systems. / Hantscher S., Etzlinger B., Reizenzahn A., Diskus C.G. // 2007. ICUWB 2007. IEEE International Conference on Ultra-Wideband. - Singapore, 24-26 Sept. 2007. - P. 590-595. ↑
- C8277.** Tan A.E.-C. Angle Accuracy of Antenna Noise Corrupted Ultra-Wideband Monopulse Receiver. / Tan A.E.-C., Chia M.Y.-W., Karumudi Rambabu. // 2007. ICUWB 2007. IEEE International Conference on Ultra-Wideband. - Singapore, 24-26 Sept. 2007. - P. 586-589. ↑
- C8278.** Schneider R.Z. Pol-dinSAR: polarimetric SAR differential interferometry using coherent scatterers. / Schneider R.Z., Papathanassiou K. // 2007. IGARSS 2007. IEEE International Geoscience and Remote Sensing Symposium. - Barcelona, 23-28 July 2007. - P. 196-199. ↑
- C8279.** Pramudita A.A. Footprint Adjustment On SFCW-GPR With Modified Dipole Array. / Pramudita A.A., Lestari A.A., Kurniawan A., Suksmono A.B. // 2007. ICUWB 2007. IEEE International Conference on Ultra-Wideband. - Singapore, 24-26 Sept. 2007. - P. 784-788. ↑
- C8280.** Aliferis I. Comparison of the diffraction stack and time-reversal imaging algorithms applied to short-range UWB scattering data. / Aliferis I., Savelyev T., Yedlin M.J., Dauvignac J.-Y., Yarovoy A., Pichot C., Ligthart L. // 2007. ICUWB 2007. IEEE International Conference on Ultra-Wideband. - Singapore, 24-26 Sept. 2007. - P. 618-621. ↑
- C8281.** Jong-Sen Lee. Evaluation and bias removal of multi-look effect on entropy/alpha/anisotropy. / Jong-Sen Lee, Ainsworth T.L., Kelly J., Lopez-Martinez C. // 2007. IGARSS 2007. IEEE International Geoscience and Remote Sensing Symposium. - Barcelona, 23-28 July 2007. - P. 172-175. ↑
- C8282.** Lopez-Martinez C. Multidimensional speckle noise reduction in synthetic aperture radar images. / Lopez-Martinez C., Fabregas X. // 2007. IGARSS 2007. IEEE International Geoscience and Remote Sensing Symposium. - Barcelona, 23-28 July 2007. - P. 176-179. ↑
- C8283.** Boerner W.-M. Review of existing monographs and books on radar polarimetry and polarimetric SAR with the aim of justifying the need of updates. / Boerner W.-M., Jong-Sen Lee. // 2007. IGARSS 2007. IEEE International Geoscience and Remote Sensing Symposium. - Barcelona, 23-28 July 2007. - P. 180-183. ↑
- C8284.** Doulgeris A. Analysis of non-Gaussian POLSAR data. / Doulgeris A., Anfinson S.N., Eltoft T. // 2007.

IGARSS 2007. IEEE International Geoscience and Remote Sensing Symposium. - Barcelona, 23-28 July 2007. - P. 160-163. ↑

C8285. Ainsworth T.L. Classification comparisons between dual-pol and quad-pol SAR imagery. / Ainsworth T.L., Lee J.-S., Chang L.W. // 2007. IGARSS 2007. IEEE International Geoscience and Remote Sensing Symposium. - Barcelona, 23-28 July 2007. - P. 164-167. ↑

C8286. Cao Fang. Analysis of fully polarimetric SAR data based on the Cloude-Pottier decomposition and the complex Wishart classifier. / Cao Fang, Hong Wen, Wu Yirong, Pottier E. // 2007. IGARSS 2007. IEEE International Geoscience and Remote Sensing Symposium. - Barcelona, 23-28 July 2007. - P. 168-171. ↑

C8287. Landes T. Monitoring temperate glaciers by high resolution Pol-InSAR data: First analysis of Argentine E-SAR acquisitions and in-situ measurements. / Landes T., Gay M., Trouve E., Nicolas J.-M., Bombrun L., Vasile G., Hajsek I. // 2007. IGARSS 2007. IEEE International Geoscience and Remote Sensing Symposium. - Barcelona, 23-28 July 2007. - P. 184-187. ↑

C8288. Songqiang. Telemedicine Center. / Songqiang, Xiaoying Tang, Weifeng Liu. // 2007. CME 2007. IEEE/ICME International Conference on Complex Medical Engineering. - Beijing, 23-27 May 2007. - P. 353-356. ↑

C8289. Li J. The Hardware Design of Three-channel EIG Monitoring System Based on S3C2410X and GPRS. / Li J., Wu S.C., Li Y.Z., Bai Y.P., Zhang S., Li D. // 2007. CME 2007. IEEE/ICME International Conference on Complex Medical Engineering. - Beijing, 23-27 May 2007. - P. 252-255. ↑

C8290. Yang Xue. An EGG wireless Monitoring Instrument Based on GPRS. / Yang Xue, Wu Shuicai, Bai Yanping. // 2007. CME 2007. IEEE/ICME International Conference on Complex Medical Engineering. - Beijing, 23-27 May 2007. - P. 238-241. ↑

C8291. Amar A. Limits on the Resolution of Closely Spaced Multipath Signals. / Amar A., Weiss A.J. // 2007. ISPA 2007. 5th International Symposium on Image and Signal Processing and Analysis. - Istanbul, 27-29 Sept. 2007. - P. 230-233. ↑

C8292. Bahari M.H. Tracking a High Maneuver Target Based on Intelligent Matrix Covariance Resetting. / Bahari M.H., Moharrami F.N., Ebrahimi Ganjeh M.A., Karsaz A. // 2007. ISPA 2007. 5th International Symposium on Image and Signal Processing and Analysis. - Istanbul, 27-29 Sept. 2007. - P. 35-40. ↑

C8293. Xu Yong. An Overview of Ultra-Wideband Technique Application for Medical Engineering. / Xu Yong, Lu Yinghua, Zhang Hongxin, Wang Yequ. // 2007. CME 2007. IEEE/ICME International Conference on Complex Medical Engineering. - Beijing, 23-27 May 2007. - P. 408-411. ↑

C8294. Xiuqiang Zhang. The Analysis And Simulation Research of Distance Resolution and Ambiguity Property of LFM Signal. / Xiuqiang Zhang, Donglin Su, Min Zhou. // 2007 International Symposium on Microwave, Antenna, Propagation and EMC Technologies for Wireless Communications. - Hangzhou, 16-17 Aug. 2007. - P. 1191-1194. ↑

C8295. Song Lizhong. Target Detection Method of the LFM Radar Signal with Multiple Polarization Agility. / Song Lizhong, Wu Qun, Mu Yinan. // 2007 International Symposium on Microwave, Antenna, Propagation and EMC Technologies for Wireless Communications. - Hangzhou, 16-17 Aug. 2007. - P. 1186-1190. ↑

C8296. Chungeng Li. The Pattern Recognition of Radar Signal by Self-Adapted Wavelet. / Chungeng Li, Cuifen Zhang. // 2007 International Symposium on Microwave, Antenna, Propagation and EMC Technologies for Wireless Communications. - Hangzhou, 16-17 Aug. 2007. - P. 1199-1203. ↑

C8297. Yang Yunfu. Direct Decomposing Modulation Phase in GSM Passive Radar. / Yang Yunfu, Wang Zhaohui, Tao Ran, Wang Yue. // 2007 International Symposium on Microwave, Antenna, Propagation and EMC Technologies for Wireless Communications. - Hangzhou, 16-17 Aug. 2007. - P. 1412-1415. ↑

C8298. Yuan Quan. A 0.35- μm BiCMOS Automatic Gain Control IF Amplifier for Radar Receivers. / Yuan Quan, Wang Zhigong, Li Qin. // 2007 International Symposium on Microwave, Antenna, Propagation and EMC Technologies for Wireless Communications. - Hangzhou, 16-17 Aug. 2007. - P. 1375-1378. ↑

C8299. Shahana T.K. Performance analysis of FIR digital filter design: RNS versus traditional. / Shahana T.K., James R.K., Jose B.R., Jacob K.P., Sasi S. // 2007. ISCIT '07. International Symposium on Communications and

Information Technologies. - Sydney,. NSW, 17-19 Oct. 2007. - P. 1-5. ↑

C8300. Kapp V. Improving cooperation between Air Traffic Controllers: a design issue. 2007. DASC '07. IEEE/AIAA 26th Digital Avionics Systems Conference. - Dallas, TX, 21-25 Oct. 2007. - P. 3.E.2-1-3.E.2-9-1. ↑

C8301. Ehrmanntraut R. Airspace design process for dynamic sectorisation. / Ehrmanntraut R., McMillan S. // 2007. DASC '07. IEEE/AIAA 26th Digital Avionics Systems Conference. - Dallas, TX, 21-25 Oct. 2007. - P. 3.D.2-1-3.D.2-9-1. ↑

C8302. Miquel T. Assessment of navigation errors on airborne state-based conflict resolution. / Miquel T., Chamayou C., Louyot P., Loscos J.-M., Anderson J., Goodchild C. // 2007. DASC '07. IEEE/AIAA 26th Digital Avionics Systems Conference. - Dallas, TX, 21-25 Oct. 2007. - P. 4.A.6-1-4.A.6-10-1. ↑

C8303. Smith E.C. Assessment of controller situation awareness in future terminal RNAV operations. 2007. DASC '07. IEEE/AIAA 26th Digital Avionics Systems Conference. - Dallas, TX, 21-25 Oct. 2007. - P. 6.B.3-1-6.B.3-13-1. ↑

C8304. Tavanti M. Augmented reality for tower: using scenarios for describing tower activities. 2007. DASC '07. IEEE/AIAA 26th Digital Avionics Systems Conference. - Dallas, TX, 21-25 Oct. 2007. - P. 5.A.4-1-5.A.4-12-1. ↑

C8305. Asada A. Development of Underwater Security Sonar System. / Asada A., Kuramoto K., Tanaka T., Oimatsu K., Kawashima Y., Nanri M., Oyagi T., Hantani K. // OCEANS 2006-Asia Pacific. - Singapore, 16-19 May 2007. - P. 1-3. ↑

C8306. Jung-Hong Cho. Optimal Acoustic Search Path Planning Based on Genetic Algorithm in Continuous Path System. / Jung-Hong Cho, Jea Soo Kim, Jun-Seok Lim, Seongil Kim, Young-Sun Kim. // OCEANS 2006-Asia Pacific. - Singapore, 16-19 May 2007. - P. 1-5. ↑

C8307. Chia-Chuen Kao. Buoy and Radar Observation Network around Taiwan. / Chia-Chuen Kao, Kuo-Ching Jao, Dong-Jiing Doong, Hui-Lin Chen, Chwen-Ling Kuo. // OCEANS 2006-Asia Pacific. - Singapore, 16-19 May 2007. - P. 1-7. ↑

C8308. Trizna D.B. Monitoring Coastal Processes and Ocean Wave Directional Spectra Using a Marine Radar. OCEANS 2006-Asia Pacific. - Singapore, 16-19 May 2007. - P. 1-4. ↑

C8309. Trizna D.B. Tsunami Detection using Multi-frequency Beam-Forming HF Radar. OCEANS 2006-Asia Pacific. - Singapore, 16-19 May 2007. - P. 1-5. ↑

C8310. Abeysekera S.S. Wideband Sonar Waveform Design using Linear FM Signals and Hermite-Rodriguez Functions. / Abeysekera S.S., Zhuquan Zang. // OCEANS 2006-Asia Pacific. - Singapore, 16-19 May 2007. - P. 1-3. ↑

C8311. Luo Ying. A Novel Method for Extraction of Micro-Doppler Signal. / Luo Ying, Chi Long, Zhang Qun, Jin Ya-qiu. // 2007 International Symposium on Microwave, Antenna, Propagation and EMC Technologies for Wireless Communications. - Hangzhou, 16-17 Aug. 2007. - P. 1458-1462. ↑

C8312. Yang Yunfu. Optimal Polarization for SINR equation in partially polarized case. / Yang Yunfu, Wang Zhaohui, Tao Ran, Wang Yue. // 2007 International Symposium on Microwave, Antenna, Propagation and EMC Technologies for Wireless Communications. - Hangzhou, 16-17 Aug. 2007. - P. 1420-1423. ↑

C8313. Chen Jiong. Super-Resolution of Polarimetric SAR Images for Ship Detection. / Chen Jiong, Yang Jian. // 2007 International Symposium on Microwave, Antenna, Propagation and EMC Technologies for Wireless Communications. - Hangzhou, 16-17 Aug. 2007. - P. 1499-1502. ↑

C8314. Yunfen Chang. Realization of the Algorithms of a Multi-static TWSR. / Yunfen Chang, Kejict Wang, Cheng Gao, Lihua Shi, Yuanzhe Xu. // 2007 International Symposium on Microwave, Antenna, Propagation and EMC Technologies for Wireless Communications. - Hangzhou, 16-17 Aug. 2007. - P. 981-984. ↑

C8315. Hu Hang. Research on Subarray Partitioning of Planar Phased Array with Adaptive Digital Beamforming. / Hu Hang, Qin Weicheng. // 2007 International Symposium on Microwave, Antenna, Propagation and EMC Technologies for Wireless Communications. - Hangzhou, 16-17 Aug. 2007. - P. 691-694. ↑

- C8316.** Tonda-Goldstein S. Slowlight in semi-conductor amplifier Application to programmable time delays for the control of microwave signals. / Tonda-Goldstein S., Berger P., Dolfi D., Chazelas J., Huignard J.P. // 2007 and the International Quantum Electronics Conference. CLEOE-IQEC 2007. European Conference on Lasers and Electro-Optics. - Munich, 17-22 June 2007. - P. 1. ↑
- C8317.** Wenlong Liu. An Efficient Method to Determine the Diagonal Loading Factor for PAM Communication System. / Wenlong Liu, Shuxue Ding. // 2007. CIT 2007. 7th IEEE International Conference on Computer and Information Technology. - Aizu-Wakamatsu, Fukushima, 16-19 Oct. 2007. - P. 116-121. ↑
- C8318.** Mackay A.J. The Theory and Design of Provably Optimal Bandwidth Radar Absorbent Materials (RAM) using Dispersive Structures and/or Frequency Selective Surfaces (FSS). 2007. ICEAA 2007. International Conference on Electromagnetics in Advanced Applications. - Torino, 17-21 Sept. 2007. - P. 157-160. ↑
- C8319.** Kaylor B.M. Adaptive Waveform Radar Enabled by S2-material Based Photonic Signal Processing Hardware. / Kaylor B.M., Berg T.J., Bekker S.H., Cole Z., Babbitt W.R., Merkel K.D., Reibel R.R. // 2007. ICEAA 2007. International Conference on Electromagnetics in Advanced Applications. - Torino, 17-21 Sept. 2007. - P. 435-438. ↑
- C8320.** Shkvarko Y.V. Unification of Descriptive Experiment Design and Worst-Case Performance Optimization-Adapted Regularization Paradigms for High-Resolution Reconstruction of Radar Imagery. 2007. ICEAA 2007. International Conference on Electromagnetics in Advanced Applications. - Torino, 17-21 Sept. 2007. - P. 340-343. ↑
- C8321.** Belbachir A.N. Object Velocity Estimation Based on Asynchronous Data from a Dual-Line Sensor System. / Belbachir A.N., Hofstatter M., Reisinger K., Donath A.N.N., Schon A.N.P. // 2007 5th IEEE International Conference on Industrial Informatics. - Vienna, 23-27 June 2007. - Vol. 1. - P. 347-352. ↑
- C8322.** Golovko M. The Evaluation of Performances of Automatic Method for the Object Detection in GPR Images. 2007. ISPA 2007. 5th International Symposium on Image and Signal Processing and Analysis. - Istanbul, 27-29 Sept. 2007. - P. 476-481. ↑
- C8323.** Chue Poh Tan. Image Processing in Polarimetric SAR Images Using a Hybrid Entropy Decomposition and Maximum Likelihood (EDML). / Chue Poh Tan, Ka Sing Lim, Hong Tat Ewe. // 2007. ISPA 2007. 5th International Symposium on Image and Signal Processing and Analysis. - Istanbul, 27-29 Sept. 2007. - P. 418-422. ↑
- C8324.** Kallfass I. A 210 GHz, Subharmonically-Pumped Active FET Mixer MMIC for Radar Imaging Applications. / Kallfass I., Massler H., Leuther A. // 2007. CSIC 2007. IEEE Compound Semiconductor Integrated Circuit Symposium. - Portland, OR, 14-17 Oct. 2007. - P. 1-4. ↑
- C8325.** Nicolson S.T. A 77-79-GHz Doppler Radar Transceiver in Silicon. / Nicolson S.T., Chevalier P., Chantre A., Sautreuil B., Voinigescu S.P. // 2007. CSIC 2007. IEEE Compound Semiconductor Integrated Circuit Symposium. - Portland, OR, 14-17 Oct. 2007. - P. 1-4. ↑
- C8326.** Tessmann A. Metamorphic HEMT Amplifier Circuits for Use in a High Resolution 210 GHz Radar. / Tessmann A., Leuther A., Massler H., Kuri M., Riessle M., Zink M., Sommer R., Wahlen A., Essen H. // 2007. CSIC 2007. IEEE Compound Semiconductor Integrated Circuit Symposium. - Portland, OR, 14-17 Oct. 2007. - P. 1-4. ↑
- C8327.** Barker D.R. Ground and flight deck alternatives for terminal merging, sequencing, and spacing for arrivals. / Barker D.R., Becher T.A., Hammer J., McCourt S., Moertl P., Smith E.C., Stock T. // 2007. DASC '07. IEEE/AIAA 26th Digital Avionics Systems Conference. - Dallas, TX, 21-25 Oct. 2007. - P. 1.D.3-1-1.D.3-14-1. ↑
- C8328.** Friberg N. Using 4DT FMS data for green approach, A-CDA, at Stockholm Arlanda airport. 2007. DASC '07. IEEE/AIAA 26th Digital Avionics Systems Conference. - Dallas, TX, 21-25 Oct. 2007. - P. 1.B.3-1-1.B.3-9-1. ↑
- C8329.** Ananda C.M. General aviation Light Transport Aircraft avionics: Integration and system tests. 2007. DASC '07. IEEE/AIAA 26th Digital Avionics Systems Conference. - Dallas, TX, 21-25 Oct. 2007. - P. 2.A.3-1-2.A.3-8-1. ↑
- C8330.** Mundra A.D. Self-separation corridors. / Mundra A.D., Simons E.M. // 2007. DASC '07. IEEE/AIAA

26th Digital Avionics Systems Conference. - Dallas, TX, 21-25 Oct. 2007. - P. 3.C.3-1-3.C.3-11-1. ↑

C8331. Sprong K.R. Analysis of RNAV arrival operations with descend via clearances at phoenix airport. / Sprong K.R., Mayer R.H. // 2007. DASC '07. IEEE/AIAA 26th Digital Avionics Systems Conference. - Dallas, TX, 21-25 Oct. 2007. - P. 3.A.5-1-3.A.5-12-1. ↑

C8332. Zhiqiang Liu. Bearing Finding and Array Error Correction in Noncooperative Passive Detection. / Zhiqiang Liu, Hongguang Ma, Xuemei Wu. // 2007 IEEE Workshop on Signal Processing Systems. - Shanghai, China, 17-19 Oct. 2007. - P. 387-390. ↑

C8333. Bradaric I. A Framework for the Analysis of Multistatic Radar Systems with Multiple Transmitters. / Bradaric I., Capraro G.T., Weiner D.D., Wicks M.C. // 2007. ICEAA 2007. International Conference on Electromagnetics in Advanced Applications. - Torino, 17-21 Sept. 2007. - P. 443-446. ↑

C8334. Blunt S.D. Diversity Aspects of Radar-Embedded Communications. / Blunt S.D., Stiles J., Allen C., Deavours D., Perrins E. // 2007. ICEAA 2007. International Conference on Electromagnetics in Advanced Applications. - Torino, 17-21 Sept. 2007. - P. 439-442. ↑

C8335. Farooq J. Application of Frequency Diverse Arrays to Synthetic Aperture Radar Imaging. / Farooq J., Temple M.A., Saville M.A. // 2007. ICEAA 2007. International Conference on Electromagnetics in Advanced Applications. - Torino, 17-21 Sept. 2007. - P. 447-449. ↑

C8336. Virone G. A waveguide/free-space measurement setup for panels and joints of large dielectric radomes. / Virone G., Tascone R., Olivieri A., Addamo G., Peverini O.A. // 2007. ICEAA 2007. International Conference on Electromagnetics in Advanced Applications. - Torino, 17-21 Sept. 2007. - P. 792-794. ↑

C8337. Goodman N.A. Closed-Loop Radar with Adaptively Matched Waveforms. 2007. ICEAA 2007. International Conference on Electromagnetics in Advanced Applications. - Torino, 17-21 Sept. 2007. - P. 468-471. ↑

C8338. Jiang Jin. A New Method for Estimating the Bandwidth using Two-Channel Narrowband Signals with Strong Interference. / Jiang Jin, Wan Qun, Wang Yan, Bai Danping. // 2007. ICCAS 2007. International Conference on Communications, Circuits and Systems. - Kokura, 11-13 July 2007. - P. 709-712. ↑

C8339. Song Yunzhao. Cluster Sorting of Radar Signals Using Intra-pulse Feature. / Song Yunzhao, Wan Qun, Liu Gang. // 2007. ICCAS 2007. International Conference on Communications, Circuits and Systems. - Kokura, 11-13 July 2007. - P. 718-721. ↑

C8340. Cao Jian-shu. A Robust Method for Censoring the Interference-targets. / Cao Jian-shu, Wang Xue-gang. // 2007. ICCAS 2007. International Conference on Communications, Circuits and Systems. - Kokura, 11-13 July 2007. - P. 653-657. ↑

C8341. Xinxiang Zhang. Noise-Linear Frequency Modulation Shared Waveform for Integrated Radar and Jammer System. / Xinxiang Zhang, Tianqi Chen. // 2007. ICCAS 2007. International Conference on Communications, Circuits and Systems. - Kokura, 11-13 July 2007. - P. 644-648. ↑

C8342. Rui Duan. Diagonal Loading Techniques to Relax Sample Support Requirement in Airborne Bistatic STAP. / Rui Duan, Xuegang Wang, Chaoshu Jiang, Zhuming Chen. // 2007. ICCAS 2007. International Conference on Communications, Circuits and Systems. - Kokura, 11-13 July 2007. - P. 649-652. ↑

C8343. Yingxi Zheng. Design of the High-powered Clutter Suppression System Based on ADSP-TS203. / Yingxi Zheng, Zhulin Zong. // 2007. ICCAS 2007. International Conference on Communications, Circuits and Systems. - Kokura, 11-13 July 2007. - P. 816-818. ↑

C8344. Bo Liu. Optimization of Orthogonal Discrete Frequency-Coding Waveform Based on Modified Genetic Algorithm for MIMO Radar. / Bo Liu, Zishu He, Qian He. // 2007. ICCAS 2007. International Conference on Communications, Circuits and Systems. - Kokura, 11-13 July 2007. - P. 966-970. ↑

C8345. Zhao Jianhong. Signal-Clutter-Noise Power Ratio of Airborne Wideband Radar. / Zhao Jianhong, Yang Jianyu. // 2007. ICCAS 2007. International Conference on Communications, Circuits and Systems. - Kokura, 11-13 July 2007. - P. 1309-1312. ↑

- C8346.** Zhou Peng. Geometry and System Aspects of Spaceborne/Airborne Hybrid Bistatic SAR. / Zhou Peng, Pi Yiming. // 2007. ICCAS 2007. International Conference on Communications, Circuits and Systems. - Kokura, 11-13 July 2007. - P. 867-871. ↑
- C8347.** Wu Haizhou. LCMV Beamforming Algorithm Based on the ractiona Fourier Transform. / Wu Haizhou, Tao Ran. // 2007. ICCAS 2007. International Conference on Communications, Circuits and Systems. - Kokura, 11-13 July 2007. - P. 826-830. ↑
- C8348.** Ling Kuang. The Influence of Random motion Errors on Bistatic SAR Resolution. / Ling Kuang, Qun Wan, Wan-lin Yang. // 2007. ICCAS 2007. International Conference on Communications, Circuits and Systems. - Kokura, 11-13 July 2007. - P. 863-866. ↑
- C8349.** Zengjiankui. Adaptive Space-time-waveform Processing for MIMO Radar. / Zengjiankui, Hezishu, Liubo. // 2007. ICCAS 2007. International Conference on Communications, Circuits and Systems. - Kokura, 11-13 July 2007. - P. 641-643. ↑
- C8350.** Khoor S. Heart Rate Analysis and Telemedicine: New concepts & Maths. / Khoor S., Kecskes I., Kovacs I., Verner D., Remete A., Jankovich P., Bartus R., Stanko N., Schramm N., Domijan M., Domijan E. // 2007. SISY 2007. 5th International Symposium on Intelligent Systems and Informatics. - Subotica, 24-25 Aug. 2007. - P. 39-43. ↑
- C8351.** Ahlander A. Architectural Challenges in Memory-Intensive, Real-Time Image Forming. / Ahlander A., Hellsten H., Lind K., Lindgren J., Svensson B. // 2007. ICPP 2007. International Conference on Parallel Processing. - Xi'an, 10-14 Sept. 2007. - P. 35. ↑
- C8352.** Ragavan S.V. A General Telematics Framework for Autonomous Service Robots. / Ragavan S.V., Ganapathy V. // 2007. CASE 2007. IEEE International Conference on Automation Science and Engineering. - Scottsdale, AZ, 22-25 Sept. 2007. - P. 609-614. ↑
- C8353.** Mohabey M. A Combinatorial Procurement Auction for QoS-Aware Web Services Composition. / Mohabey M., Narahari Y., Mallick S., Suresh P., Subrahmanya S.V. // 2007. CASE 2007. IEEE International Conference on Automation Science and Engineering. - Scottsdale, AZ, 22-25 Sept. 2007. - P. 716-721. ↑
- C8354.** Fontanelli D. A Fast RANSAC-Based Registration Algorithm for Accurate Localization in Unknown Environments using LIDAR Measurements. / Fontanelli D., Ricciato L., Soatto S. // 2007. CASE 2007. IEEE International Conference on Automation Science and Engineering. - Scottsdale, AZ, 22-25 Sept. 2007. - P. 597-602. ↑
- C8355.** Hou Xuan. Study of Detection Technique Simulation of High Resolution Radar Based on BP Neural Network. / Hou Xuan, He Mingyi. // 2007. ICNC 2007. Third International Conference on Natural Computation. - Haikou, 24-27 Aug. 2007. - Vol. 1. - P. 426-430. ↑
- C8356.** Binlu Liu. Design of Perfect Reconstruction Cosine Modulated Filter Banks with Linear Phase. / Binlu Liu, Zijing Zhang, Zhiwei Deng. // 2007. ICCAS 2007. International Conference on Communications, Circuits and Systems. - Kokura, 11-13 July 2007. - P. 633-636. ↑
- C8357.** Bin Tang. A Generalized Sidelobe Canceller Architecture for Reduced-rank Beam-space Post-Doppler STAP. / Bin Tang, Xuegang Wang. // 2007. ICCAS 2007. International Conference on Communications, Circuits and Systems. - Kokura, 11-13 July 2007. - P. 637-640. ↑
- C8358.** Bernhardt P.A. CARE: Rocket Experiments for Investigation of the Radar Scatter Proerties of a Dusty Plasma. / Bernhardt P.A., Scales W.A., Chen Chen. // 2007. ICOPS 2007. IEEE 34th International Conference on Plasma Science. - Albuquerque, NM, 17-22 June 2007. - P. 690. ↑
- C8359.** Lan Du. A Novel Statistical Recognition Method Based on Hypersphere Model for Radar HRRP ATR. / Lan Du, Hongwei Liu, Zheng Bao, Feng Chen. // 2007. ICNC 2007. Third International Conference on Natural Computation. - Haikou, 24-27 Aug. 2007. - Vol. 2. - P. 595-599. ↑
- C8360.** Sheng Lu. Implementation and Design of Auto Ranging System with Risk Estimation for Vehicles. / Sheng Lu, Xiao-Li Cao, Zhong-Jian Cai, Gao-Rong Zeng, Tan Liu. // 2007. ICNC 2007. Third International Conference on Natural Computation. - Haikou, 24-27 Aug. 2007. - Vol. 5. - P. 190-194. ↑

- C8361.** Ramos-Perez I. Synthetic Aperture PAU: a new instrument to test potential improvements for future SMOSops. / Ramos-Perez I., Camps A., Bosch-Lluis X., Marchan-Hernandez J.F., Rodriguez-Alvarez N., Valencia E., Frascella F., Campigotto P., Donadio M. // 2007. IGARSS 2007. IEEE International Geoscience and Remote Sensing Symposium. - Barcelona, 23-28 July 2007. - P. 247-250. ↑
- C8362.** Christensen J. GAS: the Geostationary Atmospheric Sounder. / Christensen J., Carlstrom A., Ekstrom H., de Maagt P., Colliander A., Emrich A., Embretsen J. // 2007. IGARSS 2007. IEEE International Geoscience and Remote Sensing Symposium. - Barcelona, 23-28 July 2007. - P. 223-226. ↑
- C8363.** Padmanabhan S. Estimation of 3-D Water vapor distribution using a network of compact microwave radiometers. / Padmanabhan S., Reising S.C., Iturbide-Sanchez F., Vivekanandan I.J. // 2007. IGARSS 2007. IEEE International Geoscience and Remote Sensing Symposium. - Barcelona, 23-28 July 2007. - P. 251-254. ↑
- C8364.** Yu Zhifu. A Multi-parameter Synthetic Signal Sorting Algorithm Based on Clustering. / Yu Zhifu, Ye Fei, Luo Jingqing. // 2007. ICEMI '07. 8th International Conference on Electronic Measurement and Instruments. - Xi'an, Aug. 16 2007-July 18 2007. - P. 2-363-2-366-363. ↑
- C8365.** Thiele A. Feature extraction of gable-roofed buildings from multi-aspect high-resolution InSAR data. / Thiele A., Cadario E., Schulz K., Thoennessen U., Soergel U. // 2007. IGARSS 2007. IEEE International Geoscience and Remote Sensing Symposium. - Barcelona, 23-28 July 2007. - P. 262-265. ↑
- C8366.** Le Roy Y. SRAL SAR radar altimeter for sentinel-3 mission. / Le Roy Y., Deschaux-Beaume M., Mavrocordatos C., Aguirre M., Heliere F. // 2007. IGARSS 2007. IEEE International Geoscience and Remote Sensing Symposium. - Barcelona, 23-28 July 2007. - P. 219-222. ↑
- C8367.** Sato R. Classification of stricken residential houses by the mid niigata prefecture earthquake based on POLSAR image analysis. / Sato R., Soma K., Yajima Y., Yamaguchi Y., Yamada H. // 2007. IGARSS 2007. IEEE International Geoscience and Remote Sensing Symposium. - Barcelona, 23-28 July 2007. - P. 200-203. ↑
- C8368.** Zhu Jun. An AMUSE-based Approach for Detection and Blind Separation of Multi-component Radar Signals. / Zhu Jun, Tang Bin, Chen Bing. // 2007. ICEMI '07. 8th International Conference on Electronic Measurement and Instruments. - Xi'an, Aug. 16 2007-July 18 2007. - P. 3-1037-3-1040-1037. ↑
- C8369.** Saunier S. The contribution of the european space agency to the ALOS PRISM / commissioning phase. / Saunier S., Santer R., Goryl P., Gruen A., Wolf K., Bouvet M., Viallefont F. // 2007. IGARSS 2007. IEEE International Geoscience and Remote Sensing Symposium. - Barcelona, 23-28 July 2007. - P. 208-211. ↑
- C8370.** Zhang Dabiao. Design of Automobile Collision Avoidance Warning System Based on LabVIEW. / Zhang Dabiao, Kang Yueyi, Liu Hongyun. // 2007. ICEMI '07. 8th International Conference on Electronic Measurement and Instruments. - Xi'an, Aug. 16 2007-July 18 2007. - P. 2-51-2-54-51. ↑
- C8371.** Rostan F. The C-SAR instrument for the GMES sentinel-1 mission. / Rostan F., Riegger S., Pitz W., Torre A., Torres R. // 2007. IGARSS 2007. IEEE International Geoscience and Remote Sensing Symposium. - Barcelona, 23-28 July 2007. - P. 215-218. ↑
- C8372.** Gao Fusheng. Simulation of Radar A/R Scope Based on Linux System. / Gao Fusheng, Wang Zhiyun, Wang Xuming. // 2007. ICEMI '07. 8th International Conference on Electronic Measurement and Instruments. - Xi'an, Aug. 16 2007-July 18 2007. - P. 2-268-2-271-268. ↑
- C8373.** Pawelec J. ICT Anti Collision Radar for Road Traffic. / Pawelec J., Kosmowski K., Krawczyk Z. // 2007. VTC-2007 Fall. 2007 IEEE 66th Vehicular Technology Conference. - Baltimore, MD, Sept. 30 2007-Oct. 3 2007. - P. 1470-1473. ↑
- C8374.** Ye Fei. Analysis of Radar Emitter Signal Feature Based on Multifractal Theory. / Ye Fei, Yu Zhifu, Luo Jingqing. // 2007. ICEMI '07. 8th International Conference on Electronic Measurement and Instruments. - Xi'an, Aug. 16 2007-July 18 2007. - P. 1-14-1-17-14. ↑
- C8375.** Nasution R.A. Technology Readiness Characteristics of 3G Subscribers in Indonesia: A Preliminary Study. / Nasution R.A., Rudito P., Syaharuddin Z. // Portland International Center for Management of Engineering and Technology. - Portland, OR, 5-9 Aug. 2007. - P. 891-898. ↑
- C8376.** Sarkar S. RADAR: Risk-and-Delay Aware Routing Algorithm in a Hybrid Wireless-Optical Broadband

Access Network (WOBAN). / Sarkar S., Hong-Hsu Yen, Sudhir Dixit, Mukherjee B. // 2007. OFC/NFOEC 2007. Conference on Optical Fiber Communication and the National Fiber Optic Engineers Conference. - Anaheim, CA, 25-29 March 2007. - P. 1-3. ↑

C8377. Valle G.D. High-power stable single-frequency waveguide laser. / Valle G.D., Festa A., Enns K., Taccheo S., Laporta P., Sorbello G. // 2007. OFC/NFOEC 2007. Conference on Optical Fiber Communication and the National Fiber Optic Engineers Conference. - Anaheim, CA, 25-29 March 2007. - P. 1-3. ↑

C8378. Zhang Zhihong. Study about Test Ammunition Terminal Effectiveness with the Velocity Radar. / Zhang Zhihong, Wang Weiming, Wu Yong, Wei Guojun. // 2007. ICEMI '07. 8th International Conference on Electronic Measurement and Instruments. - Xi'an, Aug. 16 2007-July 18 2007. - P. 1-308-1-312-308. ↑

C8379. Sun Minhong. Using Polynomial Phase Signal Modeling against Range False Targets. / Sun Minhong, Tang Bin. // 2007. ICEMI '07. 8th International Conference on Electronic Measurement and Instruments. - Xi'an, Aug. 16 2007-July 18 2007. - P. 1-712-1-716-712. ↑

C8380. Wu Gongcheng. Design of LXIbus Interface Circuit for HF Ground Wave Radar. / Wu Gongcheng, Chen Zezong, Xu Chao. // 2007. ICEMI '07. 8th International Conference on Electronic Measurement and Instruments. - Xi'an, Aug. 16 2007-July 18 2007. - P. 1-858-1-861-858. ↑

C8381. Ma Botao. TDC Based Radar Signal Reconstruction from Periodic Nonuniform Samples. / Ma Botao, Zhu Yilong, Fan Hongqi. // 2007. ICEMI '07. 8th International Conference on Electronic Measurement and Instruments. - Xi'an, Aug. 16 2007-July 18 2007. - P. 1-673-1-676-673. ↑

C8382. Chen JianYun. Wide-Band High Resolution Homing Sonar Echo Detect Based On Spread Spectrum Technology. / Chen JianYun, Zhong XiaoPen, Fen XuZhe, Yan JianWei. // 2007. ICEMI '07. 8th International Conference on Electronic Measurement and Instruments. - Xi'an, Aug. 16 2007-July 18 2007. - P. 1-588-1-590-588. ↑

C8383. Lv Junwei. A Design of the Test According to Amplitude-frequency Characteristic in the Radar Antenna Control System. / Lv Junwei, Wang Zhiyun, Xue Zhouchen. // 2007. ICEMI '07. 8th International Conference on Electronic Measurement and Instruments. - Xi'an, Aug. 16 2007-July 18 2007. - P. 1-631-1-634-631. ↑

C8384. Fabrizio G. Experimental HF radar trial of real-time STAP. / Fabrizio G., Holdsworth D., Farina A. // 2007. International Waveform Diversity and Design Conference. - Pisa, 4-8 June 2007. - P. 316-320. ↑

C8385. Morrison K. Use of frequency-randomized SAR waveforms for the detection and mitigation of small-motion effects in precision RCS measurement. 2007. International Waveform Diversity and Design Conference. - Pisa, 4-8 June 2007. - P. 321-325. ↑

C8386. Bradaric I. Signal processing and waveform selection strategies in multistatic radar systems. / Bradaric I., Capraro G.T., Wicks M.C., Zulch P. // 2007. International Waveform Diversity and Design Conference. - Pisa, 4-8 June 2007. - P. 307-311. ↑

C8387. Lombardini F. Sector interpolation for 3D SAR imaging with baseline diversity data. / Lombardini F., Pardini M., Gini F. // 2007. International Waveform Diversity and Design Conference. - Pisa, 4-8 June 2007. - P. 297-301. ↑

C8388. Baldini L. Evaluation of a fully self-consistent methodology to correct attenuation and differential attenuation at C-band. / Baldini L., Gorgucci E., Cuccoli F., Giuli D., Gherardelli M. // 2007. International Waveform Diversity and Design Conference. - Pisa, 4-8 June 2007. - P. 302-306. ↑

C8389. Varslot T. Time-reversal waveform preconditioning for clutter rejection. / Varslot T., Yazici B., Yarman C.-E., Cheney M., Scharf L. // 2007. International Waveform Diversity and Design Conference. - Pisa, 4-8 June 2007. - P. 330-334. ↑

C8390. Ashtari A. Radar signal design using chaotic signals. / Ashtari A., Thomas G., Garces H., Flores B.C. // 2007. International Waveform Diversity and Design Conference. - Pisa, 4-8 June 2007. - P. 353-357. ↑

C8391. Lo Monte L. Design and realization of a distributed vector sensor for polarization diversity applications. / Lo Monte L., Elnour B., Erricolo D., Nehorai A. // 2007. International Waveform Diversity and Design Conference. - Pisa, 4-8 June 2007. - P. 358-361. ↑

- C8392.** Baker C.J. Target classification by echo locating animals. / Baker C.J., Vespe M., Jones G.J. // 2007. International Waveform Diversity and Design Conference. - Pisa, 4-8 June 2007. - P. 348-352. ↑
- C8393.** Rangaswamy M. Model order estimation for adaptive radar clutter cancellation. / Rangaswamy M., Kay S., Cuichun Xu, Lin F.C. // 2007. International Waveform Diversity and Design Conference. - Pisa, 4-8 June 2007. - P. 339-343. ↑
- C8394.** Gray D.A. MIMO noise radar-element and beam space comparisons. / Gray D.A., Fry R. // 2007. International Waveform Diversity and Design Conference. - Pisa, 4-8 June 2007. - P. 344-347. ↑
- C8395.** Jung-Hyo Kim. Laboratory experiments for the evaluation of Digital Beamforming SAR features. / Jung-Hyo Kim, Ossowska A., Wiesbeck W. // 2007. International Waveform Diversity and Design Conference. - Pisa, 4-8 June 2007. - P. 292-296. ↑
- C8396.** Wicks M.C. Distributed and Layered Sensing. / Wicks M.C., Moore W. // 2007. International Waveform Diversity and Design Conference. - Pisa, 4-8 June 2007. - P. 233-239. ↑
- C8397.** Martorella M. Image contrast and entropy based autofocus for polarimetric ISAR. / Martorella M., Berizzi F., Palmer J., Haywood B., Bates B. // 2007. International Waveform Diversity and Design Conference. - Pisa, 4-8 June 2007. - P. 245-249. ↑
- C8398.** Setlur P. A frequency diverse Doppler radar for range-to-motion estimation in urban sensing applications. / Setlur P., Amin M., Ahmad F., Estephan H. // 2007. International Waveform Diversity and Design Conference. - Pisa, 4-8 June 2007. - P. 228-232. ↑
- C8399.** De Maio A. Code selection for radar performance optimization. / De Maio A., Farina A. // 2007. International Waveform Diversity and Design Conference. - Pisa, 4-8 June 2007. - P. 219-223. ↑
- C8400.** Fuhrmann D.R. One-step optimal measurement selection for linear gaussian estimation problems. 2007. International Waveform Diversity and Design Conference. - Pisa, 4-8 June 2007. - P. 224-227. ↑
- C8401.** Palmer J. Polarimetric ISAR autofocussing techniques: Comparison of results. / Palmer J., Martorella M., Haywood B. // 2007. International Waveform Diversity and Design Conference. - Pisa, 4-8 June 2007. - P. 250-254. ↑
- C8402.** Krieger G. Multidimensional waveform encoding for spaceborne synthetic aperture radar systems. / Krieger G., Gebert N., Moreira A. // 2007. International Waveform Diversity and Design Conference. - Pisa, 4-8 June 2007. - P. 282-286. ↑
- C8403.** Hens S. Interferometric radar waveform design and the effective interferometric wavelength. / Hens S., Madsen S.N. // 2007. International Waveform Diversity and Design Conference. - Pisa, 4-8 June 2007. - P. 287-291. ↑
- C8404.** Sturm C. Waveform communalities between digital beamforming radar and MIMO. / Sturm C., Schulteis S., Wiesbeck W. // 2007. International Waveform Diversity and Design Conference. - Pisa, 4-8 June 2007. - P. 279-281. ↑
- C8405.** Prodi F. Motion compensation for a frequency stepped radar. / Prodi F., Tilli E. // 2007. International Waveform Diversity and Design Conference. - Pisa, 4-8 June 2007. - P. 255-259. ↑
- C8406.** Hussain M.G.M. Waveform design and modulation schemes for impulse communications and radar. 2007. International Waveform Diversity and Design Conference. - Pisa, 4-8 June 2007. - P. 260-264. ↑
- C8407.** Liu Congfeng. Canonical Framework for ATI and DPCA. / Liu Congfeng, Liao Guisheng, Zeng Cao. // 2007. WiCom 2007. International Conference on Wireless Communications, Networking and Mobile Computing. - Shanghai, 21-25 Sept. 2007. - P. 714-717. ↑
- C8408.** Shentang Li. Precise Measurement of RCF in Colored Gaussian Noise. / Shentang Li, Hong wan, Yuqi Huang, Wenjun Huo. // 2007. WiCom 2007. International Conference on Wireless Communications, Networking and Mobile Computing. - Shanghai, 21-25 Sept. 2007. - P. 970-973. ↑
- C8409.** Shentang Li. Detection of Moving Target in FM Broadcast-Based Passive Radar. / Shentang Li, Hong

Wan, Haichang Yin, Yuqi Huang. // 2007. WiCom 2007. International Conference on Wireless Communications, Networking and Mobile Computing. - Shanghai, 21-25 Sept. 2007. - P. 649-652. ↑

C8410. Nelander A. Continuous coded waveforms for noise radar. 2007. International Waveform Diversity and Design Conference. - Pisa, 4-8 June 2007. - P. 438-442. ↑

C8411. Shackelford A.K. Shared-spectrum multistatic radar: Preliminary experimental results. / Shackelford A.K., de Graaf J., Talapatra S., Gerlach K., Blunt S.D. // 2007. International Waveform Diversity and Design Conference. - Pisa, 4-8 June 2007. - P. 443-447. ↑

C8412. Yu Shi. An Algorithm for 4-D Parameters Jointly Estimating of Near-Field Sources. / Yu Shi, Zhiqiang Huang, Shuxun Wang. // 2007. WiCom 2007. International Conference on Wireless Communications, Networking and Mobile Computing. - Shanghai, 21-25 Sept. 2007. - P. 1012-1015. ↑

C8413. Xujing Guo. Speckle Reduction for Remote Sensing Images Based on Nonsubsampled Contourlet. / Xujing Guo, Zulin Wang. // 2007. WiCom 2007. International Conference on Wireless Communications, Networking and Mobile Computing. - Shanghai, 21-25 Sept. 2007. - P. 2927-2930. ↑

C8414. Cunbin Li. The Research of Network Planning Risk Element Transmission Theory Model Based on Neural Network. / Cunbin Li, Kecheng Wang. // 2007. WiCom 2007. International Conference on Wireless Communications, Networking and Mobile Computing. - Shanghai, 21-25 Sept. 2007. - P. 3887-3890. ↑

C8415. Zou Xue-yu. Collaborative Detection Probability of Mobile Target for Coverage in Large-Scale WSN. / Zou Xue-yu, Cao Yang. // 2007. WiCom 2007. International Conference on Wireless Communications, Networking and Mobile Computing. - Shanghai, 21-25 Sept. 2007. - P. 2710-2714. ↑

C8416. Yanbin Shi. Research of Radar Signal Processor Based on the Software Defined Radio. / Yanbin Shi, Xianjun Gao, Zhongji Tan, Yan Wang. // 2007. WiCom 2007. International Conference on Wireless Communications, Networking and Mobile Computing. - Shanghai, 21-25 Sept. 2007. - P. 1252-1255. ↑

C8417. Chengqian Xu. Binary Sequence Pairs With Two-level Autocorrelation Functions. / Chengqian Xu, Kai Liu, Gang Li, Wangbo Yu. // 2007. WiCom 2007. International Conference on Wireless Communications, Networking and Mobile Computing. - Shanghai, 21-25 Sept. 2007. - P. 1361-1364. ↑

C8418. Gabele M. A new method to create a virtual third antenna from a two-channel SAR-GMTI system. / Gabele M., Sikaneta I. // 2007. International Waveform Diversity and Design Conference. - Pisa, 4-8 June 2007. - P. 433-437. ↑

C8419. Hurtado M. Polarization diversity for detecting targets in inhomogeneous clutter. / Hurtado M., Nehorai A. // 2007. International Waveform Diversity and Design Conference. - Pisa, 4-8 June 2007. - P. 382-386. ↑

C8420. Subotic N. Conditional and constrained joint optimization of RADAR waveforms. / Subotic N., Cooper K., Zulch P. // 2007. International Waveform Diversity and Design Conference. - Pisa, 4-8 June 2007. - P. 387-394. ↑

C8421. Searle S. A novel polyphase code for sidelobe suppression. / Searle S., Howard S. // 2007. International Waveform Diversity and Design Conference. - Pisa, 4-8 June 2007. - P. 377-381. ↑

C8422. Leshem A. Information theoretic radar waveform design for multiple targets. / Leshem A., Naparstek O., Nehorai A. // 2007. International Waveform Diversity and Design Conference. - Pisa, 4-8 June 2007. - P. 362-366. ↑

C8423. Kyriakides I. Target tracking using particle filtering and CAZAC sequences. / Kyriakides I., Konstantinidis I., Morrell D., Benedetto J.J., Papandreou-Suppappola A. // 2007. International Waveform Diversity and Design Conference. - Pisa, 4-8 June 2007. - P. 367-371. ↑

C8424. Jun Hyeong Bae. Adaptive waveforms for target class discrimination. / Jun Hyeong Bae, Goodman N.A. // 2007. International Waveform Diversity and Design Conference. - Pisa, 4-8 June 2007. - P. 395-399. ↑

C8425. Frazer G.J. Orthogonal waveform support in MIMO HF OTH radars. / Frazer G.J., Johnson B.A., Abramovich Y.I. // 2007. International Waveform Diversity and Design Conference. - Pisa, 4-8 June 2007. - P. 423-427. ↑

- C8426.** Yimin Zhang. Concurrent operation and cross-radar interference cancellation of two over-the-horizon radars. / Yimin Zhang, Amin M.G. // 2007. International Waveform Diversity and Design Conference. - Pisa, 4-8 June 2007. - P. 428-432. ↑
- C8427.** Welstead S. Characterization of diversity approaches for LFM stretch-processed waveforms. 2007. International Waveform Diversity and Design Conference. - Pisa, 4-8 June 2007. - P. 418-422. ↑
- C8428.** Gumas S. Computationally efficient waveform diversity. / Gumas S., Himed B. // 2007. International Waveform Diversity and Design Conference. - Pisa, 4-8 June 2007. - P. 400-406. ↑
- C8429.** Amuso V.J. The Strength Pareto Evolutionary Algorithm 2 (SPEA2) applied to simultaneous multi-mission waveform design. / Amuso V.J., Enslin J. // 2007. International Waveform Diversity and Design Conference. - Pisa, 4-8 June 2007. - P. 407-417. ↑
- C8430.** Yang Yang. Energy-efficient Routing for Signal Detection under the Neyman-Pearson Criterion in Wireless Sensor Networks. / Yang Yang, Blum R.S. // 2007. IPSN 2007. 6th International Symposium on Information Processing in Sensor Networks. - Cambridge, MA, 25-27 April 2007. - P. 303-312. ↑
- C8431.** Singh J. Tracking Multiple Targets Using Binary Proximity Sensors. / Singh J., Madhow U., Kumar R., Suri S., Cagley R. // 2007. IPSN 2007. 6th International Symposium on Information Processing in Sensor Networks. - Cambridge, MA, 25-27 April 2007. - P. 529-538. ↑
- C8432.** Hongkai Wang. Skeleton-Based Tornado Hook Echo Detection. / Hongkai Wang, Mercer R.E., Barron J.L., Joe P. // 2007. ICIP 2007. IEEE International Conference on Image Processing. - San Antonio, TX, Sept. 16 2007-Oct. 19 2007. - Vol. 6. - P. VI-361 - VI - 364-361. ↑
- C8433.** Imaizumi S. Collusion Attack-Resilient Hierarchical Encryption of JPEG 2000 Codestreams with Scalable Access Control. / Imaizumi S., Fujiyoshi M., Abe Y., Kiya H. // 2007. ICIP 2007. IEEE International Conference on Image Processing. - San Antonio, TX, Sept. 16 2007-Oct. 19 2007. - Vol. 2. - P. II-137 - II - 140-137. ↑
- C8434.** Hyun-chong Cho. Morphological Processing of Severely Occluded Digital Elevation Images to Extract and Connect Stream Channels. / Hyun-chong Cho, Slatton K.C. // 2007. ICIP 2007. IEEE International Conference on Image Processing. - San Antonio, TX, Sept. 16 2007-Oct. 19 2007. - Vol. 2. - P. II-241 - II - 244-241. ↑
- C8435.** Lixia Shu. SAR and SPOT Image Registration Based on Mutual Information with Contrast Measure. / Lixia Shu, Tieniu Tan. // 2007. ICIP 2007. IEEE International Conference on Image Processing. - San Antonio, TX, Sept. 16 2007-Oct. 19 2007. - Vol. 5. - P. V-429 - V - 432-429. ↑
- C8436.** Bretar F. Processing Fine Digital Terrain Models by Markovian Regularization from 3D Airborne Lidar Data. 2007. ICIP 2007. IEEE International Conference on Image Processing. - San Antonio, TX, Sept. 16 2007-Oct. 19 2007. - Vol. 4. - P. IV-125 - IV - 128-125. ↑
- C8437.** Davis B.J. Interferometric Synthetic Aperture Microscopy: Physics-Based Image Reconstruction from Optical Coherence Tomography Data. / Davis B.J., Ralston T.S., Marks D.L., Boppart S.A., Carney P.S. // 2007. ICIP 2007. IEEE International Conference on Image Processing. - San Antonio, TX, Sept. 16 2007-Oct. 19 2007. - Vol. 4. - P. IV-145 - IV - 148-145. ↑
- C8438.** Bachmann S. Polarimetric Azimuthal Spectral Histogram Exposes Types of Mixed Scatterers and the Cause for Unexpected Polarimetric Averages. / Bachmann S., Zrnic D., De Brunner V. // 2007. ICIP 2007. IEEE International Conference on Image Processing. - San Antonio, TX, Sept. 16 2007-Oct. 19 2007. - Vol. 4. - P. IV-113 - IV - 116-113. ↑
- C8439.** Christophe E. Robust Road Extraction for High Resolution Satellite Images. / Christophe E., Inglada J. // 2007. ICIP 2007. IEEE International Conference on Image Processing. - San Antonio, TX, Sept. 16 2007-Oct. 19 2007. - Vol. 5. - P. V-437 - V - 440-437. ↑
- C8440.** Qadir S.G. Digital Implementation of Pulse Compression Technique for X-band Radar. / Qadir S.G., Kayani J.K., Malik S. // 2007. IBCAST 2007. International Bhurban Conference on Applied Sciences & Technology. - Islamabad, 8-11 Jan. 2007. - P. 35-39. ↑

- C8441.** Bystrom M. A coherent fiber-optic link with optical-domain down-conversion and digital demodulation. / Bystrom M., Li Y., Vacirca N., Herczfeld P., Jemison W. // 2007 IEEE International Topical Meeting on Microwave Photonics. - Victoria, BC, 3-5 Oct. 2007. - P. 164-167. ↑
- C8442.** Yuan Quan. A Fuzzy Adaptive Fusion Algorithm for Radar/Infrared Based on Wavelet Analysis. / Yuan Quan, Dong Chaoyang, Wang Qing. // 2007. ICCA 2007. IEEE International Conference on Control and Automation. - Guangzhou, May 30 2007-June 1 2007. - P. 1344-1348. ↑
- C8443.** Yang Jim Peng. Application of neural network in Infrared-Radar Dual-mode Guidance System. / Yang Jim Peng, Zhu Xiao Ping. // 2007. ICCA 2007. IEEE International Conference on Control and Automation. - Guangzhou, May 30 2007-June 1 2007. - P. 1765-1768. ↑
- C8444.** Zhou Xiaobin. Application and Simulation of Kalman Filtering with Anti-Jamming. / Zhou Xiaobin, Fang Yangwang, Wang Yafei. // 2007. ICCA 2007. IEEE International Conference on Control and Automation. - Guangzhou, May 30 2007-June 1 2007. - P. 696-700. ↑
- C8445.** Andina D. Improved Multilayer Perceptron Design by Weighted Learning. / Andina D., Jevtic A. // 2007. ISIE 2007. IEEE International Symposium on Industrial Electronics. - Vigo, 4-7 June 2007. - P. 3424-3429. ↑
- C8446.** Shi Xiaoli. Optimization of Fighter Aircraft Evasive Trajectories for Radar Threats Avoidance. / Shi Xiaoli, Wang Xinmin, Liu Yongcai, Wang Changqing, Xu Cheng. // 2007. ICCA 2007. IEEE International Conference on Control and Automation. - Guangzhou, May 30 2007-June 1 2007. - P. 303-307. ↑
- C8447.** Shijun Ying. Ship Route Designing for Collision Avoidance Based on Bayesian Genetic Algorithm. / Shijun Ying, Chaojian Shi, Shenhua Yang. // 2007. ICCA 2007. IEEE International Conference on Control and Automation. - Guangzhou, May 30 2007-June 1 2007. - P. 1807-1811. ↑
- C8448.** Jin Zhang. Information Fusion System with GPRS module for Monitoring the Status of Driver. / Jin Zhang, Jun Dai. // 2007. ICCA 2007. IEEE International Conference on Control and Automation. - Guangzhou, May 30 2007-June 1 2007. - P. 2964-2967. ↑
- C8449.** Liu Hang. Research on Data Association in Three Passive Sensors Network. / Liu Hang, Dou Li-hua, Pan Feng, Dong Ling-xun. // 2007. ICCA 2007. IEEE International Conference on Control and Automation. - Guangzhou, May 30 2007-June 1 2007. - P. 3235-3238. ↑
- C8450.** Hai Chen. Digital Signal Processing for A Level Measurement System Based on FMCW Radar. / Hai Chen, Yan Li, Xin-min Wang. // 2007. ICCA 2007. IEEE International Conference on Control and Automation. - Guangzhou, May 30 2007-June 1 2007. - P. 2843-2847. ↑
- C8451.** Bo Qu. ART and Fuzzy K-means Clustering Based Algorithm for Packet Classification. / Bo Qu, Shuiping Gou, Licheng Jiao. // 2007. ICCA 2007. IEEE International Conference on Control and Automation. - Guangzhou, May 30 2007-June 1 2007. - P. 1987-1991. ↑
- C8452.** Yuan Dongli. A Study of Information Fusion for UAV Based on RBF Neural Network. / Yuan Dongli, Yan Jianguo, Wang Xinmin, Xi Qingbiao. // 2007. ICCA 2007. IEEE International Conference on Control and Automation. - Guangzhou, May 30 2007-June 1 2007. - P. 2839-2842. ↑
- C8453.** Sanming Hu. Measurements of UWB Antennas Backscattering Characteristics for RFID Systems. / Sanming Hu, Choi Look Law, Wenbin Dou. // 2007. ICUWB 2007. IEEE International Conference on Ultra-Wideband. - Singapore, 24-26 Sept. 2007. - P. 94-99. ↑
- C8454.** Lestari A.A. Theoretical and Experimental Analysis of a Rolled-Dipole Antenna for Low-Resolution GPR. / Lestari A.A., Yulian D., Liarto, Suksmono A.B., Bharata E., Yarovoy A.G., Ligthart L.P. // 2007. ICUWB 2007. IEEE International Conference on Ultra-Wideband. - Singapore, 24-26 Sept. 2007. - P. 294-298. ↑
- C8455.** Yugang Ma. UWB Reference-Free Self-Positioning with Electrical Scanning Directional Antenna. / Yugang Ma, Okada K., Xiaobing Sun. // 2007. ICUWB 2007. IEEE International Conference on Ultra-Wideband. - Singapore, 24-26 Sept. 2007. - P. 83-88. ↑
- C8456.** Sato M. Bistatic UWB Radar System. / Sato M., Yoshida K. // 2007. ICUWB 2007. IEEE International Conference on Ultra-Wideband. - Singapore, 24-26 Sept. 2007. - P. 62-65. ↑

- C8457.** Zhuge X. Subsurface Imaging with UWB Linear Array: Evaluation of Antenna Step and Array Aperture. / Zhuge X., Savelyev T.G., Yarovoy A.G., Ligthart L.P. // 2007. ICUWB 2007. IEEE International Conference on Ultra-Wideband. - Singapore, 24-26 Sept. 2007. - P. 66-70. ↑
- C8458.** Yarovoy A. Development of Antennas for Subsurface Radars within ACE. / Yarovoy A., Meincke P., Dauvignac J.-Y., Craddock I., Sarri A., Yi Huang. // 2007. ICUWB 2007. IEEE International Conference on Ultra-Wideband. - Singapore, 24-26 Sept. 2007. - P. 299-304. ↑
- C8459.** Wenger J. Long Range and Ultra-Wideband Short Range Automotive Radar. / Wenger J., Hahn S. // 2007. ICUWB 2007. IEEE International Conference on Ultra-Wideband. - Singapore, 24-26 Sept. 2007. - P. 518-522. ↑
- C8460.** Trotta S. SiGe Circuits for Spread Spectrum Automotive Radar. / Trotta S., Dehlink B., Knapp H., Aufinger K., Meister T.F., Bock J., Simburger W., Scholtz A.L. // 2007. ICUWB 2007. IEEE International Conference on Ultra-Wideband. - Singapore, 24-26 Sept. 2007. - P. 523-528. ↑
- C8461.** Ghahramani M. A Double Stage IPCP Detector for UWB Radars. / Ghahramani M., Mohseni R., Sheikhi A. // 2007. ICUWB 2007. IEEE International Conference on Ultra-Wideband. - Singapore, 24-26 Sept. 2007. - P. 345-348. ↑
- C8462.** Nezirovic A. Experimental Verification of Human Being Detection Dependency on Operational UWB Frequency Band. / Nezirovic A., Yarovoy A.G., Ligthart L.P. // 2007. ICUWB 2007. IEEE International Conference on Ultra-Wideband. - Singapore, 24-26 Sept. 2007. - P. 305-310. ↑
- C8463.** Jeongeun Julie Lee. Using UWB Radios as Sensors for Disaster Recovery. / Jeongeun Julie Lee, Singh S. // 2007. ICUWB 2007. IEEE International Conference on Ultra-Wideband. - Singapore, 24-26 Sept. 2007. - P. 311-315. ↑
- C8464.** Nezirovic A. Narrowband Interference Suppression in UWB Impulse Radar for Human Being Detection. / Nezirovic A., Damen I.J.P., Yarovoy A.G. // 2007. ICUWB 2007. IEEE International Conference on Ultra-Wideband. - Singapore, 24-26 Sept. 2007. - P. 56-61. ↑
- C8465.** Reinking J.T. Improving the Speed of a Class of Single Frequency Estimation Algorithms. 2007 IEEE Region 5 Technical Conference. - Fayetteville, AR, 20-22 April 2007. - P. 246-248. ↑
- C8466.** Fontana R.J. Recent Advances in Ultra Wideband Radar and Ranging Systems. / Fontana R.J., Foster L.A., Fair B., Wu D. // 2007. ICUWB 2007. IEEE International Conference on Ultra-Wideband. - Singapore, 24-26 Sept. 2007. - P. 19-25. ↑
- C8467.** Kidder C.C. Design Considerations For An Atmospheric Imaging Radar. / Kidder C.C., Yeary M.B., Palmer R.D. // 2007 IEEE Region 5 Technical Conference. - Fayetteville, AR, 20-22 April 2007. - P. 97-101. ↑
- C8468.** Starek M.J. Shoreline Based Feature Extraction and Optimal Feature Selection for Segmenting Airborne LiDAR Intensity Images. / Starek M.J., Vemula R.K., Slatton K.C., Shrestha R.L., Carter W.E. // 2007. ICIP 2007. IEEE International Conference on Image Processing. - San Antonio, TX, Sept. 16 2007-Oct. 19 2007. - Vol. 4. - P. IV-369 - IV - 372-369. ↑
- C8469.** Vazquez Alejos A. Ground Penetration Radar Using Golay Sequences. / Vazquez Alejos A., Muhammad D., Ur Rahman Mohammed H. // 2007 IEEE Region 5 Technical Conference. - Fayetteville, AR, 20-22 April 2007. - P. 318-321. ↑
- C8470.** Sakamoto T. Real-time Imaging of Human Bodies with UWB Radars using Walking Motion. / Sakamoto T., Sato T. // 2007. ICUWB 2007. IEEE International Conference on Ultra-Wideband. - Singapore, 24-26 Sept. 2007. - P. 26-30. ↑
- C8471.** Hirose A. UWB measurement, complex-amplitude texture, and Walled-LTSA array in plastic landmine visualization. / Hirose A., Masuyama S. // 2007. ICUWB 2007. IEEE International Conference on Ultra-Wideband. - Singapore, 24-26 Sept. 2007. - P. 46-49. ↑
- C8472.** Sachs J. Recent Advances and Applications of M-Sequence based Ultra-Wideband Sensors. / Sachs J., Herrmann R., Kmec M., Helbig M., Schilling K. // 2007. ICUWB 2007. IEEE International Conference on Ultra-Wideband. - Singapore, 24-26 Sept. 2007. - P. 50-55. ↑

- C8473.** Fang Guangyou. The Research Activities of Ultrawide-band (UWB) Radar in China. 2007. ICUWB 2007. IEEE International Conference on Ultra-Wideband. - Singapore, 24-26 Sept. 2007. - P. 43-45. ↑
- C8474.** Koshelev V.I. Detection and recognition of radar objects at sounding by high-power ultrawideband pulses. 2007. ICUWB 2007. IEEE International Conference on Ultra-Wideband. - Singapore, 24-26 Sept. 2007. - P. 31-36. ↑
- C8475.** Nishimoto M. UWB-GPR Data Processing for Identification of Anti-personnel Landmines under Rough Ground Surface. / Nishimoto M., Kimura Y., Tanaka T., Ogata K. // 2007. ICUWB 2007. IEEE International Conference on Ultra-Wideband. - Singapore, 24-26 Sept. 2007. - P. 37-42. ↑
- C8476.** Yimin Wei. Vehicle Frontal Collision Warning System based on Improved Target Tracking and Threat Assessment. / Yimin Wei, Huadong Meng, Hao Zhang, Xiqin Wang. // 2007. ITSC 2007. IEEE Intelligent Transportation Systems Conference. - Seattle, WA, Sept. 30 2007-Oct. 3 2007. - P. 167-172. ↑
- C8477.** Kramer K.A. Sensor Calibration Using the Neural Extended Kalman Filter in a Control Loop. / Kramer K.A., Stubberud S.C., Geremia J.A. // 2007. CIMSA 2007. IEEE International Conference on Computational Intelligence for Measurement Systems and Applications. - Ostuni, 27-29 June 2007. - P. 19-24. ↑
- C8478.** Jianxin Fang. A Low-cost Vehicle Detection and Classification System based on Unmodulated Continuous-wave Radar. / Jianxin Fang, Huadong Meng, Hao Zhang, Xiqin Wang. // 2007. ITSC 2007. IEEE Intelligent Transportation Systems Conference. - Seattle, WA, Sept. 30 2007-Oct. 3 2007. - P. 715-720. ↑
- C8479.** Nigam C. Feature Fusion for Robust Object Tracking Using Fragmented Particles. / Nigam C., Babu R.V., Raja S.K., Ramakrishnan K.R. // 2007. ICDSC '07. First ACM/IEEE International Conference on Distributed Smart Cameras. - Vienna, 25-28 Sept. 2007. - P. 283-290. ↑
- C8480.** Wolfe M. Improving Arterial Performance Measurement Using Traffic Signal System Data. / Wolfe M., Monsere C., Koonce P., Bertini R.L. // 2007. ITSC 2007. IEEE Intelligent Transportation Systems Conference. - Seattle, WA, Sept. 30 2007-Oct. 3 2007. - P. 113-118. ↑
- C8481.** Zanin M. Localization of ahead vehicles with on-board stereo cameras. 2007. ICIAP 2007. 14th International Conference on Image Analysis and Processing. - Modena, 10-14 Sept. 2007. - P. 111-116. ↑
- C8482.** Buemi M.E. Improvement in SAR Image Classification using Adaptive Stack Filters. / Buemi M.E., Mejail M., Jacobo J., Gambini J. // 2007. SIBGRAPI 2007. XX Brazilian Symposium on Computer Graphics and Image Processing. - Minas Gerais, 7-10 Oct. 2007. - P. 263-270. ↑
- C8483.** Malevich I.Yu. Radiomodule of VHF Reception Path. 2007. CriMiCo 2007. 17th International Crimean Conference Microwave & Telecommunication Technology. - Crimea, 10-14 Sept. 2007. - P. 65-66. ↑
- C8484.** Qingguo Zhou. Test bed for Remote Environmental Monitoring in Northwestern China. / Qingguo Zhou, Guanghui Cheng, Tzu-Han Kao, Wenzhong Wu, Lian Li. // 2007. ICPCA 2007. 2nd International Conference on Pervasive Computing and Applications. - Birmingham, 26-27 July 2007. - P. 705-708. ↑
- C8485.** Zingaretti P. Automatic extraction of LIDAR data classification rules. / Zingaretti P., Frontoni E., Forlani G., Nardinocchi C. // 2007. ICIAP 2007. 14th International Conference on Image Analysis and Processing. - Modena, 10-14 Sept. 2007. - P. 273-278. ↑
- C8486.** Sayrafian-Pour K. Robust Indoor Positioning Based on Received Signal Strength. / Sayrafian-Pour K., Perez J. // 2007. ICPCA 2007. 2nd International Conference on Pervasive Computing and Applications. - Birmingham, 26-27 July 2007. - P. 693-698. ↑
- C8487.** Neinhuis M. FIR-filter based equalization of ultra wideband mutual coupling on linear antenna arrays. / Neinhuis M., Held S., Solbach K. // 2007. INICA '07. 2nd International ITG Conference on Antennas. - Munich, 28-30 March 2007. - P. 115-119. ↑
- C8488.** Duan Junqi. Multicarrier Coherent Pulse Shaping for Radar and Corresponding Signal Processing. 2007. ICEMI '07. 8th International Conference on Electronic Measurement and Instruments. - Xi'an, Aug. 16 2007-July 18 2007. - P. 3-843-3-847-843. ↑
- C8489.** Zhang Ruoyu. Radar Reflected Signal Process of High Spinning Rate Projectiles. / Zhang Ruoyu,

Wang Yuanqin, Wu tao, Geng Wendong. // 2007. ICEMI '07. 8th International Conference on Electronic Measurement and Instruments. - Xi'an, Aug. 16 2007-July 18 2007. - P. 3-982-3-985-982. ↑

C8490. Chen Ting. Research on Rough Set-Neural Network and Its Application in Radar Signal Recognition. / Chen Ting, Luo Jingqing, Shen Bing. // 2007. ICEMI '07. 8th International Conference on Electronic Measurement and Instruments. - Xi'an, Aug. 16 2007-July 18 2007. - P. 3-764-3-768-764. ↑

C8491. Zhang Jie. Research of High Precision Frequency Measure Algorithm Based on LabVIEW. 2007. ICEMI '07. 8th International Conference on Electronic Measurement and Instruments. - Xi'an, Aug. 16 2007-July 18 2007. - P. 3-268-3-271-268. ↑

C8492. Zhang Yongqiang. Application of Radial Basis Function Neural Networks in Complicated Radar Signal Measurement and Sorting. / Zhang Yongqiang, Sun Guozhi. // 2007. ICEMI '07. 8th International Conference on Electronic Measurement and Instruments. - Xi'an, Aug. 16 2007-July 18 2007. - P. 3-375-3-378-375. ↑

C8493. Chunbo Ma. Password-based Dynamic Group Key Agreement. / Chunbo Ma, Jun Ao, Jianhua Li. // 2007. NPC Workshops. IFIP International Conference on Network and Parallel Computing Workshops. - Liaoning, 18-21 Sept. 2007. - P. 203-208. ↑

C8494. Hafner N. Non-Contact Cardiopulmonary Sensing with a Baby Monitor. / Hafner N., Mostafanezhad I., Lubecke V.M., Boric-Lubecke O., Host-Madsen A. // 2007. EMBS 2007. 29th Annual International Conference of the IEEE Engineering in Medicine and Biology Society. - Lyon, 22-26 Aug. 2007. - P. 2300-2302. ↑

C8495. Cvetkovic D. Inter and Intra-Hemispheric EEG Coherence Responses to Visual Stimulations. / Cvetkovic D., Cosic I. // 2007. EMBS 2007. 29th Annual International Conference of the IEEE Engineering in Medicine and Biology Society. - Lyon, 22-26 Aug. 2007. - P. 2839-2842. ↑

C8496. Lu Guohua. Study of the Ballistocardiogram signal in life detection system based on radar. / Lu Guohua, Wang Jianqi, Yue Yu, Jing Xijing. // 2007. EMBS 2007. 29th Annual International Conference of the IEEE Engineering in Medicine and Biology Society. - Lyon, 22-26 Aug. 2007. - P. 2191-2194. ↑

C8497. Prieto-Guerrero A. Lost Sample Recovering of ECG Signals in e-Health Applications. / Prieto-Guerrero A., Mailhes C., Castanie F. // 2007. EMBS 2007. 29th Annual International Conference of the IEEE Engineering in Medicine and Biology Society. - Lyon, 22-26 Aug. 2007. - P. 31-34. ↑

C8498. Dung Nguyen. Noise Considerations for Remote Detection of Life Signs with Microwave Doppler Radar. / Dung Nguyen, Yamada S., Byung-Kwon Park, Lubecke V., Boric-Lubecke O., Host-Madsen A. // 2007. EMBS 2007. 29th Annual International Conference of the IEEE Engineering in Medicine and Biology Society. - Lyon, 22-26 Aug. 2007. - P. 1667-1670. ↑

C8499. Gagnon A. Recent Developments in Ground Based Millimeter Wave Radars. / Gagnon A., Kwong M.P. // 2007 41st Annual IEEE International Carnahan Conference on Security Technology. - Ottawa, Ont., 8-11 Oct. 2007. - P. 189-192. ↑

C8500. Harman K. Experience with Ranging Buried Cable Sensing. / Harman K., Hodgins B., Patchell J. // 2007 41st Annual IEEE International Carnahan Conference on Security Technology. - Ottawa, Ont., 8-11 Oct. 2007. - P. 193-200. ↑

C8501. Butler W. Benefits of Wide Area Intrusion Detection Systems using FMCW Radar. / Butler W., Poitevin P., Bjornholt J. // 2007 41st Annual IEEE International Carnahan Conference on Security Technology. - Ottawa, Ont., 8-11 Oct. 2007. - P. 176-182. ↑

C8502. Zhi-Fei Ye. Learning Imbalanced Data Sets with a Min-Max Modular Support Vector Machine. / Zhi-Fei Ye, Bao-Liang Lu. // 2007. IJCNN 2007. International Joint Conference on Neural Networks. - Orlando, FL, 12-17 Aug. 2007. - P. 1673-1678. ↑

C8503. Linnehan Robert. Resolving Wall Ambiguities Using Angular Diverse Synthetic Arrays. / Linnehan Robert, Schindler John, Brady David, Kozma Robert, Deming Ross, Perlovsky Leonid. // 2007. IJCNN 2007. International Joint Conference on Neural Networks. - Orlando, FL, USA, 12-17 Aug. 2007. - P. 2758-2763. ↑

C8504. Modebadze Z. Effect of 8.43 Hz Frequency Magnetic Field on the Single Neuron. / Modebadze Z., Partcvania B., Surguladze T., Andriadze L., Sanablidze L., Shoshiashvili L. // 2007 XIIth International

Seminar/Workshop on Direct and Inverse Problems of Electromagnetic and Acoustic Wave Theory. - Lviv, 17-20 Sept. 2007. - P. 43-47. ↑

C8505. Gorringe C. IEEE 1641 signal modelling as a learning aid. / Gorringe C., Coles T. // 2007 IEEE Autotestcon. - Baltimore, MD, 17-20 Sept. 2007. - P. 728-734. ↑

C8506. Torres J. Radar Detection Through Wavelet Transform. / Torres J., Marcano A., Andina D. // 2007. ISIE 2007. IEEE International Symposium on Industrial Electronics. - Vigo, 4-7 June 2007. - P. 3420-3423. ↑

C8507. Damiani E. L-VCONF: A Location-Aware Infrastructure for Battlefield Videoconferences. / Damiani E., Anisetti M., Ardagna C.A., Bellandi V. // 2007. VECIMS 2007. IEEE Symposium on Virtual Environments, Human-Computer Interfaces and Measurement Systems. - Ostuni, 25-27 June 2007. - P. 160-165. ↑

C8508. Nazarchuk Z.T. The Influence of Permittivity of the Crack-Type Defects to the Scattered Far Field (TM-Case). / Nazarchuk Z.T., Kulynych Ya.P., Stadnik T.M. // 2007 XIIth International Seminar/Workshop on Direct and Inverse Problems of Electromagnetic and Acoustic Wave Theory. - Lviv, 17-20 Sept. 2007. - P. 77-80. ↑

C8509. Xiaoyan Pan. Building Learning Communities in Blended Classrooms Through an Innovative mLearning System. / Xiaoyan Pan, Ruimin Shen, Minjuan Wang. // 2007. VECIMS 2007. IEEE Symposium on Virtual Environments, Human-Computer Interfaces and Measurement Systems. - Ostuni, 25-27 June 2007. - P. 139-143. ↑

C8510. Thompson B.D. An Iterative Learning Algorithm for Multi-Channel Coherence Analysis. / Thompson B.D., Azimi-Sadjadi M.R. // 2007. IJCNN 2007. International Joint Conference on Neural Networks. - Orlando, FL, 12-17 Aug. 2007. - P. 1326-1331. ↑

C8511. Lagovsky B.A. Angular Resolution Increasing in Processing of Radionavigation Signals. 2007. CriMiCo 2007. 17th International Crimean Conference Microwave & Telecommunication Technology. - Crimea, 10-14 Sept. 2007. - P. 857-858. ↑

C8512. Chapursky V.V. Addition and Multiplication Statistics for Orthogonal Signal Processing in Multiple Antennas System. / Chapursky V.V., Kalinin V.I. // 2007. CriMiCo 2007. 17th International Crimean Conference Microwave & Telecommunication Technology. - Crimea, 10-14 Sept. 2007. - P. 863-864. ↑

C8513. Votoropin S.D. Autodyne Signal at Reflection Factor Value Modulation. / Votoropin S.D., Noskov V.Ya., Smolskiy S.M. // 2007. CriMiCo 2007. 17th International Crimean Conference Microwave & Telecommunication Technology. - Crimea, 10-14 Sept. 2007. - P. 748-750. ↑

C8514. Kolesov V.V. Elements of Fractal Radiosystems. / Kolesov V.V., Krupenin S.V., Potapov A.A. // 2007. CriMiCo 2007. 17th International Crimean Conference Microwave & Telecommunication Technology. - Crimea, 10-14 Sept. 2007. - P. 632-633. ↑

C8515. Ostapenko P.S. Analysis Features of Fast-Acting Radio Electronic Systems with Combined FM-AM Modulation. / Ostapenko P.S., Smolskiy S.M. // 2007. CriMiCo 2007. 17th International Crimean Conference Microwave & Telecommunication Technology. - Crimea, 10-14 Sept. 2007. - P. 731-732. ↑

C8516. Ying Li. Information Compression and Speckle Reduction for Multifrequency Polarimetric SAR Imagery using KPCA. / Ying Li, Xiao-Gang Lei, Ben-Du Bai, Yan-Ning Zhang. // 2007 International Conference on Machine Learning and Cybernetics. - Hong Kong, 19-22 Aug. 2007. - Vol. 3. - P. 1688-1692. ↑

C8517. Deming R. Neural Modeling Fields for Multitarget/Multisensor Tracking. / Deming R., Schindler J., Perlovsky L. // 2007. IJCNN 2007. International Joint Conference on Neural Networks. - Orlando, FL, 12-17 Aug. 2007. - P. 442-447. ↑

C8518. Hikawa H. Performance Comparison of SOM Based Hybrid Hardware Classifiers. / Hikawa H., Miyanishi T., Tamaya K. // 2007. IJCNN 2007. International Joint Conference on Neural Networks. - Orlando, FL, 12-17 Aug. 2007. - P. 1091-1096. ↑

C8519. Guan Xin. Discretization of Continuous Interval-Valued Attributes in Rough Set Theory and its Application. / Guan Xin, Yi Xiao, He You. // 2007 International Conference on Machine Learning and Cybernetics. - Hong Kong, 19-22 Aug. 2007. - Vol. 7. - P. 3682-3686. ↑

- C8520.** Xiao-Qin Wen. A Two-Stage Hybrid Space-Time Adaptive Processing Approach. / Xiao-Qin Wen, Lin-Ru You, Shu-E Bi. // 2007 International Conference on Machine Learning and Cybernetics. - Hong Kong, 19-22 Aug. 2007. - Vol. 5. - P. 2566-2571. ↑
- C8521.** Ran Yue. The Affection of MAC Protocols to Energy Consumption in the UWB-Ad hoc System. / Ran Yue, Wei-Qiang Wu, Qin-Yu Zhang, Nai-Tong Zhang. // 2007 International Conference on Machine Learning and Cybernetics. - Hong Kong, 19-22 Aug. 2007. - Vol. 6. - P. 3229-3233. ↑
- C8522.** Wang Yiding. A new encoding transponders for SAR calibration. 2007. APSAR 2007. 1st Asian and Pacific Conference on Synthetic Aperture Radar. - Huangshan, 5-9 Nov. 2007. - P. 244-248. ↑
- C8523.** Xueru Bai. Adaptive S-method based ISAR imaging of maneuvering targets. / Xueru Bai, Mengdao Xing, Feng Zhou, Bao Zheng. // 2007. APSAR 2007. 1st Asian and Pacific Conference on Synthetic Aperture Radar. - Huangshan, 5-9 Nov. 2007. - P. 249-252. ↑
- C8524.** Li Yan. ESPRIT super-resolution imaging algorithm based on external illuminators. / Li Yan, Wang Jun, Liu Jinrong. // 2007. APSAR 2007. 1st Asian and Pacific Conference on Synthetic Aperture Radar. - Huangshan, 5-9 Nov. 2007. - P. 232-235. ↑
- C8525.** Shushan Qiao. HIPERMA: A high performance and reconfigurable processor for SAR applications. / Shushan Qiao, Yong Hei, Xinfeng Xu, Bin Wu, Yumei Zhou. // 2007. APSAR 2007. 1st Asian and Pacific Conference on Synthetic Aperture Radar. - Huangshan, 5-9 Nov. 2007. - P. 240-243. ↑
- C8526.** Yang Lei. A new channel equalization method for airborne multi-channel SAR-GMTI system. / Yang Lei, Wang Tong Xing, Mengdao Bao Zheng. // 2007. APSAR 2007. 1st Asian and Pacific Conference on Synthetic Aperture Radar. - Huangshan, 5-9 Nov. 2007. - P. 271-274. ↑
- C8527.** Lifeng Zhang. A novel approach to three-channel SAR-GMTI channel equalization and moving target detection and location based on real data. / Lifeng Zhang, Tong Wang, Mengdao Xing, Zheng Bao. // 2007. APSAR 2007. 1st Asian and Pacific Conference on Synthetic Aperture Radar. - Huangshan, 5-9 Nov. 2007. - P. 284-288. ↑
- C8528.** Eunjung Yang. Non-statistical transformed data domain stap algorithm for non-homogeneous environment. / Eunjung Yang, Joohwan Chun, Jonghoon Chun. // 2007. APSAR 2007. 1st Asian and Pacific Conference on Synthetic Aperture Radar. - Huangshan, 5-9 Nov. 2007. - P. 257-261. ↑
- C8529.** Deng Haitao. A Real-time signal processing method for air-born three-channels GMTI. / Deng Haitao, Zhang Changyao. // 2007. APSAR 2007. 1st Asian and Pacific Conference on Synthetic Aperture Radar. - Huangshan, 5-9 Nov. 2007. - P. 262-265. ↑
- C8530.** Li Ming. Algorithm for the latitude and longitude of an arbitrary pixel in air-borne strip mode SAR image. / Li Ming, Guo Qing, Wu Shunjun. // 2007. APSAR 2007. 1st Asian and Pacific Conference on Synthetic Aperture Radar. - Huangshan, 5-9 Nov. 2007. - P. 180-184. ↑
- C8531.** Cui Rui. Research on jamming effect evaluation method of ISAR. / Cui Rui, Xue Lei, Li Ming-liang. // 2007. APSAR 2007. 1st Asian and Pacific Conference on Synthetic Aperture Radar. - Huangshan, 5-9 Nov. 2007. - P. 65-67. ↑
- C8532.** Li Xiaohan. Analysis of deception jamming to ISAR imaging system. / Li Xiaohan, Wang Jianguo. // 2007. APSAR 2007. 1st Asian and Pacific Conference on Synthetic Aperture Radar. - Huangshan, 5-9 Nov. 2007. - P. 68-70. ↑
- C8533.** Xin Lu. Parameter assessment for SAR image quality evaluation system. / Xin Lu, Hong Sun. // 2007. APSAR 2007. 1st Asian and Pacific Conference on Synthetic Aperture Radar. - Huangshan, 5-9 Nov. 2007. - P. 58-60. ↑
- C8534.** Hongrong Zhang. SAR deceptive jamming signal simulation. / Hongrong Zhang, Yuesheng Tang, Guan Wu, Long Sun. // 2007. APSAR 2007. 1st Asian and Pacific Conference on Synthetic Aperture Radar. - Huangshan, 5-9 Nov. 2007. - P. 61-64. ↑
- C8535.** Long Zhuang. Separable space-time pattern synthesis for SBR sparse aperture array GMTI. / Long Zhuang, Xingzhao Liu. // 2007. APSAR 2007. 1st Asian and Pacific Conference on Synthetic Aperture Radar. -

Huangshan, 5-9 Nov. 2007. - P. 119-122. ↑

C8536. Ning Li. On the influence of frequency-domain broadband beamformer on ISAR imaging. / Ning Li, Jia Xu, Yingning Peng, Jun Tang. // 2007. APSAR 2007. 1st Asian and Pacific Conference on Synthetic Aperture Radar. - Huangshan, 5-9 Nov. 2007. - P. 151-153. ↑

C8537. Wen Shilling. 1-D high resolution range profiling technique for wideband solid state active phased array radar under active jamming situations. / Wen Shilling, Lu Yaobing. // 2007. APSAR 2007. 1st Asian and Pacific Conference on Synthetic Aperture Radar. - Huangshan, 5-9 Nov. 2007. - P. 76-82. ↑

C8538. Qiu Xiaolan. Non-linear chirp scaling algorithm for one-stationary bistatic SAR. / Qiu Xiaolan, Hu Donghui, Ding Chibiao. // 2007. APSAR 2007. 1st Asian and Pacific Conference on Synthetic Aperture Radar. - Huangshan, 5-9 Nov. 2007. - P. 111-114. ↑

C8539. Ting Shu. Moving target detection in airborne SAR by a combined wigner-STFT transform. / Ting Shu, Xingzhao Liu. // 2007. APSAR 2007. 1st Asian and Pacific Conference on Synthetic Aperture Radar. - Huangshan, 5-9 Nov. 2007. - P. 298-301. ↑

C8540. Yu Hongyun. SAR ATR based on multi-subspaces of independent component analysis. / Yu Hongyun, Guan Jian, Giang Tao, Zhang Jinge. // 2007. APSAR 2007. 1st Asian and Pacific Conference on Synthetic Aperture Radar. - Huangshan, 5-9 Nov. 2007. - P. 493-496. ↑

C8541. Liya Li. Radar automatic target recognition based on InISAR images. / Liya Li, Weiming Yuan, Hongwei Liu, Bo Chen, Shunjun Wu. // 2007. APSAR 2007. 1st Asian and Pacific Conference on Synthetic Aperture Radar. - Huangshan, 5-9 Nov. 2007. - P. 497-502. ↑

C8542. Xiangdong Meng. Spatial decorrelation evaluation for interferometric SAR. / Xiangdong Meng, Tong Wang, Zheng Bao, Jinshan Ding. // 2007. APSAR 2007. 1st Asian and Pacific Conference on Synthetic Aperture Radar. - Huangshan, 5-9 Nov. 2007. - P. 439-443. ↑

C8543. Ge Xu. An improved road extraction method based on MRFs in rural areas for SAR images. / Ge Xu, Hong Sun, Wen Yang, Yongmin Shuai. // 2007. APSAR 2007. 1st Asian and Pacific Conference on Synthetic Aperture Radar. - Huangshan, 5-9 Nov. 2007. - P. 489-492. ↑

C8544. Dong Yin. Multi-scale feature analysis method for bridge recognition in SAR images. / Dong Yin, Yuqing Miao, Guiqin Li, Bin Cheng. // 2007. APSAR 2007. 1st Asian and Pacific Conference on Synthetic Aperture Radar. - Huangshan, 5-9 Nov. 2007. - P. 517-520. ↑

C8545. Li Nan. Research on jamming synthetic aperture radar technologies. / Li Nan, Qu Changwen. // 2007. APSAR 2007. 1st Asian and Pacific Conference on Synthetic Aperture Radar. - Huangshan, 5-9 Nov. 2007. - P. 563-566. ↑

C8546. Yongmin Shuai. A fast segmentation scheme based on level set for SAR images. / Yongmin Shuai, Hong Sun, Ge Xu. // 2007. APSAR 2007. 1st Asian and Pacific Conference on Synthetic Aperture Radar. - Huangshan, 5-9 Nov. 2007. - P. 503-506. ↑

C8547. Xiaoguang Lu. Two-dimensional PCA for SAR automatic target recognition. / Xiaoguang Lu, Ping Han, Renbiao Wu. // 2007. APSAR 2007. 1st Asian and Pacific Conference on Synthetic Aperture Radar. - Huangshan, 5-9 Nov. 2007. - P. 513-516. ↑

C8548. Tang Yu. Motion compensation technique for high resolution spotlight SAR. / Tang Yu, Xing Mengdao. // 2007. APSAR 2007. 1st Asian and Pacific Conference on Synthetic Aperture Radar. - Huangshan, 5-9 Nov. 2007. - P. 435-438. ↑

C8549. Yin Jian-feng. MTI processing based on dual frequencies-dual apertures spaceborne SAR. / Yin Jian-feng, Li Dao-jing, Wu Yi-rong. // 2007. APSAR 2007. 1st Asian and Pacific Conference on Synthetic Aperture Radar. - Huangshan, 5-9 Nov. 2007. - P. 318-322. ↑

C8550. Zhu Jiabing. A novel adaptive filtering algorithm for SAR speckle reduction. / Zhu Jiabing, Chen Renyuan, Hong Yi. // 2007. APSAR 2007. 1st Asian and Pacific Conference on Synthetic Aperture Radar. - Huangshan, 5-9 Nov. 2007. - P. 327-330. ↑

- C8551.** Yu Jing. An effective SAR-GMTI technique based on eigen-decomposition of the covariance matrix. / Yu Jing, Liao Guisheng. // 2007. APSAR 2007. 1st Asian and Pacific Conference on Synthetic Aperture Radar. - Huangshan, 5-9 Nov. 2007. - P. 302-305. ↑
- C8552.** Qiu Chaoyang. Ground slow-moving target adaptive processing for Airborne Radar. / Qiu Chaoyang, Hao Zhimei. // 2007. APSAR 2007. 1st Asian and Pacific Conference on Synthetic Aperture Radar. - Huangshan, 5-9 Nov. 2007. - P. 310-313. ↑
- C8553.** Yi Yu-sheng. Study on imaging algorithm for missile-borne side-looking SAR. / Yi Yu-sheng, Zhang Lin-rang, Liu Xin, Liu Nan, Shen Dong. // 2007. APSAR 2007. 1st Asian and Pacific Conference on Synthetic Aperture Radar. - Huangshan, 5-9 Nov. 2007. - P. 413-417. ↑
- C8554.** Tan Wei-xian. A novel imaging approach for multi-baseline SAR tomography. / Tan Wei-xian, Hong Wen, Wang Yan-ping, Wu Yi-rong. // 2007. APSAR 2007. 1st Asian and Pacific Conference on Synthetic Aperture Radar. - Huangshan, 5-9 Nov. 2007. - P. 423-426. ↑
- C8555.** Hee Sub Shin. Extension of range migration algorithm for airborne spotlight SAR with velocity variation. / Hee Sub Shin, Jae Han Jeon, Ho Jin Lee, Jong Tae Lim. // 2007. APSAR 2007. 1st Asian and Pacific Conference on Synthetic Aperture Radar. - Huangshan, 5-9 Nov. 2007. - P. 360-363. ↑
- C8556.** Gang Li. Improved RDM for SAR autofocus processing. / Gang Li, Jia Xu, Yingning Peng, Xiang-Gen Xia. // 2007. APSAR 2007. 1st Asian and Pacific Conference on Synthetic Aperture Radar. - Huangshan, 5-9 Nov. 2007. - P. 401-403. ↑
- C8557.** Krengel E.I. New Binary ZCZ Sequence Sets with Mismatched Filtering. 2007. IWSDA 2007. 3rd International Workshop on Signal Design and Its Applications in Communications. - Chengdu, 23-27 Sept. 2007. - P. 26-29. ↑
- C8558.** Jingye Cai. High Performance Waveform Generator Design for Full-Coherent Millimeter-Wave Radar. / Jingye Cai, Yishi Yang, Yuanwang Yang, Lianfu Liu, Xueyong Zhu. // 2007. IWSDA 2007. 3rd International Workshop on Signal Design and Its Applications in Communications. - Chengdu, 23-27 Sept. 2007. - P. 378-382. ↑
- C8559.** Thies W. A Practical Approach to Exploiting Coarse-Grained Pipeline Parallelism in C Programs. / Thies W., Chandrasekhar V., Amarasinghe S. // 2007. MICRO 2007. 40th Annual IEEE/ACM International Symposium on Microarchitecture. - Chicago, IL, 1-5 Dec. 2007. - P. 356-369. ↑
- C8560.** Moreno O. Double Periodic Arrays with Good Correlation for Applications in Watermarking. / Moreno O., Ortiz-Ubarri J. // 2007. IWSDA 2007. 3rd International Workshop on Signal Design and Its Applications in Communications. - Chengdu, 23-27 Sept. 2007. - P. 214-218. ↑
- C8561.** Taati B. Variable Dimensional Local Shape Descriptors for Object Recognition in Range Data. / Taati B., Bondy M., Jasiobedzki P., Greenspan M. // 2007. ICCV 2007. IEEE 11th International Conference on Computer Vision. - Rio de Janeiro, 14-21 Oct. 2007. - P. 1-8. ↑
- C8562.** Lu Wang. Semiautomatic registration between ground-level panoramas and an orthorectified aerial image for building modeling. / Lu Wang, Suyu You, Neumann U. // 2007. ICCV 2007. IEEE 11th International Conference on Computer Vision. - Rio de Janeiro, 14-21 Oct. 2007. - P. 1-8. ↑
- C8563.** Quang Khai Trinh. Sequence Sets with Zero Correlation Zones using Mismatched Filtering. / Quang Khai Trinh, Pingzhi Fan, Xiaohu Tang. // 2007. IWSDA 2007. 3rd International Workshop on Signal Design and Its Applications in Communications. - Chengdu, 23-27 Sept. 2007. - P. 61-64. ↑
- C8564.** Vladimir G. Synthesis Results of the Periodic Discretely Coded Sequences with the Parameters Constraints Defined on the Basis of Cyclotomic Classes. / Vladimir G., Vladimir E. // 2007. IWSDA 2007. 3rd International Workshop on Signal Design and Its Applications in Communications. - Chengdu, 23-27 Sept. 2007. - P. 9-12. ↑
- C8565.** Bar-Shalom Y. Track association and fusion with heterogeneous local trackers. / Bar-Shalom Y., Huimin Chen. // 2007 10th International Conference on Information Fusion. - Quebec, Que., 9-12 July 2007. - P. 1. ↑

- C8566.** Musicki D. Track management and PMHT. / Musicki D., Xuezhi Wang. // 2007 10th International Conference on Information Fusion. - Quebec, Que., 9-12 July 2007. - P. 1-5. ↑
- C8567.** Seeker J. Exploitation of multi-temporal SAR and EO satellite imagery for geospatial intelligence. / Seeker J., Vachon P.W. // 2007 10th International Conference on Information Fusion. - Quebec, Que., 9-12 July 2007. - P. 1-8. ↑
- C8568.** Rheaume F. Fire control-based adaptation in data fusion applications. / Rheaume F., Benaskeur A.R. // 2007 10th International Conference on Information Fusion. - Quebec, Que., 9-12 July 2007. - P. 1-8. ↑
- C8569.** Ya-Dong Wang. Gaussian mixture probability hypothesis density for visual people tracking. / Ya-Dong Wang, Jian-Kang Wu, Weimin Huang, Kassim A.A. // 2007 10th International Conference on Information Fusion. - Quebec, Que., 9-12 July 2007. - P. 1-6. ↑
- C8570.** Tsogas M. Situation refinement for vehicle maneuver identification and driver's intention prediction. / Tsogas M., Polychronopoulos A., Floudas N., Amditis A. // 2007 10th International Conference on Information Fusion. - Quebec, Que., 9-12 July 2007. - P. 1-8. ↑
- C8571.** Willett P. Quickest detection of statistical changes with application to tracking. 2007 10th International Conference on Information Fusion. - Quebec, Que., 9-12 July 2007. - P. 1. ↑
- C8572.** Barbaresco F. Radar resources optimization by adaptive search domains priority assignment based on most threatening trajectories computation. 2007 10th International Conference on Information Fusion. - Quebec, Que., 9-12 July 2007. - P. 1-8. ↑
- C8573.** Arulampalam S. Performance of the shifted Rayleigh filter in single-sensor bearings-only tracking. / Arulampalam S., Clark M., Vinter R. // 2007 10th International Conference on Information Fusion. - Quebec, Que., 9-12 July 2007. - P. 1-6. ↑
- C8574.** Moon Ting Su. Service-Oriented E-Learning System. / Moon Ting Su, Chee Shyang Wong, Chuak Fen Soo, Choon Tsun Ooi, Shun Ling Sow. // 2007. ISITAE '07. First IEEE International Symposium on Information Technologies and Applications in Education. - Kunming, 23-25 Nov. 2007. - P. 6-11. ↑
- C8575.** Yan He. Multiscale Variational Threshold SAR Image Denoising Based on Quad-tree Complex Wavelet Packets Transform. / Yan He, Cheng Wei, He Guang-min, Li Gang, Dong Shi-du. // Second Workshop on Digital Media and its Application in Museum & Heritages. - Chongqing, 10-12 Dec. 2007. - P. 57-62. ↑
- C8576.** Zhang Tianqi. Estimate and Track the PN Sequence of Weak DS-SS Signals. / Zhang Tianqi, Dai Shaosheng, Yang Liufei, Li Xuesong. // 2007 International Conference on Computational Intelligence and Security. - Harbin, 15-19 Dec. 2007. - P. 52-56. ↑
- C8577.** Mandic D.P. Why a Complex Valued Solution for a Real Domain Problem. / Mandic D.P., Javidi S., Souretis G., Goh V.S.L. // 2007 IEEE Workshop on Machine Learning for Signal Processing. - Thessaloniki, 27-29 Aug. 2007. - P. 384-389. ↑
- C8578.** Seungju Han. Robust Adaptive Minimum Entropy Beamformer in Impulsive Noise. / Seungju Han, Kyu-Hwa Jeong, Principe J. // 2007 IEEE Workshop on Machine Learning for Signal Processing. - Thessaloniki, 27-29 Aug. 2007. - P. 437-440. ↑
- C8579.** Dang Hongxing. Stepped frequency chirp signal SAR imaging. 2007. APSAR 2007. 1st Asian and Pacific Conference on Synthetic Aperture Radar. - Huangshan, 5-9 Nov. 2007. - P. 14-18. ↑
- C8580.** Xu Ye. Airborne ISAR imaging of ship side view. / Xu Ye, Daiyin Zhu, Ling Wang, Zhaoda Zhu. // 2007. APSAR 2007. 1st Asian and Pacific Conference on Synthetic Aperture Radar. - Huangshan, 5-9 Nov. 2007. - P. 41-44. ↑
- C8581.** Fan Yang. The scheme and key components design of W-band coherent doppler velocity radar front-end. / Fan Yang, Xiao-Hong Tang, Tao Wu. // 2007. ASICON '07. 7th International Conference on ASIC. - Guilin, 22-25 Oct. 2007. - P. 356-359. ↑
- C8582.** Chen Jie. Operation mode for topside ionospheric sounding based on space-borne high frequency synthetic aperture radar. / Chen Jie, Liu Wei, Zhou Yinqing, Li Chunsheng. // 2007. APSAR 2007. 1st Asian and

Pacific Conference on Synthetic Aperture Radar. - Huangshan, 5-9 Nov. 2007. - P. 1-5. ↑

C8583. Masagutov V. Vibrometry classification of moving vehicles using throttle signature analysis. / Masagutov V., Stouch D.W., Kanjilal P., Snorrason M. // 2007. ISIC. IEEE International Conference on Systems, Man and Cybernetics. - Montreal, Que., 7-10 Oct. 2007. - P. 3938-3944. ↑

C8584. Knappmeyer M. Advanced Multicast and Broadcast Content Distribution in Mobile Cellular Networks. / Knappmeyer M., Ricks B., Tonjes R., Al-Hezmi A. // 2007. GLOBECOM '07. IEEE Global Telecommunications Conference. - Washington, DC, 26-30 Nov. 2007. - P. 2097-2101. ↑

C8585. Hu Min Qiang. Follow-up control system of ultrasonic motor based on DSP. / Hu Min Qiang, Gan Yun Hua, Jin Long, Wang Xin Jian, Xu Zhi Ke, Gu Ju Ping. // 2007. ICEMS. International Conference on Electrical Machines and Systems. - Seoul, 8-11 Oct. 2007. - P. 1596-1599. ↑

C8586. Sang-hoon Yang. Automobile Advance Alarm System Based on Monocular Vision Processing. / Sang-hoon Yang, Yong-eun Kim, In-gul Jang, Jin-gyun Chung. // 2007. ISITC 2007. International Symposium on Information Technology Convergence. - Joenju, 23-24 Nov. 2007. - P. 193-197. ↑

C8587. Yun-Woong Choi. Heuristic Road Extraction. / Yun-Woong Choi, Young Woon Jang, Hyo Jong Lee, Gi-Sung Cho. // 2007. ISITC 2007. International Symposium on Information Technology Convergence. - Joenju, 23-24 Nov. 2007. - P. 338-342. ↑

C8588. Berg H. A high linearity mixed signal down converter IC for C-band radar receivers. / Berg H., Thiesies H., Hertz M., Norling F. // 2007. EuMIC 2007. European Microwave Integrated Circuit Conference. - Munich, 8-10 Oct. 2007. - P. 255-258. ↑

C8589. Chen Ting. Recognition Method of Radar Signal Based on Rough Set and Support Vector Machine. / Chen Ting, Luo Jingqing. // 2007. EMC 2007. International Symposium on Electromagnetic Compatibility. - Qingdao, 23-26 Oct. 2007. - P. 486-490. ↑

C8590. Hall J.S. Novel robotic spacecraft simulator with mini-control moment gyroscopes and rotating thrusters. / Hall J.S., Romano M. // 2007 IEEE/ASME international conference on Advanced intelligent mechatronics. - Zurich, 4-7 Sept. 2007. - P. 1-6. ↑

C8591. Allart B. Navigation paradigm of a prehensive robotics assistance. / Allart B., Marhic B., Delahoche L., Remy-Neris O. // 2007 IEEE/ASME international conference on Advanced intelligent mechatronics. - Zurich, 4-7 Sept. 2007. - P. 1-6. ↑

C8592. Milisavljevic N. Possibilistic multi-sensor fusion for humanitarian demining. / Milisavljevic N., Bloch I. // 2007. IGARSS 2007. IEEE International Geoscience and Remote Sensing Symposium. - Barcelona, 23-28 July 2007. - P. 14-17. ↑

C8593. Sato M. Hand held dual sensor ALIS and its evaluation test in Cambodia. / Sato M., Takahashi K., Fujiwara J. // 2007. IGARSS 2007. IEEE International Geoscience and Remote Sensing Symposium. - Barcelona, 23-28 July 2007. - P. 18-21. ↑

C8594. Boni G. High resolution COSMO/SkyMed SAR data analysis for civil protection from flooding events. / Boni G., Castelli F., Ferraris L., Pierdicca N., Serpico S., Siccardi F. // 2007. IGARSS 2007. IEEE International Geoscience and Remote Sensing Symposium. - Barcelona, 23-28 July 2007. - P. 6-9. ↑

C8595. Berardino P. The SBAS-DInSAR technique as a tool for the observation of active volcanic areas: Results and future perspectives. / Berardino P., Casu F., Fornaro G., Lanari R., Manunta M., Manzo M., Pepe A., Pepe S., Sansosti E., Serafino F., Solaro G., Tizzani P., Zeni G. // 2007. IGARSS 2007. IEEE International Geoscience and Remote Sensing Symposium. - Barcelona, 23-28 July 2007. - P. 10-13. ↑

C8596. Galletti M. Concept design of a near-space radar for tsunami detection. / Galletti M., Krieger G., Borner T., Marquart N., Schultz-Stellenfleth J. // 2007. IGARSS 2007. IEEE International Geoscience and Remote Sensing Symposium. - Barcelona, 23-28 July 2007. - P. 34-37. ↑

C8597. Weissman D.E. Measurements of the effect of rain-induced sea surface roughness on the satellite scatterometer radar cross section. / Weissman D.E., Bourassa M.A. // 2007. IGARSS 2007. IEEE International Geoscience and Remote Sensing Symposium. - Barcelona, 23-28 July 2007. - P. 46-49. ↑

- C8598.** Mazhar R. Use of an application-specific dictionary for matching pursuits discrimination of landmines and clutter. / Mazhar R., Wilson J.N., Gader P.D. // 2007. IGARSS 2007. IEEE International Geoscience and Remote Sensing Symposium. - Barcelona, 23-28 July 2007. - P. 26-29. ↑
- C8599.** Kovalenko V. Polarimetric feature fusion in GPR for landmine detection. / Kovalenko V., Yarovoy A., Ligthart L.P. // 2007. IGARSS 2007. IEEE International Geoscience and Remote Sensing Symposium. - Barcelona, 23-28 July 2007. - P. 30-33. ↑
- C8600.** Trivero P. High resolution COSMO-SkyMed SAR images for oil spills automatic detection. / Trivero P., Biamino W., Nirchio F. // 2007. IGARSS 2007. IEEE International Geoscience and Remote Sensing Symposium. - Barcelona, 23-28 July 2007. - P. 2-5. ↑
- C8601.** Zhi-Yu Zhang. Ridgelet transform with application in ground penetrating radar processing. / Zhi-Yu Zhang, Jiu-Long Zhang, Hai-Yan Yu, Yan-Jun Lu. // 2007. ICWAPR '07. International Conference on Wavelet Analysis and Pattern Recognition. - Beijing, 2-4 Nov. 2007. - Vol. 3. - P. 1054-1059. ↑
- C8602.** Ming Zhu. Classification of radar emitter signals based on the feature of time-frequency atoms. / Ming Zhu, Wei-Dong Jen, Yun-Wei Pu, Lai-Zhao Hu. // 2007. ICWAPR '07. International Conference on Wavelet Analysis and Pattern Recognition. - Beijing, 2-4 Nov. 2007. - Vol. 3. - P. 1232-1236. ↑
- C8603.** Shogo Tanaka. An electromagnetic coupling device for high speed running radar for non-destructive inspection. 2007 Annual Conference SICE. - Takamatsu, Japan, 17-20 Sept. 2007. - P. 2895-2900. ↑
- C8604.** Xiu-Qin Pan. A kind of trading off algorithm of object classification based on intelligent data fusion. / Xiu-Qin Pan, Yong Lu, Yue Zhao, Yong-Cun Cao, Yuan Shun. // 2007. ICWAPR '07. International Conference on Wavelet Analysis and Pattern Recognition. - Beijing, 2-4 Nov. 2007. - Vol. 3. - P. 990-993. ↑
- C8605.** Ming-Qiu Ren. Radar emitter signals classification using kernel principle component analysis and fuzzy support vector machines. / Ming-Qiu Ren, Yuan-Qing Zhu, Yan Mao, Jun Han. // 2007. ICWAPR '07. International Conference on Wavelet Analysis and Pattern Recognition. - Beijing, 2-4 Nov. 2007. - Vol. 3. - P. 1442-1446. ↑
- C8606.** Jun Han. A new method for recognising radar radiating-source. / Jun Han, Ming-Hao He, Yan Mao, Ming-Qiu Ren. // 2007. ICWAPR '07. International Conference on Wavelet Analysis and Pattern Recognition. - Beijing, 2-4 Nov. 2007. - Vol. 4. - P. 1665-1668. ↑
- C8607.** Tao-Wei Chen. Feature extraction of radar emitter signals based on symbolic time series analysis. / Tao-Wei Chen, Wei-Dong Jin. // 2007. ICWAPR '07. International Conference on Wavelet Analysis and Pattern Recognition. - Beijing, 2-4 Nov. 2007. - Vol. 3. - P. 1277-1282. ↑
- C8608.** Feng-Yun Zhu. Small-shaped space target recognition based on wavelet decomposition and support vector machine. / Feng-Yun Zhu, Shi-Yin Qin. // 2007. ICWAPR '07. International Conference on Wavelet Analysis and Pattern Recognition. - Beijing, 2-4 Nov. 2007. - Vol. 3. - P. 1397-1402. ↑
- C8609.** Brogioni M. Bistatic scattering from bare soils: Sensitivity to soil moisture and surface roughness. / Brogioni M., Macelloni G., Paloscia S., Pampaloni P., Pettinato S., Ticconi F. // 2007. IGARSS 2007. IEEE International Geoscience and Remote Sensing Symposium. - Barcelona, 23-28 July 2007. - P. 77-80. ↑
- C8610.** D'Aria D. Delay/Doppler altimeter data processing. / D'Aria D., Guccione P., Rosich B., Cullen R. // 2007. IGARSS 2007. IEEE International Geoscience and Remote Sensing Symposium. - Barcelona, 23-28 July 2007. - P. 137-140. ↑
- C8611.** Cantalloube H.M.J. Merging of the stereogrammetry and interferometry techniques as relative bandwidth grows. Illustration with VHF Carabas SAR images. / Cantalloube H.M.J., Colin-Koeniguer E., Frolind P.O., Ulander L.M.H. // 2007. IGARSS 2007. IEEE International Geoscience and Remote Sensing Symposium. - Barcelona, 23-28 July 2007. - P. 141-143. ↑
- C8612.** Santoro M. Improvement of interferometric SAR coherence estimates by slope-adaptive range common-band filtering. / Santoro M., Werner C., Wegmuller U., Cartus O. // 2007. IGARSS 2007. IEEE International Geoscience and Remote Sensing Symposium. - Barcelona, 23-28 July 2007. - P. 129-132. ↑
- C8613.** Martorella M. Polarimetric phase gradient autofocus. / Martorella M., Preiss M., Haywood B., Bates B.

// 2007. IGARSS 2007. IEEE International Geoscience and Remote Sensing Symposium. - Barcelona, 23-28 July 2007. - P. 133-136. ↑

C8614. Frey O. Tomographic processing of multi-baseline P-band SAR data for imaging of a forested area. / Frey O., Morsdorf F., Meier E. // 2007. IGARSS 2007. IEEE International Geoscience and Remote Sensing Symposium. - Barcelona, 23-28 July 2007. - P. 156-159. ↑

C8615. Meta A. Investigations on the TOPSAR acquisition mode with TerraSAR-X. / Meta A., Mittermayer J., Steinbrecher U., Prats P. // 2007. IGARSS 2007. IEEE International Geoscience and Remote Sensing Symposium. - Barcelona, 23-28 July 2007. - P. 152-155. ↑

C8616. Walterscheid I. Evaluation of the Bistatic Range migration processor. / Walterscheid I., Brenner A.R., Ender J.H.G., Loffeld O. // 2007. IGARSS 2007. IEEE International Geoscience and Remote Sensing Symposium. - Barcelona, 23-28 July 2007. - P. 144-147. ↑

C8617. Prats P. A SAR processing algorithm for TOPS imaging mode based on extended chirp scaling. / Prats P., Scheiber R., Mittermayer J., Meta A., Moreira A., Sanz-Marcos J. // 2007. IGARSS 2007. IEEE International Geoscience and Remote Sensing Symposium. - Barcelona, 23-28 July 2007. - P. 148-151. ↑

C8618. Nashashibi A.Y. Bistatic SAR imaging: A novel approach using a stationary receiver. / Nashashibi A.Y., Ulaby F.T. // 2007. IGARSS 2007. IEEE International Geoscience and Remote Sensing Symposium. - Barcelona, 23-28 July 2007. - P. 125-128. ↑

C8619. Lopez-Dekker P. Phase and temporal synchronization in bistatic SAR systems using sources of opportunity. / Lopez-Dekker P., Mallorqui J.J., Serra-Morales P., Sanz-Marcos J. // 2007. IGARSS 2007. IEEE International Geoscience and Remote Sensing Symposium. - Barcelona, 23-28 July 2007. - P. 97-100. ↑

C8620. Ender J.H.G. Space-based moving target positioning using radar with a switched aperture antenna. / Ender J.H.G., Gierull C.H., Cerutti-Maori D. // 2007. IGARSS 2007. IEEE International Geoscience and Remote Sensing Symposium. - Barcelona, 23-28 July 2007. - P. 101-106. ↑

C8621. Wenjian Ni. Improvement of 3D radar backscatter model by matrix-doubling methods. / Wenjian Ni, Zhifeng Guo, Guoqing Sun, Fang Wang. // 2007. IGARSS 2007. IEEE International Geoscience and Remote Sensing Symposium. - Barcelona, 23-28 July 2007. - P. 85-88. ↑

C8622. Pietra G.D. Feasibility of spaceborne bistatic radar missions for land applications. / Pietra G.D., Capobianco F., Falzini S., Pierdicca N., De Titta L. // 2007. IGARSS 2007. IEEE International Geoscience and Remote Sensing Symposium. - Barcelona, 23-28 July 2007. - P. 93-96. ↑

C8623. Weiss M. Position and orientation estimation of two airborne platforms towards each other. / Weiss M., Marino G. // 2007. IGARSS 2007. IEEE International Geoscience and Remote Sensing Symposium. - Barcelona, 23-28 July 2007. - P. 115-118. ↑

C8624. Fois F. Performance results of the SHARAD instrument. / Fois F., Croci R., Seu R., Picardi G., Flamini E. // 2007. IGARSS 2007. IEEE International Geoscience and Remote Sensing Symposium. - Barcelona, 23-28 July 2007. - P. 119-124. ↑

C8625. Lopez-Dekker P. Bistatic SAR interferometry using ENVISAT and a ground based receiver: Experimental results. / Lopez-Dekker P., Merlano J.C., Duque S., Sanz-Marcos J., Aguasca A., Mallorqui J.J. // 2007. IGARSS 2007. IEEE International Geoscience and Remote Sensing Symposium. - Barcelona, 23-28 July 2007. - P. 107-110. ↑

C8626. Jung-Hyo Kim. Experimental investigation of Digital Beamforming SAR Performance using a ground-based demonstrator. / Jung-Hyo Kim, Ossowska A., Wiesbeck W. // 2007. IGARSS 2007. IEEE International Geoscience and Remote Sensing Symposium. - Barcelona, 23-28 July 2007. - P. 111-114. ↑

C8627. Tang Shiyue. The detection of multi moving targets for the airborne SAR. / Tang Shiyue, Gao Xincheng. // 2007. APSAR 2007. 1st Asian and Pacific Conference on Synthetic Aperture Radar. - Huangshan, 5-9 Nov. 2007. - P. 691-694. ↑

C8628. Zhang Yanfei. Adaptive CFAR detection of range-spread targets based on SAR raw data. / Zhang Yanfei, Guan Jian, Li Xiyou, Huang Yong. // 2007. APSAR 2007. 1st Asian and Pacific Conference on

Synthetic Aperture Radar. - Huangshan, 5-9 Nov. 2007. - P. 699-703. ↑

C8629. Wu Chao. Research on real time range profile of marine targets and its characteristics. / Wu Chao, Gong Cuiling, Song Wanjie, Wu Shunjun. // 2007. APSAR 2007. 1st Asian and Pacific Conference on Synthetic Aperture Radar. - Huangshan, 5-9 Nov. 2007. - P. 683-686. ↑

C8630. Yunhua Zhang. ISAR imaging with stepped-frequency chirp signal by de-chirping processing. / Yunhua Zhang, Jie Wu. // 2007. APSAR 2007. 1st Asian and Pacific Conference on Synthetic Aperture Radar. - Huangshan, 5-9 Nov. 2007. - P. 687-690. ↑

C8631. Ling Wang. Improvements of ROPE in ISAR Motion compensation. / Ling Wang, Daiyin Zhu, Zhaoda Zhu. // 2007. APSAR 2007. 1st Asian and Pacific Conference on Synthetic Aperture Radar. - Huangshan, 5-9 Nov. 2007. - P. 735-738. ↑

C8632. Tang Yu. Two dimension chirp-Z transform for polar format imaging algorithm. / Tang Yu, Xing Mengdao. // 2007. APSAR 2007. 1st Asian and Pacific Conference on Synthetic Aperture Radar. - Huangshan, 5-9 Nov. 2007. - P. 743-746. ↑

C8633. Tao Li. Research on the technology of monopulse SAR ground moving target indication. / Tao Li, Tao Zhang. // 2007. APSAR 2007. 1st Asian and Pacific Conference on Synthetic Aperture Radar. - Huangshan, 5-9 Nov. 2007. - P. 704-708. ↑

C8634. Liu Hongya. ISAR Imaging with LFM waveforms. 2007. APSAR 2007. 1st Asian and Pacific Conference on Synthetic Aperture Radar. - Huangshan, 5-9 Nov. 2007. - P. 729-734. ↑

C8635. Xianghui Kong. Design and realization of intermediate down-sampling for SAR based on FPGA. / Xianghui Kong, Tao Zhang, Guanjie Zhang. // 2007. APSAR 2007. 1st Asian and Pacific Conference on Synthetic Aperture Radar. - Huangshan, 5-9 Nov. 2007. - P. 680-682. ↑

C8636. Cai-sheng Zhang. An experimental independent bistatic radar system for wideband application. / Cai-sheng Zhang, Jia-hui Ding. // 2007. APSAR 2007. 1st Asian and Pacific Conference on Synthetic Aperture Radar. - Huangshan, 5-9 Nov. 2007. - P. 630-633. ↑

C8637. Hu Wuming. Airborne SAR passive radar imaging algorithm based on external illuminator. / Hu Wuming, Wang Jun. // 2007. APSAR 2007. 1st Asian and Pacific Conference on Synthetic Aperture Radar. - Huangshan, 5-9 Nov. 2007. - P. 642-645. ↑

C8638. Xiong Tao. Two methods for enhancing the coherence in PolInSAR data processing. / Xiong Tao, Yang Jian, Zhang Weijie. // 2007. APSAR 2007. 1st Asian and Pacific Conference on Synthetic Aperture Radar. - Huangshan, 5-9 Nov. 2007. - P. 584-587. ↑

C8639. Shu Yong jiang. The design of waveform-generation applied to wide-band high resolution imaging radar. / Shu Yong jiang, Zhang Xu jin, Zhang Wei hua. // 2007. APSAR 2007. 1st Asian and Pacific Conference on Synthetic Aperture Radar. - Huangshan, 5-9 Nov. 2007. - P. 588-591. ↑

C8640. Sheng-Lei. Design and implementation of SAR raw data BAQ based on FPGA. / Sheng-Lei, Zheng-TaoYe, Zhang-Xu Jin. // 2007. APSAR 2007. 1st Asian and Pacific Conference on Synthetic Aperture Radar. - Huangshan, 5-9 Nov. 2007. - P. 664-666. ↑

C8641. Liu Jing. Airborne C-SAR (Synthetic Aperture Radar) real-time imaging system. / Liu Jing, Wu Jingwei, Wang Zhi-rui, Hu Qing-rong. // 2007. APSAR 2007. 1st Asian and Pacific Conference on Synthetic Aperture Radar. - Huangshan, 5-9 Nov. 2007. - P. 675-679. ↑

C8642. Chen Tao. Design of real-time processor for groundbased ISAR imaging. / Chen Tao, Sun Hai-ping, Wang Ru-qi, Kang Meng, Lei Wan-ming. // 2007. APSAR 2007. 1st Asian and Pacific Conference on Synthetic Aperture Radar. - Huangshan, 5-9 Nov. 2007. - P. 657-660. ↑

C8643. Tang Yue-sheng. Multi-DSPs SAR real-time signal processing system based on cPCI bus. / Tang Yue-sheng, Zhang Chang-yao. // 2007. APSAR 2007. 1st Asian and Pacific Conference on Synthetic Aperture Radar. - Huangshan, 5-9 Nov. 2007. - P. 661-663. ↑

C8644. Liu Hui. A simple implementation of multi-baseline INSAR. / Liu Hui, Zhou Yinqing, Xu Huaping, Li

Chunsheng. // 2007. APSAR 2007. 1st Asian and Pacific Conference on Synthetic Aperture Radar. - Huangshan, 5-9 Nov. 2007. - P. 747-750. ↑

C8645. Wen-Biao Jin. Velocity determination of single sound source based on Doppler effect. / Wen-Biao Jin, You Jun. // 2007. ICWAPR '07. International Conference on Wavelet Analysis and Pattern Recognition. - Beijing, 2-4 Nov. 2007. - Vol. 2. - P. 956-961. ↑

C8646. Nakasako N. On distance measurement using band-limited noise. / Nakasako N., Uebo T., Ohmata N., Mori A. // 2007 Annual Conference SICE. - Takamatsu, 17-20 Sept. 2007. - P. 151-156. ↑

C8647. Yi-Shu Zhai. An improved fog-degraded image enhancement algorithm. / Yi-Shu Zhai, Xiao-Ming Liu. // 2007. ICWAPR '07. International Conference on Wavelet Analysis and Pattern Recognition. - Beijing, 2-4 Nov. 2007. - Vol. 2. - P. 522-526. ↑

C8648. Hong-Qiang Wang. Maneuvering target tracking using the optimal stochastic jump filtering algorithm. / Hong-Qiang Wang, Yang-Wang Fang, You-Liwu, Xiao-Bin Zhou, Xian-Wei Zeng. // 2007. ICWAPR '07. International Conference on Wavelet Analysis and Pattern Recognition. - Beijing, 2-4 Nov. 2007. - Vol. 2. - P. 868-873. ↑

C8649. Zyada Z. 3D template based automatic landmine detection from GPR data. / Zyada Z., Fukuda T. // 2007 Annual Conference SICE. - Takamatsu, 17-20 Sept. 2007. - P. 1552-1557. ↑

C8650. Won-Yong Choi. Modeling of local search for track updates in phased array radar tracking. / Won-Yong Choi, Sun-Mog Hong, Seung-Min Song. // 2007 Annual Conference SICE. - Takamatsu, 17-20 Sept. 2007. - P. 2540-2545. ↑

C8651. Haruyama K. Development of the detection and reporting device for patients' getting out of bed using ultrasonic radar and power line communication. / Haruyama K., Tanaka K., Wakasa Y., Akashi T., Yamada Y. // 2007 Annual Conference SICE. - Takamatsu, 17-20 Sept. 2007. - P. 484-487. ↑

C8652. Yamaguchi K. Estimation of the 3D structure of road scenes from monocular images and range data. / Yamaguchi K., Kato T., Ninomiya Y. // 2007 Annual Conference SICE. - Takamatsu, 17-20 Sept. 2007. - P. 1465-1470. ↑

C8653. Wen-Chao Du. Using FRFT to estimate target radial acceleration. / Wen-Chao Du, Xue-Qiang Gao, Guo-Hong Wang. // 2007. ICWAPR '07. International Conference on Wavelet Analysis and Pattern Recognition. - Beijing, 2-4 Nov. 2007. - Vol. 1. - P. 442-447. ↑

C8654. Liu Ling. Experimental reaserch of unsupervised Cameron/ML Classification method for fully polarimetric SAR Data. / Liu Ling, Xing MengDao, Bao Zheng. // 2007. APSAR 2007. 1st Asian and Pacific Conference on Synthetic Aperture Radar. - Huangshan, 5-9 Nov. 2007. - P. 797-800. ↑

C8655. Placentino F. Measurements of length and velocity of vehicles with a low cost sensor radar Doppler operating at 24GHz. / Placentino F., Alimenti F., Battistini A., Bernardini W., Mezzanotte P., Palazzari V., Leone S., Scarponi A., Porzi N., Comez M., Roselli L. // 2007. IWASI 2007. 2nd International Workshop on Advances in Sensors and Interface. - Bari, 26-27 June 2007. - P. 1-5. ↑

C8656. Haijian Zhang. Automatic extraction of power transmission tower series from PolSAR imagery based on MRF model. / Haijian Zhang, Wen Yang, Tongyuan Zhou, Hong Sun. // 2007. APSAR 2007. 1st Asian and Pacific Conference on Synthetic Aperture Radar. - Huangshan, 5-9 Nov. 2007. - P. 788-792. ↑

C8657. Na Li. Pixel-level image fusion based on multi-to-multi turbo iterative. / Na Li, Chu He, Lei Yu, Hong Sun. // 2007. APSAR 2007. 1st Asian and Pacific Conference on Synthetic Aperture Radar. - Huangshan, 5-9 Nov. 2007. - P. 793-796. ↑

C8658. Lan-Ying Cao. An ant colony optimization approach for SAR image segmentation. / Lan-Ying Cao, Liang-Zheng Xia. // 2007. ICWAPR '07. International Conference on Wavelet Analysis and Pattern Recognition. - Beijing, 2-4 Nov. 2007. - Vol. 1. - P. 296-300. ↑

C8659. Lei Chen. Contour extraction based on improved GVF snake model in ASAR images. / Lei Chen, Xiao-Lin Zhang, Zhe Wang, Lin-Tang Fang. // 2007. ICWAPR '07. International Conference on Wavelet Analysis and Pattern Recognition. - Beijing, 2-4 Nov. 2007. - Vol. 1. - P. 301-304. ↑

- C8660.** Potgieter P.F. Inferring radar mode changes from elementary pulse features using fuzzy ARTMAP classification. / Potgieter P.F., Olivier J.C. // 2007. ICWAPR '07. International Conference on Wavelet Analysis and Pattern Recognition. - Beijing, 2-4 Nov. 2007. - Vol. 1. - P. 88-93. ↑
- C8661.** Hong-Qiao Wang. Edge-enhanced speckle suppression using curvelet transform with an optimal soft thresholding. / Hong-Qiao Wang, Fu-Chun Sun, Yan-Ning Cai, Zong-Tao Zhao. // 2007. ICWAPR '07. International Conference on Wavelet Analysis and Pattern Recognition. - Beijing, 2-4 Nov. 2007. - Vol. 1. - P. 204-209. ↑
- C8662.** Wee Chang Khor. An Experimental and Theoretical Investigation into Capabilities of a UWB Microwave Imaging Radar System to Detect Breast Cancer. / Wee Chang Khor, Hua Wang, Bialkowski M.E., Abbosh A., Seman N. // 2007. The International Conference on "EUROCONComputer as a Tool". - Warsaw, 9-12 Sept. 2007. - P. 771-776. ↑
- C8663.** Marcu M. Experimental Test Cases for Wireless Positioning Systems. / Marcu M., Fuicu S., Girban A., Popa M. // 2007. The International Conference on "EUROCONComputer as a Tool". - Warsaw, 9-12 Sept. 2007. - P. 530-537. ↑
- C8664.** Istemi Ekin Akkus. Multi-objective optimization for peer-to-peer multipoint video conferencing using layered video. / Istemi Ekin Akkus, Oznur Ozkasap, Civanlar M. Reha. // Packet Video 2007. - Lausanne, Switzerland, 12-13 Nov. 2007. - P. 182-190. ↑
- C8665.** Karuri K. Increasing data-bandwidth to instruction-set extensions through register clustering. / Karuri K., Chattopadhyay A., Hohenauer M. // 2007. ICCAD 2007. IEEE/ACM International Conference on Computer-Aided Design. - San Jose, CA, 4-8 Nov. 2007. - P. 166-171. ↑
- C8666.** Perez-Cruz F. Accurate posterior probability estimates for channel equalization using gaussian processes for classification. / Perez-Cruz F., Martinez-Olmos P., Murillo-Fuentes J.J. // 2007. SPAWC 2007. IEEE 8th Workshop on Signal Processing Advances in Wireless Communications. - Helsinki, 17-20 June 2007. - P. 1-5. ↑
- C8667.** Castaneda N. A new bearings-only tracking algorithm for ground moving targets constrained to roads. / Castaneda N., Charbit M., Moulines E. // 2007. SPAWC 2007. IEEE 8th Workshop on Signal Processing Advances in Wireless Communications. - Helsinki, 17-20 June 2007. - P. 1-5. ↑
- C8668.** Milewski A. Amplitude Weighting of Linear Frequency Modulated Chirp Signals. / Milewski A., Sedek E., Gawor S. // 2007. The International Conference on "EUROCONComputer as a Tool". - Warsaw, 9-12 Sept. 2007. - P. 383-386. ↑
- C8669.** Gaoyi Zhang. Estimation of 2D-DOAs and angular spreads for coherently distributed sources using cumulants. / Gaoyi Zhang, Tang Bin. // 2007. SPAWC 2007. IEEE 8th Workshop on Signal Processing Advances in Wireless Communications. - Helsinki, 17-20 June 2007. - P. 1-5. ↑
- C8670.** Yilmazer N. Performance analysis of direct data domain approach and Esprit method for DOA Estimation. / Yilmazer N., Burintramart S., Sarkar T.K. // 2007 IEEE Antennas and Propagation Society International Symposium. - Honolulu, HI, 9-15 June 2007. - P. 5295-5298. ↑
- C8671.** Dan Lu. A space-frequency anti-jamming algorithm for GPS. / Dan Lu, Renbiao Wu, Zhigang Su, Wei Huang. // 2007 IEEE Antennas and Propagation Society International Symposium. - Honolulu, HI, 9-15 June 2007. - P. 4216-4219. ↑
- C8672.** Rashid L.S. RCS and radar propagation near offshore wind farms. / Rashid L.S., Brown A.K. // 2007 IEEE Antennas and Propagation Society International Symposium. - Honolulu, HI, 9-15 June 2007. - P. 4605-4608. ↑
- C8673.** Ortega R. FDTD modeling of scattering from distant buried objects. / Ortega R., Chi-Chih Chen, Lee R. // 2007 IEEE Antennas and Propagation Society International Symposium. - Honolulu, HI, 9-15 June 2007. - P. 3309-3312. ↑
- C8674.** Petrochilos N. Separation of multiple secondary surveillance radar sources in a real environment for the near-far case. / Petrochilos N., Piracci E.G., Galati G. // 2007 IEEE Antennas and Propagation Society International Symposium. - Honolulu, HI, 9-15 June 2007. - P. 3988-3991. ↑

- C8675.** Inman M.J. GPU based FDTD solver with CPML boundaries. / Inman M.J., Elsherbeni A.Z., Maloney J.G., Baker B.N. // 2007 IEEE Antennas and Propagation Society International Symposium. - Honolulu, HI, 9-15 June 2007. - P. 5255-5258. ↑
- C8676.** Escot D. Application of particle swarm optimization (PSO) to single-snapshot direction of arrival (DOA) estimation. / Escot D., Poyatos D., Gonzalez I., de Adana F.S., Catedra M.F. // 2007 IEEE Antennas and Propagation Society International Symposium. - Honolulu, HI, 9-15 June 2007. - P. 5287-5290. ↑
- C8677.** Giunta G. Tolerance manufacturing effects in crossfeed monopulse radars in presence of rough sea scattering. / Giunta G., Lucci L., Pelosi G., Riminesi C., Selleri S., Serrano F. // 2007 IEEE Antennas and Propagation Society International Symposium. - Honolulu, HI, 9-15 June 2007. - P. 4817-4820. ↑
- C8678.** Ogden G. Multipath return for radar targets over a rough surface. / Ogden G., Matzner S., Zurk L.M., Blejer D. // 2007 IEEE Antennas and Propagation Society International Symposium. - Honolulu, HI, 9-15 June 2007. - P. 4825-4828. ↑
- C8679.** Khairnar D.G. Nonlinear Target Identification and Tracking Using UKF. / Khairnar D.G., Nandakumar S., Merchant S.N., Desai U.B. // 2007. GRC 2007. IEEE International Conference on Granular Computing. - Fremont, CA, 2-4 Nov. 2007. - P. 761. ↑
- C8680.** de Wit J.J.M. Concept for measuring and compensating array deformation. / de Wit J.J.M., van Rossum W.L., Otten M.P.G., Koekenberg A.G.P. // 2007. EuRAD 2007. European Radar Conference. - Munich, 10-12 Oct. 2007. - P. 55-58. ↑
- C8681.** Gorski T. Application of STAP technique to FMCW systems. / Gorski T., Kawalec A., Czarnecki W., Le Caillec J.-M., Lecornu L. // 2007. EuRAD 2007. European Radar Conference. - Munich, 10-12 Oct. 2007. - P. 63-66. ↑
- C8682.** Lievers C.M. Digital beamforming and multidimensional waveform encoding for spaceborne radar remote sensing. / Lievers C.M., van Rossum W.L., Maas A.P.M., Huizing A.G. // 2007. EuRAD 2007. European Radar Conference. - Munich, 10-12 Oct. 2007. - P. 43-46. ↑
- C8683.** Jung-Hyo Kim. Investigation of MIMO SAR for interferometry. / Jung-Hyo Kim, Ossowska A., Wiesbeck W. // 2007. EuRAD 2007. European Radar Conference. - Munich, 10-12 Oct. 2007. - P. 51-54. ↑
- C8684.** Piracci E.G. Single-antenna projection algorithm to discriminate super-imposed Secondary Surveillance Radar Mode S signals. / Piracci E.G., Petrochilos N., Galati G. // 2007. EuRAD 2007. European Radar Conference. - Munich, 10-12 Oct. 2007. - P. 75-78. ↑
- C8685.** Cristallini D. Adaptive antenna configuration for unambiguous signal reconstruction in dual-channel SAR systems. / Cristallini D., Marini J., Lombardo P. // 2007. EuRAD 2007. European Radar Conference. - Munich, 10-12 Oct. 2007. - P. 107-110. ↑
- C8686.** Ries P. Knowledge-aided array calibration for registration-based range-dependence compensation in airborne STAP radar with Conformal Antenna Arrays. / Ries P., Lesturgie M., Lapierre F.D., Verly J.G. // 2007. EuRAD 2007. European Radar Conference. - Munich, 10-12 Oct. 2007. - P. 67-70. ↑
- C8687.** Di Wu. Real-Time Space-Time Adaptive Processing on the STI CELL Multiprocessor. / Di Wu, Yi-Hsien Li, Eilert J., Dake Liu. // 2007. EuRAD 2007. European Radar Conference. - Munich, 10-12 Oct. 2007. - P. 71-74. ↑
- C8688.** Maas A.P.M. Set of X-band distributed absorptive limiter GaAs MMICs. / Maas A.P.M., Janssen J.P.B., van Vliet F.E. // 2007. EuRAD 2007. European Radar Conference. - Munich, 10-12 Oct. 2007. - P. 17-20. ↑
- C8689.** Hui Zhang. 24GHz Software-Defined Radar System for Automotive Applications. / Hui Zhang, Lin Li, Ke Wu. // 2007 European Conference on Wireless Technologies. - Munich, 8-10 Oct. 2007. - P. 138-141. ↑
- C8690.** Sinitsyn R. Signal Detection Algorithms Based on Non-Parametric Estimates of Density Function. / Sinitsyn R., Yanovsky F. // 2007 European Conference on Wireless Technologies. - Munich, 8-10 Oct. 2007. - P. 201-204. ↑
- C8691.** Nikookar H. Complex-Weighted OFDM Transmission with Low PAPR. / Nikookar H., Soehartono D. //

2007 European Conference on Wireless Technologies. - Munich, 8-10 Oct. 2007. - P. 8-11. ↑

C8692. Gierlich R. Performance Analysis of FMCW Synchronization Techniques for Indoor Radiolocation. / Gierlich R., Huttner J., Dabek A., Huemer M. // 2007 European Conference on Wireless Technologies. - Munich, 8-10 Oct. 2007. - P. 24-27. ↑

C8693. Perotoni M.B. A study on RCS of missile models using the method of moments. / Perotoni M.B., Barbin S.E. // 2007. IMOC 2007. SBMO/IEEE MTT-S International Microwave and Optoelectronics Conference. - Brazil, Oct. 29 2007-Nov. 1 2007. - P. 492-495. ↑

C8694. Ossowska A. Modeling of nonidealities in receiver front-end for a simulation of multistatic SAR system. / Ossowska A., Jung Hyo Kim, Wiesbeck W. // 2007. EuRAD 2007. European Radar Conference. - Munich, 10-12 Oct. 2007. - P. 13-16. ↑

C8695. Berg H. A High Linearity Mixed Signal Down Converter IC for C-band Radar Receivers. / Berg H., Thiesies H., Hertz M., Norling F. // 2007 European Conference on Wireless Technologies. - Munich, 8-10 Oct. 2007. - P. 335-338. ↑

C8696. El Aabbaoui H. Design of a [DC-20 GHz] Buffered Track and Hold Circuit in InP DHBT Technology. / El Aabbaoui H., Gorisse B., Rolland N., Benlarbi-Delai A., Fel N., Allouche V., Leclerc P., Riondet B., Rolland P.-A. // 2007 European Conference on Wireless Technologies. - Munich, 8-10 Oct. 2007. - P. 339-342. ↑

C8697. Svoboda P. Modeling E-Mail Traffic for 3G Mobile Networks. / Svoboda P., Karner W., Rupp M. // 2007. PIMRC 2007. IEEE 18th International Symposium on Personal, Indoor and Mobile Radio Communications. - Athens, 3-7 Sept. 2007. - P. 1-5. ↑

C8698. Loukatos D. Tools and Practices for Measurement-based Network Performance Evaluation. / Loukatos D., Sarakis L., Kontovasilis K., Skianis C., Kormentzas G. // 2007. PIMRC 2007. IEEE 18th International Symposium on Personal, Indoor and Mobile Radio Communications. - Athens, 3-7 Sept. 2007. - P. 1-5. ↑

C8699. Al-Hezmi A. Enabling IMS with Multicast and Broadcast Capabilities. / Al-Hezmi A., Knappmeyer M., Ricks B., Pinto F.C., Tonjes R. // 2007. PIMRC 2007. IEEE 18th International Symposium on Personal, Indoor and Mobile Radio Communications. - Athens, 3-7 Sept. 2007. - P. 1-5. ↑

C8700. Sandoval-Arechiga R. Teletraffic Analysis for the Performance Evaluation of De-Allocation/Re-Allocation Strategies in GSM/GPRS Cellular Networks. / Sandoval-Arechiga R., Cruz-Perez F.A., Ortigoza-Guerrero L. // 2007. PIMRC 2007. IEEE 18th International Symposium on Personal, Indoor and Mobile Radio Communications. - Athens, 3-7 Sept. 2007. - P. 1-5. ↑

C8701. Markaki O. Enhancing Quality of Experience in Next Generation Networks Through Network Selection Mechanisms. / Markaki O., Charilas D., Nikitopoulos D. // 2007. PIMRC 2007. IEEE 18th International Symposium on Personal, Indoor and Mobile Radio Communications. - Athens, 3-7 Sept. 2007. - P. 1-5. ↑

C8702. Qasem H. Enhanced Local Positioning Radar with Predictive Filters. / Qasem H., Reindl L. // 2007. PIMRC 2007. IEEE 18th International Symposium on Personal, Indoor and Mobile Radio Communications. - Athens, 3-7 Sept. 2007. - P. 1-5. ↑

C8703. Kyriazakos S. Secure Interworking in Multi-Operator, Multi-Technology Wireless Communication Environment: Issues & Challenges. 2007. PIMRC 2007. IEEE 18th International Symposium on Personal, Indoor and Mobile Radio Communications. - Athens, 3-7 Sept. 2007. - P. 1-4. ↑

C8704. Ozen M. Pilot Remote Experiment in the ERRL: Measurement of Scattering Parameters. / Ozen M., Aydin E.U., Kara A. // 2007. PIMRC 2007. IEEE 18th International Symposium on Personal, Indoor and Mobile Radio Communications. - Athens, 3-7 Sept. 2007. - P. 1-4. ↑

C8705. Prabhudesai R.G. GPRS based Real-Time Reporting and Internet Accessible Sea Level Gauge for Monitoring Storm Surge and Tsunami. / Prabhudesai R.G., Joseph A., Agarvadekar Y., Dabholkar N., Mehra P., Gouveia A., Tengali S., Vijaykumar, Parab A. // OCEANS 2006-Asia Pacific. - Singapore, 16-19 May 2007. - P. 1-4. ↑

C8706. Hunter A. Fast Fourier-domain modelling for a SAS simulator with application to time-variant targets, aspect-dependent occlusions, and Doppler effects. / Hunter A., Hayes M., Gough P. // OCEANS 2006-Asia

Pacific. - Singapore, 16-19 May 2007. - P. 1-8. ↑

C8707. Passerieux J.-M. Ambiguity Function and Cramer-Rao Lower Bounds for Passive Synthetic Aperture Sonar (SAS). OCEANS 2006-Asia Pacific. - Singapore, 16-19 May 2007. - P. 1-6. ↑

C8708. Heron M.L. VHF PortMap Sea Surface Radar Observations in a Shipping Channel. / Heron M.L., Prytz A., Page G., Mazzoldi A., Cosoli S., Gacic M., Kovacevic V. // OCEANS 2006-Asia Pacific. - Singapore, 16-19 May 2007. - P. 1-4. ↑

C8709. Barclay P. Bathymetric results from a multi-frequency InSAS sea-trial. / Barclay P., Hayes M., Gough P. // OCEANS 2006-Asia Pacific. - Singapore, 16-19 May 2007. - P. 1-6. ↑

C8710. Tong Poh Bee. Extended Towed Array Measurement: Beam-domain phase estimation and coherent summation. / Tong Poh Bee, Lim Hock Siong, Chia Chin Swee, Passerieux J.-M. // OCEANS 2006-Asia Pacific. - Singapore, 16-19 May 2007. - P. 1-6. ↑

C8711. Bouxsein P. A SONAR Simulation used to Develop an Obstacle Avoidance System. / Bouxsein P., An E., Schock S., Beaujean P.-P. // OCEANS 2006-Asia Pacific. - Singapore, 16-19 May 2007. - P. 1-7. ↑

C8712. Ura T. Dive into Myojin-sho Underwater Caldera. / Ura T., Nagahashi K., Asada A., Okamura K., Tamaki K., Sakamaki T., Iizasa K. // OCEANS 2006-Asia Pacific. - Singapore, 16-19 May 2007. - P. 1-5. ↑

C8713. Sharif M.R. Efficient Active Sonar Parameter Estimation Using Linear FM Signals via Hermite Decompositions. / Sharif M.R., Abeysekera S.S. // OCEANS 2006-Asia Pacific. - Singapore, 16-19 May 2007. - P. 1-5. ↑

C8714. Neekzad B. Comparison of Ray Tracing Simulations and Millimeter Wave Channel Sounding Measurements. / Neekzad B., Sayrafian-Pour K., Perez J., Baras J.S. // 2007. PIMRC 2007. IEEE 18th International Symposium on Personal, Indoor and Mobile Radio Communications. - Athens, 3-7 Sept. 2007. - P. 1-5. ↑

C8715. Sakamoto T. Code-division multiple transmission for high-speed UWB radar imaging with array antennas. / Sakamoto T., Sato T. // 2007 IEEE Antennas and Propagation Society International Symposium. - Honolulu, HI, 9-15 June 2007. - P. 429-432. ↑

C8716. Vazquez-Alejos A. Design and implementation of a golay-based GPR system for improved subsurface imaging. / Vazquez-Alejos A., Dawood M., Garcia-Sanchez M., Habbeeb-ur-Rehman M., Jedlicka R.P., Cuinas I. // 2007 IEEE Antennas and Propagation Society International Symposium. - Honolulu, HI, 9-15 June 2007. - P. 597-600. ↑

C8717. Dung Phuong Nguyen. A versatile through-the-wall doppler radar using BSS algorithms. / Dung Phuong Nguyen, Petrochilos N., Host-Madsen A., Lubecke V., Boric-Lubecke O. // 2007 IEEE Antennas and Propagation Society International Symposium. - Honolulu, HI, 9-15 June 2007. - P. 273-276. ↑

C8718. Rui Xu. A power-efficient CMOS UWB signal-generation module. / Rui Xu, Yalin Jin, Cam Nguyen. // 2007 IEEE Antennas and Propagation Society International Symposium. - Honolulu, HI, 9-15 June 2007. - P. 321-324. ↑

C8719. Yun Z. Detection of buried metal structures using ground penetration radar techniques: A numerical study. / Yun Z., Iskander M.F. // 2007 IEEE Antennas and Propagation Society International Symposium. - Honolulu, HI, 9-15 June 2007. - P. 1813-1816. ↑

C8720. Phu P. Multipath height finding in the presence of interference. / Phu P., Aumann H., Piou J.E. // 2007 IEEE Antennas and Propagation Society International Symposium. - Honolulu, HI, 9-15 June 2007. - P. 2025-2028. ↑

C8721. Matzner S.A. Frequency domain feature extraction from synthetic aperture radar data. / Matzner S.A., Zurk L.M. // 2007 IEEE Antennas and Propagation Society International Symposium. - Honolulu, HI, 9-15 June 2007. - P. 1489-1492. ↑

C8722. Hoi-Shun Lui. Performance analysis on subsurface target depth detection using the E-Pulse Technique. / Hoi-Shun Lui, Shuley N.V. // 2007 IEEE Antennas and Propagation Society International

Symposium. - Honolulu, HI, 9-15 June 2007. - P. 1781-1784. ↑

C8723. Yifan Chen. Human respiration rate estimation using body-worn ultra-wideband radar. / Yifan Chen, Gunawan E., Kay Soon Low, Cheong Boon, Cheong Boon Soh, Lin Lin Thi. // 2007 IEEE Antennas and Propagation Society International Symposium. - Honolulu, HI, 9-15 June 2007. - P. 265-268. ↑

C8724. Alexiou A. Evaluation of the Multicast Mode of MBMS. / Alexiou A., Bouras C., Kokkinos V., Rekkas E. // 2007. PIMRC 2007. IEEE 18th International Symposium on Personal, Indoor and Mobile Radio Communications. - Athens, 3-7 Sept. 2007. - P. 1-5. ↑

C8725. Makela J. Towards Seamless Mobility Support with Cross-Layer Triggering. 2007. PIMRC 2007. IEEE 18th International Symposium on Personal, Indoor and Mobile Radio Communications. - Athens, 3-7 Sept. 2007. - P. 1-5. ↑

C8726. Gazis V. Discovering Feasible Protocol Stack Combinations in Beyond 3G Systems: Information Model, Search Algorithms and Performance. / Gazis V., Alonistioti N., Merakos L. // 2007. PIMRC 2007. IEEE 18th International Symposium on Personal, Indoor and Mobile Radio Communications. - Athens, 3-7 Sept. 2007. - P. 1-6. ↑

C8727. Macagnano D. Tracking Multiple Dynamic Targets with Multidimensional Scaling. / Macagnano D., Thadeu G. // 2007. PIMRC 2007. IEEE 18th International Symposium on Personal, Indoor and Mobile Radio Communications. - Athens, 3-7 Sept. 2007. - P. 1-5. ↑

C8728. Chen W.C. Utilizing the energy of each of the extracted poles to identify the dominant complex natural resonances of the radar target. / Chen W.C., Shuley N. // 2007 IEEE Antennas and Propagation Society International Symposium. - Honolulu, HI, 9-15 June 2007. - P. 69-72. ↑

C8729. Speciale R.A. Design of more affordable and reliable electronically-steered phased arrays. 2007 IEEE Antennas and Propagation Society International Symposium. - Honolulu, HI, 9-15 June 2007. - P. 157-160. ↑

C8730. Almorox-Gonzalez P. Portable High Resolution LFM-CW Radar Sensor in Millimeter-Wave Band. / Almorox-Gonzalez P., Gonzalez-Partida J.-T., Burgos-Garcia M., de la Morena-Alvarez-Palencia C., Arche-Andradas L., Dorta-Naranjo B.P. // 2007. SensorComm 2007. International Conference on Sensor Technologies and Applications. - Valencia, 14-20 Oct. 2007. - P. 5-9. ↑

C8731. Neering J. Optimal Passive Source Localization. / Neering J., Bordier M., Maizi N. // 2007. SensorComm 2007. International Conference on Sensor Technologies and Applications. - Valencia, 14-20 Oct. 2007. - P. 295-300. ↑

C8732. Musicki D. Target existence based resource allocation. 2007 10th International Conference on Information Fusion. - Quebec, Que., 9-12 July 2007. - P. 1-7. ↑

C8733. Duflos E. Time allocation of a set of radars in a multitarget environment. / Duflos E., de Vilmorin M., Vanheegehe P. // 2007 10th International Conference on Information Fusion. - Quebec, Que., 9-12 July 2007. - P. 1-8. ↑

C8734. de Villers Y. A fusion study of the FAVS sensors suite. 2007 10th International Conference on Information Fusion. - Quebec, Que., 9-12 July 2007. - P. 1-6. ↑

C8735. Ray P. A novel framework for the network-wide distributed detection problem. / Ray P., Varshney P.K., Ruixin Niu. // 2007 10th International Conference on Information Fusion. - Quebec, Que., 9-12 July 2007. - P. 1-8. ↑

C8736. Hanselmann T. Multiple target tracking with asynchronous bearings-only-measurements. / Hanselmann T., Morelande M. // 2007 10th International Conference on Information Fusion. - Quebec, Que., 9-12 July 2007. - P. 1-8. ↑

C8737. McDonald M. Continuous-discrete filtering for dim manoeuvring maritime targets. / McDonald M., Balaji B. // 2007 10th International Conference on Information Fusion. - Quebec, Que., 9-12 July 2007. - P. 1-6. ↑

C8738. Yifeng Zhou. A sequential ESM track association algorithm based on the use of information theoretic criteria. / Yifeng Zhou, Mickeal J. // 2007 10th International Conference on Information Fusion. - Quebec, Que.,

9-12 July 2007. - P. 1-7. ↑

C8739. Salmond D. Ground target modelling, tracking and prediction with road networks. / Salmond D., Clark M., Vinter R., Godsill S. // 2007 10th International Conference on Information Fusion. - Quebec, Que., 9-12 July 2007. - P. 1-8. ↑

C8740. Carthel C. Multisensor tracking and fusion for maritime surveillance. / Carthel C., Coraluppi S., Grignan P. // 2007 10th International Conference on Information Fusion. - Quebec, Que., 9-12 July 2007. - P. 1-6. ↑

C8741. Panzhi Liu. Adaptive censored cell-averaging CFAR detection in distributed sensor networks. / Panzhi Liu, Chongzhao Han, Ming Lei, Zengguo Sun. // 2007 10th International Conference on Information Fusion. - Quebec, Que., 9-12 July 2007. - P. 1-8. ↑

C8742. Li-Wei Fong. Distributed data fusion algorithms for tracking a maneuvering target. 2007 10th International Conference on Information Fusion. - Quebec, Que., 9-12 July 2007. - P. 1-8. ↑

C8743. Brown K. A distributed stand-in EW hunter-killer system. / Brown K., Drake S., Mason K., Piotrowski A., Swierkowski L. // 2007 10th International Conference on Information Fusion. - Quebec, Que., 9-12 July 2007. - P. 1-8. ↑

C8744. Panzhi Liu. Distributed adaptive CCAWCA CFAR detector. / Panzhi Liu, Chongzhao Han, Yi Yang, Ming Lei. // 2007 10th International Conference on Information Fusion. - Quebec, Que., 9-12 July 2007. - P. 1-8. ↑

C8745. Ting Liu. Change detection methodology based on region classification fusion. / Ting Liu, Gigli G., Lampropoulos G.A. // 2007 10th International Conference on Information Fusion. - Quebec, Que., 9-12 July 2007. - P. 1-7. ↑

C8746. Lang T. Exploitation of bistatic doppler measurements in multistatic tracking. / Lang T., Hayes G. // 2007 10th International Conference on Information Fusion. - Quebec, Que., 9-12 July 2007. - P. 1-8. ↑

C8747. Ramdaras U. Sensor selection: the modified riccati equation approach compared with other selection schemes. / Ramdaras U., Absil F. // 2007 10th International Conference on Information Fusion. - Quebec, Que., 9-12 July 2007. - P. 1-6. ↑

C8748. Novoselsky A. Track to track fusion using out-of-sequence track information. / Novoselsky A., Sklarz S.E., Dorfman M. // 2007 10th International Conference on Information Fusion. - Quebec, Que., 9-12 July 2007. - P. 1-5. ↑

C8749. Fosbury A.M. Ground target tracking using terrain information. / Fosbury A.M., Singh T., Crassidis J.L., Springen C. // 2007 10th International Conference on Information Fusion. - Quebec, Que., 9-12 July 2007. - P. 1-8. ↑

C8750. Lindner P. Multi level fusion with confidence measures for automotive safety applications. / Lindner P., Scheunert U., Richter E., Wanielik G. // 2007 10th International Conference on Information Fusion. - Quebec, Que., 9-12 July 2007. - P. 1-7. ↑

C8751. Danu D. Fusion of over-the-horizon radar and automatic identification systems for overall maritime picture. / Danu D., Sinha A., Kirubarajan T., Farooq M., Brookes D. // 2007 10th International Conference on Information Fusion. - Quebec, Que., 9-12 July 2007. - P. 1-8. ↑

C8752. Torres-Torriti M. Automatic ship positioning and radar biases correction using the hausdorff distance. / Torres-Torriti M., Guesalaga A. // 2007 10th International Conference on Information Fusion. - Quebec, Que., 9-12 July 2007. - P. 1-8. ↑

C8753. Dorion E. Multi-source semantic integration-revisiting the theory of signs and ontology alignment principles. / Dorion E., Fortin S. // 2007 10th International Conference on Information Fusion. - Quebec, Que., 9-12 July 2007. - P. 1-6. ↑

C8754. Stakkeland M. Tracking and fusion of surveillance radar images of extended targets. / Stakkeland M., hallingstad O., Overrein O. // 2007 10th International Conference on Information Fusion. - Quebec, Que., 9-12 July 2007. - P. 1-8. ↑

- C8755.** Mellema G.R. An operator perspective on net-centric underwater warfare. 2007 10th International Conference on Information Fusion. - Quebec, Que., 9-12 July 2007. - P. 1-6. ↑
- C8756.** Oxley M.E. A Boolean Algebra of receiver operating characteristic curves. / Oxley M.E., Thorsen S.N., Schubert C.M. // 2007 10th International Conference on Information Fusion. - Quebec, Que., 9-12 July 2007. - P. 1-8. ↑
- C8757.** Mallick M. Geolocation using video sensor measurements. 2007 10th International Conference on Information Fusion. - Quebec, Que., 9-12 July 2007. - P. 1-8. ↑
- C8758.** Brookes D. A case for service-oriented architecture in support of arctic C4ISR. / Brookes D., Helleur C., Gingell M., Campbell B., Jassemi-Zargami R. // 2007 10th International Conference on Information Fusion. - Quebec, Que., 9-12 July 2007. - P. 1-8. ↑
- C8759.** Tadruri M. Drift aware wireless sensor networks. / Tadruri M., Challa S. // 2007 10th International Conference on Information Fusion. - Quebec, Que., 9-12 July 2007. - P. 1-7. ↑
- C8760.** Ho T.-J. Radar target tracking using an IMM-EV estimators-based switching scheme. 2007 10th International Conference on Information Fusion. - Quebec, Que., 9-12 July 2007. - P. 1-6. ↑
- C8761.** Li X.R. Optimal bayes joint decision and estimation. 2007 10th International Conference on Information Fusion. - Quebec, Que., 9-12 July 2007. - P. 1-8. ↑
- C8762.** Wehn H. A distributed information fusion testbed for coastal surveillance. / Wehn H., Yates R., Valin P., Guitouni A., Bosse E., Dlugan A., Zwick H. // 2007 10th International Conference on Information Fusion. - Quebec, Que., 9-12 July 2007. - P. 1-7. ↑
- C8763.** Zhenhua Li. High Level data fusion system for CanCoastWatch. / Zhenhua Li, Leung H., Valin P., Wehn H. // 2007 10th International Conference on Information Fusion. - Quebec, Que., 9-12 July 2007. - P. 1-6. ↑
- C8764.** Helleur C. Track-to-track fusion by a human operator for maritime domain awareness. / Helleur C., Mathews M., Kashyap N., Rafuse J. // 2007 10th International Conference on Information Fusion. - Quebec, Que., 9-12 July 2007. - P. 1-8. ↑
- C8765.** Ulmke M. Gaussian mixture cardinalized PHD filter for ground moving target tracking. / Ulmke M., Erdinc O., Willett P. // 2007 10th International Conference on Information Fusion. - Quebec, Que., 9-12 July 2007. - P. 1-8. ↑
- C8766.** Dahlbom A. Trajectory clustering for coastal surveillance. / Dahlbom A., Niklasson L. // 2007 10th International Conference on Information Fusion. - Quebec, Que., 9-12 July 2007. - P. 1-8. ↑
- C8767.** Kulpa K. A simple robust detection of weak target in noise radars. / Kulpa K., Misiurewicz J., Gajo Z., Malanowski M. // 2007. EuRAD 2007. European Radar Conference. - Munich, 10-12 Oct. 2007. - P. 275-278. ↑
- C8768.** Grubinger H. A low-Noise front-end with beamsteering capability at 35 GHz. / Grubinger H., Barth H., Vahldieck R. // 2007. EuRAD 2007. European Radar Conference. - Munich, 10-12 Oct. 2007. - P. 315-318. ↑
- C8769.** Volkov V.A. A Ka-band, Magnetron based, scanning radar for airborne applications. / Volkov V.A., Vavriv D.M., Kozhin R.V., Shevtsova L.V., Yong-Hoon Kim, Hoon Lee. // 2007. EuRAD 2007. European Radar Conference. - Munich, 10-12 Oct. 2007. - P. 186-189. ↑
- C8770.** Doyuran U.C. Multi-range and multi-pulse radar detection in correlated non-Gaussian clutter. / Doyuran U.C., Tanik Y. // 2007. EuRAD 2007. European Radar Conference. - Munich, 10-12 Oct. 2007. - P. 190-193. ↑
- C8771.** Lukjanov S.P. Use of the ground penetrating radar methods for paleontology on example of the mammoth fauna investigation. / Lukjanov S.P., Stepanov R.A., Chernyi I.A., Stukach O.V. // 2007. EuRAD 2007. European Radar Conference. - Munich, 10-12 Oct. 2007. - P. 468-471. ↑
- C8772.** Alimenti F. A low-cost 24GHz Doppler radar sensor for traffic monitoring implemented in standard discrete-component technology. / Alimenti F., Placentino F., Battistini A., Tasselli G., Bernardini W., Mezzanotte P., Rascio D., Palazzari V., Leone S., Scarponi A., Porzi N., Comez M., Roselli L. // 2007. European Microwave

Conference. - Munich, 9-12 Oct. 2007. - P. 1441-1444. ↑

C8773. Monti G. Dispersion analysis of a planar negative group velocity-transmission line. / Monti G., Tarricone L. // 2007. EuRAD 2007. European Radar Conference. - Munich, 10-12 Oct. 2007. - P. 365-368. ↑

C8774. Prokopenko I.G. Adaptive algorithm for moving target detection and velocity estimation. / Prokopenko I.G., Yanovsky F.J., Prokopenko K.I. // 2007. EuRAD 2007. European Radar Conference. - Munich, 10-12 Oct. 2007. - P. 452-455. ↑

C8775. Moldovan E. W-band substrate integrated waveguide radar sensor based on multi-port technology. / Moldovan E., Tatu S.O., Affes S., Bosisio R.G., Ke Wu. // 2007. EuRAD 2007. European Radar Conference. - Munich, 10-12 Oct. 2007. - P. 174-177. ↑

C8776. Winkler V. Automotive 24 GHz pulse radar extended by a DQPSK communication channel. / Winkler V., Detlefsen J. // 2007. EuRAD 2007. European Radar Conference. - Munich, 10-12 Oct. 2007. - P. 138-141. ↑

C8777. Ruggiano M. Wideband ambiguity function and optimized coded radar signals. / Ruggiano M., van Genderen P. // 2007. EuRAD 2007. European Radar Conference. - Munich, 10-12 Oct. 2007. - P. 142-145. ↑

C8778. Kostylev V.I. Analysis of the signal model for forward scattering radar in case of a small target. / Kostylev V.I., Cherniakov M. // 2007. EuRAD 2007. European Radar Conference. - Munich, 10-12 Oct. 2007. - P. 126-129. ↑

C8779. Sturm C. Two-dimensional radar imaging with scattered PSK-modulated communication signals. / Sturm C., Schulteis S., Wiesbeck W. // 2007. EuRAD 2007. European Radar Conference. - Munich, 10-12 Oct. 2007. - P. 134-137. ↑

C8780. Winkler V. Range Doppler detection for automotive FMCW radars. 2007. EuRAD 2007. European Radar Conference. - Munich, 10-12 Oct. 2007. - P. 166-169. ↑

C8781. Shen Chiu. Performance analysis of RADARSAT-2 multi-channel MODEX modes. 2007. EuRAD 2007. European Radar Conference. - Munich, 10-12 Oct. 2007. - P. 170-173. ↑

C8782. Ouacha A. Technology for ultra broadband reconfigurable beamformer and front-end. / Ouacha A., Erickson R., Malmqvist R. // 2007. EuRAD 2007. European Radar Conference. - Munich, 10-12 Oct. 2007. - P. 150-153. ↑

C8783. Alimenti F. A low-cost 24GHz doppler radar sensor for traffic monitoring implemented in standard discrete-component technology. / Alimenti F., Placentino F., Battistini A., Tasselli G., Bernardini W., Mezzanotte P., Rascio D., Palazzari V., Leone S., Scarponi A., Porzi N., Comez M., Roselli L. // 2007. EuRAD 2007. European Radar Conference. - Munich, 10-12 Oct. 2007. - P. 162-165. ↑

C8784. Winkler V. Range Doppler detection for automotive FMCW radars. 2007. European Microwave Conference. - Munich, 9-12 Oct. 2007. - P. 1445-1448. ↑

C8785. Hee-Sub Shin. Range migration algorithm with resampling in airborne bistatic spotlight SAR systems. / Hee-Sub Shin, Jong-Tae Lim. // 2007. ICCAS '07. International Conference on Control, Automation and Systems. - Seoul, 17-20 Oct. 2007. - P. 2361-2364. ↑

C8786. {no data available}. Appriou bio. 2007 10th International Conference on Information Fusion. - Quebec City, QC, Canada, 9-12 July 2007. - P. 1. ↑

C8787. Shanwen Zhang. A Detection Method of Radar Signal by Wavelet Transforms. / Shanwen Zhang, Jianbo Fan, Lidan Shou, Jinxiang Dong. // 2007. FSKD 2007. Fourth International Conference on Fuzzy Systems and Knowledge Discovery. - Haikou, 24-27 Aug. 2007. - Vol. 2. - P. 710-714. ↑

C8788. Ming Li. SAR Image Segmentation Based on Mixture Context and Wavelet Hidden-Class-Label Markov Random Field. / Ming Li, Yan Wu, Shunjun Wu. // 2007. FSKD 2007. Fourth International Conference on Fuzzy Systems and Knowledge Discovery. - Haikou, 24-27 Aug. 2007. - Vol. 3. - P. 360-365. ↑

C8789. le Roux W.H. Using a data fusion-based activity recognition framework to determine Surveillance System Requirements. / le Roux W.H., Nel J.J., Steinberg A.N. // 2007 10th International Conference on

Information Fusion. - Quebec, Que., 9-12 July 2007. - P. 1-6. ↑

C8790. Luo Zhiyong. ML Estimation of true Height in 2-D Radar Network. / Luo Zhiyong, He Jia-Zhou. // 2007 10th International Conference on Information Fusion. - Quebec, Que., 9-12 July 2007. - P. 1-7. ↑

C8791. Chun Yang. Track Fusion with Road Constraints. / Chun Yang, Blasch E. // 2007 10th International Conference on Information Fusion. - Quebec, Que., 9-12 July 2007. - P. 1-8. ↑

C8792. Chun Yang. A simple maneuver indicator from target's range-doppler image. / Chun Yang, Garber W., Mitchell R., Blasch E. // 2007 10th International Conference on Information Fusion. - Quebec, Que., 9-12 July 2007. - P. 1-8. ↑

C8793. Jain V. A CMOS 22-29GHz Receiver Front-End for UWB Automotive Pulse-Radars. / Jain V., Sundararaman S., Heydari P. // 2007. CICC '07. IEEE Custom Integrated Circuits Conference. - San Jose, CA, 16-19 Sept. 2007. - P. 757-760. ↑

C8794. Volkov V.A. A Ka-band, magnetron based, scanning radar for airborne applications. / Volkov V.A., Vavriv D.M., Kozhin R.V., Shevtsova L.V., Yong-Hoon Kim, Hoon Lee. // 2007. European Microwave Conference. - Munich, 9-12 Oct. 2007. - P. 1465-1468. ↑

C8795. Kulpa K. A simple robust detection of weak target in noise radars. / Kulpa K., Misiurewicz J., Gajo Z., Malanowski M. // 2007. European Microwave Conference. - Munich, 9-12 Oct. 2007. - P. 1554-1557. ↑

C8796. Shen Chiu. Performance analysis of RADARSAT-2 multi-channel MODEX modes. 2007. European Microwave Conference. - Munich, 9-12 Oct. 2007. - P. 1449-1452. ↑

C8797. Moldovan E. W-band substrate integrated waveguide radar sensor based on multi-port technology. / Moldovan E., Tatu S.O., Affes S., Bosisio R.G., Ke Wu. // 2007. European Microwave Conference. - Munich, 9-12 Oct. 2007. - P. 1453-1456. ↑

C8798. Prokopenko I.G. Adaptive algorithm for moving target detection and velocity estimation. / Prokopenko I.G., Yanovsky F.J., Prokopenko K.I. // 2007. European Microwave Conference. - Munich, 9-12 Oct. 2007. - P. 1731-1734. ↑

C8799. Lukjanov S.P. Use of the Ground Penetrating Radar Methods for paleontology on example of the mammoth fauna investigation. / Lukjanov S.P., Stepanov R.A., Chernyi I.A., Stukach O.V. // 2007. European Microwave Conference. - Munich, 9-12 Oct. 2007. - P. 1747-1750. ↑

C8800. Kubicke G. Comparison of bistatic signatures of octahedral and icosahedral reflectors in high-frequency domain. / Kubicke G., Bourlier C., Saillard J. // 2007. European Microwave Conference. - Munich, 9-12 Oct. 2007. - P. 1704-1707. ↑

C8801. Khraisat Y.S.H. Joint influence of rain rate and turbulence on radar signal spectrum width. / Khraisat Y.S.H., Yanovsky F.J. // 2007. European Microwave Conference. - Munich, 9-12 Oct. 2007. - P. 1708-1711. ↑

C8802. Blunt S.D. Waveform design for radar-embedded communications. / Blunt S.D., Yantham P. // 2007. International Waveform Diversity and Design Conference. - Pisa, 4-8 June 2007. - P. 214-218. ↑

C8803. Hantscher S. An UWB Wall Scanner Based on a Shape Estimating SAR Algorithm. / Hantscher S., Reizenzahn A., Diskus C.G. // 2007. IEEE/MTT-S International Microwave Symposium. - Honolulu, HI, 3-8 June 2007. - P. 1463-1466. ↑

C8804. Veenstra H. A SiGe-BiCMOS UWB Receiver for 24 GHz Short-Range Automotive Radar Applications. / Veenstra H., van der Heijden E., Notten M., Dolmans G. // 2007. IEEE/MTT-S International Microwave Symposium. - Honolulu, HI, 3-8 June 2007. - P. 1791-1794. ↑

C8805. Mostafanezhad I. Sensor Nodes for Doppler Radar Measurements of Life Signs. / Mostafanezhad I., Byung-Kwon Park, Boric-Lubecke O., Lubecke V., Host-Madsen A. // 2007. IEEE/MTT-S International Microwave Symposium. - Honolulu, HI, 3-8 June 2007. - P. 1241-1244. ↑

C8806. Fukuda T. A 26GHz Short-Range UWB Vehicular-Radar Using 2.5Gcps Spread Spectrum Modulation. / Fukuda T., Negoro N., Ujita S., Nagai S., Nishijima M., Sakai H., Tanaka T., Ueda D. // 2007. IEEE/MTT-S

International Microwave Symposium. - Honolulu, HI, 3-8 June 2007. - P. 1311-1314. ↑

C8807. Zhou De-Quan. Study of Key Techniques Applied in Radars of Locating Enemy Artilleries. 2007. ICMMT '07. International Conference on Microwave and Millimeter Wave Technology. - Builin, 18-21 April 2007. - P. 1-4. ↑

C8808. Xiong Gang. The Short-Time Multifractal Spectral Analysis Based on the Singularity Exponents. / Xiong Gang, Yang Xiaoniu, Zhao Huichang. // 2007. ICMMT '07. International Conference on Microwave and Millimeter Wave Technology. - Builin, 18-21 April 2007. - P. 1-4. ↑

C8809. Yue Hongwei. Adaptive Nulling Methods with Multiple Constraints for Transmitting DBF. / Yue Hongwei, Wang Jiegui, Luo Jingqing. // 2007. ICMMT '07. International Conference on Microwave and Millimeter Wave Technology. - Builin, 18-21 April 2007. - P. 1-4. ↑

C8810. Lingyan Dai. A Blanket Deception Jamming Rejection Approach Based on Jamming Sample Recognition. / Lingyan Dai, Rongfeng Li, Yongliang Wang, Hongbin Jin. // 2007. ICMMT '07. International Conference on Microwave and Millimeter Wave Technology. - Builin, 18-21 April 2007. - P. 1-4. ↑

C8811. Wagner C. A Fully-Automated Measurement System for 77-GHz Mixers. / Wagner C., Trembl M., Hartmann M., Stelzer A., Jaeger H. // 2007. IMTC 2007. IEEE Instrumentation and Measurement Technology Conference Proceedings. - Warsaw, 1-3 May 2007. - P. 1-4. ↑

C8812. Khrebto P. A Wireless Location System for Sensing the Relative Position between Mining Vehicles. / Khrebto P., Pottkeir A., Max S. // 2007. IMTC 2007. IEEE Instrumentation and Measurement Technology Conference Proceedings. - Warsaw, 1-3 May 2007. - P. 1-5. ↑

C8813. Stubberud S.C. Measurement Augmentation to Compensate for Sensor Registration Using a Neural Kalman Filter. / Stubberud S.C., Kramer K.A., Geremia J.A. // 2007. IMTC 2007. IEEE Instrumentation and Measurement Technology Conference Proceedings. - Warsaw, 1-3 May 2007. - P. 1-6. ↑

C8814. Horak G. A Framework for Low Data Rate, Highly Distributed Measurement Systems. / Horak G., Vasic D., Bilas V. // 2007. IMTC 2007. IEEE Instrumentation and Measurement Technology Conference Proceedings. - Warsaw, 1-3 May 2007. - P. 1-4. ↑

C8815. Chiappe M. Analytical Solution to Inverse Electromagnetic Scattering: Shape and Position Reconstruction of Dielectric Objects. / Chiappe M., Gragnani G.L. // 2007. IST '07. IEEE International Workshop on Imaging Systems and Techniques. - Krakow, 5-5 May 2007. - P. 1-6. ↑

C8816. Lubecke V.M. Through-the-Wall Radar Life Detection and Monitoring. / Lubecke V.M., Boric-Lubecke O., Host-Madsen A., Fathy A.E. // 2007. IEEE/MTT-S International Microwave Symposium. - Honolulu, HI, 3-8 June 2007. - P. 769-772. ↑

C8817. Dziadak B. Some aspects of design and measurements results prediction for a Mobile Observation Point for a hydrocarbon pollution monitoring system. / Dziadak B., Michalski A. // 2007. IMTC 2007. IEEE Instrumentation and Measurement Technology Conference Proceedings. - Warsaw, 1-3 May 2007. - P. 1-6. ↑

C8818. Salvade A. A numerical evaluation of an optimal setup for a microwave axial tomograph aimed at the inspection of wood. / Salvade A., Pastorino M., Monleone R., Randazzo A., Bartesaghi T., Bozza G. // 2007. IST '07. IEEE International Workshop on Imaging Systems and Techniques. - Krakow, 5-5 May 2007. - P. 1-6. ↑

C8819. Shuguang Liu. High Order Nyström-PO Hybrid Method for 3D EM Scattering of Arbitrary Shape. / Shuguang Liu, Xiaojuan Zhang. // 2007. ICMMT '07. International Conference on Microwave and Millimeter Wave Technology. - Builin, 18-21 April 2007. - P. 1-3. ↑

C8820. Besson O. Bayesian Estimation of Covariance Matrices in Non-Homogeneous Environments. / Besson O., Tournet J.-Y., Bidon S. // 2007. ICASSP 2007. IEEE International Conference on Acoustics, Speech and Signal Processing. - Honolulu, HI, 15-20 April 2007. - Vol. 3. - P. III-1037-III-1040-1037. ↑

C8821. Wei He-Wen. Influence of Random Carrier Phase on True Cramer-Rao Lower Bound for Time Delay Estimation. / Wei He-Wen, Ye Shangfu, Wan Qun. // 2007. ICASSP 2007. IEEE International Conference on Acoustics, Speech and Signal Processing. - Honolulu, HI, 15-20 April 2007. - Vol. 3. - P. III-1029-III-1032-1029. ↑

- C8822.** Berisha V. Sparse Manifold Learning with Applications to SAR Image Classification. / Berisha V., Shah N., Waagen D., Schmitt H., Bellofiore S., Spanias A., Cochran D. // 2007. ICASSP 2007. IEEE International Conference on Acoustics, Speech and Signal Processing. - Honolulu, HI, 15-20 April 2007. - Vol. 3. - P. III-1089-III-1092-1089. ↑
- C8823.** Sajjad N. Asymptotic Cramér-Rao Bound for Multi-Dimensional Harmonic Models. / Sajjad N., Boyer R. // 2007. ICASSP 2007. IEEE International Conference on Acoustics, Speech and Signal Processing. - Honolulu, HI, 15-20 April 2007. - Vol. 3. - P. III-1041-III-1044-1041. ↑
- C8824.** Setlur P. Cramer-Rao Bounds for Range and Motion Parameter Estimations using Dual Frequency Radars. / Setlur P., Amin M., Ahmad F. // 2007. ICASSP 2007. IEEE International Conference on Acoustics, Speech and Signal Processing. - Honolulu, HI, 15-20 April 2007. - Vol. 3. - P. III-813-III-816-813. ↑
- C8825.** Wang A. Threat Estimation of Multifunction Radars: Modeling and Statistical Signal Processing of Stochastic Context Free Grammars. / Wang A., Krishnamurthy V. // 2007. ICASSP 2007. IEEE International Conference on Acoustics, Speech and Signal Processing. - Honolulu, HI, 15-20 April 2007. - Vol. 3. - P. III-793-III-796-793. ↑
- C8826.** Christensen L.P.B. An EM-Algorithm for Band-Toeplitz Covariance Matrix Estimation. 2007. ICASSP 2007. IEEE International Conference on Acoustics, Speech and Signal Processing. - Honolulu, HI, 15-20 April 2007. - Vol. 3. - P. III-1021-III-1024-1021. ↑
- C8827.** Boufounos P. Generating Binary Processes with all-Pole Spectra. 2007. ICASSP 2007. IEEE International Conference on Acoustics, Speech and Signal Processing. - Honolulu, HI, 15-20 April 2007. - Vol. 3. - P. III-981-III-984-981. ↑
- C8828.** Song lizhong. Study on a Nonlinear Frequency Modulation Signal with Polarization-Coded Modulation. / Song lizhong, Wang Miao. // 2007. ICMMT '07. International Conference on Microwave and Millimeter Wave Technology. - Builin, 18-21 April 2007. - P. 1-4. ↑
- C8829.** Zhao Jianhong. LFM extended target echoes detecting using Radon-Wigner Method. / Zhao Jianhong, Yang Jianyu. // 2007. ICMMT '07. International Conference on Microwave and Millimeter Wave Technology. - Builin, 18-21 April 2007. - P. 1-4. ↑
- C8830.** Yin Zhiping. Imaging of space objects using space-borne millimeter wave ISAR. / Yin Zhiping, Zhang Yian, Wang Dongjin, Chen Weidong. // 2007. ICMMT '07. International Conference on Microwave and Millimeter Wave Technology. - Builin, 18-21 April 2007. - P. 1-4. ↑
- C8831.** Jin Tao. Millimeter Wave Polarimetric Monopulse Radar Debugging System. / Jin Tao, Qi Xiaohui, Zhang Min, Qiao Xiaolin, Yuan Shuqing, Zhang Qunxing. // 2007. ICMMT '07. International Conference on Microwave and Millimeter Wave Technology. - Builin, 18-21 April 2007. - P. 1-4. ↑
- C8832.** Pruvost S. Low Noise Low Cost Rx Solutions for Pulsed 24GHz Automotive Radar Sensors. / Pruvost S., Moquillon L., Imbs E., Marchetti M., Garcia P. // 2007 IEEE Radio Frequency Integrated Circuits (RFIC) Symposium. - Honolulu, HI, 3-5 June 2007. - P. 387-390. ↑
- C8833.** Abramovich Y.I. Diagonally Loaded Normalised Sample Matrix Inversion (LNSMI) for Outlier-Resistant Adaptive Filtering. / Abramovich Y.I., Spencer N.K. // 2007. ICASSP 2007. IEEE International Conference on Acoustics, Speech and Signal Processing. - Honolulu, HI, 15-20 April 2007. - Vol. 3. - P. III-1105-III-1108-1105. ↑
- C8834.** Guodong Xu. Simulation of ISAR Imaging for a Missile. / Guodong Xu, Jianjun Gao, Fulin Su. // 2007. ICMMT '07. International Conference on Microwave and Millimeter Wave Technology. - Builin, 18-21 April 2007. - P. 1-3. ↑
- C8835.** Qiao Xiaolin. Anti-Millimeter Wave Polarization Agile Active Jamming. / Qiao Xiaolin, Jin Tao, Qi Xiaohui, Zhang Min, Yuan Shuqing, Zhang Qunxing. // 2007. ICMMT '07. International Conference on Microwave and Millimeter Wave Technology. - Builin, 18-21 April 2007. - P. 1-4. ↑
- C8836.** Del Amo A. A Spatial Classification Model for Multicriteria Analysis. / Del Amo A., Garmendia L., Gomez D., Montero J. // IEEE Symposium on Computational Intelligence in Multicriteria Decision Making. - Honolulu, HI, 1-5 April 2007. - P. 348-353. ↑

- C8837.** Hatfield D.N. The Potential Value of Decentralized Trunking as Regulatory Precedent for the Introduction of Dynamic Spectrum Access Technology. / Hatfield D.N., Tenhula P.A. // 2007. DySPAN 2007. 2nd IEEE International Symposium on New Frontiers in Dynamic Spectrum Access Networks. - Dublin, 17-20 April 2007. - P. 597-605. ↑
- C8838.** Yen-Wen Lin. SIP-Based Handoff in 4G Mobile Networks. / Yen-Wen Lin, Ta-He Huang. // 2007.WCNC 2007. IEEE Wireless Communications and Networking Conference. - Kowloon, 11-15 March 2007. - P. 2806-2811. ↑
- C8839.** Zito D. Wearable System-on-a-Chip Pulse Radar Sensors for the Health Care: System Overview. / Zito D., Pepe D., Neri B., De Rossi D., Lanata A. // AINAW '07. 21st International Conference on Advanced Information Networking and Applications Workshops, 2007. - Niagara Falls, Ont., 21-23 May 2007. - Vol. 2. - P. 766-769. ↑
- C8840.** McVay J. A. Through-the-Wall Imaging and Sensing: An Electromagnetic Perspective. / McVay J. A., Yemelyanov K. M., Hoorfar A., Engheta N. // 2007. SAFE '07. IEEE Workshop on Signal Processing Applications for Public Security and Forensics. - Washington, DC, USA, 11-13 April 2007. - P. 1-4. ↑
- C8841.** Nemati S. Spectral Signature Classification Using A Support Vector Classifier For Real-Time Instrumentation. / Nemati S., Yeary M., Yu T.-Y., Wang Y., Zhai Y., Fagg A.H. // 2007. IMTC 2007. IEEE Instrumentation and Measurement Technology Conference Proceedings. - Warsaw, 1-3 May 2007. - P. 1-4. ↑
- C8842.** Lidicky L. Fourier Approach to Moving Target Indication and Detection in Multichannel SAR Data. 2007. CIISP 2007. IEEE Symposium on Computational Intelligence in Image and Signal Processing. - Honolulu, HI, 1-5 April 2007. - P. 397-402. ↑
- C8843.** Aviyente Selin. Information Theoretic Measures for Change Detection in Urban Sensing Applications. / Aviyente Selin, Ahmad Fauzia, Amin Moeness G. // 2007. SAFE '07. IEEE Workshop on Signal Processing Applications for Public Security and Forensics. - Washington, DC, USA, 11-13 April 2007. - P. 1-6. ↑
- C8844.** Hiryu S. Compensation behaviors in echolocating bats measured by a telemetry microphone during flight. / Hiryu S., Hagino T., Shiori Y., Riquimaroux H., Watanabe Y. // 2007. Symposium on Underwater Technology and Workshop on Scientific Use of Submarine Cables and Related Technologies. - Tokyo, 17-20 April 2007. - P. 535-539. ↑
- C8845.** Al-Tae M.A. Remote Monitoring of Vehicle Diagnostics and Location Using a Smart Box with Global Positioning System and General Packet Radio Service. / Al-Tae M.A., Khader O.B., Al-Saber N.A. // 2007. AICCSA '07. IEEE/ACS International Conference on Computer Systems and Applications. - Amman, 13-16 May 2007. - P. 385-388. ↑
- C8846.** Kumar D. Distributed Collaborative Adaptive Sensing: A Unifying Theme for a Junior Level Embedded Systems Course. / Kumar D., Bursleson W. // 2007. MSE '07. IEEE International Conference on Microelectronic Systems Education. - San Diego, CA, 3-4 June 2007. - P. 47-48. ↑
- C8847.** Maeda F. Development of diver detection and sensor integration for wharf surveillance software. / Maeda F., Asada A., Kuramoto K., Kurashige Y., Nanri M., Kawashima Y., Imai R., Hantani K. // 2007. Symposium on Underwater Technology and Workshop on Scientific Use of Submarine Cables and Related Technologies. - Tokyo, 17-20 April 2007. - P. 133-141. ↑
- C8848.** Chen Yixin. Vehicle Tracking and Distance Estimation Based on Multiple Image Features. / Chen Yixin, Das M., Bajpai D. // 2007. CRV '07. Fourth Canadian Conference on Computer and Robot Vision. - Montreal, Que., 28-30 May 2007. - P. 371-378. ↑
- C8849.** Weiqun Shi. Development of an Experimental Prototype Multi-Modal Netted Sensor Fence for Homeland Defense and Border Integrity. / Weiqun Shi, Arabadjis G., Bishop B., Hill P., Plasse R. // 2007 IEEE Conference on Technologies for Homeland Security. - Woburn, MA, 16-17 May 2007. - P. 221-226. ↑
- C8850.** Hamdi M. Doppler Effect on Location-Based Tracking in Mobile Sensor Networks. / Hamdi M., Bellazreg R., Boudriga N. // 2007. AICCSA '07. IEEE/ACS International Conference on Computer Systems and Applications. - Amman, 13-16 May 2007. - P. 252-257. ↑
- C8851.** Yang Xuezhi. SAR Sea Ice Image Segmentation Based on Edge-preserving Watersheds. / Yang

Xuezhi, Clausi D.A. // 2007. CRV '07. Fourth Canadian Conference on Computer and Robot Vision. - Montreal, Que., 28-30 May 2007. - P. 426-431. ↑

C8852. Ahmad Fauzia. Through-the-Wall Radar Imaging Experiments. / Ahmad Fauzia, Amin Moeness G. // 2007. SAFE '07. IEEE Workshop on Signal Processing Applications for Public Security and Forensics. - Washington, DC, USA, 11-13 April 2007. - P. 1-5. ↑

C8853. George K. Multiple Signal Detection and Measurement Using a Configurable Wideband Digital Receiver. / George K., Chien-In Henry Chen. // 2007. IMTC 2007. IEEE Instrumentation and Measurement Technology Conference Proceedings. - Warsaw, 1-3 May 2007. - P. 1-5. ↑

C8854. De Angelis A. A Low-Cost Ultra-Wideband Indoor Ranging Technique. / De Angelis A., Dionigi M., Moschitta A., Carbone P. // 2007. IMTC 2007. IEEE Instrumentation and Measurement Technology Conference Proceedings. - Warsaw, 1-3 May 2007. - P. 1-6. ↑

C8855. Cirillo L.A. Estimation of Near-Field Parameters using Spatial Time-Frequency Distributions. / Cirillo L.A., Zoubir A.M., Amin M.G. // 2007. ICASSP 2007. IEEE International Conference on Acoustics, Speech and Signal Processing. - Honolulu, HI, 15-20 April 2007. - Vol. 3. - P. III-1141-III-1144-1141. ↑

C8856. Pu Wang. Algorithm Extension of Cubic Phase Function for Estimating Quadratic FM Signal. / Pu Wang, Jianyu Yang, Djurovic I. // 2007. ICASSP 2007. IEEE International Conference on Acoustics, Speech and Signal Processing. - Honolulu, HI, 15-20 April 2007. - Vol. 3. - P. III-1125-III-1128-1125. ↑

C8857. George K. Configurable and Expandable FFT Processor for Wideband Communication. / George K., Chen C.-I.H. // 2007. IMTC 2007. IEEE Instrumentation and Measurement Technology Conference Proceedings. - Warsaw, 1-3 May 2007. - P. 1-6. ↑

C8858. van Dorp P. Local Information from Range-Speed Radar Sequences. / van Dorp P., Groen F.C.A. // 2007. IMTC 2007. IEEE Instrumentation and Measurement Technology Conference Proceedings. - Warsaw, 1-3 May 2007. - P. 1-6. ↑

C8859. Dogancay K. Profile Likelihood Estimator for Passive Scan-Based Emitter Localization. / Dogancay K., Hmam H. // 2007. ICASSP 2007. IEEE International Conference on Acoustics, Speech and Signal Processing. - Honolulu, HI, 15-20 April 2007. - Vol. 3. - P. III-1117-III-1120-1117. ↑

C8860. Noury L. A Generic ASIC Architecture for Real Time Time-Frequency Analysis of Non-stationary Large Bandwidth Signals. / Noury L., Durbin F., Mehrez H., Tissot A. // 2007. IMTC 2007. IEEE Instrumentation and Measurement Technology Conference Proceedings. - Warsaw, 1-3 May 2007. - P. 1-5. ↑

C8861. Haykin S. Cognitive Dynamic Systems. 2007. ICASSP 2007. IEEE International Conference on Acoustics, Speech and Signal Processing. - Honolulu, HI, 15-20 April 2007. - Vol. 4. - P. IV-1369-IV-1372-1369. ↑

C8862. McCree A. Multisensor Dynamic Waveform Fusion. / McCree A., Brady K., Quatieri T.F. // 2007. ICASSP 2007. IEEE International Conference on Acoustics, Speech and Signal Processing. - Honolulu, HI, 15-20 April 2007. - Vol. 4. - P. IV-577-IV-580-577. ↑

C8863. Yang Yunqiang. Near-Real-Time Data Acquisition and Beamforming for UWB See-Through-Wall System. / Yang Yunqiang, Fathy Aly E. // 2007. SAFE '07. IEEE Workshop on Signal Processing Applications for Public Security and Forensics. - Washington, DC, USA, 11-13 April 2007. - P. 1-4. ↑

C8864. Lai Chieh-Ping. Hilbert-Huang Transform (HHT) Processing of Through-Wall Noise Radar Data for Human Activity Characterization. / Lai Chieh-Ping, Ruan Qing, Narayanan Ram M. // 2007. SAFE '07. IEEE Workshop on Signal Processing Applications for Public Security and Forensics. - Washington, DC, USA, 11-13 April 2007. - P. 1-6. ↑

C8865. Sira S.P. Improving Detection in Sea Clutter using Waveform Scheduling. / Sira S.P., Cochran D., Papandreou-Suppappola A., Morrell D., Moran B., Howard S., Calderbank R. // 2007. ICASSP 2007. IEEE International Conference on Acoustics, Speech and Signal Processing. - Honolulu, HI, 15-20 April 2007. - Vol. 3. - P. III-1241-III-1244-1241. ↑

C8866. Chatelain F. Bivariate Gamma Distributions for Multisensor Sar Images. / Chatelain F., Tournet J.-Y. // 2007. ICASSP 2007. IEEE International Conference on Acoustics, Speech and Signal Processing. - Honolulu,

HI, 15-20 April 2007. - Vol. 3. - P. III-1237-III-1240-1237. ↑

C8867. Vaidyanathan P.P. Some properties of IIR power-symmetric filters. 2007. ICASSP 2007. IEEE International Conference on Acoustics, Speech and Signal Processing. - Honolulu, HI, 15-20 April 2007. - Vol. 3. - P. III-1449-III-1452-1449. ↑

C8868. Xiaoxiang Liu. Through the Wall Imaging using Chaotic Modulated Ultra Wideband Synthetic Aperture Radar. / Xiaoxiang Liu, Henry Leung. // 2007. ICASSP 2007. IEEE International Conference on Acoustics, Speech and Signal Processing. - Honolulu, HI, 15-20 April 2007. - Vol. 3. - P. III-1257-III-1260-1257. ↑

C8869. Shi Zhiguang. Joint Model Selection and Parameter Estimation of GTD Model using RJ-MCMC Algorithm. / Shi Zhiguang, Zhou Jianxiong, Zhao Hongzhong, Fu Qiang. // 2007. ICASSP 2007. IEEE International Conference on Acoustics, Speech and Signal Processing. - Honolulu, HI, 15-20 April 2007. - Vol. 3. - P. III-777-III-780-777. ↑

C8870. Jianhua Yan. A Graph Reduction Method for 2D Snake Problems. / Jianhua Yan, Keqi Zhang, Chengcui Zhang, Shu-Ching Chen, Narasimhan G. // 2007. CVPR '07. IEEE Conference on Computer Vision and Pattern Recognition. - Minneapolis, MN, 17-22 June 2007. - P. 1-6. ↑

C8871. Liebelt J. Precise Registration of 3D Models To Images by Swarming Particles. / Liebelt J., Schertler K. // 2007. CVPR '07. IEEE Conference on Computer Vision and Pattern Recognition. - Minneapolis, MN, 17-22 June 2007. - P. 1-8. ↑

C8872. Huaping Liu. Symmetry-Aided Particle Filter for Vehicle Tracking. / Huaping Liu, Fuchun Sun, Kezhong He. // 2007 IEEE International Conference on Robotics and Automation. - Roma, 10-14 April 2007. - P. 4633-4638. ↑

C8873. Price M. Training and optimization of operating parameters for flash LADAR cameras. / Price M., Kenney J., Eastman R.D., Tsai Hong. // 2007 IEEE International Conference on Robotics and Automation. - Roma, 10-14 April 2007. - P. 3408-3413. ↑

C8874. Daeheung Kwon. Methods for Seamless Vertical Handoff between UMTS and WLAN. / Daeheung Kwon, Aesoon Park. // The 9th International Conference on Advanced Communication Technology. - Gangwon-Do, 12-14 Feb. 2007. - Vol. 2. - P. 1286-1289. ↑

C8875. Ki-Seok Bang. Verifying Behavior of L4 Microkernel based Mobile Phone. / Ki-Seok Bang, Su-Young Lee, Ki-Hyuk Nam, Wan-Yeon Lee, Young-Woong Ko. // The 9th International Conference on Advanced Communication Technology. - Gangwon-Do, 12-14 Feb. 2007. - Vol. 1. - P. 113-115. ↑

C8876. Ebrahimi-Tofghi N. Investigation of the Effect of Fading Correlation on Performance of MIMO Systems Using an RCS Channel Model. / Ebrahimi-Tofghi N., Ardebilipour M., Shahabadi M., Rajabi S. // The 9th International Conference on Advanced Communication Technology. - Gangwon-Do, 12-14 Feb. 2007. - Vol. 3. - P. 1748-1751. ↑

C8877. Hao Jiang. A Linear Programming Approach for Multiple Object Tracking. / Hao Jiang, Fels S., Little J.J. // 2007. CVPR '07. IEEE Conference on Computer Vision and Pattern Recognition. - Minneapolis, MN, 17-22 June 2007. - P. 1-8. ↑

C8878. Kawamoto M. Particle Filtering Algorithms for Tracking Multiple Sound Sources using Microphone Arrays. / Kawamoto M., Asano F., Asoh H., Yamamoto K. // 2007. ICASSP 2007. IEEE International Conference on Acoustics, Speech and Signal Processing. - Honolulu, HI, 15-20 April 2007. - Vol. 1. - P. I-129-I-132-129. ↑

C8879. Yiteng Huang. Laplace Entropy and its Application to Time Delay Estimation for Speech Signals. / Yiteng Huang, Benesty J., Jingdong Chen. // 2007. ICASSP 2007. IEEE International Conference on Acoustics, Speech and Signal Processing. - Honolulu, HI, 15-20 April 2007. - Vol. 1. - P. I-113-I-116-113. ↑

C8880. Yarman C.E. Bistatic Synthetic Aperture Hitchhiker Imaging. / Yarman C.E., Yazici B., Cheney M. // 2007. ICASSP 2007. IEEE International Conference on Acoustics, Speech and Signal Processing. - Honolulu, HI, 15-20 April 2007. - Vol. 1. - P. I-537-I-540-537. ↑

C8881. Petrochilos N. Blind Separation of Human Heartbeats and Breathing by the use of a Doppler Radar Remote Sensing. / Petrochilos N., Rezk M., Host-Madsen A., Lubecke V., Boric-Lubecke O. // 2007. ICASSP

2007. IEEE International Conference on Acoustics, Speech and Signal Processing. - Honolulu, HI, 15-20 April 2007. - Vol. 1. - P. I-333-I-336-333. ↑

C8882. Ingemar Soderquist. Event Driven Data Processing Architecture. 2007. DATE '07 Design, Automation & Test in Europe Conference & Exhibition. - Nice, 16-20 April 2007. - P. 1-5. ↑

C8883. Hairion D. New safety critical radio altimeter for Airbus and related design flow. / Hairion D., Emeriau S., Combet E., Sarlotte M. // 2007. DATE '07 Design, Automation & Test in Europe Conference & Exhibition. - Nice, 16-20 April 2007. - P. 1-5. ↑

C8884. {no data available}. 2007 IEEE International Conference on Acoustics, Speech, and Signal Processing. 2007. ICASSP 2007. IEEE International Conference on Acoustics, Speech and Signal Processing. - Honolulu, HI, 15-20 April 2007. - Vol. 1. - P. i. ↑

C8885. Subramanian A. UWB Linear Quadratic Frequency Domain Frequency Invariant Beamforming and Angle of Arrival Estimation. 2007. VTC2007-Spring. IEEE 65th Vehicular Technology Conference. - Dublin, 22-25 April 2007. - P. 614-618. ↑

C8886. Harabi F. Estimation of 2-D Direction of Arrival with an Extended Correlation Matrix. / Harabi F., Changuel H., Gharsallah A. // 2007. WPNC '07. 4th Workshop on Positioning, Navigation and Communication. - Hannover, 22-22 March 2007. - P. 255-260. ↑

C8887. Schaum A. Advanced Methods of Multivariate Anomaly Detection. 2007 IEEE Aerospace Conference. - Big Sky, MT, 3-10 March 2007. - P. 1-7. ↑

C8888. Blanding W.R. Multiple Target Tracking Using Maximum Likelihood Probabilistic Data Association. / Blanding W.R., Willett P.K., Bar-Shalom Y. // 2007 IEEE Aerospace Conference. - Big Sky, MT, 3-10 March 2007. - P. 1-12. ↑

C8889. Bergin J.S. Evaluation of Knowledge-Aided STAP Using Experimental Data. / Bergin J.S., Kirk D.R., Chaney G., McNeil S., Zulch P.A. // 2007 IEEE Aerospace Conference. - Big Sky, MT, 3-10 March 2007. - P. 1-13. ↑

C8890. Wenchong Xie. Space-Time Adaptive Processing for Non-Sidelooking Airborne Radar with HPRF. / Wenchong Xie, Yongliang Wang. // 2007 IEEE Aerospace Conference. - Big Sky, MT, 3-10 March 2007. - P. 1-7. ↑

C8891. Saxena Akhilesh. RFInD: An RFID-Based System to Manage Virtual Spaces. / Saxena Akhilesh, Ganguly Samrat, Bhatnagar Sudeept, Izmailov Rauf. // 2007. PerCom Workshops '07. Fifth Annual IEEE International Conference on Pervasive Computing and Communications Workshops. - White Plains, NY, 19-23 March 2007. - P. 382-387. ↑

C8892. Brown Alan. Tork: A Variable-Hop Overlay for Heterogeneous Networks. / Brown Alan, Buford John, Kolberg Mario. // 2007. PerCom Workshops '07. Fifth Annual IEEE International Conference on Pervasive Computing and Communications Workshops. - White Plains, NY, 19-23 March 2007. - P. 104-108. ↑

C8893. Doddamani N.D. Design of SPDT Switch, 6 Bit Digital Attenuator, 6 Bit Digital Phase Shifter for L-Band T/R Module using 0.7 μ m GaAs MMIC Technology. / Doddamani N.D., Harishchandra, Nandi A.V. // 2007. ICSCN '07. International Conference on Signal Processing, Communications and Networking. - Chennai, 22-24 Feb. 2007. - P. 302-307. ↑

C8894. Tonnis Marcus. Ontology-Based Pervasive Spatial Knowledge for Car Driver Assistance. / Tonnis Marcus, Klinker Gudrun, Fischer Jan-Gregor. // 2007. PerCom Workshops '07. Fifth Annual IEEE International Conference on Pervasive Computing and Communications Workshops. - White Plains, NY, 19-23 March 2007. - P. 401-406. ↑

C8895. Bonneau R.J. Multiresolution Subspace Beam Formation Using a Partially Coherent Model. 2007 IEEE Aerospace Conference. - Big Sky, MT, 3-10 March 2007. - P. 1-11. ↑

C8896. Rooks J.W. High Performance Space Computing. / Rooks J.W., Linderman R. // 2007 IEEE Aerospace Conference. - Big Sky, MT, 3-10 March 2007. - P. 1-9. ↑

- C8897.** Qasem H. Unscented and Extended Kalman Estimators for non Linear Indoor Tracking Using Distance Measurements. / Qasem H., Reindl L. // 2007. WPNC '07. 4th Workshop on Positioning, Navigation and Communication. - Hannover, 22-22 March 2007. - P. 177-181. ↑
- C8898.** Schelkshorn S. Indoor Navigation Based on Doppler Measurements. / Schelkshorn S., Dettelsen J. // 2007. WPNC '07. 4th Workshop on Positioning, Navigation and Communication. - Hannover, 22-22 March 2007. - P. 37-40. ↑
- C8899.** Lauri A. Analysis and Emulation of FM Radio Signals for Passive Radar. / Lauri A., Colone F., Cardinali R., Bongioanni C., Lombardo P. // 2007 IEEE Aerospace Conference. - Big Sky, MT, 3-10 March 2007. - P. 1-10. ↑
- C8900.** Malas J.A. Information Theory Based Radar Signature Analysis. / Malas J.A., Pasala K.M. // 2007 IEEE Aerospace Conference. - Big Sky, MT, 3-10 March 2007. - P. 1-13. ↑
- C8901.** Sadowy G. Technology Demonstration of Ka-band Digitally-Beam formed Radar for Ice Topography Mapping. / Sadowy G., Heavey B., Moller D., Rignot E., Zawadzki M., Rengarajan S. // 2007 IEEE Aerospace Conference. - Big Sky, MT, 3-10 March 2007. - P. 1-10. ↑
- C8902.** Santori A. A Modulus Compensation Algorithm for Shape Self-Calibration of Paired Sensors Based Antennas. / Santori A., Chabriel G., Barrere J., Jauffret C., Medynski D. // 2007 IEEE Aerospace Conference. - Big Sky, MT, 3-10 March 2007. - P. 1-8. ↑
- C8903.** Moebus M. Three-Dimensional Ultrasound Imaging in Air using a 2D Array on a Fixed Platform. / Moebus M., Zoubir A.M. // 2007. ICASSP 2007. IEEE International Conference on Acoustics, Speech and Signal Processing. - Honolulu, HI, 15-20 April 2007. - Vol. 2. - P. II-961-II-964-961. ↑
- C8904.** Yuanwei Jin. TR-SAR: Time Reversal Target Focusing in Spotlight SAR. / Yuanwei Jin, Moura J.M.F. // 2007. ICASSP 2007. IEEE International Conference on Acoustics, Speech and Signal Processing. - Honolulu, HI, 15-20 April 2007. - Vol. 2. - P. II-957-II-960-957. ↑
- C8905.** Bin Liu. Blind Adaptive Algorithm for M-Ary Distributed Detection. / Bin Liu, Jeremic A., Kon Max Wong. // 2007. ICASSP 2007. IEEE International Conference on Acoustics, Speech and Signal Processing. - Honolulu, HI, 15-20 April 2007. - Vol. 2. - P. II-1025-II-1028-1025. ↑
- C8906.** Ahmad F. High-Resolution Imaging using Capon Beamformers for Urban Sensing Applications. / Ahmad F., Amin M.G. // 2007. ICASSP 2007. IEEE International Conference on Acoustics, Speech and Signal Processing. - Honolulu, HI, 15-20 April 2007. - Vol. 2. - P. II-985-II-988-985. ↑
- C8907.** Chun-Yang Chen. A Subspace Method for MIMO Radar Space-Time Adaptive Processing. / Chun-Yang Chen, Vaidyanathan P.P. // 2007. ICASSP 2007. IEEE International Conference on Acoustics, Speech and Signal Processing. - Honolulu, HI, 15-20 April 2007. - Vol. 2. - P. II-925-II-928-925. ↑
- C8908.** Chin-Heng Lim. Non-Linear Prediction of Inverse Covariance Matrix for Stap. / Chin-Heng Lim, Chong-Meng Samson See, Mulgrew B. // 2007. ICASSP 2007. IEEE International Conference on Acoustics, Speech and Signal Processing. - Honolulu, HI, 15-20 April 2007. - Vol. 2. - P. II-921-II-924-921. ↑
- C8909.** Fabrizio G.A. GLRT-Based Adaptive Doppler Processing for HF Radar Systems. / Fabrizio G.A., Farina A. // 2007. ICASSP 2007. IEEE International Conference on Acoustics, Speech and Signal Processing. - Honolulu, HI, 15-20 April 2007. - Vol. 2. - P. II-949-II-952-949. ↑
- C8910.** Coker J.D. Characteristic Phase E-Sequences in Efficient Pulse-Compression Methods using Discrete Wavelet Decomposition. / Coker J.D., Tewfik A.H. // 2007. ICASSP 2007. IEEE International Conference on Acoustics, Speech and Signal Processing. - Honolulu, HI, 15-20 April 2007. - Vol. 2. - P. II-945-II-948-945. ↑
- C8911.** Marple S.L. Multi-Channel Parametric Estimator Fast Block Matrix Inverses. / Marple S.L., Corbell P.M., Rangaswamy M. // 2007. ICASSP 2007. IEEE International Conference on Acoustics, Speech and Signal Processing. - Honolulu, HI, 15-20 April 2007. - Vol. 2. - P. II-1137-II-1140-1137. ↑
- C8912.** Wanjun Zhi. Near-Field Source Localization via Symmetric Subarrays. / Wanjun Zhi, Chia M.Y.-W. // 2007. ICASSP 2007. IEEE International Conference on Acoustics, Speech and Signal Processing. - Honolulu, HI, 15-20 April 2007. - Vol. 2. - P. II-1121-II-1124-1121. ↑

- C8913.** Vincent F. Synthetic Aperture Radar Demonstration Kit for Signal Processing Education. / Vincent F., Mouton B., Chaumette E., Nouals C., Besson O. // 2007. ICASSP 2007. IEEE International Conference on Acoustics, Speech and Signal Processing. - Honolulu, HI, 15-20 April 2007. - Vol. 3. - P. III-709-III-712-709. ↑
- C8914.** Shuangqing Wei. Spreading Sequence-Based Non-coherent Sensor Fusion and its Resulting Large Deviation Exponents. 2007. ICASSP 2007. IEEE International Conference on Acoustics, Speech and Signal Processing. - Honolulu, HI, 15-20 April 2007. - Vol. 3. - P. III-177-III-180-177. ↑
- C8915.** Bin Yang. Different Sensor Placement Strategies for TDOA Based Localization. 2007. ICASSP 2007. IEEE International Conference on Acoustics, Speech and Signal Processing. - Honolulu, HI, 15-20 April 2007. - Vol. 2. - P. II-1093-II-1096-1093. ↑
- C8916.** Subramanian A. Blind Identification and Linear Quadratic Frequency Invariant Beamforming Based Angle of Arrival Estimation. 2007. ICASSP 2007. IEEE International Conference on Acoustics, Speech and Signal Processing. - Honolulu, HI, 15-20 April 2007. - Vol. 2. - P. II-1077-II-1080-1077. ↑
- C8917.** Tong Zhao. Adaptive Polarized Waveform Design for Target Tracking using Electromagnetic Vector Sensors. / Tong Zhao, Hurtado M., Nehorai A. // 2007. ICASSP 2007. IEEE International Conference on Acoustics, Speech and Signal Processing. - Honolulu, HI, 15-20 April 2007. - Vol. 2. - P. II-1117-II-1120-1117. ↑
- C8918.** Morelande M.R. Performance Bounds and Algorithms for Tracking with a Radar Array. / Morelande M.R., Suvarova S., Moran B. // 2007. ICASSP 2007. IEEE International Conference on Acoustics, Speech and Signal Processing. - Honolulu, HI, 15-20 April 2007. - Vol. 2. - P. II-1105-II-1108-1105. ↑
- C8919.** Luzhou Xu. Waveform Optimization for MIMO Radar: A Cramér-Rao Bound Based Study. / Luzhou Xu, Jian Li, Stoica P., Forsythe K.W., Bliss D.W. // 2007. ICASSP 2007. IEEE International Conference on Acoustics, Speech and Signal Processing. - Honolulu, HI, 15-20 April 2007. - Vol. 2. - P. II-917-II-920-917. ↑
- C8920.** Durand R. SAR Processor based on a CFAR Signal or Interference Subspace Detector Matched to Man Made Target Detection in a Forest. / Durand R., Ginolhac G., Thirion L., Forster P. // 2007. ICASSP 2007. IEEE International Conference on Acoustics, Speech and Signal Processing. - Honolulu, HI, 15-20 April 2007. - Vol. 2. - P. II-293-II-296-293. ↑
- C8921.** Kennedy H.L. Detecting and Tracking Moving Objects in Sequences of Color Images. 2007. ICASSP 2007. IEEE International Conference on Acoustics, Speech and Signal Processing. - Honolulu, HI, 15-20 April 2007. - Vol. 1. - P. I-1197-I-1200-1197. ↑
- C8922.** Latombe G. Incremental Learning of Stochastic Grammars with Graphical EM in Radar Electronic Support. / Latombe G., Granger E., Dilkes F.A. // 2007. ICASSP 2007. IEEE International Conference on Acoustics, Speech and Signal Processing. - Honolulu, HI, 15-20 April 2007. - Vol. 2. - P. II-301-II-304-301. ↑
- C8923.** Lunden J. Scaled Conjugate Gradient Method for Radar Pulse Modulation Estimation. / Lunden J., Koivunen V. // 2007. ICASSP 2007. IEEE International Conference on Acoustics, Speech and Signal Processing. - Honolulu, HI, 15-20 April 2007. - Vol. 2. - P. II-297-II-300-297. ↑
- C8924.** Gurbuz A.C. Detecting Curved Underground Tunnels using Partial Radon Transforms. / Gurbuz A.C., McClellan J.H., Scott W.R. // 2007. ICASSP 2007. IEEE International Conference on Acoustics, Speech and Signal Processing. - Honolulu, HI, 15-20 April 2007. - Vol. 1. - P. I-545-I-548-545. ↑
- C8925.** Yarman C.E. Inversion of Circular Averages using the Funk Transform. / Yarman C.E., Yazici B. // 2007. ICASSP 2007. IEEE International Conference on Acoustics, Speech and Signal Processing. - Honolulu, HI, 15-20 April 2007. - Vol. 1. - P. I-541-I-544-541. ↑
- C8926.** Junjie Wu. Signal Properties of Squint Mode Bistatic SAR. / Junjie Wu, Yulin Huang, Jintao Xiong, Jianyu Yang. // 2007. ICASSP 2007. IEEE International Conference on Acoustics, Speech and Signal Processing. - Honolulu, HI, 15-20 April 2007. - Vol. 1. - P. I-881-I-884-881. ↑
- C8927.** Xin Kang. Clustering Polarimetric SAR Image Under Deorientation Theory. / Xin Kang, Chongzhao Han, Feng Xu. // 2007. ICASSP 2007. IEEE International Conference on Acoustics, Speech and Signal Processing. - Honolulu, HI, 15-20 April 2007. - Vol. 1. - P. I-877-I-880-877. ↑

- C8928.** Yao Xie. Optimal Array Pattern Synthesis via Matrix Weighting. / Yao Xie, Jian Li, Xiayu Zheng, Ward J. // 2007. ICASSP 2007. IEEE International Conference on Acoustics, Speech and Signal Processing. - Honolulu, HI, 15-20 April 2007. - Vol. 2. - P. II-885-II-888-885. ↑
- C8929.** Wai Yie Leong. Blind Extraction of Noisy Events using Nonlinear Predictor. / Wai Yie Leong, Mandic D.P., Wei Liu. // 2007. ICASSP 2007. IEEE International Conference on Acoustics, Speech and Signal Processing. - Honolulu, HI, 15-20 April 2007. - Vol. 2. - P. II-657-II-660-657. ↑
- C8930.** Neyt X. Maximum Likelihood Range Dependence Compensation for STAP. / Neyt X., Acheroy M., Verly J.G. // 2007. ICASSP 2007. IEEE International Conference on Acoustics, Speech and Signal Processing. - Honolulu, HI, 15-20 April 2007. - Vol. 2. - P. II-913-II-916-913. ↑
- C8931.** Leshem A. Adaptive Radar Waveform Design for Multiple Targets: Computational Aspects. / Leshem A., Naparstek O., Nehorai A. // 2007. ICASSP 2007. IEEE International Conference on Acoustics, Speech and Signal Processing. - Honolulu, HI, 15-20 April 2007. - Vol. 2. - P. II-909-II-912-909. ↑
- C8932.** Bachmann S. Spectral Analysis of Polarimetric Weather Radar Data with Multiple Processes in a Resolution Volume. / Bachmann S., DeBrunner V., Zrnic D., Yearly M. // 2007. ICASSP 2007. IEEE International Conference on Acoustics, Speech and Signal Processing. - Honolulu, HI, 15-20 April 2007. - Vol. 2. - P. II-309-II-312-309. ↑
- C8933.** Aittomaki T. Low-Complexity Method for Transmit Beamforming in MIMO Radars. / Aittomaki T., Koivunen V. // 2007. ICASSP 2007. IEEE International Conference on Acoustics, Speech and Signal Processing. - Honolulu, HI, 15-20 April 2007. - Vol. 2. - P. II-305-II-308-305. ↑
- C8934.** Kyu-Hwa Jeong. The Fast Correntropy Mace Filter. / Kyu-Hwa Jeong, Seungju Han, Principe J.C. // 2007. ICASSP 2007. IEEE International Conference on Acoustics, Speech and Signal Processing. - Honolulu, HI, 15-20 April 2007. - Vol. 2. - P. II-613-II-616-613. ↑
- C8935.** Buhren M. A Global Motion Model for Target Tracking in Automotive Applications. / Buhren M., Bin Yang. // 2007. ICASSP 2007. IEEE International Conference on Acoustics, Speech and Signal Processing. - Honolulu, HI, 15-20 April 2007. - Vol. 2. - P. II-313-II-316-313. ↑
- C8936.** Mazlouman S.J. A Low-Power CMOS Modulator for Ultra-Wideband Transmitters. / Mazlouman S.J., Mahanfar A., Mirabbasi S. // 2007. CCECE 2007. Canadian Conference on Electrical and Computer Engineering. - Vancouver, BC, 22-26 April 2007. - P. 381-384. ↑
- C8937.** Nickel U. Detection with Adaptive Arrays with Irregular Digital Subarrays. 2007 IEEE Radar Conference. - Boston, MA, 17-20 April 2007. - P. 635-640. ↑
- C8938.** Paine A.S. An Adaptive Beamforming Technique for Countering Synthetic Aperture Radar (SAR) Jamming Threats. 2007 IEEE Radar Conference. - Boston, MA, 17-20 April 2007. - P. 630-634. ↑
- C8939.** Abramovich Y.I. Time-varying autoregressive adaptive filtering for airborne radar applications. / Abramovich Y.I., Rangaswamy M., Johnson B.A., Corbell P., Spencer N. // 2007 IEEE Radar Conference. - Boston, MA, 17-20 April 2007. - P. 653-657. ↑
- C8940.** Montlouis W. Direction of Arrival and Angular Velocities (DOAV) Estimation using Minimum Variance Beamforming. / Montlouis W., Comely P.-R.J. // 2007 IEEE Radar Conference. - Boston, MA, 17-20 April 2007. - P. 641-646. ↑
- C8941.** Wang Yu. Spotlight SAR Raw Data Simulation Using Frequency Scaling Algorithm. / Wang Yu, Zhang Zhi-min, Deng Yun-kai. // 2007 IEEE Radar Conference. - Boston, MA, 17-20 April 2007. - P. 608-613. ↑
- C8942.** Shengchun Zhao. Self-Organizing Adaptive Radar Space-Time Adaptive Processing. 2007 IEEE Radar Conference. - Boston, MA, 17-20 April 2007. - P. 596-601. ↑
- C8943.** De Maio A. Adaptive Radar Detection: A Bayesian Approach. / De Maio A., Farina A., Foglia G. // 2007 IEEE Radar Conference. - Boston, MA, 17-20 April 2007. - P. 624-629. ↑
- C8944.** Pourrostam J. Super-Resolution Direction-of-Arrival Estimation via Blind Signal Separation Methods. / Pourrostam J., Zekavat S.A., Pourkhaatoun M. // 2007 IEEE Radar Conference. - Boston, MA, 17-20 April 2007. ↑

- P. 614-617. ↑

C8945. Picciolo M.L. Fast-Converging Adaptive Cascaded Cancellers Using A Novel Soft-Weighting and Reiteration(SWR) Technique. / Picciolo M.L., Gerlach K. // 2007 IEEE Radar Conference. - Boston, MA, 17-20 April 2007. - P. 756-761. ↑

C8946. Huaijin Gu. Angle-Tracking Adaptive Array -- Adaptive-Adaptive Array Processing. 2007 IEEE Radar Conference. - Boston, MA, 17-20 April 2007. - P. 750-755. ↑

C8947. Da-Zheng Feng. An Efficient Identification Algorithm for FIR Filtering with Noisy Data. / Da-Zheng Feng, Wei Xing Zheng. // 2007. ISCAS 2007. IEEE International Symposium on Circuits and Systems. - New Orleans, LA, 27-30 May 2007. - P. 829-832. ↑

C8948. Hjortland H.A. Thresholded samplers for UWB impulse radar. / Hjortland H.A., Wisland D.T., Lande T.S., Limbodal C., Meisal K. // 2007. ISCAS 2007. IEEE International Symposium on Circuits and Systems. - New Orleans, LA, 27-30 May 2007. - P. 1210-1213. ↑

C8949. Yao Xie. Adaptive WEighting of Signals via One Matrix Entity (AWESOME). / Yao Xie, Jian Li, Ward J. // 2007 IEEE Radar Conference. - Boston, MA, 17-20 April 2007. - P. 699-705. ↑

C8950. Xi-Zeng Dai. High Resolution Frequency MIMO Radar. / Xi-Zeng Dai, Jia Xu, Ying-Ning Peng. // 2007 IEEE Radar Conference. - Boston, MA, 17-20 April 2007. - P. 693-698. ↑

C8951. Dan Lu. A Two Stage GPS Anti-jamming processor for Interference Suppression and Multipath mitigation. / Dan Lu, Renbiao Wu, Zhigang Su, Wei Huang. // 2007 IEEE Radar Conference. - Boston, MA, 17-20 April 2007. - P. 746-749. ↑

C8952. Zebker H. InSAR Remote Sensing Over Decorrelating Terrains: Persistent Scattering Methods. / Zebker H., Shankar P., Hooper A. // 2007 IEEE Radar Conference. - Boston, MA, 17-20 April 2007. - P. 717-722. ↑

C8953. Junjie Wu. Range Migration Algorithm in Bistatic SAR Based on Squint Mode. / Junjie Wu, Yulin Huang, Jintao Xiong, Jianyu Yang. // 2007 IEEE Radar Conference. - Boston, MA, 17-20 April 2007. - P. 579-584. ↑

C8954. Cantrell B. Affordable Naval Surveillance Radar Concept. / Cantrell B., Pollock M., Alter J. // 2007 IEEE Radar Conference. - Boston, MA, 17-20 April 2007. - P. 414-420. ↑

C8955. Colone F. A spectral slope-based approach for mitigating bistatic STAP clutter dispersion. / Colone F., Fornari M., Lombardo P. // 2007 IEEE Radar Conference. - Boston, MA, 17-20 April 2007. - P. 408-413. ↑

C8956. Yong Wu. Clutter Rank of Multi-dimensional Sparse Array Radar. 2007 IEEE Radar Conference. - Boston, MA, 17-20 April 2007. - P. 463-468. ↑

C8957. Stafford W.K. MESAR, Sampson & Radar Technology for BMD. 2007 IEEE Radar Conference. - Boston, MA, 17-20 April 2007. - P. 437-442. ↑

C8958. Frazer G.J. Spatially Waveform Diverse Radar: Perspectives for High Frequency OTHR. / Frazer G.J., Abramovich Y.I., Johnson B.A. // 2007 IEEE Radar Conference. - Boston, MA, 17-20 April 2007. - P. 385-390. ↑

C8959. Wang J. Music-Enhanced CFAR for High Frequency Over-the-Horizon Radar. / Wang J., Riddolls R.J., Ponsford A.M. // 2007 IEEE Radar Conference. - Boston, MA, 17-20 April 2007. - P. 379-384. ↑

C8960. Boryssenko A.O. Ultra-Wide Band Near-Field Imaging System. / Boryssenko A.O., Craeye C., Schaubert D.H. // 2007 IEEE Radar Conference. - Boston, MA, 17-20 April 2007. - P. 402-407. ↑

C8961. Dawber W.N. Modelling of Adaptive Multifunction Radars for Trials Planning and Acceptance. / Dawber W.N., Hunter G.J., Branson J.A. // 2007 IEEE Radar Conference. - Boston, MA, 17-20 April 2007. - P. 396-401. ↑

C8962. Xian-Jun Shen. Time-Domain Planar Near-Field Measurement Simulation for Wideband RCS and Antenna. / Xian-Jun Shen, Xu Chen, Yong-Qing Zou, Yu-Mei Zhang. // 2007 IEEE Radar Conference. - Boston,

MA, 17-20 April 2007. - P. 535-540. ↑

C8963. Johnsen T. Hitchhiking bistatic radar: principles, processing and experimental findings. / Johnsen T., Olsen K.E. // 2007 IEEE Radar Conference. - Boston, MA, 17-20 April 2007. - P. 518-523. ↑

C8964. Karasev P.A. Obtaining a 35x Speedup in 2D Phase Unwrapping Using Commodity Graphics Processors. / Karasev P.A., Campbell D.P., Richards M.A. // 2007 IEEE Radar Conference. - Boston, MA, 17-20 April 2007. - P. 574-578. ↑

C8965. Ram S.S. Human Tracking Using Doppler Processing and Spatial Beamforming. / Ram S.S., Yang Li, Lin A., Hao Ling. // 2007 IEEE Radar Conference. - Boston, MA, 17-20 April 2007. - P. 546-551. ↑

C8966. Madanizadeh S.A. Signal Detection using the Correlation Coefficient in Fractal Geometry. / Madanizadeh S.A., Nayebi M.M. // 2007 IEEE Radar Conference. - Boston, MA, 17-20 April 2007. - P. 481-486. ↑

C8967. Jamali M.M. DSP Based Implementation of Direction of Arrival for Wideband Sources. / Jamali M.M., Affo A., Wilkins N., Mumford P.D., Hahn K. // 2007 IEEE Radar Conference. - Boston, MA, 17-20 April 2007. - P. 475-480. ↑

C8968. Nienhaus K. An Experimental Study on Using Electronically Scanning Microwave Radar Systems on Surface Mining Machines. / Nienhaus K., Winkel R., Mayer W., Gronau A., Menzel W. // 2007 IEEE Radar Conference. - Boston, MA, 17-20 April 2007. - P. 509-512. ↑

C8969. Jangal F. Wavelets: a Versatile Tool for the High Frequency Surface Wave Radar. / Jangal F., Saillant S., Helier M. // 2007 IEEE Radar Conference. - Boston, MA, 17-20 April 2007. - P. 497-502. ↑

C8970. Johnson B.A. Adaptive estimation of unknown phase offset between sub-arrays in distributed aperture systems. / Johnson B.A., Abramovich Y.I. // 2007. IDC '07 Information, Decision and Control. - Adelaide, Qld., 12-14 Feb. 2007. - P. 34-36. ↑

C8971. Anderson S. Optimising bistatic HF radar configurations for target and environmental signature discrimination. 2007. IDC '07 Information, Decision and Control. - Adelaide, Qld., 12-14 Feb. 2007. - P. 29-33. ↑

C8972. Davey S.J. Tracking Possibly Unresolved Targets with PMHT. 2007. IDC '07 Information, Decision and Control. - Adelaide, Qld., 12-14 Feb. 2007. - P. 47-52. ↑

C8973. Kronhamn T. Angle-Only Tracking of Manoeuvring Targets using Double Sets of Multiple Range Models and Probability Mass Diffusion. 2007. IDC '07 Information, Decision and Control. - Adelaide, Qld., 12-14 Feb. 2007. - P. 41-46. ↑

C8974. Coleman C. A Kirchhoff Integral Approach to Radar Propagation Modelling and its Application to the Estimation of Clutter. 2007 IEEE Radar Conference. - Boston, MA, 17-20 April 2007. - P. 1004-1007. ↑

C8975. Pappert S.A. RF Photonics for Radar Front-Ends. / Pappert S.A., Krantz B. // 2007 IEEE Radar Conference. - Boston, MA, 17-20 April 2007. - P. 965-970. ↑

C8976. Yu Teng. Netted Radar Theory and Experiments. / Yu Teng, Doughty S., Woodbridge K., Griffiths H., Baker C. // 2007. IDC '07 Information, Decision and Control. - Adelaide, Qld., 12-14 Feb. 2007. - P. 23-28. ↑

C8977. Griffiths H. The Signal and Interference Environment in Passive Bistatic Radar. / Griffiths H., Baker C. // 2007. IDC '07 Information, Decision and Control. - Adelaide, Qld., 12-14 Feb. 2007. - P. 1-10. ↑

C8978. Dogancay K. Optimal Receiver Trajectories for Scan-Based Radar Localization. 2007. IDC '07 Information, Decision and Control. - Adelaide, Qld., 12-14 Feb. 2007. - P. 88-93. ↑

C8979. Leong A.S. Error Exponents for Neyman-Pearson Detection of Markov Chains in Noise. / Leong A.S., Dey S., Evans J.S. // 2007. IDC '07 Information, Decision and Control. - Adelaide, Qld., 12-14 Feb. 2007. - P. 94-99. ↑

C8980. Xuezhi Wang. Enhanced Multi-Target Tracking with Doppler Measurements. / Xuezhi Wang, Musicki D., Ellem R., Fletcher F. // 2007. IDC '07 Information, Decision and Control. - Adelaide, Qld., 12-14 Feb. 2007. - P. 53-58. ↑

- C8981.** Bahari M.H. High Maneuver Target Tracking Based on Combined Kalman Filter and Fuzzy Logic. / Bahari M.H., Karsaz A., Khaloozadeh H. // 2007. IDC '07 Information, Decision and Control. - Adelaide, Qld., 12-14 Feb. 2007. - P. 59-64. ↑
- C8982.** Finn A. Design Challenges for an Autonomous Cooperative of UAVs. / Finn A., Kabacinski K., Drake S.P. // 2007. IDC '07 Information, Decision and Control. - Adelaide, Qld., 12-14 Feb. 2007. - P. 160-169. ↑
- C8983.** Marsh L. UAV Team Formation for Emitter Geolocation. / Marsh L., Gossink D., Drake S.P., Calbert G. // 2007. IDC '07 Information, Decision and Control. - Adelaide, Qld., 12-14 Feb. 2007. - P. 176-181. ↑
- C8984.** Okello N. Track Registration for Multistatic Radars with Multipath. 2007. IDC '07 Information, Decision and Control. - Adelaide, Qld., 12-14 Feb. 2007. - P. 118-123. ↑
- C8985.** Roughan M. Data fusion without data fusion: localization and tracking without sharing sensitive information. / Roughan M., Arnold J. // 2007. IDC '07 Information, Decision and Control. - Adelaide, Qld., 12-14 Feb. 2007. - P. 136-141. ↑
- C8986.** Knepp D.L. Ionospheric Propagation Effects on Ground and Space Based Radars. / Knepp D.L., Hausman M.A. // 2007 IEEE Radar Conference. - Boston, MA, 17-20 April 2007. - P. 916-921. ↑
- C8987.** Fowler J.D. Characterization of Zero-Doppler Clutter Removal Techniques for ISAR Applications. / Fowler J.D., Temple M.A., Havrilla M.J., Akerson J.J. // 2007 IEEE Radar Conference. - Boston, MA, 17-20 April 2007. - P. 800-804. ↑
- C8988.** Overrein O. A New Method for Compensation of SAR Range Cell Migration Based on the Pulse Z-Transform. 2007 IEEE Radar Conference. - Boston, MA, 17-20 April 2007. - P. 778-782. ↑
- C8989.** Goodman J. A New Approach to Achieving High-Performance Power Amplifier Linearization. / Goodman J., Miller B., Raz G., Herman M. // 2007 IEEE Radar Conference. - Boston, MA, 17-20 April 2007. - P. 840-845. ↑
- C8990.** Roman J.R. Polarization Diversity Using Mutual Information. / Roman J.R., Garnham J.W., Antonik P. // 2007 IEEE Radar Conference. - Boston, MA, 17-20 April 2007. - P. 828-833. ↑
- C8991.** Berger S.D. Map-Aided Secondary Data Selection. / Berger S.D., Melvin W.L., Showman G.A. // 2007 IEEE Radar Conference. - Boston, MA, 17-20 April 2007. - P. 762-767. ↑
- C8992.** Da-Zheng Feng. Adaptive IIR Filtering via a Recursive Total Instrumental Variable Algorithm. / Da-Zheng Feng, Wei Xing Zheng. // 2007. ISCAS 2007. IEEE International Symposium on Circuits and Systems. - New Orleans, LA, 27-30 May 2007. - P. 105-108. ↑
- C8993.** Neyt X. Maximum-likelihood based range-dependence compensation for coherent multistatic STAP radar. / Neyt X., Acheroy M., Verly J.G. // 2007 IEEE Radar Conference. - Boston, MA, 17-20 April 2007. - P. 772-777. ↑
- C8994.** Burintramart S. Multiple Constraint Space-Time Adaptive Processing Using Direct Data Domain Least Squares (D3LS) Approach. / Burintramart S., Yilmazer N., Sarkar T.K. // 2007 IEEE Radar Conference. - Boston, MA, 17-20 April 2007. - P. 768-771. ↑
- C8995.** Savage C.O. Accurate Target Geolocation using Cooperative Observers. / Savage C.O., La Scala B.F. // 2007. IDC '07 Information, Decision and Control. - Adelaide, Qld., 12-14 Feb. 2007. - P. 248-253. ↑
- C8996.** Sun-Mog Hong. Parameter Optimization for Load-Optimal Agile Beam Radar Tracking. / Sun-Mog Hong, Won-Yong Choi, Young-Hun Jung. // 2007. IDC '07 Information, Decision and Control. - Adelaide, Qld., 12-14 Feb. 2007. - P. 320-325. ↑
- C8997.** Jiaxue Liu. Training Method for Ground Bounce Removal with Ground Penetrating Radar. / Jiaxue Liu, Renbiao Wu. // 2007 IEEE Radar Conference. - Boston, MA, 17-20 April 2007. - P. 875-878. ↑
- C8998.** Hmam H. Mobile Platform Self-Localization. 2007. IDC '07 Information, Decision and Control. - Adelaide, Qld., 12-14 Feb. 2007. - P. 242-247. ↑

- C8999.** De Maio A. Challenging Issues in Multichannel Radar Array Processing. / De Maio A., Fabrizio G.A., Farina A., Melvin W.L., Timmoneri L. // 2007 IEEE Radar Conference. - Boston, MA, 17-20 April 2007. - P. 856-862. ↑
- C9000.** Akhtar J. An ECCM Scheme for Orthogonal Independent Range-Focusing of Real and False Targets. 2007 IEEE Radar Conference. - Boston, MA, 17-20 April 2007. - P. 846-849. ↑
- C9001.** Ristic B. Cramér-Rao Bound for Multiple Target Tracking Using Intensity Measurements. / Ristic B., Morelande M. // 2007. IDC '07 Information, Decision and Control. - Adelaide, Qld., 12-14 Feb. 2007. - P. 354-359. ↑
- C9002.** Perry R.P. Coherent Integration With Range Migration Using Keystone Formatting. / Perry R.P., DiPietro R.C., Fante R.L. // 2007 IEEE Radar Conference. - Boston, MA, 17-20 April 2007. - P. 863-868. ↑
- C9003.** Frazer G.J. Forward-based Receiver Augmentation for OTHR. 2007 IEEE Radar Conference. - Boston, MA, 17-20 April 2007. - P. 373-378. ↑
- C9004.** Duque S. Application of the Coherent Pixels Technique (CPT) to urban monitoring. / Duque S., Mallorqui J.J., Blanco P., Monells D. // 2007 Urban Remote Sensing Joint Event. - Paris, 11-13 April 2007. - P. 1-7. ↑
- C9005.** Fornaro G. Multipass SAR Processing for Urbanized Areas Imaging and Deformation Monitoring at Small and Large Scales. / Fornaro G., Pauciuolo A., Serafino F. // 2007 Urban Remote Sensing Joint Event. - Paris, 11-13 April 2007. - P. 1-7. ↑
- C9006.** Lee Sang-Gug. UWB and mm-Wave Communications Systems. / Lee Sang-Gug, Gharpurey Ranjit. // 2007. ISSCC 2007. Digest of Technical Papers. IEEE International Solid-State Circuits Conference. - San Francisco, CA, USA, 11-15 Feb. 2007. - P. 110-111. ↑
- C9007.** Soergel U. Extraction of Bridge Features from high-resolution InSAR Data and optical Images. / Soergel U., Thiele A., Gross H., Thoennessen U. // 2007 Urban Remote Sensing Joint Event. - Paris, 11-13 April 2007. - P. 1-6. ↑
- C9008.** Le Moigne V. Statistical Polygonal Snakes for 3D building reconstruction using High Resolution SAR data. / Le Moigne V., Tupin F. // 2007 Urban Remote Sensing Joint Event. - Paris, 11-13 April 2007. - P. 1-5. ↑
- C9009.** Matsuoka M. Damage mapping for the 2004 Niigata-ken Chuetsu earthquake using Radarsat images. / Matsuoka M., Yamazaki F., Ohkura H. // 2007 Urban Remote Sensing Joint Event. - Paris, 11-13 April 2007. - P. 1-5. ↑
- C9010.** Perissin D. Target recognition by means of spaceborne C-band SAR data. / Perissin D., Prati C. // 2007 Urban Remote Sensing Joint Event. - Paris, 11-13 April 2007. - P. 1-5. ↑
- C9011.** Lombardini F. Towards a Complete Processing Chain of Multibaseline Airborne InSAR Data for Layover Scatterers Separation. / Lombardini F., Rossing L., Ender J., Viviani F. // 2007 Urban Remote Sensing Joint Event. - Paris, 11-13 April 2007. - P. 1-6. ↑
- C9012.** Trotta S. A 79GHz SiGe-Bipolar Spread-Spectrum TX for Automotive Radar. / Trotta S., Knapp H., Dibra D., Aufinger K., Meister T.F., Bock J., Simburger W., Scholtz A.L. // 2007. ISSCC 2007. Digest of Technical Papers. IEEE International Solid-State Circuits Conference. - San Francisco, CA, 11-15 Feb. 2007. - P. 430-613. ↑
- C9013.** Schiltz Tom. Broadband RF and Radar. / Schiltz Tom, Halonen Kari. // 2007. ISSCC 2007. Digest of Technical Papers. IEEE International Solid-State Circuits Conference. - San Francisco, CA, USA, 11-15 Feb. 2007. - P. 416-417. ↑
- C9014.** Wenming Shi. A Novel Positioning Algorithm in Wireless Sensor Networks Based on Indoor Connective Information. / Wenming Shi, Chuanhe Huang, Mingkai Shao, Dandan Song, Yong Cheng, Ying Long. // 2007. SAS '07. IEEE Sensors Applications Symposium. - San Diego, CA, 6-8 Feb. 2007. - P. 1-5. ↑
- C9015.** Money D.G. Intelligent Radar Management Techniques in High Frequency Surface Wave Radar. / Money D.G., Emery D.J., Dickel G. // 2007 3rd Institution of Engineering and Technology Seminar on Intelligent Sensor Management. - London, 10-10 May 2007. - P. 1-11. ↑

- C9016.** Niknejad Ali. mm-Wave Tranceivers and Building Blocks. / Niknejad Ali, Sakai Hiroyuki. // 2007. ISSCC 2007. Digest of Technical Papers. IEEE International Solid-State Circuits Conference. - San Francisco, CA, USA, 11-15 Feb. 2007. - P. 186-187. ↑
- C9017.** Hoon Hee Chung. A Bandpass $\Delta\Sigma$ DDFS-Driven 19GHz Frequency Synthesizer for FMCW Automotive Radar. / Hoon Hee Chung, Lyles U., Copani T., Bakaloglu B., Kiaei S. // 2007. ISSCC 2007. Digest of Technical Papers. IEEE International Solid-State Circuits Conference. - San Francisco, CA, 11-15 Feb. 2007. - P. 126-591. ↑
- C9018.** Mayr P. A 90GHz 65nm CMOS Injection-Locked Frequency Divider. / Mayr P., Weyers C., Langmann U. // 2007. ISSCC 2007. Digest of Technical Papers. IEEE International Solid-State Circuits Conference. - San Francisco, CA, 11-15 Feb. 2007. - P. 198-596. ↑
- C9019.** KaChun Kwok. A 23-to-29GHz Differentially Tuned Varactorless VCO in 0.13 μ m CMOS. / KaChun Kwok, Long J.R., Pekarik J.J. // 2007. ISSCC 2007. Digest of Technical Papers. IEEE International Solid-State Circuits Conference. - San Francisco, CA, 11-15 Feb. 2007. - P. 194-596. ↑
- C9020.** Haala N. Cell Decomposition for Building Model Generation at Different Scales. / Haala N., Becker S., Kada M. // 2007 Urban Remote Sensing Joint Event. - Paris, 11-13 April 2007. - P. 1-6. ↑
- C9021.** Jerabek J. Moving Target UWB Radar Demonstration using Real-Time Sampling. / Jerabek J., Dvorak D., Mrkvica J., Siki R. // 2007. 17th International Conference Radioelektronika. - Brno, 24-25 April 2007. - P. 1-4. ↑
- C9022.** Jozsa L. Doppler Radar System for Small Objects Localization. / Jozsa L., Sebesta J. // 2007. 17th International Conference Radioelektronika. - Brno, 24-25 April 2007. - P. 1-4. ↑
- C9023.** Siki R. Comparison of Pulse and Continuous Wave Propagation Through the Wall. / Siki R., Dvorak D., Mrkvica J., Jerabek J. // 2007. 17th International Conference Radioelektronika. - Brno, 24-25 April 2007. - P. 1-4. ↑
- C9024.** Cerny P. Simulated Transient Radiation Characteristics of Optimized Ultra Wideband Printed Dipole Antennas. / Cerny P., Mazanek M. // 2007. 17th International Conference Radioelektronika. - Brno, 24-25 April 2007. - P. 1-6. ↑
- C9025.** Kurrant D.J. Tumor Estimation In Tissue Sensing Adaptive Radar (TSAR) Signals. / Kurrant D.J., Fear E.C., Westwick D.T. // 2007. CCECE 2007. Canadian Conference on Electrical and Computer Engineering. - Vancouver, BC, 22-26 April 2007. - P. 860-863. ↑
- C9026.** Errington A.F.C. Vehicle Positioning in Underground Mines. / Errington A.F.C., Daku B.L.F., Prugger A.F. // 2007. CCECE 2007. Canadian Conference on Electrical and Computer Engineering. - Vancouver, BC, 22-26 April 2007. - P. 586-589. ↑
- C9027.** Hafez A.S. A New Differential Clutter Map Processing in Modern Surveillance Radars. 2007. NRSC 2007. National Radio Science Conference. - Cairo, 13-15 March 2007. - P. 1-6. ↑
- C9028.** Emery M. IEEE 802.11 WLAN Based Real-Time Location Tracking in Indoor and Outdoor Environments. / Emery M., Denko M.K. // 2007. CCECE 2007. Canadian Conference on Electrical and Computer Engineering. - Vancouver, BC, 22-26 April 2007. - P. 1062-1065. ↑
- C9029.** Franceschetti G. Simulation Tools for Interpretation of High Resolution SAR Images of Urban Areas. / Franceschetti G., Guida R., Iodice A., Riccio D., Ruello G., Stilla U. // 2007 Urban Remote Sensing Joint Event. - Paris, 11-13 April 2007. - P. 1-5. ↑
- C9030.** Gamba P. Raster to Vector in 2D Urban Data. / Gamba P., Dell'Acqua F., Lisini G. // 2007 Urban Remote Sensing Joint Event. - Paris, 11-13 April 2007. - P. 1-6. ↑
- C9031.** Sugumaran R. Object-Oriented Classification of LIDAR-Fused Hyperspectral Imagery for Tree Species Identification in an Urban Environment. / Sugumaran R., Voss M. // 2007 Urban Remote Sensing Joint Event. - Paris, 11-13 April 2007. - P. 1-6. ↑
- C9032.** Tarsha-Kurdi F. Joint combination of point cloud and DSM for 3D building reconstruction using

airborne laser scanner data. / Tarsha-Kurdi F., Landes T., Grussenmeyer P. // 2007 Urban Remote Sensing Joint Event. - Paris, 11-13 April 2007. - P. 1-7. ↑

C9033. Ya-Qiu Jin. Reconstruction of the 3D Stereo Buildings from Polarimetric SAR Images in Two Converse Flights. / Ya-Qiu Jin, Eryan Dai. // 2007 Urban Remote Sensing Joint Event. - Paris, 11-13 April 2007. - P. 1-5. ↑

C9034. Sauer S. 3D Visualisation and Physical Feature Extraction of Urban Areas using Multibaseline POL-InSAR Data at L-Band. / Sauer S., Ferro-Famil L., Pottier E., Reigber A. // 2007 Urban Remote Sensing Joint Event. - Paris, 11-13 April 2007. - P. 1-5. ↑

C9035. Weihing D. An Integral Detection Scheme for Moving Object Indication in Dual-Channel High Resolution Spaceborne SAR Data. / Weihing D., Hinz S., Meyer F., Suchandt S., Bamler R. // 2007 Urban Remote Sensing Joint Event. - Paris, 11-13 April 2007. - P. 1-6. ↑

C9036. Del Frate F. Urban Land Cover in Rome, Italy, monitored by single-parameter multi-temporal SAR images. / Del Frate F., Pacifici F., Solimini D. // 2007 Urban Remote Sensing Joint Event. - Paris, 11-13 April 2007. - P. 1-5. ↑

C9037. Stakkeland M. Estimating instantaneous false alarm rate in a CFAR system by Bayesian and empirical Bayesian methods. / Stakkeland M., Li X.R. // 2007 IEEE Radar Conference. - Boston, MA, 17-20 April 2007. - P. 314-319. ↑

C9038. Jie Yang. Cancellation of Doppler Distortion in Pulse Compression for Targets Moving in an Arbitrary Direction. / Jie Yang, Sarkar T.K. // 2007 IEEE Radar Conference. - Boston, MA, 17-20 April 2007. - P. 297-301. ↑

C9039. Yong Liu. Computationally Efficient Angle Estimation Using Maximum Likelihood In A Digital Beam-Forming Radar. / Yong Liu, Wong G., Kennedy W. // 2007 IEEE Radar Conference. - Boston, MA, 17-20 April 2007. - P. 337-342. ↑

C9040. Pourkhaatoun M. A Novel High Resolution ICA-Based TOA Estimation Technique. / Pourkhaatoun M., Zekavat S.A., Pourrostam J. // 2007 IEEE Radar Conference. - Boston, MA, 17-20 April 2007. - P. 320-324. ↑

C9041. Jie Yang. A New Doppler-Tolerant Polyphase Pulse Compression Codes Based on Hyperbolic Frequency Modulation. / Jie Yang, Sarkar T.K. // 2007 IEEE Radar Conference. - Boston, MA, 17-20 April 2007. - P. 265-270. ↑

C9042. Lu X. A Co-Channel Signal Detector Based on Phase Tracking for Pulse Doppler Radar. / Lu X., Kiriln R.L., Wang J. // 2007 IEEE Radar Conference. - Boston, MA, 17-20 April 2007. - P. 254-258. ↑

C9043. Xia T.Q. Adaptive Regularized FOCUSS Algorithm. / Xia T.Q., Zheng Y., Wan Q., Wang X.G. // 2007 IEEE Radar Conference. - Boston, MA, 17-20 April 2007. - P. 282-284. ↑

C9044. Sammartino P.F. Adaptive MIMO radar system in clutter. / Sammartino P.F., Baker C.J., Griffiths H.D. // 2007 IEEE Radar Conference. - Boston, MA, 17-20 April 2007. - P. 276-281. ↑

C9045. Razavi B. CMOS Transceivers at 60 GHz and Beyond1. 2007. ISCAS 2007. IEEE International Symposium on Circuits and Systems. - New Orleans, LA, 27-30 May 2007. - P. 1983-1986. ↑

C9046. Wai Yie Leong. Noisy Component Extraction (Noice). / Wai Yie Leong, Mandic D.P. // 2007. ISCAS 2007. IEEE International Symposium on Circuits and Systems. - New Orleans, LA, 27-30 May 2007. - P. 3243-3246. ↑


C9047. Johnson B.A. Elevation Filtering in Wide-Aperture HF Skywave Radar. / Johnson B.A., Abramovich Y.I. // 2007 IEEE Radar Conference. - Boston, MA, 17-20 April 2007. - P. 367-372. ↑


C9048. Pados D.A. Short-data-record Adaptive Detection. / Pados D.A., Karystinos G.N., Batalama S.N., Matyjas J.D. // 2007 IEEE Radar Conference. - Boston, MA, 17-20 April 2007. - P. 357-361. ↑


C9049. Capraro C.T. Knowledge Aided Detection and Tracking. / Capraro C.T., Capraro G.T., Wicks M.C. // 2007 IEEE Radar Conference. - Boston, MA, 17-20 April 2007. - P. 352-356. ↑


- C9050.** Krikorian K.V. Inverse Precision Velocity Update for Monopulse Calibration. / Krikorian K.V., Yu-Hong Kwong, Rosen R.A. // 2007 IEEE Radar Conference. - Boston, MA, 17-20 April 2007. - P. 348-351. ↑
- C9051.** Pastorino M. Detection of defects in wood slabs by using a microwave imaging technique. / Pastorino M., Salvade A., Monleone R., Bartesaghi T., Bozza G., Randazzo A. // 2007. IMTC 2007. IEEE Instrumentation and Measurement Technology Conference Proceedings. - Warsaw, 1-3 May 2007. - P. 1-6. ↑
- C9052.** Barnes W.J. An Overlapped Scan Method for Enhanced 3D Radome Characterization. / Barnes W.J., Yeary M., Olivero K., Phillips J., Ibrahim T. // 2007. IMTC 2007. IEEE Instrumentation and Measurement Technology Conference Proceedings. - Warsaw, 1-3 May 2007. - P. 1-4. ↑
- C9053.** Loizos A. Ground Penetrating Radar: A Smart Sensor for the Evaluation of the Railway Trackbed. / Loizos A., Plati C. // 2007. IMTC 2007. IEEE Instrumentation and Measurement Technology Conference Proceedings. - Warsaw, 1-3 May 2007. - P. 1-6. ↑
- C9054.** Peer U. Compression Waveforms for Non-Coherent Radar. / Peer U., Levanon N. // 2007 IEEE Radar Conference. - Boston, MA, 17-20 April 2007. - P. 104-109. ↑
- C9055.** Kebo A. Ambiguity and sidelobe behavior of CAZAC coded waveforms. / Kebo A., Konstantinidis I., Benedetto J.J., Dellomo M.R., Sieracki J.M. // 2007 IEEE Radar Conference. - Boston, MA, 17-20 April 2007. - P. 99-103. ↑
- C9056.** Blunt S.D. Achieving Real-Time Efficiency for Adaptive Radar Pulse Compression. / Blunt S.D., Higgins T. // 2007 IEEE Radar Conference. - Boston, MA, 17-20 April 2007. - P. 116-121. ↑
- C9057.** Nunn C. Performance of Pulse Compression Code and Filter Pairs Optimized For Loss and Integrated Sidelobe Level. / Nunn C., Kretschmer F.F. // 2007 IEEE Radar Conference. - Boston, MA, 17-20 April 2007. - P. 110-115. ↑
- C9058.** Brookner E. Phased-Array and Radar Breakthroughs. 2007 IEEE Radar Conference. - Boston, MA, 17-20 April 2007. - P. 37-42. ↑
- C9059.** Loomis J.M. Army Radar Requirements for the 21st Century. 2007 IEEE Radar Conference. - Boston, MA, 17-20 April 2007. - P. 1-6. ↑
- C9060.** Hall T.M. Statistics of Clutter Residue in MTI Radars with IF Limiting. / Hall T.M., Shrader W.W. // 2007 IEEE Radar Conference. - Boston, MA, 17-20 April 2007. - P. 81-87. ↑
- C9061.** Adrian O. Future Surface Radar technology: From Air Defence to Air and Missile Defence. 2007 IEEE Radar Conference. - Boston, MA, 17-20 April 2007. - P. 49-54. ↑
- C9062.** Xia T.Q. 2-D Angle of Arrival Estimation with Two Parallel Uniform Linear Arrays for Coherent Signals. / Xia T.Q., Zheng Y., Wan Q., Wang X.G. // 2007 IEEE Radar Conference. - Boston, MA, 17-20 April 2007. - P. 244-247. ↑
- C9063.** Shackelford A.K. Adaptive Pulse Compression: Preliminary Experimental Measurements. / Shackelford A.K., de Graaf J., Talapatra S., Blunt S.D., Gerlach K. // 2007 IEEE Radar Conference. - Boston, MA, 17-20 April 2007. - P. 234-237. ↑
- C9064.** Noyer J.-C. Sequential Monte-Carlo techniques and vision-based methods for road signs detection. / Noyer J.-C., Lanvin P., Yeary M., Yan Zhai. // 2007. IMTC 2007. IEEE Instrumentation and Measurement Technology Conference Proceedings. - Warsaw, 1-3 May 2007. - P. 1-6. ↑
- C9065.** Andrzej M. Development problems of large area, web accessible, environmental pollution monitoring system. / Andrzej M., Andrzej K., Zbigniew S., Piotr P. // 2007. IMTC 2007. IEEE Instrumentation and Measurement Technology Conference Proceedings. - Warsaw, 1-3 May 2007. - P. 1-5. ↑
- C9066.** Fan Mingyi. MonoPulse Angle Measurement For An Airborne Side-Looking Phased Array PD Radar. / Fan Mingyi, Ge Jianjun, Qiu Wei, Wu Manqing. // 2007 IEEE Radar Conference. - Boston, MA, 17-20 April 2007. - P. 209-211. ↑
- C9067.** Keel B.M. A Comprehensive Review of Quasi-Orthogonal Waveforms. / Keel B.M., Heath T.H. // 2007 ↑


IEEE Radar Conference. - Boston, MA, 17-20 April 2007. - P. 122-127. 


C9068. Goldman G.H. Tracking High-Speed Targets Using a Pulse Doppler Stepped-Frequency Waveform. 2007 IEEE Radar Conference. - Boston, MA, 17-20 April 2007. - P. 229-233. 


C9069. Lin Tang. The Frequency Selection Consideration for the Low Orbit Space Based Radar. / Lin Tang, Zhongxian Chen. // 2007 IEEE Radar Conference. - Boston, MA, 17-20 April 2007. - P. 212-217. 


C9070. Gurbuz S.Z. Spectrogram-Based Methods for Human Identification in Single-Channel SAR Data. / Gurbuz S.Z., Melvin W.L., Williams D.B. // 2007. SIU 2007. IEEE 15th Signal Processing and Communications Applications. - Eskisehir, 11-13 June 2007. - P. 1-4. 


C9071. Milewski A. Amplitude Weighting of Linear Frequency Modulated Chirp Signals. / Milewski A., Sedek E., Gawor S. // 2007. SIU 2007. IEEE 15th Signal Processing and Communications Applications. - Eskisehir, 11-13 June 2007. - P. 1-4. 


C9072. Huang Yuchun. CZT-Based High Performance Frequency Estimation. / Huang Yuchun, Huang Zailu, Huang Benxiong, Xu Shuhua. // 2007. SIU 2007. IEEE 15th Signal Processing and Communications Applications. - Eskisehir, 11-13 June 2007. - P. 1-4. 


C9073. Gurbuz A.C. Detecting Features using Random Sample Theory. / Gurbuz A.C., McClellan J.H., Scott W.R. // 2007. SIU 2007. IEEE 15th Signal Processing and Communications Applications. - Eskisehir, 11-13 June 2007. - P. 1-4. 


C9074. Xylomenos G. Reducing the Transmission Power Requirements of the Multimedia Broadcast/Multicast Service. / Xylomenos G., Tsakanikas V., Polyzos G.C. // 2007. 16th IST Mobile and Wireless Communications Summit. - Budapest, 1-5 July 2007. - P. 1-5. 


C9075. Brooker G. Prototype of a Reconfigurable 94GHz Smart Radar Sensor. / Brooker G., McCouat N. // 2007. AusWireless 2007. The 2nd International Conference on Wireless Broadband and Ultra Wideband Communications. - Sydney, NSW, 27-30 Aug. 2007. - P. 26. 


C9076. Demirkol A. A Holographic Approach to Image Processing. / Demirkol A., Woodley R.S., Acar L. // 2007. SIU 2007. IEEE 15th Signal Processing and Communications Applications. - Eskisehir, 11-13 June 2007. - P. 1-4. 


C9077. Secmen M. Electromagnetic Target Recognition with the Fused MUSIC Spectrum Matrix Method: Applications and Performance Analysis for Incomplete Frequency Data. / Secmen M., Ekmekci E., Turhan-Sayan G. // 2007. SIU 2007. IEEE 15th Signal Processing and Communications Applications. - Eskisehir, 11-13 June 2007. - P. 1-4. 


C9078. Sonmez T. Development of a Software Testbed for Integrated Navigation Systems. / Sonmez T., Aslan G. // 2007. SIU 2007. IEEE 15th Signal Processing and Communications Applications. - Eskisehir, 11-13 June 2007. - P. 1-4. 

C9079. Varshney K.R. A Sparse Signal Representation-based Approach to Image Formation and Anisotropy Determination in Wide-Angle Radar. / Varshney K.R., Cetin M., Fisher J.W., Willsky A.S. // 2007. SIU 2007. IEEE 15th Signal Processing and Communications Applications. - Eskisehir, 11-13 June 2007. - P. 1-4. 

C9080. Coskun O. Adaptive Censored CFAR Performance in Nonhomogeneous Correlated Clutter. / Coskun O., Uner M. // 2007. SIU 2007. IEEE 15th Signal Processing and Communications Applications. - Eskisehir, 11-13 June 2007. - P. 1-4. 

C9081. Kocaadam Engin. LPI Radar Sinyallerinin Ozimge Yaklasimi ile Siniflandirilmesi Classification of LPI Radar Signals via Eigenimage Approach. / Kocaadam Engin, Ozkcazanc Yacup. // 2007. SIU 2007. IEEE 15th Signal Processing and Communications Applications. - Eskisehir, 11-13 June 2007. - P. 1-4. 

C9082. Ince T. On Performance of S-band FMCW Radar For Atmospheric Observation. 2007. SIU 2007. IEEE 15th Signal Processing and Communications Applications. - Eskisehir, 11-13 June 2007. - P. 1-4. 

C9083. Makal S. Classification of Cylindrical Targets above Perfectly Conducting Flat Surfaces by Statistical Neural Networks. / Makal S., Kizilay A. // 2007. SIU 2007. IEEE 15th Signal Processing and Communications Applications. - Eskisehir, 11-13 June 2007. - P. 1-4. 

Applications. - Eskisehir, 11-13 June 2007. - P. 1-3.

C9084. Yilmaz K. Non-Parametric Radar Detection In Homogeneous And Non-Homogeneous Environments. / Yilmaz K., Uner M. // 2007. SIU 2007. IEEE 15th Signal Processing and Communications Applications. - Eskisehir, 11-13 June 2007. - P. 1-4. ↑

C9085. Filik T. Design of V-shaped Array Geometry. / Filik T., Tuncer T.E., Yasar T.K. // 2007. SIU 2007. IEEE 15th Signal Processing and Communications Applications. - Eskisehir, 11-13 June 2007. - P. 1-4. ↑

C9086. Johnson D. Experimental Comparison of Two Automotive Radars for use on an Autonomous Vehicle. 2007. AusWireless 2007. The 2nd International Conference on Wireless Broadband and Ultra Wideband Communications. - Sydney, NSW, 27-30 Aug. 2007. - P. 28. ↑

C9087. Xiao Jin-Jun. Optimal Beampattern Synthesis of a Polarized Array. / Xiao Jin-Jun, Nehorai Arye. // 2007. SSP '07. IEEE/SP 14th Workshop on Statistical Signal Processing. - Madison, WI, USA, 26-29 Aug. 2007. - P. 463-467. ↑

C9088. Yang Yang. MIMO Radarwaveform Design. / Yang Yang, Blum Rick S. // 2007. SSP '07. IEEE/SP 14th Workshop on Statistical Signal Processing. - Madison, WI, USA, 26-29 Aug. 2007. - P. 468-472. ↑

C9089. Bachmann Svetlana. Detection of Small Aircraft with Doppler Weather Radar. / Bachmann Svetlana, DeBrunner Victor, Zrnic Dusan. // 2007. SSP '07. IEEE/SP 14th Workshop on Statistical Signal Processing. - Madison, WI, USA, 26-29 Aug. 2007. - P. 443-447. ↑

C9090. Bhattacharya Sujit. Fast Encoding of Synthetic Aperture Radar Raw Data using Compressed Sensing. / Bhattacharya Sujit, Blumensath Thomas, Mulgrew Bernard, Davies Mike. // 2007. SSP '07. IEEE/SP 14th Workshop on Statistical Signal Processing. - Madison, WI, USA, 26-29 Aug. 2007. - P. 448-452. ↑

C9091. Gurbuz Ali Cafer. Feature Detection in Images by Adaptive Random Sampling. / Gurbuz Ali Cafer, McClellan James H., Scott Waymond R. // 2007. SSP '07. IEEE/SP 14th Workshop on Statistical Signal Processing. - Madison, WI, USA, 26-29 Aug. 2007. - P. 591-595. ↑

C9092. Abileah R. Mapping Ocean Currents With IKONOS. OCEANS 2007-Europe. - Aberdeen, 18-21 June 2007. - P. 1-5. ↑

C9093. Pezeshki Ali. Doppler Resilient Golay Complementary Pairs for Radar. / Pezeshki Ali, Calderbank Robert, Howard Stephen D., Moran William. // 2007. SSP '07. IEEE/SP 14th Workshop on Statistical Signal Processing. - Madison, WI, USA, 26-29 Aug. 2007. - P. 483-487. ↑

C9094. Orguner Umut. Statistical Characteristics of Harris Corner Detector. / Orguner Umut, Gustafsson Fredrik. // 2007. SSP '07. IEEE/SP 14th Workshop on Statistical Signal Processing. - Madison, WI, USA, 26-29 Aug. 2007. - P. 571-575. ↑















C9095. Bidon Stephanie. Bayesian Covariance Matrix Estimation with Non-Homogeneous Snapshots. / Bidon Stephanie, Besson Olivier, Tournet Jean-Yves. // 2007. SSP '07. IEEE/SP 14th Workshop on Statistical Signal Processing. - Madison, WI, USA, 26-29 Aug. 2007. - P. 39-43. ↑

C9096. Yeste-Ojeda Omar A. Limitations of Spectral Correlation Based Detectors. / Yeste-Ojeda Omar A., Grajal Jesus. // 2007. SSP '07. IEEE/SP 14th Workshop on Statistical Signal Processing. - Madison, WI, USA, 26-29 Aug. 2007. - P. 244-248. ↑

C9097. Mostafa S.A. Estimation of the Hit Probability and its Effect on the Performance of Frequency Hopping Radar System. 2007. AusWireless 2007. The 2nd International Conference on Wireless Broadband and Ultra Wideband Communications. - Sydney, NSW, 27-30 Aug. 2007. - P. 75. ↑

C9098. Sammoura F. A Plastic W-Band MEMS Phase Shifter. / Sammoura F., Liwei Lin. // 2007. TRANSDUCERS 2007. International Solid-State Sensors, Actuators and Microsystems Conference. - Lyon, 10-14 June 2007. - P. 647-650. ↑

C9099. Jin Yuanwei. Time Reversal Target Classification from Scattered Radiation. / Jin Yuanwei, Moura Jose M.F., Jiang Yi, Stancil Dan, O'Donoghue Nick. // 2007. SSP '07. IEEE/SP 14th Workshop on Statistical Signal Processing. - Madison, WI, USA, 26-29 Aug. 2007. - P. 317-321. ↑

- C9100.** Bachmann Svetlana. Adaptive Technique for Clutter and Noise Supression in Weather Radar Exposes Weak Echoes Over an Urban Area. / Bachmann Svetlana, DeBrunner Victor, Zrnic Dusan, Yeary Mark. // 2007. SSP '07. IEEE/SP 14th Workshop on Statistical Signal Processing. - Madison, WI, USA, 26-29 Aug. 2007. - P. 438-442. 
- C9101.** Li Y. Maximizing Detection Performance with waveform Design for Sensing in Heavy Sea Clutter. / Li Y., Sira S. P., Papandreou-Suppappola A., Cochran D., Scharf L. L. // 2007. SSP '07. IEEE/SP 14th Workshop on Statistical Signal Processing. - Madison, WI, USA, 26-29 Aug. 2007. - P. 249-253. 
- C9102.** Shichuan Du. Improved Tracking of Airborne Targets Hidden in the Blind Doppler using Particle Filter. / Shichuan Du, Zhiguo Shi, Wei Zang, Kangsheng Chen. // 2007. SSP '07. IEEE/SP 14th Workshop on Statistical Signal Processing. - Madison, WI, USA, 26-29 Aug. 2007. - P. 289-293. 
- C9103.** Lodha S.K. Aerial Lidar Data Classification using AdaBoost. / Lodha S.K., Fitzpatrick D.M., Helmbold D.P. // 2007. 3DIM 07. Sixth International Conference on 3-D Digital Imaging and Modeling. - Montreal, QC, 21-23 Aug. 2007. - P. 435-442. 
- C9104.** Yeung W.M. Wireless LAN Positioning based on Received Signal Strength from Mobile device and Access Points. / Yeung W.M., Ng J.K. // 2007. RTCSA 2007. 13th IEEE International Conference on Embedded and Real-Time Computing Systems and Applications. - Daegu, 21-24 Aug. 2007. - P. 131-137. 
- C9105.** Buhren M. Extension of Automotive Radar Target List Simulation to consider further Physical Aspects. / Buhren M., Bin Yang. // 2007. ITST '07. 7th International Conference on ITS Telecommunications. - Sophia Antipolis, 6-8 June 2007. - P. 1-6. 
- C9106.** Taati B. Automatic Registration for Model Building using Variable Dimensional Local Shape Descriptors. / Taati B., Bondy M., Jasiobedzki P., Greenspan M. // 2007. 3DIM 07. Sixth International Conference on 3-D Digital Imaging and Modeling. - Montreal, QC, 21-23 Aug. 2007. - P. 265-272. 
- C9107.** Zhiguo He. A Fast SAR Target Recognition Approach Using PCA Features. / Zhiguo He, Jun Lu, Gangyao Kuang. // 2007. ICIG 2007. Fourth International Conference on Image and Graphics. - Sichuan, 22-24 Aug. 2007. - P. 580-585. 
- C9108.** Xiangqian Chen. Modeling Attack Distribution in Sensor Networks. / Xiangqian Chen, Makki K., Kang Yen, Pissinou N. // 2007. INSS '07. Fourth International Conference on Networked Sensing Systems. - Braunschweig, 6-8 June 2007. - P. 98-101. 
- C9109.** Huo Zhihua. The Application of KL Transform to Remove Direct Wave in Ground Penetrating Radar Records. / Huo Zhihua, Wang Minghui. // 2007. ICIG 2007. Fourth International Conference on Image and Graphics. - Sichuan, 22-24 Aug. 2007. - P. 133-138. 
- C9110.** Peng-wei Wang. Weighted Support Vector Machine Segmentation of SAR Images Based on MARMA model. / Peng-wei Wang, Xiu-qing Wu, Shan Yu. // 2007. ICIG 2007. Fourth International Conference on Image and Graphics. - Sichuan, 22-24 Aug. 2007. - P. 347-352. 
- C9111.** Volosyuk V.K. Spectrum Analysis of Radar Signals with Usage of Kravchenko Windows. / Volosyuk V.K., Pavlikov V.V., Sevostjanov J.V. // 2007. MSMW '07. The Sixth International Kharkov Symposium on Physics and Engineering of Microwaves, Millimeter and Submillimeter Waves and Workshop on Terahertz Technologies. - Kharkov, 25-30 June 2007. - Vol. 2. - P. 941-943. 
- C9112.** Potapov A.A. Conception of Scaling, Fractional Dimension and Deterministic Chaos in Radio Physics and Radio Electronics. 2007. MSMW '07. The Sixth International Kharkov Symposium on Physics and Engineering of Microwaves, Millimeter and Submillimeter Waves and Workshop on Terahertz Technologies. - Kharkov, 25-30 June 2007. - Vol. 2. - P. 965-967. 
- C9113.** Varavin A.V. The Signal Digital Processing in the Millimeter Band FMCW Radar. / Varavin A.V., Ermak G.P., Vasilev A.S., Popov I.V. // 2007. MSMW '07. The Sixth International Kharkov Symposium on Physics and Engineering of Microwaves, Millimeter and Submillimeter Waves and Workshop on Terahertz Technologies. - Kharkov, 25-30 June 2007. - Vol. 2. - P. 858-860. 
- C9114.** Churikov D.V. Construction of 2D Filters for Digital Signal and Image Processing on Basis of the Kravchenko Weight Functions and R-Operations in Millimeter Range. 2007. MSMW '07. The Sixth International

Kharkov Symposium on Physics and Engineering of Microwaves, Millimeter and Submillimeter Waves and Workshop on Terahertz Technologies. - Kharkov, 25-30 June 2007. - Vol. 2. - P. 935-937. ↑

C9115. Xinhan Huang. Mobile Robot's Map Reconstruction Based on DSMT and Fast-Hough Self-Localization. / Xinhan Huang, Xinde Li, Zuyu Wu, Min Wang. // 2007. ICIA '07. International Conference on Information Acquisition. - Seogwipo-si, 8-11 July 2007. - P. 590-595. ↑

C9116. Buhren M. Initialization Procedure for Radar Target Tracking without Object Movement Constraints. / Buhren M., Bin Yang. // 2007. ITST '07. 7th International Conference on ITS Telecommunications. - Sophia Antipolis, 6-8 June 2007. - P. 1-6. ↑

C9117. Kravchenko V.F. The Contour Analysis of Low-Sized Complex-Shaped Objects Based on R-Functions, Atomic Functions and Wavelets. / Kravchenko V.F., Kravchenko O.V., Yurin A.V. // 2007. MSMW '07. The Sixth International Kharkov Symposium on Physics and Engineering of Microwaves, Millimeter and Submillimeter Waves and Workshop on Terahertz Technologies. - Kharkov, 25-30 June 2007. - Vol. 2. - P. 974-976. ↑

C9118. Golikov V. CFAR Matched Detector of Signals in Autoregressive Noise. / Golikov V., Moreno A.C., Lebedeva O., Ponomaryov V. // 2007. MSMW '07. The Sixth International Kharkov Symposium on Physics and Engineering of Microwaves, Millimeter and Submillimeter Waves and Workshop on Terahertz Technologies. - Kharkov, 25-30 June 2007. - Vol. 2. - P. 995-997. ↑

C9119. Satake S. Brownie: Searching Concealed Real World Artifacts. / Satake S., Kawashima H., Imai M. // 2007. INSS '07. Fourth International Conference on Networked Sensing Systems. - Braunschweig, 6-8 June 2007. - P. 159-162. ↑

C9120. Zhaonian Zhang. Acoustic Micro-Doppler Gait Signatures of Humans and Animals. / Zhaonian Zhang, Pouliquen P., Waxman A., Andreou A.G. // 2007. CISS '07. 41st Annual Conference on Information Sciences and Systems. - Baltimore, MD, 14-16 March 2007. - P. 627-630. ↑

C9121. Akkus I.E. Peer-to-peer Multipoint Conferencing using Layered Video: Multi-objective Optimization for Extra Requests. / Akkus I.E., Ozkasap O., Civanlar M.R. // 2007. SIU 2007. IEEE 15th Signal Processing and Communications Applications. - Eskisehir, 11-13 June 2007. - P. 1-4. ↑

C9122. Stralka J.P. Constant Envelope Orthogonal Frequency-Division Multiplexing Phase Modulation for Radar Pulse Compression. / Stralka J.P., Meyer G.G.L. // 2007. CISS '07. 41st Annual Conference on Information Sciences and Systems. - Baltimore, MD, 14-16 March 2007. - P. 558. ↑

C9123. Ananthasubramaniam B. Collector Receiver Design for Data Collection and Localization in Sensor-driven Networks. / Ananthasubramaniam B., Madhow U. // 2007. CISS '07. 41st Annual Conference on Information Sciences and Systems. - Baltimore, MD, 14-16 March 2007. - P. 591-596. ↑

C9124. Arslan Z. Constant False Alarm Rate (CFAR) Detection in Weibull Environment. / Arslan Z., Uner M.K. // 2007. SIU 2007. IEEE 15th Signal Processing and Communications Applications. - Eskisehir, 11-13 June 2007. - P. 1-4. ↑

C9125. Bozdogan A.O. Application of Topographic State Constraints in Ground Target Tracking. / Bozdogan A.O., Efe M. // 2007. SIU 2007. IEEE 15th Signal Processing and Communications Applications. - Eskisehir, 11-13 June 2007. - P. 1-4. ↑

C9126. Doyuran U.Q. Detection in Heterogeneous Radar Clutter. / Doyuran U.Q., Tanikr Y. // 2007. SIU 2007. IEEE 15th Signal Processing and Communications Applications. - Eskisehir, 11-13 June 2007. - P. 1-4. ↑

C9127. Karabatak M. Texture Classification by Using Wavelet Domain Association Rules. / Karabatak M., Sengur A., Ince M.C. // 2007. SIU 2007. IEEE 15th Signal Processing and Communications Applications. - Eskisehir, 11-13 June 2007. - P. 1-4. ↑

C9128. Anatoliy. Method of Compound Object Identification in Microwave Band by Scattered Field Interference Pattern. / Anatoliy, Lobur M. // 2007. CADSM '07. 9th International Conference-The Experience of Designing and Applications of CAD Systems in Microelectronics. - Lviv-Polyana, 19-24 Feb. 2007. - P. 106-108. ↑

C9129. Wagner K.T. Proportionate-Type Steepest Descent and NLMS Algorithms. / Wagner K.T., Doroslovacki M.I. // 2007. CISS '07. 41st Annual Conference on Information Sciences and Systems. - Baltimore, MD, 14-16

March 2007. - P. 47-50. ↑

C9130. Prudyus I.N. Analysis of scattered by rain precipitation radar signals in MMW-band. / Prudyus I.N., Zakharia Y.A., Kobylanska O.V., Mymrikov D.O. // 2007. CADSM '07. 9th International Conference-The Experience of Designing and Applications of CAD Systems in Microelectronics. - Lviv-Polyana, 19-24 Feb. 2007. - P. 35-38. ↑

C9131. Zubkov A. Echo Signal Frequency Averaging as Method of Forming the Stable Criteria of Compound Object Identification in Microwave Band. / Zubkov A., Lobur M. // 2007. CADSM '07. 9th International Conference-The Experience of Designing and Applications of CAD Systems in Microelectronics. - Lviv-Polyana, 19-24 Feb. 2007. - P. 98-100. ↑

C9132. Yi Sun. Approach to Optimum Performance in Random Spreading CDMA by Linear-Complex LAS Detectors. 2007. CISS '07. 41st Annual Conference on Information Sciences and Systems. - Baltimore, MD, 14-16 March 2007. - P. 196-201. ↑

C9133. Yeshwantpur A. The Estimation and Removal of Unknown Background Signatures in Raman-Shift Spectra via SWTPE. / Yeshwantpur A., Morris J.M. // 2007. CISS '07. 41st Annual Conference on Information Sciences and Systems. - Baltimore, MD, 14-16 March 2007. - P. 462. ↑

C9134. Dayanik S. Joint Detection and Identification of an Unobservable Change in the Distribution of a Random Sequence. / Dayanik S., Goulding C., Poor H.V. // 2007. CISS '07. 41st Annual Conference on Information Sciences and Systems. - Baltimore, MD, 14-16 March 2007. - P. 68-73. ↑

C9135. Yang Yang. Minimax Robust Waveform Design for MIMO Radar in the Presence of PSD Uncertainties. / Yang Yang, Blum R.S. // 2007. CISS '07. 41st Annual Conference on Information Sciences and Systems. - Baltimore, MD, 14-16 March 2007. - P. 154-159. ↑

C9136. Legris M. Comparison between DPCA Algorithm and Inertial Navigation on the Ixsea Shadows SAS. / Legris M., Jean F. // OCEANS 2007-Europe. - Aberdeen, 18-21 June 2007. - P. 1-6. ↑

C9137. Danyu Zhang. Design of a Communication Service System for Vehicle Monitoring. / Danyu Zhang, Hongfeng Gao. // 2007 IEEE International Conference on Automation and Logistics. - Jinan, 18-21 Aug. 2007. - P. 894-897. ↑

C9138. Yuqi Hu. The Design of Vehicle Emergent Calling System Based on GPRS. / Yuqi Hu, Yang Liu, Huaquan Zang. // 2007 IEEE International Conference on Automation and Logistics. - Jinan, 18-21 Aug. 2007. - P. 1220-1224. ↑

C9139. Banks Jerry. Past, Present and Future of RFID. 2007 IEEE International Conference on Automation and Logistics. - Jinan, China, 18-21 Aug. 2007. - P. nil26-nil27. ↑

C9140. Xianwei Zeng. A New Guidance Law Based on Information Fusion and Optimal Control of Structure Stochastic Jump System. / Xianwei Zeng, Yangwang Fang, Youli Wu, Hongqiang Wang, Xiaobin Zhou, Zenghui Xie. // 2007 IEEE International Conference on Automation and Logistics. - Jinan, 18-21 Aug. 2007. - P. 624-627. ↑

C9141. {no data available}. Agenda-at-a-glance. 2007. International Waveform Diversity and Design Conference. - Pisa, Italy, 4-8 June 2007. - P. vi. ↑

C9142. Landi L. Time-orthogonal-waveform-space-time adaptive processing for distributed aperture radars. / Landi L., Adve R.S. // 2007. International Waveform Diversity and Design Conference. - Pisa, 4-8 June 2007. - P. 13-17. ↑

C9143. Jinhua Wu. Research on Cooperative Control Method of Saturation Attack. / Jinhua Wu, Peibei Ma, Jun Ji. // 2007 IEEE International Conference on Automation and Logistics. - Jinan, 18-21 Aug. 2007. - P. 1409-1413. ↑

C9144. Kashani A.H. Real-Time Robot Joint Variable Extraction from a Laser Scanner. / Kashani A.H., Owen W.S., Lawrence P.D., Hall R.A. // 2007 IEEE International Conference on Automation and Logistics. - Jinan, 18-21 Aug. 2007. - P. 2994-2999. ↑

C9145. Liu Xiankang. Satellite Recognition Base on Wavelet Denoising in HRRP Feature Extraction. / Liu

Xiankang, Gao Meiguo, Fu Xiongjun. // 2007. ICIEA 2007. 2nd IEEE Conference on Industrial Electronics and Applications. - Harbin, 23-25 May 2007. - P. 2530-2533. ↑

C9146. Jin Tao. Polarimetric Monopulse Radar Intelligent Emulator. / Jin Tao, Qi Xiaohui, Yuan Shuqing, Qiao Xiaolin, Zhang Min, Zhang Qunxing. // 2007. ICIEA 2007. 2nd IEEE Conference on Industrial Electronics and Applications. - Harbin, 23-25 May 2007. - P. 2660-2665. ↑

C9147. Zhu Ming. A Novel Feature Extraction Approach for Radar Emitter Signals. / Zhu Ming, Jin Weidong, Pu Yunwei, Hu Laizhao. // 2007. ICIEA 2007. 2nd IEEE Conference on Industrial Electronics and Applications. - Harbin, 23-25 May 2007. - P. 1785-1789. ↑

C9148. Li Lin-lin. A SAR Imaging Algorithm with Stronger Anti-jamming Capability. / Li Lin-lin, Li Jing-wen. // 2007. ICIEA 2007. 2nd IEEE Conference on Industrial Electronics and Applications. - Harbin, 23-25 May 2007. - P. 2189-2192. ↑

C9149. Guigen Nie. Research on LEO Satellites Time Synchronization with GPS Receivers Onboard. / Guigen Nie, Falin Wu, Kefei Zhang, Bo Zhu. // 2007 Joint with the 21st European Frequency and Time Forum. IEEE International Frequency Control Symposium. - Geneva, May 29 2007-June 1 2007. - P. 896-900. ↑

C9150. Puranen M. Improved Methods for Frequency Measurement of Short Radar Pulses. / Puranen M., Eskelinen P. // 2007 Joint with the 21st European Frequency and Time Forum. IEEE International Frequency Control Symposium. - Geneva, May 29 2007-June 1 2007. - P. 970-973. ↑

C9151. Jin Tao. Anti-Full Polarization Active Jamming. / Jin Tao, Qi Xiaohui, Qiao Xiaolin, Zhang Min, Yuan Shuqing, Zhang Qunxing. // 2007. ICIEA 2007. 2nd IEEE Conference on Industrial Electronics and Applications. - Harbin, 23-25 May 2007. - P. 2718-2722. ↑

C9152. Boroditsky R. Ultra Low Phase Noise 1 GHz OCXO. / Boroditsky R., Gomez J. // 2007 Joint with the 21st European Frequency and Time Forum. IEEE International Frequency Control Symposium. - Geneva, May 29 2007-June 1 2007. - P. 250-253. ↑

C9153. Soldani F. The benefits of matched illumination for radar detection of ground based targets. / Soldani F., Alabaster C.M. // 2007. International Waveform Diversity and Design Conference. - Pisa, 4-8 June 2007. - P. 23-27. ↑

C9154. Ravenni V. An approach for interference detection and rejection from other sensors by using Hough Transform and image processing. / Ravenni V., Cantini L., Bertacca M. // 2007. International Waveform Diversity and Design Conference. - Pisa, 4-8 June 2007. - P. 136-140. ↑

C9155. Ferrara M. The peak sidelobe distribution for binary codes. / Ferrara M., Kupferschmid M., Coxson G. // 2007. International Waveform Diversity and Design Conference. - Pisa, 4-8 June 2007. - P. 141-144. ↑

C9156. Lu Y.L. Air target detection and tracking using a multi-channel GSM based passive radar. / Lu Y.L., Tan D.K.P., Sun H.B. // 2007. International Waveform Diversity and Design Conference. - Pisa, 4-8 June 2007. - P. 122-126. ↑

C9157. Liu W.X. Optimal sparse waveform design for HFSWR system. / Liu W.X., Lu Y.L., Lesturgie M. // 2007. International Waveform Diversity and Design Conference. - Pisa, 4-8 June 2007. - P. 127-130. ↑

C9158. Coker J.D. Multistatic SAR image reconstruction based on an elliptical-geometry radon transform. / Coker J.D., Tewfik A.H. // 2007. International Waveform Diversity and Design Conference. - Pisa, 4-8 June 2007. - P. 204-208. ↑

C9159. Falk L. Cross-eye jamming of monopulse radar. 2007. International Waveform Diversity and Design Conference. - Pisa, 4-8 June 2007. - P. 209-213. ↑

C9160. Machowski W. Novel pulse-sequences design enables multi-user collision-avoidance vehicular radar. / Machowski W., Koutsogiannis G.S., Ratliff P.A. // 2007. International Waveform Diversity and Design Conference. - Pisa, 4-8 June 2007. - P. 155-159. ↑

C9161. Kwang June Sohn. Multichannel parametric detectors for airborne radar applications. / Kwang June Sohn, Hongbin Li, Himed B., Markow J.S. // 2007. International Waveform Diversity and Design Conference. -

Pisa, 4-8 June 2007. - P. 178-182. ↑

C9162. Magde K.M. Waveforms in virtual tomographic arrays. / Magde K.M., Wicks M.C. // 2007. International Waveform Diversity and Design Conference. - Pisa, 4-8 June 2007. - P. 83-87. ↑

C9163. Capraro G.T. Knowledge base technologies for waveform diversity and electromagnetic compatibility. / Capraro G.T., Bradaric I., Wicks M.C. // 2007. International Waveform Diversity and Design Conference. - Pisa, 4-8 June 2007. - P. 88-92. ↑

C9164. Zito D. Feasibility study of a low-cost system-on-a-chip UWB pulse radar on silicon for the heart monitoring. / Zito D., Pepe D., Neri B., De Rossi D. // 2007. International Waveform Diversity and Design Conference. - Pisa, 4-8 June 2007. - P. 32-36. ↑

C9165. Lock E. Varying FM rates in adaptive processing for distributed radar apertures. / Lock E., Adve R.S. // 2007. International Waveform Diversity and Design Conference. - Pisa, 4-8 June 2007. - P. 74-78. ↑

C9166. Yarman C.E. Waveform design for distributed aperture using Gram-Schmidt orthogonalization. / Yarman C.E., Varslot T., Yazici B., Cheney M. // 2007. International Waveform Diversity and Design Conference. - Pisa, 4-8 June 2007. - P. 111-115. ↑

C9167. Jae Woong Yi. Real-time PRF selection for medium PRF airborne pulsed-doppler radars in tracking phase. / Jae Woong Yi, Young Jin Byun. // 2007. International Waveform Diversity and Design Conference. - Pisa, 4-8 June 2007. - P. 116-121. ↑

C9168. Garnham J.W. How will waveform diversity affect electromagnetic compatibility?. / Garnham J.W., Roman J.R. // 2007. International Waveform Diversity and Design Conference. - Pisa, 4-8 June 2007. - P. 98-101. ↑

C9169. Byung Wook Jung. Discrete Suppression with $\Sigma\Delta$ -STAP. / Byung Wook Jung, Joohwan Chun, Adve R.S., Jonghoon Chun. // 2007. International Waveform Diversity and Design Conference. - Pisa, 4-8 June 2007. - P. 107-110. ↑

C9170. Kohut J.T. A Nested Multi-static HF Radar Testbed for the New York Bight and Beyond. / Kohut J.T., Glenn S.M., Roarty H.J., Schofield O.M. // OCEANS 2007-Europe. - Aberdeen, 18-21 June 2007. - P. 1-3. ↑

C9171. Mellema G.R. A Structured Approach to Passive Sonar Track Association. OCEANS 2007-Europe. - Aberdeen, 18-21 June 2007. - P. 1-6. ↑

C9172. Bilik I. Comparative Theoretical Performance of Maneuverable Unmanned Vehicles versus Conventional Towed-Arrays for Passive Sonar. / Bilik I., Krolik J. // OCEANS 2007-Europe. - Aberdeen, 18-21 June 2007. - P. 1-5. ↑

C9173. Gorski T. Target Detection Using HF Radar Data. / Gorski T., Le Caillec J.-M., Kawalec A., Czarnecki W., Lennon M., Thomas N. // OCEANS 2007-Europe. - Aberdeen, 18-21 June 2007. - P. 1-5. ↑

C9174. Weissman D.E. Measurements of the Effect of Rain-induced Sea Surface Roughness on the Satellite Scatterometer Radar Cross Section. / Weissman D.E., Bourassa M.A. // OCEANS 2007-Europe. - Aberdeen, 18-21 June 2007. - P. 1-4. ↑

C9175. Thevar T. Advances in Lidar Transmitter Sources for Ocean-Atmosphere Remote Sensing. / Thevar T., Boczar B., Rousseva I., Walling J.C., Heller D.F. // OCEANS 2007-Europe. - Aberdeen, 18-21 June 2007. - P. 1-4. ↑

C9176. Arvelyna Y. New Application of Wavelet Transform for Internal Wave Detection SAR and Optical Image: A Case Study in Japan Waters. / Arvelyna Y., Oshima M. // OCEANS 2007-Europe. - Aberdeen, 18-21 June 2007. - P. 1-6. ↑

C9177. Snyder H.D. Satellite Data Visualization on the Ocean Motion Website. / Snyder H.D., Tweedie M.S. // OCEANS 2007-Europe. - Aberdeen, 18-21 June 2007. - P. 1-3. ↑

C9178. Cotton D. MARCOAST-Operational Marine Oil Spill and Water Quality Monitoring Services. OCEANS 2007-Europe. - Aberdeen, 18-21 June 2007. - P. 1-5. ↑

- C9179.** Shay L.K. Resolving Coastal Ocean Eddy Activity in Surface Velocity Signatures from Wellen Radars and an Acoustic Doppler Current Profiler. / Shay L.K., Parks A.B., Haus B.K., Martinez-Pedraja J., Johns W.E., Gurgel K.-W., Cook T.M. // OCEANS 2007-Europe. - Aberdeen, 18-21 June 2007. - P. 1-6. ↑
- C9180.** Daun M. Multistatic Target Tracking for Non-Cooperative Illuminating by DAB/DVB-T. / Daun M., Koch W. // OCEANS 2007-Europe. - Aberdeen, 18-21 June 2007. - P. 1-6. ↑
- C9181.** Wyatt L.R. Wave and Tidal Power measurement using HF radar. OCEANS 2007-Europe. - Aberdeen, 18-21 June 2007. - P. 1-5. ↑
- C9182.** Haus B.K. HF Radar Observation of Wave Directional Spectra in a Strong Current Regime. / Haus B.K., Mei Wang, Shay L.K., Wyatt L.R. // OCEANS 2007-Europe. - Aberdeen, 18-21 June 2007. - P. 1-5. ↑
- C9183.** Gurgel K.-W. Radio Frequency Interference Suppression Techniques in FMCW Modulated HF Radars. / Gurgel K.-W., Barbin Y., Schlick T. // OCEANS 2007-Europe. - Aberdeen, 18-21 June 2007. - P. 1-4. ↑
- C9184.** Reichert K. Coastal applications of X-band radar to achieve spatial and temporal surface wave monitoring. / Reichert K., Hessner K., Lund B. // OCEANS 2007-Europe. - Aberdeen, 18-21 June 2007. - P. 1-6. ↑
- C9185.** Heron M.L. Tsunami Monitoring by HF Ocean Radar: Time and Space Scales. OCEANS 2007-Europe. - Aberdeen, 18-21 June 2007. - P. 1-5. ↑
- C9186.** Vesecky J.F. Coastal Eddies in the Ocean Wind Field as Observed by Single and Multifrequency HF Radars on Monterey Bay, California. / Vesecky J.F., Drake J., Laws K., Ludwig F.L., Teague C.C., Paduan J.D., Sinton D. // OCEANS 2007-Europe. - Aberdeen, 18-21 June 2007. - P. 1-5. ↑
- C9187.** Parikh S. Node-Replacement Policies to Maintain Threshold-Coverage in Wireless Sensor Networks. / Parikh S., Vokkarane V.M., Liudong Xing, Kasilingam D. // 2007. ICCCN 2007. Proceedings of 16th International Conference on Computer Communications and Networks. - Honolulu, HI, 13-16 Aug. 2007. - P. 760-765. ↑
- C9188.** Stoica P. On Sequences with Good Correlation Properties: A New Perspective. / Stoica P., Jian Li, Ming Xue. // 2007 IEEE Information Theory Workshop on Information Theory for Wireless Networks. - Solstrand, 1-6 July 2007. - P. 1-5. ↑
- C9189.** Chitrapu P. Evolution of GSM into the Next Generation Wireless World. / Chitrapu P., Aghili B. // 2007. LISAT 2007. IEEE Long Island Systems, Applications and Technology Conference. - Farmingdale, NY, 4-4 May 2007. - P. 1-10. ↑
- C9190.** Yiming Ji. Optimal Sniffers Deployment On Wireless Indoor Localization. / Yiming Ji, Biaz S., Shaoen Wu, Bing Qi. // 2007. ICCCN 2007. Proceedings of 16th International Conference on Computer Communications and Networks. - Honolulu, HI, 13-16 Aug. 2007. - P. 251-256. ↑
- C9191.** Liu Xiankang. Satellite Target Recognition Algorithm Based on BP Neural Networks. / Liu Xiankang, Gao Meiguo, Fu Xiongjun. // 2007. ICIEA 2007. 2nd IEEE Conference on Industrial Electronics and Applications. - Harbin, 23-25 May 2007. - P. 1775-1778. ↑
- C9192.** Huadong Sun. Parameter Estimations of SAR Moving Target Based on DPCA-FrFT Algorithm. / Huadong Sun, Fulin Su, Jianjun Gao, Xinghui Cao. // 2007. ICIEA 2007. 2nd IEEE Conference on Industrial Electronics and Applications. - Harbin, 23-25 May 2007. - P. 1779-1784. ↑
- C9193.** Leonard J.J. Challenges for Autonomous Mobile Robots. 2007. IMVIP 2007. International Machine Vision and Image Processing Conference. - Kildare, 5-7 Sept. 2007. - P. 4. ↑
- C9194.** McTavish D.J. A New Approach to Geometrical Feature Assessment for ICP-Based Pose Measurement: Continuum Shape Constraint Analysis. / McTavish D.J., Okouneva G. // 2007. IMVIP 2007. International Machine Vision and Image Processing Conference. - Kildare, 5-7 Sept. 2007. - P. 23-32. ↑
- C9195.** Danilo C. Comparisons between HF radar and SAR current measurements in the Iroise Sea. / Danilo C., Chapron B., Mouche A., Garelo R., Collard F. // OCEANS 2007-Europe. - Aberdeen, 18-21 June 2007. - P. 1-5. ↑
- C9196.** Cameron I.D. Offshore wind mapping using synthetic aperture radar and meteorological model data. /

Cameron I.D., Miller D., Woodhouse I.H. // OCEANS 2007-Europe. - Aberdeen, 18-21 June 2007. - P. 1-6. ↑

C9197. Jangal F. Remote Sensing of the Sea and Target Detection Improvement Using a Wavelet-based Extraction of Sea Echoes from High Frequency Radars. / Jangal F., Saillant S., Dorey P., Helier M. // OCEANS 2007-Europe. - Aberdeen, 18-21 June 2007. - P. 1-5. ↑

C9198. Helzel T. Features and Limitations of the Modular Oceanography Radar System WERA. / Helzel T., Kniephoff M., Petersen L. // OCEANS 2007-Europe. - Aberdeen, 18-21 June 2007. - P. 1-4. ↑

C9199. Norgard J. Detection/Imaging of Buried Objects: Using Spatial/Angular Diversity with Distributed/Embedded Sub-Surface Sensors for Reduced Mutual Coupling and Suppressed EM Emissions. / Norgard J., Magde K., Wicks M., Drozd A., Musselman R. // 2007. EMC 2007. IEEE International Symposium on Electromagnetic Compatibility. - Honolulu, HI, 9-13 July 2007. - P. 1-5. ↑

C9200. Johnk R.T. RF Electromagnetic Penetration of the Nasa Space Shuttle Endeavour Performed with an Ultra-Wideband System. / Johnk R.T., Novotny D.R., Grosvenor C.A., Canales N., Camell D.G., Koepke G.H., Scully R.C. // 2007. EMC 2007. IEEE International Symposium on Electromagnetic Compatibility. - Honolulu, HI, 9-13 July 2007. - P. 1-6. ↑

C9201. Howarth M.J. HF radar measurements in Liverpool Bay, Irish Sea. / Howarth M.J., Player R.J., Wolf J., Siddons L.A. // OCEANS 2007-Europe. - Aberdeen, 18-21 June 2007. - P. 1-6. ↑

C9202. Capraro G.T. Waveform Diversity and Electromagnetic Compatibility. / Capraro G.T., Bradaric I., Wicks M.C. // 2007. EMC 2007. IEEE International Symposium on Electromagnetic Compatibility. - Honolulu, HI, 9-13 July 2007. - P. 1-7. ↑

C9203. Abramov A. High Order Spectral Estimation Methods in Ground Penetrating Radar Applications. / Abramov A., Sugak A., Sugak V. // 2007. MSMW '07. The Sixth International Kharkov Symposium on Physics and Engineering of Microwaves, Millimeter and Submillimeter Waves and Workshop on Terahertz Technologies. - Kharkov, 25-30 June 2007. - Vol. 2. - P. 855-857. ↑

C9204. Cassidy N. J. Frequency-Dependent Attenuation and Velocity Characteristics of Magnetically Lossy Materials. 2007 4th International Workshop on Advanced Ground Penetrating Radar. - Aula Magna Partenope, 27-29 June 2007. - P. 142-146. ↑

C9205. van Kempen L. Solving the full nonlinear inverse problem for GPR using a three step method. / van Kempen L., Thanh N. T., Sahli H., Hao D. N. // 2007 4th International Workshop on Advanced Ground Penetrating Radar. - Aula Magna Partenope, 27-29 June 2007. - P. 147-152. ↑

C9206. Mangué M. FirstArrival Traveltimes Inversion Based on Minimal Number of Parameters in shallow crosswell GPR Tomography. / Mangué M., Perroud H., Rousset D. // 2007 4th International Workshop on Advanced Ground Penetrating Radar. - Aula Magna Partenope, 27-29 June 2007. - P. 132-136. ↑

C9207. Belkebir K. Characterization of inhomogeneous cylinders from transient data. / Belkebir K., Catapano I., Geffrin J. M. // 2007 4th International Workshop on Advanced Ground Penetrating Radar. - Aula Magna Partenope, 27-29 June 2007. - P. 137-141. ↑

C9208. Brancaccio A. Subsurface localization of interfaces. / Brancaccio A., Pierri R., Soldovieri F., Leone G. // 2007 4th International Workshop on Advanced Ground Penetrating Radar. - Aula Magna Partenope, 27-29 June 2007. - P. 163-168. ↑

C9209. Kuroda S. A Full Waveform Inversion Algorithm for Interpreting Crosshole Radar Data. / Kuroda S., Takeuchi M., Kim H. J. // 2007 4th International Workshop on Advanced Ground Penetrating Radar. - Aula Magna Partenope, 27-29 June 2007. - P. 169-174. ↑

C9210. di Vico M. Electromagnetic scattering by buried cylinders. / di Vico M., Martinelli P., Pajewski L., Schettini G., Frezza F. // 2007 4th International Workshop on Advanced Ground Penetrating Radar. - Aula Magna Partenope, 27-29 June 2007. - P. 153-158. ↑

C9211. Lopera O. Time-frequency domain signature analysis of GPR data for landmine identification. / Lopera O., Milisavljevic N., Daniels D., Macq B. // 2007 4th International Workshop on Advanced Ground Penetrating Radar. - Aula Magna Partenope, 27-29 June 2007. - P. 159-162. ↑

- C9212.** Lambot S. Constraining GPR data inversion using hydrodynamic laws for noninvasive soil hydraulic and electric property determination. / Lambot S., Guillaso S., Vereecken H., Slob E. // 2007 4th International Workshop on Advanced Ground Penetrating Radar. - Aula Magna Partenope, 27-29 June 2007. - P. 101-105. ↑
- C9213.** di Pasquo B. Design and construction of a large test site to characterize the GPR response in the vadose zone. / di Pasquo B., Pettinelli E., Vannaroni G., di Matteo A., Mattei E., de Santis A., Annan P.A., Redman D.J. // 2007 4th International Workshop on Advanced Ground Penetrating Radar. - Aula Magna Partenope, 27-29 June 2007. - P. 106-109. ↑
- C9214.** Saintenoy A. Evaluating GroundPenetrating Radar use for water infiltration monitoring. / Saintenoy A., Schneider S., Tucholka P. // 2007 4th International Workshop on Advanced Ground Penetrating Radar. - Aula Magna Partenope, 27-29 June 2007. - P. 91-95. ↑
- C9215.** Soldovieri F. Determination of soil permittivity from GPR data and a microwave tomography approach: a preliminary study. / Soldovieri F., Prisco G., Persico R. // 2007 4th International Workshop on Advanced Ground Penetrating Radar. - Aula Magna Partenope, 27-29 June 2007. - P. 96-100. ↑
- C9216.** Diamanti N. An Investigation into the Implementation of ADI-FDTD Subgrids in FDTD GPR Modeling. / Diamanti N., Giannopoulos A. // 2007 4th International Workshop on Advanced Ground Penetrating Radar. - Aula Magna Partenope, 27-29 June 2007. - P. 122-126. ↑
- C9217.** Crocco L. Advanced forward modeling and tomographic inversion for leaking water pipes monitoring. / Crocco L., Prisco G., Soldovieri F., Cassidy N. J. // 2007 4th International Workshop on Advanced Ground Penetrating Radar. - Aula Magna Partenope, 27-29 June 2007. - P. 127-131. ↑
- C9218.** Elkhetai S. I. Estimation of Electromagnetic of Libyan soil Properties by Stepped Frequency Radar. / Elkhetai S. I., Salem K. A. // 2007 4th International Workshop on Advanced Ground Penetrating Radar. - Aula Magna Partenope, 27-29 June 2007. - P. 110-113. ↑
- C9219.** Solimene R. Localization of thin metallic scatterers by experimental data. / Solimene R., Brancaccio A., Romano J., Pierri R. // 2007 4th International Workshop on Advanced Ground Penetrating Radar. - Aula Magna Partenope, 27-29 June 2007. - P. 117-121. ↑
- C9220.** Solimene R. Localization of small PEG spheres by multiview/single-frequency data: numerical results. / Solimene R., Buonanno A., Pierri R. // 2007 4th International Workshop on Advanced Ground Penetrating Radar. - Aula Magna Partenope, 27-29 June 2007. - P. 175-178. ↑
- C9221.** Kopeikin V.V. Experimental Verification of LOZA-V GPR Penetration Depth and Signal Quality. / Kopeikin V.V., Krashennnikov I.V., Morozov P.A., Popov A.V., Guangyou F., Xiaojun L., Bin Z. // 2007 4th International Workshop on Advanced Ground Penetrating Radar. - Aula Magna Partenope, 27-29 June 2007. - P. 230-233. ↑
- C9222.** Nuzzo L. Metal-sheet test to estimate shape and frequency content of the radar pulse. / Nuzzo L., Quarta T. // 2007 4th International Workshop on Advanced Ground Penetrating Radar. - Aula Magna Partenope, 27-29 June 2007. - P. 234-238. ↑
- C9223.** Utsi V. Design of a GPR for deep investigations. 2007 4th International Workshop on Advanced Ground Penetrating Radar. - Aula Magna Partenope, 27-29 June 2007. - P. 222-225. ↑
- C9224.** Lestari A.A. GPR Antenna Test Facility at IRCTR-IB. / Lestari A.A., Yulian D., Liarto, Soetikno T.P., Suksmonol A.B., Bharata E., Yarovoy A.G., Ligthart L.P. // 2007 4th International Workshop on Advanced Ground Penetrating Radar. - Aula Magna Partenope, 27-29 June 2007. - P. 226-229. ↑
- C9225.** Hamran S-E. A prototype for the WISDOM GPR on the ExoMars mission. / Hamran S-E, Berger T., Hanssen L., Oyan M.J., Ciarletti V., Corbel C., Plettemeier D. // 2007 4th International Workshop on Advanced Ground Penetrating Radar. - Aula Magna Partenope, 27-29 June 2007. - P. 252-255. ↑
- C9226.** Picardi G. MARSIS Data Inversion Approach. / Picardi G., Biccari D., Cartacci M., Cicchetti A., Giuppi S., Marini A., Masdea A., Noschese R., Piccari F., Seu R., Bombaci O., Calabrese D., Zampolini E., Pettinelli E., Federico C., Frigeri A., Melacci P.T., Orosei R., Marinangeli L., Flamini E. // 2007 4th International Workshop on Advanced Ground Penetrating Radar. - Aula Magna Partenope, 27-29 June 2007. - P. 256-260. ↑

- C9227.** Croci R. Calibration report of the SHARAD instrument. / Croci R., Fois F., Flamini E., Mecozzi R., Seu R. // 2007 4th International Workshop on Advanced Ground Penetrating Radar. - Aula Magna Partenope, 27-29 June 2007. - P. 241-245. ↑
- C9228.** Flamini E. Sounding Mars with SHARAD & MARSIS. / Flamini E., Fois F., Calabrese D., Bombaci O., Catallo C., Croce A., Croci R., Guelfi M., Zampolini E., Picardi G., Seu R., Mecozzi R., Biccari D., Cartacci M., Cicchetti A., Masdea A., Alberti G., Maffei S., Papa C. // 2007 4th International Workshop on Advanced Ground Penetrating Radar. - Aula Magna Partenope, 27-29 June 2007. - P. 246-251. ↑
- C9229.** Turk A. S. Investigation of Convenient Antenna Designs for Ultra-Wide Band GPR Systems. / Turk A. S., Sahinkaya D. A., Sezgin M., Nazli H. // 2007 4th International Workshop on Advanced Ground Penetrating Radar. - Aula Magna Partenope, 27-29 June 2007. - P. 192-196. ↑
- C9230.** Lestari A.A. Improved Bow-Tie Antenna for Pulse Radiation and Its Implementation in a GPR Survey. / Lestari A.A., Yulian D., Liarto, Suksmono A.B., Bharata E., Yarovoy A.G., Ligthart L.P. // 2007 4th International Workshop on Advanced Ground Penetrating Radar. - Aula Magna Partenope, 27-29 June 2007. - P. 197-202. ↑
- C9231.** Catapano I. Shape reconstruction of three dimensional buried objects from stepped frequency data. / Catapano I., Crocco L., Isernia T. // 2007 4th International Workshop on Advanced Ground Penetrating Radar. - Aula Magna Partenope, 27-29 June 2007. - P. 179-184. ↑
- C9232.** Rial F. I. Vertical and Horizontal Resolution of GPR bow-tie antennas. / Rial F. I., Pereira M., Lorenzo H., Arias P., Novo A. // 2007 4th International Workshop on Advanced Ground Penetrating Radar. - Aula Magna Partenope, 27-29 June 2007. - P. 187-191. ↑
- C9233.** Grazzini G. A Clutter Canceller for Continuous Wave GPR. / Grazzini G., Pieraccini M., Parrini F., Atzeni C. // 2007 4th International Workshop on Advanced Ground Penetrating Radar. - Aula Magna Partenope, 27-29 June 2007. - P. 212-216. ↑
- C9234.** Chubinsky N. The broadband device for nondestructive measurements of dielectric permeability of lossy media. / Chubinsky N., Filonenko V. // 2007 4th International Workshop on Advanced Ground Penetrating Radar. - Aula Magna Partenope, 27-29 June 2007. - P. 217-221. ↑
- C9235.** Garcia G. Analysis of a non Electrical Resistive GPR Antenna. / Garcia G., Casassa G., Ulloa D., Zamora R. // 2007 4th International Workshop on Advanced Ground Penetrating Radar. - Aula Magna Partenope, 27-29 June 2007. - P. 203-207. ↑
- C9236.** Bausov I. Y. Look-Ahead Radar and Horizon Sensing for Coal Cutting Drums. / Bausov I. Y., Stolarczyk G. L., Stolarczyk L. G., Koppenjan Sc.D. S. // 2007 4th International Workshop on Advanced Ground Penetrating Radar. - Aula Magna Partenope, 27-29 June 2007. - P. 208-211. ↑
- C9237.** Ambrosch K. Hardware implementation of an SAD based stereo vision algorithm. / Ambrosch K., Humenberger M., Kubinger W., Steininger A. // 2007. CVPR '07. IEEE Conference on Computer Vision and Pattern Recognition. - Minneapolis, MN, 17-22 June 2007. - P. 1-6. ↑
- C9238.** Counsell J. Displaying LiDAR Data for Interactive Web-Based Modelling of the Environment. / Counsell J., Smith S. // 2007. IV 07. 11th International Conference Information Visualization. - Zurich, 4-6 July 2007. - P. 573-578. ↑
- C9239.** Hautiere N. Towards Fog-Free In-Vehicle Vision Systems through Contrast Restoration. / Hautiere N., Tarel J.-P., Aubert D. // 2007. CVPR '07. IEEE Conference on Computer Vision and Pattern Recognition. - Minneapolis, MN, 17-22 June 2007. - P. 1-8. ↑
- C9240.** Thakoor N. Real-time Planar Surface Segmentation in Disparity Space. / Thakoor N., Sungyong Jung, Jean Gao. // 2007. CVPR '07. IEEE Conference on Computer Vision and Pattern Recognition. - Minneapolis, MN, 17-22 June 2007. - P. 1-8. ↑
- C9241.** Guo Fang Mao. Voice over Internet Protocol on Mobile Devices. / Guo Fang Mao, Talevski A., Chang E. // 2007. ICIS 2007. 6th IEEE/ACIS International Conference on Computer and Information Science. - Melbourne, Qld., 11-13 July 2007. - P. 163-169. ↑
- C9242.** {no data available}. Opinion. 2007 4th International Workshop on Advanced Ground Penetrating Radar. ↑

- Aula Magna Partenope, 27-29 June 2007. - P. v. ↑

C9243. Lin C.E. A Fast Flow Control and Approach Queuing Monitor using FDP in Excel Environment. / Lin C.E., Shao-Gang Jian, Kao J., Chang P. // 2007. ICNS '07 Integrated Communications, Navigation and Surveillance Conference. - Herndon, VA, April 30 2007-May 3 2007. - P. 1-12. ↑

C9244. Tan xin. Wireless Telemedicine Physiological Monitoring Center Based on Virtual Instruments. / Tan xin, Guo Xing-ming, Cheng min, Yan yan. // 2007. ICBBE 2007. The 1st International Conference on Bioinformatics and Biomedical Engineering. - Wuhan, 6-8 July 2007. - P. 1157-1160. ↑

C9245. Xiao Chen He. A Novel Algorithm for Estimating Vehicle Speed from Two Consecutive Images. / Xiao Chen He, Yung N.H.C. // 2007. WACV 07. IEEE Workshop on Applications of Computer Vision. - Austin, TX, Feb. 2007. - P. 12. ↑

C9246. Wei-Min Lance Kuo. Comparison of Shunt and Series/Shunt nMOS Single-Pole Double-Throw Switches for X-Band Phased Array T/R Modules. / Wei-Min Lance Kuo, Comeau J.P., Andrews J.M., Cressler J.D., Mitchell M.A. // 2007 Topical Meeting on Silicon Monolithic Integrated Circuits in RF Systems. - Long Beach, CA, 10-12 Jan. 2007. - P. 249-252. ↑

C9247. Silva M.C.J.A.A. 4G Self-Configurable System Based on Neural Networks. 2007. CONIELECOMP '07. 17th International Conference on Electronics, Communications and Computers. - Cholula, Puebla, 26-28 Feb. 2007. - P. 16. ↑

C9248. Thomas M. Vector field characterization in ERS-1 imagery of sea ice. / Thomas M., Geiger C.A., Kambhamettu C. // 2007. WACV 07. IEEE Workshop on Applications of Computer Vision. - Austin, TX, Feb. 2007. - P. 23. ↑

C9249. Knapp H. SiGe Circuits for Automotive Radar. / Knapp H., Dehlink B., Forstner H.-P., Kolmhofer E., Aufinger K., Bock J., Meister T.F. // 2007 Topical Meeting on Silicon Monolithic Integrated Circuits in RF Systems. - Long Beach, CA, 10-12 Jan. 2007. - P. 231-236. ↑

C9250. Sen Wang. An X-band Transmission Line Based CMOS VCO with FM Modulation. / Sen Wang, Hsien-Shun Wu, Tzuang C.-K.C. // 2007 Topical Meeting on Silicon Monolithic Integrated Circuits in RF Systems. - Long Beach, CA, 10-12 Jan. 2007. - P. 139-141. ↑

C9251. van der Heijden E. 16-26GHz Low Noise Amplifier for short-range automotive radar in a production SiGe:C technology. / van der Heijden E., Veenstra H., Havens R. // 2007 Topical Meeting on Silicon Monolithic Integrated Circuits in RF Systems. - Long Beach, CA, 10-12 Jan. 2007. - P. 241-244. ↑

C9252. Hartmann M. A Low-Power Micromixer with High Linearity for Automotive Radar at 77 GHz in Silicon-Germanium Bipolar Technology. / Hartmann M., Wagner C., Seemann K., Platz J., Jager H., Weigel R. // 2007 Topical Meeting on Silicon Monolithic Integrated Circuits in RF Systems. - Long Beach, CA, 10-12 Jan. 2007. - P. 237-240. ↑

C9253. Sato M. Development of the Hand held dual sensor ALIS and its evaluation. / Sato M., Takahashi K., Fujiwara J. // 2007 4th International Workshop on Advanced Ground Penetrating Radar. - Aula Magna Partenope, 27-29 June 2007. - P. 3-7. ↑

C9254. Delaney A. J. Multi-frequency ground-penetrating radar method for revealing complex sedimentary facies. / Delaney A. J., Horsman J., Prentice M. L., Arcone S. A. // 2007 4th International Workshop on Advanced Ground Penetrating Radar. - Aula Magna Partenope, 27-29 June 2007. - P. 60-63. ↑

C9255. Barone P.M. Applications of GPR to archaeology and geology: the example of the regio III in Pompeii (Naples, Italy). / Barone P.M., Bellomo T., Pettinelli E., Scarpati C. // 2007 4th International Workshop on Advanced Ground Penetrating Radar. - Aula Magna Partenope, 27-29 June 2007. - P. 64-67. ↑

C9256. Deparis J. Inversion of dispersive APVO GPR curves: a thin-layer approach for fracture characterization on a vertical cliff. / Deparis J., Garambois S. // 2007 4th International Workshop on Advanced Ground Penetrating Radar. - Aula Magna Partenope, 27-29 June 2007. - P. 49-53. ↑

C9257. Baker G. S. Ground penetrating radar imaging of a 4th Century Roman Fort, Humayma, Jordan. / Baker G. S., Ambrose H. M. // 2007 4th International Workshop on Advanced Ground Penetrating Radar. - Aula Magna Partenope, 27-29 June 2007. - P. 54-56. ↑

Magna Partenope, 27-29 June 2007. - P. 54-59. ↑

C9258. Bavusi M. Geophysical investigations in the Castle of Crotona (Calabria Region, Italy). / Bavusi M., Giocoli A., Rizzo E., Lapenna V. // 2007 4th International Workshop on Advanced Ground Penetrating Radar. - Aula Magna Partenope, 27-29 June 2007. - P. 78-81. ↑

C9259. Kooper K. Incorporating near-surface layering in GPR data inversion for improved surface water content estimates. / Kooper K., Lambot S., Slob E.C. // 2007 4th International Workshop on Advanced Ground Penetrating Radar. - Aula Magna Partenope, 27-29 June 2007. - P. 85-90. ↑

C9260. Carnevale M. Low Frequency GPR in Difficult Terrain. / Carnevale M., Hager J. // 2007 4th International Workshop on Advanced Ground Penetrating Radar. - Aula Magna Partenope, 27-29 June 2007. - P. 68-73. ↑

C9261. Pieraccini M. Masonry investigation through Very Large Bandwidth CW-SF radar. / Pieraccini M., Parrini F., Noferini L., Atzeni C. // 2007 4th International Workshop on Advanced Ground Penetrating Radar. - Aula Magna Partenope, 27-29 June 2007. - P. 74-77. ↑

C9262. Borchert O. Directional Borehole Radar Calibration. / Borchert O., Aliman M., Glasmachers A. // 2007 4th International Workshop on Advanced Ground Penetrating Radar. - Aula Magna Partenope, 27-29 June 2007. - P. 19-23. ↑

C9263. Ebihara S. Analysis of Dipole Antenna Eccentered in a Borehole for Borehole Radar. / Ebihara S., Inoue Y. // 2007 4th International Workshop on Advanced Ground Penetrating Radar. - Aula Magna Partenope, 27-29 June 2007. - P. 24-27. ↑

C9264. Slob E. General representations of electromagnetic interferometry. / Slob E., Wapenaar K. // 2007 4th International Workshop on Advanced Ground Penetrating Radar. - Aula Magna Partenope, 27-29 June 2007. - P. 8-11. ↑

C9265. Yarovoy A.G. Array-Based GPR for Shallow Subsurface Imaging. / Yarovoy A.G., Savelyev T.G., Aubry P.J., Ligthart L.P. // 2007 4th International Workshop on Advanced Ground Penetrating Radar. - Aula Magna Partenope, 27-29 June 2007. - P. 12-15. ↑

C9266. Ebihara S. Influence of Mode Conversion at Borehole on Direction Finding with Dipole Array Antenna. / Ebihara S., Inaida Y., Suzuki R. // 2007 4th International Workshop on Advanced Ground Penetrating Radar. - Aula Magna Partenope, 27-29 June 2007. - P. 36-41. ↑

C9267. Orlando L. Using GPR to Monitor Cracks in a Historical Building. 2007 4th International Workshop on Advanced Ground Penetrating Radar. - Aula Magna Partenope, 27-29 June 2007. - P. 45-48. ↑

C9268. Gundelach V. Principle of a direction sensitive borehole antenna with advanced technology and data examples. / Gundelach V., Eisenburger D. // 2007 4th International Workshop on Advanced Ground Penetrating Radar. - Aula Magna Partenope, 27-29 June 2007. - P. 28-31. ↑

C9269. Takayama T. Analysis of Directional Borehole Radar Measurement Data. / Takayama T., Sato M., Kim J. H. // 2007 4th International Workshop on Advanced Ground Penetrating Radar. - Aula Magna Partenope, 27-29 June 2007. - P. 32-35. ↑

C9270. Alberti G. SHARAD radar signal processing technique. / Alberti G., Dinardo S., Mattei S., Papa C., Santovito M.R. // 2007 4th International Workshop on Advanced Ground Penetrating Radar. - Aula Magna Partenope, 27-29 June 2007. - P. 261-264. ↑

C9271. Nielsen A.A. Complex Wishart Distribution Based Analysis of Polarimetric Synthetic Aperture Radar Data. / Nielsen A.A., Skriver H., Conradsen K. // 2007. MultiTemp 2007. International Workshop on the Analysis of Multi-temporal Remote Sensing Images. - Leuven, 18-20 July 2007. - P. 1-6. ↑

C9272. Marzahn P. Derivation of Soil Surface Roughness Dynamics from Multi-temporal and Multi-parametric Air-borne PolSAR-data. / Marzahn P., Kruger K., Ludwig R. // 2007. MultiTemp 2007. International Workshop on the Analysis of Multi-temporal Remote Sensing Images. - Leuven, 18-20 July 2007. - P. 1-5. ↑

C9273. Alberga V. Performance Estimation of Similarity Measures of Multi-Sensor Images for Change

Detection Applications. / Alberga V., Idrissa M., Lacroix V., Inglada J. // 2007. MultiTemp 2007. International Workshop on the Analysis of Multi-temporal Remote Sensing Images. - Leuven, 18-20 July 2007. - P. 1-5. ↑

C9274. Villalon-Turrubiates I.E. Dynamical Analysis of Hydrological Indexes Extracted from Remote Sensing Imagery: An Introductory Study. 2007. MultiTemp 2007. International Workshop on the Analysis of Multi-temporal Remote Sensing Images. - Leuven, 18-20 July 2007. - P. 1-4. ↑

C9275. Zhixi Li. Cross-band Inverse Synthetic Aperture Radar (ISAR) Image Fusion. / Zhixi Li, Narayanan R.M. // 2007. ISSSE '07. International Symposium on Signals, Systems and Electronics. - Montreal, Que., July 30 2007-Aug. 2 2007. - P. 111-114. ↑

C9276. Chieh-Ping Lai. Hilbert-Huang Transform (HHT) Analysis of Human Activities Using Through-Wall Noise Radar. / Chieh-Ping Lai, Qing Ruan, Narayanan R.M. // 2007. ISSSE '07. International Symposium on Signals, Systems and Electronics. - Montreal, Que., July 30 2007-Aug. 2 2007. - P. 115-118. ↑

C9277. Wang Xiong-Liang. Super-resolution Processing of SAR Images by Match Pursuit Method Based on Fourier Dictionary. / Wang Xiong-Liang, Wang Chun-Ling, Wang Zheng-Ming. // 2007. CGIV '07 Computer Graphics, Imaging and Visualisation. - Bangkok, 14-17 Aug. 2007. - P. 239-244. ↑

C9278. Hailu D.M. Sub-wavelength Microwave Radar Imaging for Detection of Breast Cancer Tumors. / Hailu D.M., Nikolova N.K., Bakr M.H. // 2007. ISSSE '07. International Symposium on Signals, Systems and Electronics. - Montreal, Que., July 30 2007-Aug. 2 2007. - P. 107-110. ↑

C9279. Tao Jin. Cross-Polarization Radar Integrated Debugging Platform. / Tao Jin, Xiaohui Qi, Shuqing Yuan, Xiaolin Qiao, Min Zhang, Qunxing Zhang. // 2007. ICIT '07. IEEE International Conference on Integration Technology. - Shenzhen, 20-24 March 2007. - P. 508-512. ↑

C9280. Haridas N. Multi-Frequency Antenna design for Space-based Reconfigurable Satellite Sensor Node. / Haridas N., El-Rayis A., Erdogan A.T., Arslan T. // 2007. AHS 2007. Second NASA/ESA Conference on Adaptive Hardware and Systems. - Edinburgh, 5-8 Aug. 2007. - P. 14-19. ↑

C9281. Fardi B. Road Border Recognition Using FIR Images and LIDAR Signal Processing. / Fardi B., Weigel H., Wanielik G., Takagi K. // 2007 IEEE Intelligent Vehicles Symposium. - Istanbul, 13-15 June 2007. - P. 1278-1283. ↑

C9282. Hirose Shigeo. Integration of Arm-equipped Mobile Robot GRYPHON for Humanitarian Demining Operation. 2007. ICIT '07. IEEE International Conference on Integration Technology. - Shenzhen, China, 20-24 March 2007. - P. nil12-nil13. ↑

C9283. Casciello D. Robust Satellite Techniques (RST) for Oil Spill Detection and Monitoring. / Casciello D., Lacava T., Pergola N., Tramutoli V. // 2007. MultiTemp 2007. International Workshop on the Analysis of Multi-temporal Remote Sensing Images. - Leuven, 18-20 July 2007. - P. 1-6. ↑

C9284. Wegmuller U. A Novel Methodology for Parameter Retrieval from Multi-temporal Data Demonstrated for Forest Biomass Retrieval from C-band SAR Backscatter. / Wegmuller U., Santoro M., Wiesmann A. // 2007. MultiTemp 2007. International Workshop on the Analysis of Multi-temporal Remote Sensing Images. - Leuven, 18-20 July 2007. - P. 1-6. ↑

C9285. Inaltekin H. A Duopoly Pricing Game for Wireless IP Services. / Inaltekin H., Wexler T., Wicker S.B. // 2007. SECON '07. 4th Annual IEEE Communications Society Conference on Sensor, Mesh and Ad Hoc Communications and Networks. - San Diego, CA, 18-21 June 2007. - P. 600-609. ↑

C9286. van der Velde R. Characterization of the Temporal and Spatial Variability of Soil Moisture through Multi-Temporal Analysis of ASAR Observations. / van der Velde R., Rientjes T., Yao-ming Ma, Yizhou Zhao, Su B. // 2007. MultiTemp 2007. International Workshop on the Analysis of Multi-temporal Remote Sensing Images. - Leuven, 18-20 July 2007. - P. 1-6. ↑

C9287. Seng Hong. Investigation on Genetic Algorithm for Countermeasure Technique Generator. / Seng Hong, Saville M.A., Simpson C., Marshall P. // 2007. ISSSE '07. International Symposium on Signals, Systems and Electronics. - Montreal, Que., July 30 2007-Aug. 2 2007. - P. 351-354. ↑

C9288. Lutsenko V.I. Statistical Model of the Signal Scattered from Sea Surface at the Grazing Feed Angles. /

Lutsenko V.I., Lutsenko I.V. // 2007. MSMW '07. The Sixth International Kharkov Symposium on Physics and Engineering of Microwaves, Millimeter and Submillimeter Waves and Workshop on Terahertz Technologies. - Kharkov, 25-30 June 2007. - Vol. 1. - P. 464-466. ↑

C9289. Ponomarenko N.N. Comparison of 3-D and 2-D DCT Based Filtering of Multichannel Images. / Ponomarenko N.N., Lukin V.V., Zelensky A.A., Koivisto P.T., Egiazarian K.O. // 2007. MSMW '07. The Sixth International Kharkov Symposium on Physics and Engineering of Microwaves, Millimeter and Submillimeter Waves and Workshop on Terahertz Technologies. - Kharkov, 25-30 June 2007. - Vol. 1. - P. 467-469. ↑

C9290. Volosuk V.K. Interpretation of an Influence of the Transmitter and Receiver Bistatic SAR Tracks to Resolution. / Volosuk V.K., Voloschuk R.P. // 2007. MSMW '07. The Sixth International Kharkov Symposium on Physics and Engineering of Microwaves, Millimeter and Submillimeter Waves and Workshop on Terahertz Technologies. - Kharkov, 25-30 June 2007. - Vol. 1. - P. 458-460. ↑

C9291. Lutsenko V.I. Polarization-Spectral Indication of the Objects. / Lutsenko V.I., Popov I.V. // 2007. MSMW '07. The Sixth International Kharkov Symposium on Physics and Engineering of Microwaves, Millimeter and Submillimeter Waves and Workshop on Terahertz Technologies. - Kharkov, 25-30 June 2007. - Vol. 1. - P. 461-463. ↑

C9292. Lukin K.A. Results of Computer Imitation Modeling of Immunity of Correlator Affected by Active Continuous Interferences at the Processing of Wideband Noise or LFM Sequences of Pulses. / Lukin K.A., Kantsedal V.M., Kulyk V.V., Konovalov V.M., Suschenko P.G. // 2007. MSMW '07. The Sixth International Kharkov Symposium on Physics and Engineering of Microwaves, Millimeter and Submillimeter Waves and Workshop on Terahertz Technologies. - Kharkov, 25-30 June 2007. - Vol. 1. - P. 487-489. ↑

C9293. Roenko A.A. SsS Process Location Parameter Adaptive Estimator Based on Data Censoring. / Roenko A.A., Lukin V.V., Djurovic I. // 2007. MSMW '07. The Sixth International Kharkov Symposium on Physics and Engineering of Microwaves, Millimeter and Submillimeter Waves and Workshop on Terahertz Technologies. - Kharkov, 25-30 June 2007. - Vol. 1. - P. 490-492. ↑

C9294. Lukin V.V. DCT Local Adaptive Filtering of Images Corrupted by Fluctuative Noise with a Priori Unknown Statistical Properties. / Lukin V.V., Fevraleev D.V., Zelensky A.A., Pogrebnyak O.B., Kildishev A.V. // 2007. MSMW '07. The Sixth International Kharkov Symposium on Physics and Engineering of Microwaves, Millimeter and Submillimeter Waves and Workshop on Terahertz Technologies. - Kharkov, 25-30 June 2007. - Vol. 1. - P. 470-472. ↑

C9295. Lukin K.A. Results of Laboratory Test of Immunity of Correlator Affected by Active Continuous Interferences at the Processing of Wideband Noise Pulses Sequences. / Lukin K.A., Kantsedal V.M., Mogyla A.A., Kulyk V.V., Konovalov V.M., Palamarchuk V.P., Suschenko P.G. // 2007. MSMW '07. The Sixth International Kharkov Symposium on Physics and Engineering of Microwaves, Millimeter and Submillimeter Waves and Workshop on Terahertz Technologies. - Kharkov, 25-30 June 2007. - Vol. 1. - P. 484-486. ↑

C9296. Chao Wang. All-Optical High-Frequency Electrical Chirped Pulse Generation using a Nonlinearly Chirped Fiber Bragg Grating. / Chao Wang, Jianping Yao. // 2007. ISSSE '07. International Symposium on Signals, Systems and Electronics. - Montreal, Que., July 30 2007-Aug. 2 2007. - P. 625-628. ↑

C9297. Vavriv D.M. High-Accuracy Doppler Signal Processing: Techniques and Applications. / Vavriv D.M., Bezvesilniy O.O., Vynogradov V.V., Volkov V.A., Kozhyn R.V., Dukhopelnykova I.V. // 2007. MSMW '07. The Sixth International Kharkov Symposium on Physics and Engineering of Microwaves, Millimeter and Submillimeter Waves and Workshop on Terahertz Technologies. - Kharkov, 25-30 June 2007. - Vol. 1. - P. 153-158. ↑

C9298. Boukari B. A Low-Cost Millimeter-Wave Six-Port Double-Balanced Mixer. / Boukari B., Moldovan E., Affes S., Ke Wu, Bosisio R.G., Tatu S.O. // 2007. ISSSE '07. International Symposium on Signals, Systems and Electronics. - Montreal, Que., July 30 2007-Aug. 2 2007. - P. 513-516. ↑

C9299. Wenig P. System Design of a 77 GHz Automotive Radar Sensor with Superresolution DOA Estimation. / Wenig P., Schoor M., Gunther O., Bin Yang, Weigel R. // 2007. ISSSE '07. International Symposium on Signals, Systems and Electronics. - Montreal, Que., July 30 2007-Aug. 2 2007. - P. 537-540. ↑

C9300. Lukin V.V. Improved Noise Parametr Estimation and Filtering of MM-Band SLAR Images. / Lukin V.V., Ponomarenko N.N., Abramov S.K., Vozel B., Chehdi K. // 2007. MSMW '07. The Sixth International Kharkov Symposium on Physics and Engineering of Microwaves, Millimeter and Submillimeter Waves and Workshop on

Terahertz Technologies. - Kharkov, 25-30 June 2007. - Vol. 1. - P. 439-441. ↑

C9301. Lukin K.A. To the Question About Estimation of Residual Fluctuation of Signal on Output of Correlation Receiver of Noise Radar. / Lukin K.A., Konovalov V.M., Scherbakov V.Ye. // 2007. MSMW '07. The Sixth International Kharkov Symposium on Physics and Engineering of Microwaves, Millimeter and Submillimeter Waves and Workshop on Terahertz Technologies. - Kharkov, 25-30 June 2007. - Vol. 1. - P. 452-454. ↑

C9302. Lukin K.A. Ka-Band Ground-Based Noise Waveform SAR. / Lukin K.A., Mogyla A.A., Vyplavin P.L., Palamarchuk V.P., Zemlyaniy O.V., Shiyan Y., Zaets N.K., Skresanov V.N., Shubniy A.I., Glamazdin V., Natarov M.P., Nechayev O.G. // 2007. MSMW '07. The Sixth International Kharkov Symposium on Physics and Engineering of Microwaves, Millimeter and Submillimeter Waves and Workshop on Terahertz Technologies. - Kharkov, 25-30 June 2007. - Vol. 1. - P. 159-164. ↑

C9303. Takano T. Performance of Falcon-I: Developed Low-Power and High-Sensitivity Cloud Profiling FM-CW Radar at 95GHz. / Takano T., Nakanishi Y., Abe H., Yamaguchi J., Yokote S.-I., Futaba K.-I., Kawamura Y., Kumagai H., Ohno Y., Takamura T., Nakajima T. // 2007. MSMW '07. The Sixth International Kharkov Symposium on Physics and Engineering of Microwaves, Millimeter and Submillimeter Waves and Workshop on Terahertz Technologies. - Kharkov, 25-30 June 2007. - Vol. 1. - P. 427-429. ↑

C9304. Grice M. Direction of Arrival Estimation using Advanced Signal Processing. / Grice M., Rodenkirch J., Yakovlev A., Hwang H.K., Aliyazicioglu Z., Lee A. // 2007. RAST '07. 3rd International Conference on Recent Advances in Space Technologies. - Istanbul, 14-16 June 2007. - P. 515-522. ↑

C9305. Ebrahimi A. Solving Multi-path Time Delay Estimation Problem in the Presence of Additive White Gaussian Noise Using a Genetic-Algorithm. / Ebrahimi A., Tabatabavakili V. // 2007. WOCN '07. IFIP International Conference on Wireless and Optical Communications Networks. - Singapore, 2-4 July 2007. - P. 1-5. ↑

C9306. Nikiforov I. Non-bayesian fault detection/isolation with nuisance parameters and constraints. 2007. ACC 07 American Control Conference. - New York, NY, 9-13 July 2007. - P. 2521-2526. ↑

C9307. Slaby A. ROC Analysis with Matlab. 2007. ITI 2007. 29th International Conference on Information Technology Interfaces. - Cavtat, 25-28 June 2007. - P. 191-196. ↑

C9308. Fasheng Wang. A Mixed Fast Particle Filter. / Fasheng Wang, Qingjie Zhao, Hongbin Deng. // 2007. SNPD 2007. Eighth ACIS International Conference on Software Engineering, Artificial Intelligence, Networking, and Parallel/Distributed Computing. - Qingdao, July 30 2007-Aug. 1 2007. - Vol. 3. - P. 932-936. ↑

C9309. Yun Jun. Experiment of Phase Unwrapping Algorithm in Interferometric Synthetic Aperture Sonar. / Yun Jun, Zhi-nong Zou, Jin-song Tang, Ai-qing Wang. // 2007. SNPD 2007. Eighth ACIS International Conference on Software Engineering, Artificial Intelligence, Networking, and Parallel/Distributed Computing. - Qingdao, July 30 2007-Aug. 1 2007. - Vol. 3. - P. 937-942. ↑

C9310. Lichao Wang. Application and Analysis of Time Domain Cross Correlation for Traffic Flow Speed Measurement. / Lichao Wang, Qiyong Lu, Xi Chen. // 2007. SNPD 2007. Eighth ACIS International Conference on Software Engineering, Artificial Intelligence, Networking, and Parallel/Distributed Computing. - Qingdao, July 30 2007-Aug. 1 2007. - Vol. 2. - P. 274-279. ↑

C9311. Pang Debin. Analysis of Sidelobe Elevation for Polyphase Complementary Codes through the Non-ideal System. / Pang Debin, Zhang Ning. // 2007. SNPD 2007. Eighth ACIS International Conference on Software Engineering, Artificial Intelligence, Networking, and Parallel/Distributed Computing. - Qingdao, July 30 2007-Aug. 1 2007. - Vol. 3. - P. 717-721. ↑

C9312. Chazelas A. J.L. EM characterization of bituminous concretes using a quadratic experimental design. / Chazelas A. J.L., Derobert B. X., Adous C. M., Villain D. G., Baltazart E. V., Laguerre F. L., Queffelec G. P. // 2007 4th International Workshop on Advanced Ground Penetrating Radar. - Aula Magna Partenope, 27-29 June 2007. - P. 278-283. ↑

C9313. Caorsi S. An innovative on-board processor for the real-time GPR monitoring of railway substructure conditions. / Caorsi S., Cevini G., Burro F., Sciotti M., Sorge S. // 2007 4th International Workshop on Advanced Ground Penetrating Radar. - Aula Magna Partenope, 27-29 June 2007. - P. 284-289. ↑

- C9314. Hugenschmidt J. The inspection of large retaining walls using GPR. / Hugenschmidt J., Mastrangelo R. // 2007 4th International Workshop on Advanced Ground Penetrating Radar. - Aula Magna Partenope, 27-29 June 2007. - P. 267-271. ↑
- C9315. Thomas A.M. A Stakeholder Led Accuracy Assessment System for Utility Location. / Thomas A.M., Rogers C.D.F., Metje N., Chapman D.N. // 2007 4th International Workshop on Advanced Ground Penetrating Radar. - Aula Magna Partenope, 27-29 June 2007. - P. 272-277. ↑
- C9316. Ranalli D. GPR signal attenuation vs. depth on damaged flexible road pavements. / Ranalli D., Scozzafava M., Tallini M., Colagrande S. // 2007 4th International Workshop on Advanced Ground Penetrating Radar. - Aula Magna Partenope, 27-29 June 2007. - P. 300-305. ↑
- C9317. {no data available}. Author Index. 2007 4th International Workshop on Advanced Ground Penetrating Radar. - Aula Magna Partenope, 27-29 June 2007. - P. 307-308. ↑
- C9318. Benedetto A. Prediction of structural damages of road pavement using GPR. 2007 4th International Workshop on Advanced Ground Penetrating Radar. - Aula Magna Partenope, 27-29 June 2007. - P. 290-294. ↑
- C9319. Roberts R. Characterizing Railroad Ballast Using GPR: Recent Experiences in the United States. / Roberts R., Schutz A., Al-Qadi I., Tutumluer E. // 2007 4th International Workshop on Advanced Ground Penetrating Radar. - Aula Magna Partenope, 27-29 June 2007. - P. 295-299. ↑
- C9320. {no data available}. 2007 15th International Conference on Digital Signal Processing. 2007 15th International Conference on Digital Signal Processing. - Cardiff, 1-4 July 2007. - P. i. ↑
- C9321. {no data available}. Conference Information. 2007 IEEE Intelligent Vehicles Symposium. - Istanbul, Turkey, 13-15 June 2007. - P. 10. ↑
- C9322. Miyake Y. Road-Shape Recognition Using On-Vehicle Millimeter-wave Radar. / Miyake Y., Natsume K., Hoshino K. // 2007 IEEE Intelligent Vehicles Symposium. - Istanbul, 13-15 June 2007. - P. 75-80. ↑
- C9323. Nabavi S. Two-Dimensional Generalized Partial Response Equalizer for Bit-Patterned Media. / Nabavi S., Vijaya Kumar B.V.K. // 2007. ICC '07. IEEE International Conference on Communications. - Glasgow, 24-28 June 2007. - P. 6249-6254. ↑
- C9324. {no data available}. 2007 IEEE Intelligent Vehicles Symposium. 2007 IEEE Intelligent Vehicles Symposium. - Istanbul, 13-15 June 2007. - P. nil1. ↑
- C9325. von Arnim A. Vehicle Identification Using Near Infrared Vision and Applications to Cooperative Perception. / von Arnim A., Perrollaz M., Bertrand A., Ehrlich J. // 2007 IEEE Intelligent Vehicles Symposium. - Istanbul, 13-15 June 2007. - P. 290-295. ↑
- C9326. Kamran S. A Multilevel Traffic Incidents Detection Approach: Identifying Traffic Patterns and Vehicle Behaviours using real-time GPS data. / Kamran S., Haas O. // 2007 IEEE Intelligent Vehicles Symposium. - Istanbul, 13-15 June 2007. - P. 912-917. ↑
- C9327. Wedel A. Monocular Video serves RADAR-based Emergency Braking. / Wedel A., Franke U. // 2007 IEEE Intelligent Vehicles Symposium. - Istanbul, 13-15 June 2007. - P. 93-98. ↑
- C9328. Bank D. Short Range Radar Signal Processing for Lateral Collision Warning in Road Traffic Scenarios. 2007 IEEE Intelligent Vehicles Symposium. - Istanbul, 13-15 June 2007. - P. 111-116. ↑
- C9329. Shkvarko Y. Finite Array Observations-Adapted Regularization Unified with Descriptive Experiment Design Approach for High-Resolution Spatial Power Spectrum Estimation with Application to Radar/SAR Imaging. 2007 15th International Conference on Digital Signal Processing. - Cardiff, 1-4 July 2007. - P. 79-82. ↑
- C9330. Amandio J. The Use of Non-Uniform Sample Phases for Array Synthesis. / Amandio J., Azevedo R. // 2007 15th International Conference on Digital Signal Processing. - Cardiff, 1-4 July 2007. - P. 95-98. ↑
- C9331. Gershman Alex. Robust Adaptive Beamforming: When the Worst Case is the Best We Can Do. 2007 15th International Conference on Digital Signal Processing. - Cardiff, UK, 1-4 July 2007. - P. 13. ↑
- C9332. Renbiao Wu. Adaptive Interference Suppression for Civil Aviation VHF Air-to-Ground Communication

Based on Constant Modulus Array. / Renbiao Wu, Qingyan Shi, Shuyan Wang, Jianli Ma. // 2007 15th International Conference on Digital Signal Processing. - Cardiff, 1-4 July 2007. - P. 67-70. ↑

C9333. Jiann-Ching Guey. Synchronization Signal Design for OFDM Based On Time-Frequency Hopping Patterns. 2007. ICC '07. IEEE International Conference on Communications. - Glasgow, 24-28 June 2007. - P. 4329-4334. ↑

C9334. Yang Yang. Routing for Emitter/Reflector Signal Detection in Wireless Sensor Network Systems. / Yang Yang, Blum R.S. // 2007. ICC '07. IEEE International Conference on Communications. - Glasgow, 24-28 June 2007. - P. 4919-4924. ↑

C9335. Gurbuz A.C. Feature Detection in Highly Noisy Images using Random Sample Theory. / Gurbuz A.C., McClellan J.H., Scott W.R. // 2007 15th International Conference on Digital Signal Processing. - Cardiff, 1-4 July 2007. - P. 423-426. ↑

C9336. Cardenete-Suriol M. VoIP Performance in SIP-Based Vertical Handovers Between WLAN and GPRS/UMTS Networks. / Cardenete-Suriol M., Mangues-Bafalluy J., Portoles-Comeras M., Requena-Esteso M., Gorricho M. // 2007. ICC '07. IEEE International Conference on Communications. - Glasgow, 24-28 June 2007. - P. 1973-1978. ↑

C9337. D'Hondt O. Quantitative analysis of texture parameter estimation in SAR images. / D'Hondt O., Lopez-Martinez C., Ferro-Famil L., Pottier E. // 2007. IGARSS 2007. IEEE International Geoscience and Remote Sensing Symposium. - Barcelona, 23-28 July 2007. - P. 274-277. ↑

C9338. Voles R. Poster Session 6d: Antennas 1. / Voles R., Stove A.G., Zheng F., Chen M., Duan B., Feng C., Moore S., Rutzel P., Feldle P., Bock M., Ostergaard A., Nandgaonkar A., Deosarkar S., Ambedkar B., Shah P., Sharp A.N., Kyprianou R., Bates B., Gill S., G w-hitehead J.R., Walbridge M.R. // 2007. RADAR 2007. The Institution of Engineering and Technology International Conference on Radar Systems. - Edinburgh, UK, 15-18 Oct. 2007. - P. 50-52. ↑

C9339. Cherniakov M. Oral Session 7a: Multistatic Radar 2. / Cherniakov M., Le Chevalier F., Kabakchiev C., Garvanov I., Whitewood A., Baker C.J., Griffiths H., Arnold-Bos A., Khenchaf A., Martin A., Chen J., Kuo C., Anderson S.J. // 2007. RADAR 2007. The Institution of Engineering and Technology International Conference on Radar Systems. - Edinburgh, UK, 15-18 Oct. 2007. - P. 53-54. ↑

C9340. Watts S. Oral Session 6b: SAR/ISAR 3. / Watts S., Kulpa K., Sjogren T., Vu V., Pettersson M., Zepernick H.J., Gustavsson A., Matthiesen D.J., Zasada D., Sanyal P., Perry R., Gonzalez-Partida J., Almorox-Gonzalez P., Burgos-Garcia M., Vigurs G., Milner C., Jarrett M. // 2007. RADAR 2007. The Institution of Engineering and Technology International Conference on Radar Systems. - Edinburgh, UK, 15-18 Oct. 2007. - P. 46-47. ↑

C9341. Ward K. Poster Session 6c: Environment 2. / Ward K., Greco M., De Miguel Vela G., Berlanga De Jesus A., Garcia Fominaya J., Stevens M.B., Olsen K.E., Johnsen T., Johnsrud S., Tansem I., Sornes P., Benham S., Murphy T.J., Burbage J.M., McDowall J., Andre D., Fuchs H., Essen H., Saillard J., Bourlier C., Hurtaud Y. // 2007. RADAR 2007. The Institution of Engineering and Technology International Conference on Radar Systems. - Edinburgh, UK, 15-18 Oct. 2007. - P. 48-49. ↑

C9342. Kinghorn A. Poster Session 7d: Antennas 2. / Kinghorn A., Rohling H., Zhuang L., Liu X., Froggatt T., Maio A.D., Fiorini M., Morini A., Moore S., Searle S., Howard S. // 2007. RADAR 2007. The Institution of Engineering and Technology International Conference on Radar Systems. - Edinburgh, UK, 15-18 Oct. 2007. - P. 59-61. ↑

C9343. Rohling H. Oral Session 8a: Radar Systems 3. / Rohling H., Teng L., Thomas G., Flores-Tapia D., Pistorius S., Cherniakov M., Gashinova M., Antoniou, Daniel L.Y., Hu C., Sizov V., Trinkle M., Gray D., Ferguson B., Brautigam B., Schwerdt M., Doring B., Sharp A.N., Bates B.D. // 2007. RADAR 2007. The Institution of Engineering and Technology International Conference on Radar Systems. - Edinburgh, UK, 15-18 Oct. 2007. - P. 62-63. ↑

C9344. Rangaswamy M. Oral Session 7b: Environment 1. / Rangaswamy M., Greco M., Tough R., Ward K., Watts S., Baker C.J., Herselman P.L., Dong Y., Haywood B., Anderson S.J., Morris J., Anderson W. // 2007. RADAR 2007. The Institution of Engineering and Technology International Conference on Radar Systems. - Edinburgh, UK, 15-18 Oct. 2007. - P. 55-56. ↑

- C9345.** Baker C.J. Poster Session 7c: Target Recognition. / Baker C.J., Farina A., Xiankang L., Meiguo G., Xiongjun F., Mishra A., Feng H., Muigrew B., Kouemou G., Opitz F., Lui H.S., Shuley N.V., Longstaff I.D. // 2007. RADAR 2007. The Institution of Engineering and Technology International Conference on Radar Systems. - Edinburgh, UK, 15-18 Oct. 2007. - P. 57-58. ↑
- C9346.** Stove A.G. Oral Session 6a: Radar Systems 2. / Stove A.G., Miceli W., Wade B., Hughes K., Mellor I.M., Adams F., Richardson P., Yamamoto K., Yonemoto N., Yamada K., Yasui H., We~i S., Biyang W., Zili L., Xiaojing H., Nickel U., Medley J.C., Briemle E. // 2007. RADAR 2007. The Institution of Engineering and Technology International Conference on Radar Systems. - Edinburgh, UK, 15-18 Oct. 2007. - P. 44-45. ↑
- C9347.** Money D. Poster Session 4c: Radar Systems 2. / Money D., Wu S., Zhang W., Jun S., Zhong T., Benito E., Rannou V., Saillant S., Bourdillon A., Nordsjo A.E., Wardell C., Patel D., Angell C., Bernhardt M., Barbaresco F., Froger J., Jeantet A., Meier U., Amin Nasrabadi M., Bastani M., Peacock C.J., Pearson G.S., Capraro G., Bradaric I., Wicks M. // 2007. RADAR 2007. The Institution of Engineering and Technology International Conference on Radar Systems. - Edinburgh, UK, 15-18 Oct. 2007. - P. 31-33. ↑
- C9348.** Ward K. Poster Session 4d: SAR/ISAR 2. / Ward K., Krieger G., Kulpa K., Misiurewicz J., Samczynski P., Smolarczyk M., Mordzonek M., Castillo-Rubio C., Burgos-Garcia M., Blanco-del-Campo A., Asensio-Lopez A., Zhong H., Liu X., Chen G., Zhou Z. // 2007. RADAR 2007. The Institution of Engineering and Technology International Conference on Radar Systems. - Edinburgh, UK, 15-18 Oct. 2007. - P. 34-35. ↑
- C9349.** Wicks M. Oral Session 4a: ECCM. / Wicks M., Le Chevalier F., Greco M., Gini, Farina A., Nelander A., Barker L.V., Threadgold M., Kauppi J.P., Martikainen K.S., Immediata S., Timmoneri L., Vigilante D. // 2007. RADAR 2007. The Institution of Engineering and Technology International Conference on Radar Systems. - Edinburgh, UK, 15-18 Oct. 2007. - P. 27-28. ↑
- C9350.** Fentem P. Oral Session 4b: Detection and Tracking 2. / Fentem P., Miceli W., Barbaresco F., Rivereau N., Li H., Sohn K., Himed B., Markow J.S., Chun J., Adve R., Yang E., Maio A.D., Nicola S.D., Farina A., Stove A.G. // 2007. RADAR 2007. The Institution of Engineering and Technology International Conference on Radar Systems. - Edinburgh, UK, 15-18 Oct. 2007. - P. 29-30. ↑
- C9351.** Cooper P. Poster Session 5c: Radar Systems 3. / Cooper P., Rohling H., Cilliers J., Smit J., Irci A., Saranh A., Baykal B., Thomsen A.C.K., Ostergaard A.C.A., Marquersen O., Moller-Hundborg C.T., Jensen L.J., Rohde R.H., Leth-Espensen P., Norland R., Gundersen R., Skjonhaug S., Skottene A., Sveli C., Dyroy B., Wang L., Borngraeber J., Winkler W., Scheytt C., Millot P., Maaref N., Pichot C., Picon O. // 2007. RADAR 2007. The Institution of Engineering and Technology International Conference on Radar Systems. - Edinburgh, UK, 15-18 Oct. 2007. - P. 40-41. ↑
- C9352.** Mulgrew B. Poster Session 5d: Detection and Tracking 3. / Mulgrew B., Kulpa K., Sjogren T., Vu V., Petterson M., Zepernick H.J., Gustavsson A., Leong H., Kovalenko V., Yarovoy A., Ligthart L., Rezazadeh A., Norouzi Y., Nayebi M. // 2007. RADAR 2007. The Institution of Engineering and Technology International Conference on Radar Systems. - Edinburgh, UK, 15-18 Oct. 2007. - P. 42-43. ↑
- C9353.** Griffiths H. Oral Session 5a: Antennas. / Griffiths H., Farina A., K wltshire M.C., Barclay M., Pietzschmann U., Gonzalez G., Tellini P., Berry P.E., Yau D., Guinvarc'h R., Finlay C., Lyon R., McCormick J., Gregson S. // 2007. RADAR 2007. The Institution of Engineering and Technology International Conference on Radar Systems. - Edinburgh, UK, 15-18 Oct. 2007. - P. 36-37. ↑
- C9354.** Lombardo P. Oral Session 5b: SAR/ISAR 2. / Lombardo P., Teng L., Flores B., Flores-Tapia D., Thomas G., Chen G., Liu X., Zhou Z., Callow H., Hansen R., Sparr T., Groen J., Gaffar M.A., Nel W., Martorella M., Berizzi F., Palmer J., Haywood B., Bates B. // 2007. RADAR 2007. The Institution of Engineering and Technology International Conference on Radar Systems. - Edinburgh, UK, 15-18 Oct. 2007. - P. 38-39. ↑
- C9355.** Zheng Yahong Rosa. A normalized Fractionally lower-order moment algorithm for Space-Time Adaptive Processing. / Zheng Yahong Rosa, Chen Genshe, Blasch Erik. // 2007. MILCOM 2007. IEEE Military Communications Conference. - Orlando, FL, USA, 29-31 Oct. 2007. - P. 1-6. ↑
- C9356.** Kim Yeejung. Detection Probability of WCDMA Based Cellular Radar System. / Kim Yeejung, Kim Seungmo, Han Youngnam, Bae Kyung Bin, Jeong Myung Deuk. // 2007. MILCOM 2007. IEEE Military Communications Conference. - Orlando, FL, USA, 29-31 Oct. 2007. - P. 1-5. ↑
- C9357.** {no data available}. Blank Page. 2007. RADAR 2007. The Institution of Engineering and Technology

International Conference on Radar Systems. - Edinburgh, UK, 15-18 Oct. 2007. - P. c3. ↑

C9358. {no data available}. Back Cover Page. 2007. RADAR 2007. The Institution of Engineering and Technology International Conference on Radar Systems. - Edinburgh, UK, 15-18 Oct. 2007. - P. c4. ↑

C9359. Liu da-xue. Fusing ladar and color image for detection grass off-road scenario. / Liu da-xue, Wu tao, Dai bin. // 2007. ICVES. IEEE International Conference on Vehicular Electronics and Safety. - Beijing, 13-15 Dec. 2007. - P. 1-4. ↑

C9360. Xun Dai. Vehicle centroid estimation based on radar multiple detections. / Xun Dai, Kummert A., Su Birm Park, Iurgel U. // 2007. ICVES. IEEE International Conference on Vehicular Electronics and Safety. - Beijing, 13-15 Dec. 2007. - P. 1-5. ↑

C9361. Blanc C. Data fusion performance evaluation for range measurements combined with cartesian ones for road obstacle tracking. / Blanc C., Checchin P., Gidel S., Trassoudaine L. // 2007. ICVES. IEEE International Conference on Vehicular Electronics and Safety. - Beijing, 13-15 Dec. 2007. - P. 1-6. ↑

C9362. Liu Zhifeng. A robust method to determine relevant target vehicle using vehicular radar. / Liu Zhifeng, Wang Jianqiang, Li Keqiang. // 2007. ICVES. IEEE International Conference on Vehicular Electronics and Safety. - Beijing, 13-15 Dec. 2007. - P. 1-5. ↑

C9363. {no data available}. RADAR 2008-First call for papers. 2007. RADAR 2007. The Institution of Engineering and Technology International Conference on Radar Systems. - Edinburgh, UK, 15-18 Oct. 2007. - P. 79-80. ↑

C9364. Watts S. Poster Session 8d: STAP and ECCM. / Watts S., Ender J., Zhu D., Shen M., Zhu Z., Akhtar J., Mulgrew B., Aboutanios E., Bell K., Trees H.V., Dikeman R.D., Moore C.A., Li W., Lu X., Da X., Liang D., Wu X., Dai D.H., Wang X.S. // 2007. RADAR 2007. The Institution of Engineering and Technology International Conference on Radar Systems. - Edinburgh, UK, 15-18 Oct. 2007. - P. 68-69. ↑

C9365. Baker C.J. Oral Session 9a: Target Recognition 2. / Baker C.J., Lnggs M.R., Ehrman L., Blair W.D., Chadwick J., Williams G.L., Aldhubaib F., Shuley N.V., Longstaff I.D., Rohling H., Ritter H., Folster F. // 2007. RADAR 2007. The Institution of Engineering and Technology International Conference on Radar Systems. - Edinburgh, UK, 15-18 Oct. 2007. - P. 70-71. ↑

C9366. Ward K. Oral Session 8b: Environment 2. / Ward K., Kwag Y., Rashid L.S., Brown A.K., Jackson C.A., Butler M.M., Nekrasov A., Rose P.S., Grieg O.W. // 2007. RADAR 2007. The Institution of Engineering and Technology International Conference on Radar Systems. - Edinburgh, UK, 15-18 Oct. 2007. - P. 64-65. ↑


















C9367. Fentem P. Poster Session 8c: Passive Radar. / Fentem P., Lesturgie M., Thomas J.M., Baker C.J., Griffiths H., Guo H., Coetzee S., Mason D., Woodbridge K., Lauri A., Cardinali R., Colone F., Lombardo P., Bucciarelli T., Meyer M. // 2007. RADAR 2007. The Institution of Engineering and Technology International Conference on Radar Systems. - Edinburgh, UK, 15-18 Oct. 2007. - P. 66-67. ↑














C9368. Le Chevalier F. Oral Session 10b: STAP. / Le Chevalier F., Klemm R., Gorski T., Le Caillec J.M., Kawalec A., Czarnecki W., Raout J., Rischette P., Neyt X., Cao T.V., Sinnott D., Melvin W., Showman G., Lim C., Mulgrew B., Kealey P.G., Carrington D.M. // 2007. RADAR 2007. The Institution of Engineering and Technology International Conference on Radar Systems. - Edinburgh, UK, 15-18 Oct. 2007. - P. 76-77. ↑

C9369. {no data available}. Blank Page. 2007. RADAR 2007. The Institution of Engineering and Technology International Conference on Radar Systems. - Edinburgh, UK, 15-18 Oct. 2007. - P. 78. ↑

C9370. Wicks M. Oral Session 9b: SAR/ISAR 4. / Wicks M., Haywood B., Bruder J., Schneible R., Jahangir M., Rollason M., Zhu D., Sedehi M., Cristallini D., Bucciarelli M., Lombardo P. // 2007. RADAR 2007. The Institution of Engineering and Technology International Conference on Radar Systems. - Edinburgh, UK, 15-18 Oct. 2007. - P. 72-73. ↑

C9371. Cherniakov M. Oral Session 10a: Passive Radar. / Cherniakov M., Colone F., Baker C.J., O'Hagan D., Griffiths H., Gould D., Tittensor P., Sarno C., Pollard R., Isohookana M., Morrison N., Lord R., Inggs M.R., Benavoli A., Lallo A.D., Farina A., Fulcoli R., Mancinelli R., Timmoneri L., Chisci L., Cardinali R. // 2007. RADAR 2007. The Institution of Engineering and Technology International Conference on Radar Systems. - Edinburgh, UK, 15-18 Oct. 2007. - P. 74-75. ↑

- C9372.** Abeysekera S.S. Hardware efficient frequency estimation and tracking using signal autocorrelations. 2007 6th International Conference on Information, Communications & Signal Processing. - Singapore, 10-13 Dec. 2007. - P. 1-5. 
- C9373.** Zhi Ning Chen. UWB antennas: Design and application. 2007 6th International Conference on Information, Communications & Signal Processing. - Singapore, 10-13 Dec. 2007. - P. 1-5. 
- C9374.** Vasantha Kumar B.P. Tunnel-accessed NATs for always-best-connected and application mobility. / Vasantha Kumar B.P., Manjunath D. // 2007 6th International Conference on Information, Communications & Signal Processing. - Singapore, 10-13 Dec. 2007. - P. 1-5. 
- C9375.** Kadambe S. 3D map generation for biometric applications using a network of multi-static radar sensors. 2007 6th International Conference on Information, Communications & Signal Processing. - Singapore, 10-13 Dec. 2007. - P. 1-5. 
- C9376.** {no data available}. Radar 2007 The Institution of Engineering and Technology International Conference on Radar Systems. 2007. RADAR 2007. The Institution of Engineering and Technology International Conference on Radar Systems. 15-18 Oct. 2007. - {no data available}. 
- C9377.** {no data available}. Copyright. 2007. RADAR 2007. The Institution of Engineering and Technology International Conference on Radar Systems. - Edinburgh, 15-18 Oct. 2007. - P. i-ii. 
- C9378.** {no data available}. The IET Radar 2007 International Conference on Radar Systems [Book of Abstracts]. 2007. RADAR 2007. The Institution of Engineering and Technology International Conference on Radar Systems. - Edinburgh, UK, 15-18 Oct. 2007. - P. c1. 
- C9379.** {no data available}. Blank Page. 2007. RADAR 2007. The Institution of Engineering and Technology International Conference on Radar Systems. - Edinburgh, UK, 15-18 Oct. 2007. - P. c2. 
- C9380.** Alkharabsheh K. Target tracking and interception in wireless sensor networks with compensation of communication delay. / Alkharabsheh K., Wendong Xiao, Lewis F., Manry M. // 2007 6th International Conference on Information, Communications & Signal Processing. - Singapore, 10-13 Dec. 2007. - P. 1-5. 
- C9381.** Gurgel Klaus-Werner. T6-High Frequency Over-the-Horizon Radar Applications I Oceanography. OCEANS 2007. - Vancouver, BC, Canada, Sept. 29 2007-Oct. 4 2007. - P. 29-30. 
- C9382.** Rodrigues N. A OFDM module for a MB-OFDM receiver. / Rodrigues N., Neto H., Sarmiento H. // 2007. DTIS. International Conference on Design & Technology of Integrated Systems in Nanoscale Era. - Rabat, 2-5 Sept. 2007. - P. 25-29. 
- C9383.** Subramanian V. Improvements in Data Management Practices within West Florida Shelf Coastal Ocean Monitoring and Prediction System. / Subramanian V., Donovan J., Atkins J., Luther M., Weisberg R. // OCEANS 2007. - Vancouver, BC, Sept. 29 2007-Oct. 4 2007. - P. 1-4. 
- C9384.** Lurton T. A Simulation of the Synthetic Aperture Radar Observation of a Manufactured Object in Sea Clutter using Finite Differences. / Lurton T., Sintès C., Garellò R., Gueriot D. // OCEANS 2007. - Vancouver, BC, Sept. 29 2007-Oct. 4 2007. - P. 1-6. 
- C9385.** Nam Trung Pham. Maintaining track continuity in GMPHD filter. / Nam Trung Pham, Weimin Huang, Ong S.H. // 2007 6th International Conference on Information, Communications & Signal Processing. - Singapore, 10-13 Dec. 2007. - P. 1-5. 
- C9386.** Albina C.M. Architecture optimization of a finite impulse response filter using toggle-based power estimation. / Albina C.M., Hackl G. // 2007 6th International Conference on Information, Communications & Signal Processing. - Singapore, 10-13 Dec. 2007. - P. 1-4. 
- C9387.** Xiumei Li. Improved ISAR imaging based on local polynomial fourier transform. / Xiumei Li, Guoan Bi, Yingtuo Ju. // 2007 6th International Conference on Information, Communications & Signal Processing. - Singapore, 10-13 Dec. 2007. - P. 1-5. 
- C9388.** Lei Lei. Robust supergain array in noise fields. / Lei Lei, Lew H. // 2007 6th International Conference on Information, Communications & Signal Processing. - Singapore, 10-13 Dec. 2007. - P. 1-4. 

- C9389.** Daniels D. Poster Session 2c: Radar Systems 1. / Daniels D., Lacomme P., Magaz B., Bencheikh M.L., Hamadouche M., Belouchrani A., Liu Y., Meng H., Zhang H., Wang X., Gallardo-Hernando B., Munoz-Ferreras J.M., Perez-Martinez F., Laizaro-Gasco J.M., Dawber W., Nichols I., Fu X., Tian L., Gao M., Murray D., Dickel G., Emery D.J., Money D.G. // 2007. RADAR 2007. The Institution of Engineering and Technology International Conference on Radar Systems. - Edinburgh, UK, 15-18 Oct. 2007. - P. 14-15. 
- C9390.** Stove A.G. Poster Session 2d: SAR/ISAR 1. / Stove A.G., Lombardo P., Munoz-Ferreras J.M., Perez-Martinez P., Amein A., Soraghan J., Wang Q., Xing M., Bao Z., Chen J., Zeng T., Teng L., Dai D., Wu X., Wang X., Xiao S., Bawar Z., Tao Z. // 2007. RADAR 2007. The Institution of Engineering and Technology International Conference on Radar Systems. - Edinburgh, UK, 15-18 Oct. 2007. - P. 16-17. 
- C9391.** Baker C.J. Oral Session 2a: Multistatic Radar 1. / Baker C.J., Bates B., Carson S., Kilfoyle D., Potter M., Vance J., Doughty S., Woodbridge K., Sandenbergh J.S., Lnggs M.R., Deng H., Himed B., Wicks W., Kulpa K., Malanowski M., Gajo Z. // 2007. RADAR 2007. The Institution of Engineering and Technology International Conference on Radar Systems. - Edinburgh, UK, 15-18 Oct. 2007. - P. 10-11. 
- C9392.** Woodbridge K. Oral Session 2b: Detection and Tracking 1. / Woodbridge K., Anderson F., Belcher D., Fabrizio G.A., Farina A., Liu Y., Meng H., Wang D., Wang X.Q., Morrison N., Lord R.T., Inggs M.R., Sammartino P.F., Baker C.J., Griffiths H., Rangaswamy M. // 2007. RADAR 2007. The Institution of Engineering and Technology International Conference on Radar Systems. - Edinburgh, UK, 15-18 Oct. 2007. - P. 12-13. 
- C9393.** Dawber W. Poster Session 3c: Environment 1. / Dawber W., Teng L., Liu N., Zhang L., Yi Y., Liu X., Jackson C.A., Holloway J., Larson R., Sarno C., Pollard R., Baker C.J., Woodbridge K., Ormondroyd R.F., Lewis M., Stove A.G., Papadopoulos S., Mulgrew B., Kwag Y.K., Yong J.Y., Jung C.H., Yamaguchi H., Suganuma W. // 2007. RADAR 2007. The Institution of Engineering and Technology International Conference on Radar Systems. - Edinburgh, UK, 15-18 Oct. 2007. - P. 22-24. 
- C9394.** Woodbridge K. Poster Session 3d: Detection and Tracking 2. / Woodbridge K., Kwag Y., Wang Q., Xing M., Machowski W., Koutsogiannis G., Potter S., Sanz-Gonzalez J., Alvarez-Vaquero F., Gonzeilez-Garcia J., Davidson G., Sheikhi A., Zamani A. // 2007. RADAR 2007. The Institution of Engineering and Technology International Conference on Radar Systems. - Edinburgh, UK, 15-18 Oct. 2007. - P. 25-26. 
- C9395.** Blacknell D. Oral Session 3a: Target Recognition 1. / Blacknell D., Cooper P., Klemm R., Smith G.E., Woodbridge K., Baker C.J., Ghaleb A., Vignaud L., Deloues T., Nicolas J.M., Abdullah R.R., Saripan M., Cherniakov M., Fang J., Meng H., Zhang H., Wang X. // 2007. RADAR 2007. The Institution of Engineering and Technology International Conference on Radar Systems. - Edinburgh, UK, 15-18 Oct. 2007. - P. 18-19. 
- C9396.** Griffiths H. Oral Session 3b: Waveform Design. / Griffiths H., Lacomme P., Antonik P., Wicks M.C., Welstead S., Ruggiano M., Genderen P.V., Magde K.M., Landi L., Adve R. // 2007. RADAR 2007. The Institution of Engineering and Technology International Conference on Radar Systems. - Edinburgh, UK, 15-18 Oct. 2007. - P. 20-21. 
- C9397.** Woodbridge K. Poster Session 1d: Detection and Tracking 1. / Woodbridge K., Anderson F., Daemi T., Jalilvand M., Shen M., Zhu D., Zhu Z., Verba V.S., Gandurin V., Sokolov A., Alabaster C., Hughes E., Worms J., Benoudnine H., Keche M., Ouamri A., Woolfson M.S. // 2007. RADAR 2007. The Institution of Engineering and Technology International Conference on Radar Systems. - Edinburgh, UK, 15-18 Oct. 2007. - P. 8-9. 
- C9398.** {no data available}. Programme. 2007. RADAR 2007. The Institution of Engineering and Technology International Conference on Radar Systems. - Edinburgh, UK, 15-18 Oct. 2007. - P. vii-xviii. 
- C9399.** {no data available}. Blank Page. 2007. RADAR 2007. The Institution of Engineering and Technology International Conference on Radar Systems. 15-18 Oct. 2007. - {no data available}. 
- C9400.** {no data available}. Radar 2007 The Institution of Engineering and Technology International Conference on Radar Systems-Committee/Members. 2007. RADAR 2007. The Institution of Engineering and Technology International Conference on Radar Systems. - Edinburgh, UK, 15-18 Oct. 2007. - P. iii-iv. 
- C9401.** {no data available}. Table of Contents. 2007. RADAR 2007. The Institution of Engineering and Technology International Conference on Radar Systems. - Edinburgh, UK, 15-18 Oct. 2007. - P. v-vi. 
- C9402.** Blacknell D. Oral Session 1b: SAR/ISAR 1. / Blacknell D., Ender J., Krieger G., Gebert N., Moreira A., Cote S., Srivastava S., Hawkins R., Dantec P.L., Fiedler H., Zink M., Hajnsek I., Younis M., Huber S., Bachmann

M., Gonzalez J.H., Werner M., Saini R., Zuo R., Cherniakov M., Barber B.C. // 2007. RADAR 2007. The Institution of Engineering and Technology International Conference on Radar Systems. - Edinburgh, UK, 15-18 Oct. 2007. - P. 4-5. ↑

C9403. Baker C.J. Poster Session 1c: Multistatic Radar. / Baker C.J., Bates B., Wnilliams L., Inggs M., Tao L., Hong Y., Zhu J., Rossum W.V., Huizing A., Lane R., Hayward S. // 2007. RADAR 2007. The Institution of Engineering and Technology International Conference on Radar Systems. - Edinburgh, UK, 15-18 Oct. 2007. - P. 6-7. ↑

C9404. {no data available}. Keynote Address. 2007. RADAR 2007. The Institution of Engineering and Technology International Conference on Radar Systems. - Edinburgh, UK, 15-18 Oct. 2007. - P. 1. ↑

C9405. Watts S. Oral Session 1a: Radar Systems 1. / Watts S., Inggs M.R., Dzvonkovskaya A., Rohling H., Dickel G., Emery D., Money D., Adrian O., Ferrier J.M., Ricci Y. // 2007. RADAR 2007. The Institution of Engineering and Technology International Conference on Radar Systems. - Edinburgh, UK, 15-18 Oct. 2007. - P. 2-3. ↑

C9406. Liang-Hwei Lee. Building Corner Feature Extraction Based on Fusion Technique with Airborne LiDAR Data and Aerial Imagery. / Liang-Hwei Lee, Shyue S.-W., Ming-Jer Huang. // 2007. IIHMSP 2007. Third International Conference on Intelligent Information Hiding and Multimedia Signal Processing. - Kaohsiung, 26-28 Nov. 2007. - Vol. 1. - P. 43-46. ↑

C9407. Daher R. A Notion of Diversity Order in Distributed Radar Networks. / Daher R., Adve R. // 2007. ACSSC 2007. Conference Record of the Forty-First Asilomar Conference on Signals, Systems and Computers. - Pacific Grove, CA, 4-7 Nov. 2007. - P. 1844-1848. ↑

C9408. Wicks M.C. RF Tomography with Application to Ground Penetrating Radar. 2007. ACSSC 2007. Conference Record of the Forty-First Asilomar Conference on Signals, Systems and Computers. - Pacific Grove, CA, 4-7 Nov. 2007. - P. 2017-2022. ↑

C9409. Lawrence Marple S. Multi-Channel Fast Parametric Algorithms and Performance for Adaptive Radar. / Lawrence Marple S., Corbell P.M., Rangaswamy M. // 2007. ACSSC 2007. Conference Record of the Forty-First Asilomar Conference on Signals, Systems and Computers. - Pacific Grove, CA, 4-7 Nov. 2007. - P. 1835-1838. ↑

C9410. Suvorova S. Doppler Resilience, Reed-MfBjller Codes and Complementary waveforms. / Suvorova S., Howard S., Moran B., Calderbank R., Pezeshki A. // 2007. ACSSC 2007. Conference Record of the Forty-First Asilomar Conference on Signals, Systems and Computers. - Pacific Grove, CA, 4-7 Nov. 2007. - P. 1839-1843. ↑

C9411. Chun Yang. A Net Track Solution to Pose-Angular Tracking of Maneuvering Targets in Clutter with HRR Radar. / Chun Yang, Blasch E., Garber W., Mitchell R. // 2007. ACSSC 2007. Conference Record of the Forty-First Asilomar Conference on Signals, Systems and Computers. - Pacific Grove, CA, 4-7 Nov. 2007. - P. 2033-2037. ↑

C9412. Bradaric I. Waveform Diversity for Different Multistatic Radar Configurations. / Bradaric I., Capraro G.T., Wicks M.C. // 2007. ACSSC 2007. Conference Record of the Forty-First Asilomar Conference on Signals, Systems and Computers. - Pacific Grove, CA, 4-7 Nov. 2007. - P. 2038-2042. ↑

C9413. Melvin W.L. Knowledge-Aided, Physics-Based Signal Processing For Next-Generation Radar. / Melvin W.L., Showman G.A. // 2007. ACSSC 2007. Conference Record of the Forty-First Asilomar Conference on Signals, Systems and Computers. - Pacific Grove, CA, 4-7 Nov. 2007. - P. 2023-2027. ↑

C9414. Pados D.A. Auxiliary-Vector RADAR on MCARM Data. / Pados D.A., Karystinos G.N., Batalama S.N., Matyjas J.D. // 2007. ACSSC 2007. Conference Record of the Forty-First Asilomar Conference on Signals, Systems and Computers. - Pacific Grove, CA, 4-7 Nov. 2007. - P. 2028-2032. ↑

C9415. Xumin Zhu. Knowledge-Aided Space-Time Adaptive Processing. / Xumin Zhu, Jian Li, Stoica P., Guerci J.R. // 2007. ACSSC 2007. Conference Record of the Forty-First Asilomar Conference on Signals, Systems and Computers. - Pacific Grove, CA, 4-7 Nov. 2007. - P. 1830-1834. ↑

C9416. Abramovich Y.I. Two-Dimensional Mixed Autoregressive Models for Space-Time Adaptive Processing. / Abramovich Y.I., Johnson B.A., Spencer N.K. // 2007. ACSSC 2007. Conference Record of the Forty-First

Asilomar Conference on Signals, Systems and Computers. - Pacific Grove, CA, 4-7 Nov. 2007. - P. 1367-1371.



C9417. Wilcox D. A Comparison of MIMO and Phased Array Radar with the Application of Music. / Wilcox D., Sellathurai M., Ratnarajah T. // 2007. ACSSC 2007. Conference Record of the Forty-First Asilomar Conference on Signals, Systems and Computers. - Pacific Grove, CA, 4-7 Nov. 2007. - P. 1529-1533.

C9418. Wage K.E. Multitaper Array Processing. 2007. ACSSC 2007. Conference Record of the Forty-First Asilomar Conference on Signals, Systems and Computers. - Pacific Grove, CA, 4-7 Nov. 2007. - P. 1242-1246.



C9419. Rubio F. Improved consistent estimation on Krylov subspaces. / Rubio F., Mestre X. // 2007. ACSSC 2007. Conference Record of the Forty-First Asilomar Conference on Signals, Systems and Computers. - Pacific Grove, CA, 4-7 Nov. 2007. - P. 1267-1271.

C9420. Yimin Zhang. A Novel Approach for Multiple Moving Target Localization Using Dual-Frequency Radars and Time-Frequency Distributions. / Yimin Zhang, Amin M., Ahmad F. // 2007. ACSSC 2007. Conference Record of the Forty-First Asilomar Conference on Signals, Systems and Computers. - Pacific Grove, CA, 4-7 Nov. 2007. - P. 1817-1821.

C9421. Ke Yong Li. A Modulation Based Approach to Wideband-STAP. / Ke Yong Li, Pillai U.S., Zulch P., Callahan M. // 2007. ACSSC 2007. Conference Record of the Forty-First Asilomar Conference on Signals, Systems and Computers. - Pacific Grove, CA, 4-7 Nov. 2007. - P. 1825-1829.

C9422. Koch L. Optimal Beamforming with Mobile Robots. / Koch L., Adve R., Francis B. // 2007. ACSSC 2007. Conference Record of the Forty-First Asilomar Conference on Signals, Systems and Computers. - Pacific Grove, CA, 4-7 Nov. 2007. - P. 1652-1656.

C9423. Yuanwei Jin. Time Reversal Synthetic Aperture Radar Imaging In Multipath. / Yuanwei Jin, Moura J.M.F., O'Donoghue N., Mulford M.T., Samuel A.A. // 2007. ACSSC 2007. Conference Record of the Forty-First Asilomar Conference on Signals, Systems and Computers. - Pacific Grove, CA, 4-7 Nov. 2007. - P. 1812-1816.



C9424. Krolik J.L. A Graph-Theoretic Approach for Constraining Floor Plan Estimation from Radar Measurements. / Krolik J.L., Hickman G. // 2007. ACSSC 2007. Conference Record of the Forty-First Asilomar Conference on Signals, Systems and Computers. - Pacific Grove, CA, 4-7 Nov. 2007. - P. 2228-2234.

C9425. Shun-Yu Chan. Application of GPRS Techniques for Wide-Area Power Quality Monitoring. / Shun-Yu Chan, Jen-Hao Teng, Chang D., Li-Yuan Chin. // 2007. PEDS '07. 7th International Conference on Power Electronics and Drive Systems. - Bangkok, 27-30 Nov. 2007. - P. 68-72.

C9426. Correll B. A Closed Form Expression for the Number of Costas Arrays of Arbitrary Order. 2007. ACSSC 2007. Conference Record of the Forty-First Asilomar Conference on Signals, Systems and Computers. - Pacific Grove, CA, 4-7 Nov. 2007. - P. 2218-2222.

C9427. Gurbuz A.C. Compressive Sensing for GPR Imaging. / Gurbuz A.C., McClellan J.H., Scott W.R. // 2007. ACSSC 2007. Conference Record of the Forty-First Asilomar Conference on Signals, Systems and Computers. - Pacific Grove, CA, 4-7 Nov. 2007. - P. 2223-2227.

C9428. Pathirana P.N. Stereo-Vision-Based Moving Object Tracking via Robust Linear Filtering. / Pathirana P.N., Bishop A.N., Savkin A.V. // ---. - Melbourne, Qld., 3-6 Dec. 2007. - P. 221-226.

C9429. Hui Ma. Distributive Target Tracking in Wireless Sensor Networks under Measurement Origin Uncertainty. / Hui Ma, Ng B.W.-H. // ---. - Melbourne, Qld., 3-6 Dec. 2007. - P. 299-304.

C9430. Sikora A. Communication and Localization for a Cooperative eSafety-System. 2007. IDAACS 2007. 4th IEEE Workshop on Intelligent Data Acquisition and Advanced Computing Systems: Technology and Applications. - Dortmund, 6-8 Sept. 2007. - P. 682-685.

C9431. Bishop A.N. Target Tracking with Range and Bearing Measurements via Robust Linear Filtering. / Bishop A.N., Pathirana P.N., Savkin A.V. // ---. - Melbourne, Qld., 3-6 Dec. 2007. - P. 131-135.

C9432. Besson O. Cramér-Rao Bound and Maximum Likelihood Estimation of Covariance Matrices With

Non-Homogeneous Snapshots. / Besson O., Bidon S., Yourneret J.Y. // 2007. ACSSC 2007. Conference Record of the Forty-First Asilomar Conference on Signals, Systems and Computers. - Pacific Grove, CA, 4-7 Nov. 2007. - P. 2213-2217. ↑

C9433. Bandiera F. Derivation and Analysis of an Adaptive Detector With Enhanced Mismatched Signals Rejection Capabilities. / Bandiera F., Besson O., Orlando D., Ricci G. // 2007. ACSSC 2007. Conference Record of the Forty-First Asilomar Conference on Signals, Systems and Computers. - Pacific Grove, CA, 4-7 Nov. 2007. - P. 2182-2186. ↑

C9434. Morris H. Morphological Component Analysis and STAP Filters. / Morris H., De Pass M.M. // 2007. ACSSC 2007. Conference Record of the Forty-First Asilomar Conference on Signals, Systems and Computers. - Pacific Grove, CA, 4-7 Nov. 2007. - P. 2187-2190. ↑

C9435. Qian He. Multibeam Amplitude Comparison Problems for MIMO Radar's Angle Measurement. / Qian He, Zishu He, Huiyong Li. // 2007. ACSSC 2007. Conference Record of the Forty-First Asilomar Conference on Signals, Systems and Computers. - Pacific Grove, CA, 4-7 Nov. 2007. - P. 2163-2167. ↑

C9436. Friedlander B. Waveform Design for MIMO Radar with Space-Time Constraints. 2007. ACSSC 2007. Conference Record of the Forty-First Asilomar Conference on Signals, Systems and Computers. - Pacific Grove, CA, 4-7 Nov. 2007. - P. 2168-2172. ↑

C9437. Yuanwei Jin. Time Reversal Transmission in MIMO Radar. / Yuanwei Jin, Moura J.M.F., O'Donoghue N. // 2007. ACSSC 2007. Conference Record of the Forty-First Asilomar Conference on Signals, Systems and Computers. - Pacific Grove, CA, 4-7 Nov. 2007. - P. 2204-2208. ↑

C9438. Sharma R. Coherent Change Detection Statistics for Multiple Polarization SAR Images. 2007. ACSSC 2007. Conference Record of the Forty-First Asilomar Conference on Signals, Systems and Computers. - Pacific Grove, CA, 4-7 Nov. 2007. - P. 2209-2212. ↑

C9439. Kazanci O. Wavefront Adaptive Raymode Processing for Over-the-Horizon HF Radar Clutter Mitigation. / Kazanci O., Bilik I., Krolík J. // 2007. ACSSC 2007. Conference Record of the Forty-First Asilomar Conference on Signals, Systems and Computers. - Pacific Grove, CA, 4-7 Nov. 2007. - P. 2191-2194. ↑

C9440. Zubeyde Gurbtiz S. Comparison of Radar-Based Human Detection Techniques. / Zubeyde Gurbtiz S., Melvin W.L., Williams D.B. // 2007. ACSSC 2007. Conference Record of the Forty-First Asilomar Conference on Signals, Systems and Computers. - Pacific Grove, CA, 4-7 Nov. 2007. - P. 2199-2203. ↑

C9441. Meng Yao. Target of Imaging Observation Based on The Wavelet Transform and GPR. / Meng Yao, Huabin Wang, Cui Wang. // 2007. IECON 2007. 33rd Annual Conference of the IEEE Industrial Electronics Society. - Taipei, 5-8 Nov. 2007. - P. 2470-2473. ↑

C9442. Solberg L.E. On the Swept-threshold Sampling in UWB Medical Radar. / Solberg L.E., Balasingham I. // 2007. BIOCAS 2007. IEEE Biomedical Circuits and Systems Conference. - Montreal, Que., 27-30 Nov. 2007. - P. 59-62. ↑

C9443. Mikhnev V.A. A Clutter Reduction Technique for Microwave Reconstruction of Shallow Underground Targets. / Mikhnev V.A., Vainikainen P. // 2007. EuCAP 2007. The Second European Conference on Antennas and Propagation. - Edinburgh, 11-16 Nov. 2007. - P. 1-4. ↑

C9444. Haina Rong. Application of S-method to Multi-component Emitter Signals. / Haina Rong, Gexiang Zhang, Weidong Jin. // 2007. IECON 2007. 33rd Annual Conference of the IEEE Industrial Electronics Society. - Taipei, 5-8 Nov. 2007. - P. 2521-2525. ↑

C9445. Gupta A. Development of a high resolution UWB Sensor for Estimation of Transfer Function of Vocal Tract Filter. / Gupta A., Saxena V., Joshi S. // 2007. WCSN '07. Third International Conference on Wireless Communication and Sensor Networks. - Allahabad, 13-15 Dec. 2007. - P. 131-134. ↑

C9446. Cho P. 3D Organization of 2D Urban Imagery. 2007. AIPR 2007. 36th IEEE Applied Imagery Pattern Recognition Workshop. - Washington, DC, 10-12 Oct. 2007. - P. 3-8. ↑

C9447. Jahangir M. Extracting information from shadows in SAR imagery. / Jahangir M., Blacknell D., Moate C.P., Hill R.D. // 2007. ICMV 2007. International Conference on Machine Vision. - Islamabad, 28-29 Dec. 2007. -

P. 107-112. ↑

C9448. Purohit N. Survivability Index for GSM Network. / Purohit N., Tokekar S. // 2007. WCSN '07. Third International Conference on Wireless Communication and Sensor Networks. - Allahabad, 13-15 Dec. 2007. - P. 105-109. ↑

C9449. Fischer C. Digital Beamforming Antenna for Synthetic Aperture Radar. / Fischer C., Schaefer C., Heer C. // 2007. EuCAP 2007. The Second European Conference on Antennas and Propagation. - Edinburgh, 11-16 Nov. 2007. - P. 1-5. ↑

C9450. Wen-Chuan Hsieh. An Architecture for the Interoperability of Multimedia Messaging Services between GPRS and PHS Cellular Networks. / Wen-Chuan Hsieh, Wei-Chung Hsu, Yu-Yuan Hsu. // 2007. IIHMSP 2007. Third International Conference on Intelligent Information Hiding and Multimedia Signal Processing. - Kaohsiung, 26-28 Nov. 2007. - Vol. 2. - P. 365-368. ↑

C9451. Fam A.T. A New Class of Interlaced Complementary Codes Based on Components with Unity Peak Sidelobes. / Fam A.T., Sarkar I. // 2007 IEEE International Symposium on Signal Processing and Information Technology. - Giza, 15-18 Dec. 2007. - P. 464-469. ↑

C9452. Chen Change Loy. Keystroke Patterns Classification Using the ARTMAP-FD Neural Network. / Chen Change Loy, Weng Kin Lai, Chee Peng Lim. // 2007. IIHMSP 2007. Third International Conference on Intelligent Information Hiding and Multimedia Signal Processing. - Kaohsiung, 26-28 Nov. 2007. - Vol. 1. - P. 61-64. ↑

C9453. Weitao Zheng. Study on the Division Tactics of Top Swimming Athletes Home and Abroad in the 400m Freestyle Swimming Race. / Weitao Zheng, Zihua Zhang, Ting Liao, Tuanjie Zhao, Yong Ma. // 2007. IIHMSP 2007. Third International Conference on Intelligent Information Hiding and Multimedia Signal Processing. - Kaohsiung, 26-28 Nov. 2007. - Vol. 2. - P. 317-320. ↑

C9454. Wei Xia. Subspace-Based Method for Multiple-Target Localization Using MIMO Radars. / Wei Xia, Zishu He, Yuyu Liao. // 2007 IEEE International Symposium on Signal Processing and Information Technology. - Giza, 15-18 Dec. 2007. - P. 715-720. ↑

C9455. Yu K.V. Application of Doppler Spectrum for Retrieval of Statistical Parameters of Sea Waves. / Yu K.V., Kanevsky M.B., Meshkov E.M. // 2007. EuCAP 2007. The Second European Conference on Antennas and Propagation. - Edinburgh, 11-16 Nov. 2007. - P. 1-6. ↑

C9456. Piracci E.G. Super-imposed Mode S signals: Single-antenna Projection Algorithm and processing architecture. / Piracci E.G., Petrochilos N., Galati G. // 2007 IEEE International Symposium on Signal Processing and Information Technology. - Giza, 15-18 Dec. 2007. - P. 166-170. ↑

C9457. Pierucci L. Improvements of radar clutter classification in air traffic control environment. / Pierucci L., Bocchi L. // 2007 IEEE International Symposium on Signal Processing and Information Technology. - Giza, 15-18 Dec. 2007. - P. 721-724. ↑

C9458. da Costa J.P.C.L. Enhanced Model Order Estimation using Higher-Order Arrays. / da Costa J.P.C.L., Haardt M., Romer F., Del Galdo G. // 2007. ACSSC 2007. Conference Record of the Forty-First Asilomar Conference on Signals, Systems and Computers. - Pacific Grove, CA, 4-7 Nov. 2007. - P. 412-416. ↑

C9459. Davis M.S. Statistical Modeling and ML Parameter Estimation of Complex SAR Imagery. / Davis M.S., Bidigare P., Chang D. // 2007. ACSSC 2007. Conference Record of the Forty-First Asilomar Conference on Signals, Systems and Computers. - Pacific Grove, CA, 4-7 Nov. 2007. - P. 500-502. ↑

C9460. Mecca V.F. Slow-Time MIMO STAP with Improved Power Efficiency. / Mecca V.F., Krolik J.L. // 2007. ACSSC 2007. Conference Record of the Forty-First Asilomar Conference on Signals, Systems and Computers. - Pacific Grove, CA, 4-7 Nov. 2007. - P. 202-206. ↑

C9461. Bliss D.W. MIMO Radar: Joint Array And Waveform Optimization. / Bliss D.W., Forsythe K.W., Richmond C.D. // 2007. ACSSC 2007. Conference Record of the Forty-First Asilomar Conference on Signals, Systems and Computers. - Pacific Grove, CA, 4-7 Nov. 2007. - P. 207-211. ↑

C9462. Boldt B.M. A Handheld Texel Camera for Acquiring Near-Instantaneous 3D Images. / Boldt B.M., Budge S.E., Pack R.T., Israelsen P.D. // 2007. ACSSC 2007. Conference Record of the Forty-First Asilomar

Conference on Signals, Systems and Computers. - Pacific Grove, CA, 4-7 Nov. 2007. - P. 953-957. ↑

C9463. Mollova G. Design of FIR LS Hilbert Transformers Through Fullband Differentiators. 2007. ACSSC 2007. Conference Record of the Forty-First Asilomar Conference on Signals, Systems and Computers. - Pacific Grove, CA, 4-7 Nov. 2007. - P. 1121-1125. ↑

C9464. Rangaswamy M. Performance Analysis of the NAMF Test in Heterogeneous Non-Gaussian Radar Clutter Scenarios. / Rangaswamy M., Lin F.C. // 2007. ACSSC 2007. Conference Record of the Forty-First Asilomar Conference on Signals, Systems and Computers. - Pacific Grove, CA, 4-7 Nov. 2007. - P. 706-710. ↑

C9465. Trump T. A robust detector for impulsive noise environment. 2007. ACSSC 2007. Conference Record of the Forty-First Asilomar Conference on Signals, Systems and Computers. - Pacific Grove, CA, 4-7 Nov. 2007. - P. 730-734. ↑

C9466. Sammartino P.F. Coverage in radar networks. / Sammartino P.F., Baker C.J., Rangaswamy M. // 2007. ACSSC 2007. Conference Record of the Forty-First Asilomar Conference on Signals, Systems and Computers. - Pacific Grove, CA, 4-7 Nov. 2007. - P. 197-201. ↑

C9467. Livingston A.R. Regional Variance Dependant Sub-frame Reduction for Face Detection in High Definition Video Frames. / Livingston A.R., Asari V.K. // 2007. AIPR 2007. 36th IEEE Applied Imagery Pattern Recognition Workshop. - Washington, DC, 10-12 Oct. 2007. - P. 89-94. ↑

C9468. Gurram P. 3D Scene Reconstruction through a Fusion of Passive Video and Lidar Imagery. / Gurram P., Rhody H., Kerekes J., Lach S., Saber E. // 2007. AIPR 2007. 36th IEEE Applied Imagery Pattern Recognition Workshop. - Washington, DC, 10-12 Oct. 2007. - P. 133-138. ↑

C9469. Schaum A. Adapting to Change: The CFAR Problem in Advanced Hyperspectral Detection. 2007. AIPR 2007. 36th IEEE Applied Imagery Pattern Recognition Workshop. - Washington, DC, 10-12 Oct. 2007. - P. 15-21. ↑

C9470. Cobb J.T. In Situ Adaptive Feature Extraction for Underwater Target Classification. / Cobb J.T., Stack J.R. // 2007. AIPR 2007. 36th IEEE Applied Imagery Pattern Recognition Workshop. - Washington, DC, 10-12 Oct. 2007. - P. 42-47. ↑

C9471. Friedlander B. On Data-Adaptive Waveform Design for MIMO Radar. 2007. ACSSC 2007. Conference Record of the Forty-First Asilomar Conference on Signals, Systems and Computers. - Pacific Grove, CA, 4-7 Nov. 2007. - P. 187-191. ↑

C9472. Chun Yang Chen. MIMO Radar Ambiguity Optimization Using Frequency-Hopping Waveforms. 2007. ACSSC 2007. Conference Record of the Forty-First Asilomar Conference on Signals, Systems and Computers. - Pacific Grove, CA, 4-7 Nov. 2007. - P. 192-196. ↑

C9473. Luzhou Xu. Parameter Estimation and Number Detection of MIMO Radar Targets. / Luzhou Xu, Stoica P., Jian Li. // 2007. ACSSC 2007. Conference Record of the Forty-First Asilomar Conference on Signals, Systems and Computers. - Pacific Grove, CA, 4-7 Nov. 2007. - P. 177-181. ↑

C9474. Aittomaki T. Signal Covariance Matrix Optimization for Transmit Beamforming in MIMO Radars. / Aittomaki T., Koivunen V. // 2007. ACSSC 2007. Conference Record of the Forty-First Asilomar Conference on Signals, Systems and Computers. - Pacific Grove, CA, 4-7 Nov. 2007. - P. 182-186. ↑

C9475. Younis M. Performance Prediction and Verification for the Synchronization Link of TanDEM-X. / Younis M., Metzsig R., Krieger G., Bachmann M., Klein R. // 2007. IGARSS 2007. IEEE International Geoscience and Remote Sensing Symposium. - Barcelona, 23-28 July 2007. - P. 5206-5209. ↑

C9476. Nicoll J. Prediction and detection of Faraday rotation in ALOS PALSAR data. / Nicoll J., Meyer F., Jehle M. // 2007. IGARSS 2007. IEEE International Geoscience and Remote Sensing Symposium. - Barcelona, 23-28 July 2007. - P. 5210-5213. ↑

C9477. Zaugg E.C. Full motion compensation for LFM-CW synthetic aperture radar. / Zaugg E.C., Long D.G. // 2007. IGARSS 2007. IEEE International Geoscience and Remote Sensing Symposium. - Barcelona, 23-28 July 2007. - P. 5198-5201. ↑

- C9478.** Brautigam B. Individual T/R module characterisation of the TerraSAR-X active phased array antenna by calibration pulse sequences with orthogonal codes. / Brautigam B., Schwerdt M., Bachmann M., Stangl M. // 2007. IGARSS 2007. IEEE International Geoscience and Remote Sensing Symposium. - Barcelona, 23-28 July 2007. - P. 5202-5205. ↑
- C9479.** Lopez-Martinez C. Analysis and improvement of polarimetric calibration techniques. / Lopez-Martinez C., Cortes A., Fabregas X. // 2007. IGARSS 2007. IEEE International Geoscience and Remote Sensing Symposium. - Barcelona, 23-28 July 2007. - P. 5224-5227. ↑
- C9480.** Tello M. Characterization of local regularity in SAR Imagery by means of multiscale techniques: application to oil spill detection. / Tello M., Lopez-Martinez C., Mallorqui J.J., Danisi A., Di Martino G., Iodice A., Ruello G., Riccio D. // 2007. IGARSS 2007. IEEE International Geoscience and Remote Sensing Symposium. - Barcelona, 23-28 July 2007. - P. 5228-5231. ↑
- C9481.** Borner T. ALOS PALSAR products verification. / Borner T., Papathanassiou K.P., Marquart N., Zink M., Meininger M., Meadows P.J., Rye A.J., Wright P., Rosich Tell B. // 2007. IGARSS 2007. IEEE International Geoscience and Remote Sensing Symposium. - Barcelona, 23-28 July 2007. - P. 5214-5217. ↑
- C9482.** Croci R. Calibration of the SHARAD Instrument. / Croci R., Fois F., Guelfi M., Noschese P., Mecozzi R., Seu R. // 2007. IGARSS 2007. IEEE International Geoscience and Remote Sensing Symposium. - Barcelona, 23-28 July 2007. - P. 5218-5223. ↑
- C9483.** Sang-Eun Park. Inversion of soil moisture content from L- and P-band AIRSAR polarimetric SAR data. / Sang-Eun Park, Moon W.M. // 2007. IGARSS 2007. IEEE International Geoscience and Remote Sensing Symposium. - Barcelona, 23-28 July 2007. - P. 5194-5197. ↑
- C9484.** Mengmeng Zhu. An improved time-frequency phase adjustment technique for ISAR. / Mengmeng Zhu, Junfeng Wang, Xingzhao Liu. // 2007. IGARSS 2007. IEEE International Geoscience and Remote Sensing Symposium. - Barcelona, 23-28 July 2007. - P. 5170-5173. ↑
- C9485.** Amein A.S. The fractional Fourier transform and its application to high resolution SAR imaging. / Amein A.S., Soraghan J.J. // 2007. IGARSS 2007. IEEE International Geoscience and Remote Sensing Symposium. - Barcelona, 23-28 July 2007. - P. 5174-5177. ↑
- C9486.** Paradella W.R. Evaluation of the altimetric information from RADARSAT-1, ASTER and SRTM data for topographic mapping in the Amazon Region. / Paradella W.R., de Oliveira C.G. // 2007. IGARSS 2007. IEEE International Geoscience and Remote Sensing Symposium. - Barcelona, 23-28 July 2007. - P. 5134-5137. ↑
- C9487.** Chen V.C. Joint time-frequency analysis for radar signal and imaging. 2007. IGARSS 2007. IEEE International Geoscience and Remote Sensing Symposium. - Barcelona, 23-28 July 2007. - P. 5166-5169. ↑
- C9488.** Duquenoy M. Characterization of scatterers by their anisotropic and dispersive behavior. / Duquenoy M., Ovarlez J.-P., Ferro-Famil L., Pottier E., Vignaud L. // 2007. IGARSS 2007. IEEE International Geoscience and Remote Sensing Symposium. - Barcelona, 23-28 July 2007. - P. 5186-5189. ↑
- C9489.** Kelly J. Subaperture analysis of polarimetric SAR imagery. / Kelly J., Ainsworth T.L., Lee J.-S. // 2007. IGARSS 2007. IEEE International Geoscience and Remote Sensing Symposium. - Barcelona, 23-28 July 2007. - P. 5190-5193. ↑
- C9490.** Kersten P.R. The cross Time-Frequency Distribution Series for Synthetic Aperture Radar (SAR) applications. / Kersten P.R., Jansen R.W., Ainsworth T.L. // 2007. IGARSS 2007. IEEE International Geoscience and Remote Sensing Symposium. - Barcelona, 23-28 July 2007. - P. 5178-5181. ↑
- C9491.** Ferro-Famil L. Complex scene analysis from Time-Frequency statistics of POLSAR data. / Ferro-Famil L., Reigber A. // 2007. IGARSS 2007. IEEE International Geoscience and Remote Sensing Symposium. - Barcelona, 23-28 July 2007. - P. 5182-5185. ↑
- C9492.** Nouvel J.F. A low-cost imaging radar: DRIVE on board ONERA motorglider. / Nouvel J.F., Roques S., du Plessis O.R. // 2007. IGARSS 2007. IEEE International Geoscience and Remote Sensing Symposium. - Barcelona, 23-28 July 2007. - P. 5306-5309. ↑
- C9493.** Klare J. Image quality analysis of the vibrating sparse MIMO antenna array of the airborne 3D imaging

radar ARTINO. / Klare J., Cerutti-Maori D., Brenner A., Ender J. // 2007. IGARSS 2007. IEEE International Geoscience and Remote Sensing Symposium. - Barcelona, 23-28 July 2007. - P. 5310-5314. ↑

C9494. Pepe A. A space-time minimum cost flow phase unwrapping algorithm for the generation of persistent scatterers deformation time-series. / Pepe A., Manunta M., Mazzarella G., Lanari R. // 2007. IGARSS 2007. IEEE International Geoscience and Remote Sensing Symposium. - Barcelona, 23-28 July 2007. - P. 5285-5288. ↑

C9495. Guarnieri A.M. A new framework for multi-pass SAR interferometry with distributed targets. / Guarnieri A.M., Tebaldini S. // 2007. IGARSS 2007. IEEE International Geoscience and Remote Sensing Symposium. - Barcelona, 23-28 July 2007. - P. 5289-5293. ↑

C9496. Kravchenko V.F. The family of atomic functions and digital signal processing in synthetic aperture radar. / Kravchenko V.F., Volosyuk V.K., Pavlikov V.V. // 2007 6th International Conference on Antenna Theory and Techniques. - Sevastopol, 17-21 Sept. 2007. - P. 20-25. ↑

C9497. Zhirnov V.V. Intellectual multisurvey processing of radar information. / Zhirnov V.V., Solonskaya S.V. // 2007 6th International Conference on Antenna Theory and Techniques. - Sevastopol, 17-21 Sept. 2007. - P. 341-343. ↑

C9498. Weiss M. A three dimensional SAR system on an UAV. / Weiss M., Peters O., Ender J. // 2007. IGARSS 2007. IEEE International Geoscience and Remote Sensing Symposium. - Barcelona, 23-28 July 2007. - P. 5315-5318. ↑

C9499. Das S. Annealed Differential Evolution. / Das S., Konar A., Chakraborty U.K. // 2007. CEC 2007. IEEE Congress on Evolutionary Computation. - Singapore, 25-28 Sept. 2007. - P. 1926-1933. ↑

C9500. Lombardini F. New potentials of differential SAR tomography: Volumetric differential interferometry and robust DEM generation. 2007. IGARSS 2007. IEEE International Geoscience and Remote Sensing Symposium. - Barcelona, 23-28 July 2007. - P. 5281-5284. ↑

C9501. Lienert B. Advances in real time lidar spectroscopy. / Lienert B., Sharma S.K., Teng Chen, Madey M.J. // 2007. IGARSS 2007. IEEE International Geoscience and Remote Sensing Symposium. - Barcelona, 23-28 July 2007. - P. 5258-5261. ↑

C9502. Tatarov B. Lidar method for determination of quartz concentration in the tropospheric mineral aerosols. / Tatarov B., Sugimoto N., Matsui I. // 2007. IGARSS 2007. IEEE International Geoscience and Remote Sensing Symposium. - Barcelona, 23-28 July 2007. - P. 5262-5265. ↑

C9503. Lambrigtsen B. Developing a GeoSTAR science mission. / Lambrigtsen B., Tanner A., Gaier T., Kangaslahti P., Brown S. // 2007. IGARSS 2007. IEEE International Geoscience and Remote Sensing Symposium. - Barcelona, 23-28 July 2007. - P. 5232-5236. ↑

C9504. Lahtinen J. Improved receiver architecture for future L-band radiometer missions. / Lahtinen J., Piironen P., Colliander A. // 2007. IGARSS 2007. IEEE International Geoscience and Remote Sensing Symposium. - Barcelona, 23-28 July 2007. - P. 5247-5250. ↑


C9505. Lachaise M. Multi baseline SAR acquisition concepts and phase unwrapping algorithms for the TanDEM-X mission. / Lachaise M., Eineder M., Fritz T. // 2007. IGARSS 2007. IEEE International Geoscience and Remote Sensing Symposium. - Barcelona, 23-28 July 2007. - P. 5272-5276. ↑


C9506. Fornaro G. Spaceborne multi-dimensional SAR imaging: Current status and perspectives. / Fornaro G., Lombardini F., Pardini M., Serafino F., Soldovieri F., Costantini M. // 2007. IGARSS 2007. IEEE International Geoscience and Remote Sensing Symposium. - Barcelona, 23-28 July 2007. - P. 5277-5280. ↑


C9507. Porter J. Lidar, sun photometer and polar nephelometer measurements: Remote sensing of aerosol size distribution properties. / Porter J., Bates D., Walterspiel J. // 2007. IGARSS 2007. IEEE International Geoscience and Remote Sensing Symposium. - Barcelona, 23-28 July 2007. - P. 5266-5267. ↑


C9508. Gimmestad G.G. A new type of lidar for atmospheric optical turbulence. / Gimmestad G.G., Roberts D.W., Stewart J.M., Wood J.W. // 2007. IGARSS 2007. IEEE International Geoscience and Remote Sensing Symposium. - Barcelona, 23-28 July 2007. - P. 5268-5271. ↑


- C9509.** Di Martino G. Disaster monitoring by extracting geophysical parameters from SAR data. / Di Martino G., Iodice A., Riccio D., Ruello G. // 2007. IGARSS 2007. IEEE International Geoscience and Remote Sensing Symposium. - Barcelona, 23-28 July 2007. - P. 4949-4952. ↑
- C9510.** Mora O. ICC's project for DInSAR terrain subsidence monitoring of the catalonian territory. / Mora O., Arbiol R., Pala V. // 2007. IGARSS 2007. IEEE International Geoscience and Remote Sensing Symposium. - Barcelona, 23-28 July 2007. - P. 4953-4956. ↑
- C9511.** Krieger G. Multidimensional radar waveforms a new paradigm for the design and operation of highly performant spaceborne synthetic aperture radar systems. / Krieger G., Gebert N., Moreira A. // 2007. IGARSS 2007. IEEE International Geoscience and Remote Sensing Symposium. - Barcelona, 23-28 July 2007. - P. 4937-4941. ↑
- C9512.** Min Wang. SBRAS-an advanced simulator of spaceborne radar. / Min Wang, Diannong Liang, Haifeng Huang, Zhen Dong. // 2007. IGARSS 2007. IEEE International Geoscience and Remote Sensing Symposium. - Barcelona, 23-28 July 2007. - P. 4942-4944. ↑
- C9513.** Omar A. Extinction-to-backscatter ratios of lofted aerosol layers observed during the first three months of CALYPSO measurements. / Omar A., Vaughan M., Liu Z., Hu Y., Reagan J., Winker D. // 2007. IGARSS 2007. IEEE International Geoscience and Remote Sensing Symposium. - Barcelona, 23-28 July 2007. - P. 4965-4968. ↑
- C9514.** Straume-Lindner A.G. ADM-Aeolus: The first space-based high spectral resolution Doppler Wind Lidar. / Straume-Lindner A.G., Ingmann P. // 2007. IGARSS 2007. IEEE International Geoscience and Remote Sensing Symposium. - Barcelona, 23-28 July 2007. - P. 4969-4974. ↑
- C9515.** Gonzalez-Huici M.A. Numerical simulation of electromagnetic-wave propagation for land mine detection using GPR. / Gonzalez-Huici M.A., Uschkerat U., Hoerdet A. // 2007. IGARSS 2007. IEEE International Geoscience and Remote Sensing Symposium. - Barcelona, 23-28 July 2007. - P. 4957-4960. ↑
- C9516.** Singh D. An efficient electromagnetic approach to train the SVM for depth estimation of shallow buried objects with microwave remote sensing data. 2007. IGARSS 2007. IEEE International Geoscience and Remote Sensing Symposium. - Barcelona, 23-28 July 2007. - P. 4961-4964. ↑
- C9517.** Belmonte A. First steps towards multimodal georeferencing of 3D VHR optical and X-band SAR imagery. / Belmonte A., Derauw D., Barbier C., Verly J.G. // 2007. IGARSS 2007. IEEE International Geoscience and Remote Sensing Symposium. - Barcelona, 23-28 July 2007. - P. 4933-4936. ↑
- C9518.** Teichrieb V. Enhancement of radar based DEMs using 3D techniques. / Teichrieb V., Kelner J. // 2007. IGARSS 2007. IEEE International Geoscience and Remote Sensing Symposium. - Barcelona, 23-28 July 2007. - P. 4902-4905. ↑
- C9519.** Blom R. Genesis of a new NASA InSAR mission concept, and natural hazards applications. / Blom R., Donnellan A., Fielding E., Freeman A., Hensley S., Johnson W.T.K., Loverro A., Lundgren P., Rosen P., Saatchi S. // 2007. IGARSS 2007. IEEE International Geoscience and Remote Sensing Symposium. - Barcelona, 23-28 July 2007. - P. 4912-4915. ↑
- C9520.** Marinkovic P. Dynamic persistent scatterers interferometry. / Marinkovic P., Hanssen R. // 2007. IGARSS 2007. IEEE International Geoscience and Remote Sensing Symposium. - Barcelona, 23-28 July 2007. - P. 4894-4897. ↑
- C9521.** Tao Wu. Ground deformation retrieval of urban and suburb areas based on multi-baseline DInSAR algorithm: A case study in Cangzhou City (China). / Tao Wu, Hong Zhang, Chao Wang. // 2007. IGARSS 2007. IEEE International Geoscience and Remote Sensing Symposium. - Barcelona, 23-28 July 2007. - P. 4898-4901. ↑
- C9522.** Faller N. TerraSAR-X and TanDEM-X: Revolution in spaceborne radar. / Faller N., Weber M. // 2007. IGARSS 2007. IEEE International Geoscience and Remote Sensing Symposium. - Barcelona, 23-28 July 2007. - P. 4924-4928. ↑
- C9523.** Mittermayer J. Verification of the TerraSAR-X system. / Mittermayer J., Younis M., Brautigam B., Fritz T., Kahle R., Metz R., Schattler B. // 2007. IGARSS 2007. IEEE International Geoscience and Remote Sensing Symposium. - Barcelona, 23-28 July 2007. - P. 4929-4932. ↑


Symposium. - Barcelona, 23-28 July 2007. - P. 4929-4932. 


C9524. Rincon R. RadSTAR L-band imaging scatterometer- performance assessment. / Rincon R., Hildebrand P.R., Hilliard L. // 2007. IGARSS 2007. IEEE International Geoscience and Remote Sensing Symposium. - Barcelona, 23-28 July 2007. - P. 4916-4919. 


C9525. Fischman M.A. Advanced control and processing capabilities in the aquarius scatterometer flight electronics. / Fischman M.A., McWatters D.A., Berkun A.C., Cheetham C.M., Chu A.J., Duong V.A., Freedman A.P., Hausmann R.W., Jourdan M.N., Kang E.C., Kobzeff P.A., Paller M. // 2007. IGARSS 2007. IEEE International Geoscience and Remote Sensing Symposium. - Barcelona, 23-28 July 2007. - P. 4920-4923. 


C9526. Buck C. Status and perspectives of GNSS-R at ESA. / Buck C., D'Addio S. // 2007. IGARSS 2007. IEEE International Geoscience and Remote Sensing Symposium. - Barcelona, 23-28 July 2007. - P. 5076-5079. 


C9527. Caparrini M. Oceanpal®: Monitoring sea state with a GNSS-R coastal instrument. / Caparrini M., Egido A., Soulat F., Germain O., Farres E., Dunne S., Ruffini G. // 2007. IGARSS 2007. IEEE International Geoscience and Remote Sensing Symposium. - Barcelona, 23-28 July 2007. - P. 5080-5083. 


C9528. Nohmi H. The repeat-pass interferometric SAR by Pi-SAR(L). / Nohmi H., Shimada M., Miyawaki M. // 2007. IGARSS 2007. IEEE International Geoscience and Remote Sensing Symposium. - Barcelona, 23-28 July 2007. - P. 5057-5060. 


C9529. Magnard C. High resolution millimeter wave SAR interferometry. / Magnard C., Meier E., Ruegg M., Brehm T., Essen H. // 2007. IGARSS 2007. IEEE International Geoscience and Remote Sensing Symposium. - Barcelona, 23-28 July 2007. - P. 5061-5064. 


C9530. Martinez-Benjamin J.J. Altimetric calibration experiences in the Western Mediterranean. / Martinez-Benjamin J.J., Garcia M.M., Davila J.M., Garate J., Castellon M.A.O., Talaya J., Baron A., Velasco G.R., Bonnefond P., Perez B. // 2007. IGARSS 2007. IEEE International Geoscience and Remote Sensing Symposium. - Barcelona, 23-28 July 2007. - P. 5121-5124. 


C9531. Vignudelli S. ALTICORE-A consortium serving european seas with coastal altimetry. / Vignudelli S., Roblou L., Snaith H.M., Cipollini P., Venuti F., Kostianoy A., Ginzburg A., Lyard F., Cretaux J.F., Birol F., Lebedev S., Sirota A., Medvedev D., Khlebnikova S., Mamedov R., Ismatova K., Alyev A., Nabiyevev T. // 2007. IGARSS 2007. IEEE International Geoscience and Remote Sensing Symposium. - Barcelona, 23-28 July 2007. - P. 5125-5128. 


C9532. Helm A. Status of GNSS reflectometry related receiver developments and feasibility studies within the German Indonesian Tsunami Early Warning System. / Helm A., Stosius R., Beyerle G., Montenbruck O., Rothacher M. // 2007. IGARSS 2007. IEEE International Geoscience and Remote Sensing Symposium. - Barcelona, 23-28 July 2007. - P. 5084-5087. 

C9533. Meehan T.K. TOGA, a prototype for an optimal orbiting GNSS-R instrument. / Meehan T.K., Esterhuizen S., Franklin G.W., Lowe S., Munson T.N., Robison D., Spitzmesser D.J., Tien J.Y.T., Young L.E. // 2007. IGARSS 2007. IEEE International Geoscience and Remote Sensing Symposium. - Barcelona, 23-28 July 2007. - P. 5109-5112. 

C9534. Thiele A. Modeling and analyzing InSAR phase profiles at building locations. / Thiele A., Cadario E., Schulz K., Thoennessen U., Soergel U. // 2007. IGARSS 2007. IEEE International Geoscience and Remote Sensing Symposium. - Barcelona, 23-28 July 2007. - P. 5053-5056. 

C9535. Mason D.C. Using airborne laser altimetry to improve river flood extents delineated from SAR data. / Mason D.C., Dall'Amico J.T., Scott T.R., Horritt M.S., Bates P.D. // 2007. IGARSS 2007. IEEE International Geoscience and Remote Sensing Symposium. - Barcelona, 23-28 July 2007. - P. 5017-5020. 

C9536. Barber B.C. Some polarimetric aspects of processing sea surface M-ATI SAR data. 2007. IGARSS 2007. IEEE International Geoscience and Remote Sensing Symposium. - Barcelona, 23-28 July 2007. - P. 5032-5036. 

C9537. Heliere A. The EarthCARE mission: Mission concept and lidar instrument pre-development. / Heliere A., Lefebvre A., Wehr T., Bezy J.-L., Durand Y. // 2007. IGARSS 2007. IEEE International Geoscience and Remote Sensing Symposium. - Barcelona, 23-28 July 2007. - P. 4975-4978. 

- C9538.** Reagan J.A. Initial CRAM aerosol retrievals from CALIPSO and supporting airborne HSRL measurements. / Reagan J.A., McPherson C.J., Hostetler C.A., Hair J.W., Ferrare R.A. // 2007. IGARSS 2007. IEEE International Geoscience and Remote Sensing Symposium. - Barcelona, 23-28 July 2007. - P. 4979-4982. ↑
- C9539.** Sauer S. Physical parameter extraction over urban areas using L-band POLSAR data and interferometric baseline diversity. / Sauer S., Ferro-Famil L., Reigber A., Pottier E. // 2007. IGARSS 2007. IEEE International Geoscience and Remote Sensing Symposium. - Barcelona, 23-28 July 2007. - P. 5045-5048. ↑
- C9540.** Okada Y. Highly accurate DSM reconstruction using Ku-band airborne InSAR. / Okada Y., Hirao C., Horiuchi T., Hara Y., Yedidia J.S., Azarbayejani A., Oishi N. // 2007. IGARSS 2007. IEEE International Geoscience and Remote Sensing Symposium. - Barcelona, 23-28 July 2007. - P. 5049-5052. ↑
- C9541.** Capozzoli A. A novel optimization approach to forest height reconstruction from multi-baseline data. / Capozzoli A., D'Elia G., Liseno A., Moreira A., Papathanassiou K.P. // 2007. IGARSS 2007. IEEE International Geoscience and Remote Sensing Symposium. - Barcelona, 23-28 July 2007. - P. 5037-5040. ↑
- C9542.** Nannini M. Height dependent motion compensation and coregistration for airborne SAR tomography. / Nannini M., Scheiber R. // 2007. IGARSS 2007. IEEE International Geoscience and Remote Sensing Symposium. - Barcelona, 23-28 July 2007. - P. 5041-5044. ↑
- C9543.** Mogyla A. SAR imaging based upon nonswitchable antenna array and noise signals. / Mogyla A., Lukin K., Vyplavin P. // 2007 6th International Conference on Antenna Theory and Techniques. - Sevastopol, 17-21 Sept. 2007. - P. 360-362. ↑
- C9544.** Shuyuan Yang. Image fusion using a NSDFB-based contourlet packet. / Shuyuan Yang, Min Wang, ZhanWen Liu, Licheng Jiao. // 2007. ISPACS 2007. International Symposium on Intelligent Signal Processing and Communication Systems. - Xiamen, Nov. 28 2007-Dec. 1 2007. - P. 690-693. ↑
- C9545.** Fang Qianxue. The arm detection based on Rao test method. / Fang Qianxue, Wang Yongliang, Wang Shouyong. // 2007. ISPACS 2007. International Symposium on Intelligent Signal Processing and Communication Systems. - Xiamen, Nov. 28 2007-Dec. 1 2007. - P. 842-845. ↑
- C9546.** Zhiwei Deng. An efficient weighted Lp algorithm for the design of non-uniform filter banks. / Zhiwei Deng, Zijing Zhang, Binlu Liu. // 2007. ISPACS 2007. International Symposium on Intelligent Signal Processing and Communication Systems. - Xiamen, Nov. 28 2007-Dec. 1 2007. - P. 482-485. ↑
- C9547.** Min Wang. Image fusion using a contourlet HMT model. / Min Wang, Dongliang Peng, ZhanWen Liu, Shuyuan Yang. // 2007. ISPACS 2007. International Symposium on Intelligent Signal Processing and Communication Systems. - Xiamen, Nov. 28 2007-Dec. 1 2007. - P. 678-681. ↑
- C9548.** Youssef E.-S.A. Simulation of pulse compression performance under influence of background noise in modern surveillance radar. / Youssef E.-S.A., Mokhtar A., Madkour M., Abdel-Latif M. // 2007. ICCES '07. International Conference on Computer Engineering & Systems. - Cairo, 27-29 Nov. 2007. - P. 205-208. ↑
- C9549.** Moreno L. Evolutionary Filter for Mobile Robot Global Localization. / Moreno L., Muoz M.L., Garrido S., Martin F. // 2007. WISP 2007. IEEE International Symposium on Intelligent Signal Processing. - Alcala de Henares, 3-5 Oct. 2007. - P. 1-6. ↑
- C9550.** Ting Cheng. Dwell scheduling of multifunction phased array radars based on genetic algorithm. / Ting Cheng, Zi-shu He, Ting Tang. // 2007. ISPACS 2007. International Symposium on Intelligent Signal Processing and Communication Systems. - Xiamen, Nov. 28 2007-Dec. 1 2007. - P. 846-849. ↑
- C9551.** Cheng Ting. An IMM-based adaptive-update-rate target tracking algorithm for phased-array radar. / Cheng Ting, He Zi-shu, Tang Ting. // 2007. ISPACS 2007. International Symposium on Intelligent Signal Processing and Communication Systems. - Xiamen, Nov. 28 2007-Dec. 1 2007. - P. 854-857. ↑
- C9552.** Shuyuan Yang. Multiscale bandelet image compression. / Shuyuan Yang, Fan Liu, Min Wang, Licheng Jiao. // 2007. ISPACS 2007. International Symposium on Intelligent Signal Processing and Communication Systems. - Xiamen, Nov. 28 2007-Dec. 1 2007. - P. 412-415. ↑
- C9553.** Fang Liu. SAR image denoising based on wedgelet and dual-tree complex wavelet transform. / Fang

Liu, Junying Liu. // 2007. ISPACS 2007. International Symposium on Intelligent Signal Processing and Communication Systems. - Xiamen, Nov. 28 2007-Dec. 1 2007. - P. 204-207. ↑

C9554. Lingyu Wang. Deriving filter parameters using dual-images for image de-noising. / Lingyu Wang, Leedham G., Siu-Yeung Cho. // 2007. ISPACS 2007. International Symposium on Intelligent Signal Processing and Communication Systems. - Xiamen, Nov. 28 2007-Dec. 1 2007. - P. 212-215. ↑

C9555. Huilin Zhou. Wrapper approach for feature subset selection using GA. / Huilin Zhou, Jianbin Wu, Yuhao Wang, Mao Tian. // 2007. ISPACS 2007. International Symposium on Intelligent Signal Processing and Communication Systems. - Xiamen, Nov. 28 2007-Dec. 1 2007. - P. 188-191. ↑

C9556. Han Li-juan. Modeling of varying geometrical scenarios of bistatic radar. / Han Li-juan, Chen Zhu-ming, Duan Rui, Jiang Chao-shu. // 2007. ISPACS 2007. International Symposium on Intelligent Signal Processing and Communication Systems. - Xiamen, Nov. 28 2007-Dec. 1 2007. - P. 196-199. ↑

C9557. Ren Lei. Implementation of STAP system for dual-channel airborne radar. / Ren Lei, Wang Yong-liang, Chen Hui, Mu Qi-yong. // 2007. ISPACS 2007. International Symposium on Intelligent Signal Processing and Communication Systems. - Xiamen, Nov. 28 2007-Dec. 1 2007. - P. 368-371. ↑

C9558. Yan Jin. A cyclostationarity based iterative algorithm for multi-component chirp signal parameter estimation. / Yan Jin, Hongbing Ji. // 2007. ISPACS 2007. International Symposium on Intelligent Signal Processing and Communication Systems. - Xiamen, Nov. 28 2007-Dec. 1 2007. - P. 388-391. ↑

C9559. Weibo Xie. Best least squares solution for Prony model. / Weibo Xie, Canhui Cai, Yongchu Wang. // 2007. ISPACS 2007. International Symposium on Intelligent Signal Processing and Communication Systems. - Xiamen, Nov. 28 2007-Dec. 1 2007. - P. 292-295. ↑

C9560. Xiaolin Tian. SAR image segmentation based on spatially adaptive weighted possibilistic c-means clustering. / Xiaolin Tian, Shuiping Gou, Licheng Jiao. // 2007. ISPACS 2007. International Symposium on Intelligent Signal Processing and Communication Systems. - Xiamen, Nov. 28 2007-Dec. 1 2007. - P. 304-307. ↑

C9561. de Paolo T. Properties of HF RADAR Compact Antenna Arrays and Their Effect on the MUSIC Algorithm. / de Paolo T., Cook T., Terrill E. // OCEANS 2007. - Vancouver, BC, Sept. 29 2007-Oct. 4 2007. - P. 1-10. ↑

C9562. Atkinson L.P. Surface Current Mapping in the Lower Chesapeake. / Atkinson L.P., Garner T., Blanco J.L. // OCEANS 2007. - Vancouver, BC, Sept. 29 2007-Oct. 4 2007. - P. 1-3. ↑

C9563. Kun-Chou Lee. An Efficient Algorithm for the Radar Recognition of Ships on the Sea Surface. / Kun-Chou Lee, Lan-Ting Wang, Jhih-Sian Ou, Chih-Wei Huang. // OCEANS 2007. - Vancouver, BC, Sept. 29 2007-Oct. 4 2007. - P. 1-6. ↑

C9564. Godin M.A. Data Exploration for Multidisciplinary Research. / Godin M.A., Bellingham J.G. // OCEANS 2007. - Vancouver, BC, Sept. 29 2007-Oct. 4 2007. - P. 1-4. ↑

C9565. Saebo T.O. Bathymetric Capabilities of the HISAS Interferometric Synthetic Aperture Sonar. / Saebo T.O., Callow H.J., Hansen R.E., Langli B., Hammerstad E.O. // OCEANS 2007. - Vancouver, BC, Sept. 29 2007-Oct. 4 2007. - P. 1-10. ↑

C9566. Gras V. Sea clutter measurement with airborne synthetic aperture radar. / Gras V., Sintes C., Garelo R. // OCEANS 2007. - Vancouver, BC, Sept. 29 2007-Oct. 4 2007. - P. 1-7. ↑

C9567. Long R.M. Surface Current Measurements During Safe Seas 2006: Comparison and Validation of Measurements from High-Frequency Radar and the Quick Release Estuarine Buoy. / Long R.M., Barrick D.E. // OCEANS 2007. - Vancouver, BC, Sept. 29 2007-Oct. 4 2007. - P. 1-7. ↑

C9568. Myers E. VDatum and Strategies for National Coverage. / Myers E., Hess K., Zhizhang Yang, Jiangtao Xu, Wong A., Doyle D., Woolard J., White S., Bang Le, Gill S., Hovis G. // OCEANS 2007. - Vancouver, BC, Sept. 29 2007-Oct. 4 2007. - P. 1-8. ↑

C9569. Cook T.M. Estimates of Radial Current Error from High Frequency Radar using MUSIC for Bearing Determination. / Cook T.M., DePaolo T., Terrill E.J. // OCEANS 2007. - Vancouver, BC, Sept. 29 2007-Oct. 4

2007. - P. 1-6. ↑

C9570. de la Mata-Moya D. Neural Network Based Approaches for Detecting Signals With Unknown Parameters. / de la Mata-Moya D., Jarabo-Amores P., Rosa-Zurera M., Vicen-Bueno R., Nieto-Borge J.C. // 2007. WISP 2007. IEEE International Symposium on Intelligent Signal Processing. - Alcala de Henares, 3-5 Oct. 2007. - P. 1-6. ↑

C9571. Hobbs C.H. Considerations in Marine Sand Mining and Beach Nourishment. OCEANS 2007. - Vancouver, BC, Sept. 29 2007-Oct. 4 2007. - P. 1-10. ↑

C9572. Moreno L. E-SLAM solution to the grid-based Localization and Mapping problem. / Moreno L., Murioz M.L., Garrido S., Martin F. // 2007. WISP 2007. IEEE International Symposium on Intelligent Signal Processing. - Alcala de Henares, 3-5 Oct. 2007. - P. 1-7. ↑

C9573. Donato P. Combined use of complementary pairs of sequences with orthogonal sequences of different length. / Donato P., Carrica D., Gonzalez S., Petrocelli R. // 2007. WISP 2007. IEEE International Symposium on Intelligent Signal Processing. - Alcala de Henares, 3-5 Oct. 2007. - P. 1-6. ↑

C9574. White S. Utilization of LIDAR and NOAA's Vertical Datum Transformation Tool (VDatum) for Shoreline Delineation. OCEANS 2007. - Vancouver, BC, Sept. 29 2007-Oct. 4 2007. - P. 1-6. ↑

C9575. Wiegert R. Demonstration of a Novel Man-Portable Magnetic STAR Technology for Real Time Localization of Unexploded Ordnance. / Wiegert R., Oeschger J., Tuovila E. // OCEANS 2007. - Vancouver, BC, Sept. 29 2007-Oct. 4 2007. - P. 1-7. ↑

C9576. Coiras E. Reliable Seabed Characterization for MCM Operations. / Coiras E., Myers V., Evans B. // OCEANS 2007. - Vancouver, BC, Sept. 29 2007-Oct. 4 2007. - P. 1-5. ↑

C9577. Wyatt L.R. Data quality and sampling requirements for reliable wave measurement with HF radar. / Wyatt L.R., Green J.J., Middleditch A. // OCEANS 2007. - Vancouver, BC, Sept. 29 2007-Oct. 4 2007. - P. 1-7. ↑

C9578. Kumar A. Generalization of Trapezoidal Vague Set and Its Use for Analyzing the Fuzzy System Reliability. / Kumar A., Yadav S.P., Kumar S. // 2007. International Conference on Conference on Computational Intelligence and Multimedia Applications. - Sivakasi, Tamil Nadu, 13-15 Dec. 2007. - Vol. 1. - P. 364-369. ↑

C9579. Manikandan J. Evaluation of Edge Detection Techniques towards Implementation of Automatic Target Recognition. / Manikandan J., Venkataramani B., Jayachandran M. // 2007. International Conference on Conference on Computational Intelligence and Multimedia Applications. - Sivakasi, Tamil Nadu, 13-15 Dec. 2007. - Vol. 2. - P. 441-445. ↑

C9580. Kumar V. Wireless Content Management (WiCoM) for Mobile Device. / Kumar V., Majumder K. // 2007. International Conference on Conference on Computational Intelligence and Multimedia Applications. - Sivakasi, Tamil Nadu, 13-15 Dec. 2007. - Vol. 4. - P. 265-269. ↑

C9581. Singh S.P. Polyphase Sequences Design-Using MSAA. / Singh S.P., Subba Rao K. // 2007. International Conference on Conference on Computational Intelligence and Multimedia Applications. - Sivakasi, Tamil Nadu, 13-15 Dec. 2007. - Vol. 4. - P. 357-362. ↑

C9582. Padilha R.S. Quantitative Evaluation of Location Systems Techniques for Short-Range RF-Based Sensor Networks. / Padilha R.S., de Souza L.M.S. // 2007. MASS 2007. IEEE International Conference on Mobile Adhoc and Sensor Systems. - Pisa, 8-11 Oct. 2007. - P. 1-6. ↑

C9583. Max Chung. Capacitive coupling return loss of a new pre-ionized monopole plasma antenna. / Max Chung, Wen-Shan Chen, Bohr-Ran Huang, Chih-Chia Chang, Kuang-Yuan Ku, Yen-Hao Yu, Tain-Wen Suen. // TENCON 2007-2007 IEEE Region 10 Conference. - Taipei, Oct. 30 2007-Nov. 2 2007. - P. 1-4. ↑

C9584. Iwashita A. Consideration of Crustal Deformation in the Adjacent Area of Plate Boundary. / Iwashita A., Muhtar Qong, Baba H., Hara M., Morohoshi T., Kudo M., Yu-Feng Lin, Wen-Qing Jiang. // 2007. ICICIC '07. Second International Conference on Innovative Computing, Information and Control. - Kumamoto, 5-7 Sept. 2007. - P. 392. ↑

C9585. Hou Yuguan. Reconstruction of Super-resolution Spectra for the Beamformed Data in HF Skywave

Radar. / Hou Yuguan, Shen Yiyang, Liu Yongtan. // 2007. ICICIC '07. Second International Conference on Innovative Computing, Information and Control. - Kumamoto, 5-7 Sept. 2007. - P. 500. ↑

C9586. Manikandan M.S. Wavelet-Based ECG and PCG Signals Compression Technique for Mobile Telemedicine. / Manikandan M.S., Dandapat S. // 2007. ADCOM 2007. International Conference on Advanced Computing and Communications. - Guwahati, Assam, 18-21 Dec. 2007. - P. 164-169. ↑

C9587. Kalgaonkar K. Acoustic Doppler sonar for gait recognition. / Kalgaonkar K., Raj B. // 2007. AVSS 2007. IEEE Conference on Advanced Video and Signal Based Surveillance. - London, 5-7 Sept. 2007. - P. 27-32. ↑

C9588. Amar A. Resolution limits of closely spaced random signals given the desired success rate. / Amar A., Weiss A.J. // 2007. AVSS 2007. IEEE Conference on Advanced Video and Signal Based Surveillance. - London, 5-7 Sept. 2007. - P. 488-492. ↑

C9589. Kazansky O.V. Radiation, scattering and receiving of pulse signals for subsurface object identification. 2007 6th International Conference on Antenna Theory and Techniques. - Sevastopol, 17-21 Sept. 2007. - P. 363-364. ↑

C9590. Andreev M.V. Localization of the reflecting centers using multifrequency and multiposition antenna scanning. / Andreev M.V., Borulko V.F. // 2007 6th International Conference on Antenna Theory and Techniques. - Sevastopol, 17-21 Sept. 2007. - P. 477-479. ↑

C9591. Kong Min. Research on Multi-mode Fusion Tracking of OTHR Based on Auction Algorithm. / Kong Min, Wang Guohong. // 2007. CISW 2007. International Conference on Computational Intelligence and Security Workshops. - Harbin, 15-19 Dec. 2007. - P. 393-396. ↑

C9592. Feng Youqian. A Method of Radar Signal Separation. / Feng Youqian, Zhang Shanwen, Li Zhengchao. // 2007. CISW 2007. International Conference on Computational Intelligence and Security Workshops. - Heilongjiang, 15-19 Dec. 2007. - P. 846-849. ↑

C9593. Jinseok Lee. Multitarget association and tracking in 3-D space based on particle filter with joint multitarget probability density. / Jinseok Lee, Byung Guk Kim, Shung Han Cho, Sangjin Hong, We-Duke Cho. // 2007. AVSS 2007. IEEE Conference on Advanced Video and Signal Based Surveillance. - London, 5-7 Sept. 2007. - P. 573-578. ↑

C9594. Zhao-hong Jia. A New Multi-objective Fully-Informed Particle Swarm Algorithm for Flexible Job-Shop Scheduling Problems. / Zhao-hong Jia, Hua-ping Chen, Jun Tang. // 2007. CISW 2007. International Conference on Computational Intelligence and Security Workshops. - Heilongjiang, 15-19 Dec. 2007. - P. 191-194. ↑

C9595. Ma Miao. SAR Image despeckling using grey system theory. / Ma Miao, Zhang Yanning, Sun Li, Yuan Hejin, Zhou Tao. // 2007. GSIS 2007. IEEE International Conference on Grey Systems and Intelligent Services. - Nanjing, 18-20 Nov. 2007. - P. 458-462. ↑

C9596. Gozalvez J. SPHERE-A Simulation Platform for Heterogeneous Wireless Systems. / Gozalvez J., Martin-Sacristan D., Lucas-Estan M., Monserrat J.F., Gonzalez-Delgado J.J., Gozalvez D., Marhuenda M. // 2007. TridentCom 2007. 3rd International Conference on Testbeds and Research Infrastructure for the Development of Networks and Communities. - Lake Buena Vista, FL, 21-23 May 2007. - P. 1-10. ↑

C9597. Guilfoos B. Web Interface for Querying/Searching RDF Database. / Guilfoos B., Samsi S., Chaves J.C., Unpingco J., Nehrbass J., Chalker A., Ahalt S., Krishnamurthy A. // 2007 DoD High Performance Computing Modernization Program Users Group Conference. - Pittsburgh, PA, 18-21 June 2007. - P. 299-301. ↑

C9598. Reuther A. Technical Challenges of Supporting Interactive HPC. / Reuther A., Kepner J., McCabe A., Mullen J., Bliss N.T., Hahn Kim. // 2007 DoD High Performance Computing Modernization Program Users Group Conference. - Pittsburgh, PA, 18-21 June 2007. - P. 403-409. ↑

C9599. Du Gang. A new method for joint estimation of three-dimensional parameters of coherent signals. / Du Gang, Zhang Yongshun, Wang Yongliang, Jiang Xinying. // 2007. ISPCS 2007. International Symposium on Intelligent Signal Processing and Communication Systems. - Xiamen, Nov. 28 2007-Dec. 1 2007. - P. 96-99. ↑

C9600. Guozhong Chen. To improve the GMAP for speckle filtering by consideration of the correlation of SAR

images. / Guozhong Chen, Yiwang Huang. // 2007. ISPACS 2007. International Symposium on Intelligent Signal Processing and Communication Systems. - Xiamen, Nov. 28 2007-Dec. 1 2007. - P. 124-127. ↑

C9601. {no data available}. 2007 International Symposium on Intelligent Signal Processing and Communications Systems Proceedings. 2007. ISPACS 2007. International Symposium on Intelligent Signal Processing and Communication Systems. - Xiamen, Nov. 28 2007-Dec. 1 2007. - P. i. ↑

C9602. Dan Lu. GPS smart jammer suppressin algorithm based on spatial APES. / Dan Lu, Renbiao Wu, Ping Li, Zhigang Su. // 2007. ISPACS 2007. International Symposium on Intelligent Signal Processing and Communication Systems. - Xiamen, Nov. 28 2007-Dec. 1 2007. - P. 88-91. ↑

C9603. Elton B. The SIP High Productivity Toolset for Parameter Sweeps and Monte Carlo Runs. / Elton B., Nehrbass J., Ahalt S., Gardiner J., Humphrey L. // 2007 DoD High Performance Computing Modernization Program Users Group Conference. - Pittsburgh, PA, 18-21 June 2007. - P. 296-298. ↑

C9604. Punchalard R. Unbiased plain gradient algorithm for adaptive 11R notch filter with constrained poles and zeros. / Punchalard R., Lorsawatsiri A., Loetwassana W., Koseeyaporn J., Wardkein P., Roeksabutr A. // TENCON 2007-2007 IEEE Region 10 Conference. - Taipei, Oct. 30 2007-Nov. 2 2007. - P. 1-4. ↑

C9605. Yong Dou. FPGA SAR Processor with Window Memory Accesses. / Yong Dou, Jie Zhou, Yuanwu Lei, Xingming Zhou. // 2007. ASAP. IEEE International Conf. on Application -specific Systems, Architectures and Processors. - Montreal, Que., 9-11 July 2007. - P. 95-100. ↑

C9606. Chen lei. A time-domain beamformer for UWB through-wall imaging. / Chen lei, Shan ouyang. // TENCON 2007-2007 IEEE Region 10 Conference. - Taipei, Oct. 30 2007-Nov. 2 2007. - P. 1-4. ↑

C9607. Fukushima C. Experimental consideration on the synthetic range-profile processing by stepped-frequency radar. TENCON 2007-2007 IEEE Region 10 Conference. - Taipei, Oct. 30 2007-Nov. 2 2007. - P. 1-4. ↑

C9608. Saqellari-Likoka A. Tropospheric signal delay estimation in repeat-pass SAR Interferometry with QR-factorization. / Saqellari-Likoka A., Karathanassi V. // 2007. MED '07. Mediterranean Conference on Control & Automation. - Athens, 27-29 June 2007. - P. 1-4. ↑

C9609. Sankaranarayanan S. On the concatenation of LDPC and RS codes in magnetic recording systems. / Sankaranarayanan S., Kuznetsov A., Sridhara D. // 2007 IEEE Globecom Workshops. - Washington, DC, 26-30 Nov. 2007. - P. 1. ↑

C9610. Xiaofu Xie. A new variable step-size equivariant adaptive source separation algorithm. / Xiaofu Xie, Qingyan Shi, Renbeso Wu. // 2007. APCC 2007. Asia-Pacific Conference on Communications. - Bangkok, 18-20 Oct. 2007. - P. 479-482. ↑

C9611. Renbiao Wu. A novel method of interference suppression for civil aviation air-ground communication based on blind signal extraction. / Renbiao Wu, Qingyan Shi, Jianyu Huang, Lunlong Zhong. // 2007. APCC 2007. Asia-Pacific Conference on Communications. - Bangkok, 18-20 Oct. 2007. - P. 81-84. ↑

C9612. Rolfe B.F. Localization with orientation using RSSI measurements: RF map based approach. / Rolfe B.F., Ekanayake S.W., Pathirana P.N., Palaniswami M. // ---. - Melbourne, Qld., 3-6 Dec. 2007. - P. 311-316. ↑

C9613. Ferguson B. Characterisation of an L-band digital noise radar. / Ferguson B., Mosel S., Brodie-Tyrrrell W., Trinkle M., Gray D. // 2007 IET International Conference on Radar Systems. - Edinburgh, UK, 15-18 Oct. 2007. - P. 1-5. ↑

C9614. Cherniakov M. Ultra wideband forward scattering radar: Concept and prospective. / Cherniakov M., Gashinova M., Cheng Hu, Antoniou M., Sizov V., Daniel L.Y. // 2007 IET International Conference on Radar Systems. - Edinburgh, UK, 15-18 Oct. 2007. - P. 1-5. ↑

C9615. Sharp Alexander N. Low noise wideband optical mixing and optical up-conversion architecture. / Sharp Alexander N., Bates Bevan D. // 2007 IET International Conference on Radar Systems. - Edinburgh, UK, 15-18 Oct. 2007. - P. 1-5. ↑

C9616. Brautigam B. Results from TerraSAR-X geometric and radiometric calibration. / Brautigam B., Schwerdt M., Bachmann M., Doring B. // 2007 IET International Conference on Radar Systems. - Edinburgh, UK, 15-18

Oct. 2007. - P. 1-5. ↑

C9617. Searle S.J. A novel nonlinear technique for sidelobe suppression in radar. / Searle S.J., Howard S.D. // 2007 IET International Conference on Radar Systems. - Edinburgh, UK, 15-18 Oct. 2007. - P. 1-5. ↑

C9618. Moore Stephen. Review of the state of the art of UK AESA technology and the future challenges faced. 2007 IET International Conference on Radar Systems. - Edinburgh, UK, 15-18 Oct. 2007. - P. 1-7. ↑

C9619. Flores-Tapia Daniel. Spatial variant apodization on subsurface imagery acquired along circular trajectories. / Flores-Tapia Daniel, Thomas Gabriel, Pistorius Stephen. // 2007 IET International Conference on Radar Systems. - Edinburgh, UK, 15-18 Oct. 2007. - P. 1-5. ↑

C9620. McLachlan A. D. T/R module design and production processes for airborne radar systems. / McLachlan A. D., Dunn M., Morrison G. D., Forbes J. G. W., Peall R., Dry R. // 2007 IET International Conference on Radar Systems. - Edinburgh, UK, 15-18 Oct. 2007. - P. 1-4. ↑

C9621. Rashid L. S. Impact modelling of wind farms on marine navigational radar. / Rashid L. S., Brown A.K. // 2007 IET International Conference on Radar Systems. - Edinburgh, UK, 15-18 Oct. 2007. - P. 1-5. ↑

C9622. Guo H. Passive radar detection using wireless networks. / Guo H., Coetzee S., Mason D., Woodbridge K., Baker C. // 2007 IET International Conference on Radar Systems. - Edinburgh, UK, 15-18 Oct. 2007. - P. 1-4. ↑

C9623. Thomas J. M. DRM signals for HF passive bistatic radar. / Thomas J. M., Baker C. J., Griffiths H. D. // 2007 IET International Conference on Radar Systems. - Edinburgh, UK, 15-18 Oct. 2007. - P. 1-5. ↑

C9624. Sahr John D. Lossy compression of voltage level samples before detection in distributed passive bistatic radar systems. 2007 IET International Conference on Radar Systems. - Edinburgh, UK, 15-18 Oct. 2007. - P. 1-4. ↑

C9625. Lauri A. A geometrically based multipath channel model for passive radar. / Lauri A., Cardinali R., Colone F., Lombardo P., Bucciarelli T. // 2007 IET International Conference on Radar Systems. - Edinburgh, UK, 15-18 Oct. 2007. - P. 1-5. ↑

C9626. Jackson C.A. Options for mitigation of the effects of windfarms on radar systems. / Jackson C.A., Butler M.M. // 2007 IET International Conference on Radar Systems. - Edinburgh, UK, 15-18 Oct. 2007. - P. 1-6. ↑

C9627. Jackson C.A. Windfarm characteristics and their effect on radar systems. 2007 IET International Conference on Radar Systems. - Edinburgh, UK, 15-18 Oct. 2007. - P. 1-6. ↑

C9628. Rose P. S. Reducing clutter in airborne radars equipped with electronically scanned array antennas. / Rose P. S., Greig D. W. // 2007 IET International Conference on Radar Systems. - Edinburgh, UK, 15-18 Oct. 2007. - P. 1-5. ↑

C9629. Nekrasov A. Measurement of the wind vector over sea by an airborne radar altimeter, which has an antenna with the modified beam shape. 2007 IET International Conference on Radar Systems. - Edinburgh, UK, 15-18 Oct. 2007. - P. 1-5. ↑

C9630. Morris J. T. Polarisation filtering for small target discrimination in ground clutter. / Morris J. T., Anderson W.C., Anderson S.J. // 2007 IET International Conference on Radar Systems. - Edinburgh, UK, 15-18 Oct. 2007. - P. 1-4. ↑

C9631. Herselman P.L. Analysis of calibrated sea clutter and boat reflectivity data at C- and X-band in South African coastal waters. / Herselman P.L., Baker C.J. // 2007 IET International Conference on Radar Systems. - Edinburgh, UK, 15-18 Oct. 2007. - P. 1-5. ↑


















C9632. Watts Simon. CFAR loss and gain in K-distributed sea-clutter and thermal noise. / Watts Simon, Ward Keith, Tough Robert. // 2007 IET International Conference on Radar Systems. - Edinburgh, UK, 15-18 Oct. 2007. - P. 1-5. ↑

C9633. Dong Y. High grazing angle X-band sea clutter distributions. / Dong Y., Haywood B. // 2007 IET International Conference on Radar Systems. - Edinburgh, UK, 15-18 Oct. 2007. - P. 1-5. ↑

- C9634. Jian-Jia Chen. Load balancing for typical radar systems with overlapping surveillance space. / Jian-Jia Chen, Chin-Fu Kuo. // 2007 IET International Conference on Radar Systems. - Edinburgh, UK, 15-18 Oct. 2007. - P. 1-5. ↑
- C9635. Arnold-Bos A. Investigating possible bistatic configurations for ship wake imaging through simulation. / Arnold-Bos A., Khenchaf A., Martin A. // 2007 IET International Conference on Radar Systems. - Edinburgh, UK, 15-18 Oct. 2007. - P. 1-5. ↑
- C9636. Tough Robert. Modelling sea clutter temporal correlation in detection calculations. / Tough Robert, Ward Keith, Watts Simon. // 2007 IET International Conference on Radar Systems. - Edinburgh, UK, 15-18 Oct. 2007. - P. 1-4. ↑
- C9637. Anderson S.J. Optimisation of bistatic HF surface wave radar configurations. 2007 IET International Conference on Radar Systems. - Edinburgh, UK, 15-18 Oct. 2007. - P. 1-4. ↑
- C9638. Liu Xiankang. Application of HRRP even rank central moments features in satellite target recognition. / Liu Xiankang, Gao Meiguo, Fu Xiongjun. // 2007 IET International Conference on Radar Systems. - Edinburgh, UK, 15-18 Oct. 2007. - P. 1-4. ↑
- C9639. Froggatt T.R. Radar interoperability with modern multi-function radars-a case study. 2007 IET International Conference on Radar Systems. - Edinburgh, UK, 15-18 Oct. 2007. - P. 1-5. ↑
- C9640. Long Zhuang. Beam pattern synthesis for spaceborne sparse aperture radar. / Long Zhuang, Xingzhao Liu. // 2007 IET International Conference on Radar Systems. - Edinburgh, UK, 15-18 Oct. 2007. - P. 1-5. ↑
- C9641. Hassani H.R. Precise full wave analysis of the slot coupled circular microstrip patch antennas. / Hassani H.R., Sadeghzade Sh. R., Jahanbakht M., Azarbar A. // 2007 IET International Conference on Radar Systems. - Edinburgh, UK, 15-18 Oct. 2007. - P. 1-5. ↑
- C9642. De Maio A. Performance analysis of sidelobe blanking system in presence of mutual coupling. / De Maio A., Farina A., Fiorini M., Morini A. // 2007 IET International Conference on Radar Systems. - Edinburgh, UK, 15-18 Oct. 2007. - P. 1-5. ↑
- C9643. Mishra A.K. Fractal feature based radar signal classification. / Mishra A.K., Feng H., Mulgrew B. // 2007 IET International Conference on Radar Systems. - Edinburgh, UK, 15-18 Oct. 2007. - P. 1-4. ↑
- C9644. Atrouz Brahim. Features influence on targets classification performance using the high range resolution profiles (HRR profiles). / Atrouz Brahim, Aait Ouazzou Hayet, Kimouche Hocine. // 2007 IET International Conference on Radar Systems. - Edinburgh, UK, 15-18 Oct. 2007. - P. 1-4. ↑
- C9645. Hoi-Shun Lui. Time-frequency analysis of late time electromagnetic transients from radar targets. / Hoi-Shun Lui, Shuley N.V., Longstaff I. D. // 2007 IET International Conference on Radar Systems. - Edinburgh, UK, 15-18 Oct. 2007. - P. 1-5. ↑
- C9646. Kouemou G. Hidden Markov Models in radar target classification. / Kouemou G., Opitz F. // 2007 IET International Conference on Radar Systems. - Edinburgh, UK, 15-18 Oct. 2007. - P. 1-5. ↑
- C9647. Melvin William L. Performance results for a knowledge-aided clutter mitigation architecture. / Melvin William L., Showman Gregory A. // 2007 IET International Conference on Radar Systems. - Edinburgh, UK, 15-18 Oct. 2007. - P. 1-5. ↑
- C9648. Lim Chin-Heng. Bistatic JDL-STAP for ground moving target detection. / Lim Chin-Heng, Mulgrew Bernard, Aboutanios Elias. // 2007 IET International Conference on Radar Systems. - Edinburgh, UK, 15-18 Oct. 2007. - P. 1-5. ↑
- C9649. Raout J. Bistatic STAP using DVB-T illuminators of opportunity. / Raout J., Neyt X., Rischette P. // 2007 IET International Conference on Radar Systems. - Edinburgh, UK, 15-18 Oct. 2007. - P. 1-5. ↑
- C9650. Cao T.V. A rare event approach to the detection of target-like signals in CFAR training data. / Cao T.V., Sinnott D. // 2007 IET International Conference on Radar Systems. - Edinburgh, UK, 15-18 Oct. 2007. - P. 1-5. ↑

- C9651. Gould Dale. Developments to a multiband passive radar demonstrator system. / Gould Dale, Pollard Robert, Sarno Carlos, Tittensor Paul. // 2007 IET International Conference on Radar Systems. - Edinburgh, UK, 15-18 Oct. 2007. - P. 1-5. ↑
- C9652. O'Hagan D.W. Passive Bistatic Radar (PBR) demonstrator. / O'Hagan D.W., Colone F., Baker C.J., Griffiths H.D. // 2007 IET International Conference on Radar Systems. - Edinburgh, UK, 15-18 Oct. 2007. - P. 1-5. ↑
- C9653. Kealey Paul G. Robust radar detection of moving ground targets with STAP. / Kealey Paul G., Carrington David M. // 2007 IET International Conference on Radar Systems. - Edinburgh, UK, 15-18 Oct. 2007. - P. 1-5. ↑
- C9654. Gui Renzhou. Suppressing radio frequency interferences with adaptive beamformer based on weight iterative algorithm. 2007. (CCWMSN07). IET Conference on Wireless, Mobile and Sensor Networks. - Shanghai, China, 12-14 Dec. 2007. - P. 648-651. ↑
- C9655. Gorski T. Space-Time Adaptive Processing in the presence of non-Gaussian sea clutter. / Gorski T., Le Caillec J-M., Kawalec A., Czarnecki W. // 2007 IET International Conference on Radar Systems. - Edinburgh, UK, 15-18 Oct. 2007. - P. 1-4. ↑
- C9656. Qi Wang. Modulus spatially variant apodization algorithm for radar images. / Qi Wang, Mengdao Xing. // 2007 IET International Conference on Radar Systems. - Edinburgh, UK, 15-18 Oct. 2007. - P. 1-5. ↑
- C9657. Moazen N. A robust CFAR algorithm in non-homogenous environments. / Moazen N., Akhavan-Sarraf M. R. // 2007 IET International Conference on Radar Systems. - Edinburgh, UK, 15-18 Oct. 2007. - P. 1-3. ↑
- C9658. Stakkeland M. The error statistics of surveillance radar position measurements. / Stakkeland M., Overrein O., Hallingstad O. // 2007 IET International Conference on Radar Systems. - Edinburgh, UK, 15-18 Oct. 2007. - P. 1-5. ↑
- C9659. Hall Stephen. Naval environment propagation characteristics and clutter suppression in a multi sensor tracker. 2007 IET International Conference on Radar Systems. - Edinburgh, UK, 15-18 Oct. 2007. - P. 1-4. ↑
- C9660. Sanz-Gonzalez Jose L. Permutation test algorithms for nonparametric radar detection. / Sanz-Gonzalez Jose L., Alvarez-Vaquero Francisco, Gonzalez-Garcia Jose E. // 2007 IET International Conference on Radar Systems. - Edinburgh, UK, 15-18 Oct. 2007. - P. 1-5. ↑
- C9661. Cardinali Roberta. Multipath cancellation on reference antenna for passive radar which exploits fm transmission. / Cardinali Roberta, Colone Fabiola, Lombardo Pierfrancesco, Crognale Omar, Cosmi Andrea, Lauri Alessandro. // 2007 IET International Conference on Radar Systems. - Edinburgh, UK, 15-18 Oct. 2007. - P. 1-5. ↑
- C9662. Zaimbashi Amir. Order statistic and Maximum Likelihood distributed CFAR detectors in Weibull background. / Zaimbashi Amir, Taban M.R., MirMohamad-Sadeghi Hamid. // 2007 IET International Conference on Radar Systems. - Edinburgh, UK, 15-18 Oct. 2007. - P. 1-4. ↑
- C9663. Machowski W. A novel approach to range profile estimation of a moving vehicle by road monitoring radar. / Machowski W., Koutsogiannis G. S., Potter S. // 2007 IET International Conference on Radar Systems. - Edinburgh, UK, 15-18 Oct. 2007. - P. 1-5. ↑
- C9664. Li Wei. Antijamming method based on orthogonal codes jittered and random initial phase for SAR. / Li Wei, Lu Xingqiang, Da Xinyu, Liang Diannong. // 2007 IET International Conference on Radar Systems. - Edinburgh, UK, 15-18 Oct. 2007. - P. 1-5. ↑
- C9665. David Dikeman R. Real Time STAP for UESA Radar. / David Dikeman R., Moore Carleton A., Bell Kristine, Van Trees Harry. // 2007 IET International Conference on Radar Systems. - Edinburgh, UK, 15-18 Oct. 2007. - P. 1-4. ↑
- C9666. Ehrman Lisa M. Impact of measurement-to-track data association errors on RCS-based target classification. / Ehrman Lisa M., Dale Blair W. // 2007 IET International Conference on Radar Systems. - Edinburgh, UK, 15-18 Oct. 2007. - P. 1-4. ↑

- C9667.** Wu X. F. Study on sar jamming measures. / Wu X. F., Dai Da-hai, Wang Xue-song. // 2007 IET International Conference on Radar Systems. - Edinburgh, UK, 15-18 Oct. 2007. - P. 1-5. ↑
- C9668.** Shen Mingwei. An efficient reduced-rank STAP based on PASTd algorithm. / Shen Mingwei, Zhu Daiyin, Zhu Zhaoda. // 2007 IET International Conference on Radar Systems. - Edinburgh, UK, 15-18 Oct. 2007. - P. 1-5. ↑
- C9669.** Meyer M. G. Ionospheric clutter modelling for VHF passive radars operating at high latitudes. 2007 IET International Conference on Radar Systems. - Edinburgh, UK, 15-18 Oct. 2007. - P. 1-2. ↑
- C9670.** Aboutanios E. Regularisation methods for covariance matrix estimation in low sample support stap. / Aboutanios E., Mulgrew B. // 2007 IET International Conference on Radar Systems. - Edinburgh, UK, 15-18 Oct. 2007. - P. 1-5. ↑
- C9671.** Akhtar Jabran. An ECCM signaling approach for deep fading of jamming reflectors. 2007 IET International Conference on Radar Systems. - Edinburgh, UK, 15-18 Oct. 2007. - P. 1-5. ↑
- C9672.** Chadwick J. Air Target Identification-concept to reality. / Chadwick J., Williams G.L. // 2007 IET International Conference on Radar Systems. - Edinburgh, UK, 15-18 Oct. 2007. - P. 1-5. ↑
- C9673.** Zhu Daiyin. A novel approach to residual video phase removal in spotlight SAR image formation. 2007 IET International Conference on Radar Systems. - Edinburgh, UK, 15-18 Oct. 2007. - P. 1-4. ↑
- C9674.** Jahangir M. Moving target detection for synthetic aperture radar via shadow detection. 2007 IET International Conference on Radar Systems. - Edinburgh, UK, 15-18 Oct. 2007. - P. 1-5. ↑
- C9675.** Sedehi M. Constrained adaptive beamforming for electromagnetic interference cancellation for a synthetic aperture radar. / Sedehi M., Cristallini D., Bucciarelli M., Lombardo P. // 2007 IET International Conference on Radar Systems. - Edinburgh, UK, 15-18 Oct. 2007. - P. 1-5. ↑
- C9676.** Chang Wenge. Airborne Multi-frequency-Band SAR system and its information processing. / Chang Wenge, Li Xiangyang, Li Yueli, Chang Yulin. // 2007 IET International Conference on Radar Systems. - Edinburgh, UK, 15-18 Oct. 2007. - P. 1-5. ↑
- C9677.** Ritter Henning. Pedestrian detection based on automotive radar. / Ritter Henning, Rohling Hermann. // 2007 IET International Conference on Radar Systems. - Edinburgh, UK, 15-18 Oct. 2007. - P. 1-4. ↑
- C9678.** Aldhubaib F. On the application of pattern recognition to identification of simple targets based on resonance and polarization diversity. / Aldhubaib F., Shuley N. V., Longstaff I.D. // 2007 IET International Conference on Radar Systems. - Edinburgh, UK, 15-18 Oct. 2007. - P. 1-5. ↑
- C9679.** Bruder J.A. Interrupted SAR waveforms for high interrupt ratios. / Bruder J.A., Schneible R. // 2007 IET International Conference on Radar Systems. - Edinburgh, UK, 15-18 Oct. 2007. - P. 1-5. ↑
- C9680.** Rohling Hermann. Lateral velocity estimation for automotive radar applications. / Rohling Hermann, Folster Florian, Ritter Henning. // 2007 IET International Conference on Radar Systems. - Edinburgh, UK, 15-18 Oct. 2007. - P. 1-4. ↑
- C9681.** Whitewood A.P. Bistatic radar using a spaceborne illuminator. / Whitewood A.P., Baker C.J., Griffiths H.D. // 2007 IET International Conference on Radar Systems. - Edinburgh, UK, 15-18 Oct. 2007. - P. 1-5. ↑
- C9682.** Zhong Hua. Four-order bi-static imaging algorithm and auto-combination technique in constellation SAR system. / Zhong Hua, Liu Xingzhao. // 2007 IET International Conference on Radar Systems. - Edinburgh, UK, 15-18 Oct. 2007. - P. 1-5. ↑
- C9683.** Castillo-Rubio Carlos. High resolution ISAR images of non-cooperative targets with a new spatially variant apodization method. / Castillo-Rubio Carlos, Burgos-Garcia Mateo, Blanco-del-Campo Alvaro, Asensio-Lopez Alberto. // 2007 IET International Conference on Radar Systems. - Edinburgh, UK, 15-18 Oct. 2007. - P. 1-4. ↑
- C9684.** Wiltshire M. C. K. Metamaterials-from magnetism to invisibility. 2007 IET International Conference on Radar Systems. - Edinburgh, UK, 15-18 Oct. 2007. - P. 1. ↑

- C9685.** Guozhong Chen. Modified frost speckle filter based on anisotropic diffusion. / Guozhong Chen, Xingzhao Liu, Zhixin Zhou. // 2007 IET International Conference on Radar Systems. - Edinburgh, UK, 15-18 Oct. 2007. - P. 1-4. 
- C9686.** Peacock C. J. Digital radar. / Peacock C. J., Pearson G. S. // 2007 IET International Conference on Radar Systems. - Edinburgh, UK, 15-18 Oct. 2007. - P. 1-5. 
- C9687.** Nasrabadi M. Amin. Exhaustive search for long low autocorrelation binary codes using length-increment algorithm. / Nasrabadi M. Amin, Bastani M. H. // 2007 IET International Conference on Radar Systems. - Edinburgh, UK, 15-18 Oct. 2007. - P. 1-4. 
- C9688.** Kulpa K. SAR image enhancement by dominant scatterer removal. / Kulpa K., Misiurewicz J., Samczynski P., Smolarczyk M., Mordzonek M. // 2007 IET International Conference on Radar Systems. - Edinburgh, UK, 15-18 Oct. 2007. - P. 1-5. 
- C9689.** Capraro G. T. Sensors as intelligent robots. / Capraro G. T., Wicks M. C., Bradaric I. // 2007 IET International Conference on Radar Systems. - Edinburgh, UK, 15-18 Oct. 2007. - P. 1-5. 
- C9690.** Barclay M. Caesar: Demonstrating AESA capability option for eurofighter captor radar. / Barclay M., Pietzschmann U., Gonzalez G., Tellini P. // 2007 IET International Conference on Radar Systems. - Edinburgh, UK, 15-18 Oct. 2007. - P. 1-5. 
- C9691.** Callow H.J. Shadow enhancement in SAR imagery. / Callow H.J., Groen J., Hansen R.E., Sparr T. // 2007 IET International Conference on Radar Systems. - Edinburgh, UK, 15-18 Oct. 2007. - P. 1-5. 
- C9692.** Guozhong Chen. Despeckling SAR images in the undecimated wavelet domain based on scale correlation and GMRF model. / Guozhong Chen, Xingzhao Liu, Zhixin Zhou. // 2007 IET International Conference on Radar Systems. - Edinburgh, UK, 15-18 Oct. 2007. - P. 1-5. 
- C9693.** Martorella M. Polarimetric hot spot processing for ISAR image autofocusing. / Martorella M., Palmer J., Bates B., Berizzi F., Haywood B. // 2007 IET International Conference on Radar Systems. - Edinburgh, UK, 15-18 Oct. 2007. - P. 1-5. 
- C9694.** Gaffar M.Y. Abdul. Investigating the effect of a target's time-varying Doppler generating axis of rotation on ISAR image distortion. / Gaffar M.Y. Abdul, Nel W. // 2007 IET International Conference on Radar Systems. - Edinburgh, UK, 15-18 Oct. 2007. - P. 1-5. 
- C9695.** Guinvarc'h R. Dual polarization wide-band interleaved spiral antenna array. 2007 IET International Conference on Radar Systems. - Edinburgh, UK, 15-18 Oct. 2007. - P. 1-5. 
- C9696.** Berry P.E. Optimal fast-time beamforming with linearly-independent waveforms. / Berry P.E., Yau D. // 2007 IET International Conference on Radar Systems. - Edinburgh, UK, 15-18 Oct. 2007. - P. 1-5. 
- C9697.** Thomas G. ISAR motion compensation using entropy metrics. / Thomas G., Flores B.C., Flores-Tapia D. // 2007 IET International Conference on Radar Systems. - Edinburgh, UK, 15-18 Oct. 2007. - P. 1-4. 
- C9698.** Finlay C. D. SPIKE a Physical Optics based code for the analysis of antenna radome interactions. / Finlay C. D., Gregson Stuart, Lyon R. W., McCormick J. // 2007 IET International Conference on Radar Systems. - Edinburgh, UK, 15-18 Oct. 2007. - P. 1-5. 
- C9699.** Kauppi J-P. An efficient set of features for pulse repetition interval modulation recognition. / Kauppi J-P., Martikainen K.S. // 2007 IET International Conference on Radar Systems. - Edinburgh, UK, 15-18 Oct. 2007. - P. 1-5. 
- C9700.** Threadgold M. Maximising the benefits of sophisticated electronic countermeasures systems. / Threadgold M., Barker L.V. // 2007 IET International Conference on Radar Systems. - Edinburgh, UK, 15-18 Oct. 2007. - P. 1-5. 
- C9701.** Barbaresco F. Diffusive CFAR & its extension for Doppler and Polarimetric data. / Barbaresco F., Rivereau N. // 2007 IET International Conference on Radar Systems. - Edinburgh, UK, 15-18 Oct. 2007. - P. 1-5. 

- C9702.** Immediata Sandro. Impact of amplitude and phase mismatch in main beam jamming cancellation for active antenna with sub-array structure. / Immediata Sandro, Timmoneri Luca, Vigilante Domenico, Farina Alfonso. // 2007 IET International Conference on Radar Systems. - Edinburgh, UK, 15-18 Oct. 2007. - P. 1-5. ↑
- C9703.** Sheikhi A. GLRT based adaptive detection for MIMO radars. / Sheikhi A., Zamani A. // 2007 IET International Conference on Radar Systems. - Edinburgh, UK, 15-18 Oct. 2007. - P. 1-4. ↑
- C9704.** Davidson Glen. Cooperation between tracking and radar resource management. 2007 IET International Conference on Radar Systems. - Edinburgh, UK, 15-18 Oct. 2007. - P. 1-4. ↑
- C9705.** Nelander A. Beamforming in terrain scattered jamming. 2007 IET International Conference on Radar Systems. - Edinburgh, UK, 15-18 Oct. 2007. - P. 1-5. ↑
- C9706.** Greco Maria. Radar detection and classification of jamming signals based on cone classes. / Greco Maria, Gini Fulvio, Farina Alfonso. // 2007 IET International Conference on Radar Systems. - Edinburgh, UK, 15-18 Oct. 2007. - P. 1-5. ↑
- C9707.** Sohn Kwang June. Performance of multichannel parametric detectors with MCARM data. / Sohn Kwang June, Hongbin Li, Himed Braham, Markow Joshua S. // 2007 IET International Conference on Radar Systems. - Edinburgh, UK, 15-18 Oct. 2007. - P. 1-5. ↑
- C9708.** Nordsjo Anders Erik. Performance bounds for tracking algorithms based on a time-varying third-order nonlinear model. 2007 IET International Conference on Radar Systems. - Edinburgh, UK, 15-18 Oct. 2007. - P. 1-5. ↑
- C9709.** Benito E. Performing inversion of HF radar backscatter ionograms. / Benito E., Bourdillon A., Rannou V., Saillant S. // 2007 IET International Conference on Radar Systems. - Edinburgh, UK, 15-18 Oct. 2007. - P. 1-5. ↑
- C9710.** Barbaresco F. Wake vortex detection & monitoring by X-band Doppler radar: Paris Orly radar campaign results. / Barbaresco F., Jeantet A., Meier U. // 2007 IET International Conference on Radar Systems. - Edinburgh, UK, 15-18 Oct. 2007. - P. 1-5. ↑
- C9711.** Wardell Colin. Sensor data association test methodology for the seawolf midlife update programme. / Wardell Colin, Angell Chris, Bernhardt Mark, Patel Dilip. // 2007 IET International Conference on Radar Systems. - Edinburgh, UK, 15-18 Oct. 2007. - P. 1-5. ↑
- C9712.** De Maio Antonio. Constrained adaptive detection of range spread targets. / De Maio Antonio, De Nicola Silvio, Farina Alfonso. // 2007 IET International Conference on Radar Systems. - Edinburgh, UK, 15-18 Oct. 2007. - P. 1-6. ↑
- C9713.** Eunjung Yang. A hybrid D3 -Sigma Delta STAP algorithm in non-homogeneous clutter. / Eunjung Yang, Joohwan Chun, Adve Raviraj, Jonghoon Chun. // 2007 IET International Conference on Radar Systems. - Edinburgh, UK, 15-18 Oct. 2007. - P. 1-5. ↑
- C9714.** Zhang Wei. System simulation for a multi-function phased array radar. / Zhang Wei, Shi Jun, Tian Zhong. // 2007 IET International Conference on Radar Systems. - Edinburgh, UK, 15-18 Oct. 2007. - P. 1-4. ↑
- C9715.** Stove A. G. Sharing false alarm rate information between disparate sensors. 2007 IET International Conference on Radar Systems. - Edinburgh, UK, 15-18 Oct. 2007. - P. 1-5. ↑
- C9716.** Olsen K.E. Multistatic and/or Quasi Monostatic Radar Measurements of propeller aircrafts. / Olsen K.E., Johnsen T., Johnsrud S., Tansem I., Sornes P. // 2007 IET International Conference on Radar Systems. - Edinburgh, UK, 15-18 Oct. 2007. - P. 1-6. ↑
- C9717.** Stevens M.B. The effect of land clutter statistics on automatic gain control. 2007 IET International Conference on Radar Systems. - Edinburgh, UK, 15-18 Oct. 2007. - P. 1-3. ↑
- C9718.** Andre D. B. Radar target-ground interaction. 2007 IET International Conference on Radar Systems. - Edinburgh, UK, 15-18 Oct. 2007. - P. 1-5. ↑
- C9719.** Benham S.P. Accurate and efficient analysis of the EM environment due to naval radars. / Benham

S.P., McDowall J.B., Murphy T.J., Burbage J.M. // 2007 IET International Conference on Radar Systems. - Edinburgh, UK, 15-18 Oct. 2007. - P. 1-3. ↑

C9720. Gonzalez-Partida J.T. Ground SAR system with tunable distance limits and low sampling rate. / Gonzalez-Partida J.T., Almorox-Gonzalez P., Burgos-Garcia M., Dorta-Naranjo B.P. // 2007 IET International Conference on Radar Systems. - Edinburgh, UK, 15-18 Oct. 2007. - P. 1-5. ↑

C9721. Zasada D. M. Detecting moving targets in multiple-channel SAR via double thresholding. / Zasada D. M., Sanyal P. K., Perry R. P. // 2007 IET International Conference on Radar Systems. - Edinburgh, UK, 15-18 Oct. 2007. - P. 1-5. ↑

C9722. de Miguel Vela Gonzalo. Prediction of low incidence angle propagation effects in ISAR images of sea targets. / de Miguel Vela Gonzalo, de Jesus Antonio Berlanga, Fominaya Javier Garcia. // 2007 IET International Conference on Radar Systems. - Edinburgh, UK, 15-18 Oct. 2007. - P. 1-5. ↑

C9723. Vigurs G.J. Accurate moving target location in SAR imagery. / Vigurs G.J., Milner C., Jarrett M.L. // 2007 IET International Conference on Radar Systems. - Edinburgh, UK, 15-18 Oct. 2007. - P. 1-5. ↑

C9724. Douvenot R. Retrieving evaporation duct heights from measured propagation factors. / Douvenot R., Fabbro V., Fuchs H.H., Essen H., Bourlier C., Saillard J., Hurtaud Y. // 2007 IET International Conference on Radar Systems. - Edinburgh, UK, 15-18 Oct. 2007. - P. 1-5. ↑

C9725. Sharp Alexander N. Sparse array systems for ultralight UAV radar. / Sharp Alexander N., Bates Bevan D. // 2007 IET International Conference on Radar Systems. - Edinburgh, UK, 15-18 Oct. 2007. - P. 1-5. ↑

C9726. Sharp Alexander N. Vivaldi Antennas: Wideband radar antennas simulation and reality. / Sharp Alexander N., Kyprianou Ross. // 2007 IET International Conference on Radar Systems. - Edinburgh, UK, 15-18 Oct. 2007. - P. 1-5. ↑

C9727. Kabakchiev Chr. Netted radar hough detector in randomly arriving impulse interference. / Kabakchiev Chr., Garvanov I., Rohling H. // 2007 IET International Conference on Radar Systems. - Edinburgh, UK, 15-18 Oct. 2007. - P. 1-5. ↑

C9728. Gill S. Quantifying the benefits of complex radar resource management techniques for airborne electronically scanned radars. / Gill S., Whitehead J.R.G., Walbridge M.R. // 2007 IET International Conference on Radar Systems. - Edinburgh, UK, 15-18 Oct. 2007. - P. 1-4. ↑

C9729. Moore Stephen. AMSAR active phased array antenna. / Moore Stephen, Rutzel Peter, Feldle Peter, Bock Markus. // 2007 IET International Conference on Radar Systems. - Edinburgh, UK, 15-18 Oct. 2007. - P. 1-4. ↑

C9730. Zheng F. Dynamic simulation of a new deployable antenna structure for space application. / Zheng F., Chen M., Wang C.S., Feng C.K. // 2007 IET International Conference on Radar Systems. - Edinburgh, UK, 15-18 Oct. 2007. - P. 1-5. ↑

C9731. Nandgaonkar A. B. Design of a low cost microstrip patch antenna for GPS applications. / Nandgaonkar A. B., Deosarkar S. B., Shah Pragnesh. // 2007 IET International Conference on Radar Systems. - Edinburgh, UK, 15-18 Oct. 2007. - P. 1-3. ↑

C9732. Ostergaard Allan. Scanner 4000/4100: Synthesis, design and manufacture of an artificial lens for an air surveillance antenna. // 2007 IET International Conference on Radar Systems. - Edinburgh, UK, 15-18 Oct. 2007. - P. 1-4. ↑

C9733. Maaref N. Through-the-wall radar using multiple UWB antennas. / Maaref N., Millot P., Pichot C., Picon O. // 2007 IET International Conference on Radar Systems. - Edinburgh, UK, 15-18 Oct. 2007. - P. 1-4. ↑

C9734. Wang Li. A 77-GHz MMIC power amplifier driver for automotive radar. / Wang Li, Borngraeber Johannes, Winkler Wolfgang, Scheytt Christoph. // 2007 IET International Conference on Radar Systems. - Edinburgh, UK, 15-18 Oct. 2007. - P. 1-4. ↑

C9735. Leong H. An estimation of radar cross sections of small vessels at HF. // 2007 IET International Conference on Radar Systems. - Edinburgh, UK, 15-18 Oct. 2007. - P. 1-4. ↑

- C9736.** Sjogren T. K. Speed estimation experiments for ground moving targets in UWB SAR. / Sjogren T. K., Vu V. T., Pettersson M. I., Zepernick H.-J., Gustavsson A. // 2007 IET International Conference on Radar Systems. - Edinburgh, UK, 15-18 Oct. 2007. - P. 1-5. ↑
- C9737.** Irci Ayhan. Resource allocation modelling using methods of feasible directions in phased array radar systems. / Irci Ayhan, Saranli Afsar, Baykal Buyurman. // 2007 IET International Conference on Radar Systems. - Edinburgh, UK, 15-18 Oct. 2007. - P. 1-5. ↑
- C9738.** Cilliers J.E. On the effects of quantization on mismatched pulse compression filters designed using L-p norm minimization techniques. / Cilliers J.E., Smit J.C. // 2007 IET International Conference on Radar Systems. - Edinburgh, UK, 15-18 Oct. 2007. - P. 1-5. ↑
- C9739.** Norland R. Polarimetric frequency agile FMCW RCS measurement radar. / Norland R., Gundersen R., Skjonhaug S., Skottene A., Sveli C., Dyroy B. // 2007 IET International Conference on Radar Systems. - Edinburgh, UK, 15-18 Oct. 2007. - P. 1-4. ↑
- C9740.** Thomsen A.C.K. SCANTER 4000/4100: A multi purpose surveillance radar. / Thomsen A.C.K., Ostergaard A., Marquersen O., Moller-Hundborg C.T., Jensen L.J., Rohde R.H., Leth-Espensen P. // 2007 IET International Conference on Radar Systems. - Edinburgh, UK, 15-18 Oct. 2007. - P. 1-4. ↑
- C9741.** Kovalenko V. An unsupervised multi-feature framework for landmine detection. / Kovalenko V., Yarovoy A., Ligthart L.P. // 2007 IET International Conference on Radar Systems. - Edinburgh, UK, 15-18 Oct. 2007. - P. 1-5. ↑
- C9742.** Nickel U. Array signal processing using digital subarrays. / Nickel U., Richardson P. G., Medley J. C., Briemle E. // 2007 IET International Conference on Radar Systems. - Edinburgh, UK, 15-18 Oct. 2007. - P. 1-5. ↑
- C9743.** Shen Wei. UHF radar system tested on the Bridge of Yangtze River. / Shen Wei, Wen Biyang, Li Zili, Huang Xiaojing. // 2007 IET International Conference on Radar Systems. - Edinburgh, UK, 15-18 Oct. 2007. - P. 1-5. ↑
- C9744.** Matthiesen Duane J. Optimal search and optimal detection. 2007 IET International Conference on Radar Systems. - Edinburgh, UK, 15-18 Oct. 2007. - P. 1-7. ↑
- C9745.** Vu V. T. Experimental results on moving target detection by focusing in UWB low frequency SAR. / Vu V. T., Sjogren T. K., Pettersson M. I., Zepernick H.-J., Gustavsson A. // 2007 IET International Conference on Radar Systems. - Edinburgh, UK, 15-18 Oct. 2007. - P. 1-5. ↑
- C9746.** Wade B. SharpEye A 'New Technology' marine radar. 2007 IET International Conference on Radar Systems. - Edinburgh, UK, 15-18 Oct. 2007. - P. 1-5. ↑
- C9747.** RezaZadeh Ahmad. Maximum likelihood CFAR for lognormal clutter with censored samples. / RezaZadeh Ahmad, Norouzi Yaser, Nayebi Mohammad Mahdi. // 2007 IET International Conference on Radar Systems. - Edinburgh, UK, 15-18 Oct. 2007. - P. 1-4. ↑
- C9748.** Yamamoto K. Power line RCS measurement at 94 GHz. / Yamamoto K., Yonemoto N., Yamada K., Yasui H. // 2007 IET International Conference on Radar Systems. - Edinburgh, UK, 15-18 Oct. 2007. - P. 1-5. ↑
- C9749.** Mellor I. M. Cross modulation cancellation for airborne phased array radar. / Mellor I. M., Adams F. J., Richardson P. G. // 2007 IET International Conference on Radar Systems. - Edinburgh, UK, 15-18 Oct. 2007. - P. 1-4. ↑
- C9750.** Setlur P. Urban target classifications using time-frequency micro-Doppler signatures. / Setlur P., Amin M., Ahmad F. // 2007. ISSPA 2007. 9th International Symposium on Signal Processing and Its Applications. - Sharjah, 12-15 Feb. 2007. - P. 1-4. ↑
- C9751.** Kirkebo J.E. Weight and layout optimized arrays using least angle regression. / Kirkebo J.E., de Campos M.L.R. // 2007. ISSPA 2007. 9th International Symposium on Signal Processing and Its Applications. - Sharjah, 12-15 Feb. 2007. - P. 1-4. ↑
- C9752.** Mubara K. Global mapping of height of bright band. / Mubara K., Dawood A., Al Dosary A. // 2007. ISSPA 2007. 9th International Symposium on Signal Processing and Its Applications. - Sharjah, 12-15 Feb.

2007. - P. 1-4. ↑

C9753. Sari F. Performance analysis of maximum likelihood CFAR detection for Gaussian mixture type clutter. / Sari F., Sari N., Celebi M.E., Kayran A.H. // 2007. ISSPA 2007. 9th International Symposium on Signal Processing and Its Applications. - Sharjah, 12-15 Feb. 2007. - P. 1-4. ↑

C9754. Li Ta-Hsin. Estimation of the Frequency of Sinusoidal Signals in Laplace Noise. / Li Ta-Hsin, Song Kai-Sheng. // 2007. ISIT 2007. IEEE International Symposium on Information Theory. - Nice, 24-29 June 2007. - P. 1786-1790. ↑

C9755. Amar Alon. Resolution of Closely Spaced Deterministic Signals with Given Success Rate. / Amar Alon, Weiss Anthony J. // 2007. ISIT 2007. IEEE International Symposium on Information Theory. - Nice, 24-29 June 2007. - P. 1791-1795. ↑

C9756. Shoeb M. Source localization in view of urban sensing applications. / Shoeb M., Ahmad F., Amin M. // 2007. ISSPA 2007. 9th International Symposium on Signal Processing and Its Applications. - Sharjah, 12-15 Feb. 2007. - P. 1-4. ↑

C9757. Napolitano A. Generalized almost-cyclostationary processes and spectrally correlated processes: Two extensions of the class of the almost-cyclostationary processes. 2007. ISSPA 2007. 9th International Symposium on Signal Processing and Its Applications. - Sharjah, 12-15 Feb. 2007. - P. 1-6. ↑

C9758. Semira H. Single snapshot projection based method for azimuth/elevation directions of arrival estimation. / Semira H., Belkacemi H., Doghmane N. // 2007. ISSPA 2007. 9th International Symposium on Signal Processing and Its Applications. - Sharjah, 12-15 Feb. 2007. - P. 1-4. ↑

C9759. Hamid A.-K. Radar cross section of a semi-elliptic channel in a ground plane loaded by multi - dielectric layerers. 2007. ISSPA 2007. 9th International Symposium on Signal Processing and Its Applications. - Sharjah, 12-15 Feb. 2007. - P. 1-4. ↑

C9760. Aissa-El-Bey A. Underdetermined audio source separation using fast parametric decomposition. / Aissa-El-Bey A., Abed-Meraim K., Grenier Y. // 2007. ISSPA 2007. 9th International Symposium on Signal Processing and Its Applications. - Sharjah, 12-15 Feb. 2007. - P. 1-4. ↑

C9761. Mathews C.P. Enhancing UCA-ESPRIT for non-circular sources. 2007. ISSPA 2007. 9th International Symposium on Signal Processing and Its Applications. - Sharjah, 12-15 Feb. 2007. - P. 1-4. ↑

C9762. Basturk A. Adaptive neuro-fuzzy inference system for speckle noise reduction in SAR images. / Basturk A., Emin Yuksel M. // 2007. ISSPA 2007. 9th International Symposium on Signal Processing and Its Applications. - Sharjah, 12-15 Feb. 2007. - P. 1-4. ↑

C9763. Farnoosh N. A hybrid MOMFD-FDTD ground penetrating radar modeling technique to detect multiple buried objects. / Farnoosh N., Shoory A., Moini R., Sadeghi S. // 2007. ISSPA 2007. 9th International Symposium on Signal Processing and Its Applications. - Sharjah, 12-15 Feb. 2007. - P. 1-4. ↑

C9764. Gutierrez R. Ladar scan preprocessing for robust motion estimation. / Gutierrez R., Gonzalez J., Blanco J.L. // 2007. ISSPA 2007. 9th International Symposium on Signal Processing and Its Applications. - Sharjah, 12-15 Feb. 2007. - P. 1-4. ↑

C9765. Laroussi T. Adaptive ML-CFAR detection for correlated chi-square targets of all fluctuation models in correlated clutter and multiple target situations. / Laroussi T., Barkat M. // 2007. ISSPA 2007. 9th International Symposium on Signal Processing and Its Applications. - Sharjah, 12-15 Feb. 2007. - P. 1-4. ↑

C9766. Alamdari M. An improved CFAR detector using wavelet shrinkage in multiple target environments. / Alamdari M., Modarres-Hashemi M. // 2007. ISSPA 2007. 9th International Symposium on Signal Processing and Its Applications. - Sharjah, 12-15 Feb. 2007. - P. 1-4. ↑

C9767. Derakhtian M. Rapid-fluctuating Radar Signal Detection with Unknown Arrival Time. / Derakhtian M., Tadaion A.A., Gazor S., Nayeibi M.M. // 2007. ICSPC 2007. IEEE International Conference on Signal Processing and Communications. - Dubai, 24-27 Nov. 2007. - P. 213-216. ↑

C9768. Alamri T.H. Serial Acquisition of DS-CDMA Signals using Smart Antennas and Adaptive Thresholding

- Constant False Alarm Rate Processing. / Alamri T.H., Alshebeili S.A., Barkat M. // 2007. ICSPC 2007. IEEE International Conference on Signal Processing and Communications. - Dubai, 24-27 Nov. 2007. - P. 468-471. ↑
- C9769.** Mezache A. A Novel Threshold Optimization Technique for CFAR Detection in Weibull Clutter using Fuzzy-Neural Networks. / Mezache A., Soltani F. // 2007. ICSPC 2007. IEEE International Conference on Signal Processing and Communications. - Dubai, 24-27 Nov. 2007. - P. 197-200. ↑
- C9770.** Zattouta B. Automatic Censoring Detection Using Binary Clutter-Map Estimation for NonGaussian Environments. / Zattouta B., Farrouki A., Barkat M. // 2007. ICSPC 2007. IEEE International Conference on Signal Processing and Communications. - Dubai, 24-27 Nov. 2007. - P. 205-208. ↑
- C9771.** Chitroub S. Independent Component Analysis of POLSAR Images. Relative Newton-Based Approach. / Chitroub S., Hachemi R. // 2007. ICSPC 2007. IEEE International Conference on Signal Processing and Communications. - Dubai, 24-27 Nov. 2007. - P. 684-687. ↑
- C9772.** Ijima H. Estimation of Motion Parameters of Moving Target using Wigner Distribution. / Ijima H., Matsuoka A., Nakajima T., Ohsumi A. // 2007. ICSPC 2007. IEEE International Conference on Signal Processing and Communications. - Dubai, 24-27 Nov. 2007. - P. 688-691. ↑
- C9773.** Al Suwaidi A.R. Determination of Earth Surface from TRMM Satellite Images. / Al Suwaidi A.R., Dawood A., Mubarak K., Matar G., Al Hammadi H. // 2007. ICSPC 2007. IEEE International Conference on Signal Processing and Communications. - Dubai, 24-27 Nov. 2007. - P. 580-583. ↑
- C9774.** Tadaion A.A. Invariant Detection of a Constant Magnitude Signal with Unknown Parameters in White Gaussian Noise. / Tadaion A.A., Derakhtian M., Gazor S., Nayebi M.M. // 2007. ICSPC 2007. IEEE International Conference on Signal Processing and Communications. - Dubai, 24-27 Nov. 2007. - P. 664-667. ↑
- C9775.** Sondur V.V. Issues in the Design of Equiripple FIR Higher Order Digital Differentiators using Weighted Least Squares Technique. / Sondur V.V., Sondur V.B., Rao D.H., Latte M.V., Ayachit N.H. // 2007. ICSPC 2007. IEEE International Conference on Signal Processing and Communications. - Dubai, 24-27 Nov. 2007. - P. 189-192. ↑
- C9776.** Uduwawala D. Gaussian vs differentiated gaussian as the input pulse for ground penetrating radar applications. 2007. ICIIS 2007. International Conference on Industrial and Information Systems. - Penadeniya, 9-11 Aug. 2007. - P. 199-202. ↑
- C9777.** Kodagoda S. Towards an enhanced driver situation awareness system. / Kodagoda S., Sehestedt S., Alempijevic A., Zhang Z., Donikian A., Dissanayake G. // 2007. ICIIS 2007. International Conference on Industrial and Information Systems. - Penadeniya, 9-11 Aug. 2007. - P. 295-300. ↑
- C9778.** Vignesh Karthik M. Building an IMS Client test bed with open source tools. / Vignesh Karthik M., Prateek S. // 2007 International Conference on IP Multimedia Subsystem Architecture and Applications. - Bangalore, 6-8 Dec. 2007. - P. 1-5. ↑
- C9779.** Roy A. Radiating element characteristics effect on the scanning performance of phased array antenna for tracking purpose. / Roy A., Ghosh S., Chakrabarty A. // 2007. ICIIS 2007. International Conference on Industrial and Information Systems. - Penadeniya, 9-11 Aug. 2007. - P. 175-180. ↑
- C9780.** Abdullah R.S.A.R. Target prediction in Forward Scattering Radar. / Abdullah R.S.A.R., Rasid M.F.A., Azis M.W., Khalafalla M. // 2007. APACE 2007. Asia-Pacific Conference on Applied Electromagnetics. - Melaka, 4-6 Dec. 2007. - P. 1-5. ↑
- C9781.** Odabae M. A new signal detection with unknown doppler in an unknown background using spectrogram. / Odabae M., Ghorbani A., Amindavar H. // 2007. ATNAC 2007. Australasian Telecommunication Networks and Applications Conference. - Christchurch, 2-5 Dec. 2007. - P. 225-229. ↑
- C9782.** Aldhubaib F. Optimal radar bistatic angle by statistical analysis of scattering patterns. / Aldhubaib F., Shuley N.V. // 2007. APACE 2007. Asia-Pacific Conference on Applied Electromagnetics. - Melaka, 4-6 Dec. 2007. - P. 1-5. ↑
- C9783.** Hoi-Shun Lui. Polarization studies in the UWB radar target response using joint Time-Frequency analysis. / Hoi-Shun Lui, Aldhubaib F., Shuley N.V.Z. // 2007. APACE 2007. Asia-Pacific Conference on Applied

Electromagnetics. - Melaka, 4-6 Dec. 2007. - P. 1-5. ↑

C9784. Shkvarko Y.V. Remote Sensing Signature Fields Reconstruction Via Robust Regularization of Bayesian Minimum Risk Technique. / Shkvarko Y.V., Villalon-Turrubiates I.E., Leyva-Montiel J.L. // 2007. CAMPSAP 2007. 2nd IEEE International Workshop on Computational Advances in Multi-Sensor Adaptive Processing. - St. Thomas, VI, 12-14 Dec. 2007. - P. 237-240. ↑

C9785. Velmurugan R. Implementation of Batch-Based Particle Filters for Multi-Sensor Tracking. / Velmurugan R., Cevher V., McClellan J.H. // 2007. CAMPSAP 2007. 2nd IEEE International Workshop on Computational Advances in Multi-Sensor Adaptive Processing. - St. Thomas, VI, 12-14 Dec. 2007. - P. 257-260. ↑

C9786. Varslot T. Waveform Preconditioning for Clutter Rejection in Multipath for Sparse Distributed Apertures. / Varslot T., Yazici B., Yarman C.-E., Cheney M., Scharf L. // 2007. CAMPSAP 2007. 2nd IEEE International Workshop on Computational Advances in Multi-Sensor Adaptive Processing. - St. Thomas, VI, 12-14 Dec. 2007. - P. 181-184. ↑

C9787. Bilik I. Wavefront Adaptive Sensing for Radar Spread Clutter Mitigation. / Bilik I., Kazanci O., Krolik J. // 2007. CAMPSAP 2007. 2nd IEEE International Workshop on Computational Advances in Multi-Sensor Adaptive Processing. - St. Thomas, VI, 12-14 Dec. 2007. - P. 185-188. ↑

C9788. Shah S.F.A. Perfectly balanced binary sequences with optimal autocorrelation. / Shah S.F.A., Tewfik A.H. // 2007. ICECS 2007. 14th IEEE International Conference on Electronics, Circuits and Systems. - Marrakech, 11-14 Dec. 2007. - P. 681-684. ↑

C9789. Ali U. Mobile Chatting Server for GPRS networks. / Ali U., Ahmed T. // 2007. ICET 2007. International Conference on Emerging Technologies. - Islamabad, 12-13 Nov. 2007. - P. 52-57. ↑

C9790. Bouleux G. A Lower Bound for Sequential Estimators. / Bouleux G., Boyer R. // 2007. CAMPSAP 2007. 2nd IEEE International Workshop on Computational Advances in Multi-Sensor Adaptive Processing. - St. Thomas, VI, 12-14 Dec. 2007. - P. 277-280. ↑

C9791. Hoehmann L. Laser range finder based obstacle tracking by means of a two-dimensional Kalman filter. / Hoehmann L., Kummert A. // 2007 International Workshop on Multidimensional (nD) Systems. - Aveiro, 27-29 June 2007. - P. 9-14. ↑

C9792. Nikolic M.M. Radar Estimation of Building Layouts Using Jump-Diffusion. / Nikolic M.M., Ortner M., Nehorai A., Djordjevic A.R. // 2007. CAMPSAP 2007. 2nd IEEE International Workshop on Computational Advances in Multi-Sensor Adaptive Processing. - St. Thomas, VI, 12-14 Dec. 2007. - P. 177-180. ↑

C9793. Blunt S.D. Hybrid Adaptive Receive Processing for Multistatic Radar. / Blunt S.D., Dower W., Gerlach K. // 2007. CAMPSAP 2007. 2nd IEEE International Workshop on Computational Advances in Multi-Sensor Adaptive Processing. - St. Thomas, VI, 12-14 Dec. 2007. - P. 5-8. ↑

C9794. Li Y. Adaptive Sensing of Dynamic Target State in Heavy Sea Clutter. / Li Y., Sira S.P., Moran B., Suvorova S., Cochran D., Morrell D., Papandreou-Suppappola A. // 2007. CAMPSAP 2007. 2nd IEEE International Workshop on Computational Advances in Multi-Sensor Adaptive Processing. - St. Thomas, VI, 12-14 Dec. 2007. - P. 9-12. ↑

C9795. Kanazaki H. Variational Bayes Data Association Filter. / Kanazaki H., Yairi T., Machida K., Kondo K., Matsukawa Y. // ---. - Melbourne, Qld., 3-6 Dec. 2007. - P. 401-406. ↑

C9796. Hendee J.C. The Integrated Coral Observing Network: Sensor Solutions for Sensitive Sites. / Hendee J.C., Gramer L., Kleypas J.A., Manzello D., Jankulak M., Langdon C. // ---. - Melbourne, Qld., 3-6 Dec. 2007. - P. 669-673. ↑

C9797. De Maio A. Adaptive Transmit/Receive Schemes for Mimo Radar. / De Maio A., Lops M. // 2007. CAMPSAP 2007. 2nd IEEE International Workshop on Computational Advances in Multi-Sensor Adaptive Processing. - St. Thomas, VI, 12-14 Dec. 2007. - P. 97-100. ↑

C9798. Sammartino P.F. Mimo Radar, Theory and Experiments. / Sammartino P.F., Baker C.J., Rangaswamy M. // 2007. CAMPSAP 2007. 2nd IEEE International Workshop on Computational Advances in Multi-Sensor Adaptive Processing. - St. Thomas, VI, 12-14 Dec. 2007. - P. 101-104. ↑

- C9799.** Jian Li. Mimo SAR Imaging: Signal Synthesis and Receiver Design. / Jian Li, Xiayu Zheng, Stoica P. // 2007. CAMPSAP 2007. 2nd IEEE International Workshop on Computational Advances in Multi-Sensor Adaptive Processing. - St. Thomas, VI, 12-14 Dec. 2007. - P. 89-92. ↑
- C9800.** Greco M. Cross-Channel Interference in Surveillance Radar Networks. / Greco M., Gini F., Farina A. // 2007. CAMPSAP 2007. 2nd IEEE International Workshop on Computational Advances in Multi-Sensor Adaptive Processing. - St. Thomas, VI, 12-14 Dec. 2007. - P. 93-96. ↑
- C9801.** Hantscher S. Application of a Surface Reconstruction Method for Material Penetrating UWB Radar. / Hantscher S., Reisenzahn A., Diskus C.G. // 2007. APMC 2007. Asia-Pacific Microwave Conference. - Bangkok, 11-14 Dec. 2007. - P. 1-4. ↑
- C9802.** Jong-Sen Lee. Polarimetric Analysis of Radar Signature of a Manmade Structure. / Jong-Sen Lee, Krogager E., Ainsworth T.L., Boerner W.-M. // 2007. APMC 2007. Asia-Pacific Microwave Conference. - Bangkok, 11-14 Dec. 2007. - P. 1-4. ↑
- C9803.** Malmqvist R. Multi-Band and Reconfigurable Front-Ends for Flexible and Multi-Functional RF Systems. / Malmqvist R., Ouacha A., Erickson R. // 2007. APMC 2007. Asia-Pacific Microwave Conference. - Bangkok, 11-14 Dec. 2007. - P. 1-4. ↑
- C9804.** Cao Fang. An Unsupervised Segmentation Using SPAN/H/γ/A initialization for Fully Polarimetric SAR Data Analysis. / Cao Fang, Hong Wen, Wu Yirong. // 2007. APMC 2007. Asia-Pacific Microwave Conference. - Bangkok, 11-14 Dec. 2007. - P. 1-3. ↑
- C9805.** Mezache A. Threshold optimization for distributed CFAR detection in Weibull clutter using genetic algorithms. / Mezache A., Soltani F. // 2007. ISSPA 2007. 9th International Symposium on Signal Processing and Its Applications. - Sharjah, 12-15 Feb. 2007. - P. 1-4. ↑
- C9806.** Hewen Wei. Influence of phase on Cramer-Rao lower bounds for joint time delay and Doppler stretch estimation. / Hewen Wei, Shangfu Ye, Qun Wan. // 2007. ISSPA 2007. 9th International Symposium on Signal Processing and Its Applications. - Sharjah, 12-15 Feb. 2007. - P. 1-4. ↑
- C9807.** Amein A.S. High resolution SAR imaging with enhanced focusing capabilities using the fractional fourier transform. 2007. ISSPA 2007. 9th International Symposium on Signal Processing and Its Applications. - Sharjah, 12-15 Feb. 2007. - P. 1-4. ↑
- C9808.** Almarshad M.N. A Monte Carlo simulation for two novel automatic censoring techniques of radar interfering targets in log-normal clutter. / Almarshad M.N., Barkat M., Alshebeili S.A. // 2007. ISSPA 2007. 9th International Symposium on Signal Processing and Its Applications. - Sharjah, 12-15 Feb. 2007. - P. 1-4. ↑
- C9809.** Fu J.S. Target Signal Extraction by Adaptive Signal Decomposition Methods. / Fu J.S., Chengjie Cai, Yichang Cheng, Wenkuan Su. // 2007. APMC 2007. Asia-Pacific Microwave Conference. - Bangkok, 11-14 Dec. 2007. - P. 1-4. ↑
- C9810.** Sahba K. A Novel Beam Deflection Method for Wide Angle Laser Scanning. / Sahba K., Alameh K.E., Smith C.L. // 2007 and the 2007 32nd Australian Conference on Optical Fibre Technology. COIN-ACOFT 2007. Joint International Conference on Optical Internet. - Melbourne, VIC, 24-27 June 2007. - P. 1-3. ↑
- C9811.** Chunhe Yu. Obstacle detection based on a four-layer laser radar. / Chunhe Yu, Danping Zhang. // 2007. ROBIO 2007. IEEE International Conference on Robotics and Biomimetics. - Sanya, 15-18 Dec. 2007. - P. 218-221. ↑
- C9812.** Hadjiloucas S. Apodisation, denoising and system identification techniques for THz transients in the wavelet domain. / Hadjiloucas S., Walker G.C., Bowen J.W., Paiva H.M., Galvao R.K.H., Dudley R. // 2007 and the 2007 15th International Conference on Terahertz Electronics. IRMMW-THz. Joint 32nd International Conference on Infrared and Millimeter Waves. - Cardiff, 2-9 Sept. 2007. - P. 212-213. ↑
- C9813.** {no data available}. Target identification and signal processing of millimeter-wave. 2007 and the 2007 15th International Conference on Terahertz Electronics. IRMMW-THz. Joint 32nd International Conference on Infrared and Millimeter Waves. - Cardiff, 2-9 Sept. 2007. - P. 926-927. ↑
- C9814.** Long Zhuang. Enhanced Resolution for Sparse Aperture Radar Imaging Using Super-SVA. / Long

Zhuang, Xingzhao Liu, Zhixin Zhou. // 2007. APMC 2007. Asia-Pacific Microwave Conference. - Bangkok, 11-14 Dec. 2007. - P. 1-4. ↑

C9815. Seungmo Kim. Detection Probability of WCDMA Based Cellular Radar System. / Seungmo Kim, Yeejung Kim, Youngnam Han, Kyung Bin Bae, Myung Deuk Jeong. // 2007. APMC 2007. Asia-Pacific Microwave Conference. - Bangkok, 11-14 Dec. 2007. - P. 1-4. ↑

C9816. Li Qian. An Iterated Extend Kalman Particle Filter for Multi-sensor based on pseudo sequential fusion. / Li Qian, Feng Jin-fu, Peng Zhi-zhuang, Lu Qing, Liang Xiao-long. // 2007. ROBIO 2007. IEEE International Conference on Robotics and Biomimetics. - Sanya, 15-18 Dec. 2007. - P. 1534-1539. ↑

C9817. Worasawate D. Durian Maturity Identification using Radar Equation Based on Support Vector Classification. / Worasawate D., Ampungart A., Krairiksh M. // 2007. APMC 2007. Asia-Pacific Microwave Conference. - Bangkok, 11-14 Dec. 2007. - P. 1-4. ↑

C9818. Lari M. Producing Pulse Compression Codes with Proper Auto Correlation Function, Regarding Pulse Shape. / Lari M., Aghaeinia H. // 2007. ICSPC 2007. IEEE International Conference on Signal Processing and Communications. - Dubai, 24-27 Nov. 2007. - P. 692-695. ↑

C9819. Murray David. DSAC report 'specification and measurement of radar performance'-have we fully exploited its findings?. 2007 IET International Conference on Radar Systems. - Edinburgh, UK, 15-18 Oct. 2007. - P. 1-4. ↑

C9820. Dickel G. The architecture and operating characteristics of a multi-frequency HF surface wave radar-part two. / Dickel G., Emery D.J., Money D.G. // 2007 IET International Conference on Radar Systems. - Edinburgh, UK, 15-18 Oct. 2007. - P. 1-5. ↑

C9821. Xiongjun Fu. Sidelobe suppression of LPI phase-coded radar signal. / Xiongjun Fu, Liyu Tian, Meiguo Gao. // 2007 IET International Conference on Radar Systems. - Edinburgh, UK, 15-18 Oct. 2007. - P. 1-5. ↑

C9822. Saeedi H. Application of neural network to pulse compression. / Saeedi H, Ahmadzadeh M.R., Akhavan M.R. // 2007 IET International Conference on Radar Systems. - Edinburgh, UK, 15-18 Oct. 2007. - P. 1-6. ↑

C9823. Qi Wang. Space debris radar imaging. / Qi Wang, Mengdao Xing, Zheng Bao. // 2007 IET International Conference on Radar Systems. - Edinburgh, UK, 15-18 Oct. 2007. - P. 1-3. ↑

C9824. Chen Juan. A new method of the high-resolution wide-swath SAR. / Chen Juan, Tao Zeng, Teng Long. // 2007 IET International Conference on Radar Systems. - Edinburgh, UK, 15-18 Oct. 2007. - P. 1-5. ↑

C9825. Munoz-Ferreras J. M. Extended envelope correlation for range bin alignment in ISAR. / Munoz-Ferreras J. M., Perez-Martinez F. // 2007 IET International Conference on Radar Systems. - Edinburgh, UK, 15-18 Oct. 2007. - P. 1-5. ↑

C9826. Amein A.S. Improved synthetic aperture radar imaging for high resolution applications. / Amein A.S., Soraghan J.J. // 2007 IET International Conference on Radar Systems. - Edinburgh, UK, 15-18 Oct. 2007. - P. 1-4. ↑

















C9827. Dawber Bill. Digital pulse compressor design for ultra-low range sidelobes for use within the eclipsed region. / Dawber Bill, Nichols Ian. // 2007 IET International Conference on Radar Systems. - Edinburgh, UK, 15-18 Oct. 2007. - P. 1-5. ↑

C9828. Liu Y.J. Optimum steady-state filter for periodic nonuniform sampling system. / Liu Y.J., Meng H.D., Wang D.S., Wang X.Q. // 2007 IET International Conference on Radar Systems. - Edinburgh, UK, 15-18 Oct. 2007. - P. 1-5. ↑

C9829. Morrison N. The Gauss-Newton algorithm applied to track-while-scan radar. / Morrison N., Lord R.T., Inggs M.R. // 2007 IET International Conference on Radar Systems. - Edinburgh, UK, 15-18 Oct. 2007. - P. 1-5. ↑

C9830. Belcher D. P. System level modelling of space based MTI performance. 2007 IET International Conference on Radar Systems. - Edinburgh, UK, 15-18 Oct. 2007. - P. 1-5. ↑

- C9831.** Fabrizio G.A. A robust adaptive detection scheme for radar Doppler processing. / Fabrizio G.A., Farina A. // 2007 IET International Conference on Radar Systems. - Edinburgh, UK, 15-18 Oct. 2007. - P. 1-5. ↑
- C9832.** Liu Y.M. Eliminating ghost images for stepped-frequency train of LFM pulses. / Liu Y.M., Meng H.D., Zhang H., Wang X.Q. // 2007 IET International Conference on Radar Systems. - Edinburgh, UK, 15-18 Oct. 2007. - P. 1-4. ↑
- C9833.** Gallardo-Hernando B. Performance evaluation for imaging laser radars with focal plane array. / Gallardo-Hernando B., Munoz-Ferreras J. M., Perez-Martinez F., Lazaro-Gasco J. M. // 2007 IET International Conference on Radar Systems. - Edinburgh, UK, 15-18 Oct. 2007. - P. 1-5. ↑
- C9834.** Sammartino P.F. Decentralized processing in radar networks. / Sammartino P.F., Baker C.J., Griffiths H.D., Rangaswamy M. // 2007 IET International Conference on Radar Systems. - Edinburgh, UK, 15-18 Oct. 2007. - P. 1-5. ↑
- C9835.** Magaz B. Optimized implementation of a parallel DSP architecture for real time stacked beam radar signal processing. / Magaz B., Bencheikh M. L., Hamadouche M., Belouchrani A. // 2007 IET International Conference on Radar Systems. - Edinburgh, UK, 15-18 Oct. 2007. - P. 1-5. ↑
- C9836.** Landi L. Range Doppler correlation for time-orthogonal distributed aperture radars. / Landi L., Adve R. S. // 2007 IET International Conference on Radar Systems. - Edinburgh, UK, 15-18 Oct. 2007. - P. 1-5. ↑
- C9837.** Liu Nan. Clutter modeling and analysis for spaceborne bistatic radar. / Liu Nan, Zhang Linrang, Yi Yusheng, Liu Xin. // 2007 IET International Conference on Radar Systems. - Edinburgh, UK, 15-18 Oct. 2007. - P. 1-5. ↑
- C9838.** Ruggiano M. Radar and communication waveform: Wideband ambiguity function and narrowband approximation. / Ruggiano M., van Genderen P. // 2007 IET International Conference on Radar Systems. - Edinburgh, UK, 15-18 Oct. 2007. - P. 1-5. ↑
- C9839.** Wicks M. C. Waveform diversity for distributed and layered sensing. / Wicks M. C., Magde K. M., Antonik P. // 2007 IET International Conference on Radar Systems. - Edinburgh, UK, 15-18 Oct. 2007. - P. 1-5. ↑
- C9840.** Kwag Y. K. Helicopter-borne mtd radar development and flight test for moving clutter measurement. / Kwag Y. K., Yang J. Y., Jung C. H. // 2007 IET International Conference on Radar Systems. - Edinburgh, UK, 15-18 Oct. 2007. - P. 1-4. ↑
- C9841.** Yamaguchi H. Predictive density of millimeter-wave backscattering based on Gamma mixture model. / Yamaguchi H., Suganuma W., Osafune T., Tanaka M., Okuda H., Aoki S. // 2007 IET International Conference on Radar Systems. - Edinburgh, UK, 15-18 Oct. 2007. - P. 1-5. ↑
- C9842.** Jackson C.A. Spectrally efficient radar systems in the L and S bands. / Jackson C.A., Holloway J.R., Pollard R., Larson R., Sarno C., Baker C., Woodbridge K., Ormondroyd R.F., Lewis M.B., Stove A.G. // 2007 IET International Conference on Radar Systems. - Edinburgh, UK, 15-18 Oct. 2007. - P. 1-6. ↑
- C9843.** Papadopoulos S. The spectrum of scattered radar signals from complex ground targets. / Papadopoulos S., Mulgrew B. // 2007 IET International Conference on Radar Systems. - Edinburgh, UK, 15-18 Oct. 2007. - P. 1-4. ↑
- C9844.** Welstead Stephen. Frequency coded waveforms from chaotic time series. 2007 IET International Conference on Radar Systems. - Edinburgh, UK, 15-18 Oct. 2007. - P. 1-5. ↑
- C9845.** Klemm R. Recognition of convoys with airborne adaptive monopulse radar. 2007 IET International Conference on Radar Systems. - Edinburgh, UK, 15-18 Oct. 2007. - P. 1-5. ↑
- C9846.** Smith G. E. Multiperspective micro-Doppler signature classification. / Smith G. E., Woodbridge K., Baker C. J. // 2007 IET International Conference on Radar Systems. - Edinburgh, UK, 15-18 Oct. 2007. - P. 1-5. ↑
- C9847.** Dai Da-hai. SAR active-decoys jamming based on DRFM. / Dai Da-hai, Wu X. F., Wang Xue-song, Xiao Shun-ping. // 2007 IET International Conference on Radar Systems. - Edinburgh, UK, 15-18 Oct. 2007. - P. 1-4. ↑

- C9848.** Bawar Zahid Hasan. Inversion of residual errors to improve insar data acquisition, processing and interpretation. / Bawar Zahid Hasan, Long Teng, Tao Zeng. // 2007 IET International Conference on Radar Systems. - Edinburgh, UK, 15-18 Oct. 2007. - P. 1-4. 
- C9849.** Fang J.X. A ground vehicle classification approach using unmodulated continuous-wave radar. / Fang J.X., Meng H.D., Zhang H., Wang X.Q. // 2007 IET International Conference on Radar Systems. - Edinburgh, UK, 15-18 Oct. 2007. - P. 1-4. 
- C9850.** Antonik P. Waveform diversity: Past, present, and future. / Antonik P., Wicks M. C. // 2007 IET International Conference on Radar Systems. - Edinburgh, UK, 15-18 Oct. 2007. - P. 1-5. 
- C9851.** Ghaleb A. Fine micro-Doppler analysis in ISAR imaging. / Ghaleb A., Vignaud L., Deloues T., Nicolas J-M. // 2007 IET International Conference on Radar Systems. - Edinburgh, UK, 15-18 Oct. 2007. - P. 1-4. 
- C9852.** Raja Abdullah R.S.A. Neural network based for automatic vehicle classification in forward scattering radar. / Raja Abdullah R.S.A., Saripan M.I., Cherniakov M. // 2007 IET International Conference on Radar Systems. - Edinburgh, UK, 15-18 Oct. 2007. - P. 1-5. 
- C9853.** Dickel G. The architecture and operating characteristics of a multi-frequency hf surfacewave radar-part one. / Dickel G., Emery D.J., Money D.G. // 2007 IET International Conference on Radar Systems. - Edinburgh, UK, 15-18 Oct. 2007. - P. 1-5. 
- C9854.** Adrian Odile. Platform concept: A breakthrough in surface radar architecture. 2007 IET International Conference on Radar Systems. - Edinburgh, UK, 15-18 Oct. 2007. - P. 1-5. 
- C9855.** Wallace William. Demonstrating the concept of using synthetic environments in radar acceptance and procurement. / Wallace William, New Chris, Branson James. // 2007 IET International Conference on Radar Systems. - Edinburgh, UK, 15-18 Oct. 2007. - P. 1-5. 
- C9856.** Dzvонkovskaya A.L. HF radar ship detection and tracking using WERA system. / Dzvонkovskaya A.L., Rohling H. // 2007 IET International Conference on Radar Systems. - Edinburgh, UK, 15-18 Oct. 2007. - P. 1-5. 
- C9857.** Cote S.J. RADARSAT calibration operations at the Canadian Space Agency: Maintaining RADARSAT-1 performance and preparations for RADARSAT-2. / Cote S.J., Srivastava S.K., Hawkins R.K., Le Dante P. // 2007 IET International Conference on Radar Systems. - Edinburgh, UK, 15-18 Oct. 2007. - P. 1-5. 
- C9858.** Krieger G. TanDEM-X: A satellite formation for high-resolution SAR interferometry. / Krieger G., Fiedler H., Zink M., Hajnsek I., Younis M., Huber S., Bachmann M., Hueso Gonzalez J., Werner M., Moreira A. // 2007 IET International Conference on Radar Systems. - Edinburgh, UK, 15-18 Oct. 2007. - P. 1-5. 
- C9859.** Adrian Odile. A combination of NLOS radar technology and LOS optical technology for Defence & Security. / Adrian Odile, Ferrier Jean-Marie, Ricci Yves. // 2007 IET International Conference on Radar Systems. - Edinburgh, UK, 15-18 Oct. 2007. - P. 1-6. 
- C9860.** Krieger G. Multidimensional waveform encoding for synthetic aperture radar remote sensing. / Krieger G., Gebert N., Moreira A. // 2007 IET International Conference on Radar Systems. - Edinburgh, UK, 15-18 Oct. 2007. - P. 1-5. 
- C9861.** Grasso G. C. Is radar still the king?. 2007 IET International Conference on Radar Systems. - Edinburgh, UK, 15-18 Oct. 2007. - P. 1. 
- C9862.** Kemouche M.S. A Hybrid Kalman/ γH^∞ Filter for Maneuvering Target Tracking. / Kemouche M.S., Aouf N., Tsourdos A., White B. // 2007. ICSPC 2007. IEEE International Conference on Signal Processing and Communications. - Dubai, 24-27 Nov. 2007. - P. 1267-1270. 
- C9863.** Khazaal A. Brightness Temperature Maps Retrieval for the SMOS Space Mission: Regularized Inversion and Bias Reduction. / Khazaal A., Anterrieu E. // 2007. ICSPC 2007. IEEE International Conference on Signal Processing and Communications. - Dubai, 24-27 Nov. 2007. - P. 1323-1326. 
- C9864.** Al-Ridha K. A Multi-Level Mobile Video Surveillance Notification System. / Al-Ridha K., Al-Qayedi A. // 2007. ICSPC 2007. IEEE International Conference on Signal Processing and Communications. - Dubai, 24-27

Nov. 2007. - P. 1171-1174. ↑

C9865. Yi Zheng. A New Algorithm for FOA and 2-D AOA Estimation. / Yi Zheng, Tieqi Xia, Xuegang Wang, Qun Wan. // 2007. ICSPC 2007. IEEE International Conference on Signal Processing and Communications. - Dubai, 24-27 Nov. 2007. - P. 1263-1266. ↑

C9866. Banani S.A. On Tracking Maneuvering Targets in 3-Dimensional Space with Online Observed Colored Glint Noise Parameter Estimation. / Banani S.A., Masnadi-Shirazi M.A. // 2007. ICSPC 2007. IEEE International Conference on Signal Processing and Communications. - Dubai, 24-27 Nov. 2007. - P. 1427-1430. ↑

C9867. Laroussi T. A Performance Comparison of Two Time Diversity Systems using TM-CFAR Detection for Partially Correlated Chi-Square Targets in Nonuniform Clutter and Multiple Target Situations. / Laroussi T., Barkat M., Benadjina N. // 2007. ICSPC 2007. IEEE International Conference on Signal Processing and Communications. - Dubai, 24-27 Nov. 2007. - P. 1511-1514. ↑

C9868. Mezache A. Fuzzy Neural Network Approach for Estimating The K-distribution Parameters. / Mezache A., Soltani F. // 2007. ICSPC 2007. IEEE International Conference on Signal Processing and Communications. - Dubai, 24-27 Nov. 2007. - P. 1335-1338. ↑

C9869. Tarlet O. Sonar Images from Well-Known Simulated Raw Data. / Tarlet O., Loussert A., Sintes C. // 2007. ICSPC 2007. IEEE International Conference on Signal Processing and Communications. - Dubai, 24-27 Nov. 2007. - P. 1423-1426. ↑

C9870. Benoudnine H. Adaptive MRIMM algorithm for tracking manoeuvring target using a phased array radar. / Benoudnine H., Keche M., Ouamri A., Woolfson M.S. // 2007 IET International Conference on Radar Systems. - Edinburgh, UK, 15-18 Oct. 2007. - P. 1-5. ↑

C9871. Carson Steven. A passive, multi-static radar system. / Carson Steven, Kilfoyle Daniel, Potter Michael, Vance James. // 2007 IET International Conference on Radar Systems. - Edinburgh, UK, 15-18 Oct. 2007. - P. 1-4. ↑

C9872. Alabaster C.M. The dependence of radar target detectability on array weighting function. / Alabaster C.M., Hughes E.J. // 2007 IET International Conference on Radar Systems. - Edinburgh, UK, 15-18 Oct. 2007. - P. 1-5. ↑

C9873. Worms Josef G. Detection of narrowband radar signals having a broadband digital receiver. 2007 IET International Conference on Radar Systems. - Edinburgh, UK, 15-18 Oct. 2007. - P. 1-5. ↑

C9874. Deng H. Target detection using orthogonal netted radar system (ONRS). / Deng H., Himed B. // 2007 IET International Conference on Radar Systems. - Edinburgh, UK, 15-18 Oct. 2007. - P. 1-4. ↑

C9875. Kulpa K. Ground clutter cancellation in MIMO and multistatic noise radars. / Kulpa K., Malanowski M., Gajo Z. // 2007 IET International Conference on Radar Systems. - Edinburgh, UK, 15-18 Oct. 2007. - P. 1-5. ↑

C9876. Doughty S.R. Improving resolution using multistatic radar. / Doughty S.R., Woodbridge K., Baker C.J. // 2007 IET International Conference on Radar Systems. - Edinburgh, UK, 15-18 Oct. 2007. - P. 1-5. ↑

C9877. Sandenbergh J.S. A common view GPSDO to synchronize netted radar. / Sandenbergh J.S., Inggs M.R. // 2007 IET International Conference on Radar Systems. - Edinburgh, UK, 15-18 Oct. 2007. - P. 1-5. ↑

C9878. Verba V.S. Efficiency of adaptive threshold detector of pulse-doppler radar. / Verba V.S., Gandurin V.A., Sokolov A.V. // 2007 IET International Conference on Radar Systems. - Edinburgh, UK, 15-18 Oct. 2007. - P. 1-3. ↑

C9879. Williams L. Low cost networked radar and sonar using open source hardware and software. / Williams L., Inggs M.R. // 2007 IET International Conference on Radar Systems. - Edinburgh, UK, 15-18 Oct. 2007. - P. 1-5. ↑

C9880. Zhu Jiabing. Adaptive beamforming passive radar based on FM radio transmitter. / Zhu Jiabing, Hong Yi, Tao Liang. // 2007 IET International Conference on Radar Systems. - Edinburgh, UK, 15-18 Oct. 2007. - P. 1-4. ↑

- C9881. Saini R. Signal synchronisation in SS-BSAR based on GLONASS Satellite emission. / Saini R., Zuo R., Cherniakov M. // 2007 IET International Conference on Radar Systems. - Edinburgh, UK, 15-18 Oct. 2007. - P. 1-5. ↑
- C9882. Barber B.C. A statistical method for processing SAR Multichannel ATI sea surface images. 2007 IET International Conference on Radar Systems. - Edinburgh, UK, 15-18 Oct. 2007. - P. 1-5. ↑
- C9883. Daemi T. Diffraction techniques in rcs prediction of an aircraft model. / Daemi T., Jalilvand M. // 2007 IET International Conference on Radar Systems. - Edinburgh, UK, 15-18 Oct. 2007. - P. 1-5. ↑
- C9884. Mingwei Shen. An improved scheme for the frequency domain $\Sigma\Delta$ -DPCA. / Mingwei Shen, Daiyin Zhu, Zhaoda Zhu. // 2007 IET International Conference on Radar Systems. - Edinburgh, UK, 15-18 Oct. 2007. - P. 1-5. ↑
- C9885. van Rossum W.L. Comparison of MIMO radar concepts: Detection performance. / van Rossum W.L., Huizing A.G. // 2007 IET International Conference on Radar Systems. - Edinburgh, UK, 15-18 Oct. 2007. - P. 1-5. ↑
- C9886. Lane R.O. Detecting personnel in wooded areas using MIMO radar. / Lane R.O., Hayward S.D. // 2007 IET International Conference on Radar Systems. - Edinburgh, UK, 15-18 Oct. 2007. - P. 1-5. ↑
- C9887. Li Z.T. DEM alignment and registration in interferometric SAR processing and evaluation. / Li Z.T., Bethel J. // 2007. IGARSS 2007. IEEE International Geoscience and Remote Sensing Symposium. - Barcelona, 23-28 July 2007. - P. 4890-4893. ↑
- C9888. Portabella M. ASCAT scatterometer ocean calibration. / Portabella M., Stoffelen A., Verspeek J., Verhoef A., Vogelzang J. // 2007. IGARSS 2007. IEEE International Geoscience and Remote Sensing Symposium. - Barcelona, 23-28 July 2007. - P. 2539-2542. ↑
- C9889. Monsivais-Huertero A. Scattering from sahelian grassland: a coherent modeling. / Monsivais-Huertero A., Chenerie I., Sarabandi K. // 2007. IGARSS 2007. IEEE International Geoscience and Remote Sensing Symposium. - Barcelona, 23-28 July 2007. - P. 2543-2545. ↑
- C9890. Hui Shen. On SAR hurricane wind speed ambiguities. / Hui Shen, Perrie W., Yijun He. // 2007. IGARSS 2007. IEEE International Geoscience and Remote Sensing Symposium. - Barcelona, 23-28 July 2007. - P. 2531-2534. ↑
- C9891. Nadai A. Dependency analysis of normalized radar cross section of ocean surface on ocean winds using an airborne dual-frequency polarimetric SAR. / Nadai A., Umehara T., Matsuoka T., Satake M., Uratsuka S. // 2007. IGARSS 2007. IEEE International Geoscience and Remote Sensing Symposium. - Barcelona, 23-28 July 2007. - P. 2535-2538. ↑
- C9892. Ehlert I. Determine the location of a thermal front in the Iroise Sea by using HF radar data and tide model results. / Ehlert I., Schlick T., Gurgel K.-W., Seille B. // 2007. IGARSS 2007. IEEE International Geoscience and Remote Sensing Symposium. - Barcelona, 23-28 July 2007. - P. 997-999. ↑
- C9893. Dehmollaian M. Refocusing through single layer building wall using synthetic aperture radar. / Dehmollaian M., Sarabandi K. // 2007. IGARSS 2007. IEEE International Geoscience and Remote Sensing Symposium. - Barcelona, 23-28 July 2007. - P. 2558-2561. ↑
- C9894. He Zhan. Half-space born approximation modeling and inversion for cross-well radar sensing of contaminants in soil. / He Zhan, Morgenthaler A., Qiuzhao Dong, Rappaport C., Miller E. // 2007. IGARSS 2007. IEEE International Geoscience and Remote Sensing Symposium. - Barcelona, 23-28 July 2007. - P. 2550-2553. ↑
- C9895. Demarty Y. Exact electromagnetic modeling of the scattering of realistic sea surfaces for HF/SWR applications. / Demarty Y., Gobin V., Thirion L., Guinvarc'h R., Lesturgie M. // 2007. IGARSS 2007. IEEE International Geoscience and Remote Sensing Symposium. - Barcelona, 23-28 July 2007. - P. 1004-1007. ↑
- C9896. Lawrence R. Differential absorption microwave radar measurements for remote sensing of atmospheric pressure. / Lawrence R., Fralick D., Harrah S., Bing Lin, Yongxiang Hu, Hunt P. // 2007. IGARSS 2007. IEEE International Geoscience and Remote Sensing Symposium. - Barcelona, 23-28 July 2007. - P. 1045-1048. ↑

- C9897.** Meta A. Sampling quantization analysis and results for FMCW SAR. / Meta A., Hoogeboom P., Ligthart L.P. // 2007. IGARSS 2007. IEEE International Geoscience and Remote Sensing Symposium. - Barcelona, 23-28 July 2007. - P. 1029-1032. ↑
- C9898.** Parrish C.E. Exploiting full-waveform lidar data and multiresolution wavelet analysis for vertical object detection and recognition. 2007. IGARSS 2007. IEEE International Geoscience and Remote Sensing Symposium. - Barcelona, 23-28 July 2007. - P. 2499-2502. ↑
- C9899.** Songxin Tan. Detection of foliage-obscured vehicle using a multiwavelength polarimetric lidar. / Songxin Tan, Stoker J., Greenlee S. // 2007. IGARSS 2007. IEEE International Geoscience and Remote Sensing Symposium. - Barcelona, 23-28 July 2007. - P. 2503-2506. ↑
- C9900.** Soisuvarn S. A geophysical model function for windsat polarimetric radiometer wind retrievals using linear polarizations. / Soisuvarn S., Jelenak Z., Chang P.S. // 2007. IGARSS 2007. IEEE International Geoscience and Remote Sensing Symposium. - Barcelona, 23-28 July 2007. - P. 2523-2526. ↑
- C9901.** Yijun He. A comparison of models for retrieving high wind speeds. / Yijun He, Hui Shen, Jie Guo, Perrie W. // 2007. IGARSS 2007. IEEE International Geoscience and Remote Sensing Symposium. - Barcelona, 23-28 July 2007. - P. 2527-2530. ↑
- C9902.** Auer S. Automatic extraction of salient geometric entities from LIDAR point clouds. / Auer S., Hinz S. // 2007. IGARSS 2007. IEEE International Geoscience and Remote Sensing Symposium. - Barcelona, 23-28 July 2007. - P. 2507-2510. ↑
- C9903.** Starek M.J. Automatic feature extraction from airborne lidar measurements to identify cross-shore morphologies indicative of beach erosion. / Starek M.J., Vemula R.K., Slatton K.C., Shrestha R.L., Carter W.E. // 2007. IGARSS 2007. IEEE International Geoscience and Remote Sensing Symposium. - Barcelona, 23-28 July 2007. - P. 2511-2514. ↑
- C9904.** Sato M. Application of Polarimetric SAR images acquired in square-loop flights. / Sato M., Iribe K., Hamasaki T. // 2007. IGARSS 2007. IEEE International Geoscience and Remote Sensing Symposium. - Barcelona, 23-28 July 2007. - P. 2632-2635. ↑
- C9905.** Shimada M. Coherence dependency of the PALSAR POLInSAR on forest in japan and amazon. 2007. IGARSS 2007. IEEE International Geoscience and Remote Sensing Symposium. - Barcelona, 23-28 July 2007. - P. 2636-2639. ↑
- C9906.** Neumann M. Multibaseline POLInSAR coherence modelling and optimization. / Neumann M., Ferro-Famil L., Reigber A. // 2007. IGARSS 2007. IEEE International Geoscience and Remote Sensing Symposium. - Barcelona, 23-28 July 2007. - P. 2624-2627. ↑
- C9907.** Chih-Tien Wang. Disaster monitoring and environmental alert in taiwan by repeat-pass spaceborne SAR. / Chih-Tien Wang, Kun-Shen Chen, Hong-Wei Lee, Jong-Sen Lee, Boerner Wolfgang M., Ruei-Yuan Wang, Hong-Sen Wan. // 2007. IGARSS 2007. IEEE International Geoscience and Remote Sensing Symposium. - Barcelona, Spain, 23-28 July 2007. - P. 2628-2631. ↑
- C9908.** Farage G. PolSAR image filtering based on feature detection using the wavelet transform. / Farage G., Foucher S., Benie G.B. // 2007. IGARSS 2007. IEEE International Geoscience and Remote Sensing Symposium. - Barcelona, 23-28 July 2007. - P. 2648-2652. ↑
- C9909.** Franceschetti G. Building feature extraction via a deterministic approach: application to real high resolution SAR images. / Franceschetti G., Guida R., Iodice A., Riccio D., Ruello G., Stilla U. // 2007. IGARSS 2007. IEEE International Geoscience and Remote Sensing Symposium. - Barcelona, 23-28 July 2007. - P. 2681-2684. ↑
- C9910.** Jun-su Kim. Estimation of physical properties of persistent scatterers using JERS-1 data. / Jun-su Kim, Moon W.M. // 2007. IGARSS 2007. IEEE International Geoscience and Remote Sensing Symposium. - Barcelona, 23-28 July 2007. - P. 2640-2643. ↑
- C9911.** Longepe N. Snow wetness monitoring using multi-temporal polarimetric ASAR data and multi-layer hybrid model. / Longepe N., Allain S., Pottier E. // 2007. IGARSS 2007. IEEE International Geoscience and Remote Sensing Symposium. - Barcelona, 23-28 July 2007. - P. 2644-2647. ↑

- C9912.** Fan Wu. Change detection and analysis with radarsat-1 SAR image. / Fan Wu, Chao Wang, Hong Zhang, Bo Zhang. // 2007. IGARSS 2007. IEEE International Geoscience and Remote Sensing Symposium. - Barcelona, 23-28 July 2007. - P. 2601-2604. ↑
- C9913.** Karvonen J. SAR-based estimation of the baltic sea ice motion. / Karvonen J., Simila M., Lehtiranta J. // 2007. IGARSS 2007. IEEE International Geoscience and Remote Sensing Symposium. - Barcelona, 23-28 July 2007. - P. 2605-2608. ↑
- C9914.** Guoqing Sun. Simulation studies of forest structure using 3D lidar and radar models. / Guoqing Sun, Ranson K.J., Dawei Liu, Koetz B. // 2007. IGARSS 2007. IEEE International Geoscience and Remote Sensing Symposium. - Barcelona, 23-28 July 2007. - P. 2562-2565. ↑
- C9915.** Demontoux F. Inversion model validation of ground emissivity. Contribution to the development of SMOS algorithm. / Demontoux F., Le Crom B., Ruffle G., Wigneron J.P., Grant J., Hernandez D.M. // 2007. IGARSS 2007. IEEE International Geoscience and Remote Sensing Symposium. - Barcelona, 23-28 July 2007. - P. 2570-2573. ↑
- C9916.** Ainsworth T.L. Quad-polarimetry and interferometry from repeat-pass dual-polarimetric SAR imagery. / Ainsworth T.L., Preiss M., Stacy N., Lee J.-S. // 2007. IGARSS 2007. IEEE International Geoscience and Remote Sensing Symposium. - Barcelona, 23-28 July 2007. - P. 2616-2619. ↑
- C9917.** Reigber A. Multi-baseline polarimetrically optimised phases and scattering mechanisms for InSAR applications. / Reigber A., Neumann M., Erten E., Jager M., Prats P. // 2007. IGARSS 2007. IEEE International Geoscience and Remote Sensing Symposium. - Barcelona, 23-28 July 2007. - P. 2620-2623. ↑
- C9918.** Aixia Dou. Technique of remote sensing image processing in active faults survey. / Aixia Dou, Xiaoqing Wang, Guoyan Wang, Dongliang Wang. // 2007. IGARSS 2007. IEEE International Geoscience and Remote Sensing Symposium. - Barcelona, 23-28 July 2007. - P. 2609-2612. ↑
- C9919.** Boerner W.-M. Need for developing repeat-pass differential POLSAR interferometry. / Boerner W.-M., Kun-Shan Chen. // 2007. IGARSS 2007. IEEE International Geoscience and Remote Sensing Symposium. - Barcelona, 23-28 July 2007. - P. 2613-2615. ↑
- C9920.** Alberga V. Comparison of similarity measures of multi-sensor images for change detection applications. / Alberga V., Idrissa M., Lacroix V., Inglada J. // 2007. IGARSS 2007. IEEE International Geoscience and Remote Sensing Symposium. - Barcelona, 23-28 July 2007. - P. 2358-2361. ↑
- C9921.** Andreoli R. Large scale change detection techniques dedicated to flood monitoring using ENVISAT wide swath mode data. / Andreoli R., Yesou H. // 2007. IGARSS 2007. IEEE International Geoscience and Remote Sensing Symposium. - Barcelona, 23-28 July 2007. - P. 2382-2385. ↑
- C9922.** Fransson J.E.S. Mapping of wind-thrown forests using VHF/UHF SAR images. / Fransson J.E.S., Magnusson M., Folkesson K., Hallberg B., Sandberg G., Smith-Jonforsen G., Gustavsson A., Ulander L.M.H. // 2007. IGARSS 2007. IEEE International Geoscience and Remote Sensing Symposium. - Barcelona, 23-28 July 2007. - P. 2350-2353. ↑
- C9923.** Villard L. Bistatic border effects modelling in forest scattering. / Villard L., Borderies P., Dubois-Fernandez P., Nouvel J.-F. // 2007. IGARSS 2007. IEEE International Geoscience and Remote Sensing Symposium. - Barcelona, 23-28 July 2007. - P. 2354-2357. ↑
- C9924.** Mercier G. Conditional copula for change detection on heterogeneous SAR data. / Mercier G., Moser G., Serpico S. // 2007. IGARSS 2007. IEEE International Geoscience and Remote Sensing Symposium. - Barcelona, 23-28 July 2007. - P. 2394-2397. ↑
- C9925.** Arnold-Bos A. Obtaining a ship's speed and direction from its Kelvin wake spectrum using stochastic matched filtering. / Arnold-Bos A., Martin A., Khenchaf A. // 2007. IGARSS 2007. IEEE International Geoscience and Remote Sensing Symposium. - Barcelona, 23-28 July 2007. - P. 1106-1109. ↑
- C9926.** Molinier M. Comparison and evaluation of polarimetric change detection techniques in aerial SAR data. / Molinier M., Rauste Y. // 2007. IGARSS 2007. IEEE International Geoscience and Remote Sensing Symposium. - Barcelona, 23-28 July 2007. - P. 2386-2389. ↑

- C9927.** Molinier M. Detecting changes in polarimetric SAR data with content-based image retrieval. / Molinier M., Laaksonen J., Rauste Y., Hame T. // 2007. IGARSS 2007. IEEE International Geoscience and Remote Sensing Symposium. - Barcelona, 23-28 July 2007. - P. 2390-2393. ↑
- C9928.** Garestier F. Vegetation modelling for height inversion using InSAR/Pol-InSAR data. / Garestier F., Thuy Le Toan. // 2007. IGARSS 2007. IEEE International Geoscience and Remote Sensing Symposium. - Barcelona, 23-28 July 2007. - P. 2322-2325. ↑
- C9929.** Watanabe M. Forest monitoring with JERS-1/SAR and ALOS/PALSAR. / Watanabe M., Shimada M., Ouchi K., Haipeng Wang, Matsuoka M., Sato M. // 2007. IGARSS 2007. IEEE International Geoscience and Remote Sensing Symposium. - Barcelona, 23-28 July 2007. - P. 2326-2329. ↑
- C9930.** Anderson L.O. Spatial patterns of the canopy stress during 2005 drought in Amazonia. / Anderson L.O., Malhi Y., Aragao L.E.O., Saatchi S. // 2007. IGARSS 2007. IEEE International Geoscience and Remote Sensing Symposium. - Barcelona, 23-28 July 2007. - P. 2294-2297. ↑
- C9931.** Ranson K.J. Using MODIS and GLAS data to develop timber volume estimates in central Siberia. / Ranson K.J., Nelson R., Kimes D., Guoqing Sun, Kharuk V., Montesano P. // 2007. IGARSS 2007. IEEE International Geoscience and Remote Sensing Symposium. - Barcelona, 23-28 July 2007. - P. 2306-2309. ↑
- C9932.** dos Santos J.R. Analysis of airborne SAR data (L-band) for discrimination land use/land cover types in the Brazilian Amazon region. / dos Santos J.R., Goncalves F.G., Dutra L.V., Mura J.C., Paradella W.R. // 2007. IGARSS 2007. IEEE International Geoscience and Remote Sensing Symposium. - Barcelona, 23-28 July 2007. - P. 2342-2345. ↑
- C9933.** Viergever K.M. backscatter and interferometry for estimating above- ground biomass in tropical savanna woodland. / Viergever K.M., Woodhouse I.H., Stuart N. // 2007. IGARSS 2007. IEEE International Geoscience and Remote Sensing Symposium. - Barcelona, 23-28 July 2007. - P. 2346-2349. ↑
- C9934.** Fransson J.E.S. Detection of forest changes using ALOS PALSAR satellite images. / Fransson J.E.S., Magnusson M., Olsson H., Eriksson L.E.B., Sandberg G., Smith-Jonforsen G., Ulander L.M.H. // 2007. IGARSS 2007. IEEE International Geoscience and Remote Sensing Symposium. - Barcelona, 23-28 July 2007. - P. 2330-2333. ↑
- C9935.** Riihela A. Estimation of the bidirectional reflectance distribution function of subarctic boreal forest using C-band SAR. / Riihela A., Manninen T. // 2007. IGARSS 2007. IEEE International Geoscience and Remote Sensing Symposium. - Barcelona, 23-28 July 2007. - P. 2334-2337. ↑
- C9936.** Alados-Arboledas L. Detection of May 2006 Saharan dust outbreak over Granada, Spain, by combination of active and passive remote sensing. / Alados-Arboledas L., Guerrero-Rascado J.L., Lyamani H., Gil J.E., Cazorla A., Olmo F.J. // 2007. IGARSS 2007. IEEE International Geoscience and Remote Sensing Symposium. - Barcelona, 23-28 July 2007. - P. 1055-1058. ↑
- C9937.** Angiuli E. Inversion algorithms comparison using L-band simulated polarimetric interferometric data for forest parameters estimation. / Angiuli E., Del Frate F., Vecchia A.D., Lavallo M., Solimini D., Licciardi G. // 2007. IGARSS 2007. IEEE International Geoscience and Remote Sensing Symposium. - Barcelona, 23-28 July 2007. - P. 2477-2480. ↑
- C9938.** Vladutescu D.V. Examination of hygroscopic properties of aerosols using a combined multiwavelength elastic-Raman lidar. / Vladutescu D.V., Yonghua Wu, Gross B., Charles L., Moshary F., Ahmed S. // 2007. IGARSS 2007. IEEE International Geoscience and Remote Sensing Symposium. - Barcelona, 23-28 July 2007. - P. 1063-1066. ↑
- C9939.** Frontoso M.G. The vertical distribution of Saharan dust over the western and central Mediterranean through dust modelling and lidar observations. / Frontoso M.G., Sicard M., Comeron A., Perez C., Baldasano J.M. // 2007. IGARSS 2007. IEEE International Geoscience and Remote Sensing Symposium. - Barcelona, 23-28 July 2007. - P. 1059-1062. ↑
- C9940.** Whitcomb J. Wetlands map of Alaska using L-Band radar satellite imagery. / Whitcomb J., Moghaddam M., McDonald K., Podest E., Kelndorfer J. // 2007. IGARSS 2007. IEEE International Geoscience and Remote Sensing Symposium. - Barcelona, 23-28 July 2007. - P. 2487-2490. ↑

- C9941.** Teague C.C. Two-dimensional surface river flow patterns measured with paired riversondes. / Teague C.C., Barrick D.E., Lilleboe P.M., Cheng R.T. // 2007. IGARSS 2007. IEEE International Geoscience and Remote Sensing Symposium. - Barcelona, 23-28 July 2007. - P. 2491-2494. ↑
- C9942.** Ketelaar G. Multi-track PS-InSAR datum connection. / Ketelaar G., van Leijen F., Marinkovic P., Hanssen R. // 2007. IGARSS 2007. IEEE International Geoscience and Remote Sensing Symposium. - Barcelona, 23-28 July 2007. - P. 2481-2484. ↑
- C9943.** Cao Fang. The Comparison of the V-Fold and the Monte-Carlo cross validation to estimate the number of clusters for the fully polarimetric sar data segmentation. / Cao Fang, Hong Wen, Wu Yirong, Pottier E. // 2007. IGARSS 2007. IEEE International Geoscience and Remote Sensing Symposium. - Barcelona, 23-28 July 2007. - P. 2485-2486. ↑
- C9944.** Singhroy V. InSAR monitoring of landslides on permafrost terrain in canada. / Singhroy V., Couture R., Alasset P.-J., Poncos V. // 2007. IGARSS 2007. IEEE International Geoscience and Remote Sensing Symposium. - Barcelona, 23-28 July 2007. - P. 2451-2454. ↑
- C9945.** Marotti L. Analysis of the temporal behavior of coherent scatterers (CSs) in ALOS PalSAR data. / Marotti L., Zandona-Schneider R., Papathanassiou K.P. // 2007. IGARSS 2007. IEEE International Geoscience and Remote Sensing Symposium. - Barcelona, 23-28 July 2007. - P. 2473-2476. ↑
- C9946.** Jumani K. An investigation of PN sequences for multistatic SAR/InSAR applications. / Jumani K., Sarabandi K. // 2007. IGARSS 2007. IEEE International Geoscience and Remote Sensing Symposium. - Barcelona, 23-28 July 2007. - P. 1102-1105. ↑
- C9947.** Bosch-Lluis X. Calibration and performance analysis of the PAU- RAD instrument. / Bosch-Lluis X., Camps A., Marchan-Hernandez J.F., Ramos-Perez I., Rodriguez-Alvarez N., Banque X., Guerrero M.A. // 2007. IGARSS 2007. IEEE International Geoscience and Remote Sensing Symposium. - Barcelona, 23-28 July 2007. - P. 2419-2422. ↑
- C9948.** Gherboudj I. Validation of a backscatter model of a river ice covers using Radarsat-1 images. / Gherboudj I., Bernier M., Leconte R. // 2007. IGARSS 2007. IEEE International Geoscience and Remote Sensing Symposium. - Barcelona, 23-28 July 2007. - P. 1087-1090. ↑
- C9949.** Williams B.A. Hurricane wind field estimation from seawinds at ultra high resolution. / Williams B.A., Long D.G. // 2007. IGARSS 2007. IEEE International Geoscience and Remote Sensing Symposium. - Barcelona, 23-28 July 2007. - P. 1075-1078. ↑
- C9950.** Sauer S. Multibaseline POL-InSAR analysis of urban scenes for 3D modeling and physical feature retrieval at L-band. / Sauer S., Ferro-Famil L., Reigber A., Pottier E. // 2007. IGARSS 2007. IEEE International Geoscience and Remote Sensing Symposium. - Barcelona, 23-28 July 2007. - P. 1098-1101. ↑
- C9951.** Ng A.H.-M. Application of persistent scatterer InSAR and GIS for urban subsidence monitoring. / Ng A.H.-M., Linlin Ge. // 2007. IGARSS 2007. IEEE International Geoscience and Remote Sensing Symposium. - Barcelona, 23-28 July 2007. - P. 1091-1094. ↑
- C9952.** Paillou P. Mapping subsurface geology in Arid Africa using L-band SAR. / Paillou P., Lopez S., Lasne Y., Rosenqvist A., Farr T. // 2007. IGARSS 2007. IEEE International Geoscience and Remote Sensing Symposium. - Barcelona, 23-28 July 2007. - P. 2685-2688. ↑
- C9953.** Churnside J.H. LIDAR detection of plankton in the ocean. 2007. IGARSS 2007. IEEE International Geoscience and Remote Sensing Symposium. - Barcelona, 23-28 July 2007. - P. 3174-3177. ↑
- C9954.** Gambardella A. Wavelet polarimetric SAR signature analysis of sea oil spills and look-alike features. / Gambardella A., Migliaccio M., De Grandi G. // 2007. IGARSS 2007. IEEE International Geoscience and Remote Sensing Symposium. - Barcelona, 23-28 July 2007. - P. 983-986. ↑
- C9955.** Wei Gong. CALIPSO-AERONET Combined Application for Weather and Climate Research. / Wei Gong, Yingying Ma, Zhongmin Zhu, Pingxiang Li, Shalei Song, Mengyu Liu, Zhongyu Hao. // 2007. IGARSS 2007. IEEE International Geoscience and Remote Sensing Symposium. - Barcelona, 23-28 July 2007. - P. 3166-3169. ↑

- C9956.** Long B. What optech's bathymetric LiDAR sees underwater. / Long B., Cottin A., Collin A. // 2007. IGARSS 2007. IEEE International Geoscience and Remote Sensing Symposium. - Barcelona, 23-28 July 2007. - P. 3170-3173. ↑
- C9957.** Jiang Jinbao. Study on inversion models for the severity of winter wheat stripe rust using hyperspectral remote sensing. / Jiang Jinbao, Chen Yunhao, Gong Adu, Li Jing. // 2007. IGARSS 2007. IEEE International Geoscience and Remote Sensing Symposium. - Barcelona, 23-28 July 2007. - P. 3186-3189. ↑
- C9958.** Rodriguez M.H. Cantarell natural seep modelling using SAR derived ocean surface wind and meteo-oceanographic buoy data. / Rodriguez M.H., Bannerman K., Caceres R.G., de Miranda F.P., Pedroso E.C. // 2007. IGARSS 2007. IEEE International Geoscience and Remote Sensing Symposium. - Barcelona, 23-28 July 2007. - P. 3257-3260. ↑
- C9959.** Collin A. Statistical classification methodology of SHOALS 3000 backscatter to mapping coastal benthic habitats. / Collin A., Cottin A., Long B., Archambault P., Kuus P., Clarke J.H., Sohn G., Miller J. // 2007. IGARSS 2007. IEEE International Geoscience and Remote Sensing Symposium. - Barcelona, 23-28 July 2007. - P. 3178-3181. ↑
- C9960.** Hyun-chong Cho. Morphological segmentation of Lidar Digital Elevation Models to extract stream channels in forested terrain. / Hyun-chong Cho, Kampa K., Slatton K.C. // 2007. IGARSS 2007. IEEE International Geoscience and Remote Sensing Symposium. - Barcelona, 23-28 July 2007. - P. 3182-3185. ↑
- C9961.** Sun Yonghua. A study on optical and SAR data fusion for extracting flooded area. / Sun Yonghua, Li Xiaojuan, Gong Huili, Zhao Wenji, Gong Zhaoning. // 2007. IGARSS 2007. IEEE International Geoscience and Remote Sensing Symposium. - Barcelona, 23-28 July 2007. - P. 3086-3089. ↑
- C9962.** Forghani A. Object-based classification of multi-sensor optical imagery to generate terrain surface roughness information for input to wind risk simulation. / Forghani A., Cechet B., Nadimpalli K. // 2007. IGARSS 2007. IEEE International Geoscience and Remote Sensing Symposium. - Barcelona, 23-28 July 2007. - P. 3090-3095. ↑
- C9963.** Ramirez N.D. An algorithm to improve the NEXRAD rain rate estimates. / Ramirez N.D., Cruz-Pol S., Xiomara Ortiz, Castro J.M., Kuliowski R. // 2007. IGARSS 2007. IEEE International Geoscience and Remote Sensing Symposium. - Barcelona, 23-28 July 2007. - P. 3060-3064. ↑
- C9964.** Lim S. Reflectivity retrieval in a networked radar environment: Demonstration from the CASA IP1 radar network. / Lim S., Chandrasekar V., Lee P., Jayasumana A.P. // 2007. IGARSS 2007. IEEE International Geoscience and Remote Sensing Symposium. - Barcelona, 23-28 July 2007. - P. 3065-3068. ↑
- C9965.** Md Reba M.N. Piece-wise variance method for signal-to-noise ratio estimation in elastic/Raman lidar signals. / Md Reba M.N., Rocadenbosch F., Sicard M., Munoz C., Tomas S. // 2007. IGARSS 2007. IEEE International Geoscience and Remote Sensing Symposium. - Barcelona, 23-28 July 2007. - P. 3158-3161. ↑
- C9966.** Gregorio E. Design methodology of a ceilometer lidar prototype. / Gregorio E., Rocadenbosch F., Comeron A. // 2007. IGARSS 2007. IEEE International Geoscience and Remote Sensing Symposium. - Barcelona, 23-28 July 2007. - P. 3162-3165. ↑
- C9967.** Lijun Zhang. Lidar application in selection and design of power line route. / Lijun Zhang, Qiu Li, Zizheng Wang, Huijie Liu, Zhongsheng Li, Yao Gui, Kletzli R., Xiaodong Yang, Shuming Chen, Yanjing Liu. // 2007. IGARSS 2007. IEEE International Geoscience and Remote Sensing Symposium. - Barcelona, 23-28 July 2007. - P. 3109-3111. ↑
- C9968.** Calla O.P.N. Comparison of measured scattering coefficient of dry soil at X-band with the scattering coefficient estimated using the dielectric constant. / Calla O.P.N., Harit K.C., Vyas R., Bohra D., Mishra S.K. // 2007. IGARSS 2007. IEEE International Geoscience and Remote Sensing Symposium. - Barcelona, 23-28 July 2007. - P. 3135-3137. ↑
- C9969.** Farquharson G. A new high-altitude airborne millimeter-wave radar for atmospheric research. / Farquharson G., Loew E., Vivekanandan J., Wen-Chau Lee. // 2007. IGARSS 2007. IEEE International Geoscience and Remote Sensing Symposium. - Barcelona, 23-28 July 2007. - P. 3313-3316. ↑
- C9970.** Nguyen C.M. A time domain clutter filter for staggered PRT and dual- PRF measurements. / Nguyen

C.M., Moiseev D.N., Chandrasekar V. // 2007. IGARSS 2007. IEEE International Geoscience and Remote Sensing Symposium. - Barcelona, 23-28 July 2007. - P. 3325-3328. ↑

C9971. Chandrasekar V. Dual-polarization spectral decompositions: Application to radar parameter estimation and quality control. / Chandrasekar V., Moiseev D.N., George J. // 2007. IGARSS 2007. IEEE International Geoscience and Remote Sensing Symposium. - Barcelona, 23-28 July 2007. - P. 3305-3308. ↑

C9972. Klugmann D. Application of single drop scattering algorithms to rain related retrieval. / Klugmann D., Fiser O. // 2007. IGARSS 2007. IEEE International Geoscience and Remote Sensing Symposium. - Barcelona, 23-28 July 2007. - P. 3309-3312. ↑

C9973. Kojima S. Wave measurements under the typhoon by 9.25MHz ocean radar. / Kojima S., Kashima M. // 2007. IGARSS 2007. IEEE International Geoscience and Remote Sensing Symposium. - Barcelona, 23-28 July 2007. - P. 979-982. ↑

C9974. Notarnicola C. Adaptive bayesian algorithm for vegetated field parameters extraction by using multi-frequency and multi-polarimetric SAR images. / Notarnicola C., Ventura B., Posa F. // 2007. IGARSS 2007. IEEE International Geoscience and Remote Sensing Symposium. - Barcelona, 23-28 July 2007. - P. 3401-3404. ↑

C9975. Shimabukuro Y.E. Mapping and monitoring land cover in Corumbiara area, Brazilian Amazonia, using JERS-1 SAR multitemporal data. / Shimabukuro Y.E., Almeida-Filho R., Kuplich T.M., de Freitas R.M. // 2007. IGARSS 2007. IEEE International Geoscience and Remote Sensing Symposium. - Barcelona, 23-28 July 2007. - P. 3370-3373. ↑

C9976. Andreoli R. Land cover analysis at a regional scale exploiting low and medium resolution ENVISAT ASAR Data: Application to Poyang Lake Area (Jianxi Province, P.R. China). / Andreoli R., Yesou H., Shifeng H., Li J., Desnos Y.-L. // 2007. IGARSS 2007. IEEE International Geoscience and Remote Sensing Symposium. - Barcelona, 23-28 July 2007. - P. 3374-3377. ↑

C9977. Cameron I.D. A novel method for estimating offshore wind fields using synthetic aperture radar and meteorological model data. / Cameron I.D., Woodhouse I.H., Walker N. // 2007. IGARSS 2007. IEEE International Geoscience and Remote Sensing Symposium. - Barcelona, 23-28 July 2007. - P. 3273-3276. ↑

C9978. Zecchetto S. Computation of wind direction from SAR images without external a priori information. / Zecchetto S., De Biasio F., Trivero P. // 2007. IGARSS 2007. IEEE International Geoscience and Remote Sensing Symposium. - Barcelona, 23-28 July 2007. - P. 3277-3280. ↑

C9979. Schulz-Stellenfleth J. Use of tandem pairs of ERS-2 and ENVISAT SAR data for the analysis of oceanographic and atmospheric processes. / Schulz-Stellenfleth J., Lehner S., Konig T., Reppucci A., Brusch S. // 2007. IGARSS 2007. IEEE International Geoscience and Remote Sensing Symposium. - Barcelona, 23-28 July 2007. - P. 3265-3268. ↑

C9980. Vesecky J.F. Measurements of eddies in the ocean surface wind field by a mix of single and multiple-frequency HF radars on monterey bay california. / Vesecky J.F., Drake J., Laws K., Ludwig F.L., Teague C.C., Paduan J.D., Sinton D. // 2007. IGARSS 2007. IEEE International Geoscience and Remote Sensing Symposium. - Barcelona, 23-28 July 2007. - P. 3269-3272. ↑

C9981. Guiting Song. Validation of a new empirical SAR algorithm. / Guiting Song, Lehner S., Schulz-Stellenfleth J., Breit H., Grassl H. // 2007. IGARSS 2007. IEEE International Geoscience and Remote Sensing Symposium. - Barcelona, 23-28 July 2007. - P. 3289-3292. ↑

C9982. Figueras i Ventura J. IDRA: A new instrument for drizzle monitoring. / Figueras i Ventura J., Russchenberg H.W.J. // 2007. IGARSS 2007. IEEE International Geoscience and Remote Sensing Symposium. - Barcelona, 23-28 July 2007. - P. 3301-3304. ↑

C9983. Konig T. Global analysis of a 2 Year ERS-2 wavemode dataset over the oceans. / Konig T., Lehner S., Schulz-Stellenfleth J. // 2007. IGARSS 2007. IEEE International Geoscience and Remote Sensing Symposium. - Barcelona, 23-28 July 2007. - P. 3281-3284. ↑

C9984. Lehner S. Validation of an X-Band SAR Wind Algorithm by SIR-C/X SAR Data. / Lehner S., Schulz-Stellenfleth J., Brusch S., Eineder M. // 2007. IGARSS 2007. IEEE International Geoscience and Remote Sensing Symposium. - Barcelona, 23-28 July 2007. - P. 3285-3288. ↑

- C9985.** Arias D. A grid based weather radar data retrieval and processing framework. / Arias D., Sanabria J., Rivera W. // 2007. IGARSS 2007. IEEE International Geoscience and Remote Sensing Symposium. - Barcelona, 23-28 July 2007. - P. 2758-2762. ↑
- C9986.** Sicard M. Intercomparison of spanish advanced lidars in the framework of EARLINET. / Sicard M., Reba M.N.M., Rocadenbosch F., Gregorio E., Kumar D., Tomas S., Comeron A., Molero F., Pujadas M., Guerrero-Rascado J.L., Pedros R., Martinez J.A. // 2007. IGARSS 2007. IEEE International Geoscience and Remote Sensing Symposium. - Barcelona, 23-28 July 2007. - P. 2763-2766. ↑
- C9987.** Colom J.G. Phase shifter system using vector modulation for xband phased array radar applications. / Colom J.G., Giraldo Castaneda L., Knapp E. // 2007. IGARSS 2007. IEEE International Geoscience and Remote Sensing Symposium. - Barcelona, 23-28 July 2007. - P. 2750-2753. ↑
- C9988.** Yuxiang Liu. Real-time three-dimensional radar mosaic in CASA IP1 testbed. / Yuxiang Liu, Yanting Wang, Chandrasekar V., Bringi V.N. // 2007. IGARSS 2007. IEEE International Geoscience and Remote Sensing Symposium. - Barcelona, 23-28 July 2007. - P. 2754-2757. ↑
- C9989.** Munoz C. Speed measurements with a continuous wave lidar prototype. / Munoz C., Rodriguez A., Comeron A., Batet O., Garcia D., Rocadenbosch F., Sicard M. // 2007. IGARSS 2007. IEEE International Geoscience and Remote Sensing Symposium. - Barcelona, 23-28 July 2007. - P. 2775-2778. ↑
- C9990.** Tomas S. A wind speed and fluctuation simulator for characterizing the wind lidar correlation method. / Tomas S., Sicard M., Masjuan J., Reba M.N.M., Munoz C., Rocadenbosch F. // 2007. IGARSS 2007. IEEE International Geoscience and Remote Sensing Symposium. - Barcelona, 23-28 July 2007. - P. 2779-2782. ↑
- C9991.** Martucci G. Lidar determination of the frequency of variations of the boundary-layer top. / Martucci G., Matthey R., Mitev V., Richner H. // 2007. IGARSS 2007. IEEE International Geoscience and Remote Sensing Symposium. - Barcelona, 23-28 July 2007. - P. 2767-2770. ↑
- C9992.** Rocadenbosch F. Statistical considerations on the extinction error variance for the raman lidar inversion algorithm. / Rocadenbosch F., Comeron A., Sicard M., Reba M.N.M. // 2007. IGARSS 2007. IEEE International Geoscience and Remote Sensing Symposium. - Barcelona, 23-28 July 2007. - P. 2771-2774. ↑
- C9993.** Trabal J.M. Rainfall estimation and rain gauge comparison for x-band polarimetric CASA radars. / Trabal J.M., McLaughlin D.J. // 2007. IGARSS 2007. IEEE International Geoscience and Remote Sensing Symposium. - Barcelona, 23-28 July 2007. - P. 2726-2729. ↑
- C9994.** Junyent F. Radar network characterization. / Junyent F., Chandrasekar V. // 2007. IGARSS 2007. IEEE International Geoscience and Remote Sensing Symposium. - Barcelona, 23-28 July 2007. - P. 2730-2733. ↑
- C9995.** Brenner A.R. Radar imaging of urban areas by means of very high resolution SAR and interferometric SAR. / Brenner A.R., Roessing L. // 2007. IGARSS 2007. IEEE International Geoscience and Remote Sensing Symposium. - Barcelona, 23-28 July 2007. - P. 2689-2693. ↑
- C9996.** Brunner D. Building characterisation in VHR SAR data acquired under controlled EMSL conditions. / Brunner D., Lemoine G., Fortuny J., Bruzzone L. // 2007. IGARSS 2007. IEEE International Geoscience and Remote Sensing Symposium. - Barcelona, 23-28 July 2007. - P. 2694-2697. ↑
- C9997.** Bharadwaj N. Evaluation of first generation CASA radar waveforms in the IP1 testbed. / Bharadwaj N., Chandrasekar V., Junyent F. // 2007. IGARSS 2007. IEEE International Geoscience and Remote Sensing Symposium. - Barcelona, 23-28 July 2007. - P. 2742-2745. ↑
- C9998.** Marrero-Fontanez V.J. Low cross-polarization antenna array for CASA's student test bed radar. / Marrero-Fontanez V.J., Rodriguez-Solis R.A. // 2007. IGARSS 2007. IEEE International Geoscience and Remote Sensing Symposium. - Barcelona, 23-28 July 2007. - P. 2746-2749. ↑
- C9999.** Donovan B.C. Simulation of minimal infrastructure short-range radar networks. / Donovan B.C., McLaughlin D.J., Zink M., Kurose J. // 2007. IGARSS 2007. IEEE International Geoscience and Remote Sensing Symposium. - Barcelona, 23-28 July 2007. - P. 2734-2737. ↑
- C10000.** Fritz J. Implementation of a new refractivity estimation algorithm on a network of S-band radars. /

Fritz J., Chandrasekar V. // 2007. IGARSS 2007. IEEE International Geoscience and Remote Sensing Symposium. - Barcelona, 23-28 July 2007. - P. 2738-2741. ↑

C10001. Jinghui Fan. Mapping subsidence in Tianjin area using ASAR images based on PS technique. / Jinghui Fan, Xiaofang Guo, Huadong Guo, Zhengmin He, Daqing Ge, Shengwei Liu. // 2007. IGARSS 2007. IEEE International Geoscience and Remote Sensing Symposium. - Barcelona, 23-28 July 2007. - P. 2975-2978. ↑

C10002. Hosokawa M. Earthquake damage detection using remote sensing data. / Hosokawa M., Byeong-pyo Jeong. // 2007. IGARSS 2007. IEEE International Geoscience and Remote Sensing Symposium. - Barcelona, 23-28 July 2007. - P. 2989-2991. ↑

C10003. Ribo S. ASAP, towards a PARIS instrument for space. / Ribo S., Arco J.C., Cardellach E., Nogues-Correig O., Rius A., Alvarez M.T., Tabero J. // 2007. IGARSS 2007. IEEE International Geoscience and Remote Sensing Symposium. - Barcelona, 23-28 July 2007. - P. 2916-2919. ↑

C10004. Gregorio E. Perspective of remote optical measurement techniques (ROMTs). / Gregorio E., Rocadenbosch F. // 2007. IGARSS 2007. IEEE International Geoscience and Remote Sensing Symposium. - Barcelona, 23-28 July 2007. - P. 2955-2958. ↑

C10005. Tomas R. DInSAR monitoring of land subsidence in Orihuela City, Spain: Comparison with geotechnical data. / Tomas R., Lopez-Sanchez J.M., Delgado J., Vicente F., Cuenca A., Mallorqui J.J., Blanco P., Duque S. // 2007. IGARSS 2007. IEEE International Geoscience and Remote Sensing Symposium. - Barcelona, 23-28 July 2007. - P. 3027-3030. ↑

C10006. Vega M.A. Student developed meteorological radar network for the western part of Puerto Rico: First node. / Vega M.A., Colom J.G. // 2007. IGARSS 2007. IEEE International Geoscience and Remote Sensing Symposium. - Barcelona, 23-28 July 2007. - P. 3057-3059. ↑

C10007. Hirn B. Improvement and validation of MODIS performance in automated detection and extent estimate of wildfires. / Hirn B., Di Bartola C., Ferrucci F. // 2007. IGARSS 2007. IEEE International Geoscience and Remote Sensing Symposium. - Barcelona, 23-28 July 2007. - P. 3004-3007. ↑

C10008. Ferrucci F. 3-D tsunami coastal hazard mapping in Sri Lanka by very-high resolution, airborne and spaceborne remote-sensing. / Ferrucci F., Rocca F., Calabretta G., Savio G., Coren F., Sterzai P., Hirn B. // 2007. IGARSS 2007. IEEE International Geoscience and Remote Sensing Symposium. - Barcelona, 23-28 July 2007. - P. 3018-3021. ↑

C10009. Shuki Chaw. Intercomparison of Calibration techniques for the 1064nm channel on a Nd:YAG elastic lidar. / Shuki Chaw, Yonghua Wu, Gross B., Moshary F., Ahmed S. // 2007. IGARSS 2007. IEEE International Geoscience and Remote Sensing Symposium. - Barcelona, 23-28 July 2007. - P. 2791-2794. ↑

C10010. Kenyi L. Comparison of SRTM-NED data to LIDAR derived canopy metrics. / Kenyi L., Dubayah R., Hofton M., Blair J.B., Schardt M. // 2007. IGARSS 2007. IEEE International Geoscience and Remote Sensing Symposium. - Barcelona, 23-28 July 2007. - P. 2825-2829. ↑

C10011. Brousmiche S. Numerical simulation of a heterodyne Doppler LIDAR for wind measurement in a turbulent atmospheric boundary layer. / Brousmiche S., Bricteux L., Sobieski P., Macq B., Winckelmans G. // 2007. IGARSS 2007. IEEE International Geoscience and Remote Sensing Symposium. - Barcelona, 23-28 July 2007. - P. 2783-2786. ↑

C10012. Lindelow P. Coherent lidar modulated with frequency stepped pulse trains for unambiguous high duty cycle range and velocity sensing in the atmosphere. / Lindelow P., Mohr J.J. // 2007. IGARSS 2007. IEEE International Geoscience and Remote Sensing Symposium. - Barcelona, 23-28 July 2007. - P. 2787-2790. ↑

C10013. Gunay A. Semi-automatic true orthophoto production by using LIDAR data. / Gunay A., Arefi H., Hahn M. // 2007. IGARSS 2007. IEEE International Geoscience and Remote Sensing Symposium. - Barcelona, 23-28 July 2007. - P. 2873-2876. ↑

C10014. Guangjian Yan. An airborne multi-angle power line inspection system. / Guangjian Yan, Junfa Wang, Qiang Liu, Lin Su, Pengxin Wang, Junming Liu, Wuming Zhang, Zhiqiang Xiao. // 2007. IGARSS 2007. IEEE International Geoscience and Remote Sensing Symposium. - Barcelona, 23-28 July 2007. - P. 2913-2915. ↑

- C10015.** Moorthy I. Extracting tree crown properties from ground-based scanning laser data. / Moorthy I., Miller J.R., Berni J.A.J., Zarco-Tejada P.J., Qingmou Li. // 2007. IGARSS 2007. IEEE International Geoscience and Remote Sensing Symposium. - Barcelona, 23-28 July 2007. - P. 2830-2832. ↑
- C10016.** Schull M. Retrieving 3D canopy structure from synergistic analysis of multi-angle and lidar data. / Schull M., Ganguly S., Samanta A., Jenkins J., Knyazikhin Y., Myneni R.B., Dong Huang. // 2007. IGARSS 2007. IEEE International Geoscience and Remote Sensing Symposium. - Barcelona, 23-28 July 2007. - P. 2833-2835. ↑
- C10017.** Waser L.T. Modeling fractional shrub/tree cover and multi-temporal changes in mire ecosystems using high-resolution digital surface models and CIR aerial images. / Waser L.T., Ginzler C., Kuechler M., Baltsavias E., Eisenbeiss H. // 2007. IGARSS 2007. IEEE International Geoscience and Remote Sensing Symposium. - Barcelona, 23-28 July 2007. - P. 2288-2293. ↑
- C10018.** Niemann K.O. Integration of first and last return LiDAR with hyperspectral data to characterize forested environments. / Niemann K.O., Frazer G., Loos R., Visintini F., Stephen R. // 2007. IGARSS 2007. IEEE International Geoscience and Remote Sensing Symposium. - Barcelona, 23-28 July 2007. - P. 1537-1540. ↑
- C10019.** Bachmann C.M. Bathymetric retrieval from manifold coordinate representations of hyperspectral imagery. / Bachmann C.M., Ainsworth T.L. // 2007. IGARSS 2007. IEEE International Geoscience and Remote Sensing Symposium. - Barcelona, 23-28 July 2007. - P. 1548-1551. ↑
- C10020.** Christoulas G. The use of ASAR data for class cover identification from small swatches. / Christoulas G., Anastassopoulos V., Petrou M. // 2007. IGARSS 2007. IEEE International Geoscience and Remote Sensing Symposium. - Barcelona, 23-28 July 2007. - P. 1513-1516. ↑
- C10021.** Pinheiro A. Evaluation of ASAR and optical data synergy for high resolution land cover mapping in Portugal. / Pinheiro A., Carrao H., Caetano M. // 2007. IGARSS 2007. IEEE International Geoscience and Remote Sensing Symposium. - Barcelona, 23-28 July 2007. - P. 1517-1520. ↑
- C10022.** Falzini S. COSMO-SkyMed active calibrator: A sophisticated tool for SAR image calibration. / Falzini S., Speziale V., De Viti E. // 2007. IGARSS 2007. IEEE International Geoscience and Remote Sensing Symposium. - Barcelona, 23-28 July 2007. - P. 1577-1580. ↑
- C10023.** Lenz R. Overview of the active TerraSAR-X calibrators and first results. / Lenz R., Wiesbeck W. // 2007. IGARSS 2007. IEEE International Geoscience and Remote Sensing Symposium. - Barcelona, 23-28 July 2007. - P. 1581-1584. ↑
- C10024.** Cereoli L. The role of performance modelling in active phased array SAR. / Cereoli L., Torre A. // 2007. IGARSS 2007. IEEE International Geoscience and Remote Sensing Symposium. - Barcelona, 23-28 July 2007. - P. 1569-1572. ↑
- C10025.** Yu Wang. A comparison of internal calibration schemes for spaceborne single-pass InSAR applications. / Yu Wang, Xing-dong Liang, Yi-rong Wu. // 2007. IGARSS 2007. IEEE International Geoscience and Remote Sensing Symposium. - Barcelona, 23-28 July 2007. - P. 1573-1576. ↑
- C10026.** Peng Xu. Emissivities of rough surface over layered media in microwave remote sensing of snow. / Peng Xu, Leung Tsang, Li Li, Kun Shan Chen. // 2007. IGARSS 2007. IEEE International Geoscience and Remote Sensing Symposium. - Barcelona, 23-28 July 2007. - P. 1436-1439. ↑
- C10027.** Stankov B.B. Empirical SWE retrieval using airborne microwave and in situ snow measurements. / Stankov B.B., Cline D., Tedesco M. // 2007. IGARSS 2007. IEEE International Geoscience and Remote Sensing Symposium. - Barcelona, 23-28 July 2007. - P. 1444-1447. ↑
- C10028.** O'Neill P. ComRAD active / passive microwave measurement of tree canopies. / O'Neill P., Joseph A., Nelson R., Lang R., Kurum M., Cosh M., Jackson T., Spicknall M. // 2007. IGARSS 2007. IEEE International Geoscience and Remote Sensing Symposium. - Barcelona, 23-28 July 2007. - P. 1420-1423. ↑
- C10029.** Vecchia A.D. A statistical and theoretical study about radar sensitivity to crop growth from S to X band. / Vecchia A.D., Ferrazzoli P., Guerriero L., Strozzi T., Wegmuller U. // 2007. IGARSS 2007. IEEE International Geoscience and Remote Sensing Symposium. - Barcelona, 23-28 July 2007. - P. 1424-1427. ↑
- C10030.** Karasakal G. Speckle noise reduction in SAR imaging using lattice filters based subband

decomposition. / Karasakal G., Erer I. // 2007. IGARSS 2007. IEEE International Geoscience and Remote Sensing Symposium. - Barcelona, 23-28 July 2007. - P. 1476-1480. ↑

C10031. Munoz-Mari J. Combination of one-class remote sensing image classifiers. / Munoz-Mari J., Camps-Valls G., Gomez-Chova L., Calpe-Maravilla J. // 2007. IGARSS 2007. IEEE International Geoscience and Remote Sensing Symposium. - Barcelona, 23-28 July 2007. - P. 1509-1512. ↑

C10032. Luzi G. Ground-based microwave interferometric measurements over a snow covered slope: an experimental data collection in Tyrol (Austria). / Luzi G., Pieraccini M., Noferini L., Mecatti D., Macaluso G., Atzeni C., Joerg P., Sailer R. // 2007. IGARSS 2007. IEEE International Geoscience and Remote Sensing Symposium. - Barcelona, 23-28 July 2007. - P. 1452-1455. ↑

C10033. Piles M. Deconvolution algorithms in image reconstruction for aperture synthesis radiometers. / Piles M., Camps A., Vall-Ilossera M., Monerris A., Talone M., Perez J.L.A. // 2007. IGARSS 2007. IEEE International Geoscience and Remote Sensing Symposium. - Barcelona, 23-28 July 2007. - P. 1460-1463. ↑

C10034. Wobbe F. Uplift rates from river profiles: methodology and case study, Oriente, Cuba. / Wobbe F., Stanek K., Gloaguen R. // 2007. IGARSS 2007. IEEE International Geoscience and Remote Sensing Symposium. - Barcelona, 23-28 July 2007. - P. 1629-1631. ↑

C10035. Pereira A.J.S. Structural lineaments in a volcanic island evaluated through remote sensing techniques The case of Santiago Island (Cape Verde). / Pereira A.J.S., Victoria S., Vicente A.M.P., Neves L.J.P. // 2007. IGARSS 2007. IEEE International Geoscience and Remote Sensing Symposium. - Barcelona, 23-28 July 2007. - P. 1632-1635. ↑

C10036. Iwashita A. Study of ground surface displacement estimation using ALOS/PALSAR D-InSAR interferometry. / Iwashita A., Kudo M., Baba H., Morohoshi T., Hara M., Yu-Feng Lin, Wen-Qing Jiang. // 2007. IGARSS 2007. IEEE International Geoscience and Remote Sensing Symposium. - Barcelona, 23-28 July 2007. - P. 1616-1617. ↑

C10037. Rauste Y. Ortho-rectification and terrain correction of polarimetric SAR data applied in the ALOS/Palsar context. / Rauste Y., Lonnqvist A., Molinier M., Henry J.-B., Hame T. // 2007. IGARSS 2007. IEEE International Geoscience and Remote Sensing Symposium. - Barcelona, 23-28 July 2007. - P. 1618-1621. ↑

C10038. Tatarov B. Stratospheric ozone layer observations over tsukuba, Japan by NIES ozone DIAL. / Tatarov B., Chan Bong Park, Nakane H., Sugimoto N., Matsui I., Sasano Y. // 2007. IGARSS 2007. IEEE International Geoscience and Remote Sensing Symposium. - Barcelona, 23-28 July 2007. - P. 1673-1676. ↑

C10039. Contreras R.F. Return from insects in the clear-air convective boundary layer. / Contreras R.F., Frasier S.J. // 2007. IGARSS 2007. IEEE International Geoscience and Remote Sensing Symposium. - Barcelona, 23-28 July 2007. - P. 1677-1679. ↑

C10040. Vicente A.M.P. Classification of satellite images applied to geological mapping (Douro Region-Northeastern Portugal). / Vicente A.M.P., Rabaca T., Pereira A.J.S. // 2007. IGARSS 2007. IEEE International Geoscience and Remote Sensing Symposium. - Barcelona, 23-28 July 2007. - P. 1661-1664. ↑

C10041. Lopes F.C.C. Recognizing salt-structures on the basis of geophysical and remote sensing data: the case of monte real salt-structure (onshore west-central portugal). / Lopes F.C.C., Pereira A.S.C., Vicente A.M.P. // 2007. IGARSS 2007. IEEE International Geoscience and Remote Sensing Symposium. - Barcelona, 23-28 July 2007. - P. 1665-1668. ↑

C10042. Fukuchi H. New polarimetric calibration proposal and its evaluation using ALOS PALSAR calibration campaign measurements. / Fukuchi H., Furuya T., Noda H., Satake M. // 2007. IGARSS 2007. IEEE International Geoscience and Remote Sensing Symposium. - Barcelona, 23-28 July 2007. - P. 1593-1595. ↑

C10043. Satake M. Polarimetric Calibration Experiment of ALOS PALSAR with Polarization-Selective Dihedrals. / Satake M., Matsuoka T., Umehara T., Fukuchi H. // 2007. IGARSS 2007. IEEE International Geoscience and Remote Sensing Symposium. - Barcelona, 23-28 July 2007. - P. 1596-1598. ↑

C10044. Ferrer P.J. Transpolarizing surfaces for polarimetric SAR systems calibration. / Ferrer P.J., Lopez-Martinez C., Fabregas X., Gonzalez-Arbesu J.M., Romeu J., Aguasca A., Craeye C. // 2007. IGARSS 2007. IEEE International Geoscience and Remote Sensing Symposium. - Barcelona, 23-28 July 2007. - P. 1585-1588. ↑



C10045. Eriksson L.E.B. ALOS PALSAR Calibration and Validation Results from Sweden. / Eriksson L.E.B., Sandberg G., Ulander L.M.H., Smith-Jonforsen G., Hallberg B., Folkesson K., Fransson J.E.S., Magnusson M., Olsson H., Gustavsson A., Flood B. // 2007. IGARSS 2007. IEEE International Geoscience and Remote Sensing Symposium. - Barcelona, 23-28 July 2007. - P. 1589-1592.

C10046. da Silva Narvaes I. Evaluation of the interaction between SAR L-band signal and structural parameters of forest cover. / da Silva Narvaes I., de Queiroz da Silva A., dos Santos J.R. // 2007. IGARSS 2007. IEEE International Geoscience and Remote Sensing Symposium. - Barcelona, 23-28 July 2007. - P. 1607-1610.

C10047. Croci R. SHARAD design and operation. / Croci R., Fois F., Calabrese D., Zampolini E.M., Seu R., Picardi G., Flamini E. // 2007. IGARSS 2007. IEEE International Geoscience and Remote Sensing Symposium. - Barcelona, 23-28 July 2007. - P. 1611-1615.

C10048. Jung C.H. Parameter based SAR simulator for image quality evaluation. / Jung C.H., Choi M.S., Kwag Y.K. // 2007. IGARSS 2007. IEEE International Geoscience and Remote Sensing Symposium. - Barcelona, 23-28 July 2007. - P. 1599-1602.

C10049. Xi Chen. Robust forest height extraction using polarimetric SAR interferometry. / Xi Chen, Chao Wang, Hong Zhang. // 2007. IGARSS 2007. IEEE International Geoscience and Remote Sensing Symposium. - Barcelona, 23-28 July 2007. - P. 1603-1606.

C10050. Hasager C.B. Satellite eye for the galathea 3 ship expedition: global tour 2006-2007. / Hasager C.B., Christiansen M.B., Sorensen P.B., Lichtenegger J., Pedersen L.T., Andersen O.B., Hoyer J.L., Jorgensen P.V., Hojerslev N.K., Nielsen R.M., Rasmussen M.S., Nyborg L. // 2007. IGARSS 2007. IEEE International Geoscience and Remote Sensing Symposium. - Barcelona, 23-28 July 2007. - P. 1232-1237.

C10051. Yamanokuchi T. Combined use of InSAR and ICESat / GLAS data for high accuracy DEM generation on antarctica. / Yamanokuchi T., Doi K., Shibuya K. // 2007. IGARSS 2007. IEEE International Geoscience and Remote Sensing Symposium. - Barcelona, 23-28 July 2007. - P. 1229-1231.

C10052. Waser L.T. Extraction of forest parameters in a mire biotope using high-resolution digital surface models and airborne imagery. / Waser L.T., Ginzler C., Kuechle M., Thee P., Baltsavias E., Eisenbeiss H. // 2007. IGARSS 2007. IEEE International Geoscience and Remote Sensing Symposium. - Barcelona, 23-28 July 2007. - P. 1265-1270.

C10053. Karvonen J. Polarview@FIMR: WWW-based delivery of baltic sea ice products to end-users. / Karvonen J., Haapala J., Lehtiranta J., Seina A. // 2007. IGARSS 2007. IEEE International Geoscience and Remote Sensing Symposium. - Barcelona, 23-28 July 2007. - P. 1242-1245.

C10054. Migliaccio M. A physically consistent stochastic model to observe oil spills and strong scatterers on SLC SAR images. / Migliaccio M., Ferrara G., Gambardella A., Nunziata F., Sorrentino A. // 2007. IGARSS 2007. IEEE International Geoscience and Remote Sensing Symposium. - Barcelona, 23-28 July 2007. - P. 1322-1325.

C10055. Malinovsky V.V. Identification of oil spills based on ratio of alternating polarization images from ENVISAT. / Malinovsky V.V., Sandven S., Mironov A.S., Korinenko A.E. // 2007. IGARSS 2007. IEEE International Geoscience and Remote Sensing Symposium. - Barcelona, 23-28 July 2007. - P. 1326-1329.

C10056. Hallikainen M. Use of quikscat ku-band scatterometer data for retrieval of seasonal snow characteristics in Finland. / Hallikainen M., Sievinen P., Yuanzhi Zhang, Halme P. // 2007. IGARSS 2007. IEEE International Geoscience and Remote Sensing Symposium. - Barcelona, 23-28 July 2007. - P. 1228.

C10057. Wiesmann A. Microwave remote sensing of alpine snow. / Wiesmann A., Strozzi T., Werner C., Wegmuller U., Santoro M. // 2007. IGARSS 2007. IEEE International Geoscience and Remote Sensing Symposium. - Barcelona, 23-28 July 2007. - P. 1223-1227.

C10058. Alpers W. Bora events over the adriatic sea and black sea studied by multi-sensor satellite imagery. / Alpers W., Ivanov A.Yu., Horstmann J. // 2007. IGARSS 2007. IEEE International Geoscience and Remote Sensing Symposium. - Barcelona, 23-28 July 2007. - P. 1307-1313.

- C10059.** Plant W.J. X-band backscatter from the ocean at low-grazing angles. / Plant W.J., Keller W.C., Hayes K. // 2007. IGARSS 2007. IEEE International Geoscience and Remote Sensing Symposium. - Barcelona, 23-28 July 2007. - P. 1303-1306. ↑
- C10060.** Pelizzari S. Oil spill segmentation of SAR images via graph cuts. / Pelizzari S., Bioucas-Dias J. // 2007. IGARSS 2007. IEEE International Geoscience and Remote Sensing Symposium. - Barcelona, 23-28 July 2007. - P. 1318-1321. ↑
- C10061.** Danisi A. SAR simulation of ocean scenes covered by oil slicks with arbitrary shapes. / Danisi A., Di Martino G., Iodice A., Riccio D., Ruello G., Tello M., Mallorqui J.J., Lopez-Martinez C. // 2007. IGARSS 2007. IEEE International Geoscience and Remote Sensing Symposium. - Barcelona, 23-28 July 2007. - P. 1314-1317. ↑
- C10062.** Karlsen S.R. Mapping and modelling the snowmelt and greening pattern in southern norway by combining microwave and optical remote sensing sensors. / Karlsen S.R., Malnes E., Haarpaintner J., Solberg R. // 2007. IGARSS 2007. IEEE International Geoscience and Remote Sensing Symposium. - Barcelona, 23-28 July 2007. - P. 1279-1282. ↑
- C10063.** Carrao H. Retrieving land cover information from MERIS and MODIS Data: a comparative study for landscape characterization in Portugal. / Carrao H., Sarmiento P., Araujo A., Caetano M. // 2007. IGARSS 2007. IEEE International Geoscience and Remote Sensing Symposium. - Barcelona, 23-28 July 2007. - P. 1271-1274. ↑
- C10064.** Cuozzo G. The role of spatial interactions for prediction of the spectral structure of the atmospheric phase screen. / Cuozzo G., di Bisceglie M., Fusco A. // 2007. IGARSS 2007. IEEE International Geoscience and Remote Sensing Symposium. - Barcelona, 23-28 July 2007. - P. 1287-1290. ↑
- C10065.** Abhyankar A.A. Qualitative approaches to rapidly identify completely submerged rice due to tropical cyclone using satellite data. / Abhyankar A.A., Patwardhan A., Inamdar A. // 2007. IGARSS 2007. IEEE International Geoscience and Remote Sensing Symposium. - Barcelona, 23-28 July 2007. - P. 1283-1286. ↑
- C10066.** Crosetto M. Uncertainty analysis in advanced differential interferometric SAR processing. / Crosetto M., Monserrat O., Agudo M., Crippa B., Rossi G. // 2007. IGARSS 2007. IEEE International Geoscience and Remote Sensing Symposium. - Barcelona, 23-28 July 2007. - P. 1171-1173. ↑
- C10067.** Perissin D. ASAR parallel-track PS analysis in urban sites. / Perissin D., Prati C., Rocca F. // 2007. IGARSS 2007. IEEE International Geoscience and Remote Sensing Symposium. - Barcelona, 23-28 July 2007. - P. 1167-1170. ↑
- C10068.** Rott H. CoRe-H2 O-A dual frequency SAR mission for hydrology and climate research. / Rott H., Pulliainen J., Cline D., Rebhan H., Nagler T., Yueh S. // 2007. IGARSS 2007. IEEE International Geoscience and Remote Sensing Symposium. - Barcelona, 23-28 July 2007. - P. 1204-1206. ↑
- C10069.** Rott H. Increased export of grounded ice after the collapse of northern Larsen ice shelf, Antarctic Peninsula, observed by Envisat ASAR. / Rott H., Rack W., Nagler T. // 2007. IGARSS 2007. IEEE International Geoscience and Remote Sensing Symposium. - Barcelona, 23-28 July 2007. - P. 1174-1176. ↑
- C10070.** Caspar C. Generation of ENVISAT ASAR Mosaics accessible on-line. / Caspar C., Colin O., Laur H., Rosich Tell B., Tandurella G., Mathot E., Goncalves P., Brito F. // 2007. IGARSS 2007. IEEE International Geoscience and Remote Sensing Symposium. - Barcelona, 23-28 July 2007. - P. 1405-1408. ↑
- C10071.** Jingsong Yang. Error analysis of Envisat ASAR level 2 algorithm based on simulation technique. / Jingsong Yang, He Wang, Weigen Huang, Qingmei Xiao. // 2007. IGARSS 2007. IEEE International Geoscience and Remote Sensing Symposium. - Barcelona, 23-28 July 2007. - P. 1409-1411. ↑
- C10072.** McNairn H. The value of SAR Multi-polarization data in delivering annual crop inventories. / McNairn H., Champagne C., Jiali Shang. // 2007. IGARSS 2007. IEEE International Geoscience and Remote Sensing Symposium. - Barcelona, 23-28 July 2007. - P. 1397-1400. ↑
- C10073.** Tell B.R. ASAR instrument performance and product quality evolution. / Tell B.R., Monti-Guarnieri A., Meadows P.J., D'Aria D., Tranfaglia M., Santuari M., Traver I.N. // 2007. IGARSS 2007. IEEE International Geoscience and Remote Sensing Symposium. - Barcelona, 23-28 July 2007. - P. 1401-1404. ↑

- C10074.** Zavorotny V.U. Comparison of geometric optics and diffraction effects in radar scattering from steep and breaking waves. / Zavorotny V.U., Voronovich A.G. // 2007. IGARSS 2007. IEEE International Geoscience and Remote Sensing Symposium. - Barcelona, 23-28 July 2007. - P. 1350-1353. ↑
- C10075.** Girard R. The RADARSAT constellation payload design. / Girard R., Plourde P., Seguin G. // 2007. IGARSS 2007. IEEE International Geoscience and Remote Sensing Symposium. - Barcelona, 23-28 July 2007. - P. 1387-1392. ↑
- C10076.** Monaldo F.M. Retrieval of wind speed using an L-band synthetic aperture radar. / Monaldo F.M., Thompson D.R., Christiansen M.B. // 2007. IGARSS 2007. IEEE International Geoscience and Remote Sensing Symposium. - Barcelona, 23-28 July 2007. - P. 1338-1341. ↑
- C10077.** Hauser D. Probability density function of ocean surface slopes from radar observations. / Hauser D., Caudal G., Guimbar S., Mouche A. // 2007. IGARSS 2007. IEEE International Geoscience and Remote Sensing Symposium. - Barcelona, 23-28 July 2007. - P. 1346-1349. ↑
- C10078.** Yuen S. Airborne Ku-band radar remote sensing of terrestrial snow cover. / Yuen S., Cline D., Elder K. // 2007. IGARSS 2007. IEEE International Geoscience and Remote Sensing Symposium. - Barcelona, 23-28 July 2007. - P. 1211-1214. ↑
- C10079.** Morrison K. The SARALPS-2007 measurement campaign on Xand Ku-Band Backscatter of snow. / Morrison K., Rott H., Nagler T., Rebhan H., Wursteisen P. // 2007. IGARSS 2007. IEEE International Geoscience and Remote Sensing Symposium. - Barcelona, 23-28 July 2007. - P. 1207-1210. ↑
- C10080.** Vachon P.W. Ship signatures in synthetic aperture radar imagery. / Vachon P.W., English R.A., Wolfe J. // 2007. IGARSS 2007. IEEE International Geoscience and Remote Sensing Symposium. - Barcelona, 23-28 July 2007. - P. 1393-1396. ↑
- C10081.** Jinyang Du. A multi-scattering and multi-layer snow model and its validation. / Jinyang Du, Shi J., Tjuatja S., Chen K.S. // 2007. IGARSS 2007. IEEE International Geoscience and Remote Sensing Symposium. - Barcelona, 23-28 July 2007. - P. 1219-1222. ↑
- C10082.** Guerrero-Rascado J.L. Atmospheric vertical profiles obtained by Lidar over Évora during CAPEX project. / Guerrero-Rascado J.L., Lyamani H., Alados-Arboledas L., Silva A.M., Wagner F., Pereira S. // 2007. IGARSS 2007. IEEE International Geoscience and Remote Sensing Symposium. - Barcelona, 23-28 July 2007. - P. 1709-1712. ↑
- C10083.** Ito Y. Development of web-based SAR processor for education. / Ito Y., Teramoto Y., Abe K. // 2007. IGARSS 2007. IEEE International Geoscience and Remote Sensing Symposium. - Barcelona, 23-28 July 2007. - P. 2185-2187. ↑
- C10084.** Marques P. A low cost testbed for synthetic aperture techniques. / Marques P., Dias I., Fernandes E. // 2007. IGARSS 2007. IEEE International Geoscience and Remote Sensing Symposium. - Barcelona, 23-28 July 2007. - P. 2195-2198. ↑
- C10085.** Huang Yulin. Vehicleborne bistatic synthetic aperture radar imaging. / Huang Yulin, Yang Jianyu, Xian Li, Yang Haiguang, Tian Zhong. // 2007. IGARSS 2007. IEEE International Geoscience and Remote Sensing Symposium. - Barcelona, 23-28 July 2007. - P. 2164-2166. ↑
- C10086.** Gimmestad G.G. Lidar education at Georgia Tech. / Gimmestad G.G., West L.L. // 2007. IGARSS 2007. IEEE International Geoscience and Remote Sensing Symposium. - Barcelona, 23-28 July 2007. - P. 2174-2176. ↑
- C10087.** Spies T. Remote sensing information visualization using volume based objects in world wind. / Spies T., Moorhead R., Brill M. // 2007. IGARSS 2007. IEEE International Geoscience and Remote Sensing Symposium. - Barcelona, 23-28 July 2007. - P. 2213-2216. ↑
- C10088.** Foucher S. Application of bootstrap techniques for the estimation of Target Decomposition parameters in RADAR polarimetry. / Foucher S., Farage G., Benie G.B. // 2007. IGARSS 2007. IEEE International Geoscience and Remote Sensing Symposium. - Barcelona, 23-28 July 2007. - P. 2224-2228. ↑
- C10089.** Lewis C. Multi-waveform radar for ice sheet measurements and classroom demonstration. / Lewis C.,

Owen H., Abi D., Hecker J., Sulzen J. // 2007. IGARSS 2007. IEEE International Geoscience and Remote Sensing Symposium. - Barcelona, 23-28 July 2007. - P. 2202-2205. ↑

C10090. Torres F. MERIT Erasmus Mundus: an opportunity for international cooperation in Remote Sensing education in Europe. / Torres F., Wiesbeck W., Beccari C., Macq B. // 2007. IGARSS 2007. IEEE International Geoscience and Remote Sensing Symposium. - Barcelona, 23-28 July 2007. - P. 2209-2210. ↑

C10091. Sharma J.J. Vertical profile reconstruction with Pol-InSAR data of a subpolar glacier. / Sharma J.J., Hajnsek I., Papathanassiou K.P. // 2007. IGARSS 2007. IEEE International Geoscience and Remote Sensing Symposium. - Barcelona, 23-28 July 2007. - P. 1147-1150. ↑

C10092. Walterscheid I. Performance analysis of a hybrid bistatic SAR system operating in the double sliding spotlight mode. / Walterscheid I., Espeter T., Ender J.H.G. // 2007. IGARSS 2007. IEEE International Geoscience and Remote Sensing Symposium. - Barcelona, 23-28 July 2007. - P. 2144-2147. ↑

C10093. Berardino P. Surface deformation analysis of the Campi Flegrei caldera, Italy, by exploiting the ENVISAT ASAR data with the SBAS-DInSAR technique. / Berardino P., Casu F., Fornaro G., Lanari R., Manunta M., Manzo M., Pepe A., Pepe S., Sansosti E., Serafino F., Solaro G., Tizzani P., Zeni G. // 2007. IGARSS 2007. IEEE International Geoscience and Remote Sensing Symposium. - Barcelona, 23-28 July 2007. - P. 1159-1162. ↑

C10094. Haiyan Li. Ship detection with the fuzzy c-mean clustering algorithm using fully polarimetric SAR. / Haiyan Li, Yijun He, Hui Shen. // 2007. IGARSS 2007. IEEE International Geoscience and Remote Sensing Symposium. - Barcelona, 23-28 July 2007. - P. 1151-1154. ↑

C10095. Nico G. Performance analysis of bistatic SAR configurations. / Nico G., Tesauro M. // 2007. IGARSS 2007. IEEE International Geoscience and Remote Sensing Symposium. - Barcelona, 23-28 July 2007. - P. 2156-2159. ↑

C10096. Espeter T. Synchronization techniques for the bistatic spaceborne/airborne SAR experiment with TerraSAR-X and PAMIR. / Espeter T., Walterscheid I., Klare J., Ender J.H.G. // 2007. IGARSS 2007. IEEE International Geoscience and Remote Sensing Symposium. - Barcelona, 23-28 July 2007. - P. 2160-2163. ↑

C10097. Cantalloube H.M.J. Elevation-dependent motion compensation for frequency-domain bistatic SAR image synthesis. / Cantalloube H.M.J., Krieger G. // 2007. IGARSS 2007. IEEE International Geoscience and Remote Sensing Symposium. - Barcelona, 23-28 July 2007. - P. 2148-2151. ↑

C10098. Ossowska A. Influence of mechanical antenna distortions on the performance of the HRWS SAR system. / Ossowska A., Jung Hyo Kim, Wiesbeck W. // 2007. IGARSS 2007. IEEE International Geoscience and Remote Sensing Symposium. - Barcelona, 23-28 July 2007. - P. 2152-2155. ↑

C10099. Montopoli M. Processing disdrometer raindrop spectra time series from various climatological regions using estimation and autoregressive methods. / Montopoli M., Vulpiani G., Anagnostou M.N., Anagnostou E.N., Marzano F.S. // 2007. IGARSS 2007. IEEE International Geoscience and Remote Sensing Symposium. - Barcelona, 23-28 July 2007. - P. 2268-2271. ↑

C10100. Ince T. Preliminary quantitative analysis of S-band FNCW radar data from atmospheric observation. 2007. IGARSS 2007. IEEE International Geoscience and Remote Sensing Symposium. - Barcelona, 23-28 July 2007. - P. 2280-2283. ↑

C10101. Angelliaume S. Compact PolInSAR for vegetation characterisation. / Angelliaume S., Dubois-Fernandez P., Souyris J.-C. // 2007. IGARSS 2007. IEEE International Geoscience and Remote Sensing Symposium. - Barcelona, 23-28 July 2007. - P. 1136-1138. ↑

C10102. Eloranta E.W. Cloud particle size measurements in Arctic clouds using lidar and radar data. / Eloranta E.W., Uttal T., Shupe M. // 2007. IGARSS 2007. IEEE International Geoscience and Remote Sensing Symposium. - Barcelona, 23-28 July 2007. - P. 2265-2267. ↑

C10103. Minnis P. Characterizing the radiation fields in the atmosphere using a cloud-aerosol-radiation product from integrated CERES, MODIS, CALIPSO and CloudSat data. / Minnis P., Wielicki B., Trepte C.A., Kato S., Sun-Mack S., Yan Chen, Gibson S., Stephens G. // 2007. IGARSS 2007. IEEE International Geoscience and Remote Sensing Symposium. - Barcelona, 23-28 July 2007. - P. 1122-1125. ↑

- C10104.** Im E. Cloud Profiling Radar Performance Eastwood Im. / Im E., Tanelli S., Durden S.L., Kyung Pak. // 2007. IGARSS 2007. IEEE International Geoscience and Remote Sensing Symposium. - Barcelona, 23-28 July 2007. - P. 5061-5064. ↑
- C10105.** Florian K. Potential of forest height estimation using X band by means of two different inversion scenarios. / Florian K., Kostas P., Irena H., Angelo C. // 2007. IGARSS 2007. IEEE International Geoscience and Remote Sensing Symposium. - Barcelona, 23-28 July 2007. - P. 1132-1135. ↑
- C10106.** Praks J. X-band extinction in boreal forest: Estimation by using E-SAR POLInSAR and HUTSCAT. / Praks J., Hallikainen M., Kugler F., Papathanassiou K.P. // 2007. IGARSS 2007. IEEE International Geoscience and Remote Sensing Symposium. - Barcelona, 23-28 July 2007. - P. 1128-1131. ↑
- C10107.** Mercier G. The use of multidimensional copulas to describe amplitude distribution of polarimetric SAR data. / Mercier G., Bouchemakh L., Smara Y. // 2007. IGARSS 2007. IEEE International Geoscience and Remote Sensing Symposium. - Barcelona, 23-28 July 2007. - P. 2236-2239. ↑
- C10108.** Ersahin K. Segmentation of polarimetric SAR data using contour information via spectral graph partitioning. / Ersahin K., Cumming I.G., Ward R.K. // 2007. IGARSS 2007. IEEE International Geoscience and Remote Sensing Symposium. - Barcelona, 23-28 July 2007. - P. 2240-2243. ↑
- C10109.** Raney R.K. Comments on hybrid-polarity SAR architecture. 2007. IGARSS 2007. IEEE International Geoscience and Remote Sensing Symposium. - Barcelona, 23-28 July 2007. - P. 2229-2231. ↑
- C10110.** Jager M. Unsupervised classification of polarimetric SAR data using graph cut optimization. / Jager M., Reigber A., Hellwich O. // 2007. IGARSS 2007. IEEE International Geoscience and Remote Sensing Symposium. - Barcelona, 23-28 July 2007. - P. 2232-2235. ↑
- C10111.** Aydin K. Dual-polarization and dual-frequency radar scattering from ice crystals. / Aydin K., Santiago E. // 2007. IGARSS 2007. IEEE International Geoscience and Remote Sensing Symposium. - Barcelona, 23-28 July 2007. - P. 2264. ↑
- C10112.** Cantalloube H. POLINSAR for FOPEN using flashlight mode images along circular trajectories. / Cantalloube H., Colin E.K. // 2007. IGARSS 2007. IEEE International Geoscience and Remote Sensing Symposium. - Barcelona, 23-28 July 2007. - P. 1139-1142. ↑
- C10113.** Loew A. Impact of surface heterogeneity on surface soil moisture retrievals from passive microwave data. 2007. IGARSS 2007. IEEE International Geoscience and Remote Sensing Symposium. - Barcelona, 23-28 July 2007. - P. 2252-2255. ↑
- C10114.** Lopez-Sanchez J.M. Volume and double-bounce decorrelation effects in the OVoG model for Single-Tx PolInSAR. / Lopez-Sanchez J.M., Ballester-Berman J.D., Marquez-Moreno Y. // 2007. IGARSS 2007. IEEE International Geoscience and Remote Sensing Symposium. - Barcelona, 23-28 July 2007. - P. 1143-1146. ↑
- C10115.** Pacifici F. Urban land cover classification: potential of high and very-high resolution SAR imagery. / Pacifici F., Del Frate F., Solimini D., Burini A. // 2007. IGARSS 2007. IEEE International Geoscience and Remote Sensing Symposium. - Barcelona, 23-28 July 2007. - P. 1982-1985. ↑
- C10116.** Bolton J. Application of random set-based clustering to landmine detection with hyperspectral imagery. / Bolton J., Gader P. // 2007. IGARSS 2007. IEEE International Geoscience and Remote Sensing Symposium. - Barcelona, 23-28 July 2007. - P. 2022-2025. ↑
- C10117.** Takaku J. High resolution DSM generation from ALOS PRISM. / Takaku J., Futamura N., Iijima T., Tadono T., Shimada M. // 2007. IGARSS 2007. IEEE International Geoscience and Remote Sensing Symposium. - Barcelona, 23-28 July 2007. - P. 1974-1977. ↑
- C10118.** Almeida-Filho R. The mega capture of the negro river, central amazonia, brazil: a novel feature revealed by SRTM data. / Almeida-Filho R., Miranda F.P., Beisl C.H. // 2007. IGARSS 2007. IEEE International Geoscience and Remote Sensing Symposium. - Barcelona, 23-28 July 2007. - P. 1978-1981. ↑
- C10119.** Sirui Tian. A wavelet based targets detection method for high resolution airborne SAR data. / Sirui Tian, Chao Wang, Hong Zhang, Bo Zhang, Fan Wu. // 2007. IGARSS 2007. IEEE International Geoscience and Remote Sensing Symposium. - Barcelona, 23-28 July 2007. - P. 2071-2073. ↑

- C10120.** Zhang Shiyu. Urban subsidence observed by InSAR in Tianjin Region. / Zhang Shiyu, Li Tao, Liu Jingnan, Xia Ye, Jiang Yanxiang, Lu Xu. // 2007. IGARSS 2007. IEEE International Geoscience and Remote Sensing Symposium. - Barcelona, 23-28 July 2007. - P. 2078-2081. ↑
- C10121.** Fulong Chen. SAR images classification using case-based reasoning method. / Fulong Chen, Chao Wang, Hong Zhang, Bo Zhang, Fan Wu. // 2007. IGARSS 2007. IEEE International Geoscience and Remote Sensing Symposium. - Barcelona, 23-28 July 2007. - P. 2048-2051. ↑
- C10122.** Pop G. Combining modern techniques for urban 3D modelling. / Pop G., Bucksch A. // 2007. IGARSS 2007. IEEE International Geoscience and Remote Sensing Symposium. - Barcelona, 23-28 July 2007. - P. 2067-2070. ↑
- C10123.** Dongryeol Ryu. Two-dimensional synthetic aperture radiometry over land surface during soil moisture experiment in 2003 (SMEX03). / Dongryeol Ryu, Jackson T.J., Bindlish R., Le Vine D.M., Haken M. // 2007. IGARSS 2007. IEEE International Geoscience and Remote Sensing Symposium. - Barcelona, 23-28 July 2007. - P. 1842-1845. ↑
- C10124.** Ruijing Sun. A method to retrieve soil moisture using ERS Scatterometer data. / Ruijing Sun, Jiancheng Shi, Lingmei Jiang. // 2007. IGARSS 2007. IEEE International Geoscience and Remote Sensing Symposium. - Barcelona, 23-28 July 2007. - P. 1857-1860. ↑
- C10125.** Edwards M.A. Assessing pine barrens soil moisture regimes using Synthetic Aperture Radar (SAR) techniques. / Edwards M.A., Winslow M. // 2007. IGARSS 2007. IEEE International Geoscience and Remote Sensing Symposium. - Barcelona, 23-28 July 2007. - P. 1828-1831. ↑
- C10126.** Arakelyan A.K. Ku-band, polarimetric, combined, short pulse scatterometer-radiometer system for stationary fixed platform, vessel and airborne applications. / Arakelyan A.K., Arakelyan A.A., Darbinyan S.A., Grigoryan M.L., Hakobyan I.K., Hambaryan A.K., Karyan V.V., Manukyan M.R., Hovhannisyan G.G., Poghosyan N.G., Clifford S.F. // 2007. IGARSS 2007. IEEE International Geoscience and Remote Sensing Symposium. - Barcelona, 23-28 July 2007. - P. 1832-1834. ↑
- C10127.** Romero R. Usage of multitemporal filtering of SAR images for change detection. / Romero R., Marcos J.S., Carrasco D., Moreno V., Valero J.L., Lafitte M. // 2007. IGARSS 2007. IEEE International Geoscience and Remote Sensing Symposium. - Barcelona, 23-28 July 2007. - P. 1955-1958. ↑
- C10128.** Junghum Yu. Accuracy comparison of Differential Interferometric Synthetic Aperture Radar using LiDAR Digital Elevation Model. / Junghum Yu, Linlin Ge, Sungheuk Jung, Lee Jeakee. // 2007. IGARSS 2007. IEEE International Geoscience and Remote Sensing Symposium. - Barcelona, 23-28 July 2007. - P. 1970-1973. ↑
- C10129.** Perez-Gutierrez C. Modeling of soil roughness using terrestrial laser scanner for soil moisture retrieval. / Perez-Gutierrez C., Martinez-Fernandez J., Sanchez N., Alvarez-Mozos J. // 2007. IGARSS 2007. IEEE International Geoscience and Remote Sensing Symposium. - Barcelona, 23-28 July 2007. - P. 1877-1880. ↑
- C10130.** Tzeng Y.C. Change detections from sar images for damage estimation based on a spatial chaotic model. / Tzeng Y.C., Chiu S.H., Chen D., Chen K.S. // 2007. IGARSS 2007. IEEE International Geoscience and Remote Sensing Symposium. - Barcelona, 23-28 July 2007. - P. 1926-1930. ↑
- C10131.** Deguchi T. Monitoring of mining induced land subsidence using L- and C-band SAR interferometry. / Deguchi T., Kato M., Akcin H., Kutoglu H.S. // 2007. IGARSS 2007. IEEE International Geoscience and Remote Sensing Symposium. - Barcelona, 23-28 July 2007. - P. 2122-2125. ↑
- C10132.** Ortiz A.M. Second-order motion compensation in bistatic airborne SAR based on a geometrical approach. / Ortiz A.M., Loffeld O., Nies H., Knedlik S. // 2007. IGARSS 2007. IEEE International Geoscience and Remote Sensing Symposium. - Barcelona, 23-28 July 2007. - P. 2126-2129. ↑
- C10133.** Fornaro G. Deformation monitoring over a large area via the ESD technique with data takes on adjacent tracks. / Fornaro G., Serafino F., Pauciuolo A. // 2007. IGARSS 2007. IEEE International Geoscience and Remote Sensing Symposium. - Barcelona, 23-28 July 2007. - P. 2114-2117. ↑
- C10134.** Xilong Sun. Research on differential interferometry for spaceborne bistatic SAR. / Xilong Sun, Anxi

Yu, Zhen Dong, Diannong Liang. // 2007. IGARSS 2007. IEEE International Geoscience and Remote Sensing Symposium. - Barcelona, 23-28 July 2007. - P. 2118-2121. ↑

C10135. Shi jun. Translational variant bistatic SAR signal space-time feature and processing method. / Shi jun, Zhang Xiaoling, Yang Jianyu. // 2007. IGARSS 2007. IEEE International Geoscience and Remote Sensing Symposium. - Barcelona, 23-28 July 2007. - P. 2140-2143. ↑

C10136. Blanco-Sanchez P. Optimizing interferogram generation, pixel selection and data processing for high non-linear deformation monitoring with Orbital DInSAR. / Blanco-Sanchez P., Duque S., Mallorqui J.J., Monells D. // 2007. IGARSS 2007. IEEE International Geoscience and Remote Sensing Symposium. - Barcelona, 23-28 July 2007. - P. 1163-1166. ↑

C10137. Duque S. A bistatic SAR interferometric simulator for fixed receiver configurations. / Duque S., Lopez-Dekker P., Mallorqui J.J., Martinez C.L. // 2007. IGARSS 2007. IEEE International Geoscience and Remote Sensing Symposium. - Barcelona, 23-28 July 2007. - P. 2130-2133. ↑

C10138. Fois F. Comparison between MARSIS & SHARAD results. / Fois F., Mecozzi R., Iorio M., Calabrese D., Bombaci O., Catallo C., Croce A., Croci R., Guelfi M., Zampolini E., Ravasi D., Molteni M., Ruggeri P., Ranieri A., Ottavianelli M., Flamini E., Picardi G., Seu R., Biccari D., Orosei R., Cartacci M., Cicchetti A., Masdea A., Giacomoni E., Cutigni M., Provenziani M., Fuga O., Alberti G., Mattei S., Papa C., Marras P., Tattarletti B., Vicari D., Bonaventura F., Paterno T., Di Placido A., Morlupi A. // 2007. IGARSS 2007. IEEE International Geoscience and Remote Sensing Symposium. - Barcelona, 23-28 July 2007. - P. 2134-2139. ↑

C10139. Hsing-Chung Chang. Radar interferometry for 3-D mining deformation monitoring. / Hsing-Chung Chang, Linlin Ge, Hua Wang, Rizos C., Milne T. // 2007. IGARSS 2007. IEEE International Geoscience and Remote Sensing Symposium. - Barcelona, 23-28 July 2007. - P. 2090-2092. ↑

C10140. Damoah-Afari P. Six years of land subsidence in shanghai revealed by JERS-1 SAR data. / Damoah-Afari P., Xiao-li Ding, Zhiwei Li, Zhong Lu, Omura M. // 2007. IGARSS 2007. IEEE International Geoscience and Remote Sensing Symposium. - Barcelona, 23-28 July 2007. - P. 2093-2097. ↑

C10141. Gernhardt S. A stability analysis of the lambda estimator for solving the ambiguity problem in persistent scatterer interferometry. / Gernhardt S., Meyer F., Bamler R., Adam N. // 2007. IGARSS 2007. IEEE International Geoscience and Remote Sensing Symposium. - Barcelona, 23-28 July 2007. - P. 2082-2085. ↑

C10142. Qiming Zeng. Correction of tropospheric water vapour effect on ASAR interferogram using synchronous MERIS data. / Qiming Zeng, Ying Li, Xiaofan Li. // 2007. IGARSS 2007. IEEE International Geoscience and Remote Sensing Symposium. - Barcelona, 23-28 July 2007. - P. 2086-2089. ↑

C10143. Poncos V. Point target interferometry for natural and artificial scatterers. / Poncos V., Mei S., Singhroy V. // 2007. IGARSS 2007. IEEE International Geoscience and Remote Sensing Symposium. - Barcelona, 23-28 July 2007. - P. 2106-2109. ↑

C10144. Qiang Chen. Evaluation of accuracy in PS-based radar interferometry with simulated data. / Qiang Chen, Xiaoli Ding, Guoxiang Liu, Yongshu Li. // 2007. IGARSS 2007. IEEE International Geoscience and Remote Sensing Symposium. - Barcelona, 23-28 July 2007. - P. 2110-2113. ↑
















C10145. Prats P. Glacier displacement field estimation using airborne SAR interferometry. / Prats P., Andres C., Scheiber R., Reigber A., Camara de Macedo K.A., Fischer J. // 2007. IGARSS 2007. IEEE International Geoscience and Remote Sensing Symposium. - Barcelona, 23-28 July 2007. - P. 2098-2101. ↑

C10146. van Leijen F.J. Persistent scatterer density improvement using adaptive deformation models. / van Leijen F.J., Hanssen R.F. // 2007. IGARSS 2007. IEEE International Geoscience and Remote Sensing Symposium. - Barcelona, 23-28 July 2007. - P. 2102-2105. ↑

C10147. Monsivais-Huertero A. Application of a coherent modeling on Sahelian grassland. / Monsivais-Huertero A., Chenerie I., Sarabandi K., Baup F. // 2007. IGARSS 2007. IEEE International Geoscience and Remote Sensing Symposium. - Barcelona, 23-28 July 2007. - P. 3405-3407. ↑

C10148. Rangwala M. Study of millimeter-wave radar for helicopter assisted landing system. / Rangwala M., Feinian Wang, Sarabandi K. // 2007. IGARSS 2007. IEEE International Geoscience and Remote Sensing Symposium. - Barcelona, 23-28 July 2007. - P. 777-780. ↑

- C10149.** Nunziata F. A simulator for SAR sea surface waves imaging. / Nunziata F., Gambardella A., Migliaccio M. // 2007. IGARSS 2007. IEEE International Geoscience and Remote Sensing Symposium. - Barcelona, 23-28 July 2007. - P. 786-789. ↑
- C10150.** Yijun He. The effect of polarization ratio on RADARSAT wind vector retrievals. / Yijun He, Biao Zhang, Hui Shen, Perrie W., Jie Guo. // 2007. IGARSS 2007. IEEE International Geoscience and Remote Sensing Symposium. - Barcelona, 23-28 July 2007. - P. 790-792. ↑
- C10151.** Komarov S.A. Pulse electromagnetic sounding of the petroleum- containing layered medium. / Komarov S.A., Mironov V.L., Muzalevsky K.V. // 2007. IGARSS 2007. IEEE International Geoscience and Remote Sensing Symposium. - Barcelona, 23-28 July 2007. - P. 766-768. ↑
- C10152.** Mironov V.L. Validation of the soil dielectric spectroscopic models with input parameters based on soil composition. / Mironov V.L., Kosolapova L.G., Fomin S.V. // 2007. IGARSS 2007. IEEE International Geoscience and Remote Sensing Symposium. - Barcelona, 23-28 July 2007. - P. 749-753. ↑
- C10153.** Morgenthaler A. Semi-Analytic Mode Matching (SAMM) algorithm for efficient computation of nearfield scattering in lossy ground from borehole sources. / Morgenthaler A., He Zhan, Rappaport C. // 2007. IGARSS 2007. IEEE International Geoscience and Remote Sensing Symposium. - Barcelona, 23-28 July 2007. - P. 754-757. ↑
- C10154.** Narvekar P.S. Polarimetric microwave emission from snow surfaces: 4th Stokes component analysis. / Narvekar P.S., Heygster G., Jackson T.J., Bindlish R. // 2007. IGARSS 2007. IEEE International Geoscience and Remote Sensing Symposium. - Barcelona, 23-28 July 2007. - P. 762-765. ↑
- C10155.** Zheng-Shu Zhou. Development of a baseband signal ATI-SAR simulator for ground moving target indication. / Zheng-Shu Zhou, Bates B.D., Yunhan Dong. // 2007. IGARSS 2007. IEEE International Geoscience and Remote Sensing Symposium. - Barcelona, 23-28 July 2007. - P. 4505-4508. ↑
- C10156.** Mecatti D. Remote sensing of glacier by ground-based radar interferometry. / Mecatti D., Noferini L., Macaluso G., Pieraccini M., Luzi G., Atzeni C., Tamburini A. // 2007. IGARSS 2007. IEEE International Geoscience and Remote Sensing Symposium. - Barcelona, 23-28 July 2007. - P. 4501-4504. ↑
- C10157.** Martinez-Espla J.J. Introduction of a grid-based filter approach for InSAR phase filtering and unwrapping. / Martinez-Espla J.J., Martinez-Marin T., Lopez-Sanchez J.M. // 2007. IGARSS 2007. IEEE International Geoscience and Remote Sensing Symposium. - Barcelona, 23-28 July 2007. - P. 4497-4500. ↑
- C10158.** Zhe Liu. Frequency domain imaging algorithm for spaceborne/airborne hybrid bistatic SAR. / Zhe Liu, Jianyu Yang, Xiaoling Zhang, Yiming Pi. // 2007. IGARSS 2007. IEEE International Geoscience and Remote Sensing Symposium. - Barcelona, 23-28 July 2007. - P. 842-845. ↑
- C10159.** Gong Zhenqiang. Automobile-based Bistatic SAR processing and experimental results. / Gong Zhenqiang, Zhang Xiaoling, Tian Zhong. // 2007. IGARSS 2007. IEEE International Geoscience and Remote Sensing Symposium. - Barcelona, 23-28 July 2007. - P. 831-834. ↑
- C10160.** Ghayourmanesh S. Shape from shading of SAR imagery in fourier space. / Ghayourmanesh S., Yun Zahng. // 2007. IGARSS 2007. IEEE International Geoscience and Remote Sensing Symposium. - Barcelona, 23-28 July 2007. - P. 835-837. ↑
- C10161.** Chang Zheng Ma. ISAR imaging of helicopter. / Chang Zheng Ma, Tat Soon Yeo, Hwee Siang Tan, Zhoufeng Liu, Xiujie Dong, Bin Zou. // 2007. IGARSS 2007. IEEE International Geoscience and Remote Sensing Symposium. - Barcelona, 23-28 July 2007. - P. 838-841. ↑
- C10162.** Braham K.A. Scattering from 2D-dielectric random surfaces effect of roughness and moisture of seedbed surfaces upon the bistatic scattering coefficient. / Braham K.A., Dusseaux R., Vannier E., Taconet O., Granet G. // 2007. IGARSS 2007. IEEE International Geoscience and Remote Sensing Symposium. - Barcelona, 23-28 July 2007. - P. 746-748. ↑
- C10163.** Chih-Tien Wang. Disaster monitoring and environmental alert in Taiwan by repeat-pass spaceborne SAR. / Chih-Tien Wang, Kun-Shen Chen, Hong-Wei Lee, Jong-Sen Lee, Boerner W.-M., Ruei-Yuan Wang, Hong-Sen Wan. // 2007. IGARSS 2007. IEEE International Geoscience and Remote Sensing Symposium. - Barcelona, 23-28 July 2007. - P. 609-612. ↑

- C10164.** Xingsong Hou. Investigation of H.264 intra coding for SAR image. / Xingsong Hou, Yujie Dun, Rongjing Ji. // 2007. IGARSS 2007. IEEE International Geoscience and Remote Sensing Symposium. - Barcelona, 23-28 July 2007. - P. 613-614. 
- C10165.** Jiang Xiao. Optimum design of antenna pattern for spaceborne SAR performance using improved NSGA-II. / Jiang Xiao, Yongqiang Chen, Xiaoqing Wang, Minhui Zhu, Liu Xiao. // 2007. IGARSS 2007. IEEE International Geoscience and Remote Sensing Symposium. - Barcelona, 23-28 July 2007. - P. 615-618. 
- C10166.** Xiuhong Sun. An advanced airborne multisensor imaging system for fast mapping and change detection applications. / Xiuhong Sun, Chen W., Fischer R.L., Jones M., Eichholz J.C., Richards J.E., Shu P., Jhabvala M., Anh La, Kahle D., Adams J. // 2007. IGARSS 2007. IEEE International Geoscience and Remote Sensing Symposium. - Barcelona, 23-28 July 2007. - P. 600-605. 
- C10167.** Jie Wei. Effects of attitude error on spaceborne ScanSAR mosaic. 2007. IGARSS 2007. IEEE International Geoscience and Remote Sensing Symposium. - Barcelona, 23-28 July 2007. - P. 586-588. 
- C10168.** Wenling Xuan. A combined sensor system of digital camera with LiDAR. / Wenling Xuan, Zhaoqiang Huang, Xiuwan Chen, Zongjian Lin. // 2007. IGARSS 2007. IEEE International Geoscience and Remote Sensing Symposium. - Barcelona, 23-28 July 2007. - P. 589-592. 
- C10169.** Zahn R. A high resolution SAR sensor for space and airborne applications. / Zahn R., Weidman K., Boukamp J. // 2007. IGARSS 2007. IEEE International Geoscience and Remote Sensing Symposium. - Barcelona, 23-28 July 2007. - P. 596-599. 
- C10170.** Bartolomeo V. Cassini RADAR: investigation of titan's surface parameters by means of Bayesian inversion technique and gravity-capillary waves modelling of liquid hydrocarbons surfaces. / Bartolomeo V., Domenico C., Claudia N., Francesco P. // 2007. IGARSS 2007. IEEE International Geoscience and Remote Sensing Symposium. - Barcelona, 23-28 July 2007. - P. 706-709. 
- C10171.** Sant'Anna S.J.S. Closed form expressions for scattering matrix of simple targets in multilayer structures. / Sant'Anna S.J.S., da S. Lacava J.C., Fernandes D. // 2007. IGARSS 2007. IEEE International Geoscience and Remote Sensing Symposium. - Barcelona, 23-28 July 2007. - P. 714-717. 
- C10172.** Mironov V.L. Dielectric spectroscopic model for tussock and shrub tundra soils. / Mironov V.L., Savin S.V. // 2007. IGARSS 2007. IEEE International Geoscience and Remote Sensing Symposium. - Barcelona, 23-28 July 2007. - P. 726-731. 
- C10173.** Blake W. A UAV avionics system to facilitate VHF depth sounding and SAR. / Blake W., Siegele K., Burns R. // 2007. IGARSS 2007. IEEE International Geoscience and Remote Sensing Symposium. - Barcelona, 23-28 July 2007. - P. 643-646. 
- C10174.** Xiaolong Dong. Surface clutter analysis and ranging sidelobe level requirements for spaceborne meteorological radars. / Xiaolong Dong, Honggang Yin, Di Zhu, Huguang Liu, Jingshan Jiang. // 2007. IGARSS 2007. IEEE International Geoscience and Remote Sensing Symposium. - Barcelona, 23-28 July 2007. - P. 626-629. 
- C10175.** Roth A. Scientific use of TerraSAR-X. / Roth A., Marschalk U. // 2007. IGARSS 2007. IEEE International Geoscience and Remote Sensing Symposium. - Barcelona, 23-28 July 2007. - P. 630. 
- C10176.** Kwag Y.K. UAV based collision avoidance radar sensor. / Kwag Y.K., Chung C.H. // 2007. IGARSS 2007. IEEE International Geoscience and Remote Sensing Symposium. - Barcelona, 23-28 July 2007. - P. 639-642. 
- C10177.** Fayard F. Matching stereoscopic SAR images for radargrammetric applications. / Fayard F., Meric S., Pottier E. // 2007. IGARSS 2007. IEEE International Geoscience and Remote Sensing Symposium. - Barcelona, 23-28 July 2007. - P. 4364-4367. 
- C10178.** Pedroso E.C. A multi-sensor approach and ranking analysis procedure for oil seeps detection in marine environments. / Pedroso E.C., de Miranda F.P., Bannerman K., HenriqueBeisl C., Rodriguez M.H., Caceres R.G. // 2007. IGARSS 2007. IEEE International Geoscience and Remote Sensing Symposium. - Barcelona, 23-28 July 2007. - P. 865-870. 

- C10179.** Xiaoqing Wang. Bistatic SAR Raw Data Simulation for Ocean. / Xiaoqing Wang, Yin Yu, Yongqiang Chen, Jiang Xiao, Minhui Zhu. // 2007. IGARSS 2007. IEEE International Geoscience and Remote Sensing Symposium. - Barcelona, 23-28 July 2007. - P. 871-874. ↑
- C10180.** Rocadenbosch F. Morphological tools for range-interval segmentation of elastic lidar signals. / Rocadenbosch F., Sicard M., Reba M.N.M., Tomas S. // 2007. IGARSS 2007. IEEE International Geoscience and Remote Sensing Symposium. - Barcelona, 23-28 July 2007. - P. 4372-4375. ↑
- C10181.** Molero F. New inversion algorithm for raman lidar without derivative of the inelastic signal. / Molero F., Pujadas M. // 2007. IGARSS 2007. IEEE International Geoscience and Remote Sensing Symposium. - Barcelona, 23-28 July 2007. - P. 4379-4382. ↑
- C10182.** Isoguchi O. Kuroshio-induced cold eddy streets in the lee of isolated islands. / Isoguchi O., Shimada M., Sakaida F., Kawamura H. // 2007. IGARSS 2007. IEEE International Geoscience and Remote Sensing Symposium. - Barcelona, 23-28 July 2007. - P. 858-861. ↑
- C10183.** Tabatabaeenejad A. Inversion of a layered rough surface model: maximizing the number of retrievable parameters for the design of future subsurface sensing radar systems. / Tabatabaeenejad A., Moghaddam M. // 2007. IGARSS 2007. IEEE International Geoscience and Remote Sensing Symposium. - Barcelona, 23-28 July 2007. - P. 4376-4378. ↑
- C10184.** Fernandez-Ordonez Y. Forest inventory applications using optical and RADARSAT-2 images in mexico. / Fernandez-Ordonez Y., Soria-Ruiz J., Woodhouse I.H. // 2007. IGARSS 2007. IEEE International Geoscience and Remote Sensing Symposium. - Barcelona, 23-28 July 2007. - P. 4350-4353. ↑
- C10185.** Magnusson M. Estimation of forest stem volume using ALOS PALSAR satellite images. / Magnusson M., Fransson J.E.S., Eriksson L.E.B., Sandberg G., Smith-Jonforsen G., Ulander L.M.H. // 2007. IGARSS 2007. IEEE International Geoscience and Remote Sensing Symposium. - Barcelona, 23-28 July 2007. - P. 4343-4346. ↑
- C10186.** Zhongmin Zhu. The active-passive remote sensing for aerosol optical depth retrieval. / Zhongmin Zhu, Wei Gong, Pingxiang Li, Liangpei Zhang, Qianqing Qin, Yingying Ma, Shalei Song, Jun Li, Mengyu Liu, Zhongyu Hao. // 2007. IGARSS 2007. IEEE International Geoscience and Remote Sensing Symposium. - Barcelona, 23-28 July 2007. - P. 4291-4294. ↑
- C10187.** Bentz C.M. Automatic recognition of coastal and oceanic environmental events with orbital radars. / Bentz C.M., Politano A.T., Ebecken N.F.F. // 2007. IGARSS 2007. IEEE International Geoscience and Remote Sensing Symposium. - Barcelona, 23-28 July 2007. - P. 914-916. ↑
- C10188.** Parmiggiani F. Surface signature of ocean convection in the greenland sea as detected by SAR and enhanced by statistical pattern analysis. / Parmiggiani F., Morales D., Moctezuma M. // 2007. IGARSS 2007. IEEE International Geoscience and Remote Sensing Symposium. - Barcelona, 23-28 July 2007. - P. 879-881. ↑
- C10189.** Reppucci A. Extreme wind conditions in tropical cyclones observed from synthetic aperture radar images. / Reppucci A., Lehner S., Schulz-Stellenfleth J., Breit H. // 2007. IGARSS 2007. IEEE International Geoscience and Remote Sensing Symposium. - Barcelona, 23-28 July 2007. - P. 894-897. ↑
- C10190.** Xiao-Ming Li. Measurement of extreme wave height by ERS-2 SAR and numerical wave model (WAM). / Xiao-Ming Li, Koenig T., Lehne S., Schulz-Stellenfleth J. // 2007. IGARSS 2007. IEEE International Geoscience and Remote Sensing Symposium. - Barcelona, 23-28 July 2007. - P. 905-908. ↑
- C10191.** Hanna R. Brightness temperature validation for SeaWinds radiometer using Advanced Microwave Scanning Radiometer on ADEOS-II. / Hanna R., Jones W.L. // 2007. IGARSS 2007. IEEE International Geoscience and Remote Sensing Symposium. - Barcelona, 23-28 July 2007. - P. 4419-4421. ↑
- C10192.** Xu Sanyuan. A quadtree algorithm for high squint SAR imaging. / Xu Sanyuan, Wang Jianguo. // 2007. IGARSS 2007. IEEE International Geoscience and Remote Sensing Symposium. - Barcelona, 23-28 July 2007. - P. 854-857. ↑
- C10193.** Boncori J.P.M. Statistical description of tropospheric delay for InSAR: Overview and a new model. / Boncori J.P.M., Mohr J.J. // 2007. IGARSS 2007. IEEE International Geoscience and Remote Sensing Symposium. - Barcelona, 23-28 July 2007. - P. 4483-4486. ↑

- C10194.** Abdelfattah R. Mixture model for the segmentation of the InSAR coherence map. / Abdelfattah R., Nicolas J.M. // 2007. IGARSS 2007. IEEE International Geoscience and Remote Sensing Symposium. - Barcelona, 23-28 July 2007. - P. 4479-4482. ↑
- C10195.** Cantalloube H.M.J. High resolution SAR imaging along circular trajectories. / Cantalloube H.M.J., Colin-Koeniguer E., Oriot H. // 2007. IGARSS 2007. IEEE International Geoscience and Remote Sensing Symposium. - Barcelona, 23-28 July 2007. - P. 850-853. ↑
- C10196.** Selva J. Image coregistration in SAR interferometry only by means of arithmetic operations. / Selva J., Lopez-Sanchez J.M. // 2007. IGARSS 2007. IEEE International Geoscience and Remote Sensing Symposium. - Barcelona, 23-28 July 2007. - P. 4493-4496. ↑
- C10197.** Darizhapov D. Investigation of creation methods of digital elevation model. / Darizhapov D., Leonov A. // 2007. IGARSS 2007. IEEE International Geoscience and Remote Sensing Symposium. - Barcelona, 23-28 July 2007. - P. 4491-4492. ↑
- C10198.** Gonzalez J.H. DEM calibration concept for TanDEM-X. / Gonzalez J.H., Bachmann M., Fiedler H., Huber S., Krieger G., Zink M. // 2007. IGARSS 2007. IEEE International Geoscience and Remote Sensing Symposium. - Barcelona, 23-28 July 2007. - P. 4487-4490. ↑
- C10199.** Awada A. Frequency impact on the bistatic radar scattering from an ocean surface. / Awada A., Khenchaf A., Coatanhay A. // 2007. IGARSS 2007. IEEE International Geoscience and Remote Sensing Symposium. - Barcelona, 23-28 July 2007. - P. 4459-4462. ↑
- C10200.** Congling Nie. Simultaneous wind and rain retrieval for ERS scatterometer measurements. / Congling Nie, Long D.G. // 2007. IGARSS 2007. IEEE International Geoscience and Remote Sensing Symposium. - Barcelona, 23-28 July 2007. - P. 4455-4458. ↑
- C10201.** Cabot F. Calibration of SMOS geolocation biases. / Cabot F., Kerr Y.H., Waldteufel P. // 2007. IGARSS 2007. IEEE International Geoscience and Remote Sensing Symposium. - Barcelona, 23-28 July 2007. - P. 4448-4450. ↑
- C10202.** Contreras R.F. The effect of rain on retrieval of C- and Ku-band scatterometer surface winds during Hurricanes Lili (2002) and Isabel (2003). / Contreras R.F., Frasier S.J., Esteban-Fernandez D., Chang P. // 2007. IGARSS 2007. IEEE International Geoscience and Remote Sensing Symposium. - Barcelona, 23-28 July 2007. - P. 4463-4466. ↑
- C10203.** Duro J. Impact of SAR impulse response function in interferometric measurement. / Duro J., Miranda N., Cooksley G., Biescas E., Arnaud A. // 2007. IGARSS 2007. IEEE International Geoscience and Remote Sensing Symposium. - Barcelona, 23-28 July 2007. - P. 4474-4478. ↑
- C10204.** Hambaryan A.K. Polarimetric, combined, short pulse scatterometer-radiometer system at 5.6GHz. / Hambaryan A.K., Arakelyan A.K., Arakelyan A.A., Darbinyan S.A., Grigoryan M.L., Hakobyan I.K., Karyan V.V., Manukyan M.R., Hovhannisyan G.G., Poghosyan T.N., Poghosyan N.G. // 2007. IGARSS 2007. IEEE International Geoscience and Remote Sensing Symposium. - Barcelona, 23-28 July 2007. - P. 4471-4473. ↑
- C10205.** Xiaolong Dong. Accuracy and resolution analysis of the pencil beam radar scatterometer onboard China's HY-2 satellite. / Xiaolong Dong, Shuyan Lang, Tao Wang, Huguang Liu. // 2007. IGARSS 2007. IEEE International Geoscience and Remote Sensing Symposium. - Barcelona, 23-28 July 2007. - P. 4467-4470. ↑
- C10206.** Reigber A. A distributed approach to efficient time-domain SAR processing. / Reigber A., Jager M., Dietzsch A., Hansch R., Weber M., Przybyl H., Prats P. // 2007. IGARSS 2007. IEEE International Geoscience and Remote Sensing Symposium. - Barcelona, 23-28 July 2007. - P. 582-585. ↑
- C10207.** Thompson P. Target separation in SAR image with the MUSIC algorithm. / Thompson P., Nannini M., Scheiber R. // 2007. IGARSS 2007. IEEE International Geoscience and Remote Sensing Symposium. - Barcelona, 23-28 July 2007. - P. 468-471. ↑
- C10208.** Jie Wei. Relationship between antenna pointing stability and spaceborne ScanSAR scalloping calibration. 2007. IGARSS 2007. IEEE International Geoscience and Remote Sensing Symposium. - Barcelona, 23-28 July 2007. - P. 482-485. ↑

- C10209.** Schulz F. Design of GMTI combining networks. / Schulz F., Saalman O. // 2007. IGARSS 2007. IEEE International Geoscience and Remote Sensing Symposium. - Barcelona, 23-28 July 2007. - P. 486-489. ↑
- C10210.** Bemad G.P. Semi-automatic fast recognition of areas of interest for SAR image interpretation. / Bemad G.P., Denise L., Refregier P. // 2007. IGARSS 2007. IEEE International Geoscience and Remote Sensing Symposium. - Barcelona, 23-28 July 2007. - P. 464-467. ↑
- C10211.** Sipelgas L. Elimination of oil spill like structures from radar image using MODIS data. / Sipelgas L., Uiboupin R. // 2007. IGARSS 2007. IEEE International Geoscience and Remote Sensing Symposium. - Barcelona, 23-28 July 2007. - P. 429-431. ↑
- C10212.** Uschkerat U. Application of 3D-SAR nearfield imaging algorithms to GPR data. 2007. IGARSS 2007. IEEE International Geoscience and Remote Sensing Symposium. - Barcelona, 23-28 July 2007. - P. 452-455. ↑
- C10213.** Tison C. Target recognition in SAR images with Support Vector Machines (SVM). / Tison C., Pourthie N., Souyris J.-C. // 2007. IGARSS 2007. IEEE International Geoscience and Remote Sensing Symposium. - Barcelona, 23-28 July 2007. - P. 456-459. ↑
- C10214.** Moon-Kyung Kang. The extraction of ocean wind, wave, and current parameters using SAR imagery. / Moon-Kyung Kang, Hoonyol Lee, Moonjin Lee, Yong-Wook Park, Wang-Jung Yoon. // 2007. IGARSS 2007. IEEE International Geoscience and Remote Sensing Symposium. - Barcelona, 23-28 July 2007. - P. 507-510. ↑
- C10215.** Gras V. Phase distortion modelling due to motion in wave scattering mechanism applied to SAR images analysis. / Gras V., Sintes C., Garelo R. // 2007. IGARSS 2007. IEEE International Geoscience and Remote Sensing Symposium. - Barcelona, 23-28 July 2007. - P. 511-515. ↑
- C10216.** Zhihua He. Spaceborne SAR raw signal simulation of ocean scene. / Zhihua He, Zhen Dong, Haifeng Huang, Anxi Yu. // 2007. IGARSS 2007. IEEE International Geoscience and Remote Sensing Symposium. - Barcelona, 23-28 July 2007. - P. 516-519. ↑
- C10217.** Sveinsson J.R. Combined wavelet and curvelet denoising of SAR images using TV segmentation. / Sveinsson J.R., Benediktsson J.A. // 2007. IGARSS 2007. IEEE International Geoscience and Remote Sensing Symposium. - Barcelona, 23-28 July 2007. - P. 503-506. ↑
- C10218.** Yixian Tang. CAESAR-XInSAR: A new software for interferometric SAR processing. / Yixian Tang, Hong Zhang, Chao Wang, Tao Wu. // 2007. IGARSS 2007. IEEE International Geoscience and Remote Sensing Symposium. - Barcelona, 23-28 July 2007. - P. 490-493. ↑
- C10219.** Aboutanios E. Evaluation of the single and two data set STAP detection algorithms using measured data. / Aboutanios E., Mulgrew B. // 2007. IGARSS 2007. IEEE International Geoscience and Remote Sensing Symposium. - Barcelona, 23-28 July 2007. - P. 494-498. ↑
- C10220.** Hwee Siang Tan. ISAR imaging of targets with moving parts using micro-doppler detection on the range profile image. / Hwee Siang Tan, Changzheng Ma, Tat Soon Yeo, Qun Zhang, Chun Sum Ng, Bin Zou. // 2007. IGARSS 2007. IEEE International Geoscience and Remote Sensing Symposium. - Barcelona, 23-28 July 2007. - P. 499-502. ↑
- C10221.** Qi Li. Steerable filter based multiscale registration method for JERS-1 SAR and ASTER images. / Qi Li, Sato I., Murakami Y. // 2007. IGARSS 2007. IEEE International Geoscience and Remote Sensing Symposium. - Barcelona, 23-28 July 2007. - P. 381-384. ↑
- C10222.** Vasile G. Coherent-stable scatterers detection in SAR multi-interferograms: Feature fuzzy fusion in Alpine glacier geophysical context. / Vasile G., Trouve E., Valet L., Nicolas J.-M., Bombrun L., Gay M., Petillot I., Bolon P., Buzuloiu V. // 2007. IGARSS 2007. IEEE International Geoscience and Remote Sensing Symposium. - Barcelona, 23-28 July 2007. - P. 4862-4865. ↑
- C10223.** Shabou A. Similarity measures between SAR and optic data. / Shabou A., Tupin F., Chaabane F. // 2007. IGARSS 2007. IEEE International Geoscience and Remote Sensing Symposium. - Barcelona, 23-28 July 2007. - P. 4858-4861. ↑
- C10224.** Moser G. Unsupervised change detection by multichannel SAR data fusion. / Moser G., Serpico S.B. // 2007. IGARSS 2007. IEEE International Geoscience and Remote Sensing Symposium. - Barcelona, 23-28 July 2007. - P. 4858-4861. ↑

July 2007. - P. 4854-4857. ↑

C10225. Prats P. Advanced D-InSAR techniques applied to a time series of airborne SAR data. / Prats P., Scheiber R., Moreira A., Reigber A., Mallorqui J.J. // 2007. IGARSS 2007. IEEE International Geoscience and Remote Sensing Symposium. - Barcelona, 23-28 July 2007. - P. 4874-4877. ↑

C10226. de Macedo K.A.C. An autofocus approach for residual motion errors with application to airborne repeat-pass SAR interferometry. / de Macedo K.A.C., Scheiber R., Moreira A. // 2007. IGARSS 2007. IEEE International Geoscience and Remote Sensing Symposium. - Barcelona, 23-28 July 2007. - P. 4886-4889. ↑

C10227. Zolotarev I.D. Research of influence of transients, non-equidistance of the taken readings, divergence of beams on characteristics of interferometric SAR. / Zolotarev I.D., Pozharsky T.O., Miller Ya.E. // 2007. IGARSS 2007. IEEE International Geoscience and Remote Sensing Symposium. - Barcelona, 23-28 July 2007. - P. 4882-4885. ↑

C10228. Perna S. X-band airborne differential interferometry over the Perugia area. / Perna S., Wimmer C., Moreira J., Fornaro G. // 2007. IGARSS 2007. IEEE International Geoscience and Remote Sensing Symposium. - Barcelona, 23-28 July 2007. - P. 4878-4881. ↑

C10229. Lidicky L. A new method for moving target indication and detection in multi-channel SAR data. 2007. IGARSS 2007. IEEE International Geoscience and Remote Sensing Symposium. - Barcelona, 23-28 July 2007. - P. 4802-4805. ↑

C10230. Solimene R. Localizing metallic small spheres by a linear distributional approach. / Solimene R., Buonanno A., Pierri R., Leone G. // 2007. IGARSS 2007. IEEE International Geoscience and Remote Sensing Symposium. - Barcelona, 23-28 July 2007. - P. 350-353. ↑

C10231. Cuinas I. Measurement and analysis of depolarization generated by scattering over constructive obstacles at 5.8 GHz. / Cuinas I., Sanchez M.G., Alejos A.V. // 2007. IGARSS 2007. IEEE International Geoscience and Remote Sensing Symposium. - Barcelona, 23-28 July 2007. - P. 354-357. ↑

C10232. Lugan S. Simulation of LIDAR-based aircraft wake vortex detection using a bi-gaussian spectral model. / Lugan S., Bricteux L., Macq B., Sobieski P., Winkelmanns G., Douchamps D. // 2007. IGARSS 2007. IEEE International Geoscience and Remote Sensing Symposium. - Barcelona, 23-28 July 2007. - P. 4806-4809. ↑

C10233. Waske B. Fusion of support vector machines for classifying SAR and multispectral imagery from agricultural areas. / Waske B., Menz G., Benediktsson J.A. // 2007. IGARSS 2007. IEEE International Geoscience and Remote Sensing Symposium. - Barcelona, 23-28 July 2007. - P. 4842-4845. ↑

C10234. Di Bisceglie M. Multiband CFAR detection of thermal anomalies using principal component analysis. / Di Bisceglie M., Episcopo R., Galdi C., Ullo S.L. // 2007. IGARSS 2007. IEEE International Geoscience and Remote Sensing Symposium. - Barcelona, 23-28 July 2007. - P. 4822-4825. ↑

C10235. Weihing D. Detecting moving targets in dual-channel high resolution spaceborne SAR images with a compound detection scheme. / Weihing D., Hinz S., Meyer F., Suchandt S., Bamler R. // 2007. IGARSS 2007. IEEE International Geoscience and Remote Sensing Symposium. - Barcelona, 23-28 July 2007. - P. 4818-4821. ↑

C10236. Yunhua Zhang. A new method for Doppler centroid estimation for spaceborne SAR based on chirp scaling algorithm. / Yunhua Zhang, Wenshuai Zhai. // 2007. IGARSS 2007. IEEE International Geoscience and Remote Sensing Symposium. - Barcelona, 23-28 July 2007. - P. 543-546. ↑

C10237. Chamundeeswari V.V. Unsupervised land cover classification of SAR images by contour tracing. / Chamundeeswari V.V., Singh D., Singh K. // 2007. IGARSS 2007. IEEE International Geoscience and Remote Sensing Symposium. - Barcelona, 23-28 July 2007. - P. 547-550. ↑

C10238. Giusti E. The equivalence of Cameron's unit disc and Poincaré's sphere for symmetric scattering characterisation and classification. / Giusti E., Martorella M., Berizzi F., Petronio C. // 2007. IGARSS 2007. IEEE International Geoscience and Remote Sensing Symposium. - Barcelona, 23-28 July 2007. - P. 551-554. ↑

C10239. Liu Hui. The analysis and compensation for the unwrapped phase error raised by the dynamic baseline of DSS-INSAR. / Liu Hui, Zhou Yingqing, Xu Huaping, Li Chunsheng, Sun Muhan, Liu Guohui. // 2007.

IGARSS 2007. IEEE International Geoscience and Remote Sensing Symposium. - Barcelona, 23-28 July 2007. - P. 540-542. ↑

C10240. Ferraioli G. Offset Phase Estimation in Multi-Channel InSAR DEM Reconstruction. / Ferraioli G., Pascasio V., Ferraiuolo G. // 2007. IGARSS 2007. IEEE International Geoscience and Remote Sensing Symposium. - Barcelona, 23-28 July 2007. - P. 4513-4516. ↑

C10241. Jie Li. A multi-baseline InSAR DEM reconstruction approach without ground control points. / Jie Li, Haifeng Huang, Diannong Liang. // 2007. IGARSS 2007. IEEE International Geoscience and Remote Sensing Symposium. - Barcelona, 23-28 July 2007. - P. 4509-4512. ↑

C10242. Kalkuhl M. Parallel computation of synthetic SAR raw data. / Kalkuhl M., Droste P., Wiechert W., Nies H., Loffeld O., Lambers M. // 2007. IGARSS 2007. IEEE International Geoscience and Remote Sensing Symposium. - Barcelona, 23-28 July 2007. - P. 536-539. ↑

C10243. Xu Feng. Region feature extraction based on improved regularization method in SAR image. / Xu Feng, Wang Chao, Zhang Hong. // 2007. IGARSS 2007. IEEE International Geoscience and Remote Sensing Symposium. - Barcelona, 23-28 July 2007. - P. 571-573. ↑

C10244. Ghaleb A. Fine micro-Doppler analysis in ISAR imaging. / Ghaleb A., Vignaud L., Nicolas J.-M. // 2007. IGARSS 2007. IEEE International Geoscience and Remote Sensing Symposium. - Barcelona, 23-28 July 2007. - P. 574-577. ↑

C10245. Bhattacharya C. Dyadic resolution multilook image generation by wavelet packet transform correlation of complex SAR signals. 2007. IGARSS 2007. IEEE International Geoscience and Remote Sensing Symposium. - Barcelona, 23-28 July 2007. - P. 578-581. ↑

C10246. Yu Wang. Spotlight-mode SAR data focusing using a modified wavenumber domain algorithm. / Yu Wang, Loffeld O., Knedlik S. // 2007. IGARSS 2007. IEEE International Geoscience and Remote Sensing Symposium. - Barcelona, 23-28 July 2007. - P. 567-570. ↑

C10247. Ya-Qiu Jin. Reconstruction of the building objects from multi-aspect high-resolution SAR images. / Ya-Qiu Jin, Feng Xu. // 2007. IGARSS 2007. IEEE International Geoscience and Remote Sensing Symposium. - Barcelona, 23-28 July 2007. - P. 555-558. ↑

C10248. Wellig P. Clutter analysis of high resolution millimeter-wave SAR-data in the spatial and wavelet domain. / Wellig P., Schmid K., Essen H., Kurz A., Schimpf H., Brehm T. // 2007. IGARSS 2007. IEEE International Geoscience and Remote Sensing Symposium. - Barcelona, 23-28 July 2007. - P. 559-562. ↑

C10249. Radius A. A velocity vector estimation algorithm tested on simulated SAR raw data. / Radius A., Solimini D. // 2007. IGARSS 2007. IEEE International Geoscience and Remote Sensing Symposium. - Barcelona, 23-28 July 2007. - P. 563-566. ↑

C10250. Meglio F. DEM estimation from multi-Baseline ENVISAT- ASAR interferometric data through maximum likelihood techniques. / Meglio F., Schirizzi G. // 2007. IGARSS 2007. IEEE International Geoscience and Remote Sensing Symposium. - Barcelona, 23-28 July 2007. - P. 4517-4520. ↑

C10251. Hieu Duong. Error analysis of ICESat waveform processing by investigating overlapping pairs over Europe. / Hieu Duong, Lindenbergh R., Pfeifer N., Vosselman G. // 2007. IGARSS 2007. IEEE International Geoscience and Remote Sensing Symposium. - Barcelona, 23-28 July 2007. - P. 4753-4756. ↑

C10252. Taejung Kim. Semiautomatic reconstruction of building height and footprints from single satellite images. / Taejung Kim, Javzandulam T., Tae-Yoon Lee. // 2007. IGARSS 2007. IEEE International Geoscience and Remote Sensing Symposium. - Barcelona, 23-28 July 2007. - P. 4737-4740. ↑

C10253. Yunqing Jiao. Uncertainty analysis of flood disaster assessment using radar imagery. / Yunqing Jiao, Shixin Wang, Yi Zhou, Litao Wang. // 2007. IGARSS 2007. IEEE International Geoscience and Remote Sensing Symposium. - Barcelona, 23-28 July 2007. - P. 4729-4732. ↑

C10254. Chaomin Shen. Variational-based speckle noise removal of SAR imagery. / Chaomin Shen, Yaxin Peng, Ling Pi, Zhibin Li. // 2007. IGARSS 2007. IEEE International Geoscience and Remote Sensing Symposium. - Barcelona, 23-28 July 2007. - P. 532-535. ↑

- C10255.** Tzong-Dar Wu. Geological lineament and shoreline detection in SAR images. / Tzong-Dar Wu, Lee M.T. // 2007. IGARSS 2007. IEEE International Geoscience and Remote Sensing Symposium. - Barcelona, 23-28 July 2007. - P. 520-523. ↑
- C10256.** Andres C. A multiprocessing framework for SAR image processing. / Andres C., Keil T., Herrmann R., Scheiber R. // 2007. IGARSS 2007. IEEE International Geoscience and Remote Sensing Symposium. - Barcelona, 23-28 July 2007. - P. 524-527. ↑
- C10257.** Meglio F. Three dimensional SAR image focusing from non-uniform samples. / Meglio F., Panariello G., Schirinz G. // 2007. IGARSS 2007. IEEE International Geoscience and Remote Sensing Symposium. - Barcelona, 23-28 July 2007. - P. 528-531. ↑
- C10258.** Andreoli R. Inland lake monitoring using low and medium resolution ENVISAT ASAR and optical data: Case study of Poyang Lake (Jiangxi, P.R. China). / Andreoli R., Yesou H., Li J., Desnos Y.-L. // 2007. IGARSS 2007. IEEE International Geoscience and Remote Sensing Symposium. - Barcelona, 23-28 July 2007. - P. 4578-4581. ↑
- C10259.** Esch T. Analysis of urban land use pattern based on high resolution radar imagery. / Esch T., Roth A., Dech S. // 2007. IGARSS 2007. IEEE International Geoscience and Remote Sensing Symposium. - Barcelona, 23-28 July 2007. - P. 4525. ↑
- C10260.** Norland R. Improving interferometric radar measurement accuracy using local meteorological data. 2007. IGARSS 2007. IEEE International Geoscience and Remote Sensing Symposium. - Barcelona, 23-28 July 2007. - P. 4521-4524. ↑
- C10261.** Renzong Ruan. Identification of inland fresh water wetland using SAR and ETM+ data. / Renzong Ruan, Liliang Ren. // 2007. IGARSS 2007. IEEE International Geoscience and Remote Sensing Symposium. - Barcelona, 23-28 July 2007. - P. 4592-4595. ↑
- C10262.** Chen Yun. Typhoon monitoring/operational forecasting and services 2005 in China. / Chen Yun, Li Qiang, Li Zechun, Xu zhi-fang. // 2007. IGARSS 2007. IEEE International Geoscience and Remote Sensing Symposium. - Barcelona, 23-28 July 2007. - P. 4675-4678. ↑
- C10263.** Lee C.-W. SAR measurements of surface displacements at Augustine volcano, Alaska from 1992 to 2005. / Lee C.-W., Lu Z., Kwoun O.-I. // 2007. IGARSS 2007. IEEE International Geoscience and Remote Sensing Symposium. - Barcelona, 23-28 July 2007. - P. 4671-4674. ↑
- C10264.** Elias P. Small scale surface deformation detection of the Gulf of Corinth (Hellas) using Permanent Scatterers technique. / Elias P., Kontoes C., Papoutsis I., Kotsis I. // 2007. IGARSS 2007. IEEE International Geoscience and Remote Sensing Symposium. - Barcelona, 23-28 July 2007. - P. 4659-4662. ↑
- C10265.** Lasne Y. Effect of salinity on the dielectric properties of geological materials: implication for soil moisture detection by means of remote sensing. / Lasne Y., Paillou P., Ruffle G., Serradilla C., Demontoux F., Freeman A., Farr T., McDonald K., Chapman B., Malezieux J.-M. // 2007. IGARSS 2007. IEEE International Geoscience and Remote Sensing Symposium. - Barcelona, 23-28 July 2007. - P. 3689-3693. ↑
- C10266.** Naeimi V. Evaluation of the influence of land cover on the noise level of ERS-scatterometer backscatter. / Naeimi V., Kuenzer C., Hasenauer S., Bartalis Z., Wagner W. // 2007. IGARSS 2007. IEEE International Geoscience and Remote Sensing Symposium. - Barcelona, 23-28 July 2007. - P. 3685-3688. ↑
- C10267.** Jinsong Chen. A semi-empirical backscattering model for estimation of leaf area index (LAI) of rice in southern China. / Jinsong Chen, Hui Lin, Aixia Liu, Yun Shao, Limin Yang. // 2007. IGARSS 2007. IEEE International Geoscience and Remote Sensing Symposium. - Barcelona, 23-28 July 2007. - P. 3667-3680. ↑
- C10268.** Marzano F.S. Potential of X-band spaceborne synthetic aperture radar for precipitation retrieval over land. / Marzano F.S., Poccia G., Cantelmi R., Pierdicca N., Weinman J.A., Chandrasekar V., Mugnai A. // 2007. IGARSS 2007. IEEE International Geoscience and Remote Sensing Symposium. - Barcelona, 23-28 July 2007. - P. 3694-3697. ↑
- C10269.** Khadhra K.B. Soil parameter estimation and analysis of bistatic scattering X-band controlled measurements. / Khadhra K.B., Boerner T., Chandra M., Zink M., Hounam D. // 2007. IGARSS 2007. IEEE International Geoscience and Remote Sensing Symposium. - Barcelona, 23-28 July 2007. - P. 3706-3709. ↑

- C10270.** Bartsch A. Application of C and Ku-Band scatterometer data for catchment hydrology in northern latitudes. / Bartsch A., Wagner W., Rupp K., Kidd R. // 2007. IGARSS 2007. IEEE International Geoscience and Remote Sensing Symposium. - Barcelona, 23-28 July 2007. - P. 3702-3705. ↑
- C10271.** Loew A. Integration of L-band SAR data into land surface models. / Loew A., Hoekman D., Hajnsek I., Davison M. // 2007. IGARSS 2007. IEEE International Geoscience and Remote Sensing Symposium. - Barcelona, 23-28 July 2007. - P. 3698-3701. ↑
- C10272.** Jin-Young Hong. Polarimetric measurements of radar backscatters of a wet-land rice field throughout a growth period at L- and C-bands. / Jin-Young Hong, Yisok Oh, Sukyoung Hong. // 2007. IGARSS 2007. IEEE International Geoscience and Remote Sensing Symposium. - Barcelona, 23-28 July 2007. - P. 3663-3666. ↑
- C10273.** Colliander A. Ground calibration of SMOS: NIR and CAS. / Colliander A., Lemmetyinen J., Uusitalo J., Suomela J., Veijola K., Kontu A., Kempainen S., Pihlflyckt J., Rautiainen K., Hallikainen M., Lahtinen J. // 2007. IGARSS 2007. IEEE International Geoscience and Remote Sensing Symposium. - Barcelona, 23-28 July 2007. - P. 3631-3634. ↑
- C10274.** Rosenqvist A. The ALOS Kyoto & Carbon Initiative. / Rosenqvist A., Shimada M., Milne A.K. // 2007. IGARSS 2007. IEEE International Geoscience and Remote Sensing Symposium. - Barcelona, 23-28 July 2007. - P. 3614-3617. ↑
- C10275.** Lucas R.M. ALOS PALSAR for characterizing wooded savannas in Northern Australia. / Lucas R.M., Armston J.D. // 2007. IGARSS 2007. IEEE International Geoscience and Remote Sensing Symposium. - Barcelona, 23-28 July 2007. - P. 3610-3613. ↑
- C10276.** Duffo N. Some results of the MIRAS-SMOS demonstrator campaigns. / Duffo N., Torres F., Corbella I., Gonzalez V., Blanch S., Camps A., Vall-Ilossera M., Alvarez J.L., Ribo S., Martin-Neira M. // 2007. IGARSS 2007. IEEE International Geoscience and Remote Sensing Symposium. - Barcelona, 23-28 July 2007. - P. 3639-3642. ↑
- C10277.** Soria-Ruiz J. Corn monitoring and crop yield using optical and RADARSAT-2 images. / Soria-Ruiz J., McNairn H., Fernandez-Ordóñez Y., Bugden-Storie J. // 2007. IGARSS 2007. IEEE International Geoscience and Remote Sensing Symposium. - Barcelona, 23-28 July 2007. - P. 3655-3658. ↑
- C10278.** Schiavon G. Sensitivity of multi-temporal high resolution polarimetric C and L-band SAR to grapes in vineyards. / Schiavon G., Solimini D., Burini A. // 2007. IGARSS 2007. IEEE International Geoscience and Remote Sensing Symposium. - Barcelona, 23-28 July 2007. - P. 3651-3654. ↑
- C10279.** Heinzl V. Remote sensing data assimilation for regional crop growth modelling in the region of Bonn (Germany). / Heinzl V., Waske B., Braun M., Menz G. // 2007. IGARSS 2007. IEEE International Geoscience and Remote Sensing Symposium. - Barcelona, 23-28 July 2007. - P. 3647-3650. ↑
- C10280.** Crisp D.J. Polarimetric analysis of maritime SAR data collected with the DSTO ingara X-Band radar. / Crisp D.J., Stacy N.J.S., Hudson D.A., Pincus P.B., Goh A.S. // 2007. IGARSS 2007. IEEE International Geoscience and Remote Sensing Symposium. - Barcelona, 23-28 July 2007. - P. 3870-3873. ↑
- C10281.** Dupuis X. Very high resolution interferogram acquisition campaign and processing. / Dupuis X., Angelliaume S., Oriot H., Dubois-Fernandez P., Cantalloube H., Coulombeix C., du Plessis O., Fromage P., Bonin G., Heuze D. // 2007. IGARSS 2007. IEEE International Geoscience and Remote Sensing Symposium. - Barcelona, 23-28 July 2007. - P. 3866-3869. ↑
- C10282.** Liu He-Guang. Theoretic error analysis of split-gate tracker in satellite radar altimetry. / Liu He-Guang, Xu Xi-Yu, Xu Ke. // 2007. IGARSS 2007. IEEE International Geoscience and Remote Sensing Symposium. - Barcelona, 23-28 July 2007. - P. 3832-3835. ↑
- C10283.** Avolio S. Integrating point, curve and area descriptors into geospatial databases for metric resolution SAR image analysis. / Avolio S., Galli L., Passaro D., Quartulli M., Sagona M., Sinatra G., Zelli C. // 2007. IGARSS 2007. IEEE International Geoscience and Remote Sensing Symposium. - Barcelona, 23-28 July 2007. - P. 3874-3877. ↑
- C10284.** Bertacca M. A FEXP model Short Range Dependence analysis for improving oil slicks and low-wind areas discrimination in sea SAR imagery. 2007. IGARSS 2007. IEEE International Geoscience and Remote

Sensing Symposium. - Barcelona, 23-28 July 2007. - P. 959-962. ↑

C10285. Alparone L. Robust change analysis of SAR data through information-theoretic multitemporal features. / Alparone L., Aiazzi B., Baronti S., Garzelli A., Nencini F. // 2007. IGARSS 2007. IEEE International Geoscience and Remote Sensing Symposium. - Barcelona, 23-28 July 2007. - P. 3883-3886. ↑

C10286. Foucher S. Multiscale filtering of SAR images using scale and space consistency. 2007. IGARSS 2007. IEEE International Geoscience and Remote Sensing Symposium. - Barcelona, 23-28 July 2007. - P. 3878-3882. ↑

C10287. Xu Xi-Yu. An innovative algorithm for radar altimeter acceleration bias compensation. / Xu Xi-Yu, Liu He-Guang. // 2007. IGARSS 2007. IEEE International Geoscience and Remote Sensing Symposium. - Barcelona, 23-28 July 2007. - P. 3829-3831. ↑

C10288. Martinez-Vazquez A. Snow avalanche detection and classification algorithm for GB-SAR imagery. / Martinez-Vazquez A., Fortuny-Guasch J. // 2007. IGARSS 2007. IEEE International Geoscience and Remote Sensing Symposium. - Barcelona, 23-28 July 2007. - P. 3740-3743. ↑

C10289. Pierdicca N. Optimal configurations of bistatic radar for retrieving soil moisture and vegetation biomass. / Pierdicca N., Pulvirenti L., Guerriero L., Della Pietra G. // 2007. IGARSS 2007. IEEE International Geoscience and Remote Sensing Symposium. - Barcelona, 23-28 July 2007. - P. 3715-3718. ↑

C10290. Hoekman D. ALOS PALSAR radar observation of tropical peat swamp forest as a monitoring tool for environmental protection and restoration. / Hoekman D., Vissers M. // 2007. IGARSS 2007. IEEE International Geoscience and Remote Sensing Symposium. - Barcelona, 23-28 July 2007. - P. 3710-3714. ↑

C10291. Marzano F.S. Microwave radar remote sensing of Plinian volcanic ash clouds for aviation hazard and civil protection applications. / Marzano F.S., Barbieri S., Picciotti E., Vulpiani G. // 2007. IGARSS 2007. IEEE International Geoscience and Remote Sensing Symposium. - Barcelona, 23-28 July 2007. - P. 3748-3751. ↑

C10292. Ke Xu. A new tracker for ocean-land compatible radar altimeter. / Ke Xu, Jingshan Jiang, Huguang Liu. // 2007. IGARSS 2007. IEEE International Geoscience and Remote Sensing Symposium. - Barcelona, 23-28 July 2007. - P. 3825-3828. ↑

C10293. Yunhua Zhang. An interferometric imaging altimeter applied for both ocean and land observation. / Yunhua Zhang, Xiangkun Zhang, Xin Meng, Wei Luo, Zhixin Zhou, Jingshan Jiang. // 2007. IGARSS 2007. IEEE International Geoscience and Remote Sensing Symposium. - Barcelona, 23-28 July 2007. - P. 3821-3824. ↑

C10294. Jin-King Liu. Lidar DEM for characterizing the volcanic landforms of tatan volcanoes in metropolitan taipei. / Jin-King Liu, Yu-Chang Chan, Tian-Yuan Shih, Yu-Chung Hsieh. // 2007. IGARSS 2007. IEEE International Geoscience and Remote Sensing Symposium. - Barcelona, 23-28 July 2007. - P. 3752-3755. ↑

C10295. Isoguchi O. Relationship between wind vectors and L-band radar cross sections examined using PALSAR. / Isoguchi O., Shimada M. // 2007. IGARSS 2007. IEEE International Geoscience and Remote Sensing Symposium. - Barcelona, 23-28 July 2007. - P. 3598-3601. ↑

C10296. Ma Jianwen. Land use changes driven by 2008 beijing olympic playground constructions and depicted by landsat temporal data. / Ma Jianwen, Chen Xue, Dai Qin, Li Liwei. // 2007. IGARSS 2007. IEEE International Geoscience and Remote Sensing Symposium. - Barcelona, 23-28 July 2007. - P. 3456-3457. ↑

C10297. Nonaka T. A comparison of the methods for the urban land cover change detection by high-resolution SAR data. / Nonaka T., Shibayama T., Umakawa H., Uratsuka S. // 2007. IGARSS 2007. IEEE International Geoscience and Remote Sensing Symposium. - Barcelona, 23-28 July 2007. - P. 3470-3473. ↑

C10298. Banal S. Canadian Space Agency's Hurricane Watch Program: Archive contents, Data Access and improved planning strategies. / Banal S., Iris S., Saint-Jean R. // 2007. IGARSS 2007. IEEE International Geoscience and Remote Sensing Symposium. - Barcelona, 23-28 July 2007. - P. 3494-3497. ↑

C10299. Hee-Young Yoo. Implementation of 3D discrete wavelet scheme for space-borne imagery classification and its application. / Hee-Young Yoo, Kiwon Lee, Byung-Doo Kwon. // 2007. IGARSS 2007. IEEE International Geoscience and Remote Sensing Symposium. - Barcelona, 23-28 July 2007. - P. 3437-3440. ↑

- C10300.** Mavrocordatos C. The Sentinel-3 mission and its topography element. / Mavrocordatos C., Berruti B., Aguirre M., Drinkwater M. // 2007. IGARSS 2007. IEEE International Geoscience and Remote Sensing Symposium. - Barcelona, 23-28 July 2007. - P. 3529-3532. ↑
- C10301.** Enjolras V. An assessment of the Ka band interferometric radar altimeter for monitoring rivers and lakes with the WatER mission. / Enjolras V., Rodriguez E. // 2007. IGARSS 2007. IEEE International Geoscience and Remote Sensing Symposium. - Barcelona, 23-28 July 2007. - P. 3525-3528. ↑
- C10302.** Shimada T. Wind jet transition and its localized impact on wave height distribution along the Pacific Coast of Northern Japan. / Shimada T., Kawamura H. // 2007. IGARSS 2007. IEEE International Geoscience and Remote Sensing Symposium. - Barcelona, 23-28 July 2007. - P. 3521-3524. ↑
- C10303.** Irisov V. Simultaneous X-band radar and Ka -band radiometer observations of the ocean. / Irisov V., Plant W.J. // 2007. IGARSS 2007. IEEE International Geoscience and Remote Sensing Symposium. - Barcelona, 23-28 July 2007. - P. 3498-3501. ↑
- C10304.** Gauthier M.-F. Integrated satellite tracking of pollution: A new operational program. / Gauthier M.-F., Weir L., Ziqiang Ou, Arkett M., De Abreu R. // 2007. IGARSS 2007. IEEE International Geoscience and Remote Sensing Symposium. - Barcelona, 23-28 July 2007. - P. 967-970. ↑
- C10305.** Hwang P.A. Statistical characterization of radar sea scatter for breaking wave detection. / Hwang P.A., Sletten M.A., Toporkov J.V. // 2007. IGARSS 2007. IEEE International Geoscience and Remote Sensing Symposium. - Barcelona, 23-28 July 2007. - P. 3517-3520. ↑
- C10306.** Essen H. High resolution millimeterwave SAR for the remote sensing of wave patterns. / Essen H., Fuchs H.-H., Pagels A. // 2007. IGARSS 2007. IEEE International Geoscience and Remote Sensing Symposium. - Barcelona, 23-28 July 2007. - P. 963-966. ↑
- C10307.** Jian Sun. A case study on swell modulation caused by surface winds using spaceborne Synthetic Aperture Radar. / Jian Sun, Kawamura H. // 2007. IGARSS 2007. IEEE International Geoscience and Remote Sensing Symposium. - Barcelona, 23-28 July 2007. - P. 975-978. ↑
- C10308.** Ahmad K.A. Oceanic Rainfall Retrievals using passive and active measurements from SeaWinds Remote Sensor. / Ahmad K.A., Jones W.L., Kasparis T. // 2007. IGARSS 2007. IEEE International Geoscience and Remote Sensing Symposium. - Barcelona, 23-28 July 2007. - P. 3502-3506. ↑
- C10309.** Hasager C.B. QuikSCAT and SSM/I ocean surface winds for wind energy. / Hasager C.B., Astrup P., Nielsen P. // 2007. IGARSS 2007. IEEE International Geoscience and Remote Sensing Symposium. - Barcelona, 23-28 July 2007. - P. 3507-3512. ↑
- C10310.** Portabella M. Towards a high-resolution ASCAT scatterometer wind product. / Portabella M., Stoffelen A., Vogelzang J., Verhoef A., Verspeek J. // 2007. IGARSS 2007. IEEE International Geoscience and Remote Sensing Symposium. - Barcelona, 23-28 July 2007. - P. 3513-3516. ↑
- C10311.** Anagnostou M.N. Evaluation of X-band polarimetric radar estimates of drop size distributions from coincident S-band polarimetric estimates and measured raindrop spectra. / Anagnostou M.N., Anagnostou E.N., Vulpiani G., Montopoli M., Vivekanandan J. // 2007. IGARSS 2007. IEEE International Geoscience and Remote Sensing Symposium. - Barcelona, 23-28 July 2007. - P. 3575-3578. ↑
- C10312.** Chandrasekar V. Waveform coding for dual polarization weather radars. / Chandrasekar V., Bharadwaj N., George J. // 2007. IGARSS 2007. IEEE International Geoscience and Remote Sensing Symposium. - Barcelona, 23-28 July 2007. - P. 3571-3574. ↑
- C10313.** Cerutti-Maori D. Wide area traffic monitoring with the PAMIR system. / Cerutti-Maori D., Klare J., Burger W., Brenner A.R., Ender J.H.G. // 2007. IGARSS 2007. IEEE International Geoscience and Remote Sensing Symposium. - Barcelona, 23-28 July 2007. - P. 3567-3570. ↑
- C10314.** Flampouris S. Survey of bathymetry and current fields by radar image series acquired by shore based x-band radar. / Flampouris S., Ziemer F., Seemann J. // 2007. IGARSS 2007. IEEE International Geoscience and Remote Sensing Symposium. - Barcelona, 23-28 July 2007. - P. 3579-3582. ↑
- C10315.** Papathanassiou K.P. Pol-InSAR Results from ALOS-PalSAR. / Papathanassiou K.P., Marotti L.,

Schneider R.Z., Hajnsek I. // 2007. IGARSS 2007. IEEE International Geoscience and Remote Sensing Symposium. - Barcelona, 23-28 July 2007. - P. 3597. ↑

C10316. Shimada M. PALSAR CALVAL summary and update 2007. / Shimada M., Isoguchi O., Tadono T., Higuchi R., Isono K. // 2007. IGARSS 2007. IEEE International Geoscience and Remote Sensing Symposium. - Barcelona, 23-28 July 2007. - P. 3593-3596. ↑

C10317. Iwata T. Advanced land observing satellite (ALOS): On-orbit status and platform calibration. 2007. IGARSS 2007. IEEE International Geoscience and Remote Sensing Symposium. - Barcelona, 23-28 July 2007. - P. 3583-3588. ↑

C10318. Berizzi F. Synthetic range profile focusing via contrast optimization. / Berizzi F., Martorella M., Cacciamano A. // 2007. IGARSS 2007. IEEE International Geoscience and Remote Sensing Symposium. - Barcelona, 23-28 July 2007. - P. 3563-3566. ↑

C10319. Roca M. The RA-2 individual echoes processing description and some scientific results. / Roca M., Martinez D., Reche M. // 2007. IGARSS 2007. IEEE International Geoscience and Remote Sensing Symposium. - Barcelona, 23-28 July 2007. - P. 3541-3546. ↑

C10320. Richard J. An advanced concept of radar altimetry over oceans with improved performances and ocean sampling: AltiKa. / Richard J., Phalippou L., Robert F., Stenou N., Thouvenot E., Sengenès P. // 2007. IGARSS 2007. IEEE International Geoscience and Remote Sensing Symposium. - Barcelona, 23-28 July 2007. - P. 3537-3540. ↑

C10321. Phalippou L. Re-tracking of SAR altimeter ocean power-waveforms and related accuracies of the retrieved sea surface height, significant wave height and wind speed. / Phalippou L., Enjolras V. // 2007. IGARSS 2007. IEEE International Geoscience and Remote Sensing Symposium. - Barcelona, 23-28 July 2007. - P. 3533-3536. ↑

C10322. Schwaller M.R. Prototype of NASA's global precipitation measurement mission ground validation system. / Schwaller M.R., Morris K.R., Petersen W.A. // 2007. IGARSS 2007. IEEE International Geoscience and Remote Sensing Symposium. - Barcelona, 23-28 July 2007. - P. 3547-3550. ↑

C10323. Scheiber R. Surface clutter suppression for ice sounding radars by coherent combination of repeat-pass data. / Scheiber R., Prats P. // 2007. IGARSS 2007. IEEE International Geoscience and Remote Sensing Symposium. - Barcelona, 23-28 July 2007. - P. 3559-3562. ↑

C10324. Gorgucci E. Rain microphysics estimation using X-band dual polarization radar measurements. / Gorgucci E., Baldini L., Chandrasekar V. // 2007. IGARSS 2007. IEEE International Geoscience and Remote Sensing Symposium. - Barcelona, 23-28 July 2007. - P. 3555-3558. ↑

C10325. Furukawa K. Preliminary design of the spaceborne dual-frequency precipitation radar for the global precipitation measurement. / Furukawa K., Hanado H., Hyakusoku Y., Ishii Y., Kojima M., Takahashi N., Iguchi T., Okumura M. // 2007. IGARSS 2007. IEEE International Geoscience and Remote Sensing Symposium. - Barcelona, 23-28 July 2007. - P. 3551-3554. ↑

C10326. Jingsong Yang. Simulation of SAR image cross spectra from mixed ocean waves. / Jingsong Yang, He Wang, Qingmei Xiao, Weigen Huang. // 2007. IGARSS 2007. IEEE International Geoscience and Remote Sensing Symposium. - Barcelona, 23-28 July 2007. - P. 952-954. ↑

C10327. Souyris J.-C. Multi-look polar decomposition of polarimetric SAR images. / Souyris J.-C., Tison C. // 2007. IGARSS 2007. IEEE International Geoscience and Remote Sensing Symposium. - Barcelona, 23-28 July 2007. - P. 4144-4147. ↑

C10328. Zuberbuhler L. The dependence of polarimetric decomposition parameters on biophysical forest parameters, frequency and methodology. / Zuberbuhler L., Meier E. // 2007. IGARSS 2007. IEEE International Geoscience and Remote Sensing Symposium. - Barcelona, 23-28 July 2007. - P. 4148-4151. ↑

C10329. Soldovieri F. Experimental validation of a Kirchhoff based shape reconstruction algorithm in realistic conditions: a test case for buried pipes. / Soldovieri F., Brancaccio A., Prisco G., Sglavo D., Pierri R., Leone G. // 2007. IGARSS 2007. IEEE International Geoscience and Remote Sensing Symposium. - Barcelona, 23-28 July 2007. - P. 4105-4108. ↑

- C10330.** Villard L. Bistatic foliage penetration modelling. / Villard L., Borderies P. // 2007. IGARSS 2007. IEEE International Geoscience and Remote Sensing Symposium. - Barcelona, 23-28 July 2007. - P. 4109-4112. ↑
- C10331.** Margarit G. Grecosar, a SAR simulator for complex targets: Application to urban environments. / Margarit G., Mallorqui J.J., Lopez-Martinez C. // 2007. IGARSS 2007. IEEE International Geoscience and Remote Sensing Symposium. - Barcelona, 23-28 July 2007. - P. 4160-4163. ↑
- C10332.** Burini A. A neural approach to unsupervised classification of very-high resolution polarimetric SAR data. / Burini A., Putignano C., Del Frate F., Del Greco M., Schiavon G., Solimini D. // 2007. IGARSS 2007. IEEE International Geoscience and Remote Sensing Symposium. - Barcelona, 23-28 July 2007. - P. 4164-4166. ↑
- C10333.** Schimpf H. Properties of polarimetric sea clutter at 35 GHz. / Schimpf H., Fuchs H.-H. // 2007. IGARSS 2007. IEEE International Geoscience and Remote Sensing Symposium. - Barcelona, 23-28 July 2007. - P. 4152-4155. ↑
- C10334.** Marzano F.S. Bayesian classification of hydrometeors from polarimetric radars at S- and X- bands: algorithm design and experimental comparisons. / Marzano F.S., Scaranari D., Montopoli M., Vulpiani G., Anagnostou M.N., Anagnostou E.N. // 2007. IGARSS 2007. IEEE International Geoscience and Remote Sensing Symposium. - Barcelona, 23-28 July 2007. - P. 4156-4159. ↑
- C10335.** Kaab A. Glacier volume changes using ASTER optical stereo. A test study in Eastern Svalbard. 2007. IGARSS 2007. IEEE International Geoscience and Remote Sensing Symposium. - Barcelona, 23-28 July 2007. - P. 3994-3996. ↑
- C10336.** Toyota T. Retrieval of ice thickness distribution in the seasonal ice zone from L-band SAR. / Toyota T., Ohshima K.I., Ebuchi N., Nakamura K., Uto S. // 2007. IGARSS 2007. IEEE International Geoscience and Remote Sensing Symposium. - Barcelona, 23-28 July 2007. - P. 3997-4000. ↑
- C10337.** Makynen M. Interpretation of C-band SAR backscattering coefficient time series for the Baltic Sea landfast sea ice using a 1-D thermodynamic snow/ice model. / Makynen M., Bin Cheng, Simila M., Vihma T., Hallikainen M. // 2007. IGARSS 2007. IEEE International Geoscience and Remote Sensing Symposium. - Barcelona, 23-28 July 2007. - P. 3983-3986. ↑
- C10338.** Shokr M. A new algorithm to calculate sea ice concentration from the SSM/I 85GHz observations. / Shokr M., Lambe A., Agnew T. // 2007. IGARSS 2007. IEEE International Geoscience and Remote Sensing Symposium. - Barcelona, 23-28 July 2007. - P. 3987-3990. ↑
- C10339.** Iorio M. GPR missions on mars. / Iorio M., Fois F., Mecozzi R., Seu R., Picardi G. // 2007. IGARSS 2007. IEEE International Geoscience and Remote Sensing Symposium. - Barcelona, 23-28 July 2007. - P. 4095-4100. ↑
- C10340.** Redadaa S. Focusing problems of subsurface imaging by a low-frequency SAR. / Redadaa S., Le Caillec J.-M., Solaiman B., Benslama M. // 2007. IGARSS 2007. IEEE International Geoscience and Remote Sensing Symposium. - Barcelona, 23-28 July 2007. - P. 4101-4104. ↑
- C10341.** Lambers M. GPU-based framework for interactive visualization of SAR data. / Lambers M., Kolb A., Nies H., Kalkuhl M. // 2007. IGARSS 2007. IEEE International Geoscience and Remote Sensing Symposium. - Barcelona, 23-28 July 2007. - P. 4076-4079. ↑
- C10342.** Huneycutt B. Active remote sensing applications to disaster management with implications to spectrum management. 2007. IGARSS 2007. IEEE International Geoscience and Remote Sensing Symposium. - Barcelona, 23-28 July 2007. - P. 4091-4094. ↑
- C10343.** Ya-Qiu Jin. Retrieval of fully polarimetric mueller matrix under Faraday rotation effect at P band in space-borne polarimetric SAR observation. / Ya-Qiu Jin, Ren-Yuan Qi. // 2007. IGARSS 2007. IEEE International Geoscience and Remote Sensing Symposium. - Barcelona, 23-28 July 2007. - P. 4167-4170. ↑
- C10344.** Nakamura K. Ice flow estimation of Shirase Glacier by using JERS-1/SAR image correlation. / Nakamura K., Wakabayashi H., Doi K., Shibuya K. // 2007. IGARSS 2007. IEEE International Geoscience and Remote Sensing Symposium. - Barcelona, 23-28 July 2007. - P. 4213-4216. ↑

- C10345.** Cea C. An improved methodology to map Snow Cover by means of Landsat and MODIS imagery. / Cea C., Cristobal J., Pons X. // 2007. IGARSS 2007. IEEE International Geoscience and Remote Sensing Symposium. - Barcelona, 23-28 July 2007. - P. 4217-4220. ↑
- C10346.** Luoju K. Assimilating spaceborne radar and ground-based weather station data for operational snow-covered area estimation. / Luoju K., Pulliainen J., Metsamaki S., Anttila S., Hallikainen M. // 2007. IGARSS 2007. IEEE International Geoscience and Remote Sensing Symposium. - Barcelona, 23-28 July 2007. - P. 4202-4205. ↑
- C10347.** Hudier E. Diurnal SAR variability due to ice and snow air interface wetness overnight changes. / Hudier E., Gosselin J.-S., Febres D. // 2007. IGARSS 2007. IEEE International Geoscience and Remote Sensing Symposium. - Barcelona, 23-28 July 2007. - P. 4206-4208. ↑
- C10348.** Erten E. Robust measurement of glacier surface motion from multiscale speckle tracking using local constraints. / Erten E., Reigber A., Jaeger M., Hellwich O. // 2007. IGARSS 2007. IEEE International Geoscience and Remote Sensing Symposium. - Barcelona, 23-28 July 2007. - P. 4237-4240. ↑
- C10349.** Byong Jun Hwang. Passive microwave signatures of autumnal sea ice types from ship-based observation. / Byong Jun Hwang, Ehn J.K., Galley R., Barber D.G. // 2007. IGARSS 2007. IEEE International Geoscience and Remote Sensing Symposium. - Barcelona, 23-28 July 2007. - P. 4245-4248. ↑
- C10350.** Dall J. P-sounder: an airborne P-band ice sounding radar. / Dall J., Skou N., Kusk A., Kristensen S.S., Krozer V. // 2007. IGARSS 2007. IEEE International Geoscience and Remote Sensing Symposium. - Barcelona, 23-28 July 2007. - P. 4225-4228. ↑
- C10351.** Strozzi T. Potential of a C-band SAR mission with 12-day repeat cycle to derive ice surface velocity with interferometry and offset tracking. / Strozzi T., Wegmuller U., Werner C., Wiesmann A., Santoro M. // 2007. IGARSS 2007. IEEE International Geoscience and Remote Sensing Symposium. - Barcelona, 23-28 July 2007. - P. 4229-4232. ↑
- C10352.** Kurz A. The problem of parameter estimation for spatially correlated polarimetric ground clutter at millimeterwave frequencies. / Kurz A., Schimpf H. // 2007. IGARSS 2007. IEEE International Geoscience and Remote Sensing Symposium. - Barcelona, 23-28 July 2007. - P. 4179-4182. ↑
- C10353.** Rangwala M. Design of FMCW millimeter-wave radar for helicopter assisted landing. / Rangwala M., Juseop Lee, Sarabandi K. // 2007. IGARSS 2007. IEEE International Geoscience and Remote Sensing Symposium. - Barcelona, 23-28 July 2007. - P. 4183-4186. ↑
- C10354.** Li Xiaowei. A ship detection method for dual polarization SAR data based on whitening filtering. / Li Xiaowei, Chong Jinsong, Zhu Minhui. // 2007. IGARSS 2007. IEEE International Geoscience and Remote Sensing Symposium. - Barcelona, 23-28 July 2007. - P. 4171-4174. ↑
- C10355.** Goh A.S. Comparison of parameter estimation accuracy of distributed-target polarimetric calibration techniques. / Goh A.S., Preiss M., Gray D.A., Stacy N.J.S. // 2007. IGARSS 2007. IEEE International Geoscience and Remote Sensing Symposium. - Barcelona, 23-28 July 2007. - P. 4175-4178. ↑
- C10356.** Skriver H. Signatures of polarimetric parameters and their implications on land cover classification. 2007. IGARSS 2007. IEEE International Geoscience and Remote Sensing Symposium. - Barcelona, 23-28 July 2007. - P. 4195-4198. ↑
- C10357.** de Souza Soler L. An approach to classify polarimetric P-band SAR images for land use and land cover mapping in the. / de Souza Soler L., Joao S., Sant'Anna S. // 2007. IGARSS 2007. IEEE International Geoscience and Remote Sensing Symposium. - Barcelona, 23-28 July 2007. - P. 4199-4201. ↑
- C10358.** Galletti M. Degree of polarization for weather radars. / Galletti M., Chandra M., Borner T., Bebbington D.H.O. // 2007. IGARSS 2007. IEEE International Geoscience and Remote Sensing Symposium. - Barcelona, 23-28 July 2007. - P. 4187-4190. ↑
- C10359.** Colin E.K. Polarimetric optical tools and decompositions applied to SAR images. 2007. IGARSS 2007. IEEE International Geoscience and Remote Sensing Symposium. - Barcelona, 23-28 July 2007. - P. 4191-4194. ↑
- C10360.** Benavoli A. Design and development of a signal and data processor test bed for a passive radar in

the FM band. / Benavoli A., Chisci L., Di Lallo A., Farina A., Fulcoli R., Mancinelli R., Timmoneri L. // 2007 IET International Conference on Radar Systems. - Edinburgh, UK, 15-18 Oct. 2007. - P. 1-5. ↑

C10361. Khajonrat D. Simultaneous radar observations of tropical cyclones by space-based and ground-based radar. / Khajonrat D., Chandrasekar V., Viswanathan G., Shellar V. // 2007. IGARSS 2007. IEEE International Geoscience and Remote Sensing Symposium. - Barcelona, 23-28 July 2007. - P. 3899-3902. ↑

C10362. Surussavadee C. Comparison of NOWRAD, AMSU, AMSR-E, TMI, and SSM/I surface precipitation rate Retrievals over the united states great plains. / Surussavadee C., Staelin D.H., Chadarong V., McLaughlin D., Entekhabi D. // 2007. IGARSS 2007. IEEE International Geoscience and Remote Sensing Symposium. - Barcelona, 23-28 July 2007. - P. 3923-3926. ↑

C10363. Zhang Yafei. Distributed target detection in SAR images using improved chaos-based method. / Zhang Yafei, Zhu Minhui, Chong Jinsong. // 2007. IGARSS 2007. IEEE International Geoscience and Remote Sensing Symposium. - Barcelona, 23-28 July 2007. - P. 929-932. ↑

C10364. Werninghaus R. TerraSAR-X Mission Status. / Werninghaus R., Buckreuss S., Pitz W. // 2007. IGARSS 2007. IEEE International Geoscience and Remote Sensing Symposium. - Barcelona, 23-28 July 2007. - P. 3927-3930. ↑

C10365. Jackson G.S. Observational data set in support of falling snow retrieval algorithm development. / Jackson G.S., Johnson B., Tokay A., Petersen W. // 2007. IGARSS 2007. IEEE International Geoscience and Remote Sensing Symposium. - Barcelona, 23-28 July 2007. - P. 3903-3906. ↑

C10366. Morrison N. The Gauss-Newton algorithm in passive aircraft tracking using doppler and bearings. / Morrison N., Lord R.T., Inggs M.R. // 2007 IET International Conference on Radar Systems. - Edinburgh, UK, 15-18 Oct. 2007. - P. 1-5. ↑

C10367. Isohookana M.A. Impact of air target altitude and co-channel interference to coverage area of GSM and DVB-T based passive radar. 2007 IET International Conference on Radar Systems. - Edinburgh, UK, 15-18 Oct. 2007. - P. 1-5. ↑

C10368. Tagawa T. Modification of the beam mismatch correction algorithm. / Tagawa T., Shimizu S., Oki R. // 2007. IGARSS 2007. IEEE International Geoscience and Remote Sensing Symposium. - Barcelona, 23-28 July 2007. - P. 3920-3922. ↑

C10369. Zafar B. Adjustment of cross-track dependence of TRMM Precipitation Radar observation. / Zafar B., Chandrasekar V. // 2007. IGARSS 2007. IEEE International Geoscience and Remote Sensing Symposium. - Barcelona, 23-28 July 2007. - P. 3907-3909. ↑

C10370. Takahashi N. Analysis of densely observed TRMM/PR data during 180-degree yaw maneuver. / Takahashi N., Iguchi T. // 2007. IGARSS 2007. IEEE International Geoscience and Remote Sensing Symposium. - Barcelona, 23-28 July 2007. - P. 3914-3919. ↑

C10371. Zink M. The TanDEM-X mission: Overview and status. / Zink M., Krieger G., Fiedler H., Moreira A. // 2007. IGARSS 2007. IEEE International Geoscience and Remote Sensing Symposium. - Barcelona, 23-28 July 2007. - P. 3944-3947. ↑

C10372. Suchandt S. First results of ground moving target analysis in TerraSAR-X data. / Suchandt S., Runge H., Eineder M., Breit H., Kotenkov A., Balss U. // 2007. IGARSS 2007. IEEE International Geoscience and Remote Sensing Symposium. - Barcelona, 23-28 July 2007. - P. 3943. ↑

C10373. Chaabouni-Chouayakh H. Linear versus non-linear analysis of relevant scatterers in high resolution SAR images. / Chaabouni-Chouayakh H., Datcu M. // 2007. IGARSS 2007. IEEE International Geoscience and Remote Sensing Symposium. - Barcelona, 23-28 July 2007. - P. 3895-3898. ↑

C10374. Soccorsi M. Stochastic models of SLC HR SAR images. / Soccorsi M., Datcu M. // 2007. IGARSS 2007. IEEE International Geoscience and Remote Sensing Symposium. - Barcelona, 23-28 July 2007. - P. 3887-3890. ↑

C10375. Benboudjema D. Unsupervised segmentation of SAR images using Triplet Markov fields and fisher noise distributions. / Benboudjema D., Tupin F., Pieczynski W., Sigelle M., Nicolas J.-M. // 2007. IGARSS 2007.

IEEE International Geoscience and Remote Sensing Symposium. - Barcelona, 23-28 July 2007. - P. 3891-3894.



C10376. Adam N. TerraSAR-X interferometry: report on a first assessment. / Adam N., Eineder M., Schattler B., Bamler R. // 2007. IGARSS 2007. IEEE International Geoscience and Remote Sensing Symposium. - Barcelona, 23-28 July 2007. - P. 3942.

C10377. Schwerdt M. TerraSAR-X calibration-first results. / Schwerdt M., Brautigam B., Bachmann M., Doring B. // 2007. IGARSS 2007. IEEE International Geoscience and Remote Sensing Symposium. - Barcelona, 23-28 July 2007. - P. 3932-3935.

C10378. Marquez-Martinez J. In-orbit SAR performance of TerraSAR-X. / Marquez-Martinez J., Gonzalez C., Younis M., Wollstadt S., Metzger R. // 2007. IGARSS 2007. IEEE International Geoscience and Remote Sensing Symposium. - Barcelona, 23-28 July 2007. - P. 3931.

C10379. Breit H. TerraSAR-X payload data processing-First Experiences. / Breit H., Fritz T., Schattler B., Borner E., Lachaise M., Niedermeier A., Eineder M., Balss U. // 2007. IGARSS 2007. IEEE International Geoscience and Remote Sensing Symposium. - Barcelona, 23-28 July 2007. - P. 3936.

C10380. Schmidt N. TerraSAR-X value added image products. / Schmidt N., Janoth J., Raggam J., Gutjahr K., Wimmer A. // 2007. IGARSS 2007. IEEE International Geoscience and Remote Sensing Symposium. - Barcelona, 23-28 July 2007. - P. 3938-3941.

C10381. Huber M. Quality of orthorectified TerraSAR-X products. / Huber M., Wessel B., Habermeyer M., Roth A. // 2007. IGARSS 2007. IEEE International Geoscience and Remote Sensing Symposium. - Barcelona, 23-28 July 2007. - P. 3937.

© В.И. Карнышев, 2011

Тематический реферативный сборник сгенерирован в автоматическом режиме
с использованием специализированного программного модуля (ПАО ТУСУР)